

# **MICROWAVE MOLECULAR SPECTRA**

**WALTER GORDY**

Duke University  
Durham, North Carolina

**ROBERT L. COOK**

Mississippi State University  
Mississippi State, Mississippi

A WILEY-INTERSCIENCE PUBLICATION

**JOHN WILEY & SONS**

New York • Chichester • Brisbane • Toronto • Singapore

Copyright © 1984 by John Wiley & Sons, Inc.

All rights reserved. Published simultaneously in Canada.

Reproduction or translation of any part of this work beyond that permitted by Section 107 or 108 of the 1976 United States Copyright Act without the permission of the copyright owner is unlawful. Requests for permission or further information should be addressed to the Permissions Department, John Wiley & Sons, Inc.

Library of Congress Catalogue Card Number: 84-40367

ISBN 0-471-08681-9

Printed in the United States of America

10 9 8 7 6 5 4 3 2 1

## ***TO THE DUKE MICROWAVERS***

The more than one hundred graduate students  
and research associates who have contributed much  
to the development of microwave spectroscopy.

# INTRODUCTION TO THE SERIES

---

Techniques of Chemistry is the successor to the Technique of Organic Chemistry Series and its companion—Technique of Inorganic Chemistry. Because many of the methods are employed in all branches of chemical science, the division into techniques for organic and inorganic chemistry has become increasingly artificial. Accordingly, the new series reflects the wider application of techniques, and the component volumes for the most part provide complete treatments of the methods covered. Volumes in which limited areas of application are discussed can be easily recognized by their titles.

Like its predecessors, the series is devoted to a comprehensive presentation of the respective techniques. The authors give the theoretical background for an understanding of the various methods and operations and describe the techniques and tools, their modifications, their merits and limitations, and their handling. It is hoped that the series will contribute to a better understanding and a more rational and effective application of the respective techniques.

Authors and editors hope that readers will find the volumes in this series useful and will communicate to them any criticisms and suggestions for improvements.

ARNOLD WEISSBERGER

*Research Laboratories  
Eastman Kodak Company  
Rochester, New York*

# PREFACE

---

Many exciting new developments in microwave spectroscopy have occurred since the earlier edition of this book was published in 1970. The frequency coverage of coherent microwave spectroscopy is still expanding. Although not comparable to the fourfold expansion that occurred in the 17 years preceding the 1970 edition, the millimeter wave range has been extended from 800 GHz to above 1000 GHz since 1970. Subtle new techniques continue to improve the sensitivity and resolving power of microwave spectrometers as well as their applicability to new types of spectra.

Detection of the microwave spectra of nonpolar, spherical-top molecules such as  $\text{CH}_4$  and of "forbidden"  $\Delta K$  transitions in symmetric-top molecules such as  $\text{PH}_3$  has been achieved. Microwave "molecular ion" spectroscopy has become a practical reality since 1970. The observation of rotational spectra of weak, hydrogen-bonded complexes and rare gas atom—molecule complexes (van der Waals molecules) has become widespread. New techniques for observation of molecules in highly excited vibrational states have been devised. Significant advances in the theory of complex microwave molecular spectra have been made. In the last 15 years microwave spectroscopy has advanced from observation of molecules in laboratory cells to observation of molecules in interstellar space. An important new field, microwave molecular astronomy, has been created. Microwave sources and techniques have been combined with infrared and optical lasers to form the new and rapidly advancing field of microwave-optical double resonance spectroscopy.

Although the spectra described in the earlier edition are in no sense out of date, the new developments made the revision of *Microwave Molecular Spectra* desirable if not necessary. The basic theory and measurements of microwave spectroscopy have a remarkable durability which results from the high resolution and accuracy of measurement that characterize all coherent radiation spectroscopy of sharp line spectra. Because we could not justifiably delete nor significantly reduce the basic material of the earlier edition, a moderate expansion of the volume was necessary to achieve an adequate coverage of microwave molecular spectra in the 1980s.

As was true for the earlier edition, we are indebted to many people for assistance in the revision of this book. Again, Vida Miller Gordy graciously assisted with every phase of the manuscript preparation. We have benefited by discussions with Frank De Lucia, Eric Herbst, Paul Helminger, and K. V. L. N. Sastry. The Winnewissers—Manfred, Brenda, and Gisbert—have helped to

keep us informed about the latest results in the field. M. C. L. Gerry read parts of the manuscript and made helpful suggestions. We are also grateful to other spectroscopists for sending us preprints and reprints describing results obtained in their laboratories. Among them are Lisa Nygaard, E. Tiemann, H. Dreizler, H. D. Rudolph, A. F. Krupnov, and J. L. Destombes.

Finally, we wish to express a tribute to the memory of Dr. William West, editor of the earlier edition. He was a great person, a considerate and competent editor, and a treasured friend.

WALTER GORDY  
ROBERT L. COOK

*Durham, North Carolina  
July 1984*

# PREFACE TO THE SECOND EDITION

---

In the 17 years since the first book on microwave spectroscopy was written, the field has developed so extensively that it is not possible to give a comprehensive coverage of all its aspects within a single volume of manageable size. Not only have the applications been increased enormously and the instruments and techniques diversified, but the microwave region itself has also been greatly expanded. The frequency range in which spectral measurements can be made with microwave methods has increased more than fourfold since 1953. Many measurements are now made at submillimeter wavelengths. With the molecular beam maser the already ultrahigh resolution of microwave spectroscopy has been increased by more than an order of magnitude. Rapidly recording, highly sensitive microwave spectrometers have become commercially available. High-speed computers have taken much of the labor out of the analysis and have made the study of complex molecules more feasible. New theoretical developments have increased the possibility of understanding complex spectra and have also increased the usefulness of such spectra. Microwave spectral measurements on short-lived gaseous free radicals and on substances with vaporization temperatures of the order of a thousand degrees are commonly made. Spectral frequencies are measured to accuracies of the order of one part in  $10^8$ . Accurate molecular structures and other properties have been found for molecules numbering into the thousands.

In this volume we have sought to provide a basis for the understanding of microwave spectra in the gas phase. In doing this we have developed the theory from what we considered to be the simplest approach consistent with essential correctness and applicability. Although we make no effort to include all the useful information about molecules that has been derived from the spectra—a hardly achievable goal—we have included a variety of types of information about selected molecules. A reasonably complete listing of the molecular structures derived up to 1969 is given in the appendix. Although the book is a member of the *Technique of Organic Chemistry* series, we have by no means limited the coverage to organic molecules. To do so would have been too wasteful because the theory applicable to organic molecules is generally applicable to inorganic molecules. The book is written for chemical physicists and physical chemists as well as for organic chemists—if indeed such separate classifications are *bona fide* in this age. We have not included a discussion of the determination of nuclear moments and masses, subjects that

are perhaps of more interest to physicists than to chemists. Most nuclear moments and isotopic masses that can be measured to advantage with microwave spectra have already been measured. Rather we have treated nuclear hyperfine structure and isotopic shifts of spectral lines with the aim of using them to gain information about molecules. To achieve more thorough coverage of gases we have omitted solid-state studies, which are made primarily with microwave paramagnetic resonance (included in another volume of this series) and liquid-state studies made chiefly through dielectric dispersion and absorption. For the same reason we have omitted discussion of instruments and techniques of measurement.

Nevertheless we have tried to serve the dual purpose of providing a convenient source and reference book for much of the valuable information gained about molecules through microwave spectroscopy and of providing a textbook that explains essential theory for interpretation of the spectra and derivation of information from spectra. Although not written specifically for the purpose, the book can be used as a text for a course or seminar on microwave spectra. A quantitative study of microwave spectroscopy provides numerous, rather elegant examples of the application of quantum mechanics to problems of molecular dynamics. Although the quantum mechanical treatment can in some cases be somewhat complicated in its details, much of the information derivable from microwave spectra of molecules is of such importance that it justifies more than casual attention.

Several people have assisted considerably in the preparation of the volume. Vida Miller Gordy has helped persistently and effectively in the preparation and proofreading of the manuscript. Jean Luffman's typing of the entire manuscript presented us with a beautiful final copy from the many revisions given her in the course of the writing. Janet Jackel drew most of the illustrations. Several research associates and graduate students at Duke University—James Cederberg, Frank De Lucia, Steve Guastafson, Paul Helminger, Sam McKnight, William Oelfke, Edward Pearson, David Straub, Gisbert Winnewisser, Ray Winton, and Fred Wyse—have read sections of the book and made helpful suggestions. To each one we offer our thanks.

WALTER GORDY  
ROBERT L. COOK

*Durham, North Carolina  
April 20, 1969*

# CONTENTS

---

## CHAPTERS

I. Introduction	1
II. Theoretical Aspects of Molecular Rotation	11
III. Microwave Transitions—Line Intensities and Shapes	37
IV. Diatomic Molecules	71
V. Linear Polyatomic Molecules	125
VI. Symmetric-top Molecules	175
VII. Asymmetric-top Molecules	227
VIII. The Distortable Rotor	297
IX. Nuclear Hyperfine Structure in Molecular Rotational Spectra	391
X. Effects of Applied Electric Fields	451
XI. Effects of Applied Magnetic Fields	505
XII. Internal Motions	569
XIII. Derivation of Molecular Structures	647
XIV. Quadrupole Couplings, Dipole Moments, and the Chemical Bond	725
XV. Irreducible Tensor Methods for Calculation of Complex Spectra	803

## APPENDIXES

A. Notes on Matrix Mechanical Methods	841
B. Calculation of the Eigenvalues and Eigenvectors of a Hermitian Tridiagonal Matrix by the Continued Fraction Method	849
C. The Van Vleck Transformation	853
D. Fundamental Constants and Conversion Factors	857
E. Isotopic Abundances, Masses, and Moments	859

<b>F. Bond Radii</b>	<b>873</b>
<b>G. Electronegativities of the Elements</b>	<b>875</b>
<b>H. Computational Procedure for the Vibrational Eigenvalue Problem</b>	<b>879</b>
<b>I. Energies and Relative Intensities of Nuclear Quadrupole Hyperfine Structure</b>	<b>881</b>
<b>J. Nuclear Quadrupole Second-Order Correction Energies for Linear or Symmetric-top Molecules</b>	<b>895</b>
<b>Author Index</b>	<b>897</b>
<b>Subject Index</b>	<b>917</b>

# INTRODUCTION

---

Microwave and radiofrequency spectroscopy are branches of spectroscopy in which the spectral transitions are measured with coherent radiation sources. The radiation sources employed are phase-coherent oscillators which provide energy in a frequency band so narrow that in comparison with most spectral lines they can be considered monochromatic sources. These essentially monochromatic sources are tunable and can be swept over a spectral line to be measured or can be conveniently tuned over wide regions in search of unknown spectral lines. The resolution easily obtainable with these tuned radio electronic oscillators is thousands of times greater than that of conventional infrared spectrometers employing noncoherent sources, with prisms or gratings for dispersion.

Figure 1.1 shows the extent of the microwave region of the electromagnetic spectrum. This region is designated as extending from wavelengths of approximately 30 cm to those of 0.3 mm, or from frequencies of 1 GHz to those of 1000 GHz, or 1 THz. The GHz unit (gigacycles per second), now commonly used by microwave spectroscopists, represents  $10^9$  Hz, or a thousand megacycles per second.

In the initial period of microwave spectroscopy, measurements were made in the centimeter wave region with oscillators and detectors developed for microwave radar during World War II. The experimental techniques and extensive results for this period are described in the earlier books on microwave spectroscopy [1, 2]. In later years the range of microwave measurements has been extended throughout the millimeter and into the submillimeter wavelengths, to 0.3 mm (1000 GHz or 1 THz).

In 1954, coherent microwave spectral measurements by Burrus and Gordy [3] were made to overlap the far-infrared grating measurements of Genzel and Eckhardt [4]. This extension of microwave spectroscopy into the submillimeter wave region was made possible by a crystal harmonic generator and a

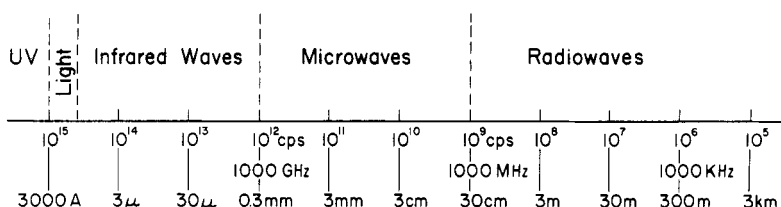
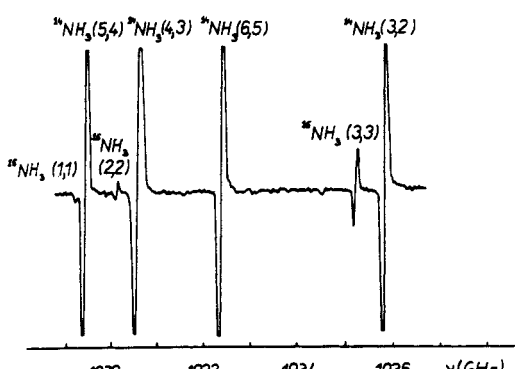


Fig. 1.1 Chart showing the extent of the microwave region of the electromagnetic spectrum.

crystal diode detector designed by King and Gordy [5]. Later refinement of the harmonic generators and improvement in the sensitivity of the submillimeter wave detectors led to further extension of coherent, tunable, microwave spectroscopy [6–9] to frequencies of 800 GHz (0.37 mm) by 1970 [8] and to 1037 GHz (0.38 mm) by 1983 [9]. Since harmonics are exact multiples of the fundamental frequency of the source power, this type of generator carries with it a precise frequency-measuring chain to the highest detectable harmonic. For example, the  $J=8 \rightarrow 9$  transition of CO was detected and measured [9] at 1,036,312.35 MHz with a Doppler-limited accuracy of about  $\pm 0.15$  MHz. Among the later improvements of the submillimeter wave spectrometers at Duke was the use of ion-bombarded [10] silicon crystals in the harmonic generators and replacement of the crystal diode detector with detectors operating at low temperatures, particularly by an indium–antimonide photoconducting detector [8] and by a silicon bolometer [11].

Very impressive submillimeter wave spectral observations with primary radiation from tunable, submillimeter wave, backward-wave oscillators (BWO's) are now made by A. F. Krupnov [12, 13] and his group working in Gorky, USSR. For detection of the spectra, they employ an acoustic detector that depends on the thermal expansion of the gaseous sample produced by the resonant absorption of the radiation at the frequency of the spectral absorption line. They designate this type of spectrometer by RAD, which signifies “radio-spectroscope with acoustic detector.” Their experiments, initiated about 1970, have resulted in high-resolution measurements in the submillimeter wave region to frequencies above 1000 GHz, or to wavelengths of 0.3 mm. An illustration of the remarkable performance of this spectrometer [14] is given in Fig. 1.2. A description of the spectrometer with a discussion of its performance is given in reviews by Krupnov and Burenin [12] and by Krupnov [13].

The development of effective microwave instruments and techniques for measurements in the shorter millimeter and the submillimeter wave region



**Fig. 1.2** Part of the submillimeter wave spectrum of  $\text{NH}_3$  in the 1 THz region (1000 GHz). From Belov et al. [14].

from 3 mm to approximately 0.3 mm (100 to 1000 GHz) has not only increased the coverage of molecular rotational spectra but has also made possible the use of semioptical techniques [15] for the focusing and direction of radiation without any sacrifice in the resolution and accuracy of the microwave source and detector. It has also made possible the use of free-space cells for corrosive or unstable molecules and ions, the use of molecular-beam, high-temperature absorption spectrometers for molecules having high vaporization temperatures, and the use of precision parallel-plate cells for measurement of Stark components. The increase in the abundance and the strength of microwave molecular lines with increase of frequency insures that the last explored region of the electromagnetic spectrum, the submillimeter wave region, will continue to be a region of interest and value to the chemist and the physicist. Experimental methods and descriptions of the results obtained with millimeter and submillimeter wave spectroscopy are available in several reviews [15–19]. Treatments of selected results will be found throughout this volume.

Because of their low intensity, spontaneous emission lines are not observable in the microwave or radiofrequency region. Since the invention of the maser, however, observation of certain microwave spectral lines through stimulated emission has become common. To make such an observation one must in some way upset the Boltzmann distribution so as to obtain an excess population in the upper of two quantum levels involved in the transition. In the first operating maser, Gordon, Zeiger, and Townes [20] accomplished this by removal of the molecules in the lower state through deflection of a molecular beam by an inhomogeneous electric field. Several other methods have since been devised for achievement of excess population in the upper state sufficient for observation of stimulated emission spectroscopy. Perhaps those most widely used are optical pumping [21] and chemical pumping [22].

The exceptional resolution in a beam-maser spectrometer makes it of great advantage in the study of specialized problems. The resolution obtainable in microwave spectroscopy with the molecular beam maser is illustrated [23] by Fig. 1.3, which shows the triplet hyperfine structure due to the deuterium nucleus superimposed upon a hyperfine component of  $^{14}\text{N}$  in the  $J=0\leftarrow 1$  rotational transition of DCN. The total width of this triplet which occurs at a frequency of 72,414 MHz is only 68.7 kHz, and the two closest components are separated by only 23 kHz. These frequencies are measured to an accuracy of better than a kilohertz, or to one part in  $10^8$ . Application of this beam maser has been extended into the upper submillimeter region by Garvey and De Lucia [24] to measure with comparable resolution the hyperfine structure of the  $J=0\leftarrow 1$  transition of  $\text{ND}_3$  at 309 GHz and of the  $1_{10}\rightarrow 1_{01}$  transition of  $\text{D}_2\text{O}$  at 317 GHz. Developments in techniques and applications of molecular beam masers up to 1975 are described in an excellent review by Lainé [25].

Since the publication of the earlier edition of this book (1970), microwave-optical laser double resonance has become increasingly important in measurement of the rotational structure of excited vibrational and electronic levels of molecules [26–30]. Harold Jones gives a thorough review of the important

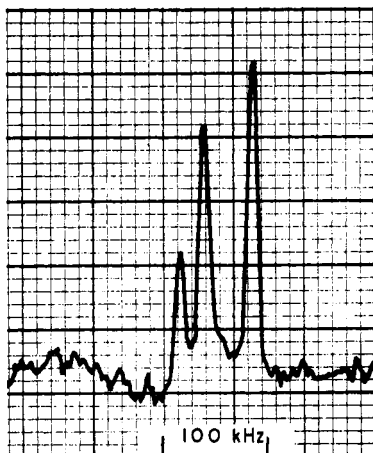


**Fig. 1.3** Illustration of the exceptional resolution obtainable with the molecular beam maser. The spectra, observed at 72,414 MHz, represent a part of the hyperfine structure of the  $J=0 \rightarrow 1$  transition of DCN. The splitting is due to the nuclear quadrupole coupling of deuterium. From De Lucia and Gordy [23].

infrared-microwave double resonance technique [30]. The development of tunable dye-lasers and the expansion of microwave techniques for the millimeter and submillimeter wave lengths have made microwave-optical double resonance increasingly feasible. An excellent monograph on laser spectroscopy by Demtroder [31] explains experimental techniques and spectral applications. Microwave-microwave double resonance has become a powerful technique for study of special problems such as molecular collision processes. Experimental methods and applications are described in a review by Baker [32]. The use of this technique for identification of spectral transitions in asymmetric rotors is described in Chapter VII, Section 5.

Lines of the strong HCN laser source [33, 34] in the 0.337 mm wave region have been accurately measured in frequency units by Hocker et al. [35, 36], who detected beat notes between the laser frequencies and the harmonics of a calibrated microwave source. A laser source thus calibrated was later used to give measurable beat notes with a laser operating at a higher frequency [37]; the second laser thus calibrated could be used for measurement of beat notes with a laser operating at a still higher frequency, and so on. With this method, optical laser sources have been measured indirectly, but precisely, in absolute frequency units. By this means the microwave harmonic frequency-measuring chain has been projected to the optical region.

Reviews of various types of lasers, with references to numerous monographs on lasers and their various applications, may be found in *Quantum Electronics*, a 1979 volume of *Methods in Experimental Physics* [38].

This book is primarily concerned with interpretation of observed spectra.

Descriptions of instruments and experimental procedures must be obtained from other sources. An excellent treatment (1979) of modern microwave spectrometers and experimental methods is given by Roussy and Chantry [39]. The pulsed, coherent microwave Fourier-transform spectrometer introduced by Ekkers and Flygare [40] holds much promise for subtle observations requiring exceptional sensitivity and resolution [41]. Interferometric methods for non-coherent (black-body) millimeter and submillimeter spectroscopy described by Fleming [42] are convenient and useful for applications where very high resolution is not required.

A technique that has evolved since the earlier edition is the adaptation of the "supersonic free jet" [43] in the study of van der Waals molecules with microwave spectroscopy [41] (Chapter V, Section 9). The method also makes possible observation of very weak hydrogen-bonded complexes that are unstable at ordinary temperatures (Chapter V, section 8) and the study of rotational transitions in normal molecules at very low temperatures, at which they would solidify in a normal absorption cell. The cooling in the supersonic jet is caused by the expansion of a highly pressurized gas as it escapes through a restricting nozzle into an evacuated microwave cavity. The restricting nozzle also collimates the escaping gas into a beam [43].

Applications of microwave spectroscopy to the study of molecular fragments, gaseous free radicals, and molecules in excited electronic states with unpaired electron spins have significantly increased since the earlier edition. Carrington's monograph on the microwave spectroscopy of gaseous free radicals (1974) describes both spectra and experimental methods [44]. The developments in microwave-optical double resonance have greatly facilitated the measurement of paramagnetic transitions of molecules in excited triplet states [45]. Since the initial observations of the microwave rotational spectra of ionized molecules such as  $\text{CO}^+$  and  $\text{HCO}^+$  by R. C. Woods and his associates [46, 47] in 1975, the spectroscopy of molecular ions has become a rapidly developing component of microwave spectroscopy [48].

The extensive observation of microwave spectral lines of molecules in interstellar space is an exciting development, most of which has occurred since the earlier edition. Lines from molecular free radicals and ions, as well as from stable molecules, are being observed with microwave spectral telescopes, operated primarily in the millimeter wave range. Many of these are emission lines originating through a cosmological laser action. The first molecular species to be detected in interstellar space through measurement of its microwave spectral lines was the OH free radical observed in 1963 [49]. The first of the stable molecules thus to be observed [50] in outer space (1968) was ammonia,  $\text{NH}_3$ , which, it is interesting to recall, was the first terrestrial molecule to be observed with microwave spectroscopy, the first to control the frequencies of an atomic clock, and the molecule used in the first operating maser. Within a few years after these initial microwave observations of molecules in outer space, microwave spectroscopy had become a powerful new technique for astronomical investigations. Laboratory measurement and identification of the

observed interstellar transitions greatly facilitated the astronomical applications. Late reviews of this rapidly developing field are available [51–53].

The interesting microwave spectrum in Fig. 1.4, the  $J=0\rightarrow 1$  rotational transition of  $(\text{NNH})^+$  showing the  $^{14}\text{N}$  nuclear quadrupole structure, was recorded from the Orion molecular cloud [54]. This molecular species had not been previously observed in the laboratory. Identification of the species was confirmed by comparison of the observed hyperfine pattern with a theoretically calculated pattern, as shown in the figure. Preliminary observations [55] and a tentative identification [56] had been made earlier.

Discrete spectral transitions that are measured primarily in the radio-frequency region up to 1 GHz (1000 MHz) are nuclear resonances (magnetic and electric quadrupole) and molecular beam resonances (electric and magnetic). Measurable pure rotational spectra of gaseous molecules fall predominantly in the microwave region; electron spin magnetic resonance is most

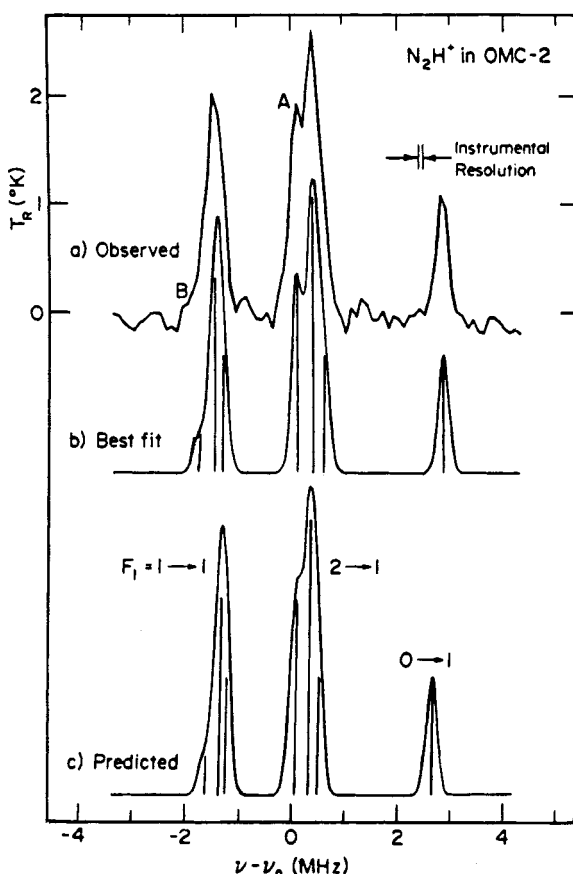


**Fig. 1.4** The 93.174 GHz lines in OMC-2, compared with theoretical calculations of the hyperfine structure of the  $J=1\rightarrow 0$  transition of  $\text{N}_2\text{H}^+$ . From Thaddeus and Turner [54].

advantageously observed in this region. The mathematical methods for treating these types of spectra, the procedures for calculating the energy eigenvalues, line intensities, selection rules, and so on, are basically similar. They all include momentum or intrinsic spin operators, dipole moment or direction cosine matrix elements, and state populations that depend on similar statistical mechanisms. The applications described in this volume are primarily rotational spectra of gaseous molecules. Microwave electron spin resonance spectra in condensed matter is treated in a companion volume of this series [57].

The development and increased availability of high-speed computers have paralleled the improvements in techniques and the expanding frequency coverage of microwave spectroscopy. These computers have greatly augmented the contributions in microwave spectroscopy by facilitating the interpretation of complex spectra.

We make no attempt to give a complete or comprehensive treatment of microwave spectroscopy. The field is now so large that such a treatment is impossible in a single volume. We shall limit our coverage mainly to problems of interest to chemists and chemical physicists. The tabulations and references we give are not intended to be complete but to be illustrative of what has been done and what can be done in the field. There are other books that describe instruments and techniques as well as spectra [58–63]. Extensive tabulations of line frequencies measured with microwave spectroscopy are given in a series of volumes published under the auspices of the National Bureau of Standards [64]. Extensive tabulations of molecular structures and constants derived from microwave spectroscopy are available in the Landolt-Börnstein series [65]. *Molecular Spectroscopy*, an annual review published by the Chemical Society (London), covers “Microwave Spectroscopy” from 1970 [66]. A book by Mizushima [67] on the theory of rotating diatomic molecules contains many applications to microwave spectra. A tabulation of the constants of diatomic molecules (to 1978) has been provided by Huber and Herzberg [68]. The valuable book *Modern Aspects of Microwave Spectroscopy*, edited by Chantry, is already referenced several times [13, 30, 32, 39, 42, 52]. Advances in the application of microwave spectroscopy to the area of chemical analysis are reviewed elsewhere [69, 70].

## References

1. W. Gordy, W. V. Smith, and R. F. Trambarulo, *Microwave Spectroscopy*, Wiley, New York, 1953. Republication by Dover, New York, 1966.
2. C. H. Townes and A. L. Schawlow, *Microwave Spectroscopy*, McGraw-Hill, New York, 1955.
3. C. A. Burrus and W. Gordy, *Phys. Rev.*, **93**, 897 (1954).
4. L. Genzel and W. Eckhardt, *Z. Physik*, **139**, 592 (1954).
5. W. C. King and W. Gordy, *Phys. Rev.*, **90**, 319 (1953).
6. M. Cowan and W. Gordy, *Phys. Rev.*, **111**, 209 (1958).
7. G. Jones and W. Gordy, *Phys. Rev.*, **135**, A295 (1964).
8. P. Helminger, F. C. De Lucia, and W. Gordy, *Phys. Rev. Lett.*, **25**, 1397 (1970).

9. P. Helminger, J. K. Messer, and F. C. De Lucia, *Appl. Phys. Lett.*, **42**, 309 (1983).
10. R. S. Ohl, P. P. Budenstein, and C. A. Burrus, *Rev. Sci. Instrum.*, **30**, 765 (1959).
11. W. Steinbach and W. Gordy, *Phys. Rev.*, **A8**, 1753 (1973).
12. A. F. Krupnov and A. V. Burenin, "New Methods in Submillimeter Microwave Spectroscopy," in *Molecular Spectroscopy: Modern Research*, Vol. 2, K. N. Rao and C. W. Mathews, Eds., Academic, New York, 1976, pp. 93-126.
13. A. F. Krupnov, "Modern Submillimetre Microwave Scanning Spectrometry," in *Modern Aspects of Microwave Spectroscopy*, G. W. Chantry, Ed., Academic, London, 1979, pp. 217-256.
14. S. P. Belov, L. I. Gershstein, A. F. Krupnov, A. V. Maslovskij, S. Urban, V. Špirko, and D. Papoušek, *J. Mol. Spectrosc.*, **84**, 288 (1980).
15. W. Gordy, "Microwave Spectroscopy in the Region of 4-0.4 Millimetres," in *Pure and Applied Chemistry*, Vol. 11, Butterworths, London, 1965, pp. 403-434.
16. G. Winnewisser, M. Winnewisser, and B. P. Winnewisser, "Millimetre Wave Spectroscopy," in *MTB International Review of Science, Physical Chemistry*, Vol. 3, *Spectroscopy*, D. A. Ramsey, Ed., Butterworths, London, 1972, pp. 241-296.
17. F. C. De Lucia, "Millimeter and Submillimeter Wave Spectroscopy," in *Molecular Spectroscopy: Modern Research*, K. N. Rao and C. W. Mathews, Eds., Vol. 2, Academic, New York, 1976, pp. 69-92.
18. Y. Morino and S. Saito, "Microwave Spectroscopy," in *Molecular Spectroscopy: Modern Research*, K. N. Rao and C. W. Mathews, Eds., Vol. 1, Academic, New York, 1972, pp. 9-28.
19. D. R. Johnson and R. Pearson, Jr., "Microwave Region," in *Methods in Experimental Physics*, Vol. 13, *Spectroscopy*, Part B, D. Williams, Ed., Academic, New York, 1976, pp. 102-133.
20. J. P. Gordon, H. J. Zeiger, and C. H. Townes, *Phys. Rev.*, **99**, 59 (1955).
21. J. Brossel and A. Kastler, *Compt. Rendu Acad. Sci. (Paris)*, **229**, 1213 (1949); F. Bitter, *Phys. Rev.*, **76**, 833 (1949).
22. T. A. Cool, "Chemically Pumped Lasers," in *Methods in Experimental Physics*, Vol. 15, *Quantum Electronics*, Part B, C. L. Tang, Ed., Academic, New York, 1979, pp. 95-142.
23. F. C. De Lucia and W. Gordy, *Phys. Rev.*, **187**, 58 (1969).
24. R. M. Garvey and F. C. De Lucia, *Can. J. Phys.*, **55**, 1115 (1977).
25. D. C. Lainé, "Advances in Molecular Beam Maser," in *Advances in Electronics and Electron Physics*, Vol. 39, L. Marton, Ed., Academic, New York, 1975, pp. 183-251.
26. T. Shimizu and T. Oka, *J. Chem. Phys.*, **53**, 2536 (1970).
27. M. Takami and K. Shimoda, *J. Mol. Spectrosc.*, **59**, 35 (1976).
28. I. Botskor and H. Jones, *J. Mol. Spectrosc.*, **81**, 1 (1980).
29. F. Kohler, H. Jones, and H. D. Rudolph, *J. Mol. Spectrosc.*, **80**, 56 (1980).
30. H. Jones, "Infrared Microwave Double Resonance Techniques," in *Modern Aspects of Microwave Spectroscopy*, G. W. Chantry, Ed., Academic, London, 1979, pp. 123-216.
31. W. Demtroder, *Laser Spectroscopy*, Springer-Verlag, New York, 1980.
32. J. G. Baker, "Microwave-Microwave Double Resonance," in *Modern Aspects of Microwave Spectroscopy*, G. W. Chantry, Ed., Academic, London, 1979, pp. 65-122.
33. H. A. Gebbie, N. W. B. Stone, and F. D. Findlay, *Nature*, **202**, 685 (1964).
34. D. R. Lide and A. G. Maki, *Appl. Phys. Lett.*, **11**, 62 (1967).
35. L. O. Hocker, A. Javan, D. R. Rao, L. Frankel, and T. Sullivan, *Appl. Phys. Lett.*, **10**, 147 (1967).
36. L. O. Hocker and A. Javan, *Phys. Lett.*, **A25**, 489 (1967).
37. L. O. Hocker and A. Javan, *Phys. Lett.*, **A26**, 255 (1968).
38. C. L. Tang, Ed., *Quantum Electronics*, Vol. 15, Part B of *Methods of Experimental Physics*, Academic, New York, 1979.

39. G. Roussy and G. W. Chantry, "Microwave Spectrometers," in *Modern Aspects of Microwave Spectroscopy*, G. W. Chantry, Ed., Academic, London, 1979, pp. 1-63.
40. J. Ekkers and W. H. Flygare, *Rev. Sci. Instrum.*, **47**, 448 (1976).
41. T. J. Balle, E. J. Campbell, M. R. Keenan, and W. H. Flygare, *J. Chem. Phys.*, **72**, 922 (1980).
42. J. W. Fleming, "Interferometric Spectrometry at Millimetre and Submillimetre Wavelengths," in *Modern Aspects of Microwave Spectroscopy*, G. W. Chantry, Ed., Academic, London, 1979, pp. 257-309.
43. D. H. Levy, "The Spectroscopy of Very Cold Gases," *Science*, **214**, 263-269 (1981).
44. A. Carrington, *Microwave Spectroscopy of Free Radicals*, Academic, New York, 1974.
45. M. A. El-Sayed, "Phosphorescence-Microwave Multiple Resonance Spectroscopy," in *MTB International Review of Science, Physical Chemistry*, Vol. 3, *Spectroscopy*, D. A. Ramsey, Ed., Butterworths, London, 1972, pp. 119-153.
46. T. A. Dixon and R. C. Woods, *Phys. Rev. Lett.*, **34**, 61 (1975).
47. R. C. Woods, T. A. Dixon, J. R. Saykally, and P. G. Szanto, *Phys. Rev. Lett.*, **35**, 1269 (1975).
48. R. J. Saykally and R. C. Woods, "High Resolution Spectroscopy of Molecular Ions," *Ann. Rev. Phys. Chem.*, **32**, 403-431 (1981).
49. S. Weinreb, A. H. Barrett, M. L. Meeks, and J. C. Henry, *Nature*, **200**, 829 (1963).
50. A. C. Cheung, D. M. Rank, C. H. Townes, D. D. Thornton, and W. J. Welch, *Phys. Rev. Lett.*, **21**, 1701 (1968).
51. W. B. Somerville, "Interstellar Radio Spectrum Lines," *Rep. Prog. Phys.*, **40**, 483-565 (1977).
52. G. Winnewisser, E. Churchwell, and C. M. Walmsley, "Astrophysics of Interstellar Molecules," in *Modern Aspects of Microwave Spectroscopy*, G. W. Chantry, Ed., Academic, London, 1979, pp. 313-503.
53. A. Carrington and D. A. Ramsey, Eds., *Molecules in Interstellar Space*, The Royal Society, London, 1982.
54. P. Thaddeus and B. F. Turner, *Astrophys. J. (Letters)*, **201**, L25 (1975).
55. B. F. Turner, *Astrophys. J. (Letters)*, **193**, L83 (1974).
56. S. Green, J. A. Montgomery, Jr., and P. Thaddeus, *Astrophys. J. (Letters)*, **193**, L89 (1974).
57. W. Gordy, *Theory and Applications of Electron Spin Resonance*, Wiley-Interscience, New York, 1980.
58. M. W. P. Strandberg, *Microwave Spectroscopy*, Methuen, London, 1954.
59. D. J. E. Ingram, *Spectroscopy at Radio and Microwave Frequencies*, Butterworths, London, 1955. Second Ed., Plenum Press, New York, 1967.
60. T. M. Sugden and C. N. Kenney, *Microwave Spectroscopy of Gases*, Van Nostrand, London, 1965.
61. J. B. Wollrab, *Rotational Spectra and Molecular Structure*, Academic, New York, 1967.
62. J. G. Baker gives an excellent treatment of harmonic generators and semiconductor detectors for millimeter and submillimeter waves in *Spectroscopic Techniques for Far Infra-red, Sub-millimetre and Millimetre Waves*, D. H. Martin, Ed., North Holland Publishing Co., Amsterdam, 1967, Ch. 5. E. H. Putley and D. H. Martin give a thorough treatment of bolometer detectors as well as point detectors. Op cit., Ch. 4.
63. H. W. Kroto, *Molecular Rotation Spectra*, John Wiley, London, 1975.
64. *Microwave Spectra Tables*, National Bureau of Standards, U.S. Department of Commerce, Washington, D.C. From 1964.
65. Landolt-Börnstein, *Numerical Data and Functional Relationships in Science and Technology, Group II, Atomic and Molecular Physics*, K.-H. Hellwege and A. M. Hellwege, Eds. Vol. 4, *Molecular Constants from Microwave Spectroscopy*, by B. Starck, Springer-Verlag, Berlin, 1967. Vol. 6, (Supplement and Extension to Vol. 4), *Molecular Constants from Microwave, Molecular Beam, and Electron Spin Resonance Spectroscopy*, Contributors: J. Demaison, W. Hüttner, B. Starck/I. Buck, R. Tischer, and M. Winnewisser. Springer-Verlag, Berlin, 1974.

- Vol. 7, *Structure Data of Free Polyatomic Molecules*, J. H. Callomon, E. Hirota, K. Kuchitsu, W. J. Lafferty, A. G. Maki, and C. S. Pote, with assistance of I. Buck and B. Starck. Springer-Verlag, Berlin, 1976. Vol. 14 (Supplement to Vols. II/4 and II/6), *Molecular Constants Mostly from Microwave, Molecular Beam, and Electron Resonance Spectroscopy*, J. Demaison, A. Dubrulle, W. Hüttner, and E. Tiemann. Springer-Verlag, Berlin, 1982.
66. *Molecular Spectroscopy: Specialized Periodical Reports*, The Chemical Society, London. "Microwave Spectroscopy," A. C. Ligon and D. J. Millen, Vol. 1 (1973), pp. 1-61; Vol. 2 (1974), pp. 1-99; Vol. 3 (1975), pp. 1-103. J. N. Macdonald and J. Sheridan, Vol. 4 (1976), pp. 1-69; Vol. 5 (1977), pp. 1-59; Vol. 6 (1979), pp. 1-45.
  67. M. Mizushima, *The Theory of Rotating Diatomic Molecules*, Wiley, New York, 1975.
  68. K. P. Huber and G. Herzberg, *Molecular Spectra and Molecular Structure*, Vol. IV, *Constants of Diatomic Molecules*, Van Nostrand Reinhold, New York, 1979.
  69. R. L. Cook and G. E. Jones, "Microwave Spectroscopy," in *Systematic Materials Analysis*, J. H. Richards and R. V. Peterson, Eds., Vol. 2, Academic, New York, 1974.
  70. R. Varma and L. W. Hrubesh, "Chemical Analysis by Microwave Rotational Spectroscopy," in *Chemical Analysis*, Vol. 52, P. J. Elving and J. D. Winefordner, Eds., John Wiley, New York, 1979.

# THEORETICAL ASPECTS OF MOLECULAR ROTATION

---

1	CLASSICAL ANGULAR MOMENTA AND ROTATIONAL ENERGY	11
2	ANGULAR MOMENTUM OPERATORS AND MATRIX ELEMENTS	15
	Spin Operators and Matrix Elements	19
	The Symmetric-Top Rotor	20
	Squared Operators	21
3	MATRIX ELEMENTS OF ROTATIONAL HAMILTONIAN OPERATORS	22
4	METHODS OF FINDING EIGENVALUES OF HAMILTONIAN OPERATORS	24
5	EIGENFUNCTIONS OF ANGULAR MOMENTUM OPERATORS	27
6	MATRIX ELEMENTS OF DIPOLE MOMENTS AND DIRECTION COSINES	29

## 1 CLASSICAL ANGULAR MOMENTA AND ROTATIONAL ENERGY

Derivation of the quantum mechanical properties of molecular rotors, including their microwave spectra, begins with the classical expressions for the angular momenta and rotational energy. Likewise, the final derivation of the molecular structure from the observed spectral constants requires a knowledge of classical moments of inertia. Hence we begin with a brief summary of the classical mechanics of rotating bodies.

The classical angular momentum of a rigid system of particles

$$\mathbf{P} = \mathbf{I} \cdot \boldsymbol{\omega} \quad (2.1)$$

where  $\boldsymbol{\omega}$  is the angular velocity and  $\mathbf{I}$  is the moment of inertia tensor which in dyadic notation is written as

$$\begin{aligned} \mathbf{I} = & I_{xx}\hat{\mathbf{u}}\hat{\mathbf{u}} + I_{xy}\hat{\mathbf{u}}\hat{\mathbf{j}} + I_{xz}\hat{\mathbf{u}}\hat{\mathbf{k}} \\ & + I_{yx}\hat{\mathbf{j}}\hat{\mathbf{u}} + I_{yy}\hat{\mathbf{j}}\hat{\mathbf{j}} + I_{yz}\hat{\mathbf{j}}\hat{\mathbf{k}} \\ & + I_{zx}\hat{\mathbf{k}}\hat{\mathbf{u}} + I_{zy}\hat{\mathbf{k}}\hat{\mathbf{j}} + I_{zz}\hat{\mathbf{k}}\hat{\mathbf{k}} \end{aligned} \quad (2.2)$$

with

$$\begin{aligned}
 I_{xx} &= \sum m(y^2 + z^2) \\
 I_{yy} &= \sum m(z^2 + x^2) \\
 I_{zz} &= \sum m(x^2 + y^2) \\
 I_{xy} = I_{yx} &= -\sum mxz \\
 I_{zx} = I_{xz} &= -\sum myz \\
 I_{yz} = I_{zy} &= -\sum myz
 \end{aligned} \tag{2.3}$$

in which  $m$  is the mass of a particular particle and  $x, y, z$  are its positional coordinates relative to a rectangular coordinate system fixed in the body and with its origin at the center of gravity of the body. The summation is taken over all the particles of the body. The origin of the coordinate system is chosen at the center of mass because this choice allows the total kinetic energy to be written as the sum of the kinetic energy of translational motion of the center of mass plus the kinetic energy of the motion relative to the center of mass. The translational and rotational motions can hence be treated separately. It is always possible to choose the coordinate axes in such a way that the products of inertia vanish, leaving only the diagonal elements, called the principal moments of inertia. The principal moments are the three roots  $I$  of the cubic equation

$$\begin{vmatrix} I_{xx} - I & I_{xy} & I_{xz} \\ I_{yx} & I_{yy} - I & I_{yz} \\ I_{zx} & I_{zy} & I_{zz} - I \end{vmatrix} = 0 \tag{2.4}$$

When the notation  $x, y, z$  represents the principal axes system, the components of angular momentum become

$$P_x = I_x \omega_x, \quad P_y = I_y \omega_y, \quad P_z = I_z \omega_z \tag{2.5}$$

The rotational kinetic energy is

$$\begin{aligned}
 E_r &= \frac{1}{2} \boldsymbol{\omega} \cdot \mathbf{I} \cdot \boldsymbol{\omega} \\
 &= \frac{1}{2} (I_{xx} \omega_x^2 + I_{yy} \omega_y^2 + I_{zz} \omega_z^2 + 2I_{xy} \omega_x \omega_y + 2I_{xz} \omega_x \omega_z + 2I_{yz} \omega_y \omega_z)
 \end{aligned} \tag{2.6}$$

which in the principal axes system becomes

$$\begin{aligned}
 E_r &= \frac{1}{2} I_x \omega_x^2 + \frac{1}{2} I_y \omega_y^2 + \frac{1}{2} I_z \omega_z^2 \\
 &= \frac{1}{2} \left( \frac{P_x^2}{I_x} \right) + \frac{1}{2} \left( \frac{P_y^2}{I_y} \right) + \frac{1}{2} \left( \frac{P_z^2}{I_z} \right)
 \end{aligned} \tag{2.7}$$

Now suppose that the body is subjected to a torque

$$\boldsymbol{\tau} = i\tau_x + j\tau_y + k\tau_z \tag{2.8}$$

relative to the space-fixed axes  $X, Y, Z$ . The time rate of change of angular momentum relative to the space-fixed axes is equal to the applied torque,

$$\frac{d\mathbf{P}}{dt} = \mathbf{i} \left( \frac{dP_x}{dt} \right) + \mathbf{j} \left( \frac{dP_y}{dt} \right) + \mathbf{k} \left( \frac{dP_z}{dt} \right) = \boldsymbol{\tau} \quad (2.9)$$

where  $X, Y, Z$  are space-fixed axes. When no torque is applied, it is evident that

$$\mathbf{P} = i P_x + j P_y + k P_z = \text{constant} \quad (2.10)$$

also that the components, and hence  $P_x^2, P_y^2$ , and  $P_z^2$  are each constant. Thus

$$P^2 = P_x^2 + P_y^2 + P_z^2 = \text{constant} \quad (2.11)$$

The rate of change of the total angular momentum with reference to a system  $x, y, z$ , fixed in a rotating body, caused by a torque relative to that system, consists of two parts. One part is due to the time rate of change of the components  $P_x, P_y, P_z$ ; the other is due to the fact that the body-fixed axes  $x, y, z$  are themselves rotating with angular velocities  $\omega_x, \omega_y, \omega_z$ . The latter contributes a term  $\boldsymbol{\omega} \times \mathbf{P}$  to the rate of change of the angular momentum. Thus

$$i \frac{dP_x}{dt} + j \frac{dP_y}{dt} + k \frac{dP_z}{dt} + \boldsymbol{\omega} \times \mathbf{P} = \boldsymbol{\tau} \quad (2.12)$$

Note that  $i, j, k$  are now unit vectors of the body-fixed system. The corresponding component equations are

$$\begin{aligned} \frac{dP_x}{dt} + \omega_y P_z - \omega_z P_y &= \tau_x \\ \frac{dP_y}{dt} + \omega_z P_x - \omega_x P_z &= \tau_y \\ \frac{dP_z}{dt} + \omega_x P_y - \omega_y P_x &= \tau_z \end{aligned} \quad (2.13)$$

Now  $x, y, z$  are chosen as the principal axes of the body so that  $P_x = I_x \omega_x, P_y = I_y \omega_y, P_z = I_z \omega_z$ . Substitution of the values of  $\omega$  from these equations, upon the assumption that the body is rotating freely, with no torque applied ( $\boldsymbol{\tau} = 0$ ) leads to these equations

$$\begin{aligned} \frac{dP_x}{dt} + \left( \frac{1}{I_y} - \frac{1}{I_z} \right) P_y P_z &= 0 \\ \frac{dP_y}{dt} + \left( \frac{1}{I_z} - \frac{1}{I_x} \right) P_z P_x &= 0 \\ \frac{dP_z}{dt} + \left( \frac{1}{I_x} - \frac{1}{I_y} \right) P_x P_y &= 0 \end{aligned} \quad (2.14)$$

These are known as Euler's equations of motion. Multiplication of the first by  $P_x$ , the second by  $P_y$ , and the third by  $P_z$ , followed by addition of the three,

yields

$$P_x \left( \frac{dP_x}{dt} \right) + P_y \left( \frac{dP_y}{dt} \right) + P_z \left( \frac{dP_z}{dt} \right) = 0 \quad (2.15)$$

which upon integration and multiplication by 2 yields

$$P_x^2 + P_y^2 + P_z^2 = \text{constant} = P^2 \quad (2.16)$$

This shows that when no torque is applied, the square of the total angular momentum expressed in the body-fixed axes is constant. Multiplication of the respective equations (2.14) by

$$\frac{P_x}{I_x}, \quad \frac{P_y}{I_y}, \quad \text{and} \quad \frac{P_z}{I_z}$$

followed by addition and integration yields

$$E_r = \frac{1}{2} \left( \frac{P_x^2}{I_x} + \frac{P_y^2}{I_y} + \frac{P_z^2}{I_z} \right) = \text{constant} \quad (2.17)$$

which shows that with no torque applied the kinetic energy of rotation remains constant.

In angular momentum space with  $P_x$ ,  $P_y$ , and  $P_z$  as the coordinates of a point, it is evident that (2.16) is an equation of a sphere with radius  $P$ . In the same momentum coordinates, (2.17) represents an ellipsoid with principal semi-axes of  $(2I_x E_r)^{1/2}$ ,  $(2I_y E_r)^{1/2}$ , and  $(2I_z E_r)^{1/2}$ . Since the values of  $P_x$ ,  $P_y$ , and  $P_z$  must satisfy both equations, it is evident that end points of  $\mathbf{P}$  can only be along the intersection of the sphere and the ellipsoid. If the sphere and the ellipsoid are to intersect, the values of  $P$  must be between those of the minimum and maximum axes of the ellipsoid. This is illustrated by the prolate, symmetric-top case (Fig. 2.1) for which the two smaller semi-axes of the energy ellipsoid are equal ( $I_x = I_y$ ).

The energy ellipsoid is fixed in the body, whereas  $\mathbf{P}$  is fixed in magnitude and in direction in space. Therefore the body must rotate in such a manner that the fixed vector  $\mathbf{P}$  continues to terminate on the surface of the ellipsoid. For a symmetric top, this motion is such that the terminal of  $\mathbf{P}$  traces circles around the symmetrical ellipsoid, as indicated by Fig. 2.1. For the asymmetric

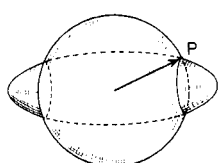


**Fig. 2.1** Diagram illustrating the restrictions on the motions of a prolate symmetric top. The allowed values of  $P$  are described by the intersection of the momentum sphere (Eq. 2.16) and the energy ellipsoid (Eq. 2.17).

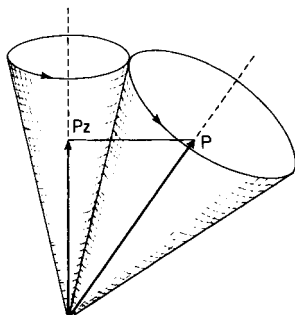


**Fig. 2.2** Simulation of the classical motions of a prolate symmetric top.

rotor in which none of the semi-axes are equal, the curve traced out by  $\mathbf{P}$  on the surface of the ellipsoid is more complicated, but the stable motions are still highly restricted.

The rotational motions of a symmetric top are simulated by a cone that rolls without slipping around the surface of a second cone that is fixed in space. The total momentum vector  $\mathbf{P}$  is along the axis of the fixed cone, and the component  $P_z$  is along the axis of the rolling cone, as indicated by Fig. 2.2 for the prolate top.

That  $P_z$  is a constant of the motion of a symmetric top is easily proved by the substitution of  $I_x = I_y$  in (2.14). One obtains

$$\frac{dP_z}{dt} = 0 \quad \text{hence} \quad P_z = \text{constant} \quad (2.18)$$

For the asymmetric rotor  $I_x \neq I_y \neq I_z$  there is, in contrast, no internal axis about which the rotation is constant, although  $P^2$  is a constant for the asymmetric rotor and is independent of the coordinate system in which it is expressed.

## 2 ANGULAR MOMENTUM OPERATORS AND MATRIX ELEMENTS

Most of the problems treated in this volume involve angular momentum operators. The characteristic energy levels required for finding the microwave spectral frequencies are eigenvalues of the Hamiltonian operators which usually can be expressed in terms of the angular momentum operators of a particle or system of particles. The matrix elements of these angular momentum operators are therefore useful in finding the characteristic energies of the system, that is, the eigenvalues of the Hamiltonian operator.

The classical angular momentum of a system of particles can be expressed by

$$\mathbf{P} = \sum_n \mathbf{r}_n \times \mathbf{p}_n \quad (2.19)$$

where  $\mathbf{p}_n$  is the instantaneous linear momentum  $m_n \mathbf{v}_n$  of the  $n$ th particle and  $\mathbf{r}_n$  is its radius vector from the center of rotation assumed to be fixed in space. Expanded in terms of its components in space-fixed rectangular coordinates  $X, Y, Z$ , it is

$$\begin{aligned}\mathbf{P} &= i P_X + j P_Y + k P_Z \\ &= \sum_n [i(Yp_Z - Zp_Y)_n + j(Zp_X - Xp_Z)_n + k(Xp_Y - Yp_X)_n]\end{aligned}\quad (2.20)$$

To derive the corresponding quantum mechanical angular momentum operators one substitutes the relations  $X \rightarrow X$ , and so on, and  $p_X \rightarrow (\hbar/i)(\partial/\partial X)$ , and so on. Thus the component angular momentum operators are

$$\begin{aligned}P_X &= \sum_n \frac{\hbar}{i} \left[ Y \left( \frac{\partial}{\partial Z} \right) - Z \left( \frac{\partial}{\partial Y} \right) \right]_n \\ P_Y &= \sum_n \frac{\hbar}{i} \left[ Z \left( \frac{\partial}{\partial X} \right) - X \left( \frac{\partial}{\partial Z} \right) \right]_n \\ P_Z &= \sum_n \frac{\hbar}{i} \left[ X \left( \frac{\partial}{\partial Y} \right) - Y \left( \frac{\partial}{\partial X} \right) \right]_n\end{aligned}\quad (2.21)$$

where  $i = (-1)^{1/2}$  and  $\hbar = h/2\pi$ . In spherical coordinates these component operators are

$$\begin{aligned}P_X &= \frac{\hbar}{i} \left[ -\sin \phi \left( \frac{\partial}{\partial \theta} \right) - \cot \theta \cos \phi \left( \frac{\partial}{\partial \phi} \right) \right] \\ P_Y &= \frac{\hbar}{i} \left[ \cos \phi \left( \frac{\partial}{\partial \theta} \right) - \cot \theta \sin \phi \left( \frac{\partial}{\partial \phi} \right) \right] \\ P_Z &= \frac{\hbar}{i} \left( \frac{\partial}{\partial \phi} \right)\end{aligned}\quad (2.22)$$

and the important operator conjugate to the square of the total angular momentum is

$$P^2 = -\hbar^2 \left\{ \left( \frac{1}{\sin \theta} \right) \left( \frac{\partial}{\partial \theta} \right) \left[ \sin \theta \left( \frac{\partial}{\partial \theta} \right) \right] + \frac{1}{\sin^2 \theta} \left( \frac{\partial^2}{\partial \phi^2} \right) \right\} \quad (2.23)$$

It is easily shown from the foregoing expression that  $P^2$  commutes with its component operators, for example,

$$P^2 P_Z - P_Z P^2 = 0 \quad (2.24)$$

The component operators do not commute among themselves, however. The following commutation rules are easily shown to hold

$$P_X P_Y - P_Y P_X = i\hbar P_Z$$

$$\begin{aligned} P_Y P_Z - P_Z P_Y &= i\hbar P_X \\ P_Z P_X - P_X P_Z &= i\hbar P_Y \end{aligned} \quad (2.25)$$

These important commutation relations for the components can be expressed most compactly by the vector equation

$$\mathbf{P} \times \mathbf{P} = i\hbar \mathbf{P} \quad (2.26)$$

Also of convenience for some manipulations are the operators defined by

$$P_+ = P_X + iP_Y \quad (2.27)$$

$$P_- = P_X - iP_Y \quad (2.28)$$

The rules for commutation of these operators are

$$P_+ P_- - P_- P_+ = 2\hbar P_Z \quad (2.29)$$

$$P_Z P_+ - P_+ P_Z = \hbar P_+ \quad (2.30)$$

$$P_Z P_- - P_- P_Z = -\hbar P_- \quad (2.31)$$

Since the component operators  $P_X$  and  $P_Y$  commute with  $P^2$ , it is evident that  $P_+$  and  $P_-$  commute with  $P^2$ .

It is one of the principles of quantum mechanics that operators which commute have common sets of eigenfunctions. Therefore  $P^2$  and  $P_Z$  have common eigenfunctions, which we designate as  $\psi_{J,M}$ . Thus we can write

$$P^2 \psi_{J,M} = k_J \psi_{J,M} \quad (2.32)$$

$$P_Z \psi_{J,M} = k_M \psi_{J,M} \quad (2.33)$$

where  $k_J$  and  $k_M$  represent temporarily the eigenvalues of  $P^2$  and  $P_Z$  corresponding to the eigenstate described by  $\psi_{J,M}$ . By application of  $P_+$  and  $P_-$  (called raising and lowering operators) to (2.33) and various other manipulations [1] the quantized values  $k_J = \hbar^2 J(J+1)$  and  $k_M = \hbar M$  are obtained, where  $M$  and  $J$  have integral values and  $|M| \leq J$ . Thus (2.32) and (2.33) can be expressed as

$$P^2 \psi_{J,M} = \hbar^2 J(J+1) \psi_{J,M} \quad (2.34)$$

$$P_Z \psi_{J,M} = \hbar M \psi_{J,M} \quad (2.35)$$

where

$$J = 0, 1, 2, 3, \dots \quad \text{and} \quad M = J, J-1, J-2, \dots, -J \quad (2.36)$$

With the commutation rules it can be shown that

$$P_+ \psi_{J,M} = C_+ \psi_{J,M+1} \quad (2.37)$$

$$P_- \psi_{J,M} = C_- \psi_{J,M-1} \quad (2.38)$$

where  $C_+$  and  $C_-$  are scalar constants. Thus  $P_+$  and  $P_-$  are raising and lowering operators in the sense that operation with  $P_+$  on  $\psi_{J,M}$  raises the  $M$  sub-

script by one, whereas operation with  $P_-$  lowers it by one. The constant  $C$  can be evaluated upon the condition that the wave function be properly normalized. Multiplication of (2.37) and (2.38) by their complex conjugates and integration over all coordinates with the use of (2.34) and (2.35) and the normalizations

$$\int \psi_{J,M+1}^* \psi_{J,M+1} d\tau = 1 \quad \text{and} \quad \int \psi_{J,M-1}^* \psi_{J,M-1} d\tau = 1 \quad (2.39)$$

yield the values

$$C_+ = i\hbar [J(J+1) - M(M+1)]^{1/2} \quad (2.40)$$

$$C_- = -i\hbar [J(J+1) - M(M-1)]^{1/2} \quad (2.41)$$

Consequently (2.37) and (2.38) become

$$P_+ \psi_{J,M} = i\hbar [J(J+1) - M(M+1)]^{1/2} \psi_{J,M+1} \quad (2.42)$$

$$P_- \psi_{J,M} = -i\hbar [J(J+1) - M(M-1)]^{1/2} \psi_{J,M-1} \quad (2.43)$$

The particular choice of the  $C$ 's as imaginary is discussed at the end of this section. Multiplication of (2.42) by  $\psi_{J,M+1}^*$  and (2.43) by  $\psi_{J,M-1}^*$  and integration over all the coordinates yield the nonvanishing matrix elements of  $P_+$  and  $P_-$  given below, (2.45) and (2.46).

For convenience, we shall use in most applications the abbreviated bracket notation for indication of wave functions and matrix elements. For example, the matrix elements  $\int \psi_{J,M+1}^* P_+ \psi_{J,M} d\tau$  of the operator  $P_+$  in the representation  $J, M$  is indicated by

$$\int \psi_{J,M+1}^* P_+ \psi_{J,M} d\tau \equiv (J, M+1 | P_+ | J, M) \quad (2.44)$$

The nonvanishing matrix elements of  $P_+$  and  $P_-$  found from (2.42) and (2.43) are

$$(J, M+1 | P_+ | J, M) = i\hbar [J(J+1) - M(M+1)]^{1/2} \quad (2.45)$$

$$(J, M-1 | P_- | J, M) = -i\hbar [J(J+1) - M(M-1)]^{1/2} \quad (2.46)$$

That these are all the nonvanishing matrix elements of  $P_+$  and  $P_-$  can be seen by the fact that multiplication by any other member of the orthogonal set of functions, say by  $\psi_{J,M+2}^*$ , would have reduced the right-hand side of the equation to zero because of the orthogonality requirement,  $\int \psi_{J,M}^* \psi_{J',M'} d\tau = 0$  when either  $J \neq J'$  or  $M \neq M'$ . All eigenfunctions of Hermitian operators having different eigenvalues must be orthogonal, and the functions  $\psi_{J,M}$  are eigenfunctions of the Hermitian operators  $P^2$  and  $P_z$ .

From (2.34) and (2.35) it is evident that the nonvanishing matrix elements of  $P^2$  and  $P_z$  are

$$(J, M | P^2 | J, M) = \hbar^2 J(J+1) \quad (2.47)$$

$$(J, M | P_z | J, M) = \hbar M \quad (2.48)$$

It is, of course, always true that the matrix of an operator in the representation of its eigenfunctions is diagonal.

The operators  $P_X$  and  $P_Y$  are not diagonal in the  $J, M$  representation, that is, in the eigenfunctions of  $P^2$  and  $P_Z$ , because they do not commute with  $P_Z$ . Since  $P_X$  or  $P_Y$  commutes with  $P^2$ , we could have chosen a set of eigenfunctions common to  $P^2$  and  $P_X$ , or to  $P^2$  and  $P_Y$ , but then the matrix elements of  $P_Z$  would not have been diagonal in either of these representations. The choice of the particular pair  $P^2$  and  $P_Z$  is, of course, completely arbitrary.

From algebraic manipulation of (2.27), (2.28), (2.45), and (2.46) and with the condition

$$(J, M | P_i | J', M') = (J', M' | P_i | J, M)^* \quad (2.49)$$

that the quantum mechanical operators of all physically real quantities must be Hermitian, the nonvanishing matrix elements of  $P_X$  and  $P_Y$  in the  $J, M$  representation are found to be

$$(J, M | P_Y | J, M \pm 1) = \frac{\hbar}{2} [J(J+1) - M(M \pm 1)]^{1/2} \quad (2.50)$$

$$(J, M | P_X | J, M \pm 1) = \mp \frac{i\hbar}{2} [J(J+1) - M(M \pm 1)]^{1/2} \quad (2.51)$$

These elements are seen to be diagonal in  $J$ , but not in  $M$ . The phase choice here is consistent with that usually selected for the body-fixed angular momentum components [see (2.63) and (2.64)], that is,  $P_Y$  is real and positive and  $P_X$  is imaginary. The choice made for  $P_X$  and  $P_Y$  in most books on quantum mechanics is just the reverse of this, since  $C_{\pm}$  is chosen to be real rather than imaginary as we have done in (2.40) and (2.41). The choice of phase is, however, completely arbitrary and has no effect on physical observables.

### Spin Operators and Matrix Elements

Although intrinsic spin angular momentum has no classical counterpart, the electronic spin vector  $\mathbf{S}$  and the nuclear spin vector  $\mathbf{I}$  are assigned similar angular momentum operators which obey the same commutation rules as those for  $\mathbf{P}$ :

$$\mathbf{S} \times \mathbf{S} = i\hbar \mathbf{S} \quad (2.52)$$

$$\mathbf{I} \times \mathbf{I} = i\hbar \mathbf{I} \quad (2.53)$$

One can then in a similar way find the nonvanishing matrix elements of  $S^2$ ,  $I^2$ , and their various components. These have the same form as those for the operator  $\mathbf{P}$  since they are derived from the same commutation rules. The justification for the assumption of the analogous commutation rules is the test of experience. The consequences of these assumptions are borne out by all measurements of fine or hyperfine structure in atomic or molecular spectra and likewise by electronic spin and nuclear resonance experiments. There is

one important difference, however. Whereas the quantum numbers for  $P_z$  have only integral values, those for  $S_z$  or  $I_z$  may take half-integral values also. This difference does not violate in any way the derivations of the angular properties from the commutation rules, which require only that the values of  $M$  must differ by integral steps and that the values must be symmetrical about zero. If the smallest numerical value of  $M$  is zero, as found for molecular end-over-end rotation, the values of  $M$ , hence of  $J$ , can be integers only. Note, however, that it is possible to have a ladder of nonintegral values of  $M$  separated by integral units and symmetric about zero when—and only when—the nonzero values of  $M$  are odd integral multiples of a half. Certain particles or systems of particles are found to have intrinsic spin values which are half-integrals. It follows that  $(\frac{1}{2})\hbar$  is the smallest observable component of this momentum. The most notable of such particles is the free electron which has an intrinsic spin of  $S=1/2$ ; hence  $M_S=1/2$  and  $-1/2$ . Organic molecules are commonly observed in triplet states for which  $S=1$ . Nuclear spin values as high as  $I=6$  (for  $^{50}\text{V}$ ) have been observed, but the most common ones are  $9/2$  or less.

Matrix elements of the spin operators can be found from (2.47), (2.48), (2.50), and (2.51) by substitution of the  $I$  or  $S$  for  $J$  and of  $M_I$  or  $M_S$  for  $M$ .

### The Symmetric-Top Rotor

The symmetric-top rotor has a component of its angular momentum about the internal symmetry axis of inertia which is a constant of the motion (see Section 1). If the body-fixed coordinate system is chosen as  $x, y, z$  with  $z$  as the axis of symmetry, then the operator  $P_z$  will commute with  $P^2$  since both are constants of the motion, that is, are simultaneously defined. Furthermore,  $P_z$  still commutes with  $P^2$  since the latter is independent of the coordinate system employed

$$P^2 = P_x^2 + P_y^2 + P_z^2 = P_x^2 + P_y^2 + P_z^2 \quad (2.54)$$

Thus, both  $P_z$  and  $P_z$  commute with  $P^2$  and hence with each other and have a common set of eigenfunctions,  $\psi_{J,K,M}$ . Therefore, in the bracket  $\psi_{J,K,M} \equiv |J, K, M\rangle$  notation

$$P^2(J, K, M) = k_J |J, K, M\rangle \quad (2.55)$$

$$P_z(J, K, M) = k_K |J, K, M\rangle \quad (2.56)$$

$$P_z(J, K, M) = k_M |J, K, M\rangle \quad (2.57)$$

The eigenvalues  $k_J$  and  $k_M$  must be the same as those previously determined for the rotor in spaced-fixed coordinates without regard to symmetry, or with  $k_J = \hbar^2 J(J+1)$  and  $k_M = M\hbar$ .

In a similar way, the values of  $k_K$  can be found from the commutation rules of the angular momentum operators expressed in the internal coordinate system. These rules are similar to those for the space-fixed system except

for a change in sign of  $i$ . In this system  $P_z$ , of course, commutes with  $P^2$ , and

$$\begin{aligned} P_x P_y - P_y P_x &= -i\hbar P_z \\ P_y P_z - P_z P_y &= -i\hbar P_x \\ P_z P_x - P_x P_z &= -i\hbar P_y \end{aligned} \quad (2.58)$$

The change in the sign of  $i$  has the additional effect of making  $P_-$  a raising and  $P_+$  a lowering operator in opposition to the corresponding space-fixed operators.

From these rules the value of  $k_K$  is found, as for  $k_M$ , to be  $K\hbar$ , where  $|K|$  is an integer equal to, or less than,  $J$ . Since  $P^2$  is independent of the coordinate system,  $k_J$  is found to be as before,  $\hbar^2 J(J+1)$ . Thus for the symmetric top the diagonal matrix elements are

$$(J, K, M | P^2 | J, K, M) = \hbar^2 J(J+1) \quad (2.59)$$

$$(J, K, M | P_z | J, K, M) = K\hbar \quad (2.60)$$

$$(J, K, M | P_z | J, K, M) = M\hbar \quad (2.61)$$

where

$$J = 0, 1, 2, \dots$$

$$K = J, J-1, J-2, \dots, -J \quad (2.62)$$

$$M = J, J-1, J-2, \dots, -J$$

The matrix elements of  $P_x$  and  $P_y$  found from the commutation rules in the body-fixed system are independent of  $M$ , but we retain the  $M$  subscript to indicate the common eigenfunction

$$(J, K, M | P_x | J, K \pm 1, M) = \pm \frac{i\hbar}{2} [J(J+1) - K(K \pm 1)]^{1/2} \quad (2.63)$$

$$(J, K, M | P_y | J, K \pm 1, M) = \frac{\hbar}{2} [J(J+1) - K(K \pm 1)]^{1/2} \quad (2.64)$$

The nonvanishing matrix elements of  $P_x$  and  $P_y$  are the same as those already stated in (2.50) and (2.51) since they are independent of the internal coordinates and hence of  $K$ .

### Squared Operators

In finding the eigenvalues of the Hamiltonian operator we shall often have need of the matrix elements of the squared operators  $P_x^2$ ,  $P_y^2$ , and so on, of the angular momentum operators. These can be found from the matrix elements already given by application of the matrix product rule

$$\begin{aligned} (J, K, M | P_g^2 | J', K', M') &= \sum_{J'', K'', M''} (J, K, M | P_g | J'', K'', M'') \\ &\quad \times (J'', K'', M'' | P_g | J', K', M') \end{aligned} \quad (2.65)$$

The matrix elements of  $P^4$  and  $P_z^2$  are:

$$(J, K, M|P^4|J', K', M') = (J, K, M|P^2|J, K, M)^2 = \hbar^4 J^2(J+1)^2 \quad (2.66)$$

and

$$(J, K, M|P_z^2|J, K, M) = K^2 \hbar^2 \quad (2.67)$$

However, the matrix elements for  $P_x^2$  and  $P_y^2$  are both diagonal and off-diagonal

$$\begin{aligned} (J, K, M|P_y^2|J', K', M') &= [(J, K, M|P_y|J, K+1, M)(J, K+1, M|P_y|J, K, M) \\ &\quad + (J, K, M|P_y|J, K-1, M)(J, K-1, M|P_y|J, K, M)]\delta_{K'K} \\ &\quad + [(J, K, M|P_y|J, K+1, M)(J, K+1, M|P_y|J, K+2, M)]\delta_{K'K+2} \\ &\quad + [(J, K, M|P_y|J, K-1, M)(J, K-1, M|P_y|J, K-2, M)]\delta_{K'K-2} \end{aligned} \quad (2.68)$$

The first two terms on the right are diagonal, and with the aid of the Hermetian property and (2.64) they can be combined to give

$$(J, K, M|P_y^2|J, K, M) = \frac{\hbar^2}{2} [J(J+1) - K^2] \quad (2.69)$$

The last two terms are off-diagonal by two units of  $K$  and with (2.64) can be written as

$$\begin{aligned} (J, K, M|P_y^2|J, K \pm 2, M) &= \frac{\hbar^2}{4} [J(J+1) - K(K \pm 1)]^{1/2} \\ &\quad \times [J(J+1) - (K \pm 1)(K \pm 2)]^{1/2} \end{aligned} \quad (2.70)$$

where the upper plus signs are to be taken together and the lower minus signs together. In a similar way, the matrix elements of  $P_x^2$  are seen to be

$$(J, K, M|P_x^2|J, K, M) = \frac{\hbar^2}{2} [J(J+1) - K^2] \quad (2.71)$$

$$\begin{aligned} (J, K, M|P_x^2|J, K \pm 2, M) &= -\frac{\hbar^2}{4} [J(J+1) - K(K \pm 1)]^{1/2} \\ &\quad \times [J(J+1) - (K \pm 1)(K \pm 2)]^{1/2} \end{aligned} \quad (2.72)$$

### 3 MATRIX ELEMENTS OF ROTATIONAL HAMILTONIAN OPERATORS

The Hamiltonian operator is obtained from the classical Hamiltonian when the momenta are replaced by their conjugate operators. When no torques are applied, the classical Hamiltonian of the rigid rotor consists of only kinetic energy which can be expressed in terms of the components of angular momentum in the principal axes, as in (2.7). To find the corresponding Hamiltonian operator, one simply substitutes for the  $P$ 's the conjugate angular momentum operators. In the body-fixed principal axes,  $x, y, z$ , this operator is

$$\mathcal{H}_r = \frac{1}{2} \left( \frac{P_x^2}{I_x} + \frac{P_y^2}{I_y} + \frac{P_z^2}{I_z} \right) \quad (2.73)$$

where

$$P_x = \frac{\hbar}{i} \left( y \frac{\partial}{\partial z} - z \frac{\partial}{\partial y} \right), \quad P_y = \frac{\hbar}{i} \left( z \frac{\partial}{\partial x} - x \frac{\partial}{\partial z} \right), \quad P_z = \frac{\hbar}{i} \left( x \frac{\partial}{\partial y} - y \frac{\partial}{\partial x} \right) \quad (2.74)$$

The eigenvalues of the Hamiltonian operators represent the quantized energies from which the microwave spectral frequencies are determined. Finding these eigenvalues is therefore one of our most important problems. The Hamiltonian operators dealt with in this volume can usually be expressed in terms of angular momentum operators or intrinsic spin operators which are of the same form as angular momentum operators. For this reason one often makes use of the matrix elements of angular momentum operators and spin operators when finding the energy levels involved in microwave spectral transitions.

If the Hamiltonian operator is found to commute with the angular momentum operators, it will be diagonal in the representation in which those operators are diagonal. Its matrix elements can then be readily found from the known diagonal matrix elements of the angular momentum operators.

As a simple example, let us consider the rigid spherical-top rotor for which the three principal moments of inertia are equal,  $I_x = I_y = I_z = I$ . The Hamiltonian operator  $\mathcal{H}_r$  becomes

$$\mathcal{H}_r = \frac{1}{2I} (P_x^2 + P_y^2 + P_z^2) = \frac{P^2}{2I} \quad (2.75)$$

Since  $I$  is a constant, the Hamiltonian obviously commutes with  $P^2$ . The nonvanishing matrix elements of  $\mathcal{H}_r$ , in this case the eigenvalues of  $\mathcal{H}_r$ , that is, the quantized energy values, are

$$E_J = (J, M | \mathcal{H}_r | J, M) = \frac{1}{2I} (J, M | P^2 | J, M) = \frac{\hbar^2 J(J+1)}{2I} \quad (2.76)$$

The Hamiltonian of the symmetric-top rotor commutes with  $P_z$  and  $P_z$  as well as with  $P^2$  and is therefore diagonal in the  $J, K, M$  representation. This can be easily seen if  $I_x$  is set equal to  $I_y$  in (2.73); the Hamiltonian for the symmetric top can then be expressed as

$$\mathcal{H}_r = \frac{P^2}{2I_y} + \left( \frac{1}{2I_z} - \frac{1}{2I_y} \right) P_z^2 \quad (2.77)$$

Since  $P^2$  and  $P_z^2$  commute with  $P_z$  and are diagonal in the  $J, K, M$  representation,  $\mathcal{H}_r$  is also diagonal in the same representation, with matrix elements

$$E_{J,K} = (J, K, M | \mathcal{H}_r | J, K, M) = \frac{\hbar^2}{2} \left[ \frac{J(J+1)}{I_y} + \left( \frac{1}{I_z} - \frac{1}{I_y} \right) K^2 \right] \quad (2.78)$$

which represent the characteristic rotational energies. Note that these diagonal elements of  $\mathcal{H}$ , do not depend on  $M$ , in agreement with the classical principle that the rotational energy in the absence of torques is independent of the direction in which the angular momentum vector points in space.

The Hamiltonian operator for the asymmetric-top rotor for which  $I_x \neq I_y \neq I_z$  does not commute with the operator  $P_z$  or with the other component operators  $P_x$  or  $P_y$ . It is thus not diagonal in the symmetric-top  $J, K, M$  representation. Its matrix elements may be easily found in the symmetric-top eigenfunctions, as is done later; but the resulting matrix will not be diagonal, and the elements will not represent eigenvalues of  $\mathcal{H}_r$ . However,  $\mathcal{H}_r$  does commute with  $P^2$  and  $P_z$ , and hence the matrix will be diagonal in the  $J$  and  $M$  quantum numbers. In principle, and in practice for  $J$  not too high, it is possible to diagonalize the resulting matrix and thus to obtain the eigenvalues of  $\mathcal{H}_r$ . This is equivalent to the setting up and solving of the secular equation as described in Section 4. For this purpose the matrix elements of  $\mathcal{H}$ , in the  $J, K, M$  representation as given below will be needed.

By substitution of the matrix elements of  $P_x^2$ ,  $P_y^2$ , and  $P_z^2$  from (2.67) and (2.69) to (2.72) into the Hamiltonian operator for the asymmetric rotor, (2.73), expressed in the coordinates of its principal axes of inertia, the nonvanishing matrix elements of  $\mathcal{H}$ , are found to be

$$(J, K | \mathcal{H}_r | J, K) = \frac{\hbar^2}{4} \left[ J(J+1) \left( \frac{1}{I_x} + \frac{1}{I_y} \right) + K^2 \left( \frac{2}{I_z} - \frac{1}{I_x} - \frac{1}{I_y} \right) \right] \quad (2.79)$$

and

$$(J, K | \mathcal{H}_r | J, K \pm 2) = \frac{\hbar^2}{8} [J(J+1) - K(K \pm 1)]^{1/2} \times [J(J+1) - (K \pm 1)(K \pm 2)]^{1/2} \left( \frac{1}{I_y} - \frac{1}{I_x} \right) \quad (2.80)$$

Thus there are diagonal elements of  $\mathcal{H}_r$ , (2.79), but these do not represent eigenvalues of  $\mathcal{H}$ , because in this representation there are also nonvanishing, off-diagonal elements, (2.80), in  $K$ .

#### 4 METHODS OF FINDING EIGENVALUES OF HAMILTONIAN OPERATORS

Certain systems such as symmetric-top rotors have sufficient symmetry that the Schrödinger equation

$$\mathcal{H}\psi = E\psi \quad (2.81)$$

is solvable for the eigenfunctions  $\psi$  and the eigenvalues  $E$  of the Hamiltonian operators. Alternately, it is possible to find the eigenvalues of  $\mathcal{H}$ , also the direction cosine matrix elements for such systems from the commutation rules of

the component operators as indicated in Sections 3 and 6, even without a specific knowledge of the eigenfunctions.

When the symmetry of the Hamiltonian operator does not allow direct solution of the Schrödinger equation, the customary procedure is to expand the unknown eigenfunction in terms of a known orthogonal set such as those of the symmetric top; for example, let us assume the eigenfunction of (2.81) to be expressed by

$$\psi = \sum_n c_n \psi_n \quad (2.82)$$

where  $\psi_n$  represents a member of a normalized orthogonal set of functions and the  $c_n$  are weighting constants. Substitution of (2.82) into (2.81) yields

$$\sum_n c_n \mathcal{H} \psi_n = E \sum_n c_n \psi_n \quad (2.83)$$

By multiplication of this equation by the  $\psi_m^*$ , or the conjugate of a member of the orthogonal set, and integration over all coordinates, one obtains

$$\sum_n c_n \int \psi_m^* \mathcal{H} \psi_n d\tau = E \sum_n c_n \int \psi_m^* \psi_n d\tau \quad (2.84)$$

Since the assumed set is orthogonal  $\int \psi_m^* \psi_n d\tau = 0$  except when  $m=n$  and since they are assumed to be normalized, this quantity is unity when  $m=n$ . For convenience, the matrix of  $\mathcal{H}$  may be expressed in the bracket notation  $\int \psi_m^* \mathcal{H} \psi_n d\tau = (m| \mathcal{H} |n)$ . In many texts it is written simply as  $\mathcal{H}_{m,n}$ . Thus (2.84) can be written as

$$\sum_n c_n [(m| \mathcal{H} |n) - E \delta_{m,n}] = 0 \quad (2.85)$$

where  $\delta_{m,n}=1$  when  $m=n$  and  $\delta_{m,n}=0$  when  $m \neq n$ . The expression (2.85) represents a set of  $l$  linear equations containing  $l$  unknown coefficients which have a nontrivial solution only if the determinant of the coefficient vanishes, where  $l$  is the number of functions in the set. If this determinant is set equal to zero, the secular equation,

$$|(m| \mathcal{H} |n) - E \delta_{m,n}| = 0 \quad (2.86)$$

is obtained. If the matrix elements  $(m| \mathcal{H} |n)$  are known or can be found, this equation can, in principle, be solved for the values of  $E$ . These values, which are the various roots of the secular equation with  $E$  considered as the unknown, represent the eigenvalues of  $\mathcal{H}$ . By substitution of each of these values of  $E$  into (2.87) with the known value of  $(m| \mathcal{H} |n)$ , ratios of the various coefficients  $c_n/c_{n-1}$ , and so on, can be found; and with the auxiliary equation,

$$\sum |c_n|^2 = 1 \quad (2.87)$$

obtained from normalization of the  $\psi$  of (2.82), the values of the  $c_n$  coefficients

can be obtained. Thus the eigenfunction  $\psi_j$  corresponding to the particular root  $j$  of the secular equation or particular value  $E_j$  can be found in terms of the assumed functions  $\psi_n$  of some other operator.

It should be noted that a knowledge of the assumed eigenfunctions  $\psi_n$  is not actually required for the setting up of the secular equation and hence for the finding of the energy values  $E_j$ ; only the matrix elements  $(m|\mathcal{H}|n)$  are required. These matrix elements (Section 2) can often be found from commutation rules without a specific knowledge of the eigenfunctions. For simplicity we have assumed that only the one quantum number  $n$  is required for the labeling of the assumed set of functions preceding; but for the problems considered in this volume additional ones will usually be required.

It is apparent that operators such as  $\mathcal{H}$  can be represented by matrices and their eigenvalues can be found by diagonalization of the corresponding matrix. The matrix formulation of quantum mechanics has been developed by Heisenberg. In Appendix A some important features of matrix mechanics pertinent to microwave spectroscopy are reviewed.

A classical example of the application of the secular equation is in the finding of the eigenvalues of the field-free, rigid, asymmetric rotor. As we have seen in Section 3, the matrix elements of the Hamiltonian operator of the asymmetric rotor in the  $J, K$  representation, that is, the representation in which the Hamiltonian of the symmetric-top rotor is diagonal, can be readily found. Because these elements are diagonal in  $J$ , the secular equation factorizes into subequations corresponding to the different values of  $J$ . Since the values of  $K$  range in unit steps from  $J$  to  $-J$ , the subdetermined equations have the form

$$\begin{array}{c|ccccccc} K/K' & J & J-1 & J-2 & J-3 & \cdots & -J \\ \hline J & \mathcal{H}_J^J - E & 0 & \mathcal{H}_{J-2}^{J-2} & 0 & \cdots & 0 \\ J-1 & 0 & \mathcal{H}_{J-1}^{J-1} - E & 0 & \mathcal{H}_{J-1}^{J-3} & \cdots & 0 \\ J-2 & \mathcal{H}_{J-2}^J & 0 & \mathcal{H}_{J-2}^{J-2} - E & 0 & \cdots & 0 \\ J-3 & 0 & \mathcal{H}_{J-3}^{J-1} & 0 & \mathcal{H}_{J-3}^{J-3} - E & \cdots & 0 \\ \cdots & \cdots & \cdots & \cdots & \cdots & \cdots & \cdots \\ -J & 0 & 0 & 0 & 0 & \cdots & \mathcal{H}_{-J}^{-J} - E \end{array} = 0 \quad (2.88)$$

in which we have, for convenience, designated  $(J, K|\mathcal{H}|J, K') = \mathcal{H}_K^K$ . From (2.79) and (2.80) we see that nonvanishing elements of  $\mathcal{H}$  occur only for  $K = K'$  and for  $K = K \pm 2$ . It is evident that the secular determinant has the dimension of  $2J+1$  and will therefore have  $2J+1$  roots or energy values  $E$  corresponding to each value of  $J$ . Although the required matrix elements and secular equation can be found easily, solution of this equation becomes increasingly difficult as  $J$  increases. It can be solved only with approximation methods and most advantageously with modern computers.

As a more specific illustration, let us solve the secular equation of a rigid asymmetric rotor when  $J=1$ . From the matrix elements obtained from (2.79)

and (2.80) with  $A = \hbar^2/2I_x$ ,  $B = \hbar^2/2I_y$ , and  $C = \hbar^2/(2I_z)$ , the secular equation is seen to be

$$\begin{array}{c|ccc} K/K' & 1 & 0 & -1 \\ \hline 1 & \left(\frac{A+B}{2}+C\right)-E & 0 & -\frac{A-B}{2} \\ 0 & 0 & (A+B)-E & 0 \\ -1 & -\frac{A-B}{2} & 0 & \left(\frac{A+B}{2}+C\right)-E \end{array} = 0 \quad (2.89)$$

Solution of this cubic equation yields the three values of  $E$  as

$$\begin{aligned} E_0 &= A + B \\ E_+ &= B + C \\ E_- &= A + C \end{aligned} \quad (2.90)$$

In the treatment of the higher  $J$  values of the asymmetric rotor we change the form of the Hamiltonian to take advantage of the symmetric properties in the reduced energies. These more involved levels are treated in Chapter VII.

## 5 EIGENFUNCTIONS OF ANGULAR MOMENTUM OPERATORS

The eigenfunction  $\psi_{J,M}$  of the angular momentum operators  $P^2$  and  $P_z$  in space-fixed coordinates are most easily found by use of these operators expressed in spherical coordinates. Application of  $P_z$  from (2.22) in (2.35) yields

$$\frac{\hbar}{i} \frac{\partial \psi_{J,M}}{\partial \phi} = M\hbar\psi_{J,M} \quad (2.91)$$

We assume that

$$\psi_{J,M} = \Phi \cdot \Theta \quad (2.92)$$

where  $\Phi$  is a function of  $\phi$  only and  $\Theta$  a function of  $\theta$  only. Then (2.91) can be written

$$\frac{\partial \Phi}{\partial \phi} = iM\Phi \quad (2.93)$$

The solution is:

$$\Phi_M = N_M e^{iM\phi} \quad (2.94)$$

and, with  $M$  an integer,  $\Phi$  is insured of being single valued, that is,  $\Phi(\phi) = \Phi(\phi + 2\pi)$ . Normalization of the eigenfunction requires

$$\int \Phi * \Phi d\tau = N_M^2 \int_0^{2\pi} d\phi = 1 \quad (2.95)$$

Thus  $N_M = 1/(2\pi)^{1/2}$  and

$$\psi_{J,M} = (1/2\pi)^{1/2} e^{iM\phi} \Theta \quad (2.96)$$

To find the  $\theta$ -dependent part of the function we apply the operator  $P^2$  from (2.23) in (2.34) and obtain

$$\frac{1}{\sin \theta} \frac{\partial}{\partial \theta} \left( \sin \theta \frac{\partial \psi_{J,M}}{\partial \theta} \right) + \frac{1}{\sin^2 \theta} \frac{\partial^2 \psi_{J,M}}{\partial \phi^2} + J(J+1)\psi_{J,M} = 0 \quad (2.97)$$

which, upon substitution of  $\psi_{J,M}$  from (2.92) and transformation, becomes

$$\frac{1}{\sin \theta} \frac{\partial}{\partial \theta} \left( \sin \theta \frac{\partial \Theta}{\partial \theta} \right) - \frac{M^2}{\sin^2 \theta} \Theta + J(J+1)\Theta = 0 \quad (2.98)$$

This is the well-known Legendre equation, solution of which is

$$\Theta_{J,M} = N_{J,M} P_J^{|M|}(\cos \theta) \quad (2.99)$$

where  $P_J^{|M|}(\cos \theta)$  represents the associated Legendre polynomials and  $N_{J,M}$  is a constant which is determined by the normalizing condition

$$\int \Theta_{J,M}^* \Theta_{J,M} d\theta = N_{J,M}^2 \int [P_J^{|M|}(\cos \theta)]^* [P_J^{|M|}(\cos \theta)] d\theta = 1 \quad (2.100)$$

to be

$$N_{J,M} = \left[ \frac{(2J+1)}{2} \cdot \frac{(J-|M|)!}{(J+|M|)!} \right]^{1/2} \quad (2.101)$$

Combination of these various factors gives the normalized eigenfunction of the angular momentum operators  $P^2$  and  $P_z$  to be

$$\psi_{J,M} = \frac{1}{\sqrt{2\pi}} \left[ \frac{2J+1}{2} \cdot \frac{(J-M)!}{(J+M)!} \right]^{1/2} e^{iM\phi} P_J^{|M|}(\cos \theta) \quad (2.102)$$

which are commonly called the surface spherical harmonics.

The operators  $P^2$  and  $P_z$  commute with the Hamiltonian operator of the rigid linear rotor, and the functions of (2.102) are also rotational energy state functions of linear molecules when centrifugal distortion is neglected. The same eigenfunctions  $\psi_{J,M}$  are obtained from a solution of the Schrödinger wave equation  $\mathcal{H}_r \psi = E \psi$  for the rigid linear molecule.

Subsequent discussion of spin statistics (Chapter III, Section 4) will require a knowledge of the effect on the wave function of an exchange of the nuclei in a linear rotor. This operation is equivalent to the transformation  $(\theta, \phi) \rightarrow (\pi - \theta, \phi + \pi)$ . Replacement of  $\phi$  by  $\phi + \pi$  in (2.102) multiplies the function by  $(-1)^M$ . The  $P_J^{|M|}(\cos \theta)$  is a polynomial of  $\cos \theta$  of order  $J-|M|$ , involving even (odd) powers of  $\cos \theta$  if  $J-|M|$  is even (odd). Replacement of  $\theta$  by  $\pi - \theta$  hence multiplies the function by  $(-1)^{J-|M|}$ . The net result is that the total function is multiplied by  $(-1)^J$ .

To obtain the common eigenfunctions  $\psi_{J,K,M}$  for the symmetric-top operators  $P^2$ ,  $P_z$ , and  $P_z$ , one can express the angular momentum operators in

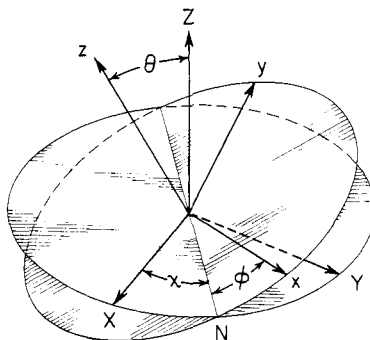


**Fig. 2.3** Euler's angles defining the orientation of the body-fixed ( $x, y, z$ ) axes relative to the space-fixed ( $X, Y, Z$ ) axes. The line  $N$  represents the intersection of the  $xy$  plane with the  $XY$  plane and is called the line of nodes.

Euler's angles  $\theta, \phi, \chi$ , and proceed in a manner similar to that followed previously, but the calculations are much more involved. Dennison [2] has obtained the symmetric-top eigenvalues with matrix methods; Reiche and Radmacher [3] and Kronig and Rabi [4], by solution of the Schrödinger equation for the symmetric top. The resulting eigenfunctions are

$$\psi_{J,K,M} = \Theta_{J,K,M} e^{iK\phi} e^{iM\chi} \quad (2.103)$$

where

$$\Theta_{J,K,M} = N_{J,K,M} \left( \sin \frac{\theta}{2} \right)^{|K-M|} \left( \cos \frac{\theta}{2} \right)^{|K+M|} F \left( \sin^2 \frac{\theta}{2} \right) \quad (2.104)$$

The function  $F(\sin^2 \theta/2)$  is a hypergeometric series, and  $N_{J,K,M}$  is a normalizing factor determined by the condition  $N_{J,K,M}^2 \int \psi_{J,K,M} \psi_{J,K,M}^* d\tau = 1$ . Euler's angles are illustrated in Fig. 2.3.

Eigenfunctions of asymmetric rotors can be obtained by expansion of these functions in terms of those for the symmetric top and evaluation of the coefficients in the expansion with the aid of energy values obtained from solution of the secular equation as described in Section 4. However, most of the quantities needed for microwave spectroscopic analysis are obtained from matrix elements derived from commutation rules without a specific knowledge of the eigenfunctions.

## 6 MATRIX ELEMENTS OF DIPOLE MOMENTS AND DIRECTION COSINES

Particularly for calculating transition probabilities and Stark and Zeeman effects, we shall need the direction cosine matrix elements of body-fixed axes of a rotor relative to space-fixed axes. Microwave spectral transitions are in-

duced by interaction of the electric or magnetic components of the radiation fixed in space with the electric or magnetic dipole components fixed in the rotating body. Likewise, the Stark and Zeeman effects arise from interaction of space-fixed electric or magnetic fields with components of the dipole moment fixed in the rotors. These interactions can be considered as occurring between the spaced-fixed fields with components of the dipole moments resolved along the space-fixed axes, but it is evident that the magnitude of the space-fixed components will depend on the state of rotation. In finding these interactions one needs matrix elements of the components of the dipole moment referred to the space-fixed axes. These elements must be expressed in the eigenfunctions of the particular energy states between which the transition occurs.

In spinning electrons and nuclei, the body-fixed magnetic dipole moments are along the spin axis and are constants in all magnetic resonance experiments because  $S$  and  $I$  do not change. Thus the components of  $\mu$  resolve along space-fixed axes as the components of  $\mathbf{S}$  and  $\mathbf{I}$  and can be readily found from the angular momentum matrix elements of the components of  $\mathbf{S}$  and  $\mathbf{I}$ .

The electric dipole moments matrix elements in space-fixed axes of rotating molecules are more complicated than those of electronic or nuclear spin magnetic moments for a number of reasons, the most important of which is that the electric dipole moment of the rotating molecule does not lie along  $\mathbf{P}$  as it does along  $\mathbf{S}$  or  $\mathbf{I}$  and hence has matrix elements that are off-diagonal in  $J$ , whereas the matrix elements of the spin magnetic moments are diagonal in the corresponding quantum number  $S$  or  $I$ . The electric dipole moment of the linear molecule is perpendicular to  $\mathbf{P}$  and has no matrix elements diagonal in  $J$ . It consequently has no resolvable component along a space-fixed axis and hence no first-order Stark effect. Another complication arises from the lower symmetry possible in molecules, especially in the asymmetric rotor which may have dipole components along each of the principal inertial axes fixed in the rotating body and for which the eigenfunctions of high  $J$  transitions are exceedingly complicated. Also, in rotating molecules the body-fixed electric dipole components are not independent of the electronic and vibrational states although these latter states do not generally change with the pure rotational transitions observed in the microwave region. Therefore we can treat the electric dipole moment components in the rotating, body-fixed system as constants. The problem is to find the nonvanishing matrix elements resolved on space-fixed axes in the representation that diagonalizes the rotational Hamiltonian operator.

Without loss of generality, we can choose the body-fixed dipole components along the principal axes of inertia. We designate the space-fixed axes by  $F = X, Y, Z$ , the body-fixed principal axes of inertia by  $g = x, y, z$ , and the cosine of the angle between  $F$  and  $g$  as  $\Phi_{F,g}$ . For example, a molecule with constant dipole moment components in the body-fixed principal axes of  $\mu_x, \mu_y, \mu_z$  would have components along the space-fixed  $Z$  axes of

$$\mu_Z = \mu_x \Phi_{Zx} + \mu_y \Phi_{Zy} + \mu_z \Phi_{Zz} \quad (2.105)$$

If  $\psi_r$  represents the rotational eigenfunctions, the matrix elements of the dipole moment with reference to the space-fixed axes would be

$$\int \psi_r^* \mu_z \psi_r' d\tau = \mu_x \int \psi_r^* \Phi_{Zx} \psi_r' d\tau + \mu_y \int \psi_r^* \Phi_{Zy} \psi_r' d\tau + \mu_z \int \psi_r^* \Phi_{Zz} \psi_r' d\tau \quad (2.106)$$

or, more generally

$$\int \psi_r^* \mu_F \psi_r' d\tau = \sum_g \mu_g \int \psi_r^* \Phi_{Fg} \psi_r' d\tau \quad (2.107)$$

Thus the matrix elements required are those for the direction cosine  $\Phi_{Fg}$ . For the linear or symmetric-top molecule, the eigenfunctions are known, and the integrals  $\int \psi_r^* \Phi_{Fg} \psi_r' d\tau$  can be evaluated in a straightforward manner. For the linear molecule this procedure is relatively simple, but for the symmetric top it is very tedious because of the complex form of the eigenfunctions. These matrix elements can be found in a simpler way from commutation rules between the angular momentum operators and the direction cosines [5], or between the angular momentum operators and the vector operators [1]. The somewhat involved derivations will not be given here, only the needed results.

The nonvanishing direction cosine matrix elements in the symmetric-top representation  $J, K, M$  are most useful. They are given in Table 2.1. These elements are separated into factors that depend on the different quantum numbers as follows

$$(J, K, M | \Phi_{Fg} | J', K', M') = (J | \Phi_{Fg} | J')(J, K | \Phi_{Fg} | J', K')(J, M | \Phi_{Fg} | J', M') \quad (2.108)$$

Those for the linear molecule may be obtained from them if  $K$  is set equal to zero. Those for the asymmetric rotor are obtained from them by methods [5] similar to those described for the finding of the energy eigenvalues of the asymmetric rotor (see Chapter VII).

As an illustration of the use of the elements of Table 2.1, let us employ them to find the dipole moment matrix elements that correspond to rotational absorption transitions  $J \rightarrow J+1$  for the symmetric-top molecule in which the permanent dipole moment lies wholly along the axis of symmetry,  $\mu = \mu_z$ . The accidentally symmetric-top in which  $I_x = I_y$  might have  $\mu_x$  or  $\mu_y$  which is not zero, but an accidentally symmetric-top molecule is exceedingly rare. Using (2.106) with  $\mu_x = 0$ ,  $\mu_y = 0$  and the  $J' = J+1$  column of Table 2.1 we find

$$(J, K, M | \mu_z | J+1, K, M) = \mu \frac{[(J+1)^2 - K^2]^{1/2} [(J+1)^2 - M^2]^{1/2}}{(J+1)[(2J+1)(2J+3)]^{1/2}} \quad (2.109)$$

$$(J, K, M | \mu_x | J+1, K, M \pm 1)$$

$$= + \frac{i\mu}{2} \frac{[(J+1)^2 - K^2]^{1/2} [(J \pm M + 1)(J \pm M + 2)]^{1/2}}{(J+1)[(2J+1)(2J+3)]^{1/2}} \quad (2.110)$$

$$(J, K, M | \mu_y | J+1, K, M \pm 1)$$

$$= \mp \frac{\mu}{2} \frac{[(J+1)^2 - K^2]^{1/2} [(J \pm M + 1)(J \pm M + 2)]^{1/2}}{(J+1)[(2J+1)(2J+3)]^{1/2}} \quad (2.111)$$

**Table 2.1** Factors of Direction Cosine Matrix Elements<sup>a</sup> of Symmetric-Top Rotors<sup>b</sup>

Matrix Element Factor	Value of $J'$		
	$J+1$	$J$	$J-1$
$(J \Phi_{Fg} J')$	$\{4(J+1)[(2J+1)(2J+3)]^{1/2}\}^{-1}$	$[4J(J+1)]^{-1}$	$[4J(4J^2-1)^{1/2}]^{-1}$
$(J, K \Phi_{Fz} J', K)$	$2[(J+1)^2 - K^2]^{1/2}$	$2K$	$-2(J^2 - K^2)^{1/2}$
$(J, K \Phi_{Fy} J', K \pm 1) = \mp i(J, K \Phi_{Fx} J', K \pm 1)$	$\mp [(J \pm K+1)(J \pm K+2)]^{1/2}$	$[J(J+1) - K(K \pm 1)]^{1/2}$	$\mp [(J \mp K)(J \mp K-1)]^{1/2}$
$(J, M \Phi_{Zg} J', M)$	$2[(J+1)^2 - M^2]^{1/2}$	$2M$	$-2(J^2 - M^2)^{1/2}$
$(J, M \Phi_{Yg} J', M \pm 1) = \pm i(J, M \Phi_{Xg} J', M \pm 1)$	$\mp [(J \pm M+1)(J \pm M+2)]^{1/2}$	$[J(J+1) - M(M \pm 1)]^{1/2}$	$\mp [(J \mp M)(J \mp M-1)]^{1/2}$

<sup>a</sup>Cross et al. [5].

<sup>b</sup>The matrix elements are obtained from the factors with the relation:  $(J, K, M|\Phi_{Fg}|J', K', M') = (J|\Phi_{Fg}|J')(J, K|\Phi_{Fg}|J', K')(J, M|\Phi_{Fg}|J', M')$ ,  $F = X, Y, Z$ , and  $g = x, y, z$ .

Transitions  $J \rightarrow J+1$  and  $M \rightarrow M+1$ , and  $M \rightarrow M-1$  are induced by interactions of the radiation with rotating components of the dipole moment in the  $XY$  plane. This is evident from the fact that the nonvanishing matrix elements from these two transitions can be expressed as

$$(J, K, M | \mu_Y - i\mu_X | J+1, K, M-1) = \frac{\mu [(J+1)^2 - K^2]^{1/2} [(J-M+1)(J-M+2)]^{1/2}}{(J+1)[(2J+1)(2J+3)]^{1/2}} \quad (2.112)$$

$$(J, K, M | \mu_Y + i\mu_X | J+1, K, M+1) = -\mu \frac{[(J+1)^2 - K^2]^{1/2} [(J+M+1)(J+M+2)]^{1/2}}{(J+1)[(2J+1)(2J+3)]^{1/2}} \quad (2.113)$$

Transitions of the type  $M \rightarrow M$  require radiation with the electric field in the  $Z$  direction.

The corresponding matrix elements for the linear molecule can be obtained from those for the symmetric top if  $K$  is set equal to zero in (2.109)–(2.113) or in Table 2.1.

The transition probabilities for induced absorption or stimulated emission are proportional to the squared dipole moment matrix elements with reference to the space-fixed axis (Chapter III, Section 1) as expressed by the Einstein  $B$  coefficient

$$B_{J,K,M \rightarrow J',K',M'} = \frac{8\pi^3}{3h^2} \sum_{F=X,Y,Z} |(J, K, M | \mu_F | J', K', M')|^2 \quad (2.114)$$

This equation provides a basis for the selection rules of dipole absorption or emission and is a factor in the calculation of intensities of spectral lines. Dipole transitions occur only between levels for which the matrix elements expressed by (2.109)–(2.113) do not all vanish. The dipole matrix elements for stimulated emission between the same levels can be found in a similar manner from Table 2.1 or simply by a reversal of the quantum numbers in the various elements,  $J'$ ,  $K'$ ,  $M'$  for  $J$ ,  $K$ ,  $M$ . This follows from the fact that the matrices are Hermitian or that the value of  $B$  is the same for induced absorption as for stimulated emission.

It is of interest that dipole matrix elements corresponding to  $J \rightarrow J$  occur for the symmetric top, but not for the linear molecule. From Table 2.1 it is seen that when  $\mu$  is along the  $z$  axis as before, the  $J \rightarrow J$  elements of the symmetric top are

$$(J, K, M | \mu_Z | J, K, M) = \frac{\mu KM}{J(J+1)} \quad (2.115)$$

$$(J, K, M | \mu_Y - i\mu_X | J, K, M-1) = \mu \frac{K[J(J+1) - M(M-1)]^{1/2}}{J(J+1)} \quad (2.116)$$

$$(J, K, M | \mu_Y + i\mu_X | J, K, M+1) = \mu \frac{K[J(J+1) - M(M+1)]^{1/2}}{J(J+1)} \quad (2.117)$$

From the nonvanishing matrix elements thus obtained from Table 2.1, the selection rules for the genuine symmetric top ( $\mu$  along  $z$ ) are found to be

$$\Delta J = 0, \pm 1, \quad \Delta K = 0, \quad \Delta M = 0, \pm 1 \quad (2.118)$$

Note, however, that the  $J \rightarrow J$ ,  $K \rightarrow K$ ,  $M \rightarrow M$  for the rigid molecule gives rise to a constant, space-fixed component, an eigenvalue of  $\mu$  along  $Z$  that cannot give resonance coupling with an ac electric field. Also, this transition for the strictly rigid top does not connect different energy states and is therefore trivial. When, however, there is an inversion vibration, as for  $\text{NH}_3$ , the dipole moment does not remain constant but changes with the inversion from  $+\mu_z$  to  $-\mu_z$  and thus can couple through resonance with an ac electric field component along  $Z$  which has the same frequency as that of the inversion. The inversion gives rise to a splitting of the rotational levels that have opposite symmetry, plus and minus, with transition probabilities proportional to the square of the foregoing matrix elements for  $\Delta J = 0, \Delta K = 0$ . It should also be noted that (2.116) and (2.117) indicate that when a field is applied, electric dipole transitions corresponding to  $J \rightarrow J$ ,  $K \rightarrow K$ ,  $M \rightarrow M \pm 1$  can be observed between the nondegenerate Stark or Zeeman components of a given rotational state, even when there is no inversion or other vibration.

For an accidentally symmetric top in which  $\mu$  does not lie exactly along  $z$ , the selection rules for  $K$  must also include the possibility  $\Delta K = \pm 1$ , but such cases are rare.

By substitution of  $K = 0$  in the matrix elements for the symmetric top, the dipole moment matrix elements corresponding to rotational absorption transitions of linear molecules are found to be

$$(J, M | \mu_z | J+1, M) = \mu \left[ \frac{(J+1+M)(J+1-M)}{(2J+1)(2J+3)} \right]^{1/2} \quad (2.119)$$

$$(J, M | \mu_y - i\mu_x | J+1, M-1) = \mu \left[ \frac{(J+1-M)(J+2-M)}{(2J+1)(2J+3)} \right]^{1/2} \quad (2.120)$$

$$(J, M | \mu_y + i\mu_x | J+1, M+1) = -\mu \left[ \frac{(J+1+M)(J+2+M)}{(2J+1)(2J+3)} \right]^{1/2} \quad (2.121)$$

Note that the  $J \rightarrow J$  transitions are zero when  $K = 0$ . Those for  $J \rightarrow J-1$  are not zero and can be found in a similar way from Table 2.1. From the nonvanishing elements the selection rules for the rigid linear molecular rotor are seen to be

$$\Delta J = \pm 1, \quad \Delta M = 0, \pm 1 \quad (2.122)$$

Transition probabilities for the particular Stark or Zeeman components are proportional to the squares of the foregoing matrix elements. In the field-free molecular rotor, the Stark components are degenerate, and the intensities of the unsplit, pure rotational lines are proportional to the squares of these matrix elements summed over all  $M$  values of the final  $J$  levels and, if the stimulating radiation is isotropic, over the three coordinates,  $X$ ,  $Y$ ,  $Z$ . The summation can be achieved simply by addition of the squared component

matrices. The  $M$  dependency cancels. The result for linear molecules is

$$\begin{aligned} |(J|\mu|J+1)|^2 &= \sum_{F=X,Y,Z} \sum_{M'} |(J, M|\mu_F|J+1, M')|^2 \\ &= (J, M|\mu_Z|J+1, M)^2 + \frac{1}{2} [(J, M|\mu_Y - i\mu_X|J+1, M-1)^2 \\ &\quad + (J, M|\mu_Y + i\mu_X|J+1, M+1)^2] \\ &= \mu^2(J+1)/(2J+1) \end{aligned} \quad (2.123)$$

Similarly, the dipole moment matrix elements for the field-free symmetric top must be summed over the  $M'$  degeneracies of the final state when the effective transition probabilities for the rotational absorption lines are obtained. The result for the  $J, K \rightarrow J+1, K$  transition is

$$\begin{aligned} |(J, K|\mu|J+1, K)|^2 &= \sum_{F=X,Y,Z} \sum_{M'} |(J, K, M|\mu_F|J+1, K, M')|^2 \\ &= \mu^2 \frac{(J+1)^2 - K^2}{(J+1)(2J+1)} \end{aligned} \quad (2.124)$$

For the  $J \rightarrow J$  or the inversion type of transition the result is

$$|(J, K^-|\mu|J, K^+)|^2 = \sum_{F=X,Y,Z} \sum_{M'} |(J, K^-, M|\mu_F|J, K^+, M')|^2 = \mu^2 \frac{K^2}{J(J+1)} \quad (2.125)$$

The (+) and (-) symbols represent the two inversion states.

When plane-polarized radiation is used, coupling with molecules occurs only along one axis, and the foregoing squared sums must be reduced by  $\frac{1}{3}$  for calculation of the line intensities.

Dipole moment matrices and selection rules for the asymmetric rotor are described in Chapter VII.

## References

1. E. Feenberg and G. E. Pake, *Notes on the Quantum Theory of Angular Momentum*, Addison-Wesley, Cambridge, Mass., 1953.
2. D. M. Dennison, *Phys. Rev.*, **28**, 318 (1926); *Rev. Mod. Phys.*, **3**, 280 (1931).
3. F. Reiche and H. Rademacher, *Z. Physik*, **39**, 444 (1927).
4. R. de L. Kronig and I. I. Rabi, *Phys. Rev.*, **29**, 262 (1927).
5. P. C. Cross, R. M. Hainer, and G. C. King, *J. Chem. Phys.*, **12**, 210 (1944).

## Chapter III

# MICROWAVE TRANSITIONS —LINE INTENSITIES AND SHAPES

---

1	LINE STRENGTHS	37
2	LINE SHAPES AND WIDTHS	44
	Natural Line Width	44
	Doppler Broadening	45
	Pressure Broadening	47
	Instrumental Distortion	50
3	POPULATION OF ENERGY STATES	54
	Molecular Vibrational and Rotational States	55
4	SYMMETRY PROPERTIES	58
	Inversion of the Coordinates	58
	Symmetry of Momental Ellipsoid	60
	Effects of Nuclear Spin	61

Microwave spectral lines arise from transitions between quantized energy levels of which the separations  $\Delta E$  correspond to the microwave quanta  $h\nu$ , where  $\nu$  is the frequency of the microwave radiation. If the molecule, particle, or system of particles has a dipole moment, electric or magnetic, the radiation field will couple with it to induce transitions when the frequency of the radiation corresponds to the Bohr condition  $h\nu = \Delta E$ . An electric dipole will couple with the electric vector; a magnetic dipole, with the magnetic component of the radiation. Electric dipole coupling is generally the mechanism for inducing molecular rotational transitions; magnetic dipole coupling, the mechanism for inducing transitions between states of electron spin resonance. Since electric quadrupole transitions and spontaneous emission are too weak in the microwave region to be of interest, we shall be concerned with induced dipole transitions.

## 1 LINE STRENGTHS

Consider two discrete, nondegenerate levels of a substance between which microwave transitions can occur. For simplicity, we designate each level by

only one quantum number,  $m$  for the lower level and  $n$  for the upper one. To be specific, we assume that the substance is made up of molecules, although the theory described applies equally well to spinning electrons, to nuclei oriented in magnetic fields, or to any quantum mechanical system considered in this volume. Now suppose that the substance is exposed to radiation at the resonant frequency

$$\nu_{mn} = \frac{E_n - E_m}{h} \quad (3.1)$$

A molecule originally in state  $m$  will have a probability

$$p_{m \rightarrow n} = \rho(\nu_{mn}) B_{m \rightarrow n} \quad (3.2)$$

of absorbing a quantum  $\hbar\nu_{mn}$  and of undergoing a transition  $m \rightarrow n$  in unit time, where  $\rho(\nu_{mn})$  represents the density of the radiation and  $B_{m \rightarrow n}$  represents the Einstein coefficient of absorption for the particular transition of the substance. A molecule originally in state  $n$  will have a probability

$$p_{m \leftarrow n} = \rho(\nu_{mn}) B_{m \leftarrow n} + A_{m \leftarrow n} \quad (3.3)$$

of emitting a quantum  $\hbar\nu_{mn}$  and of undergoing the transition  $m \leftarrow n$  in unit time, where  $B_{m \leftarrow n}$  is the Einstein coefficient of induced emission and  $A_{m \leftarrow n}$  is the Einstein coefficient of spontaneous emission for the transition.

Einstein originally assumed the coefficients of induced emission and absorption to be equal, an assumption later verified by quantum mechanical calculations and by experiments. From time-dependent perturbation theory it can be shown (see, for example, Pauling and Wilson [1]) that for isotropic radiation the probability of absorption in unit time is

$$p_{m \rightarrow n} = \left( \frac{8\pi^3}{3h^2} \right) [(m|\mu_F|n)|^2 + (m|\mu_Y|n)|^2 + (m|\mu_Z|n)|^2] \rho(\nu_{mn}) \quad (3.4)$$

where

$$(m|\mu_F|n) = \int \psi_m^* \mu_F \psi_n d\tau \quad (3.5)$$

and where  $F = X, Y, Z$  represents the matrix elements of the dipole moment component of the molecule or other particle referred to space-fixed axes for the transition  $m \rightarrow n$ . The dipole moment matrix is Hermitian  $(m|\mu_F|n) = (n|\mu_F|m)^*$ . Thus the Einstein  $B$  coefficients are

$$B_{mn} = B_{m \rightarrow n} = B_{m \leftarrow n} = \left( \frac{8\pi^3}{3h^2} \right) [(m|\mu_X|n)|^2 + (m|\mu_Y|n)|^2 + (m|\mu_Z|n)|^2] \quad (3.6)$$

The quantities  $(m|\mu_F|n)$  are the matrix elements of the dipole moment components resolved on the space-fixed axes in the representation that diagonalizes the energy matrix of the molecule. For most molecules, the dipole moment components can be considered as constant in the rotating body-fixed axes, and the matrix elements may then be expressed only in molecular rota-

tional eigenfunctions. Dipole moment matrix elements for molecular rotational transitions are given in Chapter II, Section 6. Since the  $B$  coefficients are equal, we shall hereafter drop the arrow subscripts.

The coefficient of spontaneous emission  $A$  is relatively inconsequential at microwave and radiofrequencies. A rigorous derivation is difficult, but the coefficient may be found easily from the  $B$  coefficients by use of Planck's radiation law with the assumption that the only mechanism for exchange of energy between levels is through radiation-induced or spontaneous emission. For isolated units in which no collision or like thermal process occurs, this assumption is obviously justifiable, and we assume this idealized condition when finding the coefficient  $A$ . It is possible, however, to treat relaxation processes such as collisions as arising from radiation components generated by the collisions that contribute to  $\rho(v_{mn})$ .

If  $N_m$  represents the number of molecules per unit volume in the lower state, the number per unit volume undergoing transitions to the upper state in time  $\Delta t$  will be

$$\Delta N_{m \rightarrow n} = N_m B_{mn} \rho(v_{mn}) \Delta t \quad (3.7)$$

The number per unit volume making the reverse transition in time  $\Delta t$  is

$$\Delta N_{m \leftarrow n} = N_n [B_{mn} \rho(v_{mn}) + A_{m \leftarrow n}] \Delta t \quad (3.8)$$

If thermal equilibrium is maintained by these processes,  $(\Delta N_{m \rightarrow n})/(\Delta t) = (\Delta N_{m \leftarrow n})/(\Delta t)$ , and (3.7) with (3.8) yields

$$\frac{N_n}{N_m} = \frac{B_{mn} \rho(v_{mn})}{B_{mn} \rho(v_{mn}) + A_{m \leftarrow n}} \quad (3.9)$$

At thermal equilibrium the Boltzmann law requires:

$$\frac{N_n}{N_m} = e^{-hv_{mn}/kT} \quad (3.10)$$

Combination of the Boltzmann relation with (3.9) yields upon transformation

$$\rho(v_{mn}) = \frac{A_{m \leftarrow n}}{B_{mn}} \frac{1}{\exp(hv_{mn}/kT) - 1} \quad (3.11)$$

Conformity of this expression with Planck's radiation law

$$\rho(v) = \left( \frac{8\pi h v^3}{c^3} \right) \left( \frac{1}{\exp(hv/kT) - 1} \right) \quad (3.12)$$

requires

$$A_{m \leftarrow n} = \left( \frac{8\pi h v_{mn}^3}{c^3} \right) B_{mn} \quad (3.13)$$

With  $B_{mn}$  from (3.6), this gives

$$A_{m \leftarrow n} = \frac{64\pi^4 v_{mn}^3}{3hc^3} [(m|\mu_x|n)^2 + (m|\mu_y|n)^2 + (m|\mu_z|n)^2] \quad (3.14)$$

In the optical region spontaneous emission is of comparable importance with stimulated emission. However, the variation of the  $A$  coefficient with the cube of the radiation frequency makes spontaneous emission insignificant in the microwave and radiofrequency regions. In these regions we can neglect it in comparison with other relaxation processes.

Suppose now that the radiation density  $\rho(v_{mn})$  is the coherent radiation from a controlled microwave or radiofrequency oscillator. If  $V$  is the volume of the sample, the total number of molecules undergoing the transition  $m \rightarrow n$  per second is  $VN_m p_{m \rightarrow n}$ . Since each of them absorbs an energy  $h\nu_{mn}$ , the total energy per second (power) required for this transition is

$$P_{m \rightarrow n} = VN_m p_{m \rightarrow n} h\nu_{mn} = VN_m B_{mn} \rho(v_{mn}) h\nu_{mn} \quad (3.15)$$

and the total power returned to the radiation field through stimulated emission is

$$P_{m \leftarrow n} = VN_n B_{mn} \rho(v_{mn}) h\nu_{mn} \quad (3.16)$$

The emitted power will be in phase with the coherent radiation that stimulates it and thus will add power of the same frequency and in phase with that from the original source. As a result of these processes, there will be a net change in the coherent power in the radiation field of

$$\Delta P = P_{m \leftarrow n} - P_{m \rightarrow n} = V(N_n - N_m)B_{mn} \rho(v_{mn}) h\nu_{mn} \quad (3.17)$$

Usually the population of the lower state is the greater,  $N_m > N_n$ , and the  $\Delta P$  of (3.17) is negative, that is, there will be a net absorption of power. If, as in maser spectrometers, the upper state has the greater population,  $N_n > N_m$ , the  $\Delta P$  will be positive, that is, there will be a net gain of power or amplification. It is evident, however, that application of resonant coherent power causes more transitions from the state having the greater population and hence tends to equalize the population of the two states. When  $N_n = N_m$ , there will be no net change in power,  $\Delta P = 0$ . It is further evident that continuous observation of either absorption or amplification of the applied radiation would require that some other process be operative to preserve a difference in populations, to offset the equalizing tendency of the applied power. Thermal motions that cause interactions between the molecules or particles most commonly serve this function. However, the thermal process always tends to produce a greater population of the lower energy level so that under conditions of thermal equilibrium the states have a difference in population given by the Boltzmann law, (3.10). Clearly, application of coherent resonant power will tend to upset the thermal equilibrium between the two levels so that the relative populations will no longer be given by Boltzmann's law. If, however, the thermal relaxation is rapid as compared with the rate of exchange of energy of the molecules with the applied radiation field, the thermal processes will dominate and thermal equilibrium will be maintained, or nearly so. Since most microwave absorption spectrometers operate under conditions of approximate thermal equilibrium, we shall calculate the peak absorption coefficients for this condition. We can

achieve this condition by lowering the applied radiation  $\rho(v_{mn})$  so as to decrease the probability of radiation-induced transitions or by increasing the rate of thermal relaxation through some process such as an increase of temperature or pressure of the sample.

Under conditions of thermal equilibrium we can employ Boltzmann's law with (3.17) to find the power absorbed

$$P_{\text{abs}} = -\Delta P = VN_m(1 - e^{-hv_{mn}/kT})B_{mn}\rho(v_{mn})hv_{mn} \quad (3.18)$$

A quantity more useful to spectroscopists than the absorbed power is the absorption coefficient  $\alpha$  defined by

$$\alpha = -\left(\frac{1}{P}\right)\left(\frac{\Delta P}{\Delta x}\right) \quad (3.19)$$

where  $\Delta P$  represents the power absorbed in an element of cell length  $\Delta x$  where the total power is  $P$ .

The element of volume  $\Delta V$  of the sample can be expressed as  $\Delta V = S\Delta x$  where  $S$  represents the crosssection of the absorption cell; the energy density in this section as  $\rho(v) = P/cS$  where  $P$  is the power at the input and  $c$  is the velocity of propagation; and the number of particles in the lower state as  $N_m = NF_m$  where  $N$  is the number of particles per unit volume of the sample and  $F_m$  is the fraction of these which are in the state  $m$ . Substitution of these relations into (3.18) and transformation give

$$\alpha_{mn} = -\frac{1}{P} \frac{\Delta P}{\Delta x} = \frac{NF_m}{c} (1 - e^{-hv_{mn}/kT}) B_{mn} hv_{mn} \quad (3.20)$$

For microwave spectroscopy, where  $hv < kT$ , the expression for the difference in population of the energy states can be expanded in a converging series and  $\alpha_{mn}$  expressed as

$$\begin{aligned} \alpha_{mn} &= \frac{NF_m(hv_{mn})^2}{ckT} \left(1 - \frac{1}{2} \frac{hv_{mn}}{kT} + \dots\right) B_{mn} \\ &\approx \frac{NF_m(hv_{mn})^2}{ckT} B_{mn} \end{aligned} \quad (3.21)$$

In convenient units for numerical computations,

$$\frac{hv}{kT} = 1.44 \frac{v(\text{cm}^{-1})}{T} = 48 \times 10^{-6} \frac{v(\text{MHz})}{T} \quad (3.22)$$

where  $T$  is measured on the absolute scale ( $^{\circ}\text{K}$ ).

Except at low temperatures or very high submillimeter wave frequencies,  $hv_{mn} \ll kT$ , and we can negelect higher terms in the expansion and employ the approximate form of (3.21). For example, with measurements made with 1-cm wavelength at room temperature ( $300^{\circ}\text{K}$ ) neglect of the  $hv_{mn}/2kT$  term would cause an error in the calculated value of only 0.2%; for measurements at the same frequency, but at liquid helium temperature ( $4.3^{\circ}\text{K}$ ) the error would be

5%. In the  $\frac{1}{2}$ -mm region ( $v = 20 \text{ cm}^{-1}$ ) and at dry ice temperatures, neglect of the higher terms in the expansion would cause an error of the order of 7%. Note that the predicted absorption with this approximation is greater than the actual absorption.

So far we have assumed that frequencies  $v_{mn}$  for transitions between  $m$  and  $n$  are the same for all particles of the samples. This is, of course, not true; no spectral line is infinitely sharp. The mutual interactions between particles, Doppler broadening, and other factors discussed in Section 2 cause the different molecules in the indicated states to have slightly different energies and transition frequencies. Thus the absorption will be distributed over a range of frequencies, and the absorption coefficient will be a function of the frequencies within the absorption range. This function, called the line-shape function, will vary according to type and degree of perturbation, but most microwave and radiofrequency absorption lines considered in this volume are sharp and have approximately the Lorentzian shape function, (3.44). The formula for absorption coefficients  $\alpha_v$  for isotropic radiation of any frequency  $v$  under conditions of thermal equilibrium can be found from (3.21) upon substitution of  $B_{mn}$  and upon multiplication by the properly normalized shape function  $S(v, v_0)$  discussed in Section 2. The resulting formula is

$$\alpha_v = \frac{8\pi^3 NF_m v^2}{3ckT} \left(1 - \frac{1}{2} \frac{hv}{kT}\right) [|(m|\mu_x|n)|^2 + |(m|\mu_y|n)|^2 + |(m|\mu_z|n)|^2] S(v, v_0) \quad (3.23)$$

where  $v_0$  is the frequency for the peak absorption and  $v$  is any frequency within the range of absorption.

With plane polarized radiation commonly employed in microwave spectroscopy we can without loss of generality choose the coupling vector of the radiation along the  $Z$  axis and can drop the  $X$  and  $Y$  components from the dipole moment matrix elements if we multiply the preceding expression for isotropic radiation by the factor of 3. However, the net result is the same if we keep all components of (3.23) and do not multiply by 3. With the Lorentzian shape function, (3.44), the absorption coefficient is

$$\alpha_v = \frac{8\pi^2 NF_m v^2}{3ckT} \left(1 - \frac{1}{2} \frac{hv}{kT}\right) |(m|\mu|n)|^2 \frac{\Delta v}{(v_0 - v)^2 + (\Delta v)^2} \quad (3.24)$$

where

$F_m$  = fraction of molecules in the lower state of the transition (Section 3)

$N$  = number of molecules per unit volume

For gaseous samples

$$N = 9.68 \times 10^{18} p_{\text{mm}}/T \quad (3.25)$$

where  $p_{\text{mm}}$  is the pressure in mm of Hg and  $T$  is the absolute temperature

$\Delta v$  = half-width of line measured between half-intensity points

For pressure broadened lines (see Section 2)

$$\Delta v \approx 300 p_{\text{mm}} \frac{(\Delta v)_1}{T} \quad (3.26)$$

where  $(\Delta v)_1$  is the line breadth measured at  $T = 300^\circ\text{K}$  and 1 mm of Hg pressure.

An important quantity often measured is the absorption coefficient at the resonant frequency  $v_0$ , called the peak absorption coefficient  $\alpha_{\text{max}}$ . When  $v = v_0$  is substituted in (3.24), the peak absorption coefficient is seen to be

$$\alpha_{\text{max}} = \frac{8\pi^2 N F_m v_0^2}{3ckT(\Delta v)} \left(1 - \frac{1}{2} \frac{hv_0}{kT}\right) |(m|\mu|n)|^2 \quad (3.27)$$

The peak absorptions are useful for quick measurements of relative intensities of lines having similar shape and width. The absolute or integrated intensity defined by

$$I = \int_0^{\infty} \alpha_v dv \quad (3.28)$$

is independent of the line width.

From the absorption coefficient  $\alpha_v$  one can calculate the power absorbed at the frequency  $v$  for an absorption cell of given length  $x$ . Upon integration of (3.19) and evaluation of the constant of integration with the condition that at  $x=0$ ,  $P=P_0$ , one obtains

$$P_x = P_0 \exp(-\alpha_v x) \quad (3.29)$$

where  $P_0$  is the power at the input and  $P_x$  is the power at the output of the cell of length  $x$  and the power absorbed is  $P_{\text{abs}} = P_0 - P_x$ . If the power attenuation constant in the absorption cell walls is  $\alpha_c$ , the transmitted power is

$$P_x = P_0 \exp[-(\alpha_v + \alpha_c)x] \quad (3.30)$$

For experimental evaluation of the spectral absorption coefficient from the measured ratio  $P_x/P_0$ , one can use the integrated expression

$$\alpha_v = -\alpha_c - \frac{1}{x} \ln \left( \frac{P_x}{P_0} \right) \quad (3.31)$$

The constant  $\alpha_c$  can be measured by the power loss when no absorbing gas is in the cell, but in actual practice it is simpler to measure  $\alpha_c$  not by removing the gas from the cell but simply by tuning the oscillator out of the region of absorption of the gas where  $\alpha_v \approx 0$ . Since  $\alpha_c$  does not vary significantly with frequency over the region of absorption of the usually sharp spectral line, its effects are not apparent in the typical frequency-sweep spectrometer, which responds only to a variation of power with frequency. The power loss in the cell does, however, affect the sensitivity of the spectrometer, and  $\alpha_c$  must be known for an absolute measurement of  $\alpha_v$ .

## 2 LINE SHAPES AND WIDTHS

In this volume we shall not be concerned with physical theories of line shapes as such, but primarily with the effects of line width and shape on the detectability, resolution, and accuracy of measurement of the line frequency. Most microwave measurements are made on gaseous absorption lines having widths ranging from a few kilohertz to a few megahertz. We shall discuss briefly the factors which determine width of this range.

### Natural Line Width

The natural width of a molecular line may be considered to arise from the probability of spontaneous emission which would limit the lifetime in the upper state  $n$  if the molecule were completely isolated from interaction with radiation fields or with other molecules or particles. The lifetime in the state and the energy spread of the state is related by the uncertainty principle

$$\Delta t \cdot \Delta E \approx \hbar \quad (3.32)$$

The corresponding frequency spread is

$$\Delta v = \frac{\Delta E}{h} \approx \frac{1}{2\pi(\Delta t)} \quad (3.33)$$

For a molecule in a state  $n$  that can only make spontaneous transitions to a lower state  $m$ , the "natural" lifetime in the state can be taken as

$$\Delta t = \frac{1}{A_{mn}} = \frac{3hc^3}{64\pi^4 v_{mn}^3 |(m|\mu|n)|^2} \quad (3.34)$$

where  $A_{mn}$  is the probability of spontaneous emission given by (3.14). Substitution of this  $\Delta t$  into (3.33) gives

$$\Delta v \approx \frac{32\pi^3 v_{mn}^3}{3hc^3} |(m|\mu|n)|^2 \quad (3.35)$$

When the dipole moment is expressed in convenient debye units ( $1 \text{ D} = 10^{-18} \text{ esu}$ ), this becomes

$$\Delta v \approx 1.86 \times 10^{-38} v_{mn}^3 |(m|\mu|n)|^2 \quad (3.36)$$

Typically for polar molecules, the dipole moment matrix elements for rotational transitions are of the order of 1 D. With  $|(m|\mu|n)|^2 \approx 1$  and for molecules in ground vibrational and electronic states, the natural half-width  $\Delta v$  of a rotational line in the 3-mm wave region,  $v_{mn} = 10^{11} \text{ Hz}$ , is of the order of  $10^{-5} \text{ Hz}$ ; that of a line in the 3-cm wave region, of the order of  $10^{-8} \text{ Hz}$ . It is evident that such line widths are entirely negligible in comparison with line width arising from other factors described later.

If a molecule in state  $m$  can undergo a transition through spontaneous emission to more than one lower state, the natural line width will depend on the sum of the probabilities of the transition to the lower states. If the

lower states are represented by  $i = 1, 2, \dots$ ,

$$\Delta v \approx \frac{1}{2\pi} \sum_i A_{im} \approx \frac{32\pi^3}{3hc^3} \sum_i v_{im}^3 |(m|\mu|i)|^2 \quad (3.37)$$

In the observation of microwave transitions between rotational sublevels of excited vibrational or electronic states, the lifetime in the state  $m$  is determined predominantly by the probability of spontaneous emission to the ground vibrational or the ground electronic state; and the spread of the level, hence the natural microwave line width, is correspondingly greater. The natural width can be estimated from (3.37) with  $v$  and the dipole moment matrix elements corresponding to the transition to the ground vibrational or ground electronic state: for example, suppose we are observing rotational lines in the first excited vibrational state of HCl. The frequency corresponding to a transition to the ground vibrational state is  $8.65 \times 10^{13}$  Hz. The matrix elements corresponding to this vibrational transition are still of the order of a Debye unit. Thus the natural line width, from (3.37), is of the order of 12 or 24 Hz if we consider the line spread of the lower rotational level. This broadening is still smaller than that caused by molecular collisions, Doppler broadening, and so on, in the usual microwave experiment. For molecules or atoms in excited electronic states, however, this "natural broadening" factor can be the dominant one unless the excited electronic state is a metastable state, for which  $|(m|\mu|n)|^2$  is zero in the first approximation. For  $v_{mn}$  in the visible region at  $4000 \text{ \AA}$  and  $|(m|\mu|n)|^2 \approx 1$ , the broadening would be of the order of 24 MHz.

### Doppler Broadening

The frequency of radiation absorbed by a molecule in motion depends to some extent on the velocity of the molecule relative to that of the radiation. If  $v_0$  represents the resonant absorption frequency of the molecule at rest, the frequency that it will absorb when moving with a velocity  $v$  relative to that of the radiation will be  $v = v_0(1 + v/c)$ , where  $c$  is the velocity of the radiation. The change in frequency  $v_0(v/c)$  is called the Doppler shift of the frequency. For molecules moving in opposite direction to the radiation ( $v$  negative), the absorption frequency will be lower than  $v_0$ ; for those moving in the direction of the radiation ( $v$  positive), the absorption frequency will be higher than  $v_0$ . Molecules moving at right angles to the path of the radiation will have no Doppler shift.

Similar shifts are observed for emission of radiation, with  $v$  representing the molecular velocity relative to that of the emitted radiation which is detected. The molecules of a gas at thermal equilibrium will have a Maxwell-Boltzmann distribution of velocities, and the various Doppler shifts of all the molecular frequencies will give rise to a line-shape function

$$S_d(v, v_0) = S_0 \exp \left[ -\frac{mc^2}{2kT} \left( \frac{v-v_0}{v_0} \right)^2 \right] \quad (3.38)$$

where  $k$  is the Boltzmann constant and  $T$  is the absolute temperature. The Doppler line width  $2(\Delta v)_d$ , the width between half-intensity points caused by Doppler broadening alone, is seen from (3.38) to be

$$2(\Delta v)_d = \frac{2v_0}{c} \left( \frac{2NkT \ln 2}{M} \right)^{1/2} = 7.15 \times 10^{-7} \left( \frac{T}{M} \right)^{1/2} v_0 \quad (3.39)$$

where  $M$  represents the molecular weight in atomic mass units and  $N$  is Avogadro's number. The line breadth  $\Delta v$  is usually defined as the width between the peak frequency  $v_0$  and the frequency at half-intensity, so that the line width measured between half-intensity points is  $2(\Delta v)$ .

By solving (3.39) for  $v_0$  in terms of  $(\Delta v)_d$  and substituting this value for  $v_0$  into (3.38), one obtains the more convenient expression

$$S_d(v, v_0) = S_0 \exp \left\{ -(\ln 2) \left[ \frac{v - v_0}{(\Delta v)_d} \right]^2 \right\} \quad (3.40)$$

for the line-shape function. Substituting this expression for the shape function in (3.23) with  $N$  in terms of pressure  $p$  from (3.25) when  $hv \ll kT$  and using  $\ln 2 = 0.693$ , one obtains

$$\alpha_v(p \leq p_c) = Cv^2 p \exp \left\{ -0.693 \left[ \frac{v - v_0}{(\Delta v)_d} \right]^2 \right\} \quad (3.41)$$

for the absorption coefficient in the pressure range below  $p_c$  above which collision broadening begins to be significant (see Pressure Broadening in Section 2). Here  $C$  is a constant independent of the pressure and frequency. At the critical pressure and resonant frequency, the Doppler broadened line has its maximum absorption coefficient

$$(\alpha_{\max})_d = Cv_0^2 p_c \quad (3.42)$$

as is seen from substitution of  $p = p_c$  and  $v = v_0$  into (3.41). Substitution of  $C$  from (3.42) into (3.41) yields

$$\left( \frac{\alpha_v}{\alpha_{\max}} \right)_d = \frac{p}{p_c} \left( \frac{v}{v_0} \right)^2 \exp \left\{ -0.693 \left[ \frac{v - v_0}{(\Delta v)_d} \right]^2 \right\} \quad (3.43)$$

where  $p \leq p_c$ . The  $(\alpha_{\max})_d$  as defined here has the same numerical value as does the  $\alpha_{\max}$  for the pressure-broadened line described in Section 2. The function of (3.43) represents the normalized shape function of the Doppler-broadened line. It is plotted in Fig. 3.1 for a few values of  $p/p_c$  with an assumed Doppler width  $(\Delta v)_d = 0.5$  MHz. Note that the width is constant and that the peak intensity decreases directly with the pressure. Since one gains nothing in resolution while losing peak intensity, it is usually undesirable to reduce the pressure below  $p_c$ , or that for which the Doppler broadening becomes a dominant factor.

Doppler broadening of gaseous lines is much smaller than pressure broadening under the usual conditions of observation in the centimeter wave region. Because of its increase with frequency, however, Doppler broadening is some-

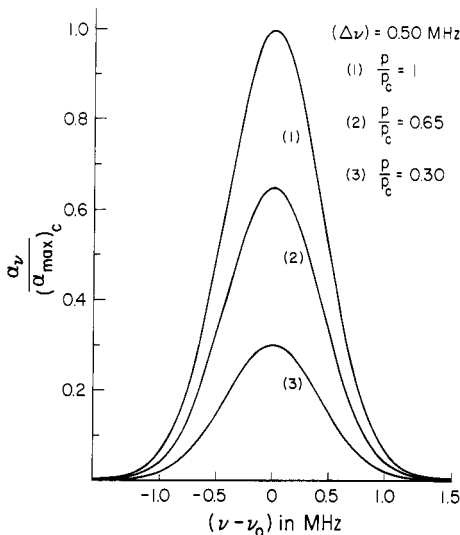


Fig. 3.1 Shape of Doppler-broadened lines.

times the dominant factor in the broadening of submillimeter wave spectral lines. As an example, let us consider NH<sub>3</sub>, which has a molecular weight of 17. At  $T = 300^{\circ}\text{K}$ , the ammonia inversion lines in the centimeter wave region,  $\nu_0 \approx 24,000$  MHz, have a Doppler width of 72 kHz; the  $J=0 \rightarrow 1$  rotational line [2] of NH<sub>3</sub> with  $\nu_0 = 572,053$  MHz has a Doppler width  $2(\Delta\nu)_d$  of 1.7 MHz. Although this increase of Doppler broadening with increase of  $\nu_0$  does not reduce the absolute accuracy of measurement of the resonant frequency, which depends on  $\Delta\nu/\nu_0$ , it interferes with resolution of the hyperfine structure, the separation of which does not increase with  $\nu_0$ .

The Doppler broadening can be circumvented or greatly reduced by the use of a molecular beam absorption spectrometer in which the absorbing molecules are sprayed across the path of the microwave radiation. Fortunately, the greater absorption of molecules at higher frequencies makes this method more feasible at the submillimeter wave frequencies where Doppler broadening becomes significant. Since the absolute resolution and accuracy of measurement depend on  $\Delta\nu/\nu_0$ , it is evident that with a molecular beam spectrometer to reduce  $\Delta\nu$ , exceptionally high precision can be achieved in the submillimeter wave region with microwave electronic methods.

### Pressure Broadening

At the pressures usually employed in the measurement of microwave spectral lines of gases,  $\sim 1$  to  $10^{-3}$  mm of Hg, pressure arising from binary collisions of the molecules is the predominant line-broadening factor. If the collision is considered as abruptly terminating the life of the molecule in a particular rotational energy state, the line width can be calculated from (3.33)

with the  $\Delta t$ 's representing the times between collisions. The line-shape function would be expected to have the same form as that for the distribution of the collision times between the molecules, which would in turn depend upon the Maxwell-Boltzmann distribution of velocities. If  $\tau$  is the mean time between collisions that end the lifetime in the state, (3.33) indicates a line breadth of  $\Delta v = 1/(2\pi\tau)$ .

All collisions do not cause transitions. Furthermore, transitions may be induced by long-range resonance interactions in which the molecules do not collide in the usual sense. Also, a molecule can experience a Stark perturbation of its energy levels from the dipole field of a molecule which approaches closely. The pressure broadening thus depends on properties of the molecules as well as on velocity distribution and collision times. Theoretically, the line shape might be used for measurement of dipole moments, but such measurements would be much more difficult to make and the resulting dipole moments much less accurate than those obtained from the Stark effect of rotational lines. However, collisions between polar and nonpolar molecules have been used for approximate measurements of molecular quadrupole moments [3] of nonpolar molecules for which no other measurements are available.

At the low pressures commonly used in microwave measurements where the half-width  $\Delta v \ll v_0$ , collision-broadened lines have the Lorentzian shape function [4]:

$$S(v, v_0) = \frac{1}{\pi} \left[ \frac{\Delta v}{(v_0 - v)^2 + (\Delta v)^2} \right] \quad (3.44)$$

where

$$\Delta v = 1/(2\pi\tau)$$

$\tau$  = mean time between collisions

$v_0$  = the peak resonant frequency

Over the range of very low pressures considered, 1 mm of Hg or less, the mean collision time  $\tau$  varies inversely as the pressure, and therefore  $\Delta v$  increases linearly with the pressure. The number of absorbing particles also increases linearly with pressure. Hence, within the range of pressures sufficiently high that molecular collisions are the dominant cause of broadening and sufficiently low that the line width is directly proportional to pressure, we can by substitution of (3.25) and (3.26) into (3.24) express the absorption coefficient as a function of frequency and pressure

$$\alpha_v = Cv^2 \left[ \frac{(\Delta v)_1 p^2}{(v - v_0)^2 + (\Delta v)_1^2 p^2} \right] \quad (3.45)$$

where  $p$  is the pressure,  $(\Delta v)_1$  is the line breadth for  $p = 1$  mm pressure,  $T = 300^\circ\text{K}$ , and  $C$  is a constant that represents other intensity factors in (3.24) that do not depend on pressure or frequency. Note that the peak absorption coefficient  $\alpha_{\max}$  obtained when  $v$  equals  $v_0$  is independent of pressure

$$\alpha_{\max} = \frac{Cv_0^2}{(\Delta v)_1} \quad (3.46)$$

This is an important property in the observation of spectra since the detectability of an absorption line generally depends on the peak intensity rather than on the integrated intensity. Thus one gains resolution without losing detectability by decreasing the pressure until other broadening factors that do not depend on pressure (mainly Doppler broadening) become significant. As the pressure is reduced to the point at which the Doppler broadening becomes dominant, the line shape changes to the Maxwell-Boltzmann shape described earlier, and the peak intensity  $\alpha_{\max}$  does not remain constant but decreases directly with the decrease in pressure.

By substituting  $Cv_0^2 = \alpha_{\max}(\Delta\nu)_1$  from (3.46) into (3.45) and rearranging the terms, one obtains

$$\frac{\alpha_v}{\alpha_{\max}} = \frac{(v/v_0)^2}{[(v - v_0)/p(\Delta\nu)_1]^2 + 1} \quad (3.47)$$

Equation 3.47 represents the normalized-shape function of pressure-broadened lines in the pressure range for which the linewidth is directly proportional to pressure, the range in which most microwave lines of gases are measured. Figure 3.2 shows plots of (3.47) for a typical line-breadth parameter  $(\Delta\nu)_1 = 10 \text{ MHz/mm of Hg}$  and for three different pressures ranging from 1 to  $10^{-1} \text{ mm of Hg}$ . These curves represent the Lorentzian line shape.

In the higher range of pressures, above 10 mm of Hg, deviations from the Lorentzian-shape function become evident. The more general Van Vleck-

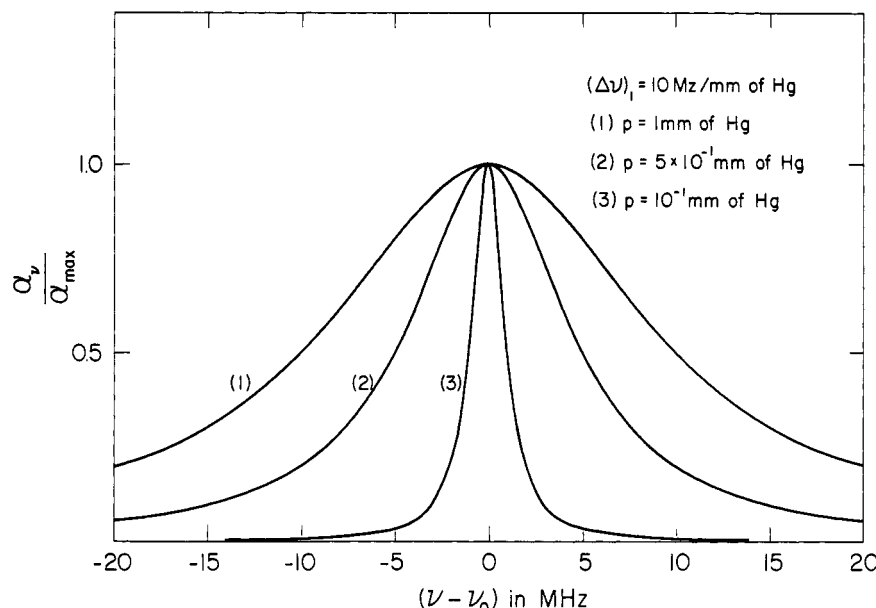


**Fig. 3.2** Microwave line shapes of pressure-broadened lines in the typical pressure range where the line width is directly proportional to pressure. The line-shape function is Lorentzian.

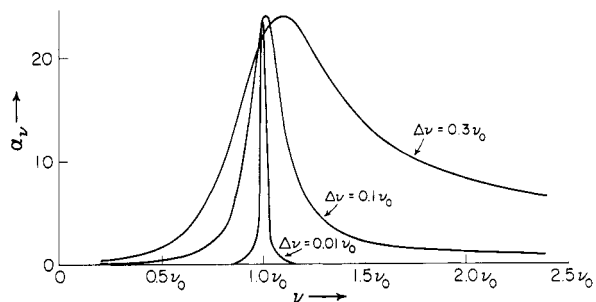


**Fig. 3.3** Microwave line shapes of pressure-broadened lines in the relatively high pressure range—the Van Vleck–Weisskopf shape function [7]. From *Microwave Spectroscopy* by Townes and Schawlow. Copyright 1955 by McGraw-Hill, Inc. Used with permission of McGraw-Hill Book Company.

Weisskopf [5] line-shape function

$$S(v, v_0) = \frac{v}{\pi v_0} \left[ \frac{\Delta v}{(v_0 - v)^2 + (\Delta v)^2} + \frac{\Delta v}{(v_0 + v)^2 + (\Delta v)^2} \right] \quad (3.48)$$

is found to fit satisfactorily the observed microwave line shapes at low gas pressures as well as at relatively high ones, of the order of an atmosphere. Figure 3.3 shows graphically the Van Vleck–Weisskopf line shape with different relative values of  $\Delta v$  and  $v_0$ . For  $v_0$  in the microwave region, these curves all correspond to relatively high pressures. For low pressures where  $\Delta v \ll v_0$ , the second term of (3.48) becomes very small in comparison with the first, and the expression reduces to the Lorentzian-shape function, (3.44), in the region of significant absorption where  $v \approx v_0$ .

In Table 3.1 illustrative line-breadth parameters are given for a few gases. These represent the half-widths of the lines between half-intensity points for a pressure of 1 mm of Hg of the gas. From these examples one can estimate roughly the line width to expect for other, unmeasured lines.

A rigorous treatment of pressure broadening is given by Anderson [6]. His theory relates the line shapes to the various types of intermolecular forces between the colliding molecules and provides a mechanistic understanding of line broadening. Discussion of collision broadening can be found in books on microwave spectroscopy by Townes and Schawlow [7] and by Gordy et al. [8]. A comprehensive review of the subject is given by Birnbaum [9].

### Instrumental Distortion

#### POWER EFFECTS

At low pressures with cells of small volume it is relatively easy to distort the line noticeably by power saturation of the molecules. In the center of the line where the absorption is greatest, the molecules at first absorb power at a rate greater than that at which they can return to the lower state through thermal

**Table 3.1** Self-broadening Line-breadth Parameters of Rotational Lines ( $T = 300^\circ\text{K}$ )

Molecule	Transition	$(\Delta\nu)_1 \text{ MHz/mm of Hg}$	Reference
OCS	$J=0 \rightarrow 1$	6.44	a
$\text{N}_2\text{O}$	$1 \rightarrow 2$	5.22	a
CICN	$1 \rightarrow 2$	25.0	b
BrCN	$2 \rightarrow 3$	22.0	c
$\text{CH}_3\text{F}$	$0 \rightarrow 1$	20.0	d
	$2 \rightarrow 3 \ K=0$	17.2	e
	$K=1$	17.2	
	$K=2$	17.2	
	$K=3$	17.2	
$\text{CHF}_3$	$0 \rightarrow 1$	35.1	f
	$6 \rightarrow 7 \ K=3$	9.0	e
	$K=4$	9.0	
	$K=5$	9.0	
	$K=6$	9.0	
$\text{H}_2\text{O}$	$2_2 \rightarrow 3_{-2}$	19.1	g

<sup>a</sup>B. T. Berendths, Thesis, Catholic Univ. of Nijmegen (Netherlands), 1966. (Quoted by G. Birnbaum [9].)

<sup>b</sup>C. H. Townes, A. N. Holden, and F. R. Merritt, *Phys. Rev.*, **74**, 1113 (1948).

<sup>c</sup>S. L. Srivastava and V. Prakash, *J. Chem. Phys.*, **42**, 3738 (1965).

<sup>d</sup>O. R. Gilliam, H. D. Edwards, and W. Gordy, *Phys. Rev.*, **75**, 1014 (1949).

<sup>e</sup>G. Birnbaum, E. R. Cohn, and J. R. Rusk, *J. Chem. Phys.*, **49**, 5150 (1968).

<sup>f</sup>C. O. Britt and J. E. Boggs, *J. Chem. Phys.*, **45**, 3877 (1966).

<sup>g</sup>J. R. Rusk, *J. Chem. Phys.*, **42**, 493 (1965).

relaxation processes. As a result, difference in population of the two states  $\Delta N = N_n - N_m$  becomes less than that for thermal equilibrium, and hence the power absorption is less than that which would occur if thermal equilibrium could be maintained. In the event of complete saturation, the amount of power absorbed is determined completely by the rate of relaxation, and a further increase of incident power will cause no further power absorption. Because of its greater probability of absorption, the center of the line becomes saturated more completely than the wings, and a broadening of the line occurs. The power density at which saturation broadening becomes noticeable depends on the Einstein coefficient  $B$  or the squared dipole moment matrix elements for the transitions as well as on the pressure of the gas.

For low pressures and incomplete saturation, Karplus and Schwinger [10] have modified the Lorentzian-shape function to take account of power effects. The resulting line-shape function is

$$S(v, v_0) = \frac{1}{\pi} \left[ \frac{\Delta\nu}{(v_0 - v)^2 + (\Delta\nu)^2 + B_{mn}P/c\pi^2} \right] \quad (3.49)$$

where  $B_{mn}$  is the Einstein coefficient and  $P$  is the power density. The presence of saturation will decrease  $\alpha_v$ , as is apparent from (3.49) and (3.23).

In the shorter millimeter wave region and particularly in the submillimeter wave region, the absorption coefficients of many molecules are so large that absorption approaching 100% of the power occurs in the center of the line for cell lengths of only a few centimeters. Since the absorption is less in the wings of the line, this nearly complete absorption in the center causes a flattening of the line peak and an increase in the indicated line width. Unlike the power saturation effects, this distortion is not lessened but increased by increase of pressure, but it can be eliminated by a severe decrease in pressure or by a decrease in the effective cell length.

#### COLLISION WITH CELL WALLS

In an absorption cell of small dimensions, broadening caused by collision with cell walls can become a significant factor when the pressure is so low that the cell dimensions become comparable to the mean free path between the molecules. The half-width caused by cell-wall broadening can be calculated by the formula  $\Delta v = 1/(2\pi\tau)$ , where  $\tau$  is the mean time between collisions of the molecules with the cell walls. If  $a$ ,  $b$ , and  $c$  are dimensions of a rectangular cell, the line width caused by collision with the cell walls [11] is approximately

$$2(\Delta v) = 10 \left( \frac{1}{a} + \frac{1}{b} + \frac{1}{c} \right) \left( \frac{T}{M} \right)^{1/2} \quad (3.50)$$

where  $(2\Delta v)$  is in kHz units and  $a$ ,  $b$ ,  $c$  are in cm units.  $T$  is the absolute temperature, and  $M$  is the molecular weight. Because the length  $c$  is large in the usual waveguide cell, the factor  $1/c$  is negligible. Usually the cross-sectional dimensions of the absorption cell are made sufficiently large that the cell-wall broadening is negligible. However,  $G$ -band waveguide which supports only the dominant mode for 3-mm wave radiation has the cross-sectional dimensions of approximately  $0.2 \times 0.1$  cm. In an observation of carbon monoxide gas (molecular weight  $M=28$ ) at room temperature ( $T=300^\circ\text{K}$ ) in a cell made of  $G$ -band waveguide, the cell broadening would be a half-megahertz.

#### BROADENING IN MOLECULAR BEAMS

In molecular-beam spectrometers in which the molecules undergoing transitions are sprayed across the path of the radiation, there is a broadening that results from the limited time the molecules are in the radiation field. This broadening can also be approximated by the formula  $\Delta v = 1/(2\pi\tau)$  where  $\tau$  is the mean time the molecules are in the radiation. If  $\bar{v}$  is the mean velocity of the molecules of the beam and  $d$  is their path length in the radiation field,  $\tau=d/\bar{v}$ , and the broadening is

$$\Delta v \approx \frac{\bar{v}}{2\pi d} \quad (3.51)$$

If  $\bar{v}$  is in cm/sec and  $d$  is in cm,  $\Delta v$  will be in Hz units.

## DISTORTION BY MODULATORS, DETECTORS, AND AMPLIFIERS

Spectral lines are often deliberately distorted by Stark or Zeeman modulation so that their sensitivity to detection may be increased and so that they may be distinguished from sharp reflections of electronic resonances caused by impedance mismatch in the microwave components. Similar distortions of the apparent line shape are produced by frequency modulation of the radiation source to aid detection. The most common types of these distorted presentations represent the first and second derivatives of the contour of the actual line. These derivative curves for a line having the typical Lorentzian shape are illustrated in Fig. 3.4. Experimentally, the first derivative curve is obtained by a frequency modulation of the source or spectrum line and the tuning of a phase-lock-in detector to the fundamental frequency of the modulation. The second derivative curve is obtained from a tuning of the phase-lock-in detector to a frequency twice that of the modulation. To prevent further distortion, in both instances the frequency of the modulation as well as its range of variation must be small compared with the line width. The first derivative is the more sensitive form for detection; the second derivative, the more convenient for measurement of the

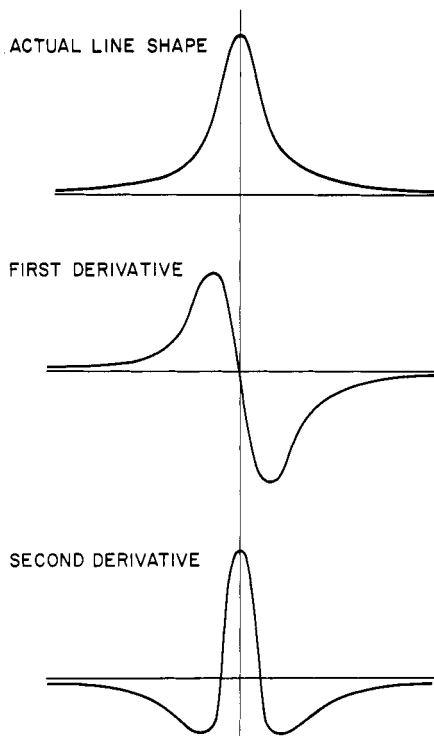


**Fig. 3.4** Comparison of the line shape obtained by a high-fidelity recording of a typical microwave line with those obtained by detection systems that display the first or second derivatives of the true line shape function (assumed to be Lorentzian).

line center and the half-width. Note from comparisons in Fig. 3.4 that the second derivative curve has an artificially sharpened peak which occurs at the center of the actual line, also minima which occur approximately at the half-intensity points. The center of the line occurs at a zero-point of the first derivative curve. Broad-banded receivers required for a high-fidelity cathode-ray-scope display of an absorption line like that of Fig. 3.4 are less sensitive than either the first- or the second-derivative detectors, but many microwave spectral lines are so strong that their detection is no problem.

When the rate of frequency modulation is not small compared with the line width, other distortion effects are encountered. This distortion also depends on the type of modulation, that is, whether sine-wave, square-wave, and so on. These effects are discussed by Karplus [12]; also by Townes and Schawlow [13].

In the typical crystal video-type spectrometer [8] the source frequency is swept completely over the spectral line at a constant rate and repeated at a constant rate, usually many times a second. A cathode-ray trace synchronized with this sweep is used to display the line which is detected with a crystal receiver and is amplified with a video-frequency receiver. The degree and type of distortion depend on the rate of frequency modulation relative to the band width of the receiver. A high-fidelity receiver must amplify equally all the Fourier components of the modulated signal. Such a receiver is not the most sensitive one for detection of the lines within thermal noise, nor will it discriminate against the spurious signals caused by impedance mismatch in the microwave components. Generally the choice of sweep-rate is a compromise between fidelity and sensitivity, depending on the strength and width of the line to be measured and the degree of mismatch in the microwave system.

### 3 POPULATION OF ENERGY STATES

The absorption line strength formula developed previously includes a factor  $N_m$  which represents the number of particles per unit volume of sample that are in the lower energy state involved in the transition. For spin resonance—electronic or nuclear—which is not split by interactions with other states, the calculation of this number  $N_m$  is relatively simple, but for molecular rotational spectra it can be complicated by the multiplicity of populated states having different energies. Under conditions of thermal equilibrium the relative population of the different states is determined by the Boltzmann law, (3.10), and by the degeneracies of the different states.

Let us assume first a spectrum of nondegenerate energy levels 0, 1, 2, 3, . . . of particles in thermal equilibrium. If  $N_0$  represents the population of the lowest level, the populations of the various other levels relative to that of the lowest level will be

$$N_1 = N_0 e^{-E_1/kT}, \quad N_2 = N_0 e^{-E_2/kT}, \quad N_3 = N_0 e^{-E_3/kT} \quad (3.52)$$

where  $E_1, E_2, E_3, \dots$  are the energies of the various levels relative to the energy

of the ground state. The total number  $N$  of particles per unit volume will be

$$N = N_0 + N_1 + N_2 + N_3 + \dots = N_0 \sum_i e^{-E_i/kT} \quad (3.53)$$

where the summation is taken over all the states. If the  $i$ th level has the degeneracy  $g_i$ , the sum total population in all states per unit volume will then be

$$N = N_0 \sum_i g_i e^{-E_i/kT} \quad (3.54)$$

and the number in the state  $m$  with degeneracy  $g_m$  and energy  $E_m$  is

$$N_m = N_0 g_m e^{-E_m/kT} \quad (3.55)$$

The fractional part  $F_m$  of the particles in state  $m$  is

$$F_m = \frac{N_m}{N} = \frac{g_m e^{-E_m/kT}}{\sum_i g_i e^{-E_i/kT}} = \frac{g_m e^{-E_m/kT}}{Q} \quad (3.56)$$

The denominator in the final expression, designated

$$Q = \sum_i g_i e^{-E_i/kT} \quad (3.57)$$

is called the partition function. It is of great significance in the calculation of spectral-line intensities. Note that  $N_0$  cancels from the ratio and that neither  $Q$  nor the numerator contains the actual number of particles in any state. Nevertheless, one can use this factor to obtain immediately the actual number of particles in any given state of known quantity of sample. The  $Q$  is a function of all the different forms of energies that the particles or system of particles may have.

### Molecular Vibrational and Rotational States

The partition function for free gaseous molecules is a function of the electronic, the vibrational, the rotational, and the nuclear spin states. If interactions between these various states are neglected, it can be expressed as the product

$$Q = Q_e Q_v Q_r Q_n \quad (3.58)$$

Most stable organic molecules at ordinary temperatures are in ground electronic singlet  $\Sigma$  states, and for them we can set  $Q_e = 1$ . For this reason we are here concerned mainly with the last three factors.

If anharmonicities are neglected, the vibrational partition function, with the energy levels measured with respect to the ground vibrational state, can be expressed as

$$Q_v = \left( \sum_{v_1} e^{-v_1 \hbar \omega_1 / kT} \right) \left( \sum_{v_2} e^{-v_2 \hbar \omega_2 / kT} \right) \left( \sum_{v_3} e^{-v_3 \hbar \omega_3 / kT} \right) \dots \quad (3.59)$$

where  $v_1, v_2, v_3, \dots$ , the vibrational quantum numbers, can each have the values 0, 1, 2, 3, ... and where  $\omega_1, \omega_2, \omega_3, \dots$  are the frequencies of the funda-

mental modes of vibration. The summation is taken over all values of  $v_1, v_2, v_3, \dots$ , and each fundamental mode of vibration is counted separately. This product by evaluation of the summations can be expressed in the more convenient form

$$Q_v = (1 - e^{-\hbar\omega_1/kT})^{-d_1} (1 - e^{-\hbar\omega_2/kT})^{-d_2} (1 - e^{-\hbar\omega_3/kT})^{-d_3} \dots \quad (3.60)$$

where  $\omega_1, \omega_2, \omega_3, \dots$  are the fundamental frequencies and each different frequency appears only once and where  $d_1, d_2, d_3, \dots$  are the degeneracies of the fundamental vibrations, that is, the number of modes having the same frequency.

The fraction of molecules in a given vibrational state specified by the set of quantum numbers  $v_1, v_2, v_3, \dots \equiv v$ , at a temperature  $T$ , is

$$F_v = \frac{d_v e^{-\hbar\Sigma_i v_i \omega_i / kT}}{Q_v} = d_v e^{-\hbar\Sigma_i v_i \omega_i / kT} (1 - e^{-\hbar\omega_1/kT})^{d_1} (1 - e^{-\hbar\omega_2/kT})^{d_2} \dots \quad (3.61)$$

When, as is customary, the vibrational frequencies are expressed in  $\text{cm}^{-1}$ , the exponent can be numerically written

$$\frac{\hbar\omega_i}{kT} = 1.439 \frac{\omega_i (\text{cm}^{-1})}{T (\text{°K})} \quad (3.62)$$

The fraction  $F_{J,i}$  of molecules in the rotational state  $|J, i\rangle$  with rotational energy  $E_{J,i}$  and in vibrational state  $v$  is given by

$$F_{J,i} = \frac{N_{J,i}}{N} = \frac{F_v g_J g_i e^{-E_{J,i}/kT}}{Q_r} \quad (3.63)$$

where

$$Q_r = \sum_J \sum_i g_J g_i e^{-E_{J,i}/kT}$$

Here  $J$  is the usual total angular momentum quantum number, and  $i$  signifies any internal quantum numbers such as  $K$  of the symmetric top. The degeneracies  $g_J = 2J + 1$  (when no external field is applied) associated with the "outer" quantum number  $M_J$  are the same for all classes of molecules. The degeneracy factor  $g_i$  is that associated with all inner quantum numbers and includes, in addition to the  $K$  degeneracy of the symmetric top, all degeneracies caused by nuclear spins, inversion, and internal rotation. Usually, however, the inversion and internal rotation degeneracies are the same for the different levels and cancel from the ratio  $g_i/Q_r$ . Except for molecules having certain symmetries described later, the effects of nuclear spins also cancel from the ratio  $g_i/Q_r$ , and hence need not be included in either. Any nuclear hyperfine splitting of the levels can be neglected in the calculation of the integrated population of the rotational level.

Linear molecules have no  $K$  degeneracy; and polar-linear molecules, which are the only ones having an observable rotational spectrum, have no center of symmetry. Therefore  $g$  (nuclear) cancels from the ratio  $g_i/Q_r$ , and we can set  $g_i = 1$  and can drop the  $i$  subscripts in (3.63). The rotational energy relative to the lowest level is adequately expressed by the rigid rotor approximation

of (5.3). Thus for diatomic or linear polyatomic molecules with no center of symmetry [14]

$$\begin{aligned} Q_r &= \sum_J (2J+1) \exp \left[ -\frac{hBJ(J+1)}{kT} \right] \\ &= \frac{kT}{hB} + \frac{1}{3} + \frac{1}{15} \left( \frac{hB}{kT} \right) + \frac{4}{315} \left( \frac{hB}{kT} \right)^2 + \dots \\ &\approx \frac{kT}{hB} \text{ (linear molecules)} \end{aligned} \quad (3.64)$$

Therefore, for linear and diatomic molecules in the vibrational state  $v$ ,

$$F_J = \frac{N_J}{N} \approx F_v \left( \frac{hB}{kT} \right) (2J+1) \exp \left[ -\frac{hBJ(J+1)}{kT} \right] \quad (3.65)$$

For a symmetric-top molecule there are degeneracies associated with the internal quantum number  $K$  as well as nuclear spin degeneracies  $g$  (nuclear) that do not cancel from (3.63) and must therefore be included. Although  $g$  (nuclear), which would appear in the definition of  $Q_r$ , can depend on the rotational state, in the high-temperature approximation the correct result is obtained if  $g$  (nuclear) is replaced by the total statistical weight factor  $g_n$  [see (3.74)] divided by the symmetry number  $\sigma$ . By definition of a reduced statistical weight factor  $g_I$  which includes the  $g_n$  factor, the fraction of molecules in a given rotational state  $J, K$  can be expressed as

$$F_{J,K} = \frac{N_{J,K}}{N} = \frac{F_v g_J g_K g_I e^{-E_{J,K}/kT}}{Q_r} \quad (3.66)$$

where  $F_v$  = fraction of molecules in the particular vibrational state being considered

$$g_J = 2J+1$$

$$g_K = 1 \text{ for } K=0 \text{ and } 2 \text{ for } K \neq 0$$

$$g_I = \text{reduced nuclear spin weight factor defined by (3.77)}$$

$$E_{J,K} = h[BJ(J+1) + (A-B)K^2]$$

and the rotational partition function is defined as

$$Q_r = \frac{1}{\sigma} \sum_{J=0}^{J=\infty} \sum_{K=-J}^{K=J} (2J+1) e^{-E_{J,K}/kT} \quad (3.67)$$

where  $\sigma$  is a measure of the degree of symmetry, discussed further in Section 4. For the usual symmetric top which has  $C_3$  or  $C_{3v}$  symmetry,  $\sigma=3$ . To a good approximation, the summation can be expressed [14] as

$$Q_r \approx \frac{1}{\sigma} \left[ \left( \frac{\pi}{B^2 A} \right) \left( \frac{kT}{h} \right)^3 \right]^{1/2} = \left( \frac{5.34 \times 10^6}{\sigma} \right) \left( \frac{T^3}{B^2 A} \right)^{1/2} \text{ (symmetric top)} \quad (3.68)$$

In the last expression the spectral constants  $B$  and  $A$  are in MHz units.

A similarly approximate formula for the partition function for the asymmetric rotor is

$$Q_r = \left( \frac{5.34 \times 10^6}{\sigma} \right) \left( \frac{T^3}{ABC} \right)^{1/2} \text{ (asymmetric top)} \quad (3.69)$$

Furthermore, in (3.66) the  $E_{J,\tau}$  term for the particular asymmetric rotor (Chapter VII) must be employed rather than the  $E_{J,K}$  term. Since there is no  $K$  degeneracy for the asymmetric rotor,  $g_K = 1$ . Many asymmetric rotors have no symmetry that allows exchange of identical nuclei with a turning of the rigid molecule. For such molecules,  $\sigma = 1$  and  $g_I = 1$ . Effects of symmetry will be described in Section 4.

#### 4 SYMMETRY PROPERTIES

Symmetry operations, such as inversion of all the coordinates at the origin or exchange of identical nuclei which leave the overall wave function of a molecule either unchanged or changed only in sign, have important consequences in the determination of selection rules and statistical weights of energy levels. The classification of the overall wave function on the basis of such symmetry operations is indicated as parity. The function that is changed in sign has a different parity from one that is left unchanged by the symmetry operation. Selection rules based on symmetry properties are called parity selection rules or symmetry selection rules.

In determination of parity it can be assumed that eigenfunctions corresponding to various energy operators of the molecule—electronic, vibrational, molecular rotational, and nuclear spin—can be used to represent the complete wave function

$$\psi_{\text{overall}} = \psi_e \psi_v \psi_r \psi_n \quad (3.70)$$

where  $\psi_e$  represents the electronic function,  $\psi_v$  the vibrational function,  $\psi_r$  the molecular rotational wave function, and  $\psi_n$  the nuclear spin function. Later we shall describe various symmetry operations on which the parity classifications are based.

##### Inversion of the Coordinates

If the coordinates of all the particles of the molecules, expressed in the Cartesian system with the origin at the center of mass, are changed in sign ( $x_i \rightarrow -x_i$ ,  $y_i \rightarrow -y_i$ ,  $z_i \rightarrow -z_i$ ), an equivalent equilibrium configuration of the molecule is achieved. For this operation, called inversion or reflection of the coordinates at the origin, the part of the product  $\psi_e \psi_v \psi_r$  must remain unchanged or be changed in sign only. Whether this product function changes sign or not depends on the behavior of each factor with respect to inversion. This part of the wave function does not include the nuclear spin function and is often referred to as the coordinate function although it does include the electron spin.

Generally, reflection of the coordinates at the origin chosen as the center of mass of the molecule does not exchange identical nuclei but may do so in molecules having certain symmetries such as  $\text{CO}_2$ . However, such linear symmetrical molecules have no dipole moment and hence no observable microwave spectra. The effect of exchange of identical nuclei is described later in this section.

In linear or planar polyatomic molecules in general, the new configuration achieved by inversion of the coordinates can also be achieved by rotation of the molecule. Inversion doubling of the levels does not occur. For nonplanar molecules, however, the new, inverted configuration cannot be achieved by rotation alone about any succession of axes; it can be achieved only if a potential barrier is overcome. When the barrier is very high, stable right and left configurations of molecules called optical isomers may occur. The two inverted configurations for nonplanar molecules (not achievable by rotation) lead to a doubling of all rotational levels, called inversion doubling. For almost all nonplanar molecules, the barrier to inversion is so high that this doubling is not resolvable, and the rotational levels are, in effect, doubly degenerate. The term  $g_{\text{inv}}=2$  would occur in both the numerator and the denominator of (3.63); hence it does not affect the term  $F_{Ji}$ , the fraction of molecules in a particular rotational state. In a few molecules, most notably ammonia, the barrier to inversion is sufficiently low that the molecule oscillates back and forth between the two equilibrium configurations, giving rise to a measurable separation of the inversion doublets and to an inversion spectrum, as described in Chapter VI, Section 3.

The functions that are unchanged upon reflection of the coordinates at the origin are designated as positive (+) functions; those that are changed in sign, as negative (-) functions. Selection rules that depend on these properties are easily derived. The dipole moment matrix elements between the states, represented by  $\psi_i$  and  $\psi_j$ , upon which the transition probability depends, can be expressed as

$$\mu_{ij} = \int \psi_i \mu_x \psi_j d\tau + \int \psi_i \mu_y \psi_j d\tau + \int \psi_i \mu_z \psi_j d\tau \quad (3.71)$$

Now for a reflection of the coordinates of all the particles at the center of mass, the components  $\mu_x$ ,  $\mu_y$ , and  $\mu_z$  change sign; and unless the functions  $\psi_i$  and  $\psi_j$  have opposite parity (opposite sign) with respect to this operation, the integrals will change sign. Since these are definite integrals, they cannot change sign unless they are identically zero. Thus for dipole-induced transitions, only positive and negative functions can combine. The parity selection rules are therefore

$$+ \leftrightarrow - \quad + \not\leftrightarrow + \quad - \not\leftrightarrow - \quad (3.72)$$

In practically all nonplanar molecules the inversion doubling is not resolvable, and these selection rules place no restrictions on the intercombinations of the rotational levels because the two components of each level have opposite symmetry.

The rotational levels of linear or planar molecules do not have the inversion degeneracy because the inverted state can be achieved also by rotation. Nevertheless, the alternate rotational levels have opposite parity with respect to the reflection of the coordinates at the center of gravity. This can readily be seen for linear molecules by an examination of the eigenfunctions of (2.102). Reflection at the origin is achieved by the transformation  $\theta \rightarrow \pi - \theta$  and  $\phi \rightarrow \pi + \phi$ . The functions of (3.70) remain unchanged for these transformations when  $J$  is even but are changed in sign when  $J$  is odd. Therefore the selection rules  $+ \leftrightarrow -, + \not\leftrightarrow +, - \not\leftrightarrow -$  are the same as those already proved,  $J \rightarrow J \pm 1$ .

The parity of the coordinate function depends on  $\psi_e$  and  $\psi_v$  as well as upon  $\psi_r$ . Most molecules have completely paired electronic systems with positive  $\psi_e$ . Likewise, the ground vibrational states of molecules in general have positive  $\psi_v$ . Thus most molecules for which rotational spectra are observed have positive  $\psi_e \psi_v$ , and the parity of  $\psi_r$  determines the parity of the overall coordinate function  $\psi_e \psi_v \psi_r$ . For these cases of linear molecules, the coordinate functions with  $J = 0, 2, 4, \dots$  are plus, and those with  $J = 1, 3, 5, \dots$  are minus.

### Symmetry of Momental Ellipsoid

Classification of the rotational levels on the basis of the symmetry properties of the momental ellipsoid is of importance in determination of the selection rules and line intensities for an asymmetric rotor.

Because of the symmetry of the momental ellipsoid, the probability density  $\psi_r^2$  of a rigid asymmetric rotor does not change for a rotation of  $\pi$  degrees about any of the principal axes of inertia. Conventionally, these axes are designated  $a, b, c$  and are chosen so that the principal moments of inertia have the order  $I_a < I_b < I_c$ . The rotational wave function either is unchanged (is even) or is changed (is odd) in sign by an operation that turns the molecule  $\pi$  degrees about a principal axis. Because a rotation of  $\pi$  about any two principal axes in succession is equivalent to a rotation of  $\pi$  about the third,  $\psi_r$  either must be odd with respect to two of the operations and even with respect to the third or must be even with respect to all three. There are thus two classes of functions. Those which are symmetric or even with respect to all three operations are sometimes designated  $A$  functions; those which are even with respect to one axis and odd with respect to the other two are designated  $B$  functions. Since there are three axes, it is evident that the  $B$  functions can be further divided into three subclasses:  $B_a, B_b$ , and  $B_c$  where the subscripts designate the particular principal axis of inertia  $a, b$ , or  $c$  with respect to which  $\psi_r$  is symmetric. Thus there are four species of functions. In microwave spectroscopy these functions are conventionally designated by two indices which refer to the operation  $C_2^a$  about the axis of least moment of inertia  $a$  and the operation  $C_2^c$  about the axis of greatest moment of inertia  $c$ , with the operation about  $a$  being designated first. For example, the designation  $eo$  means that  $\psi_r$  is symmetric (even) with respect to a rotation of  $\pi$  about the axis of least moment of inertia  $a$  and is antisymmetric (odd) with respect to a similar rotation about the axis of largest moment of inertia  $c$ . This function is evidently a  $B_a$  function. Similarly,  $ee \equiv A$ ,

$oo \equiv B_b$ , and  $oe \equiv B_c$ . In the  $J_{K_{-1}, K_1}$  designation of the asymmetric rotor levels, the evenness or oddness of the integral subscripts  $K_{-1}$  and  $K_1$  reveals the parity of the levels (see Chapter VII, Section 2). If  $K_{-1}$  is an odd integral, the rotational eigenfunction for the state is odd with respect to a rotation of  $\pi$  about  $a$ ; if  $K_{-1}$  is zero or an even integral, the function is even with respect to this operation. The  $K_1$  subscript has a similar relation to this operation about  $c$ . Thus a  $J_{2,5}$  level has the parity  $eo$ ; a  $J_{2,4}$  level,  $ee$ ; a  $J_{3,1}$  level,  $oo$ .

The foregoing symmetry operations  $C_2^a$ ,  $C_2^b$ ,  $C_2^c$  (with the identity operation  $E$ ), under which the asymmetric rotor functions are classified, form a symmetry group known as the Four group, see Table 7.4. The symbols  $A$ ,  $B_a$ ,  $B_b$ , and  $B_c$ , introduced to distinguish the symmetry of the functions, correspond to the designations of the symmetry species of the group.

Selection rules based on the symmetry properties of the momental ellipsoid depend on which principal axis has a component of dipole moment. These rules are described in Chapter 7. The symmetry of the rotational levels with respect to rotation of  $\pi$  about a principal axis is of importance in the determination of the parity of the overall wave function with respect to exchange of identical nuclei. It will be discussed in the section to follow.

### Effects of Nuclear Spin

For an exchange of identical nuclei the overall wave function of the molecule expressed by (3.70) must either remain unchanged or change sign or phase only. Those which remain unchanged by this operation are designated as symmetric functions and those which change sign as antisymmetric. It is found by experience that for particles having spins of zero or an integer (Bose particles) the overall functions are symmetric, and for particles having spins of half-integers (Fermi particles) the overall functions are antisymmetric with regard to an operation that exchanges the identical particles.

Selection rules based on the symmetric-antisymmetric classification are derived in a manner similar to those of (3.71). If  $\psi_i$  and  $\psi_j$  represent the overall wave function of two states  $i$  and  $j$ , the transition dipole moment between the states is

$$\mu_{ij} = \sum_F \int \psi_i \mu_F \psi_j d\tau \quad (3.73)$$

where  $F = X, Y, Z$ .

For an operator that merely exchanges two identical nuclei, the sign of  $\mu_F$  does not change, and therefore the integral will change sign unless  $\psi_i$  and  $\psi_j$  have the same symmetry. Since the definite integral cannot change sign unless it is zero, the transition moment  $\mu_{ij}$  is zero and the transition probability is also zero unless  $\psi_i$  and  $\psi_j$  have the same parity. Not only the dipole moment but all higher induced moments, quadrupole, and so on, are unchanged in sign for an operation that involves only exchange of identical nuclei. Therefore the parity selection rules based on this classification of the overall functions

are

$$\begin{array}{ccc} \text{symmetric} \leftrightarrow \text{symmetric} & & \text{antisymmetric} \leftrightarrow \text{antisymmetric} \\ & \text{symmetric} \not\leftrightarrow \text{antisymmetric} & \end{array}$$

These rules hold rigorously for all possible mechanisms of induced transitions. However, the selection rules derived on the basis of the nonvanishing of the matrix elements of the dipole moments (Chapter II, Section 6) are sufficient for most applications in microwave spectroscopy.

The presence of identical nuclei in the molecule can have important consequences in the determination of the statistical weights of energy levels and the relative intensities of rotational lines. When there is no symmetry and no nuclear hyperfine splitting, each molecular rotational level will have a degeneracy

$$g_n = (2I_1 + 1)(2I_2 + 1)(2I_3 + 1) \cdots = \prod_i (2I_i + 1) \quad (3.74)$$

where  $I_i$  represents the spin of the  $i$ th nucleus and where the product is taken over all nuclei of the molecule. With no symmetry, however, this product will cancel from the numerator and denominator in (3.63) and thus need not be considered in the calculations of population of the rotational states. Even when there is nuclear coupling which gives rise to a splitting of the rotational levels, it is more convenient to neglect the nuclear splitting in the calculation of the overall, integrated number of molecules in the rotational state and then to take account of the molecular distribution among the hyperfine levels in a separate calculation.

In certain nonlinear molecules there are symmetries that give rise to inequivalent nuclear statistical weights for different rotational levels, and hence these weights do not cancel from the formula for calculation of population of rotational levels. For such molecules the rotational partition function must be divided by a symmetry number  $\sigma$ , defined as the number of indistinguishable positions that can be achieved through simple rotation of the rigid molecule.

The reduction in  $Q$  by the factor  $\sigma$  arises from the symmetry properties of the overall wave function for the molecule which must be symmetric for an exchange of identical particles obeying the Bose-Einstein statistics (zero or integral spins) and must be antisymmetric for an exchange of particles obeying Fermi-Dirac statistics (spins of odd integral multiples of  $\frac{1}{2}$ ). In the determination of these symmetries the overall function of the molecule can be expressed as the product of (3.70). Except when the spins of the identical particles are zero, both symmetric and antisymmetric nuclear spin functions  $\psi_n$  can be chosen from combinations of those of the identical nuclei. Thus when  $I \neq 0$ , one can choose  $\psi_n$ 's that make the product  $\psi_r \psi_n$  either symmetric or antisymmetric whatever the symmetry of  $\psi_r$ . However, the number of symmetric and antisymmetric nuclear spin functions that can be thus formed are not equivalent, and the weights of the rotational levels that can be matched with them to satisfy the required overall symmetry will not be equal. When  $I=0$ , the nuclear spin functions are all symmetric, and only symmetric  $\psi$ , can be multiplied with them

to give the symmetric, overall function required for Bose particles. In this instance the odd rotational levels will be entirely missing when  $\psi_e\psi_v$  is even, and the even rotational levels will be missing when that product is odd.

Although both symmetric and antisymmetric spin functions can be chosen from combinations of the separate spin functions of the identical nuclei, not all of the possible combinations can be paired with a  $\psi_r$  to give the proper symmetry of the overall functions. If there are  $n$  such identical nuclei, there will be  $(2I+1)^n$  possible functions, but on the average only  $(2I+1)^n/\sigma$  combinations of them will form the correct overall symmetry with the  $\psi_r$  functions. Although the nuclear statistical weight factor for various rotational levels will be different in the summation of the levels for determination of  $Q_r$ , we can simply multiply each level by the averaged nuclear degeneracy  $(2I+1)^n/\sigma$ . This is completely satisfactory except for very light molecules or extremely low temperatures.

Diatomc molecules with identical nuclei have no electric dipole moment that gives rise to an observable microwave spectrum; but an important one, O<sub>2</sub>, has a magnetic spin dipole moment that gives rise to an observable microwave spectrum. It provides a simple illustration of the effects of nuclear spin statistics on the population of rotational states. Its ground electronic state  $\psi_e$  is antisymmetric for the exchange of the nuclei, and its vibrational states are symmetric. Therefore  $\psi_e\psi_v$  is odd. Because O<sub>2</sub> has a spin angular momentum, the rotational quantum number is represented by  $N$  rather than  $J$  (see Chapter IV, Section 2). The rotational wave functions are symmetric when  $N$  is even (0, 2, 4, etc.) and antisymmetric when  $N$  is odd (1, 3, 5, etc.). The nuclear spin  $I$  of <sup>16</sup>O is zero, and hence for <sup>16</sup>O<sup>16</sup>O,  $\psi_n$  is symmetric. Furthermore, the overall wave function must be symmetric for the operation which exchanges the two identical Bose particles (for a rotation of  $\pi$ ). Since the product  $\psi_e\psi_v$  is antisymmetric, it is obvious that only the  $\psi_r$  functions having odd  $N$  satisfy this condition. The rotational levels corresponding to even values of  $N$  are entirely missing. Since only half of the possible energy levels exist, it is evident that the expression for  $Q_r$  must be divided by  $\sigma=2$ .

When the spin of the identical nuclei of a diatomic molecule is not zero, all the rotational levels will be populated, but with different weights. This condition, which does not give rise to a microwave spectrum, is most simply illustrated by H<sub>2</sub>, for which  $I=\frac{1}{2}$ . Let us designate the individual spin states corresponding to  $M_I=+\frac{1}{2}$  as  $\alpha$  and those corresponding to  $M_I=-\frac{1}{2}$  as  $\beta$ . Obviously the combined spin functions  $\psi_n$  for the two-proton system corresponding to  $|\alpha\alpha\rangle$  and  $|\beta\beta\rangle$  will not change sign and therefore will be symmetric upon exchange of the identical nuclei. The combinations  $|\alpha\beta\rangle$  or  $|\beta\alpha\rangle$ , where the two proton spins differ, cannot be distinguished, and the acceptable functions are independent linear combinations:

$$\psi_s = \frac{1}{\sqrt{2}} [|\alpha\beta\rangle + |\beta\alpha\rangle] \quad (3.75)$$

$$\psi_a = \frac{1}{\sqrt{2}} [|\alpha\beta\rangle - |\beta\alpha\rangle] \quad (3.76)$$

The first of these is symmetric under proton exchange, and the second is antisymmetric. There are thus three symmetric spin functions and one anti-symmetric spin function. The total spin angular momentum quantum number is  $T=1$  for the symmetric spin functions and  $T=0$  for the antisymmetric spin function. For  $H_2$ ,  $\psi_e\psi_v$  is symmetric, and  $\psi_e\psi_v\psi_r$  is symmetric for even  $J$  and antisymmetric for odd  $J$ . The overall function must be antisymmetric for the operator that exchanges the identical Fermi particles. This requirement can be met by a combination of the odd  $J$  rotational levels (odd  $\psi_e\psi_v\psi_r$ ) with the even or symmetric spin states (weight 3) or by a combination of even rotational levels (even  $\psi_e\psi_v\psi_r$ ) with the odd spin states (weight 1). Consequently, all the rotational levels occur, but the ones with  $J=1, 3, 5, \dots$  have three times the weight of those with  $J=0, 2, 4, \dots$ . The average weight of the levels  $(3+1)/2=2$  is again only one-half the total number of spin states  $(2I+1)^2=4$ .

For diatomic molecules having identical nuclei with spin  $I$ , there are  $(I+1)(2I+1)$  symmetric (even) spin functions and  $I(2I+1)$  antisymmetric (odd) spin functions. The relative weights of adjacent rotational levels will be  $I/(I+1)$ , and the average weights of the levels will be  $(2I+1)^2/2$ . The symmetry of  $\psi_e\psi_v$  and the conformity of  $I$  to Bose or Fermi statistics (as explained previously) determine whether the  $J$  even or the  $J$  odd rotational levels will have the greater weight. A summary and values of  $g$  (nuclear) are given in Table 3.2.

For determination of nuclear statistical weights in symmetric-top rotors, the rotational levels are conveniently classified under the rotational subgroup of the full point group of the molecule. This rotational subgroup is comprised of the identity operation and the rotational operations that exchange identical nuclei. The rotational subgroup for symmetric tops belonging to the point group  $C_{3v}$  is  $C_3$ , the symmetry species of which are  $A$  and  $E$  (see Table 12.1). Similarly,  $\psi_e$  and  $\psi_v$  may be classified with respect to the given rotational subgroup. Although the calculation of nuclear statistical weights in symmetric polyatomic molecules is appreciably more involved than that for diatomic molecules, nevertheless, it is based on the same principle, requiring the proper symmetry of the overall wave function. Nuclear statistical weights  $g$  (nuclear)

**Table 3.2** Symmetry of the Eigenfunctions and Nuclear Statistical Weights for Exchange of Two Identical Nuclei

Statistics	Spin $I$	Total Function $\psi$ Overall	Coordinate Function $\psi_e\psi_v\psi_r$	Spin Function $\psi_n$	Statistical Weight <sup>a</sup> $g(\text{nuclear})$
Fermi-Dirac	$\frac{1}{2}, \frac{3}{2}, \dots$	asym	sym	asym	$(2I+1)I$
Bose-Einstein	$0, 1, 2, \dots$	sym	asym	sym	$(2I+1)(I+1)$

<sup>a</sup> $g_I = g(\text{nuclear})/(2I+1)^2$ .

for the largest class of symmetrical molecules, those having  $C_{3v}$  symmetry ( $\text{NH}_3$ ,  $\text{CH}_3\text{Cl}$ ,  $\text{CH}_3\text{CCH}$ , etc.) are listed in Table 3.3. These have been obtained with group theory by Dennison [15] and by Wilson [16]. Other derivations are described in books by Townes and Schawlow [7] and by Sugden and Kenney [17]. Because of the opposite symmetry of the doubly degenerate components of the levels when  $K \neq 0$ , the same statistical weight formulas hold for either Bose or Fermi particles. However, when  $K=0$ , the weights for the different inversion levels depend on the nature of the nuclear statistics as indicated in Table 3.3. These formulas hold for symmetric vibrational and electronic states,  $\psi_e \psi_v$  even. They also hold for molecules in degenerate vibrational states with  $\psi_e$  even if  $K$  is replaced by  $K-l$ . If the inversion doubling is not resolved, the statistical weights would be the sum of those for the sublevels.

**Table 3.3** Nuclear Statistical Weights<sup>a</sup> for Symmetric-top Molecules Having  $C_{3v}$  Symmetry

Statistics	<i>J</i>	<i>K</i>	Inversion Level	Statistical Weight <i>g</i> (nuclear)
<i>When Inversion Levels Are Separated<sup>b</sup></i>				
Either	Even or odd	Not 0 and multiple of 3	Either	$\frac{1}{3}(2I+1)(4I^2+4I+3)$
Either	Even or odd	Not 0 and not multiple of 3	Either	$\frac{1}{3}(2I+1)(4I^2+4I)$
Fermi-Dirac	Even {	0	Lower	$\frac{1}{3}(2I+1)(2I-1)I$
Bose-Einstein	Odd {			
Fermi-Dirac	Even {	0	Upper	$\frac{1}{3}(2I+1)(2I+3)(I+1)$
Bose-Einstein	Odd {			
Fermi-Dirac	Odd {	0	Lower	$\frac{1}{3}(2I+1)(2I+3)(I+1)$
Bose-Einstein	Even {			
Fermi-Dirac	Odd {	0	Upper	$\frac{1}{3}(2I+1)(2I-1)I$
Bose-Einstein	Even {			
<i>When Inversion Levels Are Not Separated<sup>c</sup></i>				
Either	Even	0 or multiple of 3		$\frac{1}{3}(2I+1)(4I^2+4I+3)$
Either	Even or odd	Not multiple of 3		$\frac{1}{3}(2I+1)(4I^2+4I)$

<sup>a</sup>These statistical weights are for rotational lines of symmetric-top molecules with three off-axis atoms having nuclear spin  $I$  when the molecule is in a nondegenerate vibrational level and in  ${}^1\Sigma$  electronic state. The values apply for a degenerate vibrational level if  $K$  is replaced by  $K-l$ . The reduced statistical weight  $g_I$  is obtained from division of the  $g$  (nuclear) by the total number of spin functions  $(2I+1)^3$ .

<sup>b</sup>In (3.66),  $g_K=1$  for all  $K$ .

<sup>c</sup>In (3.66),  $g_K=1$  for  $K=0$  and  $g_K=2$  for  $K \neq 0$ .

Theoretically, the averaged nuclear statistical weight factor involved in  $Q_r$  is  $g_n/\sigma$  where  $g_n$  is the total spin degeneracy and  $\sigma$  is the symmetry number as explained previously. However, it is more convenient in numerical calculations to omit the factor  $g_n$  from the expression for  $Q_r$  and to employ a reduced nuclear statistical weight  $g_I$  in the numerator of (3.66). This reduced factor is defined as

$$g_I = \frac{g(\text{nuclear})}{g_n} \quad (3.77)$$

Values of  $g_I$  for symmetric-top molecules having  $C_{3v}$  and  $C_3$  symmetry are also given in Chapter VI.

A number of asymmetric rotors studied with microwave spectroscopy have two identical nuclei and  $C_{2v}$  symmetry. Examples are  $\text{H}_2\text{O}$  and  $\text{SO}_2$ . The identical nuclei can be exchanged and the molecule changed into an indistinguishable configuration by rotation of  $\pi$  degrees about the symmetry axis. With respect to this operation, there are  $(I+1)(2I+1)$  symmetric and  $I(2I+1)$  antisymmetric nuclear spin functions, just as for diatomic molecules. If  $\psi_e\psi_v$  is positive, the symmetric nuclear spin functions must be paired with the even rotational levels when  $I=0, 1, 2, \dots$  (Bose-Einstein statistics) and with the odd rotational levels when  $I=\frac{1}{2}, \frac{3}{2}, \frac{5}{2}, \dots$  (Fermi-Dirac statistics). Thus far the conditions are exactly those which were described for the diatomic molecule. The difference in the two cases arises not from the nuclear statistics but from the greater difficulty in determination of the parity (odd or even character) of the wave functions  $\psi$ , of the asymmetric rotor with respect to the operation which exchanges the identical nuclei. This procedure will be briefly described.

To determine the effects of nuclear statistical weights on a particular level, one must know which of the axes,  $a$ ,  $b$ , or  $c$ , is the symmetry axis and must then ascertain the parity of  $\psi$ , with respect to this axis. One then chooses the nuclear spin functions  $\psi_n$  which with the particular  $\psi$ , will give the correct symmetry for the overall wave function  $\psi$ . For illustration, let us choose a molecule with  $C_{2v}$  symmetry for which  $\psi_e\psi_v$  is even and the symmetry axis is the intermediate axis  $b$ . If spins of the two identical nuclei are zero or integrals (Bose-Einstein statistics), the overall wave function must be symmetric with respect to a rotation of  $\pi$  about the symmetry axis  $b$ . Now the level  $J_{4,5}$  will be antisymmetric (odd) with respect to this operation; since the  $\psi_e\psi_v$  is even, only the antisymmetric nuclear spin function will give the required overall symmetry (even). The nuclear statistical weight for the level will then be  $I(2I+1)$ . When  $I=0$  it is evident that the level does not occur. If the symmetry axis had been the  $a$  axis, the symmetric spin function would have been required and the weights would have been  $(I+1)(2I+1)$ . For nuclei obeying the Fermi-Dirac statistics,  $I=\frac{1}{2}, \frac{3}{2}, \dots$ , these weights would be reversed, that is, weights  $(I+1)(2I+1)$  when  $b$  is the symmetry axis and  $I(2I+1)$  when  $a$  is the symmetry axis. To obtain the corresponding reduced statistical weights, one divides these numbers by  $(2I+1)^2$ .

When there is more than one pair of equivalent nuclei, the statistical weights

can be obtained by an extension of the foregoing discussion. For a molecule such as  $\text{CH}_2\text{F}_2$ , a rotation about the twofold axis of symmetry simultaneously exchanges the two hydrogens and the two fluorines. The resultant statistics, whether Bose-Einstein or Fermi-Dirac, depends on the statistics of the individual pairs and can be obtained by consideration of the effect of exchanging each pair separately. Exchange of the two hydrogens which are fermions must change the sign of the total wave function. The same holds for the exchange of two fluorines. Therefore a simultaneous exchange of both pairs of nuclei must leave the total wave function for  $\text{CH}_2\text{F}_2$  unchanged, and the resultant statistics is Bose-Einstein statistics. On the other hand, for  $\text{CD}_2\text{F}_2$ , where deuterium is a boson, the resultant statistics is Fermi-Dirac; and the nuclear spin functions must be combined with the coordinate function in such a way as to yield a total wave function which changes sign for a rotation about the twofold axis.

For one pair of identical nuclei having spins  $I_1$  there are a total of  $(2I_1 + 1)^2$  spin functions, of which  $(I_1 + 1)(2I_1 + 1)$  are symmetric spin functions and  $I_1(2I_1 + 1)$  are antisymmetric. Likewise, the other pair of identical nuclei having spins  $I_2$  have in all  $(2I_2 + 1)^2$  spin functions, of which  $(I_2 + 1)(2I_2 + 1)$  are symmetric and  $I_2(2I_2 + 1)$  are antisymmetric. The total spin functions for the system of two pairs of identical nuclei will be product functions composed of the spin functions associated with  $I_1$  and those associated with  $I_2$ . Products composed of the symmetric spin functions of the two types of nuclei will give total spin functions which are symmetric. Similarly, products of anti-symmetric spin functions give symmetric total spin functions. There are thus for the composite system the following number of symmetric spin functions

$$\begin{aligned} g^s(\text{nuclear}) &= (I_1 + 1)(2I_1 + 1)(I_2 + 1)(2I_2 + 1) + I_1(2I_1 + 1)I_2(2I_2 + 1) \\ &= (2I_1 + 1)(2I_2 + 1)(2I_1 I_2 + I_1 + I_2 + 1) \end{aligned} \quad (3.78)$$

If the symmetric spin functions of one type of nuclei are combined with the anti-symmetric spin functions of the other, the total spin functions will be anti-symmetric. The total number of such combinations will be

$$\begin{aligned} g^a(\text{nuclear}) &= (I_1 + 1)(2I_1 + 1)I_2(2I_2 + 1) + I_1(2I_1 + 1)(I_2 + 1)(2I_2 + 1) \\ &= (2I_1 + 1)(2I_2 + 1)(2I_1 I_2 + I_1 + I_2) \end{aligned} \quad (3.79)$$

The total number of spin functions in all will be  $(2I_1 + 1)^2(2I_2 + 1)^2$ . For the case of  $\text{CH}_2\text{F}_2$  with  $\psi_e \psi_v$  even and the symmetry axis the  $b$  axis, we find from (3.78) and (3.79) that the  $ee$  and  $oo$  levels will have a statistical weight of 10 while the  $eo$  and  $oe$  levels have a statistical weight of 6.

An instructive illustration of the effects of nuclear statistics on the relative intensities of the lines of asymmetric rotors is provided by Fig. 3.5, which represents a number of lines corresponding to different  $J$  values for the  ${}^RQ_{K_{1,1}=0}$  branch of  $\text{D}_2\text{S}_2$  observed by Winnewisser et al. [18]. For the  $\text{D}^{32}\text{S}^{32}\text{SD}$  species it is readily apparent that the lines alternate in intensity in the ratio 1:2. Those for  $J$  even are the stronger set. This intensity alternation is due to the nuclear statistics of the identical D nuclei which are exchanged by a rota-

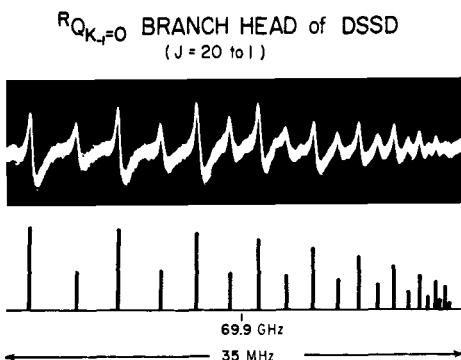


**Fig. 3.5** Illustration of the effects of nuclear statistical weights on the relative intensities of the rotational lines of the  $R_{Q_{K_1=0}}$  branch of  $D_2S_2$ . From Winnewisser, Winnewisser, and Gordy [18].

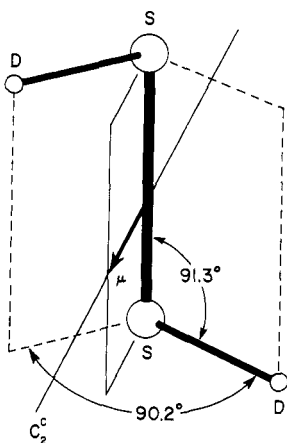


**Fig. 3.6** Structural diagram of the  $D_2S_2$  molecule.

tion of  $\pi$  degrees about the  $c$  axis, which is perpendicular to the SS bond as is indicated by Fig. 3.6. The operation  $C_2^c$  also exchanges two identical  $^{32}S$  nuclei, but because they have zero spins the resultant spin of the identical nuclei exchanged by the operation is  $I=1$ , and the overall wave function must conform to the Bose-Einstein statistics. The molecules observed are in symmetric ground electronic and ground vibrational states. Thus  $\psi_e\psi_v$  is even, and the product  $\psi_r\psi_n$  must be symmetric with respect to the operation  $C_2^c$  which rotates the molecule about the symmetry axis  $c$ . This means that only even spin functions can combine with the even  $\psi_r$ , and that only odd spin functions can combine with the odd  $\psi_r$ .

The  $D_2S_2$  molecule is an almost accidentally prolate symmetric top with  $I_b \approx I_c$ . In the symmetric-top approximation the observed transitions correspond to  $J \rightarrow J$  and  $K=0 \rightarrow 1$ . Classically, this corresponds to a rotation of the

deuteriums and the dipole moment about the SS bond. In the asymmetric-top  $J_{K_1, K_1}$  notation, the transitions are  $J_{K_1=0, K_1=J} \rightarrow J_{K_1=1, K_1=J}$ . Because the dipole moment is along  $c$ , the parity of  $K_1$  does not change, and the allowed transitions are  $eo \rightarrow oo$  and  $ee \rightarrow oe$ . The first type is between wave functions  $\psi$ , that are antisymmetric with respect to  $C_2^e$  ( $K_1$  odd), and the second is between functions that are symmetric with respect to this operation ( $K_1$  even). Also note that for the  $J_{0, K_1=J}$  levels or the  $J_{K_1=1, K_1=J}$  levels the parity of  $K_1$  is even when  $J$  is even and odd when  $J$  is odd. Thus to achieve an overall wave function that is symmetric with respect to  $C_2^e$  we must combine the symmetric nuclear spin functions, weight  $(I+1)(2I+1)=6$ , with even  $J$  levels and must combine the antisymmetric nuclear spin functions, weight  $I(2I+1)=3$ , with the odd  $J$  levels. Therefore the transitions involving levels of even  $J$  are expected to have twice the strength of the transitions involving levels of odd  $J$ , in agreement with the observations.

Substitution of  $^{34}\text{S}$  for  $^{32}\text{S}$  in one position, to form  $\text{D}^{32}\text{S}^{34}\text{SD}$ , destroys the symmetry and the alternation in the line intensities. Although  $^{34}\text{S}$ , like  $^{32}\text{S}$ , has  $I=0$ , the difference in mass causes the center of mass to shift so that the nuclei are no longer exchanged by a rotation of  $\pi$  about a principal axis. Since  $I=\frac{1}{2}$  for H, the  $\text{H}^{32}\text{S}^{32}\text{SH}$  obeys the Fermi-Dirac statistics, and the alternation of the line intensity is  $(I+1)/I=3:1$ , with those for  $J$  odd being the stronger set. This case was also observed by Winnewisser et al. [18]. Table 3.2 indicates the nuclear statistical weights for exchange of two identical nuclei of any spin value  $I$ .

## References

1. L. Pauling and E. B. Wilson, *Introduction to Quantum Mechanics*, McGraw-Hill, New York, 1935, Chap. XI.
2. P. Helminger and W. Gordy, *Bull. Am. Phys. Soc.*, **11**, 543 (1967).
3. W. V. Smith and R. R. Howard, *Phys. Rev.*, **79**, 132 (1950); C. Greenhow and W. V. Smith, *J. Chem. Phys.*, **19**, 1298 (1951).
4. H. A. Lorentz, *Proc. Amsterdam Acad.*, **8**, 591 (1906).
5. J. H. Van Vleck and V. F. Weisskopf, *Rev. Mod. Phys.*, **17**, 227 (1945). See also H. Fröhlich, *Nature*, **157**, 478 (1946).
6. P. W. Anderson, *Phys. Rev.*, **76**, 647 (1949). See also H. Margenau, *Phys. Rev.*, **76**, 1423 (1949).
7. C. H. Townes and A. L. Schawlow, *Microwave Spectroscopy*, McGraw-Hill, New York, 1955.
8. W. Gordy, W. V. Smith, and R. F. Trambarulo, *Microwave Spectroscopy*, Wiley, New York, 1953. Republication by Dover, New York, 1966.
9. G. Birnbaum, "Microwave Pressure Broadening" in *Intermolecular Forces*, J. O. Hirschfelder, Ed. (*Adv. Chem. Phys.*, **12**), Wiley, New York, 1967, pp. 487-548.
10. R. Karplus and J. Schwinger, *Phys. Rev.*, **73**, 1020 (1948).
11. R. H. Johnson and M. W. P. Strandberg, *Phys. Rev.*, **86**, 811 (1952).
12. R. Karplus, *Phys. Rev.*, **73**, 1027 (1948).
13. See Chap. 10 of [7].
14. G. Herzberg, *Infrared and Raman Spectra of Polyatomic Molecules*, Van Nostrand, New York, 1945. Chap. V.
15. D. M. Dennison, *Rev. Mod. Phys.*, **3**, 280 (1931).

16. E. B. Wilson, Jr., *J. Chem. Phys.*, **3**, 276 (1935).
17. T. M. Sugden and C. N. Kenney, *Microwave Spectroscopy of Gases*, Van Nostrand, London, 1965.
18. G. Winnewisser, M. Winnewisser, and W. Gordy, *J. Chem. Phys.*, **49**, 3465 (1968).

## Chapter IV

# DIATOMIC MOLECULES

---

1	MOLECULES WITHOUT ELECTRONIC ANGULAR MOMENTUM	71
	Gross Rotational Spectrum—Rigid Rotor Approximation	71
	Nonrigid Molecules—The Vibrating Rotor	73
	Dunham's Solution	78
	Higher-order Corrections of the Theory	80
	Applications of Dunham's Theory	81
	Observations at High Temperatures and High Frequencies	82
	Molecular Constants from High-temperature Spectroscopy	85
2	MOLECULES WITH ELECTRONIC ANGULAR MOMENTUM	90
	Hund's Coupling Cases	91
	Molecules in the $^2\Sigma$ State	94
	Molecules in $^3\Sigma$ States	98
	Molecules in $\Pi$ and $\Delta$ States	107
3	LINE INTENSITIES	117

## 1 MOLECULES WITHOUT ELECTRONIC ANGULAR MOMENTUM

### Gross Rotational Spectrum—Rigid Rotor Approximation

Most stable diatomic molecules have a  $^1\Sigma$  ground electronic state with no unbalanced electronic angular momentum. When there is no nuclear coupling, the angular momentum arises wholly from the end-over-end rotation. If small effects caused by centrifugal distortion and by interaction between vibration and rotation are neglected and if no external field is applied, the rotational spectra of these molecules are simple. To provide an understanding of the gross rotational spectra of diatomic molecules we shall first describe the rigid rotor approximation.

The Hamiltonian for the rigid rotor is given by (2.73). For diatomic, or linear polyatomic, molecules in  $^1\Sigma$  states, the principal moment of inertia about the molecular bond axis is zero, and the moments of inertia for rotation in two orthogonal planes about an axis normal to the bond are equal. Thus

$I_a=0$ , and from (2.5),  $P_z=P_a=0$ ;  $I_b=I_c=I$ , and

$$\mathcal{H}_r = \frac{1}{2I} (P_x^2 + P_y^2) = \frac{P^2}{2I} \quad (4.1)$$

Therefore, from (2.59),

$$E_J = \frac{\hbar^2}{2I} J(J+1) = hBJ(J+1) \quad (4.2)$$

With the selection rules  $\Delta J = \pm 1$  for dipole transitions (see Chapter II, Section 6), the rotational absorption lines are

$$\nu_r = \frac{E_{J+1} - E_J}{h} = 2B(J+1) \quad (4.3)$$

where  $J=0, 1, 2, \dots$  and where

$$B = \frac{h}{8\pi^2 I} \quad (4.4)$$

is the rotational spectral constant. The gross rotational spectrum then consists of a harmonic series of lines having frequencies

$$\nu = 2B, 4B, 6B, \dots \quad (4.5)$$

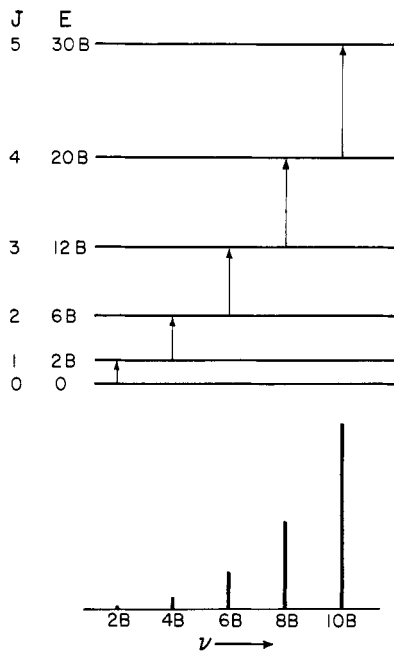


Fig. 4.1 Diagram indicating the sequence of the rotational levels and corresponding absorption lines for a diatomic molecule. This diagram also applies to linear polyatomic molecules discussed in Chapter 5.

The first few energy levels, transitions, and corresponding absorption lines are indicated in Fig. 4.1. The heights of the bars indicate the relative intensities that are assumed to increase as the cube of the frequency (see Section 3).

Note that the lowest rotational frequency corresponds to  $2B$ . Thus, if  $B$  is too large, that is,  $I$  too small, the molecule might have its rotational spectrum originating in the infrared region outside the region of observation with microwave techniques. However, all the diatomic molecules, except the lightest halogen hydride HF, for which  $v(J=0 \rightarrow 1) = 2B = 1233$  GHz or  $\lambda = 0.243$  mm, have their rotational spectra originating in the region presently observable with microwave spectroscopy. The light  $H_2$  molecule has no dipole moment and no microwave spectrum. Free radicals such as CH and OH have  $B$  values comparable to that of HF, but they have A doublet spectra (see Section 2) which can be observed at microwave frequencies. Lithium hydride has its lowest rotational frequency in the 0.68 mm wave region. The  $J=0 \rightarrow 1$  transition of LiD in the 1.2-mm wave region [1] and that of HCl in the 0.48-mm region [2] have been measured. Essentially all diatomic molecules are now accessible to microwave spectral measurements although the lighter diatomic hydrides have only one or two rotational lines falling in the microwave region.

### Nonrigid Molecules—The Vibrating Rotor

Diatomc molecules in  ${}^1\Sigma$  ground states (no electronic angular momentum) are sufficiently simple that they can be treated as distortable vibrating rotors. A wave equation can be set up and solved for their vibrational and rotational energies. The solution yields directly the effects of centrifugal distortion and of interaction between vibration and rotation, which for polyatomic molecules must be calculated with perturbation theory. To obtain such a solution, however, one must know or assume the potential function for the interaction of the two atoms. We shall give the spectral constants obtained from solution of the wave equation with the familiar Morse potential function [3] and with the Dunham potential function [4], which is a series expansion having many adjustable potential parameters. Only the essential results will be given here. Descriptions of the solution of the equations, which are rather lengthy, can be found elsewhere [4–6].

In spherical coordinates the wave equation describing the rotationvibration motion of a nonrigid diatomic molecule, without interaction of electronic angular momentum ( ${}^1\Sigma$  electronic states) and without nuclear couplings, is

$$\frac{1}{r^2} \frac{\partial}{\partial r} \left( r^2 \frac{\partial \psi}{\partial r} \right) + \frac{1}{r^2 \sin \theta} \frac{\partial}{\partial \theta} \left( \sin \theta \frac{\partial \psi}{\partial \theta} \right) + \frac{1}{r^2 \sin^2 \theta} \left( \frac{\partial^2 \psi}{\partial \phi^2} \right) + \frac{8\pi^2 \mu}{h^2} [E - U(r)] \psi = 0 \quad (4.6)$$

where the origin of the coordinate system is chosen at the center of mass and where  $r$  represents the internuclear distance. The reduced mass is

$$\mu = \frac{m_1 m_2}{m_1 + m_2} \quad (4.7)$$

where  $m_1$  and  $m_2$  are the masses of the individual atoms. With the assumption of a suitable potential function  $U(r)$ , it is possible to obtain a detailed solution of the equation and to find the eigenfunctions and the energy eigenvalues.

The most commonly used potential function is the Morse potential,

$$U(r) = \mathcal{D} [1 - e^{-a(r - r_e)}]^2 \quad (4.8)$$

where  $\mathcal{D}$  is the energy of dissociation measured from the bottom of the potential well,  $r_e$  is the equilibrium distance between the nuclei, and  $a$  is a constant. This function is represented approximately by the curve of Fig. 4.2. Solution of (4.6) with a Morse-type potential has been obtained by Morse [3] for  $J=0$  and by Pekeris [6] for higher values of  $J$ . The energy eigenvalues obtained from the solution can be expressed in the form

$$\frac{E_{v,J}}{\hbar} = \omega_e(v + \frac{1}{2}) - \omega_e x_e(v + \frac{1}{2})^2 + B_v J(J+1) - D_v J^2(J+1)^2 + H_v J^3(J+1)^3 + \dots \quad (4.9)$$

in which  $v$  represents the vibrational quantum number  $v=0, 1, 2, \dots$ ,  $J$  represents the rotational quantum number  $J=0, 1, 2, \dots$ ;  $\omega_e$  is the fundamental vibrational frequency; and  $\omega_e x_e$  is the anharmonicity constant. The vibrational transitions are not observable in the microwave region. We are concerned here with pure rotational transitions occurring within a given vibrational state and observed in absorption for which the selection rules are  $\Delta v=0$  and  $J \rightarrow J+1$ . Application of these rules with the Bohr postulate,  $h\nu=\Delta E$ , to (4.9) yields the rotational frequencies

$$\nu = 2B_v(J+1) - 4D_v(J+1)^3 + H_v(J+1)^3[(J+2)^3 - J^3] + \dots \quad (4.10)$$

$$B_v = B_e - \alpha_e(v + \frac{1}{2}) + \gamma_e(v + \frac{1}{2})^2 + \dots \quad (4.11)$$

$$D_v = D_e + \beta_e(v + \frac{1}{2}) + \dots \quad (4.12)$$

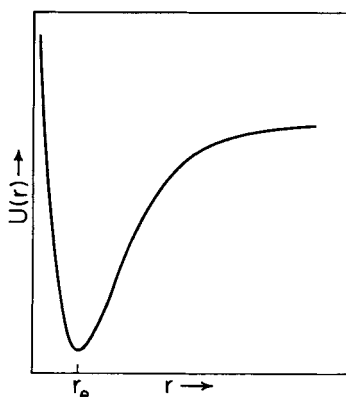


Fig. 4.2 Graph of the typical Morse potential function.

$$H_v \approx H_e = \frac{2D_e}{3\omega_e^2} (12B_e^2 - \omega_e \alpha_e) \quad (4.13)$$

The  $\alpha_e$  and  $\gamma_e$  represent rotation-vibration interaction constants. The  $\gamma_e$ , which is small as compared with the  $\alpha_e$ , can be neglected in some applications. The  $D_v$  represents the first-order centrifugal stretching term, and the term  $\beta_e(v + \frac{1}{2})$  corrects for the effects of vibration on the centrifugal stretching constant. Because the higher-order centrifugal stretching correction (the term in  $H_v$ ) is so small that its effects are barely observable in the microwave region, it is usually neglected.

For measurement of  $D_v$  for any given vibrational state, at least two rotational lines of molecules in that state must be measured. When  $H_v$  is not negligible, additional lines must be measured. For accurate measurement of  $D_v$ , one of the measured lines should be of a relatively high  $J$  transition, preferably in the shorter millimeter or submillimeter range where the centrifugal stretching effects are large. For an increase in accuracy and as a check on the consistency of the results, measurements are often made on many different transitions. An illustration is given in Table 4.1 of the use of (4.10) for evaluation of  $B_0$  and  $D_0$  for  $^{12}\text{C}^{16}\text{O}$  from precise measurements of the first seven rotational transitions of the ground vibrational state. Effects of the higher-order terms at these frequencies are too small to permit a meaningful evaluation of  $H_0$ . Note that these lowest rotational frequencies of CO fall primarily in the submillimeter wave region. Millimeter or submillimeter wave measurements on all the hydrogen halides have now been made. The resulting  $B_0$  and  $D_0$  values are listed in Table 4.2.

**Table 4.1** Rotational Frequencies and Derived Rotational Constants for  $^{12}\text{C}^{16}\text{O}$  in the Ground Vibrational State

Transition	Observed Frequency (MHz)	Calculated Frequency (MHz)	$v_{obs} - v_{calc}$ (MHz)
0→1	115,271.204 <sup>a</sup>	115,271.206	-0.002
1→2	230,537.974 <sup>b</sup>	230,538.005	-0.031
2→3	345,795.989 <sup>c</sup>	345,795.993	-0.004
3→4	461,040.811 <sup>c</sup>	461,040.764	+0.047
4→5	576,267.934 <sup>c</sup>	576,267.910	+0.024
5→6	691,472.978 <sup>c</sup>	691,473.027	-0.049
6→7	806,651.719 <sup>c</sup>	806,651.708	+0.011
<i>Derived Rotational Constants</i>			
$B_0 = 57,635.970 \pm 0.006 \text{ MHz}$			
$D_0 = 0.18358 \pm 0.00014$			

<sup>a</sup>Rosenblum et al. [9].

<sup>b</sup>M. Cowan and W. Gordy, *Bull. Am. Phys. Soc.*, **2**, 212 (1957).

<sup>c</sup>P. Helmlinger, F. C. De Lucia, and W. Gordy, *Phys. Rev. Lett.*, **25**, 1397 (1970).

**Table 4.2** Rotational Constants  $B_0$  and  $D_0$  and Equilibrium Internuclear Distances  $r_e$  for the Hydrogen Halides<sup>a</sup>

Halides	$B_0$ (MHz)	$D_0$ (MHz)	$r_e$
$^2\text{H}^{19}\text{F}$	325,584.98(30)	17.64	0.916914
$^1\text{H}^{35}\text{Cl}$	312,989.297(20)	15.863	1.2745991
$^1\text{H}^{37}\text{Cl}$	312,519.121(20)	15.788	1.2745990
$^2\text{H}^{35}\text{Cl}$	161,656.238(14)	4.196(3)	1.2745990
$^2\text{H}^{37}\text{Cl}$	161,183.122(16)	4.162(3)	1.2745998
$^3\text{H}^{35}\text{Cl}$	111,075.84	1.977	1.2745997
$^3\text{H}^{37}\text{Cl}$	110,601.62	1.960	1.2745985
$^1\text{H}^{79}\text{Br}$	250,358.51(15)	10.44(6)	1.4144691
$^1\text{H}^{81}\text{Br}$	250,280.58(15)	10.44(6)	1.4144705
$^2\text{H}^{79}\text{Br}$	127,357.639(12)	2.6529(14)	1.4144698
$^2\text{H}^{81}\text{Br}$	127,279.757(17)	2.6479(20)	1.4144698
$^3\text{H}^{79}\text{Br}$	86,251.993	1.234	1.4144705
$^3\text{H}^{81}\text{Br}$	86,174.078	1.232	1.4144691
$^1\text{H}^{127}\text{I}$	192,657.577(19)	6.203(3)	1.609018
$^2\text{H}^{127}\text{I}$	97,537.092(9)	1.578(1)	1.609018
$^3\text{H}^{127}\text{I}$	65,752.305	0.7150	1.609018

<sup>a</sup>These constants were derived by De Lucia, Helminger, and Gordy [Phys. Rev., A3, 1849 (1971)] from their submillimeter wave measurements with the aid of earlier millimeter wave measurements of the tritium halides and with some of the  $D_0$  values derived from infrared data, as cited by them. The  $r_e$  values have higher-order corrections applied (Chapter XIII, Section 6). The last three figures given for  $r_e$  have only relative significance because of the limited accuracy of Planck's constant.

If  $B_e$ ,  $\alpha_e$ , and  $\gamma_e$  are to be obtained entirely from microwave rotational spectra, measurements must be made on rotational lines in three vibrational states. Enough lines must be measured for each vibrational state so that the effects of centrifugal stretching on  $B_v$  can be determined. Normally, the ground state and the first two excited vibrational states ( $v=0, 1$ , and  $2$ ) are observed, and the corresponding rotational constants  $B_0$ ,  $B_1$ , and  $B_2$  are obtained. From (4.11) one finds that

$$\begin{aligned} B_e &= \frac{1}{8}(15B_0 - 10B_1 + 3B_2) \\ \alpha_e &= 2B_0 - 3B_1 + B_2 \\ \gamma_e &= \frac{1}{2}(B_0 - 2B_1 + B_2) \end{aligned} \quad (4.14)$$

Because of low population the second vibrational state for molecules with high  $\omega_e$  may not be observable. Then  $\gamma_e$  may be neglected, and reasonably accurate values of  $B_e$  and  $\alpha_e$  may be obtained from  $B_0$  and  $B_1$  only.

Theoretically,

$$B_e = \frac{h}{(8\pi^2 I_e)} = \frac{h}{(8\pi^2 \mu r_e^2)} \quad (4.15)$$

where  $r_e$  represents the equilibrium internuclear distance, the separation of the nuclei corresponding to the minimum on the potential energy curve (Fig. 4.2), and where  $I_e$  is the moment of inertia that the molecule would have if the nuclei actually were separated by the distance  $r_e$  with an effective reduced mass of  $\mu$ . Thus a determination of  $B_e$  from the spectral data provides an evaluation of  $r_e$ . However, one should be aware of the fact that  $B_e$  obtained as just described depends on an assumed potential function and neglects the effects caused by electronic motions and displacements. Although gross effects of electronic interaction with rotation occur only when there is an unbalanced electronic spin or orbital momentum as described in Section 2, there are slight interactions between the electronic and rotational motions even for molecules in  ${}^1\Sigma$  states. Because of unequal sharing of the bonding electrons and the distortion of the electronic clouds of each atom by the chemical bonding, the effective reduced mass is not exactly that obtained by substitution of the atomic masses of the neutral atoms into (4.7). These slight electronic effects on  $r_e$  are treated in Chapter XI, Section 7 and Chapter XIII, Section 6. Corrections for these higher-order effects were included in the calculation of the  $r_e$  values for the hydrogen halides listed in Table 4.2. As a result, the  $r_e$  values listed for the different isotopic species of the same molecule are the same, within the accuracy of the measurements. The largest effects on the interatomic distances are due to the vibrational motions and to centrifugal stretching by rotation. These effects are taken into account in the preceding theory. The determination of  $B_e$  with the assumption of a different potential function, the Dunham series function, is described later.

The equilibrium values  $B_e$ ,  $I_e$ , and  $r_e$  have the advantage of being independent of the vibrational motions, and hence  $r_e$  is independent of isotopic substitution. However, these values are purely theoretical. Because of the asymmetry in the potential curve they do not correspond to averaged values of the internuclear distance for any eigenstate. Perhaps of more real significance for the chemist are the averaged values  $I^*$  and  $\langle r \rangle$  for the ground vibrational state and for a particular isotopic species of the molecule. Evaluation of these from  $B_0$  is discussed in Chapter XIII.

The vibrational constants  $\omega_e$  and  $\omega_e x_e$  are related to the rotational constants  $B_e$ ,  $\alpha_e$ , and  $D_e$  through the auxiliary relations derived by Pekeris [6]

$$\omega_e^2 = \frac{4B_e^3}{D_e} \quad (4.16)$$

$$\omega_e x_e = B_e \left( \frac{\alpha_e \omega_e}{6B_e^2} + 1 \right)^2 \quad (4.17)$$

with the assumption of the Morse potential function. Also, this assumption leads to the prediction,

$$\mathcal{D} = \frac{\omega_e^2}{4\omega_e x_e} \quad (4.18)$$

for the dissociation energy of the molecule. Equation 4.18 provides only an approximate value of  $\mathcal{D}$ . For the lighter diatomic molecules for which  $\omega_e$

is large, the sparse population of excited vibrational states makes it difficult to obtain enough microwave data for a complete evaluation of  $B_e$ ,  $\alpha_e$ , and  $D_e$ . When this is true, (4.16) and (4.17) make possible the use of  $\omega_e$  and  $\omega_e x_e$  from vibrational spectra with microwave data on the ground vibrational state for an accurate determination of these constants. For such light molecules, the vibrational frequencies fall in the near-infrared region where  $\omega_e$  and  $\omega_e x_e$  can be measured very accurately. In contrast,  $\omega_e$  and  $\omega_e x_e$  for the heavier molecules cannot be measured very accurately with optical spectroscopy, but the smallness of  $\omega_e$  and consequently the greater population of their excited vibrational states make possible the measurements of rotational transitions in a sufficient number of vibrational states for precise evaluation of  $B_e$ ,  $\alpha_e$ , and  $D_e$  from microwave data only. Then, (4.16) and (4.17) give the vibrational frequency  $\omega_e$  and the anharmonicity constant  $\omega_e x_e$ . The values of these vibrational constants for the heavier molecules are usually more precise when measured in this manner from the rotational spectra than when measured directly in the infrared region. For such molecules, however, it is advantageous to apply the more elaborate Dunham theory, which is described next.

### Dunham's Solution

Employing the Wentzel-Kramers-Brillouin method, Dunham [4] has solved the wave equation for the diatomic molecule with the assumption of a series expansion of the potential function in the form

$$U(\xi) = a_0 \xi^2 (1 + a_1 \xi + a_2 \xi^2 + a_3 \xi^3 + \dots) + B_e J(J+1)(1 - 2\xi + 3\xi^2 - 4\xi^3 + \dots) \quad (4.19)$$

where  $\xi = (r - r_e)/r_e$  and where  $a_0, a_1, a_2, \dots$  are potential constants. The resulting expression which he obtained for the energy levels is

$$\begin{aligned} \frac{E_{vJ}}{\hbar} &= \sum_{l,m} Y_{l,m} (v + \frac{1}{2})^l J^m (J+1)^m \\ &= Y_{10}(v + \frac{1}{2}) + Y_{20}(v + \frac{1}{2})^2 + Y_{01}J(J+1) \\ &\quad + Y_{11}(v + \frac{1}{2})J(J+1) + Y_{21}(v + \frac{1}{2})^2 J(J+1) \\ &\quad + Y_{31}(v + \frac{1}{2})^3 J(J+1) + Y_{02}J^2(J+1)^2 \\ &\quad + Y_{12}(v + \frac{1}{2})J^2(J+1)^2 + Y_{03}J^3(J+1)^3 + \dots \end{aligned} \quad (4.20)$$

where the  $Y$ 's are observable constants known as Dunham's constants. Usually only five of the Dunham constants are required for a fitting of the observable microwave rotational spectra. To seven terms, the rotational frequency formula is

$$\begin{aligned} v &= 2Y_{01}(J+1) + 2Y_{11}(v + \frac{1}{2})(J+1) + 2Y_{21}(v + \frac{1}{2})^2(J+1) \\ &\quad + 2Y_{31}(v + \frac{1}{2})^3(J+1) + 4Y_{02}(J+1)^3 + 4Y_{12}(v + \frac{1}{2})(J+1)^3 \\ &\quad + Y_{03}(J+1)^3[(J+2)^3 - J^3] + \dots \end{aligned} \quad (4.21)$$

One must measure at least seven spectral lines to evaluate the seven constants, but in practice it is desirable to measure more than this and to obtain a least-

squares fitting of the formula to the measured frequency. For this task it is desirable to use a high-speed computer. The terms in  $Y_{31}$  and  $Y_{03}$  are very small and often are negligible.

With the possible exception of  $Y_{01}$ , the Dunham constants are equivalent within the accuracy of the usual microwave measurements to the more familiar constants of (4.9)–(4.13). The relationships are

$$\begin{aligned} Y_{01} &\approx B_e, & Y_{02} &= -D_e, & Y_{03} &= H_e, & Y_{11} &= -\alpha_e, & Y_{12} &= -\beta_e \\ Y_{21} &= \gamma_e, & Y_{10} &= \omega_e, & \text{and} & & Y_{20} &= -\omega_e x_e \end{aligned} \quad (4.22)$$

From a comparison of (4.11) and (4.21) it is evident that

$$B_v = Y_{01} + Y_{11}(v + \frac{1}{2}) + Y_{21}(v + \frac{1}{2})^2 + Y_{31}(v + \frac{1}{2})^3 + \dots \quad (4.23)$$

The more precise relationship of  $Y_{01}$  and  $B_e$  is

$$Y_{01} = B_e \left[ 1 + C_{01} \left( \frac{B_e^2}{\omega_e^2} \right) \right] \quad (4.24)$$

where

$$C_{01} = Y_{10}^2 \left( \frac{Y_{21}}{4Y_{01}^3} \right) + 16a_1 \left( \frac{Y_{20}}{3Y_{01}} \right) - 8a_1 - 6a_1^2 + 4a_1^3 \quad (4.25)$$

Dunham gives equations relating the various  $Y$ 's to the potential constants  $a_0$ ,  $a_1$ ,  $a_2$ , and so on. Generally, these equations are rather involved, and all need not be repeated here. The expressions most often needed are those which give the first few potential constants in terms of the  $Y$ 's that can be obtained directly from the measured spectral lines. The first four potential constants can be evaluated from

$$\begin{aligned} a_0 &= \frac{\omega_e^2}{4B_e} = \frac{B_e^2}{D_e} \approx -\frac{Y_{01}^2}{Y_{02}} \\ a_1 &= \frac{Y_{11}Y_{10}}{6Y_{01}^2} - 1 = \frac{Y_{11}}{3(-Y_{02}Y_{01})^{1/2}} - 1 \\ a_2 &= \frac{Y_{12}}{6} \left( \frac{Y_{01}}{-Y_{02}^3} \right)^{1/2} + \frac{9}{8}a_1(2+a_1) + \frac{19}{8} \\ a_3 &= -\frac{2}{15} \frac{Y_{21}}{Y_{02}} + \frac{a_2}{5} (3 + 13a_1) - \frac{a_1}{2} [4 + 3a_1(1 + a_1)] - 1 \end{aligned} \quad (4.26)$$

The vibrational constants  $Y_{10}$  and  $Y_{20}$  are not obtained directly from the rotational frequencies but can be derived with use of the relations,

$$\begin{aligned} Y_{10} &= 2 \left( \frac{B_e^3}{-Y_{02}} \right)^{1/2} \approx 2 \left( \frac{Y_{01}^3}{-Y_{02}} \right)^{1/2} \\ Y_{20} &= \frac{3}{2} B_e (a_2 - \frac{5}{4}a_1^2) \end{aligned} \quad (4.27)$$

## Higher-order Corrections of the Theory

There are three small deviations of  $Y_{01}$  from the equilibrium constant  $B_e$  which are detectable with highly precise microwave measurements for some diatomic molecules in  ${}^1\Sigma_0$  ground states. These are generally designated as  $\delta_1$ ,  $\delta_2$ , and  $\delta_3$  in the probable order of their decreasing significance. The  $\delta_3$ , called Dunham's correction, is included in Dunham theory and is calculable with (4.24). Mechanistically, it arises from an anharmonicity generated by rotation-vibration interactions. The deviations  $\delta_1$  and  $\delta_2$ , not included in Dunham's solutions, result, in principle, from the inadequacy of the Born-Oppenheimer approximation [7] employed by Dunham. Mechanistically,  $\delta_1$  may be ascribed to electron-cloud distortions and to electronic components in the total angular momentum induced by the end-over-end rotation of the molecule. These effects also give rise to the molecular rotational  $g$  factor for  ${}^1\Sigma$  molecules, and the  $\delta_1$  correction may be calculated from the experimentally measured  $g_{\text{mol}}$ , as is shown in Chapter XI, Section 7 and Chapter XIII, Section 6 (See Eq. 11.115). The deviation  $\delta_2$ , although related to  $\delta_1$ , differs from it mechanistically. The induced, second-order, electronic component in the total angular momentum (which contributes to  $\delta_1$ ) causes the rotating internuclear frame to wobble, thus inducing a slight stretching force that in diatomic molecules is along the internuclear axis. The theory for this effect, known as wobble-stretching, was first derived by Van Vleck [8] and was further developed and applied by Rosenblum et al. [9] in their early microwave spectral measurements of CO. Applications to other molecules are described in Chapter XIII, Section 6.

In summary, the precise  $B_e$  value for a diatomic molecule in a  ${}^1\Sigma$  electronic ground state is related to  $Y_{01}$  by

$$B_e = Y_{01} + \delta_1 + \delta_2 + \delta_3 \quad (4.28)$$

where  $\delta_1$  is the correction for electronic distortion and electronic angular momentum components ( $L$ -uncoupling) described in Chapter XI, Section 7,  $\delta_2$  is the wobble-stretch correction described in Chapter XIII, Section 6, and  $\delta_3$  is the Dunham correction given by (4.24). In calculation of  $\delta_1$  for diatomic molecules with (11.115),  $Y_{01}$  may be substituted for  $B_{\text{eff}}$  and  $B_e - (\delta_2 + \delta_3)$  for  $B$ . Thus, for this case (11.115) becomes

$$B_e - (\delta_2 + \delta_3) = \frac{Y_{01}}{1 + (m/M_p)g} \cong Y_{01} + \delta_1 \quad (4.29)$$

and hence

$$\delta_1 = -\left(\frac{m}{M_p}\right)g Y_{01} = -\frac{g Y_{01}}{1836} \quad (4.30)$$

There is no direct method for calculation of  $\delta_2$ , but because of its  $1/\mu^2$  dependence it may be obtained from reduced mass ratios when more than one isotopic species of the molecule is measured (See Chapter XIII, Section 6).

Because of the proportionality relationship,

$$Y_{lm} \propto \left(\frac{1}{\mu}\right)^{(l+2m)/2} \quad (4.31)$$

between spectral constants  $Y_{lm}$  and the reduced mass  $\mu = m_1 m_2 / (m_1 + m_2)$  of the molecule, the very useful relationship

$$\frac{Y_{lm}}{Y'_{lm}} = \left(\frac{\mu'}{\mu}\right)^{(l+2m)/2} \quad (4.32)$$

exists between the corresponding constants  $Y_{lm}$  and  $Y'_{lm}$  and the reduced masses  $\mu$  and  $\mu'$  of different isotopic species of the same diatomic molecule. The relationship holds to the accuracy of most microwave measurements except for  $Y_{01}$  which does not always correspond to  $B_e$  within the accuracy of the measurements. The relationship can be used for calculation of  $Y_{lm}$  values for isotopic species of low abundance for which the rotational lines cannot be measured as completely or as accurately as those of a more abundant species. When sufficient lines can be accurately measured for different isotopic species, the relationship can be used to give accurate isotopic mass ratios of atoms. In this way, precise isotopic ratios have been obtained for some of the heavier elements [10–12].

### Applications of Dunham's Theory

Successful application of Dunham's theory requires measurements on different rotational transitions in at least two, and preferably more, excited vibrational states. For an accurate evaluation of the stretching constant, molecules should be measured over a range of  $J$  values that includes some relatively high ones. It is evident that a wide frequency coverage is needed, including millimeter or even submillimeter waves, and that the required range of data is not easily obtainable for molecules with high values of  $B$  and  $\omega$ . Nevertheless, sufficient data have been obtained for useful application of Dunham's theory to the alkali halides, including the lightest of the group  ${}^6\text{LiF}$ . Table 4.3 illustrates the close fitting of the frequencies calculated with (4.21) to observed rotational lines of three vibrational states measured over a wide range of millimeter and submillimeter wave frequencies. The six Dunham constants obtained from this fitting are those listed for  ${}^6\text{LiF}$  in Table 4.4. The  $Y$  values of Table 4.4 have been used with (4.26) for calculation of the first four potential constants in the series expansion of (4.19). The resulting constants are listed in Table 4.5. With (4.19) these constants provide accurate description of the potential curve in the region where  $|r - r_e| \ll r$ . The series of (4.19) does not converge rapidly when  $|r - r_e|$  is large, and the description becomes less precise. In Table 4.4, note the accuracy of the indirectly measured vibrational constants,  $\omega_e$  and  $\omega_{ex_e}$ .

During the early years of microwave spectroscopy, the lower  $J$  rotational transitions of the mixed diatomic halides,  $\text{ClF}$ ,  $\text{BrF}$ ,  $\text{BrCl}$ ,  $\text{ICl}$ , and  $\text{IBr}$ , were measured in the centimeter wave region. These measurements provided valuable

**Table 4.3** Comparison of Observed Frequencies of  ${}^6\text{LiF}$  with Those Calculated from (4.21) with Constants from Table 4.4

Vibration <i>v</i>	Transition <i>J</i> → <i>J</i> +1	Measured Frequency <sup>a</sup> (MHz)	Calculated Frequency <sup>a</sup> (MHz)	Difference
0	0→1	89,740.46 <sup>b</sup>	89,740.47	-0.01
0	1→2	179,470.35	179,470.37	-0.02
0	2→3	269,179.18	269,179.12	0.06
0	3→4	358,856.19	358,856.16	0.03
0	4→5	448,491.07	448,490.92	0.15
0	5→6	538,072.65	538,072.83	-0.18
1	0→1	88,319.18 <sup>b</sup>	88,319.19	-0.01
1	1→2	176,627.91	176,627.92	-0.01
1	2→3	264,915.79	264,915.74	0.05
1	3→4	353,172.23	353,172.19	0.04
1	4→5	441,386.83	441,386.82	0.01
2	0→1	86,921.20 <sup>b</sup>	86,921.20	0.00
2	1→2	173,832.04	173,832.06	-0.02
2	2→3	260,722.24	260,722.23	0.01
2	3→4	347,581.39	347,581.38	0.01
3	1→2	171,082.27	171,082.26	0.01
3	2→3	256,597.84	256,597.82	0.02
3	3→4	342,082.66	342,082.71	-0.05

<sup>a</sup>All measured frequencies (except those indicated by *b*) and all calculated frequencies are taken from Pearson and Gordy [1].

<sup>b</sup>L. Wharton, W. Klemperer, L. P. Gold, J. J. Gallagher, and V. E. Derr, *J. Chem. Phys.*, **38**, 1203 (1963).

information about nuclear coupling, but the transitions measured were insufficient to permit accurate evaluation of  $B_e$ ,  $r_e$ , and other molecular constants. In 1980, Willis and Clark [13] measured the higher millimeter wave rotational transitions of the entire group in excited as well as ground vibrational states. Some of the halides were heated to temperatures of several hundred degrees to populate the higher vibrational states. The spectral constants obtained for the different isotopic species appear in the various tables of the paper. The molecular constants obtained, in addition to the Dunham  $Y$ 's, include accurate Dunham potential constants,  $a_0$ ,  $a_1$ ,  $a_2$ ,  $a_3$ , and  $r_e$  values for the entire group. References to the earlier microwave papers on these molecules may also be found in their paper. Tabulation of the earlier measurements of frequencies and the constants derived from them are given by Lovas and Tiemann [14].

#### Observations at High Temperatures and High Frequencies

The development of high-temperature cells for microwave spectroscopy has made possible the study of many diatomic molecules which have too low

**Table 4.4** Observed and Derived Molecular Constants of Lithium Fluoride<sup>a</sup>

Constants	${}^6\text{Li}{}^{19}\text{F}$	${}^7\text{Li}{}^{19}\text{F}$
<i>Observed</i>		
$Y_{01} (\approx B_e)$ MHz	45,230.848(13)	40,329.808(14)
$Y_{11} (= -\alpha_e)$ MHz	-722.417(28)	-608.182(29)
$Y_{21} (= \gamma_e)$ MHz	5.918(16)	4.670(17)
$Y_{31} (= \delta_e)$ MHz	-0.212(28)	-0.0104(28)
$Y_{02} (= -D_e)$ kHz	-442.95(16)	-352.36(17)
$Y_{12} (= -\beta_e)$ kHz	4.81(12)	3.73(9)
<i>Derived</i>		
$\omega_e \text{ cm}^{-1}$	964.24(18)	910.25(22)
$\omega_e \chi_e \text{ cm}^{-1}$	9.136(45)	8.104(42)
$B_e$ MHz	45,230.556	40,329.768
$r_e \text{ \AA}$	1.563857(21)	1.563857(21)
$a_0 \text{ cm}^{-1}$	154,053(57)	153,976(74)
$a_1 \text{ cm}^{-1}$	-2.70127(38)	-2.70062(49)
$a_2 \text{ cm}^{-1}$	5.084(17)	5.101(18)
$a_3 \text{ cm}^{-1}$	-7.85(15)	-7.98(15)

<sup>a</sup>Pearson and Gordy [1].**Table 4.5** Molecular Constants of Lithium and Sodium Hydroxides

Constants	${}^6\text{LiD}^a$	${}^7\text{LiD}^a$	$\text{NaH}^b$	$\text{NaD}^b$
$Y_{01}$ (MHz)	131,615.07(4)	126,905.36(4)	146,999.10(30)	76,659.59(20)
$Y_{11}$ (MHz)	-2,898.90(4)	-2,744.61(4)	-4,108.99(80)	-1,546.94(40)
$Y_{21}$ (MHz)			32.83(50)	8.76(20)
$Y_{31}$ (MHz)			-0.96(7)	-0.16(4)
$Y_{02}$ (MHz)			-10.307(20)	-2.802(6)
$B_e$ (MHz)	131,673(4)	126,961(4)	147,076(10)	76,680(2)
$r_e$ ( $\text{\AA}$ )		1.59490(2)		1.88654(10)

<sup>a</sup>From Pearson and Gordy [1].<sup>b</sup>From Sastry et al. [32].

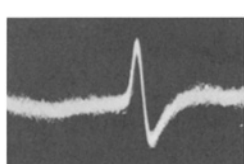
a vapor pressure for observation at room temperature. Even the light diatomic molecule LiD must be heated to a temperature of a few hundred degrees C before it has a vapor pressure adequate for microwave measurements. The earliest high-temperature microwave spectrometer, developed by Townes and his co-workers [15], operated at centimeter wavelengths and employed a waveguide cell heated to the desired temperature. A number of spectrometers have

since been constructed with heated Stark modulation cells which operate very effectively in the centimeter and upper millimeter wave regions. Particularly noteworthy is the work of Lide [16] and his co-workers at the Bureau of Standards, also that by Fitzky [17], Törring [18], and Hoeft [19] in Germany. High-temperature spectrometers of great convenience and effectiveness have been developed for the shorter millimeter and submillimeter wavelengths [20–27].

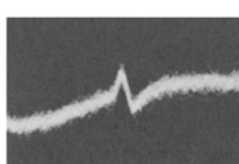
Many of the nonvolatile substances now being studied cannot be observed simply by vaporization of the substance in a hot cell, as was done for the alkali halides [15, 20, 21]. At the elevated temperatures required for evaporation, the molecules usually dissociate, if not completely, so much that the products of dissociation prevent detection of the much lower concentrations of the undisassociated molecules. Special techniques have been developed for production of the molecules in the vapor state by reactions that occur within the absorption cell. An example of these techniques is the flowing of halide gas over hot chips of copper metal to produce the copper halides [28]. Measurable SiO vapor was produced by the heating of homogeneous mixtures of silicon dioxide to 1350°C directly within the absorption cell [10]. In the hot cell developed in the laboratory of M. Winnewisser at Giessen [23, 24], the metal atoms are vaporized into the microwave absorption chamber where they interact with flowing gases to produce the desired product such as BaO [29] or BaS [25].

The advantage of the higher frequencies for high-temperature spectroscopy lies partly in the greater ease with which short waves can be focused with horns and lenses. This, in turn, makes practical the use of free-space cells in which the molecules are simply vaporized into, or across, the path of the focused radiation. A further advantage comes from the rapid increase of absorption of the molecule with increase of frequency, which makes possible the use of a much shorter absorbing path. Fig. 4.3, showing the spectra of  ${}^6\text{LiF}$ , illustrates the detection and display of absorption lines at high temperature in the submillimeter wave region. These spectra were obtained when the submillimeter waves were simply focused with horns and lenses through the central region of a cylindrical, stainless steel pipe, the central region of which was heated to vaporize the salt. Usually the rotational transitions observed in the millimeter and submillimeter wave regions are of such high  $J$  that the nuclear hyperfine structure treated in Chapter IX is not resolvable.

$v = 0$



$v = 1$



$v = 2$

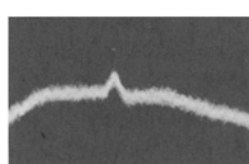


Fig. 4.3 Cathode ray display of submillimeter wave rotational lines of  ${}^6\text{LiF}$  observed at a temperature of 950°K. The lines represent the  $J=3 \rightarrow 4$  transition at  $\lambda=0.85$  in different vibrational states as indicated. The line widths are approximately 1.6 MHz. From Pearson and Gordy [1].

## Molecular Constants from High-temperature Spectroscopy

Many diatomic molecules in  ${}^1\Sigma$  ground states have been studied with microwave rotational spectroscopy at high temperatures. These include the light molecules LiD and NaH and many heavier ones such as AgCl, TiCl, PbO, and GeS. The different isotopic species were measured for most of them. From these measurements were evaluated such molecular properties as moments of inertia, internuclear distances, fundamental vibrational frequencies, anharmonicities, potential constants, centrifugal distortion constants, molecular dipole moments, and nuclear quadrupole couplings. Although not all such quantities were evaluated for all the molecules studied, the moments of inertia and internuclear distances were obtained for each one. The dipole moments and nuclear couplings of some of these molecules will be treated in later chapters. Also, the evaluation of the internuclear distances will be described in Chapter XIII.

Probably the most comprehensive investigations are those made on the alkali halides, the first group of molecules to be observed at high temperatures with microwave spectroscopy [15]. Measurements on these molecules have been extended into the millimeter and submillimeter regions with spectrometers designed to reduce the excessive pressure and Doppler broadening at the elevated temperatures required for vaporization of these halides. By application of Dunham's theory, vibrational as well as rotational constants, internuclear distances, and potential constants were obtained. As an illustration, the constants for LiF are given in Table 4.4. Those for the other alkali halides may be found in the literature [21, 22, 30, 31].

Although the rotational transitions of LiD were measured [1] with molecules produced by vaporization of solid lithium deuteride in a hot cell, early effort to observe the heavier alkali hydrides in this way failed, apparently because of rapid dissociation of the molecules at the high temperature required for their vaporization. Sastry et al. [32] have now succeeded in measuring sharp lines of NaH and NaD by producing the molecules directly in the microwave absorption cell from flowing hydrogen gas and sodium vapor that were caused to react by a glow discharge. The important molecular constants they obtained are listed in Table 4.5, together with those previously measured for LiD. Higher-order corrections (earlier in Section 1) were applied for determination of  $r_e$  and  $B_e$  values.

Thorough studies of the diatomic halides of silver, copper, aluminum, and bismuth have now been made. Some of the molecular constants derived from these measurements are listed in Table 4.6. Other constants may be obtained from the original sources cited in the table. At the temperatures required for vaporization of these substances, excited vibrational levels are significantly populated. This makes possible the measurement of rotational transitions for several vibrational states and accurate evaluation of the rotation-vibration interactions, the vibrational frequencies, and the anharmonic constants. Note that  $\omega_e$  for these molecules is obtained to 5 or 6 significant figures and  $\omega_{ex_e}$  to 3 or 4 figures. As an example, the rotational structure of 14 vibrational states was measured for aluminum iodide [33].

**Table 4.6** Selected Molecular Constants of Diatomic Halides of Silver, Copper, Aluminum, and Bismuth

Diatomc Halide	$Y_{01} \approx B_e$ (MHz)	$\omega_e$ (cm $^{-1}$ )	$\omega_e \chi_e$ (cm $^{-1}$ )	$r_e$ (Å)	Ref.
$^{107}\text{Ag}^{19}\text{F}$	7,965.545(9)	514.6(111)	2.95(9)	1.983171(23)	<sup>a</sup>
$^{107}\text{Ag}^{35}\text{Cl}$	3,686.9639(6)	353.52(4)	1.169(3)	2.28078(31)	<sup>b,c,d</sup>
$^{107}\text{Ag}^{79}\text{Br}$	1,943.6420(15)			2.393100(3)	<sup>d,e</sup>
$^{107}\text{Ag}^{127}\text{I}$	1,345.1103(25)			2.544611(3)	<sup>d</sup>
$^{63}\text{Cu}^{19}\text{F}$	11,374.214(20)	622.65	3.95	1.744923(20)	<sup>a</sup>
$^{63}\text{Cu}^{35}\text{Cl}$	5,343.768(20)	417.599(42)	1.617(6)	2.051177(8)	<sup>f</sup>
$^{63}\text{Cu}^{79}\text{Br}$	3,055.707(16)	314.816(12)	0.955(1)	2.173435(6)	<sup>g</sup>
$^{63}\text{Cu}^{127}\text{I}$	2,197.102(2)	264.897(18)	0.715(2)	2.338317(2)	<sup>h</sup>
$^{27}\text{Al}^{19}\text{F}$	16,562.930(6)	802.85(25)	4.86(6)	1.65436(2)	<sup>i,j,k</sup>
$^{27}\text{Al}^{35}\text{Cl}$	7,313.206(4)	481.67(14)	2.07(4)	2.13011(3)	<sup>i,j,k</sup>
$^{27}\text{Al}^{79}\text{Br}$	4,772.825(2)	378.19(6)	1.327(9)	2.2980(3)	<sup>l</sup>
$^{27}\text{Al}^{127}\text{I}$	3,528.5533(8)	316.25(2)	0.981(2)	2.53709(3)	<sup>l</sup>
$^{209}\text{Bi}^{35}\text{Cl}$	2,761.8538(13)	308.18	1.09	2.47155(7)	<sup>m</sup>
$^{209}\text{Bi}^{79}\text{Br}$	1,295.5609(12)	209.62	0.52	2.60953(7)	<sup>n</sup>
$^{209}\text{Bi}^{127}\text{I}$	816.11943(13)	164.12	0.321	2.80053(8)	<sup>o</sup>

<sup>a</sup>F. J. Hoeft, F. J. Lovas, E. Tiemann, and T. Törring, *Z. Naturforsch.*, **25a**, 35 (1970).<sup>b</sup>Pearson and Gordy [22].<sup>c</sup>L. C. Krisher and W. G. Norris, *J. Chem. Phys.*, **44**, 391 (1966).<sup>d</sup>J. Hoeft, F. J. Lovas, E. Tiemann, and T. Törring, *Z. Naturforsch.*, **26a**, 240 (1971).<sup>e</sup>L. C. Krisher and W. G. Norris, *J. Chem. Phys.*, **44**, 974 (1966).<sup>f</sup>Manson et al. [28].<sup>g</sup>E. L. Manson, F. C. De Lucia, and W. Gordy, *J. Chem. Phys.*, **63**, 2724 (1975).<sup>h</sup>E. L. Manson, F. C. De Lucia, and W. Gordy, *J. Chem. Phys.*, **62**, 4796 (1975).<sup>i</sup>F. C. Wyse, W. Gordy, and E. F. Pearson, *J. Chem. Phys.*, **52**, 3887 (1970).<sup>j</sup>J. Hoeft, F. J. Lovas, E. Tiemann, and T. Törring, *Z. Naturforsch.*, **25a**, 1029 (1970).<sup>k</sup>D. R. Lide, *J. Chem. Phys.*, **38**, 2027 (1963); **42**, 1013 (1965).<sup>l</sup>Wyse and Gordy [33].<sup>m</sup>Kuijpers et al. [27].<sup>n</sup>P. Kuijpers and A. Dymanus, *Chem. Phys. Lett.*, **39**, 217 (1976).<sup>o</sup>Kuijpers et al. [26].

Microwave spectra of the alkaline earth oxides, CaO, SrO, and BaO, likewise the sulfide BaS, have been observed. For each of them, numerous rotational transitions of several vibrational states were measured in the millimeter wave range. An example of the observed spectra, that for BaS, is shown in Fig. 4.4 (on page 90). Accurate values of the molecular constants were obtained, some of which are listed in Table 4.7.

Pure rotational spectra of a large number of diatomic molecules formed by combinations of elements of Group IV with elements of Group VI have been

measured for several vibrational states. All these substances, except those formed with carbon, are solids at room temperature and require elevated temperature for production of measurable vapors. Some of the molecular constants obtained are listed in Table 4.8 with references to the original sources, from which more complete results may be learned. Note that all of the very heavy lead group, PbO, PbS, PbSe, and PbTe, have been measured. It is of interest that maser emission lines corresponding to the first three rotational transitions of SiO in the first excited vibrational state,  $v=1$ , and the  $J=1 \rightarrow 0$  transition in the  $v=2$  state have been observed in a large number of astronomical sources [34]. Laboratory measurements aided in the identification of these interstellar lines. Rotational lines of the related molecule CO have also been detected [35] from interstellar sources.

The interesting diatomic molecule PN, first observed with optical spectroscopy [36] in 1933, was not measured with microwave spectroscopy [37, 38] until 1972, following its observation in the  $J=1$  rotational state with molecular beam electric resonance (MBER) [39] in 1971. Millimeter wave rotational transitions were measured [37] for the ground state and for four excited vibrational states at temperatures of approximately 800°C. The MBER measurements yielded accurate hyperfine coupling constants and the precise dipole moment, 2.7471 D. The millimeter wave measurement yielded accurate Dunham  $Y$ 's, potential constants  $a_0, a_1, a_2, a_3$ , and the equilibrium values  $B_e = 23,578.34(8)$  MHz and  $r_e = 1.49086(2)$  Å.

**Table 4.7** Molecular Constants of Some Alkaline Earth Oxides and Sulfides

Constants	$^{40}\text{Ca}^{16}\text{O}^a$	$^{88}\text{Sr}^{16}\text{O}^b$	$^{138}\text{Ba}^{16}\text{O}^{b,c}$	$^{138}\text{Ba}^{32}\text{S}^{d,e}$
<i>Observed</i>				
$Y_{01}$ (MHz)	13,324.3578(32)	10,132.5841(16)	9,371.9403(12)	3,097.28216(26)
$Y_{11}$ (MHz)	-99.3110(28)	-65.8012(26)	-41.7482(21)	-9.44620(33)
$Y_{21}$ (MHz)			-0.12522(60)	-0.013323(66)
$Y_{02}$ (kHz)	-19.623(33)	-10.848(11)	-8.1555(68)	-0.918568(63)
$Y_{12}$ (kHz)	-0.203(30)	-0.108(19)	-0.024(10)	0.001554(93)
<i>Derived</i>				
$\omega_e(\text{cm}^{-1})$	732.48(62)	653.30(33)	670.24(28)	379.42
$\omega_e\chi_e(\text{cm}^{-1})$	4.71(14)	3.74(14)	2.26(10)	0.8710
$r_e(\text{\AA})$	1.822203(68)	1.919809(95)	1.939630(7)	2.5073184(15)

<sup>a</sup>R. A. Creswell, W. H. Hocking, and E. F. Pearson, *Chem. Phys. Lett.*, **48**, 369 (1977).

<sup>b</sup>Hocking et al. [29].

<sup>c</sup>J. Hoefl, F. J. Lovas, E. Tiemann, and T. Törring, *Z. Naturforsch.*, **25a**, 1750 (1970).

<sup>d</sup>Helms et al. [25].

<sup>e</sup>E. Tiemann, C. Ryzlewicz, and T. Törring, *Z. Naturforsch.*, **31a**, 128 (1976).

**Table 4.8** Selected Molecular Constants of Diatomic Molecules Formed by Si, Ge, Sn, and Pb with O, S, Se, and Te

<i>Diatomict Molecules</i>	$Y_{01}(\cong B_e)(MHz)$	$Y_{11}(MHz)$	$-Y_{02}(kHz)$	$\omega_e(cm^{-1})$	$\omega_e\chi_e(cm^{-1})$	$r_e(\text{\AA})$	<i>Ref</i>
$^{28}\text{Si}^{16}\text{O}$	21,787.453(11)	151.026(11)	29.38(13)	1252(3)	5.96(71)	1.50973(4)	<sup>a,b</sup>
$^{28}\text{Si}^{32}\text{S}$	9,099.5365(12)	44.1616(11)	5.997(59)			1.929320(57)	<sup>c,d</sup>
$^{28}\text{Si}^{80}\text{Se}$	5,756.365(11)	23.286(10)	2.524			2.058326(60)	<sup>e</sup>
$^{74}\text{Ge}^{16}\text{O}$	14,560.872(16)	92.306(27)				1.624647(5)	<sup>f,g</sup>
$^{74}\text{Ge}^{32}\text{S}$	5,593.1019(22)	22.4569(19)	2.41(11)	569(13)	1.723(53)	2.0120772(12)	<sup>h</sup>
$^{74}\text{Ge}^{80}\text{Se}$	2,888.218(3)	8.669(2)	0.60(6)			2.134632(63)	<sup>i</sup>
$^{74}\text{Ge}^{130}\text{Te}$	1,958.7903(15)	5.1702(12)	0.353(33)	308(15)	0.62(4)	2.3401556(26)	<sup>j</sup>
$^{120}\text{Sn}^{16}\text{O}$	10,664.189(17)	64.243(37)	7.98(2)	882	3.93	1.832198(38)	<sup>k</sup>
$^{120}\text{Sn}^{32}\text{S}$	4,103.0013(12)	15.1585(17)	1.272(32)	491.6(63)	1.412(25)	2.2090172(7)	<sup>l</sup>
$^{120}\text{Sn}^{80}\text{Se}$	1,948.584(5)	5.111(5)	0.33(8)			2.325603(70)	<sup>m</sup>
$^{120}\text{Sn}^{130}\text{Te}$	1,273.4936(10)	2.8609(10)	0.165(10)	237.6(75)	0.408(17)	2.5228035(28)	<sup>n</sup>
$^{208}\text{Pb}^{16}\text{O}$	9,212.791(12)	57.405(14)				1.921813(60)	<sup>o</sup>
$^{208}\text{Pb}^{32}\text{S}$	3,487.1435(24)	13.0373(52)	1.012(27)	431.8(58)	1.277(24)	2.2868535(13)	<sup>l</sup>
$^{208}\text{Pb}^{80}\text{Se}$	1,516.9358(19)	3.8952(15)	0.210(19)	272.3(50)	0.552(14)	2.402223(32)	<sup>p</sup>
$^{208}\text{Pb}^{130}\text{Te}$	938.5824(18)	2.02160(72)	0.080(16)	214(22)	0.374(55)	2.594969(13)	<sup>q</sup>

<sup>a</sup>T. Töring, *Z. Naturforsch.*, **23a**, 777 (1968).

<sup>b</sup>Manson et al. [10].

<sup>c</sup>E. Tiemann, E. F. Renwanz, J. Hoeft, and T. Töring, *Z. Naturforsch.*, **27a**, 1566 (1972).

<sup>d</sup>J. Hoeft, *Z. Naturforsch.*, **20a**, 1327 (1965).

<sup>e</sup>J. Hoeft, *Z. Naturforsch.*, **20a**, 1122 (1965).

<sup>f</sup>R. Honerjager and R. Tischer, *Z. Naturforsch.*, **28a**, 1374 (1973).

<sup>g</sup>T. Töring, *Z. Naturforsch.*, **21a**, 287 (1966).

<sup>h</sup>J. Hoeft, F. J. Lovas, E. Tiemann, R. Tischer, and T. Töring, *Z. Naturforsch.*, **24a**, 1217 (1969).

<sup>i</sup>J. Hoeft, *Z. Naturforsch.*, **21a**, 1240 (1966).

<sup>j</sup>J. Hoeft and H.-P. Nolting, *Z. Naturforsch.*, **22a**, 1121 (1967).

<sup>k</sup>T. Töring, *Z. Naturforsch.*, **22a**, 1234 (1967).

<sup>l</sup>Hoeft et al. [11].

<sup>m</sup>J. Hoeft, *Z. Naturforsch.*, **21a**, 437 (1966).

<sup>n</sup>J. Hoeft and E. Tiemann, *Z. Naturforsch.*, **23a**, 1034 (1968).

<sup>o</sup>Töring [18].

<sup>p</sup>J. Hoeft and K. Manns, *Z. Naturforsch.*, **21a**, 1884 (1966).

<sup>q</sup>Tiemann et al. [12].

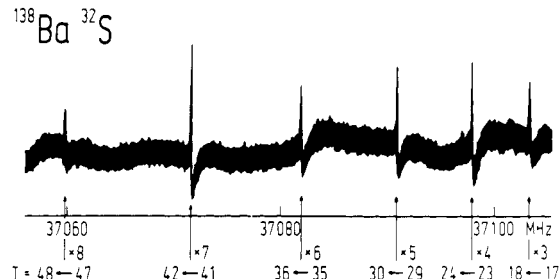


**Fig. 4.4** Video oscilloscope display of a sequence of rotational transitions in  $^{138}\text{Ba}^{32}\text{S}$ . The third through the eighth harmonic of the klystron fundamental are shown covering simultaneously portions of the spectrum between 110 and 297 GHz. From Helms, Winnewisser and Winnewisser [25].

## 2 MOLECULES WITH ELECTRONIC ANGULAR MOMENTUM

Because of the interaction of the electronic angular momentum with the molecular rotation, molecules having unbalanced electronic angular spin or orbital momentum cannot be treated with the theory presented in Section 1. The nature of the microwave spectra of such molecules depends on the type of electronic state and upon the degree of coupling among the various angular momentum vectors (electronic spin, orbital angular momentum, and molecular end-over-end rotation). There are only a few stable diatomic molecules with unbalanced angular momentum, but with the microwave techniques now available the spectra of a number of unstable diatomic radicals such as CH and CN may be observable in the microwave region. The unstable species OH and OD have been successfully investigated, as have the moderately unstable molecules NO, SO, and ClO. A number of others have been observed with paramagnetic resonance, as described in Chapter XI.

If a diatomic molecule has orbital electronic angular momentum  $L \neq 0$ , this will be coupled strongly to the internuclear axis by the electrical forces of the chemical bond. As a result, the  $\mathbf{L}$  vector will not be fixed in space but will precess rapidly about the internuclear axis. Thus  $\mathbf{L}$  itself is not a constant of the motion and is not defined as it is in free atoms. However, the components of the orbital angular momentum are resolved along the bond axis and have definite quantized values. The electrical forces of the bond can be regarded as giving rise to a strong internal Stark effect which lifts the  $L$  degeneracy and resolves the components  $M_L$  along the bond axis. Because this is a second-order effect, the states corresponding to  $+M_L$  and  $-M_L$  are degenerate, and only the magnitude of  $M_L$  is required in labeling the states of different energy. Conventionally, the magnitudes are designated by  $\Lambda$  and have the values

$$\Lambda = |M_L| = 0, 1, 2, \dots, L \quad (4.33)$$

Molecules for which  $\Lambda = 0$  have  $\Sigma$  states; those for which  $\Lambda = 1$  have  $\Pi$  states; those for which  $\Lambda = 2$  have  $\Delta$  states, and so on.

Electrical forces do not couple directly to the resultant electronic spin angular momentum  $\mathbf{S}$  since its associated moment is a purely magnetic dipole, but when  $\Lambda \neq 0$ , the magnetic field generated by the orbital motion which is directed along the bond axis will interact with the spin magnetic moment and, in the absence of other magnetic fields such as that generated by molecular rotation, will resolve it into quantized components along the bond axis. This internal "Zeeman" splitting of the  $S$  levels is a first-order effect, and the levels corresponding to the plus and minus components are not degenerate, as are those of  $L$ . The components of  $S$  along the axis, in units of  $\hbar$ , are designated by  $\Sigma$  (not to be confused with the  $\Sigma$  state), the possible values of which are

$$\Sigma = S, S - 1, \dots, -S \quad (4.34)$$

When  $\Lambda = 0$ ,  $\Sigma$  is not defined. The resultant angular momentum along the molecular axis (in units of  $\hbar$ ) is

$$\Omega = |\Lambda + \Sigma| \quad (4.35)$$

where  $\Omega$  is the quantum number of the total electronic angular momentum for the nonrotating molecule corresponding to the quantum number  $J$  for the atom. Even when there is molecular rotation,  $\Omega$  is still defined in some molecules.

Conventionally,  $J$  is used for designation of the quantum number for the total angular momentum of the molecule (or of the free atom) exclusive of nuclear spin. When there is nuclear coupling, the total angular momentum including nuclear spin is designated by  $\mathbf{F}$ . Thus for an atom,  $\mathbf{J} = \mathbf{L} + \mathbf{S}$ ; but for a molecule,  $\mathbf{J}$  represents the sum of the electronic angular momentum and the angular momentum for the end-over-end rotation of the molecule, which is designated by  $\mathbf{O}$ . When the molecule has no electronic angular momentum—when in the  ${}^1\Sigma$  state— $J = O$ , and only the quantum number  $J$  is required. The symbol  $\mathbf{N}$  is used to designate the angular momentum exclusive of spin, that is,  $\mathbf{N} = \Lambda + \mathbf{O}$ .

As we have observed, the term symbols  $\Sigma$ ,  $\Pi$ ,  $\Delta$ ,  $\Phi$ , and so on, are employed to denote, respectively, the value of  $\Lambda = 0, 1, 2, 3, \dots$ . To this is added as a left superscript the multiplicity  $2S + 1$  and as a right subscript the value of  $\Lambda + \Sigma$ . Note that  $\Lambda + \Sigma$  may be negative in comparison to  $\Omega$ . For  $\Lambda = 1, S = 1$ , we have the states  ${}^3\Pi_0, {}^3\Pi_1, {}^3\Pi_2$ .

### Hund's Coupling Cases

#### CASE (a)

When  $\Lambda \neq 0$  and the magnetic field generated by the rotation is not large,  $\mathbf{S}$  as well as  $\mathbf{L}$  is resolved along the molecular axis, and  $\Omega$  is a good quantum number even when  $O \neq 0$ . Then  $\mathbf{O}$  and  $\Omega$  form a resultant  $\mathbf{J}$ , as indicated in the vector diagram of Fig. 4.5. This condition of coupling in which both  $\mathbf{L}$  and  $\mathbf{S}$  are resolved along the molecular axis in the presence of rotation, is known as Hund's case (a).

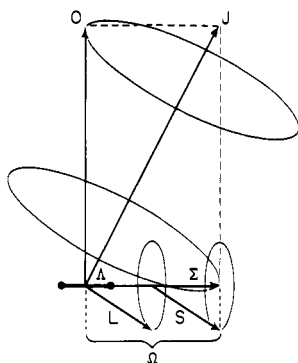


Fig. 4.5 Vector diagram of coupling for Hund's case (a).

It is evident from the vector diagram that for this case the molecular axis will precess about the direction of  $\mathbf{J}$ , as does the symmetry axis  $z$  for the polyatomic symmetric-top molecule (Chapter V). Indeed, the eigenvalues for the rotational energy can be found by the same methods as those for the symmetric top: let  $I_a$  be the moment of inertia associated with the orbital angular momentum about the bond axis, and let  $I_b$  be the moment of inertia for rotation about an axis normal to the bond. The rotational Hamiltonian will then be

$$\mathcal{H}_r = \frac{1}{2} \left( \frac{\mathbf{O}^2}{I_b} + \frac{\boldsymbol{\Omega}^2}{I_a} \right) \quad (4.36)$$

However, from the vector diagram, Fig. 4.5,

$$\mathbf{O}^2 = \mathbf{J}^2 - \boldsymbol{\Omega}^2 \quad (4.37)$$

Hence,

$$\mathcal{H}_r = \frac{1}{2} \left[ \frac{\mathbf{J}^2}{I_b} + \boldsymbol{\Omega}^2 \left( \frac{1}{I_a} - \frac{1}{I_b} \right) \right] \quad (5.38)$$

Thus  $\mathcal{H}_r$  is diagonal in the representation in which  $\mathbf{J}^2$  and  $\boldsymbol{\Omega}^2$  are diagonal. Therefore,

$$\begin{aligned} E_{J,\Omega} &= \frac{\hbar^2}{2} \left[ \frac{J(J+1)}{I_b} + \boldsymbol{\Omega}^2 \left( \frac{1}{I_a} - \frac{1}{I_b} \right) \right] \\ &= \hbar [B_v J(J+1) + \Omega^2 (A - B)] \end{aligned} \quad (4.39)$$

where

$$J = \Omega, \Omega + 1, \Omega + 2, \dots \quad (4.40)$$

Thus values of  $J$  begin with  $\Omega$ , and levels for  $J < \Omega$  do not occur.

The selection rules for dipole-induced transitions are

$$\Delta J = 0, \pm 1, \quad \Delta \Omega = 0, \pm 1 \quad (4.41)$$

However, those transitions corresponding to a change in the electronic quantum number  $\Delta\Omega = \pm 1$  represent such large changes in energy that the frequencies do not fall in the microwave region. The transitions that give rise to observable microwave absorption frequencies are therefore

$$\Delta J = 1, \quad \Delta\Omega = 0 \quad (4.42)$$

The corresponding frequencies are

$$v = 2B_v(J+1) \quad (4.43)$$

This formula is the same as that obtained for the rigid diatomic molecule or the linear polyatomic molecule without electronic angular momentum. Superficially, the electronic motions appear to have no effect on the frequencies, but this is not true. The values of the quantum number  $J$  are no longer restricted to integral values beginning with zero. The lowest value of  $J$  is not zero but  $\Omega$ ; and when  $\Omega$  is a half-integral,  $J$  is also a half-integral.

Equation 4.43 applies only to the idealized coupling case (a), which never holds strictly. There are noticeable effects on the microwave spectra which are due to interactions of the end-over-end rotation and to centrifugal stretching. Before describing these effects we shall consider the second important coupling case known as Hund's case (b).

#### CASE (b)

When  $\Lambda = 0$  but  $S \neq 0$ , the electronic momentum is due to spin only. Since there is no orbital field to couple the spin moment to the internuclear axis, the spin moment becomes coupled to the axis of rotation  $N$  through a weak magnetic field generated by the end-over-end rotation of the molecule. For certain light molecules such as OH, the molecular field generated by the rotation becomes so large for high rotational states that the spin  $S$  is resolved along  $J$  rather than along the molecular axis, even if  $\Lambda \neq 0$ . The idealized coupling case in which  $S$  is coupled to  $N$  to form a resultant  $J$ , as illustrated by the vector diagram of Fig. 4.6, is known as Hund's case (b). When  $\Lambda = 0$ ,  $N$  becomes equivalent to  $O$ , and for molecules in multiplet  $\Sigma$  states such as O<sub>2</sub> the spin is coupled to  $N$ , which is now perpendicular to the internuclear axis, to form the rotational axis  $J$ . The significant numbers are

$$N = \Lambda, \Lambda + 1, \Lambda + 2, \dots \quad (4.44)$$

and

$$J = N + S, N + S - 1, N + S - 2, \dots, |N - S| \quad (4.45)$$

#### OTHER CASES

The molecules that have been investigated with microwave spectroscopy, as well as most of those likely to be investigated, are in  $\Pi$  or  $\Sigma$  states which can be classified as approximately Hund's case (a) or (b), or else as intermediate between these two cases. Hund proposes other idealized cases such as those

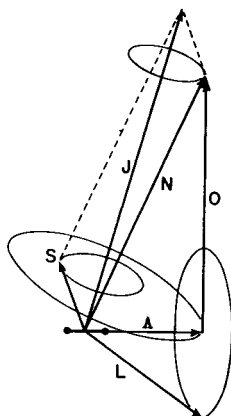


Fig. 4.6 Vector diagram of coupling for Hund's case (b).

in which both  $\mathbf{L}$  and  $\mathbf{S}$  are coupled to form a resultant which is, in turn, coupled to the molecular axis or to the axis of rotation. These infrequent cases are described by Herzberg in his treatise on diatomic molecules [40].

### Molecules in the ${}^2\Sigma$ State

Molecules having electronic spin, but no orbital momentum and no strong nuclear coupling, approximate closely Hund's case (b). The spin is coupled to the rotational axis through interaction of the spin magnetic moment with the weak magnetic field generated by the molecular rotation. To a good approximation, this field is directly proportional to the end-over-end rotational momentum  $\mathbf{N}$ , and the spin magnetic moment is  $g_s \beta \mathbf{S}$ . When there is more than one unpaired electron in the molecule, the individual spins are coupled to form a resultant spin greater than  $\frac{1}{2}$  and multiplet states greater than the doublet  $\Sigma$  considered in this section. Although the coupling model still conforms to that of Fig. 4.7, the Hamiltonians of the higher spin states,  ${}^3\Sigma$ ,  ${}^4\Sigma$ , and so on, are complicated by a spin–spin interaction considered for  ${}^3\Sigma$  states in the next section. The  ${}^2\Sigma$  molecules treated in this section have only one unpaired electron and hence no electron spin–spin interaction.

The Hamiltonian operator for the rotating  ${}^2\Sigma^+$  molecule, including the spin–rotation interaction and the first term in the centrifugal distortion perturbation energy but not the nuclear interactions, may be expressed as

$$\mathcal{H} = B_v \mathbf{N}^2 - D_v \mathbf{N}^4 + \gamma_v \mathbf{S} \cdot \mathbf{N} \quad (4.46)$$

Here  $\mathbf{N}$  is the end-over-end rotational operator,  $\mathbf{S}$  is the electron spin operator;  $B_v$  is the rotational constant,  $D_v$  the centrifugal distortion constant, and  $\gamma_v$  the spin–rotation coupling constant for the vibrational state  $v$ . Without nuclear moments, the angular momentum  $\mathbf{J}$ , the vector sum of  $\mathbf{N}$  and  $\mathbf{S}$ , is the total angular momentum. From the vector diagram of Fig. 4.7 it is apparent that

$$\mathbf{J}^2 = \mathbf{N}^2 + \mathbf{S}^2 - 2\mathbf{S} \cdot \mathbf{N}$$

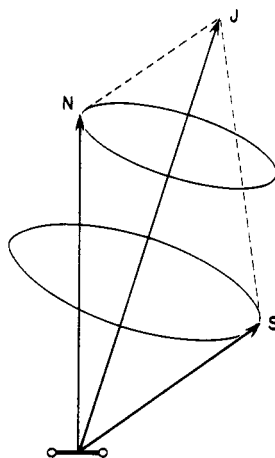


Fig. 4.7 Vector diagram of coupling for Hund's case (b) when molecules are in  $\Sigma$  states.

and thus

$$\mathbf{S} \cdot \mathbf{N} = \frac{1}{2}(\mathbf{J}^2 - \mathbf{N}^2 - \mathbf{S}^2) \quad (4.47)$$

Therefore, the  $\mathcal{H}$  operator of (4.46) can be expressed as

$$\mathcal{H} = (B_v - D_v N^2) \mathbf{N}^2 + \frac{1}{2} \gamma_v (\mathbf{J}^2 - \mathbf{N}^2 - \mathbf{S}^2) \quad (4.48)$$

For the assumed coupling model the Hamiltonian, (4.48), is diagonal in  $J$ ,  $N$ ,  $S$ , and the diagonal elements yield the energies

$$E_{J,N,S} = B_v N(N+1) - D_v N^2(N+1)^2 + \frac{1}{2} \gamma_v [J(J+1) - N(N+1) - S(S+1)] \quad (4.49)$$

in which the quantum numbers are

$$N = 0, 1, 2, 3, \dots$$

$$S = \pm \frac{1}{2}$$

$$J = N + \frac{1}{2} \quad \text{and} \quad N - \frac{1}{2}$$

Substitution of these values of  $S$  and  $J$  in (4.49) gives the two sets of levels

$$\left( \frac{E_N}{h} \right)_{J=N+(1/2)} = B_v N(N+1) - D_v N^2(N+1)^2 + \frac{\gamma_v N}{2} \quad (4.50)$$

$$\left( \frac{E_N}{h} \right)_{J=N-(1/2)} = B_v N(N+1) - D_v N^2(N+1)^2 - \frac{\gamma_v}{2}(N+1) \quad (4.51)$$

The sets of levels given by these expressions are illustrated in Fig. 4.8a which shows that the rotational levels are split into doublets by the spin rotation interaction and that the lowest level corresponds to  $J = \frac{1}{2}$ .

Selection rules for electric dipole, rotational transitions are

$$\Delta N = \pm 1, \quad \Delta J = 0, \pm 1$$

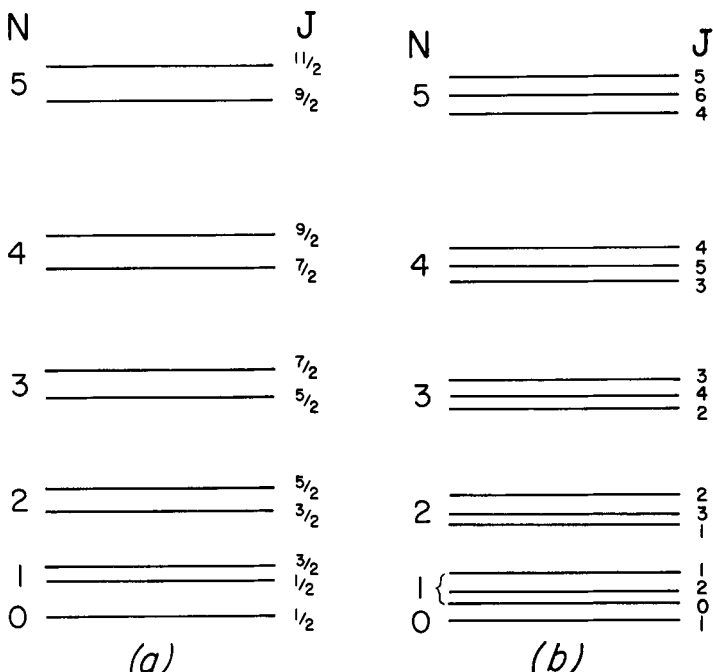


Fig. 4.8 Energy level diagram illustrating fine structure of rotational levels of diatomic molecules: (a) in  $^2\Sigma$  electronic states and (b) in  $^3\Sigma$  electronic states.

Thus the lowest rotational transition,  $N=0 \rightarrow 1$ , is a doublet; higher transitions are triplets, but the  $\Delta J=0$  component is weak and diminishes rapidly with increasing  $N$ . Only the doublet corresponding to  $\Delta J=1$  is likely to be detected for the higher  $N$  transitions. The relative intensities of these fine-structure components can be found from Appendix I by substitution of  $N$  for  $J$ ,  $J$  for  $F$ , and  $S$  for  $I=\frac{1}{2}$ .

An important application of the above theory is the analysis of the observed microwave transitions of the molecular ion  $^{12}\text{C}^{16}\text{O}^+$  which has a  $^2\Sigma^+$  electronic ground state and no nuclear spin moments. The  $N=0 \rightarrow 1$  transition of  $\text{CO}^+$ , reported by Dixon and Woods [41] in 1975, was the first microwave spectral observation of molecular ions in the laboratory. This observation aided in the detection of a pair of lines from interstellar space tentatively assigned as fine-structure components of the  $N=1 \rightarrow 2$  transition of  $\text{CO}^+$  and confirmed later by measurement of these components of the  $N=1 \rightarrow 2$  transition in the laboratory by Sastry et al. [42]. The  $N=0 \rightarrow 1$  doublet of  $^{12}\text{C}^{16}\text{O}^+$ , accurately measured by Piltch et al. [43], falls at 117,692.29 MHz ( $J=\frac{1}{2} \rightarrow \frac{1}{2}$ ) and 118,101.89 MHz ( $J=\frac{1}{2} \rightarrow \frac{3}{2}$ ) for ions in the ground vibrational state. The somewhat lower frequencies for the corresponding transitions for the  $v=1$  and  $v=2$  vibrational states have been measured by Bogey et al. [44] at Lille.

Sastry et al. [42] measured the fine-structure lines for the three transitions  $N=1 \rightarrow 2$ ,  $2 \rightarrow 3$ ,  $3 \rightarrow 4$ , which extend into the submillimeter frequencies to 471,952.34 MHz. These various measurements were analyzed by the investigators to give the rotational and fine-structure constants of (4.50) and (4.51) listed for  $^{12}\text{C}^{16}\text{O}^+$  in Table 4.9.

The analysis of the  $X^2\Sigma^+$  spectrum of  $^{12}\text{C}^{14}\text{N}$  and of  $^{28}\text{Si}^{14}\text{N}$  involves the  $^{14}\text{N}$  hyperfine structure caused by nuclear magnetic and nuclear quadrupole coupling. Microwave rotational transitions of CN were first measured for interstellar molecules [45], and the first analysis of the  $^{14}\text{N}$  hyperfine structure was made of the interstellar spectrum by Penzias, Wilson, and Jefferts [46]. The effective Hamiltonian including the hyperfine interaction is

$$\mathcal{H} = \mathcal{H}_{N,S-N} + \mathcal{H}_{MHS} + \mathcal{H}_Q \quad (4.52)$$

where  $\mathcal{H}_{N,S-N}$  is the rotational and spin-rotation  $\mathcal{H}$  of (4.46),  $\mathcal{H}_{MHS}$  is the operator for the nuclear magnetic interaction, and  $\mathcal{H}_Q$  is that for nuclear quadrupole interactions.

The nuclear magnetic operator of (4.52) has the form

$$\mathcal{H}_{MHS} = b\mathbf{I} \cdot \mathbf{S} + cI_zS_z + C_I\mathbf{N} \cdot \mathbf{I} \quad (4.53)$$

where  $b$ ,  $c$ , and  $C_I$  are the nuclear magnetic coupling constants as designated by Frosch and Foley [47], who originally worked out the theory of the magnetic hyperfine structure. The nuclear quadrupole interaction has the general form of that described for axially symmetric  $^1\Sigma$  molecules in Chapter IX, but its specific form depends on the nature of the coupling vectors. Usually the quadrupole coupling is very weak compared with the magnetic interactions and can be treated with first-order perturbation theory.

The nature of the solution of the  $\mathcal{H}$  of (4.52) depends on the relative magnitudes of the various coupling terms. When the nuclear coupling terms are at least moderately smaller than the spin-rotation term, the coupling scheme  $\mathbf{N}+\mathbf{S}=\mathbf{J}$  may still be used, but now  $\mathbf{J}$  couples with the nuclear spin  $\mathbf{I}$  to form the resultant  $\mathbf{F}=\mathbf{J}+\mathbf{I}$ , as illustrated in Fig. 9.3. These conditions hold for both  $^{12}\text{C}^{14}\text{N}$  and  $^{28}\text{Si}^{14}\text{N}$ .

Dixon and Woods [48], who were first to measure microwave rotational transitions of CN in the laboratory, tabulated matrix elements for the various terms in  $\mathcal{H}$  which one may use to obtain the energy matrix required for a precise solution for its energies. Solution of the rather complex secular equation that results can be achieved with numerical computer methods. The  $\mathcal{H}_{MHS}$  for  $^{28}\text{Si}^{14}\text{N}$  is like that for  $^{12}\text{C}^{14}\text{N}$ , and the methods for its solution are similar [49]. The rotational and coupling constants for both these molecules are listed in Table 4.9.

The hyperfine structure of the species  $^{13}\text{C}^{16}\text{O}^+$ , which has  $^{13}\text{C}$  magnetic hyperfine structure but no nuclear quadrupole interaction, has been measured and analyzed by Piltch et al. [43]. In this ion the  $^{13}\text{C}$  magnetic coupling is much stronger than the spin-rotation interaction,  $b_0=14.58$  MHz compared

# LINEAR POLYATOMIC MOLECULES

---

1	THEORETICAL FORMULATIONS: ENERGIES AND FREQUENCIES	126
	Molecules in the Ground Vibrational State	126
	Molecules in Excited Vibrational States	128
	<i>I</i> -Type Doublet Spectra	133
	Fermi Resonance	136
	Nuclear Effects	136
2	LINE INTENSITIES	138
	Optimum Regions for Observations	139
3	MEASUREMENTS WITH SPECIAL HIGH-RESOLUTION TECHNIQUES	141
4	OBSERVATIONS ON LINEAR TRIATOMIC MOLECULES	143
	Alkali Hydroxides	143
	Boron Compounds	144
	Cyanides and Phosphides	144
	Hydrogen Isocyanide HNC	145
5	LONG LINEAR MOLECULES ON EARTH AND IN OUTER SPACE	146
6	EQUILIBRIUM STRUCTURES	147
7	QUASI-LINEAR MOLECULES	149
8	HYDROGEN-BONDED DIMERS	153
9	RARE GAS ATOM-MOLECULE COMPLEXES	160
10	LINEAR MOLECULAR IONS: INTERSTELLAR AND LABORATORY	163
11	LINEAR FREE RADICALS: LABORATORY AND INTERSTELLAR	166

Because the potential functions of nonrigid polyatomic molecules are more complicated than those of diatomic molecules, it is generally not feasible to solve their wave equations by the same methods as were used for the diatomic molecules. Instead, the customary procedure is to find a first solution for the polyatomic molecule with the assumption that it is a completely rigid, field-free rotor and then to treat centrifugal distortion, Stark and Zeeman interactions with perturbation theory. For these calculations, specific eigenfunctions are not required; only the matrix elements of angular momentum

operators and the direction cosine matrix elements, as given in Chapter II, are required. These elements can be derived from matrix methods without specific knowledge of the eigenfunctions. Thus one need not solve the wave equation to find the required spectral formulas and selection rules. Even though the wave equation for a rigid, linear rotor is readily solvable, the desired eigenvalues of the rotational energy can be obtained more easily from the matrix elements of the angular momentum operators derived from the commutation rules of these operators. In this chapter we shall treat only unperturbed, field-free rotors, leaving the Stark and Zeeman effects and the nuclear hyperfine structure to later chapters. Methods for calculation of molecular structures from the spectra are given in Chapter XIII.

## 1 THEORETICAL FORMULATIONS: ENERGIES AND FREQUENCIES

### Molecules in the Ground Vibrational State

For a rigid, linear, polyatomic molecule with no resultant electronic angular momentum, the angular momentum about the figure axis  $a$  is zero, just as for the diatomic molecule, and  $I_b = I_c = I$ . Therefore the rotational Hamiltonian can be expressed as

$$\mathcal{H}_0 = \frac{P^2}{2I} \quad (5.1)$$

where  $I$  is the moment of inertia and  $P^2$  is the operator conjugate to the square of the total angular momentum. Since the nonvanishing matrix elements of the operator  $P^2$  are  $(J|P^2|J) = \hbar^2 J(J+1)$  (see Chapter II, Section 2) the Hamiltonian operator  $\mathcal{H}_0$  has only diagonal elements, and the energy eigenvalues are therefore

$$E_J^0 = (J|\mathcal{H}_0|J) = \left( \frac{1}{2I} \right) (J|P^2|J) = \frac{\hbar^2 J(J+1)}{8\pi^2 I} \quad (5.2)$$

With the substitution of the spectral constant  $B \equiv \hbar/8\pi^2 I$ , this becomes

$$E_J^0 = hBJ(J+1) \quad (5.3)$$

The bracket notation signifies  $(J|\mathcal{H}_0|J) = \int \psi_J^0 * \mathcal{H}_0 \psi_J^0 d\tau$  where  $\psi_J^0$  represents the eigenfunctions of the unperturbed operator  $\mathcal{H}_0$ . Since  $\mathcal{H}_0$ ,  $P^2$ , and  $P_z$  are commuting operators, they have a common set of eigenfunctions  $\psi_{JM}^0$ . The eigenfunctions for the rigid diatomic or linear polyatomic molecule are the same as those of (2.102) and can be obtained from solution of Schrödinger's wave equation. Furthermore, the component of the angular momentum of the linear rotor that can be resolved along a fixed axis by a Stark or Zeeman field is

$$P_z = \frac{\hbar}{2\pi} M_J \quad (5.4)$$

The quantum number of the angular momentum, as was found earlier, can take only the integral values

$$J=0, 1, 2, 3, \dots \quad (5.5)$$

and  $M_J$ , which measures in units of  $\hbar$  the components of the angular momentum along a space-fixed axis, can take the values

$$M_J = J, J-1, J-2, \dots, -J \quad (5.6)$$

The selection rules for dipole absorption of radiation (see Chapter II, Section 6), based on the condition that the matrix elements of the molecular dipole moment  $\int \psi_{JM} \mu \psi_{J'M'} d\tau$  must not vanish, are found to be

$$J' = J \pm 1, \quad M_{J'} = M_J \text{ or } M_J \pm 1 \quad (5.7)$$

just as they are for diatomic molecules. The selection rules for  $M_J$  are of interest only when an external field is applied (see Chapter X). The transitions  $J \rightarrow J+1$  correspond to absorption of radiation of the field-free rotor. Hence the absorption line frequencies are

$$\nu = 2B(J+1) \quad (5.8)$$

where the spectral constant  $B$  is expressed in frequency units.

From (5.8) it is seen that the rotational frequencies of the rigid, linear, polyatomic molecule, like those of the diatomic molecule, form a series of  $2B, 4B, 6B$ , and so on. The lowest rotational frequency  $2B$  for most polyatomic molecules, falls in the centimeter wave region, although for HCN it occurs in the 3-mm wave region.

The corresponding Hamiltonian for the nonrigid rotor can be written as

$$\mathcal{H} = \mathcal{H}_0 + \mathcal{H}_d \quad (5.9)$$

where  $\mathcal{H}_d$  represents the centrifugal distortion energy. For the linear molecule there is only one axis of distortion, and  $(P_x^2 + P_y^2)^2 = P^4$ ,  $P_z^2 = 0$ . With these conditions, (8.35) for  $\mathcal{H}_d$  takes the simple form

$$\mathcal{H}_d = -\left(\frac{\hbar}{\hbar^4}\right) DP^4 \quad (5.10)$$

in which  $D$  is a constant. The first-order perturbation energy is the average of  $\mathcal{H}_d$  over the eigenfunction  $\psi_0^0$  of the unperturbed Hamiltonian  $\mathcal{H}_0$ , or

$$E^{(1)} = \langle J | \mathcal{H}_d | J \rangle = -\left(\frac{\hbar}{\hbar^4}\right) D \langle J | P^4 | J \rangle = -\hbar D J^2 (J+1)^2 \quad (5.11)$$

where  $D$ , the centrifugal stretching constant, depends on the potential functions of the various bonds and can, in principle, be expressed as a function of the vibrational frequencies or force constants. For a triatomic linear molecule, Nielsen [1] has shown that

$$D = 4B^3 \left( \frac{\zeta_{21}^2}{\omega_3^2} + \frac{\zeta_{23}^2}{\omega_1^2} \right) \quad (5.12)$$

where  $\omega_1$  and  $\omega_3$  are the bond-stretching frequencies and  $\zeta_{21}$  and  $\zeta_{23}$  are Coriolis coupling constants.

The next higher-order term in the expression has the form,  $H_0 J^3(J+1)^3$ , where  $H_0 \approx H_e \ll D_0$ . Thus the rotational energy for the linear molecules in the ground vibrational state may be expressed as

$$\frac{E_J}{\hbar} = B_0 J(J+1) - D_0 J^2(J+1)^2 + H_0 J^3(J+1)^3 \quad (5.13)$$

With the selection rules for dipole absorption of radiation,  $J \rightarrow J+1$ , the rotational frequencies are

$$\nu = 2B_0(J+1) - 4D_0(J+1)^3 + H_0(J+1)^3[(J+2)^3 - J^3] \quad (5.14)$$

This equation is found to be adequate for most microwave measurements of linear molecules in the ground vibrational state. It has the same form as (4.10) for diatomic molecules.

### Molecules in Excited Vibrational States

Theory for the rotational spectra of linear polyatomic molecules in excited vibrational states is more complicated than that for diatomic molecules, not only because of the greater number of vibrating modes but also because of the special type of interaction of rotation with the degenerate bending modes of vibration.

A linear molecule with  $n$  atoms has  $(3n-5)$  modes of vibration. Not all these modes have different frequencies  $\omega_i$ , however. The bending modes are always doubly degenerate; that is, there are two bending modes of vibration, both of which have the same frequency; and in molecules with  $n > 3$  there is more than one degenerate mode. A nonsymmetric, triatomic linear molecule such as OCS or HCN has two nondegenerate parallel modes  $v_1$  and  $v_3$  and a doubly degenerate bending mode  $v_2$ , as indicated in Fig. 5.1. The parallel modes correspond essentially to the stretching vibrations of the two bonds, XY and YZ.

As in diatomic molecules, the averaged or effective bond lengths tend to be slightly longer in the excited parallel modes because of the asymmetry in the Morse-type potential curve (anharmonicity). This leads to a slightly increasing moment of inertia and a consequent lowering of  $B_v$  and the rotational frequency with increasing vibrational quantum number for the parallel modes. In contrast, linear molecules in bending vibrational modes are slightly shorter, on the average, than are the molecules of the ground vibrational states. Their effective  $B_v$  and their rotational frequencies are expected therefore to be slightly higher than the corresponding ones for molecules in the ground vibrational states.

Except for deviations caused by  $I$ -type resonances or Fermi resonances (discussed later in this section), the effects of the vibration on  $B_v$  are to first order given by

$$B_v = B_e - \sum_i \alpha_i \left( v_i + \frac{d_i}{2} \right) \quad (5.15)$$

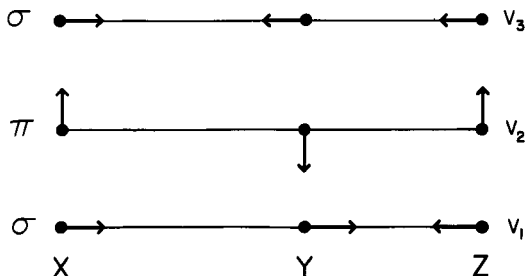


**Fig. 5.1** Indication of the vibrational modes of a triatomic linear molecule. The bending mode  $v_2$  is doubly degenerate because the molecule is free to bend in two orthogonal planes.

where  $v_i$  is the vibrational quantum number for the  $i$ th excited mode,  $d_i$  is the degeneracy of that mode, and  $\alpha_i$  is a small interaction constant that gives the first-order correction of  $B_v$  for the  $i$ th mode. For reasons given previously,  $\alpha_i$  is generally positive for parallel modes and negative for perpendicular modes. Vibrational modes having the same fundamental frequency, degenerative modes, are counted only once in the summation. For nondegenerate modes,  $d_i=1$ ; for doubly degenerate modes,  $d_i=2$ , and so on. Note that  $B_v$  for the ground vibrational state differs from  $B_e$  by  $\sum \alpha_i d_i / 2$ . Thus the evaluation of  $B_e$  to first order requires measurement of rotational lines of the molecule in at least one excited vibrational level for each of the fundamental modes. Interactions among the different modes of excitation give rise to higher-order cross terms included in (5.25).

Likewise, the centrifugal stretching constants differ slightly for the excited vibrational states. To first order, this difference is expressed by

$$D_v = D_e + \sum_i \beta_i \left( v_i + \frac{d_i}{2} \right) \quad (5.16)$$

Since  $D_v$  is already a very small constant in comparison with  $B_v$ , the changes in the higher-order stretching constant  $H_v$  with vibrational state are usually negligible.

In addition to the shifts in the lines described above, there are other effects of interaction of rotation with the degenerate bending vibrational modes. If  $z$  is chosen along the figure axis, the degenerate vibrations of the nonrotating molecules can be considered as orthogonal bending motions of the molecule in the  $xz$  and  $yz$  planes. In the rotating molecule the degeneracy is lifted by the interaction between vibration and rotation. The vibrational states can be represented as combinations of the two idealized states of the nonrotating molecule. Two such orthogonal vibrations with a  $90^\circ$  phase difference are equivalent to rotations, clockwise and counterclockwise, about the figure axis  $z$ . Thus a degenerate bending vibrational state with vibrational quantum number  $v_i$  can be regarded as having components of angular momentum  $p_z = \pm \hbar$  with rotational quantum numbers

$$l_i = v_i, v_i - 2, v_i - 4, \dots, -v_i \quad (5.17)$$

For a first excited degenerate bending mode,  $v_i=1$  and  $l_i=\pm 1$ ; for a second,  $v_i=2$ , and  $l_i=0, \pm 2$ ; for a third,  $v_i=3$ ,  $l_i=\pm 1, \pm 3$ , and so on. The various vibrational states are indicated by a sequence of their vibrational quantum numbers. For example, the vibrational states of a triatomic molecule would be indicated by  $v_1 v_2^{(1)} v_3$ , where the subscripts indicate the fundamental modes specified in Fig. 5.1 and the corresponding  $v$  numbers indicate their states of excitation. Examples are

$$0\ 1^1\ 0,\quad 0\ 2^0\ 0,\quad 0\ 2^2\ 0,\quad 1\ 1^1\ 0.$$

When more than one bending vibrational state is excited, the quantum number for the total vibrational angular momentum,  $l=\sum_i l_i$ , characterizes the component of angular momentum about the molecular axis. Since the angular momentum thus generated is about the figure axis,  $l$  is analogous to the  $K$  quantum number of the symmetric top or the  $\Lambda$  component in diatomic molecules with electronic orbital momentum. Following a proposal by Mulliken [2], the vibrational states of linear polyatomic molecules are often designated as are those of diatomic molecules, with the value of  $|l|$  replacing that for  $\Lambda$ , that is, vibrational states  $l=0$  are designated as  $\Sigma$  states; with  $|l|=1$ , as  $\pi$  states; with  $|l|=2$ , as  $\Delta$  states, and so on.

In an excited degenerate bending mode, the rotating linear molecule has an effective moment of inertia  $I_a$  as well as a component of angular momentum about the figure axis. As for the rigid symmetric top (to be discussed in Chapter VI), its rotational Hamiltonian can be expressed as

$$\mathcal{H}_r = \frac{P^2}{2I_b} + \frac{1}{2} \left( \frac{1}{I_a} - \frac{1}{I_b} \right) p_z^2 \quad (5.18)$$

Since  $p_z^2$  has eigenvalues  $\hbar^2 l^2$ , the allowed energy values are

$$\frac{E_r}{\hbar} = B_v J(J+1) + (A_v - B_v) l^2 \quad (5.19)$$

The term  $A_v l^2$  is usually treated as vibrational energy, and the rotational energy is expressed by

$$\frac{E_r}{\hbar} = B_v [J(J+1) - l^2] \quad (5.20)$$

For pure rotational transitions, the selection rules are  $J \rightarrow J+1$  and  $l \rightarrow l$ ; the rotational frequencies in this approximation are

$$\nu = 2B_v(J+1) \quad (5.21)$$

where  $J$  represents the total angular momentum quantum number including the vibrational angular momentum. Thus  $J$  has the values

$$J = |l|, |l|+1, |l|+2, \dots \quad (5.22)$$

Except for the small change in  $B_v$  given by (5.15), (5.21) is like that for the rigid molecule in the ground vibrational state. There is, however, an important

effect which is due to the fact that  $J$  must now include  $l$ . In an excited bending mode when  $|l|=1$ , the lowest value of  $J$  is 1. As a result, the line corresponding to  $J=0 \rightarrow 1$  of the ground vibrational state does not occur. For a higher excited vibrational state when  $l=2$ , the first two rotational states are missing and the  $J=0 \rightarrow 1$  and  $1 \rightarrow 2$  levels are missing, and so on. In addition to these effects and the  $l$ -doubling effects to be described later, there are slight effects of the vibrational angular momentum in the centrifugal stretching term which are altered to  $-D_v[J(J+1)-l^2]^2$  and  $H_v[J(J+1)-l^2]^3$ .

Because of the Coriolis coupling force proportional to  $\mathbf{v} \times \boldsymbol{\omega}$  between the vibrational motion  $\mathbf{v}$  and the angular rotational motion  $\boldsymbol{\omega}$  in orthogonal planes, the  $\pm l$  degeneracy of (5.19) is lifted, and a doublet splitting of the rotational lines (called  $l$  doubling) is produced. As a result of this interaction, the effective moment of inertia generated about the  $z$  axis is not quite symmetric, and the molecule behaves like a slightly asymmetric rotor in which there is a small splitting of the  $K$  levels which are degenerate in the corresponding symmetric top. For the  $\Pi$  state,  $|l|=1$ , and the  $l$  splitting  $\Delta E_l$  is approximately proportional to the square of the angular momentum and is expressed by [3, 4]

$$(\Delta E)_{|l|=1} = h \left( \frac{q_i}{2} \right) (v_i + 1) J(J+1) \quad (5.23)$$

where  $v_i$  is the vibrational quantum number of the  $i$ th degenerate bending mode and  $q_i$  is the coupling constant of the vibration and rotation for this mode when  $|l|=1$ .

For linear molecules in degenerate bending modes when the splitting for  $|l|=1$  is included, the rotational energies may be expressed as

$$\begin{aligned} \frac{E_r^\pm}{h} = & B_v [J(J+1)-l^2] \pm \left( \frac{q_i}{4} \right) (v_i + 1) J(J+1) - D_v [J(J+1)-l^2]^2 \\ & + H_v [J(J+1)-l^2]^3 \end{aligned} \quad (5.24)$$

If the lower and upper component levels of an  $l$  doublet are signified by subscripts  $L$  and  $U$ , respectively, the possible transitions are  $J, l_U \rightarrow J+1, l_U$  and  $J, l_L \rightarrow J+1, l_L$ . The squared dipole matrix elements, upon which the probabilities of these transitions depend, may be obtained from (2.124) by replacement of  $K$  with  $l_L$  or  $l_U$ . With the omission of the usually negligible term in  $H_v$ , the rotational frequencies are

$$\nu_\pm = 2B_v(J+1) \pm \frac{1}{2}q_i(v_i + 1)(J+1) - 4D_v(J+1)[(J+1)^2 - l^2] \quad (5.25)$$

where

$$\begin{aligned} B_v = & B_e - \sum_i \alpha_i (v_i + \frac{1}{2}d_i) + \sum_{ij} \gamma_{ij} (v_i + \frac{1}{2}d_i)(v_j + \frac{1}{2}d_j) \\ & + \sum_{ijk} \epsilon_{ijk} (v_i + \frac{1}{2}d_i)(v_j + \frac{1}{2}d_j)(v_k + \frac{1}{2}d_k) + \gamma_{ll} l^2 \end{aligned} \quad (5.26)$$

and

$$D_v = D_e + \sum_i \beta_i (v_i + \frac{1}{2} d_i) \quad (5.27)$$

In (5.26) the factors  $\alpha_i$ ,  $\gamma_{ij}$ ,  $\epsilon_{ijk}$ , and  $\gamma_{ll}$  are interaction constants which are a measure of the effects of the vibration-rotation interactions on  $B_v$ , and  $l = \sum_i l_i$  is the quantum number for the total vibrational angular momentum about the molecular axis.

In measurements on the lower vibrational states, those most often investigated, the terms in  $\alpha_i$  and  $\gamma_{ij}$  in the expansion of  $B_v$ , (5.26), are usually adequate for a fitting of the observed spectra. However, De Lucia and Helminger [3], who measured rotational transitions of 12 excited vibrational states of HCN in active laser plasmas, found the term  $\epsilon_{ijk}$  of (5.26) to be required for a fitting of the data of some relatively low excited states. For example, they found that  $\epsilon_{222}$  makes a significant contribution to the  $B_v$  value for the lower bending modes of HCN. The various parameters of (5.26) that they evaluated from their measurements are reproduced in Table 5.1.

The theory of the interactions of rotation with bending vibrations in linear molecules has been developed by Nielsen and Shaffer [4, 5]. For the linear  $XYZ$  molecules with  $|l|=1$  for the degenerate bending mode  $v_2$  they derive the following expression for the coupling constant in (5.23).

$$q_2 = 2 \frac{B_e^2}{\omega_2} \left[ 1 + 4 \sum_i \zeta_{2i}^2 \left( \frac{\omega_2^2}{\omega_i^2 - \omega_2^2} \right) \right] \approx 2.6 \frac{B_e^2}{\omega_2} \quad (5.28)$$

**Table 5.1** Equilibrium Rotational Constants of  $H^{12}C^{14}N$  as Derived from (5.26) with Experimental Values of  $B_v$  for 12 Excited Vibrational States<sup>a</sup>

Constant	Value (MHz)	Standard Deviation $\sigma$
$B_e$	44,511.62	0.03
$\alpha_1$	300.028	0.03
$\alpha_2$	-108.369	0.05
$\alpha_3$	312.983	0.03
$\gamma_{11}$	-0.893	0.009
$\gamma_{12}$	-3.583	0.033
$\gamma_{13}$	6.448	0.027
$\gamma_{22}$	0.762	0.027
$\gamma_{23}$	6.332	0.033
$\gamma_{33}$	-4.521	0.018
$\epsilon_{222}$	0.094	0.003
$\gamma_{ll}$	-6.224	0.006

<sup>a</sup>From De Lucia and Helminger [3].

where  $\omega_2$  signifies the vibrational frequency of the degenerate bending mode and  $\omega_i$ , the frequencies of other vibrational modes, and where  $\zeta_{2i}$ , the Coriolis coupling constants, are parameters that depend on the force constants, atomic mass, and so on. Expressions for  $\zeta_{2i}$ , which are relatively involved, may be found in the original papers. When  $|l| > 1$ , the  $l$  splitting is much less than when  $|l|=1$  and is usually not observable when  $|l| > 2$ . For the alkali hydroxides, Kuijpers et al. [6] found the  $l$  doubling to be measurable for  $|l|=1$  and 2, but not detectable for  $|l|=3$ .

Bogey and Bauer [7], who measured rotational transitions of very high vibrational states of OCS, excited through active transfer from N<sub>2</sub>, used the theoretical formalism of Amat et al. [8] for their analysis. They give particular formulas for the frequencies of the  $v_i=3, 4$ , and 5 degenerate bending modes with the allowed values of  $|l|$  for each mode. These formulas should be useful in the analysis of the microwave spectra of other linear triatomic molecules in highly excited bending modes, but they require too much space for reproduction here.

An observational scan [9] displaying the  $J=2 \rightarrow 3$  rotational line of FCP in seven different vibrational states, shown in Fig. 5.2 illustrates the nature of the experimental observations from which vibrational effects on rotational spectra are evaluated.

### $l$ -Type Doublet Spectra

As Shulman and Townes [10] proved, direct transitions between  $l$ -type doublet levels  $l_L \leftrightarrow l_U$  with no change in  $J$  can be observed. The squared dipole moment matrix elements upon which the transition probabilities depend are

$$|(J, l_L | \mu | J, l_U)|^2 = \frac{\mu^2 l^2}{J(J+1)} \quad (5.29)$$

These elements are obtainable from (2.125) by replacement of  $K$  by  $l$ . For light molecules such as HCN, these transitions correspond to frequencies in the microwave region and provide the most precise measurements available of the coupling constant  $q$ . When  $q$  is measured in frequency units, the  $l$ -doublet transitions, according to Eq. (5.23), correspond to frequencies of

$$(v_l)_i = \left( \frac{q_i}{2} \right) (v_i + 1) J(J+1) \quad (5.30)$$

For a given molecule  $q_i$  is approximately constant; therefore for a given bending mode  $v_i$ , the  $l$ -doublet frequencies should be proportional to  $J(J+1)$ . That this is nearly true was shown by the early measurements of Shulman and Townes [10] on HCN. However, measurable deviations [11, 12] from this formula occur as  $J$  becomes large. Nielsen and Amat [13] have shown that this deviation can be attributed to a change of  $q_i$  by centrifugal distortion. To first order, the dependence of  $q_i$  on  $J$  is expressed by

$$q_i = q_i^{(0)} - q_i^{(1)} J(J+1) \quad (5.31)$$

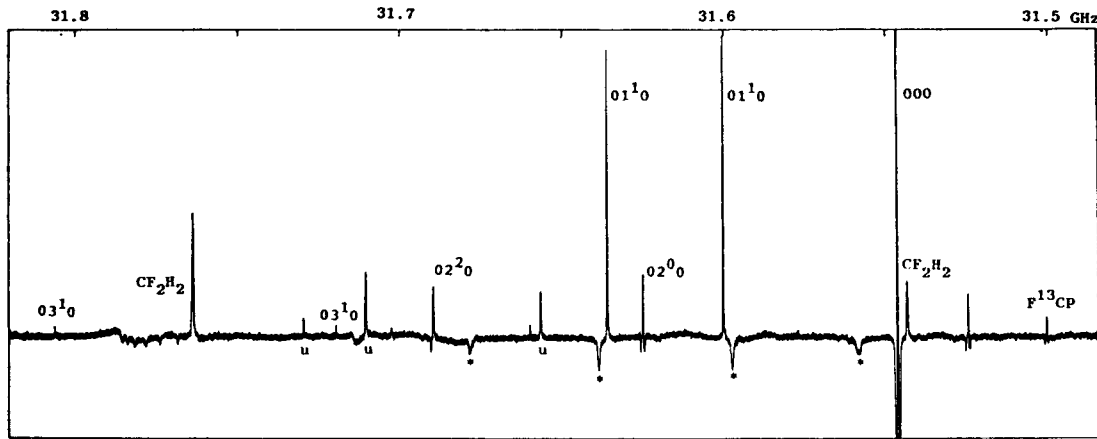


**Fig. 5.2** Moderate resolution scan of the  $J = 3 \leftarrow 2$  transition of  $\text{FC}\equiv\text{P}$  observed with a  $2800 \text{ V cm}^{-1}$  Stark modulation. Unassigned lines are labeled  $u$  and the  $l$ -doublet Stark lobes by an asterisk. Note that  $\text{CF}_2\text{H}_2$  impurity lines are also detected as indicated. From Kroto, Nixon, and Simmons [9].

so that the  $l$ -type doublet frequencies are expressed by

$$(v_l)_i = \left( \frac{q_l^{(0)}}{2} \right) (v_i + 1) J(J+1) - \left( \frac{q_l^{(1)}}{2} \right) (v_i + 1) J^2 (J+1)^2 \quad (5.32)$$

Törning [12] found that the several  $l$ -type doublet transition frequencies which they observed for the degenerate bending mode  $v_2$  in HCN and DCN when  $v_2=1$  and  $|l|=1$ , could be fitted to the formulas with  $v_l$  in kHz

$$v_l(\text{H}^{12}\text{C}^{12}\text{N}) = 224,478 J(J+1) - 0.002666 J^2 (J+1)^2 \quad (5.33)$$

and

$$v_l(\text{D}^{12}\text{C}^{12}\text{N}) = 186,192 J(J+1) - 0.00220 J^2 (J+1)^2 \quad (5.34)$$

Winnewisser and Bodenseh [14] have found that still higher order terms were required for satisfactory agreement with their precise measurements on  $l$ -type doublet transitions of the degenerate bending vibrations  $v_4=1$  and  $v_5=1$  of HCNO over a wide range of  $J$  values. They employed the expression

$$(v_l)_i = q_l^{(0)} J(J+1) - q_l^{(1)} J^2 (J+1)^2 + q_l^{(2)} J^3 (J+1)^3 - q_l^{(3)} J^4 (J+1)^4 + \dots \quad (5.35)$$

which was indicated by the theoretical work of Ramadier and Amat [15]. The fitting of the observed frequencies with those calculated from (5.35) was very close. The values obtained for the various  $q$ 's are listed in Table 5.2. Figure 5.3 shows plots of the observed  $l$ -doublet transition frequencies as a function of  $J$ . The  $v_4$  and  $v_5$  for HCNO correspond to the HCN and the CNO bending modes, respectively.

Later investigations [16–20] of the interesting molecule HCNC (fulminic acid) provide a basis for understanding the anomalies of the doublet splitting described above. Yamada et al. [18] have shown that the abnormal splitting arises partly from accidental resonances among some excited vibrational levels. Near coincidences were found to occur between levels of two bending modes,  $v_4$  and  $v_5$ , and the lowest-lying stretching mode,  $v_3$ . The accidental resonances were found to be less normal and the  $l$ -type splitting more nearly normal [19]

**Table 5.2**  $l$ -Type Doublet Constants of  $\text{H}^{12}\text{C}^{14}\text{N}^{16}\text{O}$  Obtained by Application of (5.35) to the  $l$ -Type Doublet Spectra for the  $v_5=1$  and the  $v_4=1$  Vibrational States<sup>a</sup>. Values are given in MHz units

$v_5 = 1$	$v_4 = 1$
$q_5^{(0)} = 34.6391 \pm 0.0001$	$q_4^{(0)} = 23.6722 \pm 0.0009$
$q_5^{(1)} = (0.1623 \pm 0.0002) 10^{-3}$	$q_4^{(1)} = (0.6139 \pm 0.0032) 10^{-3}$
$q_5^{(2)} = (1.00 \pm 0.11) 10^{-9}$	$q_4^{(2)} = (0.1417 \pm 0.0034) 10^{-6}$
	$q_4^{(3)} = (0.199 \pm 0.012) 10^{-10}$

<sup>a</sup>From Winnewisser and Bodenseh [14].

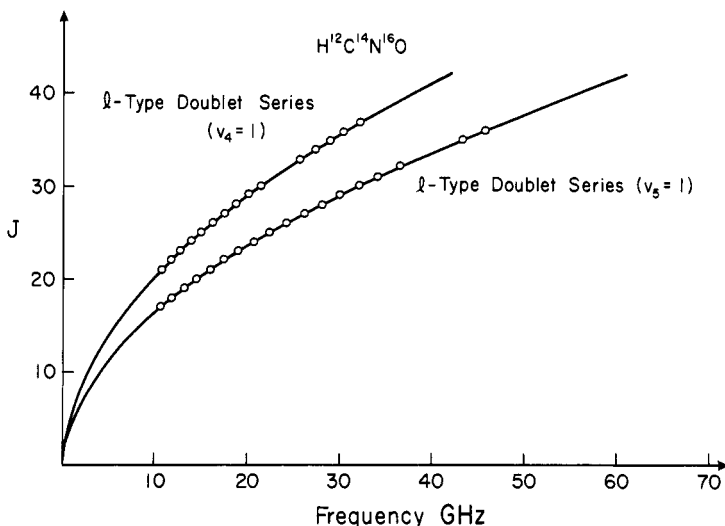


**Fig. 5.3** Plots of observed frequencies of *l*-type doublet transitions of HCNO as a function of *J*. From Winnewisser and Bodenseh [14].

in DCNO than in HCNO. The abnormalities are also enhanced by the quasi-linearity of the molecule (Section 7). Bunker et al. [20] conclude that the equilibrium structure of HCNO is linear but that in the zero-point vibrational state and in the  $v_1$  and  $v_2$  vibrational states the HCN bending potential has its minimum off the internuclear axis. This would seem to be the cause of its quasi-linear behavior.

Table 5.3 shows a comparison of the  $q_i^{(0)}$  values for the first excited bending modes ( $v_i=1$ ) for a few linear molecules.

### Fermi Resonance

In addition to the effects of vibrations on rotational spectra, described earlier, there are smaller and less frequently encountered perturbations caused by Fermi resonance between the two vibrational levels of the same symmetry that have nearly the same energy. As Fermi predicted [21], such an interaction gives rise to a repulsion which further separates the vibrational levels. Such displacements in the vibrational levels will be accompanied by changes in the  $\alpha_i$  and  $B_v$  values.

### Nuclear Effects

Practically all stable linear molecules have singlet sigma electronic ground states and hence no molecular magnetic field except a weak one generated by the molecular rotation. For this reason most linear molecules observed with microwave spectroscopy do not have a resolvable nuclear magnetic hyperfine structure. However, hyperfine structure due to nuclear quadrupole

**Table 5.3** *l*-Type Doublet Constants for First Excited Bending Modes ( $v_i=1$ ) of Some Linear Molecules. Values are Given in MHz Units

Molecule <sup>a</sup>	$q_2$	Ref.	Molecule <sup>a</sup>	$q_2$	Ref.
HCN	224.47	<sup>b</sup>	OCS	6.344	<sup>e</sup>
DCN	186.19	<sup>b</sup>	<sup>79</sup> BrCN	3.915	<sup>c</sup>
NNO	23.73	<sup>c</sup>	OC <sup>80</sup> Se	3.172	<sup>c</sup>
FCN	19.85	<sup>d</sup>	ICN	2.688	<sup>e</sup>
<sup>35</sup> ClCN	7.459	<sup>c</sup>	SCTe	0.659	<sup>f</sup>
	$q_4$	$q_5$			
HCCF	19.12	12.57			<sup>d</sup>
DCCF	15.33	13.26			<sup>d</sup>
	$q_5$	$q_6$	$q_7$		
HCCCN	2.56	3.57	6.54		<sup>d</sup>
DCCCN	2.68	3.10	5.97		<sup>d</sup>

<sup>a</sup>Atomic symbols are for the most abundant species where not specified.

<sup>b</sup>T. Töring [12].

<sup>c</sup>C. A. Burrus and W. Gordy, *Phys. Rev.*, **101**, 599 (1956).

<sup>d</sup>J. K. Tyler and J. Sheridan, *Trans. Faraday Soc.*, **59**, 2661 (1963).

<sup>e</sup>C. H. Townes, A. N. Holden, and F. R. Merritt, *Phys. Rev.*, **74**, 1113 (1948).

<sup>f</sup>W. A. Hardy and G. Silvey, *Phys. Rev.*, **95**, 385 (1954).

coupling is often resolved in the microwave rotational spectra. Nuclear quadrupole moments are electric moments, and their coupling to the molecular frame depends on the molecular electric field gradient. Thus large nuclear quadrupole splittings can occur for molecules in "nonmagnetic" singlet sigma states, but only nuclei with spins greater than  $\frac{1}{2}$  can have quadrupole moments. For this reason the rotational spectra of many linear organic molecules do not have resolvable hyperfine structure.

When there is nuclear hyperfine splitting of the rotational lines, it must be analyzed, and the hypothetical unsplit rotational frequencies corresponding to those which would occur if there were no nuclear splitting must be found before the preceding formulas are applied for calculation of the spectral constant  $B$  and the corresponding moment of inertia. Methods for analysis of the hyperfine structure are given in Chapter IX. Because of its rapid decrease with increase of  $J$ , the hyperfine splitting is frequently negligible for transitions observed at millimeter wave frequencies and almost always negligible for those observed in the submillimeter wave region.

The effect of nuclear isotopic substitution is to change the moment of inertia of the molecule and hence to shift all the rotational lines. Each isotopic species of a given molecule has a complete rotational spectrum that with microwave spectrometers can be easily resolved from that of other isotopic species except when the isotopic difference occurs only in an atom that happens to occur at,

or very near, the center of gravity of the molecule. The different isotopic species are very useful in the determination of the interatomic distances of polyatomic molecules from microwave spectroscopy. See Chapter XIII. The rotational transitions of an isotopic species have their particular rotational spectra and nuclear hyperfine structure, which must be analyzed separately.

## 2 LINE INTENSITIES

The formula for calculation of the rotational absorption coefficients of a linear polyatomic molecule is the same as that for a diatomic molecule (Chapter IV, Section 3). The molecule OCS is often used for tuning or monitoring of spectrometers. Furthermore, its dipole moment,  $B$  value, and other constants, upon which the absorption coefficient depends, are in the middle range of those of linear polyatomic molecules. As an example, we shall calculate the peak absorption coefficients of its microwave rotational lines for the ground vibrational state. For this purpose we apply (4.110), for which pressure-broadened lines are assumed to be in the range where the peak intensities are independent of pressure. In the computation it is more convenient to express  $\alpha_{\max}$  as a function of  $J$ . Hence we substitute  $v_0 = 2B(J+1)$  into (4.110) and obtain

$$\alpha_{\max} = X(J+1)^3 \left[ 1 - \frac{0.048B(J+1)}{T} \right] e^{-0.048BJ(J+1)/T} \quad (5.36)$$

where

$$X = \alpha_{\max}(0 \rightarrow 1) = \frac{3.95 \times 10^{-2} i_c F_v \mu^2 B^3}{(\Delta v)_1 T^2} \quad (5.37)$$

In this equation the spectral constant  $B$  is expressed in GHz (kilomegahertz), but the line breadth parameter  $(\Delta v)_1$  is in MHz per mm of Hg at 300°K. For OCS,  $B = 6.08$  GHz and  $(\Delta v)_1 = 6.44$  MHz. The isotopic concentration of the species is indicated by  $i_c$ . We shall choose  $T$  as 195°K, the temperature of dry ice. For  $^{16}\text{O}^{12}\text{C}^{32}\text{S}$  in its natural abundance,  $i_c = 0.94$ . The dipole moment  $\mu = 0.709$  D. There are three fundamental vibrational modes, but only the degenerate bending mode  $\omega_2 = 527 \text{ cm}^{-1}$  and the CS stretching mode  $\omega_1 = 859 \text{ cm}^{-1}$  have significant populations at  $T = 195^\circ\text{K}$ . The CO stretching mode  $\omega_3 = 2079 \text{ cm}^{-1}$ . Therefore the population of the ground vibrational state given by (3.56) for  $v = 0$  is

$$F_{v=0} = (1 - e^{-1.44\omega_1/T})^{d_1} (1 - e^{-1.44\omega_2/T})^{d_2} (1 - e^{-1.44\omega_3/T})^{d_3} = 0.96 \quad (5.38)$$

With these values

$$\alpha_{\max}(0 \rightarrow 1) = 1.65 \times 10^{-5} \text{ cm}^{-1}$$

and

$$\alpha_{\max}(\text{OCS}) = 1.65 \times 10^{-5} (J+1)^3 [1 - 15 \times 10^{-4} (J+1)] \times e^{-1.5 \times 10^{-4} J(J+1)} \quad (5.39)$$

This function is plotted in Fig. 5.4. The graph shows that OCS at dry-ice temperature has its strongest rotational absorption lines in the region of  $\lambda=0.77$  mm, for which  $J=31\rightarrow 32$ , approximately. The frequency for this strongest transition is  $\nu_{\text{opt}}=390$  GHz, and the absorption coefficient at the line peak  $\alpha_{\text{max}}(31\rightarrow 32)=1.15 \times 10^{-1} \text{ cm}^{-1}$ . In comparison with such a large absorption, the losses to the cell walls are negligible, and the power absorption fractional in a cell 20 cm in length is

$$\frac{P_{\text{abs}}}{P_0} = 1 - e^{-\alpha x} = 1 - e^{-2.3} = 0.90 \quad (5.40)$$

Thus, in the optimum region 90% of the power is absorbed in a cell only 20 cm in length. Although an absorption coefficient of  $1.65 \times 10^{-5} \text{ cm}^{-1}$  (that for the  $J=0\rightarrow 1$  line) can be detected easily with conventional microwave spectrometers, the  $J=0\rightarrow 1$  line of the isotopic species  $^{18}\text{OCS}$  in its natural abundance of 0.2% would have a peak absorption coefficient of only  $3.3 \times 10^{-8} \text{ cm}^{-1}$  and could be detected with only the more sensitive spectrometers. In the region of optimum absorption,  $\lambda=0.77$  mm, the peak absorption coefficient for this rare isotopic species is  $2.3 \times 10^{-4} \text{ cm}^{-1}$ , and the lines can be readily detected without isotopic concentration.

### Optimum Regions for Observations

Now that the microwave region has been extended well into the submillimeter wave region, it covers the frequency range where most molecules have their strongest rotational lines. With such coverage available, it is of advantage to know in what regions the different molecules have their optimum detectability. This is particularly desirable when one is searching for lines of molecules

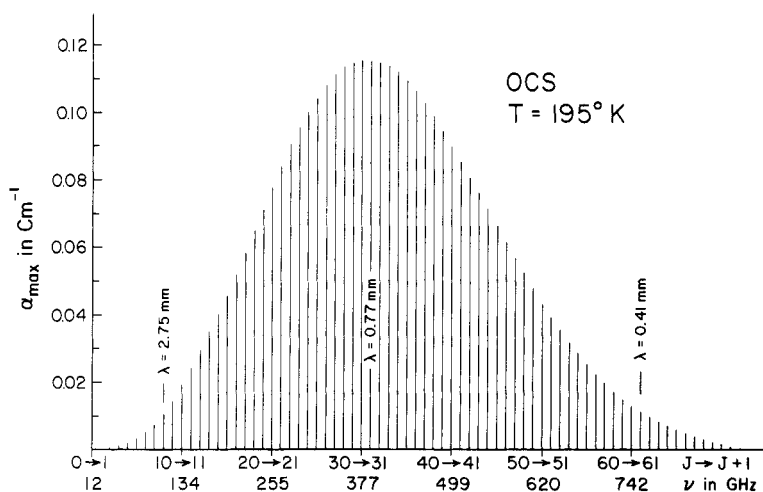


**Fig. 5.4** Theoretical peak absorption coefficients of rotational lines of OCS in the ground vibrational state.

with very small dipole moments, for lines of rare isotopic species, or for rotational lines of molecules in sparsely populated vibrational states. To find the  $J$  value of the strongest  $J \rightarrow J+1$  transition we differentiate  $\alpha_{\max}$  with respect to  $J$  in (5.36), set the derivative equal to zero, and solve for  $J$ . With the omission of some very small terms, the result is

$$J_{\text{opt}} \text{ (for strongest line)} \approx 5.5 \left( \frac{T \text{ (K}^{\circ})}{B \text{ (GHz)}} \right)^{1/2} \quad (5.41)$$

Having obtained  $J_{\text{opt}}$ , one can readily find the optimum frequency region from the relation

$$\nu \text{ (for strongest line)} = 2B(J_{\text{opt}} + 1) \quad (5.42)$$

It is apparent from examination of Table 5.4 and the similar one for symmetric-top molecules in Chapter VI that the optimum region for observation of most molecular rotational spectra is already accessible to the high-resolution, high-precision methods of microwave spectroscopy. Only the very lightest linear polyatomic molecules, HCN and HCP, have their greatest absorption coefficient in the infrared region, beyond the range of microwave spectrometers, and by observing these molecules at reduced temperatures one can shift their region of optimum absorption to the edge of the microwave region. Although one can obtain better resolution of nuclear hyperfine structure on low  $J$  transitions, which usually fall in the lower frequency microwave region, the optimum region for observation of microwave rotational spectra is that from about 5 to 0.5 mm wavelength.

**Table 5.4**  $J$  Transitions and Frequencies for Regions of Greatest Absorption Line Strengths of Linear Molecules at  $T = 300^{\circ}\text{K}$

Molecule	$B \text{ (GHz)}$	$J \rightarrow J+1$	$\nu_{\text{opt}} \text{ (GHz)}$	$\lambda_{\text{opt}} \text{ (mm)}$
HCN	44.31	14→15	1330	0.23
HCP	19.97	21→22	877	0.34
NNO	12.56	27→28	703	0.43
HCNO	11.47	28→29	665	0.45
FCN	10.55	29→30	634	0.47
HCCF	9.70	30→31	600	0.50
OCS	6.08	39→40	496	0.60
$^{35}\text{ClCN}$	5.97	39→40	478	0.63
HCC $^{35}\text{Cl}$	5.68	40→41	465	0.65
HCCCN	4.55	44→45	400	0.75
$^{79}\text{BrCN}$	4.12	47→48	394	0.76
OC $^{78}\text{Se}$	4.04	47→48	388	0.77
ICN	3.22	53→54	348	0.86
SCTe	1.56	76→77	240	1.25

### 3 MEASUREMENTS WITH SPECIAL HIGH-RESOLUTION TECHNIQUES

The Doppler-broadened line width, which increases directly with the transition frequency [see (3.39)], becomes an important factor in limiting the accuracy of transitions measured with conventional spectrometers at high frequencies. Three effective devices for circumventing effects of Doppler broadening are the molecular beam maser, the collimated molecular beam spectrometer, and the Lamb-dip method.

A section of the DCN spectrum in the shorter millimeter wave region, shown in Fig. 1.3, demonstrates the remarkable resolution of the beam maser. In an ordinary spectrometer, the well-resolved hyperfine structure of the deuterium, shown in this figure within a span of 100 kHz, would have been completely masked by Doppler broadening. The values of  $B_0$  and  $D_0$  for  $\text{H}^{12}\text{C}^{14}\text{N}$  that are obtained from these beam measurements [22] are listed later, in Table 5.7. The frequencies of the  $J=0 \leftarrow 1$  and  $1 \leftarrow 2$  transitions from which they are derived were measured to a precision of one part in  $10^8$ . The first HCN maser operation was achieved on the  $J=0 - 1$  transition by Marcuse [23], who did not use it for accurate measurement of the molecular constants.

A collimated molecular beam absorption spectrometer was developed [24, 25] in the early years of microwave spectroscopy for reduction of line broadening in the alkali halides at their high vaporization temperatures. Since that time, Dymanus and his associates at Nijmegen [26-28] have developed a Stark-modulation, molecular-beam absorption spectrometer that is operable for gases at ordinary or lowered temperatures. It has resolution comparable to that of the beam maser and offers the advantage of being simpler to operate.

Another effective means of combating the limitations to measurement caused by Doppler broadening is the Lamb-dip method [29-31]. It does not require collimated molecular beams, but it does require sufficient source power to saturate the molecules in the center of the Doppler-broadened line and an absorption cell in which the source power is so reflected as to pass through the absorbing molecules in opposite directions. A relatively simple qualitative explanation for the dip can be given. Because the molecules absorbing at the center of the Doppler band have zero velocity relative to that of the transmitted radiation, they absorb, at the same resonant frequency  $v_0$ , the power traveling in either the forward or the reverse direction. In contrast, molecules having a velocity  $v$  relative to the forward direction will have a velocity  $-v$  relative to the reverse direction and will thus absorb the forward and the reverse radiation at different frequencies,  $v_0 + \Delta v$  and  $v_0 - \Delta v$ , on opposite sides of the center frequency  $v_0$ . Thus the molecules absorbing at the center frequency  $v_0$  are subjected to twice as much resonant power as are those absorbing at slightly higher or slightly lower frequencies. If the power can be critically adjusted to saturate the molecules absorbing at the center of the band without complete saturation of those absorbing at frequencies on either side, the result is a "hole-burning" at the exact center of the band. The "burned hole," or Lamb dip, can

be used for precise measurement of the resonant frequency  $v_0$ . This effect is illustrated in Fig. 5.5 by the Lamb dip in a Doppler-broadened OCS line. Several rotational frequencies of OCS as measured with the method are listed in Table 5.5, together with the rotational constants derived from them. These measurements were made with a klystron-driven harmonic generator, a source

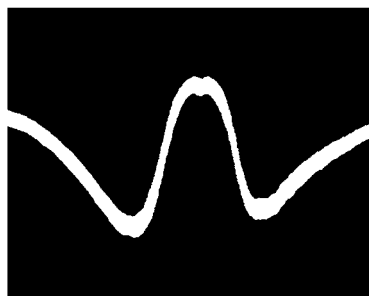


**Fig. 5.5** Lamb dip in the  $J=15 \rightarrow 16$  rotational line of OCS at 194,586.4333 MHz. The broad downward curve is the Fabry-Perot cavity resonance; the broad upward curve is the Doppler-broadened line (width about 310 kHz); the small, sharp depression at the center of the line is the Lamb dip (width about 10 kHz). From Winton and Gordy [31].

**Table 5.5** Ground-state Rotational Frequencies and Constants of  $^{16}\text{O}^{12}\text{C}^{32}\text{S}$  from Measurements of Lamb Dips<sup>a</sup>

$J^b$	Frequencies in MHz		
	Measured	Calculated	Difference
8	109,463.063	109,463.064	-0.001
9	121,624.638	121,624.638	0.000
10	133,785.900	133,785.900	0.000
11	145,946.821	145,946.818	+0.003
12	158,107.360	158,107.361	-0.001
13	170,267.494	170,267.498	-0.004
14	182,427.198	182,427.198	0.000
15	194,586.433	194,586.433	0.000
16	206,745.161	206,745.161	0.000
19	243,218.040	243,218.042	-0.002
20	255,374.461	255,374.460	+0.001

#### Molecular Constants in MHz

$$B_0 = 6081.49205 \pm 0.0002$$

$$D_J = (1.3008 \pm 0.0006) \times 10^{-3}$$

$$H_J = (-0.85 \pm 0.8) \times 10^{-9}$$

<sup>a</sup>From Winton and Gordy [31].

<sup>b</sup>Rotational quantum number for lower level.

of relatively low power; the saturation power was achieved through amplification with a high-*Q*, Fabry-Perot cell.

Cazzoli et al. [32] have used Lamb-dip spectroscopy to measure the first two rotational transitions of D<sup>12</sup>C<sup>15</sup>N. The Lamb dips of the D hyperfine structure are well resolved. The value they obtained for  $(eQq)_D$ , 0.207 MHz, compares favorably with 0.194 MHz, that from the beam maser experiments [22].

Microwave-microwave double resonance is becoming an increasingly important method, not only for ultra-high resolution, but also for special types of measurements, particularly for study of line shapes and molecular collision processes. Notable studies by Oka [33] and by Lees [34] have been made on the linear molecules HCN and OCS. These studies, the experimental techniques, and their potentialities are described in an excellent review by Baker [35].

## 4 OBSERVATIONS ON LINEAR TRIATOMIC MOLECULES

### Alkali Hydroxides

Through measurements of rotational transitions of KOH and CsOH vapors in a high-temperature microwave spectrometer, Kuczkowski et al. [36] gained the first evidence of the linear configuration of these molecules. This preliminary finding was confirmed by more complete measurements on RbOH and CsOH by Lide and his associates [37, 38], who obtained, with isotopic substitution, accurate values for the internuclear distances. The ground-state rotational constants and structures are given in Table 5.6. The dipole moments of these

**Table 5.6** Molecular Constants of Alkali Hydroxides

Hydroxide MOH	<i>B</i> <sub>0</sub> (MHz)	<i>D</i> <sub>0</sub> (kHz)	<i>r</i> <sub>0</sub> and <i>r</i> <sub>e</sub> (Å)	
			MO	OH
NaOH	12,567.054(10) <sup>a</sup>	28.72(5) <sup>b</sup>	<i>r</i> <sub>0</sub> 1.95 <sup>b</sup>	(0.96) <sup>b</sup>
<sup>39</sup> KOH	8,208.679(10) <sup>c</sup>	12.19(6) <sup>c</sup>	<i>r</i> <sub>0</sub> 2.212 <sup>c</sup>	0.912 <sup>c</sup>
<sup>39</sup> KOD	7,494.827(10) <sup>c</sup>	9.46(6) <sup>c</sup>	<i>r</i> <sub>e</sub> 2.200 <sup>d</sup>	0.968 <sup>d</sup>
<sup>85</sup> RbOH	6,290.10 <sup>e</sup>		<i>r</i> <sub>0</sub> 2.316 <sup>e</sup>	0.913 <sup>e</sup>
<sup>85</sup> RbOD	5,720.77 <sup>e</sup>		<i>r</i> <sub>e</sub> 2.301(2) <sup>f</sup>	0.957(10) <sup>f</sup>
CsOH	5,501.08 <sup>g</sup>		<i>r</i> <sub>0</sub> 2.403 <sup>g</sup>	0.920 <sup>g</sup>
CsOD	4,996.83 <sup>g</sup>		<i>r</i> <sub>e</sub> 2.391(2) <sup>f</sup>	0.960(10) <sup>f</sup>

<sup>a</sup>Pearson and Trueblood [39].

<sup>b</sup>Kuijpers et al. [42].

<sup>c</sup>Pearson and Trueblood [40].

<sup>d</sup>Pearson et al. [43].

<sup>e</sup>Matsumura and Lide [38].

<sup>f</sup>Lide and Matsumura [41].

<sup>g</sup>Lide and Kuczkowski [37].

structures are very high, 7.1 D for CsOH for example, indicating a completely ionic structure of the form  $\text{Cs}^+\text{O}^- \text{H}$ , as would be expected for the electronegativity differences of Cs and OH. Pearson and Trueblood [39, 40] made similarly thorough measurements on NaOH, KOH, and KOD. The accurate values they obtained for the ground-state constants are listed in Table 5.6. Other measurements on alkali hydroxides in several vibrational states have led to accurate values for the equilibrium structures and rotation-vibration interaction constants [41-43]. The  $r_e$  values are listed with the  $r_0$  values in Table 5.6 for all except NaOH. Generally, the  $r_e$  distances are found to be shorter than  $r_0$  for MO and longer than that for OH. A preliminary study with molecular-beam electric resonance [44] has been made on LiOH, but details apparently are not yet published. Its structure may not be linear.

### Boron Compounds

The millimeter wave spectra of several isotopic species of the unstable thioborine molecule HBS have been measured by Pearson and McCormick [45], who proved that the molecule has a linear structure. They obtained the accurate substitutional structure,  $r_s(\text{HB}) = 1.1692 \text{ \AA}$  and  $r_s(\text{SB}) = 1.5994 \text{ \AA}$ . They produced the HBS by causing the  $\text{H}_2\text{S}$  (or  $\text{D}_2\text{S}$ ) to flow over solid boron at  $1100^\circ\text{C}$  in a "free-space" hot cell. Afterward, microwave spectra were measured for four isotopic species of CIBS by Kirby and Kroto [46], who showed that it also has a linear structure, with  $r_s(\text{CIB}) = 1.681 \text{ \AA}$  and  $r_s(\text{BS}) = 1.606 \text{ \AA}$ .

### Cyanides and Phosphides

Table 5.7 displays the bond lengths and ground-state rotational constants for the most abundant isotopic species of some related cyanides and phosphides. Since the first observation [47] in 1948, hydrogen cyanide has been observed many times with millimeter wave spectroscopy; its ground-state rotational constants for the various isotopic combinations [48], including the tritium species [49], are accurately known. Those for its most abundant species, listed in Table 5.7, were measured precisely with a molecular beam maser. It was one of the earlier molecules to be detected with microwave spectroscopy in interstellar space [50], and it has proved to be very useful in various types of interstellar observations. It is responsible for the strong, much used, submillimeter maser source [51, 52] at 0.33 mm.

It is interesting to compare the lengths of the same bonds in the cyanides and phosphides of Table 5.7. The CF bond is significantly shorter in FCN than in FCP, primarily because of the greater conjugation of the single and triple bonds formed with the first-row elements. This conjugation, which may be represented as contribution of valence structures of the form  $\text{F}^+ \equiv \text{C}=\text{N}^-$ , has much more influence in shortening the single bond than in lengthening the triple bond. The CN length of FCN is only slightly longer than that of HCN. Note that the lengths of the CN bonds in all the cyanides listed are quite close, as are the CP lengths also. There is, of course, considerable conjugation of the bonds in FCP, although less than in FCN. With no such conjugation, the FC

**Table 5.7** Rotational Constants and Bond Lengths of Some Linear Cyanides and Phosphides for the Ground Vibrational State and the Most Abundant Isotopic Species

Bond Lengths (Å)	$B_0$ (MHz)	$D_0$ (kHz)	Ref.
H— <sup>1.063</sup> C— <sup>1.155</sup> N	44,315.9757(4)	87.24(6)	<sup>a</sup>
H— <sup>0.987</sup> N— <sup>1.171</sup> C	45,332.005(40)	101.9(50)	<sup>b</sup>
H— <sup>1.067</sup> C— <sup>1.542</sup> P	19,976.005(9)	21.23(10)	<sup>c,d</sup>
F— <sup>1.262</sup> C— <sup>1.159</sup> N	10,554.20(2)	5.3(5)	<sup>e</sup>
F— <sup>1.285</sup> C— <sup>1.541</sup> P	5,257.80(3)	1.0	<sup>f</sup>
N— <sup>1.159</sup> C— <sup>1.378</sup> C— <sup>1.544</sup> P	2,704.4803(19)	0.216(13)	<sup>g</sup>

<sup>a</sup>De Lucia and Gordy [22].

<sup>b</sup>Creswell et al. [53]; also, Pearson et al. [48].

<sup>c</sup>J. W. C. Johns, J. M. R. Stone, and G. Winnewisser, *J. Mol. Spectrosc.*, **38**, 437 (1971).

<sup>d</sup>J. K. Tyler, *J. Chem. Phys.*, **40**, 1170 (1964).

<sup>e</sup>J. K. Tyler and J. Sheridan, *Trans. Faraday Soc.*, **59**, 2661 (1963).

<sup>f</sup>Kroto et al. [9].

<sup>g</sup>T. A. Cooper, H. W. Kroto, J. F. Nixon, and O. Ohashi, *J. Chem. Soc., Chem. Commun.*, No. 8, 333 (1980).

bond would be much longer than 1.285 Å; the CF single-bond length in  $\text{CH}_3\text{F}$  is 1.38 Å. Without reduction by contributions from structures of the form  $\text{F}^+=\text{C}=\text{P}^-$ , the dipole moment of FCP would be expected to be appreciably larger than the observed value [9] of 0.279 D.

### Hydrogen Isocyanide HNC

Not until 1976 was the microwave rotational spectrum of HNC, hydrogen isocyanide observed in the laboratory [53–55], and that only after this elusive species had been discovered six years earlier in interstellar space through observation of its  $J=0 \rightarrow 1$  transition [56, 57] with a rest frequency of 90,663.9 MHz and tentative identification of the line by use of a theoretically calculated structure [58]. Although the series  $\text{CH}_3\text{NC}$ ,  $\text{C}_2\text{H}_5\text{NC}$ , and so on, are commonly known chemicals studied in the gas phase by microwave spectroscopy, the first evidence for the existence of HNC was the infrared spectral observation by Milligan and Jacox [59] made in 1963 on photolized methylazide in an argon matrix at 4°K. Creswell et al. [53] measured the  $J=0 \rightarrow 1$  and  $1 \rightarrow 2$  rotational transitions of HNC, DNC, and  $\text{HN}^{13}\text{C}$ ; they obtained precise values of the ground-state rotational constants and structural parameters. The  $J=0 \rightarrow 1$  line was measured at 90,663.602 MHz, thus providing experimental confirmation of the correct assignment of 90,663.9(5) MHz as the rest frequency of HNC in the earlier radio-astronomical observation. Pearson et al. [48] extended the laboratory observations to the  $J=2 \rightarrow 3$  transitions and included species containing the  $^{13}\text{C}$  isotope. The constants of HNC are recorded in Table 5.7.

## 5 LONG LINEAR MOLECULES ON EARTH AND IN OUTER SPACE

Much interest in long linear molecules has been generated by the discovery with microwave spectroscopy of carbon-chain cyanides in interstellar space. The ground-state rotational constants and bond lengths for these cyanides, as derived from spectral measurements in the laboratory, are listed in Table 5.8. The constants of HCN are repeated for comparison.

All molecules listed in Table 5.8 have been observed in interstellar space. The longest of them,  $\text{HC}_9\text{N}$  and  $\text{HC}_{11}\text{N}$ , have been observed only in interstellar space. Detection of their microwave rotational lines and their assignment were achieved by means of a theoretical model based on the projections of the measured constants of the preceding members of the  $\text{HC}_n\text{N}$  series recorded in Table 5.8. Because of the orderliness of this sequence, the projections proved reliable and provided a close fitting of the interstellar lines observed. The lines of  $\text{HC}_9\text{N}$  and  $\text{HC}_{11}\text{N}$  from outer space are very weak. To this time, it is the longest molecule to be observed in outer space. Whether either of these mole-

**Table 5.8** Rotational Constants and Bond Lengths of Some Linear  $\text{HC}_n\text{N}$  Molecules for their Ground Vibrational States and Most Abundant Isotopic Species

$\text{HC}_n\text{N}$	$B_0$ (MHz)	$D_0$ (kHz)	Ref.
HCN	44,315.9757(4)	87.24(6)	<sup>a</sup>
$\text{HC}_3\text{N}$	4,549.0579(4)	0.54311(45)	<sup>b</sup>
$\text{HC}_5\text{N}$	1,331.332714(46)	0.0301016(58)	<sup>c,d</sup>
$\text{HC}_7\text{N}$	564.00074(16)	0.003821(87)	<sup>e</sup>
$\text{HC}_9\text{N}$ (Detected only in interstellar space)			<sup>f</sup>
$\text{HC}_{11}\text{N}$ (Detected only in interstellar space)			<sup>g</sup>
Bond Lengths in Å			
H—C≡N	1.0631 1.155		<sup>h</sup>
H—C≡C—C≡N	1.058 1.205 1.378 1.159		<sup>i</sup>
H—C≡C—C≡C—C≡N	1.0569 1.2087 1.3623 1.2223 1.3636 1.1606		<sup>d</sup>
H—C≡C—C≡C—C≡C—C≡N	1.0569 1.2087 1.3623 1.2223 1.348 1.2223 1.3636 1.1606		<sup>e</sup>

<sup>a</sup>De Lucia and Gordy [22].

<sup>b</sup>R. A. Creswell, G. Winnewisser, and M. C. L. Gerry, *J. Mol. Spectrosc.*, **65**, 4201 (1977).

<sup>c</sup>M. Winnewisser, *J. Chem. Soc., Faraday Discussions* **71**, 1 (1981).

<sup>d</sup>Alexander et al. [63].

<sup>e</sup>Kirby et al. [64].

<sup>f</sup>Broton et al. [60].

<sup>g</sup>M. B. Bell, P. A. Feldman, S. Kwok, and H. E. Matthews, *Nature*, **295**, 399 (1982).

<sup>h</sup>G. Winnewisser, A. H. Maki, and D. R. Johnson, *J. Mol. Spectrosc.*, **39**, 149 (1971).

<sup>i</sup>J. K. Tyler and J. Sheridan, *Trans. Faraday Society*, **59**, 266 (1963).

cules is sufficiently stable under achievable earth conditions to be observed in an absorption cell in a laboratory seems problematical.

Broten et al. [60], who detected the  $\text{HC}_9\text{N}$ , speculate on the possibility of detection in interstellar space of still longer members of the chain, to  $\text{HC}_{13}\text{N}$ , and conclude that this would be extremely difficult with the equipment presently available. The highly significant discoveries of the long molecules,  $\text{HC}_5\text{N}$ ,  $\text{HC}_7\text{N}$ , and  $\text{HC}_9\text{N}$ , in outer space [60–62] have resulted from a fortunate collaboration between Oka et al., of the Herzberg Institute in Ottawa, and Kroto et al., at the University of Sussex. The laboratory synthesis and measurement of  $\text{HC}_5\text{N}$  and  $\text{HC}_7\text{N}$  by the Kroto group greatly aided the astronomical observations. The shorter members of this series,  $\text{HCN}$  and  $\text{HC}_3\text{N}$ , were among the first molecules to be discovered in interstellar space [50, 65]. Their discovery was aided by the frequencies that were accurately known from previous measurements in the laboratory.

Although rotational transitions in highly excited bending vibrational states of the long, linear molecules  $\text{HC}_n\text{N}$  are observed in the laboratory, only transitions of the ground vibrational state were detected for molecules in the cold interstellar spaces. Like most other lines of interstellar molecules, those of the long-chain cyanides were observed through maser emission. The mechanisms of the required population inversion of the rotational states are not certain, but collisional interactions and radiative transfer are possible causes [66]. The mechanisms of formation of such long-chain molecules in outer space and their role in the history of the evolving universe are challenging problems.

The microwave rotational spectrum of the rather long molecule  $\text{O}=\text{C}=\text{C}=\text{S}$  (tricarbon oxide sulfide) has been measured for the first time by Winnewisser and Christiansen [67]. Their measurements prove that its structure is strictly linear, in contrast to the similar molecule  $\text{OCCCO}$ , which is quasi-linear (see Section 7). Rotational constants for the ground vibrational state and most abundant isotopic combination are  $B_0 = 1,413.898$  MHz and  $D_0 = 0.046$  kHz. A later study [68] of the molecule in excited bending states yielded the equilibrium constants:  $B_e = 1,407.230$  MHz and  $D_e = 0.0347$  kHz. Values for  $q$ ,  $\gamma$ , and  $x_{ll}$  were also obtained. The dipole moment for the ground state was found to be 0.662 D. Knowledge of these constants should be helpful in the search for this long molecule in interstellar space.

## 6 EQUILIBRIUM STRUCTURES

An important objective for measurement of the rotational structure of excited vibrational states is to obtain the equilibrium structures of the molecule. Descriptions of the various types of structures of polyatomic molecules—equilibrium,  $r_e$ , ground state,  $r_0$ , substitutional,  $r_s$ , and so on—and methods for their calculation from the spectral measurements are described in Chapter XIII. Although it is not particularly difficult to obtain equilibrium structures for diatomic molecules, the measurements required for even the simplest polyatomic molecules are an order of magnitude greater. Nevertheless, many

accurate equilibrium structures have now been obtained for linear triatomic molecules, most of them since the earlier edition of this book in 1970. The progress is accelerating partly because of the improved sensitivity and the increased frequency range of microwave spectrometers and partly because of new techniques for excitation of the higher vibrational states.

Since there are two independent structural parameters of nonsymmetrical linear triatomic molecules, measurements on two isotopic species are required for determination of their structures. For calculation of  $r_e$  structures, the  $B_e$  value for each of these species is required. To obtain each  $B_e$  value, one must measure rotational transitions in excited levels of each of the three fundamental vibrational modes and over a sufficient frequency range for evaluation of the centrifugal distortions. Theoretically, only the lowest excited levels must be measured, but for greater accuracy, especially where there are Fermi resonances or other complications, it is desirable to make more extended measurements. Also, it is desirable for a consistency test to include more than one isotopic pair.

The minimum of data for giving accurate  $B_e$  values of the two isotopic species necessary for evaluation of the equilibrium structures of a linear triatomic molecule is illustrated by the constants of ICN in Table 5.9. Although accurate measurements on excited  $v_1$  and  $v_2$  states of ICN were measured in 1972 by Simpson et al. [69], the necessary measurements on an excited level of  $v_3$ , which corresponds to the CN vibration, were accomplished much later, in 1978, by Cazzoli et al. [70], who excited the  $v_3$  states by energy transfer from activated N<sub>2</sub>.

Equilibrium structures for ICN and a few other linear triatomic molecules are given in Table 5.10 as an illustration of the accuracy obtainable. Even though considerable microwave data were available, some data from infrared rotation-vibration spectra were included in the solutions for HCN and OCS. The degree of consistency of the derivations for different isotopic combinations of OCSe is illustrated in Table 5.11.

**Table 5.9** Equilibrium Constants for ICN<sup>a</sup>

Constants	I <sup>12</sup> C <sup>14</sup> N	I <sup>13</sup> C <sup>14</sup> N
$B_e$ (MHz)	3229.159(6)	3180.674(6)
$\alpha_1$	11.895(4) <sup>b</sup>	11.634(5)
$\alpha_2$	-9.497(2) <sup>b</sup>	-8.861(3)
$\alpha_3$	14.332(7)	13.353(5)
$D_e$ (kHz)	0.587(27)	0.570(9)
$\beta_1$	0.022 <sup>b</sup>	0.028
$\beta_2$	0.011 <sup>b</sup>	0.008
$\beta_3$	-0.040	-0.021

<sup>a</sup>Cazzoli et al. [70].

<sup>b</sup>Simpson et al. [69].

**Table 5.10** Examples of Equilibrium Structures of Linear Triatomic Molecules

Molecule XYZ	Equilibrium Distance		Ref.
	$r_e(XY)$	$r_e(YZ)$	
HCN	1.06549(24)	1.15321(5)	<sup>a</sup>
ICN	1.99209(22)	1.16044(33)	<sup>b</sup>
OCS	1.15446	1.56295	<sup>c</sup>
OCSe	1.1535(1)	1.7098(1)	<sup>d</sup>

<sup>a</sup>G. Winnewisser, A. G. Maki, and R. D. Johnson, *J. Mol. Spectrosc.*, **39**, 149 (1971).

<sup>b</sup>Cazzoli *et al.* [70].

<sup>c</sup>Y. Morino and T. Nakagawa, *J. Mol. Spectrosc.*, **26**, 496 (1968).

<sup>d</sup>A. G. Maki, R. L. Sams, and R. Pearson, Jr., *J. Mol. Spectrosc.*, **64**, 452 (1977).

**Table 5.11** Equilibrium Structures for Carbonyl Selenide as Derived from Various Isotopic Pairs<sup>a</sup>

Isotopic Pairs	$r_e(\text{C}-\text{O}) (\text{\AA})$	$r_e(\text{C}-\text{Se}) (\text{\AA})$
$r_e(^{18}\text{O}^{12}\text{C}^{80}\text{Se}-^{16}\text{O}^{13}\text{C}^{80}\text{Se})^b$	1.15347(4)	1.70978(3)
$r_e(^{18}\text{O}^{12}\text{C}^{80}\text{Se}-^{16}\text{O}^{12}\text{C}^{80}\text{Se})^b$	1.15333(21)	1.70989(16)
$r_e(^{16}\text{O}^{12}\text{C}^{80}\text{Se}-^{16}\text{O}^{13}\text{C}^{80}\text{Se})^b$	1.15372(36)	1.70960(26)
$r_e(^{18}\text{O}^{12}\text{C}^{80}\text{Se}-^{16}\text{O}^{13}\text{C}^{80}\text{Se})^c$	1.15341(4)	1.70971(3)
$r_e(^{18}\text{O}^{12}\text{C}^{80}\text{Se}-^{16}\text{O}^{12}\text{C}^{80}\text{Se})^c$	1.15356(23)	1.70959(18)
$r_e(^{16}\text{O}^{12}\text{C}^{80}\text{Se}-^{16}\text{O}^{13}\text{C}^{80}\text{Se})^c$	1.15313(40)	1.70991(29)

<sup>a</sup>From A. G. Maki, R. L. Sams, and R. Pearson, *J. Mol. Spectrosc.*, **64**, 452 (1977).

<sup>b</sup>Excited states used: (10<sup>0</sup>0, 01<sup>1</sup>0, 00<sup>0</sup>1).

<sup>c</sup>Excited states used: (10<sup>0</sup>0, 02<sup>0</sup>0, 00<sup>0</sup>1).

Equilibrium structures have now been obtained for most of the alkali hydroxides. Their  $r_e$  values are given in Table 5.6, where they are compared with the ground state structures,  $r_0$ .

## 7 QUASI-LINEAR MOLECULES

The quasi-linear characterization of certain molecules apparently was made first by Thorson and Nakagawa [71] in 1960. They based their criteria for quasi linearity on a theoretical model of a two-dimensional harmonic oscillator with a superimposed barrier at the minimum of the harmonic potential. Specifically, the model was designed to simulate deviation in the behavior of a triatomic

linear molecule when barriers of different heights are superimposed at the minimum of the bending potential. A computer program was made for calculation of the energy levels, eigenfunctions, dipole transition moments, and other significant properties as a function of the imposed barrier heights. Not surprisingly, Thorson and Nakagawa found that in the high barrier limit the calculated properties are those of a nonlinear, or bent, triatomic molecule. However, the calculations for the low-to-moderate barriers and those for anharmonic vibrations in a well with no barrier, revealed properties that could not be assigned either to bent or to strictly linear molecules. They concluded that certain molecules cannot be correctly classified as either bent or linear and are best classified as quasi-linear molecules. Their theory has been applied by Johns [72] to HCN in an excited bending state and to certain bent triatomic molecules such as  $\text{H}_2\text{O}$  in their lowest bending state. He found that the effects of quasi linearity give rise to large anharmonicities in the bending vibrations.

Yamada and M. Winnewisser [73] have proposed a relatively simple test for quasi linearity which is based on the degree of separation of the coordinates of the rotational and vibrational motions in the Born-Oppenheimer approximation [74]. The degree of separation required by the approximation is based on the ratio of the differences of the rotational energy levels  $\Delta E_r$ , and those of the vibrational levels  $\Delta E_v$ , and is approximately

$$\frac{\Delta E_r}{\Delta E_v} \sim \sqrt{\frac{m_e}{m_p}} \approx 10^{-2} \quad (5.43)$$

where  $m_e$  and  $m_p$  signify electron and proton masses. Yamada and Winnewisser label the energy ratio as

$$\gamma = \frac{\Delta E_r}{\Delta E_v} \quad (5.44)$$

and show that the parameter  $\gamma_0$  as defined by

$$\gamma_0 = 1 - 4\gamma \quad (5.45)$$

is a measure of quasi linearity when the  $\Delta E_r$  and  $\Delta E_v$  are properly chosen.

The proposed relationship is suggested by consideration of the limiting cases of the ideal linear molecule and the ideal bent molecule. In an ideal linear molecule the coordinates of one of the three rotational degrees of freedom is not separable from those of the bending vibrations, with the result that a completely linear molecule has only two rotational degrees of freedom. In contrast, an ideal bent molecule has three rotational degrees of freedom; that is, the rotational coordinates are completely separable from the coordinates for vibration. The parameter  $\gamma_0$ , defined by (5.45), gives a measure of the allowed departure of "well-behaved" molecules from these ideal cases.

An ideal bent molecule has  $A \ll v_{\text{bend}}$  and  $\gamma \approx 0$ ; consequently, from (5.46),  $\gamma_0 \approx 1$ . An ideal linear molecule, which conforms to the harmonic approximation of a two-dimensional isotropic oscillator, has  $E(02^00) = 2E(01^10)$ ; thus from (5.47)  $\gamma = \frac{1}{2}$ . Likewise, (5.46) gives  $\gamma = \frac{1}{2}$  for this case. With this  $\gamma$  value, (5.45) gives  $\gamma_0 = -1$  for the idealized linear molecule.

## Chapter VI

# SYMMETRIC-TOP MOLECULES

---

1	MOLECULES IN THE GROUND VIBRATIONAL STATE	175
	The Rigid Rotor Approximation	175
	The Distortable Rotor	177
2	MOLECULES IN EXCITED VIBRATIONAL STATES	182
3	MOLECULAR INVERSIONS	187
4	"FORBIDDEN" ROTATIONAL TRANSITIONS	194
	Molecules with $C_{3v}$ Symmetry	196
	Avoided-crossing, Molecular Beam Resonance Method for Measurement of <i>K</i> -level Separations	202
	Tetrahedral, Spherical-top Molecules	205
5	LINE INTENSITIES	208
	Optimum Regions for Detection of Symmetric-top Rotational Spectra	212
6	MOLECULAR STRUCTURES	213
	Ground-state Structures	213
	Equilibrium Structures	216
	Hydrogen-bonded Symmetric-top Complexes	221

A molecule in which two of the principal moments of inertia are equal is a symmetric-top rotor. This condition is generally met when the molecule has an axis of symmetry that is trigonal or greater. The molecules PH<sub>3</sub>, CH<sub>3</sub>F, CH<sub>3</sub>CCH, CH<sub>3</sub>SiH<sub>3</sub>, and CF<sub>3</sub>SF<sub>5</sub> are examples of symmetric-top molecules. A linear molecule can be treated as a special case of a symmetric top in which the angular momentum about the symmetry axis is zero. The rotational energies of the symmetric-top molecule were calculated first by Dennison [1] with matrix mechanical methods and later by Reiche and Rademacher [2] and by Kronig and Rabi [3] with the Schrödinger wave equation.

## 1 MOLECULES IN THE GROUND VIBRATIONAL STATE

### The Rigid Rotor Approximation

The classical mechanics of the symmetric top is discussed in Chapter II, Section 1. Classically, the molecule rotates about the symmetry axis while this

axis in turn precesses about a fixed direction in space corresponding to the direction of the total angular momentum  $\mathbf{P}$ . This motion is illustrated by Fig. 6.1.

In a symmetric top, one of the principal axes of inertia must lie along the molecular axis of symmetry. The principal moments of inertia which have their axes perpendicular to this axis are equal. If  $a$ , the axis of least moment of inertia ( $I_a < I_b = I_c$ ), lies along the symmetry axis, the molecule is a prolate symmetric top ( $\text{CH}_3\text{CCH}$ , for example). If  $c$ , the axis of the greatest moment of inertia ( $I_a = I_b < I_c$ ), lies along the symmetry axis, the molecule is an oblate symmetric top ( $\text{BCl}_3$ , for example). Most of the symmetric-top molecules observed in the microwave region are prolate. With the  $a$  axis chosen along the symmetry axis ( $I_c = I_b$ ) and with  $P^2 = P_a^2 + P_b^2 + P_c^2$ , the Hamiltonian operator of (2.17) may be expressed as

$$\mathcal{H}_r = \frac{P^2}{2I_b} + \frac{1}{2} \left( \frac{1}{I_a} - \frac{1}{I_b} \right) P_a^2 \quad (6.1)$$

Eigenvalues for the angular momentum operators  $P^2$ ,  $P_z$ , and  $P_z$  for the symmetric-top rotor (Chapter II, Section 2) are

$$(J, K, M | P^2 | J, K, M) = \hbar^2 J(J+1) \quad (6.2)$$

$$(J, K, M | P_z | J, K, M) = \hbar K \quad (6.3)$$

$$(J, K, M | P_z | J, K, M) = \hbar M \quad (6.4)$$

where

$$J = 0, 1, 2, 3, \dots$$

$$K = 0, \pm 1, \pm 2, \pm 3, \dots, \pm J$$

$$M = 0, \pm 1, \pm 2, \pm 3, \dots, \pm J$$

In the  $x, y, z$  system,  $z$  is chosen as the symmetry axis of the top. In the  $a, b, c$  system used here for designation of the principal axes of inertia,  $z$  becomes  $a$

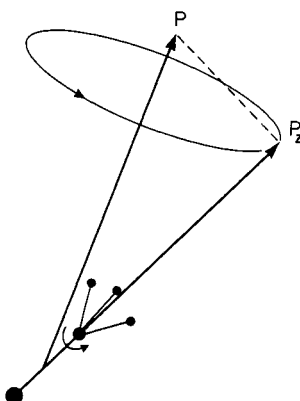


Fig. 6.1 Vector diagram of a symmetric rotor.

for the prolate top, and  $z$  becomes  $c$  for the oblate top. In the field-free rotor, the rotational energies do not depend on  $M$ . It is evident that the Hamiltonian of (6.1) commutes with  $P^2$  and  $P_a$  and is therefore diagonal in the  $J, K$  representation. Its eigenvalues, which are the quantized rotational energies of the rigid prolate symmetric top, are therefore

$$\begin{aligned} E_{J,K} &= (J, K | \mathcal{H}_r | J, K) = \frac{1}{2I_b} (J, K | P^2 | J, K) + \frac{1}{2} \left( \frac{1}{I_a} - \frac{1}{I_b} \right) (J, K | P_a^2 | J, K) \\ &= \left( \frac{\hbar^2}{8\pi^2 I_b} \right) J(J+1) + \left( \frac{\hbar^2}{8\pi^2} \right) \left( \frac{1}{I_a} - \frac{1}{I_b} \right) K^2 \end{aligned} \quad (6.5)$$

With the designation  $A = \hbar/(8\pi^2 I_a)$  and  $B = \hbar/(8\pi^2 I_b)$ ,  $E_{J,K}$  can be written

$$E_{J,K} = \hbar [BJ(J+1) + (A-B)K^2] \quad (6.6)$$

Since  $P_a$  is a component of  $P$ , the values of  $K$  cannot exceed those of  $J$  in magnitude. Although  $K$  can have both negative and positive values, the  $+$  and  $-$  values do not lead to separate sets of energy levels because  $K$  appears only as a squared term in (6.6). Thus all  $K$  levels except those for  $K=0$  are doubly degenerate. This  $K$  degeneracy cannot be removed by either external or internal fields. In addition to the  $K$  degeneracy, there is a  $(2J+1)$ ,  $M$  degeneracy in the field-free symmetric rotor as in the linear molecule. Unlike the  $K$  degeneracy, the  $M$  degeneracy can be lifted completely by the application of an external electric or magnetic field (see Chapters X and XI).

In a true symmetric top, any permanent dipole moment must of necessity lie along the symmetry axis. All matrix elements of this dipole moment resolved along a space-fixed axis vanish except those between states corresponding to  $J \rightarrow J$  or  $J \pm 1$ ,  $K \rightarrow K$ . See Chapter II, Section 6. The selection rules for the field-free rotor are therefore

$$\Delta J = 0, \pm 1 \quad \Delta K = 0 \quad (6.7)$$

The rule corresponding to absorption of radiation is  $J \rightarrow J+1$  and  $K \rightarrow K$ . Application of these rules to (6.6) gives the formula for the absorption frequencies for the rigid symmetric top

$$\nu = 2B(J+1) \quad (6.8)$$

which is exactly that for the linear molecule. However, as we shall see below, centrifugal stretching separates the lines corresponding to different  $|K|$  by small frequency differences which are usually sufficient to make these lines resolvable in the microwave region.

### The Distortable Rotor

Centrifugal stretching is treated as a perturbation on the eigenstates of the rigid rotor. If  $\mathcal{H}_r$  represents the Hamiltonian of the rigid rotor and  $\mathcal{H}_d$  represents that of the distortional energy, the rotational Hamiltonian is

$$\mathcal{H} = \mathcal{H}_r + \mathcal{H}_d \quad (6.9)$$

In Chapter VIII it is shown that the centrifugal distortion Hamiltonian has the form

$$\mathcal{H}_d = \frac{\hbar^4}{4} \sum_{\alpha\beta\gamma\delta} \tau_{\alpha\beta\gamma\delta} P_\alpha P_\beta P_\gamma P_\delta \quad (6.10)$$

where  $\alpha, \beta, \gamma, \delta$  represent the principal coordinate axes of the moments of inertia and where each must be summed over all three coordinate axes. However, in the first-order perturbation treatment, the terms with odd powers in any angular momentum which occur in the sum average to zero. Furthermore, by use of the angular momenta commutation rules and the fact that many of the  $\tau$ 's are equal, the Hamiltonian can be further simplified. This is discussed in Chapter VIII. For the first-order treatment, which is adequate for the usual microwave measurements, the Hamiltonian can be written as

$$\begin{aligned} \mathcal{H}_d^{(1)} &= \frac{1}{4} \sum \tau'_{\alpha\alpha\beta\beta} P_\alpha^2 P_\beta^2 \\ &= \frac{1}{4} [\tau'_{xxxx} P_x^4 + \tau'_{yyyy} P_y^4 + \tau'_{zzzz} P_z^4 + \tau'_{xxyy} (P_x^2 P_y^2 + P_y^2 P_x^2) \\ &\quad + \tau'_{xxzz} (P_x^2 P_z^2 + P_z^2 P_x^2) + \tau'_{yyzz} (P_y^2 P_z^2 + P_z^2 P_y^2)] \end{aligned} \quad (6.11)$$

in which  $x, y, z$  represent the principal axes and  $z$  represents the symmetry axis of the top. The  $\tau'$ 's are defined in Table 8.4. To first order, the distortion energy is

$$E_d^{(1)} = \langle J, K | \mathcal{H}_d^{(1)} | J, K \rangle \quad (6.12)$$

With the angular momentum matrix elements given in Table 8.19, this expression can be evaluated readily. The resulting expression can be condensed because of the fact that for the symmetric top certain of the coefficients  $\tau'$  are equal, that is,  $\tau'_{xxxx} = \tau'_{xxyy} = \tau'_{yyyy}$ . Therefore, the terms which contain contributions from  $\langle P_x^4 \rangle$  and  $\langle P_y^4 \rangle$  which are not simple functions of  $P^2$  and  $K^2$  cancel with those from  $\langle P_x^2 P_y^2 + P_y^2 P_x^2 \rangle$ . The nonvanishing terms can be combined in an expression of the form

$$E_d^{(1)} = -h[D_J J^2 (J+1)^2 + D_{JK} J(J+1)K^2 + D_K K^4] \quad (6.13)$$

in which the  $D_J$ ,  $D_{JK}$ , and  $D_K$  are the usual first-order centrifugal stretching constants of the symmetric-top molecule expressed in frequency units. The  $D$ 's obviously represent a combination of the  $\tau$ 's. For molecules of  $C_{3v}$  symmetry, expressions of the centrifugal stretching constants in terms of  $\tau$ 's are given in Table 8.11 and 8.12.

Addition of  $E_d^{(1)}$  to the rigid rotor values of (6.6) gives the usual expression for the rotational energy of the nonrigid prolate symmetric-top molecule

$$E_{J,K} = h[B_0 J(J+1) + (A_0 - B_0)K^2 - D_J J^2 (J+1)^2 - D_{JK} J(J+1)K^2 + D_K K^4] \quad (6.14)$$

For the oblate symmetric top, the expression in the parentheses of the second term becomes  $(C - B)$  instead of  $(A - B)$ . With the selection rules  $J \rightarrow J+1$ ,

$K \rightarrow K$ , this equation gives the rotational frequencies as

$$\nu = 2B_0(J+1) - 4D_J(J+1)^3 - 2D_{JK}(J+1)K^2 \quad (6.15)$$

This frequency equation holds for both the prolate and the oblate tops. Note that neither the second nor the last term in the energy expression of (6.14) influences the pure rotational frequencies. These terms involve only rotation about the symmetry axis. The last term of (6.15) splits the rotational transition into  $J+1$  closely spaced components whose separation increases as  $K^2$ .

The next higher order correction for centrifugal stretching leads to the expression

$$\begin{aligned} \nu = & h\{2B_0(J+1) - 4D_J(J+1)^3 - 2D_{JK}(J+1)K^2 \\ & + H_J(J+1)^3[(J+2)^3 - J^3] + 4H_{JK}(J+1)^3K^2 + 2H_{KJ}(J+1)K^4\} \end{aligned} \quad (6.16)$$

for the ground-state rotational frequencies of symmetric-top molecules. The first-order expression, (6.15), has been found entirely adequate for most measurements. Small, higher-order terms have been detected in a few cases [4, 5].

Figure 6.2 indicates the appearance of the first few rotational transitions of a symmetric-top molecule. The  $K$  splitting is greatly exaggerated. Figure 6.3 shows the  $K$  lines of the  $J=8 \rightarrow 9$  transition of  $\text{CF}_3\text{H}$ . Generally, pyramidal molecules such as  $\text{NH}_3$  and  $\text{PH}_3$  have  $D_{JK}$  negative so that the lines of a given  $J$  transition occur at higher frequencies as  $K$  increases, whereas those for which the symmetrical group occurs on the end of a linear group, such as  $\text{CH}_3\text{CN}$  and  $\text{CH}_3\text{CCH}$ , have  $D_{JK}$  positive and have the lines of increasing  $K$  falling at lower frequencies. Those such as  $\text{CF}_3\text{H}$  (shown in Fig. 6.3) and  $\text{CCl}_3\text{H}$ , which have a heavy symmetrical group and the light H atom attached to a central carbon, have negative  $D_{JK}$  like the pyramidal molecules, whereas those with the lighter H atoms forming the symmetrical group of  $\text{CH}_3\text{F}$ ,  $\text{CH}_3\text{Cl}$ , and so on, have  $D_{JK}$  positive. The values of  $B_0$ , of  $D_J$ , and of  $D_{JK}$  for selected molecules of different types are compared in Table 6.1. For all types,  $D_J$  is positive; therefore the  $D_J$  term shifts the different  $J$  transitions to lower frequencies.

The centrifugal stretching constants of symmetric-top molecules are related to the bond force constants and fundamental vibrational frequencies, but the

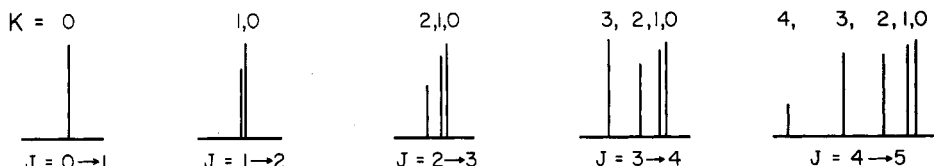
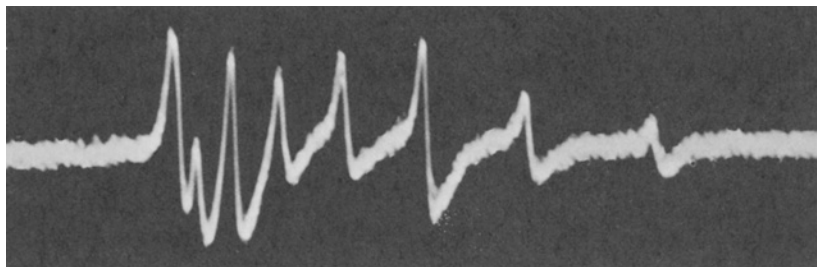
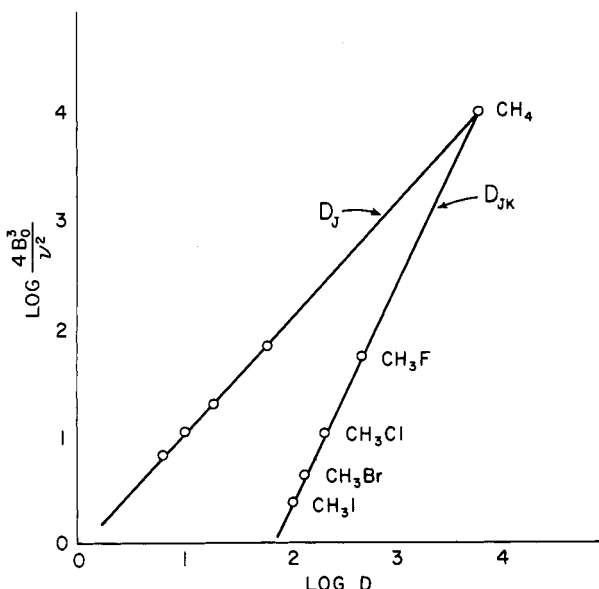


Fig. 6.2 Diagram indicating the general appearance of the rotational spectrum of a symmetric-top molecule. The lines of different  $K$  for the same  $J$  transition are separated by centrifugal distortion. This separation is extremely small compared with the separation of the different  $J$  transitions.



**Fig. 6.3** Cathode ray display of the eight  $K$  lines of the  $J=8\rightarrow 9$  transition of  $\text{CF}_3\text{H}$  occurring at  $\lambda=1.61$  mm. The centrifugal distortion constant  $D_{JK}$  is negative ( $-18$  kHz) so that the higher  $K$  components fall at higher frequencies to the right. The total frequency spread of the multiplet is 21 MHz. From C. A. Burrus and W. Gordy, *J. Chem. Phys.* **26**, 391 (1957).



**Fig. 6.4** Plots of  $\log D_J$  and of  $\log D_{JK}$  versus  $\log (4B_0^3/v^2)$  for the methyl halides where  $v$  represents the fundamental vibrational frequency of the parallel mode  $v_3$  for the  $D_J$  plot and the fundamental frequency of the perpendicular mode  $v_6$  for the  $D_{JK}$  plot. From Orville-Thomas, Cox, and Gordy [7].

**Table 6.1** Selected Rotational Constants of Some Symmetric-top Molecules in the Ground Vibrational State

Molecule	$B_0$ (MHz)	$D_J$ (kHz)	$D_{JK}$ (kHz)	Ref.
$\text{PH}_3$	133,480.15	3950	-5180	<sup>a</sup>
$\text{AsH}_3$	112,470.59(3)	2925(3)	-3718(4)	<sup>b</sup>
$^{121}\text{SbH}_3$	88,038.99(3)	1884(4)	-2394(15)	<sup>b</sup>
$\text{NF}_3$	10,681.02(1)	14.53(7)	-22.69(10)	<sup>c,d</sup>
$\text{N}^{35}\text{Cl}$	3,468.603(3)	1.863(2)	-3.015(6)	<sup>e</sup>
$\text{CH}_3\text{F}$	25,536.147(2)	59.87(20)	420.3(4)	<sup>f,g</sup>
$\text{CH}_3^{35}\text{Cl}$	13,292.869(10)	18.0	198(3)	<sup>g</sup>
$\text{CH}_3^{79}\text{Br}$	9,568.19(5)	9.87	128(1)	<sup>g</sup>
$\text{CH}_3\text{I}$	7,501.276(5)	6.31	98.7(1)	<sup>g</sup>
$\text{CH}_3\text{CN}$	9,198.897(6)	3.81(8)	176.9(2)	<sup>h</sup>
$\text{SiH}_3\text{CN}$	4,973.009(15)	1.48(10)	63(2)	<sup>i</sup>
$\text{CH}_3\text{CCH}$	8,545.869	2.875	163.0	<sup>j,k</sup>
$\text{SiH}_3\text{CCH}$	4,828.687	2.1	63	<sup>l</sup>
$\text{CH}_3\text{CNO}$	3,914.796(4)	0.42(2)	153.1(3)	<sup>m</sup>
$\text{SiH}_3\text{NCO}$	2,517.888(14)	0.9(2)	641(13)	<sup>n</sup>
$\text{SiH}_3\text{NCS}$	1,516.040(1)	0.037(4)	41.958(6)	<sup>o</sup>

<sup>a</sup> Helminger and Gordy [77].

<sup>b</sup> Helminger et al. [78].

<sup>c</sup> A. M. Mirri and G. Cazzoli, *J. Chem. Phys.*, **47**, 1197 (1967).

<sup>d</sup> Otake et al. [117].

<sup>e</sup> G. Cazzoli, P. G. Favero, and A. Dal Borgo, *J. Mol. Spectrosc.*, **50**, 82 (1974).

<sup>f</sup> R. S. Winton and W. Gordy, *Phys. Lett.*, **A 32**, 219 (1970).

<sup>g</sup> T. E. Sullivan and L. Frenkel, *J. Mol. Spectrosc.*, **39**, 185 (1971).

<sup>h</sup> A. Bauer and S. Maes, *J. Phys. (Paris)*, **30**, 169 (1968).

<sup>i</sup> Careless and Kroto [31].

<sup>j</sup> C. A. Burrus and W. Gordy, *J. Chem. Phys.*, **26**, 391 (1957).

<sup>k</sup> A. Bauer and J. Burie, *Compt. Rend.*, **268B**, 1569 (1969).

<sup>l</sup> Gerry and Sugden [30].

<sup>m</sup> H. K. Bodenseh and K. Morgenstern, *Z. Naturforsch.*, **25a**, 150 (1970).

<sup>n</sup> M. C. L. Gerry, J. C. Thompson, and T. M. Sugden, *Nature*, **211**, 846 (1966).

<sup>o</sup> K. F. Dössel and A. G. Robiette, *Z. Naturforsch.*, **32a**, 462 (1977).

relationship is generally quite complicated because of the many vibrational degrees of freedom of the polyatomic molecules (see Chapter VIII). The methyl halides provide perhaps the simplest group of organic symmetric-top molecules for which attempts at relating the vibrational frequencies with the stretching constants have been made. From the infrared vibrational spectra Chang and Dennison [6] have calculated values of  $D_J=18.4$  kHz and  $D_{JK}=189$  kHz for  $\text{CH}_3^{35}\text{Cl}$  which agree very well with the observed microwave values [7], 18.1 and 198 kHz, respectively.

One can, to a useful approximation, treat the methyl halides as diatomic molecules in which the  $\text{CH}_3$  group as a unit vibrates against the halogen. To

this simplified model one can then apply (4.16) for diatomic molecules

$$D_J = \frac{4B^3}{\omega_i^2} \quad (6.17)$$

where  $\omega_i$  represents the fundamental parallel vibrational frequency corresponding to the stretching of the C—X bond. Figure 6.4 shows a plot [7] of  $\log D_J$  versus  $\log(B^3/\omega_i^2)$  for the methyl halides with  $\omega_i$  taken as the parallel frequency  $\omega_3$ . The relationship is linear as expected from (6.17). In the same figure is given a plot of  $\log D_{JK}$  versus  $\log(B^3/\omega_i^2)$  with  $\omega_i$  taken as the frequency of the mode  $\omega_6$  in which the atoms vibrate in planes perpendicular to the symmetry axis. This relationship is also found to be linear. As the mass of X is reduced to that of H, both the frequencies  $\omega_3$  and  $\omega_6$  go over into the deformation frequency  $\omega_4$  in methane [8]. Likewise, the parameters  $D_J$  and  $D_{JK}$  go over into a single distortion parameter  $D$  for the spherical-top molecule. It is therefore interesting to note that the two plots of Fig. 6.4 intersect at the point for methane if  $\omega_i$  is taken as its deformation frequency  $\omega_4$  and if  $D_J = D_{JK} = D$  represents the distortion constant of  $\text{CH}_4$  from optical spectroscopy.

## 2 MOLECULES IN EXCITED VIBRATIONAL STATES

For symmetric-top molecules in excited vibrational states the effective rotational constants differ somewhat from those of the ground state. The effective values of the constants in excited states are expected to have, in the first approximation, variation with the vibrational quantum number similar to that for linear molecules. To the approximation usually required,

$$B_v = B_e - \sum \alpha_i^b \left( v_i + \frac{d_i}{2} \right) \quad (6.18)$$

$$A_v = A_e - \sum \alpha_i^a \left( v_i + \frac{d_i}{2} \right) \quad (6.19)$$

The higher-order expression  $B_v$  is similar to that for the linear molecule, (5.26). In these relations  $B_e$  and  $A_e$  are the equilibrium values,  $v_i$  is the vibrational quantum number for the  $i$ th mode,  $\alpha_i^a$  and  $\alpha_i^b$  are small anharmonic constants, and  $d_i$  represents the degeneracy of the  $i$ th mode. Slight differences in the stretching constants from those of the ground vibrational state are also expected. These differences, which are usually negligible, may be represented by a formula similar to that of (4.12). Silver and Shaffer [9, 10] have shown that (6.18) and (6.19) hold for pyramidal molecules; Shaffer [11], for axially symmetric molecules. Nielsen [12] has given a general treatment of the subject.

For molecules in nondegenerate vibrational modes, the rotational frequencies of either the prolate or the oblate symmetric top can be expressed by

$$\nu = 2B_v(J+1) - 4D_J^{(v)}(J+1)^3 - 2D_{JK}^{(v)}(J+1)K^2 \quad (6.20)$$

where  $B_v$  is given by (6.18), with  $d_i=1$ . For molecules in degenerate vibrational modes,  $d_i>1$ , the change in  $B_v$  can also be expressed by (6.18), but (6.20) does

not adequately predict the rotational spectrum. In addition to the change in  $A$ ,  $B$ , or  $C$  for the degenerate vibrational modes, there is a splitting of the rotational lines, which is similar to the  $l$ -type doubling for linear molecules.

The displacement of rotational lines of symmetric-top molecules by vibrational excitation is illustrated in Fig. 6.5. This recording shows  $J=11\rightarrow 12$  rotational transitions in the 21 GHz region of  $(\text{CH}_3)_3\text{C}-\text{C}\equiv\text{C}^{35}\text{Cl}$  in excited vibrational states up to  $v=5$  of the fundamental mode believed to be that corresponding to a bending mode between the tertiary C atom and the acetylene group [13]. The labeling on the figure indicates the main peaks of the rotational lines in the vibrational states  $v=0$  to  $v=5$  which have unresolved  $l$ -type doubling as described later, also unresolved nuclear quadrupole structure and  $K$  structure. From a fitting of the relative intensities of the lines with those expected from the Boltzmann relation (Chapter III), the fundamental frequency of the vibration was found to be  $120 \text{ cm}^{-1}$ , approximately.

For symmetric-top molecules such as  $\text{CH}_3\text{CCH}$  which have a linear group along the symmetry axis, there are degenerate bending vibrational modes which give rise to  $l$ -type doubling of the rotational levels similar to that described for linear molecules in Chapter V. Also, degenerate vibrational modes involving perpendicular motions of the atoms which are off the axis can give rise to components of vibrational angular momentum along the symmetry axis. Thus degenerate modes leading to vibrational angular momentum occur in pyramidal  $XY_3$  molecules and even in planar  $XY_3$  molecules. Because of Coriolis interaction between vibration and rotation, a splitting of the levels occurs which is known as  $l$ -type doubling. There is a component of this vibrational angular momentum along the figure axis which adds to, or subtracts from, the pure rotational angular momentum about the symmetry axis. This component has the value  $\zeta l\hbar$ , where  $\zeta$  is the Coriolis coupling constant and

$$l = v_d, v_d - 2, \dots, -v_d \quad (6.21)$$

where  $v_d$  is the vibrational quantum number of the degenerate mode. For the most important case,  $v_d=1$  and  $l=\pm 1$ . When the vibrating motions are perpendicular to the symmetry axis,  $\zeta=1$  and the vibrational component along  $z$  is  $l\hbar$ , just as in the linear molecules. In the symmetric top, however, the

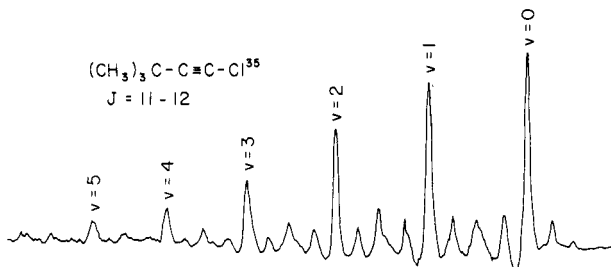


**Fig. 6.5** Recording of the  $J=11\rightarrow 12$  rotational transition of  $(\text{CH}_3)_3\text{C}-\text{C}\equiv\text{C}^{35}\text{Cl}$  in excited states up to  $v=5$  of a bending vibrational mode. The substructure of the lines caused by  $l$ -type doubling, centrifugal distortion, and nuclear coupling is not resolved. From Bodenseh, Gegenheimer, Mennicke, and Zeil [13].

component along the symmetry axis can, in general, be less than  $l\hbar$ , or  $0 \leq |\zeta| \leq 1$ . In any event, the quantum mechanics of the symmetric top requires that the overall angular momentum along the symmetry axis, that is, the sum of that caused by pure rotation and vibration, must be an integral multiple of  $\hbar$  instead of that caused by vibration or rotation alone. Likewise, the square of the overall angular momentum including that arising from the degenerate vibrational modes is quantized with values  $J(J+1)\hbar^2$ .

If  $P_x$ ,  $P_y$ , and  $P_z$  represent the overall angular momentum about the principal axis including that caused by pure rotation of the molecule and that caused by vibration, the pure rotational Hamiltonian can be expressed as

$$\mathcal{H}_r = \frac{(P_x - p_x)^2}{2I_x} + \frac{(P_y - p_y)^2}{2I_y} + \frac{(P_z - p_z)^2}{2I_z} \quad (6.22)$$

where  $p_x$ ,  $p_y$ , and  $p_z$  represent the components of the angular momentum which arises from the degenerate vibratory motions. Let us assume a prolate symmetric top with  $I_x = I_y = I_b$ ,  $I_z = I_a$ , and  $p_x = p_y = 0$ . The  $\mathcal{H}_r$  can then be expressed as

$$\begin{aligned} \mathcal{H}_r &= \frac{P^2}{2I_b} - \frac{P_z^2}{2I_b} + \frac{(P_z - p_z)^2}{2I_a} \\ &= \frac{P^2}{2I_b} + \frac{1}{2} \left( \frac{1}{I_a} - \frac{1}{I_b} \right) P_z^2 - \frac{P_z p_z}{I_a} \end{aligned} \quad (6.23)$$

In the last expression we neglect the term  $p_z^2/(2I_a)$ , which represents pure vibrational energy and which does not change with the rotational state. Since

$$P^2 = \hbar^2 J(J+1), \quad P_z = K\hbar, \quad \text{and} \quad p_z = \zeta l\hbar \quad (6.24)$$

$$\frac{E_r}{\hbar} = B_v J(J+1) + (A_v - B_v) K^2 - 2\zeta l K A_v \quad (6.25)$$

where

$$\begin{aligned} J &= 0, 1, 2, 3, \dots \\ K &= 0, \pm 1, \pm 2, \dots, \pm J \end{aligned} \quad (6.26)$$

and where  $l$  values are given by (6.21). To obtain the formula for the oblate symmetric top one simply replaces the  $A_v$  by  $C_v$ . A formula like that of (6.25) was originally derived by Teller [14] and by Johnston and Dennison [15].

Since both  $K$  and  $l$  can take plus and minus values, (6.25) indicates a doublet splitting of the levels with each component retaining a double degeneracy. However, certain of the levels may be further split by interactions of higher order. When  $|K|=3n+1$  where  $n$  is an integer including zero, the term with  $K/l$  positive represents two coinciding levels of species  $A$  whereas the term with  $K/l$  negative represents a doubly degenerate level of species  $E$ . For  $|K|=3n+2$ , the reverse is true. When  $|K|=3n$  but not including zero, the terms with  $K/l$  positive or negative represent separately doubly degenerate levels of species  $E$ .

The double degeneracy of the levels of species  $E$  cannot be removed [16], but the coinciding levels of species  $A$  may be split by interactions of higher order. H. H. Nielsen [17] has shown that the further splitting of the levels of species  $A$  can be appreciable for  $K=1$ , but that it is negligible for other  $K$  values.

More complete treatments of the interaction of degenerate vibrations with rotation in symmetric-top molecules have been given by Nielsen [17, 18], by Grenier-Beeson and Amat [19], and by others [20–22]. For singly excited degenerate bending, with  $v_d=1$ ,  $l=\pm 1$ , Nielsen's formula for the rotational energy which includes stretching as well as higher-order interaction with the degenerate vibration is

$$\begin{aligned} E_{JK} = & h\{B_v J(J+1) + (A_v - B_v)K^2 - 2A_v Kl\zeta - D_J J^2(J+1)^2 \\ & - D_{JK} J(J+1)K^2 - D_K K^4 + 2 \\ & \times [(2D_J + D_{JK})J(J+1) + (2D_K + D_{JK})K^2] Kl\zeta + P(J, K, l)\} \end{aligned} \quad (6.27)$$

where for  $K=l=\pm 1$

$$P = \pm \frac{1}{2} J(J+1)q \quad (6.28)$$

where  $q \approx 2B^2/\omega$ , and  $\omega$  is the fundamental bending vibrational frequency. For  $K \neq l = \pm 1$ ,

$$P = \pm \frac{[J(J+1) - K(K \mp 1)][J(J+1) - (K \mp 1)(K \mp 2)]}{8(K \mp 1)[(1 - \zeta)A_v - B_v]} q^2 \quad (6.29)$$

The upper signs are taken when  $K$  and  $l$  have the same sign; the lower signs, when  $K$  and  $l$  are of different sign. With the selection rules,

$$J \rightarrow J+1, \quad K \rightarrow K, \quad l \rightarrow l \quad (6.30)$$

the predicted frequencies are

$$\begin{aligned} \nu = & 2B_v(J+1) - 4D_J(J+1)^3 - 2D_{JK}(J+1)K^2 \\ & + 4(2D_J + D_{JK})(J+1)Kl\zeta + \Delta P(J, K, l) \end{aligned} \quad (6.31)$$

where

$$\Delta P = \pm q(J+1) \quad (6.32)$$

for  $K=l=\pm 1$ , and

$$\Delta P = \pm \frac{(J+1)[(J+1)^2 - (K \mp 1)^2]}{4(K \mp 1)[(1 - \zeta)A_v - B_v]} q^2 \quad (6.33)$$

for  $K \neq l = \pm 1$ . Upper signs are taken when  $K$  and  $l$  have the same sign; the lower signs hold when  $K$  and  $l$  have different signs.

The qualitative features predicted by Nielsen's theory, including the rather wide separation of the  $K=l=\pm 1$  lines by  $2q(J+1)$ , were verified [23] by early measurements on  $\text{CH}_3\text{CCH}$ . The theory has been applied to a number of other symmetric-top molecules [24], including  $\text{SiH}_3\text{NCS}$  which, surprisingly, is a symmetric top, and to several different rotational transitions of  $\text{CH}_3\text{CN}$ .

[25]. Table 6.2 illustrates the extent of agreement of the calculated with the observed frequencies of the  $J=10 \rightarrow 11$  lines of the  $v_8=1$  bending vibrational state of CH<sub>3</sub>CN. Although it was found that the positions of the various doublets for CH<sub>3</sub>CN were given adequately by Nielsen's theory, the separations of the individual doublets were not satisfactorily predicted. Venkateswarlu et al. [25] found that these separations could be closely predicted, as in Table 6.2, if the term  $4\epsilon K\zeta(J+1)$  where  $\epsilon \approx 0.034$  is inserted into (6.31). Values of interaction constants were found to be  $\zeta = 0.878$  and  $q = 17.775$  MHz. Measurements and analysis of CH<sub>3</sub>CN have been extended by Bauer [26] to include several rotational transitions of the second excited state,  $v_8=2$ .

Nielsen's theoretical work on  $l$ -type doubling has been extended and improved by others. Formulas for  $J \rightarrow J+1$  rotational frequencies including  $l$ -type doubling are provided by Grenier-Beeson and Amat [19] for first excited states,  $v_t=1$ , of molecules having  $C_{3v}$  symmetry. The formulation is extended by Tarrago [27] to second excited vibrations having  $l=1$ , that is,  $v_t=2^1$  states.

**Table 6.2** The Observed and Calculated Frequencies and the Assignments of the  $J=10 \rightarrow 11$  Lines Corresponding to the Molecules in the Excited State  $v_8=1$  of CH<sub>3</sub>CN<sup>a</sup>

<i>J</i>	<i>Transition</i>		<i>Observed Frequency (MHz)</i>	<i>Calculated Frequency (MHz)</i>
	<i>K</i>	<i>l</i>		
10→11	±1	±1	203,161.23	203,161.53
			202,769.94	202,770.08
	±2	±1	202,972.63	202,972.53
	0	±1	202,950.97	202,950.87
	±3	±1	202,956.31	202,956.28
	±1	±1	202,943.39	202,943.68
	±4	±1	202,935.67	202,935.61
	±2	±1	202,924.94	202,925.23
	±5	±1	202,907.98	202,907.97
	±3	±1	202,897.68	202,898.15
	±6	±1	202,872.91	202,872.87
	±4	±1	202,862.38	202,862.88
	±7	±1	202,830.05	202,830.11
	±5	±1	202,819.06	202,819.63
	±8	±1	202,779.70	202,779.64
	±6	±1	202,768.06	202,768.47
	±9	±1	202,721.62	202,721.40
	±7	±1	202,709.07	202,709.43
	±10	±1	202,655.71	202,655.39
	±8	±1	202,642.27	202,642.51

<sup>a</sup>From Venkateswarlu et al. [25].

The formulas by Grenier-Beeson and Amat were applied by them [19] to the available data on  $\text{F}_3\text{CC}\equiv\text{CH}$  and found to provide consistent agreement. Others have successfully applied their theory: Otake et al. [28], to measurements on the degenerate  $v_3$  and  $v_4$  modes of  $\text{NF}_3$ ; Whittle et al. [29], to the degenerate  $v_7$  and  $v_8$  modes of  $\text{CF}_3\text{CN}$ ; Gerry and Sugden [30], to the degenerate bending mode  $v_{10}$  of  $\text{SiH}_3\text{CCH}$ , as examples. The formulation of Tarrago [27] has been applied with consistent fitting to rotational transitions of a number of  $C_{3v}$  molecules in  $v=2^1$  states: to  $\text{CH}_3\text{CN}$ , by Bauer [26]; to  $\text{SiH}_3\text{CN}$ , by Careless and Kroto [31]. The latter work extends the formulation to include  $v_8=3$  and 4 states of  $\text{SiH}_3\text{CN}$ .

Direct transitions between the  $l$ -type doublets in the  $J=17$  to 24 rotational levels of the  $v_4=1$  state of  $\text{PF}_3$  have been observed and analyzed by Hirota [32]. The  $l$ -type doubling constant,  $q_4=29.49270(8)$  MHz, and the 2-1 interaction constant,  $r_4=3.013(5)$  MHz, were obtained. Direct  $l$ -type doublet transitions have also been measured and analyzed in rotational levels of the  $v_6=1$  state of  $\text{CF}_3\text{H}$  and  $\text{CF}_3\text{D}$  by Kawashima and Cox [33]. The values,  $|q_6|=36.27917(13)$  MHz and  $|r_6|=0.97(2)$  MHz, were obtained. These papers provide instructive examples of the analysis of  $l$ -type doublet spectra in symmetric-top molecules.

An example of Fermi resonance between different vibrational states is provided by the work of Morino and Hirose [34] in the measurement of shifts in the lines due to interaction of the  $v_5$  and  $v_3+v_6$  vibrational states of  $\text{CH}_3\text{I}$ . Accidentally strong resonances between certain rotational levels of the  $v=2$  vibrational states of both  $\text{CH}_3^{12}\text{CN}$  and  $\text{CH}_3^{13}\text{CN}$  have been observed by Bauer and Maes [35].

### 3 MOLECULAR INVERSIONS

According to quantum mechanics, pyramidal  $XY_3$  symmetric-top molecules can execute inversion motion in which the  $X$  atom moves through the  $Y_3$  plane to achieve an identical but inverted pyramidal configuration. The inverted configuration is obtained mathematically by a change of sign of the coordinates of all the particles measured from the center of mass. Theoretically, such inversion is possible in any nonplanar molecule (Chapter III, Section 4), but, practically, it is of significance for only a very few. The inversion potential curve of the  $\text{NH}_3$  molecule is illustrated by Fig. 6.6. The potential energy of the molecule plotted as a function of the distance between the N atom and the  $\text{H}_3$  plane has double minima corresponding to the two equivalent equilibrium configurations.

The wave functions of the molecule can be expressed as linear combinations of  $\phi_L$  and  $\phi_R$  of those of the molecule in the equivalent right and left configurations. These functions,

$$\psi_+ = \frac{1}{\sqrt{2}} (\phi_L + \phi_R) \quad (6.34)$$

$$\psi_- = \frac{1}{\sqrt{2}} (\phi_L - \phi_R) \quad (6.35)$$

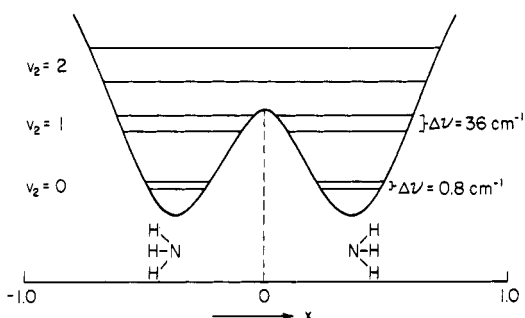


Fig. 6.6 Potential curve of the  $\text{NH}_3$  inversion.

have opposite symmetry. For an infinitely high barrier they represent degenerate states; but when the barrier is sufficiently low, as in  $\text{NH}_3$ , the two states are separated by a measurable interaction energy. Selection rules (Chapter III, Section 4) allow transitions  $+ \leftrightarrow -$  between the states giving rise to inversion spectra. The transition moment is given by (2.125).

In addition to the inversion motion, the molecule has a symmetrical vibrational mode in which the  $X$  atom moves back and forth along the symmetry axis in opposition to the motions of the  $Y_3$  atoms. In the first and second excited symmetrical modes this vibrational energy for  $\text{NH}_3$  is lower than the potential energy barrier between the two minima. In all other  $XY_3$  molecules the potential hill between the vibrational and potential energy is much greater relative to the vibrational energy. Thus, in lower symmetrical vibrational modes the  $XY_3$  molecule executes vibrational motions in the potential valley on either side of the potential barrier. Classically, it is not possible for the molecule to invert when in these vibrational states which lie below the potential maximum. Quantum mechanically, though, it is possible for the molecule to achieve inversion transition through "barrier tunneling." In  $\text{NH}_3$ , the N atom tunnels through the  $\text{H}_3$  plane at approximately 23 GHz to give rise to the well-known inversion spectrum in the 1.3-cm wave region, the first spectrum to be observed in the microwave region [36–38]. The corresponding inversion frequency of  $\text{ND}_3$  is approximately 1.7 GHz, and for  $\text{NT}_3$  it is 0.306 GHz. No other symmetric-top molecules have inversion frequencies that fall in the microwave region. The next highest inversion frequency [39, 40], that of  $\text{PH}_3$ , is predicted to be very small. So far, the inversion splitting of the rotational lines of  $\text{PH}_3$  has proved undetectable with the highest resolution available. Other related molecules such as  $\text{AsH}_3$  are predicted to have such long inversion time, of the order of days [40], that no observable effects on microwave spectra are expected. However, related barrier-tunneling effects associated with internal rotation and torsional oscillation of groups within symmetric-top and asymmetric-top molecules are observable in microwave spectra. These effects are treated in Chapter XII.

Theoretically, one can obtain the inversion frequencies from a solution of the wave equation for the vibrating rotor, as is done for diatomic molecules with the assumption of a double minima potential of the appropriate form. This is a very difficult problem, however. In a first-order approximation one can neglect the interaction between vibration and rotation and can obtain separate solutions of the wave equation for the vibration and rotation and can then, with the perturbation theory, correct for the interaction. The simplest model that accounts for the inversion is one which treats the three hydrogens in a plane as a unit vibrating against the N atom, somewhat as a diatomic molecule. The reduced mass of the vibration is  $\mu = 3mM/(3m+M)$ . The wave equation for this simple model is

$$\frac{d^2\psi}{dx^2} + \frac{8\pi^2\mu}{h^2} [E_v - V(x)]\psi = 0 \quad (6.36)$$

With a double minima potential function, the solution yields the vibrational levels split by inversion. Solutions have been obtained by Manning [41], also by Dennison and Uhlenbeck [42], whose solutions for inversion energies and frequencies are

$$\frac{\Delta E_{\text{inv.}}}{\Delta E_v} = \frac{1}{\pi A^2} \quad \text{or} \quad v_{\text{inv}} = v_{\text{vib}} \left( \frac{1}{\pi A^2} \right) \quad (6.37)$$

where

$$A = \exp \left\{ \frac{2\pi}{h} \int_0^{x_1} [2\mu(V(x) - E_v)]^{1/2} dx \right\} \quad (6.38)$$

in which

$\Delta E_v$  = separation of the vibrational levels

$\Delta E_{\text{inv}}$  = inversion splitting of the vibrational levels

$v_{\text{inv}}$  = the inversion frequency

$v_{\text{vib}}$  = the fundamental vibrational frequency

$E_v$  = the total vibrational energy

$x = x_1$  when  $V = E_v$

The quantity  $A$  measures the area under the potential curve between the potential minima and is not particularly sensitive to the exact shape of the curve. Dennison and Uhlenbeck used the *W-K-B* method and assumed the curves in the region of the minima to be parabolic. Manning assumed a potential function of the form

$$V (\text{in cm}^{-1}) = 66,551 \operatorname{sech}^4 \frac{x}{2\rho} - 109,619 \operatorname{sech}^2 \frac{x}{2\rho} \quad (6.39)$$

where  $\rho = 6.98 \times 10^{-8}/\mu^{1/2}$ . This formula was found to predict the frequencies quite well. It allows, through the effects of  $\mu$ , the prediction of the isotopic shifts of the inversion frequency.

The effects of rotation on the inversion splitting have been taken into account in various semiempirical formulas, the nature of which is suggested by the centrifugal stretching terms of the noninverting symmetric-top rotor or by the nature of the function  $A$  of (6.38). The various constants in these expressions are then evaluated by a fitting of them to the accurately measured rotational fine structure of the inversion. The formula that fits most closely all the accurately measured fine structure is an exponential function suggested by Costain [43] from a consideration of the nature of the function of (6.37) as well as the nature of the centrifugal stretching terms in symmetric-top rotors. It is evident that centrifugal distortion would alter slightly both  $V$  and  $E_v$  of (6.38). Costain's formula was extended to higher order by Schnabel et al. [44] and its various constants determined by a fitting of the formula to the most complete and accurate measurements on the  $\text{NH}_3$  available to 1965. Their formula and values for the constants are given in the earlier edition of this book.

Because the lowest rotational frequency of  $\text{NH}_3$  and  $\text{ND}_3$  falls in the submillimeter wave region, the many early microwave measurements on these symmetric molecules were limited to their inversion spectra, although combined rotation-inversion transitions were observed for the mixed species  $\text{NHD}_2$ ,  $\text{NH}_2\text{D}$  which are asymmetric rotors. In 1957, observation of the  $J=0 \rightarrow 1$  rotational transition of  $\text{ND}_3$ , which occurs at  $\lambda=0.97$  mm, was reported [45], but the corresponding rotational transitions of  $^{14}\text{NH}_3$  and  $^{15}\text{NH}_3$ , which occur in the 0.52-mm wave region, were not observed until 1967 [46]. In 1974, the rotation-inversion spectrum of  $\text{NT}_3$  in the  $v_2=0$  states was measured [47].

Figure 6.7 shows the energy level diagram of the first few rotation-inversion levels of  $\text{NH}_3$  and  $\text{ND}_3$  with the observable transitions indicated. Note that for  $\text{NH}_3$ , only one of the inversion levels occurs when  $K=0$ , whereas for  $\text{ND}_3$

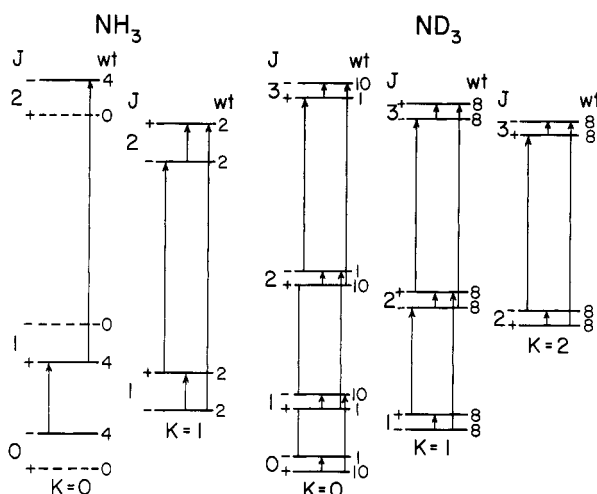


Fig. 6.7 Diagram of the lower rotation-inversion levels and transitions of  $\text{NH}_3$  and  $\text{ND}_3$  with the allowed transitions indicated.

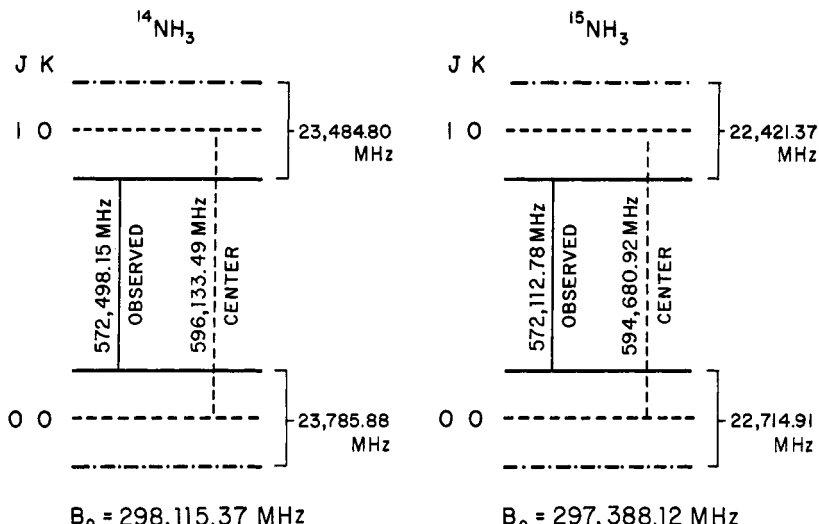
both the + and - levels occur, but with differing statistical weights. This difference is due to the effects of nuclear spin statistics discussed in Chapter III, Section 4 and conforms to the statistical weight formula given in Table 3.3.

Figure 6.8 indicates how the measured centimeter wave inversion frequencies for the upper and lower levels were combined with the  $J=0 \rightarrow 1$  submillimeter wave rotation-inversion frequencies [48] to give accurate values for the rotational constants  $B_0$  for  $^{14}\text{NH}_3$  and  $^{15}\text{NH}_3$ . After correction of the rotational frequencies for inversion effects, they were used in (6.15) with infrared  $D_J$  values for calculation of the  $B_0$  values listed on Fig. 6.8. Measured inversion frequencies of  $\text{ND}_3$  in the 2-GHz microwave region [49, 50] have also been combined with the observed submillimeter wave rotation-inversion transitions for derivation of the rotational constants [48]  $B_0$ ,  $D_J$ , and  $D_{JK}$  for the  $^{14}\text{ND}_3$  and  $^{15}\text{ND}_3$ , entirely from microwave data.

The inversion splitting of  $\text{NT}_3$ , together with its rotational constants, has been obtained by Helmlinger et al. [47], entirely from measurements of millimeter and submillimeter wave rotation-inversion transitions. They used the frequency formula

$$\nu = 2B_0(J+1) - 4D_J(J+1)^3 - 2D_{JK}(J+1)K^2 \pm [(v_i)_0 + C_1(J+1)^2 + C_2 K^2] \quad (6.40)$$

and adjusted the constants by the least-squares method to reproduce the observed frequencies as shown in Table 6.3. The resulting constants are given at the bottom of Table 6.3. The  $J=0 \rightarrow 1$  frequency is corrected for  $^{14}\text{N}$  nuclear quadrupole splitting. The bracketed term in (6.40) represents the inversion



**Fig. 6.8** Illustration of the derivation of  $B_0$  from the observed rotational frequencies of  $^{14}\text{NH}_3$  and  $^{15}\text{NH}_3$  as measured. From Helmlinger et al. [48].

**Table 6.3** Rotation-Inversion Frequencies and Derived Spectral Constants of  $^{14}\text{NT}_3^a$ 

<i>Transition</i>	<i>Inversion Component</i>	<i>Observed Frequency (MHz)</i>	<i>Calculated Frequency (MHz)</i>	<i>Difference (MHz)</i>
$J=0 \rightarrow 1, K=0$	lower	210,814.885	210,815.023	-0.138
$J=1 \rightarrow 2, K=1$	lower	421,891.743	421,891.608	0.135
$J=1 \rightarrow 2, K=0$	upper	422,482.040	422,482.014	0.026
$J=1 \rightarrow 2, K=1$	upper	422,500.800	422,500.871	-0.071
$J=2 \rightarrow 3, K=0$	lower	632,810.839	632,810.768	0.071
$J=2 \rightarrow 3, K=1$	lower	632,836.513	632,836.626	-0.113
$J=2 \rightarrow 3, K=2$	lower	632,914.199	632,914.202	-0.003
$J=2 \rightarrow 3, K=1$	upper	633,440.324	633,440.321	0.003
$J=2 \rightarrow 3, K=2$	upper	633,523.744	633,523.724	0.020

<i>Inversion Constants (MHz)</i>	<i>Rotation Constants (MHz)</i>
$(v_i)_0 = 305.89 \pm 0.11$	$B_0 = 105,565.373 \pm 0.034$
$C_1 = -0.557 \pm 0.020$	$D_J = 2.5981 \pm 0.0024$
$C_2 = 0.971 \pm 0.038$	$D_{JK} = -4.472 \pm 0.006$

<sup>a</sup>From Helminger et al. [47].

splitting;  $(v_i)_0$  is the inversion frequency; the  $C_1$  and  $C_2$  terms correct the inversion frequency for centrifugal distortion effects.

The effective and substitution structures for the ground state of ammonia, as derived from the  $B_0$  values of various isotopic species, are given in Section 6, Table 6.7.

The inversion doubling frequencies  $(v_i)_0$  for the ground state are now known accurately from microwave measurements for all three species,  $\text{NH}_3$ ,  $\text{ND}_3$ , and  $\text{NT}_3$ . The much larger inversion frequencies for the  $v_2=1$  excited state have been measured with infrared vibration-rotation spectroscopy: for  $\text{NH}_3$  and  $\text{ND}_3$  by Benedict and Plyler [51] and for  $\text{NT}_3$  by Rao et al. [52]. Figure 6.9 shows the relationship between  $\log_{10}(v_i/v_0)$  and  $\mu^{1/2}$ , where  $v_i$  is the inversion frequency,  $v_0$  is the fundamental vibrational frequency of the  $v_2$  mode, and  $\mu$  is the reduced mass of the particular isotopic species of the ammonia. The relationship in each state,  $v_2=0$  or 1, is approximately linear.

The relationship revealed in Fig. 6.9 is suggested by the Dennison-Uhlenbeck formula, (6.37). Substitution of (6.38) into (6.37) shows that

$$\frac{v_{\text{inv}}}{v_{\text{vib}}} = \frac{1}{\pi} \exp \left( -\frac{2}{\hbar} \int_0^{x_1} [2\mu(V(x) - E_v)]^{1/2} dx \right) \quad (6.41)$$

and thus

$$\ln \left( \frac{v_{\text{inv}}}{v_{\text{vib}}} \right) \sim \sqrt{\mu} \left( \int_0^{x_1} [V(x) - E_v]^{1/2} dx \right) \quad (6.42)$$

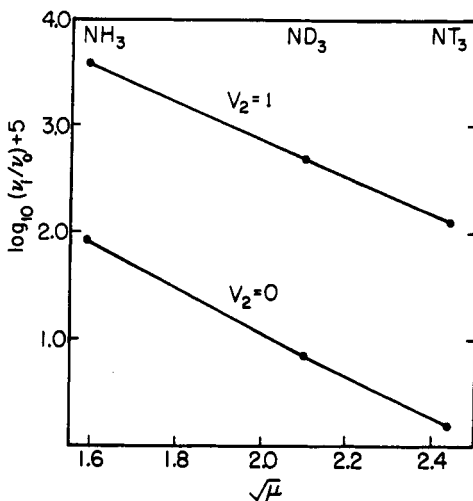
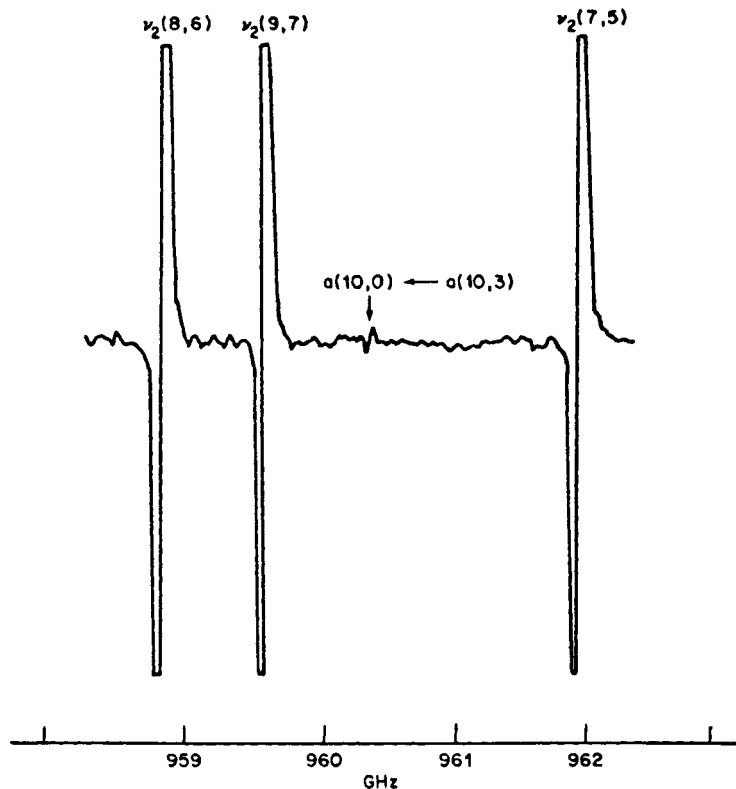


Fig. 6.9 Correlation of the inversion splitting with the reduced molecular mass for the three isotopic species of ammonia in different  $v_2$  vibrational states. From Helminger, De Lucia, Gordy, Morgan, and Staats [47].

where, in Fig. 6.9,  $v_i \equiv v_{\text{inv}}$  and  $v_0 \equiv v_{\text{vib}}$ . The fact that the experimental relationship for each vibrational state,  $v^2 = 0$  or  $v^2 = 1$ , is approximately linear indicates that the quantity expressed by the integral varies little with the change of isotopic species, that is, approximately  $\ln(v_i/v_0) \sim \mu^{1/2}$  for a given  $v_2$  vibrational state.

The simple, one-dimensional, double-minimum potential model of Dennison and Uhlenbeck [42] and Manning [41], (6.37)–(6.39), has been extended and refined by Swalen and Ibers [53] and by Damburg and Propin [54]. A more comprehensive, vibration–inversion–rotation Hamiltonian that includes centrifugal distortion and Coriolis interactions in the ground and excited inversion states has been developed by Papoušek et al. [55]. The Hamiltonian is a logical extension of one developed by Hougen et al. [56] for triatomic molecules. Further development of this Hamiltonian has been carried out by Špirko et al. [57], who give procedures for a least-squares fitting of its solution to the vibration–inversion–rotation energy levels of  $\text{NH}_3$ ,  $\text{ND}_3$ , and  $\text{NT}_3$ . This later form of the ammonia Hamiltonian is related to the one for the inversion–rotation of triatomic molecules with large-amplitude bending motions, developed earlier by Hoy and Bunker [58].

The effective vibration–inversion–rotation Hamiltonian developed by Papoušek et al. [55, 57] has been used in successful analyses of extensive submillimeter wave measurements on the inversion and inversion–rotation spectrum of  $\text{NH}_3$  in the  $v_2 = 1$  vibration state by Belov et al. [59]. A section of the submillimeter wave spectrum of  $^{14}\text{NH}_3$  in the  $v_2 = 1$  vibrational state, obtained with the Krupnov spectrometer, is shown in Fig. 6.10. Scappini and Guarnieri



**Fig. 6.10** Part of the submillimeter microwave spectrum of  $^{14}\text{NH}_3$ . The three strong lines result from inversion transitions,  $s(J, K) \rightarrow a(J, K)$ , of the excited  $v_2=1$  state. The weak line, denoted  $a(10,0) \leftarrow a(10,3)$ , is a perturbation-allowed transition of the ground state,  $v_2=0$ . From S. Urban, V. Špirko, D. Papoušek, J. Kauppinen, S. P. Belov, L. I. Gershtein, and A. F. Krupnov, *J. Mol. Spectrosc.*, **88**, 274 (1981).

[60] have measured the millimeter wave spectrum of  $\text{ND}_3$  in the  $v_i=1$  vibrational state and obtained the accurate value of 106,354.35(3) MHz for  $(v_i)_1$  in that state.

#### 4 "FORBIDDEN" ROTATIONAL TRANSITIONS

Because there is no permanent dipole component perpendicular to the symmetry axis, resonance radiation does not normally induce changes in the  $K$  quantum number of symmetric-top rotors; that is, the selection rule  $\Delta K=0$  applies in first order. Thus, from normal rotational spectra, only one inertial constant,  $I_b$  or  $B$ , can be obtained for symmetric-top rotors, whereas three independent inertial constants can be obtained for most asymmetric rotors. Because of theoretical developments and considerable improvement in experimental techniques and spectrometer sensitivity, it has become possible to detect

in polar, symmetric-top rotors the "forbidden" rotational transitions of the ground vibrational state corresponding to changes in the  $K$  quantum number. Likewise, it has become possible to detect  $\Delta J=1, \Delta K=0$  rotational transitions of the ground vibrational states for certain nonpolar, spherical-top molecules. These advances, which came after publication of the earlier edition of this book (1970), have led to the precise microwave measurement of the spectral constant  $C_0$  (or  $A_0$  for prolate-top rotors) of several symmetric-top molecules and  $B_0$  values for some spherical tops such as  $\text{CH}_4$ . For pyramidal  $XY_3$  molecules, such as  $\text{PH}_3$ , that have only two structural parameters, these developments have made possible complete determination of the molecular structure of the ground state without isotopic substitution. Examples are given in Section 6, Table 6.8.

The possibility of observing forbidden rotational transitions in the ground state of symmetric-top molecules was apparently reported first by Hansen [61]. In the same year, Oka [62] considered collision-induced  $\Delta K=\pm 3$  transitions of  $\text{NH}_3$  in mixtures with rare gases. Pure rotational spectra of spherical-top molecules in their ground vibrational states were theoretically predicted by Fox [63] and Watson [64] in 1971. Mizushima and Venkateswarlu [65] had predicted earlier that nonpolar, symmetric-top molecules having  $T_d$  symmetry ( $\text{CH}_4$ ,  $\text{CF}_4$ ,  $\text{SiH}_3$ , etc.) can have vibrationally induced dipole moments and possibly observable pure rotational spectra when in excited, degenerate vibrational states. Their theory was extended to other molecular types by Mills et al. [66]. Pure rotational spectra of nonpolar molecules in excited vibrational states would be very difficult to observe because of the relatively low populations of the excited states. So far as we know, none have been observed.

The first detection of the forbidden  $\Delta J=0, \Delta K=\pm 3$  rotational transitions in symmetric-top molecules was achieved by Chu and Oka [67], who observed  $\Delta J=0, \Delta K=\pm 3$  ( $K=\pm 1 \rightarrow \pm 2$ ) transitions in  $\text{PH}_3$ ,  $\text{PD}_3$ , and  $\text{AsH}_3$ . The first observation of the forbidden rotational transitions in a nonpolar molecule of  $T_d$  symmetry,  $\text{CH}_4$ , was achieved by Rosenberg et al. [68] in far infrared spectroscopy. The first microwave detection of pure rotational of  $\text{CH}_4$  was accomplished by Holt et al. [69]. An excellent review of the earlier work on forbidden rotational transitional is given by Oka [70].

A general theory of ground-state, forbidden rotational transitions in polyatomic molecules, with predictions of the selection rules and transition probabilities, has been developed by Watson [64]. The theory for ground-state transitions of tetrahedral molecules like  $\text{CH}_4$  was developed independently by Fox [63, 71] and was extended to other molecular types by Aliev and Mikhaylov [72]. Generally, the ground-state transition moment results from centrifugal distortions of the molecules. For those with  $C_{3v}$  symmetry, the rotation of the molecule about the  $b$  axis produces a small distortion moment perpendicular to the symmetry axis which can give rise to observable  $\Delta J=\pm 1, \Delta K=\pm 3$  transitions. In molecules having  $T_d$  symmetry and no permanent dipole moment ( $\text{CH}_4$ ,  $\text{SiH}_4$ , etc.), rotation about a bond axis distorts the molecule so as to produce a weak dipole moment along that axis which can give rise to observ-

able  $\Delta J = \pm 1$ ,  $\Delta K = 0$  transitions. In addition to the ground-state, centrifugal-distortion mechanism, Watson [64] has shown that vibration-rotation interaction of the ground state with an excited, degenerate vibrational mode can also contribute to the probability of a forbidden transition.

Watson [64] defined an effective dipole-moment operator which includes the induced distortion moments as well as any fixed dipole components. The operator for the effective dipole moment is expressed as a power series in the vibrational and rotational operators in a manner similar to that used in Chapter VIII, Section 2 for development of the Wilson-Howard Hamiltonian, (8.10). In the molecule-fixed axes, Watson's effective dipole operator is expressed by

$$\mu_x = \mu_x^{(e)} + \sum_{\beta\gamma} \theta_x^{\beta\gamma} P_\beta P_\gamma \quad (6.43)$$

where  $\mu_x^{(e)}$  signifies the components of the fixed dipole operator, and the last term signifies the components of the induced dipole operator in which  $P_\beta$ ,  $P_\gamma$  are molecule-fixed components of the total angular-momentum operator. The symmetrized, space-fixed components of the operator of (6.43) are

$$\mu_F = \frac{1}{2} \sum (\Phi_{fx} \mu_x + \mu_x \Phi_{fx}) \quad (6.44)$$

where  $\Phi_{Fx}$  are the direction cosines of the molecule-fixed axes with the space-fixed axes. In calculation of the intensities of the spectra lines, Watson used the matrix elements of the effective dipole operator  $\mu_F$  of (6.44) in the representation that diagonalizes the Wilson-Howard rotational Hamiltonian, (8.10).

### Molecules with $C_{3v}$ Symmetry

Molecules having  $C_{3v}$  symmetry comprise the largest class of symmetric tops investigated with microwave spectroscopy. Forbidden  $\Delta K = \pm 3$  transitions have been observed in a number of the simpler ones. The  $\Delta K = 3$  selection rule for these not-strictly-forbidden transitions arises from the nature of the molecular wave function for the  $C_{3v}$  symmetry and an intramolecular interaction  $\mathcal{H}_d$  such as rotational distortion that mixes the  $K$  and  $K' = K \pm 3$  states. Exclusive of the  $M$  dependency, which we omit for simplicity, the undistorted symmetric-top rotational function may be expressed, (2.103), by

$$\psi_{JK} = e^{i\phi K} e^{i\phi K} \Theta_{JK} \quad (6.45)$$

where  $K$  has both + and - values and  $\phi$  is the angle about the symmetry axis. For a molecule of  $C_{3v}$  symmetry, a rotation of  $120^\circ$  exchanges two pairs of identical nuclei. The two configurations are indistinguishable. Thus,  $\psi_{JK} \psi_{JK}^*$  is left unchanged for an operation that simply rotates the molecules through  $\pm 120^\circ$  or  $\pm 2\pi/3$  about the symmetry axis. Under the  $C_s$  operation

$$\psi_{JK} = e^{(\pm 2\pi i/3)K} \Theta_{JK} \quad (6.46)$$

If  $J$ , the total angular quantum number exclusive of nuclear spin, is assumed to remain a good quantum number, the degree of admixture of the  $K$  and  $K'$

states is measured by  $\langle J, K | \mathcal{H}_d | J, K' \rangle$ , where  $\mathcal{H}_d$  is the Hamiltonian for the admixing interaction. With the restricted  $\psi_{JK} = |JK\rangle$  of (6.46), this can be expressed [70]

$$\langle J, K | \mathcal{H}_d | J, K' \rangle = e^{(2\pi i/3)(K' - K)} \langle J, K | \mathcal{H}_d | J, K' \rangle \quad (6.47)$$

Only when  $K - K' = 3n$  where  $n$  is an integer including zero or when the interaction  $\langle J, K | \mathcal{H}_d | J, K' \rangle$  is zero, are the two sides of (6.47) equal. Thus, with a finite interaction, the selection rules  $\Delta K = \pm 3, \pm 6$ , and so on, may occur in addition to the normal  $\Delta K = 0$  rule.

The interaction  $\mathcal{H}_d$ , responsible for admixing of the  $|J, K\rangle$  and  $|J, K \pm 3\rangle$  levels of the ground vibrational state of symmetric-top rotors having  $C_{3v}$  symmetry, is the centrifugal distortion term

$$\mathcal{H}_d = \left( \frac{\hbar^4 \tau_{xxxx}}{4} \right) [(P_+^3 + P_-^3)P_z + P_z(P_+^3 + P_-^3)] \quad (6.48)$$

where  $\tau_{xxxx}$  is the centrifugal distortion constant and  $P_{\pm} = P_x \pm iP_y$  are the rotational ladder operators. The  $|J, K\rangle$  levels of the ground state can also intermix slightly with  $|J, K \pm 2, l \mp 1\rangle$  levels of excited degenerate vibrational states by means of the vibration-rotation interaction term of the form [70]

$$\mathcal{H}_{v-r} = -2\pi B a_{t_1}^{(xx)} (q + P_-^2 + q_- P_+^2) \left( \frac{ch}{v_t} \right)^{1/2} \quad (6.49)$$

where  $v_t$  is the frequency of the degenerate vibration,  $B$  is the rotational constant,  $a_{t_1}^{(xx)} = (\partial I_{xx}/\partial Q_{t_1})$ ,  $Q_{t_1}, Q_{t_2}$  are the pair of degenerate coordinates, and  $q_{\pm}$  and  $P_{\pm}$  are the vibrational and rotational operators.

Watson [64] shows that the effective dipole-moment operator of (6.44) may be expressed for molecules of  $D_{3h}$  or  $C_{3v}$  symmetry by

$$\mu_F = \frac{1}{2} (\theta_x^{xx})_{\text{eff}} [(\Phi_{Fx} + i\Phi_{Fy})P_+^2 + (\Phi_{Fx} - i\Phi_{Fy})P_-^2] \quad (5.50)$$

where

$$(\theta_x^{xx})_{\text{eff}} = \theta_x^{xx} + \frac{\hbar^4 \tau_{xxxx} \mu_z^{(e)}}{2hc(B_x - B_z)} \quad (6.51)$$

In (6.51)  $\mu_z^{(e)}$  is the permanent dipole moment,  $\tau_{xxxx}$  is the centrifugal distortion constant, and  $B_x$  and  $B_z$  are rotational constants. The  $z$  coordinate is along the symmetry axis; hence,  $B_x = B$  and  $B_z = C$  for the oblate top and  $A$  for the prolate top. It should be noted that for molecules of  $D_{3h}$  symmetry, which have no permanent dipole moment, the last term of (6.51) vanishes and  $(\theta_x^{xx})_{\text{eff}} = \theta_x^{xx}$ .

The line strength  $S$  is proportional to the squared transition matrix elements of  $\mu_F$ . These squared matrix elements of the  $\mu_F$  of (6.50) were derived by Watson [64] for molecules of  $D_{3h}$  symmetry, planar  $XY_3$ -type. The line-strength factors of the allowed transitions (those for which the matrix elements are nonvanishing) are given in Table I of Watson's paper. These nonvanishing matrix elements prove the  $\Delta K = \pm 3$  selection rules for molecules of  $D_{3h}$  and  $C_{3v}$  symmetry. By a unitary transformation of the  $\mathcal{H}_d$  of (6.48) and of the  $\mu_F$  expressed by (6.50), he

derived the  $(\theta_x^{xx})_{\text{eff}}$  for molecules of  $C_{ev}$  symmetry given by (6.51). Thus, by substitution of  $(\theta_x^{xx})_{\text{eff}}$  from (6.51) for  $\theta_x^{xx}$  in the formulas of his Table I, the corresponding line strengths for symmetric-top molecules of  $C_{3v}$  symmetry are obtained. For example, the line strengths for the  $\Delta J=0$ ,  $\Delta K=\pm 3$  transitions of phosphine or arsine are

$$\Phi(J, K \leftrightarrow J, K \pm 3) = \frac{1}{4}(\theta_x^{xx})_{\text{eff}}^2 (J \mp K)(J \mp K - 1)(J \mp K - 2) \\ \times (J \pm K + 1)(J \pm K + 2)(J \pm K + 3)(2J + 1)/J(J + 1) \quad (6.52)$$

where

$$(\theta_x^{xx})_{\text{eff}} = \theta_x^{xx} + \frac{\hbar^4 \tau_{xxxz} \mu_z}{2h(B - C)} \quad (6.53)$$

and

$$\theta_x^{xx} = 2B^2 \left[ \frac{a_3^{xx}}{v_3^2} \left( \frac{\partial \mu_x}{\partial Q_3} \right) + \frac{a_4^{xx}}{v_4^2} \left( \frac{\partial \mu_x}{\partial Q_4} \right) \right] \quad (6.54)$$

is the induced dipole component resulting from the admixture of the excited degenerate vibrational modes  $v_3$  and  $v_4$  with the ground vibrational states. Note that Watson [64], also Oka [70], uses  $k$  for  $+$  and  $-$  values of  $K$  and defines  $K=|k|$ , whereas we allow  $K$  to have  $+$  or  $-$  values defined by (2.62).

Chu and Oka [67] used (6.52) in calculations of the intensities of forbidden  $(J, K) \rightarrow (J, \pm 1) \leftarrow (J, \mp 2)$  rotational transitions of  $\text{PH}_3$  for  $J$  values ranging from 6 to 17 which they observed in the frequency range of 47.4 to 43.7 GHz. The intensities ranged in strength from  $2.1 \times 10^{-9} \text{ cm}^{-1}$  for  $J=6$  to  $5.5 \times 10^{-9} \text{ cm}^{-1}$  for  $J=10$  and dropped to  $1.1 \times 10^{-9} \text{ cm}^{-1}$  for  $J=17$ . Helms and Gordy [73] observed  $(J, 0) \leftarrow (J, 3)$  transitions of  $\text{PH}_3$  for  $J$  values from 3 to 14 which range in frequency from 143.7 to 134.6 GHz. The intensity distribution of the observed lines, as calculated with (6.52), is shown in Fig. 6.11. The maximum intensity,  $48.5 \times 10^{-9} \text{ cm}^{-1}$ , occurs for  $J=10$ . Intensities for the same transitions in  $\text{PD}_3$  are an order of magnitude lower than those for  $\text{PH}_3$ . For  $\text{AsH}_3$ , they are still lower [74], with the maximum intensity for the  $J \rightarrow J, K=\pm 2 \rightarrow \mp 1$  transitions only  $2 \times 10^{-10} \text{ cm}^{-1}$ .

It is obvious that millimeter wave spectrometers of high sensitivity are required for observation of these forbidden spectra. The spectrometer used at Duke for measurement of the  $\Delta K=\pm 3$  transition in phosphine [73] and arsine [74] employed a high- $Q$ , Stark-modulated Fabry-Perot absorption cavity and had an estimated sensitivity of  $2 \times 10^{-10} \text{ cm}^{-1}$  at 144 GHz for a time constant of 1 sec. Figure 6.12 shows four  $^{75}\text{As}$  hyperfine components of a  $\Delta J=0, \Delta K=\pm 3$  transition of  $\text{AsH}_3$  recorded with this spectrometer.

For  $C_{3v}$  molecules such as phosphine and arsine having a relatively large  $\mu_z$  and high degenerate vibrational frequencies,  $v_3$  and  $v_4$ , the intensities of the  $\Delta K=\pm 3$  transitions are due primarily to centrifugal distortion in the ground vibrational state. For example, Chu and Oka [67] calculated  $\theta_x^{xx}=1.6 \times 10^{-5} \text{ D}$  and the distortion moment, last term of (6.53), to be  $8.3 \times 10^{-5} \text{ D}$ . Thus the

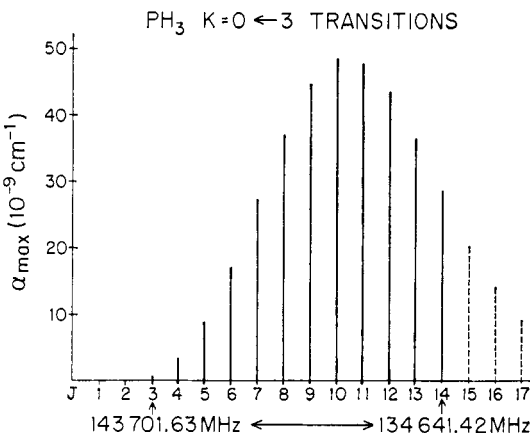


**Fig. 6.11** Calculated intensities of the  $J \leftarrow J$ ,  $K=0 \leftarrow 3$  rotational lines of  $\text{PH}_3$  in the ground vibrational state. The solid lines indicate observed transitions. From Helms and Gordy [73].

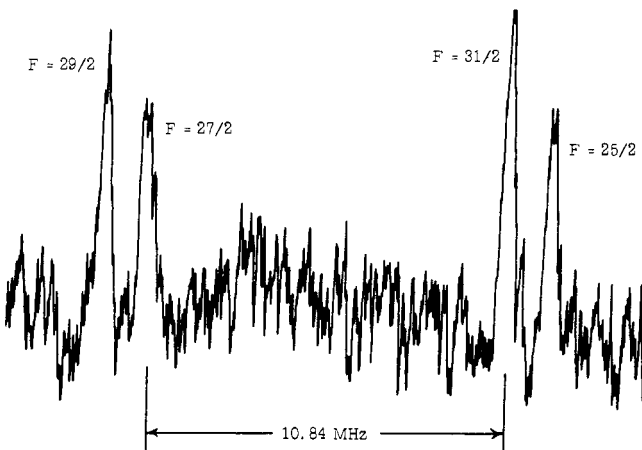


**Fig. 6.12** Single scan of the "forbidden"  $J=14$ ,  $K=\pm 5 \rightarrow \pm 2$  rotational transition of  $\text{AsH}_3$  showing  $F \rightarrow F$  components of the  $^{75}\text{As}$  hyperfine structure. From Helms and Gordy [74].

contribution of the vibration-rotation interaction to the line intensities is only  $(1.6)^2 / [(1.6)^2 + (8.3)^2] = 3.6\%$ . Oka [70] describes the contribution from centrifugal distortion, which mixes the  $(J, K)$  and  $(J, K \pm 3)$  rotational levels of the ground vibrational states, as "rotational intensity borrowing" from the normal  $\Delta J=1$ ,  $\Delta K=0$  transitions. The contribution of the vibration-rotation interaction, (6.49), which mixes the ground-state rotational levels with those of excited, degenerate vibrational states, he describes as "vibrational intensity borrowing." In this description, the observed  $\Delta K = \pm 3$  transitions in phosphine

and arsine are due primarily to “rotational intensity borrowing” within the ground vibrational state.

In the rigid-rotor approximation, Section 1, the  $|K|$  levels of the symmetric-top molecule are all doubly degenerate except for  $K=0$ . In the distortable rotor, the  $|K|$  levels, except for  $|K|=3$ , remain degenerate with  $E$  symmetry but are displaced by centrifugal distortion. The  $K=0$  and  $|K|=3, 6, \dots$  have symmetry  $A$ . In addition to displacement, the  $|K|=3$  levels are split into two components with symmetry  $A$ , designated as  $A_1$  and  $A_2$ . These designations indicate the symmetric or antisymmetric classification of the coordinate wave function (exclusive of nuclear spin) under exchange of two identical atoms. The selection rules  $A \leftrightarrow A$  and  $E \leftrightarrow E$  conform to the  $\Delta K = \pm 3$  rule. Within the transitions for the split  $K=3$  levels,  $A_1 \leftrightarrow A_2$  are allowed. The signs + and - are used for designation of the symmetry of the wave function with respect to inversion of the coordinates (Chapter III, Section 4). In addition to the  $K = \pm 3$  rule, the transitions must comply with the parity selection rules, sym  $\leftrightarrow$  sym and antisym  $\leftrightarrow$  antisym, for the overall wave function including nuclear spin, as described in Chapter III, Section 4. The effects of nuclear-spin statistics on the intensities of the transitions for symmetric-top molecules having  $C_{3v}$  symmetry are given in Table 3.3. In measurements on  $\text{PH}_3$ ,  $\text{PD}_3$ , and  $\text{AsH}_3$ , the inversion levels were not separated, and hence the weights given at the bottom of Table 3.3 apply.

In addition to the determination of the moments of inertia about the symmetry axis, measurements of the forbidden transitions in  $C_{3v}$  symmetric-top molecules have provided considerable new information about the centrifugal distortion of the molecule in the ground vibrational state including the splitting of the  $K=3$  levels. Because the transitions can be measured over a wide range of  $J$  values (see Fig. 6.11), accurate evaluations of the centrifugal distortion constants can be made for relatively light symmetric tops such as  $\text{PH}_3$  without need for measurement of very high frequencies extending into the submillimeter and infrared regions. The most extensive measurements of forbidden spectra to date have been made on  $\text{PH}_3$ ,  $\text{PD}_3$ , and  $\text{AsH}_3$ . Vibration-rotation transitions, including  $\Delta(K-l)=\pm 3$ , have been measured by Maki et al. [75] for  $\text{PH}_3$  and by Olsen et al. [76] for  $\text{AsH}_3$ . The first measurements of ground state,  $\Delta K=\pm 3$ , transitions are those by Chu and Oka [67] the  $J \rightarrow J$ ,  $K=\pm 2 \rightarrow \mp 1$  transitions of  $\text{PH}_3$ ,  $\text{PD}_3$ , and  $\text{AsH}_3$ . Helms and Gordy [73, 74] extended these measurements to include:  $J \rightarrow J$ ,  $K=3 \rightarrow 0$  in  $\text{PH}_3$ ;  $J \rightarrow J$ ,  $K=3 \rightarrow 0$ , and  $K=\pm 4 \rightarrow \pm 1$  in  $\text{PD}_3$ ;  $J \rightarrow J$ ,  $K=\pm 4 \rightarrow \pm 1$ , and  $K=\pm 5 \rightarrow \pm 2$  in  $\text{AsH}_3$ . Each  $K$  transition was measured for several  $J$  values. Helms and Gordy combined the measured frequencies of all these forbidden transitions with those measured earlier [77, 78] for the normal  $\Delta J=1$ ,  $\Delta K=0$  of these molecules in a computer analysis to obtain the values of their rotational constants, listed in Table 6.4. The molecular structures obtained from this analysis are given in Table 6.8.

The analysis of the phosphine and arsine data consists of a least-squares computer fitting of the involved spectral parameters to the observed frequencies. The computer program was made to include all frequencies of the different types of transitions measured. It was designed to compute the differences in the

## Chapter VII

# ASYMMETRIC-TOP MOLECULES

---

1	QUALITATIVE DESCRIPTION	227
2	ENERGIES OF THE RIGID ASYMMETRIC ROTOR	232
	Factorization of the Energy Matrix from Symmetry Properties	237
	Symmetry Classification of the Energy Levels	241
	Evaluation of the Energy Levels, Wave Functions, and Average Values	244
3	SLIGHTLY ASYMMETRIC ROTORS	250
4	SELECTION RULES AND INTENSITIES	254
5	IDENTIFICATION AND ANALYSIS OF ROTATIONAL SPECTRA	264
	Common Aids for Identification of Observed Transitions	264
	Computer Assignment and Analysis	269
	Double Resonance as an Aid to Spectral Assignment	273
6	EFFECTS OF VIBRATION	281
	Rotation-Vibration Hamiltonian	282
	Coriolis Perturbations	289
7	ASYMMETRIC ROTOR STRUCTURES	291

## 1 QUALITATIVE DESCRIPTION

When none of the three principal moments of inertia of a molecule is zero and if no two are equal, considerable complexity is encountered in its pure rotational spectrum. The rotational frequencies can no longer be expressed in convenient equations, as can be done for linear or symmetric-top molecules. Only for certain low  $J$  values can the energy levels of the asymmetric rotor be expressed in closed form, even if centrifugal distortion effects are neglected. The increased complexity of the pure rotational spectrum over that of the symmetric-top rotor is illustrated in Fig. 7.1. The various methods that have been used to give the energy levels and wave functions for the asymmetric rotor are considerably more involved than are those for symmetric rotors. The general procedure is to assume that the wave functions can be expanded in terms of an orthogonal set of functions (a natural basis would be the symmetric-top functions) and to set up the secular equations for the unknown coefficients and energies. The resulting secular determinant can be broken down into a number

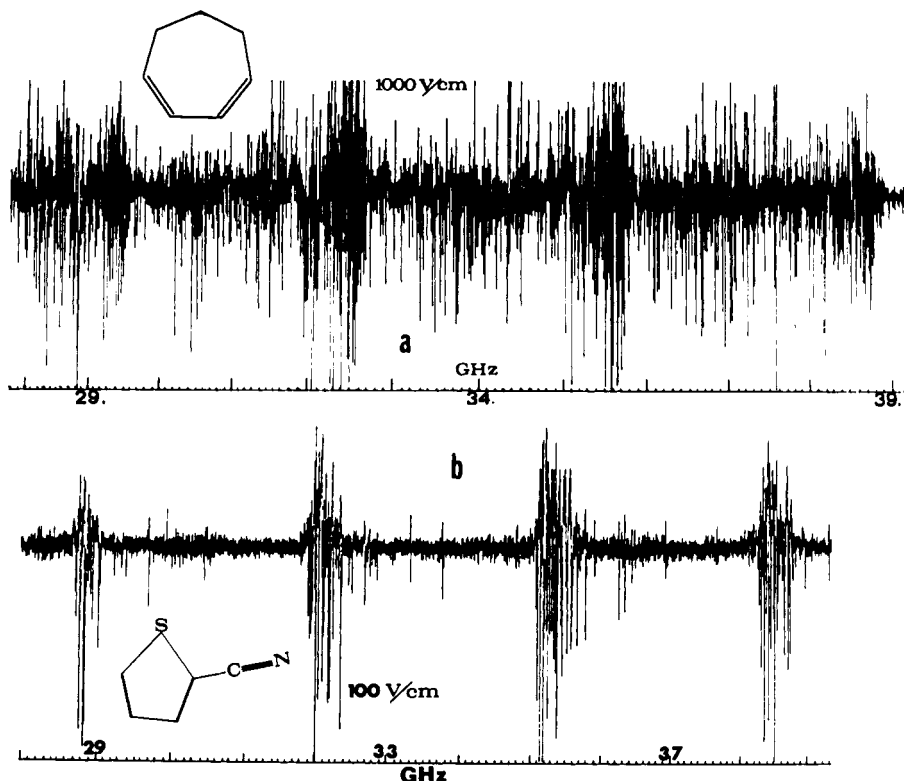


**Fig. 7.1 (a)** A condensed-scale scan of the spectrum of 1,3-cycloheptadiene ( $\kappa \approx 0.85$ ) which has "b"-type transitions. Frequency markers are spaced 100 MHz apart and the sweep rate was about 5 MHz/sec. The zero field lines are down, Stark lobes are up. The separation between the  ${}^bQ_{1-1}$  band heads is approximately 3110 MHz.  $A = 3419.424$ ,  $B = 3297.290$ , and  $C = 1799.961$  MHz. From Avirah et al. [48]. (b) Condensed-scale, *R*-band spectrum of 2-cyanothiophene. The sample pressure was about  $30 \mu\text{m}$  and the scan was about 3 MHz/sec. The Stark lobes are up and the zero field lines are down. Groups of closely spaced absorption lines ( $J \rightarrow J+1$ ,  $K_{-1} \rightarrow K_{-1}$ ) are observed separated by approximately 3175 MHz ( $\approx B+C$ ). From T. K. Avirah, T. B. Malloy Jr., and R. L. Cook, *J. Mol. Struct.*, **29**, 47 (1975).

of subdeterminants, the order of which increases with  $J$ . The solution of these subdeterminants yields the required energy levels and expansion coefficients. Details of these energy level calculations will be discussed in the next section.

Despite this complexity, much information useful to the chemist can be obtained from the microwave spectrum of an asymmetric-top molecule, in many instances without long labor or advanced mathematical skill. This is a fortunate circumstance since most molecules are of the asymmetric-top class. In the first place, both qualitative and quantitative spectrochemical analysis can be accomplished by measurements of microwave rotational spectra without an interpretation of their patterns. Second, somewhere in the wide span of the now workable microwave region there are usually low  $J$  transitions whose

frequency can be expressed with closed algebraic equations, from which the principal moments of inertia can be immediately evaluated. Furthermore, except for a few very light molecules such as H<sub>2</sub>O, the centrifugal distortion effects on very low  $J$  transitions can usually be neglected. These lines cannot be identified from the simple pattern of the rotational spectrum as they can for the symmetric-top rotor, but the low  $J$  transitions can be readily identified by their Stark patterns from which the electric dipole moment can also be obtained (see Chapter X). In some cases, the transition can be identified by nuclear quadrupole hyperfine structure. Third, extensive tables are available from which energy levels for various degrees of asymmetry can be obtained to a useful degree of approximation for high  $J$  values.

To apply the equations and selection rules developed in the following sections, one must first become familiar with the notation used to designate the levels. Here we shall outline briefly the qualitative characteristics of the asymmetric rotor energy levels. In an asymmetric rotor there is no internal component of the angular momentum that is a constant of the motion; that is  $P_z$  no longer commutes with  $\mathcal{H}$  and only  $J$  and  $M$  are "good" quantum numbers. As for the symmetric rotor, we can write  $P^2 = (h/2\pi)^2 J(J+1)$  and  $P_z = \hbar M / 2\pi$ , where  $J$  and  $M$  are integers as previously defined. Pseudo-quantum numbers, customarily designated by subscripts on  $J$ , are employed in the designation of the levels. The double subscript system of King et al. [1] is perhaps the most descriptive and useful; it will be employed extensively. Their system is best understood by a comparison of the limiting prolate and oblate symmetric tops. In the conventional order,  $I_a < I_b < I_c$ . Thus, when  $I_b \rightarrow I_c$ , the prolate symmetric top is approached; and when  $I_b \rightarrow I_a$ , the oblate symmetric top is approached. We can describe the behavior of the asymmetric rotor in terms of the parameter:

$$\kappa = \frac{2B - A - C}{A - C} \quad (7.1)$$

which is a measure of its asymmetry, with  $A, B, C$ , the rotational constants with respect to the  $a, b, c$  axes. The limiting values for  $\kappa$ ,  $-1$  and  $+1$ , correspond to the prolate and oblate symmetric tops, respectively. The most asymmetric top has  $\kappa = 0$ . The energy levels of asymmetric rotors ( $\kappa \approx -1$  or  $\approx +1$ ) differ from the limiting symmetric-top ones essentially in that the levels corresponding to  $-K$  and  $+K$ , which are always degenerate in the symmetric rotor, are separated in the asymmetric rotor. Thus, an asymmetric rotor has  $(2J+1)$  distinct rotational sublevels for each value of  $J$ , whereas the symmetric rotor has only  $(J+1)$  distinct sublevels for each value of  $J$ . With an increase in asymmetry, the "K splitting" increases until there is no longer any close correspondence between the two levels and the degenerate  $K$  levels of the symmetric top. Nevertheless, by connecting the  $K$  levels for a given  $J$  of the limiting prolate symmetric top with those of the limiting oblate symmetric top in the ordered sequence—highest to highest, next highest to next highest, and so on, as indicated in Fig. 7.2—one may obtain a qualitative indication of the levels of the asymmetric rotor. This chart also reveals the significance of the King-Hainer-Cross notation,

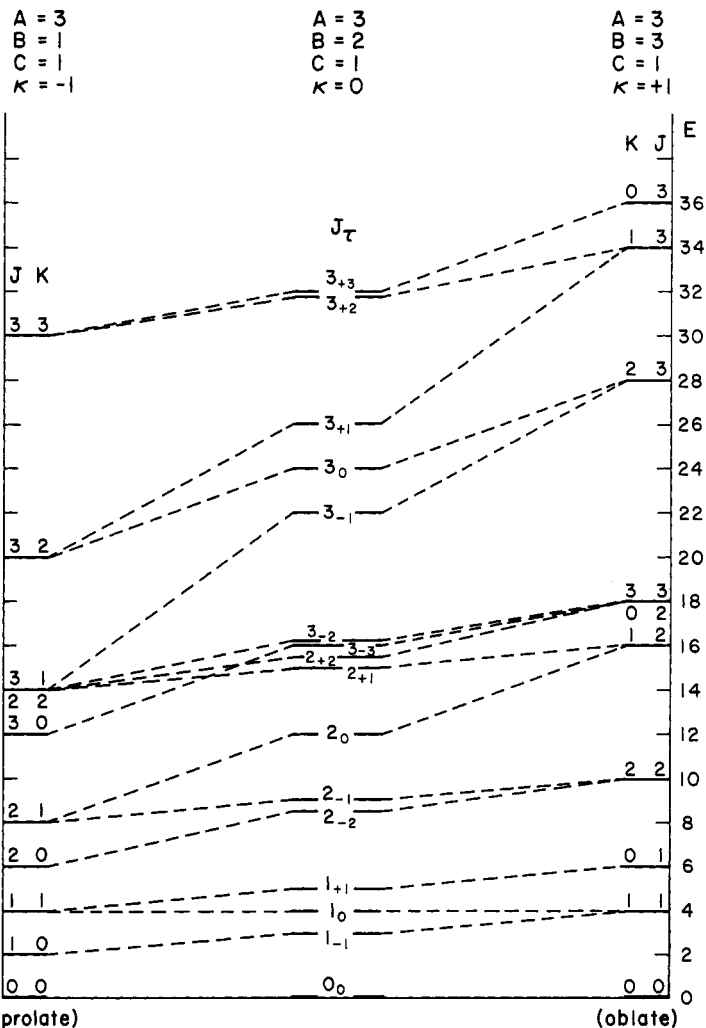


**Fig. 7.2** Relation of the asymmetric rotor energy levels to those of the limiting prolate and oblate symmetric top. Note there is no crossing of sublevels of a given  $J$  although those of different  $J$  may cross. Also, the straight-line representation of the variation of the energy levels with  $k$  is only approximate.

$J_{K-1, K_1}$ . The first subscript,  $K_{-1}$ , represents the  $K$  value of the limiting prolate top (left side in Fig. 7.2) with which the asymmetric-top level connects as  $\kappa$  approaches  $-1$ . The second subscript,  $K_1$ , represents the  $K$  value of the limiting oblate top with which the particular level connects as  $\kappa$  approaches  $1$ . Note that the highest sublevels of the prolate symmetric top have the highest  $K$  values, whereas the highest sublevels for the oblate symmetric top have the lowest  $K$  values. Another important point evident from Fig. 7.2 is that the asymmetry

**Table 7.1** Effective Rigid-Rotor Constants for the Ground Vibrational State of Some Asymmetric-top Molecules

Molecule	$A_0$ (MHz)	$B_0$ (MHz)	$C_0$ (MHz)	Ref.
CH <sub>3</sub> OCl	42,064.35	6,296.88	5,670.62	<sup>b</sup>
CH <sub>2</sub> F <sub>2</sub>	49,138.4	10,603.89	9,249.20	<sup>c</sup>
CH <sub>2</sub> (CN) <sub>2</sub>	20,882.137	2,942.477	2,616.774	<sup>d</sup>
CH <sub>3</sub> CH <sub>2</sub> F	36,070.30	9,364.54	8,199.74	<sup>e</sup>
CH <sub>3</sub> CHO <sup>a</sup>	56,920.5	10,165.1	9,100.0	<sup>f</sup>
CH <sub>3</sub> COF	11,039.28	9,685.65	5,322.05	<sup>g</sup>
CH <sub>2</sub> =CHF	64,582.7	10,636.83	9,118.18	<sup>h</sup>
CH <sub>3</sub> N=CH <sub>2</sub> <sup>a</sup>	52,523.75	10,666.13	9,377.19	<sup>i</sup>
CH <sub>3</sub> CH <sub>2</sub> CH <sub>3</sub>	29,207.36	8,446.07	7,458.98	<sup>j</sup>
CH <sub>3</sub> CH <sub>2</sub> CH <sub>2</sub> Cl ( <i>gauche</i> )	11,829.22	3,322.58	2,853.06	<sup>k</sup>
CH <sub>3</sub> CH=CHF ( <i>cis</i> )	17,826.09	5,656.57	4,406.91	<sup>l</sup>
CH <sub>3</sub> CH=C=O	38,920	4,507.349	4,136.983	<sup>m</sup>
(CH <sub>3</sub> ) <sub>2</sub> O	38,788.5	10,056.6	8,886.9	<sup>n</sup>
(CH <sub>3</sub> ) <sub>2</sub> CO	10,165.60	8,514.95	4,910.17	<sup>o</sup>
C <sub>4</sub> H <sub>4</sub> O (furan)	9,446.96	9,246.61	4,670.88	<sup>p</sup>
C <sub>6</sub> H <sub>5</sub> F	5,663.54	2,570.64	1,767.94	<sup>q</sup>
C <sub>6</sub> H <sub>5</sub> OH	5,650.46	2,619.20	1,789.84	<sup>r</sup>
<i>p</i> -CH <sub>3</sub> C <sub>6</sub> H <sub>4</sub> F	5,702.722	1,430.322	1,143.551	<sup>s</sup>

<sup>a</sup>Rotational constants of the *A* lines which have not been corrected for internal rotation effects.

<sup>b</sup>J. S. Rigden and S. S. Butcher, *J. Chem. Phys.*, **40**, 2109 (1964).

<sup>c</sup>D. R. Lide, Jr., *J. Am. Chem. Soc.*, **74**, 3548 (1952).

<sup>d</sup>E. Hirota and Y. Morino, *Bull. Chem. Soc. Japan*, **33**, 158 (1960).

<sup>e</sup>J. Kraitchman and B. P. Dailey, *J. Chem. Phys.*, **23**, 184 (1955).

<sup>f</sup>R. W. Kilb, C. C. Lin, and E. B. Wilson, Jr., *J. Chem. Phys.*, **26**, 1695 (1957).

<sup>g</sup>L. Pierce and L. C. Krisher, *J. Chem. Phys.*, **31**, 875 (1959).

<sup>h</sup>A. M. Mirri, A. Guarneri, and P. Favero, *Nuovo Cim.*, **19**, 1189 (1961).

<sup>i</sup>K. V. L. N. Sastry and R. F. Curl, Jr., *J. Chem. Phys.*, **41**, 77 (1964).

<sup>j</sup>D. R. Lide, Jr., *J. Chem. Phys.*, **33**, 1514 (1960).

<sup>k</sup>T. N. Sarachman, *J. Chem. Phys.*, **39**, 469 (1963).

<sup>l</sup>R. A. Beaudet and E. B. Wilson, Jr., *J. Chem. Phys.*, **37**, 1133 (1962).

<sup>m</sup>B. Bak, J. J. Christiansen, K. Kunstmann, L. Nygaard, and J. Rastrup-Andersen, *J. Chem. Phys.*, **45**, 883 (1966).

<sup>n</sup>U. Blukis, P. H. Kasai, and R. J. Myers, *J. Chem. Phys.*, **38**, 2753 (1963).

<sup>o</sup>R. Nelson and L. Pierce, *J. Mol. Spectrosc.*, **18**, 344 (1965).

<sup>p</sup>B. Bak, D. Christensen, W. B. Dixon, L. Hansen-Nygaard, J. Rastrup-Andersen and M. Schottlander, *J. Mol. Spectrosc.*, **9**, 124 (1962).

<sup>q</sup>B. Bak, D. Christensen, L. Hansen-Nygaard, and E. Tannenbaum, *J. Chem. Phys.*, **26**, 134 (1957).

<sup>r</sup>T. Kojima, *J. Phys. Soc. Japan.*, **15**, 284 (1960).

<sup>s</sup>H. D. Rudolph and H. Seiler, *Z. Naturforsch.*, **20a**, 1682 (1965).

splitting of the  $K$  levels decreases as  $K$  increases, and for a given  $K$ , increases as  $J$  increases. The double subscript notation also gives the symmetry of the wave functions of the level, which is useful information for the application of the symmetry selection rules to be given later.

In the older notation still used widely in the literature, a single subscript on  $J$ , designated  $\tau$ , is employed. For the highest sublevels of a given  $J$ , the subscript  $\tau$  is given the value  $J$ ; for the next highest,  $J - 1$ , and so on to the lowest level for which the subscript  $\tau$  is assigned the value of  $-J$ . Since there are  $(2J + 1)$  discrete rotational sublevels for a given value of  $J$ , there are  $(2J + 1)$  values of  $\tau$  ranging from  $\tau = J$  for the highest, to  $\tau = -J$  for the lowest level. From Fig. 7.2 it is clear that

$$\tau = K_{-1} - K_1 \quad (7.2)$$

It should be emphasized that  $\tau$  is not a quantum number (nor is  $K_{-1}$  or  $K_1$ ); it is simply a number used to designate the sequence of the sublevels. It is often called a pseudo-quantum number.

Characteristic rotational energies of the rigid asymmetric rotor for  $J$  values up to 15 have been obtained [2] in the form of algebraic equations which, in general, increase in power as  $J$  increases. For very low  $J$  values, only linear and quadratic equations are involved, and these can be readily solved to give the desired energies. Expressions for the energies for such cases have been given in terms of the rotational constants [3]  $A$ ,  $B$ , and  $C$ , and in terms of the asymmetry parameter [1]  $\kappa$ . These are collected in Tables 7.6 and 7.7. The values of  $A$ ,  $B$ , and  $C$  for some selected molecules are listed in Table 7.1. One can obtain the microwave rotational frequencies, as before, by finding the difference in the energies of the two levels between which a transition occurs. Various expansions can be employed for finding the energies of special classes of asymmetric rotors, such as those near the prolate or near the oblate limits. These methods will be discussed in Section 3 after a more complete description of the asymmetric rotor energy levels is given.

## 2 ENERGIES OF THE RIGID ASYMMETRIC ROTOR

The qualitative behavior of the energy levels of an asymmetric rotor has been described; however, quantitative calculations of the rotational energies require a discussion of the quantum mechanics of the system.

In general, the rotational problem is treated in terms of a Cartesian axis system ( $x$ ,  $y$ ,  $z$ ) tied, so to speak to the molecule so that it rotates with the molecule and has its origin located at the center of mass of the system. Furthermore, the molecule-fixed axis system is usually oriented so that its axes coincide with the principal axes of inertia, designated as  $a$ ,  $b$ , and  $c$ . The quantum mechanical Hamiltonian describing the rotation of a rigid asymmetric body is then

$$\mathcal{H} = AP_a^2 + BP_b^2 + CP_c^2 \quad (7.3)$$

where  $A = h^2/(8\pi^2 I_a)$ ,  $B = h^2/(8\pi^2 I_b)$ , and  $C = h^2/(8\pi^2 I_c)$ . This Hamiltonian is analogous to the classical Hamiltonian except that the components of the angular momentum of rotation  $P_a$ ,  $P_b$ ,  $P_c$  are replaced in quantum mechanics by their corresponding operators. For convenience, the  $\hbar$  factor has been included in the definition of the rotational constants so that the angular momenta are now expressed in units of  $\hbar$ . The calculation of the energy levels is facilitated by rearrangement of (7.3) as proposed by Ray [4]:

$$\mathcal{H} = \frac{1}{2}(A + C)P^2 + \frac{1}{2}(A - C)\mathcal{H}(\kappa) \quad (7.4)$$

$$\mathcal{H}(\kappa) = P_a^2 + \kappa P_b^2 - P_c^2 \quad (\text{Reduced Hamiltonian}) \quad (7.5)$$

with  $P^2 = P_a^2 + P_b^2 + P_c^2$  and  $\kappa$  a dimensionless number measuring the degree of asymmetry. That this expression is equivalent to (7.3) is readily seen by substitution of the definition of Ray's asymmetry parameter, (7.1) and collection of terms. The advantage of this formulation is that the reduced energies, which are the eigenvalues of  $\mathcal{H}(\kappa)$ , depend only on the inertial asymmetry parameter  $\kappa$  and not on the individual rotational constants, and are hence easily tabulated. It may be noted that the reduced energies are simply eigenvalues of (7.3) for a hypothetical rotor with  $A = +1$ ,  $B = \kappa$ ,  $C = -1$ .

Unlike the symmetric rotor Hamiltonian, this Hamiltonian is such that the Schrödinger wave equation cannot be solved directly; thus, a closed general expression for the asymmetric rotor wave functions is not possible. However, they may be represented by a linear combination of symmetric rotor functions, that is,

$$\psi_{J,M} = \sum_{J,K,M} a_{JKM} \psi_{JKM} \quad (7.6)$$

where the  $a_{JKM}$ 's are numerical constants and where  $\psi_{JKM}$  is given by (2.103). The symmetric rotor wave functions are orthonormal:

$$(J', K', M' | J, K, M) = \begin{cases} 0 & \text{if } J'K'M' \neq JKM \\ 1 & \text{if } J'K'M' = JKM \end{cases} \quad (7.7)$$

and characterize a representation in which  $P^2$ ,  $P_z$ , and  $P_z$  are simultaneously diagonal. Since  $\mathcal{H}$  is a function of  $P_x^2$ ,  $P_y^2$ , and  $P_z^2$ , the matrix elements of these operators will be required. In Table 7.2 we summarize the angular momenta matrix elements, with angular momentum measured in units of  $\hbar$ . These have been discussed in Chapter II, Section 2.

Following the procedure outlined in Chapter II, Section 4, and noting that the Hamiltonian matrix elements vanish unless  $J' = J$ ,  $M' = M$  (see Table 7.2), we obtain the following set of homogeneous linear equations in the coefficients  $a_{JKM}$ :

$$\sum_{K=-J}^{+J} (\mathcal{H}_{K'K} - \delta_{K'K}\lambda) a_{JKM} = 0 \quad K' = -J, \dots, +J \quad (7.8)$$

where  $\mathcal{H}_{K'K} = (J, K', M | \mathcal{H} | J, K, M)$ . The square array  $[\mathcal{H}_{K'K}]$  is in particular

**Table 7.2** Angular Momentum Matrix Elements in a Symmetric Rotor Representation<sup>a</sup>*Molecule-fixed Axis System*

$$(J, K, M|P_z|J, K, M) = K$$

$$(J, K, M|P_y|J, K \pm 1, M) = \mp i(J, K, M|P_x|J, K \pm 1, M) = \frac{1}{2}[J(J+1) - K(K \pm 1)]^{1/2}$$

$$(J, K, M|P_x^2|J, K, M) = J(J+1)$$

$$(J, K, M|P_z^2|J, K, M) = K^2$$

$$(J, K, M|P_y^2|J, K, M) = (J, K, M|P_x^2|J, K, M) = \frac{1}{2}[J(J+1) - K^2]$$

$$(J, K, M|P_x^2|J, K \pm 2, M) = -(J, K, M|P_x^2|J, K \pm 1, M) = \frac{1}{4}\{[J(J+1) - K(K \pm 1)][J(J+1) - (K \pm 1)(K \pm 2)]\}^{1/2}$$

<sup>a</sup>Phase choice is that of King et al. [1] and the angular momentum is measured in units of  $\hbar$ . Note the matrices are Hermitian, i.e., the elements are related by  $(R|P_a|R') = (R'|P_a|R)^*$  where  $R$  stands for the totality of quantum numbers  $JKM$  and the asterisk stands for the complex conjugate. The  $P_x^2$  matrix elements are obtained by the ordinary matrix multiplication rule:  $(R|P_x^2|R') = \sum_{R''} (R|P_x|R'') \times (R''|P_x|R')$ .

a matrix representation of the Hamiltonian operator (energy matrix) with respect to the symmetric rotor basis functions. The foregoing set of equations has nontrivial solutions for the expansion coefficients only for certain values of  $\lambda$ . The special values of  $\lambda$  (the allowed energy levels for an asymmetric rotor) are those for which the secular determinant vanishes  $|\mathcal{H} - \mathbf{I}\lambda| = 0$  where  $\mathbf{I}$  is a unit matrix. Because there are no off-diagonal matrix elements in  $J$ , the matrices for each value of  $J$  are independent and may be treated separately (see Fig. 7.3). The fact that the energy matrix is diagonal in  $J$  is to be expected since we noted previously that the total angular momentum is a constant of motion. Moreover, the matrix elements are independent of the value of  $M$  (the energy independent of the spacial orientation of  $\mathbf{P}$ ) so that its value need not concern us further. Consequently, we will have a secular determinant to solve for each value of  $J$ ; and since  $K$  takes on all integral values from  $-J$  to  $+J$ , each determinant will have  $2J+1$  rows and columns. The energy eigenvalues or characteristic values are obtained by solution of the secular determinant.

To set up the energy matrix explicitly for a given  $J$ , it is necessary to know the nonvanishing matrix elements of the Hamiltonian, (7.4). These may be obtained from Table 7.2. Since  $\frac{1}{2}(A+C)P^2$  contributes only a constant diagonal term, being independent of  $K$ , and since the factor  $\frac{1}{2}(A-C)$  multiplies each matrix element of  $\mathcal{H}(\kappa)$ , a reduced energy matrix  $\mathbf{E}(\kappa)$  may be defined, involving only the operator  $\mathcal{H}(\kappa)$ , with the secular determinant

$$|\mathbf{E}(\kappa) - \mathbf{I}\lambda| = 0 \quad (7.9)$$

The total rotational energy for a particular level is given by

$$E = \frac{1}{2}(A+C)J(J+1) + \frac{1}{2}(A-C)E_{J\tau}(\kappa) \quad (7.10)$$

Here the  $2J+1$  solutions of (7.9) are labeled by  $E_{J\tau}(\kappa)$  where the magnitude of the subscript  $\tau$  increases as the magnitude of the reduced energy increases. The nonvanishing matrix elements of  $\mathbf{E}(\kappa)$  are

$$E_{K,K'} = \langle J, K, M | \mathcal{H}(\kappa) J, K, M \rangle = F[J(J+1) - K^2] + GK^2 \quad (7.11)$$

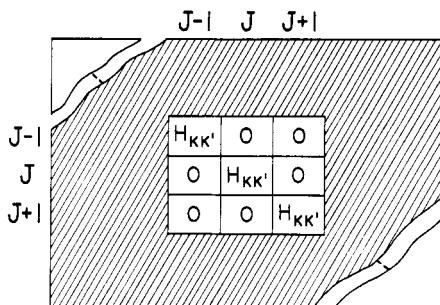


Fig. 7.3 Factoring of the infinite order energy matrix into  $J$ -blocks.

$$E_{K,K\pm 2} = (J, K, M | \mathcal{H}(\kappa) | J, K \pm 2, M) = H[f(J, K \pm 1)]^{1/2} \quad (7.12)$$

where

$$f(J, K \pm 1) = \frac{1}{4}[J(J+1) - K(K \pm 1)][J(J+1) - (K \pm 1)(K \pm 2)] \quad (7.13)$$

with the fact that

$$E_{K,K} = E_{-K,-K}, \quad E_{K,K+2} = E_{K+2,K} = E_{-K,-K-2} = E_{-K-2,-K} \quad (7.14)$$

The values of  $f(J, K \pm 1)$  have been tabulated [1] up to  $J=30$ . The constants  $F$ ,  $G$ , and  $H$  depend on the particular way in which the  $a$ ,  $b$ , and  $c$  axes are identified with the axes  $x$ ,  $y$ , and  $z$ . There are six possible ways to make this identification, which are summarized in Table 7.3, along with the possible values of  $F$ ,  $G$ , and  $H$ . The I' and III' type representation are sufficient to handle conveniently most asymmetric tops. Both identifications, of course, give the same energy levels; however, each identification has a particular advantage for certain ranges of  $\kappa$ . For example, if we consider a prolate rotor where  $\kappa = -1$  and where the unique axis, the symmetry axis  $z$ , is associated with the  $a$  axis, that is, type I', the energy matrix becomes diagonal,  $H=0$ . The diagonal matrix elements are simply

$$-J(J+1) + 2K_{-1}^2$$

and from (7.10) the rotational energies of a prolate symmetric top are

$$E = CJ(J+1) + (A - C)K_1^2 \quad (7.15)$$

Thus for an asymmetric rotor with  $\kappa$  near  $-1$ , type I' is the most convenient form to use in determining the energy levels since the matrix has small off-diagonal elements and thus is nearly diagonal. For an oblate rotor where  $\kappa = +1$  with  $z=c$ , that is, type III', the energy matrix is again diagonal with elements

$$J(J+1) - 2K_1^2$$

and the oblate top energy levels are given by

$$E = AJ(J+1) - (A - C)K_1^2 \quad (7.16)$$

**Table 7.3** Identification of  $a$ ,  $b$ ,  $c$  with  $x$ ,  $y$ ,  $z$  and the Coefficients for the Matrix Elements of  $E(\kappa)$

I'	II'	III'	I'	II'	III'
$x$	$b$	$c$	$a$	$c$	$a$
$y$	$c$	$a$	$b$	$b$	$c$
$z$	$a$	$b$	$c$	$a$	$c$
$F$	$\frac{1}{2}(\kappa-1)$	0	$\frac{1}{2}(\kappa+1)$	$\frac{1}{2}(\kappa-1)$	0
$G$	1	$\kappa$	-1	1	$\kappa$
$H$	$-\frac{1}{2}(\kappa+1)$	1	$\frac{1}{2}(\kappa-1)$	$\frac{1}{2}(\kappa+1)$	-1

Therefore for an asymmetric oblate type top with  $\kappa$  close to +1 type III<sup>t</sup> is the most useful form to employ.

The explicit form of the secular determinant, (7.9), for  $J=3$  is

$$\begin{array}{|c|ccccccc|} \hline K' | K & -3 & -2 & -1 & 0 & 1 & 2 & 3 \\ \hline -3 & E_{-3-3}-\lambda & 0 & E_{-3-1} & 0 & 0 & 0 & 0 \\ -2 & 0 & E_{-2-2}-\lambda & 0 & E_{-20} & 0 & 0 & 0 \\ -1 & E_{-1-3} & 0 & E_{-1-1}-\lambda & 0 & E_{-11} & 0 & 0 \\ 0 & 0 & E_{0-2} & 0 & E_{00}-\lambda & 0 & E_{02} & 0 \\ 1 & 0 & 0 & E_{1-1} & 0 & E_{11}-\lambda & 0 & E_{13} \\ 2 & 0 & 0 & 0 & E_{20} & 0 & E_{22}-\lambda & 0 \\ 3 & 0 & 0 & 0 & 0 & E_{31} & 0 & E_{33}-\lambda \\ \hline \end{array} = 0 \quad (7.17)$$

where, for clarity, the rows and columns are labeled in terms of the possible values of  $K$ . The numerical values of the matrix elements  $E_{KK'}$  are obtained directly from (7.11) and (7.12) once a value of  $\kappa$  is specified. It may be pointed out that this determinant can be factored into two subdeterminants made up, respectively, of even and odd  $K$  indices, because there are no matrix elements connecting even and odd  $K$ . However, a further factoring is possible, which is suggested by the additional symmetry of the energy matrix about the secondary diagonal, and this will be discussed in the next section.

### Factorization of the Energy Matrix from Symmetry Properties

Although the energy levels can be found from a solution of (7.9) and thus, in principle, the energy level calculation for an asymmetric rotor has been solved, a further simplification can be obtained by consideration of the symmetry properties of the Hamiltonian. The symmetry properties of the rotational problem may be deduced from its ellipsoid of inertia. The ellipsoid of inertia is symmetric not only to an identity operation  $E$  but also to a rotation of  $180^\circ$ ,  $C_2$ , about any one of its principal axes of inertia. This set of symmetry operations form a group which in the language of group theory is known as the Four-group designated by  $V(a, b, c)$ . These symmetry operations cause the angular momentum to transform in the following manner:

$$E: P_a \rightarrow P_a, P_b \rightarrow P_b, P_c \rightarrow P_c$$

$$C_2^a: P_a \rightarrow P_a, P_b \rightarrow -P_b, P_c \rightarrow -P_c$$

$$C_2^b: P_a \rightarrow -P_a, P_b \rightarrow P_b, P_c \rightarrow -P_c$$

$$C_2^c: P_a \rightarrow -P_a, P_b \rightarrow -P_b, P_c \rightarrow P_c$$

The Hamiltonian of a rigid asymmetric rotor is invariant under these operations and, therefore, has the symmetry of the Four-group. The symmetry group of the Hamiltonian is extremely important in quantum mechanics because a knowledge of it allows the classification of quantum states, simplification thereby of the energy matrix, and the determination of selection rules with

relative ease. In the present case, each asymmetric rotor wave function may be classified according to its behavior under  $V(a, b, c)$ , the symmetry group of the asymmetric rotor Hamiltonian. The character table for the Four-group is given in Table 7.4. The notation for the symmetry species of  $V$  indicates the axis about which the rotation has a character of +1. A wave function which is, for example, symmetric (multiplied by +1) for a twofold rotation about axis  $a$  and anti-symmetric (multiplied by -1) for a twofold rotation about the other two axes may be classified as belonging to species  $B_a$  of the group. A function that is invariant with respect to all symmetry operations of the group obviously belongs to species  $A$ .

It would be advantageous to use a set of basis functions in the calculations of the rotational energies which also belong to this group. Each wave function could then be classified according to one of the symmetry species  $A$ ,  $B_a$ ,  $B_b$ ,  $B_c$  of  $V$ , and hence the matrix elements of the Hamiltonian ( $\psi_i | \mathcal{H} | \psi_j$ ) would be nonzero only between states of the same symmetry. This follows since the matrix elements are just numerical quantities and hence must be invariant under a transformation of coordinates such as the group symmetry operations that carry the system into an equivalent configuration, that is, one which is indistinguishable from the original. Therefore, since  $\mathcal{H}$  belongs to the species  $A$  being unchanged by any symmetry operations of the group, the wave functions must both have the same symmetry; otherwise, the matrix elements will change sign for two of the symmetry operations and must then vanish. (See also the discussion at the end of Appendix A.) As a consequence, the secular determinant for any value of  $J$  will factor into four independent subdeterminants, one for each of the symmetry species of the Four-group (see Fig. 7.4). This, of course, considerably simplifies the diagonalization problem and has the further advantage that pairs of degenerate or nearly degenerate  $K$  levels are separated into different submatrices. Without this separation of near degeneracies, the numerical evaluation of the roots by continued fraction techniques become more difficult.

This factoring of the secular determinant is a typical example of the simplification that can result if basis functions are chosen which may be classified according to the symmetry species of the group which reflects the symmetry

**Table 7.4** Character Table of the Four-Group  $V(a, b, c)$

Symmetry Species	$E$	$C_2^a$	$C_2^b$	$C_2^c$
$A$	1	1	1	1
$B_a$	1	1	-1	-1
$B_b$	1	-1	1	-1
$B_c$	1	-1	-1	1

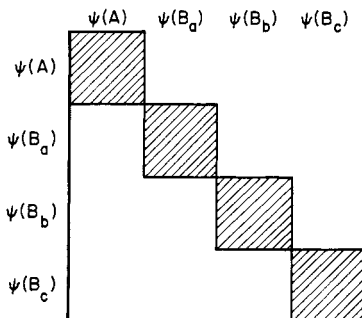


**Fig. 7.4** Schematic illustration of the maximum factoring of the energy matrix by proper choice of basis functions.  $\psi(A)$ , for example, signifies a set of basis functions with symmetry  $A$ . Nonzero matrix elements of the Hamiltonian are present only in the shaded blocks. Each of the smaller submatrices may be solved separately since there are no connecting elements present.

of the problem. Molecular orbital calculations, which are of particular interest to the chemist, are greatly aided by exploitation of the symmetry of the molecule.

The symmetric rotor wave functions which have been used as the basis functions do not belong to  $V$  but to the continuous two-dimensional rotation group  $D_\infty$ , which is comprised of  $C_\infty^z$ , indicating full rotational symmetry about the  $z$  axis and an infinite number of twofold axes of symmetry,  $C_2$ 's, at right angles to the principal symmetry axis  $z$ . This group has an infinite number of symmetry species. However, as pointed out by Mulliken [5], the Wang [6] linear combinations of symmetric rotor functions do belong to the Four-group. The appropriate linear combinations are constructed from functions of the doubly degenerate  $K$ -states which differ in the sign of  $K$  and are defined for a given  $J$  and  $M$  as follows

$$S_{JKM\gamma} = \frac{1}{\sqrt{2}} [\psi_{JKM}^\chi + (-1)^\gamma \psi_{J-KM}^\chi], \quad \text{for } K \neq 0$$

$$S_{J0M0} = \psi_{J0M}^\chi, \quad \text{for } K = 0 \quad (7.18)$$

where  $\gamma$  is 0 or 1 and  $K$  now takes on only positive values. The  $\gamma=0$  functions are the symmetric Wang functions whereas those with  $\gamma=1$  are the antisymmetric Wang functions. Here  $\psi_{JKM}^\chi = (-1)^\beta \psi_{JKM}$  with  $\beta = K$  if  $K \geq M$  or  $\beta = M$  if  $K \leq M$ . This latter modification was suggested by Van Vleck [7] in discussing the phase of the wave functions. The phases of the symmetric rotor wave functions, of course, have no effect on the energies. However, they are important when the symmetry classification of Wang's functions are considered [5].

The foregoing equations relate the old basis (the symmetric rotor functions) to the new basis (the Wang functions or symmetrized functions) and may be written in matrix form,  $\mathbf{S} = \hat{\mathbf{X}}\psi^\chi$ , in terms of the Wang symmetrizing transformation matrix,  $\mathbf{X}$ , which defines the change of basis. For a given  $J$  we have explicitly:

$$\begin{bmatrix} \vdots \\ S_{21} \\ S_{11} \\ S_{00} \\ S_{10} \\ S_{20} \\ \vdots \end{bmatrix} = \frac{1}{\sqrt{2}} \begin{bmatrix} \ddots & & & & & & \vdots \\ -1 & 0 & 0 & 0 & 1 & & \psi_{-2}^x \\ 0 & -1 & 0 & 1 & 0 & & \psi_{-1}^x \\ 0 & 0 & \sqrt{2} & 0 & 0 & & \psi_0^x \\ 0 & 1 & 0 & 1 & 0 & & \psi_1^x \\ 1 & 0 & 0 & 0 & 1 & & \psi_2^x \\ \ddots & & & & & & \vdots \end{bmatrix} \quad (7.19)$$

where all the subscripts except  $K$  and  $\gamma$  are suppressed and where the square matrix  $\tilde{\mathbf{X}} = \mathbf{X}^{-1} = \mathbf{X}$  (the tilde indicates the transpose).

Each asymmetric rotor wave function may now be expressed as a linear combination of the symmetrized wave functions

$$A_{J,\gamma,M} = \sum_K a_K^{J,M} S_{JKM,\gamma} \quad (7.20)$$

Alternately, we might use the notation  $A_{J_{K-1},K_1,M}$  to designate the asymmetric rotor wave function. The index  $M$  is not necessary since, as we have seen, the energy does not depend on the spatial orientation, at least in the absence of external fields, and is included only for completeness. Since the symmetrized functions can be classified to particular symmetry species of the asymmetric rotor group, the sum over  $K$  is to be carried out only over these  $S_{JKM,\gamma}$ 's that belong to the same symmetry species of  $V$  as does  $A_{J,\gamma,M}$ . Thus, the number of terms in (7.20) is much less than in (7.6). The change from an expansion in terms of the  $\psi_{JKM}$  to an expansion in terms of the  $S_{JKM,\gamma}$  will affect the form of the energy matrix. The new energy matrix  $\mathbf{E}'(\kappa)$  may be readily obtained by the following transformation on the original energy matrix  $\mathbf{E}(\kappa)$  (see Appendix A):

$$\mathbf{E}'(\kappa) = \tilde{\mathbf{X}} \mathbf{E}(\kappa) \mathbf{X} = \mathbf{E}^+(\kappa) + \mathbf{O}^+(\kappa) + \mathbf{E}^-(\kappa) + \mathbf{O}^-(\kappa) \quad (7.21)$$

This is the usual rule for relating the matrix representation of an operator (here the Hamiltonian) in an old basis to that in a new basis. The result of the matrix multiplication [use being made of (7.14)] is that  $\mathbf{E}(\kappa)$  splits into two submatrices corresponding to  $\gamma=0$  and  $\gamma=1$ . Each of these can be further factored as noted previously by arrangement of rows and columns so that even values of  $K$  are grouped together and odd values of  $K$  are grouped together. Thus in the notation used in (7.21)  $E$  and  $O$  refer to the evenness or oddness of the  $K$  values involved in the matrix elements and + and - to the evenness or oddness of  $\gamma$ . Portions of the four submatrices are:

$$\mathbf{E}^+(\kappa) = \begin{bmatrix} E_{00} & \sqrt{2}E_{02} & 0 & . & . \\ \sqrt{2}E_{02} & E_{22} & E_{24} & 0 & . \\ 0 & E_{24} & E_{44} & E_{46} & . \\ . & 0 & E_{46} & E_{66} & . \\ . & . & . & . & . \end{bmatrix},$$

$$\mathbf{E}^-(\kappa) = \begin{bmatrix} E_{22} & E_{24} & 0 & . & . \\ E_{24} & E_{44} & E_{46} & 0 & . \\ 0 & E_{46} & E_{66} & E_{68} & . \\ . & 0 & E_{68} & E_{88} & . \\ . & . & . & . & . \end{bmatrix}, \quad (7.22)$$

$$\mathbf{O}^+(\kappa) = \begin{bmatrix} E_{11} + E_{-11} & E_{13} & 0 & . & . \\ E_{13} & E_{33} & E_{35} & 0 & . \\ 0 & E_{35} & E_{55} & E_{57} & . \\ . & 0 & E_{57} & E_{77} & . \\ . & . & . & . & . \end{bmatrix},$$

$$\mathbf{O}^-(\kappa) = \begin{bmatrix} E_{11} - E_{-11} & E_{13} & 0 & . & . \\ E_{13} & E_{33} & E_{35} & 0 & . \\ 0 & E_{35} & E_{55} & E_{57} & . \\ . & 0 & E_{57} & E_{77} & . \\ . & . & . & . & . \end{bmatrix}$$

where the elements are calculable from (7.11)–(7.14). Each of these submatrices may now be diagonalized independently to give the reduced energies,  $E_{J,\kappa}(\kappa)$ . Therefore, by symmetry considerations, the size of the secular determinant has been reduced; the order of the submatrices being approximately  $J/2$ .

### Symmetry Classification of the Energy Levels

We have seen that the energy levels are conveniently labeled in terms of the limiting prolate and oblate  $K$  values, that is,  $J_{K_{-1},K_1}$ . This particular notation has the added advantage that the symmetry classification of a level to the species of  $V(a, b, c)$  is given uniquely in terms of the parities of these limiting  $K$  indices. Consider the limiting case of a symmetric prolate rotor. If  $K_{-1}$  is an even integer ( $0, \pm 2, \dots$ ), the rotational wave function  $\psi_{JKM}$  is symmetric with respect to a rotation of  $\pi$  degrees about  $a$ ; that is, it is an even function, not changing in sign with the rotation. The even characteristic is indicated by  $e$ . This is easily seen because such a rotation about the molecule-fixed symmetry axis (the  $a$  axis) changes the angle  $\phi$  into  $\phi = \phi + \pi$ , while leaving the other angles unaffected (see Chapter II, Section 5, Fig. 2.3). Since the angle  $\phi$  enters  $\psi_{JKM}$  through the factor  $e^{iK\phi}$ , we obtain

$$C_2^a: \psi_{JKM} \rightarrow e^{iK\pi} \psi_{JKM} = (-1)^K \psi_{JKM}$$

If  $K_{-1} = \pm 1, \pm 3, \dots$  (odd integer),  $\psi_{JKM}$  is antisymmetric [changes sign, odd ( $o$ ) function] with respect to this operation. Similarly, for an oblate rotor, if  $K_1$  is an even integer,  $\psi_{JKM}$  is symmetric ( $e$  function) with respect to a rotation of  $\pi$  degrees about the symmetry axis, that is, the  $c$  axis; and if  $K_1$  is an odd

integer,  $\psi_{JKM}$  is antisymmetric with respect to this operation. Now the symmetry of an asymmetric-top level must be invariant to changes in the moments of inertia, that is,  $\kappa$ . It must then possess the behavior of the two limiting cases with which it correlates. Therefore, if  $K_{-1}$  is  $e$  and  $K_1$  is  $o$ , then the asymmetric wave function is symmetric with respect to a rotation about  $a$  and antisymmetric with respect to a rotation about  $c$ . Since a rotation about any two of the axes in succession is equivalent to a rotation about the third, a rotation about the  $b$  axis in the present case must yield an antisymmetric result. From Table 7.4 this implies that the function belongs to species  $B_a$ . Similarly, if  $K_{-1}K_1$  is  $ee$ ,  $oo$ , or  $oe$ , the wave function must belong to  $A$ ,  $B_b$ , and  $B_c$ , respectively. Thus a knowledge of the evenness or oddness of  $K_{-1}$ ,  $K_1$  gives us the symmetry classification of the level directly.

Another important point is the symmetry classification of each submatrix which has been discussed by King et al. [1]. The symmetrized functions  $S_{JKM\gamma}$  that occur in any particular submatrix must all belong to the same symmetry species of the Four-group. This fact may be used for classification of the submatrices. However, the symmetrized functions are constructed relative to the axes  $x$ ,  $y$ ,  $z$  and not relative to the axes  $a$ ,  $b$ ,  $c$ , that is, the  $z$  axis is always taken as the symmetry axis which may coincide with  $a$  if the rotor is a prolate top or with  $c$  if it is an oblate top. Therefore, the functions are characterized by the representation  $A$ ,  $B_x$ ,  $B_y$ ,  $B_z$  of the Four-group  $V(x, y, z)$  (here as before the species notation shows directly the axis of rotation for which the character is +1). To classify the symmetrized functions one must find their behavior with respect to the group operations  $E$ ,  $C_2^x$ ,  $C_2^y$ ,  $C_2^z$ , of  $V(x, y, z)$ , as Mulliken [5] has done, with the result

$$\begin{aligned} E: S_{JKM\gamma} &\rightarrow S_{JKM\gamma} \\ C_2^x: S_{JKM\gamma} &\rightarrow (-1)^{J+K+\gamma} S_{JKM\gamma} \\ C_2^y: S_{JKM\gamma} &\rightarrow (-1)^{J+\gamma} S_{JKM\gamma} \\ C_2^z: S_{JKM\gamma} &\rightarrow (-1)^K S_{JKM\gamma} \end{aligned} \quad (7.23)$$

The parities are seen to depend only on the even or odd character of  $J+\gamma$  and  $K$ , and this character is readily determined from the designation of each submatrix. Consider, for example, the  $E^+$  submatrix where  $K$  and  $\gamma$  are even; therefore, for  $J_{\text{even}}$ , all of the  $S_{JKM\gamma}$ 's of  $E^+$  are symmetric with respect to all operations of the group and must belong to symmetric species  $A$ . The symmetry classification of the various submatrices in  $V(x, y, z)$  are collected in Table 7.5.

The symmetry classification of the submatrices with respect to  $V(a, b, c)$  will depend on the correlation of  $x$ ,  $y$ ,  $z$  with  $a$ ,  $b$ ,  $c$ ; in particular,  $A$  corresponds to  $A$ , and  $B_a$ ,  $B_b$ ,  $B_c$  correspond to  $B_x$ ,  $B_y$ ,  $B_z$  in the same way as  $a$ ,  $b$ ,  $c$  are related to  $x$ ,  $y$ ,  $z$ . The symmetry classification in  $V(a, b, c)$  is also given in Table 7.5 along with the parities of  $K_{-1}$ ,  $K_1$  which are included in parenthesis for the assignments considered. Thus a knowledge of the symmetry of a particular level also tells us in which of the four submatrices the level may be found.

**Table 7.5** Symmetry Classification of the Submatrices in  $V(x, y, z)$  and  $V(a, b, c)$

Symmetry Species in $V(x, y, z)$							
		$K$		$\gamma$		$J + \gamma$	
Submatrix		$J_{\text{even}}$	$J_{\text{odd}}$	$J_{\text{even}}$	$J_{\text{odd}}$		
$\mathbf{E}^+$	$e$	$e$	$e$	$o$	$A$	$B_z$	
$\mathbf{E}^-$	$e$	$o$	$o$	$e$	$B_z$	$A$	
$\mathbf{O}^+$	$o$	$e$	$e$	$o$	$B_y$	$B_x$	
$\mathbf{O}^-$	$o$	$o$	$o$	$e$	$B_x$	$B_y$	

Symmetry Species in $V(a, b, c)$ <sup>a</sup>													
Type:	I'		II'		III'								
Submatrix	$J_{\text{even}}$	$J_{\text{odd}}$	$J_{\text{even}}$	$J_{\text{odd}}$	$J_{\text{even}}$	$J_{\text{odd}}$							
$\mathbf{E}^+$	$A(ee)$	$B_d(oe)$	$A(ee)$	$B_b(oo)$	$A(ee)$	$B_c(oe)$	$A(ee)$	$B_a(oe)$	$A(ee)$	$B_b(oo)$	$A(ee)$	$B_c(oe)$	
$\mathbf{E}^-$	$B_a(oe)$	$A(ee)$	$B_b(oo)$	$A(ee)$	$B_c(oe)$	$A(ee)$	$B_d(oe)$	$A(ee)$	$B_b(oo)$	$A(ee)$	$B_c(oe)$	$A(ee)$	
$\mathbf{O}^+$	$B_c(oe)$	$B_b(oo)$	$B_a(oe)$	$B_c(oe)$	$B_b(oo)$	$B_a(oe)$	$B_b(oo)$	$B_c(oe)$	$B_c(oe)$	$B_a(oe)$	$B_a(oe)$	$B_b(oo)$	
$\mathbf{O}^-$	$B_b(oo)$	$B_c(oe)$	$B_c(oe)$	$B_a(oe)$	$B_a(oe)$	$B_b(oo)$	$B_c(oe)$	$B_b(oo)$	$B_a(oe)$	$B_c(oe)$	$B_b(oo)$	$B_a(oe)$	

<sup>a</sup>Symmetry classification of the levels are indicated with the parities of  $K_{-1}K_1$  indicated in parenthesis for various representations.

## Evaluation of the Energy Levels, Wave Functions, and Average Values

For relatively low values of  $J$  one can find the energy levels by expanding the determinant of each submatrix of (7.22) and finding the roots of the resulting polynomial. Explicit expressions for  $E(\kappa)$ , for certain low  $J$  values, are given in Table 7.6. Explicit expressions for the total rotational energy in terms of the rotational constants are given in Table 7.7. From a knowledge of the energy eigenvalues, the eigenvectors of the energy matrix can then be obtained by solution of a set of simultaneous equations, similar to (7.8), for each submatrix.

**Table 7.6** Explicit Expressions for the Reduced Energy  $E(\kappa)^a$

$J_{K_{-1}K_1}$	$E(\kappa)$
$0_{00}$	0
$1_{10}$	$\kappa + 1$
$1_{11}$	0
$1_{01}$	$\kappa - 1$
$2_{20}$	$2[\kappa + (\kappa^2 + 3)^{1/2}]$
$2_{21}$	$\kappa + 3$
$2_{11}$	$4\kappa$
$2_{12}$	$\kappa - 3$
$2_{02}$	$2[\kappa - (\kappa^2 + 3)^{1/2}]$
$3_{30}$	$5\kappa + 3 + 2(4\kappa^2 - 6\kappa + 6)^{1/2}$
$3_{31}$	$2[\kappa + (\kappa^2 + 15)^{1/2}]$
$3_{21}$	$5\kappa - 3 + 2(4\kappa^2 + 6\kappa + 6)^{1/2}$
$3_{22}$	$4\kappa$
$3_{12}$	$5\kappa + 3 - 2(4\kappa^2 - 6\kappa + 6)^{1/2}$
$3_{13}$	$2[\kappa - (\kappa^2 + 15)^{1/2}]$
$3_{03}$	$5\kappa - 3 - 2(4\kappa^2 + 6\kappa + 6)^{1/2}$
$4_{40}$	—
$4_{41}$	$5\kappa + 5 + 2(4\kappa^2 - 10\kappa + 22)^{1/2}$
$4_{31}$	$10\kappa + 2(9\kappa^2 + 7)^{1/2}$
$4_{32}$	$5\kappa - 5 + 2(4\kappa^2 + 10\kappa + 22)^{1/2}$
$4_{22}$	—
$4_{23}$	$5\kappa + 5 - 2(4\kappa^2 - 10\kappa + 22)^{1/2}$
$4_{13}$	$10\kappa - 2(9\kappa^2 + 7)^{1/2}$
$4_{14}$	$5\kappa - 5 - 2(4\kappa^2 + 10\kappa + 22)^{1/2}$
$4_{04}$	—
$5_{42}$	$10\kappa + 6(\kappa^2 + 3)^{1/2}$
$5_{24}$	$10\kappa - 6(\kappa^2 + 3)^{1/2}$

<sup>a</sup>In general, the sum rule for the reduced energy levels of a given  $J$  is  $\sum_i E_{J,i}(\kappa) = \frac{1}{3} J(J+1)(2J+1)\kappa$ .

**Table 7.7** Explicit Expressions for the Total Rotational Energy in Terms of the Rotational Constants<sup>a</sup>

$J_{K_1, K_2}$	$E(A, B, C)$
$0_{00}$	0
$1_{10}$	$A + B$
$1_{11}$	$A + C$
$1_{01}$	$B + C$
$2_{20}$	$2A + 2B + 2C + 2[(B - C)^2 + (A - C)(A - B)]^{1/2}$
$2_{21}$	$4A + B + C$
$2_{11}$	$A + 4B + C$
$2_{12}$	$A + B + 4C$
$2_{02}$	$2A + 2B + 2C - 2[(B - C)^2 + (A - C)(A - B)]^{1/2}$
$3_{30}$	$5A + 5B + 2C + 2[4(A - B)^2 + (A - C)(B - C)]^{1/2}$
$3_{31}$	$5A + 2B + 5C + 2[4(A - C)^2 - (A - B)(B - C)]^{1/2}$
$3_{21}$	$2A + 5B + 5C + 2[4(B - C)^2 + (A - B)(A - C)]^{1/2}$
$3_{22}$	$4A + 4B + 4C$
$3_{12}$	$5A + 5B + 2C - 2[4(A - B)^2 + (A - C)(B - C)]^{1/2}$
$3_{13}$	$5A + 2B + 5C - 2[4(A - C)^2 - (A - B)(B - C)]^{1/2}$
$3_{03}$	$2A + 5B + 5C - 2[4(B - C)^2 + (A - B)(A - C)]^{1/2}$
$4_{40}$	—
$4_{41}$	$10A + 5B + 5C + 2[4(B - C)^2 + 9(A - C)(A - B)]^{1/2}$
$4_{31}$	$5A + 10B + 5C + 2[4(A - C)^2 - 9(A - B)(B - C)]^{1/2}$
$4_{32}$	$5A + 5B + 10C + 2[4(A - B)^2 + 9(A - C)(B - C)]^{1/2}$
$4_{22}$	—
$4_{23}$	$10A + 5B + 5C - 2[4(B - C)^2 + 9(A - C)(A - B)]^{1/2}$
$4_{13}$	$5A + 10B + 5C - 2[4(A - C)^2 - 9(A - B)(B - C)]^{1/2}$
$4_{14}$	$5A + 5B + 10C - 2[4(A - B)^2 + 9(A - C)(B - C)]^{1/2}$
$4_{04}$	—
$5_{42}$	$10A + 10B + 10C + 6[(B - C)^2 + (A - B)(A - C)]^{1/2}$
$5_{24}$	$10A + 10B + 10C - 6[(B - C)^2 + (A - B)(A - C)]^{1/2}$

<sup>a</sup>In general, the sum rule for the energy levels of a given  $J$  is  $\sum_r E_{J,r}(A, B, C) = \frac{1}{2}J(J+1)(2J+1)(A+B+C)$ .

As pointed out in Appendix A, the matrix formed from the normalized eigenvectors (each column corresponding to an eigenvector associated with a particular energy level) constitutes a transformation matrix  $T$  which diagonalizes the reduced energy matrix, that is,

$$\tilde{T}ET = \Lambda \quad (7.24)$$

where  $\Lambda$  is a diagonal matrix formed by the eigenvalues of  $E$ . A knowledge of  $T$  is required whenever matrix elements of operators in the asymmetric rotor basis are needed.

Obviously, this technique of direct expansion becomes impractical for all but small  $J$  values, and iterative matrix diagonalization procedures must be

used. The rapid development of high-speed digital computers has, however, made possible the relatively easy solution of such mathematical problems by the use of iterative procedures. A very useful diagonalization procedure due to Jacobi [8] determines the eigenvalues and eigenvectors simultaneously. This method is applicable to symmetric matrices and is unaffected by the presence of degenerate eigenvalues. The method consists in the application of a series of plane rotations (in a space of  $n$ -dimensions) which are chosen to reduce the size of the off-diagonal elements, the process being continued until the off-diagonal elements are small enough for the matrix to be considered diagonal. The product of the rotation matrices thus constitutes a transformation matrix which diagonalizes the energy matrix and hence is the matrix of eigenvectors.

Alternately, since the four submatrices are of tridiagonal form, that is, with nonzero elements along the diagonal and immediately above and below the principal diagonal, the secular determinant may be cast into a continued fraction form. The continued fraction expansion is particularly efficient for numerical evaluation of the eigenvalues and allows the roots to be determined very accurately. Both first- [1, 9] and second-order [10] iterative techniques for the continued fraction method have been described, as well as efficient procedures for evaluation of eigenvectors. This method is discussed in Appendix B.

A number of tables are available which give numerical values of  $E_{J,\kappa}$  for values of  $\kappa$  in steps of 0.1 [1, 11] and 0.01 [12] with values of  $J$  up to 12. Also available are tables for values of  $\kappa$  in steps of 0.1 [13] and 0.001 [14] up to  $J=40$  and  $J=18$ , respectively. These tables provide a convenient means by which the energies of any asymmetric rotor may be approximated. To calculate the characteristic rotational energy for a particular level, one merely selects from the table the reduced energy,  $E_{J,\kappa}$ , corresponding to the desired  $J_\tau$  and  $\kappa$  values, and then makes use of (7.10). Interpolation between tabulated values of  $\kappa$  may be used, but in most tables the intervals in  $\kappa$  are not small enough to give the required accuracy for microwave work. However, the tabulation for intervals of 0.001 in  $\kappa$  are sufficiently close to allow accurate interpolation. Usually only positive or negative values are tabulated since the reduced energy matrix has a form such that

$$E_{J,\kappa} = -E_{J,-\kappa} \quad (7.25)$$

or

$$E_{J_{K-1},K_1}(\kappa) = -E_{J_{K_1},K_{-1}}(-\kappa)$$

The quantities of interest in the calculation are, of course, the rotational transition frequencies, obtained by division of the energy difference by Planck's constant. It is common practice to express the rotational spectroscopic constants in units of megahertz so that

$$A = \frac{h}{8\pi^2 I_a}, \text{ etc.}$$

or

(7.26)

$$A \text{ (MHz)} = \frac{5.05376 \times 10^5}{I_a(\text{amu} \cdot \text{\AA}^2)}, \text{ etc.}$$

This conversion factor is based on the  $^{12}\text{C}$  atomic mass scale and constants of Appendix D.

In (7.20) the asymmetric rotor wave functions were synthesized from the symmetrized symmetric rotor wave functions by means of the expansion coefficients  $a_K^{J\tau}$ , which give the relative contributions of the various symmetric rotor states to the asymmetric rotor state with their squares giving the probability for rotation with a particular angular momentum  $J$  and  $\pm K$ . For a very slightly asymmetric rotor, one of the  $a_K^{J\tau}$ 's approaches unity while the others approach zero and each asymmetric rotor wave function  $A_{J\tau}$  will be closely approximated by one  $S_{JK\gamma}$ . The different sets of coefficients, the eigenvectors of the energy matrix, are discriminated by means of the index  $\tau$ . The eigenvectors are required for the calculation of line strengths of asymmetric rotors. They are also useful for calculation of the average values of  $P_z^2$  and  $P_z^4$ , that is, the values of  $P_z^2$  and  $P_z^4$  averaged over the asymmetric rotor wave functions. Such quantities find frequent use particularly in the analysis of centrifugal distortion, quadrupole and internal rotation effects. Consider, for example, the average value of  $P_z^2$ , where  $z$  represents the unique molecule-fixed axis of quantization, we have

$$\langle P_z^2 \rangle = (J, \tau | P_z^2 | J, \tau) \quad (7.27)$$

where  $\langle P_z^2 \rangle$  is the average value of  $P_z^2$  associated with the level  $J, \tau$ . From (7.20) which gives  $A_{J\tau}$  in terms of  $S_{JK\gamma}$ 's, recalling the definition of  $S_{JK\gamma}$  and the fact that  $P_z^2$  is diagonal in the  $\psi_{JK}^x$  basis, we obtain

$$\langle P_z^2 \rangle = \sum_K (a_K^{J\tau})^2 K^2 \quad (7.28)$$

The summation over  $K$  will be only over those  $K$ 's that occur along the main diagonal of the submatrix to which the level  $J, \tau$  belongs. A similar expression would result for  $\langle P_z^4 \rangle$  except that  $K^2$  would be replaced by  $K^4$ . Usually only a limited number of terms in the sum are required to give results of sufficient accuracy. For a slightly asymmetric rotor, where one of the  $a_K^{J\tau}$ 's approaches unity and the others approach zero, the  $\langle P_z^2 \rangle$  approaches the value of  $K^2$  for the limiting symmetric rotor level. Tables of  $\langle P_z^2 \rangle$  and  $\langle P_z^4 \rangle$  tabulated in increments of 0.1 [15] and 0.002 [16] in  $\kappa$  are available. Formulas for  $\langle P_z^2 \rangle$  and  $\langle P_z^4 \rangle$  based on continued fractions have been given [17], which are very convenient when the rigid rotor energy levels are calculated by the continued fraction method. It is also possible to express the  $\langle P_z^4 \rangle$  simply in terms of  $P^2$ ,  $E$ , and  $\langle P_g^2 \rangle$ ,  $g=x, y, z$  (see Chapter VIII, Section 3).

The average values of  $P_x^2$ ,  $P_y^2$ , and  $P_z^2$  are also directly related to the derivatives of the rotational energy with respect to the rotational constants. Specifically,

it has been shown by Bragg and Golden [18, 19] that

$$\langle P_a^2 \rangle = \frac{\partial E}{\partial A} \quad (7.29)$$

$$\langle P_b^2 \rangle = \frac{\partial E}{\partial B} \quad (7.30)$$

$$\langle P_c^2 \rangle = \frac{\partial E}{\partial C} \quad (7.31)$$

Therefore, on differentiating (7.10) with respect to  $A$ ,  $B$ , and  $C$ , we find the following convenient expressions

$$\langle P_a^2 \rangle = \frac{\partial E}{\partial A} = \frac{1}{2} \left[ J(J+1) + E(\kappa) - (\kappa+1) \frac{\partial E(\kappa)}{\partial \kappa} \right] \quad (7.32)$$

$$\langle P_b^2 \rangle = \frac{\partial E}{\partial B} = \frac{\partial E(\kappa)}{\partial \kappa} \quad (7.33)$$

$$\langle P_c^2 \rangle = \frac{\partial E}{\partial C} = \frac{1}{2} \left[ J(J+1) - E(\kappa) + (\kappa-1) \frac{\partial E(\kappa)}{\partial \kappa} \right] \quad (7.34)$$

The  $\langle P_x^2 \rangle$ ,  $\langle P_y^2 \rangle$ ,  $\langle P_z^2 \rangle$  are identified with the  $\langle P_a^2 \rangle$ ,  $\langle P_b^2 \rangle$ ,  $\langle P_c^2 \rangle$  according to the way  $a$ ,  $b$ ,  $c$  are related to  $x$ ,  $y$ ,  $z$ . The values of  $\partial E / \partial \kappa$  may be obtained from Tables of  $E(\kappa)$  if differences of  $E(\kappa)$  between two appropriate values of  $\kappa$  are taken. Tables with small increments in  $\kappa$  should be employed.

To indicate the use of Table 7.5 and to illustrate some of the previous concepts, we look at a simple example. Consider the case of a prolate asymmetric rotor in a type I' representation for  $J=2$ . The allowed energy levels are  $2_{02}$ ,  $2_{12}$ ,  $2_{11}$ ,  $2_{21}$ , and  $2_{20}$ . We see from the Table 7.5 that the levels will be found in the following submatrices:  $2_{02}$ ,  $2_{20}$  in  $\mathbf{E}^+$ ;  $2_{21}$  in  $\mathbf{E}^-$ ;  $2_{12}$  in  $\mathbf{O}^+$ , and  $2_{11}$  in  $\mathbf{O}^-$ .  $\mathbf{E}^+$  gives a  $2 \times 2$  secular determinant, and the others are all one-dimensional. The wave functions associated with the levels in the various submatrices have the symmetry:  $\mathbf{E}^+ \leftrightarrow A$ ,  $\mathbf{E}^- \leftrightarrow B_a$ ,  $\mathbf{O}^+ \leftrightarrow B_c$ , and  $\mathbf{O}^- \leftrightarrow B_b$ . The largest eigenvalue in  $\mathbf{E}^+$  will be associated with  $2_{20}$  level and the other with the  $2_{02}$  level. The  $\mathbf{E}^+$  matrix has the following secular equation:

$$\begin{vmatrix} E_{00} - \lambda & \sqrt{2}E_{02} \\ \sqrt{2}E_{02} & E_{22} - \lambda \end{vmatrix} = \begin{vmatrix} 3(\kappa-1) - \lambda & -\sqrt{3}(\kappa+1) \\ -\sqrt{3}(\kappa+1) & (\kappa+3) - \lambda \end{vmatrix} = 0$$

Upon expansion, the determinant yields a quadratic equation in  $\lambda$  with the roots:

$$E_{2_{20}} = E_{2_2} = 2[\kappa + (\kappa^2 + 3)^{1/2}]$$

$$E_{2_{02}} = E_{2_{-2}} = X[\kappa - (\kappa^2 + 3)^{1/2}]$$

The asymmetric rotor wave functions for the two states have the form:

$$A_{2_2} = a_0^{2_2} S_{200} + a_2^{2_2} S_{220}$$

$$A_{2_{-2}} = a_0^{2_{-2}} S_{200} + a_2^{2_{-2}} S_{220}$$

where the  $M$  index is suppressed. The coefficients  $a_K^J$  in the above expressions are determined from the simultaneous equations:

$$(E_{00} - \lambda)a_0^{2\tau} + \sqrt{2}E_{02}a_2^{2\tau} = 0$$

$$\sqrt{2}E_{02}a_0^{2\tau} + (E_{22} - \lambda)a_2^{2\tau} = 0$$

A system of equations such as these do not determine the  $a_K^J$ 's uniquely, but give only their ratios. We can evaluate an arbitrary or relative set from either of the foregoing equations by setting one  $a_K^J = 1$  and solving for the remaining one. Using the first of the foregoing equations and setting  $\lambda = E_2$ , we find the relative eigenvectors to be

$$a_0^{2\tau} = 1 \quad \text{and} \quad a_2^{2\tau} = \frac{(\kappa - 3) - 2(\kappa^2 + 3)^{1/2}}{\sqrt{3}(\kappa + 1)}$$

The values are fixed by means of the relation,

$$a_K^J = \frac{a_K^J \text{ (relative)}}{\{\sum_K [a_K^J \text{ (relative)}]^2\}^{1/2}}$$

which ensures the eigenvectors will be normalized, that is,  $\sum_K (a_K^J)^2 = 1$ . The normalized set of eigenvectors are:

$$a_0^{2\tau} = \frac{(\sqrt{3}/2)(\kappa + 1)}{\{(\kappa^2 + 3)^{1/2}[2(\kappa^2 + 3)^{1/2} + (3 - \kappa)]\}^{1/2}}$$

$$a_2^{2\tau} = -\frac{1}{2} \left[ 2 + \frac{(3 - \kappa)}{(\kappa^2 + 3)^{1/2}} \right]^{1/2}$$

Likewise, we find for the  $2_{02}$  level that

$$a_2^{2-2} = a_0^{2\tau} \quad \text{and} \quad a_0^{2-2} = -a_2^{2\tau}$$

If for example,  $\kappa = -0.968$ , we find that

$$E_{22} = 2.0324, \quad a_0^{2\tau} = 0.00698, \quad a_2^{2\tau} = -0.99998$$

$$E_{2-2} = -5.9044, \quad a_0^{2-2} = 0.99998, \quad a_2^{2-2} = 0.00698$$

By means of the eigenvectors we calculate

$$\langle P_z^2 \rangle_{22} = 3.9998 \quad \text{and} \quad \langle P_z^2 \rangle_{2-2} = 0.0002$$

As mentioned previously, the original energy matrix can be brought to diagonal form by a similarity transformation, (7.23), with the matrix of eigenvectors. In the present case, we have explicitly:

$$\tilde{T} \quad E^+ \quad T$$

$$\begin{bmatrix} 0.99998 & 0.00698 \\ 0.00698 & -0.99998 \end{bmatrix} \begin{bmatrix} -5.9040 & -0.0554 \\ -0.0554 & 2.0320 \end{bmatrix} \begin{bmatrix} 0.99998 & 0.00698 \\ 0.00698 & -0.99998 \end{bmatrix}$$

$$= \begin{bmatrix} -5.9044 & 0.0000 \\ 0.0000 & 2.0324 \end{bmatrix}$$

which provides a check of our calculations.

### 3 SLIGHTLY ASYMMETRIC ROTORS

It would be convenient to have expressions that give the explicit dependence of the energies on the rotational quantum numbers. This is not possible for molecules with large asymmetry; however, there are a large number of molecules that may be classified as slightly asymmetric tops, for example,  $\text{HN}_3$ ,  $\text{HNCO}$ ,  $\text{CH}_2\text{DBr}$ ,  $\text{NOBr}$ ,  $\text{CH}_3\text{SH}$ ,  $\text{H}_2\text{S}_2$ ,  $\text{P}^{35}\text{Cl}_2\text{Cl}^{37}$ , etc. The spectrum of a slightly asymmetric rotor is illustrated in Fig. 7.5. For this type, the energies can be expressed with sufficient accuracy as a series expansion in powers of an asymmetry parameter. Various asymmetry parameters have been employed for finding the energies of this special class of asymmetric rotors. An asymmetry parameter introduced by Wang [6] is particularly useful for such expansions. The rotational Hamiltonian for a near-prolate rotor type I', in terms of Wang's asymmetry parameter is written in the form

$$\mathcal{H} = AP_a^2 + BP_b^2 + CP_c^2 = \frac{1}{2}(B+C)P^2 + [A - \frac{1}{2}(B+C)]\mathcal{H}(b_p) \quad (7.35)$$

with

$$\mathcal{H}(b_p) = P_a^2 + b_p(P_c^2 - P_b^2) \quad (7.36)$$

where the  $a$  axis is the unique axis of quantization and the asymmetry parameter is defined as

$$b_p = \frac{C-B}{2A-B-C} = \frac{\kappa+1}{\kappa-3} \quad (7.37)$$

in which  $-1 \leq b_p \leq 0$  with  $b_p = -\frac{1}{3}$  corresponding to the maximum degree of asymmetry. In a symmetric rotor representation the nonvanishing matrix elements are:

$$(J, K, M|P^2|J, K, M) = J(J+1) \quad (7.38)$$

$$(J, K, M|\mathcal{H}(b_p)|J, K, M) = K^2 \quad (7.39)$$

$$(J, K, M|\mathcal{H}(b_p)|J, K \pm 2, M) = b_p[f(J, K \pm 1)]^{1/2} \quad (7.40)$$

As with Ray's formulation, the determination of the eigenvalues of  $\mathcal{H}$  is reduced to finding those of  $\mathcal{H}(b_p)$ . If the matrix of the Wang operator, (7.39) and (7.40),

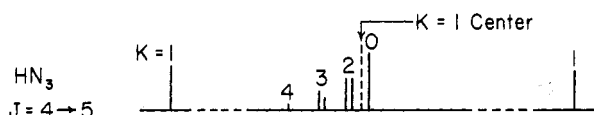


**Fig. 7.5** Illustration of the rotational spectrum of the slightly asymmetric prolate rotor  $\text{HN}_3$  ( $b_p = -20.9 \times 10^{-5}$ ) observed in the millimeter region. The frequencies of the absorption lines increase from left to right. Separation of the lines for different values of  $K$  is due to centrifugal distortion effects. The  $K=1$  and  $K=2$  lines are split (1263.1 and 1.5 MHz, respectively) because of the small asymmetry of the molecule. The  $K=3$  line shows quadrupole splitting which is unresolved in the other lines. After R. Kewley, K. V. L. N. Sastry, and M. Winnewisser, *J. Mol. Spectrosc.* **12**, 387 (1964).

is subjected to the Wang transformation, four matrices will result similarly to the  $\mathbf{E}^\pm$ ,  $\mathbf{O}^\pm$  matrices, discussed previously. The only difference is that now the matrix elements are given by (7.39) and (7.40). The roots of these secular determinants are the reduced energies  $W_{J,\tau}(b_p)$  with the characteristic rotational energy being given by:

$$E = \frac{1}{2}(B+C)J(J+1) + [A - \frac{1}{2}(B+C)]W_{J,\tau}(b_p) \quad (7.41)$$

All of the symmetry properties given previously are still valid. For the prolate symmetric limit,  $B=C$ , we have  $b_p=0$  and  $W_{J,\tau}=K_{-1}^2$  so that the energy expression reduces to that given for a symmetric top. Alternately, near the symmetric rotor limit, that is,  $b_p \approx 0$ , the reduced energies may be expressed as:

$$W_{J,\tau}(b_p) = K_{-1}^2 + C_1 b_p + C_2 b_p^2 + C_3 b_p^3 + \dots \quad (7.42)$$

where  $K_{-1}$  is the limiting prolate index of the level. The coefficients  $C_i$  for the powers of  $b_p$  can be evaluated by standard perturbation techniques, with the term in  $b_p$  of  $\mathcal{H}(b_p)$  being treated as the perturbation operator. The Wang linear combinations of symmetric rotor wave functions are used as the basis functions, with the coefficient of  $b_p^n$  being provided by  $n$ th order perturbation. The expressions for the coefficients [13, 20] up to  $C_5$  are given in Table 7.8. They depend only on the rotational quantum numbers. Numerically tabulated coefficients for various energy levels have also been reported [12, 20].

We may, for example, by use of Table 7.8 immediately write down the asymmetry splitting between the two  $K=1$  levels of a slightly asymmetric rotor. We find (retaining terms up to  $b_p^2$ )

$$\Delta W(b_p) = b_p J(J+1)$$

which indicates directly that the degenerate level splitting increases with  $J$ . An approximate general expression for the asymmetry splitting of the  $K$  levels has been given by Wang [6]

$$\Delta W(b) = \frac{b^K (J+K)!}{8^{K-1} (J-K)! [(K-1)!]^2} \quad (7.43)$$

in which  $\Delta W$  is the reduced energy difference with  $b$  and  $K$ , respectively,  $b_p$  and  $K_{-1}$  for a near prolate top, or  $b_o$  and  $K_1$  for a near oblate top. Equation 7.43 reveals that the degenerate level splitting decreases with increasing  $K$  (see Fig. 7.2). A more accurate expression, correct to  $(K+2)$ -power of  $b$ , is also available [21].

The energy expression for a near-oblate top, type III<sup>l</sup>, is obtained by a simple interchange of  $A$  and  $C$  in the preceding relations. The total rotational energy for an asymmetric oblate top is then:

$$E = \frac{1}{2}(A+B)J(J+1) + [C - \frac{1}{2}(A+B)]W_{J,\tau}(b_o) \quad (7.44)$$

with

$$b_o = \frac{A-B}{2C-B-A} = \frac{\kappa-1}{\kappa+3} \quad (7.45)$$

**Table 7.8** General Expressions for the Coefficients  $C_l$  for a Near Prolate Top<sup>a</sup>


---

$C_1 = \pm \frac{J(J+1)}{2}$	for $K=1, \mathbf{O}^\pm$
$C_1 = 0$	for all other $K$ values
$C_2 = \left[ \frac{f(J, K-1)}{4(K-1)} - \frac{f(J, K+1)}{4(K+1)} \right]$	for all $K$ values
$C_3 = \pm \frac{J(J+1)f(J, 2)}{128}$	for $K=1, \mathbf{O}^\mp$
$C_3 = \pm \frac{J(J+1)f(J, 2)}{128}$	for $K=3, \mathbf{O}^\pm$
$C_3 = 0$	for all other $K$ values
$C_4 = C'_4 - \frac{J^2(J+1)^2 f(J, 2)}{2048}$	for $K=1, C'_4$ given below
$C_4 = C'_4 + \frac{J^2(J+1)^2 + f(J, 2)}{2048}$	for $K=3, C'_4$ given below
$C_4 = C'_4 = \frac{f(J, K-1)}{128(K-1)^2} \left[ \frac{2f(J, K+1)}{(K+1)} - \frac{2f(J, K-1)}{(K-1)} + \frac{f(J, K-3)}{(K-2)} \right] - \frac{f(J, K+1)}{128(K+1)^2} \left[ \frac{2f(J, K-1)}{(K-1)} - \frac{2f(J, K+1)}{(K+1)} + \frac{f(J, K+3)}{(K+2)} \right]$	for all other $K$ values
$C_5 = \frac{\pm J(J+1)f(J, 2)}{294,912} [108f(J, 2) - 9J^2(J+1)^2 - 28f(J, 4)]$	for $K=1, \mathbf{O}^\pm$
$C_5 = \frac{\pm J(J+1)f(J, 2)}{294,912} [108f(J, 2) - 9J^2(J+1)^2 - 27f(J, 4)]$	for $K=3, \mathbf{O}^\mp$
$C_5 = \frac{\pm J(J+1)f(J, 2)f(J, 4)}{294,912}$	for $K=5, \mathbf{O}^\pm$
$C_5 = 0$	for all other $K$ values

---

<sup>a</sup>Here  $K$  refers to the limiting prolate index of a level. The symbol  $\mathbf{O}^\pm$  identifies the submatrix to which a level belongs, see Table 7.5, and indicates which sign to use; for example, if level in  $\mathbf{O}^+$  for  $K=1$ , minus sign is to be used for calculation of  $C_3$ . The functions  $f(J, K \pm 1)$  are given by (7.13) of text, except that  $f(J, 1) = \frac{1}{2}J(J+1)[J(J+1)-2]$ . Furthermore,  $f(J, 1)$  must be taken to be zero in computation of  $C_2$  or  $C_4$  for the  $\mathbf{E}^-$  levels. Also  $f(J, 0)$  and  $f(J, -1)$  must always be set equal to zero. After Allen and Cross [13].

The range is the same as  $b_o$ , that is,  $-1 \leq b_o \leq 0$  and the most symmetric case is again represented by the value  $-\frac{1}{3}$ . For an oblate limit  $A=B$ , we have  $b_0=0$ , so that an expansion in terms of  $b_o$  is the most appropriate for expressing the reduced energy of a slightly asymmetric oblate rotor

$$W_{J_t}(b_o) = K_1^2 + C_1 b_o + C_2 b_o^2 + C_3 b_o^3 + \dots \quad (7.46)$$

where  $K_1$  is the appropriate limiting oblate index. The  $C$ 's for the oblate case may be obtained from Table 7.8 for the prolate case as follows: If the

oblate level of interest is  $J_{K-1, K_1}$ , then one computes the coefficients for the prolate rotor level  $J_{K_1, K-1}$ . The use of such expansions for energy level calculations are, of course, dictated by the size of the asymmetry parameter  $b$  and the accuracy that is desired. If the asymmetry is too large, the series expansion, (7.42) or (7.46), will not converge rapidly enough. The expansions are, in general, most accurate for very small asymmetries and become progressively worse with increasing asymmetry.

For asymmetric rotors where the power series expansion is not appropriate, the Wang formulation suffers from the fact that extensive tables of reduced energies are available in terms of  $\kappa$  rather than Wang's asymmetry parameter. However, if necessary, Wang's reduced energy can be calculated from the tabulated values of Ray's reduced energy by means of the relation

$$E_{J_t}(\kappa) = F J(J+1) + (G - F) W_{J_t}(b) \quad (7.47)$$

where  $b$  is either  $b_p$  or  $b_o$ , depending on whether one is considering a prolate or oblate asymmetric rotor. The values of  $F$  and  $G$  are given in Table 7.2 for the two possible cases. This relation can be obtained simply by equating the different expressions for the total energy.

In cases where the expansion can be used satisfactorily, we can write the average values of  $P_z^2$  in an asymmetric rotor basis as an expansion in terms of the asymmetry parameter, thereby circumventing the more laborious calculations using the eigenvectors. As an example, consider the derivation of  $\langle P_z^2 \rangle$ . For the  $a$  axis identified with the  $z$  axis, type I', we have from (7.41), on differentiating with respect to  $A$ ,

$$\left( \frac{\partial E}{\partial A} \right) = W(b_p) + [A - \frac{1}{2}(B+C)] \left( \frac{\partial W(b_p)}{\partial A} \right) \quad (7.48)$$

Now

$$\left( \frac{\partial W(b_p)}{\partial A} \right) = \left( \frac{\partial W(b_p)}{\partial b_p} \right) \left( \frac{\partial b_p}{\partial A} \right) = \frac{-b_p}{A - \frac{1}{2}(B+C)} \left( \frac{\partial W(b_p)}{\partial b_p} \right)$$

Therefore

$$\langle P_z^2 \rangle = W(b_p) - b_p \left( \frac{\partial W(b_p)}{\partial b_p} \right) \quad (7.49)$$

This is a general expression for  $\langle P_z^2 \rangle$ . If, however, we assume  $W(b_p)$  is given by (7.42), we obtain the following expression

$$\langle P_z^2 \rangle = K_{-1}^2 + \sum_{n=1} (1-n) C_n b_p^n \quad (7.50)$$

From a knowledge of  $\langle P_z^2 \rangle$ , we can calculate  $\langle P_x^2 \rangle$  and  $\langle P_y^2 \rangle$  from the relations

$$\frac{\partial E}{\partial B} = \langle P_x^2 \rangle = \frac{1}{2} [J(J+1) - (1+\sigma) \langle P_z^2 \rangle + \sigma W(b_p)] \quad (7.51)$$

$$\frac{\partial E}{\partial C} = \langle P_y^2 \rangle = \frac{1}{2} [J(J+1) + (\sigma - 1)\langle P_z^2 \rangle - \sigma W(b_p)] \quad (7.52)$$

with  $\sigma = -1/b_p$ . The method of calculation of  $\langle P_z^2 \rangle$  and  $W(b_p)$  in the foregoing expressions is, of course, dictated by the size of the asymmetry. For slightly asymmetric rotors, the  $\langle P_z^4 \rangle$  can be roughly approximated by

$$\langle P_z^4 \rangle \approx \langle P_z^2 \rangle^2 \quad (7.53)$$

A more accurate approximation has been given by Kivelson and Wilson [17] for slightly asymmetric rotors.

#### 4 SELECTION RULES AND INTENSITIES

The allowed changes in  $J$  for dipole absorption of radiation are:

$$\Delta J = 0, \pm 1 \quad (7.54)$$

As in previous instances, these "permitted" transitions result from the nonvanishing property of the dipole matrix elements,  $\int A_{J_1} \mu A_{J_2} dt$ , when  $J' = J$  or  $J' = J \pm 1$ . For other values of  $J'$ , all matrix elements of the dipole components along fixed axes in space are found to be zero. This is to be expected since the asymmetric rotor wave functions are expressed as linear combinations of symmetric rotor functions, all having the same value of  $J$ . Therefore, only those matrix elements will be nonvanishing for change of  $J$  which were nonvanishing for the symmetric rotor. In an asymmetric rotor, each of the three changes might give rise to an absorption line, whereas, for a symmetric rotor, the level with higher  $J$  always lies highest, and only  $\Delta J = +1$  gives rise to rotational absorption. The  $\Delta J = -1$  transitions are designated as *P*-branch; the  $\Delta J = 0$ , as *Q*-branch; and the  $\Delta J = +1$ , as *R*-branch transitions.

In addition to these selection rules for  $J$ , there are also restrictions on the changes that can occur in the subscripts of  $J$ , in the pseudo-quantum numbers. These restrictions result from the symmetry properties of the ellipsoid of inertia. To discuss these selection rules, we must again inquire into the nonvanishing property of the matrix elements of the dipole components along axes fixed in space. The component of the electric moment along a space-fixed axis  $F$ , can be written as

$$\mu_F = \sum_g \cos(Fg) \mu_g \quad F = X, Y, Z; g = a, b, c \quad (7.55)$$

where  $\mu_g$  are the components of the permanent molecular dipole moment resolved along the principal axes of inertia. The  $\cos(Fg)$  are the cosines of the angles between the nonrotating  $F$  and rotating  $g$  axes. These quantities may be expressed as explicit functions of the Eulerian angles  $\theta, \phi, \chi$  which specify the orientation of the molecule-fixed axis system with respect to the space-fixed

axis system. The direction cosines are commonly indicated by the symbol  $\Phi_{Fg}$ . They find extensive use whenever it is desirable to refer a vector whose components are known in the rotating coordinate system to the nonrotating system, or vice versa. For the case where the electric moment lies only along one of the principal axes, say the  $a$  axis, since the direction cosines are functions of the rotational coordinates, the dipole matrix element is

$$(J, K_{-1}, K_1 | \mu_F | J', K'_{-1}, K'_1) = \mu_a (J, K_{-1}, K_1 | \cos(Fa) | J', K'_{-1}, K'_1) \quad (7.56)$$

If this integral is not to vanish, it must be unchanged (no change in sign) for any operation that carries the system into a configuration indistinguishable from the original. This is tantamount to saying that the integrand  $A_j^* K_{-1, K_1} \cos(Fa) A_{J' K'_{-1, K'_1}}$  transforms according to the totally symmetric representation  $A$ . The symmetry in which we are interested is not the molecular symmetry but the symmetry of the inertia ellipsoid, which for the asymmetric rotor is characterized by the Four-group operations. If the integrand is to belong to species  $A$ , then for each symmetry operation of  $V$  either each term of the integrand is even, or one term is even and the other two are odd. Under the Four-group operations, the direction cosines have  $B$  symmetries. For a rotation of  $180^\circ$  about  $a$ ,  $C_a^a$ , the  $\cos(Fa)$  does not change, but it does change sign for a rotation about  $b$  or  $c$  since the angle changes from  $Fa$  to  $\pi - Fa$ . It transforms, therefore, according to the  $B_a(eo)$  representation. Likewise,  $\cos(Fb)$ , does not change sign for the  $C_2^b$  symmetry operation but does change sign for the  $C_2^a$  and  $C_2^c$  operations and thus transforms as the species  $B_b(oo)$ . For similar reasons,  $\cos(Fc)$  has  $B_c(oe)$  symmetry. For the case under consideration ( $\mu_a \neq 0$  with  $\mu_b = \mu_c = 0$ ) where the direction cosine transforms as  $B_a$ , it is readily apparent from Table 7.3 that if the integrand is to have symmetry  $A$ , the functions  $A_j^* K_{-1, K_1}$  and  $A_{J' K'_{-1, K'_1}}$  must be of symmetry  $A$  and  $B_a$ , or of symmetry  $B_b$  and  $B_c$ . The allowed transitions are then  $A \leftrightarrow B_a$ , and  $B_b \leftrightarrow B_c$ . The other selection rules for electric dipole components along the  $b$  and  $c$  axes are similarly established. For  $\mu_b \neq 0$  with  $\mu_a = \mu_c = 0$ , the allowed transitions are  $A \leftrightarrow B_b$  and  $B_a \leftrightarrow B_c$ , whereas for  $\mu_c \neq 0$  and  $\mu_a = \mu_b = 0$  they are  $A \leftrightarrow B_c$  and  $B_a \leftrightarrow B_b$ . Often, the symmetry selection rules are stated in terms of the evenness or oddness of the  $K_{-1}, K_1$  subscripts. In this notation they are:

Dipole Component	Permitted Transitions
$\mu_a \neq 0$ (along axis of least moment of inertia)	$ee \leftarrow \rightarrow eo$ $oe \leftarrow \rightarrow oo$
$\mu_b \neq 0$ (along axis of intermediate moment of inertia)	$ee \leftarrow \rightarrow oo$ $oe \leftarrow \rightarrow eo$
$\mu_c \neq 0$ (along axis of greatest moment of inertia)	$ee \leftarrow \rightarrow oe$ $eo \leftarrow \rightarrow oo$

In terms of permitted changes in the  $K_{-1}$  and  $K_1$  subscripts, the selection rules are:

Dipole Component	$\Delta K_{-1}$	$\Delta K_1$
$\mu_a \neq 0$ (along axis of least moment of inertia)	$0, \pm 2, \dots$	$\pm 1, \pm 3, \dots$
$\mu_b \neq 0$ (along axis of intermediate moment of inertia)	$\pm 1, \pm 3, \dots$	$\pm 1, \pm 3, \dots$
$\mu_c \neq 0$ (along axis of greatest moment of inertia)	$\pm 1, \pm 3, \dots$	$0, \pm 2, \dots$

If the dipole moment lies wholly along one of the principal inertial axes, only those changes in the subscript notation listed in the preceding tables for that component are allowed. If there are dipole components along each of the principal inertial axes, all changes listed in the tables are allowed. Any given transition will be due to only one component of the molecular dipole, for example,  $\mu_a$ ,  $\mu_b$ , or  $\mu_c$ . The transitions due to the  $\mu_a$  component are designated as "*a*"-type transitions, those due to  $\mu_b$  as "*b*"-type, and those due to  $\mu_c$  as "*c*"-type transitions.

The presence of different types of transitions for asymmetric rotors, although at times creating additional complexity, can also be an advantage. For instance, with moderately large organic molecules one or more rotational isomers may exist, and one conformation might, from preliminary information, be expected to exhibit "*a*"-type transitions whereas another both "*a*"- and "*b*"-type transitions. This information can be of great aid in distinguishing the isomers and in the assignment of the spectrum. The dependence of the type of transition on the structure in the asymmetric rotor [22] is illustrated with  $\text{H}_2\text{S}_2$  in Fig. 7.6 (see also Fig. 12.19).

While any changes indicated in the previous stable are permitted by the selection rules, it is found that absorption lines corresponding to large changes in either subscript ( $K_{-1}$  or  $K_1$ ) are weak. Also, if the dipole along a particular principal axis is small, the transitions arising from this component will be weak. Furthermore, if the rotor is near the limiting prolate symmetric-top case ( $\kappa \approx -1$ ), the changes in  $K_{-1}$  which correspond to the symmetric-top selection rules,  $\Delta K_{-1} = 0, \pm 1$ , will be the only ones of significant strength, but those for larger changes in  $\Delta K_1$  may have observable strength. Conversely, if the molecule approximates the oblate symmetric rotor ( $\kappa \approx 1$ ), only the lines corresponding to  $\Delta K_1 = 0, \pm 1$  will have significant strength, but relatively large changes in  $K_{-1}$  can give rise to measurable lines. When neither symmetric-top case is approached ( $\kappa \approx 0$ , or asymmetry large), the strongest lines will correspond to 0 and  $\pm 1$  change in both  $K_{-1}$  and  $K_1$ , but lines of significant strength may occur which correspond to larger changes in either or both subscripts. It should also be pointed out that when the dipole moment lies wholly along the symmetry axis, the symmetric-top selection rule is simply  $\Delta K = 0$  (commonly referred to

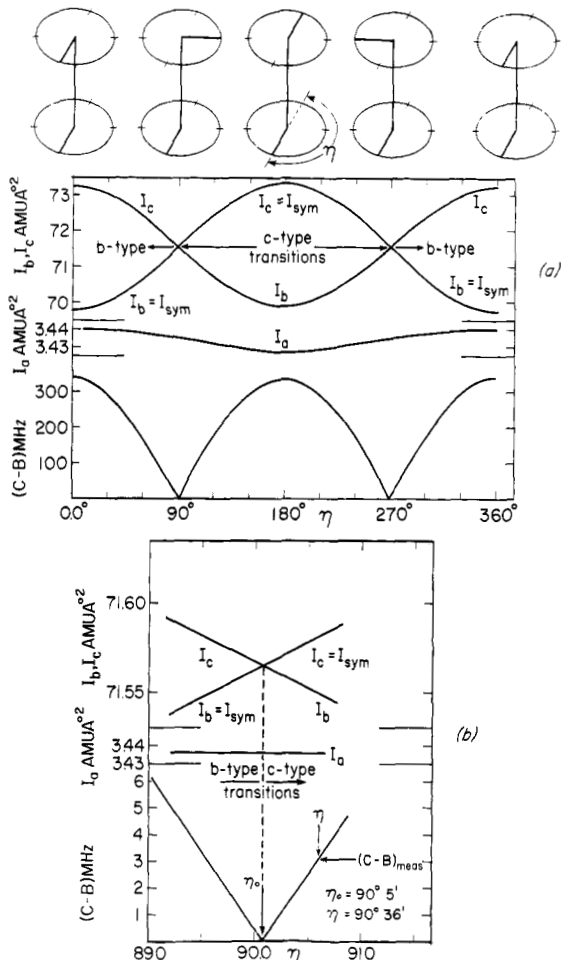


**Fig. 7.6** The dependence on the dihedral angle of the moments of inertia and of the difference of the rotational constants ( $C - B$ ) for HSSH. (a) The dihedral angle varies from 0 to  $360^\circ$ . (b) The dihedral angle varies from  $89.0$  to  $91.0$ . After Winnewisser et al. [22].

as parallel-type transitions), and that when it is entirely perpendicular to the symmetry axis,  $\Delta K = \pm 1$  (perpendicular-type transitions). Hence, we can obtain further information about the probable intensity of a transition by noting the direction of the dipole moment with reference to that principal inertial axis which would in the limit become the symmetry axis.

It is often convenient in the analysis of spectra to group transitions into series or branches which are characterized by the changes in  $J$ ,  $K_{-1}$  and  $K_1$ . The notation used to specify each branch, which is frequently found in the literature, is

$${}^gQ_{\Delta K_{-1}\Delta K_1}, {}^gR_{\Delta K_{-1}\Delta K_1}, {}^gP_{\Delta K_{-1}\Delta K_1}$$

Here  $Q(\Delta J=0)$  and  $R(\Delta J=+1)$  indicate the changes in  $J(J \rightarrow J)$  and  $J \rightarrow J+1$  while the change in  $K_{-1}$  is indicated by the first subscript. The second subscript gives  $\Delta K_1$ . The dipole component responsible for the transition is given as a superscript,  $g=a, b$ , and  $c$ . A summary of the stronger asymmetric rotor transitions is provided in Table 7.9. These stronger branches can often provide more easily recognized spectral patterns which are useful in the assignment of rotational spectra.

The intensities of absorption lines are proportional to the squares of absolute values of direction cosine matrix elements. As shown in (2.108), the direction cosine matrix elements in a symmetric rotor basis may be written as a product of three factors. Each factor depends only on the rotational quantum numbers indicated. The various factors have been given in Table 2.1. They are also seen to depend on the internal axes  $g$  and the external axes  $F$ . For the linear and symmetric-top molecules, the electric moment could be assumed to be along the axis  $z$  so that only the matrix elements of  $\Phi_{F_z}$  were required. In contrast, the asymmetric rotor often has components of its dipole moment along all three principal axes  $x, y, z$ .

For an asymmetric rotor basis the direction cosine matrix elements may also be written in a form similar to (2.108). Each asymmetric rotor wave function is expressed as a linear combination of Wang symmetric rotor functions all

**Table 7.9** Stronger Asymmetric Rotor Transitions<sup>a</sup>

*Near-Oblate Rotor*

<sup>a</sup> $Q_{01}, {}^aQ_{0-1}, {}^aQ_{2-1}, {}^aQ_{-21}$   
<sup>a</sup> $R_{01}, {}^aP_{0-1}, {}^bR_{2-1}, {}^aP_{-21}$   
<sup>b</sup> $Q_{1-1}, {}^bQ_{-11}$   
<sup>b</sup> $R_{11}, {}^bP_{-1-1}, {}^bR_{3-1}, {}^bP_{-31}$   
<sup>c</sup> $Q_{10}, {}^cQ_{-10}$   
<sup>c</sup> $R_{10}, {}^cP_{-10}$

*Near-Prolate Rotor*

<sup>a</sup> $Q_{01}, {}^aQ_{0-1}$   
<sup>a</sup> $R_{01}, {}^aP_{0-1}$   
<sup>b</sup> $Q_{1-1}, {}^bQ_{-11}$   
<sup>b</sup> $R_{11}, {}^bP_{-1-1}, {}^bR_{-13}, {}^bP_{1-3}$   
<sup>c</sup> $Q_{10}, {}^cQ_{-10}, {}^cQ_{-12}, {}^cQ_{1-2}$   
<sup>c</sup> $R_{10}, {}^cP_{-10}, {}^cP_{1-2}, {}^cR_{-12}$

<sup>a</sup>The stronger branches are indicated. Here the “ $g$ ”-type,  $\Delta J=0$  and  $\Delta J=+1$  branches are specified with the notation  ${}^aQ_{\Delta K_{-1}\Delta K_1}$  and  ${}^aR_{\Delta K_{-1}\Delta K_1}$  respectively.

<sup>b</sup>Such reverse transitions are designated by  $P(\Delta J=-1)$ .

having the same value of  $J$  and  $M$  but different values of  $K$ . The  $J$  and  $M$  dependence of the matrix elements in an asymmetric rotor basis will thus be the same as that for a symmetric rotor basis, and we may write

$$(J, \tau, M|\Phi_{Fg}|J', \tau', M') = (J|\Phi_{Fg}|J') \cdot (J, \tau|\Phi_{Fg}|J'\tau') \cdot (J, M|\Phi_{Fg}|J', M') \quad (7.57)$$

The calculation of the  $(J, \tau|\Phi_{Fg}|J', \tau')$  factor requires a knowledge of the eigenvectors associated with the two states  $J_\tau$  and  $J_{\tau'}$ . Evaluation of this direction cosine matrix has been discussed by Cross et al. [23] and by Schwendeman [24]. The latter author has given the matrix elements of the direction cosines in the Wang symmetric rotor basis and has discussed the properties of the matrices, symmetry, and so on. Also the forms chosen for the matrix elements are convenient for transformation to the asymmetric rotor basis by means of a digital computer. In the case of slightly asymmetric rotors, perturbation theory may be used to give the asymmetric rotor wave functions by use of the Wang functions as basis functions. Simple expressions may then be obtained for the direction cosine matrix elements in terms of the symmetric rotor matrix elements and correction terms dependent on the asymmetry. This has been carried out by Lide [25] to second-order, and the results applicable to molecules with  $|\kappa| \geq 0.9$  are collected in Table 7.10.

For a transition  $J, \tau \rightarrow J', \tau'$  caused by a component of the electric moment  $\mu_g$ , a convenient quantity called the line strength is defined as

$$\lambda_g(J, \tau; J', \tau') = \sum_{FMM'} |(J, \tau, M|\Phi_{Fg}|J', \tau', M')|^2 \quad (7.58)$$

where the sum extends over the three directions of the space-fixed system and over all values of  $M$  and  $M'$ . The latter sum over  $M$  and  $M'$  takes into account all possible transitions which in the absence of external fields will be degenerate. The line strength depends only on the inertial asymmetry parameter  $\kappa$  and not on the individual rotational constants; thus it is easily tabulated. Extensive tables of line strengths for various values of  $\kappa$  are available [23, 26–28]. The summation over  $F$  in the absence of external fields can be accomplished by multiplying the results for a given  $F$  by 3, that is,

$$\lambda_g(J, \tau; J'\tau') = 3 \sum_{MM'} |(J, \tau, M|\Phi_{Fg}|J', \tau', M')|^2 \quad (7.59)$$

The dipole moment matrix element appearing in (3.24) may be expressed in terms of the line strength. We have for a field-free rotor

$$\begin{aligned} |(J, \tau|\mu|J', \tau')|^2 &= \sum_{M'F} |(J, \tau, M|\mu_F|J', \tau', M')|^2 \\ &= \mu_g^2 \sum_{M'F} |(J, \tau, M|\Phi_{Fg}|J', \tau', M')|^2 \end{aligned} \quad (7.60)$$

since  $\mu_F = \sum_g \mu_g \Phi_{Fg}$  and for a given transition only one term in the sum over  $g$

**Table 7.10** Coefficients Required to Evaluate the Direction Cosine Matrix Elements of a Slightly Asymmetric Prolate Type Rotator<sup>a,b</sup>

Coefficients	$\alpha$	$\beta$
$K=0$	0	$\frac{\sqrt{2}}{8} [f(J, 1)]^{1/2} \left\{ \delta + \frac{\delta^2}{2} \right\}$
$K=1, \gamma=0$	0	$\frac{1}{16} [f(J, 2)]^{1/2} \left\{ \delta + \frac{[16+J(J+1)]\delta^2}{32} \right\}$
$K=1, \gamma=1$	0	$\frac{1}{16} [f(J, 2)]^{1/2} \left\{ \delta + \frac{[16-J(J+1)]\delta^2}{32} \right\}$
$K=2, \gamma=0$	$-\frac{\sqrt{2}}{8} [f(J, 1)]^{1/2} \left\{ \delta + \frac{\delta^2}{2} \right\}$	$\frac{1}{24} [f(J, 3)]^{1/2} \left\{ \delta + \frac{\delta^2}{2} \right\}$
$K=2, \gamma=1$	0	$\frac{1}{24} [f(J, 3)]^{1/2} \left\{ \delta + \frac{\delta^2}{2} \right\}$
$K=3, \gamma=0$	$-\frac{1}{16} [f(J, 2)]^{1/2} \left\{ \delta + \frac{[16+J(J+1)]\delta^2}{32} \right\}$	$\frac{1}{32} [f(J, 4)]^{1/2} \left\{ \delta + \frac{\delta^2}{2} \right\}$
$K=3, \gamma=1$	$-\frac{1}{16} [f(J, 2)]^{1/2} \left\{ \delta + \frac{[16-J(J+1)]\delta^2}{32} \right\}$	$\frac{1}{32} [f(J, 4)]^{1/2} \left\{ \delta + \frac{\delta^2}{2} \right\}$
$K > 3$	$-\frac{[f(J, K-1)]^{1/2}}{8(K-1)} \left\{ \delta + \frac{\delta^2}{2} \right\}$	$\frac{[f(J, K+1)]^{1/2}}{8(K+1)} \left\{ \delta + \frac{\delta^2}{2} \right\}$

<sup>a</sup>From Lide [25].

<sup>b</sup>Here  $K$  stands for  $K_{-1}$  and  $\gamma=0$  if  $J+K+K_1$  is even and  $\gamma=1$  if  $J+K+K_1$  is odd. The parameter  $\delta=(B-C)/(A-C)$ . The direction cosine matrix elements are evaluated from the relations:

$$(J, K, K_1|\Phi_{Fg}|J', K, K'_1) = [1 - (\alpha^2 + \beta^2 + \alpha'^2 + \beta'^2)/2](J, K|\Phi_{Fg}^0|J', K) + \alpha\alpha'(J, K-2|\Phi_{Fg}^0|J', K-2) \\ + \beta\beta'(J, K+2|\Phi_{Fg}^0|J', K+2)$$

and       $(J, K, K_1|\Phi_{Fg}|J', K+1, K'_1) = [1 - (\alpha^2 + \beta^2 + \alpha'^2 + \beta'^2)/2](J, K|\Phi_{Fg}^0|J', K+1) + \alpha'(J, K|\Phi_{Fg}^0|J', K-1) \\ + \beta(J, K+2|\Phi_{Fg}^0|J', K+1) + \alpha\alpha'(J, K-2|\Phi_{Fg}^0|J', K-1) \\ + \beta\beta'(J, K+2|\Phi_{Fg}^0|J', K+3)$

The  $(J, K|\Phi_{Fg}^0|J', K')$  are the symmetric rotor direction cosine matrix elements and  $\alpha, \beta$ , calculable from the above table, refer to the level  $J, K, K_1$ , and  $\alpha', \beta'$  to the level  $J', K', K'_1$ . For  $(J, 0|\Phi_{Fg}^0|J', 1)$  the expression given in Table 2.1 must, in this particular case, be multiplied by  $2^{1/2}$ .

remains from symmetry arguments. The results are

$$\begin{aligned}\lambda_g(J, \tau; J', \tau') &= (2J+1) \sum_{FM'} |(J, \tau, M|\Phi_{Fg}|J', \tau', M')|^2 \\ &= (2J+1)|(J, \tau|\mu|J', \tau')|^2/\mu_g^2\end{aligned}\quad (7.61)$$

$$\begin{aligned}&= (2J'+1) \sum_{FM} |(J', \tau', M'|\Phi_{Fg}|J, \tau, M)|^2 \\ &= (2J'+1)|(J', \tau'|\mu|J, \tau)|^2/\mu_g^2\end{aligned}\quad (7.62)$$

The direction cosine matrix elements can also be conveniently expressed in terms of the line strengths. For  $F=Z$  and any  $g$ , the line strength can be expressed in terms of the matrix elements  $|(J, \tau|\Phi_{Zg}|J', \tau')|^2$  by use of (7.57), Table 2.1, and carrying out the summation. Note that the sum over  $M'$  reduces to one term since  $\Phi_{Zg}$  is diagonal in  $M$  [see (10.71)–(10.73)]. We find

$$\lambda_g(J, \tau; J', \tau') = \frac{1}{4} R |(J, \tau|\Phi_{Zg}|J', \tau')|^2 \quad (7.63)$$

where  $R$  is defined as  $1/J$ ,  $(2J+1)/J(J+1)$ , or  $1/(J+1)$  for  $J'=J-1$ ,  $J$ , or  $J+1$ , respectively. Since from (7.57)

$$|(J, \tau|\Phi_{Zg}|J', \tau')|^2 = \frac{|(J, \tau, M|\Phi_{Zg}|J', \tau', M)|^2}{|(J|\Phi_{Zg}|J')|^2 \cdot |(J, M|\Phi_{Zg}|J', M)|^2} \quad (7.64)$$

one obtains from (7.63) and Table 2.1

$$|(J, \tau, M|\Phi_{Zg}|J-1, \tau', M)|^2 = \frac{J^2 - M^2}{J(2J-1)(2J+1)} \lambda_g(J, \tau; J-1, \tau') \quad (7.65)$$

$$|(J, \tau, M|\Phi_{Zg}|J, \tau', M)|^2 = \frac{M^2}{J(J+1)(2J+1)} \lambda_g(J, \tau; J, \tau') \quad (7.66)$$

$$|(J, \tau, M|\Phi_{Zg}|J+1, \tau', M)|^2 = \frac{(J+1)^2 - M^2}{(J+1)(2J+1)(2J+3)} \lambda_g(J, \tau; J+1, \tau') \quad (7.67)$$

These expressions multiplied by  $\mu_g^2$  represent the dipole matrix elements for particular Stark or Zeeman components with the field along  $Z$  analogous to (2.109) and (2.115) for a symmetric top

$$|(J, \tau, M|\mu_Z|J', \tau', M)|^2 = \mu_g^2 |(J, \tau, M|\Phi_{Zg}|J', \tau', M)|^2 \quad (7.68)$$

It may also be readily shown that

$$\sum_{M=-J}^{+J} |(J, \tau, M|\Phi_{Zg}|J', \tau', M)|^2 = \frac{1}{3} \lambda_g(J, \tau; J', \tau') \quad (7.69)$$

since  $\sum M^2 = \frac{1}{3} J(J+1)(2J+1)$ . A number of useful sum rules exist because of the orthogonal properties of the direction cosine matrices [23]. Rudolph [29, 30]

has also derived a number of additional relations involving the line strengths, reduced energy, and average of  $P_g^2$ .

A knowledge of the line strength is important in assessing the intensity of a given line and how the intensity can be expected to change with  $\kappa$  or variations in  $J$  or  $K$ . The larger  $|\Delta\tau|$  in the transition the smaller the value of the corresponding  $\lambda$ . The line strength is independent of the direction of the transition. For a given  $\kappa$

$$\lambda_g(J, \tau; J', \tau') = \lambda_g(J', \tau'; J, \tau) \quad (7.70)$$

Also the line strength for an oblate asymmetric rotor transition  $J_{K-1, K_1} \rightarrow J'_{K'-1, K'_1}$  can be obtained from the prolate asymmetric rotor transition  $J_{K, K-1} \rightarrow J'_{K'_1, K'-1}$  with the subscripts reversed by the means of the relation

$$\lambda_g(J, \tau; J', \tau'; \kappa) = \lambda_g(J, -\tau; J', -\tau'; -\kappa) \quad (7.71)$$

Here the explicit dependence on  $\kappa$  is indicated, and the axes change  $g \rightarrow g'$  as follows:  $a \rightarrow c$ ,  $b \rightarrow b$ , and  $c \rightarrow a$ .

For small asymmetry the direction cosine matrix elements may be evaluated with the aid of Table 7.10 and hence the line strengths [see (7.63)]. Explicit expressions for the line strengths of low  $J$  rotational transitions have been given by Gora [31]. The line strengths for the symmetric top limit, which are useful simple approximations to the line strengths for near asymmetric tops, follow from (7.63) and Table 7.10 with  $\delta=0$  and Table 2.1.

The dipole matrix element factor appearing in (3.27) for the absorption coefficient is related to the line strength from (7.61) as follows:

$$|(J, \tau | \mu | J', \tau')|^2 = \frac{\mu_g^2 \lambda_g(J, \tau; J', \tau')}{(2J+1)} \quad (7.72)$$

If (7.72) and (3.25), (3.26), and (3.66) (the latter equation modified for an asymmetric rotor as indicated in Chapter III, Section 3) are inserted into (3.27), the peak absorption coefficient for the transition  $J, \tau \rightarrow J', \tau'$  may be written as

$$\alpha_{\max} = 3.85 \times 10^{-14} F_v \sigma(ABC)^{1/2} \mu_g^2 \lambda_g(J, \tau; J', \tau') \left( \frac{v_0^2}{(\Delta v)_1 T^{5/2}} \right) g_I e^{-EJ\tau/kT} \quad (7.73)$$

where it is assumed that  $hv_0 \ll kT$ . The rotational constants  $A$ ,  $B$ ,  $C$ , the resonant frequency  $v_0$ , and the line breadth  $(\Delta v)_1$  are in megahertz, with  $\mu_g$  in debye units and  $\alpha_{\max}$  in  $\text{cm}^{-1}$ . If the lowest vibrational frequency is much greater than  $kT$  (say  $1000 \text{ cm}^{-1}$  for room temperature), the vibrational partition function is nearly equal to unity, and, for the ground vibrational state,  $F_v$  may hence be taken to be unity. Other things being equal (such as the Boltzmann factor), the strongest lines of a spectrum will be those which have the largest line strength. For asymmetric rotors with no symmetry  $\sigma$ ,  $g_I=1$ . When equivalent nuclei may be exchanged, the rotational level populations are affected and hence the relative intensities. The effects of nuclear spin statistics and the evaluation of  $g_I$  have been discussed in Chapter III, Section 4.

## Chapter VIII

# THE DISTORTABLE ROTOR

---

1	INTRODUCTION	297
2	HAMILTONIAN FOR THE DISTORTABLE ROTOR	301
	Calculation of the $\tau$ 's	305
3	FIRST-ORDER PERTURBATION TREATMENT OF ROTATIONAL DISTORTION	313
	Simplifications for Planar Asymmetric Rotors and Symmetric Tops	322
4	REDUCED HAMILTONIAN	324
	Asymmetric Top Reduction ( $A$ )	329
	Symmetric Top Reduction ( $S$ )	333
	Determinable Combinations of Coefficients	335
	Symmetric and Spherical Tops	337
5	EVALUATION OF THE DISTORTION CONSTANTS FROM OBSERVED SPECTRA	339
	Symmetric and Spherical Tops	357
	Choice of Hamiltonian	361
6	PLANARITY RELATIONS FOR CONSTANTS OF THE REDUCED HAMILTONIAN	366
7	EFFECTS OF VIBRATION	368
	Centrifugal Defect	370
8	CENTRIFUGAL DISTORTION CONSTANTS AND MOLECULAR FORCE FIELDS	372
	Calculation of the Sextic Distortion Constants	382
9	ALTERNATE FORMULATIONS	382
	Large Amplitude Motion—Rotation Hamiltonian	382
	The Padé Hamiltonian	383

## 1 INTRODUCTION

In the initial treatment of the asymmetric rotor we regarded the nuclear framework as rigid. This has proved to be a very useful approximation in the interpretation of rotational spectra. However, in reality, the nuclei are held together by finite restoring forces. Thus, bond distances and angles will vary because of the centrifugal force produced by rotation, which gives rise to a

centrifugal distortion. The rotating molecule will no longer be in its equilibrium configuration but in a distorted configuration. Rotation of CH<sub>3</sub>F, for example, about the symmetry axis would lead to a spreading of the hydrogens and a lengthening of the C—H bond, while end-over-end rotation would produce a closing of the methyl group umbrella and a stretching of the C—F bond. The centrifugal distortion of the molecular parameters of a few molecules for various rotational states is illustrated in Table 8.1. A general expression for the centrifugally induced changes in molecular geometry has been given [1]. Specific application has been made [2] to various isotopic forms of water and hydrogen sulfide which allows calculation of the geometric changes for any rotational level. The effects are usually large for light molecules because of the small moments of inertia. As a consequence of this distortion, the moments of inertia can no longer be considered constant and independent of the rotational state. Therefore, the rotational spectrum will not be simply that of a rigid rotor characterized by a set of equilibrium moments of inertia. Even for low-lying levels with relatively small rotational energies, the precision of microwave measurements is such that the effects of centrifugal distortion can be observed.

**Table 8.1** Centrifugal Distortion of Molecular Parameters<sup>a</sup>

<i>Molecule</i>	<i>Equilibrium Configuration</i>		<i>Change due to Centrifugal Distortion</i>	
			<i>J</i> = 10	30
OH <sup>b</sup>	<i>r</i> (Å)	0.9706	0.0109	0.0922
HCl <sup>b</sup>	<i>r</i> (Å)	1.2746	0.0070	0.0595
CO <sub>2</sub> <sup>b</sup>	<i>r</i> (Å)	1.1615	0.0000	0.0004
		<i>J, K</i> = 10, 10	10, 5	10, 0
NH <sub>3</sub> <sup>c</sup>	<i>r</i> (Å)	1.0124	0.00093	0.00246
	$\alpha$ (deg)	106.67	0.237	-0.337
	$\beta$ (deg)		0.217	-0.308
		<i>J<sub>K-1, K1</sub></i> = 10 <sub>0,10</sub>	10 <sub>3,7</sub>	10 <sub>10,0</sub>
H <sub>2</sub> O <sup>d</sup>	<i>r</i> (Å)	0.9572	0.00283	0.00352
	$\alpha$ (deg)	104.52	0.016	-5.741

<sup>a</sup>From M. Toyama et al. [1].

<sup>b</sup>The rotational state is indicated by the value of *J*.

<sup>c</sup>The rotational state is indicated by the value of *J, K*; *r* denotes N—H bond distance;  $\alpha$ , the H—N—H bond angle; and  $\beta$ , the angle between the N—H bond and the symmetry axis.

<sup>d</sup>The rotational state is indicated by the value of *J<sub>K-1, K1</sub>*; *r* denotes O—H bond distance; and  $\alpha$ , the H—O—H bond angle.

The theory of centrifugal distortion is considerably more complex for asymmetric rotors, and the effects are in general larger for them than for linear or symmetric-top molecules. In asymmetric rotors numerous transitions between levels of large rotational energies can occur in the microwave region, especially for perpendicular-type transitions. On the other hand, for symmetric tops and linear molecules, transitions involving high  $J$  values usually are observed for molecules with large moments of inertia and consequently small rotational energies. In Table 8.2 we show for the asymmetric rotor NSF the shift of the observed frequencies because of centrifugal distortion for various rotational transitions. It is apparent from the table that the spectrum varies significantly from that of a rigid rotor.

Although we must consider the influence of centrifugal distortion in order to accurately account for the positions of rotational transitions, its effects still represent only a small fraction of the rotational energy which is accounted for mainly by the rigid rotor term. Therefore in many cases it can be treated as a perturbation of the rigid rotor Hamiltonian.

Besides introducing a complication in the rotational spectrum, the study of centrifugal distortion provides useful kinds of information. First of all, such a study provides very accurate ground-state spectroscopic constants. For small molecules these data can be profitably combined with infrared vibration-rotation measurements to yield even more accurate values for the rotational energy levels of the excited vibrational states. Such results are important in the study of the fundamental processes of complex molecular laser systems; see, for example, De Lucia et al. [3, 4]. Second, a study of distortion effects allows

**Table 8.2** Comparison of Observed and Rigid Rotor Frequencies for the Asymmetric Rotor NSF (MHz)<sup>a</sup>

Transition	Observed Frequency	Calculated Rigid Rotor Frequency	Distortion Shift <sup>b</sup>
$1_{0,1} \leftarrow 0_{0,0}$	16,105.42	16,105.45	-0.03
$2_{1,2} \leftarrow 1_{0,1}$	71,897.10	71,898.95	-1.85
$4_{2,3} \leftarrow 5_{1,4}$	34,757.97	34,780.70	-22.73
$9_{3,7} \leftarrow 10_{2,8}$	36,366.59	36,418.53	-51.94
$14_{2,12} \leftarrow 15_{1,15}$	13,904.62	14,014.98	-110.36
$15_{2,14} \leftarrow 14_{3,11}$	11,267.85	11,267.46	0.39
$21_{2,20} \leftarrow 20_{3,17}$	39,528.46	39,281.63	246.83
$24_{4,20} \leftarrow 23_{5,19}$	34,948.10	35,440.36	-492.26
$25_{2,24} \leftarrow 24_{3,21}$	16,312.53	15,373.17	939.36
$28_{3,25} \leftarrow 29_{2,28}$	39,307.27	41,451.29	-2,144.02
$30_{7,24} \leftarrow 31_{6,25}$	27,957.29	27,938.85	18.44

<sup>a</sup>After Cook and Kirchhoff [163].

<sup>b</sup>Observed frequency minus rigid rotor frequency.

one to predict unmeasured transition frequencies, in many cases, with a high degree of confidence. The more varied the sample data set, the lower will be the calculated uncertainty limits in the predicted frequencies. This is particularly useful for the transitions of molecules of potential astrophysical interest. Radio astronomers have discovered to date some 50 molecules, and it can be expected that many more will be found as the sensitivity of radio telescopes increases. Contrary to previous expectations, which considered only diatomic molecules as likely to be found in interstellar space, most of the molecules found have been considerably more complex. The importance of laboratory measurements of accurate spectroscopic constants to aid in the detection of molecules in interstellar space through observation of rotational transitions is well documented in reviews on the subject by Winnewisser et al. [5] and Snyder [6]. Third, lines of most interest in a distortion analysis are also particularly useful in the application of microwave spectroscopy to chemical analysis. The location of absorption lines provides the basis for qualitative analysis. The transitions of most use for analytical identification purposes are naturally the most intense transitions. These strong transitions will usually be high  $J$  transitions, the ones assigned and employed in the analysis of distortion effects, but not the ones most likely used to evaluate just the rotational constants. However, if a distortion analysis is performed, high  $J$  lines can be assigned, and one can be sure that these lines belong to the molecule in question and not to a possible impurity. This is illustrated in Fig. 8.1, which shows a small portion of the  $R$ -band spectrum of methylene cyanide [7]. The spectrum extends some 800 MHz with the major frequency markers separated by 100 MHz. The three strongest lines correspond to transitions with  $J > 30$ . The two lower  $J$  transitions are shifted around 300 MHz from their rigid rotor positions while the higher  $J$  transition is shifted around 1900 MHz. These transitions have been measured and assigned on the basis of the distortion analysis. It perhaps should be noted that the rigid rotor positions of these lines cannot even be indicated in Fig. 8.1 since the limited frequency range shown does not encompass these frequency positions. Such

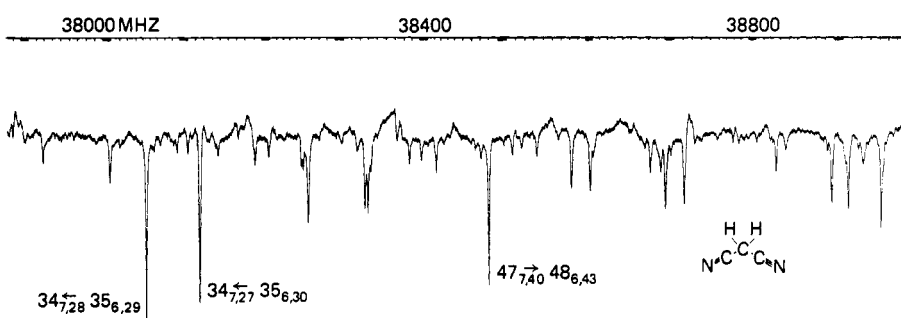


**Fig. 8.1** A small portion of the microwave spectrum of methylene cyanide. The Stark modulation voltage is 800 V. The three stronger transitions are high  $J$  lines. The  $J = 47 \rightarrow 48$  transition is shifted about 1900 MHz from its rigid-rotor position. From Cook et al. [7].

strong lines would naturally be most useful for compilation in a microwave atlas. With the continued interest in microwave spectroscopy as an analytical tool, it might prove useful for molecules where the distortion effects have been studied, to specifically note some of the most intense lines of the spectrum. Finally, the distortion constants themselves provide direct information on the vibrational potential function. This has proved particularly useful in the case of small molecules. A knowledge of the molecular force constants provides fundamental information for the elucidation of interatomic forces and bonding. Examples of this application are reviewed in Section 8.

## 2 HAMILTONIAN FOR THE DISTORTABLE ROTOR

Before we can discuss the perturbation treatment of rotational distortion for a semirigid rotor, a knowledge of the quantum mechanical Hamiltonian is required. The general theory of centrifugal distortion of asymmetric rotors has been formulated by Wilson and Howard [8] and by Nielsen [9]. A simpler derivation, similar to that given earlier by Wilson [10], is described here.

In general, three coordinates are required to describe the translational motion of the center of mass of a molecule. In addition, three coordinates are needed for a nonlinear molecule (two for a linear molecule) to describe the rotational motion about the center of mass. Therefore, for an  $N$ -atom molecule a total of  $3N-6$  (or  $3N-5$  for a linear molecule) coordinates are necessary to describe the vibrations of the molecule. The molecule-fixed Cartesian coordinate system rotating with the molecule provides the reference framework for description of the vibrational motions. Various coordinates can be employed which measure the displacements of the atoms from their equilibrium positions, and since the potential energy is a function of the distortion of the molecule from its equilibrium configuration it can be expressed as a power series expansion in terms of the displacement coordinates. For our purposes it is convenient to set up the vibrational problem in terms of a set of  $3N-6$  independent internal displacement coordinates.

Consider a set of  $3N-6$  internal parameters (e.g., bond distances  $r_i$  and angles  $\alpha_i$ ) required to describe the molecular configuration of a polyatomic molecule. Let  $\{R_i\}$  be a set of  $3N-6$  internal displacement coordinates that describe the displacements of the internuclear distances and bond angles of the molecule from their equilibrium values (e.g.,  $R_1 = \delta r_1 = r_1 - r_1^e$ ,  $R_2 = \delta r_2 = r_2 - r_2^e$ ,  $R_3 = \delta \alpha_1 = \alpha_1 - \alpha_1^e, \dots$ ). If harmonic forces are assumed, that is, only terms quadratic in the displacements are retained, the potential energy can be expressed as

$$V = \frac{1}{2} \sum_{i,j} f_{ij} R_i R_j \quad (8.1)$$

with  $f_{ij}$  the harmonic force constants and  $f_{ij} = f_{ji}$ . The nature of the internal coordinates  $R_i$  and  $R_j$  determines whether the force constant  $f_{ij}$  will represent a bond-stretching or angle-bending force constant, or an interaction force

constant, for example, a stretch-bend interaction constant. For small displacements this potential function is a good approximation to the actual potential of the molecule. Thus the classical Hamiltonian for a vibrating rotating polyatomic molecule may be written approximately as

$$\mathcal{H} = \frac{1}{2} \sum_{\alpha, \beta} \mu_{\alpha\beta} P_\alpha P_\beta + \frac{1}{2} \sum_{i,j} G_{ij} p_i p_j + V \quad (8.2)$$

where  $\alpha$  and  $\beta$  take on the values  $x$ ,  $y$ , or  $z$  of the molecule-fixed Cartesian coordinate system, where  $i$  and  $j$  enumerate the various internal coordinates, and where  $V$  is given by (8.1). The first term represents the rotational energy of the system with  $\mu_{\alpha\beta}$  as an element of the inverse moment of inertia tensor and  $P_\alpha$  as the  $\alpha$  component of the total angular momentum. At this point the  $\mu_{\alpha\beta}$  coefficients must be considered to be functions of the vibrational coordinates, since the requirement that the molecule be rigid has been dropped. The last two terms made up of kinetic and potential energy terms represent the vibrational energy of the molecular system. Here  $p_i$  is the momentum conjugate to the internal coordinate  $R_i$ , and  $G_{ij}$  are the elements of the well-known  $G$ -matrix that arises when internal coordinates are used in molecular vibration problems [11]. The  $G$ -matrix elements are simply functions of the masses and molecular geometry.

In the present discussion we are interested in the situation where the molecular system is not vibrating but only rotating. This rotational motion will result in a distortion of the molecule because of the stretching effects of the centrifugal forces and the nonrigidity of the molecular framework. One of Hamilton's equations of motion,  $\dot{p}_i = -\partial \mathcal{H} / \partial R_i$ , when applied to (8.2), with  $\mu_{\alpha\beta}$  depending on the  $R_i$ 's, yields

$$\frac{1}{2} \sum_{\alpha, \beta} \frac{\partial \mu_{\alpha\beta}}{\partial R_i} P_\alpha P_\beta + \frac{\partial V}{\partial R_i} = 0, \quad i = 1, 2, \dots, 3N-6 \quad (8.3)$$

since both  $p_i$  and  $\dot{p}_i$  are zero under the assumption of no vibration. This relation expresses the equilibrium condition between the restoring potential forces and the centrifugal forces due to rotation.

The coefficient  $\mu_{\alpha\beta}$  can be approximated by a series expansion about the equilibrium value  $\mu_{\alpha\beta}^e$  (i.e., the value when all displacement coordinates  $R_i$  are zero, which corresponds physically here to no rotation), as follows

$$\mu_{\alpha\beta} = \mu_{\alpha\beta}^e + \sum_i \mu_{\alpha\beta}^{(i)} R_i + \dots \quad (8.4)$$

with

$$\mu_{\alpha\beta}^{(i)} = \left( \frac{\partial \mu_{\alpha\beta}}{\partial R_i} \right)_e \quad (8.5)$$

This latter quantity, which is the partial derivative of the  $\alpha\beta$  component of the reciprocal moment of inertia tensor with respect to the internal coordinate  $R_i$ , is to be evaluated at the equilibrium position. In the expansion, only linear

terms are retained since the displacements are assumed to be small. From this expansion in conjunction with the potential energy expression, (8.1), one immediately obtains from (8.3)

$$\frac{1}{2} \sum_{\alpha, \beta} \mu_{\alpha \beta}^{(i)} P_\alpha P_\beta + \sum_j f_{ij} R_j = 0, \quad i=1, 2, \dots, 3N-6 \quad (8.6)$$

This set of linear equations may be solved for  $R_j$  giving

$$R_j = -\frac{1}{2} \sum_{i, \alpha, \beta} (f^{-1})_{ji} \mu_{\alpha \beta}^{(i)} P_\alpha P_\beta \quad (8.7)$$

where  $(f^{-1})_{ji}$  is an element of the matrix inverse to the matrix of force constants  $f_{ji}$ . Inserting this in (8.4) allows one to express the instantaneous values of  $\mu_{\alpha \beta}$  in terms of the components of the total angular momentum as follows

$$\mu_{\alpha \beta} = \mu_{\alpha \beta}^e - \frac{1}{2} \sum_{i, j, \gamma, \delta} \mu_{\alpha \beta}^{(i)} (f^{-1})_{ij} \mu_{\gamma \delta}^{(j)} P_\gamma P_\delta \quad (8.8)$$

If (8.7) is inserted into (8.1), the potential energy becomes

$$V = \frac{1}{8} \sum_{i, j, \alpha, \beta, \gamma, \delta} \mu_{\alpha \beta}^{(i)} (f^{-1})_{ij} \mu_{\gamma \delta}^{(j)} P_\alpha P_\beta P_\gamma P_\delta \quad (8.9)$$

Note  $\sum_i f_{ii} (f^{-1})_{ij} = \delta_{ij}$ . When these expressions for  $\mu_{\alpha \beta}$  and  $V$  are substituted in (8.2) one obtains

$$\mathcal{H} = \frac{1}{2} \sum_{\alpha, \beta} \mu_{\alpha \beta}^e P_\alpha P_\beta + \frac{1}{4} \sum_{\alpha, \beta, \gamma, \delta} \tau_{\alpha \beta \gamma \delta} P_\alpha P_\beta P_\gamma P_\delta \quad (8.10)$$

with

$$\tau_{\alpha \beta \gamma \delta} = -\frac{1}{2} \sum_{ij} \mu_{\alpha \beta}^{(i)} (f^{-1})_{ij} \mu_{\gamma \delta}^{(j)} \quad (8.11)$$

This is the classical rotational Hamiltonian for a semirigid nonvibrating molecule; it represents the quantum mechanical Hamiltonian when the angular momentum components are taken as the corresponding angular momentum operators.

The first term on the right in (8.10) represents the usual rigid rotor energy while the second term represents the energy of distortion. The  $\tau_{\alpha \beta \gamma \delta}$  are the distortion constants, and the distortion contribution will involve angular momentum about all three axes. The dependence of the distortion constants on the inverse elements of the molecular force constant matrix is physically reasonable, since, all things being equal, one would expect that weaker bonds with small force constants should show larger distortion effects than the strong bonds with large force constants.

The equilibrium rotational and centrifugal distortion constants in  $\mathcal{H}$  which are independent of the rotational coordinates are also seen to be independent of the vibrational coordinates. Within the approximation considered here, we have a rigid rotor with a correction term for centrifugal distortion. However,

in an actual molecule, vibrational motion is unavoidable, and the rotational and distortion constants must be considered as functions of the vibrational coordinates and thus dependent on the vibrational state in which the rotational spectrum is observed. In practice then, the principal moments of inertia obtained from the ground state spectrum are moments averaged over the ground vibrational state, that is, effective moments of inertia. The general vibration-rotation quantum mechanical Hamiltonian operator of a polyatomic molecule has been discussed by Wilson and Howard [8] and by Darling and Dennison [12]. Perturbation treatments to various order have been given for the evaluation of the vibration-rotation energy levels [8, 9, 13, 14]. These general formulations admit vibration-rotation interaction terms in the Hamiltonian from which the vibrational dependence of the rotational constants and centrifugal distortion constants arises as well as other vibration-rotation interactions such as Coriolis coupling. We may also cite some of the more recent discussions [15-20] on the rotation-vibration Hamiltonian (see also Chapter VII).

As a simple application of (8.10), let us consider the case of a semirigid diatomic rotor. The rotation of a diatomic molecule is mathematically equivalent to the rotation of a single particle of reduced mass  $\mu$  at a distance  $r$  from the axis of rotation and we have

$$\mu = \frac{1}{I}; \quad I = mr^2 = \frac{m_1 m_2}{m_1 + m_2} r^2 \quad (8.12)$$

The distortion term of (8.10) with the aid of (8.11) reduces to

$$-\frac{1}{8} \left( \frac{\partial \mu}{\partial R} \right)_e^2 \left( \frac{1}{f} \right) P^4 \quad (8.13)$$

where  $f$  is the force constant appearing in the potential energy which is simply  $V = \frac{1}{2} f R^2$  where  $R = \delta r = r - r_e$ ,  $r_e$  is the equilibrium bond distance, and  $r$  is the instantaneous value. Now the partial derivative, evaluated at equilibrium, of the reciprocal moment of inertia is

$$\left( \frac{\partial \mu}{\partial R} \right)_e = \left( \frac{\partial \mu}{\partial r} \right)_e = \frac{-2}{mr_e^3} = \frac{-2}{m} \left( \frac{m}{I^e} \right)^{3/2} \quad (8.14)$$

In the case of polyatomic molecules the evaluation of such quantities is more complicated. If we now impose the quantum mechanical restriction that the angular momentum must be quantized in units of  $\hbar$ , that is,  $P^2 = \hbar^2 J(J+1)$ , then (8.13) may be written in the familiar form  $-hD_J J^2(J+1)^2$  with the distortion constant defined as

$$D_J = \frac{\hbar^4}{2h} \frac{m}{f(I^e)^3} = \frac{4B_e^3}{\omega_e^2} \quad (8.15)$$

where (8.14) and the relations  $B_e = \hbar/(8\pi^2 I^e)$  and  $\omega_e = (1/2\pi)(f/m)^{1/2}$  have been utilized. This is the usual definition of  $D_J$  given for a diatomic molecule.

### Calculation of the $\tau$ 's

The distortion constants can either be evaluated from the rotational spectrum (this will be discussed in the next section) or if the force constants are known they may be obtained by means of (8.11) once the derivatives, which depend on the molecular geometry, are evaluated. For a general molecule the partial derivatives appearing in (8.11) are most easily determined by the method proposed by Kivelson and Wilson [21]. They first express the partial derivatives of the inverse inertia tensor components in terms of the partial derivatives of the components of the inertia tensor. In the matrix notation we have, since  $\mu = \mathbf{I}^{-1}$ , the equation  $\mu \mathbf{I} = \mathbf{E}$  with  $\mathbf{E}$  the unit matrix, and taking partial derivatives we obtain

$$\frac{\partial \mu}{\partial R_i} \mathbf{I} + \mu \frac{\partial \mathbf{I}}{\partial R_i} = 0 \quad (8.16)$$

thus

$$\frac{\partial \mu}{\partial R_i} = -\mu \frac{\partial \mathbf{I}}{\partial R_i} \mu \quad (8.17)$$

The coordinate axes are now so chosen that the undistorted molecule will be in its principal axis system with origin at the center of mass. Then the inertia matrix is diagonal with equilibrium elements  $I_{xx}^e$ ,  $I_{yy}^e$ ,  $I_{zz}^e$ , and we find for the components of (8.17) evaluated at equilibrium

$$\left( \frac{\partial \mu_{\alpha\beta}}{\partial R_i} \right)_e = - \frac{[J_{\alpha\beta}^{(i)}]_e}{I_{\alpha\alpha}^e I_{\beta\beta}^e} \quad (8.18)$$

since  $\mu_{\alpha\alpha}^e = 1/I_{\alpha\alpha}^e$ , etc. Here

$$J_{\alpha\beta}^{(i)} = \frac{\partial I_{\alpha\beta}}{\partial R_i} \quad (8.19)$$

If (8.18) is inserted into (8.11), the distortion constants may be re-expressed as

$$\tau_{\alpha\beta\gamma\delta} = -\frac{1}{2}(I_{\alpha\alpha}^e I_{\beta\beta}^e I_{\gamma\gamma}^e I_{\delta\delta}^e)^{-1} \sum_{i,j} [J_{\alpha\beta}^{(i)}]_e (f^{-1})_{ij} [J_{\gamma\delta}^{(j)}]_e \quad (8.20)$$

An alternate definition in terms of partial derivatives with respect to the normal coordinates has been given in Chapter VII, Section 6.

Evaluation of the partial derivatives of components of the inertia matrix requires special consideration. The components of the inertia matrix are given by

$$I_{\alpha\alpha} = \sum_l m_l (\beta_l^2 + \gamma_l^2) \quad (8.21)$$

$$I_{\alpha\beta} = I_{\beta\alpha} = - \sum_l m_l \alpha_l \beta_l \quad (8.22)$$

where  $m_l$  and  $\alpha_l$  are, respectively, the mass and the  $\alpha$ -coordinate of the  $l$ th atom as measured in the body-fixed axis system. Here, and in the following equations,

$\alpha$ ,  $\beta$ , and  $\gamma$  are taken in cyclic order; that is, if  $\alpha_i = x_i$ , then  $\beta_i$  and  $\gamma_i$  stand for  $y_i$  and  $z_i$ , respectively. What is required are the variations of the components of the inertia tensor when the molecule is distorted from its equilibrium configuration. Now the variations in the  $3N$  Cartesian coordinates,  $\delta\alpha_i$ ,  $\delta\beta_i$ ,  $\delta\gamma_i$ , cannot be made arbitrarily but must satisfy the six Eckart conditions [22, 23] which serve to define the rotating coordinate system so as to provide maximum separation of rotation and vibration. Physically, we may view these as restrictions on the distortions that insure that the center of mass of the molecule does not change and that no angular momentum is imparted to the molecule. With the Eckart conditions it can be shown that [21]

$$J_{\alpha\alpha}^{(i)} = \frac{2}{\delta R_i} \sum_l m_l (\beta_l \delta\beta_l + \gamma_l \delta\gamma_l) \quad (8.23)$$

$$J_{\alpha\beta}^{(i)} = -\frac{2}{\delta R_i I_{yy}} \left\{ I_\alpha \sum_l m_l \beta_l \delta\alpha_l + I_\beta \sum_l m_l \alpha_l \delta\beta_l \right\} \quad (8.24)$$

with  $I_\alpha = \sum_k m_k \alpha_k^2$ , and so on, and  $I_{yy}$  given by (8.21). These relations allow the displacements  $\delta\alpha_i$ , and so on, to be entirely arbitrary while still satisfying the Eckart conditions. The expressions are to be evaluated at the equilibrium configuration of the molecule ( $R_i = 0$ ,  $i = 1, \dots, 3N - 6$ ) and are referred to the rotating principal axis system. The Cartesian coordinates  $\alpha_i$  are thus measured from the center of mass in the principal axis system.

For the finding of a derivative, the principal axis system may be translated to a convenient position in the molecule. Small displacements are then given to the nuclei so that the set of increments  $\delta\alpha_i$  will change the angle or internuclear distance that is involved in a given internal coordinate  $R_i$ , in such a way that the internal coordinate will change by an increment  $\delta R_i$  while leaving all other internal coordinates with their equilibrium values (see Fig. 8.2). The coordinates  $\alpha_i$  are related to those of the displaced coordinate system ( $x'$ ,  $y'$ ,  $z'$ ) by  $\alpha_i = \alpha'_i - \bar{\alpha}$ , where  $\bar{\alpha}$  is the  $\alpha$  component of the center of mass in the displaced system.

When there are more internal displacement coordinates than vibrational degrees of freedom, that is, redundancies are present, additional considerations are necessary. These have been discussed by Gold et al. [24]. If the molecule has symmetry, calculation of the distortion constants can be simplified by use of a set of internal symmetry coordinates  $\{S_i\}$  which are particular orthonormal linear combinations of the internal displacement coordinates. These symmetry coordinates are chosen so that, under the symmetry operations of the molecular point group, each coordinate may be classified as belonging to one of the symmetry species of the group. Equation 8.20 is still applicable when both the partial derivatives and the force constant matrix are expressed in terms of the symmetry coordinates. To obtain the  $J_{\alpha\beta}^{(i)}$ , we choose increments  $\delta\alpha_i$  so as to produce an increment  $\delta S_i$  in a particular symmetry coordinate while the other symmetry coordinates are left unchanged. When symmetry coordinates are used, the matrix of force constants, and its inverse, will factor into submatrices

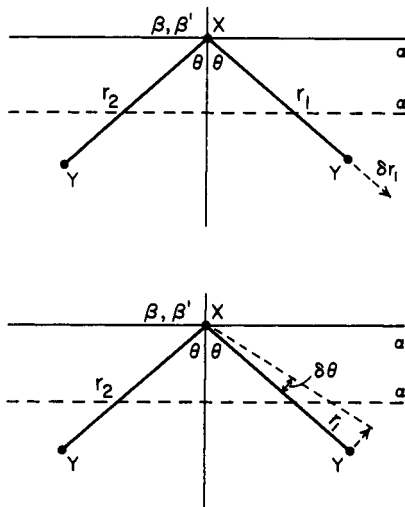


**Fig. 8.2** Principal and translated axes for bent  $XY_2$ -type molecule. Displacement of  $r_1$  bond length (top figure). Displacement of valence bond angle (bottom figure).

corresponding to different symmetry species of the group; there will be no coupling between  $J_{\alpha\beta}^{(i)}$  and  $J_{\alpha\beta}^{(j)}$  if the  $i$ th and  $j$ th symmetry coordinates belong to different symmetry species [21]. In Table 8.3 (on pages 308–311) explicit expressions for the derivatives of some common types of molecules are given. Expressions for other types such as axially symmetric  $ZX_3Y$  molecules [25], pyramidal  $XYZ_2$  molecules [26], and axially symmetric  $ZX_3YW$  molecules [27] have also been reported. General expressions for a number of commonly used internal displacement coordinates may be found in [21]. Corrections for non-tetrahedral angles in the symmetric tops  $ZX_3Y$  and  $XY_3$  have been described [28].

Since calculation of the  $J_{\alpha\beta}^{(i)}$  elements is somewhat tedious, alternate methods of evaluation that are more convenient have been formulated. The Cartesian displacements in the principal inertial axis system can be conveniently expressed, as pointed out by Parent and Gerry [29], in terms of the  $\rho$  vectors ( $\rho_i = \rho_i^{(x)}, \rho_i^{(y)}, \rho_i^{(z)}, \rho_{i1}^{(x)}, \rho_{i1}^{(y)}, \dots, \rho_{iN}^{(z)}$ )

$$\delta\alpha_i = \rho_{il}^{(\alpha)} \quad (8.25)$$

with  $\rho_{il}^{(\alpha)}$  the  $\alpha$  component of the  $\rho$  vector for the  $l$ th atom associated with the  $i$ th internal coordinate. These  $\rho$  vectors, introduced by Polo [30], can also be used to evaluate the inverse kinetic energy matrix  $\mathbf{G}^{-1}$ , which is useful in the solution of the vibrational problem. An alternate formulation which makes use of the Wilson  $s$  vectors has been discussed by a number of authors (see Aliev and Aleksanyan [31], Cyvin et al. [32–34], Pulay and Sawodny [35], and Klauss and Strey [36]).

Let  $R_i$  denote an internal displacement coordinate and  $\delta\alpha_i = \alpha_i - \alpha_i^e$ , the Cartesian displacement coordinate of the  $i$ th atom ( $\alpha = x, y$ , or  $z$ ). These are

related by the well-known transformation

$$R_i = \sum_{l,\alpha} B_{il}^{(\alpha)} \delta\alpha_l \quad \begin{cases} l=1, \dots, N; \alpha=x, y, z \\ i=1, \dots, 3N-6 \end{cases} \quad (8.26)$$

The **B** matrix elements are constructed from the Wilson **s** vectors and give the kinetic energy matrix **G**,

$$G_{ij} = \sum_{\alpha,l} \left( \frac{1}{m_l} \right) B_{il}^{(\alpha)} B_{jl}^{(\alpha)} \quad (8.27)$$

with the three components  $B_{il}^{(x)}$ ,  $B_{il}^{(y)}$ ,  $B_{il}^{(z)}$  associated with atom  $l$  and coordinate  $R_i$ . The inverse transformation is denoted by

$$\delta\alpha_l = \sum_i A_{li}^{(\alpha)} R_i \quad (8.28)$$

The matrix **A** is not simple  $\mathbf{B}^{-1}$  since **B** cannot be inverted because it is a rectangular matrix. However, Crawford and Fletcher [37] have shown that if the six Eckart conditions are added, the desired transformation is given by

$$A_{li}^{(\alpha)} = \sum_k \frac{1}{m_l} B_{kl}^{(\alpha)} G_{ki}^{-1} \quad (8.29)$$

This relation forms the basis for evaluating the derivatives of  $I_{\alpha\beta}$  satisfying the Eckart conditions. Taking the partial derivatives of the components of the inertia tensor, with respect to the internal coordinates, gives

$$\begin{aligned} \frac{\partial I_{\alpha\alpha}}{\partial R_i} &= 2 \sum_l m_l \left( B_l \frac{\partial \beta_l}{\partial R_i} + \gamma_l \frac{\partial \gamma_l}{\partial R_i} \right) \\ \frac{\partial I_{\alpha\beta}}{\partial R_i} &= - \sum_l m_l \left( \alpha_l \frac{\partial \beta_l}{\partial R_i} + \beta_l \frac{\partial \alpha_l}{\partial R_i} \right) \end{aligned} \quad (8.30)$$

From (8.28)

$$\frac{\partial \alpha_l}{\partial R_i} = A_{li}^{(\alpha)} \quad (8.31)$$

and substitution in (8.30), with cognizance of (8.29), gives

$$\begin{aligned} \frac{\partial I_{\alpha\alpha}}{\partial R_i} &= 2 \sum_k \sum_l (\beta_l B_{kl}^{(\beta)} + \gamma_l B_{kl}^{(\gamma)}) G_{ki}^{-1} = \sum_k G_{ik}^{-1} T_{\alpha\alpha}^{(k)} \\ \frac{\partial I_{\alpha\beta}}{\partial R_i} &= - \sum_k \sum_l (\alpha_l B_{kl}^{(\beta)} + \beta_l B_{kl}^{(\alpha)}) G_{ki}^{-1} = \sum_k G_{ik}^{-1} T_{\alpha\beta}^{(k)} \end{aligned} \quad (8.32)$$

The definitions of  $T_{\alpha\alpha}^{(k)}$  and  $T_{\alpha\beta}^{(k)}$  are apparent from the foregoing equations. Evaluation of these in the equilibrium configuration yields the desired quantities

$$J_{\alpha\beta}^{(i)} = \left( \frac{\partial I_{\alpha\beta}}{\partial R_i} \right)_e \quad (8.33)$$

**Table 8.3** The  $[J_{\alpha\beta}^{(i)}]_e$  Expressions for Some Particular Cases

	$[J_{xx}^{(i)}]_e$	$[J_{zz}^{(i)}]_e$	$[J_{xz}^{(i)}]_e$
<b>Internal Coordinate</b>			
	<i>For Nonlinear XY<sub>2</sub> Molecules<sup>a</sup></i>		
$\delta r_1$	$2m_Y rs^2$	$\frac{2m_X m_Y rc^2}{M}$	$\frac{2m_Y rsc}{1 + 2m_Y m_X^{-1}s^2}$
$\delta r_2$	$2m_Y rs^2$	$\frac{2m_X m_Y rc^2}{M}$	$\frac{-2m_Y rsc}{1 + 2m_Y m_X^{-1}s^2}$
$\delta\alpha$	$2m_Y r^2 sc$	$\frac{-2m_X m_Y r^2 sc}{M}$	0
<b>Symmetry Coordinate</b>			
$S_1$	$2\sqrt{2}m_Y rs^2$	$\frac{2\sqrt{2}m_X m_Y rc^2}{M}$	0
$S_2$	$2m_Y r^2 sc$	$\frac{-2m_X m_Y r^2 sc}{M}$	0
$S_3$	0	0	$\frac{2\sqrt{2}m_Y rsc}{1 + 2m_Y m_X^{-1}s^2}$
<i>Definition of Symmetry Coordinates for XY<sub>2</sub></i>			
	<i>A<sub>1</sub> species</i>	<i>B<sub>1</sub> species</i>	
	<hr/>	<hr/>	
	$S_1 = \frac{\delta r_1 + \delta r_2}{\sqrt{2}}$	$S_3 = \frac{\delta r_1 - \delta r_2}{\sqrt{2}}$	
	$S_2 = \delta\alpha$		
<i>For Planar XYZ<sub>2</sub> Molecules<sup>b</sup></i>			
$S_1$	$\sqrt{8}m_Z(l+r_1c)c$	$\sqrt{8}m_Z r_1 s^2$	0
$S_2$	$2m_Y(r_3-l)$	0	0
$S_3$	$\frac{-4m_Z r_1 s(l+r_1c)}{\sqrt{6}}$	$\frac{4m_Z r_1^2 sc}{\sqrt{6}}$	0
$S_4$	0	0	$\frac{-\sqrt{8}m_Z [I_x s(l+r_1c) + I_z r_1 sc]}{I_{yy}}$
$S_5$	0	0	$\frac{-\sqrt{2}m_Y I_x r_3(r_3-l)}{I_{yy}}$

Table 8.3 Continued

	$[J_{xx}^{(i)}]_e$	$[J_{zz}^{(i)}]_e$	$[J_{xz}^{(i)}]_e$
<i>Definition of Symmetry Coordinates for XYZ<sub>2</sub></i>			
<i>A<sub>1</sub> species</i>		<i>B<sub>1</sub> species</i>	
$S_1 = \frac{\delta r_1 + \delta r_2}{\sqrt{2}}$		$S_4 = \frac{\delta r_1 - \delta r_2}{\sqrt{2}}$	$S_6 = \delta \tau$
$S_2 = \delta r_3$		$S_5 = \frac{\delta \beta_1 - \delta \beta_2}{\sqrt{2}}$	
$S_3 = \frac{2\delta \alpha - \delta \beta_1 - \delta \beta_2}{\sqrt{6}}$			
<i>For Pyramidal XY<sub>3</sub> Molecules<sup>c</sup></i>			
$S_1$	$\frac{m_Y r^2 t (3m_Y - m_X)}{\sqrt{3}M}$	$\frac{2}{\sqrt{3}} m_Y r^2 t$	0
$S_2$	$\frac{\sqrt{3}rm_Y}{M} [M + (m_X - 3m_Y)c^2]$	$2\sqrt{3}m_Y rs^2$	0
$S_{1x}$	$\frac{\sqrt{2}}{\sqrt{3}} m_Y r^2 t$	0	$\frac{-4m_X m_Y r^2 ct I_x}{\sqrt{6}MsI_{yy}}$
$S_{2x}$	$\frac{\sqrt{6}}{2} m_Y rs^2$	0	$\frac{\sqrt{6}m_Y rsc(m_X I_x + MI_z)}{MI_{yy}}$
$S_{1y}, S_{2y}$	0	0	0
<i>Definition of Symmetry Coordinates for XY<sub>3</sub></i>			
<i>A<sub>1</sub> species</i>		<i>E species</i>	
$S_1 = \frac{\delta \alpha_{12} + \delta \alpha_{13} + \delta \alpha_{23}}{\sqrt{3}}$		$S_{1x} = \frac{2\delta \alpha_{12} - \delta \alpha_{13} - \delta \alpha_{23}}{\sqrt{6}}$	
$S_2 = \frac{\delta r_1 + \delta r_2 + \delta r_3}{\sqrt{3}}$		$S_{2x} = \frac{-2\delta r_3 + \delta r_1 + \delta r_2}{\sqrt{6}}$	
		$S_{1y} = \frac{\delta \alpha_{13} - \delta \alpha_{23}}{\sqrt{2}}$	
		$S_{2y} = \frac{\delta r_1 - \delta r_2}{\sqrt{2}}$	

The Eckart conditions are satisfied automatically, and the  $G$ -matrix elements and the  $J_{\alpha\beta}^{(i)}$  can be calculated together with a set of  $s$  vectors evaluated in the principal inertial axis system of the equilibrium configuration. The equilibrium coordinates  $\alpha_i^e$ , however, need not refer to the center of gravity of the molecule as their origin [33].

If desired, (8.20) may be written in an alternate form in terms of the  $T_{\alpha\beta}^{(k)}$ . The vibrational eigenvalue problem may be expressed as  $\mathbf{G}\mathbf{F}\mathbf{L} = \mathbf{L}\Lambda$ , where  $\Lambda$  is a diagonal matrix of eigenvalues  $\lambda_i = 4\pi^2 c^2 \omega_i^2$  and  $\mathbf{L}$  relates the internal coordinates  $R_i$  to the normal coordinates  $Q_i$ ,  $\mathbf{R} = \mathbf{L}\mathbf{Q}$ . Since in matrix notation  $\tilde{\mathbf{L}}\mathbf{F}\mathbf{L} = \Lambda$  and  $\tilde{\mathbf{L}}\mathbf{G}^{-1}\mathbf{L} = \mathbf{E}$ , with  $\mathbf{E}$  a unit matrix, it follows that  $\mathbf{G}^{-1}\mathbf{F}^{-1}\mathbf{G}^{-1} = \tilde{\mathbf{L}}^{-1}\Lambda^{-1}\mathbf{L}^{-1}$ . By use of (8.32), (8.20) may be rewritten as

$$\tau_{\alpha\beta\gamma\delta} = -\frac{1}{2}(I_{\alpha\alpha}^e I_{\beta\beta}^e I_{\gamma\gamma}^e I_{\delta\delta}^e)^{-1} \sum_{k,k'} T_{\alpha\beta}^{(k)} T_{\gamma\delta}^{(k')} \theta_{kk'} \quad (8.34)$$

with

$$\theta_{kk'} = \sum_{ij} G_{ki}^{-1} F_{ij}^{-1} G_{jk'}^{-1} = \sum_i \frac{L_{ik}^{-1} L_{ik'}^{-1}}{\lambda_i} \quad (8.35)$$

The elements of  $\theta_{kk'}$  are obtained from the usual normal-coordinate analysis of the molecular vibrations. (See Appendix H).

Application of Table 8.3 may be illustrated by considering a symmetrical bent triatomic molecule, for example,  $\text{SO}_2$ , for which there are four force constants and four independent  $\tau$ 's. From (8.20) and the  $[J_{\alpha\beta}^{(i)}]_e$ 's of Table 8.3, with introduction of the factor  $\hbar^4/h$ , the explicit relations between the distortion constants (equilibrium values) and the force constants are found to be [38]

$$\frac{-\tau_{aaaa} R}{A^2} = 2(F^{-1})_{11} + \tan^2 \theta (F^{-1})_{22} - 2\sqrt{2} \tan \theta (F^{-1})_{12} \quad (8.36)$$

<sup>a</sup>After Kivelson and Wilson [21]. The  $xz$  plane is taken as the molecular plane with the  $x$  axis parallel to the  $C_2$  axis, and  $M = 2m_Y + m_X$ ,  $c = \cos \theta$ ,  $s = \sin \theta$ , where  $\theta$  is one-half the  $Y-X-Y$  angle ( $\alpha$ ) and  $r$  is the  $Y-X$  equilibrium bond distance. Derivatives of  $I_{yy}$  with respect to  $S_1$  and  $S_2$  can be obtained from the table since  $I_{yy} = I_{xx} + I_{zz}$  for a planar molecule.

<sup>b</sup>From M. G. K. Pillai and F. F. Cleveland, *J. Mol. Spectrosc.*, **6**, 465 (1961). The symbols are defined as follows:  $m_Z$  = mass of  $Z$  atom,  $m_Y$  = mass of  $Y$  atom,  $r_1$  is the  $X-Z$  bond distance and  $r_3$  is the  $X-Y$  bond distance,  $c = \cos(\alpha/2)$ ,  $s = \sin(\alpha/2)$  with  $\alpha$  the  $Z-X-Z$  angle,  $l$  is the distance between the center of mass and the  $X$  atom, measured along the  $X-Y$  bond, which is taken as the  $z$  axis. For symmetry coordinates:  $r_1$  and  $r_2$  are the  $X-Z_i$  bond distances;  $r_3$ , the  $X-Y$  bond distance;  $\alpha$ , the  $Z-X-Z$  angle;  $\beta_i$ , the  $Y-X-Z_i$  angle; and  $\tau$ , out-of-plane angle. Derivatives of  $I_{yy}$  with respect to  $S_1$ ,  $S_2$ , and  $S_3$  are easily obtained from the table since the molecule is planar. All other derivatives vanish.

<sup>c</sup>From P. N. Schatz, *J. Chem. Phys.*, **29**, 481 (1958). Here the  $C_3$  axis has been chosen as the  $z$  axis. The symbols are defined as follows:  $c = \cos \theta$ ,  $s = \sin \theta$ , with  $\theta$  the angle between the  $C_3(z)$  axis and an  $X-Y$  bond ( $\theta > 90^\circ$ ),  $m_X$  = mass of  $X$  atom,  $m_Y$  = mass of  $Y$  atom,  $M$  = total mass,  $r = X-Y$  bond distance,  $t = \sin \alpha$ , where  $\alpha = Y-X-Y$  angle.

$$\frac{-\tau_{bbbb}R}{B^2} = 2(F^{-1})_{11} + \cot^2 \theta (F^{-1})_{22} + 2\sqrt{2} \cot \theta (F^{-1})_{12} \quad (8.37)$$

$$\frac{-\tau_{aabb}R}{AB} = 2(F^{-1})_{11} - (F^{-1})_{22} + \sqrt{2}(\cot \theta - \tan \theta)(F^{-1})_{12} \quad (8.38)$$

$$\frac{-\tau_{abab}R}{AB} = 2Mm_X^{-1}(1 + 2m_Ym_X^{-1}\sin^2 \theta)^{-2}(F^{-1})_{33} \quad (8.39)$$

Here  $h$  is in erg-sec, masses are in amu and

$$R = \frac{r^2 \times 10^{-22}}{2h}$$

with  $\theta$  as one-half the  $Y-X-Y$  angle,  $M=2m_Y+m_X$ ,  $r$  as the  $X-Y$  bond distance expressed in angstrom units, and with the  $\tau$ 's and rotational constants in megahertz. The  $(F^{-1})_{ij}$  are the elements of the matrix inverse to the potential constant matrix  $\mathbf{F}$  (dynes/cm) written in terms of the symmetry coordinates given in Table 8.3 [see (8.199)]. It is clear that the observed  $\tau$ 's provide a basis for evaluation of the force constant matrix. Since  $\tau_{abab}$  depends only on  $\omega_3(B_1)$ , an even simpler expression may be written [39] in terms of the vibrational frequency

$$\tau_{abab} = -\frac{16cABC}{\omega_3^2} \quad (8.40)$$

with  $\tau_{abab}$  in Hz and  $A, B, C, \omega_3$  in  $\text{cm}^{-1}$ , and  $c$  the speed of light in cm/sec.

From these relations it is apparent that for triatomic planar molecules, where the  $C_{2v}$  symmetry is unaltered by isotopic substitution, the distortion constants for the isotopic species can be calculated from the distortion constants of the parent species. In particular, for  $Y^*-X^*-Y^*$  we have

$$\tau_{aaaa}^* = \left( \frac{A^*}{A} \right)^2 \tau_{aaaa} \quad (8.41)$$

$$\tau_{bbbb}^* = \left( \frac{B^*}{B} \right)^2 \tau_{bbbb} \quad (8.42)$$

$$\tau_{aabb}^* = \left( \frac{A^*B^*}{AB} \right) \tau_{aabb} \quad (8.43)$$

$$\tau_{abab}^* = \left( \frac{A^*B^*}{AB} \right) \left( \frac{M^*m_X}{Mm_X^*} \right) \times \left[ \frac{1 + (2m_Y/m_X)\sin^2 \theta}{1 + (2m_Y^*/m_X^*)\sin^2 \theta} \right]^2 \tau_{abab} \quad (8.44)$$

where  $A, B$ , and  $C$  are the rotational constants; the asterisk refers to the isotopically substituted molecule. It can be noted that for the isotope  $X^*Y_2$ , where  $X$  is on the  $C_2$  symmetry axis ( $\alpha$ ), the corresponding moment of inertia is unchanged, and hence the corresponding  $\tau_{aaaa}$  is unchanged. An even simpler isotopic relation follows from (8.40) for  $\tau_{abab}$ . Isotopic relations for the  $\tau$  constants

of various type molecules have been given [40, 41], as well as relations for the  $P^6$  constants of tetrahedral  $XY_4$  molecules [42].

From an examination of the extremal properties of  $\tau_{xxxx}$  and  $\tau_{x\beta x\beta}$ , it has been shown that these constants are always negative [43]. Simple empirical [44] and theoretical [45] relationships between the distortion constants  $\tau_{xxxx}$  and the rotational constants  $B_z$  have been discussed to obtain order-of-magnitude estimates of the distortion constants. Relations for the upper and lower limits of  $\tau_{xxxx}$ ,  $\tau_{xx\beta\beta}$ , and  $\tau_{x\beta x\beta}$  have been developed [43, 46, 47] that are determined from the values of the rotational constants and the lowest and highest frequency vibration.

The relation for  $(-\tau_{xxxx})_{\max} = 16B_z^3/\omega_{\min}^2$  is particularly simple, and interchanging  $\max \leftrightarrow \min$  gives the lower bound,  $(-\tau_{xxxx})_{\min}$ . These relations may be employed to calculate an approximate value of a constant which can help in deciding whether such a constant should be included in the distortion Hamiltonian or whether the observed constant is consistent with the observed vibrational frequencies. Bounds for the spectroscopic constants  $D_J$ ,  $D_{JK}$ ,  $D_K$  for symmetric tops [46, 47] and  $\Delta_J$ ,  $\Delta_{JK}$ , and so on, for asymmetric tops [47] have been discussed. From these results it may be concluded that  $D_J$  is positive and  $D_{JK}$ ,  $D_K$  may be positive or negative. For a planar symmetric top  $D_{JK}$  and  $D_K$  are negative and positive, respectively. The linear combinations  $(\Delta_J + 2\delta_J)$ ,  $(\Delta_J - 2\delta_J)$ , and  $(\Delta_J + \Delta_{JK} + \Delta_K)$  are necessarily positive. For linear triatomic molecules, the experimental values of  $D_J$  are very close to their upper limits and thus are not very useful as supplemental data for force constant evaluations. In this regard, a very simple formula for  $D_J$ , applicable to a triatomic molecule with a very low stretching frequency, has been obtained [48]. This is particularly useful for linear van der Waals molecules. For nonlinear triatomic molecules, however, the experimental values are not close to their upper limits and hence are useful in force field evaluations, as has been found. The fact that the lower frequency vibrational modes are primarily responsible for the centrifugal distortion effects has been used to give information on the skeletal motions of some molecules of moderate size [49].

### 3 FIRST-ORDER PERTURBATION TREATMENT OF ROTATIONAL DISTORTION

Taking the quantum mechanical Hamiltonian for a semirigid rotor in the form of (8.10) and choosing the principal axes system for the rigid rotor problem, we may express the Hamiltonian as

$$\mathcal{H}' = \mathcal{H}'_r + \mathcal{H}'_d \quad (8.45)$$

$$\mathcal{H}'_r = A'P_z^2 + B'P_x^2 + C'P_y^2 \quad (8.46)$$

$$\mathcal{H}'_d = \frac{\hbar^4}{4} \sum_{\alpha, \beta, \gamma, \delta} \tau_{\alpha\beta\gamma\delta} P_\alpha P_\beta P_\gamma P_\delta \quad (8.47)$$

with the angular momentum in units of  $\hbar$ , with  $\alpha, \beta, \gamma, \delta = x, y, \text{ or } z$ , and with  $A' = \hbar^2/2I_z$ , and so on. As mentioned previously, a rigorous treatment of the problem indicates that the rotation and distortion constants in the foregoing Hamiltonian must be regarded as effective constants and thus dependent on the vibrational state. The effects of centrifugal distortion on the rotational spectra will depend on both the constants  $\tau_{\alpha\beta\gamma\delta}$  and the angular momentum operators. A simple closed-form expression for the effect of these operators, like that obtained for a symmetric rotor, cannot be obtained for an asymmetric rotor. However, the distortion effects for a large number of asymmetric rotors may be treated to a good approximation by first-order perturbation theory. Furthermore, the first-order energy expression is particularly convenient for analysis of the rotational spectrum for the distortion constants, since these constants enter linearly into the energy expression. A first-order treatment of centrifugal distortion has been discussed by Kivelson and Wilson [50] and more recently by Watson [51]. The first-order perturbation treatment will involve averaging the perturbing operator  $\mathcal{H}'_d$  over the wave functions associated with  $\mathcal{H}'_r$ , that is, the asymmetric rigid rotor wave functions. The first-order distortion energy for a particular level  $J_\tau$  is then

$$E_d = \langle \mathcal{H}'_d \rangle = (J, \tau | \mathcal{H}'_d | J, \tau) \quad (8.48)$$

In the following discussion it will be seen that by consideration of only a first-order approximation, or molecules with particular symmetry, the general distortion Hamiltonian, (8.47), may be greatly simplified. In Section 4, order-of-magnitude arguments are used to provide a more general simplified Hamiltonian.

As noted before, an important quantum mechanical property of angular momentum components is that they do not commute. When the total angular momentum is referred to axes fixed in the molecule ( $x, y, z$ ), the following commutation rules are found to exist:

$$\begin{aligned} P_x P_y - P_y P_x &= -i P_z \\ P_y P_z - P_z P_y &= -i P_x \\ P_z P_x - P_x P_z &= -i P_y \end{aligned} \quad (8.49)$$

where  $P_\alpha$  is in units of  $\hbar$ . Except for the sign change on the right-hand side of the equations, these are similar to the set of commutation rules that apply for the components of the angular momentum resolved along the space-fixed (nonrotating) axes ( $X, Y, Z$ ). Because of the noncommuting character of the angular momentum components  $P_\alpha$ , there is a total of 81 terms in the sum of (8.47). However, from (8.20) it is seen that many distortion constants are equivalent, and we have, in fact,

$$\tau_{\alpha\beta\gamma\delta} = \tau_{\alpha\beta\delta\gamma} = \tau_{\beta\alpha\delta\gamma} = \tau_{\beta\alpha\gamma\delta} = \tau_{\gamma\delta\alpha\beta} = \tau_{\gamma\delta\beta\alpha} = \tau_{\delta\gamma\beta\alpha} = \tau_{\delta\gamma\alpha\beta} \quad (8.50)$$

Furthermore, many of the terms will not contribute to first-order. The rigid asymmetric rotor wave functions are classified according to the Four-group  $V$ , and hence if the integral (8.48) is to be nonvanishing, the product of the

angular momentum components must be invariant to the symmetry operations of the group, that is, belong to the totally symmetric species  $A$ . The transformation properties of  $P_x$ ,  $P_y$ ,  $P_z$  have already been given (see Chapter VII, Section 2), and we may summarize the results by saying that under the group  $V$ ,  $P_a$  transforms according to  $B_a$ ,  $P_b$  according to  $B_b$ , and  $P_c$  according to  $B_c$ . The symmetry of a given angular momentum term will be given by the direct product of the symmetries of the individual members of the term. It follows, therefore, that all terms involving odd powers of any angular momentum component will not contribute to first-order because such terms will belong to one of the  $B$  symmetry species and their average values will vanish. Thus, for any asymmetric top only 21 constants (many of which are equal to each other) will contribute to a first-order approximation. Moreover, when the symmetry of the molecule is taken into account ( $\mathcal{H}'$  and thus  $\mathcal{H}'_d$  must be invariant under the symmetry operations of the molecular point group), it is found that the distortion constants of these odd-power terms must vanish identically for molecules of orthorhombic symmetry [52, 53]. Orthorhombic symmetry includes molecules belonging to either the  $C_{2v}$ ,  $V_h$ , or  $V$  point groups. The eight asymmetric rotor point groups are summarized in Table 8.4. Noting that  $P_\alpha$  transforms as the corresponding rotation  $R_\alpha$  of the point group, and carrying out the symmetry operations of the group on  $P_\alpha P_\beta P_\gamma P_\delta$ , Parker [53] found that the nonvanishing  $\tau_{\alpha\beta\gamma\delta}$  are as given in Table 8.4. All other terms are antisymmetric under one or more symmetry operations of the particular group. As a consequence, for molecules of orthorhombic symmetry there are only 21 nonvanishing coefficients in  $\mathcal{H}'_d$  to any approximation; since many of these constants are equal, one is left finally with only nine different quartic distortion constants:

$$\tau_{\alpha\alpha\alpha\alpha} = \tau_{\alpha\alpha\beta\beta} = \tau_{\beta\beta\alpha\alpha} = \tau_{\alpha\beta\alpha\beta} = \tau_{\alpha\beta\beta\alpha} = \tau_{\beta\alpha\beta\alpha} = \tau_{\beta\alpha\alpha\beta} \quad (\alpha, \beta = x, y, \text{ or } z) \quad (8.51)$$

with  $\alpha \neq \beta$ . Therefore, the various surviving  $P_\alpha P_\beta P_\gamma P_\delta$  terms of  $\mathcal{H}'_d$  may be arranged into nine groups, each of which has the same  $\tau$  coefficient.

A further reduction of the distortion Hamiltonian to six groups of terms is still possible by an appeal to the commutation rules. By means of the commutation rules, (8.49), the following relations may be derived [48]:

$$(P_\alpha P_\beta + P_\beta P_\alpha)^2 = 2(P_\alpha^2 P_\beta^2 + P_\beta^2 P_\alpha^2) + 3P_\gamma^2 - 2P_\alpha^2 - 2P_\beta^2 \quad (8.52)$$

here  $\alpha \neq \beta \neq \gamma$  and with  $\alpha, \beta, \gamma$  to be taken in cyclic order. Note that since  $P_\alpha P_\beta$  do not commute, there will be four different  $P^4$  terms when the left-hand side is multiplied out. From these three relations, further simplification results, since one can eliminate the  $\tau_{\alpha\beta\alpha\beta}(P_\alpha P_\beta + P_\beta P_\alpha)^2$  terms of  $\mathcal{H}'_d$ . As a result of this simplification, the coefficients  $\tau_{\alpha\beta\alpha\beta}$  are folded into those of  $(P_\alpha^2 P_\beta^2 + P_\beta^2 P_\alpha^2)$ , and terms in  $P_\alpha^2$ ,  $P_\beta^2$ , and  $P_\gamma^2$  are introduced which can be absorbed into the rigid rotor part of the Hamiltonian  $\mathcal{H}_r'$ , thus giving a new definition to the rotational constants. This procedure leads to the following form of the Hamiltonian

$$\mathcal{H} = \mathcal{H}_r + \mathcal{H}_d \quad (8.53)$$

**Table 8.4** Asymmetric-Rotator Point Groups and Nonvanishing  $\tau$  Constants<sup>a</sup>

Crystallographic Nomenclature	Group Symbol	Group Operations Other Than Identity Operation	Sets with Nonzero Distortion Constants <sup>b</sup>
Triclinic	$C_1$	None	$I_1, I_2, II_1, II_2$
	$C_i = S_2$	$i$	$I_1, I_2, II_1, II_2$
Monoclinic	$C_S = C_{1h}$	$\sigma, \begin{array}{l} (a) \sigma(xy) \\ (b) \sigma(yz) \\ (c) \sigma(zx) \end{array}$	$I_1, I_2$
	$C_2$	$C_2, \begin{array}{l} (a) C_2(z) \\ (b) C_2(x) \\ (c) C_2(y) \end{array}$	$I_1, I_2$
	$C_{2h}$	$C_2, \sigma_h, i, \begin{array}{l} (a) C_2(z), \sigma(xy) \\ (b) C_2(x), \sigma(yz) \\ (c) C_2(y), \sigma(zx) \end{array}$	$I_1, I_2$
Orthorhombic	$C_{2v}$	$C_2, \text{two } \sigma_v,$	$I_1$
	$V = D_2$	three mutually $\perp C_2$	$I_1$
	$V_h = D_{2h}$	$\begin{cases} \text{three mutually } \perp C_2, i, \\ \text{three mutually } \perp \sigma, \end{cases}$	$I_1$
<i>Nonvanishing <math>\tau_{\alpha\beta\gamma\delta}</math></i>			<i>Set</i>
1	$\tau_{xxxx}$		
2	$\tau_{yyyy}$		
3	$\tau_{zzzz}$		
4	$\tau_{yyzz} = \tau_{zzyy}$		
5	$\tau_{zzxx} = \tau_{xxzz}$		$I_1$
6	$\tau_{xyyy} = \tau_{yyxx}$		
7	$\tau_{yzyz} = \tau_{zyzy} = \tau_{yzyy} = \tau_{zyyz}$		
8	$\tau_{zxzx} = \tau_{xzxz} = \tau_{zxzx} = \tau_{xzzx}$		
9	$\tau_{xyxy} = \tau_{yxxy} = \tau_{xyyy} = \tau_{yxyx}$		
10	$\tau_{xxxy} = \tau_{xxyx} = \tau_{xyxx} = \tau_{yxxx}$		
11	$\tau_{yyxy} = \tau_{yyxy} = \tau_{yxyy} = \tau_{xyyy}$		$I_2$
12	$\tau_{xyzx} = \tau_{yxzz} = \tau_{zzyx} = \tau_{zzyz}$		
13	$\tau_{xzyy} = \tau_{yzzx} = \tau_{zxyz} = \tau_{zyxz} = \tau_{zxyz} = \tau_{zyzx} = \tau_{xzyz} = \tau_{yzxz}$		
14	$\tau_{yyyz} = \tau_{yyzy} = \tau_{yzyy} = \tau_{zyyy}$		
15	$\tau_{zzzy} = \tau_{zzyz} = \tau_{zyzz} = \tau_{zyzz}$		
16	$\tau_{yzxx} = \tau_{zyxx} = \tau_{xxyz} = \tau_{xxzy}$		$II_1$
17	$\tau_{yxzx} = \tau_{zxxxy} = \tau_{xyzx} = \tau_{xzyx} = \tau_{xyxz} = \tau_{xzxy} = \tau_{yxzx} = \tau_{zxyx}$		
18	$\tau_{xxxx} = \tau_{xxzx} = \tau_{xzxz} = \tau_{zxxx}$		
19	$\tau_{zzzx} = \tau_{zzxz} = \tau_{zxzx} = \tau_{xzzz}$		
20	$\tau_{zxyy} = \tau_{xzyy} = \tau_{yyzx} = \tau_{yxyz}$		$II_2$
21	$\tau_{zyyx} = \tau_{xyyz} = \tau_{yzyy} = \tau_{yzyx} = \tau_{yzyx} = \tau_{yxyz} = \tau_{zyxy} = \tau_{xyzy}$		

<sup>a</sup>From Parker [53].

<sup>b</sup>Corresponding angular momentum operators of Set I may have nonvanishing matrix elements in a symmetric rotor basis of the type  $(K|K)$ ,  $(K|K \pm 2)$ ,  $(K|K \pm 4)$ ; whereas Set II operators may have nonvanishing elements of the type  $(K|K \pm 1)$  and  $(K|K \pm 3)$  only.

$$\mathcal{H}_r = AP_z^2 + BP_x^2 + CP_y^2 \quad (8.54)$$

$$\mathcal{H}_d = \frac{1}{4} \sum_{\alpha, \beta} \tau'_{\alpha\alpha\beta\beta} P_\alpha^2 P_\beta^2 \quad (8.55)$$

This Hamiltonian is applicable for molecules with orthorhombic symmetry or for any molecule to a first order of approximation. The relations between the old and new coefficients are given in Table 8.5. From the table we see that the corrected rotational constants  $A$ ,  $B$ , and  $C$  depend on the distortion constants. This introduces another ambiguity into the definition of the moments of inertia in addition to that arising from the vibrational effects. If the distortion constants are not known, with the result that  $A'$ ,  $B'$ ,  $C'$  cannot be obtained, additional uncertainty is transmitted to the derived structural parameters although this effect is very small.

The first-order distortion energy may now be written from (8.55) in the following form

$$E_d = \frac{1}{8} \sum_{\alpha, \beta} \tau'_{\alpha\alpha\beta\beta} \langle P_\alpha^2 P_\beta^2 + P_\beta^2 P_\alpha^2 \rangle \quad (\alpha, \beta = x, y, \text{ or } z) \quad (8.56)$$

with  $\tau'_{\alpha\alpha\beta\beta} = \tau'_{\beta\beta\alpha\alpha}$  and with  $\langle P_\alpha^2 P_\beta^2 + P_\beta^2 P_\alpha^2 \rangle$  as the average value of the appropriate operators. To proceed further, one needs explicit expressions for the various average values appearing in the above equation. These are usually expressed in terms of  $P^2$ ,  $\langle P_z^n \rangle$  ( $n=2$  and 4), and the rigid rotor energy  $E_r$ , since the latter quantities are easily determined from the diagonalization of the rigid rotor problem. Employing the expressions for  $\mathcal{H}_r$  and  $P^2$ , one may write

$$P_x^2 = \frac{[\mathcal{H}_r - (A - C)P_z^2 - CP^2]}{(B - C)} \quad (8.57)$$

$$P_y^2 = \frac{[\mathcal{H}_r - (A - B)P_z^2 - BP^2]}{(C - B)} \quad (8.58)$$

**Table 8.5** Definition of the Coefficients in the Distortion Hamiltonian

$\tau'_{xxxx} = \hbar^4 \tau_{xxxx}$	$\tau'_{xxzz} = \hbar^4 (\tau_{xxzz} + 2\tau_{xzxz})$
$\tau'_{yyyy} = \hbar^4 \tau_{yyyy}$	$\tau'_{xxyy} = \hbar^4 (\tau_{xxyy} + 2\tau_{xyxy})$
$\tau'_{zzzz} = \hbar^4 \tau_{zzzz}$	$\tau'_{yyzz} = \hbar^4 (\tau_{yyzz} + 2\tau_{yzyz})$
$A = A' + \frac{\hbar^4}{4} (3\tau_{xyxy} - 2\tau_{xzxz} - 2\tau_{yzyz})$	
$B = B' + \frac{\hbar^4}{4} (3\tau_{yzyz} - 2\tau_{xyxy} - 2\tau_{xzxz})$	
$C = C' + \frac{\hbar^4}{4} (3\tau_{xzxz} - 2\tau_{xyxy} - 2\tau_{yzyz})$	

from which one may construct the desired average value equations noting that with  $P$  in units of  $\hbar$

$$\begin{aligned}\langle P^4 \rangle &= J^2(J+1)^2 \\ \langle \mathcal{H}_r^2 \rangle &= E_r^2 \\ \langle \mathcal{H}_r P^2 + P^2 \mathcal{H}_r \rangle &= 2E_r J(J+1) \\ \langle \mathcal{H}_r P_z^2 + P_z^2 \mathcal{H}_r \rangle &= 2E_r \langle P_z^2 \rangle \\ \langle P^2 P_z^2 + P_z^2 P^2 \rangle &= 2J(J+1) \langle P_z^2 \rangle\end{aligned}\quad (8.59)$$

The average values of these operators are evaluated in a rigid asymmetric rotor basis, the basis in which the matrix representation of  $\mathcal{H}_r$  is diagonal with diagonal elements  $E_r = \langle \mathcal{H}_r \rangle = A \langle P_z^2 \rangle + B \langle P_x^2 \rangle + C \langle P_y^2 \rangle$ . The appropriate average value equations of the quartic angular momentum terms are listed in Table 8.6. It may be pointed out that the average value equations can also be expressed as desired in terms of Ray's  $E(\kappa)$  or Wang's  $W(b_p)$  reduced energy by simple definition of  $A$ ,  $B$ ,  $C$  in the appropriate manner, that is,  $A \rightarrow 1$ ,  $B \rightarrow \kappa$ ,  $C \rightarrow -1$ ,  $E_r \rightarrow E(\kappa)$  or  $A \rightarrow 1$ ,  $B \rightarrow -b_p$ ,  $C \rightarrow b_p$ ,  $E_r \rightarrow W(b_p)$ .

Watson [51] has shown that, in addition to the five equations of (8.59), another relation may be obtained from the average over the commutation relation

$$\begin{aligned}i[\mathcal{H}_r, (P_x P_y P_z + P_z P_y P_x)] &= 2(C-B)(P_x^2 P_y^2 + P_y^2 P_x^2 + 2P_z^2) \\ &\quad + 2(A-C)(P_y^2 P_z^2 + P_z^2 P_y^2 + 2P_x^2) \\ &\quad + 2(B-A)(P_x^2 P_z^2 + P_z^2 P_x^2 + 2P_y^2)\end{aligned}\quad (8.60)$$

Here the following relations,

$$\begin{aligned}[P_\alpha^2, (P_x P_y P_z + P_z P_y P_x)] &= 2i(P_\alpha^2 P_\beta^2 + P_\beta^2 P_\alpha^2) - 2i(P_\alpha^2 P_\gamma^2 + P_\gamma^2 P_\alpha^2) \\ &\quad + 4i(P_\gamma^2 - P_\beta^2)\end{aligned}\quad (8.61)$$

(with  $\alpha, \beta, \gamma = x, y$ , or  $z$ ;  $\alpha \neq \beta \neq \gamma$ , and  $\alpha, \beta$ , and  $\gamma$  taken in cyclic order) derived from the angular momentum commutation rules, have been used to reduce the right-hand side of (8.60). Now the average value of the commutator  $\langle [\mathcal{H}, O_p] \rangle$  vanishes for any operator  $O_p$  averaged over eigenfunctions of  $\mathcal{H}$ . Therefore, the average value of the commutator on the left-hand side of (8.60) vanishes, and one obtains a relation between the average values of the quartic and quadratic angular momentum terms in the rigid rotor basis. The vanishing of such commutators has also found application to internal rotation problems [54].

By insertion of the appropriate average value equations given in Table 8.6, the following expression is attained [51]

$$\begin{aligned}E_r^2 &= (B-C)^2 \langle P_z^2 \rangle + (A-C)(C-B) \langle P_x^2 \rangle + (A-B)(B-C) \langle P_y^2 \rangle \\ &\quad + (B+C)E_r J(J+1) - BCJ^2(J+1)^2 - 2(AB+AC-2BC) \\ &\quad \times J(J+1) \langle P_z^2 \rangle - 3(A-B)(A-C) \langle P_z^4 \rangle \\ &\quad + 2(2A-B-C)E_r \langle P_z^2 \rangle\end{aligned}\quad (8.62)$$

This relation may now be used to eliminate  $E_r^2$  from the average value equations of Table 8.6 so that any given average value will at most be a function of five different terms,  $P^4$ ,  $P^2 \langle P_z^2 \rangle$ ,  $\langle P_z^4 \rangle$ ,  $P^2 E_r$ , and  $E_r \langle P_z^2 \rangle$ . As a result, the distortion

**Table 8.6** The Average Values of the Distortion Operators in the Asymmetric Rigid Rotor Basis<sup>a</sup>

---


$$\langle P_x^4 \rangle = \left( \frac{1}{B-C} \right)^2 [C^2 P^4 + 2C(A-C)P^2 \langle P_z^2 \rangle + (A-C)^2 \langle P_z^4 \rangle - 2CP^2 E_r - 2(A-C)E_r \langle P_z^2 \rangle + E_r^2]$$

$$\langle P_y^4 \rangle = \left( \frac{1}{B-C} \right)^2 [B^2 P^4 + 2B(A-B)P^2 \langle P_z^2 \rangle + (A-B)^2 \langle P_z^4 \rangle - 2BP^2 E_r - 2(A-B)E_r \langle P_z^2 \rangle + E_r^2]$$

$$\langle P_x^2 P_y^2 + P_y^2 P_x^2 \rangle = -2 \left( \frac{1}{B-C} \right)^2 [BCP^4 + (AB+AC-2BC)P^2 \langle P_z^2 \rangle + (A-B)(A-C) \langle P_z^4 \rangle - (B+C)P^2 E_r - (2A-B-C)E_r \langle P_z^2 \rangle + E_r^2]$$

$$\langle P_x^2 P_z^2 + P_z^2 P_x^2 \rangle = -2 \left( \frac{1}{B-C} \right) [CP^2 \langle P_z^2 \rangle + (A-C) \langle P_z^4 \rangle - E_r \langle P_z^2 \rangle]$$

$$\langle P_y^2 P_z^2 + P_z^2 P_y^2 \rangle = 2 \left( \frac{1}{B-C} \right) [BP^2 \langle P_z^2 \rangle + (A-B) \langle P_z^4 \rangle - E_r \langle P_z^2 \rangle]$$


---

<sup>a</sup>  $P^2 = J(J+1)$ ,  $E_r$  is the rigid rotor energy and  $\langle P_z^n \rangle$  is the average value of  $P_z^n$  in the rigid asymmetric rotor basis.

energy to first order will depend on only five combinations of the  $\tau'_{\alpha\beta\beta\beta}$ . The terms in  $\langle P_x^2 \rangle$ ,  $\langle P_y^2 \rangle$ , and  $\langle P_z^2 \rangle$  introduced by the elimination of  $E_r^2$  can be absorbed into  $E_r$ , thus resulting in a redefinition of the effective rotational constants  $A$ ,  $B$ , and  $C$ . This will not significantly affect the average values of the quartic terms, and the average values in (8.64) may be identified with the asymmetric rotor basis specified by (8.65). This produces, however, another small ambiguity in the definition of the moments of inertia, since the quantities  $A'$ ,  $B'$ , and  $C'$  should define the effective moments of inertia, whereas those of (8.65) are determined in practice.

By use then of (8.62) and Table 8.6 and by insertion of the average values in (8.56) followed by collection of terms and considerable manipulation, one arrives at the following first-order expression for the energy of a semirigid asymmetric rotor [50, 51]

$$E = E_r + E_d \quad (8.63)$$

$$E_d = -d_J J^2 (J+1)^2 - d_{JK} J(J+1) \langle P_z^2 \rangle - d_K \langle P_z^4 \rangle - d_{EJ} E_r J(J+1) - d_{EK} E_r \langle P_z^2 \rangle \quad (8.64)$$

Here  $E_r$  is the energy of a rigid rotor with the following rotational constants

$$\mathcal{A} = A + 16R_6$$

$$\mathcal{B} = B - \frac{16R_6(A-C)}{B-C}$$

$$\mathcal{C} = C + \frac{16R_6(A-B)}{B-C} \quad (8.65)$$

The  $d$  coefficients of Watson [51] are defined in Table 8.7 in terms of the  $D$ 's,  $R$ 's, and  $\delta_J$  used by Kivelson and Wilson [50]. These latter constants are linear combinations of the  $\tau$ 's and are also defined in Table 8.7. Equation (8.61) could equally well have been used for elimination of  $\langle P_z^4 \rangle$  rather than  $E_r^2$ . The calculation of  $\langle P_z^4 \rangle$  could therefore be avoided, but the analogy with the symmetric top would be lost. The energy expression obtained by elimination of  $\langle P_z^4 \rangle$  may be found elsewhere [55]. By application of (8.60) it is possible to express the average values of the quartic terms,  $\langle P_z^2 P_\beta^2 \rangle = \langle P_\beta^2 P_z^2 \rangle$ , in terms of the average values of the quadratic terms,  $\langle P_z^2 \rangle$ . The detailed expressions are given elsewhere [55]. Results for the  $d$  coefficients of some asymmetric rotors are collected in Table 8.8.

It has been found [56–58] in studies of a number of nonplanar molecules with the first-order expression, (8.63), that there is high correlation between  $d_K$  and  $d_{EK}$  and between  $d_{JK}$  and  $d_{EK}$ . Also, for  $\kappa < -0.97$ , the normal equations become highly ill-conditioned (see Section 4). Equation 8.64 can be written in a more suitable form involving the  $\Delta$  coefficients to be introduced later. In particular, elimination of  $E_r$  from (8.64) by means of the relations

$$\mathcal{H}_r = \frac{1}{2}(\mathcal{B} + \mathcal{C})J(J+1) + [\mathcal{A} - \frac{1}{2}(\mathcal{B} + \mathcal{C})]P_z^2 + \frac{1}{2}(\mathcal{B} - \mathcal{C})(P_x^2 - P_y^2) \quad (8.66)$$

and

$$\langle \mathcal{H}_r P_z^2 + P_z^2 \mathcal{H}_r \rangle = 2E_r \langle P_z^2 \rangle, \langle \mathcal{H}_r \rangle = E_r \quad (8.67)$$

**Table 8.7** Distortion Coefficients of the First-Order Energy Expression

---

$d_J = D_J - \frac{2\delta_J(B+C)}{B-C} - 2R_6$
$d_{JK} = D_{JK} - 2\sigma\delta_J + 4(R_5 + 2\sigma R_6) \frac{B+C}{B-C} + 12R_6$
$d_K = D_K + 4\sigma(R_5 + 2\sigma R_6) - 10R_6$
$d_{EJ} = \frac{4\delta_J}{B-C}$
$d_{EK} = \frac{-8(R_5 + 2\sigma R_6)}{B-C}$
$\sigma = \frac{2A - B - C}{B - C}$
$D_J = -\frac{1}{32}\{3\tau_{xxxx} + 3\tau_{yyyy} + 2(\tau_{xxyy} + 2\tau_{xyxy})\}\hbar^4$
$D_K = D_J - \frac{1}{4}\{\tau_{zzzz} - (\tau_{xxzz} + 2\tau_{xzxz}) - (\tau_{yyzz} + 2\tau_{yzyz})\}\hbar^4$
$D_{JK} = -D_J - D_K - \frac{1}{4}\tau_{zzzz}\hbar^4$
$R_5 = -\frac{1}{32}\{\tau_{xxxx} - \tau_{yyyy} - 2(\tau_{xxzz} + 2\tau_{xzxz}) + 2(\tau_{yyzz} + 2\tau_{yzyz})\}\hbar^4$
$R_6 = \frac{1}{64}\{\tau_{xxxx} + \tau_{yyyy} - 2(\tau_{xxyy} + 2\tau_{xyxy})\}\hbar^4$
$\delta_J = -\frac{1}{16}\{\tau_{xxxx} - \tau_{yyyy}\}\hbar^4$

---

**Table 8.8** Rotational and Centrifugal Distortion Constants (*d* Coefficients) of Some Asymmetric Rotors (MHz)<sup>a</sup>

Molecule	<i>A</i>	<i>B</i>	<i>C</i>	<i>d<sub>J</sub></i>	<i>d<sub>JK</sub></i>	<i>d<sub>K</sub></i>	<i>d<sub>EJ</sub></i> ( $\times 10^6$ )	<i>d<sub>EK</sub></i> ( $\times 10^6$ )	Ref.
(CH <sub>3</sub> ) <sub>2</sub> SO	7,036.49	6,910.93	4,218.78	0.043	10.550	-4.172	-5.20	-1517	<i>d</i>
(CH <sub>3</sub> ) <sub>2</sub> S <sup>c</sup>	17,809.73	7,621.10	5,717.77	-0.03158	-0.1503	0.058	5.943	7.280	<i>d</i>
CH <sub>2</sub> (OH)CHO <sup>b</sup>	18,446.41	6,525.04	4,969.27	-0.02714	-0.0732	0.0883	5.648	-3.40	<i>e</i>
CH <sub>2</sub> FCONH <sub>2</sub> <sup>c</sup>	9,884.36	4,059.67	2,932.47	-0.00206	-0.0312	-0.0507	0.801	8.41	<i>f</i>
1, 3 Dioxane <sup>b</sup>	4,999.93	4,807.61	2,757.11	0.00198	-0.2088	0.09118	-0.1839	42.21	<i>g</i>
Pyridine	6,029.28	5,804.95	2,959.25	0.00367	0.1738	-0.0868	-0.22	-29.87	<i>h</i>
3-Fluorophenol <sup>c</sup>	3,748.49	1,797.71	1,215.05	0.00023	-0.0110	-0.0150	-0.20	7.2	<i>i</i>
trans-CH <sub>3</sub> CHCH <sub>2</sub> NH <sup>c</sup>	16,892.44	6,533.61	5,761.30	-0.00457	0.020	0.020	1.228	-5.0	<i>j</i>
CH <sub>3</sub> SCl	17,341.83	4,603.78	3,719.10	-0.01167	-0.2087	-0.3692	3.468	37.23	<i>k</i>
HBF <sub>2</sub> <sup>c</sup>	52,896.09	10,498.29	8,740.46	-0.0386	-1.134	-2.96	4.91	89.5	<i>l</i>
N <sub>2</sub> F <sub>4</sub>	5,576.19	3,189.42	2,813.16	-0.01389	-0.2566	-0.2087	4.7984	81.164	<i>m</i>

<sup>a</sup>Note constants *d<sub>EJ</sub>* and *d<sub>EK</sub>* are dimensionless.

<sup>b</sup>III' representation.

<sup>c</sup>I' representation.

<sup>d</sup>H. Dreizler, *Z. Naturforsch.*, **21a**, 1719 (1966).

<sup>e</sup>K. M. Marstokk and H. Møllendal, *J. Mol. Struct.*, **5**, 205 (1970).

<sup>f</sup>K. M. Marstokk and H. Møllendal, *J. Mol. Struct.*, **22**, 287 (1974).

<sup>g</sup>R. S. Lowe and R. Kewley, *J. Mol. Spectrosc.*, **60**, 312 (1976).

<sup>h</sup>R. R. Filgueira, A. C. Fantoni, and L. M. Boggia, *J. Mol. Spectrosc.*, **78**, 175 (1979).

<sup>i</sup>A. I. Jaman, R. N. Nandi, and D. K. Ghosh, *J. Mol. Spectrosc.*, **86**, 269 (1981).

<sup>j</sup>C. F. Su and E. B. Beason, *J. Chem. Phys.*, **59**, 759 (1973).

<sup>k</sup>A. Guarnieri, *Z. Naturforsch.*, **25a**, 18 (1970).

<sup>l</sup>T. Kasuya, W. J. Lafferty, and D. R. Lide, *J. Chem. Phys.*, **48**, 1 (1968).

<sup>m</sup>V. K. Kaushik and P. Venkateswarlu, *Chem. Phys. Lett.*, **46**, 426 (1977).

**Table 8.9** Relations Between the  $d$ - and  $\Delta$  Distortion Coefficients<sup>a</sup>

---

$d_J = \Delta_J - \frac{2\delta_J(\mathcal{B} + \mathcal{C})}{\mathcal{B} - \mathcal{C}}$
$d_{JK} = \Delta_{JK} - \frac{2\delta_K(\mathcal{B} + \mathcal{C})}{\mathcal{B} - \mathcal{C}} - \frac{2\delta_J(2\mathcal{A} - \mathcal{B} - \mathcal{C})}{\mathcal{B} - \mathcal{C}}$
$d_K = \Delta_K - \frac{2\delta_K(2\mathcal{A} - \mathcal{B} - \mathcal{C})}{\mathcal{B} - \mathcal{C}}$
$d_{EJ} = \frac{4\delta_J}{\mathcal{B} - \mathcal{C}}$
$d_{EK} = \frac{4\delta_K}{\mathcal{B} - \mathcal{C}}$

---

<sup>a</sup>Here  $(x, y, z) \equiv (b, c, a)$ , alternate choices made by reidentification of  $\mathcal{A}, \mathcal{B}, \mathcal{C}$ .

yields

$$E_d = -\Delta_J J^2(J+1)^2 - \Delta_{JK} J(J+1)\langle P_z^2 \rangle - \Delta_K \langle P_z^4 \rangle - 2\delta_J J(J+1)\langle P_x^2 - P_y^2 \rangle - \delta_K \langle P_z^2(P_x^2 - P_y^2) + (P_x^2 - P_y^2)P_z^2 \rangle \quad (8.68)$$

The relations between the  $d$ - and  $\Delta$  coefficients are given in Table 8.9. In the present discussion we have used an  $I'$  representation ( $x \rightarrow b, y \rightarrow c, z \rightarrow a$ ) for  $\mathcal{H}_r$ . Alternate choices are readily obtained by reidentification of  $\mathcal{A}, \mathcal{B}, \mathcal{C}$ .

### Simplifications for Planar Asymmetric Rotors and Symmetric Tops

For planar asymmetric rotor molecules, significant simplification results, as is shown by Dowling [59]. For a planar, prolate-type rotor, the unique symmetric-top axis  $z$  will lie in the plane of the molecule, whereas for an oblate top the limiting symmetric-top axis will be perpendicular to this plane. For purposes of discussion, assume that the molecule lies in the  $xz$  plane. Then if  $\alpha$  or  $\beta$  is  $y$  in (8.24), all the  $J_{\alpha\beta}^{(i)}$ 's will be zero since all the  $y_l$  coordinates of the atoms are zero at equilibrium. Therefore it follows from (8.20) that  $\tau_{xyxy} = \tau_{zyyz} = 0$ . Similarly, (8.23) yields  $J_{xx}^{(i)} + J_{zz}^{(i)} = J_{yy}^{(i)}$  when all  $y_l$  coordinates are set equal to zero. This relation in conjunction with (8.20) provides three relations among the  $\tau$ 's. The relations summarized in Table 8.10 are appropriate for both prolate, type  $I'$ , and oblate, type  $III'$ , cases. These relations can be used to reduce the number of independent  $\tau$ 's to only four, for example,  $\tau_{xxxx}, \tau_{zzzz}, \tau_{xxzz}$ , and  $\tau_{xzxz}$ . In this particular case the first-order energy expression can be written in terms of four  $\tau$ 's. The coefficients of the four  $\tau$ 's in the energy expression can be easily found by use of the average values of Table 8.6 and the relations of Table 8.10 in conjunction with (8.56). Evaluation of the four  $\tau$ 's from the

**Table 8.10** Distortion Constant Relationships for Planar Asymmetric Rotor Molecules<sup>a</sup>

---


$$\begin{aligned}\tau_{bcbc} &= \tau_{acac} = 0 \\ \tau_{cccc} &= \left(\frac{C}{A}\right)^4 \tau_{aaaa} + 2 \frac{C^4}{A^2 B^2} \tau_{aabb} + \left(\frac{C}{B}\right)^4 \tau_{bbbb} \\ \tau_{bbcc} &= \left(\frac{C}{B}\right)^2 \tau_{bbbb} + \left(\frac{C}{A}\right)^2 \tau_{aabb} \\ \tau_{aacc} &= \left(\frac{C}{A}\right)^2 \tau_{aaaa} + \left(\frac{C}{B}\right)^2 \tau_{aabb}\end{aligned}$$


---

<sup>a</sup>The coordinate axes are to be assigned  $a \leftrightarrow z$ ,  $b \leftrightarrow x$ ,  $c \leftrightarrow y$  for the prolate case and  $a \leftrightarrow y$ ,  $b \leftrightarrow x$ , and  $c \leftrightarrow z$  in the oblate case; in each case the molecule lies in the  $ab$  plane.

**Table 8.11** Rotational Distortion Constants for Molecules of  $C_{3v}$  Symmetry<sup>a</sup>

---

*Nonvanishing τ's*

$$\begin{array}{ll} \tau_{xxxx} = \tau_{yyyy} & \tau_{zzzz} \\ \tau_{xxzz} = \tau_{yyzz} & \tau_{xxyy} = \tau_{xxxx} - 2\tau_{xyxy} \\ \tau_{xzzz} = \tau_{yyzz} & \tau_{yyyy} = -\tau_{xyzx} = -\tau_{xxyz}^b \end{array}$$

*Distortion Coefficients*

$$D_J = -\frac{\hbar^4}{4} \tau_{xxxx} \quad D_{JK} = -2D_J - \frac{\hbar^4}{2} \{\tau_{xxzz} + 2\tau_{xzzz}\}$$

$$D_K = -D_J - D_{JK} - \frac{\hbar^4}{4} \tau_{zzzz}$$


---

<sup>a</sup> $y$  axis lies in a symmetry plane with  $I_{xx}^c = I_{yy}^c$ ,  $R_5 = R_6 = \delta_J = 0$ . The symmetry axis is  $z$ .

<sup>b</sup>Do not contribute in a first-order approximation.

spectrum and use of the relations allows direct evaluation of the seven individual  $\tau$ 's. The rotational constants to be used in the relations of Table 8.10 should be the equilibrium rotational constants, but in practice these usually must be replaced by the effective rotational constants. Also, if the harmonic approximation is not adequate, then the relations are not strictly correct.

For a  $C_{pv}$  ( $p \neq 4$ ) symmetric rotor,  $R_5$ ,  $R_6$ , and  $\delta_J$  are identically zero while the factors multiplying these constants remain finite in this limit. Furthermore,  $\langle P_z^2 \rangle = K^2$  and  $\langle P_z^4 \rangle = K^4$  and hence the first-order (8.64) will reduce to that given previously for a symmetric rotor. For molecules with  $C_{3v}$  symmetry,

**Table 8.12** Distortion Coefficients for Planar Symmetric Rotors<sup>a</sup>


---

$D_J = -\frac{\hbar^4}{4} \tau_{xxxx}$	$D_K = -\frac{\hbar^4}{4} \{ \tau_{xxxx} - 3\tau_{zzzz} \}$
$D_{JK} = \frac{\hbar^4}{2} \{ \tau_{xxxx} - 2\tau_{zzzz} \}$	$D_{JK} = -\frac{2}{3} (D_J + 2D_K)$

---

<sup>a</sup>The  $z$  axis is taken as the symmetry axis that is perpendicular to the plane of the molecule.

symmetric rotors, direct calculation [60] or group theoretical considerations [21] lead to the nonvanishing  $\tau$ 's listed in Table 8.11, and the explicit definitions of  $D_J$ ,  $D_K$ , and  $D_{JK}$  in terms of the  $\tau$ 's can be simplified [25]. These results are also included in Table 8.11. For planar symmetric rotors (oblate tops) additional relations exist between the  $\tau$ 's, with further simplification of the distortion coefficients [59]. These are given in Table 8.12. For this case it is evident that if any two distortion constants are determined, the remaining one may be immediately evaluated.

#### 4 REDUCED HAMILTONIAN

From (8.64) it is apparent that no more than five linear combinations of the nine possible  $\tau$ 's can be obtained from an analysis of the rotational spectrum of an asymmetric rotor. It might appear from (8.56) and Table 8.6 that six linear combinations of  $\tau$ 's could be determined from the observed spectrum; because of the linear relation (8.62), however, the resulting energy level equation would have an inherent indeterminacy and would thus not be satisfactory for evaluation of unique values of the distortion constants, although it would be applicable to calculation of the distortion effects with known constants. In (8.64) this indeterminacy has been removed by application of (8.62), leaving five determinable distortion coefficients. Such a problem does not arise for planar molecules when the planarity conditions (see the previous section) are applied, since this effectively removes the indeterminacy resulting from the linear relation between the average values. Most early analysis of centrifugal distortion employed the planar relations and thus avoided the problem. This indeterminacy was first reported by Dreizler, Dendl, and Rudolph [61, 62] in their analysis of dimethylsulfoxide and dimethylsulfide for six quartic distortion constants. They found the least-squares equations to be quite ill-conditioned, and determinate values for the constants could not be obtained.

This is an example of a more general problem that can arise when one attempts to evaluate parameters in any Hamiltonian from the corresponding eigenvalues. The eigenvalues may depend on only certain linear combinations of the parameters. To properly fit the experimental data, one must employ a

Hamiltonian that has any experimentally indeterminable parameters removed from it. This Hamiltonian, which may be obtained by a contact transformation, is termed a "reduced Hamiltonian." The reduced Hamiltonian is to be used to fit experimental data. On the other hand, to interpret the quantities in terms of fundamental molecular parameters, the experimentally determined coefficients must be related to the constants in the original "first-principles Hamiltonian." These relations are, of course, specified by the contact transformation which relates the two Hamiltonians.

The nature of the problem can be readily appreciated by consideration of the rigid rotor Hamiltonian. For a general asymmetric top only three principal moments of inertia can be obtained from the eigenvalues of  $\mathcal{H}_r$ . For an arbitrary orientation of the molecule-fixed axis, however, the rotational Hamiltonian contains six terms corresponding to six elements of the inertia tensor; see (2.6). But, by application of a unitary transformation a particular axis orientation can be selected for which the inertia tensor has a diagonal form;  $\tilde{\mathcal{H}}$ , then depends on only three independent constants, the three principal moments of inertia, and it is these parameters that can be evaluated from the observed spectrum.

A unitary operator ( $U^{-1} = U^\dagger$ ) can be conveniently written as

$$U = e^{iS} \quad (8.69)$$

where  $S$  is Hermitian. The transformed Hamiltonian is given by

$$\tilde{\mathcal{H}} = U^{-1} \mathcal{H} U \quad (8.70)$$

The result of applying the appropriate transformation is that the form and eigenvalues of  $\tilde{\mathcal{H}}$  are unchanged from  $\mathcal{H}$ , but the individual coefficients are altered. This fact, along with order of magnitude arguments, have been used by Watson in a series of papers [55, 63, 64] to obtain the reduced Hamiltonian. Since the eigenvalues must remain the same, only those linear combinations of coefficients which remain invariant to the transformation can be evaluated from the eigenvalues, and hence are determinable coefficients.

The most general form of the rotational Hamiltonian, correct to terms in  $P^6$ , is given by

$$\mathcal{H} = \sum_{\alpha} B_{\alpha}^2 P_{\alpha}^2 + \frac{\hbar^4}{4} \sum \tau_{\alpha\beta\gamma\delta} P_{\alpha} P_{\beta} P_{\gamma} P_{\delta} + \hbar^6 \sum \tau_{\alpha\beta\gamma\delta\eta} P_{\alpha} P_{\beta} P_{\gamma} P_{\delta} P_{\varepsilon} P_{\eta} \quad (8.71)$$

where we denote the rotational constants by  $B_{\alpha} = \hbar^2 / 2I_{\alpha}$ . From our previous discussion of the  $P^4$  terms we have shown that for orthorhombic symmetry there are nine independent  $\tau_{\alpha\beta\gamma\delta}$  (Table 8.4) and that reduction of the fourth-power angular momentum terms  $P_{\alpha} P_{\beta} P_{\gamma} P_{\delta}$  of  $\mathcal{H}_d$  by means of the commutation relations yields a Hamiltonian with six terms, (8.55). Similar simplifications are possible for the  $P^6$  terms. Initially, there are a total of  $3^6 = 729$  coefficients in the  $P^6$  sum.  $\mathcal{H}$  must, however, be invariant under all symmetry operations of the point group of the molecule, and a number of coefficients in the  $P^6$  sum must vanish. Application of the group operations of the asymmetric-top point groups

to the Hamiltonian reveals that for the orthorhombic point groups ( $C_{2v}, D_2, D_{2h}$ ) a total of 183 coefficients are nonzero, for the monoclinic point groups ( $C_{1h}, C_2, C_{2h}$ ) 365 coefficients are nonzero, and for the triclinic point groups ( $C_1, C_i$ ) all 729 coefficients are nonzero. Enumeration of the  $P^6$  distortion constants,  $\tau_{\alpha\beta\gamma\delta\eta}$ , for the orthorhombic point groups has been discussed by Chung and Parker [65]. They show that, in general

$$\tau_{\alpha\beta\gamma\delta\eta} = \tau_{\eta\delta\gamma\beta\alpha} \quad (8.72)$$

The 183 coefficients are hence reduced to 105 distinct ones as follows:

1. Three coefficients of the type  $\tau_{\alpha\alpha\alpha\alpha\alpha\alpha}$ .
2. Fifty-four coefficients of the type  $\tau_{\alpha\alpha\alpha\alpha\beta\beta} (\alpha \neq \beta)$ , with the subscripts occurring in any order, taking (8.72) into account.
3. Forty-eight coefficients of the type  $\tau_{\alpha\alpha\beta\beta\gamma\gamma} (\alpha \neq \beta \neq \gamma)$ , with the subscripts occurring in any order, with (8.72) taken into account.

Because of (8.72), coefficients such as  $\tau_{xyyyxy}$  and  $\tau_{xyyyyx}$  occurring in (2) are equal, and likewise coefficients such as  $\tau_{xyyxzz}$  and  $\tau_{zzyyxx}$  occurring in (3) are equal. Compilation of all 105 distinct coefficients may be found elsewhere [65].

Reduction of the sixth-power angular momentum terms of the rotational Hamiltonian appropriate to an orthorhombic molecule by means of the commutation relations has been discussed by Kneizys et al. [66]. This reduction results in various  $P^6$  coefficients being folded into other coefficients. It is found that the Hamiltonian can be written in the form [63]

$$\begin{aligned} \mathcal{H} = & \sum_{\alpha} B_{\alpha} P_{\alpha}^2 + \sum_{\alpha, \beta} T_{\alpha\beta} P_{\alpha}^2 P_{\beta}^2 + \sum_{\alpha} \Phi_{\alpha\alpha\alpha} P_{\alpha}^6 \\ & + \sum_{\alpha \neq \beta} \Phi_{\alpha\alpha\beta} (P_{\alpha}^4 P_{\beta}^2 + P_{\beta}^2 P_{\alpha}^4) \\ & + \Phi_{xyz} (P_x^2 P_y^2 P_z^2 + P_z^2 P_y^2 P_x^2) \end{aligned} \quad (8.73)$$

where the coefficients are all real. (See also Table 8.13 for an alternate form.) The rotational constants  $B_{\alpha}$  are defined in Table 8.5, as

$$B_{\alpha} = (\hbar^2/2I_{\alpha}) + (\hbar^2/4)(3\tau_{\beta\beta\beta\gamma} - 2\tau_{\alpha\beta\alpha\beta} - 2\tau_{\alpha\gamma\alpha\gamma}), \alpha \neq \beta \neq \gamma \equiv (x, y, \text{ or } z) \quad (8.74)$$

Once a particular choice of representation has been made, the various  $B_x, B_y, B_z$  can be identified with the  $A, B, C$  in a particular order. Here an alternate notation has been adopted for the effective quartic distortion coefficients

$$T_{\alpha\alpha} = \frac{1}{4} \tau'_{\alpha\alpha\alpha\alpha} = \frac{\hbar^4}{4} \tau_{\alpha\alpha\alpha\alpha} \quad (8.75)$$

$$T_{\alpha\beta} = \frac{1}{4} \tau'_{\alpha\alpha\beta\beta} = \frac{\hbar^4}{4} (\tau_{\alpha\alpha\beta\beta} + 2\tau_{\alpha\beta\alpha\beta}), \alpha \neq \beta \quad (8.76)$$

with  $T_{\alpha\beta} = T_{\beta\alpha}$ . The 10  $\Phi_{\alpha\beta\gamma}$  coefficients are the effective sextic distortion coefficients. They are linear combinations of the various 105  $P^6$  distortion constants mentioned previously, and explicit expressions are available [66]. The

subscripts on the distortion coefficients are indicative of the angular momentum operator associated with the coefficient.

An alternate and more convenient form of the general power series of (8.71) has been introduced by Watson [55], the so-called standard form, that is,

$$\mathcal{H}_{st} = \sum_{p,q,r=0}^{\infty} h_{pqr} (P_x^p P_y^q P_z^r + P_z^r P_y^q P_x^p) \quad (8.77)$$

Any term in the general Hamiltonian, (8.71), can, by means of the commutation relations, be cast into this form at the expense of introducing terms of lower degree. There is one term for each combination of powers of  $P_x$ ,  $P_y$ ,  $P_z$ . Equation 8.55 is hence in standard form, and the fact that  $\tau_{\alpha\beta\alpha\beta}$  cannot be separated from  $\tau_{\alpha\alpha\beta\beta}$  is taken care of automatically by writing the Hamiltonian in the standard form. (Note, e.g.,  $T_{xy} = h_{220}$ .)

If one exploits the requirement that the Hamiltonian is invariant to the operation of Hermitian conjugation and time reversal [55], only terms with even values of  $n=p+q+r$  are allowed, with the corresponding coefficients  $h_{pqr}$  real. The number of terms of total degree  $n=p+q+r$  is  $\frac{1}{2}(n+1)(n+2)$ . Thus, for  $n=2, 4$ , and  $6$ , there are  $6, 15$ , and  $28$  terms, respectively. Of these terms for a given  $n$ , there are  $\frac{1}{8}(n+2)(n+4)$  terms with  $pqr=eee$  ( $e$  even) and  $\frac{1}{8}n(n+2)$  terms each with  $pqr=eoo, oeo$ , and  $ooo$  ( $o$  odd). Since the Hamiltonian must belong to the totally symmetric symmetry species of the molecular point group, one finds [55] for molecules of orthorhombic symmetry that  $p$ ,  $q$ , and  $r$  are, in addition, each required to be even in (8.77). Thus, it is clear that for  $n=2, 4$ , and  $6$ , there are in the standard form  $\frac{1}{8}(n+2)(n+4)=3, 6$ , and  $10$  terms, respectively, in agreement with (8.73).

It should be noted that the Hamiltonian (8.73) holds even for molecules of non-orthorhombic symmetry. For such molecules, additional terms such as  $ooo$  appear in the standard form, for example,  $h_{310}, h_{112}$ , and these contribute in higher order. Elements of the unitary transformation  $S_3$  ( $S_5$  for  $\mathcal{H}_d^{(6)}$ ) can, however, be chosen to eliminate such terms, and thereby to give a Hamiltonian of orthorhombic form with coefficients modified from their original values. The important changes occur in the higher-order  $P^6$  coefficients, and the modified definitions of the  $\Phi_{\alpha\beta\gamma}$  are given elsewhere [64].

The orthorhombic form of the Hamiltonian can be further reduced by means of a unitary transformation as indicated previously. The transformation is conveniently represented as two successively applied transformations

$$U = e^{iS_3} e^{iS_5} \quad (8.78)$$

where terms to  $P^6$  are to be considered. The invariant properties discussed previously show that  $S$  has a form similar to (8.77) with  $p+q+r=n$ , and  $n$  odd, viz.

$$S = \sum s_{pqr} (P_x^p P_y^q P_z^r + P_z^r P_y^q P_x^p) \quad (8.79)$$

Terms of the same degree are denoted by  $S_n$ . For molecules of orthorhombic symmetry, only the terms [55]

$$S_3 = s_{111} (P_x P_y P_z + P_z P_y P_x) \quad (8.80)$$

and

$$S_5 = s_{311}(P_x^3 P_y P_z + P_z P_y P_x^3) + s_{131}(P_x P_y^3 P_z + P_z P_y^3 P_x) \\ + s_{113}(P_x P_y P_z^3 + P_z^3 P_y P_x) \quad (8.81)$$

are required. The  $s_{pqr}$  are real coefficients and are the parameters of the unitary transformation that are to be chosen to achieve the reduction. Other terms of  $S_3$  and  $S_5$  come into play when one wishes to remove nonorthorhombic terms in (8.77) as mentioned previously. For such molecules, the terms in  $\mathcal{H}$  that are not totally symmetric in the Four-group are removed by non-totally symmetric terms in  $S$  and they appear in terms of higher degree in the Hamiltonian.

Now the order of magnitude of the terms in (8.77) may be taken approximately as

$$h_{pqr} \sim \kappa^{2(p+q+r)} E_e \quad (8.82)$$

where the rotational, vibrational, and electronic energy are related approximately by  $E_r \sim \kappa^2 E_v \sim \kappa^4 E_e (\kappa \ll 1)$ . The rigid rotor Hamiltonian is thus of order  $\kappa^4 E_e$ . Likewise, the quartic distortion Hamiltonian is of order  $\kappa^8 E_e$ , and the sextic distortion Hamiltonian is of order  $\kappa^{12} E_e$ . The  $s_{pqr}$  satisfy the order-of-magnitude relation

$$s_{pqr} \sim \kappa^{2(p+q+r-1)} \quad (8.83)$$

Thus, for example,  $s_{111}$  is of order of magnitude  $\kappa^4$ , which is on the order of the ratio of a quartic distortion coefficient to a rotational constant ( $\tau/B$ ). Expressing the exponentials in (8.70) as a power series expansion (see Appendix C) and arranging by order of magnitude, one finds

$$\tilde{\mathcal{H}} = U^{-1} \mathcal{H} U = \tilde{\mathcal{H}}_r + \tilde{\mathcal{H}}_d^{(4)} + \tilde{\mathcal{H}}_d^{(6)} \quad (8.84)$$

where

$$\tilde{\mathcal{H}}_r = \mathcal{H}_r \quad (8.85)$$

$$\tilde{\mathcal{H}}_d^{(4)} = \mathcal{H}_d^{(4)} + i[\mathcal{H}_r, S_3] \quad (8.86)$$

$$\tilde{\mathcal{H}}_d^{(6)} = \mathcal{H}_d^{(6)} + i[\mathcal{H}_r, S_5] + i[\mathcal{H}_d^{(4)}, S_3] - \frac{1}{2}[[\mathcal{H}_r, S_3], S_3] \quad (8.87)$$

which is correct to order  $\kappa^{12} E_e$ , where  $[A, B]$  is the commutator  $AB - BA$ . Note, for example, that  $\mathcal{H}_d^{(4)}$  and  $[\mathcal{H}_r, S_3]$  are both of order  $\kappa^8 E_e$ . Here  $s_{111}$  specifies the reduction of  $\mathcal{H}_d^{(4)}$ , whereas  $s_{311}, s_{131}$ , and  $s_{113}$  specify the reduction of  $\mathcal{H}_d^{(6)}$ . Once a choice of the  $s_{pqr}$  parameters has been made to eliminate the maximum number of terms from  $\mathcal{H}$ , the transformed Hamiltonian becomes a reduced Hamiltonian. In principle, an infinite number of reductions are possible, and a number have been discussed in the literature [55, 63, 64, 67–71]. In the next section two specific reductions will be considered.

The most general Hamiltonian for a symmetric-top and the procedure for obtaining the corresponding reduced Hamiltonian via (8.84), which depends on the molecular symmetry, are discussed elsewhere [64], though the particular results will be given here.

### Asymmetric Top Reduction ( $A$ )

For simplicity we consider only the reduction of  $\tilde{\mathcal{H}}_d^{(4)}$  in demonstrating the procedure. The results for the reduction of  $\tilde{\mathcal{H}}_d^{(6)}$  will be simply quoted. Consult [63] for further details. Evaluation of the commutator in (8.86) has been given in (8.60), and with a change in notation we have

$$\begin{aligned} i[\mathcal{H}_r, S_3] = & 2s_{111}\{(B_y - B_x)(P_x^2 P_y^2 + P_y^2 P_x^2 + 2P_z^2) \\ & + (B_z - B_y)(P_y^2 P_z^2 + P_z^2 P_y^2 + 2P_x^2) \\ & + (B_x - B_z)(P_z^2 P_x^2 + P_x^2 P_z^2 + 2P_y^2)\} \end{aligned} \quad (8.88)$$

and hence, from (8.73) and (8.84),

$$\tilde{\mathcal{H}} = \sum_{\alpha} \tilde{B}_{\alpha} P_{\alpha}^2 + \sum_{\alpha, \beta} \tilde{T}_{\alpha \beta} P_{\alpha}^2 P_{\beta}^2 \quad (8.89)$$

This has the same form as  $\mathcal{H}$ ; however, the coefficients are modified as follows:

$$\begin{aligned} \tilde{B}_x &= B_x + 4(B_z - B_y)s_{111} \\ \tilde{B}_y &= B_y + 4(B_x - B_z)s_{111} \\ \tilde{B}_z &= B_z + 4(B_y - B_x)s_{111} \end{aligned} \quad (8.90)$$

and

$$\begin{aligned} \tilde{T}_{xx} &= T_{xx} \\ \tilde{T}_{xy} &= T_{xy} + 2(B_y - B_x)s_{111} \\ \tilde{T}_{yz} &= T_{yz} + 2(B_z - B_y)s_{111} \\ \tilde{T}_{xz} &= T_{xz} + 2(B_x - B_z)s_{111} \end{aligned} \quad (8.91)$$

It will be convenient to recast (8.73) into a form involving the constants  $D_J$ ,  $D_{JK}$ ,  $D_K$ ,  $\delta_J$ ,  $R_5$ , and  $R_6$  defined in Table 8.7, which is more suitable for numerical calculations. With considerable manipulations one finds [64]

$$\begin{aligned} \mathcal{H} = & (B_x - 4R_6)P_x^2 + (B_y - 4R_6)P_y^2 + (B_z + 6R_6)P_z^2 \\ & - D_J P^4 - D_{JK} P^2 P_z^2 - D_K P_z^4 - \delta_J P^2 (P_+^2 + P_-^2) \\ & + R_5 \{P_z^2 (P_+^2 + P_-^2) + (P_+^2 + P_-^2) P_z^2\} \\ & + R_6 (P_+^4 + P_-^4) \end{aligned} \quad (8.92)$$

with  $P_{\pm} = (P_x \pm iP_y)$  and  $P^2 = P_x^2 + P_y^2 + P_z^2$ . A more compact notation [72] for this Hamiltonian is found in Table 8.13. The relations between the coefficients of the cylindrical tensor form and that of (8.73) are also given in Table 8.13. The form of  $\tilde{\mathcal{H}}$  of (8.92) will also be the same, with the coefficients identified by a tilde, however; with use of (8.90), (8.91), and Table 8.7, they are defined as

$$\begin{aligned} \tilde{D}_J &= D_J + \frac{1}{2}(B_x - B_y)s_{111} \\ \tilde{D}_{JK} &= D_{JK} - 3(B_x - B_y)s_{111} \\ \tilde{D}_K &= D_K + \frac{5}{2}(B_x - B_y)s_{111} \\ \tilde{\delta}_J &= \delta_J \\ \tilde{R}_5 &= R_5 + \frac{1}{2}(B_x + B_y - 2B_z)s_{111} \\ \tilde{R}_6 &= R_6 + \frac{1}{4}(B_x - B_y)s_{111} \end{aligned} \quad (8.93)$$

Table 8.13 Relations Between the Cylindrical and Cartesian Coefficients

Cylindrical Tensor Form of  $\mathcal{H}^a$

$$H = \sum_{l,m} \Phi_{2l,2m,0} P^{2l} P_z^{2m} + \frac{1}{2} \sum_{l,n,m} \Phi_{2l,2m,2n} P^{2l} \left( P_z^{2m} (P_+^{2n} + P_-^{2n}) + (P_+^{2n} + P_-^{2n}) P_z^{2m} \right)$$

$$\Phi_{2l,2m,2n} = \begin{cases} = B_{2l,2m,2n} & \text{for } 2l+2m+2n=2 \\ = T_{2l,2m,2n} & \text{for } 2l+2m+2n=4 \end{cases}$$

$P^2$  Terms<sup>b</sup>

$$B_{200} = \frac{1}{2}(B_x + B_y) - 4T_{004}$$

$$B_{020} = B_z - B_{200} + 6T_{004}$$

$$B_{002} = \frac{1}{4}(B_x - B_y)$$

$P^4$  Terms<sup>b</sup>

$$T_{400} = \frac{1}{8}(3T_{xx} + 3T_{yy} + 2T_{xy}) = -D_J$$

$$T_{220} = (T_{xz} + T_{yz}) - 2T_{400} = -D_{JK}$$

$$T_{040} = T_{zz} - T_{220} - T_{400} = -D_K$$

$$T_{202} = \frac{1}{4}(T_{xx} - T_{yy}) = -\delta_J$$

$$T_{022} = \frac{1}{2}(T_{xz} - T_{yz}) - T_{202} = 2R_5$$

$$T_{004} = \frac{1}{16}(T_{xx} + T_{yy} - 2T_{xy}) = R_6$$

$P^6$  Terms<sup>b</sup>

$$\Phi_{600} = \frac{5}{16}(\Phi_{xxx} + \Phi_{yyy}) + \frac{1}{8}(\Phi_{xxy} + \Phi_{yyx})$$

$$\Phi_{420} = \frac{3}{4}(\Phi_{xxz} + \Phi_{yyz}) + \frac{1}{4}\Phi_{xyz} - 3\Phi_{600}$$

$$\Phi_{240} = (\Phi_{zxx} + \Phi_{zzy}) - 2\Phi_{420} - 3\Phi_{600}$$

$$\Phi_{060} = \Phi_{zzz} - \Phi_{240} - \Phi_{420} - \Phi_{600}$$

$$\Phi_{402} = \frac{15}{64}(\Phi_{xxx} - \Phi_{yyy}) + \frac{1}{32}(\Phi_{xxy} - \Phi_{yyx})$$

$$\Phi_{222} = \frac{1}{2}(\Phi_{xxz} - \Phi_{yyz}) - 2\Phi_{402}$$

$$\Phi_{042} = \frac{1}{2}(\Phi_{zxx} - \Phi_{zzy}) - \Phi_{222} - \Phi_{402}$$

$$\Phi_{204} = \frac{3}{32}(\Phi_{xxx} + \Phi_{yyy}) - \frac{1}{16}(\Phi_{xxy} + \Phi_{yyx})$$

$$\Phi_{024} = \frac{1}{8}(\Phi_{xxz} + \Phi_{yyz} - \Phi_{xyz}) - \Phi_{204}$$

$$\Phi_{006} = \frac{1}{64}(\Phi_{xxx} - \Phi_{yyy}) - \frac{1}{32}(\Phi_{xxy} - \Phi_{yyx})$$

<sup>a</sup> $P_{\pm} = (P_x \pm iP_y)$ ,  $P^2 = P_x^2 + P_y^2 + P_z^2$ . Note the subscripts  $2l$ ,  $2m$ , and  $2n$  refer, respectively, to the powers of  $P$ ,  $P_z$ , and  $P_{\pm}$ .

<sup>b</sup>From Watson [64].

with the effective rotational constants

$$\tilde{B}_x - 4\tilde{R}_6, \tilde{B}_y - 4\tilde{R}_6, \tilde{B}_z + 6\tilde{R}_6 \quad (8.94)$$

The most advantageous reduction, initially introduced by Watson, involves choosing  $s_{111}$  so that  $R_6 = 0$ . In this case, the  $(K/K \pm 4)$  matrix elements of  $\mathcal{H}$  in a symmetric rotor basis are eliminated.  $\mathcal{H}_d^{(4)}$  then contains only five terms, and the matrix of  $\mathcal{H}_d^{(4)}$  has the same tridiagonal form as that for a rigid rotor. The condition  $\tilde{R}_6 = 0$  requires

$$s_{111} = -\frac{4R_6}{B_x - B_y} \quad (8.95)$$

and the coefficients in the reduced form are

$$\begin{aligned} \Delta_J &= \tilde{D}_J = D_J - 2R_6 \\ \Delta_{JK} &= \tilde{D}_{JK} = D_{JK} + 12R_6 \\ \Delta_K &= \tilde{D}_K = D_K - 10R_6 \\ \delta_J &= \tilde{\delta}_J \end{aligned}$$

$$\delta_K = -2\tilde{R}_5 = -2R_5 - \frac{4(2B_z - B_x - B_y)R_6}{B_x - B_y} \quad (8.96)$$

where the determinable constants  $\tilde{D}_J$  and so on, are given an alternate notation.

Note that  $\Delta_K$  is invariant to a permutation of axes, whereas  $\Delta_J$ ,  $\Delta_{JK}$ ,  $\delta_J$ , and  $\delta_K$  change on permuting axes. Hence these latter constants depend on the axis representation used in the analysis. From (8.92) with  $P_+^2 + P_-^2 = 2(P_x^2 - P_y^2)$ , the reduced Hamiltonian for the  $A$  reduction including the  $P^6$  terms is, therefore,

$$\tilde{\mathcal{H}}^{(A)} = \mathcal{H}_r + \mathcal{H}_d^{(4)} + \mathcal{H}_d^{(6)} \quad (8.97)$$

$$\begin{aligned} \mathcal{H}_r &= B_x^{(A)} P_x^2 + B_y^{(A)} P_y^2 + B_z^{(A)} P_z^2 \\ &= \frac{1}{2}(B_x^{(A)} + B_y^{(A)})P^2 + [B_z^{(A)} - \frac{1}{2}(B_x^{(A)} + B_y^{(A)})]P_z^2 \\ &\quad + \frac{1}{2}(B_x^{(A)} - B_y^{(A)})(P_x^2 - P_y^2) \end{aligned} \quad (8.98)$$

$$\begin{aligned} \mathcal{H}_d^{(4)} &= \Delta_J P^4 - \Delta_{JK} P^2 P_z^2 - \Delta_K P_z^4 - 2\delta_J P^2(P_x^2 - P_y^2) \\ &\quad - \delta_K [P_z^2(P_x^2 - P_y^2) + (P_x^2 - P_y^2)P_z^2] \end{aligned} \quad (8.99)$$

$$\begin{aligned} \mathcal{H}_d^{(6)} &= \Phi_J P^6 + \Phi_{JK} P^4 P_z^2 + \Phi_{KJ} P^2 P_z^4 + \Phi_K P_z^6 + 2\phi_J P^4(P_x^2 - P_y^2) \\ &\quad + \phi_{JK} P^2 [P_z^2(P_x^2 - P_y^2) + (P_x^2 - P_y^2)P_z^2] \\ &\quad + \phi_K [P_z^4(P_x^2 - P_y^2) + (P_x^2 - P_y^2)P_z^4] \end{aligned} \quad (8.100)$$

where  $\Delta_J$ ,  $\Delta_{JK}$ ,  $\Delta_K$ ,  $\delta_J$ , and  $\delta_K$  are the quartic distortion coefficients defined in terms of various notations in Table 8.14, and where  $\Phi_J$ ,  $\Phi_{JK}$ ,  $\Phi_{KJ}$ ,  $\Phi_K$ ,  $\phi_J$ ,  $\phi_{JK}$ , and  $\phi_K$  are the sextic distortion coefficients. Note  $P_z^2$  and  $(P_x^2 - P_y^2)$  do not commute. The notation  $H_J$ ,  $H_{JK}$ ,  $H_{KJ}$ ,  $H_K$ ,  $h_J$ ,  $h_{JK}$ ,  $h_K$  has been used in the past for the  $P^6$  constants, and many constants have been reported with this notation using the  $A$  reduction. However, as has been suggested [64], we have used the

**Table 8.14** Quartic Distortion Coefficients of the Reduced Distortion Hamiltonian<sup>a</sup>

---

$\Delta_J = -\frac{1}{8}\{\tau'_{xxxx} + \tau'_{yyyy}\} = D_J - 2R_6$
$\Delta_{JK} = \frac{3}{8}\{\tau'_{xxxx} + \tau'_{yyyy}\} - \frac{1}{4}\{\tau'_{yyzz} + \tau'_{xxzz} + \tau'_{xxyy}\} = D_{JK} + 12R_6$
$\Delta_K = -\frac{1}{4}\{\tau'_{xxxx} + \tau'_{yyyy} + \tau'_{zzzz}\} + \frac{1}{4}\{\tau'_{yyzz} + \tau'_{xxzz} + \tau'_{xxyy}\} = D_K - 10R_6$
$\delta_J = -\frac{1}{16}\{\tau'_{xxxx} - \tau'_{yyyy}\}$
$\delta_K = \frac{\frac{1}{8}\tau'_{xxxx}(B_x - B_z)}{B_x - B_y} + \frac{\frac{1}{8}\tau'_{yyyy}(B_y - B_z)}{B_x - B_y} + \frac{1}{8}\left\{\tau'_{yyzz} - \tau'_{xxzz} + \frac{\tau'_{xxyy}(2B_z - B_x - B_y)}{B_x - B_y}\right\}$
$= -2\left[R_5 + \frac{2R_6(2B_z - B_x - B_y)}{B_x - B_y}\right]$
$\Delta_J = -\frac{1}{2}(T_{xx} + T_{yy})$
$\Delta_{JK} = \frac{3}{2}(T_{xx} + T_{yy}) - (T_{yz} + T_{xz} + T_{xy})$
$\Delta_K = -(T_{xx} + T_{yy} + T_{zz}) + (T_{yz} + T_{xz} + T_{xy})$
$\delta_J = -\frac{1}{4}(T_{xx} - T_{yy})$
$\delta_K = -\frac{1}{2}(T_{xz} - T_{yz}) + \frac{1}{4}(T_{xx} - T_{yy}) - \frac{(2B_z - B_x - B_y)}{4(B_x - B_y)}(T_{xx} + T_{yy} - 2T_{xy})$

---

<sup>a</sup> $\tau'_{xxxx} = \hbar^4 \tau_{xxxx}$ ,  $T_{xx} = \frac{1}{4} \tau'_{xxxx}$ ,  $\tau'_{\alpha\beta\beta\beta} = \hbar^4 (\tau_{\alpha\beta\beta\beta} + 2\tau_{\alpha\beta\beta\beta})$ ,  $T_{\alpha\beta} = \frac{1}{4} \tau'_{\alpha\beta\beta\beta}$  with  $(\alpha \neq \beta)$ .  $B_z$  are the rotational constants.

alternate notation  $\Phi_J$ ,  $\Phi_{JK}$ ,  $\Phi_{KJ}$ ,  $\Phi_K$ ,  $\phi_J$ ,  $\phi_{JK}$ , and  $\phi_K$  in order to retain the  $H_J, \dots, H_K$  notation for the symmetric-top reduced Hamiltonian of the next section, since the diagonal  $P^6$  constants for the  $A$  reduction do not correlate appropriately with the symmetric-top constants. The  $P^6$  spectroscopic constants are defined in Table 8.15 in terms of the  $\Phi_{\alpha\beta\gamma}$ . The effective rotational constants are defined as

$$\begin{aligned} B_x^{(A)} &= B_x - \frac{16R_6(B_z - B_y)}{B_x - B_y} \\ &= B_x - 2\Delta_J - \Delta_{JK} + 2\delta_J + 2\delta_K \end{aligned} \quad (8.101)$$

$$\begin{aligned} B_y^{(A)} &= B_y + \frac{16R_6(B_z - B_x)}{B_x - B_y} \\ &= B_y - 2\Delta_J - \Delta_{JK} - 2\delta_J - 2\delta_K \end{aligned} \quad (8.102)$$

$$\begin{aligned} B_z^{(A)} &= B_z + 16R_6 \\ &= B_z - 2\Delta_J \end{aligned} \quad (8.103)$$

where  $B_x$ ,  $B_y$ , and  $B_z$  are given in (8.118) and are readily derivable from the effective rotational constants using the  $\Delta$ -constants obtained from the spectrum. This Hamiltonian has been found to be applicable to a large range of asymmetric tops. It is apparent that the effective Hamiltonian has been reduced to one that contains only determinable constants and is appropriate for fitting purposes. The reduced Hamiltonian in general contains  $(n+1)$  distortion coefficients for each degree  $n$  in the angular momentum. There are  $(n/2+1)$  purely diagonal angular momentum operators, and the remaining ones are off-diagonal, involving  $(P_x^2 - P_y^2)$ .

For light molecules higher-order effects are important, and numerous distortion coefficients are required to adequately fit the spectrum. The reduced

**Table 8.15** Sextic Distortion Coefficients of the Reduced Distortion Hamiltonian in Terms of the Cylindrical Tensor Coefficients<sup>a</sup>

---


$$\begin{aligned} \Phi_J &= \Phi_{600} + 2\Phi_{204} \\ \Phi_{JK} &= \Phi_{420} - 12\Phi_{204} + 2\Phi_{024} + 16\sigma\Phi_{006} + 8T_{022}T_{004}/B_{002} \\ \Phi_{KJ} &= \Phi_{240} + \frac{10}{3}\Phi_{420} - 30\Phi_{204} - \frac{10}{3}\Phi_{JK} \\ \Phi_K &= \Phi_{060} - \frac{7}{3}\Phi_{420} + 28\Phi_{204} + \frac{7}{3}\Phi_{JK} \\ \phi_J &= \Phi_{402} + \Phi_{006} \\ \phi_{JK} &= \Phi_{222} + 4\sigma\Phi_{204} - 10\Phi_{006} + 2(T_{220} - 2\sigma T_{202} - 4T_{004})T_{004}/B_{002} \\ \phi_K &= \Phi_{042} + \frac{4\sigma}{3}\Phi_{024} + \left(\frac{32}{3}\sigma^2 + 9\right)\Phi_{006} + 4\left[T_{040} + \frac{\sigma}{3}T_{022} - 2(\sigma^2 - 2)T_{004}\right]T_{004}/B_{002} \end{aligned}$$


---

<sup>a</sup>See Table 8.13 for definition of the coefficients in the cylindrical tensor form of  $\mathcal{H}$  in terms of  $\Phi_{\alpha\beta\gamma}$  of (8.73). From Watson [64].

Hamiltonian can be readily generalized to include  $P^8$  and  $P^{10}$  effects, and the following terms are added to the Hamiltonian

$$\begin{aligned}\mathcal{H}_d^{(8)} = & L_J P^8 + L_{JJK} P^6 P_z^2 + L_{JK} P^4 P_z^4 + L_{KKJ} P^2 P_z^6 + L_K P_z^8 + 2l_J P^6 (P_x^2 - P_y^2) \\ & + l_{JK} P^4 [P_z^2 (P_x^2 - P_y^2) + (P_x^2 - P_y^2) P_z^2] + l_{KJ} P^2 [P_z^4 (P_x^2 - P_y^2) + (P_x^2 - P_y^2) P_z^4] \\ & + l_K [P_z^6 (P_x^2 - P_y^2) + (P_x^2 - P_y^2) P_z^6],\end{aligned}\quad (8.104)$$

$$\begin{aligned}\mathcal{H}_d^{(10)} = & P_J P^{10} + P_{JJK} P^8 P_z^2 + P_{JK} P^6 P_z^4 + P_{KJ} P^4 P_z^6 + P_{KKJ} P^2 P_z^8 + P_K P_z^{10} \\ & + 2p_J P^8 (P_x^2 - P_y^2) + p_{JJK} P^6 [P_z^2 (P_x^2 - P_y^2) + (P_x^2 - P_y^2) P_z^2] \\ & + P_{JK} P^4 [P_z^4 (P_x^2 - P_y^2) + (P_x^2 - P_y^2) P_z^4] \\ & + p_{KKJ} P^2 [P_z^6 (P_x^2 - P_y^2) + (P_x^2 - P_y^2) P_z^6] + p_K [P_z^8 (P_x^2 - P_y^2) + (P_x^2 - P_y^2) P_z^8]\end{aligned}\quad (8.105)$$

The  $L, l$  are octic centrifugal distortion constants, and the  $P, p$  are the corresponding decitic constants. These coefficients must be regarded at this point as empirical constants in the sense that they have not as yet been theoretically related to the vibrational potential constants. On the other hand, the quartic and sextic distortion constants have been related to the potential constants, in particular to the quadratic and cubic force constants, respectively.

### Symmetric Top Reduction ( $S$ )

For very slightly asymmetric tops, the previous reduction can present problems. It is clear from the definition of  $s_{111}$  that if  $B_x \approx B_y$ ,  $s_{111}$  gets very large and the order-of-magnitude arguments employed previously no longer apply. Specifically, the breakdown depends on the ratio of a  $P^4$  distortion constant to  $(B_x - B_y)$ . Different representations can be chosen to minimize this effect by making  $(B_x - B_y)$  larger and  $R_6$  as small as possible. However, it is preferable to employ an alternate reduction that reduces in a well-defined way to the symmetric top limit. In this case it is convenient to take  $\tilde{R}_5 = 0$  which requires

$$s_{111} = \frac{2R_5}{2B_z - B_x - B_y} \quad (8.106)$$

This reduction has been proposed by Winnewisser [69] and Van Eijck [70]. It has been demonstrated by Van Eijck [70], who discussed  $\mathcal{H}_d^{(4)}$ , and by Typke [71] who extended the results to  $\mathcal{H}_d^{(6)}$ , that a more satisfactory analysis can be obtained for slightly asymmetric tops with this reduction. Watson [64] also was instrumental in the introduction of this form of the reduction.

The coefficients in the reduced form of (8.92) are now

$$\begin{aligned}\tilde{D}_J = & D_J + \frac{R_5}{\sigma} \\ = & \Delta_J - \frac{\delta_K}{2\sigma}\end{aligned}$$

$$\begin{aligned}
\tilde{D}_{JK} &= D_{JK} - \frac{6R_5}{\sigma} \\
&= \Delta_{JK} + \frac{3\delta_K}{\sigma} \\
\tilde{D}_K &= D_K + \frac{5R_5}{\sigma} \\
&= \Delta_K - \frac{5\delta_K}{2\sigma} \\
\tilde{\delta}_J &= \delta_J \\
\tilde{R}_6 &= R_6 + \frac{R_5}{2\sigma} \\
&= -\frac{\delta_K}{4\sigma}
\end{aligned} \tag{8.107}$$

where

$$\sigma = \frac{2B_z - B_x - B_y}{B_x - B_y} \tag{8.108}$$

for an I' and III' representation,  $\sigma = -1/b_p$  and  $-1/b_0$ , respectively. The notation adopted to retain the similarity of the reduced Hamiltonian to that of a symmetric top is

$$D_J = \tilde{D}_J, D_{JK} = \tilde{D}_{JK}, D_K = \tilde{D}_K, d_1 = -\delta_J, d_2 = \tilde{R}_6 \tag{8.109}$$

The reduced Hamiltonian for the S reduction is therefore

$$\hat{\mathcal{H}}^{(S)} = \mathcal{H}_r + \mathcal{H}_d^{(4)} + \mathcal{H}_d^{(6)} \tag{8.110}$$

$$\begin{aligned}
\mathcal{H}_r &= B_x^{(S)} P_x^2 + B_y^{(S)} P_y^2 + B_z^{(S)} P_z^2 \\
&= \frac{1}{2}(B_x^{(S)} + B_y^{(S)}) P^2 + [B_z^{(S)} - \frac{1}{2}(B_x^{(S)} + B_y^{(S)})] P_z^2 + \frac{1}{4}(B_x^{(S)} - B_y^{(S)})(P_+^2 + P_-^2)
\end{aligned} \tag{8.111}$$

$$\mathcal{H}_d^{(4)} = -D_J P^4 - D_{JK} P^2 P_z^2 - D_K P_z^4 + d_1 P^2 (P_+^2 + P_-^2) + d_2 (P_+^4 + P_-^4) \tag{8.112}$$

$$\begin{aligned}
\mathcal{H}_d^{(6)} &= H_J P^6 + H_{JK} P^4 P_z^2 + H_{KJ} P^2 P_z^4 + H_K P_z^6 \\
&\quad + h_1 P^4 (P_+^2 + P_-^2) + h_2 P^2 (P_+^4 + P_-^4) + h_3 (P_+^6 + P_-^6)
\end{aligned} \tag{8.113}$$

where the  $P^6$  terms have also been included. Note, however, that the constants  $D_J$ ,  $D_{JK}$ , and  $D_K$  used in the foregoing Hamiltonian are not the same constants as those defined in Table 8.7. The effective rotational constants, with cognizance of (8.90), are

$$\begin{aligned}
B_x^{(S)} &= \tilde{B}_x - 4\tilde{R}_6 = B_x - 4R_6 + 4R_5 + \frac{2R_5}{\sigma} \\
&= B_x - 2D_J - D_{JK} - 2d_1 - 4d_2
\end{aligned} \tag{8.114}$$

$$\begin{aligned} B_y^{(S)} &= \hat{B}_y - 4\hat{R}_6 = B_y - 4R_6 - 4R_5 + \frac{2R_5}{\sigma} \\ &= B_y - 2D_J - D_{JK} + 2d_1 - 4d_2 \end{aligned} \quad (8.115)$$

$$\begin{aligned} B_z^{(S)} &= \hat{B}_z + 6\hat{R}_6 = B_z + 6R_6 - \frac{5R_5}{\sigma} \\ &= B_z - 2D_J - 6d_2 \end{aligned} \quad (8.116)$$

where  $B_x$ ,  $B_y$ ,  $B_z$  are defined in (8.118). The coefficients in  $\mathcal{H}^{(A)}$  and  $\mathcal{H}^{(S)}$  can be related to each other (see Table 8.16), and the coefficients of the two reduced Hamiltonians provide the same information.

It is apparent that this Hamiltonian can be readily generalized to include higher-order constants. If we extend the Hamiltonian to  $P^8$  terms, the following terms must be added

$$\begin{aligned} \tilde{\mathcal{H}}^{(8)} &= L_J P^8 + L_{JJK} P^6 P_z^2 + L_{JK} P^4 P_z^4 + L_{KKJ} P^2 P_z^6 + L_K P_z^8 \\ &\quad + l_1 P^6 (P_+^2 + P_-^2) + l_2 P^4 (P_+^4 + P_-^4) + l_3 P^2 (P_+^6 + P_-^6) + l_4 (P_+^8 + P_-^8) \end{aligned} \quad (8.117)$$

### Determinable Combinations of Coefficients

From (8.90) and (8.91)  $s_{111}$  can be eliminated from the nine equations to give eight linear combinations of quadratic and quartic coefficients. These coefficients are the determinable combinations of coefficients since the energies cannot depend on  $s_{111}$ . The experimentally determinable coefficients can be conveniently taken as

$$\begin{aligned} B_x &= B_x - 2T_{yz} \\ B_y &= B_y - 2T_{zx} \\ B_z &= B_z - 2T_{xy} \end{aligned} \quad (8.118)$$

**Table 8.16** Relations Between the Distortion Coefficients in the  $A$  and  $S$  Reduced Hamiltonians<sup>a</sup>

$B_x^{(A)} = B_x^{(S)} - 4(2\sigma + 1)d_2$	$B_z^{(A)} = B_z^{(S)} + 10d_2$	$B_y^{(A)} = B_y^{(S)} + 4(2\sigma - 1)d_2$
$\Delta_J = D_J - 2d_2$	$\Delta_{JK} = D_{JK} + 12d_2$	$\Delta_K = D_K - 10d_2$
$\delta_J = -d_1$		$\delta_K = -4\sigma d_2$
$\Phi_J = H_J + 2h_2$		$\Phi_{JK} = H_{JK} - 12h_2 + 16\sigma h_3$
$\Phi_{KJ} = H_{KJ} + 10h_2 - (160\sigma/3)h_3$		$\Phi_K = H_K + (112\sigma/3)h_3$
$\phi_J = h_1 + h_3$		
$\phi_{JK} = 4\sigma h_2 - 10h_3 - 8d_2 \{D_{JK} + 2\sigma d_1 + 4d_2\}/(B_x - B_y)$		
$\phi_K = (32\sigma^2/3 + 9)h_3 - 16d_2 \{D_K + 2(\sigma^2 - 2)d_2\}/(B_x - B_y)$		

<sup>a</sup> $\sigma = (2B_z - B_x - B_y)/(B_x - B_y)$ . From Watson [140].

$$\begin{aligned} & T_{xx}, T_{yy}, T_{zz}, \\ & T_1 = T_{yz} + T_{xz} + T_{xy} \\ & T_2 = B_x T_{yz} + B_y T_{xz} + B_z T_{xy} \end{aligned} \quad (8.119)$$

In terms of the  $\tau$  notation, the determinable coefficients are

$$\begin{aligned} B_x &= B_x - \frac{1}{2}\tau'_{yyzz} \\ B_y &= B_y - \frac{1}{2}\tau'_{xxzz} \\ B_z &= B_z - \frac{1}{2}\tau'_{xxyy} \end{aligned} \quad (8.120)$$

$$\begin{aligned} & \tau'_{xxxx}, \tau'_{yyyy}, \tau'_{zzzz}, \\ & \tau_1 = \tau'_{yyzz} + \tau'_{xxzz} + \tau'_{xxyy} \\ & \tau_2 = B_x \tau'_{yyzz} + B_y \tau'_{xxzz} + B_z \tau'_{xxyy} \end{aligned} \quad (8.121)$$

The  $T_1$  (or  $\tau_1$ ) and  $T_2$  (or  $\tau_2$ ) have the same value for any permutation of the axes. The constant  $T_2$  (or  $\tau_2$ ) is often scaled so that it has same units as the other constants, that is,

$$T_2 \rightarrow \frac{T_2}{S} \quad \text{or} \quad \tau_2 \rightarrow \frac{\tau_2}{S} \quad (8.122)$$

with  $S = B_x + B_y + B_z$ . Likewise the  $P^6$  determinable coefficients can be taken as [64]

$$\begin{aligned} & \Phi_{xxx}, \Phi_{yyy}, \Phi_{zzz}, \\ & \Phi_1 = 3 \sum_{\alpha \neq \beta} \Phi_{\alpha\alpha\beta} + \Phi_{xyz} \\ & \Phi_2 = (B_x - B_z) \Phi_{xxy} + (B_x - B_y) \Phi_{xxz} - 2(T_{xx} - T_{xy})(T_{xx} - T_{xz}) \\ & \Phi_3 = (B_y - B_x) \Phi_{yyz} + (B_y - B_z) \Phi_{yyx} - 2(T_{yy} - T_{yz})(T_{yy} - T_{yx}) \\ & \Phi_4 = (B_z - B_y) \Phi_{zzx} + (B_z - B_x) \Phi_{zzy} - 2(T_{zz} - T_{zx})(T_{zz} - T_{zy}) \end{aligned} \quad (8.123)$$

These determinable combinations of constants are hence directly related to the constants of the first-principles Hamiltonian and can thus be directly related to the molecular force field.

The foregoing determinable combinations may be expressed in terms of the constants evaluated from the rotational spectrum via the Hamiltonians of (8.97) and (8.110). These relations are given in Tables 8.17 and 8.18. Once an axis representation is chosen, those relations yield the constants  $T_{aa}$ ,  $T_{bb}$ , ..., referred to the principal inertial axis system.

In reporting the rotation and distortion constants, the effective rotational constants  $\mathcal{A}$ ,  $\mathcal{B}$ ,  $\mathcal{C}$  and  $A$ ,  $B$ ,  $C$  should be listed. The type of reduction ( $A$  or  $S$ ) used and the representation I', II', and so on, that is employed should be indicated in the table of constants. In the cases where large numbers of constants are required in the fit, the addition of an  $A$  or  $S$  superscript to the constants would avoid the need for two sets of symbols for the higher-order constants, for example,  $P^8$  constants ( $L_J^{(S)}$  or  $L_J^{(A)}$ ).

**Table 8.17** Determinable Combinations in Terms of the Spectroscopic Constants of the *A* Reduction<sup>a</sup>


---

$B_x = B_x^{(A)} + 2\Delta_J + \Delta_{JK} - 2\delta_J - 2\delta_K$
$B_y = B_y^{(A)} + 2\Delta_J + \Delta_{JK} + 2\delta_J + 2\delta_K$
$B_z = B_z^{(A)} + 2\Delta_J$
$T_{xx} = -\Delta_J - 2\delta_J, T_{yy} = -\Delta_J + 2\delta_J, T_{zz} = -\Delta_J - \Delta_{JK} - \Delta_K$
$T_1 = -3\Delta_J - \Delta_{JK}$
$T_2 = -(B_x + B_y + B_z)\Delta_J - \frac{1}{2}(B_x + B_y)\Delta_{JK} + (B_x - B_y)(\delta_J + \delta_K)$
$\Phi_{xxx} = \Phi_J + 2\phi_J, \Phi_{yyy} = \Phi_J - 2\phi_J$
$\Phi_{zzz} = \Phi_J + \Phi_{JK} + \Phi_{KJ} + \Phi_K$
$\Phi_1 = 30\Phi_J + 10\Phi_{JK} + 3\Phi_{KJ}$
$\Phi_2 + \Phi_3 = -3[B_z - \frac{1}{2}(B_x + B_y) + 10R_6]\Phi_J + (B_x - B_y)(5\phi_J + 2\phi_{JK}) - 8\delta_J(\delta_J - \delta_K)$
$\Phi_2 - \Phi_3 = -2[B_z - \frac{1}{2}(B_x + B_y) + 10R_6]\phi_J + \frac{1}{2}(B_x - B_y)(9\Phi_J + 2\Phi_{JK}) + 4\delta_J\Delta_{JK}$
$\Phi_4 = [B_z - \frac{1}{2}(B_x + B_y) + 10R_6](3\Phi_J + 2\Phi_{JK} + \Phi_{KJ}) + (B_x - B_y)(\phi_J + \phi_{JK} + \phi_K) - \frac{1}{2}(\Delta_{JK} + 2\Delta_K)^2 + 2(\delta_J + \delta_K)^2$

---

<sup>a</sup>  $R_6 = \frac{1}{16}(T_{xx} + T_{yy} - 2T_{xy})$ . From Watson [64].

**Table 8.18** Determinable Combinations in Terms of the Spectroscopic Constants of the *S* Reduction<sup>a</sup>


---

$B_x = B_x^{(S)} + 2D_J + D_{JK} + 2d_1 + 4d_2$
$B_y = B_y^{(S)} + 2D_J + D_{JK} - 2d_1 + 4d_2$
$B_z = B_z^{(S)} + 2D_J + 6d_2$
$T_{xx} = -D_J - 2d_1 + 2d_2, T_{yy} = -D_J - 2d_1 + 2d_2$
$T_{zz} = -D_J - D_{JK} - D_K, T_1 = -3D_J - D_{JK} - 6d_2$
$T_2 = -(B_x + B_y + B_z)D_J - \frac{1}{2}(B_x + B_y)D_{JK} - (B_x - B_y)d_1 - 6B_zd_2$
$\Phi_{xxx} = H_J + 2h_1 + 2h_2 + 2h_3$
$\Phi_{yyy} = H_J - 2h_1 + 2h_2 - 2h_3$
$\Phi_{zzz} = H_J + H_{JK} + H_{KJ} + H_K$
$\Phi_1 = 30H_J + 10H_{JK} + 3H_{KJ} - 30h_2$
$\Phi_2 + \Phi_3 = -[B_z - \frac{1}{2}(B_x + B_y) + 10R_6](3H_J - 10h_2) + 5(B_x - B_y)(h_1 - 3h_3) - 8d_1^2 - 16d_2(D_{JK} + 4d_2)$
$\Phi_2 - \Phi_3 = -2[B_z - \frac{1}{2}(B_x + B_y) + 10R_6](h_1 - 15h_3) + \frac{1}{2}(B_x - B_y)(9H_J + 2H_{JK} - 6h_2) - 4d_1(D_{JK} + 12d_2)$
$\Phi_4 = [B_z - \frac{1}{2}(B_x + B_y) + 10R_6](3H_J + 2H_{JK} + H_{KJ}) + (B_x - B_y)h_1 - \frac{1}{2}(D_{JK} + 2D_K)^2 + 2d_1^2$

---

<sup>a</sup>  $R_6 = \frac{1}{16}(T_{xx} + T_{yy} - 2T_{xy})$ . From Watson [64].

## Symmetric and Spherical Tops

For a symmetric rotor  $B_x^{(S)} = B_y^{(S)}$ , and the reduced Hamiltonian has the form

$$\begin{aligned} \tilde{\mathcal{H}} = & B_x P^2 + (B_z - B_x)P_z^2 - D_J P^4 - D_{JK} P^2 P_z^2 - D_K P_z^4 \\ & + H_J P^6 + H_{JK} P^4 P_z^2 + H_{KJ} P^2 P_z^4 + H_K P_z^6 + \tilde{\mathcal{H}}_{\text{split}} \end{aligned} \quad (8.124)$$

The  $D$ 's have their usual meaning for a symmetric top. The  $\tilde{\mathcal{H}}_{\text{split}}$  term arises from the off-diagonal terms in  $\mathcal{H}^{(S)}$  and leads to splitting of the  $K$ -degenerate levels of a symmetric top. The form of the reduced splitting term depends on the molecular point group. In particular, correct to  $P^6$  terms

$$\tilde{\mathcal{H}}_{\text{split}} = (d_2 + h_2 P^2)(P_+^4 + P_-^4) + h_3(P_+^6 + P_-^6) \quad (8.125)$$

where, for a  $p$ -fold axis of rotation [61]

$$d_2 = h_2 = h_3 = 0, \quad \text{if } p = 5 \text{ or } \geq 7 \quad (8.126)$$

$$d_2 = h_2 = 0, \quad \text{if } p = 3 \text{ or } 6 \quad (8.127)$$

$$h_3 = 0, \quad \text{if } p = 4 \quad (8.128)$$

The constants  $d_2$ ,  $h_2$ , and  $h_3$  are particularly important in the splitting of the  $K = \pm 2$  and  $K = \pm 3$  levels, respectively. For a  $C_{3v}$  molecule [72]

$$\begin{aligned} H_J &= \frac{1}{2}(\Phi_{xxx} + \Phi_{yyy}) \\ H_{JK} &= 2\Phi_{zxx} - 3H_J \\ H_{KJ} &= 2\Phi_{zzx} - 2H_{JK} - 3H_J \\ H_K &= \Phi_{zzz} - H_{KJ} - H_{JK} - H_J \\ 2h_3 &= \frac{1}{2}(\Phi_{xxx} - \Phi_{yyy}) \end{aligned} \quad (8.129)$$

The Hamiltonian for a spherical rotor has been discussed by a number of authors [73–80]. It may be conveniently written in terms of spherical tensor operators  $\Omega_l$  of rank  $l$  ( $l = 0, 2, 4, 6, \dots$ ) [78]

$$\mathcal{H} = BP^2 - D_S P^4 + D_{4T} \Omega_4 + H_S P^6 + H_{4T} P^2 \Omega_4 + H_{6T} \Omega_6 \quad (8.130)$$

where the  $D$ 's and  $H$ 's are, respectively, the effective quartic and sextic distortion constants. The subscript  $T$  indicates a coefficient of a tensor operator,  $l \neq 0$ , and  $S$  indicates coefficients of the scalar terms,  $l = 0$ . For a  $T_d$  molecule [72]

$$\begin{aligned} H_S &= \frac{1}{105}(45\Phi_{xxx} + 36\Phi_{xxy} + 2\Phi_{xyz}) \\ H_{4T} &= \frac{1}{110}(-15\Phi_{xxx} + 8\Phi_{xxy} + \Phi_{xyz}) \\ H_{6T} &= \frac{1}{231}(6\Phi_{xxx} - 12\Phi_{xxy} + 4\Phi_{xyz}) \end{aligned} \quad (8.131)$$

The energy levels are conveniently labeled by  $J, M_J, C, t$ , where  $J, M_J$  have their usual meaning,  $C$  specifies the irreducible symmetry representation of the level, and  $t$  distinguishes different levels of the same representation. Precise measurements [81] have indicated the need for higher-order terms in the Hamiltonian. The  $P^8$  effects add the following terms

$$\mathcal{H}^{(8)} = L_S P^8 + L_{4T} P^4 \Omega_4 + L_{6T} P^2 \Omega_6 + L_{8T} \Omega_8 \quad (8.132)$$

It has been shown that this can be written in an alternate form [80]

$$\mathcal{H}^{(8)} = L_S P^8 + L_{4T} P^4 \Omega_4 + L_{6T} P^2 \Omega_6 + L_{44T} \Omega_4^2 \quad (8.133)$$

which replaces the evaluation of the matrix of  $\Omega_8$  with that for  $\Omega_4^2$ . The latter matrix is readily constructed from that for  $\Omega_4$ . The coefficients of lower degree are also modified slightly by this formulation. In a similar way one obtains the following additional terms to higher-order for the reduced Hamiltonian to twelfth degree [80]

$$\begin{aligned} \mathcal{H}^{(10)} = & P_S P^{10} + P_{4T} P^6 \Omega_4 + P_{6T} P^4 \Omega_6 + P_{44T} P^2 \Omega_4^2 \\ & + P_{46T} (\Omega_4 \Omega_6 + \Omega_6 \Omega_4) \end{aligned} \quad (8.134)$$

$$\begin{aligned} \mathcal{H}^{(12)} = & R_S P^{12} + R_{4T} P^8 \Omega_4 + R_{6T} P^6 \Omega_6 + R_{44T} P^4 \Omega_4^2 \\ & + R_{46T} P^2 (\Omega_4 \Omega_6 + \Omega_6 \Omega_4) + R_{444T} \Omega_4^3 \end{aligned} \quad (8.135)$$

where the  $P$ 's and  $R$ 's are additional distortion constants.

A discussion of the evaluation of the energy levels is found in Section 5 (see also Chapter VI). The tensor operators in the foregoing expressions are constructed from the angular momentum components  $P_x$  so as to be totally symmetric under the operations of the molecular point group, for example, [77]

$$\Omega_4 = 6P^4 - 10(P_x^4 + P_y^4 + P_z^4) - 2P^2 \quad (8.136)$$

and

$$\Omega_6 = 15P^6 + \frac{77}{2}(P_x^6 + P_y^6 + P_z^6) - \frac{35}{2}(P_x^4 + P_y^4 + P_z^4)(3P^2 - 7) - \frac{135}{2}P^4 + 19P^2 \quad (8.137)$$

## 5 EVALUATION OF THE DISTORTION CONSTANTS FROM OBSERVED SPECTRA

For molecules with very small moments of inertia (e.g.,  $H_2O$ ,  $H_2S$ ) or levels with high rotational quantum numbers, a first-order treatment of centrifugal distortion may not be adequate. A detailed study of the distortion effects in  $OF_2$  by Pierce et al. [82] has shown that at high  $J$  values,  $20 \leq J \leq 40$ , second- and higher-order distortion effects, though small compared to the first-order effects, are nevertheless significant. For these cases, as with the rigid rotor problem, the complete energy matrix can be set up and diagonalized directly to give the total energy of the molecule, including distortion corrections. Earlier distortion studies employed the Hamiltonian of (8.53) and were carried out on planar molecules; the planarity relations were used to reduce the number of  $\tau$  constants from six to four, for example,  $\tau_{aaaa}$ ,  $\tau_{bbbb}$ ,  $\tau_{aabb}$ , and  $\tau_{abab}$ . The indeterminacy mentioned previously was thus removed. For the case of molecules with orthorhombic symmetry, (8.53), the Hamiltonian matrix in a symmetric rotor basis is diagonal in  $J$  and  $M$ , with nonvanishing matrix elements in  $K$  of the type  $(K|K)$ ,  $(K|K \pm 2)$ , and  $(K|K \pm 4)$ . For molecules with non-orthorhombic symmetry, additional distortion constants (e.g.,  $\tau_{axz\beta}$ ) are introduced which also contribute in higher order [50, 64, 72, 83]. In the reduced

Hamiltonian, these constants do not appear explicitly but rather modify the definitions of the higher-order reduced constants. The matrix elements for the distortion Hamiltonian (8.55) may be obtained, as before, by matrix multiplication and use of the matrix elements given previously. Explicit expressions are given in Table 8.19. The matrix will still factor into four submatrices upon application of the Wang symmetrizing transformation [84]. Portions of the submatrices in terms of the original matrix elements are:

$$\mathbf{E}^{\pm} = \begin{bmatrix} E_{00} & \sqrt{2}E_{02} & \sqrt{2}E_{04} & 0 & \cdot & \cdot & \cdot \\ \sqrt{2}E_{02} & E_{22} \pm E_{-2,2} & E_{24} & E_{26} & 0 & \cdot & \cdot \\ 2E_{04} & E_{24} & E_{44} & E_{46} & E_{48} & 0 & \cdot \\ 0 & E_{26} & E_{46} & E_{66} & E_{68} & E_{6,10} & \cdot \\ \cdot & \cdot & \cdot & \cdot & \cdot & \cdot & \cdot \end{bmatrix} \quad (8.138)$$

$$\mathbf{O}^{\pm} = \begin{bmatrix} E_{11} \pm E_{-1,1} & E_{13} \pm E_{-1,3} & E_{15} & 0 & \cdot & \cdot & \cdot \\ E_{13} \pm E_{-1,3} & E_{33} & E_{35} & E_{37} & 0 & \cdot & \cdot \\ E_{15} & E_{35} & E_{55} & E_{57} & E_{59} & 0 & \cdot \\ 0 & E_{37} & E_{57} & E_{77} & E_{79} & E_{7,11} & \cdot \\ \cdot & \cdot & \cdot & \cdot & \cdot & \cdot & \cdot \end{bmatrix}$$

**Table 8.19** Matrix Elements of  $P_x^2 P_y^2$  in a Symmetric Rotor Representation<sup>a</sup>

$$(K|P_z^4|K) = K^4$$

$$(K|P_y^4|K) = \frac{1}{4}[(P^2 - K^2)^2 + \frac{1}{4}\{f_+(0)f_+(1) + f_-(0)f_-(1)\}]$$

$$(K|P_x^4|K) = (K|P_y^4|K)$$

$$(K|P_x^2 P_y^2 + P_y^2 P_x^2|K) = \frac{1}{2}[(P^2 - K^2)^2 - \frac{1}{4}\{f_+(0)f_+(1) + f_-(0)f_-(1)\}]$$

$$(K|P_y^2 P_z^2 + P_z^2 P_y^2|K) = K^2[P^2 - K^2]$$

$$(K|P_x^2 P_z^2 + P_z^2 P_x^2|K) = (K|P_y^2 P_z^2 + P_z^2 P_y^2|K)$$

$$(K|P_y^4|K \pm 2) = \frac{1}{8}\{2P^2 - K^2 - (K \pm 2)^2\}\{f_{\pm}(0)f_{\pm}(1)\}^{1/2}$$

$$(K|P_x^4|K \pm 2) = -(K|P_y^4|K \pm 2)$$

$$(K|P_y^2 P_z^2 + P_z^2 P_y^2|K \pm 2) = \frac{1}{4}\{K^2 + (K \pm 2)^2\}\{f_{\pm}(0)f_{\pm}(1)\}^{1/2}$$

$$(K|P_x^2 P_z^2 + P_z^2 P_x^2|K \pm 2) = -(K|P_y^2 P_z^2 + P_z^2 P_y^2|K \pm 2)$$

$$(K|P_y^4|K \pm 4) = \frac{1}{16}\{f_{\pm}(0)f_{\pm}(1)f_{\pm}(2)f_{\pm}(3)\}^{1/2}$$

$$(K|P_x^4|K \pm 4) = (K|P_y^4|K \pm 4)$$

$$(K|P_x^2 P_y^2 + P_y^2 P_x^2|K \pm 4) = -2(K|P_y^4|K \pm 4)$$

$$P^2 = J(J+1); f_{\pm}(l) = \{P^2 - (K \pm l)(K \pm l \pm 1)\}$$

<sup>a</sup>The phase choice used here is that of G. W. King, R. M. Hainer, and P. C. Cross, *J. Chem. Phys.*, **11**, 27 (1943). For simplicity we do not display the  $J$  and  $M$  labeling, it being understood the matrix elements are diagonal in these quantum numbers.

For  $E^-$ , the first row and column must be deleted as indicated by the dashed lines. In these derivations, use has been made of the relations

$$E_{K,K} = E_{-K,-K}; \quad E_{K,K+l} = E_{K+l,K} = E_{-K,-K-l} = E_{-K-l,-K} \quad (8.139)$$

with  $l=2$  or  $4$ . Table 7.5 is still applicable for identification of the explicit energy levels contained in each submatrix. Each matrix element of (8.138) will be made up of contributions from  $\mathcal{H}$ , and  $\mathcal{H}_d$ . Diagonalization of the complete energy matrix gives the rotational energy, including distortion corrections. For sufficiently low values of  $J$ , the subdeterminants of (8.138) may be solved directly to give expressions for the energy levels, including the effects of centrifugal distortion. Oka and Morino [85] and Chung and Parker [19] have reported expressions for the rotational energies of particular low  $J$  levels which are in the form of linear or quadratic expressions. In Table 8.20 we give explicit expressions for the energy levels that can be expressed in linear forms. By use of this table, the frequency for certain low  $J$  transitions can be easily evaluated if the  $\tau$ 's are known.

Sum rules involving the rotational and distortion constants have also been obtained [86-90]. These are derived by use of the invariance of the trace of a matrix to a similarity transformation. Thus, for each  $J$ , the trace of a submatrix of, for example, (8.138) equals the sum of the corresponding energy levels.

**Table 8.20** Linear Expressions for the Rotational Energy Levels Including Centrifugal Distortion Effects<sup>a</sup>

$J_{K-1,K_1}$	$E$
$0_{0,0}$	0
$1_{0,1}$	$B + C + \frac{\hbar^4}{4} \{ \tau_{bbbb} + \tau_{cccc} + 2(\tau_{bbcc} + 2\tau_{bcbc}) \}$
$1_{1,1}$	$A + C + \frac{\hbar^4}{4} \{ \tau_{aaaa} + \tau_{cccc} + 2(\tau_{aacc} + 2\tau_{acac}) \}$
$1_{1,0}$	$A + B + \frac{\hbar^4}{4} \{ \tau_{aaaa} + \tau_{bbbb} + 2(\tau_{aabb} + 2\tau_{abab}) \}$
$2_{1,2}$	$A + B + 4C + \frac{\hbar^4}{4} \{ \tau_{aaaa} + \tau_{bbbb} + 16\tau_{cccc} + 8(\tau_{bbcc} + 2\tau_{bcbc}) + 8(\tau_{aacc} + 2\tau_{acac}) + 2(\tau_{aabb} + 2\tau_{abab}) \}$
$2_{1,1}$	$A + 4B + C + \frac{\hbar^4}{4} \{ \tau_{aaaa} + 16\tau_{bbbb} + \tau_{cccc} + 8(\tau_{bbcc} + 2\tau_{bcbc}) + 2(\tau_{aacc} + 2\tau_{acac}) + 8(\tau_{aabb} + 2\tau_{abab}) \}$
$2_{2,1}$	$4A + B + C + \frac{\hbar^4}{4} \{ 16\tau_{aaaa} + \tau_{bbbb} + \tau_{cccc} + 2(\tau_{bbcc} + 2\tau_{bcbc}) + 8(\tau_{aacc} + 2\tau_{acac}) + 8(\tau_{aabb} + 2\tau_{abab}) \}$
$3_{2,2}$	$4(A + B + C) + 4\hbar^4 \{ \tau_{aaaa} + \tau_{bbbb} + \tau_{cccc} + 2(\tau_{bbcc} + 2\tau_{bcbc}) + 2(\tau_{aacc} + 2\tau_{acac}) + 2(\tau_{aabb} + 2\tau_{abab}) \}$

<sup>a</sup>From Oka and Morino [85]. Note that for planar molecules  $\tau_{acac} = \tau_{bcbc} = 0$ .

Because the latter information is often unavailable, however, the sum rules are hence of limited value. Sum rules for the reduced Hamiltonian are also available [64].

For higher values of  $J$ , the order of the secular determinant requires numerical diagonalization techniques. To set up the energy matrix, (8.138), the numerical values of the  $\tau$ 's are required. If the force constants and structural parameters are available, the distortion constants may be calculated directly, and the corresponding energy matrix diagonalized to give the effects of centrifugal distortion. The centrifugal distortion constants are, however, best evaluated from the experimental data of the rotational spectrum. An approximate set of rotation and distortion constants may be obtained by use of the first-order expression (8.56) for a planar molecule; all seven individual  $\tau$ 's may be obtained from the analysis (if the relations of Table 8.10 are assumed). These constants along with the rotational constants are used for setting up the complete energy matrix, (8.138), and the higher effects may be taken into account by use of the rigid-rotor basis distortion analysis to be discussed later. Distortion constants of some earlier studies, as well as more recent ones employing the planar relations in the analysis, are listed in Table 8.21.

Although the form of  $\mathcal{H}_d$ , (8.55), is applicable to planar molecules with use of the planarity conditions, it is not suitable for the general case. The maximum number of quartic distortion coefficients that can be obtained from the experimental data is five, whereas  $\mathcal{H}_d$  of (8.55) contains six coefficients. Furthermore, as we shall see, use of the planarity relations usually introduces significant model errors. To remove this problem, the Hamiltonian was transformed by means of a unitary operator to a form that contains only five independent terms in the angular momenta. The coefficients of each term are combinations of the original coefficients. This reduced Hamiltonian, which has been discussed in Section 4, has been given correct to  $P^{10}$  terms in the Hamiltonian of (8.97)–(8.105)

$$\mathcal{H}^{(A)} = \mathcal{H}_r + \mathcal{H}_d \quad (8.140)$$

$$\mathcal{H}_d = \mathcal{H}_d^{(4)} + \mathcal{H}_d^{(6)} + \mathcal{H}_d^{(8)} + \mathcal{H}_d^{(10)} \quad (8.141)$$

This form is particularly suited to the empirical determination of the centrifugal distortion constants if higher-order effects are to be considered in nonplanar molecules or in planar molecules where the planarity conditions are not employed. The energy matrix, like the rigid rotor energy matrix, has only  $(K|K)$  and  $(K|K \pm 2)$  matrix elements in a symmetric rotor basis, and the Wang transformation gives four separate submatrices  $\mathbf{E}^+$ ,  $\mathbf{E}^-$ ,  $\mathbf{0}^+$ ,  $\mathbf{0}^-$  for each  $J$ , the form of which is specified by (7.22). Furthermore, the continued-fraction technique, which is particularly efficient, may be used for diagonalization of the matrix (see Appendix B). Thus, if a program applicable to calculation of the rigid rotor energy levels is available, it can be readily applied to the analysis of distortion effects by modification of the matrix elements. In particular, the matrix elements of (7.22) contain terms arising from the various distortion constants

$$E_{KK'} = (J, K | \mathcal{H} | J, K') = (J, K | \mathcal{H}_r | J, K') + (J, K | \mathcal{H}_d | J, K') \quad (8.142)$$

**Table 8.21** Rotational Distortion Constants for Some Planar Asymmetric Rotors<sup>a</sup>

Molecule	$\tau_{aaaa}$ (MHz)	$\tau_{bbbb}$ (MHz)	$\tau_{aabb}$ (MHz)	$\tau_{abab}$ (MHz)	Ref.
SO <sub>2</sub>	-10.1557	-0.0356	0.4644	-0.0485	c
O <sub>3</sub>	-23.2588	-0.0762	0.4538	-0.3009	d
OF <sub>2</sub>	-6.6154	-0.0950	0.3996	-0.1625	e
ClO <sub>2</sub>	-7.8422	-0.0433	0.4748	-0.0416	f
Cl <sub>2</sub> O	-5.3889	-0.0091	0.1146	-0.0188	g
S(CN) <sub>2</sub>	-0.5838	-0.0144	0.0833	-0.0023	h
NF <sub>2</sub>	-7.75	-0.081	0.297	-0.126	i
NOF	-15.5869	-0.0996	0.4186	-0.2896	j
NSF	-8.8343	-0.0564	0.4480	-0.0896	k
NOCl	-17.322	-0.0292	0.2555	-0.1101	l
NO <sub>2</sub> Cl	-0.0427	-0.0173	0.0038	-0.0253	m
H <sup>11</sup> BF <sub>2</sub>	-9.04	-0.0563	0.409	-0.099	n
CINCO	-59.138	-0.0107	0.6923	-0.0101	o
CHO-COOH	-0.0397	-0.0033	0.0018	-0.0368	p
<sup>11</sup> BH <sub>2</sub> OH	-25.64	-0.362	0.54	-1.676	q
ArCO <sub>2</sub>	-0.0160 <sup>b</sup>	-0.0983	0 <sup>b</sup>	-0.907	r

<sup>a</sup>The planarity conditions have been invoked in these analyses.

<sup>b</sup>Fixed.

<sup>c</sup>Kivelson [38].

<sup>d</sup>Pierce [153].

<sup>e</sup>Pierce et al. [82].

<sup>f</sup>M. G. K. Pillai and R. F. Curl, Jr., *J. Chem. Phys.*, **37**, 2921 (1962).

<sup>g</sup>Herberich et al. [138].

<sup>h</sup>L. Pierce, R. Nelson, and C. Thomas, *J. Chem. Phys.*, **43**, 3423 (1965).

<sup>i</sup>R. D. Brown, F. R. Burden, P. D. Godfrey, and I. R. Gillard, *J. Mol. Spectrosc.*, **52**, 301 (1974).

<sup>j</sup>Cook [157].

<sup>k</sup>Cook and Kirchhoff [163].

<sup>l</sup>G. Cazzoli, R. Cervellati, and A. M. Mirri, *J. Mol. Spectrosc.*, **56**, 422 (1975).

<sup>m</sup>R. R. Filgueira, P. Forti, and G. Corbelli, *J. Mol. Spectrosc.*, **57**, 97 (1975).

<sup>n</sup>Robiette and Gerry [178].

<sup>o</sup>W. H. Hocking and M. C. L. Gerry, *J. Mol. Spectrosc.*, **42**, 547 (1972).

<sup>p</sup>K. M. Marstokk and H. Møllendal, *J. Mol. Struct.*, **15**, 137 (1973).

<sup>q</sup>Y. Kawashima, H. Takeo, and C. Matsumura, *J. Chem. Phys.*, **74**, 5430 (1981).

<sup>r</sup>J. M. Steed, T. A. Dixon, and W. Klemperer, *J. Chem. Phys.*, **70**, 4095 (1979).

The matrix elements required for  $\mathcal{H}_d$  in a symmetric rotor basis are summarized in Table 8.22. Those for the rigid rotor part,  $\mathcal{H}_r$ , have been given in Chapter VII. The terms independent of  $(P_x^2 - P_y^2)$  are purely diagonal in the symmetric top basis, while those involving  $(P_x^2 - P_y^2)$  are off-diagonal with  $\Delta K = \pm 2$ .

For evaluating the centrifugal distortion constants from the rotational spectrum, two procedures are particularly convenient—a rigid rotor basis [91, 92] and a semirigid rotor basis [93] distortion analysis. The former procedure makes use of the rigid rotor basis, that is, the basis in which  $\mathcal{H}_r$  is diagonal, to derive a first-order energy expression from which the

## Chapter IX

# NUCLEAR HYPERFINE STRUCTURE IN MOLECULAR ROTATIONAL SPECTRA

---

1	INTRODUCTION	392
2	CLASSICAL HAMILTONIAN FOR NUCLEAR QUADRUPOLE COUPLING	392
3	NUCLEAR QUADRUPOLE INTERACTIONS IN FIXED MOLECULES OF SOLIDS	395
4	QUADRUPOLE INTERACTIONS BY A SINGLE COUPLING NUCLEUS IN A ROTATING MOLECULE	399
	General Theory of the Interaction	399
	Diatom and Linear Polyatomic Molecules	407
	Symmetric-top Molecules	412
	Asymmetric Rotors	413
5	QUADRUPOLE COUPLING BY MORE THAN ONE NUCLEUS IN A ROTATING MOLECULE	423
	Coupling by Two Nuclei	423
	Coupling by Three or More Nuclei	425
6	SECOND-ORDER EFFECTS IN NUCLEAR QUADRUPOLE INTERACTIONS	426
7	MAGNETIC HYPERFINE STRUCTURE OF MOLECULES IN SINGLET $\Sigma$ STATES	429
	Theory of Magnetic Interaction	429
	Diatom and Linear Polyatomic Molecules	432
	Symmetric-top Molecules	433
	Asymmetric Rotors	435
8	PLURAL NUCLEAR COUPLING—QUADRUPOLE AND MAGNETIC	436
	Hybrid Coupling by Two Nuclei: Strong Quadrupole and Weak Magnetic Coupling	436
	Coupings of Comparable Strength	437
	Coupling by Identical Nuclei	440
	Spin-Spin Interactions	441
	Observed Spectra in Asymmetric Rotors—Maser Resolutions	441
9	MOLECULES WITH UNBALANCED ELECTRONIC ANGULAR MOMENTUM	444
10	MOLECULES IN EXCITED VIBRATIONAL STATES	444
11	SELECTION RULES AND RELATIVE INTENSITIES OF HYPERFINE COMPONENTS	445

## 1 INTRODUCTION

Nuclear hyperfine structure in molecular rotational spectra may arise from either magnetic or electric interactions of the molecular fields with the nuclear moments, or from a combination of the two. The most important of these interactions is that of the molecular field gradient with the electric quadrupole moments of the nuclei. Such an interaction is not possible, however, for isotopes with nuclear spins of 0 or  $\frac{1}{2}$  since such nuclei are spherically symmetric and hence have no quadrupole moments. The nuclear quadrupole hyperfine structure provides a measure of the molecular field gradients from which much information about the electronic structure and chemical bonds can be obtained. Nuclear quadrupole interaction in molecules was first detected in molecular beam experiments on diatomic molecules in the radiofrequency region [1, 2]. The basic theory worked out by Casimer<sup>3</sup> was extended to diatomic molecules by Nordsieck [4] and by Feld and Lamb [5]. The first detection of quadrupole hyperfine structure in the microwave region was that of the ammonia inversion spectrum by Good [6]. The theory for the interaction was extended to symmetric tops by Coles and Good [7] and by Van Vleck [8], to asymmetric rotors by Bragg and Golden [9, 10].

Practically all stable molecules, particularly organic molecules, have singlet  $\Sigma$  electronic ground states. All their electrons are paired, either in the atomic subshells or in the molecular orbital valence shells, so that in the first-order approximation their electronic magnetism whether from electronic spin or from orbital motion is canceled. When the molecules are not rotating, the molecular magnetism is canceled even in the higher orders of approximation. The end-over-end rotation of the molecule, however, generates weak magnetic fields which can interact with the nuclear magnetic moments to produce a slight magnetic splitting or displacement of the lines. Although the complexity of this slight magnetic field generated by rotation usually prevents measurements sufficiently accurate to give reliable information about chemical bonding like that given by nuclear quadrupole interactions, one must evaluate these small magnetic displacements when they are evident if the evaluation of the nuclear quadrupole coupling and rotational constants is to be the most precise. A general theory for nuclear magnetic interactions of rotating molecules in  $\Sigma$  singlet states has been worked out by Gunther-Mohr et al. [11].

For convenience in the prediction of hyperfine structure we have provided a table of nuclear moments (Appendix E).

## 2 CLASSICAL HAMILTONIAN FOR NUCLEAR QUADRUPOLE COUPLING

The nuclear quadrupole interaction results from a nonspherical distribution of nuclear charge which gives rise to a nuclear quadrupole moment and a nonspherical distribution of electronic charge about the nucleus which gives rise to an electric field gradient at the nucleus. If either the nuclear charge or the

electronic charge about the nucleus is spherically symmetric, no such interaction is observed. The interaction puts a twisting torque on the nucleus, tending to align its spin moment in the direction of the field gradient. As a result of this torque, the spin axis will precess about the direction of the resultant field gradient, giving rise to precessional frequencies and nuclear quadrupole spectra. In solids, the field gradients are fixed in direction, and pure nuclear quadrupole spectra analogous to nuclear magnetic resonance are observable. In gases, the field gradients at the nucleus depend on the rotational state of the molecule; the nuclear quadrupole interaction differs for each rotational state and leads to a hyperfine structure of the rotational levels.

Let us first consider the classical interaction energy of a nuclear charge with a static potential  $V$  arising from extranuclear charges. Suppose  $V(XYZ)$  to be the potential at a point with coordinates  $X, Y, Z$  in a cartesian system fixed in space and having its origin at the center of the nucleus, as indicated in Fig. 9.1. The value of  $V$  at the origin is  $V_0$ . To a first approximation, the electrical energy is  $ZeV_0$ , the usual energy that holds the electrons in their orbits. Because of the finite size of the nucleus, however, the electrical energy is correctly expressed by

$$E = \int \rho_n V d\tau_n \quad (9.1)$$

where  $\rho_n = \rho(X, Y, Z)$  represents the density of the nuclear charge in the elemental volume  $d\tau_n = dX dY dZ$  and where the integration is taken over the

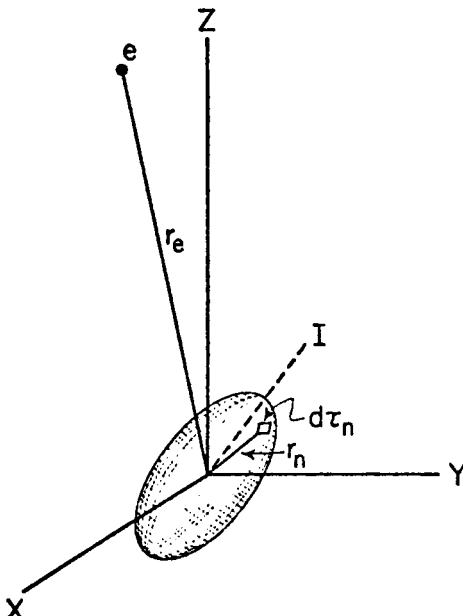


Fig. 9.1 Reference system for expressing nuclear interaction with extra-nuclear charges.

nuclear volume. The charge density  $\rho_n$  can be taken as uniform throughout the volume. In evaluation of the integral it is convenient to express the potential as a Taylor's expansion. In this expansion,

$$\begin{aligned} V = V_0 + & \left( \frac{\partial V}{\partial X} \right)_0 X_n + \left( \frac{\partial V}{\partial Y} \right)_0 Y_n + \left( \frac{\partial V}{\partial Z} \right)_0 Z_n + \frac{1}{2} \left( \frac{\partial^2 V}{\partial X^2} \right)_0 X_n^2 \\ & + \frac{1}{2} \left( \frac{\partial^2 V}{\partial Y^2} \right)_0 Y_n^2 + \frac{1}{2} \left( \frac{\partial^2 V}{\partial Z^2} \right)_0 Z_n^2 + \left( \frac{\partial^2 V}{\partial X \partial Y} \right)_0 X_n Y_n \\ & + \left( \frac{\partial^2 V}{\partial X \partial Z} \right)_0 X_n Z_n + \left( \frac{\partial^2 V}{\partial Y \partial Z} \right)_0 Y_n Z_n \dots \end{aligned} \quad (9.2)$$

where  $X_n = \Delta X$ ,  $Y_n = \Delta Y$ , and  $Z_n = \Delta Z$  represent the nuclear coordinates at the point of the elemental volume  $d\tau_n$  in the nucleus. Substitution of  $V$  from (9.2) into (9.1) shows the first term in the expansion

$$E_0 = V_0 \int \rho_n d\tau_n \quad (9.3)$$

to be the usual monopole interaction which is independent of nuclear orientation. The second or dipole term,

$$E_d = \left( \frac{\partial V}{\partial X} \right)_0 \int X_n \rho_n d\tau_n + \left( \frac{\partial V}{\partial Y} \right)_0 \int Y_n \rho_n d\tau_n + \left( \frac{\partial V}{\partial Z} \right)_0 \int Z_n \rho_n d\tau_n = 0 \quad (9.4)$$

vanishes because  $\rho(X, Y, Z)$  is a symmetric function, and the integral with + and - values of the coordinates cancels. This is in agreement with the fact that no nuclear electric dipole moment has ever been observed experimentally. The term of next higher order represents the quadrupole interaction,

$$\begin{aligned} E_Q = & \frac{1}{2} \left( \frac{\partial^2 V}{\partial X^2} \right)_0 \int \rho_n X_n^2 d\tau_n + \frac{1}{2} \left( \frac{\partial^2 V}{\partial Y^2} \right)_0 \int \rho_n Y_n^2 d\tau_n \\ & + \frac{1}{2} \left( \frac{\partial^2 V}{\partial Z^2} \right)_0 \int \rho_n Z_n^2 d\tau_n + \left( \frac{\partial^2 V}{\partial X \partial Y} \right)_0 \int \rho_n X_n Y_n d\tau_n \\ & + \left( \frac{\partial^2 V}{\partial X \partial Z} \right)_0 \int \rho_n X_n Z_n d\tau_n + \left( \frac{\partial^2 V}{\partial Y \partial Z} \right)_0 \int \rho_n Y_n Z_n d\tau_n \end{aligned} \quad (9.5)$$

Let us now choose a body-fixed system  $x, y, z$  with  $z$  along the spin axis **I**. As a consequence of rotational symmetry about the spin axis;  $x, y, z$  are principal axes; the integrals of the cross terms vanish; and

$$\int \rho_n x_n^2 d\tau_n = \int \rho_n y_n^2 d\tau_n = \frac{1}{2} \int \rho_n (x_n^2 + y_n^2) d\tau_n = \frac{1}{2} \int \rho_n (r_n^2 - z_n^2) d\tau_n \quad (9.6)$$

Consequently, (9.5) can be expressed as

$$E_Q = \frac{1}{4} \left[ \left( \frac{\partial^2 V}{\partial x^2} \right)_0 + \left( \frac{\partial^2 V}{\partial y^2} \right)_0 \right] \int \rho_n (r_n^2 - z_n^2) d\tau_n + \frac{1}{2} \left( \frac{\partial^2 V}{\partial z^2} \right)_0 \int \rho_n z_n^2 d\tau_n \quad (9.7)$$

Because the charge giving rise to the field gradient can be considered to be zero over the nuclear volume, Laplace's equation  $\nabla^2 V = 0$  holds, and

$$\left(\frac{\partial^2 V}{\partial x^2}\right)_0 + \left(\frac{\partial^2 V}{\partial y^2}\right)_0 = - \left(\frac{\partial^2 V}{\partial z^2}\right)_0 \quad (9.8)$$

With this relation, the classical interaction can be expressed as

$$E_Q = \frac{1}{4} \left( \frac{\partial^2 V}{\partial z^2} \right)_0 \int \rho_n (3z_n^2 - r_n^2) d\tau_n \quad (9.9)$$

The quantity

$$Q^* = \frac{1}{e} \int \rho_n (3z_n^2 - r_n^2) d\tau_n \quad (9.10)$$

is defined as the intrinsic nuclear quadrupole moment. Hence

$$E_Q = \frac{1}{4} \left( \frac{\partial^2 V}{\partial z^2} \right)_0 e Q^* \quad (9.11)$$

In this classical expression  $z$  is along the spin axis. Quantum mechanically, however, the spin  $\mathbf{I}$  and  $Q^*$  are not observable quantities since only  $\mathbf{I}^2$  and its components along a fixed direction in space have eigenvalues. However, the value of  $Q^*$  can be obtained from the observable quantity  $Q$  with the relationship, (9.20), derived later.  $Q^*$  is a measure of the deviation of the nuclear shape from spherical symmetry. A positive  $Q^*$  indicates that the nucleus is elongated along the spin axis, is prolate; a negative  $Q^*$  indicates that the nucleus is flattened along this axis, is oblate. For a spherical nucleus  $Q^*$  vanishes.

### 3 NUCLEAR QUADRUPOLE INTERACTIONS IN FIXED MOLECULES OF SOLIDS

Let us now transform the field gradient of (9.11) to a space-fixed system  $X, Y, Z$ , with its origin at the center of the nucleus and chosen so that  $X, Y$ , and  $Z$  are principal axes of the field gradient. In the principal system the cross terms vanish, and the transformation is expressed by

$$\begin{aligned} \frac{\partial^2 V}{\partial z^2} &= \frac{\partial^2 V}{\partial X^2} \left( \frac{\partial X}{\partial z} \right)^2 + \frac{\partial^2 V}{\partial Y^2} \left( \frac{\partial Y}{\partial z} \right)^2 + \frac{\partial^2 V}{\partial Z^2} \left( \frac{\partial Z}{\partial z} \right)^2 \\ &= \frac{\partial^2 V}{\partial X^2} \left( \frac{I_X}{|\mathbf{I}|} \right)^2 + \frac{\partial^2 V}{\partial Y^2} \left( \frac{I_Y}{|\mathbf{I}|} \right)^2 + \frac{\partial^2 V}{\partial Z^2} \left( \frac{I_Z}{|\mathbf{I}|} \right)^2 \end{aligned} \quad (9.12)$$

The last form follows from the fact that  $\mathbf{I}$  is along  $z$  and  $I_X, I_Y$ , and  $I_Z$  are components of  $\mathbf{I}$ ; hence the direction cosines are

$$\frac{\partial X}{\partial z} = \cos(X, z) = \frac{I_X}{|\mathbf{I}|}, \dots \quad (9.13)$$

By treating the spin components as quantum mechanical operators and substituting for  $\mathbf{I}^2$  its eigenvalue  $I(I+1)$ , one can obtain a spin Hamiltonian operator by substitution of (9.12) into (9.11). Thus

$$\mathcal{H}_Q = \frac{eQ^*}{4I(I+1)} \left[ \left( \frac{\partial^2 V}{\partial X^2} \right)_0 I_X^2 + \left( \frac{\partial^2 V}{\partial Y^2} \right)_0 I_Y^2 + \left( \frac{\partial^2 V}{\partial Z^2} \right)_0 I_Z^2 \right] \quad (9.14)$$

When the field gradient is axially symmetric about  $Z$ ,

$$\left( \frac{\partial^2 V}{\partial X^2} \right)_0 = \left( \frac{\partial^2 V}{\partial Y^2} \right)_0 = -\frac{1}{2} \left( \frac{\partial^2 V}{\partial Z^2} \right)_0 \quad (9.15)$$

where use is made of Laplace's equation  $\nabla^2 V = 0$ . With (9.15) and  $I^2 = I_X^2 + I_Y^2 + I_Z^2$ , (9.14) becomes, for the axially symmetric coupling,

$$\mathcal{H}_Q = \frac{eQ^*}{8I(I+1)} \left( \frac{\partial^2 V}{\partial Z^2} \right)_0 (3I_Z^2 - I^2) \quad (9.16)$$

and

$$(E_Q)_{M_I} = \frac{eQ^*(\partial^2 V / \partial Z^2)_0}{8I(I+1)} [3M_I^2 - I(I+1)] \quad (9.17)$$

where  $M_I$  is the eigenvalue of  $I_Z$  in units of  $\hbar$ . Except for the use of the intrinsic quadrupole moment  $Q^*$ , (9.14) and (9.16) are the usual Hamiltonians for pure quadrupole resonance in the solid state.

A simple, if not rigorous, derivation of the relationship between  $Q^*$  and the observable  $Q$  can be found by comparison of (9.17) with the classical energy, (9.11), derived for axially symmetric coupling about  $z$ , the spin axis. Conventionally,  $Q$  is defined as the effective component for the most complete alignment along  $Z$ , that is, the component for  $M_I = I$ . From (9.17),

$$(E_Q)_{M_I=I} = \frac{eQ^*(\partial^2 V / \partial Z^2)_0 (2I-1)}{8(I+1)} \quad (9.18)$$

Since the effective quadrupole moment for coupling with  $(\partial^2 V / \partial Z^2)$  is  $Q$ , the coupling energy found by analogy with (9.11) is

$$E_Q = \frac{1}{4} \left( \frac{\partial^2 V}{\partial Z^2} \right)_0 eQ \quad (9.19)$$

Equation of this energy to  $(E_Q)_{M_I=I}$  from (9.18) yields

$$Q^* = \frac{2(I+1)}{(2I-1)} Q \quad (9.20)$$

Substitution of this value into (9.14) gives the solid state Hamiltonian operator in the form

$$\mathcal{H}_Q = \frac{1}{2I(2I-1)} (\chi_{XX} I_X^2 + \chi_{YY} I_Y^2 + \chi_{ZZ} I_Z^2) \quad (9.21)$$

where the customary designations for the principal values of the coupling constants have been made:

$$\chi_{xx} \equiv eQq_{xx}, \quad \chi_{yy} \equiv eQq_{yy}, \quad \chi_{zz} \equiv eQq_{zz} \quad (9.22)$$

where

$$q_{xx} \equiv \left( \frac{\partial^2 V}{\partial X^2} \right)_0, \quad q_{yy} \equiv \left( \frac{\partial^2 V}{\partial Y^2} \right)_0, \quad q_{zz} \equiv \left( \frac{\partial^2 V}{\partial Z^2} \right)_0 \quad (9.23)$$

With axial symmetry about  $Z$ , it is evident from (9.17) that

$$E_Q = \frac{\chi_{zz}}{4I(2I-1)} [3M_I^2 - I(I+1)] \quad (9.24)$$

where

$$M_I = I, I-1, I-2, \dots, -I \quad (9.25)$$

In the general case when there is no axial symmetry, the secular equation must be set up and solved as described in Chapter II, Section 4, or perturbation methods must be used. The required matrix elements of the squared operators of (9.21) are

$$\begin{aligned} (I, M_I | I_Z^2 | I, M_I) &= M_I^2 \\ (I, M_I | I_X^2 | I, M_I) &= (I, M_I | I_Y^2 | I, M_I) = \frac{1}{2}[I(I+1) - M_I^2] \\ (I, M_I | I_X^2 | I, M_I \pm 2) &= -(I, M_I | I_Y^2 | I, M_I \pm 2) \\ &= -\frac{1}{4}[I(I+1) - M_I(M_I \pm 1)]^{1/2} \\ &\times [I(I+1) - (M_I \pm 1)(M_I \pm 2)]^{1/2} \end{aligned} \quad (9.26)$$

These matrix elements have the same form as those for  $P_x^2$ ,  $P_y^2$ , and  $P_z^2$  in the symmetric-top representation if  $I$  is identified with  $J$  and  $M_I$  with  $K$ . However,  $I$  and  $M_I$  may have half-integral as well as integral values, whereas  $J$  and  $K$  have only integral values. Note that (9.21) for  $\mathcal{H}_Q$  has the same form as the Hamiltonian for the rigid asymmetric rotor if the couplings are related to the moments of inertia by

$$\frac{\chi_{xx}}{2I(2I-1)} \rightarrow \frac{1}{2I_x}, \quad \frac{\chi_{yy}}{2I(2I-1)} \rightarrow \frac{1}{2I_y}, \quad \frac{\chi_{zz}}{2I(2I-1)} \rightarrow \frac{1}{2I_z} \quad (9.27)$$

With these relations the various solutions already obtained for the rigid asymmetric rotor can be used for the finding of quadrupole coupling energies for integral spin values. This relationship was first pointed out by Bersohn [12]. Because the values of  $I$  are small, exceeding  $\frac{9}{2}$  for only a very few isotopes, the problem of finding the quadrupole coupling energies in solid state asymmetric field gradients is simpler than that of calculating the energies of the asymmetric rotor for which populated states with high values are possible. Solutions for various spin values are given by Cohen and Reif [13] and by Das and Hahn [14].

Frequently, the field gradient is almost axially symmetric, if not completely so, about a bond to the coupling atom. Such cases are most conveniently

treated by perturbation theory in a manner similar to that for treatment of the slightly asymmetric rotor. The most nearly symmetric axis is defined as the  $Z$  axis, and the asymmetry parameter is defined by

$$\eta = \frac{\chi_{xx} - \chi_{yy}}{\chi_{zz}} \quad (9.28)$$

Because Laplace's equation holds,  $\chi_{xx} + \chi_{yy} + \chi_{zz} = 0$ , there are only two independent coupling parameters. These are chosen as  $\chi_{zz}$  and  $\eta$ . The Hamiltonian can then be expressed so that the off-diagonal terms contain  $\eta$  as a coefficient. The off-diagonal terms can then be evaluated with perturbation theory. The asymmetry parameter  $\eta$  has been related by Das and Hahn [14] to the asymmetry parameter  $b$  of the slightly asymmetric rotor so that the energy formula for the slightly asymmetric rotor (Chapter VII) can be used to give the quadrupole energies when  $\eta \ll 1$ .

Transitions between the quadrupole hyperfine levels in solids can be observed through coupling of the magnetic dipole moment of the nucleus to the radiation field. The selection rule for pure quadrupole absorption spectra is  $|\Delta M_I| = 1$ . For an axially symmetric field, the frequencies from (9.24) are

$$\nu = |\chi_{zz}| \left[ \frac{3}{4I(2I-1)} \right] (2|M_I|-1) \quad (9.29)$$

where  $M_I$  is the larger of the two quantum numbers involved. Figure 9.2 shows an energy level diagram indicating the transitions and pure quadrupole spectrum for a nucleus with spin  $I = \frac{7}{2}$  which is in an axially symmetric field.

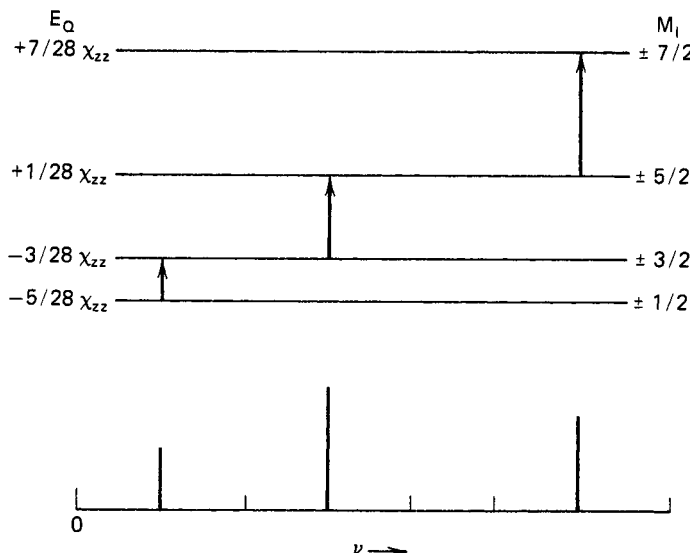


Fig. 9.2 Energy level diagram and predicted pure quadrupole resonance spectrum for a nucleus with spin  $I = \frac{7}{2}$ .

Pure quadrupole resonance frequencies of solids, first detected by Dehmelt and Krüger [15], generally occur at radiofrequencies below those of the microwave region. For this reason we shall not discuss them further. Comprehensive treatments are given by Cohen and Reif [13], and by Das and Hahn [14]. The coupling values obtained are closely related to those measured by microwave spectroscopy of gases, and in Chapter XIV we shall discuss some of the solid-state results. Pure quadrupole resonance in solids is a simpler phenomenon than quadrupole coupling in gases, where the coupling gradient is a function of the rotational state. This is particularly true when there is more than one coupling nucleus in the molecule. In solids, the interaction of one nucleus does not perturb the field gradient at the other coupling nuclei, and the theory derived for a single coupling nucleus applies when there are other coupling nuclei in the same molecule. In contrast, plural coupling greatly complicates the problem in rotating molecules.

#### 4 QUADRUPOLE INTERACTIONS BY A SINGLE COUPLING NUCLEUS IN A ROTATING MOLECULE

##### General Theory of the Interaction

The quadrupole coupling of a nucleus in a rotating molecule of a gas is more complicated than that in frozen molecules of a solid because the field gradients depend upon the rotation. For an external-field-free molecule, the nuclear spin **I** is coupled to the molecular rotational angular momentum **J** to form a resultant **F**. In the vector model, **J** and **I** can be considered as precessing about **F**, as indicated in Fig. 9.3. The total angular momentum of the molecule with nuclear coupling is thus represented by **F** rather than **J**, which designates the total angular momentum exclusive of nuclear spin. However, in the first-order treatment, which is adequate for most coupling cases,  $\mathbf{J}^2$  is still a constant of the motion. The good quantum numbers are thus  $F$ ,  $M_F$ ,  $J$ , and  $I$ . The new angular momentum quantum numbers are

$$F = J + I, J + I - 1, J + I - 2, \dots, |J - I| \quad (9.30)$$

and

$$M_F = F, F - 1, F - 2, \dots, -F \quad (9.31)$$

where  $J$  and  $I$  have the values assigned previously in Chapter II. In units of  $\hbar$  the eigenvalues of the square of the total angular momentum and its components along an axis in space are

$$(F, M_F | \mathbf{F}^2 | F, M_F) = F(F+1) \quad (9.32)$$

$$(F, M_F | F_Z | F, M_F) = M_F \quad (9.33)$$

Let us consider again the general expansion of (9.5) for the classical quadrupole interaction. By subtraction and addition of  $\frac{1}{6}\nabla^2 V \int \rho_n R_n^2 d\tau_n$  to the right

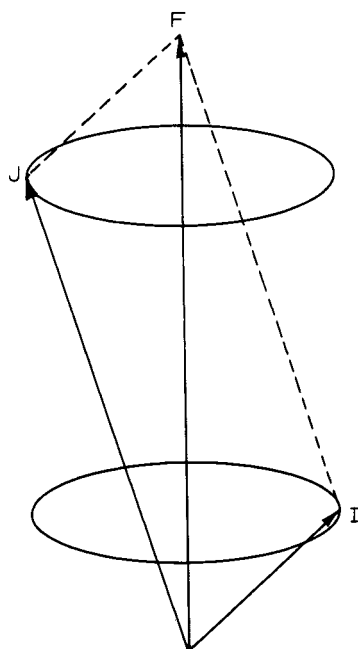


**Fig. 9.3** Vector diagram of coupling of a nuclear spin  $\mathbf{I}$  with molecular rotational momentum  $\mathbf{J}$ .

side, this expression can be put into the form:

$$\begin{aligned}
 E_Q = & \frac{1}{6} \left[ \left( \frac{\partial^2 V}{\partial X^2} \right)_0 \int (3X_n^2 - R_n^2) \rho_n d\tau_n + \left( \frac{\partial^2 V}{\partial Y^2} \right)_0 \int (3Y_n^2 - R_n^2) \rho_n d\tau_n \right. \\
 & + \left( \frac{\partial^2 V}{\partial Z^2} \right)_0 \int (3Z_n^2 - R_n^2) \rho_n d\tau_n + 6 \left( \frac{\partial^2 V}{\partial X \partial Y} \right)_0 \int X_n Y_n \rho_n d\tau_n \\
 & + 6 \left( \frac{\partial^2 V}{\partial X \partial Z} \right)_0 \int X_n Z_n \rho_n d\tau_n + 6 \left( \frac{\partial^2 V}{\partial Y \partial Z} \right)_0 \int Y_n Z_n \rho_n d\tau_n \Big] \\
 & + \frac{1}{6} \left[ \left( \frac{\partial^2 V}{\partial X^2} \right)_0 + \left( \frac{\partial^2 V}{\partial Y^2} \right)_0 + \left( \frac{\partial^2 V}{\partial Z^2} \right)_0 \right] \int R_n^2 \rho_n d\tau_n
 \end{aligned} \tag{9.34}$$

For reasons already given, Laplace's equation  $\nabla^2 V = 0$  holds over the nuclear volume; hence the last term is vanishingly small and can be omitted. The remaining expression can be written as the scalar product (double-dot product) of two symmetric dyadics

$$E_Q = -\frac{1}{6} \mathbf{Q} : \nabla \mathbf{E} = \frac{1}{6} \sum_{i,j=X,Y,Z} Q_{ij} V_{ij} \tag{9.35}$$

where  $V_{ij} = -\nabla E_{ij}$  and where the dyadic  $\nabla \mathbf{E}$  is the gradient of the electric field

of the extra nuclear charges

$$\nabla \mathbf{E} = e_x \frac{\partial \mathbf{E}}{\partial X} + e_y \frac{\partial \mathbf{E}}{\partial Y} + e_z \frac{\partial \mathbf{E}}{\partial Z} \quad (9.36)$$

and  $\mathbf{Q}$  is the quadrupole moment dyadic

$$\mathbf{Q} = \int \rho_n [3\mathbf{R}_n \mathbf{R}_n - \mathbb{I} R_n^2] d\tau_n \quad (9.37)$$

Here  $\mathbf{R}_n$  represents the vector locating points of the nuclear volume in the space-fixed  $X$ ,  $Y$ ,  $Z$  reference system.  $\mathbb{I} = e_x e_x + e_y e_y + e_z e_z$  is the unit dyadic and  $e_x$ ,  $e_y$ , and  $e_z$  are unit vectors along  $X$ ,  $Y$ , and  $Z$ .

We now develop the quantum mechanical operator for the quadrupole interaction energy. The potential  $V$  at the nucleus arises from all the various extra nuclear charges of the molecule, but we need consider only the extra nuclear electrons since the charges of other nuclei are well screened. We can therefore express the potential as

$$V = \sum_k e \left( \frac{1}{R_e} \right)_k \quad (9.38)$$

where  $(1/R_e)_k$  represents the distance from the  $k$ th electron to the nucleus and where the summation is taken over all electrons contributing to  $V$ . Let us substitute this value of  $V$  into the tensor  $V_{ij}$ . We consider only one component because the transformations of other components of the tensor are similar. Since

$$\frac{\partial^2}{\partial X^2} \left( \frac{1}{R} \right) = \left( \frac{\partial^2}{\partial X^2} \right) (X^2 + Y^2 + Z^2)^{-1/2} = \left( \frac{3X^2 - R^2}{R^5} \right) \quad (9.39)$$

Thus it is evident that

$$\begin{aligned} V_{XX} &= \left( \frac{\partial^2 V}{\partial X^2} \right)_0 = e \sum_k \left\langle \left( \frac{1}{R_e^3} \right)_k \right\rangle \left\langle \left[ 3 \left( \frac{X_e}{R_e} \right)^2 - 1 \right]_k \right\rangle \\ &= e \sum_k \left\langle \left( \frac{1}{R_e^3} \right)_k \right\rangle \langle (3 \cos^2 \theta_X - 1)_k \rangle \end{aligned} \quad (9.40)$$

where  $\theta_X$  is the angle between  $R_e$  and the  $X$  axis fixed in space (see Fig. 9.1). The average is taken over the electronic orbitals and over the vibrational and rotational states of the molecule. However,  $\langle (1/R_e^3)_k \rangle$  is independent of the rotation and in a particular vibrational state may be treated as a constant. We can then write

$$V_{XX} = \sum_k C_k \left\langle \left( \frac{3X_e^2}{R_e^2} - 1 \right)_k \right\rangle \quad (9.41)$$

Because the orbitals of all the electrons are fixed in the molecule and rotate with the molecular frame about the axis of  $\mathbf{J}$ , the angular dependence of their averaged sum will be the same as that of  $\mathbf{J}$ , and their resultant field gradient

will resolve along space-fixed axes in the same proportions as the components of  $\mathbf{J}$ ; the rapid rotation about  $\mathbf{J}$  will effectively average out the components of the field gradient perpendicular to  $\mathbf{J}$  and make  $\mathbf{J}$  an axis of symmetry for the gradient. From (9.41) one thus obtains

$$(V_{XX})_{\text{op}} = C \left( 3 \frac{J_X^2}{\mathbf{J}^2} - 1 \right) \quad (9.42)$$

where  $C$  is a proportionality constant to be evaluated, a constant which depends on the electronic distribution in the whole molecule but primarily in the atom of the particular coupling nucleus. In units of  $\hbar$ , the eigenvalues of  $\mathbf{J}^2$  are  $J(J+1)$ , and hence (9.42) can be written

$$(V_{XX})_{\text{op}} = \frac{C}{J(J+1)} [3J_X^2 - J(J+1)] \quad (9.43)$$

The expressions for  $V_{YY}$  and  $V_{ZZ}$  are similar. Because the component operators do not commute, however, the analogous operators for the cross-product terms must be symmetrized. For example,

$$V_{XY} = \sum_k C_k \left\langle \left( 3 \frac{X_e Y_e}{R_e^2} \right)_k \right\rangle \quad (9.44)$$

and the conjugate operator is

$$(V_{XY})_{\text{op}} = \frac{C}{J(J+1)} \left( 3 \frac{J_X J_Y + J_Y J_X}{2} \right) \quad (9.45)$$

It is customary to evaluate the constant  $C$  by defining the coupling constant  $q_J$  as that observed for the maximum projection of  $\mathbf{J}$  along a space-fixed axis, that is, for the state  $M_J = J$ . Hence from the  $ZZ$  component

$$q_J = (J, J | V_{ZZ} | J, J) = \frac{C}{J(J+1)} [3J^2 - J(J+1)] \quad (9.46)$$

and

$$C = \frac{J+1}{2J-1} q_J \quad (9.47)$$

Hence

$$(V_{ZZ})_{\text{op}} = \frac{q_J}{J(2J-1)} [3J_Z^2 - J(J+1)] \quad (9.48)$$

The generalized expression for the elements of the tensor operator of the field gradient is consequently

$$-(\nabla E_{ij})_{\text{op}} = (V_{ij})_{\text{op}} = \frac{q_J}{J(2J-1)} \left( 3 \frac{J_i J_j + J_j J_i}{2} - \delta_{ij} \mathbf{J}^2 \right) \quad (9.49)$$

where  $i, j = X, Y$ , or  $Z$  and  $\delta_{ij} = 1$  when  $i = j$  and 0 when  $i \neq j$ .

Since the nuclear quadrupole tensor  $Q_{ij}$ , (9.37), has rotational symmetry about the spin axis, it can be treated in a manner similar to  $V_{ij}$ . Accordingly, the nuclear quadrupole operator can be expressed as

$$(Q_{ij})_{\text{op}} = C_n \left( 3 \frac{I_i I_j + I_j I_i}{2} - \delta_{ij} \mathbf{I}^2 \right) \quad (9.50)$$

where  $C_n$  is the proportionality constant evaluated by definition of  $Q$  as the value for maximum resolution along a space-fixed axis, that is, when  $M_I = I$ . Thus

$$eQ \equiv (I, I | Q_{zz} | I, I) = C_n (I, I | 3I_z^2 - I(I+1) | I, I) = C_n [3I^2 - I(I+1)] \quad (9.51)$$

Therefore

$$C_n = \frac{eQ}{I(2I-1)} \quad (9.52)$$

and

$$(Q_{ij})_{\text{op}} = \frac{eQ}{I(2I-1)} \left( 3 \frac{I_i I_j + I_j I_i}{2} - \delta_{ij} \mathbf{I}^2 \right). \quad (9.53)$$

Substitution of the operators of (9.49) and (9.53) into (9.35) yields the Hamiltonian operator for the quadrupole interaction

$$\mathcal{H}_Q = \frac{1}{6} \frac{eq_J Q}{J(2J-1)I(2I-1)} \sum_{i,j=X,Y,Z} \left( 3 \frac{I_i I_j + I_j I_i}{2} - \delta_{ij} \mathbf{I}^2 \right) \left( 3 \frac{J_i J_j + J_j J_i}{2} - \delta_{ij} \mathbf{J}^2 \right) \quad (9.54)$$

If the indicated multiplication is performed and the results expressed in terms of vector products, this Hamiltonian can be put into a more convenient form. Because the components of  $\mathbf{I}$  commute with those of  $\mathbf{J}$ , the term

$$\begin{aligned} \sum_{i,j} I_i I_j J_i J_j &= \sum_i (I_i J_i) \sum_j (I_j J_j) \\ &= (I_X J_X + I_Y J_Y + I_Z J_Z)(I_X J_X + I_Y J_Y + I_Z J_Z) = (\mathbf{I} \cdot \mathbf{J})^2 \end{aligned} \quad (9.55)$$

The sum of all such terms is  $\frac{9}{2}(\mathbf{I} \cdot \mathbf{J})^2$ . Because  $\delta_{ij}=0$  when  $i \neq j$ , the terms

$$\begin{aligned} - \sum_{i,j} \frac{3}{2}(J_i J_j + J_j J_i) \delta_{ij} \mathbf{I}^2 &= -3 \mathbf{J}^2 \mathbf{I}^2 \\ - \sum_{i,j} \frac{3}{2}(I_i I_j + I_j I_i) \delta_{ij} \mathbf{J}^2 &= -3 \mathbf{J}^2 \mathbf{I}^2 \end{aligned}$$

and

$$\sum_{i,j} \delta_{ij} \mathbf{I}^2 \delta_{ij} \mathbf{J}^2 = 3 \mathbf{J}^2 \mathbf{I}^2 \quad (9.56)$$

Because the components of  $\mathbf{J}$  and of  $\mathbf{I}$  do not commute among themselves, that is,  $J_i J_j \neq J_j J_i$  and  $I_i I_j \neq I_j I_i$  when  $i \neq j$ , the commutation rules given in Chapter II must be applied for evaluation of the remaining terms which are of the form  $I_i I_j J_j J_i$ . The transformations, which are rather lengthy, are given by Ramsey [16]. The results are

$$\sum_{i,j} I_i I_j J_j J_i = (\mathbf{I} \cdot \mathbf{J})^2 + \mathbf{I} \cdot \mathbf{J} \quad (9.57)$$

and the total of such terms is  $\frac{9}{2}[(\mathbf{I} \cdot \mathbf{J})^2 + (\mathbf{I} \cdot \mathbf{J})]$ . Collection of all these terms, with slight simplification, yields the quadrupole Hamiltonian in the compact form,

$$\mathcal{H}_Q = \frac{eQq_J}{2J(2J-1)I(2I-1)} [3(\mathbf{I} \cdot \mathbf{J})^2 + \frac{3}{2}\mathbf{I} \cdot \mathbf{J} - \mathbf{I}^2 \mathbf{J}^2] \quad (9.58)$$

This Hamiltonian, originally derived by Casimer [3], is applicable to a coupling nucleus in any type of molecule, or to a free atom if  $\mathbf{J}$  is treated as the total electronic angular momentum exclusive of nuclear spin. The quantity  $q_J$  depends on the particular type of molecule, whether linear, symmetric rotor, or asymmetric rotor.

The advantage of the general Hamiltonian of (9.58) is that its eigenvalues for the terms in the bracket can be obtained easily for the field-free rotor in which  $\mathbf{J}$  and  $\mathbf{I}$  are coupled to form a resultant  $\mathbf{F}$ , as indicated in Fig. 9.3. Since  $\mathbf{F}$  is the vector sum of  $\mathbf{J}$  and  $\mathbf{I}$ ,

$$\mathbf{F}^2 = (\mathbf{J} + \mathbf{I})^2 = \mathbf{J}^2 + 2\mathbf{I} \cdot \mathbf{J} + \mathbf{I}^2 \quad (9.59)$$

and

$$\mathbf{I} \cdot \mathbf{J} = \frac{1}{2}(\mathbf{F}^2 - \mathbf{J}^2 - \mathbf{I}^2) \quad (9.60)$$

The eigenvalues of  $\mathbf{I} \cdot \mathbf{J}$  are therefore

$$(F, J, I | \mathbf{I} \cdot \mathbf{J} | F, J, I) = \frac{1}{2}[F(F+1) - J(J+1) - I(I+1)] = \frac{1}{2}C \quad (9.61)$$

and

$$(F, J, I | (\mathbf{I} \cdot \mathbf{J})^2 | F, J, I) = \frac{1}{4}C^2 \quad (9.62)$$

Substitution of these values with  $\mathbf{J}^2 \mathbf{I}^2 = J(J+1)I(I+1)$  into (9.58) yields

$$E_Q = \frac{eQq_J}{2J(2J-1)I(2I-1)} [\frac{3}{4}C(C+1) - J(J+1)I(I+1)] \quad (9.63)$$

where

$$C = F(F+1) - J(J+1) - I(I+1) \quad (9.64)$$

Let us now evaluate the quantity  $q_J$ . To do this we must first transform the field gradient to a reference system fixed in the molecule. Although later transformations will be made to special axes chosen to coincide with the bond axis to the coupling nucleus, the principal inertial axes  $a$ ,  $b$ ,  $c$  at this stage in the

development have the advantage of applying to molecules of all classes. The cross terms in the field gradient, such as  $(\partial^2 V / \partial a \partial b)$ , vanish when averaged over the rotational state, as will be explained later.

As defined previously,

$$q_J = \left\langle \left( \frac{\partial^2 V}{\partial Z^2} \right)_0 \right\rangle_{M_J=J} = \int \psi_{J,i}^{* M_J=J} \frac{\partial^2 V}{\partial Z^2} \psi_{J,i}^{M_J=J} d\tau = \left\langle J, i, J \left| \frac{\partial^2 V}{\partial Z^2} \right| J, i, J \right\rangle \quad (9.65)$$

where  $Z$  is fixed in space and where  $i$  represents any internal rotational quantum numbers such as  $K$ . In the inertial axes  $a, b, c$ ,

$$\begin{aligned} \frac{\partial^2 V}{\partial Z^2} &= \frac{\partial^2 V}{\partial a^2} \left( \frac{\partial a}{\partial Z} \right)^2 + \frac{\partial^2 V}{\partial b^2} \left( \frac{\partial b}{\partial Z} \right)^2 + \frac{\partial^2 V}{\partial c^2} \left( \frac{\partial c}{\partial Z} \right)^2 \\ &+ 2 \frac{\partial^2 V}{\partial a \partial b} \left( \frac{\partial a}{\partial Z} \right) \left( \frac{\partial b}{\partial Z} \right) + 2 \frac{\partial^2 V}{\partial a \partial c} \left( \frac{\partial a}{\partial Z} \right) \frac{\partial c}{\partial Z} \\ &+ 2 \frac{\partial^2 V}{\partial b \partial c} \left( \frac{\partial b}{\partial Z} \right) \left( \frac{\partial c}{\partial Z} \right) \end{aligned} \quad (9.66)$$

The quantities

$$\frac{\partial a}{\partial Z} = \cos \theta_{Z,a} = \Phi_{Z,a}, \dots \quad (9.67)$$

are the direction cosines of the principal axes with the space-fixed  $Z$  axis. The quantities

$$\frac{\partial^2 V}{\partial a^2} = q_{aa}, \quad \frac{\partial^2 V}{\partial a \partial b} = q_{ab}, \dots \quad (9.68)$$

are the field gradients with reference to the principal inertial axes. They depend on the electronic state and to a slight extent on the vibrational state of the molecule, but to a high order of approximation they are independent of the molecular rotational state and can in the present evaluation be treated as constants. Thus

$$\begin{aligned} \frac{\partial^2 V}{\partial Z^2} &= q_{aa} \Phi_{Za}^2 + q_{bb} \Phi_{Zb}^2 + q_{cc} \Phi_{Zc}^2 + 2q_{ab} \Phi_{Za} \Phi_{Zb} \\ &+ 2q_{ac} \Phi_{Za} \Phi_{Zc} + 2q_{bc} \Phi_{Zb} \Phi_{Zc} \end{aligned} \quad (9.69)$$

To obtain  $q_J$  we must average the terms on the right side of (9.69) over the rotational wave function  $\Psi_r^{M_J=J}$ . The factors  $q_{aa}, q_{ab}, \dots$ , are constant and can be removed from the integral. When averaged over the rotational state, the off-diagonal terms for an asymmetric rotor vanish, for example,

$$q_{ab} \int \Psi_r^{* M_J=J} \Phi_{Za} \Phi_{Zb} \Psi_r^{M_J=J} d\tau = 0, \dots \quad (9.70)$$

This results from the symmetry properties of the momental ellipsoid (see Chapter III). Either  $\Psi_r$  must be symmetric (+) or antisymmetric (-) with respect to a

rotation of  $\pi$  degrees about a principal axis. In either case, however, the product  $\Psi, \Psi^*$  will be positive for the same rotational function. It is evident that for a rotation of  $\pi$  about the  $a$  axis,  $\Phi_{za}$  will be unchanged while  $\Phi_{zb}$  will change sign only. Similar relationships apply for  $b$  and  $c$ . Thus the integrals of (9.70) must change in sign for at least two of the operations  $C_2^a, C_2^b, C_2^c$ . However, these definite integrals cannot change sign for such operations as change the system into an indistinguishable one. They are therefore identically zero. The off-diagonal terms, however, are not zero in the second-order approximation. For linear and symmetric-top molecules the principal inertial axes are principal axes of the quadrupole coupling tensor, and hence the cross terms vanish automatically since  $q_{ab}, \dots$  vanish.

Expressed in the principal inertial axes,  $q_J$  becomes

$$q_J = q_{aa}(J, i, M_J = J | \Phi_{Za}^2 | J, i, M_J = J) + q_{bb}(J, i, M_J = J | \Phi_{Zb}^2 | J, i, M_J = J) \\ + q_{cc}(J, i, M_J = J | \Phi_{Zc}^2 | J, i, M_J = J) \quad (9.71)$$

where  $q_{aa}$ ,  $q_{bb}$ , and  $q_{cc}$  are the molecular field gradients at the coupling nucleus with reference to the inertial axes.

For brevity, the coupling constant  $eQq$  is often designated by  $\chi$ . With this designation the general expression for the quadrupole coupling energy is obtained by substitution of (9.71) into (9.63)

$$E_Q = \sum_{g=a,b,c} \chi_{gg}(J, i, M_J = J | \Phi_{Zg}^2 | J, i, M_J = J) \left[ \frac{\frac{3}{4}C(C+1) - J(J+1)I(I+1)}{2J(2J-1)I(2I-1)} \right] \quad (9.72)$$

where

$$\chi_{aa} = eQq_{aa}, \quad \chi_{bb} = eQq_{bb}, \quad \chi_{cc} = eQq_{cc} \quad (9.73)$$

Because of the relationship

$$(J, i, M_J = J | \Phi_{Zg}^2 | J, i, M_J = J) = \frac{2}{(J+1)(2J+3)} (J, i | J_g^2 | J, i) + \frac{1}{2J+3} \quad (9.74)$$

which exists between the diagonal matrix elements of  $\Phi_{Zg}^2$  when  $M_J = J$  and the diagonal matrix elements of  $J_g^2$  in the  $J, i, M_J$  representation of the unperturbed rotor, (9.72) can be put in the alternative form

$$E_Q = \frac{2}{(J+1)(2J+3)} \sum_{g=a,b,c} \chi_{gg}(J, i | J_g^2 | J, i) \left[ \frac{\frac{3}{4}C(C+1) - J(J+1)I(I+1)}{2J(2J-1)I(2I-1)} \right] \quad (9.75)$$

The term  $(2J+3)^{-1}$  of (9.74) does not enter in this expression since we have used Laplace's relation, (9.76). This expression of the quadrupole coupling energies, which was first obtained by Bragg and Golden [10], is particularly useful in the calculation of the nuclear quadrupole perturbation in the asymmetric rotor. Equation 9.74 can be readily proved for the symmetric-top wave functions and hence for the asymmetric-top functions by comparison of the matrix elements derived from Table 2.1 ( $J, K, M = J | \Phi_{Zg}^2 | J, K, M_J = J$ ) with those for the symmetric top ( $J, K | J_g^2 | J, K$ ), which are given in Chapter II.

Because Laplace's equation holds,

$$\chi_{aa} + \chi_{bb} + \chi_{cc} = 0 \quad (9.76)$$

and there are only two independent coupling constants in the most general case. These are usually expressed in terms of the coupling constant with reference to one of the axes and an asymmetric parameter  $\eta$ . If the reference axis is chosen as the  $c$  axis, the two coupling constants would be  $\chi_{cc}$  and

$$\eta = \frac{\chi_{aa} - \chi_{bb}}{\chi_{cc}} \quad (9.77)$$

The reference axis is usually chosen as the one for which the coupling is the most nearly symmetric, that is, for which  $\eta$  is smallest.

The matrix elements of the squared direction cosines differ for the different classes of molecules. For diatomic or linear polyatomic molecules and for symmetric-top molecules they can be evaluated explicitly, as will be done below. For asymmetric rotors a closed-form evaluation can be made only for low  $J$  states, but values can be obtained by numerical techniques (especially with computers) for higher  $J$  values.

It should be appreciated that the values of  $q_J$  as expressed in the preceding formulas are not exact, but are first-order perturbation values obtained when the field gradient is averaged over the wave functions of the unperturbed rotor. However, the off-diagonal elements that are omitted in the average are entirely negligible except for the coupling by the few nuclei that have large quadrupole moments. For them, the second-order corrections described in Section 6 are adequate.

### Diatom and Linear Polyatomic Molecules

In a linear molecule, diatomic or polyatomic, the molecular field gradient is symmetric about the bond axis. Let us designate a molecule-fixed coordinate system  $x, y, z$  with  $z$  along the bond axis. Obviously, this system coincides with the principal axes of inertia with  $a \rightarrow z$ . From the symmetry and from Laplace's equation

$$q_{xx} = q_{yy} = -\frac{1}{2}q_{zz} \quad (9.78)$$

Because there is only one coupling axis it is customary to drop the subscript and to set  $q_{zz} = q$ . Substitution of these relations into (9.71) gives

$$\begin{aligned} q_J &= q(J, M_J = J | \Phi_{zz}^2 - \frac{1}{2}[\Phi_{zx}^2 + \Phi_{zy}^2] | J, M_J = J) \\ &= q \left( J, M_J = J \left| \frac{3\Phi_{zz}^2 - 1}{2} \right| J, M_J = J \right) \end{aligned} \quad (9.79)$$

The matrix elements of  $\Phi_{zz}$  for the linear molecule correspond to those of the symmetric top with  $K=0$ . Although the diagonal matrix elements of  $\Phi$  for a linear molecule are zero, those of  $\Phi^2$  are not. From the matrix product rule,

$$(J, M_J = J | \Phi_{zz}^2 | J, M_J = J) = \sum_{J'} (J, J | \Phi_{zz} | J', J)(J', J | \Phi_{zz} | J, J) = \frac{1}{2J+3} \quad (9.80)$$

where the elements of the product are evaluated from Table 2.1 with  $K=0$  and  $M_J=J$ . Substitution of (9.80) into (9.79) yields

$$q_J = -\frac{qJ}{2J+3} \quad (9.81)$$

The first-order quadrupole coupling energies for a single coupling nucleus in a linear molecule are found from combination of (9.63) and (9.81) or (9.72) and (9.80) to be

$$E_Q = -eQqY(J, I, F) = -\chi Y(J, I, F) \quad (9.82)$$

where

$$Y(J, I, F) = \frac{\frac{3}{4}C(C+1) - I(I+1)J(J+1)}{2(2J-1)(2J+3)I(2I-1)} \quad (9.83)$$

For convenience in the calculation of hyperfine structure, numerical tabulations of  $Y(J, I, F)$  and of the relative intensities of the hyperfine components for  $J \rightarrow J+1$  transitions are given in Appendix I.

Selection rules for hyperfine transitions in rotational absorption spectra are

$$J \rightarrow J+1, \quad F \rightarrow F, \quad F \rightarrow F \pm 1, \quad I \rightarrow I$$

The rotational frequencies perturbed by quadrupole coupling are

$$\nu = \frac{E_r(J+1) - E_r(J)}{h} + \frac{E_Q(J+1, I, F') - E_Q(J, I, F)}{h} \quad (9.84)$$

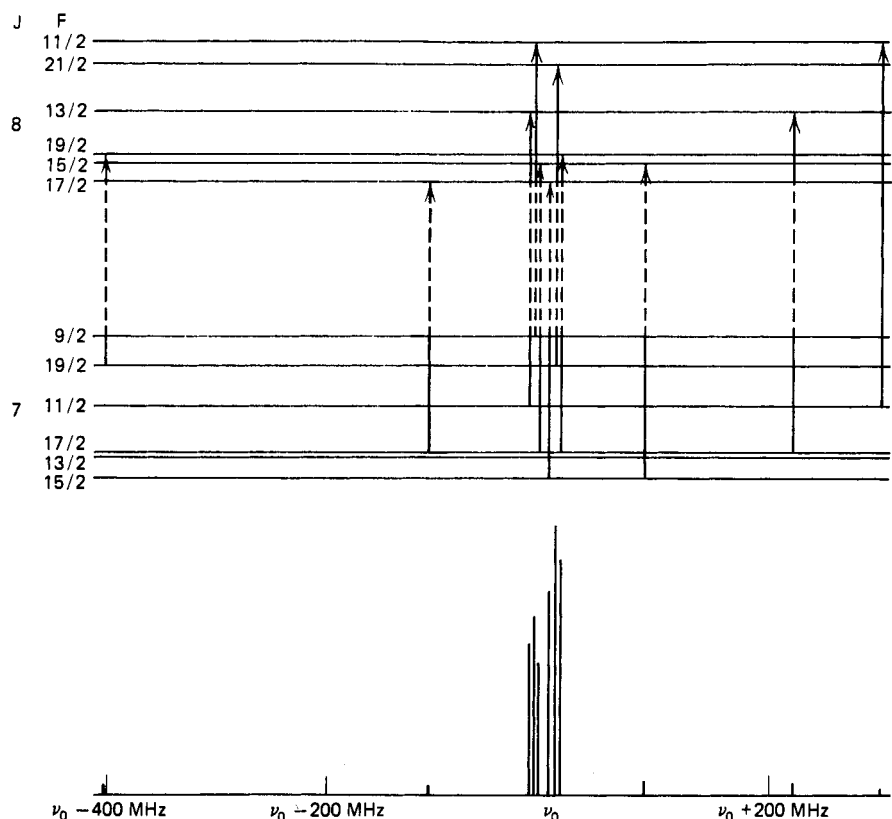
where  $F'=F$ ,  $F \pm 1$ . It is customary to express the coupling constants in frequency units so that

$$\nu = \nu_0 - eQq[Y(J+1, I, F') - Y(J, I, F)] \quad (9.85)$$

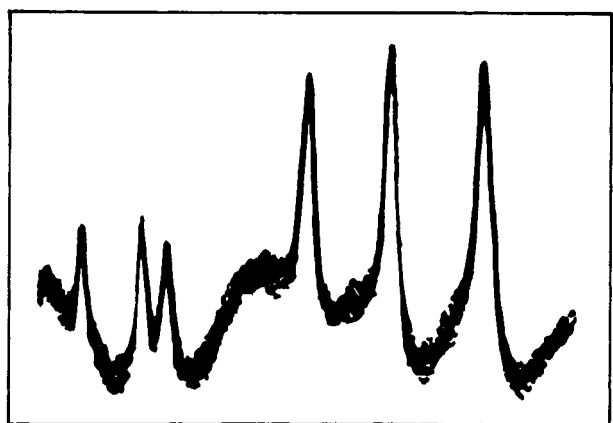
where  $\nu_0$  is the "unperturbed" rotational frequency that would be observed if there were no quadrupole coupling. By measurement of only two frequencies of the hyperfine multiplet,  $\chi \equiv eQq$  and  $\nu_0$  may be obtained. For best accuracy one should measure the most widely spaced components provided that they are sufficiently strong for precise measurement. As a test of the accuracy, other components are usually measured. It is evident that wherever the rotational transitions have resolved hyperfine structure one must measure  $eQq$  in order to obtain  $\nu_0$  and hence the rotational constant  $B_0$  described in Chapters IV and V.

Figure 9.4 illustrates the calculation of the frequencies of the hyperfine components caused by  $^{127}\text{I}$  in the  $J=7 \rightarrow 8$  rotational transition of  $^{127}\text{ICN}$ . The spin of  $^{127}\text{I}$  is  $\frac{5}{2}$ , and the total number of components for all transitions for which  $J > I$  is 15. However, it will be noted that only the six  $F \rightarrow F+1$  components are of significant strength. Figure 9.5 shows these six  $F \rightarrow F+1$  components as they appear on the cathode ray scope. The splitting caused by  $^{14}\text{N}$  ( $I=1$ ) is not resolvable for this  $J$  transition.

For transitions where  $J > I$ , the variation in the hyperfine pattern is rather uniform with increasing  $J$ . The  $F \rightarrow F-1$  components become weaker and



**Fig. 9.4** Energy level diagram and calculated nuclear quadrupole hyperfine structure for the  $J = 7 \rightarrow 8$  rotational transition of a linear molecule with a single coupling nucleus having a spin of  $\frac{5}{2}$ . All  $F \rightarrow F - 1$  components are less than one-thousandth the strength of the strongest component and hence are omitted. Here  $eQq$  is assumed to be  $-2400$  MHz, as it is for ICN in Fig. 9.5.



**Fig. 9.5** The  $F \rightarrow F + 1$  components of the  $J = 7 \rightarrow 8$  transition of ICN observed at 5.87 mm wavelength (compare with the theoretical components of Fig. 9.4). The observed components are due to  $^{127}\text{I}$  (spin  $\frac{5}{2}$ ,  $eQq = -2400$  MHz). The substructure caused by  $^{14}\text{N}$  (spin 1,  $eQq = -3.8$  MHz) is not resolved.

eventually undetectable; the  $F \rightarrow F+1$  components remain strong but converge in frequency and eventually become unresolvable as  $J$  continues to increase. Thus for high  $J$  values only a single line is observable except when the coupling is very large. When  $J > I$ , there are  $2I+1$  components for  $F \rightarrow F+1$ ,  $2I$  components for  $F \rightarrow F$ , and  $2I-1$  components for  $F \rightarrow F-1$ . However, for the  $J=0 \rightarrow 1$  transition, there are only three hyperfine components whatever the value of  $I$ .

These variations are illustrated in Fig. 9.6 for a coupling nucleus with  $I=\frac{3}{2}$ . Although there are four  $F \rightarrow F+1$  transitions expected for  $I=\frac{3}{2}$  when  $J > I$ , two pairs of the four lines coincide so that only two  $F \rightarrow F+1$  lines are observable.

Table 9.1 illustrates some of the nuclear quadrupole coupling constants of linear molecules that have been measured from analysis of rotational hyperfine structure. Note the rather large differences in the  $^{14}\text{N}$  coupling of the related molecules FCN, ClCN, and BrCN. Also note the large difference between the

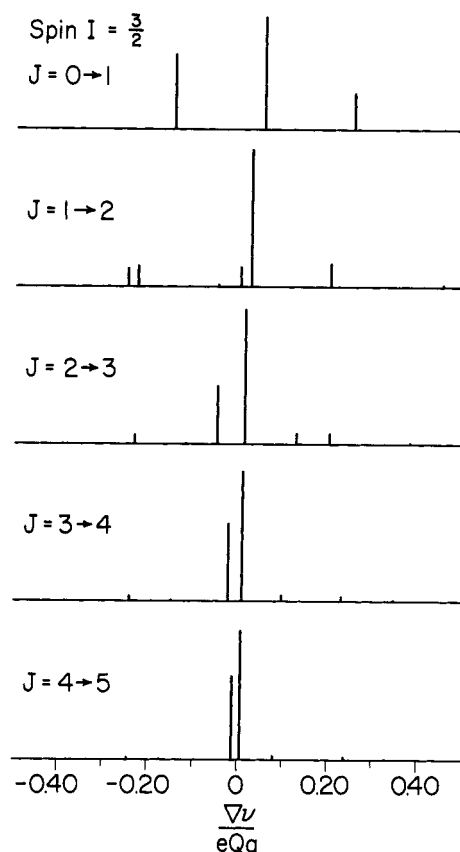


**Fig. 9.6** Theoretical patterns of the first five rotational transitions of a linear molecule resulting from quadrupole interactions by a single nucleus with spin  $I=\frac{3}{2}$ .

**Table 9.1** Nuclear Quadrupole Coupling in Some Diatomic and Linear Polyatomic Molecules in the Ground Vibrational State

Molecule	$eQq$ (MHz)	Ref.	Molecule	$eQq$ (MHz)	Ref.
<i>D coupling</i>			<i><sup>33</sup>S coupling</i>		
DBr	0.1469(14)	<sup>a</sup>	CS	12.83(3)	<sup>m</sup>
DCN	0.1944(25)	<sup>b</sup>	SiS	10.90(20)	<sup>n</sup>
DCP	0.233(40)	<sup>c</sup>	GeS	6.96(30)	<sup>n</sup>
DCCF	0.212(10)	<sup>d</sup>	OCS	-29.07(1)	<sup>o</sup>
<i><sup>11</sup>B coupling</i>			<i><sup>35</sup>Cl coupling</i>		
BF	4.5(4)	<sup>e</sup>	HCl	-67.80(10)	<sup>p</sup>
HBS	-3.71(3)	<sup>f</sup>	ClCn	-83.2752(4)	<sup>q</sup>
<i><sup>14</sup>N coupling</i>			HCCl	-79.67	<sup>r</sup>
<i><sup>79</sup>Br coupling</i>			<i><sup>127</sup>I coupling</i>		
PN	-5.2031(5)	<sup>g</sup>	HI	-1828.42(20)	<sup>p</sup>
HCN	-4.7091(15)	<sup>b</sup>	ICN	-2418.8(5)	<sup>t</sup>
FCN	-2.67(5)	<sup>h</sup>	HCCI	-2250.6(55)	<sup>u</sup>
HCNO	0.245(5)	<sup>i</sup>			
HCCN	-4.28(5)	<sup>j</sup>			
<i><sup>17</sup>O coupling</i>					
CO	4.48(10)	<sup>k</sup>			
OCS	-1.32(7)	<sup>l</sup>			

<sup>a</sup>B. P. Van Eijck, *J. Mol. Spectrosc.*, **53**, 246 (1974).

<sup>b</sup>F. C. De Lucia and W. Gordy, *Phys. Rev.*, **187**, 58 (1969).

<sup>c</sup>S. L. Harford, W. C. Allen, C. L. Allen, C. L. Harris, E. F. Pearson, and W. H. Flygare, *Chem. Phys. Lett.*, **18**, 153 (1973).

<sup>d</sup>V. W. Weiss and W. H. Flygare, *J. Chem. Phys.*, **45**, 8 (1966).

<sup>e</sup>F. J. Lovas and D. R. Johnson, *J. Chem. Phys.*, **55**, 41 (1971).

<sup>f</sup>E. F. Pearson, C. L. Norris, and W. H. Flygare, *J. Chem. Phys.*, **60**, 1761 (1974).

<sup>g</sup>J. Raymonda and W. Klemperer, *J. Chem. Phys.*, **55**, 232 (1971).

<sup>h</sup>J. Sheridan, J. K. Tyler, E. E. Aynsley, R. E. Dodd, and R. Little, *Nature*, **185**, 96 (1960).

<sup>i</sup>W. Hüttner, H. K. Bodenseh, P. Nowicki, and K. Morgenstern, *J. Mol. Spectrosc.*, **71**, 246 (1978).

<sup>j</sup>J. K. Tyler and J. Sheridan, *Trans. Faraday Soc.*, **59**, 2661 (1963).

<sup>k</sup>W. H. Flygare and V. W. Weiss, *J. Chem. Phys.*, **45**, 2785 (1966).

<sup>l</sup>S. Geschwind, R. Gunther-Mohr, and J. Silvey, *Phys. Rev.*, **85**, 474 (1952).

<sup>m</sup>M. Bogey, C. Demuynck, and J. L. Destombes, *Chem. Phys. Lett.*, **81**, 256 (1981).

<sup>n</sup>J. Hoeft, F. J. Lovas, E. Tiemann, and T. Törring, *J. Chem. Phys.*, **53**, 2736 (1970).

<sup>o</sup>C. H. Townes and S. Geschwind, *Phys. Rev.*, **74**, 626 (1948).

<sup>p</sup>F. C. De Lucia, P. Helmlinger, and W. Gordy, *Phys. Rev. A*, **3**, 1849 (1971).

<sup>q</sup>J. M. L. J. Reinartz, W. L. Meerts, A. Dymanus, *Chem. Phys.*, **45**, 387 (1980).

<sup>r</sup>H. Jones, M. Takami, and J. Sheridan, *Z. Naturforsch.*, **33a**, 156 (1978).

<sup>s</sup>A. P. Porter and P. D. Godfrey, *J. Mol. Spectrosc.*, **68**, 492 (1977).

<sup>t</sup>T. Oka, H. Hirakawa and A. Miyahara, *J. Phys. Soc. Japan*, **12**, 39 (1957).

<sup>u</sup>E. Schafer and J. J. Christiansen, *J. Mol. Struct.*, **97**, 101 (1983).

coupling of the middle nitrogen and that of the end nitrogen in NNO, as well as that between the  $^{33}\text{S}$  coupling in CS and in OCS. It is evident that the nuclear quadrupole coupling depends upon the nature of the chemical bonding to the coupling atom. This relationship is treated in Chapter XIV.

### Symmetric-top Molecules

The most commonly studied symmetric-top hyperfine structure arises from a single coupling nucleus on the symmetry axis. A single coupling isotope, or two such isotopes which are off the axis, would destroy the symmetry and convert the molecule into an asymmetric rotor. It is possible, however, to have three off-axis coupling isotopes, for example,  $^{35}\text{Cl}$  in  $^{35}\text{Cl}_3\text{CH}$ , in a symmetric top. At this point we consider the simpler case of a single coupling nucleus that is on the symmetry axis.

The symmetry axis will, of course, be a principal axis of inertia, either  $a$  (prolate top) or  $c$  (oblate top). To include both cases we designate this axis as  $z$  and the other two body-fixed axes as  $x$  and  $y$ . With (9.78), which also holds for symmetric tops, (9.71) becomes

$$q_J = q \left( J, K, M_J = J \left| \frac{3\Phi_{zz}^2 - 1}{2} \right| J, K, M_J = J \right) \quad (9.86)$$

From the matrix elements given in Table 2.1

$$\begin{aligned} (J, K, M_J = J | \Phi_{zz}^2 | J, K, M_J = J) &= (J, K, J | \Phi_{zz} | J, K, J)^2 \\ &\quad + (J, K, J | \Phi_{zz} | J+1, K, J)^2 + (J, K, J | \Phi_{zz} | J-1, K, J)^2 \\ &= \frac{K^2}{(J+1)^2} + \frac{(J+1)^2 - K^2}{(J+1)^2(2J+3)} \end{aligned} \quad (9.87)$$

Substitution of these values into (9.86) gives

$$q_J = q \frac{J}{2J+3} \left[ \frac{3K^2}{J(J+1)} - 1 \right] \quad (9.88)$$

The resulting formula for the quadrupole energy of the symmetric top is, from (9.63),

$$E_Q = eQq \left[ \frac{3K^2}{J(J+1)} - 1 \right] Y(J, I, F) \quad (9.89)$$

where  $Y(J, I, F)$  is the function of Eq. (9.83), which is numerically tabulated in Appendix I, and

$$eQq = eQ \left\langle \frac{\partial^2 V}{\partial z^2} \right\rangle = \chi \quad (9.90)$$

is the coupling constant with reference to the molecular axis of symmetry. Selection rules are  $\Delta J = \pm 1$ ;  $\Delta K = 0$ ;  $\Delta F = 0 \pm 1$ ;  $\Delta I = 0$ .

It is evident from examination of (9.89) that each  $K$  component of a  $J \rightarrow J+1$  rotational transition of a symmetric top will have its own hyperfine multiplet.

For  $K=0$  the equation reduces to that for the linear molecule, and the pattern for this component alone will be similar to those illustrated in Figs. 9.4–9.6. The splitting of other  $K$  components differs by a scale factor only and hence individually resembles the patterns for the linear molecule. When, as is often true, the separation of the  $K$  components by centrifugal stretching is less than the quadrupole splitting, the multiplets for the different  $K$  components are scrambled so that they produce a rather complicated spectrum, such as is illustrated in Fig. 9.7. Comparison of these various patterns was used for proof that the nuclear spin of radioactive  $^{129}\text{I}$  is  $\frac{7}{2}$ . The slight disagreement between the observed and calculated patterns for  $I=\frac{7}{2}$  are due to second-order effects, described in Section 6, which were not included in the calculations. Since the spin of the stable isotope  $^{127}\text{I}$  is  $\frac{5}{2}$ , the hyperfine structure of the  $J=2 \rightarrow 3$  transition of normal methyl iodide is like that for the theoretical pattern for  $I=\frac{5}{2}$ .

Selected values of quadrupole couplings in symmetric-top molecules as obtained from microwave spectroscopy are given in Table 9.2.

### Asymmetric Rotors

The general expression for nuclear quadrupole interaction, (9.72), applies to all classes of molecules. By multiplication and division of this equation by  $J/(2J+3)$  it can be expressed as

$$E_Q = eQq_J \frac{2J+3}{J} Y(J, I, F) \quad (9.91)$$

In the asymmetric-top representation,

$$q_J = \sum_{g=a,b,c} q_{gg}(J_{K-1K_1}, M_J=J | \Phi_{Zg}^2 | J_{K-1K_1}, M_J=J) \quad (9.92)$$

The function  $Y(J, I, F)$  is expressed by (9.83) and is tabulated in Appendix I. Except for low  $J$  values, the matrix elements of the squared direction cosines in (9.92) cannot be expressed in closed form; hence  $q_J$  cannot be expressed in closed form. Because the line intensities depend on the squared matrix elements, the problem of calculation of  $q_J$  can, however, be reduced to that already encountered in the calculation of line intensities. For example, from the matrix product rule

$$(J_{K-1K_1}, J) \Phi_{Za}^2 | J_{K-1K_1}, J) = \sum_{J'_{K'-1K'_1}} |(J_{K-1K_1}, M_J=J | \Phi_{Za} | J'_{K'-1K'_1}, M_J=J)|^2 \quad (9.93)$$

If the dipole moment is along the principal axis  $a$ , the line strength of the transitions  $(J_{K-1K_1}, M_J=J) \rightarrow (J'_{K'-1K'_1}, M_J=J)$  is proportional to the squared matrix elements of this expression. By thus relating the diagonal matrix elements of

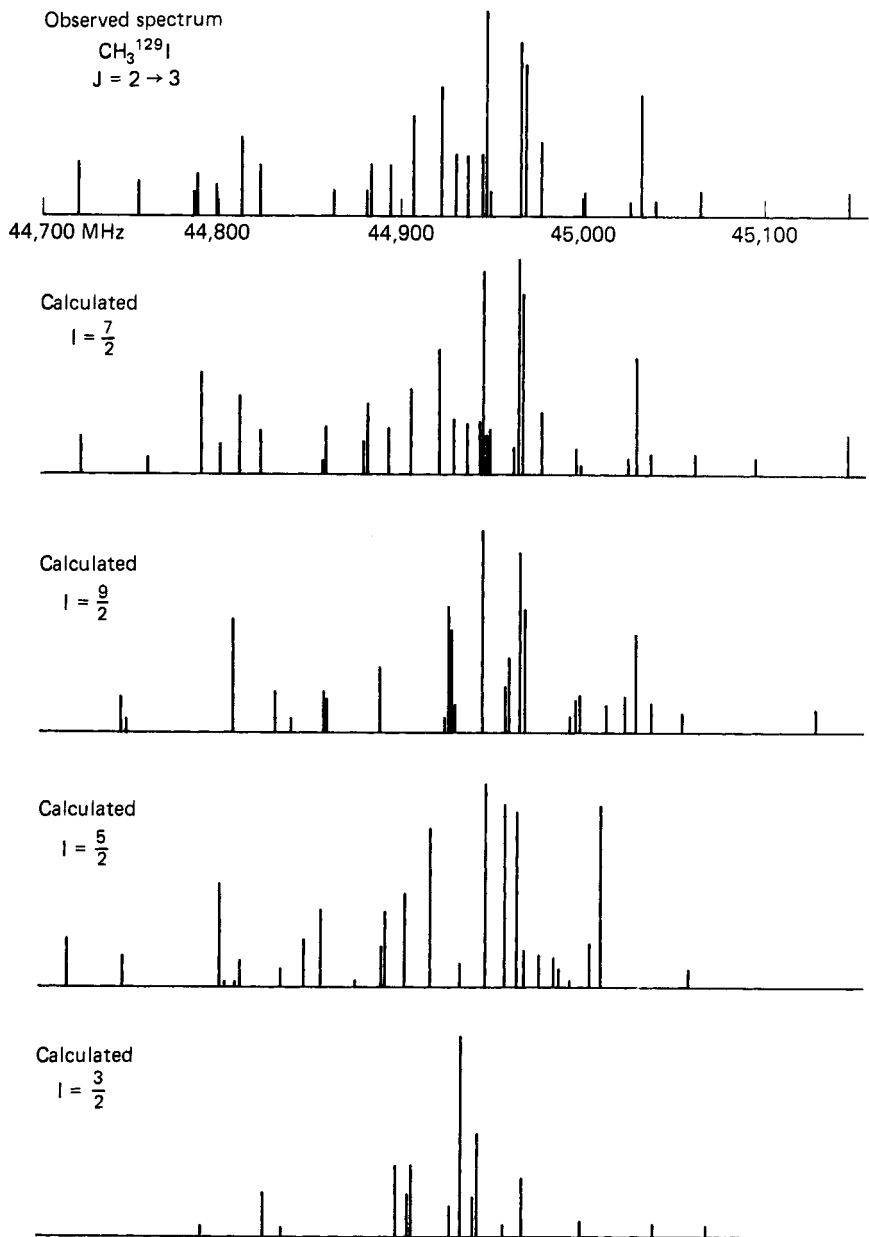


**Fig. 9.7** Observed nuclear quadrupole hyperfine pattern for the  $J = 2 \rightarrow 3$  rotational transition of  $\text{CH}_3^{129}\text{I}$  (top figure) compared with the patterns predicted with first-order theory for various nuclear spin values assumed for the iodine (lower figures). The close similarity of the two top patterns proved that the spin of  $^{129}\text{I}$  is  $\frac{7}{2}$ . From R. Livingston, O. R. Gilliam, and W. Gordy, *Phys. Rev.*, **76**, 149 (1949).

**Table 9.2** Nuclear Quadrupole Coupling in Some Symmetric-top Molecules in the Ground Vibrational State

Molecule	$eQq$ (MHz)	Ref.	Molecule	$eQq$ (MHz)	Ref.			
<i>D coupling</i>								
$\text{CH}_3\text{D}$	0.192	<sup>a</sup>	$\text{NCl}_3$	-108(3)	<sup>l</sup>			
$\text{CF}_3\text{D}$	0.171(2)	<sup>b</sup>	$\text{CH}_3\text{Cl}$	-74.77(10)	<sup>m</sup>			
$\text{CD}_3\text{CN}$	0.168(4)	<sup>c</sup>	$\text{SiH}_3\text{Cl}$	-40.0	<sup>n</sup>			
<i><sup>11</sup>B coupling</i>								
$\text{BH}_3\text{CO}$	1.60(10)	<sup>d</sup>	$\text{GeH}_3\text{Cl}$	-46.95(2)	<sup>o</sup>			
$\text{CH}_3\text{BS}$	-3.714(20)	<sup>e</sup>	$\text{SnH}_3\text{Cl}$	-41.6(3)	<sup>p</sup>			
<i><sup>14</sup>N coupling</i>								
$\text{NH}_3$	-4.0842(3)	<sup>f</sup>	$\text{CH}_3\text{Br}$	577.15(10)	<sup>m</sup>			
$\text{NF}_3$	-7.07(10)	<sup>g</sup>	$\text{SiH}_3\text{Br}$	334.970(6)	<sup>q</sup>			
$\text{CH}_3\text{CN}$	-4.2244(15)	<sup>c</sup>	$\text{GeH}_3\text{Br}$	384(2)	<sup>r</sup>			
$\text{CH}_3\text{NC}$	-0.4885(10)	<sup>h</sup>	$\text{SnH}_3\text{Br}$	350(6)	<sup>s</sup>			
$\text{SiH}_3\text{CN}$	-4.77(3)	<sup>i</sup>	<i><sup>127</sup>I coupling</i>					
<i><sup>73</sup>Ge coupling</i>								
$\text{GeH}_3\text{F}$	-93.0(1)	<sup>j</sup>	$\text{CH}_3\text{I}$	-1940.41(7)	<sup>t</sup>			
$\text{GeH}_3\text{CCH}$	+32.5	<sup>k</sup>	$\text{SiH}_3\text{I}$	-1240(30)	<sup>u</sup>			
			$\text{GeH}_3\text{I}$	-1381(4)	<sup>r</sup>			
			$\text{SnH}_3\text{I}$	-1273(8)	<sup>v</sup>			

<sup>a</sup>S. C. Wofsy, J. S. Muenter, and W. Klemperer, *J. Chem. Phys.*, **53**, 4005 (1970).

<sup>b</sup>S. G. Kukolich, A. C. Nelson, and D. J. Ruben, *J. Mol. Spectrosc.*, **40**, 33 (1971).

<sup>c</sup>S. G. Kukolich, D. J. Ruben, J. H. S. Wang, and J. R. Williams, *J. Chem. Phys.*, **58**, 3155 (1973).

<sup>d</sup>A. C. Venkatachar, R. C. Taylor, and R. L. Kuczkowski, *J. Mol. Struct.*, **38**, 17 (1977).

<sup>e</sup>C. Kirby and H. W. Kroto, *J. Mol. Spectrosc.*, **83**, 1 (1980).

<sup>f</sup>Gunther-Mohr et al. [41].

<sup>g</sup>J. Sheridan and W. Gordy, *Phys. Rev.*, **79**, 513 (1950).

<sup>h</sup>S. G. Kukolich, *Chem. Phys. Lett.*, **10**, 52 (1971).

<sup>i</sup>A. J. Careless and H. W. Kroto, *J. Mol. Spectrosc.*, **57**, 198 (1975).

<sup>j</sup>L. C. Krisher, J. A. Morrison, and W. A. Watson, *J. Chem. Phys.*, **57**, 1357 (1972).

<sup>k</sup>E. C. Thomas and V. C. Laurie, *J. Chem. Phys.*, **44**, 2602 (1966).

<sup>l</sup>G. Cazzoli, P. G. Favero, and A. Dal Borgo, *J. Mol. Spectrosc.*, **50**, 82 (1974).

<sup>m</sup>J. Kraitchman and B. P. Dailey, *J. Chem. Phys.*, **22**, 1477 (1954).

<sup>n</sup>A. H. Sharbaugh, *Phys. Rev.*, **74**, 1870 (1948).

<sup>o</sup>S. Geshwind, R. Gunther-Mohr, and C. H. Townes, *Phys. Rev.*, **81**, 288 (1951).

<sup>p</sup>L. C. Krisher, R. A. Gsell, and J. M. Bellama, *J. Chem. Phys.*, **54**, 2287 (1971).

<sup>q</sup>K. F. Dössel and D. H. Sutter, *Z. Naturforsch.*, **32a**, 1444 (1977).

<sup>r</sup>S. N. Wolf and L. C. Krisher, *J. Chem. Phys.*, **56**, 1040 (1971).

<sup>s</sup>S. N. Wolf, L. C. Krisher, and R. A. Gsell, *J. Chem. Phys.*, **54**, 4605 (1971).

<sup>t</sup>A. Dubrulle, J. Burie, D. Boucher, F. Herlemont, and J. Demaison, *J. Mol. Spectrosc.*, **88**, 394 (1981).

<sup>u</sup>A. H. Sharbaugh, G. A. Heath, L. F. Thomas, and J. Sheridan, *Nature*, **171**, 87 (1953).

<sup>v</sup>S. N. Wolf, L. C. Krisher, and R. A. Gsell, *J. Chem. Phys.*, **55**, 2106 (1971).

$\Phi_{Zg}^2$  to those of the transition dipole moments, Bragg [9] has derived the expression

$$q_J = \frac{2J}{(2J+1)(2J+3)} \sum_{K'_{-1} K'_1} [q_{aa}\lambda_a(J_{K_{-1} K_1}; J_{K'_{-1} K'_1}) + q_{bb}\lambda_b(J_{K_{-1} K_1}; J_{K'_{-1} K'_1}) \\ + q_{cc}\lambda_c(J_{K_{-1} K_1}; J_{K'_{-1} K'_1})] \quad (9.94)$$

in which the  $\lambda$ 's are the line strength factors for the transitions  $J_{K_{-1} K_1} \rightarrow J_{K'_{-1} K'_1}$  tabulated by Cross et al. [17]. Although these tables include only values for line strengths of molecules having an asymmetry parameter  $\kappa$  of  $\mp 1$ ,  $\mp 0.5$ ,  $0$ ,  $\pm 0.5$ , and  $\pm 1$ , these can be interpolated to give reasonably approximate values of  $q_J$  for other degrees of asymmetry. More extensive tabulations are referenced in Chapter VII.

A second, and perhaps more useful, expression of  $q_J$  in terms of the reduced energies and Ray's asymmetry parameter  $\kappa$  has been derived by Bragg and Golden [10]. This derivation is based upon the relationship between the matrix elements of the direction cosines and the angular momentum expressed by (9.74), which allows  $q_J$  to be expressed by

$$q_J = \frac{2}{(J+1)(2J+3)} \sum_{g=a,b,c} q_{gg} \langle J_g^2 \rangle \quad (9.95)$$

where the asymmetric-top representation is used for the average values

$$\langle J_g^2 \rangle = (J, K_{-1}, K_1 | J_g^2 | J, K_{-1}, K_1) \quad (9.96)$$

As discussed in Chapter VII,

$$\langle J_a^2 \rangle = \frac{1}{2} \left[ J(J+1) + E(\kappa) - (\kappa+1) \frac{\partial E(\kappa)}{\partial \kappa} \right] \quad (9.97)$$

$$\langle J_b^2 \rangle = \frac{\partial E(\kappa)}{\partial \kappa} \quad (9.98)$$

$$\langle J_c^2 \rangle = \frac{1}{2} \left[ J(J+1) - E(\kappa) + (\kappa-1) \frac{\partial E(\kappa)}{\partial \kappa} \right] \quad (9.99)$$

which lead to an expression for the quadrupole energy in the form

$$E_Q = \frac{1}{J(J+1)} \left\{ \chi_{aa} \left[ J(J+1) + E(\kappa) - (\kappa+1) \frac{\partial E(\kappa)}{\partial \kappa} \right] + 2\chi_{bb} \frac{\partial E(\kappa)}{\partial \kappa} \right. \\ \left. + \chi_{cc} \left[ J(J+1) - E(\kappa) + (\kappa-1) \frac{\partial E(\kappa)}{\partial \kappa} \right] \right\} Y(J, I, F) \quad (9.100)$$

in which  $E(\kappa)$  is the reduced energy of the asymmetric rotor described in Chapter VII and Ray's parameter is

$$\kappa = \frac{2B-A-C}{A-C} \quad (9.101)$$

where  $A$ ,  $B$ , and  $C$  are the rotational constants with regard to the respective  $a$ ,  $b$ , and  $c$  axes. The reduced energies for various values of  $\kappa$  have been tabulated (see Chapter VII). For low  $J$  values, for which nuclear quadrupole coupling is best resolved, explicit expressions for  $E(\kappa)$  have been obtained. Selection rules  $\Delta F=0, \pm 1$  and  $\Delta I=0$  apply with those given for  $J_{K-1, K_1}$  in Chapter VII.

We illustrate the application of (9.100) with a simple example, the  $1_{01} \rightarrow 1_{10}$  transition of  $H_2^{32}S$ . For the  $1_{01}$  level:

$$E(\kappa)=\kappa-1, \quad \frac{\partial E(\kappa)}{\partial \kappa}=1 \quad (9.102)$$

and

$$E_Q(1_{01})=(\chi_{bb}+\chi_{cc})Y(F)=-\chi_{aa}Y(F) \quad (9.103)$$

For the  $1_{10}$  level:

$$E(\kappa)=\kappa+1, \quad \frac{\partial E(\kappa)}{\partial \kappa}=1 \quad (9.104)$$

and

$$E_Q(1_{10})=(\chi_{aa}+\chi_{bb})Y(F)=-\chi_{cc}Y(F) \quad (9.105)$$

For both levels:

$$\begin{aligned} J &= 1, & I &= \frac{3}{2}, & F &= \frac{5}{2}, \frac{3}{2}, \frac{1}{2} \\ Y(1, \frac{3}{2}, \frac{5}{2}) &= \frac{1}{20}, & Y(1, \frac{3}{2}, \frac{3}{2}) &= -\frac{1}{5}, & Y(1, \frac{3}{2}, \frac{1}{2}) &= \frac{1}{4} \end{aligned}$$

The resulting energy levels, allowed transitions, and predicted lines are indicated in Fig. 9.8. Comparison of theoretical with observed frequencies [18] leads to the values

$$\begin{aligned} \chi_{aa} &= -32 \text{ MHz}, & \chi_{bb} &= -8 \text{ MHz}, & \chi_{cc} &= 40 \text{ MHz}, \\ v_0 &= 168,322.63 \text{ MHz} \end{aligned}$$

and hence the asymmetry parameter of the quadrupole coupling is

$$\eta = \frac{\chi_{aa} - \chi_{bb}}{\chi_{cc}} = -0.60$$

For slightly asymmetric rotors, (9.100) can be expressed in a more convenient form by the use of expansions for  $W(b)$  given in Chapter VII. The resulting expression for the nearly prolate or oblate symmetric top is

$$\begin{aligned} E_Q &= \frac{\chi}{J(J+1)} [3K^2 - J(J+1) - 3b^2(C_2 + 2C_3b) \\ &\quad + \eta(C_1 + 2C_2b + 3C_3b^2 + 4C_4b^3)]Y(J, I, F) \end{aligned} \quad (9.106)$$

where the  $b$ 's are the inertial parameters defined in Chapter VII, Section 3 and where the  $C$ 's are parameters given in Table 7.8. For a prolate rotor  $b=b_p$ ,

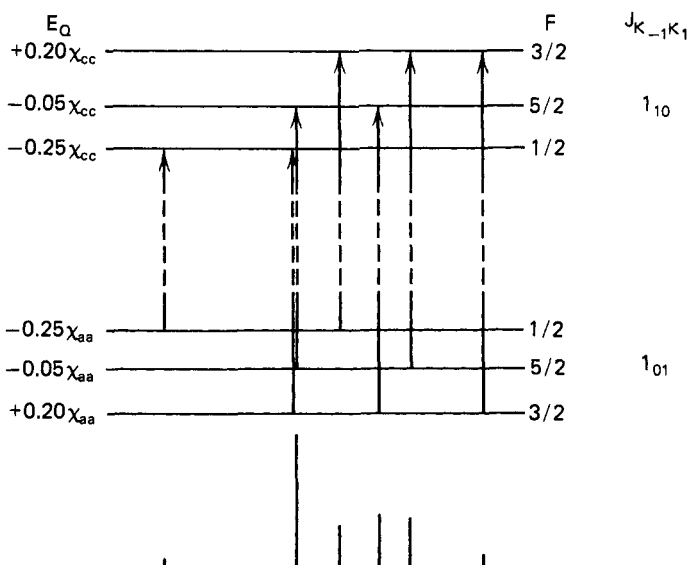


**Fig. 9.8** Energy level diagram and predicted nuclear quadrupole hyperfine structure caused by  $^{33}\text{S}$  ( $I=\frac{3}{2}$ ) in the  $1_{01} \rightarrow 1_{10}$  rotational transition of  $\text{H}_2^{33}\text{S}$ .

$\chi = \chi_{aa}$  and  $\eta = (\chi_{cc} - \chi_{bb})/\chi_{aa}$ , whereas for an oblate rotor  $b = b_o$ ,  $\chi = \chi_{cc}$ , and  $\eta = (\chi_{aa} - \chi_{bb})/\chi_{cc}$ .

Although the diagonal elements  $\chi_{aa}$ ,  $\chi_{bb}$ , and  $\chi_{cc}$  of the coupling with reference to the principal inertial axes are the coupling constants directly observable from the rotational hyperfine structure, they are not necessarily the most convenient for interpretation of the quadrupole coupling in terms of the properties of chemical bonds. While the cross terms  $\chi_{ab}, \dots$ , are averaged out by the relation [see (9.70)], the principal inertial axes are not generally principal axes of the nuclear coupling in the tensor, even though they may be in special cases, such as linear molecules. Let us therefore transform  $\chi_{aa}$ ,  $\chi_{bb}$ , and  $\chi_{cc}$  to the principal axes of the quadrupole coupling tensor which we shall designate by  $x$ ,  $y$ ,  $z$ . Since  $eQ$  is constant, we need only to transform  $q$ .

$$q_{aa} = \left( \frac{\partial^2 V}{\partial a^2} \right) = \left( \frac{\partial^2 V}{\partial x^2} \right) \left( \frac{\partial x}{\partial a} \right)^2 + \left( \frac{\partial^2 V}{\partial y^2} \right) \left( \frac{\partial y}{\partial a} \right)^2 + \left( \frac{\partial^2 V}{\partial z^2} \right) \left( \frac{\partial z}{\partial a} \right)^2 \quad (9.107)$$

with similar expressions for  $q_{bb}$  and  $q_{cc}$ . Cross terms such as  $(\partial^2 V / \partial x \partial y)$  are zero because  $x$ ,  $y$ ,  $z$  are principal axes of the field gradient.

Now

$$\frac{\partial x}{\partial a} = \cos \theta_{xa}, \dots$$

$$\frac{\partial^2 V}{\partial x^2} = q_{xx}, \dots$$

and

$$\chi_x = eQq_{xx}, \dots \quad (9.108)$$

Therefore

$$\chi_{aa} = \chi_x \cos^2 \theta_{xa} + \chi_y \cos^2 \theta_{ya} + \chi_z \cos^2 \theta_{za} \quad (9.109)$$

$$\chi_{bb} = \chi_x \cos^2 \theta_{xb} + \chi_y \cos^2 \theta_{yb} + \chi_z \cos^2 \theta_{zb} \quad (9.110)$$

$$\chi_{cc} = \chi_x \cos^2 \theta_{xc} + \chi_y \cos^2 \theta_{yc} + \chi_z \cos^2 \theta_{zc} \quad (9.111)$$

The difficulty in the solution for the principal elements is apparent from these equations. In the general case where the angles as well as the magnitudes  $\chi_x$ ,  $\chi_y$ , and  $\chi_z$  are unknown, there are too few equations linking these unknowns with observable quantities. To diagonalize the tensor in the usual way we must also know the off-diagonal elements  $\chi_{ab}$ ,  $\chi_{ac}$ , and so on. However, these off-diagonal elements are not directly observable in the first-order quadrupole hyperfine structure usually measured. For nuclei with large quadrupole coupling it is sometimes possible to obtain very approximate values of off-diagonal elements from measurement of the second-order displacements in the hyperfine component (Section 6), but only diagonal elements in the inertial system are usually measured. Devious methods for use of these diagonal elements to give information about the principal elements are described later.

In some molecules the directions of one or more of the principal axes in the coupling can be ascertained from a consideration of the symmetry of the electronic structure around the coupling nucleus. Then, with the molecular structure and the inertial axes  $a$ ,  $b$ , and  $c$  known from analysis of the rotational spectra, the angles  $\theta$  can be found; hence the coupling constants  $\chi_x$ ,  $\chi_y$ , and  $\chi_z$  can be obtained from the measured quantities  $\chi_{aa}$ ,  $\chi_{bb}$ , and  $\chi_{cc}$  by solution of (9.109)–(9.111). In some cases the coupling has axial symmetry about a bond axis or other axis. If  $z$  is chosen as such an axis of symmetry,  $\chi_x = \chi_y = -\frac{1}{2}\chi_z$ . There is then only one independent coupling constant, and (9.109)–(9.111) can be put in the form

$$\chi_{aa} = \frac{1}{2}\chi_z(3 \cos^2 \theta_{za} - 1) \quad (9.112)$$

$$\chi_{bb} = \frac{1}{2}\chi_z(3 \cos^2 \theta_{zb} - 1) \quad (9.113)$$

$$\chi_{cc} = \frac{1}{2}\chi_z(3 \cos^2 \theta_{zc} - 1) \quad (9.114)$$

where  $\chi_z$  represents the coupling constant with reference to the symmetry axis.

In a molecule having a plane of symmetry, the axis perpendicular to the plane will be a principal axis of inertia and also a principal axis of the field gradient or coupling. We assume that this is the  $c$  axis of the inertial moment and that it coincides with the principal axis  $y$  of the field gradient. Then (9.109)–(9.111) reduce to the form

$$\chi_{aa} = \chi_x \sin^2 \theta_{za} + \chi_z \cos^2 \theta_{za} \quad (9.115)$$

$$\chi_{bb} = \chi_x \cos^2 \theta_{za} + \chi_z \sin^2 \theta_{za} \quad (9.116)$$

## Chapter X

# EFFECTS OF APPLIED ELECTRIC FIELDS

---

1	LINEAR AND SYMMETRIC-TOP MOLECULES WITHOUT NUCLEAR COUPLING	451
2	LINEAR AND SYMMETRIC-TOP MOLECULES WITH NUCLEAR QUADRUPOLE COUPLING	458
	The Weak-field Case	459
	The Strong-field Case: Single or Plural Nuclear Coupling	462
	The Intermediate-field Case	465
3	ASYMMETRIC-TOP MOLECULES WITHOUT NUCLEAR COUPLING	468
	The Nondegenerate Case	469
	The Degenerate Case	474
4	ASYMMETRIC-TOP MOLECULES WITH NUCLEAR QUADRUPOLE COUPLING	478
5	MOLECULES IN EXCITED VIBRATIONAL STATES—INVERSION DOUBLETS AND / DOUBLETS	481
6	ANISOTROPIC POLARIZABILITIES FROM THE STARK EFFECT	484
7	RELATIVE INTENSITIES	489
8	IDENTIFICATION AND MODULATION OF ROTATIONAL LINES WITH THE STARK EFFECT	491
9	DIPOLE MOMENTS FROM THE STARK EFFECT	493

The Stark effect is a particularly useful auxiliary in microwave spectroscopy. From it, the most accurate evaluation of electric dipole moments of gaseous molecules can be made. It is also useful in the identification of pure rotational lines, particularly of asymmetric-top molecules, and it is widely employed as an aid to the detection of spectral lines [1].

## 1 LINEAR AND SYMMETRIC-TOP MOLECULES WITHOUT NUCLEAR COUPLING

Classically, the interaction energy of a dipole moment  $\mu$  in a field  $\mathcal{E}$  is  $-\mu \cdot \mathcal{E}$ . In the Stark effect of rotational spectra,  $\mathcal{E}$  is an electric field fixed in space, and

$\mu$  is an electric dipole moment fixed in the molecule. Here  $\mathcal{E}$  is assumed to be constant in magnitude and to have the fixed direction  $Z$  in space, and  $\mu$  is assumed to be constant in the molecule-fixed reference system chosen as the principal inertial axes  $x, y, z$ . With these conditions, the Stark effect Hamiltonian operator can then be expressed as

$$\mathcal{H}_{\mathcal{E}} = -\mathcal{E} \sum_{g=x,y,z} \mu_g \Phi_{Zg} \quad (10.1)$$

where  $\Phi_{Zg}$  are the direction cosines of the  $x, y, z$  axes with reference to the space-fixed  $Z$  axis. A small term  $\alpha\mathcal{E}^2\Phi_{Zg}$  caused by anisotropic polarizability of the molecule which is neglected in (10.1) is treated in Section 6. Linear and symmetric-top molecules have a dipole moment component only along the symmetry axis  $z$ . For them,  $\mu_z = \mu$ ,  $\mu_x = \mu_y = 0$ ; the Hamiltonian then becomes simply

$$\mathcal{H}_{\mathcal{E}} = -\mu\mathcal{E}\Phi_{zz} \quad (10.2)$$

where  $\mu$  and  $\mathcal{E}$  are constants and where  $\Phi_{zz}$  is the direction cosine of the axis of molecular symmetry with reference to the direction of the applied field. Although the magnitude of the field is periodically changed in a Stark modulation spectrometer, a square-wave modulation of low frequency is generally employed so that  $\mathcal{E}$  can still be considered constant in value during the time interval when the Stark components are displaced. In comparison to the effects of the permanent dipole moment which must be present for detection of rotational spectra, those of the much small polarization moments induced through electronic displacements by the applied field are entirely negligible. We can consider  $\mu$  as having a constant value in the molecule-fixed reference system even though centrifugal distortion causes it to vary slightly with vibrational state. In the present treatment we shall neglect these small effects and consider only  $\Phi$  as varying with rotation.

For rotational lines observed in the microwave region with the field values usually applicable, the Stark energies can be evaluated with significant accuracy from perturbation theory. The first-order energy is simply the average of  $\mathcal{H}_{\mathcal{E}}$  over the unperturbed rotational state. Since the linear molecule can be treated as a special case of the symmetric top with  $K=0$ , we shall express the average first in the unperturbed symmetric-top wave functions. In this representation the first-order Stark energies are

$$\begin{aligned} E_{\mathcal{E}}^{(1)} &= (J, K, M_J | \mathcal{H}_{\mathcal{E}} | J, K, M_J) \\ &= -\mu\mathcal{E}(J, K, M_J | \Phi_{zz} | J, K, M_J) \\ &= -\frac{\mu\mathcal{E}KM_J}{J(J+1)} \end{aligned} \quad (10.3)$$

where the direction cosine matrix elements are evaluated from Table 2.1. Note that  $M_J$  is designated by  $M$  in Table 2.1.

When  $K=0$ , it is seen from (10.3) that  $E_{\mathcal{E}}^{(1)}=0$ . Thus there is no first-order Stark effect for a linear molecule nor for the  $K=0$  levels of a symmetric-top

molecule. We can also prove this by averaging  $\Phi_{zz}$  over the wave function  $\psi_{J,M_J}$  of the linear molecule.

The first-order energy can be obtained from the vector model of Fig. 10.1 which we shall describe because of the insight it gives into the Stark effect. In this model,  $\mathbf{K}$  represents the direction of the symmetry axis and hence the direction of  $\mu$ . In the normal motion of a symmetric top,  $\mathbf{K}$ , which is a component of  $\mathbf{J}$ , precesses about the direction of  $\mathbf{J}$  while  $\mathbf{J}$  precesses about the direction of the applied field, as indicated in the diagram. When the rotational energy is large as compared with the Stark energy, the precession of  $\mathbf{K}$  about  $\mathbf{J}$  is so rapid compared with that of  $\mathbf{J}$  about  $\mathcal{E}$  that the components of  $\mu$  normal to  $\mathbf{J}$  are averaged out, leaving only the component  $\mu_J$  along  $\mathbf{J}$  which effectively interacts with the field. Therefore the first-order Stark energy can be expressed as

$$E_{\mathcal{E}}^{(1)} = -\mathcal{E}\mu_J \cos \theta_{z,J} \quad (10.4)$$

where

$$\cos \theta_{z,J} = \frac{J_z}{|\mathbf{J}|} = \frac{M_J}{[J(J+1)]^{1/2}} \quad (10.5)$$

and

$$\mu_J = \mu \cos \theta_{z,J} = \mu \frac{J_z}{|\mathbf{J}|} = \frac{\mu K}{[J(J+1)]^{1/2}} \quad (10.6)$$

Substitution of these values into (10.4) gives the expression already obtained, (10.3). It is seen that the vanishing of the first-order effect when  $K=0$  can be attributed to the fact that  $\cos \theta_{z,J}=0$  and hence that the molecular axis  $z$  is normal to  $\mathbf{J}$ .

The second-order term of the Stark perturbation for the symmetric-top molecule is

$$\begin{aligned} E_{\mathcal{E}}^{(2)} &= \sum'_{J'} \frac{|(J, K, M_J | \mathcal{H}_{\mathcal{E}} | J', K, M_J)|^2}{E_{J,K} - E_{J',K}} \\ &= \mu^2 \mathcal{E}^2 \left[ \frac{(J, K, M_J | \Phi_{zz} | J+1, K, M_J)^2}{E_{J,K} - E_{J+1,K}} + \frac{(J, K, M_J | \Phi_{zz} | J-1, K, M_J)^2}{E_{J,K} - E_{J-1,K}} \right] \end{aligned} \quad (10.7)$$

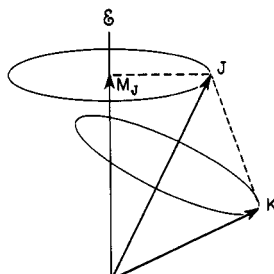


Fig. 10.1 Vector model of a symmetric-top molecule in an electric field.

The direction cosine matrix elements are found from Table 2.1 and the energy differences

$$E_{J,K} - E_{J+1,K} = -2hB(J+1) \quad (10.8)$$

$$E_{J,K} - E_{J-1,K} = 2hBJ \quad (10.9)$$

are evaluated from (6.6). Substitution of the values into (10.7) shows that the second-order Stark energy of the symmetric-top molecule is

$$E_{\mathcal{E}}^{(2)} = \frac{\mu^2 \mathcal{E}^2}{2hB} \left\{ \frac{(J^2 - K^2)(J^2 - M_J^2)}{J^3(2J-1)(2J+1)} - \frac{[(J+1)^2 - K^2][(J+1)^2 - M_J^2]}{(J+1)^3(2J+1)(2J+3)} \right\} \quad (10.10)$$

The Stark energy for the linear molecule, obtained by setting  $K=0$  in (10.10) is

$$E_{\mathcal{E}}^{(2)} = \frac{\mu^2 \mathcal{E}^2}{2hB} \frac{[J(J+1) - 3M_J^2]}{J(J+1)(2J-1)(2J+3)} \quad (10.11)$$

Although the  $J=0$  level cannot be split by the field since for it  $M_J=0$ , it has a second-order Stark displacement which is given by

$$E_{\mathcal{E}}^{(2)}(J=0) = -\frac{\mu^2 \mathcal{E}^2}{6hB} \quad (10.12)$$

as can be seen by substitution of  $J=0$ ,  $K=0$ , and  $M_J=0$  into (10.10).

The  $M_J$  selection rules for rotational lines are

$$M_J \rightarrow M_J \quad \text{and} \quad M_J \rightarrow M_J \pm 1 \quad (10.13)$$

The first of these transitions  $\Delta M_J=0$ , sometimes designated as  $\pi$  components, are observed when the Stark field is parallel to the electric vector of the microwave radiation. The  $\Delta M_J=\pm 1$  transitions, designated as  $\sigma$  components, are observed when the dc field is perpendicular to the electric vector of the radiation. The most commonly observed are the  $\Delta M_J=0$  components. The first-order frequency displacement of the  $K \neq 0$  lines of these components are seen from (10.3) to be

$$\Delta v^{(1)}(\Delta M_J=0) = 2 \left( \frac{\mu \mathcal{E}}{h} \right) \frac{KM_J}{J(J+1)(J+2)} \quad (10.14)$$

To this must be added the small second-order corrections when the splitting becomes large (when  $\mu \mathcal{E}$  is large). For linear molecules or for symmetric-top molecules with  $K=0$ , the displacement of the  $\Delta M_J=0$  components caused by the second-order effect are

$$\Delta v^{(2)}(\Delta M_J=0, J=0 \rightarrow 1) = \frac{8}{15} \frac{\mu^2 \mathcal{E}^2}{h^2 v_0} \quad (10.15)$$

and

$$\Delta v^{(2)}(\Delta M_J=0, J \rightarrow J+1, J \neq 0)$$

$$= \frac{2\mu^2 \mathcal{E}^2}{h^2 v_0} \left[ \frac{3M_J^2(8J^2 + 16J + 5) - 4J(J+1)^2(J+2)}{J(J+2)(2J-1)(2J+1)(2J+3)(2J+5)} \right] \quad (10.16)$$

In these equations  $v_0$  represents the frequency of the unsplit rotational line observed when no field is applied;  $\Delta v$  represents the displacements caused by the applied field  $E$ . If the factor  $2/h^2$  in (10.16) is replaced by 0.5069 and the factor  $8/15h^2$  in (10.15) is replaced by 0.1352, the equations give  $\Delta v$  in MHz when  $v_0$  is in MHz units,  $\mu$  is in debye units, and  $E$  is in volts per centimeter.

It is evident from the foregoing equations that the magnitude of the Stark splitting of the rotational levels decreases with increase in  $J$ . The largest displacement occurs for  $M_J = J$ . For high  $J$  values the maximum second-order displacement varies inversely with  $J^2$  approximately. It also varies inversely with  $B$  so that the second-order Stark effect becomes increasingly difficult to observe as the submillimeter wave region is approached. If one chooses a light molecule so that high-frequency transitions occur at low  $J$  values, the large  $B$  value then makes low the second-order Stark sensitivity. Note, however, that the first-order effect, (10.3), which is very much more sensitive than the second-order effect, is independent of  $B$ . The maximum first-order  $\Delta v$ , which occurs for  $K = J$ ,  $M_J = J$ , varies approximately as  $1/J$ ; but, because of the great sensitivity of the first-order effect, the splittings of symmetric-top lines for  $K \neq 0$  can be observed with ease for very high  $J$  values of transitions occurring in the submillimeter wave region. Figure 10.2 illustrates the first-order Stark effect

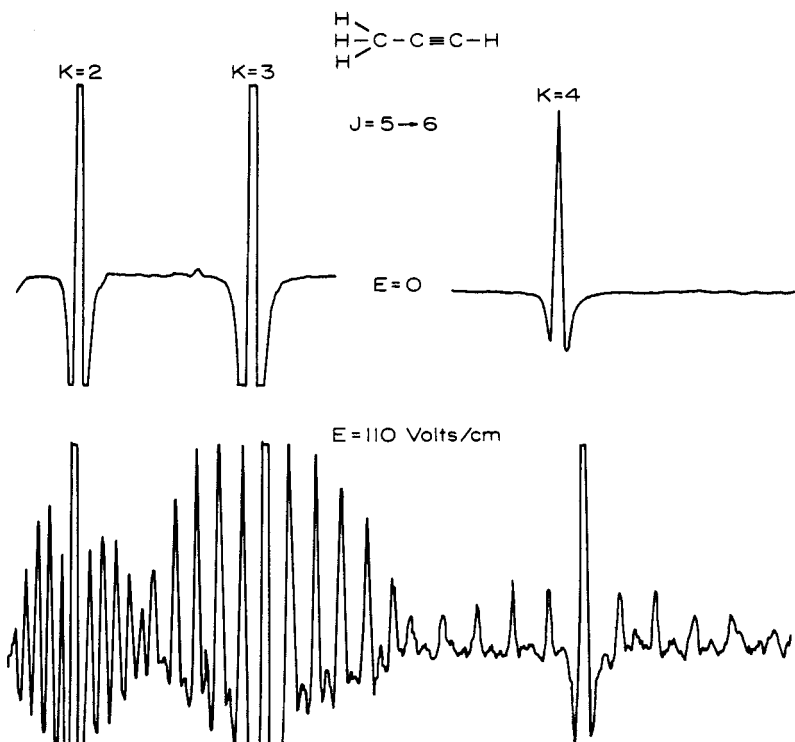
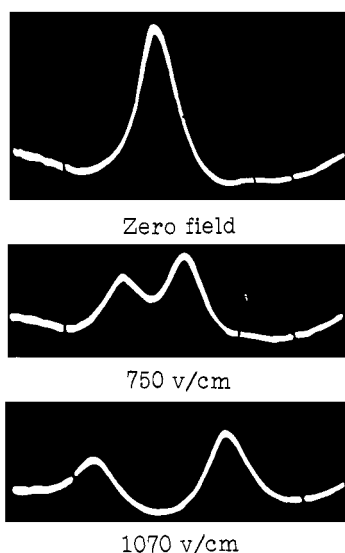


Fig. 10.2 Illustration of the first-order Stark effect of a symmetric-top molecule. The  $J = 5 \rightarrow 6$  transition of  $\text{CH}_3\text{CCH}$ . From P. A. Steiner, Ph.D. dissertation, Duke University, 1964.

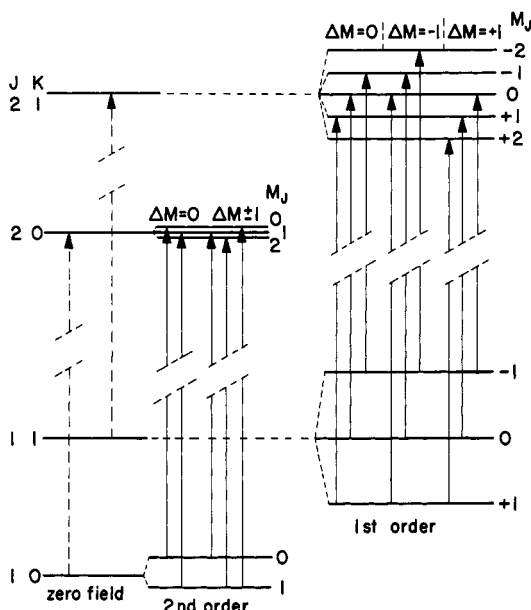
of a symmetric-top molecule observed in the 2.9-mm wave region with a field of 110 v/cm. Figure 10.3 illustrates the second-order effect for a linear molecule as observed in the centimeter wave region with a field up to 1070 v/cm.

Figure 10.4 shows an energy level diagram of the Stark splitting of the  $J=1 \rightarrow 2$  transition of a symmetric-top molecule with the  $\pi$  and  $\sigma$  absorption transitions indicated by solid arrows. Such a diagram cannot be drawn to scale because the separations of the rotational levels are generally of the order of 100 times greater than the Stark splitting; and for the same field value, the first-order splitting of the  $K=1$  lines is of the order of 10 to 100 times that of the second-order splitting of the  $K=0$  lines. Nevertheless, the diagram gives a qualitative indication of the expected Stark effect. The  $K=0$ ,  $\Delta M_J=0$  transitions correspond to the observed components shown for a linear molecule in Fig. 10.3.

Because the field orientations required for observations of the  $\pi$  and  $\sigma$  components are different, these components are generally not observed at the same time. Nearly all measurements in the past have been made on  $\Delta M_J=0$  components, which require the dc electric field to be parallel to the electric vector of the microwave radiation. These are the components observed with a rectangular waveguide Stark cell having for the Stark electrode a metal strip held by dielectric supports in the center of the waveguide. The development of the parallel-plate, millimeter-wave Stark cell made possible the observation of the  $\Delta M_J=\pm 1$  components, which require that the dc electric field be imposed at right angles to the electric vector of the microwave radiation.



**Fig. 10.3** Illustration of the second-order Stark effect in the splitting of the  $J=1 \rightarrow 2$  rotational line of OCS. From T. W. Dakin, W. E. Good, and D. K. Coles, *Phys. Rev.*, **70**, 560 (1946).



**Fig. 10.4** Diagram (not drawn to scale) of the Stark effect of the  $J=1 \rightarrow 2$  transitions of a symmetric-top molecule.

Perturbation theory to second order is sufficient to account for the Stark splitting within the accuracy of most measurements which are made with an imposed field of a few thousand volts/centimeter. When there is a first-order effect, one needs to apply only a few hundred volts/centimeter to obtain a very wide separation of the Stark components ( $\sim 100$  MHz or more), and first-order plus second-order terms are completely adequate. When there is no first-order effect, one often finds it advantageous to apply several thousand volts/centimeter to obtain sufficiently large displacements for precise measurement of  $\Delta v$ . With voltage of the order of 5000 v/cm, Muenter and Laurie [2] detected deviations of as much as 1% from the second-order theory in  $K=0$  transitions of some symmetric-top molecules. For linear molecules or symmetric tops with  $K=0$ , all odd perturbation terms are zero. Hence the next term of significance is of fourth order. To correct for the fourth-order perturbation in the precise measurement of a dipole moment it is fortunately not necessary to employ explicitly the complicated fourth-order formula. The displacement of a particular Stark component for which there is no odd-order effect can be expressed by the simple equation

$$\Delta v = a\mu^2 \mathcal{E}^2 + b\mu^4 \mathcal{E}^4 + \dots \quad (10.17)$$

where  $a$  and  $b$  are constants. The constant  $a$  can be obtained from the second-order formula, (10.11), or for the  $\Delta M_J=0$  component more simply from (10.16).

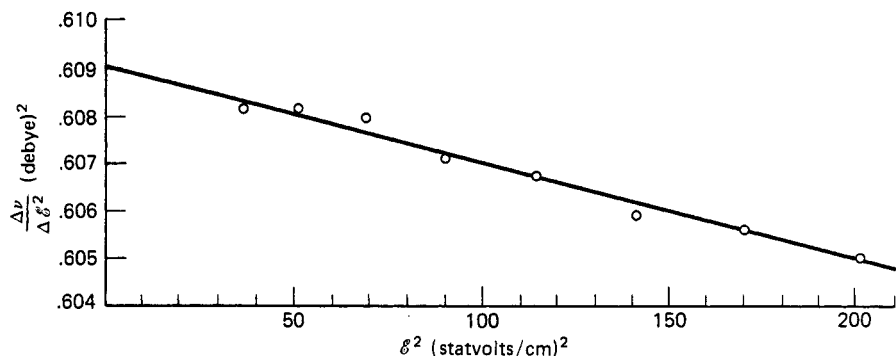


Fig. 10.5 Plot demonstrating fourth-order Stark effect in the  $J=1 \rightarrow 2$ ,  $K=0$ ,  $\Delta M_J=0$  transition of methyl acetylene. From Muenter and Laurie [2].

If one expresses (10.17) in the form

$$\frac{\Delta v}{a\epsilon^2} = \left( \frac{b\mu^4}{a} \right) \epsilon^2 + \mu^2 \quad (10.18)$$

it is seen  $(b\mu^4/a)$  is the slope and  $\mu^2$  is the intercept of a straight line obtained by a plotting of  $(\Delta v/a\epsilon^2)$  versus  $\epsilon^2$ . Figure 10.5 shows such a plot for the  $J=1 \rightarrow 2$ ,  $K=0$  transition of  $\text{CH}_3\text{CCH}$  by Muenter and Laurie. From projection of the straight line one obtains  $\mu^2$  as the intercept. With this value one can then obtain  $b$  from the slope if this is desirable.

Effects of anisotropic polarization, detectable in some molecules at very high field values, are treated in Section 6.

The relative intensities of the Stark components of molecules without hyperfine structure depend only on  $J$  and  $M_J$  and hence are the same for all classes of molecules. The relative intensity formulas given in Section 7 are simply the  $M_J$ -dependent terms of the squared direction-cosine matrix elements given in Chapter II.

## 2 LINEAR AND SYMMETRIC-TOP MOLECULES WITH NUCLEAR QUADRUPOLE COUPLING

The theory of the Stark effect in the rotational spectra of linear molecules with nuclear quadrupole coupling was first treated by Fano [3]; that of symmetric-top molecules, by Low and Townes [4]. Buckingham and Stephens [5] developed this theory further to take into account such cross-product terms as  $\mathcal{H}_S \mathcal{H}_Q$  and  $\mathcal{H}_S^2 \mathcal{H}_Q$  which have measurable effects for molecules having large nuclear quadrupole coupling. Coester [6] has treated the combined Stark-Zeeman effect for symmetric-top molecules with nuclear quadrupole coupling.

The complete Hamiltonian for a rotating molecule having nuclear quadrupole coupling with an imposed electric field can be expressed as

$$\mathcal{H} = \mathcal{H}_r + \mathcal{H}_Q + \mathcal{H}_S \quad (10.19)$$

where  $\mathcal{H}_r$  is the Hamiltonian operator for the pure rotational energy described in Chapter II,  $\mathcal{H}_Q$  is that for the nuclear quadrupole interaction described in Chapter IX, and  $\mathcal{H}_{\mathcal{E}}$  is that just described for the Stark interaction of molecules without hyperfine structure. In finding the characteristic energies it is convenient to consider three cases separately. First is the weak-field case, in which  $\mathcal{H}_{\mathcal{E}} \ll \mathcal{H}_Q$ ; second, the intermediate-field case, in which  $\mathcal{H}_{\mathcal{E}} \sim \mathcal{H}_Q$ ; and third, the strong-field case, in which  $\mathcal{H}_{\mathcal{E}} \gg \mathcal{H}_Q$ . The weak- and strong-field cases are simpler than the intermediate one, and the greater number of measurements of Stark effect and dipole moments have been made with applied fields such that one or the other of these simple cases holds. When the nuclear coupling is relatively strong, as that for Br or I in organic molecules, the weak-field case can be used; when the coupling is relatively weak, as that for B or N, the strong-field case can be easily achieved. Perturbation theory allows the derivation of a closed formula for weak- and strong-field cases; for the intermediate field-cases a secular equation must be solved. Plural nuclear coupling will be treated in the strong-field case only, for which the effect is particularly simple.

### The Weak-field Case

When  $\mathcal{H}_{\mathcal{E}} \ll \mathcal{H}_Q$ , the Stark interaction can be treated as a perturbation on the hyperfine state. The first-order Stark energy of a symmetric-top is then the average of the  $\mathcal{H}_{\mathcal{E}}$  over the wave function  $\psi(J, K, I, F, M_F)$  of the nuclear-coupled molecule unperturbed by the Stark field, that is, the wave function of the operator  $\mathcal{H}_r + \mathcal{H}_Q$ . This wave function can be expanded in terms of the function for the molecule without nuclear coupling:

$$\psi(J, K, I, F, M_F) = \sum_{M_J} C(JIF; M_J M_I M_F) \psi(J, K, M_J) \phi(I, M_I) \quad (10.20)$$

where the  $C$ 's are known as Clebsch-Gordon coefficients, values of which are given by Condon and Shortley [7]. (See also Rose [8].) These coefficients arise when, as here, the problem of combining two commuting angular momenta to form a resultant is considered, in particular  $\mathbf{F} = \mathbf{J} + \mathbf{I}$ . These coefficients are independent of  $K$  and vanish unless  $M_F = M_J + M_I$  and unless  $F$  is one of the following values (see Chapter XV for further discussion).

$$F = J + I, J + I - 1, \dots, |J - I|$$

The first-order Stark term is

$$\begin{aligned} E_{\mathcal{E}}^{(1)} &= (J, K, I, F, M_F | \mathcal{H}_{\mathcal{E}} | J, K, I, F, M_F) \\ &= -\mu \mathcal{E} \sum_{M_J} |C(JIF; M_J M_I M_F)|^2 (J, K, M_J | \Phi_{zz} | J, K, M_J) \end{aligned} \quad (10.21)$$

Since the direction cosine operator  $\Phi_{zz}$  is independent of the nuclear spin function  $\phi(I, M_I)$ , these spin functions are factored out and normalized to unity ( $\phi|\phi\rangle = 1$ ). The quantity  $(J, K, M_J | \Phi_{zz} | J, K, M_J)$  has been evaluated as

$KM_J/[J(J+1)]$  in (10.3). Therefore

$$\begin{aligned} E_{\mathbf{F}}^{(1)} &= -\mu\epsilon \sum_{M_J} |C(JIF; M_J M_I M_F)|^2 \frac{KM_J}{J(J+1)} \\ &= -\frac{\mu\epsilon K}{J(J+1)} \sum_{M_J} |C(JIF; M_J M_I M_F)|^2 M_J \end{aligned} \quad (10.22)$$

The quantity in the summation is the average of  $M_J$  over the function  $\psi(J, K, I, F, M_F)$  which is simply the component of  $J$  along the space-fixed axis in the  $\mathbf{I} \cdot \mathbf{J}$ -coupled vector model of Fig. 10.6. This value can easily be found from the vector model. For example, the component of  $\mathbf{J}$  along  $\mathbf{F}$  is  $|\mathbf{J}| \cos(\mathbf{F}, \mathbf{J})$ , and the averaged component along  $Z$  is

$$\langle M_J \rangle = |\mathbf{J}| \cos(\mathbf{F}, \mathbf{J}) \cos(\mathbf{F}, \mathbf{Z}) \quad (10.23)$$

From application of the law of the cosine with the vector model

$$\cos(\mathbf{F}, \mathbf{J}) = \frac{\mathbf{F}^2 + \mathbf{J}^2 - \mathbf{I}^2}{2|\mathbf{F}||\mathbf{J}|} = \frac{F(F+1) + J(J+1) - I(I+1)}{2[F(F+1)]^{1/2}[J(J+1)]^{1/2}} \quad (10.24)$$

also

$$\cos(\mathbf{F}, \mathbf{Z}) = \frac{M_F}{|\mathbf{F}|} = \frac{M_F}{[F(F+1)]^{1/2}} \quad (10.25)$$

and hence

$$\langle M_J \rangle = M_F \frac{F(F+1) + J(J+1) - I(I+1)}{2F(F+1)} \quad (10.26)$$

Substitution of this value for  $\langle M_J \rangle$  for the summation into (10.22) shows the first-order Stark energy to be

$$E_{\mathbf{F}}^{(1)} = -\frac{\mu\epsilon KM_F[F(F+1) + J(J+1) - I(I+1)]}{2J(J+1)F(F+1)} \quad (10.27)$$

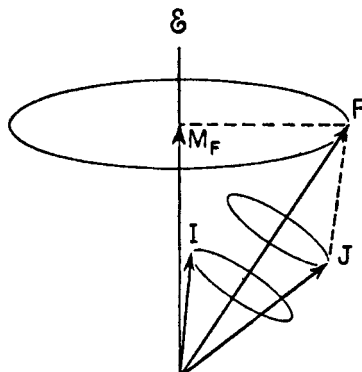


Fig. 10.6 Vector model of the weak-field Stark effect of a symmetric-top molecule with nuclear coupling.

One can derive (10.27) entirely from the vector model of Fig. 10.6 by first resolving the component  $\mu$ , which is wholly along the symmetry axis **K**, from **K** to **J**. Thus,

$$\mu_J = \mu \frac{K}{[J(J+1)]^{1/2}} \quad (10.28)$$

$$\mu_F = \mu_J \cos (\mathbf{F}, \mathbf{J}) \quad (10.29)$$

and

$$\mu_{\mathcal{E}} = \mu_F \cos (\mathbf{F}, \mathbf{Z}) = \mu_F \frac{M_F}{[F(F+1)]^{1/2}} \quad (10.30)$$

The Stark energy is just  $-\mathcal{E}$  times the average dipole moment in the direction of the field. Therefore

$$E_{\mathcal{E}} = -\mu_{\mathcal{E}} \mathcal{E} = -\frac{\mu \mathcal{E} K M_F}{[J(J+1)]^{1/2} [F(F+1)]^{1/2}} \cos (\mathbf{F}, \mathbf{J}) \quad (10.31)$$

Substitution of the value of  $\cos (\mathbf{F}, \mathbf{J})$  from (10.24) into (10.31) yields (10.27).

It should be noted that the first-order Stark effect vanishes when  $K=0$ , as it does for molecules without nuclear coupling. This condition also applies for linear molecules. When  $M_F=F=J+I$ , the first-order formula reduces to the simple form,

$$E_{\mathcal{E}}^{(1)} = -\frac{\mu \mathcal{E} K}{J+1} \quad \text{when } M_F=F=J+I \quad (10.32)$$

which is equivalent to (10.3) for molecules without quadrupole coupling when  $M_J=J$ .

The second-order term in the weak-field case is

$$E_{\mathcal{E}}^{(2)} = \sum'_{F', J'} \frac{|(J, K, I, F, M_F | \mathcal{H}_{\mathcal{E}} | J', K, I, F', M_F)|^2}{E_{J, K, I, F, M_F} - E_{J', K, I, F', M_F}} \quad (10.33)$$

Note that the term  $F=F'$ ,  $J=J'$  is to be excluded from the sum. This expression can be separated into two sums. By substitution of the  $\mathcal{H}_{\mathcal{E}}$  from (10.2) it becomes

$$\begin{aligned} E_{\mathcal{E}}^{(2)} = & \mu^2 \mathcal{E}^2 \sum_{F' \neq F} \frac{|(J, K, I, F, M_F | \Phi_{zz} | J, K, I, F', M_F)|^2}{E_Q(F) - E_Q(F')} \\ & + \mu^2 \mathcal{E}^2 \sum_{F', J' \neq J} \frac{|(J, K, I, F, M_F | \Phi_{zz} | J', K, I, F', M_F)|^2}{E_r(J) - E_r(J')} \end{aligned} \quad (10.34)$$

where the approximation  $E_{J, K, F} - E_{J', K, F'} \approx E_{J, K} - E_{J', K}$  has been made. The first of these expressions is the larger because of the smaller energy difference in the denominator. To evaluate the terms on the right, one expresses the functions of  $|J, K, I, F, M_F\rangle$  in terms of those of the field-free rotor with the nucleus decoupled, as in the expansion of (10.20). When evaluated, the first term on the right contains the factor  $K$  and hence vanishes when  $K=0$ . The second term gives the second-order correction for symmetric-top levels when  $K=0$ , or for

linear molecules. It has the values [3, 4]

$$E_{\mathcal{E}}^{(2)}(K=0) = - \frac{\mu^2 \mathcal{E}^2 [3M_F^2 - F(F+1)][3D(D-1) - 4F(F+1)J(J+1)]}{hB2J(J+1)(2J-1)(2J+3)2F(F+1)(2F-1)(2F+3)} \quad (10.35)$$

in which

$$D = F(F+1) - I(I+1) + J(J+1) \quad (10.36)$$

As before, the case where  $M_F = F = J + I$  is particularly simple since the Stark effect is independent of the effects of nuclear quadrupole coupling. As noted previously, because of the smaller energy difference in its denominator, the first term on the right of (10.34) is larger than the second term, but it is absent unless the much larger, first-order effect of (10.27) is present. Since the field values must be sufficiently small to insure that the Stark splitting is small compared with the quadrupole splitting for the weak field case to apply, the second-order terms are not of much value except when  $K=0$ . Hence we shall not reproduce here the rather complicated second-order term which vanishes when  $K=0$ . An explicit formula for the term is given by Coester [6]. In addition to the above terms, Buckingham and Stephens [5] show that for strong nuclear quadrupole coupling, which is necessary for practical application of the weak-field case, cross terms of the form

$$2 \sum_{J' \neq J} \frac{(J, K, I, F, M_F | \mathcal{H}_{\mathcal{E}} | J', K, I, F, M_F)(J', K, I, F, M_F | \mathcal{H}_Q | J, K, I, F, M_F)}{E(J) - E(J')}$$

are important. With this term included, the Stark displacement of a particular component in the weak-field case can be expressed [5] as

$$\Delta v = a\mu\mathcal{E} + b \frac{(\mu\mathcal{E})(eQq)}{B} + c \frac{\mu^2 \mathcal{E}^2}{eQq} \quad (10.37)$$

where  $a$ ,  $b$ , and  $c$  depend only on the quantum numbers for the transition.

The  $M_F$  selection rules are

$$M_F \rightarrow M_F \quad \text{and} \quad M_F \rightarrow M_F \pm 1 \quad (10.38)$$

The  $\Delta M_F = 0$  transitions are observed when the dc Stark field is parallel to the radiofrequency electric field, while  $\Delta M_F = \pm 1$  transitions are observed when these fields are perpendicular.

### The Strong-field Case: Single or Plural Nuclear Coupling

The simplest and probably the most useful case is that in which the applied field  $\mathcal{E}$  is sufficiently strong to break down the nuclear coupling between  $\mathbf{I}$  and  $\mathbf{J}$  but not large enough to perturb significantly the rotational state. This case occurs when  $\mathcal{H}_Q \ll \mathcal{H}_{\mathcal{E}} \ll \mathcal{H}_r$ . It is represented by the vector model of Fig. 10.7 in which both  $\mathbf{J}$  and  $\mathbf{I}$  precess about the direction of the field. This model is similar to that of the familiar Paschen-Back effect observed with strong magnetic fields in atomic spectra.

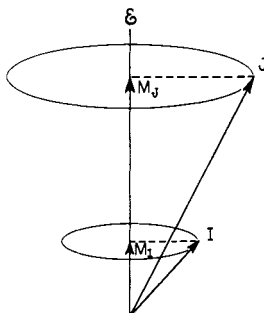


**Fig. 10.7** Vector model of the strong-field Stark effect of a molecule with nuclear coupling.

Since  $\mathbf{J}$  and  $\mathbf{I}$  are decoupled, the quantum number  $F$  is destroyed as a good quantum number and the  $J, I, F$  scheme is no longer appropriate. The representation appropriate to the strong-field case is  $J, K, I, M_J, M_I$ , and in this representation the required matrix elements of  $\mathcal{H}_r$ ,  $\mathcal{H}_Q$ , and  $\mathcal{H}_S$  are easily found. The rotational Hamiltonian  $\mathcal{H}_r$  is independent of  $I$  and  $M_I$ , and the values are those already obtained in Chapter VI. Since the matrix elements of  $\mathcal{H}_S$  are likewise independent of the nuclear spin functions  $|I, M_I\rangle$  in this decoupled case, the values of the Stark energy are the same as those for molecules without nuclear coupling described in Section 1. Hence we have only to evaluate  $\mathcal{H}_Q$ .

Under the assumed conditions, only the  $Z$  component of the molecular field component, or  $V_{ZZ} = (\partial^2 V / \partial Z^2)$ , interacts with the nuclear quadrupole moment, and only with the  $Z$  component of  $eQ_{ZZ}$ . The precession of  $\mathbf{J}$  about  $\mathbf{Z}$  is so rapid relative to that of  $\mathbf{I}$  that the  $X$  and  $Y$  components are averaged out. The quadrupole Hamiltonian can be expressed as

$$\mathcal{H}_Q = \frac{1}{4} Q_{ZZ} V_{ZZ} \quad (10.39)$$

With the value of  $(Q_{ZZ})_p$  obtained from (9.53) with  $i=j=Z$  and with  $V_{ZZ}$  given by (9.48), it is seen that

$$(\mathcal{H}_Q)_{ZZ} = \frac{eQq_J}{4J(2J-1)I(2I-1)} [3J_Z^2 - J(J+1)][3I_Z^2 - I(I+1)] \quad (10.40)$$

This Hamiltonian is diagonal in the specified representation with  $J_Z$  and  $I_Z$  having the eigenvalues  $M_J$  and  $M_I$ , respectively. The quantity  $q_J$ , which is independent of  $M_J$  and  $M_I$ , has already been evaluated in Chapter IX, Section 7. For the symmetric top, its values are given to first order by (9.88). Thus for the symmetric top in the strong-field case the quadrupole energies are

$$E_Q = \frac{eQq}{4(2J-1)(2J+3)I(2I-1)} \left[ \frac{3K^2}{J(J+1)} - 1 \right] \times [3M_J^2 - J(J+1)][3M_I^2 - I(I+1)] \quad (10.41)$$

which for the linear molecule becomes

$$E_Q = - \frac{eQq[3M_J^2 - J(J+1)][3M_I^2 - I(I+1)]}{4(2J-1)(2J+3)I(2I-1)} \quad (10.42)$$

The nuclear quadrupole interaction in the strong-field case is very similar to the interaction of a quadrupole moment with an axially symmetric field in a solid. If  $q_{zz}$  of (9.24) for the solid state is replaced by the value of  $V_{zz}$  from (9.48), it is seen that the same value of  $E_Q$  is obtained as is given by (10.41).

The strong-field Stark effect has the great advantage that coupling by more than one nucleus causes no theoretical complication, as it does for field-free molecules or for the weak-field or intermediate-field Stark effect. The value for the  $E_Q$  of each coupling nucleus is calculated from (10.41), and the results are added:

$$E_Q = E_{Q_1}(I_1) + E_{Q_2}(I_2) + \dots$$

The presence of magnetic hyperfine structure also causes no particular complication in the strong-field case, for which all nuclear coupling is broken down. For molecules in  ${}^1\Sigma$  states the magnetic coupling is weak and easily decoupled. The strong-field energies are given by

$$E_m = (J, K, M_J, M_I | \mathcal{H}_m | J, K, M_J, M_I) = C_{J,K} M_J M_I \quad (10.43)$$

where  $C_{J,K}$  depends only on the quantum numbers  $J$  and  $K$  and is given by (9.158). The magnetic energy for the different nuclei are additive, like those for the quadrupole energy. This simplification is possible because the precession of  $\mathbf{J}$  is so dominated by the Stark field that coupling by a given nucleus does not significantly alter the value of the electric field gradient or the magnetic field value at the other nuclei. This is similar to the situation in solids where the nuclear coupling does not alter the field gradient because the directions of the field gradients are "frozen in." Hence the quadrupole couplings by the different nuclei of the solid state are simply additive, as in the strong-field case. In addition to the usual selection rules for  $M_J$ , we have  $\Delta M_{I_i} = 0$ .

The resultant energy for the strong-field case is the sum

$$E = E_r + E_{\mathcal{E}}^{(1)} + E_{\mathcal{E}}^{(2)} + \sum_i E_{Q_i} + \sum_i E_{m_i} \quad (10.44)$$

where the values of  $E_{\mathcal{E}}^{(1)}$  and  $E_{\mathcal{E}}^{(2)}$  are those given in Section 1 and where  $E_{Q_i}$  and  $E_{m_i}$  are those given above.

Although the strong-field case can generally be achieved when  $eQq$  is not large, there is one important exception for  $K=0$  which occurs for integral spin values. When  $M_J = \pm 1$  and also  $M_I = \pm 1$ , there is an admixture of the  $M_J = \pm 1$  and the  $M_I = \mp 1$  states which causes a breakdown in the  $M_J = \pm 1$  degeneracy and hence a failure of the strong-field formulas. To obtain the energy for this case one must solve the secular equation

$$\begin{vmatrix} E_{\mathcal{E}}(M_J=1) + (1, -1 | \mathcal{H}_Q | 1, -1) - E & (1, -1 | \mathcal{H}_Q | -1, 1) \\ (-1, 1 | \mathcal{H}_Q | 1, -1) & E_{\mathcal{E}}(M_J=-1) + (-1, 1 | \mathcal{H}_Q | -1, 1) - E \end{vmatrix} = 0 \quad (10.45)$$

for the intermediate-field case described in the next section. The abbreviation  $|M_J, M_I\rangle$  is used for  $|J, I, M_J, M_I\rangle$ . It is apparent from (10.45) that there are off-diagonal matrix elements that directly connect  $M_J = +1$  and  $M_J = -1$ . For  $E_{\mathcal{S}}(|M_J| = 1)$ , the values from (10.10) can be used. The matrix elements of  $\mathcal{H}_Q$  are obtained from (10.53). Solution of this equation is like that for (10.55).

### The Intermediate-field Case

When the applied field is such as to make  $\mathcal{H}_{\mathcal{S}}$  of comparable magnitude to  $\mathcal{H}_Q$ , one must treat  $\mathcal{H}_Q + \mathcal{H}_{\mathcal{S}}$  as a common perturbation on the pure rotational states instead of treating  $\mathcal{H}_{\mathcal{S}}$  as a perturbation on the functions of  $\mathcal{H}_r + \mathcal{H}_Q$ , as was done for weak fields. This can be achieved by solution of a secular equation which is obtained from

$$\mathcal{H}\psi = E\psi \quad (10.46)$$

where

$$\mathcal{H} = \mathcal{H}_r + \mathcal{H}_Q + \mathcal{H}_{\mathcal{S}} \quad (10.47)$$

To find  $E$ , it is convenient to express  $\psi$  in the eigenfunctions of the operator  $\mathcal{H}_r$  of the unperturbed rotor

$$\psi = \sum_i C_i \psi_i(J, K, I, M_J, M_I) \quad (10.48)$$

Substitution of these functions into (10.46), multiplication by  $\psi_j$ , followed by integration and transformation, yield

$$\sum_i C_i [(\psi_j | \mathcal{H}_r + \mathcal{H}_{\mathcal{S}} + \mathcal{H}_Q | \psi_i) - E \delta_{ij}] = 0 \quad (10.49)$$

Since  $\mathcal{H}_r$  is diagonal in all the quantum numbers  $J, K, I, M_J, M_I$ , and since  $\mathcal{H}_Q$  is diagonal in  $J, K, I$ , (10.49) can be expressed as

$$\begin{aligned} & \sum_i C_i [(J, K, I, M_J, M_I | \mathcal{H}_{\mathcal{S}} | J', K, I, M_J, M_I) \\ & \quad + (J, K, I, M_J, M_I | \mathcal{H}_Q | J, K, M'_J, M'_I) + (E_{J,K} - E) \delta_{ij}] = 0 \end{aligned} \quad (10.50)$$

where  $E_{J,K}$  is the unperturbed rotational energy. Because  $\mathcal{H}_{\mathcal{S}}$  has off-diagonal elements only in  $J$ , the matrix can be conveniently reduced by a procedure that begins with evaluation of  $\mathcal{H}_{\mathcal{S}}$  for the rotor without nuclear coupling, as was made in Section 1. Let the resulting values be

$$E_{\mathcal{S}}(M_J) = E_{\mathcal{S}}^{(1)}(M_J) + E_{\mathcal{S}}^{(2)}(M_J) \quad (10.51)$$

where  $E_{\mathcal{S}}^{(1)}(M_J)$  and  $E_{\mathcal{S}}^{(2)}(M_J)$  are given by (10.3) and (10.10). The secular equation can then be expressed as

$$|(J, K, I, M_J, M_I | \mathcal{H}_Q | J, K, I, M'_J, M'_I) + [E_{J,K} + E_{\mathcal{S}}(M_J) - E] \delta_{M_J M'_J} \delta_{M_I M'_I}| = 0 \quad (10.52)$$

This simplification is possible because the second-order perturbation in  $J$  by the Stark effect can be neglected in the evaluation of the matrix elements of

$\mathcal{H}_Q$ . The required matrix elements [9, 6] are

$$\begin{aligned}
 & (J, K, I, M_J, M_I | \mathcal{H}_Q | J, K, I, M'_J, M'_I) \\
 &= P(J, K, I) \{ \delta_{M'_J, M_J} \delta_{M'_I, M_I} [3M_I^2 - I(I+1)] \\
 &\quad \times [3M_J^2 - J(J+1)] + (\delta_{M'_J, M_J \pm 1} \delta_{M'_I, M_I \mp 1}) \\
 &\quad \times [\frac{3}{2} + 3M_I M_J + 3(M_I \mp 1)(M_J \pm 1)] \\
 &\quad \times ([J(I+1) - M_I(M_I \mp 1)][J(J+1) - M_J(M_J \pm 1)])^{1/2} + (\delta_{M_J M_J \pm 2} \delta_{M_I M_I \mp 2}) \\
 &\quad \times \frac{3}{2} ([J(J+1) - M_J(M_J \pm 1)] \times [J(J+1) - (M_J \pm 1)(M_J \pm 2)]) \\
 &\quad \times [I(I+1) - M_I(M_I \mp 1)] \times [I(I+1) - (M_I \mp 1)(M_I \mp 2)])^{1/2} \} \quad (10.53)
 \end{aligned}$$

where

$$P = \frac{eqQ}{4(2J-1)(2J+3)I(2I-1)} \left( \frac{3K^2}{J(J+1)} - 1 \right)$$

and where the  $\delta$ 's are all zero except when the indicated subscript values are equal. Because  $\mathcal{H}_Q$  is diagonal in  $J, K, I$ , an independent set of equations is obtained for each  $J, K, I$  combination. Furthermore,  $\mathcal{H}_Q$  is diagonal in  $M \equiv M_J + M_I$ , and hence the matrix can be factored into submatrices with common values of  $M_J + M_I$ . In writing out the matrix it is convenient to group together the common values  $M = M_J + M_I$ .

For the maximum values  $M_J = J$ ,  $M_I = I$ , and  $M = I + J$ , the secular equation is of first degree and gives

$$E = E_{J,K} + E_{\epsilon}(M_J = J) + (M_J = J, M_I = I | \mathcal{H}_Q | M_J = J, M_I = I) \quad (10.54)$$

when  $M = I + J - 1$ , the secular equation is the quadratic

$M_J, M_I$	$M_J = J, M_I = I - 1$	$M_J = J - 1, M_I = I$	= 0
$\begin{cases} M_J = J \\ M_I = I - 1 \end{cases}$	$E_{J,K} + E_{\epsilon}(M_J = J)$ $+ (J, I - 1   \mathcal{H}_Q   J, I - 1) - E$	$(J - 1, I   \mathcal{H}_Q   J, I - 1)$	
$\begin{cases} M_J = J - 1 \\ M_I = I \end{cases}$	$(J - 1, I   \mathcal{H}_Q   J, I - 1)$	$E_{J,K} + E_{\epsilon}(M_J = J - 1)$ $+ (J - 1, I   \mathcal{H}_Q   J - 1, I) - E$	

(10.55)

In these equations we have used the abbreviation  $|M_J, M_I\rangle$  for  $|J, K, I, M_J, M_I\rangle$ . The equation of next higher order, that for  $M = M_J + M_I = J + I - 2$ , is a cubic; the next, for  $M = J + I - 3$ , is a quartic. High-speed computers can be used for solution of these equations of higher power when it is desirable. However, one can often employ transitions involving only the energy values obtained from equations of first and second power for accurate evaluation of dipole moments. The relevant selection rules for  $M$  are  $\Delta M = 0, \pm 1$ ;  $M_J$  and  $M_I$  are no longer good quantum numbers.

Explicit values of  $E$  for symmetric rotors ( $K \neq 0$ ) for which  $M = M_J + M_I = J + I$  are derived from (10.54).

$$E_{J,K,M_J=J,M_I=I} = E_{J,K} - \frac{\mu\mathcal{E}K}{J+1} - \frac{\mu^2\mathcal{E}^2[(J+1)^2 - K^2]}{2hB(J+1)^3(2J+3)} + \frac{eQq[3K^2 - J(J+1)]}{4(J+1)(2J+3)} \quad (10.56)$$

For linear molecules this equation reduces to

$$E_{J,M_J=J,M_I=I} = E_J - \frac{\mu^2\mathcal{E}^2}{2hB(J+1)(2J+3)} - \frac{eQqJ}{4(2J+3)} \quad (10.57)$$

With a Stark spectrometer which permits measurement of the  $\sigma$  component  $M \rightarrow M' (=M+1)$  of the  $J \rightarrow J' (=J+1)$  transition, one can measure frequency shifts determined entirely by (10.56) or (10.57). From these shifts one can obtain  $\mu$  and  $eQq$ .

The quadratic equation (10.55) is readily solvable and yields energies of the levels for  $M = M_J + M_I = J + I - 1$  which are

$$E_{\pm} = E_{J,K} + \frac{1}{2}(\alpha + \beta + a + b) \pm \frac{1}{2}[(\alpha - \beta + a - b)^2 + 4c^2]^{1/2} \quad (10.58)$$

where

$$\alpha = E_{\mathcal{E}}(M_J=J) = -\frac{\mu\mathcal{E}K}{J+1} - \frac{(\mu\mathcal{E})^2}{2hB} \frac{[(J+1)^2 - K^2]}{(J+1)^3(2J+3)} \quad (10.59)$$

$$\begin{aligned} \beta &= E_{\mathcal{E}}(M_J=J-1) \\ &= -\frac{\mu\mathcal{E}K(J-1)}{J(J+1)} + \frac{(\mu\mathcal{E})^2}{2hB} \left\{ \frac{(J^2 - K^2)}{J^3(2J+1)} - \frac{4J[(J+1)^2 - K^2]}{(J+1)^3(2J+1)(2J+3)} \right\} \end{aligned} \quad (10.60)$$

$$\begin{aligned} a &= (M_J=J, M_I=I-1 | \mathcal{H}_Q | M_J=J, M_I=I-1) \\ &= P(J)(2J-1)(2I^2 - 7I + 3) \end{aligned} \quad (10.61)$$

$$\begin{aligned} b &= (M_J=J-1, M_I=I | \mathcal{H}_Q | M_J=J-1, M_I=I) \\ &= P(I)(2I-1)(2J^2 - 7J + 3) \end{aligned} \quad (10.62)$$

$$\begin{aligned} c &= (M_J=J-1, M_I=I | \mathcal{H}_Q | M_J=J, M_I=I-1) \\ &= 3P[(2J-1)(2I-1)](IJ)^{1/2} \end{aligned} \quad (10.63)$$

$$P = \frac{eQq}{4(2J-1)(2J+3)I(2I-1)} \left[ \frac{3K^2}{J(J+1)} - 1 \right] \quad (10.64)$$

The levels corresponding to  $E_+$  and  $E_-$  in (10.58) represent a mixture of  $M_J=J$  and  $M_J=J-1$  states. The  $\pi$ -type transitions ( $\Delta M=0$ ) are possible from, or to, either the plus or minus levels to other levels having the same  $M$  values, provided that the selection rules for  $J$  and  $K$  are not violated. A commonly observed transition for measurement of dipole moments is a  $\pi$ -type one from the  $M=M_J+M_I=J+I$  (the energy of which can be calculated with 10.56) to the next highest rotational level, represented by  $J'=J+1$ ,  $M'=J'+I-1=J+I$ . Since  $M=M'$ , this is a  $\Delta M=0$  transition which is observed with the dc electric field parallel to the electric vector of the microwave radiation. However, a doublet

will be observed that corresponds to transitions to the plus and minus substates having the same  $M$  value. The relative intensities of the doublet will depend on the relative weights of the  $M'_J = J'$  and  $M'_J = J' - 1$  components in the admixed states. These weights can be found by substitution of the  $E_{\pm}$  values into (10.50) followed by solution for the  $C_i^2$  values. The relative intensities will be proportional to the  $C_i^2$  values of the two admixed functions.

In deriving the secular equation for the intermediate-field values Low and Townes [4] used the representation  $J, I, F, M$  in which  $\mathcal{H}_Q$  is diagonal and  $\mathcal{H}_S$  is therefore not diagonal. This representation is a bit complicated since one must then express the basis function in terms of the set  $|J, K, I, M_J, M_I\rangle$  in which the matrix elements of  $\mathcal{H}_S$  are known. This transformation can be achieved by use of (10.20) with the Clebsch-Gordon [7, 8] coefficients.

### 3 ASYMMETRIC-TOP MOLECULES WITHOUT NUCLEAR COUPLING

The theory of the Stark effect for asymmetric rotors has been developed by Penney [10] and by Golden and Wilson [11]. The Stark effect for asymmetric-top molecules is calculated with perturbation theory in a manner similar to that for linear or symmetric rotors. However, the evaluation of the direction cosine matrix elements becomes more involved since the wave functions for asymmetric rotors are considerably more complicated. With symmetric or linear molecules the dipole moment was associated with one of the axes, whereas for asymmetric rotors we have now the possibility of permanent molecular dipole components along each of the three principal axes of inertia. The Stark effect Hamiltonian operator will thus have the form given in (10.1). The application of an electric field will, via the interaction of the dipole moment and the field, perturb the rotational motion and thus the rotational energy levels. In particular, the levels will no longer be  $(2J+1)$ -fold degenerate in the space orientation quantum number  $M_J$ . Each energy level of the asymmetric rotor consequently splits up into a number of sublevels corresponding to various values of  $|M_J|$ .

In a perturbation treatment of  $\mathcal{H}_S$ , the asymmetric rotor functions  $|J, \tau, M_J\rangle$  for the unperturbed or field-free rotor are used to give the matrix elements of the direction cosines. The relevant direction cosine matrix elements in an asymmetric rotor basis may be expressed as

$$(J, \tau, M_J | \Phi_{Zg} | J', \tau', M_J) = (J | \Phi_{Zg} | J') (J, \tau | \Phi_{Zg} | J', \tau') (J, M_J | \Phi_{Zg} | J', M_J) \quad (10.65)$$

The  $J$  and  $J, M_J$  dependent factors are the same as for a symmetric rotor basis and are found in Table 2.1. The direction cosine matrix elements will be non-vanishing only if the product of the symmetries of  $\psi_{J, M_J}$ ,  $\Phi_{Zg}$ , and  $\psi_{J', M_J}$  belongs to species  $A$ . The symmetries of the direction cosines (see Chapter VII, Section 4) and their products, under the rotation group  $V(x, y, z)$ , are summarized in Table 10.1. The correlation of the species of  $V(x, y, z)$  with those of  $V(a, b, c)$  may be readily found by use of Table 7.5. With the aid of Table 10.1 the possible

**Table 10.1** The Direction Cosine Symmetries in  $V(x, y, z)$

Direction Cosine	Symmetry
$\Phi_{zx}, \Phi_{zy}\Phi_{zz}$	$B_x$
$\Phi_{zy}, \Phi_{zx}\Phi_{zz}$	$B_y$
$\Phi_{zz}, \Phi_{zx}\Phi_{zy}$	$B_z$
$\Phi_{zx}^2, \Phi_{zy}^2, \Phi_{zz}^2$	$A$

nonvanishing matrix elements of  $\mathcal{H}_g$  may be found. These are listed in Table 10.2. It is apparent that the perturbation connects the various diagonal blocks of  $\mathcal{H}_r$ . From (10.71)–(10.73), which give the direction cosine matrix elements in terms of the line strengths, we see that the connections are of the type  $(J|J)$  and  $(J|J\pm 1)$ . The complete energy matrix with  $\mathcal{H}_g$  included can, of course, be constructed and subsequently diagonalized to give the energy levels [12]. Usually, however, perturbation techniques are sufficiently accurate. The diagonal elements of  $\mathcal{H}_g$ , in the basis which diagonalizes  $\mathcal{H}_r$ , are the first-order perturbation corrections. However, since  $\mathcal{H}_g$  has (from Table 10.2) no diagonal matrix elements, there should be no first-order effects. Usually the Stark effect for asymmetric rotors will be of second-order, that is, proportional to  $\mathcal{E}^2$ . It frequently happens, however, that a pair of interacting levels for the unperturbed rotor are degenerate or nearly degenerate. Under these conditions a first-order effect can arise. This situation will be deferred until consideration is given to the case where the unperturbed energy levels are nondegenerate, that is, widely separated.

### The Nondegenerate Case

From Table 2.1 it is seen that the  $\Phi_{Zg}$  matrix elements are diagonal in  $M_J$ ; hence, the total rotational energy with a Stark field perturbation can be expressed for a specific value of  $M_J$  as:

$$E_{J, M_J} = E_{J, M_J}^0 + \sum_g [E_g^{(2)}]_{J, M_J} \quad (10.66)$$

**Table 10.2** Structure of the  $\mathcal{H}_g$  Matrix

$\psi_{J_i} \psi_{J'_i}$	$A$	$B_x$	$B_y$	$B_z$
$A$	...	$\mu_x\Phi_{zx}$	$\mu_y\Phi_{zy}$	$\mu_z\Phi_{zz}$
$B_x$	$\mu_x\Phi_{zx}$	...	$\mu_z\Phi_{zz}$	$\mu_y\Phi_{zy}$
$B_y$	$\mu_y\Phi_{zy}$	$\mu_z\Phi_{zz}$	...	$\mu_x\Phi_{zx}$
$B_z$	$\mu_z\Phi_{zz}$	$\mu_y\Phi_{zy}$	$\mu_x\Phi_{zx}$	...

where  $E_{J_t}^0$  is the rotational energy of the unperturbed rotor, and the second-order Stark energy is given by the conventional nondegenerate perturbation expression as

$$[E_g^{(2)}]_{J, M_J} = \mu_g^2 \mathcal{E}^2 \sum'_{J', \tau'} \frac{|(J, \tau, M_J | \Phi_{Zg} | J', \tau', M_J)|^2}{E_{J_t}^0 - E_{J', \tau'}^0} \quad (10.67)$$

The summation over  $J', \tau'$  includes all states that interact with the state  $J_t$ , that is to say, all states which are connected by a nonvanishing direction cosine matrix element. The level  $J_t$ , however, is to be excluded as indicated by the prime on the summation. There are no cross products of dipole components in (10.67) because of symmetry restrictions (see Table 10.1). The total Stark energy of a level characterized by  $J, \tau, M_J$  is the sum of the contributions arising from each dipole component.

As mentioned previously, the only nonvanishing direction cosine matrix elements are those for which  $J' = J-1, J$ , and  $J+1$ . If (10.65) is used to separate out the  $J$  and  $M_J$  factors, the energy shift arising from the  $g$ th component of the permanent dipole is [11]

$$\begin{aligned} [E_g^{(2)}]_{J, M_J} = & \mu_g^2 \mathcal{E}^2 \left[ \frac{(J^2 - M_J^2)}{4J^2(4J^2 - 1)} \sum'_{\tau'} \frac{|(J, \tau | \Phi_{Zg} | J-1, \tau')|^2}{E_{J_t}^0 - E_{J-1, \tau'}^0} \right. \\ & + \frac{M_J^2}{4J^2(J+1)^2} \sum'_{\tau'} \frac{|(J, \tau | \Phi_{Zg} | J, \tau')|^2}{E_{J_t}^0 - E_{J, \tau'}^0} \\ & \left. + \frac{(J+1)^2 - M_J^2}{4(J+1)^2(2J+1)(2J+3)} \sum'_{\tau'} \frac{|(J, \tau | \Phi_{Zg} | J+1, \tau')|^2}{E_{J_t}^0 - E_{J+1, \tau'}^0} \right] \end{aligned} \quad (10.68)$$

This expression in conjunction with (10.66) yields to second order the rotational energies in the presence of an applied electric field. The Stark energies are seen to depend on  $M_J^2$ , and hence the  $(2J+1)$ -fold degeneracy in  $M_J$  is partially removed, a given rotational level being split into  $(J+1)$  distinct sublevels. To calculate the Stark shifts one must know the dipole moment, the direction cosine matrix elements, and the energy level differences. In many instances, some of the energy differences will not correspond to observed frequencies and will have to be evaluated by known rotational constants. Conversely, when the energy levels and Stark shifts are known, the dipole moment may be calculated. The evaluation of  $|(J, \tau | \Phi_{Zg} | J', \tau')|^2$  in an asymmetric rotor basis is rather tedious for any except the lowest  $J$  values. Separating the  $M_J^2$  dependence, Golden and Wilson [11] write (10.68) in the equivalent form,

$$[E_g^{(2)}]_{J, M_J} = \frac{2\mu_g^2 \mathcal{E}^2}{A+C} [A_{J_t}(\kappa, \alpha) + M_J^2 B_{J_t}(\kappa, \alpha)] \quad (10.69)$$

where  $\alpha = (A-C)/(A+C)$  and the  $(A+C)/2$  dependence of the  $E^0$ 's has been factored out. They have tabulated these reduced Stark coefficients  $A_{J_t}$  and  $B_{J_t}$  for various values of  $\alpha$  and  $\kappa$  up to  $J=2$ . By means of these tabulated quantities, the second-order Stark energies may be calculated with a minimum of effort.

For higher values of  $J$ , the calculations can be further simplified if it is noted that the matrix elements of interest are related to the line strengths, (7.58), for which extensive tables are available. In the absence of external fields,  $X$ ,  $Y$ , and  $Z$  are equivalent, and the line strengths may be written as

$$\begin{aligned}\lambda_g(J, \tau; J', \tau') &= 3 \sum_M |(J, \tau, M_J | \Phi_{Zg} | J', \tau', M_J)|^2 \\ &= \left[ 3 |(J | \Phi_{Zg} | J')|^2 \cdot \sum_{M_J} |(J, M_J | \Phi_{Zg} | J', M_J)|^2 \right] |(J, \tau | \Phi_{Zg} | J', \tau')|^2\end{aligned}\quad (10.70)$$

In writing this expression we have taken cognizance of the fact that  $\Phi_{Zg}$  has nonvanishing elements only for  $M'_J = M_J$ . The term in brackets may be readily evaluated. Using Table 2.1 and carrying out the sum over  $M_J$ , noting that  $\sum_{M_J=-J}^{+J} M_J^2 = (\frac{1}{3})J(J+1)(2J+1)$ , one obtains:

$$\lambda_g(J, \tau; J+1, \tau') = \left[ \frac{1}{4(J+1)} \right] |(J, \tau | \Phi_{Zg} | J+1, \tau')|^2 \quad (10.71)$$

$$\lambda_g(J, \tau; J, \tau') = \left[ \frac{2J+1}{4J(J+1)} \right] |(J, \tau | \Phi_{Zg} | J, \tau')|^2 \quad (10.72)$$

$$\lambda_g(J, \tau; J-1, \tau') = \left( \frac{1}{4J} \right) |(J, \tau | \Phi_{Zg} | J-1, \tau')|^2 \quad (10.73)$$

Thus the required matrix elements  $|(J, \tau | \Phi_{Zg} | J', \tau')|^2$  may be evaluated from the foregoing equation and the tabulated line strengths [13]. Interpolation of the line strength tables may be used when necessary. As  $J$  increases, the number of possible interacting levels increases rapidly, especially when there is more than one dipole component. However, in many cases certain of the matrix elements or line strengths connecting two levels will be vanishingly small and can be neglected.

Usually the electric field applied is such that  $\Delta M_J = 0$  transitions are observed. A completely resolved spectral line with  $\Delta J = \pm 1$  will have  $(J+1)$  Stark components, while for  $\Delta J = 0$  there will be  $J$  components, where  $J$  is the smaller of the two  $J$ 's involved in the transition. These cases are illustrated in Fig. 10.8. The loss of one component for  $\Delta J = 0$  transition is due to the vanishing intensity of the  $M_J = 0$  component which is apparent from the intensity expressions given later. According to the magnitude and sign of the Stark coefficients for the two levels involved in the transition, the Stark components may be on one or both sides of the zero-field line. When the Stark coefficient differences, that is,  $\Delta A$  and  $\Delta B$ , have the same sign, the largest displacement will occur for the Stark component associated with the largest possible  $M_J$  value.

The evaluation of the  $|M_J|$  associated with a particular Stark component can be made if necessary from measurements on the frequency displacements [11]. Let the frequency shift for a given  $M_J$  component be expressed as

$$\Delta v_{M_J} = \mathcal{E}^2 (A' + B' M_J^2) \quad (10.74)$$

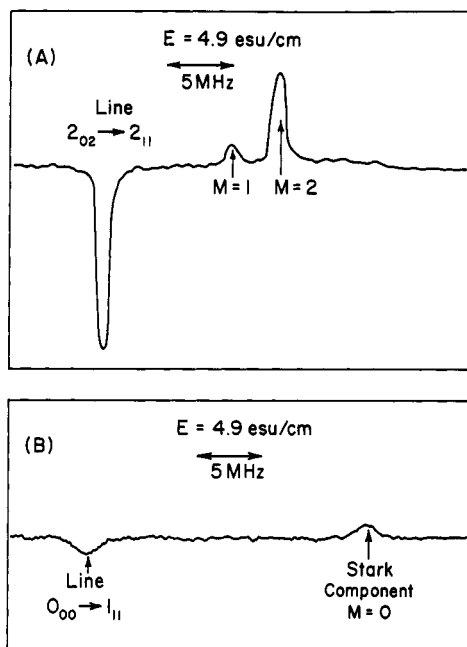


**Fig. 10.8** (A) Recording of the  $2_{02} \rightarrow 2_{11}$  transition of  $\text{SO}_2$  at 53,529 MHz. (B) Recording of the  $0_{00} \rightarrow 1_{11}$  transition of  $\text{SO}_2$  at 69,576 MHz. Obtained with a Stark-modulation spectrometer, employing phase-sensitive detection. After Crable [15].

The  $M_J$  value for successive components will differ by unity and the following relations for three consecutive components may be written

$$\Delta v_{M_J} - \Delta v_{M_J \pm 1} = \mp \mathcal{E}^2 B'(2M_J \pm 1) \quad (10.75)$$

$$\Delta v_{M_J \pm 1} - \Delta v_{M_J \pm 2} = \mp \mathcal{E}^2 B'(2M_J \pm 3) \quad (10.76)$$

Taking the ratio of the component separations gives

$$r = \frac{\Delta v_{M_J} - \Delta v_{M_J \pm 1}}{\Delta v_{M_J \pm 1} - \Delta v_{M_J \pm 2}} = \frac{2M_J \pm 1}{2M_J \pm 3} \quad (10.77)$$

which in turn yields

$$M_J = \pm \left( \frac{3r - 1}{2 - 2r} \right) \quad (10.78)$$

The values of  $M_J$  can also be related to the relative intensities of the components [11]; however, frequency measurements can be made with greater accuracy, and hence the  $|M_J|$  can be most satisfactorily estimated from the frequency displacements.

With very large electric fields, higher-order Stark corrections may need to be considered. For nondegenerate levels the odd-order corrections vanish [11],

and hence the next correction will be proportional to  $\mathcal{E}^4$ . If fourth-order Stark corrections are important, the procedure for handling the data discussed in Section 1 can be employed which, although explicitly including fourth-order effects, does not require a knowledge of the fourth-order Stark coefficients. The second-order Stark coefficients in (10.18) are obtained from (10.68). This method may be generalized for the case where the Stark effect depends on more than one dipole component  $\mu_g$ , but additional intercepts from different transitions (e.g., different  $M_J$  values) will be required in the solution for the dipole components.

As an illustration of the application of (10.68), consider the evaluation of the dipole moment of  $\text{SO}_2$  from the Stark splitting of the  $0_{00} \rightarrow 1_{11}$  transition for which only one Stark component is observed, viz.,  $M_J=0$  (see Fig. 10.8), and no near-degeneracies occur. The symmetry of  $\text{SO}_2$  is such that the dipole moment will be entirely along the twofold axis of symmetry which is the  $b$  axis. Therefore, the levels which perturb the  $0_{00}$  level by means of the dipole component  $\mu_b$  must have symmetry  $B_b$ . Thus only the  $1_{11}$  level perturbs the  $0_{00}$  level. On the other hand, the  $1_{11}$  level interacts via the Stark perturbation with the  $0_{00}$ ,  $2_{02}$ , and  $2_{20}$  levels. The spectroscopic constants of  $\text{SO}_2$  are [14]:  $A=60,778.79$  MHz,  $B=10,318.10$  MHz, and  $C=8,799.96$  MHz. Keeping only three decimal places we find  $\kappa=-0.942$ . The reduced energies of the various levels may be obtained from the expressions of Tables 7.6 and 7.7 or existing reduced energy tables. The total rigid-rotor energy of the various levels is found to be (MHz):

$$E_{0_{00}}=0$$

$$E_{1_{11}}=A+C=69,578.75$$

$$E_{2_{02}}=3(A+C)+\frac{(A-C)}{2}(-5.8273)=57,288.13$$

$$E_{2_{20}}=3(A+C)+\frac{(A-C)}{2}(2.0593)=262,256.25$$

The appropriate matrix elements of the direction cosines are obtainable from the tabulated line strengths and (10.71)–(10.73). The necessary quantities may be summarized as follows:

$J_{K'-1,K_1} - J'_{K'-1,K'_1}$	$\lambda_b(J_{K'-1,K_1}; J'_{K'-1,K'_1})$	$ (J_{K'-1,K_1} \Phi_{zb} J'_{K'-1,K'_1}) ^2$
$0_{00}-1_{11}$	1.0000	4.0000
$1_{11}-2_{02}$	0.5191	4.1528
$1_{11}-2_{20}$	1.4809	11.8472

These are for a  $\kappa$  of  $-0.95$  from [13] which is sufficiently accurate for our purpose. In practice, however, an interpolation would be carried out to give the values corresponding to the observed  $\kappa$ . With these results, the Stark energy for the  $0_{00}$  and  $1_{11}$  levels may be readily calculated from (10.68). The

separation  $\Delta\nu$  of the Stark component ( $M_J=0$ ) from the zero-field rotational transition is given by the following expression

$$\Delta\nu = [E_b^{(2)}]_{1_{11}} - [E_b^{(2)}]_{0_{00}} = (0.50344)^2 \mu_b^2 \mathcal{E}^2 [9.3973 - (-4.7907)] \times 10^{-6}$$

$$= \mu_b^2 \mathcal{E}^2 (0.50344)^2 (14.1880 \times 10^{-6})$$

Here the conversion factor 0.50344 (MHz) (debye volt/cm) $^{-1}$  is included so that the Stark splittings may be expressed in megahertz with  $\mu_b$  in debye units, and  $\mathcal{E}$  in v/cm. For  $\mathcal{E}=2005.1$  v/cm, the observed Stark splitting is found to be  $\Delta\nu=36.2$  MHz [15], and one obtains from the above expression  $\mu=\mu_b=1.58$  D for the dipole moment. The dipole moment obtained with interpolation and measurement of different splittings is  $1.59 \pm 0.01$  D [16].

### The Degenerate Case

In asymmetric rotors degeneracies frequently occur; both approximate symmetric-rotor degeneracy and various types of accidental degeneracies are possible. Table 10.3 indicates for  $J \leq 3$  which pairs of levels can become accidentally degenerate. When degeneracies are present, (10.68) obviously fails, since it will contain terms with vanishing denominators. Thus, if rotational degeneracies or near-degeneracies are encountered, a simple second-order perturbation treatment is not applicable. Van Vleck [17], however, has developed a convenient perturbation technique which is very effective for dealing

**Table 10.3** Possible Degeneracies in the Asymmetric Rotor<sup>a</sup>

$J_{K-1} K_1$	$0_{00}$	$1_{01}$	$1_{11}$	$1_{10}$	$2_{02}$	$2_{12}$	$2_{11}$	$2_{21}$	$2_{20}$
$0_{00}$									
$1_{01}$									
$1_{11}$		$\mu_c$							
$1_{10}$			$\mu_a$						
$2_{02}$				$\mu_b$	$\mu_c$				
$2_{12}$						$\mu_c$			
$2_{11}$							$\mu_a$		
$2_{21}$								$\mu_c$	
$2_{20}$									$\mu_a$
$3_{03}$						$\mu_c$	$\mu_b$	*	$\mu_a$
$3_{13}$							*	$\mu_c$	$\mu_b$
$3_{12}$								$\mu_b$	$\mu_c$
$3_{22}$									
$3_{21}$									
$3_{31}$									
$3_{30}$									

<sup>a</sup>From Golden and Wilson [11]. Entries indicate which component of the dipole moment becomes important in the accidental degeneracy. The asterisk denotes no coupling term. Blanks indicate no accidental degeneracy possible.

with the problem of degeneracies or near-degeneracies. It consists of application of a transformation to the energy matrix, that is, the matrix of  $\mathcal{H}_r + \mathcal{H}_s$  evaluated in an asymmetric-rotor basis. The transformation is so constructed that the elements connecting degenerate blocks after the transformation are reduced to second order and can hence be neglected for results correct up to fourth order in the energy. This perturbation technique is discussed in more detail in Appendix C and in the section on internal rotation. The net result of the transformation is that one obtains a number of small submatrices, each associated with a group of degenerate or nearly degenerate levels. The diagonal elements of these submatrices contain correction terms from the Van Vleck transformation and are given by (10.66) and (10.68), except that in the case of degeneracies or near-degeneracies the summation is only over those levels for which  $E_{J',M_J}^0$  is not near  $E_{J,M_J}^0$ . The perturbed energies are then found from solution of the usual secular determinant. Usually the degeneracy occurs only between a pair of levels; the secular equation then has the form

$$\begin{vmatrix} E_{J,M_J} - E & \mathcal{E}\xi \\ \mathcal{E}\xi^* & E_{J',M_J} - E \end{vmatrix} = 0 \quad (10.79)$$

where  $\xi$  is the appropriate off-diagonal matrix element. The two possible solutions are

$$E_{\pm} = \frac{E_{J,M_J} + E_{J',M_J}}{2} \pm \left[ \left( \frac{E_{J,M_J} - E_{J',M_J}}{2} \right)^2 + \mathcal{E}^2 |\xi|^2 \right]^{1/2} \quad (10.80)$$

where for  $E_{J,M_J} > E_{J',M_J}$ , the plus sign is associated with the level  $J,M_J$  and the minus sign is associated with the level  $J',M_J$ , since two such interacting states repel one another. The off-diagonal elements are made up of the Stark coupling term for the levels and correction terms from the transformation

$$\mathcal{E}\xi = (J, \tau, M_J | \mathcal{H}_s | J', \tau', M_J) + \text{Correction terms} \quad (10.81)$$

These off-diagonal elements depend on the two levels under consideration, and Golden and Wilson [11] have given expressions for various types of near-degeneracies.

We shall discuss only the case of near-degeneracies between asymmetry doublet states, which is often encountered even in rather asymmetric rotors. These levels will appear in pairs having different symmetry, except for the  $K=0$  level which is nondegenerate in  $K$ . For a near-prolate rotor the pairs of  $K$  levels will have either symmetries  $A, B_a$  or symmetries  $B_b, B_c$ , whereas for a near-oblate rotor the symmetries will be  $B_a, B_b$  or  $A, B_c$ . For two members of an asymmetry doublet,  $J_\tau$  and  $J_{\tau'}$ , which interact in the presence of an electric field by means of a dipole component  $\mu_g$ , the off-diagonal matrix element connecting the two states will have the simple form

$$\mathcal{E}^2 |\xi|^2 = |(J, \tau, M_J | \mathcal{H}_s | J, \tau', M_J)|^2 = \mu_g^2 \mathcal{E}^2 \frac{M_J^2}{4J^2(J+1)^2} |(J, \tau | \Phi_{Zg} | J, \tau')|^2 \quad (10.82)$$

where  $g$  is  $a$  or  $c$  depending on the symmetry of the two near-degenerate  $K$  levels. The secular determinant, (10.79), with the off-diagonal elements given

by (10.82), is just what is expected from conventional perturbation theory for two such nearby levels, except that the diagonal elements here contain, in addition, the second-order Stark contributions of the remaining nondegenerate levels. Each of the two levels,  $J_{\tau}$  and  $J_{\tau'}$ , splits into  $(J+1)$  distinct sublevels given by (10.80) and (10.82), the  $+M_J$  and  $-M_J$  levels coinciding. If  $|E_{J_{\tau} M_J} - E_{J_{\tau'} M_J}| \ll |\mathcal{E}\xi|$ , then (10.80) may be expanded to give an energy that is a linear function of the electric field

$$E_{\pm} = \frac{1}{2}(E_{J_{\tau}}^0 + E_{J_{\tau'}}^0) \pm \mathcal{E}|\xi| \quad (10.83)$$

or explicitly for the two levels

$$E(J_{\tau} M_J) = \frac{1}{2}(E_{J_{\tau}}^0 + E_{J_{\tau'}}^0) + \mu_g \mathcal{E} \frac{|M_J|}{2J(J+1)} (J, \tau | \Phi_{Zg} | J, \tau') \quad (10.84)$$

$$E(J_{\tau'} M_J) = \frac{1}{2}(E_{J_{\tau}}^0 + E_{J_{\tau'}}^0) - \mu_g \mathcal{E} \frac{|M_J|}{2J(J+1)} (J, \tau | \Phi_{Zg} | J, \tau') \quad (10.85)$$

In this approximation, the asymmetry splitting has been ignored along with possible second-order Stark effects. If, on the other hand,  $|E_{J_{\tau} M_J} - E_{J_{\tau'} M_J}| \gg |\mathcal{E}\xi|$ , the expansion will give the conventional second-order result, although possibly a large second-order effect because of the presence of a small energy denominator. If the separation of the levels is such that for a given field neither expansion is sufficiently accurate, that is, an intermediate case is attained, then the complete energy expression, (10.80), must be employed. Under the appropriate conditions it is possible with increasing electric field to observe a transition from a Stark-effect quadratic in the electric field to one linear in  $\mathcal{E}$ .

As with the nondegenerate case, the  $M_J$  value can be expressed in terms of the Stark-component separations. For the first-order Stark effect in asymmetry doublets one finds

$$M_J = \pm \frac{\Delta v_{M_J}}{\Delta v_{M_J} - \Delta v_{M_J \pm 1}} \quad (10.86)$$

For slightly asymmetric rotors, the direction cosine matrix elements are given to a good approximation by those for symmetric tops. Hence the off-diagonal matrix element would reduce to

$$\mathcal{E}^2 |\xi|^2 = \left[ \frac{\mu_g \mathcal{E} K M_J}{J(J+1)} \right]^2 \quad (10.87)$$

with  $K$  the appropriate quantum number for the limiting symmetric top. When the asymmetry splitting vanishes,  $E_{J_{\tau}}^0 = E_{J_{\tau'}}^0$  (levels degenerate), it is apparent that (10.83), with the aid of (10.87), reduces to the first-order expression given for a symmetric rotor.

Figure 10.9 illustrates both a first- and second-order Stark pattern for the nearly prolate asymmetric rotor HNCO. The asymmetry splitting is very small, and the  $3_{22} \rightarrow 4_{23}$  and  $3_{21} \rightarrow 4_{22}$  ( $K=2$ ) transitions appear as a single line in the absence of an electric field. This  $K$  degeneracy leads to a first-order Stark pattern like that of a symmetric top, and  $(2J+1)$  Stark components are

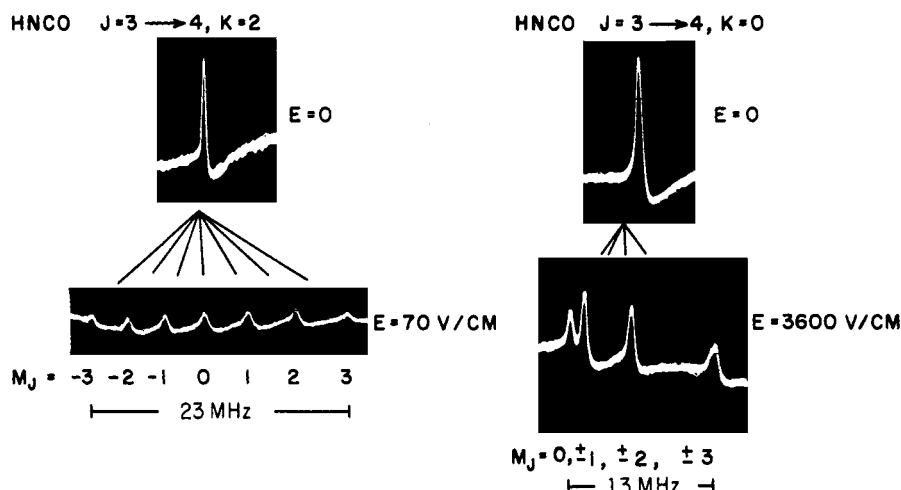


**Fig. 10.9** Oscilloscope tracing of the field-free lines and the  $\Delta M_J = 0$  Stark components of the  $J=3 \rightarrow 4, K=2$  transition (first-order) and the  $J=3 \rightarrow 4, K=0$  transition (second-order) for the slightly asymmetric rotor HNCO. The frequency increases from left to right. Obtained with a parallel-plate Stark cell operating in the millimeter wave region. From K. White, Ph.D. dissertation, Duke University, 1965.

obtained. For the  $3_{03} \rightarrow 4_{04}$  ( $K=0$ ) transition, which is a nondegenerate case, a typical second-order pattern is observed. For the  $J=3 \rightarrow 4, K=1$  lines (not pictured) an intermediate case is found. A Stark pattern similar to the  $K=0$  transition is obtained for each  $K=1$  line, except that the Stark components for the high-frequency  $K=1$  line are on the low-frequency side whereas for the low-frequency  $K=1$  line they are on the high-frequency side.

A case of a highly degenerate Stark effect has been observed in the near-oblate rotor  $\text{CH}_3\text{CHF}_2$  by Kwei and Herschbach [18]. Here the Stark effect exhibits strong perturbations arising from the two components of the dipole moment ( $\mu_a, \mu_c$ ) and all three of the  $J=1$  rotational levels and all five of the  $J=2$  levels had to be treated as degenerate. The Van Vleck transformation is used to separate the blocks of different  $J$ , giving a  $3 \times 3$  secular equation for  $J=1$  and a  $5 \times 5$  secular equation for  $J=2$ .

For molecules with internal rotation it is possible for  $E$  levels with  $K > 0$  to exhibit a first-order Stark effect that is dependent on the barrier height. This is discussed more fully in Chapter XII. It suffices to say here that because of the presence in the Hamiltonian of a linear term in the angular momentum, the  $\pm M_J$  degeneracy can be removed and a first-order Stark effect obtained. This splitting between the  $+M_J$  and the  $-M_J$  Stark components is sensitive to the barrier height and thus allows a means of its evaluation.

The degree of planarity of molecules and the nature of the potential function which governs the out-of-plane bending vibration are questions in which the Stark effect can yield valuable information. A discussion of this may be found elsewhere [19, 20].

## Chapter XI

# EFFECTS OF APPLIED MAGNETIC FIELDS

---

1	ZEEMAN EFFECT IN MOLECULES WITHOUT NUCLEAR COUPLING	506
	Interaction Energies	506
	Linear Molecules	509
	Symmetric-top Molecules	512
	Asymmetric Rotors	515
2	ZEEMAN EFFECT OF NUCLEAR HYPERFINE STRUCTURE	518
	Weak-field Case	518
	Strong-field Case	521
3	THEORY OF MAGNETISM IN CLOSED-SHELL MOLECULES ( ${}^1\Sigma$ STATES)	523
4	ANISOTROPIC MAGNETIC SUSCEPTIBILITIES	528
	Measurement of Molecular Anisotropies	528
	Calculation of Molecular Susceptibilities from Local Atomic Components	536
5	SECOND MOMENTS AND MOLECULAR QUADRUPOLE MOMENTS FROM THE ZEEMAN EFFECT	538
	Molecular Quadrupole Moments	538
	Second Moments of the Electron Charge Distributions	542
6	SIGN OF THE ELECTRIC DIPOLE MOMENT FROM THE ZEEMAN EFFECT	544
7	ELECTRONIC EFFECTS ON INERTIAL CONSTANTS: RELATION TO $g$ FACTOR	546
8	MOLECULES WITH ELECTRONIC ANGULAR MOMENTUM	549
	Molecules with Orbital Angular Momentum ( $\Pi$ or $\Delta$ States)	550
	Molecules with Electronic Spin but Not Orbital Angular Momentum ( ${}^2\Sigma$ or ${}^3\Sigma$ States)	551
	Hyperfine Structure in Molecules with Electronic Angular Momentum	551
9	GAS-PHASE ELECTRON PARAMAGNETIC RESONANCE SPECTRA	552
	Molecules with Orbital Angular Momentum	553
	Molecules in Multiplet $\Sigma$ States	560
10	STARK EFFECT OF GAS-PHASE ELECTRON PARAMAGNETIC RESONANCE	561

Most stable molecules have  $\Sigma$  singlet ground electronic states and hence when not rotating are nonmagnetic in the sense that they have no permanent magnetic dipole moment exclusive of nuclear moments. However, magnetic moments are generated by molecular rotation which gives rise to Zeeman splittings [1–3], usually resolvable with fields of several kilogauss. Magnetic moments are also induced by the applied field because of the magnetic susceptibility of the molecules, but these induced moments are very much smaller than those caused by rotation, and only the anisotropic components can affect the observed spectra [4]. The nuclear magnetic moments influence the rotational Zeeman effect only when the moments are coupled to the molecular axes so that an observable hyperfine structure results. First we shall consider molecules in  ${}^1\Sigma$  states without nuclear coupling.

## 1 ZEEMAN EFFECT IN MOLECULES WITHOUT NUCLEAR COUPLING

### Interaction Energies

The classical Hamiltonian for the interaction of a magnetic dipole with a field  $\mathbf{H}$  is

$$\mathcal{H}_H = -\mu \cdot \mathbf{H} \quad (11.1)$$

In the molecular rotational Zeeman effect the magnetic moment is fixed in the molecular frame, and  $\mathbf{H}$  is fixed in space. The component of the molecular magnetic moment along the total angular momentum vector  $\mathbf{J}$  (or along  $\mathbf{F}$  when there is nuclear coupling) interacts with  $\mathbf{H}$ , causing  $\mathbf{J}$  to precess about the direction of  $\mathbf{H}$ , as indicated by the vector diagram of Fig. 11.1. With the

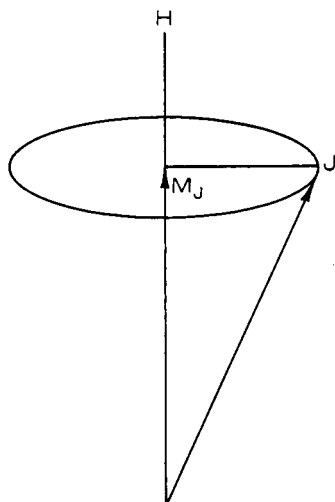


Fig. 11.1 Vector model of the first-order Zeeman effect.

weak magnetic moments of molecules in  $\Sigma$  states, the precession of  $\mathbf{J}$  about  $\mathbf{H}$  is very much slower than the molecular rotation, and only the components of  $\mu$  along  $\mathbf{J}$  effectively interact with  $\mathbf{H}$ . Those normal to  $\mathbf{H}$  are averaged out by the rotation. Even in molecules with unbalanced electronic moments this approximation holds for ordinary field strengths. If  $\langle \mu_J \rangle$  represents the averaged value of the molecular magnetic moment along  $\mathbf{J}$ , the Zeeman Hamiltonian can be expressed as

$$\mathcal{H}_H = -\langle \mu_J \rangle \frac{\mathbf{J} \cdot \mathbf{H}}{|\mathbf{J}|} = -\langle \mu_J \rangle H \cos(\mathbf{J}, \mathbf{H}) \quad (11.2)$$

From the vector diagram of Fig. 11.1 it is seen that

$$\cos(\mathbf{J}, \mathbf{H}) = \frac{J_z}{|\mathbf{J}|} = \frac{M_J}{[J(J+1)]^{1/2}} \quad (11.3)$$

Therefore (11.2) can be expressed as

$$E_H = -\langle \mu_J \rangle \frac{HM_J}{[J(J+1)]^{1/2}} \quad (11.4)$$

Although (11.4) is a rather general first-order expression which applies to molecules of different types, symmetric tops or asymmetric rotors, the quantity  $\langle \mu_J \rangle$  varies with molecular type and rotational state. Therefore, if we are to find the specific value of  $E_H$  in (11.4), we must find the corresponding operator for  $\mu_J$  and average it over the molecular wave function.

When the principal magnetic axes are the same as the inertial axes  $x$ ,  $y$ ,  $z$ , the components of  $\mu$  generated along the axes are proportional to the respective components of rotational momentum, as verified in Section 3. They can be expressed as

$$\mu_x = \beta_I g_{xx} J_x, \quad \mu_y = \beta_I g_{yy} J_y, \quad \mu_z = \beta_I g_{zz} J_z \quad (11.5)$$

where  $\beta_I g_{xx}$ , and so on, are proportionality constants. The nuclear magneton  $\beta_I$  is introduced so that  $g$  will represent the ratio of  $\mu$  in nuclear magneton units to the angular momentum  $J$  in units of  $\hbar$ , the customary designation used in the definition of the dimensionless gyromagnetic ratio of the nuclei. It gives the  $g$  factors in numbers of convenient magnitude for molecules in  $\Sigma$  states. The magnitude of  $\mu_J$  is found by resolution of the components of (11.5) along  $\mathbf{J}$ :

$$\begin{aligned} \mu_J &= \mu_x \cos(x, J) + \mu_y \cos(y, J) + \mu_z \cos(z, J) \\ &= \mu_x \frac{J_x}{|\mathbf{J}|} + \mu_y \frac{J_y}{|\mathbf{J}|} + \mu_z \frac{J_z}{|\mathbf{J}|} \\ &= \frac{\beta_I}{[J(J+1)]^{1/2}} (g_{xx} J_x^2 + g_{yy} J_y^2 + g_{zz} J_z^2) \end{aligned} \quad (11.6)$$

When the principal magnetic axes are not the same as the inertial axes, off-diagonal elements in the magnetic moment are generated so that

$$\begin{aligned}\mu_x &= \beta_I(g_{xx}J_x + g_{xy}J_y + g_{xz}J_z) \\ \mu_y &= \beta_I(g_{yx}J_x + g_{yy}J_y + g_{yz}J_z) \\ \mu_z &= \beta_I(g_{zx}J_x + g_{zy}J_y + g_{zz}J_z)\end{aligned}\quad (11.7)$$

Resolution of these components along  $\mathbf{J}$  gives

$$\mu_J = \frac{\beta_I}{[J(J+1)]^{1/2}} \sum_{g,g'} g_{gg'} J_g J_{g'} \quad (11.8)$$

When, however,  $\mu_J$  is averaged over the rotational wave functions, the off-diagonal elements will vanish, leaving only the diagonal elements of the  $\mathbf{g}$  tensor. Thus,

$$\langle \mu_J \rangle = \frac{\beta_I}{[J(J+1)]^{1/2}} \sum_{g=x,y,z} g_{gg} \langle J_g^2 \rangle \quad (11.9)$$

Because  $\langle \mu_J \rangle$  is independent of  $M_J$ , it is possible to define an effective  $g$  factor for the particular rotational state  $|J, \tau\rangle$  by

$$g_{J,\tau} = \frac{\langle \mu_J \rangle / \beta_I}{[J(J+1)]^{1/2}} = \frac{1}{J(J+1)} \sum_g g_{gg} \langle J, \tau | J_g^2 | J, \tau \rangle \quad (11.10)$$

and hence

$$\langle \mu_J \rangle = g_{J,\tau} \beta_I [J(J+1)]^{1/2} \quad (11.11)$$

where  $\tau$  becomes  $K$  for symmetric tops, is zero for linear molecules, and represents the pseudo-quantum numbers  $K_{-1} - K_1$  for the asymmetric rotor. Substitution of this value of  $\langle \mu_J \rangle$  from (11.11) into (11.4) gives the Zeeman energies as

$$E_H(\mu_J) = -g_{J,\tau} \beta_I H M_J \quad (11.12)$$

in which

$$g_{J,\tau} = \frac{1}{J(J+1)} (g_{xx} \langle J_x^2 \rangle + g_{yy} \langle J_y^2 \rangle + g_{zz} \langle J_z^2 \rangle) \quad (11.13)$$

where  $g_{xx}$ ,  $g_{yy}$ , and  $g_{zz}$  are the diagonal elements of the  $\mathbf{g}$  tensor with reference to the inertial axes and where the averages are taken over the wave functions of the unperturbed rotors. The quantity  $g_{J,\tau}$  is called the rotational  $g$  factor or the spectroscopic splitting factor. As shown in Section 3, its origin in  ${}^1\Sigma$  molecules is due partly to the rotation of formal charges and partly to a slight admixture of electronic states having orbital angular momentum with the  $\Sigma$  singlet ground electronic state.

We did not include in (11.1) a small term arising from the moments induced in the molecule by the applied field. At very high fields this term can have detectable effects on the Zeeman displacements when the magnetic susceptibility of the molecules is anisotropic. These effects are discussed in Section 4.

Strictly speaking, we should include in (11.1) the Hamiltonian for the nuclear magnetic interaction with the applied field

$$\mathcal{H}_n = -\beta_I \sum_i g_{I_i} \mathbf{I}_i \cdot \mathbf{H} \quad (11.14)$$

where the sum is taken over all nuclei having nonzero spins. On the other hand, when the nuclear coupling is negligible, as for nuclei with no quadrupole interaction, the perturbation of the molecular rotation can be neglected, and the allowed values of  $\mathcal{H}_n$  are

$$E_H(\mu_I) = -\beta_I H \sum_i g_{I_i} M_{I_i} \quad (11.15)$$

Because of the selection rule  $\Delta M_{I_i} = 0$ , there is no observable effect of  $E_H(\mu_I)$  on the observed microwave spectra.

### Linear Molecules

The remaining problem in the evaluation of the Zeeman splitting is the specialization of (11.13) to the particular molecular type under consideration. For linear molecules  $J_z = 0$ ,  $g_{zz} = 0$ , and from symmetry  $g_{xx} = g_{yy} = g$ . Since  $J_x^2 + J_y^2 = J^2$  and, in units of  $\hbar$ ,  $\langle J^2 \rangle = J(J+1)$ ,

$$g_J = \frac{1}{J(J+1)} g \langle J^2 \rangle = g \quad (11.16)$$

Therefore, in the first-order treatment for linear molecules  $g_J$  is a constant, independent of the rotational state. The associated magnetic moment  $\langle \mu_J \rangle$  is perpendicular to the molecular axis and gives rise to a first-order Zeeman effect. The level splitting is given by (11.12). In contrast, there is no first-order Stark effect for linear molecules because the electric dipole moment is parallel to the molecular axis.

The  $M_J$  selection rules for the Zeeman effect are the same as those for the Stark effect

$$M_J \rightarrow M_J \quad \text{and} \quad M_J \rightarrow M_J \pm 1 \quad (11.17)$$

For transitions which are induced by electric dipole coupling with the radiation, the magnetic field must be parallel to the electric vector of the radiation for observation of the  $M_J \rightarrow M_J$  transitions, called  $\pi$  components; for observation of the  $M_J \rightarrow M_J \pm 1$  transitions, called  $\sigma$  components, it must be imposed perpendicular to the electric vector of the radiation.

With the foregoing selection rules and with (11.12), the frequencies of the Zeeman components of the  $J \rightarrow J+1$  rotational transition are

$$v(\pi) = v_0 \quad (11.18)$$

$$v(\sigma) = v_0 \pm \frac{g_J \beta_I H}{\hbar} \quad (11.19)$$

where  $v_0$  is the frequency of the line when no field is applied. Since from (11.16)  $g_J$  is a constant, these first-order effects of a linear molecule are independent of  $J$ . One therefore expects the same Zeeman pattern for all the lines of an unsplit  $\pi$  component and for a doublet  $\sigma$  component, as shown in Fig. 11.2. Together they form the normal Zeeman triplet. Since it does not depend on  $J$ , the  $\sigma$  splitting can be observed for very high  $J$  transitions. Only the undisplaced rotational line, the  $\pi$  component, is observable when the magnetic field is parallel to the microwave  $\mathbf{E}$  vector.

In the higher-order approximations,  $g_J$  is not exactly the same for all values of  $J$ . The frequency expressions for this situation may be obtained from (11.23) and (11.24) by replacement of  $g_{J,K}$  and  $g_{J+1,K}$  with  $g_J$  and  $g_{J+1}$ , respectively. When  $g_J \neq g_{J+1}$ , there are  $(2J+1)\pi$  components corresponding to the possible values of  $M_J$ . Although  $g_J$  and  $g_{J+1}$  are not likely to differ sufficiently to make this structure resolvable, they may differ enough to cause a detectable broadening of the line in some molecules. Likewise, a difference in  $g_J$  and  $g_{J+1}$  would cause each component of the  $\sigma$  doublet to be split into  $2J+1$  components, but such a splitting has not been resolved. Nevertheless, differences in  $g_J$  and  $g_{J+1}$  might cause a distortion of this line shape, as indicated by the theoretical pattern of Fig. 11.3. The difference between  $g_J$  and  $g_{J+1}$  assumed in these patterns is much greater than that likely to be encountered for linear molecules. Note that the center of the sub-multiplet structure does not occur at the peak absorption and that the asymmetry reverses when  $g_{J+1}$  changes from greater than  $g_J$  to smaller than  $g_J$ . If  $2\Delta\nu$  represents the frequency difference between the centers of the  $\sigma$  doublet multiplets,  $g_{J+1}$  can be found from

$$g_{J+1} = \frac{h\Delta\nu}{\beta_I H} \quad (11.20)$$

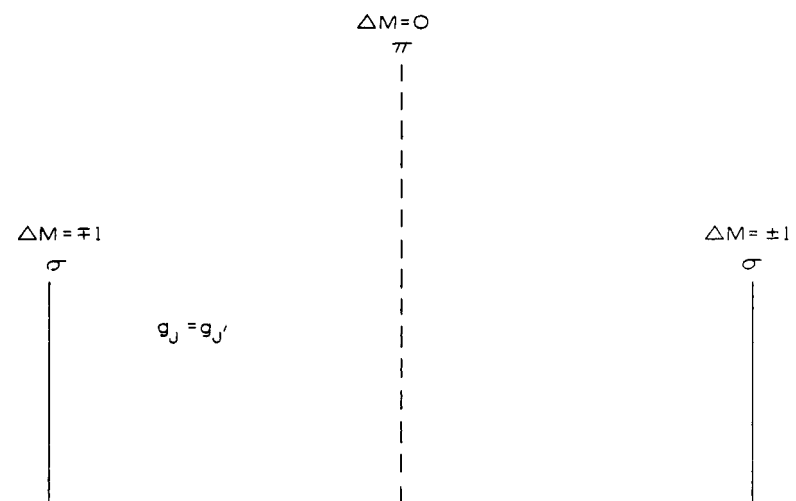


Fig. 11.2 Theoretical Zeeman components for a  $J \rightarrow J'$  transition when  $g_J = g_{J'}$ .

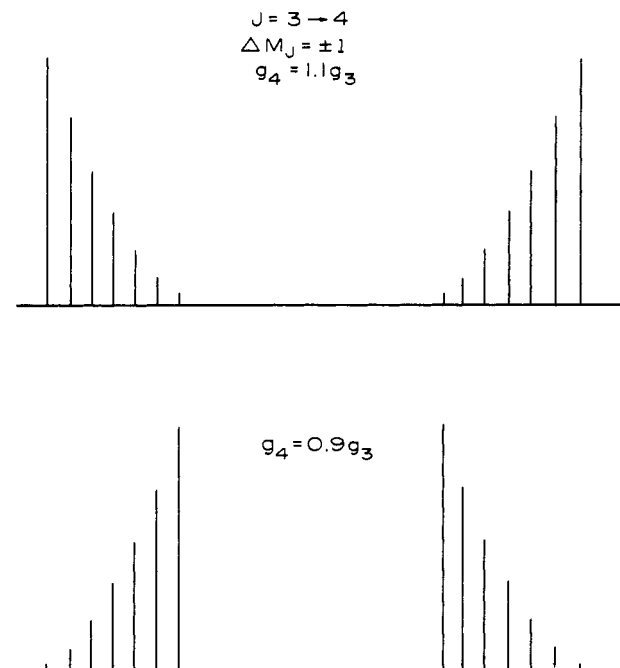


Fig. 11.3 The  $\Delta M = \pm 1$  Zeeman pattern ( $\sigma$  components) for a  $J \rightarrow J + 1$  transition when  $g_J \neq g_{J+1}$ .

The most complete data available are for OCS. The  $\Delta M = \pm 1$  components of the Zeeman splitting have been observed for several OCS transitions, and the simple doublet pattern expected from (11.19) is found for each. That  $g_J$  does not vary significantly with the rotational state is demonstrated more quantitatively in Table 11.1, where the effective  $g_J$  values observed for different transitions are shown. Not surprisingly, the greatest deviation is observed for the  $J=0 \rightarrow 1$  transition. This doublet splitting was first observed by Jen [5], who found the  $g$  value from  $J=1 \rightarrow 2$  transition to be  $0.029 \pm 0.006$ . By use of circularly polarized radiation, Eshbach and Strandberg [3] later established the sign of  $g_J$  as negative and found for the  $J=1 \rightarrow 2$  transition the average  $g_J = -0.0251 \pm 0.002$ . The magnitude of their value appears too small in comparison to other values, and its deviation is well outside the estimated limits of error of the highly accurate value later measured by Flygare et al. which is given in Table 11.1.

The  $g_J$  factor of CO is an order of magnitude larger than that of OCS. It has been measured from the  $J=0 \rightarrow 1$  transition by three different groups of workers [6–8]. All the values are in good agreement. Rosenblum et al. [7], who made measurements on different isotopic species, obtained measurably different  $g_J$  values for them. Burrus [8] extended the measurements on  $^{12}\text{C}^{16}\text{O}$  to  $J=1 \rightarrow 2$  transition and found  $g_J$  to be independent of  $J$  within the accuracy of measurement. The  $g_J$  measured for the  $J=0 \rightarrow 1$  transition is strictly that for

**Table 11.1** Molecular Rotational *g* Factors for Selected Diatomic and Linear Molecules<sup>a</sup>

Molecule	<i>J State</i>	$g_J = g_{\perp}$	Ref.
$^{12}\text{C}^{16}\text{O}$	1	-0.2691(5)	b
$^{12}\text{C}^{17}\text{O}$	1	-0.2623(5)	b
$^{13}\text{C}^{16}\text{O}$	1	-0.2570(5)	b
$^{12}\text{C}^{18}\text{O}$	1	-0.2562(5)	b
$^{14}\text{C}^{16}\text{O}$	1	-0.2466(5)	b
$^{13}\text{C}^{18}\text{O}$	1	-0.2442(5)	b
$^{12}\text{C}^{32}\text{S}$	1	-0.272(2)	c,d
$^{12}\text{C}^{80}\text{Se}$	1	-0.2431(16)	e
D <sup>79</sup> Br	1	+0.181(15)	f
D <sup>81</sup> Br	1	+0.184(15)	f
D <sup>127</sup> I	1	+0.096(10)	f
$^{16}\text{O}^{12}\text{C}^{32}\text{S}$	1	-0.02871(4)	g,h
$^{16}\text{O}^{12}\text{C}^{34}\text{S}$	1	-0.02813(4)	h
$^{16}\text{O}^{12}\text{C}^{79}\text{Se}$	1	-0.0195(2)	i
H <sup>12</sup> C <sup>14</sup> N	1	-0.0962	j
H <sup>12</sup> C <sup>15</sup> N	1	-0.0917(7)	k
H <sup>12</sup> CP	1	-0.430(10)	e
$^{15}\text{N}^{15}\text{N}^{16}\text{O}$	1	+0.07606(10)	l
F <sup>12</sup> C <sup>12</sup> CH	1	-0.0077(2)	m
$^{35}\text{Cl}^{12}\text{C}^{12}\text{CH}$	1	-0.00630(14)	n

<sup>a</sup>The *g* factors are consistent with the magnetic moment expressed in nuclear magneton units.

<sup>b</sup>Rosenblum et al. [7].

<sup>c</sup>Gustafson and Gordy [31].

<sup>d</sup>H. F. Bates, J. J. Gallagher, and V. E. Derr, *J. Appl. Phys.*, **39**, 3218 (1968).

<sup>e</sup>McGurk et al. [40].

<sup>f</sup>Burrus [8].

<sup>g</sup>Hüttner et al. [17].

<sup>h</sup>Flygare et al. [20].

<sup>i</sup>Shoemaker and Flygare [30].

<sup>j</sup>B. N. Bhattacharya, Ph.D. dissertation, Duke University, 1958.

<sup>k</sup>Gustafson and Gordy [41].

<sup>l</sup>Flygare et al. [22].

<sup>m</sup>Shoemaker and Flygare [18].

<sup>n</sup>Allen and Flygare [36].

the  $J=1$  state since  $M_J$  equals zero in the lower state. The  $g_J$  measured for the  $J=1 \rightarrow 2$  transition is essentially that for the  $J=2$  state, as indicated by (11.20).

### Symmetric-top Molecules

For the symmetric top, as for the linear molecule,  $z$  represents the symmetry axis, and we can set  $g_{xx}=g_{yy}=g_{\perp}$ ,  $g_{zz}=g_K$ , and  $\tau=K$ . Since  $J_x^2+J_y^2=J^2-J_z^2$ ,

the average is  $(J, K, M_J | J_x^2 + J_y^2 | J, K, M_J) = J(J+1) - K^2$ . Equation 11.10 specialized to the symmetric top becomes

$$g_{J,K} = g_{\perp} + (g_K - g_{\perp}) \frac{K^2}{J(J+1)} \quad (11.21)$$

and from (11.12) we get

$$E_{J,K,M_J} = -g_{J,K}\beta_I H M_J \quad (11.22)$$

Equation 11.21 can also be derived from the vector model of the symmetric top in an applied field, Fig. 10.1.

The selection rules governing  $M_J$  are the same as those for a linear molecule, (11.17), and for a rotational transition  $J \rightarrow J+1$  and  $K \rightarrow K$ . Since  $K$  does not change,  $g_K$  is the same for both upper and lower transitions. Furthermore, the assumption that  $g_{\perp}(J, K) = g_{\perp}(J+1, K) = g_{\perp}$  seems justified from the data on linear molecules, Table 11.1. From (11.22) the Zeeman frequencies are found to be

$$\nu_{\pi}(M_J \rightarrow M_J) = \nu_0 + \frac{\beta_I H}{h} (g_{J,K} - g_{J+1,K}) M_J \quad (11.23)$$

$$\nu_{\sigma}(M_J \rightarrow M_J \pm 1) = \nu_0 + \frac{\beta_I H}{h} (g_{J,K} - g_{J+1,K}) M_J \mp \frac{\beta_I H g_{J+1,K}}{h} \quad (11.24)$$

where  $\nu_0$  is the rotational frequency when no field is applied. When  $g_K$  and  $g_{\perp}$  are constants

$$g_{J,K} - g_{J+1,K} = \frac{2(g_K - g_{\perp})K^2}{J(J+1)(J+2)} \quad (11.25)$$

Because  $g_K - g_{\perp}$  is not negligible for many molecules, the  $\pi$  splitting is observable for low  $J$  values. It vanishes for  $K=0$  and for a given  $K$  decreases approximately as  $1/J^3$ , but for  $K=J$  it decreases only as  $1/J$ , approximately.

We illustrate the application of the foregoing theory with  $\text{CH}_3\text{CCH}$ . The upper curve of Fig. 11.4 shows the zero field and the components of the  $J=3 \rightarrow 4$  transition. The different  $K$  lines are separated by centrifugal distortion. The bottom curve shows the same transition with a field of 10 kG imposed at right angles to the electric vector of the microwave radiation polarized in such a way that only the  $M_J \rightarrow M_J \pm 1$  components are observable. Note that the  $K=0$  line is unsplit and not even measurably broadened by the field. When  $K=0$ , the splitting is due entirely to  $g_{\perp}$ , as may be readily seen from (11.21). The expected splitting is like that for a linear molecule with  $g_J = g_{\perp}$ . Thus the failure to observe splitting or broadening of the  $K=0$  line proves that  $g_{\perp}$  is small. For the other components we can set  $g_{\perp} \approx 0$  and obtain

$$g_{J,K} = \frac{g_K K^2}{J(J+1)} \quad gg_{J+1,K} = \frac{g_K K^2}{(J+1)(J+2)} \quad (11.26)$$

The splitting is best resolved for the  $K=3$  line for which

$$g_{33} = \frac{3g_K}{4} \quad \text{and} \quad g_{43} = \frac{9g_K}{20}$$

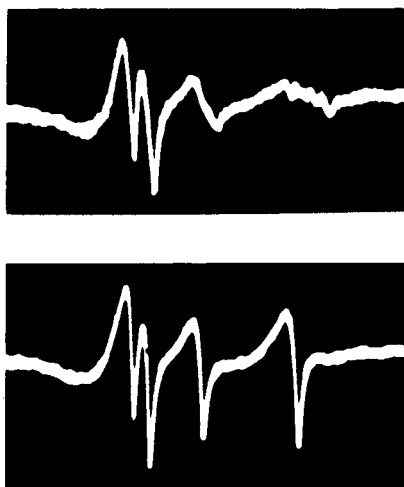


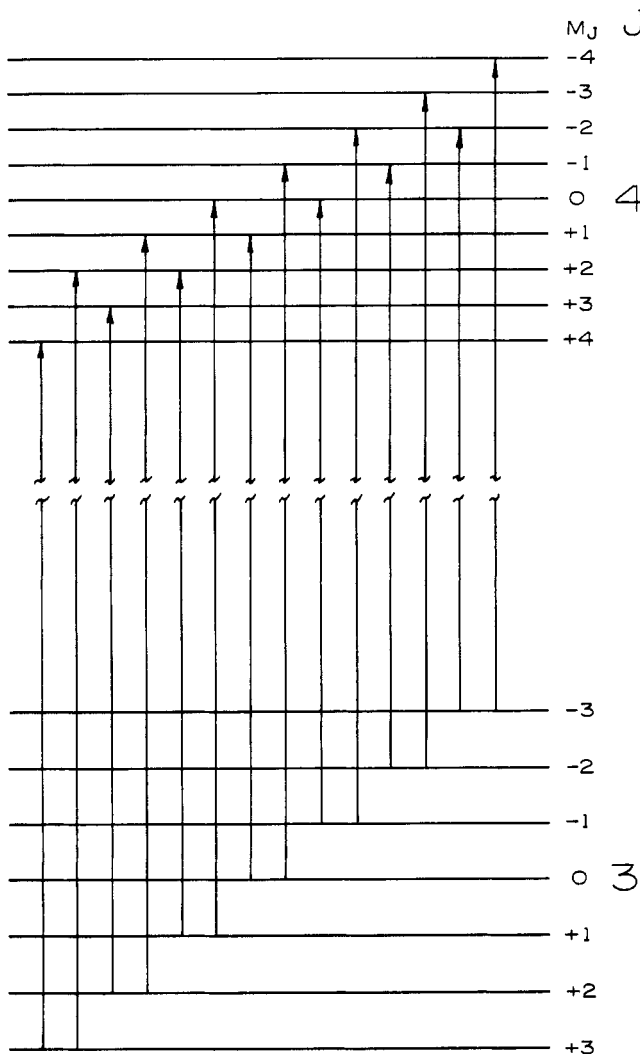
**Fig. 11.4** Zeeman effect of a symmetric-top molecule. The  $J=3 \rightarrow 4$  transition ( $K=0, 1, 2, 3$  components from right to left) of  $\text{CH}_3\text{CCH}$  with the field arranged for observation of the  $\Delta M_J = \pm 1$  components. The upper figure is for zero field; the lower, for a field of 10 kgauss. From Cox and Gordy [6].

The splittings of the two energy levels are given by

$$E_{33} = -\frac{3g_K\beta_I HM_J}{4h} \quad \text{and} \quad E_{43} = -\frac{9g_K\beta_I HM_J}{20h}$$

in frequency units. The energy level diagram (not drawn to scale) and the indicated  $M_J \rightarrow M_J \pm 1$  transitions are shown in Fig. 11.5. The spacing of the upper multiplet level is only  $\frac{3}{5}$  that of the lower multiplet. The relative intensities of the  $M_J \rightarrow M_J - 1$  components with increasing frequencies are 2, 6, 12, 20, 42, and 56 as calculated from (10.127). Those of the  $M_J \rightarrow M_J + 1$  components are the same, but in reverse order. The superimposed  $M_J \rightarrow M_J - 1$  and  $M_J \rightarrow M_J + 1$  components obtained when  $g_{43} = (\frac{3}{5})g_{33}$  are shown in Fig. 11.6. The four observed Zeeman components of the  $K=3$  line shown in Fig. 11.4 correspond to the four strong lines of the theoretical pattern. The others are too weak to be observable. From the separation of the outer of the four observed lines,  $g_K$  is found [6] to be  $0.298 \pm 0.006$ . The corresponding  $g_{J,K}$  factor for the  $K=2$  line is only  $\frac{4}{5}$  that for the  $K=3$  line, and the spread of the unresolved multiplet is about one-half that of the  $K=3$  line. The  $g$  factor for the  $K=1$  line, only  $\frac{1}{5}$  that of the  $K=3$  line, is too small for any resolution of the splitting.

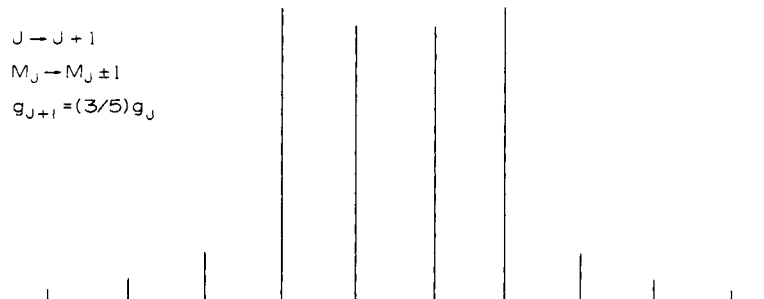
Shoemaker and Flygare [9] have remeasured the Zeeman effect of methyl acetylene with a magnetic field of 30,000 G and obtained the more accurate value  $g_{\parallel} = +0.312 \pm 0.002$ . They were also able to measure the small  $g_{\perp}$  for  $\text{CH}_3\text{CCH}$ . These and  $g$  factors for some other symmetric-top molecules are listed in Table 11.2. The  $g$  value caused by rotation of the methyl group in different symmetric tops appears to have the approximately constant value of 0.310.



**Fig. 11.5** Energy level diagram of the Zeeman splitting of the  $J = 3 \rightarrow 4$  transition when  $g_4 = (\frac{2}{3})g_3$  with indicated  $\Delta M_J = \pm 1$  transition. This diagram corresponds to that for the  $K = 3$  line shown for  $\text{CH}_3\text{CCH}$  in Fig. 11.4 and to the theoretical spectrum shown in Fig. 11.6.

### Asymmetric Rotors

The first-order Zeeman perturbation energies of asymmetric-top molecules are given by (11.12) with the  $g_{J,\tau}$  given by (11.13). The problem of obtaining the average  $\langle J_g^2 \rangle$  over the wave functions of the asymmetric rotor is the same as that already encountered in the evaluation of the rigid rotor energies. The values given in terms of the reduced energies, (9.97)–(9.99), can be employed.

Fig. 11.6 The theoretical pattern of the  $J = 3 \rightarrow 4$ ,  $\Delta M_J = \pm 1$  Zeeman components when  $g_4 = (\frac{3}{5})g_3$ .**Table 11.2** Molecular Rotational *g* Factors for Some Symmetric-top Molecules

Molecule	$g_{\perp}$	$g_{\parallel} = g_K$	Ref.
$^{15}\text{NH}_3$	0.563(2)	0.500(2)	<sup>b</sup>
$\text{PH}_3$	-0.033(1)	0.017(1)	<sup>c</sup>
$\text{PF}_3$	-0.0659(3)	-0.0815(20)	<sup>d</sup>
$\text{CH}_3\text{F}$	-0.062(5)	[0.31(3)] <sup>a</sup>	<sup>e,f</sup>
$\text{CH}_3^{35}\text{Cl}$	-0.01653(28)	[0.305(20)]	<sup>g</sup>
$\text{CH}_3^{79}\text{Br}$	-0.00569(30)	0.294(16)	<sup>g,h</sup>
$\text{CH}_3\text{I}$	-0.00677(40)	0.310(16)	<sup>g</sup>
$\text{SiH}_3^{81}\text{Br}$	-0.02185(13)	-0.3185(5)	<sup>h</sup>
$\text{CH}_3\text{CN}$	-0.0338(8)	[0.31(3)]	<sup>i</sup>
$\text{CH}_3\text{NC}$	-0.0546(15)	[0.31(3)]	<sup>i</sup>
$\text{CH}_3\text{CCH}$	0.00350(15)	0.312(2)	<sup>j</sup>
$\text{SiH}_3\text{NCS}$	-0.01521(10)	-0.315(5)	<sup>k</sup>

<sup>a</sup>Values in brackets are assumed from methyl group contribution of 0.31. See Flygare and Benson [57].

<sup>b</sup>S. G. Kukolich and W. H. Flygare, *Mol. Phys.*, **17**, 127 (1969).

<sup>c</sup>Kukolich and Flygare [28].

<sup>d</sup>Stone et al. [23].

<sup>e</sup>Cox and Gordy [6].

<sup>f</sup>Shoemaker, Kukolich, and Flygare, reported by Flygare and Benson [57].

<sup>g</sup>VanderHart and Flygare [21].

<sup>h</sup>Dössel and Sutter [51].

<sup>i</sup>Pochan et al. [32].

<sup>j</sup>Shoemaker and Flygare [24].

<sup>k</sup>Dössel and Sutter [52].

With these expressions we have

$$g_{J,\tau} = \frac{1}{2J(J+1)} \left\{ g_{aa} \left[ J(J+1) + E_{J,\tau}(\kappa) - (\kappa+1) \frac{\partial E_{J,\tau}(\kappa)}{\partial \kappa} \right] + 2g_{bb} \left[ \frac{\partial E_{J,\tau}(\kappa)}{\partial \kappa} \right] + g_{cc} \left[ J(J+1) - E_{J,\tau}(\kappa) + (\kappa-1) \frac{\partial E_{J,\tau}(\kappa)}{\partial \kappa} \right] \right\} \quad (11.27)$$

where  $a$ ,  $b$ , and  $c$  are the principal axes of inertia,  $E(\kappa)$  is the reduced rotational energy,  $\kappa = (2B - A - C)/(A - C)$  is the asymmetry parameter, and  $A$ ,  $B$ , and  $C$  are the usual spectral constants (see Chapter VII). In analysis of the spectra and evaluation of  $g_{aa}$ ,  $g_{bb}$ , and  $g_{cc}$ , it is convenient to use first the frequency equations

$$\nu_\pi(M_J \rightarrow M_J) = \nu_0 + \frac{\beta_I H}{h} (g_{J,\tau} - g_{J',\tau'}) M_J \quad (11.28)$$

$$\nu_\sigma(M_J \rightarrow M_J \pm 1) = \nu_0 + \frac{\beta_I H}{h} (g_{J,\tau} - g_{J',\tau'}) M_J \mp \frac{\beta_I H}{h} g_{J',\tau'} \quad (11.29)$$

to find the  $g_{J,\tau}$  values for different states from the observed Zeeman patterns and then to employ these values with (11.27) to solve for  $g_{aa}$ ,  $g_{bb}$ , and  $g_{cc}$ . Obviously,  $g_{J,\tau}$  must be measured for three different states for evaluation of these elements.

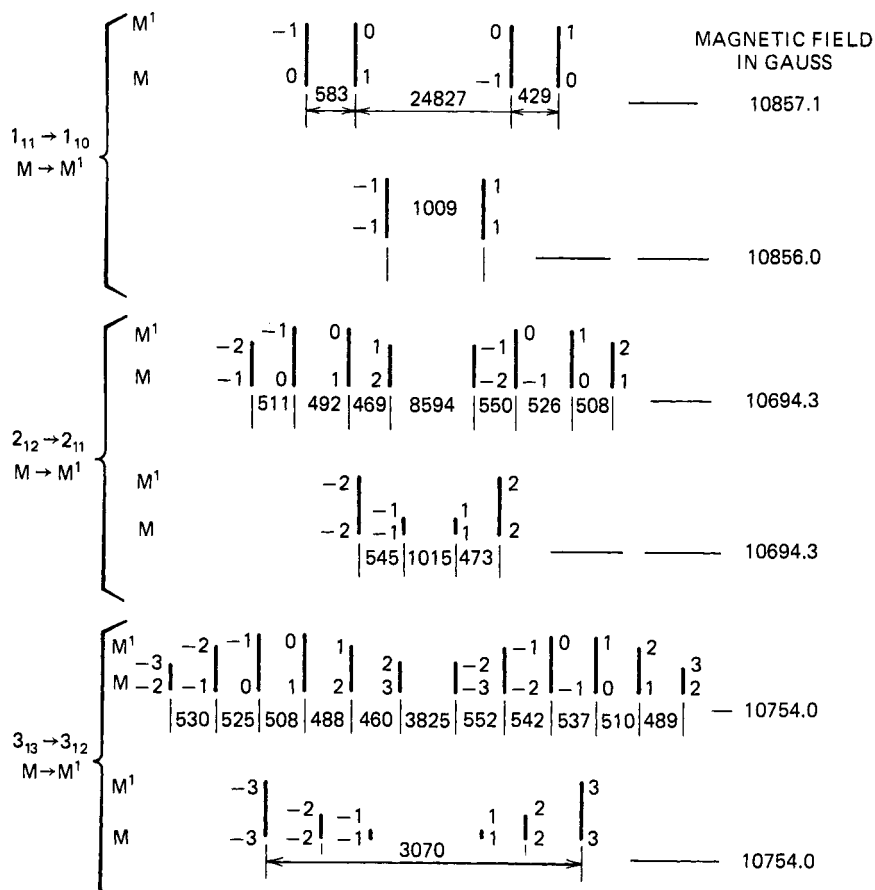


Fig. 11.7 Theoretical  $Q$ -branch ( $\Delta J = 0$ ) Zeeman pattern with observed splittings for  $\text{H}_2\text{CO}$ . From Hüttner et al. [17].

Because  $J$  does not appear explicitly in the energy formula (11.12), the foregoing frequency formulas are applicable to  $J \rightarrow J$  transitions as well as the  $J \rightarrow J \pm 1$  transitions, all of which may occur in asymmetric rotors. Since the intensity formulas are different, (10.125)–(10.129), the appearance of the Zeeman patterns for the  $Q$ ,  $P$ , and  $R$  branches are generally different. Figure 11.7 illustrates the types of patterns which occur for the  $\Delta J = 0$ ,  $Q$ -branch transition. The small differences in the observed component spacings of a particular set are due to effects of anisotropic susceptibility, described in Section 4.

Table 11.5, in Section 4, gives examples of principal  $g$  values of asymmetric rotors measured with the microwave Zeeman effect. For these molecules that have a plane of symmetry normal to the molecular plane, the magnetic axes,  $x$ ,  $y$ , and  $z$ , coincide with the inertial axes, and the diagonal elements  $g_{aa}$ ,  $g_{bb}$ ,  $g_{cc}$  can be taken as principal values of the  $\mathbf{g}$  tensor.

## 2 ZEEMAN EFFECT OF NUCLEAR HYPERFINE STRUCTURE

### Weak-field Case

When the nuclear coupling energy is much stronger than the Zeeman interaction, the rotational angular momentum  $\mathbf{J}$  will form with the various coupled nuclear spin vectors a resultant angular momentum  $\mathbf{F}$  which will precess about the direction of the field, as indicated in Fig. 10.6. In this weak-field case only the averaged values of the magnetic moment along  $\mathbf{F}$  will effectively interact with  $\mathbf{H}$  since the components of  $\mu_J$  or of  $\mu_I$  normal to  $\mathbf{F}$  will be averaged out by the precession about  $\mathbf{F}$ . The Zeeman interaction energy will then be

$$E_H(M_F) = -\langle \mu_F \rangle H \cos(\mathbf{F}, \mathbf{H}) = -\frac{\langle \mu_F \rangle H M_F}{[F(F+1)]^{1/2}} \quad (11.30)$$

By comparison with (11.11)  $g_F$  is so defined that

$$\langle \mu_F \rangle = g_F \beta_I [F(F+1)]^{1/2} \quad (11.31)$$

Hence

$$E_H(M_F) = -g_F \beta_I H M_F \quad (11.32)$$

where

$$M_F = F, F-1, F-2, \dots, -F \quad (11.33)$$

where  $F$  is the hyperfine quantum number defined in Chapter IX. The selection rules for  $M_F$  are the same as those for  $M_J$ , that is,  $\Delta M_F = 0, \pm 1$ . The frequencies of the Zeeman component can be expressed as

$$\nu = \nu_0 + \frac{\beta_I H}{h} [(g_F - g_{F'}) M_F - g_{F'} \Delta M_F] \quad (11.34)$$

where  $v_0$  represents the frequency of the  $F \rightarrow F'$  component when no field is applied and where  $M_F$  and  $g_F$  are for the lower rotational level. When the magnetic field is parallel to the electric vector of the microwave radiation, only the  $\pi$  components corresponding to  $\Delta M_F = 0$  are observable. When the field is perpendicular to this vector, the  $\Delta M_F = \pm 1$  or  $\sigma$  components are observable.

The relative intensity formulas are the same as those for the Stark effect (10.130) and (10.131) and are like those for molecules without hyperfine structure if  $J$  is replaced by  $F$  and  $M_J$  by  $M_F$ .

From analysis of the observed Zeeman patterns with (11.34) values of  $g_F$  for the different hyperfine states can be obtained. From them it is possible to derive the nuclear  $g$  factor and the diagonal elements of the molecular  $g$  factor with reference to the inertial axes. To do this we must resolve both  $\mu_I$  and  $\mu_J$  along  $\mathbf{F}$ . When  $\mathbf{I}$  and  $\mathbf{J}$  are coupled, the nuclear magnetic moment  $\mu_I$  which is along  $\mathbf{I}$  contributes to the Zeeman splitting of the lines, whereas it does not when the coupling is negligible. In fact, the contribution of  $\mu_I$  to the Zeeman splitting of the hyperfine components is of the same order of magnitude as that of  $\mu_J$ .

We now express  $g_F$  in terms of  $g_J$  and  $g_I$ . First let us consider a molecule with a single coupling nucleus. The derivation is independent of the type of coupling (magnetic or quadrupole), but only quadrupole coupling is sufficiently strong to prevent decoupling of  $\mathbf{J}$  and  $\mathbf{I}$  for fields sufficiently strong for resolution of the Zeeman patterns. For the weak-field case the vector model of Fig. 10.6 applies. The angles between  $\mathbf{J}$  and  $\mathbf{F}$  and between  $\mathbf{I}$  and  $\mathbf{F}$  are constant, and with the relation  $\langle \mu_F \rangle = g_J \beta_I [J(J+1)]^{1/2} \cos(\mathbf{J}, \mathbf{F}) + g_I \beta_I [I(I+1)]^{1/2} \cos(\mathbf{I}, \mathbf{F})$  we find

$$g_F = g_J \alpha_J + g_I \alpha_I \quad (11.35)$$

where

$$\alpha_J = \frac{[J(J+1)]^{1/2}}{[F(F+1)]^{1/2}} \cos(\mathbf{J}, \mathbf{F}) \quad \text{and} \quad \alpha_I = \frac{[I(I+1)]^{1/2}}{[F(F+1)]^{1/2}} \cos(\mathbf{I}, \mathbf{F})$$

From the law of the cosine applied to Fig. 10.6,

$$\alpha_J = \frac{F(F+1) + J(J+1) - I(I+1)}{2F(F+1)} \quad (11.36)$$

$$\alpha_I = \frac{F(F+1) + I(I+1) - J(J+1)}{2F(F+1)} \quad (11.37)$$

where

$$F = J + I, J + I - 1, \dots, |J - I| \quad (11.38)$$

Equation 11.32 for the Zeeman energies can now be expressed in the more explicit form

$$E_H(M_F) = -(g_J \alpha_J + g_I \alpha_I) \beta_I H M_F \quad (11.39)$$

For a linear molecule,  $g_J \equiv g_{\perp}$  is approximately constant, independent of the rotational state (Section 1). For symmetric-top molecules, the value of  $g_J \equiv g_{J,K}$  is given by Eq. 11.21; for asymmetric rotors,  $g_J \equiv g_{J,\tau}$  is given by (11.27).

With the  $g_I$  measured from the Zeeman effect one can obtain values for the nuclear magnetic moment from

$$\mu_I = g_I \beta_I I \quad (11.40)$$

The value of  $\mu_I$  for radioactive  $^{131}\text{I}$  was first measured with this method [10], also that of  $^{33}\text{S}$  [11]. However, the Zeeman effect cannot compete with the more accurate nuclear resonance method, which has already been used for measurement of  $\mu_I$  for essentially all known isotopes in their ground states. It is common practice to use these known nuclear moments (tabulated in Appendix E) to simplify the determination of  $g_J$  from (11.39).

When there is a second nucleus with coupling weaker than the first, one first finds

$$g_{F_1} = g_J \alpha_J + g_{I_1} \alpha_{I_1} \quad (11.41)$$

by resolution of  $\mu_J$  and  $\mu_{I_1}$ , along  $\mathbf{F}_1$  the resultant of  $\mathbf{J}$  and  $\mathbf{I}_1$ , as described above; one then resolves  $\mu_{F_1}$  and  $\mu_{I_2}$  along  $\mathbf{F}$ , which is the resultant of  $\mathbf{F}_1$  and  $\mathbf{I}_2$  (see vector diagram of Fig. 9.9). The result is

$$g_F = g_{F_1} \alpha_{F_1} + g_{I_2} \alpha_{I_2} \quad (11.42)$$

where

$$\alpha_{F_1} = \frac{F(F+1) + F_1(F_1+1) - I_2(I_2+1)}{2F(F+1)} \quad (11.43)$$

$$\alpha_{I_2} = \frac{F(F+1) + I_2(I_2+1) - F_1(F_1+1)}{2F(F+1)} \quad (11.44)$$

The Zeeman splitting of the hyperfine level designated by  $F$  is given by (11.32) with the  $g_F$  of (11.42). Note that  $g_F$  is a function of  $g_J$ ,  $g_{I_1}$ , and  $g_{I_2}$ . Definition of the quantum numbers is given by (9.122) and (9.123). When there is a third nucleus with still weaker coupling, derivation of  $g_F$  is accomplished by a further compounding of the vectors in the same manner.

Jen [2] first observed the Zeeman effect of rotational hyperfine structure in the  $0 \rightarrow 1$  transition of  $\text{CH}_3\text{Cl}$ . Burrus [8] has observed the effect in hyperfine components of DBr and DI. Figure 11.8 shows the  $\sigma$  and  $\pi$  components which he observed for the  $F = \frac{5}{2} \rightarrow \frac{7}{2}$  transitions of  $\text{D}^{132}\text{I}$ . The measured values of  $g_J$  are listed in Table 11.1. Note that the sign as well as the magnitude of  $g_J$  is given. The known sign of  $g_I$  makes possible the determination of the sign of the molecular  $g$  factor from application of (11.35). For molecules without nuclear coupling, determination of the sign of  $g_J$  requires the use of circularly polarized radiation [3].

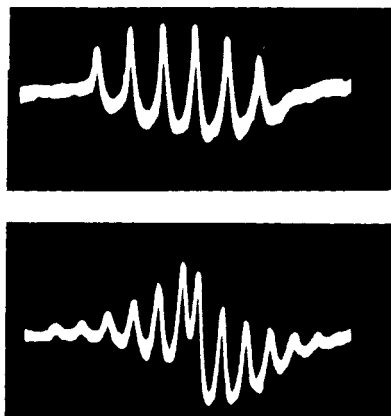


**Fig. 11.8** Zeeman pattern observed for the  $J=0\rightarrow 1$ ,  $F=\frac{5}{2}\rightarrow \frac{7}{2}$  transition of DI at 195 GHz. The upper trace shows the  $\pi$  components ( $\Delta M_F=0$ ). The lower trace shows the  $\sigma$  components ( $\Delta M_F=\pm 1$ ). From Burrus [8].

### Strong-field Case

When the strength of the magnetic field is such as to make the Zeeman energy large as compared with the nuclear hyperfine energy, the nuclear coupling is broken down, and  $\mathbf{J}$  and  $\mathbf{I}$  precess separately about the field direction, as indicated in Fig. 10.7. The resultant  $\mathbf{F}$  is not formed, and  $F$  and  $M_F$  are no longer good quantum numbers. Instead, the quantum numbers which describe the state are  $J$ ,  $M_J$ ,  $I$ , and  $M_I$ . The strong-field case is often called the Paschen-Back effect from analogy with the breaking down of the spin-orbit coupling in atoms by strong magnetic fields or the Back-Goudsmit effect, which applies to the similar breaking of the nuclear and the electron coupling in atomic spectra. It is very similar to the strong-field Stark case described in this section.

The Zeeman energy for the decoupled, strong-field case *per se* is the same as that for molecule without nuclear coupling, Section 1. However, the nuclear coupling energies are not canceled but simply altered by the applied field, and they must still be taken into account. The nuclear magnetic coupling energy in strong fields is very simple:

$$E_{\mu}^{(1)}(M_J M_I) = C_{J,\tau} M_J M_I \quad (11.45)$$

where  $C_{J,\tau}$  is the coupling constant for the particular rotational state  $J$ ,  $\tau$  derived for various molecular types in Chapter IX, Section 7. The nuclear quadrupole coupling energy for the strong-field case, which is the average  $\langle J, M_J, I, M_I | \mathcal{H}_Q | J, M_J, I, M_I \rangle$ , already evaluated in Chapter X, Section 2, is

$$E_Q^{(1)}(M_J M_I) = \frac{e Q q_J}{4 J(2J-1) I(2I-1)} [3M_J^2 - J(J+1)][3M_I^2 - I(I+1)] \quad (11.46)$$

where  $q_J$  for different molecular types is given in Chapter IX. If there is more than one coupling nucleus, the  $E_Q$  for each one is calculated with the same

formula, (11.46), and the results are added. The total first-order perturbation energy of the rotating molecule in the strong-field case is

$$E^{(1)} = -g_{J,\tau}\beta_I H M_J - \beta_I H \sum_i g_{I_i} M_{I_i} + \sum_i (C_{J,\tau})_i M_J M_{I_i} + \sum_i E_Q(M_J M_{I_i}) \quad (11.47)$$

where the sums are taken over all nuclei with coupling moments. The strong-field Zeeman effect has the same advantage as the strong-field Stark effect in simplifying the hyperfine structure caused by more than one coupling nucleus. The selection rules are

$$M_J \rightarrow M_J \quad M_I \rightarrow M_I \quad \pi \text{ components} \quad (11.48)$$

$$M_J \rightarrow M_J \pm 1 \quad M_I \rightarrow M_I \quad \sigma \text{ components} \quad (11.49)$$

Because  $g_{I_i}$  is the same for all states and because the nuclear spin does not change orientation;  $\Delta M_{I_i} = 0$ , the second term on the right, has no influence on the spectrum and can be dropped. For molecules in  ${}^1\Sigma$  states the term in  $C_{J,\tau}$  is usually negligible. Since the first term corresponding to  $E_H(M_J)$  is larger than  $E_Q(M_J M_I)$ , it is convenient to calculate first the splitting caused by this term and then to superimpose the hyperfine splitting on each of the Zeeman states.

The relative intensities of the gross components of the Zeeman pattern are the same as those for molecules without hyperfine structure. Each gross Zeeman component is split into a hyperfine substructure. Because of the selection rules  $\Delta M_I = 0$ , there is no reorientation of the nuclei during a transition, and the nuclear orientation states are equally populated or very nearly so. Thus the hyperfine components corresponding to different values of  $M_I$  are all of equal intensity. However, for nuclear quadrupole interaction the levels corresponding to  $+M_I$  and  $-M_I$  are degenerate. For this reason the components for  $M_I$  not zero are twice as strong as those for  $M_I = 0$ . When there is a single nucleus with quadrupole coupling having  $I = \frac{3}{2}$ , each Zeeman component will be split into a doublet of equal intensity corresponding to  $M_I = \pm \frac{1}{2}$  and  $M_I = \pm \frac{3}{2}$ . For  $I = 1$ , the substructure would still be a doublet, but the components would have intensity ratios of 1 to 2 corresponding to  $M_I = 0$  and  $M_I = \pm 1$ . If the molecule has two nuclei with quadrupole coupling, it is convenient to calculate first the hyperfine pattern which is due to the stronger coupling nucleus and then to calculate the substructure of each of its components caused by the coupling of the second nucleus. Each calculation is independent of the other. Suppose, for example, that the stronger coupling nucleus has  $I = \frac{5}{2}$ . Each Zeeman component would have a calculated triplet substructure of equal intensity caused by this nucleus. If the second coupling nucleus has  $I = 1$ , each component of this triplet is further split into doublets with intensity ratios of 1:2.

Figure 11.9 illustrates the strong-field spectrum [12] for  $N_2O$  in which there are two  ${}^{14}N$  nuclei with weak but unequal quadrupole coupling. The

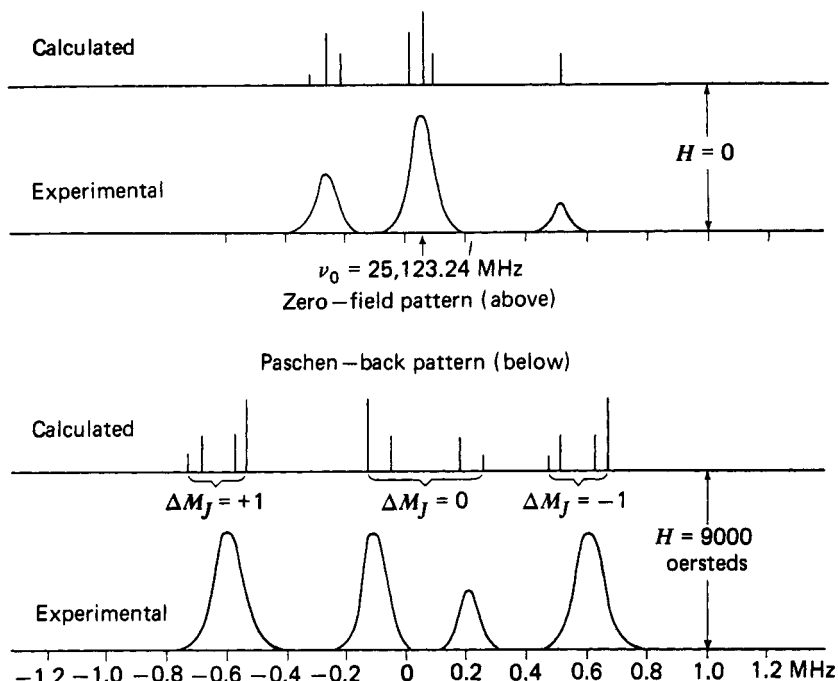


**Fig. 11.9** Theoretical and observed strong-field Zeeman effect of the hyperfine structure of the  $J=0 \rightarrow 1$  transition of  $^{14}\text{N}^{14}\text{NO}$ . From Jen [12].

nuclear magnetic coupling is negligible. The gross triplet is due to the  $\pi$  and  $\sigma$  components arising from the term  $-g_J\beta_I HM_J$ , the substructure to the nuclear quadrupole coupling. The coupling by one  $^{14}\text{N}$  splits each Zeeman component into a doublet with intensity ratios 1:2; the second  $^{14}\text{N}$  further splits each of these into doublets with intensity ratios 1:2, thus giving each Zeeman component a four-line substructure. The splitting by the end nitrogen is the greater.

Because of its infrequent application we shall not treat the intermediate-field case in which the Zeeman and the nuclear coupling energies are of comparable magnitude. The treatment is similar to that described for the intermediate-field Stark effect in Chapter X, Section 2. Usually the external field may be adjusted so that either the weak- or strong-field case applies.

### 3 THEORY OF MAGNETISM IN CLOSED-SHELL MOLECULES ( $^1\Sigma$ STATES)

The most common molecules have closed electronic shells ( $^1\Sigma$  states) and have no magnetic moments when field-free and not rotating. Molecular rotation, however, generates a small magnetic moment which is proportional to the rotational angular momentum, as is assumed in Section 1. Also, an externally imposed magnetic field may generate a magnetic moment caused by the

molecular susceptibility which is proportional to the strength of the magnetic field, as is assumed in Section 11.4. The magnetic susceptibility is a familiar quantity which is treated thoroughly in Van Vleck's classic work on magnetic and electric susceptibilities [13]. The susceptibility per molecule consists of a diamagnetic as well as a paramagnetic contribution, the principal elements of which can be expressed as

$$\chi_{xx} = -\frac{e^2}{4mc^2} \left( 0 \left| \sum_i (y_i^2 + z_i^2) \right| 0 \right) + \frac{e^2}{2m^2c^2} \sum_{n \neq 0} \frac{|(n|L_x|0)|^2}{E_n - E_0} \quad (11.50)$$

$$\chi_{yy} = -\frac{e^2}{4mc^2} \left( 0 \left| \sum_i (z_i^2 + x_i^2) \right| 0 \right) + \frac{e^2}{2m^2c^2} \sum_{n \neq 0} \frac{|(n|L_y|0)|^2}{E_n - E_0} \quad (11.51)$$

$$\chi_{zz} = -\frac{e^2}{4mc^2} \left( 0 \left| \sum_i (x_i^2 + y_i^2) \right| 0 \right) + \frac{e^2}{2m^2c^2} \sum_{n \neq 0} \frac{|(n|L_z|0)|^2}{E_n - E_0} \quad (11.52)$$

In these expressions  $|0\rangle$  represents the ground electronic wave function of the molecule; and  $|n\rangle$ , that of the excited state;  $L_g$  represents the electronic orbital angular momentum operator; and  $E_n - E_0$ , the difference in energy between the states  $|n\rangle$  and the ground state. The subscripts signify the coordinates of the  $i$ th electron, and the summation is taken over all electrons in the molecule. The constants  $e$ ,  $m$ , and  $c$  represent the charge and mass of the electron and the velocity of light, respectively. The molar susceptibility may be obtained by multiplication of the susceptibility per molecule by Avogadro's number  $N$ . The quantity measured in the usual bulk susceptibility experiments is the average

$$\chi = \frac{1}{3}(\chi_{xx} + \chi_{yy} + \chi_{zz}) \quad (11.53)$$

The first term on the right of Eqs. (11.50)–(11.52) arises from the Larmor precession of the electronic charge about the applied field and represents the diamagnetic component. The last term is the paramagnetic component that arises from an induced admixture of excited paramagnetic states with the nonmagnetic ground states. Although these excited states have orbital angular momentum, this momentum is counterbalanced by the opposite circulation of charges giving the diamagnetic term so that the total, overall angular momentum remains zero. The electronic spins remain paired and thus make no contribution to the magnetism.

Condon [14] originally treated rotational magnetic moments as caused by the rotation of charges fixed in the molecule. However, the early measurements of rotational magnetism by the molecular beam resonance method showed that the concept of fixed charges rotating with the molecular frame was inadequate. Wick [15] considered the separate contribution of the electron and nuclei and showed that the measured moment of  $H_2$  could be explained if the electrons were considered as having angular momentum apart from their rotation with the molecular frame. Jen [5] extended this theory to polyatomic molecules and assumed that the inner-shell electrons rotate with the nuclei and that only the valence electrons have angular momentum relative to the molecular frame.

With the Wick theory one can consider the rotation of the charges as generating a magnetic field which then induces a magnetic moment in the electronic cloud because of its magnetic susceptibility. In the Hamiltonian for the rotating molecule Eshbach and Strandberg [3] approached the problem in a more basic manner by considering separately the angular momentum due to the nuclear system from that due to the electrons. Their treatment, which does not explicitly employ the concept of magnetic susceptibility, is followed here.

Rotating molecules in  ${}^1\Sigma$  states can have a slight component of orbital electronic angular momentum which is due to a rotation-induced admixture of electronic states having orbital angular momentum with the ground electronic state. Because of the rigorous requirement that the total angular momentum must be a constant of the motion, no such components are possible in the nonrotating molecule, for which the electronic orbital angular momentum must either be exactly zero, as for  ${}^1\Sigma$  states, or must have the magnitude  $\hbar[L(L+1)]^{1/2}$  where  $L$  is an integer, as for  $\Pi$  states.

In the rotating molecule let us represent the total angular momentum by

$$\mathbf{J} = \mathbf{N} + \mathbf{L} \quad (11.54)$$

where  $\mathbf{N}$  represents the angular momentum caused by rotation of the nuclei alone and  $\mathbf{L}$ , that due to the electrons. Only  $\mathbf{J}$ , the total angular momentum, must be precisely quantized. The rotational Hamiltonian for the nuclear system plus the Hamiltonian for the unperturbed electronic energies is

$$\begin{aligned} \mathcal{H} &= \frac{1}{2} \sum_g \frac{N_g^2}{I_g} + \mathcal{H}_e = \frac{1}{2} \sum_g \frac{(J_g - L_g)^2}{I_g} + \mathcal{H}_e \\ &= \frac{1}{2} \sum_g \frac{J_g^2}{I_g} - \sum_g \frac{J_g L_g}{I_g} + \frac{1}{2} \sum_g \frac{L_g^2}{I_g} + \mathcal{H}_e \end{aligned} \quad (11.55)$$

where  $g = x, y, z$  represents the principal inertial axes and where  $I_g$  represents the principal moments of inertia due to the nuclear masses alone. We have assumed the nuclear frame to be rigid, that is, have neglected the effects of vibration and centrifugal distortion. Since  $L_g$  is very small, the third term in (11.55) can be neglected, and the second term can be treated as a perturbation. Therefore

$$\mathcal{H} = \mathcal{H}^0 + \mathcal{H}' \quad (11.56)$$

where

$$\mathcal{H}^0 = \frac{1}{2} \sum_g \frac{J_g^2}{I_g} + \mathcal{H}_e \quad (11.57)$$

and

$$\mathcal{H}' = - \sum_g \frac{J_g L_g}{I_g} \quad (11.58)$$

Here the first term in  $\mathcal{H}^0$  is like the Hamiltonian of the rigid rotor considered in earlier chapters except that  $I_g$  represents the moment of inertia resulting

from the nuclear masses alone, whereas in the earlier chapters the electronic masses were lumped with the nuclear masses in determination of  $I_g$ . See the discussion in Section 7. The electronic Hamiltonian is a function of the kinetic and potential energy of the electrons; however, the exact form of  $\mathcal{H}_e$  is not required for our discussion. The angular momentum of the electrons will have an associated magnetic moment

$$\mu_L = -\frac{e}{2mc} \mathbf{L} \quad (11.59)$$

Averaged over the unperturbed ground electronic state (pure  $\Sigma$  state), this will be zero.

$$\langle 0 | \mu_L | 0 \rangle = -\frac{e}{2mc} \langle 0 | \mathbf{L} | 0 \rangle = 0 \quad (11.60)$$

However, the term  $\mathcal{H}'$  perturbs the ground electronic state when the molecule is rotating. To obtain the electronic contribution to the rotational magnetic moment one may correct the electronic basis functions for the perturbation term. According to perturbation theory the first-order perturbed wave function is

$$\psi_0^{(1)} = \psi_0^{(0)} - \sum_{n \neq 0} \frac{\langle n | \mathcal{H}' | 0 \rangle}{E_n - E_0} \psi_n^{(0)} \quad (11.61)$$

where  $\psi_0^{(0)}$  signifies the wave function of the unperturbed state and  $\psi_n^{(0)}$  signifies those of other states for which the matrix elements of  $\mathcal{H}'$  are not zero. The  $E_n$  are the unperturbed electronic energies. Since the unperturbed electronic functions are independent of the  $J_g$  operators, the first-order perturbed electronic function is found from (11.58) and (11.61) to be

$$\psi_0^{(1)} = \psi_0^{(0)} + \sum_{n \neq 0} \sum_g \frac{J_g}{I_g} \frac{\langle n | L_g | 0 \rangle}{E_n - E_0} \psi_n^{(0)} \quad (11.62)$$

with  $I_g$  assumed to be constant. The averaged component  $\langle \mu \rangle_{\text{electronic}}$  along the  $g$  axis caused by the electronic angular momentum is

$$\begin{aligned} \langle \mu_g \rangle_{\text{electronic}} &= -\frac{e}{2mc} (\psi_0^{(1)} | L_g | \psi_0^{(1)}) \\ &= -\frac{e}{2mc} (\psi_0^{(0)} | L_g | \psi_0^{(0)}) - \frac{e}{2mc} \sum_{n \neq 0} \sum_{g'} \frac{J_{g'}}{I_{g'}} \\ &\quad \times \frac{\langle 0 | L_g | n \rangle \langle n | L_{g'} | 0 \rangle + \langle 0 | L_{g'} | n \rangle \langle n | L_g | 0 \rangle}{E_n - E_0} \end{aligned} \quad (11.63)$$

where higher-order terms are omitted. The first term on the right is zero, from (11.60). The second term is a tensor quantity, the diagonal elements of which give the observable quantities along the principal axes of inertia.

These are

$$\langle \mu_g \rangle_{\text{electronic}} = -2\beta \frac{J_g}{I_g} \sum_{n \neq 0} \frac{|(n|L_g|0)|^2}{E_n - E_0} = \beta_I g_{gg}^e J_g \quad (11.64)$$

where  $\beta (=e\hbar/2mc)$  is the Bohr magneton,  $\beta_I$  is the nuclear magneton, and  $J_g$  is now in units of  $\hbar$ . The electronic contribution is seen to arise purely from an admixture with paramagnetic states. There is no diamagnetic contribution to the rotational magnetic moment from the precessional motions of the electronic cloud.

The contribution to  $\mu_g$  by the rotating nuclei is easy to calculate because it need not be averaged over the electronic functions. It is simply the classical expression for the magnetic moment produced by the fixed nuclear charges  $Z_k e$  rotating about the principal axes with angular velocity  $\omega_g = \hbar J_g / I_g$ . The component about the principal axis  $x$  is, for example,

$$\langle \mu_x \rangle_{\text{nuclear}} = M_p \beta_I \frac{J_x}{I_x} \sum_k Z_k (y_k^2 + z_k^2) = \beta_I g_{xx}^n J_x \quad (11.65)$$

where  $M_p$  is the proton mass,  $\beta_I$  is the nuclear magneton  $e\hbar/2M_p c$ ,  $Z_k$  is the atomic number, and  $y_k$  and  $z_k$  are the coordinates of the  $k$ th nucleus in the principal inertial axes, and the summation is taken over all nuclei in the molecule. The  $y$  and  $z$  components are similar. The foregoing equation defines the diagonal elements of the  $\mathbf{g}^n$  tensor;  $\mathbf{g}^n$ , like  $\mathbf{g}^e$ , is, in general, a tensor quantity, but in first-order only the diagonal elements enter, as observed previously. When the inertial axes and the magnetic axes are the same, as in symmetric-top molecules, the diagonal elements of  $\mathbf{g}$  represent the principal values. The total rotational moment along the principal inertial axis  $g$  is

$$\mu_g = \langle \mu_g \rangle_{\text{nuclear}} + \langle \mu_g \rangle_{\text{electronic}} \quad (11.66)$$

where the values on the right are obtained from (11.64) and (11.65). It is seen that  $\mu_g$  is proportional to  $J_g$ , as assumed in Section 1. The diagonal elements of the molecular rotational  $g$  factor in the principal inertial axes are readily obtainable from these values of  $\mu_g$  and from (11.5) which defines  $g_{gg} = g_{gg}^e + g_{gg}^n$ . These elements are

$$g_{xx} = \frac{M_p}{I_x} \sum_k Z_k (y_k^2 + z_k^2) - \frac{2M_p}{mI_x} \sum_{n \neq 0} \frac{|(n|L_x|0)|^2}{E_n - E_0} \quad (11.67)$$

$$g_{yy} = \frac{M_p}{I_y} \sum_k Z_k (z_k^2 + x_k^2) - \frac{2M_p}{mI_y} \sum_{n \neq 0} \frac{|(n|L_y|0)|^2}{E_n - E_0} \quad (11.68)$$

$$g_{zz} = \frac{M_p}{I_z} \sum_k Z_k (x_k^2 + y_k^2) - \frac{2M_p}{mI_z} \sum_{n \neq 0} \frac{|(n|L_z|0)|^2}{E_n - E_0} \quad (11.69)$$

The first term on the right in these expressions is easily calculable from the moments of inertia and the molecular structures which are found from analysis of the rotational spectra. Since  $I_x \approx \sum M_p Z_k (y_k^2 + z_k^2)$ , and so on, these quantities are very closely equal to unity. The last, the paramagnetic term, can then be

measured from the principal elements of the  $g$  factors. These values of the paramagnetic terms can then be substituted into (11.50)–(11.52). When the corresponding elements of paramagnetic susceptibility are measured, the summed averages of all the electrons  $\sum_i \langle 0 | y_i^2 + z_i^2 | 0 \rangle$  over the electronic ground state function can be obtained. From the sum of these expressions  $\sum_i \langle 0 | r_i^2 | 0 \rangle$  can be evaluated. For this, it is convenient to eliminate the paramagnetic term between these expressions and to solve for the summed averages. Thus

$$\sum_i \langle 0 | y_i^2 + z_i^2 | 0 \rangle = \sum_k Z_k (y_k^2 + z_k^2) - \frac{I_x}{M_p} g_{xx} - \frac{4mc^2}{e^2} \chi_{xx} \quad (11.70)$$

$$\sum_i \langle 0 | z_i^2 + x_i^2 | 0 \rangle = \sum_k Z_k (z_k^2 + x_k^2) - \frac{I_y}{M_p} g_{yy} - \frac{4mc^2}{e^2} \chi_{yy} \quad (11.71)$$

$$\sum_i \langle 0 | x_i^2 + y_i^2 | 0 \rangle = \sum_k Z_k (x_k^2 + y_k^2) - \frac{I_z}{M_p} g_{zz} - \frac{4mc^2}{e^2} \chi_{zz} \quad (11.72)$$

For a linear molecule,  $g_{xx} = g_{yy} = g$  and (11.67)–(11.69) reduce to the simpler expression

$$g = \frac{M_p}{I} \sum_k Z_k z_k^2 - \frac{2M_p}{mI} \sum_{n \neq 0} \frac{|(n|L_x|0)|^2}{E_n - E_0} \quad (11.73)$$

where  $z_k$  is the distance of the  $k$ th nucleus from the center of gravity. For a linear molecule the summed average from (11.70) to (11.72) is

$$\sum_i \langle 0 | r_i^2 | 0 \rangle = \sum_k Z_k z_k^2 - \frac{gI}{M_p} - \frac{6mc^2}{e^2} \chi \quad (11.74)$$

where  $\chi = \frac{1}{3}(x_{\parallel} + 2\chi_{\perp})$ ,  $z_k$  is the distance of the  $k$ th nucleus from the center of gravity,  $I$  is the moment of inertia due to the nuclear masses alone, and  $r_i^2 = x_i^2 + y_i^2 + z_i^2$ .

## 4 ANISOTROPIC MAGNETIC SUSCEPTIBILITIES

### Measurement of Molecular Anisotropies

In addition to the molecular magnetic moments generated by rotation, which were considered previously, there are much smaller magnetic moments introduced in the molecule by the applied Zeeman field. When the magnetic susceptibility of the molecule is completely isotropic the induced moment is independent of the rotational state, and there is no detectable effect on the spectra. An anisotropic component can, in sufficiently strong fields, produce a measurable effect on the Zeeman pattern. Essentially all molecules, except the spherically symmetric ones which generally have no observable rotational spectra, do have anisotropic susceptibility.

The effects of anisotropic susceptibility on the Zeeman effect are very similar to those of anisotropic polarizability on the Stark effect considered in

Chapter X, Section 6. It is convenient to express the induced moments with reference to the inertial axes. Although these axes are not necessarily the principal axes of magnetic susceptibility, the off-diagonal elements will average out in the first-order treatment so that we need to consider only the diagonal elements. The induced value of the moment along the principal inertial axis  $x$  is

$$\begin{aligned}\mu_x(\chi) &= \frac{1}{2}(\chi_{xx}H_x + \chi_{xy}H_y + \chi_{xz}H_z) \\ &= \frac{1}{2}H(\chi_{xx}\Phi_{Zx} + \chi_{xy}\Phi_{zy} + \chi_{xz}\Phi_{zz})\end{aligned}\quad (11.75)$$

with  $H$  taken along the space-fixed  $Z$  axis. The interaction of this component with the field will be

$$\begin{aligned}-\mu_x \cdot \mathbf{H} &= -\mu_x H \Phi_{Zx} \\ &= -\frac{1}{2}H^2(\chi_{xx}\Phi_{Zx}^2 + \chi_{xy}\Phi_{Zx}\Phi_{zy} + \chi_{xz}\Phi_{Zx}\Phi_{zz})\end{aligned}\quad (11.76)$$

The interactions with  $\mu_y$  and  $\mu_z$  are similar, and the total interaction is

$$\mathcal{H}(\chi) = -\frac{1}{2}H^2 \sum_{g,g' = x,y,z} \chi_{gg'} \Phi_{Zg} \Phi_{Zg'} \quad (11.77)$$

where  $\chi_{gg'}$  are elements of the magnetic-susceptibility tensor referred to the principal inertial axis system. The first-order energy is the average of this Hamiltonian over the wave function of the rotor. In this average the off-diagonal terms do not contribute; only the diagonal terms are involved. Thus

$$E_H(\chi) = -\frac{1}{2}H^2[\chi_{xx}\langle\Phi_{Zx}^2\rangle + \chi_{yy}\langle\Phi_{Zy}^2\rangle + \chi_{zz}\langle\Phi_{Zz}^2\rangle] \quad (11.78)$$

in a symmetric-top or linear molecule the principal inertial axes are also principal axes of  $\chi$ , and  $\chi_{xx} = \chi_{yy} = \chi_{\perp}$ ,  $\chi_{zz} = \chi_{\parallel}$ , where  $z$  is the symmetry axis. Therefore we write

$$E_H(\chi) = -\frac{1}{2}H^2[\chi_{\perp}\langle\Phi_{Zx}^2 + \Phi_{Zy}^2\rangle + \chi_{\parallel}\langle\Phi_{Zz}^2\rangle] \quad (11.79)$$

With  $\Phi_{Zx}^2 + \Phi_{Zy}^2 = 1 - \Phi_{Zz}^2$  and with neglect of the term  $-\frac{1}{2}\chi_{\perp}H^2$  which does not depend on the rotational quantum numbers, we obtain

$$E_H(\chi) = -\frac{1}{2}H^2(\chi_{\parallel} - \chi_{\perp})\langle\Phi_{Zz}^2\rangle \quad (11.80)$$

where for a symmetric rotor basis

$$\langle\Phi_{Zz}^2\rangle = \langle J, K, M_J | \Phi_{Zz}^2 | J, K, M_J \rangle = \sum_{J'} | \langle J, K, M_J | \Phi_{Zz} | J', K, M_J \rangle |^2 \quad (11.81)$$

The required cosine matrix elements are given in Table 2.1. Substitution of these matrix elements gives the perturbation energy for the symmetric top,

$$\begin{aligned}E_{J,K,M_J}(\chi) &= -\frac{1}{2}(\chi_{\parallel} - \chi_{\perp})H^2 \left\{ \frac{[(J+1)^2 - K^2][(J+1)^2 - M_J^2]}{(J+1)^2(2J+1)(2J+3)} \right. \\ &\quad \left. + \frac{K^2 M_J^2}{J^2(J+1)^2} + \frac{(J^2 - K^2)(J^2 - M_J^2)}{J^2(4J^2 - 1)} \right\}\end{aligned}\quad (11.82)$$

The formula for a linear molecule is obtained when  $K=0$  is set in (11.82), which then becomes

$$E_{J,M_J}(\chi) = -\frac{1}{2}(\chi_{\parallel} - \chi_{\perp})H^2 \left[ \frac{(J+1)^2 - M_J^2}{(2J+1)(2J+3)} + \frac{J^2 - M_J^2}{4J^2 - 1} \right] \quad (11.83)$$

One must add  $E_H(\chi)$  to  $E_H(\mu)$  to obtain the total perturbation of a magnetic field. The total energy of the rotating molecule in a magnetic field is

$$E_H = E_r^0 + E_H(\mu) + E_H(\chi) \quad (11.84)$$

where  $E_r^0$  is the energy of the unperturbed rotor. With the magnetic fields commonly available in the laboratory, one is not justified in extending the calculations to higher order. Here  $E_H(\mu)$  represents the first-order magnetic interaction derived in Section 1.

The anisotropic susceptibility energies for asymmetric-top molecules are obtained from the average of the squared direction cosines of (11.78) over the functions of the asymmetric rotor. These averages can be expressed in terms of the line strengths. However, a more usable formula is obtained by expression of the average values of the squared direction cosines in terms of the average values of the squared angular momentum components. The resulting formula can be expressed in the form [16]

$$E_{J,\tau}(\chi) = -H^2 \left[ \frac{3M_J^2 - J(J+1)}{(2J-1)(2J+3)J(J+1)} \right] \sum_{g=a,b,c} (\chi_{gg} - \chi) \langle J_g^2 \rangle \quad (11.85)$$

where

$$\chi = \frac{1}{3}(\chi_{aa} + \chi_{bb} + \chi_{cc}) \quad (11.86)$$

is the isotropic component and where  $a$ ,  $b$ , and  $c$  represent the principal axes of inertia. Values of  $\langle J_g^2 \rangle$  in terms of the reduced rotational energies and their derivatives are given by (9.97)–(9.99). See also Chapter VII.

The total energy of the asymmetric rotor in a strong magnetic field, exclusive of nuclear interactions, may be expressed by (11.84) with  $E_H(\mu)$  from (11.12) and  $E_H(\chi)$  from (11.85). Thus

$$E_H(J, \tau, M_J) = E_0(J, \tau, M_J) - \frac{H\beta_I M_J}{J(J+1)} \sum_{g=a,b,c} g_{gg} \langle J_g^2 \rangle - H^2 \left[ \frac{3M_J^2 - J(J+1)}{(2J-1)(2J+3)J(J+1)} \right] \sum_{g=a,b,c} (\chi_{gg} - \chi) \langle J_g^2 \rangle \quad (11.87)$$

where the first term on the right,  $E_0(J, \tau, M_J)$ , is the field-free rotational energy which may be found as described in Chapter IX. A term,  $-\frac{1}{2}H^2$ , is omitted because it displaces all levels equally and has no influence on the spectra. The Zeeman splitting of the rotational lines caused by the second term on the right is described in Section 1. Further shifts of these components resulting from the last term are measured as a function of the field  $H$ . From these measurements are found the magnitudes of the three components,  $g_{aa}$ ,  $g_{bb}$ , and  $g_{cc}$ ,

along the principal inertial axes,  $a$ ,  $b$ , and  $c$ , of the asymmetric rotor, together with the anisotropies.

$$3(\chi_{aa} - \chi) = 2\chi_{aa} - \chi_{bb} - \chi_{cc} \quad (11.88)$$

$$3(\chi_{bb} - \chi) = 2\chi_{bb} - \chi_{aa} - \chi_{cc} \quad (11.89)$$

$$3(\chi_{cc} - \chi) = 2\chi_{cc} - \chi_{aa} - \chi_{bb} \quad (11.90)$$

These expressions are easily derived by addition of  $\chi_{aa}$ ,  $\chi_{bb}$ , or  $\chi_{cc}$  to both sides of (11.86) and rearrangement of the terms. The third  $3(\chi_{cc} - \chi)$  is seen to be the negative sum of the first two. Because of the relationship of (11.86), there are only two independent molecular anisotropies. These are usually expressed by the right-hand sides of (11.88) and (11.89). When  $\chi$  can be reliably calculated or derived from bulk susceptibility measurements, the diagonal elements,  $\chi_{aa}$ ,  $\chi_{bb}$ , and  $\chi_{cc}$ , can be obtained from (11.88)–(11.90).

As indicated in Section 3, the molecular susceptibilities defined by (11.50)–(11.52) have diamagnetic as well as paramagnetic components.

$$\chi_{gg} = \chi_{gg}^d + \chi_{gg}^p \quad (11.91)$$

The diamagnetic components correspond to the first terms on the right in (11.50)–(11.52), and in the asymmetric rotor, inertial axes,  $a$ ,  $b$ , and  $c$ , are

$$\chi_{aa}^d = -\frac{e^2}{4mc^2} \sum_i^{\text{electrons}} \langle 0 | b_i^2 + c_i^2 | 0 \rangle \quad (11.92)$$

$$\chi_{bb}^d = -\frac{e^2}{4mc^2} \sum_i^{\text{electrons}} \langle 0 | c_i^2 + a_i^2 | 0 \rangle \quad (11.93)$$

$$\chi_{cc}^d = -\frac{e^2}{4mc^2} \sum_i^{\text{electrons}} \langle 0 | a_i^2 + b_i^2 | 0 \rangle \quad (11.94)$$

If these values are substituted in (11.70)–(11.72) with the coordinate change  $x \rightarrow a$ ,  $y \rightarrow b$ ,  $z \rightarrow c$ , solutions for  $\chi_{aa} - \chi_{aa}^d$ , and so on, yield the paramagnetic components

$$\chi_{aa}^p = -\frac{e^2}{4mc^2} \left[ \frac{hg_{aa}}{8\pi^2 AM_p} - \sum_k^{\text{nuclei}} Z_k(b_k^2 + c_k^2) \right] \quad (11.95)$$

$$\chi_{bb}^p = -\frac{e^2}{4mc^2} \left[ \frac{hg_{bb}}{8\pi^2 BM_p} - \sum_k^{\text{nuclei}} Z_k(c_k^2 + a_k^2) \right] \quad (11.96)$$

$$\chi_{cc}^p = -\frac{e^2}{4mc^2} \left[ \frac{hg_{cc}}{8\pi^2 CM_p} - \sum_k^{\text{nuclei}} Z_k(a_k^2 + b_k^2) \right] \quad (11.97)$$

where we have substituted  $I_a = h/8\pi^2 A$ , and so on. In these expressions  $Z_k$  is the atomic number of the  $k$ th nucleus, and the summation is taken over all nuclei in the molecule. To express the susceptibility components in mole units, the terms on the right are multiplied by Avagadro's number,  $N$ .

Because of their symmetry, the principal axes of magnetic susceptibility of linear and symmetric-top molecules coincide with their principal inertial axes, indicated simply as the parallel and perpendicular axes in (11.82) and (11.83) and in the tabulated values for these quantities. See Tables 11.3 and 11.4. The axes,  $a$ ,  $b$ , and  $c$ , in which  $g_{gg}$  or  $\chi_{gg}$  are expressed for the asymmetric rotors, as in (11.87), are principal axes of inertia and do not necessarily coincide with the principal magnetic axes. In general, the derived magnetic quantities  $g_{gg}$  and  $\chi_{gg}$  are diagonal elements of magnetic tensors that may have nonzero, off-diagonal elements. However, any such off-diagonal elements of  $\chi$  are averaged out by the molecular rotation and hence are not detected in these experiments. In planar molecules having  $C_{2v}$  symmetry, such as those listed in Table 11.5, the principal magnetic axes designated as  $x$ ,  $y$ ,  $z$ , coincide with the principal inertial axes  $a$ ,  $b$ ,  $c$ ; for these, the principal values of the magnetic quantities are obtained directly from the analysis of the spectra.

**Table 11.3** Anisotropy in Magnetic Susceptibility and Molecular Quadrupole Moment of Some Linear Molecules

Molecule	Susceptibility Anisotropy, $\chi_{\perp} - \chi_{\parallel}$ ( $10^{-6}$ erg/ $G^2 \cdot \text{mole}$ )	Quadrupole Moment, $Q_{\parallel}$ ( $10^{-26}$ esu $\cdot$ cm $^2$ )	Ref.
CO	8.2(9)	-2.0(10)	<sup>a</sup>
CS	24(3)	0.8(14)	<sup>a,b</sup>
CSe	27.8(14)	-2.6(16)	<sup>b</sup>
SiO	11.1(9)	-4.6(11)	<sup>c</sup>
AlF	5.2(5)	-5.9(5)	<sup>d</sup>
CuF	6.5(7)	-6.1(8)	<sup>e</sup>
OCS	9.27(10)	-0.88(15)	<sup>f</sup>
OCSe	10.06(18)	-0.32(24)	<sup>g</sup>
HC <sup>15</sup> N	7.6(8)	3.5(9)	<sup>h</sup>
HCP	8.4(9)	4.4(9)	<sup>b</sup>
NNO	10.15(15)	-3.65(25)	<sup>i</sup>
FCCH	5.19(15)	3.96(14)	<sup>j</sup>
<sup>35</sup> CICCH	9.3(5)	8.8(4)	<sup>k</sup>

<sup>a</sup>Gustafson and Gordy [31].

<sup>b</sup>McGurk et al. [40].

<sup>c</sup>Hornerjäger and Tischer [38].

<sup>d</sup>Hornerjäger and Tischer [42].

<sup>e</sup>Hornerjäger and Tischer [45].

<sup>f</sup>Flygare et al. [20].

<sup>g</sup>Shoemaker and Flygare [30].

<sup>h</sup>Gustafson and Gordy [41].

<sup>i</sup>Flygare et al. [22].

<sup>j</sup>Shoemaker and Flygare [18].

<sup>k</sup>Allen and Flygare [36].

**Table 11.4** Anisotropy in Magnetic Susceptibility and Molecular Quadrupole Moment of Some Symmetric-top Molecules

Molecule	Susceptibility Anisotropy, $\chi_{\perp} - \chi_{\parallel}$ ( $10^6$ erg/ $G^2 \cdot$ mole)	Molecular Quadrupole Moment, $Q_{\parallel}$ ( $10^{-26}$ esu $\cdot$ cm $^2$ )	Ref.
NH <sub>3</sub>	-0.37(4)	-2.32(7)	a
PH <sub>3</sub>	2.7(8)	-2.1(10)	b
PF <sub>3</sub>	1.3(5)	24(3)	c
CH <sub>3</sub> Cl	8.0(5)	1.2(8)	d
CH <sub>3</sub> Br	8.5(4)	3.4(8)	d
CH <sub>3</sub> I	11.0(5)	5.4(9)	d
HCN	10.2(10)	-1.8(12)	e
CH <sub>3</sub> NC	13.5(17)	-2.7(16)	e
CH <sub>3</sub> CCH	7.70(14)	4.82(23)	f
CH <sub>3</sub> CCCCH	13.1(2)	9.9(8)	g
SiH <sub>3</sub> Br	2.7(3)	-0.1(4)	h
SiH <sub>3</sub> NCS	28.0(30)	16.6(37)	i

<sup>a</sup>Kukolich [29].<sup>b</sup>Kukolich and Flygare [28].<sup>c</sup>Stone et al. [23].<sup>d</sup>VanderHart and Flygare [21].<sup>e</sup>Pochan et al. [32].<sup>f</sup>Shoemaker and Flygare [24].<sup>g</sup>Shoemaker and Flygare, reported by Sutter and Flygare [58].<sup>h</sup>Dössel and Sutter [51].<sup>i</sup>Dössel and Sutter [52].

Taft and Dailey [4] have measured the anisotropic susceptibility for OCS from the  $J=1 \rightarrow 2$ ,  $M_J \rightarrow M_J$  transition with a magnitude field of 23 kG. The  $M_J \rightarrow M_J$  or  $\pi$  transitions are observed with the field imposed parallel to the microwave electric vector. With this arrangement no shift or broadening of the rotational lines is caused by the rotational magnetic moment when  $g_J = g_{J+1}$ . For linear molecules the  $g$  value for the different rotational states is expected to be the same except for very slight effects caused by centrifugal distortion. In OCS the possible difference in the  $g$  value observed for different rotational states can give rise to a splitting of the  $\pi$  components of only a few hertz, even at the 23 kG fields employed by Taft and Dailey. However, it is seen from Eq. (11.82) that the magnetic states have a slight  $J$  dependence caused by the anisotropic susceptibility. As a result, the  $J=1 \rightarrow 2$ ,  $M_J=0 \rightarrow 0$  component is separated from the  $J=1 \rightarrow 2$ ,  $M_J=\pm 1 \rightarrow \pm 1$  component. Taft and Dailey observed that the  $\pm 1 \rightarrow \pm 1$  component was shifted from the position of the zero-field line by 132 kHz. Using this observation they obtained the anisotropic susceptibility from (11.83) as  $\chi_{\perp} - \chi_{\parallel} = 8.35 \times 10^{-6}$  erg/( $G^2 \cdot$  mole). A remeasurement by Flygare et al. with a field of 30 kG gives the more accurate value listed in Table 11.3.

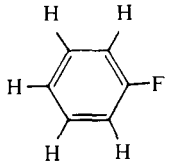
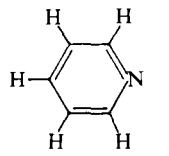
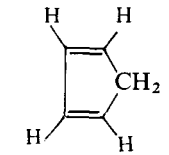
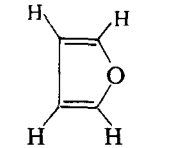
In an asymmetric rotor the molecular  $g$  factor differs according to the rotational state, and therefore the  $\Delta M_J=0$  transitions are split, even in the absence of anisotropic susceptibility. Without anisotropic effects, however, all the Zeeman components of a given multiplet (whether  $\pi$  or  $\sigma$ ) are equally spaced. Addition of the quadratic term  $E_H(\chi)$  of (11.85) cause a difference in the spacing which allows measurement of the  $(\chi_{gg} - \chi)$ . Hüttner et al. [17] were the first to measure the components of the magnetic susceptibilities of an asymmetric rotor, H<sub>2</sub>CO, from the differences in the spacing of the Zeeman components, as shown in Fig. 11.7. Later values of the magnetic constants of H<sub>2</sub>CO obtained with magnetic fields of 30 kG are listed in Table 11.5.

Following the experiments just discussed, there have been a large number of measurements of anisotropies in magnetic susceptibilities, some of which are cited here [18–56]. Description of the method and review of the essential results to 1970 are given by Flygare and Benson [57] and to 1976, by Sutter and Flygare [58]. Selected experimental values are given in Tables 11.3, 11.4, and

**Table 11.5** Zeeman Parameters and Molecular Quadrupole Moments for Selected Asymmetric-top Molecules<sup>a</sup>

Molecule	$g_{xx}$	$2\chi_{xx} - \chi_{yy} - \chi_{zz}$ ( $10^{-6}$ erg/G <sup>2</sup> ·mole)	$Q_{xx}$	Ref.
H \ O /    H	0.718(7) 0.657(1) 0.645(6)	-0.199(48) 0.464(24) -2.50(2)	-0.13(3) 2.63(2) -2.50(2)	b,c
H \ C=O /    H	-2.9017(8) -0.2243(1) -0.0994(1)	25.5(5) -3.9(3) -0.1(5)	-0.1(3) 0.2(2) -0.1(5)	d
H \ C=C=O /    H	-0.4182(9) -0.0356(13) -0.0238(6)	-5.0 -0.2(6) -3.1(4)	-0.7(3) 3.8(4) -3.1(4)	e,f
H              F \      / C=C /    \ H      F	-0.0421(5) -0.0466(4) -0.0119(4)	-2.3(6) 7.7(5) -1.5(8)	2.4(5) -0.9(4) -1.5(8)	d

**Table 11.5** (Continued)

<i>Molecule</i>	$g_{xx}$	$2\chi_{xx} - \chi_{yy} - \chi_{zz}$	$Q_{xx}$	
	$g_{yy}$	$2\chi_{yy} - \chi_{xx} - \chi_{zz}$	$Q_{yy}$	
	$g_{zz}$	( $10^{-6}$ erg/G $^2$ · mole)	$Q_{zz}$	<i>Ref.</i>
	-0.06892(22) -0.04161(13) -0.02627(9)	51.68(26) 61.69(45)	-1.52(36) 7.34(48) -5.82(62)	<sup>a</sup>
	-0.0770(5) -0.1010(8) 0.0428(4)	54.3(6) 60.5(8)	-3.5(9) 9.7(11) -6.2(15)	<sup>b</sup>
	-0.0827(3) -0.0700(3) 0.0385(2)	37.8(3) 30.7(3)	3.7(4) 1.4(4) -5.1(5)	<sup>i</sup>
	-0.0911(7) -0.0913(2) 0.0511(1)	43.0(2) 34.4(2)	0.2(4) 5.9(3) -6.1(4)	<sup>j</sup>

<sup>a</sup>In these molecules the principal axes of susceptibility, *x*, *y*, and *z*, coincide with the inertial axes, *a*, *b*, and *c*.

<sup>b</sup>J. Verhoeven and A. Dynamus, *J. Chem. Phys.*, **52**, 3222 (1970).

<sup>c</sup>S. G. Kukolich, *J. Chim. Phys.*, **50**, 3751 (1969).

<sup>d</sup>Blickensderfer et al. [26].

<sup>e</sup>Lo et al. [19].

<sup>f</sup>Hüttner et al. [25].

<sup>g</sup>Stolze et al. [56].

<sup>h</sup>Wang and Flygare [33].

<sup>i</sup>Benson and Flygare [34].

<sup>j</sup>Sutter and Flygare [27].

11.5. In these tables are also given molecular quadrupole moments derived from the anisotropies and measured *g* values, described in Section 5. Certain of the molecules listed have nuclear quadrupole coupling which can complicate the interpretation of the Zeeman patterns, as described in Section 2. Treatment of these complications for particular molecules may be found in the references cited. Diamagnetic and paramagnetic susceptibility components from (11.92)–(11.97) are illustrated in Table 11.7 in Section 5.

## Calculation of Molecular Susceptibilities from Local Atomic Components

Early in the century (1910) Pascal [59] proposed the concept of additive, local susceptibilities for calculation of bulk susceptibilities from atomic contributions. In 1970 Benson and Flygare [60] broadened the concept to include tensor elements of local atomic susceptibilities for calculation of anisotropic susceptibility components of molecules. This concept became increasingly useful with the widespread applications of microwave spectroscopy for accurate measurement of anisotropic molecular susceptibilities, beginning in 1968. For the calculations, useful sets of atomic susceptibility elements have been developed and published in convenient tables. The first such table, by Schmalz et al. [61] in 1973, was revised and extended by Sutter and Flygare [58] in 1976.

The tabulated local-atom susceptibility elements are empirically obtained by adjustment of assumed local parameter elements for the best overall fitting of calculated with observed susceptibility elements  $\chi_{aa}$ ,  $\chi_{bb}$ ,  $\chi_{cc}$ , of a large number of open-chain or nonaromatic molecules for which contributions from delocalized  $\pi$ -type bonds can be assumed negligible. For determination of the original set of local elements by Schmalz et al. [61], 14 molecules were used, for which good values of  $\chi_{aa}$ ,  $\chi_{bb}$ , and  $\chi_{cc}$  were available from microwave spectroscopy and bulk susceptibility measurements. Since that time the values have been improved and extended by inclusion of additional molecules from later microwave Zeeman measurements [54, 55, 58].

The molecular susceptibilities are calculated by summation of the atomic components resolved along the molecular inertial axes,  $a$ ,  $b$ , and  $c$ . For example,

$$\chi_{aa}^{\text{mol}} = \sum_i \{ \chi_{xx}^i \cos^2(a, x^i) + \chi_{yy}^i \cos^2(a, y^i) + \chi_{zz}^i \cos^2(a, z^i) \} \quad (11.98)$$

where  $x^i$ ,  $y^i$ ,  $z^i$  are the principal axes of the local atomic tensor  $\chi^i$  of the  $i$ th atom and where the summation is taken over all the local tensors contribution to the  $\chi_{aa}^{\text{mol}}$ . The expressions for  $\chi_{bb}^{\text{mol}}$  and  $\chi_{cc}^{\text{mol}}$  are similar. For obtaining the cosines in (11.98), the directions of the diagonal elements of the local tensors relative to the molecular frame must be known. Their directions are related to the bond directions formed by the atoms within the molecule. Generally, the complete structure of the molecule must be known for resolution of all the local tensor elements along  $a$ ,  $b$ , and  $c$ . Atoms forming different types of localized bonds, such as  $sp$ ,  $sp_2$ , and  $sp_3$  bonds, are assigned different atomic elements for each type of bonding. Some of the more commonly used elements are reproduced in Table 11.6.

Two examples of calculated (local atomic) and experimental  $\chi_{gg}$  values for molecules having negligible delocalized contributions are methyl formate [61] for which

$$\begin{array}{lll} \chi_{aa}^{\text{calc}} = -28.6 & \chi_{bb}^{\text{calc}} = -29.8 & \chi_{cc}^{\text{calc}} = -36.7 \\ \chi_{aa}^{\text{exp}} = -28.3(5) & \chi_{bb}^{\text{exp}} = -30.9(6) & \chi_{cc}^{\text{exp}} = -36.7(8) \end{array}$$

## Chapter XII

# INTERNAL MOTIONS

---

1	INTRODUCTION	570
2	POTENTIAL FUNCTION FOR INTERNAL ROTATION	572
3	TORSIONAL ENERGY LEVELS	574
4	HAMILTONIAN FOR INTERNAL AND OVERALL ROTATION	581
5	HIGH-BARRIER APPROXIMATION	585
6	HIGH-BARRIER ASYMMETRIC ROTORS	591
	Energy Levels and Spectra of the Pseudorigid Rotor	591
	Higher-order Effects	593
	Rotational Spectra of the Ground Torsional State	598
	Rotational Spectra in Excited Torsional States: $V_6$ Effects	600
	Stark Effect	603
	Example of a Barrier Calculation	605
7	HIGH-BARRIER SYMMETRIC ROTORS	606
8	LOW-BARRIER APPROXIMATION	607
	Energy Levels and Spectra: Free Rotation	609
	Energy Levels and Spectra: Hindered Rotation with a Low Sixfold Barrier	612
9	OTHER METHODS FOR EVALUATION OF BARRIER HEIGHTS	617
	Method Based on Satellite Frequency Pattern	617
	Relative Intensity Method	618
	Avoided-Crossing Method	620
10	MOLECULES HAVING TWO INTERNAL ROTORS WITH $C_{3v}$ SYMMETRY: TWO-TOP MOLECULES	621
11	MOLECULES HAVING INTERNAL ASYMMETRIC-TOP ROTORS: TWO-FOLD BARRIERS	622
12	SOME OBSERVED PROPERTIES OF MOLECULES THAT UNDERGO INTERNAL ROTATION	623
	Barrier Heights	623
	Methyl Group Tilt	625
		569

13	ROTATIONAL ISOMERISM AND RING CONFORMATIONS	627
	Examples of Rotational Isomers	630
	Application of Low-resolution Spectroscopy	633
	Effects of Intramolecular Hydrogen Bonding on Conformation	635
14	RING-PUCKERING VIBRATIONS	636
15	HINDERED PSEUDOROTATION	639

## 1 INTRODUCTION

In this chapter we consider hindered internal motions essentially of large amplitude, such as internal rotation and ring puckering, which may be effectively separated from the other vibrational modes. Inversion motion considered in Chapter VI is another example of large amplitude motion. Numerous threefold barriers to internal rotation for molecules with methyl groups have been evaluated from a study of the microwave spectrum. For molecules with asymmetric tops, the most stable conformations have been obtained, and in certain cases, the potential function governing interconversion. Similarly for ring compounds, a microwave study provides the preferred conformations. In the case of certain small rings, the conformation and the ring puckering potential function have been evaluated. Studies of potential functions, barrier heights, stability of rotational isomers and ring conformations all provide basic information for testing and improving predictive methods and for understanding the origin of barriers and the forces responsible for conformational preference.

The most active of these areas in microwave spectroscopy is the study of internal rotation. The phenomenon of internal rotation has for many years been a subject of considerable interest to both chemists and physicists. For molecules which consist of two groups connected by a single bond, the groups can rotate with respect to one another about the single bond. In ethane,  $\text{H}_3\text{C}-\text{CH}_3$ , one  $\text{CH}_3$  group rotates with respect to the other about the C—C bond. If the barrier were very high, the internal motion of the methyl groups about the C—C bond would correspond to simple harmonic torsional oscillation, whereas if the barrier were very low the internal motion would be essentially free rotation about the C—C bond. For a long time, this rotation about a single bond was believed to be completely free because it had been impossible to separate any isomers which could arise from different orientations of one part of the molecule relative to the other. In contrast, for two groups connected by a double bond, the relative rotation of the two groups requires uncoupling of the  $\pi$ -electrons and is expected to be very difficult. This is reflected in the fact that stable isomers can be isolated, for example, *cis*- and *trans*-1, 2 dichloroethylene.

In 1936 Kemp and Pitzer [1] concluded, on the basis of thermodynamic evidence, that the relative rotation of the two methyl groups in ethane is not entirely free but is restricted by a potential barrier. In Fig. 12.1 are shown the

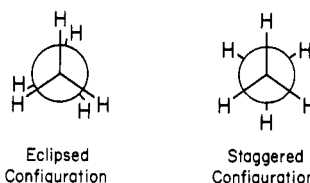


Fig. 12.1 Newman projection formulas for ethane.

configurations of ethane where the two methyl groups are in an eclipsed and staggered position relative to each other. Within one complete revolution there are three equivalent staggered and eclipsed configurations. The staggered configuration turns out to be the one of minimum energy [2] while the eclipsed configuration corresponds to an energy maximum. In the transition from a staggered to an eclipsed conformation an energy barrier of about 3000 cal/mole [3] has to be surmounted. Soon after the work of Kemp and Pitzer it became apparent that rotation about single bonds is restricted in many molecules, although the barriers (on the order of a few thousand calories) are not large enough to permit chemical isolation.

For over 30 years the method of microwave spectroscopy has been employed to study the problem of hindered internal rotation. It has the great advantage that potential barriers can be obtained with an accuracy of 5% or better and that other important information is obtainable, such as the structural parameters and the equilibrium configuration of the methyl group. It is applicable to polar molecules with barriers ranging from several calories/mole to about 4000 cal/mole. In most of the remaining part of this chapter a quantitative study of the effects of internal rotation on the rotational spectrum of a molecule will be considered. In short, the effect of internal rotation on the rotational spectrum is that each rotational transition will exhibit a fine structure caused by the interaction of internal and overall rotation. This fine structure depends on the height of the potential barrier hindering internal rotation. Analysis of this fine structure with the high resolution and accurate measurements of microwave spectroscopy leads to the evaluation of the potential barrier.

A typical spectrum is illustrated in Fig. 12.2 which shows the main features of the  $J=2 \rightarrow 3$  spectrum of thioacetaldehyde,  $\text{CH}_3\text{CHS}$  [4]. Thioacetaldehyde is a near-prolate asymmetric rotor. The lines are doublets made up of *A* and *E* components. The ground state  $K_{-1}=0, 1$ , and 2 lines are split by approximately 0.7, 4, and 7 MHz, respectively. Strong satellite lines with larger splittings are also observed. The *A* torsional state lines were fit as a usual semirigid rotor (rigid rotor plus distortion effects) and the barrier height was then varied such that the observed splitting between *A* and *E* components for each line was obtained. This gave a barrier,  $V_3 = 1572 \pm 30$  cal/mole.

For a general discussion of the field of internal rotation in molecules the reader is directed to books by Mizushima [5] and Orville-Thomas [6]. Since the initial derivation of the potential barrier of methyl alcohol by Burkhard and Dennison [7], considerable progress has been made in the application of

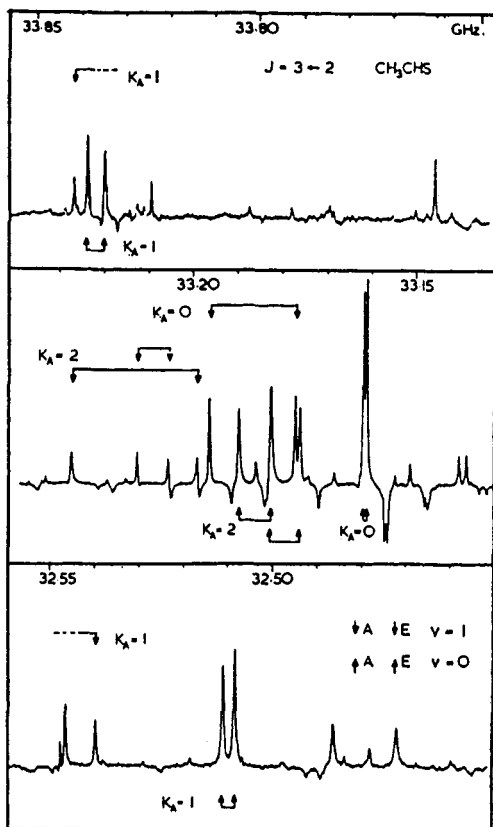


**Fig. 12.2** The  $J = 3 \leftarrow 2$  transitions of  $\text{CH}_3\text{CHS}$  under moderate resolution. The  $K_A = 1$  E torsional satellites are subject to large shifts of the order of 400 MHz and are not shown in the traces. From Kroto and Landsberg [4].

microwave spectroscopy to the elucidation of potential barriers. An excellent review article on the theory and application of microwave spectroscopy to the problem of internal rotation has been given by Lin and Swalen [8], by Dreizler [9], and most recently by Lister et al. [10].

## 2 POTENTIAL FUNCTION FOR INTERNAL ROTATION

The internal rotation of two parts of a molecule relative to each other can be described by the angle  $\alpha$ , called the angle of internal rotation or the torsional angle. For example, in ethane the torsional angle may be taken as the angle between two planes: one defined by the C-C bond and a specifically chosen C-H bond of one  $\text{CH}_3$  group, and the other plane defined by the C-C bond and a C-H bond of the other  $\text{CH}_3$  group. As the two parts rotate relative to one another, the potential energy will vary as a function of  $\alpha$ . In molecules such as  $\text{CH}_3-\text{CH}_3$  or  $\text{CH}_3-\text{CF}_3$ , there are three equivalent positions into which

one methyl group can rotate relative to the other group. The same is true for  $\text{CH}_3\text{—CHO}$ , whereas for  $\text{CH}_3\text{—NO}_2$  there are six such equivalent positions, and for  $\text{CH}_2=\text{CH}_2$  there are two. The number of equivalent configurations  $N$  for a complete internal revolution is obviously dependent on the symmetry of the molecule. It is natural to require that the potential function be a periodic function in  $\alpha$ , which repeats itself  $N$  times in the interval  $\alpha=0$  to  $\alpha=2\pi$ . Such a periodic function may be represented by a Fourier series expansion. If the potential is taken as an even function of  $\alpha$ , a periodic potential function, with period  $2\pi/N$ , can be expressed in the form:

$$V(\alpha) = a_0 + \sum_{k=1}^{\infty} a_k \cos k N \alpha \quad (12.1)$$

where with

$$a_0 = - \sum_{k=1}^{\infty} a_k \quad (12.2)$$

$V(\alpha)$  is zero at  $\alpha=0, \pm 2\pi/N, \pm 4\pi/N$ , and soon. This potential function for a barrier with  $N$ -fold symmetry may be written as:

$$V(\alpha) = \frac{V_N}{2} (1 - \cos N\alpha) + \frac{V_{2N}}{2} (1 - \cos 2N\alpha) + \dots \quad (12.3)$$

We will at first be concerned with molecules having a threefold barrier, which have been extensively studied; we shall consider sixfold barriers in Section 8. For a threefold barrier one would have

$$V(\alpha) = \frac{V_3}{2} (1 - \cos 3\alpha) + \frac{V_6}{2} (1 - \cos 6\alpha) + \dots \quad (12.4)$$

Usually only the first term of the cosine expansion is retained:

$$V(\alpha) = \frac{V_3}{2} (1 - \cos 3\alpha) \quad (12.5)$$

The sinusoidal shape of this periodic hindering potential is depicted in Fig. 12.3.

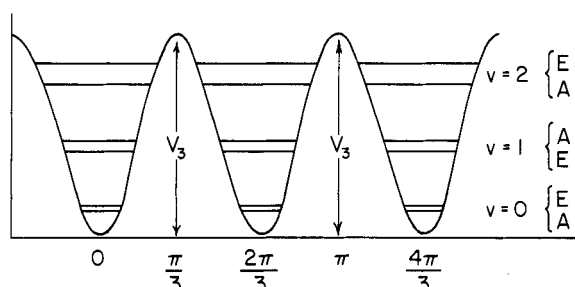


Fig. 12.3 Schematic representation of the potential function and torsional energy levels. A simple cosine potential is depicted with three identical minima and maxima. Each torsional energy level is labeled by the torsional quantum number  $v$ . The torsional sublevels are denoted by their symmetry  $A$  or  $E$  under the  $C_3$  group.

This has a minimum value of zero at  $\alpha=0, \pm 2\pi/3, \pm 4\pi/3, \dots$ , and a maximum value of  $V_3$  at  $\alpha=\pm\pi/3, \pm\pi, \pm 5\pi/3, \dots$ . This simple potential function has proved to be a rather accurate representation of the actual potential, because in many cases the higher terms in the expansion are very small. Investigation of some threefold-barrier molecules has, in fact, indicated that the  $V_6$  term is much smaller than  $V_3$  [11–14], usually less than 3% of  $V_3$ . This is further suggested from results on molecules such as  $\text{CH}_3\text{NO}_2$  where  $V_6$  is the leading term of the expansion and has been found to be very small (6 cal/mole, see Sections 6 and 8).

### 3 TORSIONAL ENERGY LEVELS

If the variation of the potential energy with respect to  $\alpha$  is taken as given in (12.5), the wave equation for the internal rotation is

$$-F \frac{d^2 U(\alpha)}{d\alpha^2} + \left[ \frac{V_3}{2} (1 - \cos 3\alpha) - E \right] U(\alpha) = 0 \quad (12.6)$$

where in this one-dimensional Schrödinger equation,  $\alpha$  is the angle of internal rotation,  $V_3$  is the height of the barrier having threefold symmetry which hinders the internal rotation, and  $F = \hbar^2/2I$ , with  $I$ , the reduced moment of inertia for the relative motion of the two groups. Solution of this differential equation yields the torsional eigenvalues  $E$  and eigenfunctions  $U(\alpha)$ .

For the case of two symmetrical coaxial tops, such as  $\text{CH}_3-\text{CH}_3$  or  $\text{CH}_3-\text{CF}_3$ , the reduced moment for internal rotation is

$$I_r = \frac{I_\alpha I_\beta}{I_\alpha + I_\beta} \quad (12.7)$$

where  $I_\alpha$  and  $I_\beta$  are the moments of inertia of the two tops about the axis of internal rotation. The expression for the reduced moment of inertia of more complex cases is given in the next section.

In examination of the torsional energy levels it is helpful to consider first two extremes,  $V_3$  very small and  $V_3$  very large. For a very small barrier such that  $V_3 \rightarrow 0$  (free rotation), (12.6) reduces to:

$$\frac{d^2 U(\alpha)}{d\alpha^2} + \left( \frac{1}{F} \right) E U(\alpha) = 0 \quad (12.8)$$

This has the form of a spatial rotator with fixed axis of rotation. The solution is

$$U(\alpha) = A e^{im\alpha} = A (\cos m\alpha + i \sin m\alpha) \quad (12.9)$$

with  $A$  an appropriate normalization factor and with the energy given by

$$E = Fm^2 \quad (12.10)$$

For the function (12.9) to be well behaved, it must satisfy the appropriate boundary condition. Applying the boundary condition

$$U(\alpha) = U(\alpha + 2\pi)$$

we see from (12.9) that  $m$  is required to take on the values

$$m=0, \pm 1, \pm 2, \pm 3, \dots$$

The constant  $A$  may be evaluated from the normalization condition giving  $A=1/2^{1/2}\pi$ . The free rotor states, specified by the quantum number  $m$ , are doubly degenerate except for the state  $m=0$ . The functions of (12.9) are also eigenfunctions of the angular momentum operator  $p=-i\hbar(\partial/\partial\alpha)$ , the eigenvalues of  $p$  being  $m\hbar$ . For the state  $m$  the two possible values of  $p$ , namely  $|m|\hbar$  and  $-|m|\hbar$ , correspond to the two possible directions of internal rotation.

In the case of a very high barrier,  $V_3 \rightarrow \infty$ , the internal motions will be restricted to small oscillations, torsional oscillations, about the minima of the barrier. The cosine function in (12.6) may be expanded for small values of  $\alpha$  as:

$$\cos 3\alpha = 1 - (\frac{9}{2})\alpha^2 + (\frac{27}{8})\alpha^4 + \dots \quad (12.11)$$

and thus:

$$V(\alpha) = (\frac{9}{4})V_3\alpha^2 - (\frac{27}{16})V_3\alpha^4 + \dots \quad (12.12)$$

For a harmonic approximation we retain only the first term of the expansion. With this potential, the torsional wave equation reduces to:

$$\frac{d^2 U(\alpha)}{d\alpha^2} + \frac{1}{F} [E - \frac{1}{2}(\frac{9}{2}V_3)\alpha^2] U(\alpha) = 0 \quad (12.13)$$

which has the same form as the simple harmonic oscillator wave equation. The solutions are well behaved if

$$E = 3(V_3 F)^{1/2}(v + \frac{1}{2}) \quad (12.14)$$

with

$$v = 0, 1, 2, 3, \dots$$

The torsional energy levels thus approximate those of a harmonic oscillator. The frequency of torsional oscillation,

$$\nu = \frac{3}{2\pi} \left( \frac{V_3}{2I_r} \right)^{1/2}$$

is related to the barrier, and this relationship provides the basis for determination of the barrier by infrared studies or microwave intensity studies.

In the limit of an infinite barrier each torsional state  $v$  is threefold degenerate since the internal motion is torsional oscillation in any one of the three equivalent potential wells. For a finite barrier, the quantum-mechanical tunneling effect leads to a splitting of this threefold degeneracy because the probability of tunneling through the barrier is now finite since  $V_3$  is finite. This is purely a quantum effect since classically if  $V_3 > E$  there is no possibility of passage from one potential well to another because the system does not have enough energy to surmount the barrier. Quantum mechanically, however, the molecule may pass from one configuration to another by tunneling through the barrier since

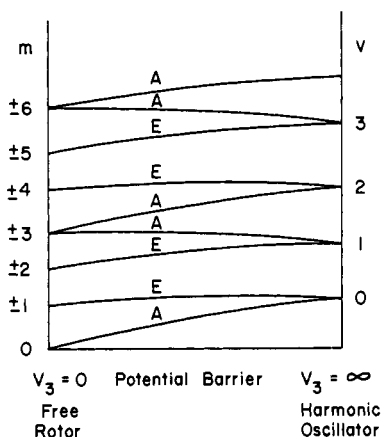


**Fig. 12.4** Correlation between the energy levels of free internal rotation specified by the quantum numbers  $m$ , and those for harmonic torsional oscillation which are labeled by the quantum numbers  $v$ . For barriers between the two extremes some of the degeneracy of the two limiting cases is removed. The degeneracy of the torsional sublevels is indicated by  $A$  and  $E$ , the  $E$  levels being doubly degenerate whereas the  $A$  levels are nondegenerate.

the wave functions extend through the classically forbidden regions. The tunneling rate depends on both height and width of the barrier. The effect of tunneling through the potential barrier is to split the triply degenerate torsional level  $v$  into two levels, a nondegenerate level designated as an  $A$  level and a doubly degenerate level designated as an  $E$  level. The connections between the harmonic oscillator limit and the free rotor limit are shown schematically in Fig. 12.4. That each triply degenerate level of the harmonic oscillator limit is split into two levels is apparent. For the free-rotor states, with  $m$  a multiple of three, the  $\pm m$  degeneracy is removed. For the other values of  $m$  this degeneracy remains. The symmetry of the torsional energy levels (the  $A$  and  $E$  designations) will be considered later.

In Fig. 12.3 the internal rotational energy levels are shown superimposed on the potential curve. Note that the torsional sublevel spacing increases as the torsional energy increases, that is, as  $v$  increases. The greater the sublevel splitting, the faster the rate of tunneling. Near the bottom of the well the energy levels approximate those of a harmonic oscillator. When the torsional energy  $E$  is greater than the barrier height  $V_3$ , the energy levels go over to those of a free rotor.

The qualitative aspects of the torsional energy levels have been presented, but quantitative discussion for intermediate values of the barrier height requires consideration of the solutions of the original torsional wave equation, (12.6). A knowledge of the torsional eigenfunctions and eigenvalues is useful for the evaluation of various perturbation sums that arise in the perturbation treatment of internal rotation, which will be described subsequently.

Because of the choice of the potential function, (12.6) can be transformed to

Mathieu's equation by the substitutions:

$$\begin{aligned} U(\alpha) &= M(x) & 3\alpha + \pi &= 2x \\ E &= (\frac{9}{4})Fb & V_3 &= (\frac{9}{4})Fs \end{aligned} \quad (12.15)$$

giving

$$\frac{d^2 M(x)}{dx^2} + (b - s \cos^2 x) M(x) = 0 \quad (12.16)$$

where  $b$  is an eigenvalue,  $s$  is a parameter termed the reduced barrier height, and  $M(x)$  a Mathieu function.

The eigenfunctions  $U(\alpha)$  of interest must satisfy the boundary condition  $U(\alpha) = U(\alpha + 2\pi)$  or for the Mathieu functions,  $M(x) = M(x + 3\pi)$ . The Mathieu functions which meet this boundary condition are those with period  $\pi$  in  $x$  (period  $2\pi/3$  in  $\alpha$ ) and period  $3\pi$  in  $x$  (period  $2\pi$  in  $\alpha$ ). The eigenvalues and eigenfunctions of the torsional wave equation can hence be obtained from existing tables [15-19] on periodic Mathieu functions with the aid of (12.15). The solutions with period  $\pi$  are associated with nondegenerate eigenvalues while those of period  $3\pi$  are associated with doubly degenerate eigenvalues. For distinction between the eigenvalues ( $E_{v\sigma}$  or  $b_{v\sigma}$ ) and the wave functions, the labels  $v$  and  $\sigma$  are introduced. The series of degenerate and nondegenerate solutions obtained are ordered in terms of increasing size. The lowest degenerate and nondegenerate eigenvalues are then labeled by  $v=0$ . The next lowest degenerate and nondegenerate eigenvalues are labeled by the index  $v=1$  and so on. For a high barrier, the degenerate and nondegenerate states corresponding to a given  $v$  have nearly the same energy, whereas those of different  $v$  are more widely separated. The degenerate and nondegenerate energy levels associated with a given  $v$  are regarded as the torsional sublevels. As  $V_3 \rightarrow \infty$ , the different energies of the torsional sublevels coalesce, and  $v$  becomes the quantum number for the limiting harmonic oscillator state. The usefulness of the label  $v$  is thus readily apparent; it is called the principal torsional quantum number. The index  $\sigma=0, \pm 1$ , which gives the symmetry or periodicity of the torsional wave functions, serves to distinguish the torsional sublevels. The  $\sigma=0$  levels are the nondegenerate  $A$  levels, and the  $\sigma=\pm 1$  are the degenerate  $E$  levels. Appropriate solution of the torsional wave equation, therefore, leads to a set of torsional levels  $v$ , each of which is split into two sublevels with one nondegenerate and the other twofold degenerate.

A periodic solution of (12.6) or (12.16) may be represented by a Fourier expansion. A solution of the torsional equation, for example, can be written in the following convenient form

$$U_{v\sigma}(\alpha) = \sum_{k=-\infty}^{\infty} A_k^{(v)} e^{i(3k+\sigma)\alpha} \quad (12.17)$$

where  $\sigma$  is an integer. For the appropriate periodic solutions of a threefold barrier  $\sigma$  takes on the three values  $-1, 0$ , and  $+1$ . As mentioned previously, the index  $\sigma$  gives the symmetry of the torsional wave functions. The torsional

**Table 12.1** Character Table for the Group  $C_3^a$

Symmetry Species	$E$	$C_3$	$C_3^2$
$A$	1	1	1
$E$	$E_1$	1	$\varepsilon$
	$E_2$	1	$\varepsilon^*$

<sup>a</sup>Here  $\varepsilon = \exp(i2\pi/3)$  where  $\varepsilon^*$  designates the complex conjugate and  $\varepsilon\varepsilon^* = 1$ ,  $(\varepsilon)^2 = \varepsilon^*$ ,  $(\varepsilon^*)^2 = \varepsilon$ .

functions may be conveniently classified under the rotational subgroup  $C_3$  of the torsional Hamiltonian. The character table of this group is given in Table 12.1. For classification according to the symmetry species of the group, it is necessary to know how the functions, (12.17), transform under the symmetry operations  $C_3$  and  $C_3^2$ . The operations  $C_3$  and  $C_3^2$  on  $U_{v\sigma}(\alpha)$  will affect only the angle  $\alpha$ , transforming it in the following manner— $C_3: \alpha \rightarrow \alpha + 2\pi/3$ ;  $C_3^2: \alpha \rightarrow \alpha + 4\pi/3 = \alpha - 2\pi/3$ . The identity operation, of course, leaves the function unchanged; the effects of the remaining operations on  $U_{v\sigma}(\alpha)$  are

$$\begin{aligned} C_3: U_{v\sigma}(\alpha) &\rightarrow \varepsilon^\sigma U_{v\sigma}(\alpha) \\ C_3^2: U_{v\sigma}(\alpha) &\rightarrow (\varepsilon^*)^\sigma U_{v\sigma}(\alpha) \end{aligned}$$

From the foregoing relations and the character table, it is evident that the  $U_{v\sigma}$  with  $\sigma = 0$  belong to the nondegenerate species  $A$  and give rise to the non-degenerate eigenvalues. The functions with  $\sigma = +1$  belong to one part of the doubly degenerate  $E$  species, viz.,  $E_1$ ; those with  $\sigma = -1$  belong to the other part,  $E_2$ , and they give rise to the pairs of degenerate eigenvalues.

Some insight into the nature of the  $A(\sigma = 1)$  and  $E(\sigma = \pm 1)$  internal torsional states may be obtained from the following considerations. The internal motion for the  $A$  states [ $U(\alpha)$  periodic in  $2\pi/3$ ] resembles a back-and-fourth oscillation localized in the potential wells. For these states the  $\pm m$  degeneracy of the free-rotor states is removed (see Fig. 12.4). The internal motion of the  $E$  states [ $U(\alpha)$  periodic in  $2\pi$ ] has some of the character of free rotation passing from one potential well to another by tunneling, the  $\pm m$  degeneracy of the free rotor which remains for the  $E$  states being related to the two possible directions of internal rotation.

In general, for a molecule with  $N$  equivalent internal configurations the appropriate periodic solutions [17, 18]

$$U_{v\sigma}(\alpha) = e^{i\sigma\alpha} \sum_{k=-\infty}^{\infty} A_k^{(v)} e^{iNk\alpha} \quad (12.18)$$

are obtained by choice of  $N$  integer values of  $\sigma$ , such that  $-N/2 < \sigma \leq N/2$

with  $\sigma \neq -N/2$  for  $N$  even. Except for  $\sigma = 0$  or  $\sigma = N/2$  ( $N$  even) which give nondegenerate solutions, the remaining values of  $\sigma$  give pairs of degenerate solutions corresponding to  $\pm\sigma$ . The number of distinct eigenvalues for any  $v$  are  $(N+2)/2$  for  $N$  even and  $(N+1)/2$  for  $N$  odd. In the limit  $V_N \rightarrow \infty$  the sublevels coalesce, leading to an  $N$ -fold degeneracy. For finite barriers the  $N$ -fold degeneracy is lifted by the effect of tunneling.

Explicit solutions of (12.6) or (12.16) can be obtained by numerical iterative techniques similar to those employed in the determination of the eigenvalues of a rigid rotor (see Appendix B). Substitution of the expansion equation (12.17) into (12.6) and subsequent multiplication by  $e^{-i(3k+\sigma)\alpha}$  and integration from 0 to  $2\pi$  gives

$$A_{k-1} + (\lambda - M_k) A_k + A_{k+1} = 0 \quad (12.19)$$

where

$$\begin{aligned} M_k &= \frac{4F}{V_3} (3k + \sigma)^2 = \left(\frac{16}{9s}\right) (3k + \sigma)^2 \\ \lambda &= 4 \left(\frac{E}{V_3} - \frac{1}{2}\right) = \left(\frac{4}{s}\right) \left(b - \frac{s}{2}\right) \end{aligned}$$

and

$$k = 0, \pm 1, \pm 2, \pm 3, \dots$$

Here the  $v$  labeling of the Fourier expansion coefficients has for the present been omitted, and the substitution of  $\cos 3\alpha = (e^{i3\alpha} + e^{-i3\alpha})/2$  and the fact that  $\int_0^{2\pi} e^{i(k-k')\alpha} d\alpha = 0$ , unless  $k = k'$  with  $k$  and integer, have been used for derivation of Eq. (12.19). If this infinite set of linear homogeneous equations is to have a nontrivial solution for the  $A$ 's, the determinant of the coefficients must vanish. The infinite order determinantal equation has the form:

$$\begin{vmatrix} M_{k-1} - \lambda & -1 & & & \\ -1 & M_k - \lambda & -1 & & \\ & -1 & M_{k+1} - \lambda & & \\ & & & \ddots & \\ & & & & \ddots \end{vmatrix} = 0 \quad (12.20)$$

There will be three separate determinants, one for each value of  $\sigma$ . However, it is apparent that the determinants corresponding to  $\pm\sigma$  have the same eigenvalues and thus constitute the degenerate  $E$  species solutions with  $U_{v,-1}(\alpha) = U_{v1}^*(\alpha)$ . The eigenvalues  $\lambda$ , and thus the torsional energies associated with a particular value of  $\sigma$ , may be conveniently obtained by solution of the appropriate determinant by the method of continued fractions [8, 17-20]. Once the eigenvalues are known, the Fourier coefficients of the expansion

can be determined by means of the recursion relations between the  $A$ 's, (12.19). Solving these relations and making use of the normalization requirement,  $\int_0^{2\pi} U^*(\alpha)U(\alpha) d\alpha = 1$ , or  $2\pi \sum A_k^2 = 1$ , one obtains the torsional eigenfunctions. Both the eigenvalues and the expansion coefficients depend on the reduced barrier height  $s$ . Since the values of  $k$  are not bounded, a truncated Fourier expansion which leads to a determinant of finite size must be used if the problem is to be mathematically tractable. The number of terms to be retained in the Fourier expansion is dictated by the accuracy desired in the eigenvalues and eigenfunctions.

In the limit of free rotation only one of the Fourier coefficients will be non-vanishing and

$$U_{v\sigma}(\alpha) = \frac{1}{\sqrt{2\pi}} e^{i(3k+\sigma)\alpha} \quad (12.21)$$

while the eigenvalues are given by the diagonal elements of (12.20):

$$E_{v\sigma} = F(3k + \sigma)^2 \quad (12.22)$$

Since  $(3k + \sigma)$  can have any integral value, a comparison of (12.22) with (12.10) reveals that  $m = \sigma$ , modulo 3 (see Fig. 12.4). In the high barrier limit the energies are those of a harmonic oscillator and are given by (12.14) as

$$E_v = 3(V_3 F)^{1/2}(v + \frac{1}{2})$$

The energies are independent of  $\sigma$  and hence are threefold degenerate. Each torsional function is a linear combination of three harmonic oscillator functions, each centered about one of the potential minima [8]

$$U_{v0}(\alpha) = \frac{1}{\sqrt{3}} [H_v^{(1)} + H_v^{(2)} + H_v^{(3)}] \quad (12.23)$$

$$U_{v1}(\alpha) = \frac{1}{\sqrt{3}} [H_v^{(1)} + \varepsilon H_v^{(2)} + \varepsilon^2 H_v^{(3)}] \quad (12.24)$$

$$U_{v,-1}(\alpha) = \frac{1}{\sqrt{3}} [H_v^{(1)} + \varepsilon^2 H_v^{(2)} + \varepsilon H_v^{(3)}] \quad (12.25)$$

where  $\varepsilon = \exp(i2\pi/3)$  and where  $H_v^{(1)}$ ,  $H_v^{(2)}$ , and  $H_v^{(3)}$  are harmonic oscillator functions centered, respectively, about 0,  $2\pi/3$ , and  $4\pi/3$ .

Fortunately, the detailed calculations outlined here are usually not necessary because the required perturbation sums, which can be obtained from a knowledge of the torsional eigenfunctions and eigenvalues, have been tabulated for various values of  $s$ , and interpolation of these tables is sufficiently accurate for barrier determinations.

Up to this point we have been concerned with the torsional energy levels for a molecule undergoing hindered internal rotation. However, besides these levels, there is a set of energy levels arising from the overall rotation of the entire molecule which will be associated with each of the torsional sublevels. The interaction between overall and internal rotation provides the major

mechanism (for asymmetric rotors) by which the splittings of the internal torsional levels are transmitted to the rotational spectrum. Since it turns out that the coupling effect differs for the two torsional sublevels, a given rotational transition associated with the *A* and *E* sublevels of a particular torsional state *v* will appear as a doublet rather than a single line. This doublet separation is a sensitive function of the barrier height, and it is from these splittings that the barrier height may be determined.

The ensuing discussion will be concerned with the derivation of the Hamiltonian that describes a molecule undergoing both internal and overall rotation. From this Hamiltonian, a quantitative discussion of the effects of internal rotation on the rotational spectrum can be made.

#### 4 HAMILTONIAN FOR INTERNAL AND OVERALL ROTATION

The formulation of the internal rotation problem follows the usual procedure which first requires choice of a molecular model from which the classical kinetic and potential energies are developed and subsequently the classical Hamiltonian. The transition to the quantum-mechanical Hamiltonian is then usually accomplished in a straightforward way.

The model chosen for the problem of internal rotation is comprised of a rigid symmetric top (e.g., a CH<sub>3</sub> group) attached to a rigid frame, which may or may not be asymmetric. The two rigid parts rotate about the bond connecting them. The symmetric top (CH<sub>3</sub>) is regarded as rotating with respect to the other part which is taken as the framework. The other modes of internal vibration are ignored. This separation of the internal rotation from the remaining (3*N* - 6 - 1) modes of vibration has proved to be a satisfactory approximation for most of the molecules investigated. The separation is expected to be valid if the torsional frequency is not close to any of the other vibrational frequencies. The entire molecule made up of symmetric top and framework is also rotating and translating in space. The translational motion may be readily separated, and there are then four degrees of freedom—three for overall rotation, which may be described by the three Eulerian angles  $\theta$ ,  $\phi$ ,  $\chi$  of the framework; and one for hindered rotation of the two groups, which is described by the relative angle  $\alpha$  between the two groups.

Two methods of approach have been used to handle the problem of internal rotation. These methods differ in choice of coordinate system, and each leads to a somewhat different mathematical formalism. The method introduced by Wilson [21] and Crawford [22] uses the principal axes of the whole molecule as the coordinate system. The axis of the internal rotation coincides with the symmetry axis of the top, but this axis may not be coincident with any one of the principal axes. The terms in the Hamiltonian which describe the interaction between internal and overall rotation are treated by perturbation theory. The boundary condition of invariance under  $\alpha \rightarrow \alpha + 2\pi$  applied to the total wave function requires that  $U(\alpha) = U(\alpha + 2\pi)$ , as applied previously. Physically, this

implies that when the original configuration of the system is restored, the wave function describing the system must take on its initial value, that is, be single-valued. This leads to torsional eigenfunctions corresponding to periodic Mathieu functions which have been tabulated. This method is commonly referred to as the principal-axis method (PAM).

An alternate method developed by Nielsen [23] and Dennison et al. [7, 24–26] uses a coordinate system in which the symmetry axis of the top is chosen as one of the coordinate axes. The other two axes are fixed with respect to the framework, and their orientation may be judiciously chosen. One or more coordinate transformations are employed to eliminate or minimize the rotation-torsion coupling; the interactions are then more readily treated by perturbation theory. Some complications, however, arise because the coordinate system chosen is, in general, not a principal axis system and the products of inertia do not vanish. Also the boundary condition of invariance now requires nonperiodic Mathieu functions which have not been tabulated. This method is usually referred to as the internal-axis method (IAM).

In many cases either method is equally applicable, but for slightly asymmetric molecules with light frames, such as methyl alcohol, the internal axis method is to be preferred. The review article by Lin and Swalen [8] discusses these two methods of approach in detail. We shall limit consideration to the principal axis method by which a large class of molecules can be handled. One advantage of the principal axis method is that the necessary perturbation sums have been extensively tabulated; hence analysis of the spectra can be carried out by use of these tables and those developed for rigid rotor molecules. Only the theory for molecules with one internal rotor which is a symmetric top will be treated in detail. Two-top molecules are discussed briefly in Section 10.

For the model of a rigid symmetric top attached to a rigid asymmetric framework (an asymmetric molecule), the principal-axis method uses a coordinate system  $x$ ,  $y$ ,  $z$  rigidly attached to the framework, the origin of which is located at the center of mass of the molecule and the orientation of which coincides with that of the principal axes of the entire molecule. The model is

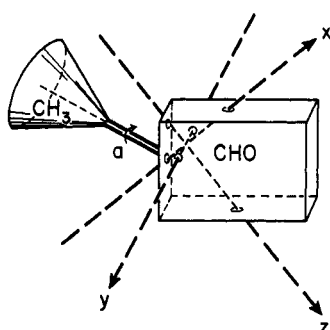


Fig. 12.5 Model used to treat overall and internal rotation.

illustrated in Fig. 12.5. The products of inertia therefore vanish since the coordinate axes are principal axes. Because of the cylindrical symmetry of the top, the principal axes of the molecule are not altered by the rotation of the top relative to the frame, and the moments of inertia of the entire molecule are constants independent of the angle of internal rotation. The moments of inertia, however, would not be independent of  $\alpha$  if the internal rotor were not a symmetric top, for example,  $\text{CH}_2\text{DCHO}$ . One of the first molecules whose microwave spectrum was analyzed by means of the PAM is acetaldehyde, studied by Kilb et al. [27].

With the system of coordinates described above, the kinetic energy for a general type of asymmetric molecule (no symmetry apart from that of the  $\text{CH}_3$  group) can be written as [22]:

$$T = \frac{1}{2} \sum_g I_g \omega_g^2 + \frac{1}{2} I_\alpha \dot{\alpha}^2 + I_\alpha \dot{\alpha} \sum_g \lambda_g \omega_g \quad (g=x, y, z) \quad (12.26)$$

where  $I_g$  are the principal moments of inertia of the entire molecule,  $I_\alpha$  is the moment of inertia of the top about its symmetry axis,  $\omega_g$  are components along the principal axes of the angular velocity of the framework,  $\dot{\alpha}$  is the angular velocity of the top relative to the framework, and  $\lambda_g$  are direction cosines between the symmetry axis of the top and the principal axes of the entire molecule. The first term in the kinetic energy expression represents the energy of overall rotation of the molecule. The second term is the kinetic energy of internal rotation of the top, and the last term represents the coupling between internal and external rotation.

To obtain the Hamiltonian we re-express the kinetic energy as a function of the angular momenta. The angular momenta are defined classically by the relations:

$$P_g = \frac{\partial T}{\partial \omega_g} = I_g \omega_g + \lambda_g I_\alpha \dot{\alpha} \quad (12.27)$$

$$p = \frac{\partial T}{\partial \dot{\alpha}} = I_\alpha \dot{\alpha} + I_\alpha \sum_g \lambda_g \omega_g \quad (12.28)$$

From these relations it is evident that the components  $P_g$  of the total angular momentum of the molecule contain a contribution from the internal rotation of the top, whereas  $p$ , the total angular momentum of the internal rotor, contains contributions from both internal ( $I_\alpha \dot{\alpha}$ ) and overall rotation. Employing (12.27) and the expression for the kinetic energy, (12.26), we may write

$$2T - \sum \frac{P_g^2}{I_g} = r I_\alpha \dot{\alpha}^2 \quad (12.29)$$

The coefficient  $r I_\alpha$  is interpreted as the reduced moment of inertia for internal rotation of the two rigid parts of the molecule with  $r$  a reducing factor defined as

$$r = 1 - \sum_g \frac{\lambda_g^2 I_g}{I_\alpha} \quad (12.30)$$

For the case of two coaxial symmetric tops,  $rI_\alpha = I_z(I_z - I_\alpha)/I_z = I_z I_\beta/I_z$ , in which  $I_z$  is the total moment of inertia of the two tops about the symmetry axis. This is equivalent to the reduced moment expression given previously in (12.7). From (12.27) and (12.28) it is seen that

$$p - \mathcal{P} = rI_\alpha \dot{\alpha} \quad (12.31)$$

with

$$\mathcal{P} = \sum_g \rho_g P_g \quad \left( \rho_g = \frac{\lambda_g I_\alpha}{I_g} \right) \quad (12.32)$$

The quantity  $p - \mathcal{P}$  represents the relative angular momentum of the top and frame. By substituting (12.31) into (12.29), we obtain the kinetic energy in the following convenient form given by Herschbach [28]

$$T = \frac{1}{2} \sum_g \frac{P_g^2}{I_g} + \frac{1}{2} \frac{(p - \mathcal{P})^2}{rI_\alpha} \quad (12.33)$$

If the internal motion is frozen, that is,  $\dot{\alpha} = 0$ , then the relative angular momentum vanishes, and (12.33) or (12.29) yields the usual expression for the kinetic energy of a rigid rotor in terms of the total angular momentum components. In addition, the angular momenta would no longer include contributions from internal rotation.

Addition of the potential energy to the above kinetic energy expression gives the classical Hamiltonian. The coefficients appearing in (12.33) are constants; therefore the classical kinetic energy becomes a quantum mechanical operator if  $P_g$  and  $p$  are simply considered as operators. If the angular momentum is measured in units of  $\hbar$ , the Hamiltonian operator is expressed as

$$\mathcal{H} = \mathcal{H}_r + F(p - \mathcal{P})^2 + V(\alpha) \quad (12.34)$$

in which the potential energy restricting internal rotation is usually assumed to have the form given in (12.5). The  $\mathcal{H}_r$  is the usual rigid rotor Hamiltonian and  $F(-\frac{1}{2}\hbar^2/rI_\alpha)$  is the reduced rotational constant for internal rotation. The operator  $\mathcal{P}$ , a reduced angular momentum, is a linear combination of the  $P_g$  as defined by (12.32).

The commutation rules for the angular momenta  $P_g$  are the standard ones for components of the total angular momentum along the molecule-fixed axis [see (2.58)]. In addition, there is the commutation relation:

$$pP_g - P_gp = 0 \quad (g=x, y, z) \quad (12.35)$$

This follows from the fact that as a quantum mechanical operator [29]

$$p = -i \left( \frac{\partial}{\partial \alpha} \right)_{\theta, \phi, \chi} \quad (12.36)$$

whereas the corresponding operators for  $P_g$  involve the Eulerian angles  $\theta, \phi, \chi$  but not  $\alpha$ . Moreover, it follows from (12.35) that the operators  $p$  and  $\mathcal{P}$  commute with each other.

## 5 HIGH-BARRIER APPROXIMATION

The Hamiltonian, (12.34), can be divided into three parts as follows

$$\mathcal{H} = \mathcal{H}_R + \mathcal{H}_T + \mathcal{H}_{TR} \quad (12.37)$$

with

$$\mathcal{H}_R = \mathcal{H}_r + F \mathcal{P}^2 \quad (12.38)$$

$$\mathcal{H}_T = F p^2 + \frac{1}{2} V_3 (1 - \cos 3\alpha) \quad (12.39)$$

$$\mathcal{H}_{TR} = -2F \mathcal{P}p \quad (12.40)$$

where we shall write

$$\mathcal{H}_r = A_x P_x^2 + B_y P_y^2 + C_z P_z^2 \quad (12.41)$$

in which  $A_x = \hbar^2/2I_x$ , and so on. The terms  $\mathcal{H}_R$  and  $\mathcal{H}_T$  are, respectively, the rotational and torsional parts, and  $\mathcal{H}_{TR}$  represents the coupling between angular momenta of internal and overall rotation. The internal rotation or torsional Hamiltonian  $\mathcal{H}_T$  leads to Mathieu's differential equation and hence to eigenvalues and eigenfunctions discussed in Section 3. The term  $\mathcal{H}_R$  is simply a quadratic form in the total angular momentum. The term  $F \mathcal{P}^2$  in  $\mathcal{H}_R$  introduces terms of the type  $P_g P_{g'}$  and  $P_g^2$ . The latter terms can be absorbed into the usual rigid rotor expression ( $\mathcal{H}_r$ ) by a modification of the definition of the rigid-rotor rotational constants. As long as the coupling term  $\mathcal{H}_{TR}$  is ignored, the Hamiltonian is separable into torsional and rotational parts, and the internal rotation does not directly affect the rotational spectrum. This follows since  $\mathcal{H}_T$  is a function only of  $\alpha$  and is hence independent of the rotational quantum numbers, whereas  $\mathcal{H}_R$  is independent of the internal coordinate  $\alpha$  and therefore of the torsional quantum numbers. Inclusion of  $-2F \mathcal{P}p$  prevents the Hamiltonian from being separable, since this term depends on both sets of quantum numbers. For molecules with sufficiently large barriers, so that the separation of torsional levels of different  $v$  is large compared with the rotational levels, this coupling term can be conveniently treated as a perturbation.

For evaluation of the energy levels, the matrix formulation is employed in which the matrix of  $\mathcal{H}$  is constructed in a suitable representation. If the unperturbed Hamiltonian is taken as  $\mathcal{H}_R + \mathcal{H}_T$ , a convenient basis would be the product functions  $\psi_R \psi_T$ , with  $\psi_R$  a rotational eigenfunction of  $\mathcal{H}_R$  with energy  $E_R$  and  $\psi_T (\equiv U_{v\sigma})$  a torsional eigenfunction of  $\mathcal{H}_T$  with energy  $E_T (\equiv E_{v\sigma})$ . Here the set of rotational quantum numbers is represented by  $R$  and the set of torsional quantum numbers by  $T$ . In this basis both  $\mathcal{H}_R$  and  $\mathcal{H}_T$  are diagonal, but  $\mathcal{H}_{TR}$  contributes off-diagonal elements. In particular, for the functions  $U_{v\sigma}$  the operator  $p$  of  $\mathcal{H}_{TR}$  is diagonal in  $\sigma$  but has both diagonal and off-diagonal elements in the principal torsional quantum number  $v$  [30]. The infinite-order Hamiltonian matrix can be grouped into blocks corresponding to different  $v$ . Within each block are the matrix elements of  $\mathcal{H}$ , all of which are diagonal in  $v$  and  $\sigma$ , but not necessarily in  $R$ . Associated with each block corresponding to a given  $v$  there are different submatrices corresponding to the dif-

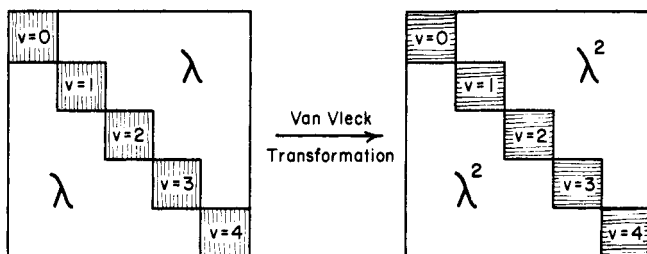


**Fig. 12.6** A portion of the energy matrix before and after the Van Vleck transformation. The blocks along the diagonal contain the matrix elements of internal and overall rotation, which are diagonal in the torsional quantum number  $T$ , in particular, in  $v$  and  $\sigma$ . The unshaded area contains the matrix elements connecting the rotational levels of the various torsional states  $v$ . After the transformation these elements are reduced to second order,  $\lambda^2$ , and corrections are introduced within each diagonal block. If the nondiagonal terms in  $v$  are now neglected, the transformed diagonal blocks can be diagonalized separately to give the rotational energy levels for each torsional state correct to second order in the separation of rotation and torsion.

ferent torsional sublevels. Blocks of different  $v$  are connected by matrix elements of  $\mathcal{H}_{TR}$ , the nondiagonal elements in  $v$  coming from the factor  $p$ . A portion of the energy matrix is illustrated in Fig. 12.6. To proceed with the solution further, we must attain some simplification of the matrix. To achieve approximate  $v$  diagonalization of this matrix we use a Van Vleck transformation [31, 32]. The effect of this transformation will be to reduce the off-diagonal matrix elements in  $v$  from  $\mathcal{H}_{TR}$  so that they may be neglected. With neglect of the reduced off-diagonal elements, the transformed matrix may be factored into smaller rotational submatrices, one for each torsional state (see Fig. 12.6). We are then left with the problem of diagonalizing smaller submatrices. The transformation has the effect of modifying the elements diagonal in  $v$  by folding the elements off-diagonal in  $v$  into the  $v$  blocks.

To second order, the matrix elements of  $\mathcal{H}$  within a  $T$  block, from Appendix C, will be replaced after the Van Vleck transformation by:

$$(R, T | \mathcal{H} | R' T') + \frac{1}{2} \sum'_{R'', T''} (R, T | \mathcal{H}' | R'', T'') (R'' T'' | \mathcal{H}' | R' T') \\ \times \left( \frac{1}{E_{RT}^0 - E_{R''T''}^0} + \frac{1}{E_{R'T'}^0 - E_{R''T''}^0} \right) \quad (12.42)$$

where  $E_{RT}^0 = E_R + E_T$  and  $\mathcal{H}'$  is the perturbation giving rise to nondiagonal elements in  $T$ . The term  $T'' = T$  is to be excluded from the sum over  $R''$  and  $T''$ . The perturbation term  $\mathcal{H}'$  is to be taken as  $\mathcal{H}_{TR} (= -2F\mathcal{P}p)$ . Since the perturbation is diagonal in  $\sigma$  and hence no degenerate or near-degenerate torsional states are connected, it is a good approximation, for reasonably high barriers, to neglect the energy spacing between rotational levels compared to that between torsional states, i.e.,  $E_{RT}^0 - E_{R''T''}^0 \approx E_T - E_{T''} = E_{v\sigma} - E_{v''\sigma}$ . This will allow us to express the energies of a given torsional state in terms of an effective Hamiltonian involving only operators of the total angular momentum.

If the rotational energy differences are neglected, the denominators of (12.42) will no longer involve  $R$ , and the summation in  $R''$  and  $T''$  can be separated. Since each matrix element in the numerator can be factored as  $(R|\mathcal{P}|R'') \cdot (T|p|T'')$ , the  $R''$  summation is simply matrix multiplication giving a factor  $(R|\mathcal{P}^2|R')$ . Explicitly, we obtain for the matrix elements of a given  $v\sigma$  block:

$$(R, v, \sigma | \mathcal{H}_R + \mathcal{H}_T + \mathcal{H}_{TR} | R', v, \sigma) + 4F^2(R|\mathcal{P}^2|R') \sum_{v'} \frac{|(v, \sigma | p | v', \sigma)|^2}{\Delta_{vv'}} \quad (12.43)$$

where  $\Delta_{vv'} = E_{v\sigma} - E_{v'\sigma}$ . This is just the  $RR'$ 'th matrix element of the following effective rotational Hamiltonian operator for the torsional state  $v\sigma$ :

$$\mathcal{H}_{v\sigma} = \mathcal{H}_r + F [W_{v\sigma}^{(0)} + W_{v\sigma}^{(1)} \mathcal{P} + W_{v\sigma}^{(2)} \mathcal{P}^2] \quad (12.44)$$

where  $F = \frac{1}{2}\hbar^2/rI_x$ ,  $\mathcal{P} = \sum \rho_g P_g$  and where

$$W_{v\sigma}^{(0)} = \frac{E_{v\sigma}}{F} \quad (12.45)$$

$$W_{v\sigma}^{(1)} = -2(v, \sigma | p | v, \sigma) \quad (12.46)$$

$$W_{v\sigma}^{(2)} = 1 + 4F \sum_{v'} \frac{|(v, \sigma | p | v', \sigma)|^2}{\Delta_{vv'}} \quad (12.47)$$

with

$$\Delta_{vv'} = E_{v\sigma} - E_{v'\sigma} = \frac{9}{4}F(b_{v\sigma} - b_{v'\sigma}) \quad (12.48)$$

and

$$(v, \sigma | p | v', \sigma) = -i \int_0^{2\pi} U_{v\sigma}^*(\alpha) \frac{\partial}{\partial \alpha} U_{v'\sigma}(\alpha) d\alpha \quad (12.49)$$

This effective rotational Hamiltonian is correct to second order. The  $W$  coefficients introduced by Herschbach [28] depend on the barrier, in particular on the ratio  $V_3/F$ . The Hamiltonian of (12.44) can also be written in the equivalent form [33, 8]:

$$\begin{aligned} \mathcal{H}_{v\sigma} = & A_{v\sigma} P_x^2 + B_{v\sigma} P_y^2 + C_{v\sigma} P_z^2 + FW_{v\sigma}^{(1)} \sum_g \rho_g P_g \\ & + \frac{1}{2}FW_{v\sigma}^{(2)} \sum_{g,g'} \rho_g \rho_{g'} (P_g P_{g'} + P_{g'} P_g) + E_{v\sigma} \quad (g = x, y, z) \end{aligned} \quad (12.50)$$

where

$$\rho_g = \frac{\lambda_g I_x}{I_g} \quad (12.51)$$

and

$$\begin{aligned} A_{v\sigma} = & A_x + W_{v\sigma}^{(2)} F \rho_x^2 \\ B_{v\sigma} = & B_y + W_{v\sigma}^{(2)} F \rho_y^2 \\ C_{v\sigma} = & C_z + W_{v\sigma}^{(2)} F \rho_z^2 \end{aligned} \quad (12.52)$$

**Table 12.2** Perturbation Coefficients for a Threefold Barrier<sup>a,b</sup>

s	Nondegenerate Sublevel ( <i>A</i> symmetry)				Degenerate Sublevel ( <i>E</i> symmetry)			
	<i>n</i> =0	<i>n</i> =2	<i>n</i> =4	<i>n</i> =0	<i>n</i> =1	<i>n</i> =2	<i>n</i> =3	<i>n</i> =4
<i>Ground Torsional Level (<i>v</i>=0)</i>								
8	5.5936	0.280631	-0.0799	5.7972	-0.2617257	-0.137544	0.213762	0.0308
10	6.4056	0.180716	-0.05725	6.5335	-0.1602753	-0.089791	0.124274	0.02676
12	7.1226	0.117586	-0.03948	7.2047	-0.1014166	-0.058664	0.077241	0.019312
16	8.3688	0.052068	-0.01841	8.4047	-0.0437764	-0.026025	0.032531	0.009178
20	9.4499	0.024473	-0.008819	9.4667	-0.0203828	-0.012236	0.015012	0.004408
28	11.3091	0.006261	-0.002281	11.3134	-0.0051860	-0.003130	0.003797	0.001141
36	12.9096	0.001856	-0.000678	12.9108	-0.0015359	-0.000928	0.001123	-0.0003391
40	13.6418	0.001055	-0.000386	13.6425	-0.0008723	-0.0005272	0.0006379	0.0001928
48	15.0029	0.0003643	-0.0001331	15.0031	-0.0003012	-0.0001819	0.0002202	0.0000666
56	16.2539	0.0001354	-0.0000495	16.2540	-0.0001120	-0.00006769	0.0000819	0.00002469
60	16.8457	0.0000845	-0.0000309	16.8457	-0.00006992	0.00004227	0.00005112	0.00001545
68	17.9726	0.0000343	-0.00001252	17.9726	-0.00002835	-0.00001714	0.00002074	0.00000626
72	18.5111	0.00002220	-0.00000812	18.5111	-0.00001838	-0.00001111	0.00001345	0.00000406
80	19.5449	0.00000963	-0.00000352	19.5449	-0.00000796	-0.00000482	0.00000582	0.00000176
88	20.5280	0.00000433	-0.00000158	20.5280	-0.00000358	-0.00000217	0.00000262	0.00000079
92	21.0028	0.00000294	-0.00000107	21.0028	-0.00000243	-0.00000147	0.00000178	0.00000054
100	21.9222	0.00000140	-0.00000051	21.9222	-0.00000115	-0.00000069	0.00000084	0.00000026

First Excited Torsional Level ( $v=1$ )								
16	24.1805	-1.27334	0.7870	23.4277	0.7977206	0.590647	-0.42680	-0.2421
20	27.2238	-0.654112	0.31265	26.8077	0.4695574	0.319985	-0.294937	-0.13408
28	32.6645	-0.200728	0.07947	32.5300	0.1594403	0.100170	-0.111855	-0.03905
36	37.4427	-0.069411	0.02603	37.3955	0.0566696	0.034699	-0.040897	-0.012993
40	39.6401	-0.042117	0.015628	39.6114	0.0345699	0.021057	-0.0250835	-0.007809
48	43.7320	-0.0162968	0.005989	43.7209	0.0134408	0.0081484	-0.0097997	-0.002995
56	47.4959	-0.0066663	0.002442	47.4914	0.0055072	0.0033332	-0.0040219	-0.0012210
60	49.2765	-0.0043405	0.0015888	49.2735	0.00358727	0.0021702	-0.0026207	-0.0007944
68	52.6667	-0.0018985	0.0006942	52.6654	0.00156961	0.0009493	-0.0011471	-0.0003472
72	54.2864	-0.0012734	0.0004655	54.2855	0.00105298	0.0006367	-0.0007698	-0.0002327
80	57.3951	-0.0005876	0.0002148	57.3947	0.00048597	0.0002938	-0.0003553	-0.0001074
88	60.3509	-0.0002796	0.0001022	60.3507	0.00023119	0.0001398	-0.001690	-0.0000511
92	61.7780	-0.0001948	0.0000712	61.7779	0.00016112	0.0000974	-0.0001178	-0.0000356
100	64.5416	-0.0000964	0.0000352	64.5415	0.00007974	0.0000482	-0.0000583	-0.000017
Second Excited Torsional Level ( $v=2$ )								
36	58.4614	0.890641	-0.2370	59.1178	-0.8593042	-0.428291	0.721421	0.06245
40	62.3641	0.619322	-0.18380	62.8093	-0.5670974	-0.304883	0.456080	0.07625
48	69.4772	0.291871	-0.09759	69.6812	-0.2522742	-0.145546	0.192538	0.04752
56	75.9067	0.137167	-0.04822	76.0014	-0.1156628	-0.068549	0.086201	0.02400
60	78.9255	0.09449	-0.03365	78.9905	-0.0791721	-0.047238	0.058634	0.016791
68	84.6483	0.045504	-0.016435	84.6795	-0.0378571	-0.022751	0.027842	0.008215
72	87.3744	0.031829	-0.011540	87.3962	-0.02643006	-0.0159144	0.0194013	0.005769
80	92.5971	0.0158271	-0.005763	92.6080	-0.01311438	-0.0079136	0.0096063	0.002882
88	97.5549	0.0080372	-0.002932	97.5604	-0.00665303	-0.0040186	0.0048686	0.001466
92	99.9466	0.0057707	-0.002107	99.9505	-0.00477549	-0.0028885	0.0034936	0.001053
100	104.5751	0.0030175	-0.001102	104.5772	-0.00249627	-0.0015088	0.0018255	0.000552

<sup>a</sup>From Herschbach [28].

<sup>b</sup>The coefficients,  $W_{\nu\sigma}^{(n)}$ , are tabulated as functions of the dimensionless parameter  $s = \frac{4}{9}(V_3/F)$ .

Note that the rotational constants of the rigid molecule  $A_x, \dots$ , are modified by the internal rotation terms arising from  $W_{v\sigma}^{(2)} \mathcal{P}^2$ .

The perturbation treatment of  $\mathcal{H}_{TR}$  can be carried to higher order by application of successive Van Vleck transformations. The effective rotational Hamiltonian for a given torsional state obtained from an  $n$ th order perturbation calculation can be expressed simply as [28]

$$\mathcal{H}_{v\sigma} = \mathcal{H}_r + F \sum_n W_{v\sigma}^{(n)} \mathcal{P}^n \quad (12.53)$$

The first term is the rigid asymmetric rotor Hamiltonian, and the last term, which is a power series in  $\mathcal{P}$ , represents the effect of internal motion on the rotational motion. The  $W_{v\sigma}^{(n)}$  are the usual  $n$ th order perturbation sums, except for  $n=2$  which contains an added contribution arising from the  $F \mathcal{P}^2$  term in the original Hamiltonian [see (12.47)].

The dimensionless perturbation coefficients  $W_{v\sigma}^{(n)}$  depend on the reduced barrier height  $s$ , and these coefficients (except  $n=0$ ) decrease in size with increasing barrier, becoming proportional to the torsional sublevel splittings ( $E_{vE} - E_{vA}$ ) and hence vanishing at the limit of infinite barrier height [28]. At this limit,  $\mathcal{H}_{v\sigma}$  reduces to the rigid rotor Hamiltonian plus the energy of a torsional harmonic oscillator, and a usual rigid rotor spectrum would be obtained.

The zeroth order term  $W_{v\sigma}^{(0)}$  is just the torsional energy contribution from  $\mathcal{H}_T$ , and does not affect the rotational spectrum. The first-order term  $W_{v\sigma}^{(1)}$  is nonzero only for the degenerate  $E$  sublevels. The second-order term  $W_{v\sigma}^{(2)}$  differs both in sign and magnitude for the  $A$  and  $E$  sublevels of a given torsional state  $v$ . The following properties of the perturbation coefficients may be listed [28]:

$$W_{v0}^{(n)} = 0 \quad \text{for } n \text{ odd} \quad (12.54)$$

$$W_{v1}^{(n)} = (-1)^n W_{v,-1}^{(n)} \quad (12.55)$$

$$W_{v0}^{(n)} \approx -2W_{v1}^{(n)} \quad \text{for } n > 0 \text{ and even} \quad (12.56)$$

$$\frac{W_{v1}^{(n+2)}}{W_{v1}^{(n)}} \approx \frac{-(2\pi/3)^2}{[(n+1)(n+2)]} \quad \text{for } n > 0 \quad (12.57)$$

The first two relations are true in general, whereas the latter two relations hold for relatively high barriers. The perturbation coefficients have been tabulated for various values of  $n$  and  $v$  and for a wide range of the parameter  $s$  [18, 19, 28]. The recent tabulation by Hayashi and Pierce [19] lists the perturbation coefficients for  $v=0, 1, 2$  and  $n=0, 1, \dots, 6, d$  for  $s$  values from 4 to 200 with the interval in  $s$  being 2 for  $s < 100$  and 4 for  $s > 100$ . These tables have also been reproduced in the book by Wallrab [121]. A short tabulation of the perturbation coefficients for the  $v=0, 1$ , and 2 torsional levels are given in Table 12.2. A discussion of the method for evaluating these perturbation coefficients, which avoids the laborious evaluation of the perturbation sums, may be found

elsewhere [28, 34]. This is the so-called "bootstrap" procedure which is based on the fact the  $W_{v\sigma}^{(n)}$  are not dependent on the molecular asymmetry.

In the derivation of the effective rotational Hamiltonian the rotational energy differences were neglected in comparison with the torsional energy differences. This approximation is adequate for molecules with high barriers but may not be so for those with low and intermediate barriers or small moments of inertia. The error caused by ignoring rotational spacing can be corrected by expansion of the denominators in a Taylor series. This has been discussed by Herschbach [28] and by Stelman [35] and its consideration requires introducing another perturbation coefficient  $W_{v\sigma}^{(d)}$  into the effective rotational Hamiltonian. These denominator corrections have no appreciable effect on the determination of the barrier height for high barrier cases [see, e.g., (12.61)] because the contributions to the rotational constants are essentially the same for both torsional sublevels. Nevertheless, they can contribute several megahertz to the rotational constants.

## 6 HIGH-BARRIER ASYMMETRIC ROTORS

We have seen, by treating the coupling of internal and overall rotation by the degenerate perturbation theory of Van Vleck, that an effective rotational Hamiltonian may be obtained for each torsional level. For a particular torsional state  $v$  there will be a set of rotational energy levels associated with each of the two torsional sublevels  $\sigma=0$  or  $A$  and  $\sigma=\pm 1$  or  $E(\sigma=+1 \text{ or } -1 \text{ lead to the same energy levels})$ . The two sets of rotational energy levels are obtained by solution of the effective Hamiltonians  $\mathcal{H}_{vA}$  and  $\mathcal{H}_{vE}$  of (12.53). The number of correction terms to  $\mathcal{H}$ , that must be retained in (12.53) for analysis of the effects of internal rotation varies significantly from molecule to molecule and is dependent on the barrier height and the asymmetry. Also the complexity of the operator  $\mathcal{P}$  depends on the molecular geometry. For molecules with a plane of symmetry containing the internal rotor axis, for example,  $\text{CH}_3\text{CHO}$ , some simplification results since the direction cosine  $\lambda_y$  vanishes ( $y$  axis perpendicular to the symmetry plane). For two planes of symmetry, for example,  $\text{CH}_3\text{BF}_2$ , both  $\lambda_x$  and  $\lambda_y$  vanish, and  $\mathcal{P}$  reduces to  $\rho_z P_z$ . Even when the molecule has only one plane of symmetry, the internal rotor axis may lie so close to one of the principal axes in the plane that the direction cosine referring to the other principal axis in the plane will be negligibly small and  $\mathcal{P}$  will again depend only on the component  $P_z$ . It may be mentioned that it is usually convenient to choose the axis of quantization, the  $z$  axis, to be the axis making the smallest angle with the top axis, even if this is not the best choice for evaluation of the asymmetric rigid rotor energy levels. Hence in dealing with specific molecules the symbols  $A_{v\sigma}$ ,  $B_{v\sigma}$ , and  $C_{v\sigma}$  [e.g., in (12.50)] may have to be permuted to satisfy the usual convention  $A \geq B \geq C$ .

### Energy Levels and Spectra of the Pseudorigid Rotor

When barriers are relatively high ( $s > 30$ ) [36], terms up to  $n=2$  in (12.53) are often sufficient, and the Hamiltonian is then given by (12.50). The cross

terms of the form  $(P_g P_{g'} + P_{g'} P_g)$  present in this expression can be eliminated as usual by a rotation of the coordinate axes to obtain a new set of principal axes in which these terms vanish. If, for example, only one such cross term were present, a simple  $2 \times 2$  rotation in the  $gg'$  plane may be chosen to remove the term. The orientation of the new coordinate system, referred to as the "effective principal-axis system" will vary with the torsional state since the coefficients of the cross terms contain  $W_{v\sigma}^{(2)}$ . This transformation alters the rotational constants and the coefficients of the linear terms [8, 27]. Often the modifications produced by such a rotation of coordinate axes is small, and negligible error is introduced by just ignoring the cross terms. The linear terms in  $P_g$ , present only for the degenerate  $E$  levels since  $W_{vA}^{(1)}=0$ , can be neglected for a barrier greater than 1000 cal/mole and an asymmetry of  $|\kappa|<0.8$  [27]. Therefore, in the cases where the linear terms may be neglected, the effective rotational Hamiltonian may be put into pseudorigid rotor form for both the  $A(\sigma=0)$  and  $E(\sigma=1)$  sublevels. The Hamiltonians are

$$\mathcal{H}_{vA} = A_{vA} P_x^2 + B_{vA} P_y^2 + C_{vA} P_z^2 \quad (12.58)$$

$$\mathcal{H}_{vE} = A_{vE} P_x^2 + B_{vE} P_y^2 + C_{vE} P_z^2 \quad (12.59)$$

where the effective rotational constants contain contributions from internal rotation, that is,

$$A_{vA} = \frac{\hbar^2}{2I_x} + F\rho_x^2 W_{vA}^{(2)} \quad (12.60)$$

etc. Since the  $W_{v\sigma}^{(2)}$  differ for the  $A$  and  $E$  levels, the effective rotational constants will differ. Thus there is a set of pseudorigid rotor energy levels,  $E_{J,v\sigma}$ , associated with the  $A$  torsional sublevel and with the  $E$  sublevel.

The usual selection rules apply for the rotational transitions with the additional restriction that  $\Delta\sigma=0$ , which results because the dipole moment is independent of the internal rotation angle. Transitions from one internal sublevel to another ( $vA \leftrightarrow vE$ ) are thus not allowed, and the  $vA$  and  $vE$  sublevels have separate rigid-rotorlike rotational spectra. Each rotational transition ( $J_t \rightarrow J'_t$ ) in a torsional state  $v$  will hence appear as a doublet rather than as a single line. The  $A$  and  $E$  lines are interpreted by the Hamiltonians of (12.58) and (12.59), and two separate sets of rotational constants are found to fit the doublets by interpolation of existing tables of rigid rotor energy levels. The analysis is therefore no more involved than that discussed previously in Chapter VII for an ordinary rigid asymmetric rotor except the rigid rotor energy is now a so-called pseudorigid rotor energy computed with the effective rotational constants of (12.60). The barrier may be evaluated from the differences in these pseudorigid rotor rotational constants. For example,

$$\Delta A = A_{vA} - A_{vE} = F\rho_x^2 [W_{vA}^{(2)} - W_{vE}^{(2)}] \quad (12.61)$$

determines the quantity  $W_{vA}^{(2)} - W_{vE}^{(2)}$ , once the moment of inertia of the methyl group and the direction cosines are established. From this, the barrier height  $V_3$  can be obtained by comparison with the tabulated perturbation coefficients.

From (12.56) the rigid rotor rotational constants which contain the structural information are found to be given by the expressions

$$A_x = \frac{\hbar^2}{2I_x} = \frac{1}{3}(A_{vA} + 2A_{vE}) \quad (12.62)$$

and so on. Furthermore, if (12.56) is a valid approximation, it follows that the shift of the *A* line from the unperturbed or rigid rotor position is twice that of the *E* line.

Another procedure is to obtain the barrier height directly from the separation of each doublet [33]. This is particularly useful if the differences in the pseudo-rotational constants are very small. The energy separation between the *A* and *E* levels may be expanded as

$$\Delta E = E_A - E_E = \left( \frac{\partial E}{\partial A} \right) \Delta A + \left( \frac{\partial E}{\partial B} \right) \Delta B + \left( \frac{\partial E}{\partial C} \right) \Delta C \quad (12.63)$$

where  $E_A$  and  $E_E$  are the rigid rotor energy of the levels *A* and *E*, respectively, and  $\Delta A$ , etc., are given by (12.61). Any centrifugal distortion correction is assumed to be the same for both the *A* and *E* levels. With the rigid rotor energy expressed by

$$E = \frac{1}{2}(A + C)J(J+1) + \frac{1}{2}(A - C)E(\kappa) \quad (12.64)$$

we find

$$\frac{\partial E}{\partial A} = \frac{1}{2} \left[ J(J+1) + E(\kappa) - (\kappa+1) \left( \frac{\partial E(\kappa)}{\partial \kappa} \right) \right] \quad (12.65)$$

$$\frac{\partial E}{\partial B} = \frac{\partial E(\kappa)}{\partial \kappa} \quad (12.66)$$

$$\frac{\partial E}{\partial C} = \frac{1}{2} \left[ J(J+1) - E(\kappa) + (\kappa-1) \left( \frac{\partial E(\kappa)}{\partial \kappa} \right) \right] \quad (12.67)$$

The values of  $\partial E(\kappa)/\partial \kappa$  may be obtained from tables of  $E(\kappa)$ . These relations and those of (12.61) will give the energy level differences,  $\Delta E$ . The difference in the  $\Delta E$  values for the two levels  $J_\tau, J'_\tau$  involved in the transition will give the frequency separation of the doublet as a function of the structural parameters, reduced energies, and so on, times the factor  $[W_{vA}^{(2)} - W_{vE}^{(2)}]$ . Thus, the barrier may be found directly from the observed splittings. If the splittings contain contributions from higher-order effects (see the next section) these contributions would be removed before application of (12.63). It should be noted that in (12.64) the rotational constants have been chosen such that  $A \geq B \geq C$ , although this, as indicated previously, is not necessarily the order of  $A_{v\sigma}, B_{v\sigma}$ , and  $C_{v\sigma}$ ; and hence these latter constants must be permuted accordingly.

### Higher-order Effects

When the linear terms in  $P_g$  are not small compared with the energy spacing between the pseudorigid rotor levels they connect (e.g., the barrier is such that

the coefficients,  $F\rho_g W_{v\sigma}^{(1)}$ , are large or if the asymmetry is small), the energy levels for the  $E$  states will not be like that of a rigid rotor. The energy levels may be obtained by diagonalization of the matrix of  $\mathcal{H}_{v\sigma}$ . With the symmetric rotor functions as basis functions, the Hamiltonian of (12.50) which is correct to second order has the following matrix elements for the torsional state  $v\sigma$  [33].

$$\begin{aligned}(K|\mathcal{H}_{v\sigma}|K) &= \frac{1}{2}(A_{v\sigma} + B_{v\sigma})J(J+1) + [C_{v\sigma} - \frac{1}{2}(A_{v\sigma} + B_{v\sigma})]K^2 \\ &\quad + FW_{v\sigma}^{(1)}\rho_z K \\ (K|\mathcal{H}_{v\sigma}|K \pm 1) &= \frac{1}{2}F[W_{v\sigma}^{(2)}\rho_z(\rho_y \pm i\rho_x)(2K \pm 1) + W_{v\sigma}^{(1)}(\rho_y \pm i\rho_x)] \\ &\quad \times [J(J+1) - K(K \pm 1)]^{1/2} \\ (K|\mathcal{H}_{v\sigma}|K \pm 2) &= \frac{1}{4}[(B_{v\sigma} - A_{v\sigma}) \pm 2iFW_{v\sigma}^{(2)}\rho_x\rho_y] \\ &\quad \times \{[J(J+1) - K(K \pm 1)][J(J+1) - (K \pm 1)(K \pm 2)]\}^{1/2}\end{aligned}\quad (12.68)$$

The indices  $J, M$  in the matrix elements have been omitted, since  $\mathcal{H}_{v\sigma}$  is diagonal in these quantum numbers. Also, the constant term  $E_{v\sigma}$  has been dropped because the torsional state does not change in a rotational transition. This matrix differs from that obtained for a rigid rotor in the appearance of the  $(K|K \pm 1)$  matrix elements.

For the  $A$  levels,  $W_{vA}^{(1)} = 0$ , and the  $(K|K \pm 1)$  elements arise only from the quadratic cross terms ( $P_g P_{g'} + P_{g'} P_g$ ). These terms also contribute to the  $(K|K \pm 2)$  elements. They can be neglected or eliminated by choice of a new principal-axis system, as discussed before. As a consequence, the matrix will reduce to that of a rigid rotor with corrected rotational constants, and the energies are obtainable by the usual rigid rotor techniques.

For the  $E$  levels the  $(K|K \pm 1)$  matrix elements cannot be completely removed even with a rotation of coordinate axes because  $W_{vE}^{(1)} \neq 0$ , and this complicates the calculation of the  $\mathcal{H}_{vE}$  energy levels. The usual factoring obtainable for the rigid rotor matrix is no longer possible, and for a given  $J$  one has a  $(2J+1)$  by  $(2J+1)$  secular determinant to solve. Diagonalization of the secular equation is difficult except for low  $J$ . Expressions for some of the low  $J$  energy levels are available [8, 12, 37]. Procedures for handling the  $n=1$  terms for certain cases have been described [11, 12, 38]. If, for example, the associated direction cosines of the  $P_x$  and  $P_y$  terms are small enough that these terms may be neglected, then the  $(K|K \pm 1)$  matrix elements will arise only from the quadratic cross terms in the angular momentum components, which can be removed by a preliminary transformation, or neglected. The matrix of  $\mathcal{H}_{vE}$  with only contributions from the linear term in  $P_z$  can now be factored into two submatrices, one for even  $K$  and one for odd  $K$ , since without the  $(K|K \pm 1)$  matrix elements even and odd  $K$  are no longer connected. Use of the Wang functions will not, however, lead to additional factoring because of the presence of the linear  $K$  term on the diagonal. The eigenvalues of these somewhat smaller secular equations can be more readily determined; for example, see the modified continued fraction procedure of Reference 11. For some of the low  $J$  energy levels the matrices are only  $2 \times 2$  and can be easily solved to give the results of Table 12.3.

**Table 12.3** Some Low  $J$  Energy Levels<sup>a</sup>

---


$$\begin{aligned}E_{00} &= 0 \\E_{10} &= A_{v\sigma} + B_{v\sigma} \\E_{11} &= C_{v\sigma} + \frac{1}{2}(A_{v\sigma} + B_{v\sigma}) \pm [(F\rho_z W_{v\sigma}^{(1)})^2 + \frac{1}{4}(A_{v\sigma} - B_{v\sigma})^2]^{1/2} \\E_{21} &= C_{v\sigma} + \frac{3}{2}(A_{v\sigma} + B_{v\sigma}) \pm [(F\rho_z W_{v\sigma}^{(1)})^2 + \frac{9}{4}(A_{v\sigma} - B_{v\sigma})^2]^{1/2}\end{aligned}$$


---

<sup>a</sup>Energy levels for the Hamiltonian of the  $E$  levels in the form  $\mathcal{H}_{v\sigma} = A_{v\sigma} P_x^2 + B_{v\sigma} P_y^2 + C_{v\sigma} P_z^2 + FW_{v\sigma}^{(1)} \rho_z P_z$ .  $K$ , though not a good quantum number, is used to label the energy levels which are designated as  $E_{JK}$ .

In many applications, the linear terms can be satisfactorily treated by perturbation theory. In particular, the linear terms are treated as a perturbation of the pseudorigid rotor Hamiltonian ( $\mathcal{H}_r$ ):

$$\mathcal{H}_{vE} = \mathcal{H}_r + \mathcal{H}' \quad (12.69)$$

$$\mathcal{H}_r = A_{vE} P_x^2 + B_{vE} P_y^2 + C_{vE} P_z^2 \quad (12.70)$$

$$\mathcal{H}' = FW_{vE}^{(1)} \sum_g \rho_g P_g \quad (12.71)$$

where  $A_{vE}, \dots$  are the pseudorigid rotor rotational constants. In the pseudorigid asymmetric rotor representation (basis in which  $\mathcal{H}_r$  is diagonal) the  $P_g$  have only off-diagonal matrix elements (diagonal in  $J$ , off-diagonal in  $\tau$ ) and  $\mathcal{H}'$  contributes only in a second- or higher-order perturbation calculation. If  $\mathcal{H}'$  is treated with second-order nondegenerate perturbation theory, the rotational energies for the torsional state  $vE$  are given by

$$E_{J,\tau} = E_{J,\tau}^0 + (FW_{vE}^{(1)})^2 \sum_g \rho_g^2 \sum_{\tau'} \frac{|(J, \tau | P_g | J, \tau')|^2}{E_{J,\tau}^0 - E_{J,\tau'}^0} \quad (12.72)$$

where  $E_{J,\tau}^0$  is the pseudorigid rotor energy of the  $J_\tau$  level. It frequently happens that for a given  $J$  near-degeneracies occur between asymmetry doublets  $J_\tau, J_{\tau'}$  (pairs of adjacent  $K$  states); when such levels are coupled by  $P_g$ , the nondegenerate perturbation treatment of the linear terms is not applicable. The linear terms can, however, be handled in a manner similar to the way in which the Stark effect for such a situation was treated, that is, by means of a second-order Van Vleck transformation. This leads to a  $2 \times 2$  secular equation to be solved [39]. The necessary matrix elements and perturbation sums required for solution of the secular equation or application of (12.72) have been tabulated by Dobyns [39] in increments of 0.05 in the asymmetry parameter  $\kappa$  for  $J \leq 12$ .

It has also been pointed out by Rudolph [40] that the required matrix elements of  $P_g$  can be expressed in terms of the line strengths, which have been extensively tabulated. In particular, the following relation can be shown to exist [41]

$$\lambda_g(J, \tau; J, \tau') = \frac{2J+1}{J(J+1)} |(J, \tau | P_g | J, \tau')|^2 \quad (12.73)$$

This relation may be used to express (12.72) in terms of the line strengths.

Although it is often sufficient to consider only terms up to  $n=2$  in the analysis of internal rotation, higher-order terms in the angular momentum operators become important when the barrier is not sufficiently high. Furthermore, even for a relatively high barrier, higher-order terms may have to be considered. When such terms will be required can be seen by examination of (12.53) in the limit of a symmetric top. In this limiting case  $\mathcal{P}^n$  may be expressed as  $(\rho K)^n$  where  $\rho = I_x/I_z$ . Although the  $W_{v\sigma}^{(n)}$  terms decrease rapidly as  $s$  increases, the convergence of the power series for a given barrier depends on the magnitude of  $\rho K$ , because for a given barrier the  $W_{v\sigma}^{(n)}$  do not converge very rapidly with increasing  $n$ . Therefore, the perturbation series converges rapidly only if energy levels have low values of  $K$  or if  $\rho$  is small. The latter condition is satisfied for molecules with light tops and heavy frames, and hence the PAM method is best suited to this class of molecules. As a rough guide to the number of terms to retain in the Hamiltonian of (12.53), it may be stated that if  $\rho K < 0.25$ , terms through  $n=2$  are sufficient, but if  $0.25 < \rho K < 0.55$ , terms through  $n=4$  should be retained [28].

The matrix elements in a symmetric rotor basis for the Hamiltonian of (12.53) up to  $n=4$  are available [28, 42]. The  $n=3$  and 4 terms introduce additional matrix elements of the type  $(K|K \pm 3)$  and  $(K|K \pm 4)$ . The solution of such a secular determinant is, however, seldom required since the  $n=3$  and 4 terms can usually be treated by perturbation techniques.

For the case where two of the three direction cosines are zero, or negligible, a first-order treatment yields a very simple energy expression. If we choose the asymmetric rigid rotor basis we have

$$E_{v\sigma} = E_r + F \sum_n \rho_z^n W_{v\sigma}^{(n)} \langle P_z^n \rangle \quad n=2, 4, \dots \quad (12.74)$$

where all correction terms of (12.53) are treated as first-order perturbations of  $\mathcal{H}_r$ . To this approximation, all odd  $n$  terms vanish. This is particularly convenient when the barrier is high enough that the odd order corrections for the  $E$  levels need not be considered. The particularly simple form of the  $n=4$  term (and others) in (12.74) arises because  $\mathcal{P}$  has been taken to depend significantly only on the  $P_z$  component. If this is not the case and all of the  $n=4$  terms are required, a term of the type

$$F W_{v\sigma}^{(4)} (\rho_x P_x + \rho_y P_y + \rho_z P_z)^4$$

would appear, one which is comprised of a sum of 81 terms, each a product of four angular momentum components. This term may be written in the equivalent form

$$F W_{v\sigma}^{(4)} \sum \rho_g \rho_{g'} \rho_{g''} \rho_{g'''} P_g P_{g'} P_{g''} P_{g'''}$$

From this form it is immediately evident that these terms have the same form as the centrifugal distortion corrections for an asymmetric rotor (see Chapter VIII). As a consequence, the techniques which have been developed for the

handling of centrifugal distortion effects can be employed for the  $n=4$  terms with the formal correspondence [28]

$$\frac{\hbar}{4} \tau_{gg'g''g'''} \leftrightarrow F W_{v\sigma}^{(4)} \rho_g \rho_{g'} \rho_{g''} \rho_{g'''} \quad (12.75)$$

As before, use of the commutation rules will introduce quadratic terms in the angular momentum components, and hence the rotational constants are modified by terms in  $W_{v\sigma}^{(4)}$  in addition to those involving  $W_{v\sigma}^{(2)}$  from  $\mathcal{P}^2$ . For a first-order perturbation treatment with the pseudorigid rotor basis the contribution of the  $n=4$  terms to the energy would have the form given in (8.64) for ordinary centrifugal distortion. The distortion coefficients are defined in terms of  $D_J$ , and so on, which are now modified as given in Table 12.4. The rotational constants as modified by contributions from both the second- and fourth-order internal rotation terms are also given in Table 12.4. The results of Table 12.4 may also be used to define the reduced pseudocentrifugal distortion constants  $\Delta_J, \dots$ . Definitions of the reduced quartic and sextic constants for  $\rho_c=0$  may be found elsewhere [43]. Dealing with these pseudocentrifugal distortion terms,  $W_{v\sigma}^{(4)} \mathcal{P}^4$ , is thus no more complicated than dealing with ordinary centrifugal distortion.

Since the most important contribution usually arises from coupling along one inertial axis,  $g$ , the major third-order contribution ( $n=3$ ) will arise from the term  $P_g^3$ . Such a term may be included in a perturbation treatment [38, 39]. Fortunately, in many cases the odd  $n$  terms, which are more difficult to handle, are not as important as the even  $n$  terms. Furthermore, when such terms are important in certain transitions, one can usually find other transitions for the barrier evaluation where the effect of these terms is small.

As mentioned previously for molecules with heavy tops, the internal rotation effects are best treated by the IAM method. A computer program, based on the IAM method, has been described by Woods [44] for treatment of heavy-top molecules such as  $\text{CF}_3\text{CHO}$ . The program is also applicable to molecules with light tops. Extension of the program to molecules with several tops has also been given [45].

**Table 12.4** Pseudocentrifugal Distortion Coefficients for Fourth-order Internal Rotation Effects<sup>a</sup>

---


$$\begin{aligned}
 D_J &= -(\frac{3}{8})(\rho_x^2 + \rho_y^2)^2 F W_{v\sigma}^{(4)} \\
 D_{JK} &= -2D_J - 3\rho_z^2(\rho_x^2 + \rho_y^2) F W_{v\sigma}^{(4)} \\
 D_K &= -D_J - D_{JK} - \rho_z^4 F W_{v\sigma}^{(4)} \\
 \delta_J &= (\frac{1}{4})(\rho_y^4 - \rho_x^4) F W_{v\sigma}^{(4)} \\
 R_5 &= (\frac{1}{2})\delta_J - (\frac{3}{4})\rho_z^2(\rho_y^2 - \rho_x^2) F W_{v\sigma}^{(4)} \\
 R_6 &= (\frac{1}{2})D_J + (\frac{1}{2})(\rho_x^4 + \rho_y^4) F W_{v\sigma}^{(4)} \\
 A &= A_x + F \rho_x^2 W_{v\sigma}^{(2)} + F(3\rho_y^2 \rho_z^2 - 2\rho_x^2 \rho_y^2 - 2\rho_x^2 \rho_z^2) W_{v\sigma}^{(4)} \\
 B &= B_y + F \rho_y^2 W_{v\sigma}^{(2)} + F(3\rho_x^2 \rho_z^2 - 2\rho_x^2 \rho_y^2 - 2\rho_y^2 \rho_z^2) W_{v\sigma}^{(4)} \\
 C &= C_z + F \rho_z^2 W_{v\sigma}^{(2)} + F(3\rho_x^2 \rho_y^2 - 2\rho_x^2 \rho_z^2 - 2\rho_y^2 \rho_z^2) W_{v\sigma}^{(4)}
 \end{aligned}$$


---

<sup>a</sup>After Herschbach [28].

Continued refinements in the theory of internal rotation of methyl groups have appeared in the literature over the last 10 years, particularly by Dreizler and co-workers and by Bauder and Günthard and co-workers. With the availability of faster and larger capacity computers, powerful direct diagonalization procedures rather than perturbation techniques have been developed [see, e.g., (46–54)].

### Rotational Spectra of the Ground Torsional State

From the preceding discussions it is apparent that the appropriate Hamiltonian and procedures for evaluation of the energy levels can range from the relatively simple to the rather complex. In any event, one should remember that the barrier height  $V_3$  is determined by finding the value of  $s (=4V_3/9F)$  which in conjunction with the appropriate Hamiltonian satisfactorily accounts for the observed rotational splittings arising from internal rotation. An example of a barrier height calculation is considered later.

Figure 12.7 gives a schematic representation of the energy levels and parallel type ( $\Delta K = 0$ ) transitions for different asymmetries and barrier heights. Internal rotation effects in asymmetric rotors lead to doublets consisting of the  $A$  and  $E$

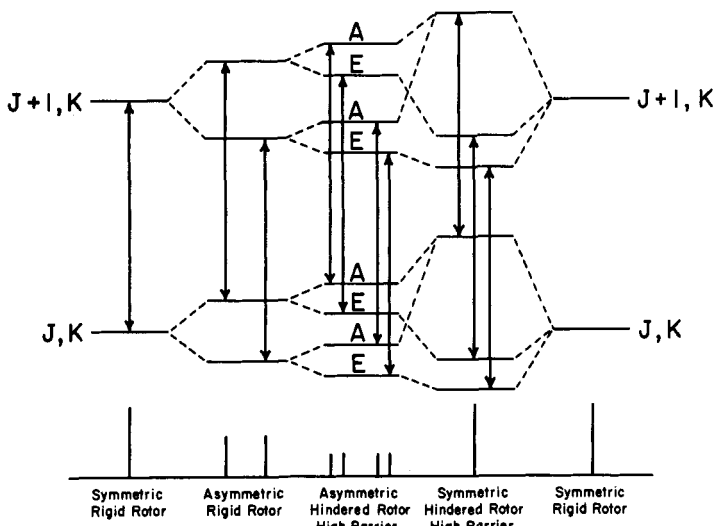


**Fig. 12.7** Illustration of the energy levels and rotational transitions ( $\Delta K = 0$ ) for a hindered symmetric and asymmetric rotor. For an infinitely high threefold barrier, each  $J, K$  level of a symmetric rotor is sixfold degenerate corresponding to the twofold  $K$  degeneracy and the threefold torsional level degeneracy. These levels are each split into two asymmetric rotor levels with the introduction of an asymmetry, and two lines are observed. If the barrier is lowered, each asymmetric rotor level is split into two levels, a nondegenerate  $A$  level and a degenerate  $E$  level, and two doublets are observed. If the asymmetry is removed, the energy levels of a symmetric hindered rotor are obtained. The presence of a high barrier splits each  $J, K$  level of a symmetric rotor into three two fold degenerate levels as indicated. The three levels correspond to  $\sigma = 0, \pm K; \sigma = +1, +K; \sigma = -1, -K; \sigma = +1, -K, \sigma = -1, +K$ . However, because of the selection rules only one line is observed.

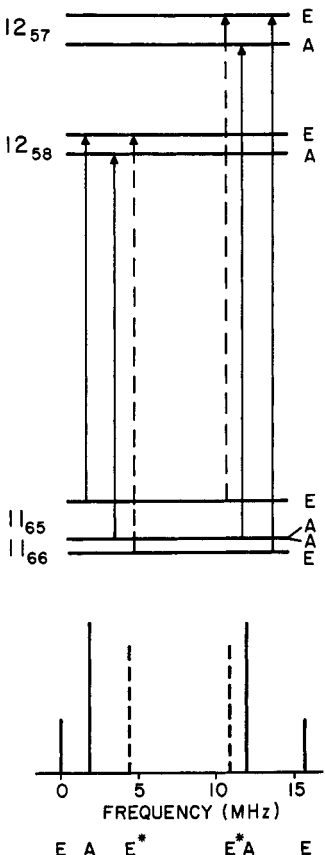


**Fig. 12.8** Forbidden transitions in propylene oxide where the asymmetry splitting and internal rotation splittings are comparable. The  $E^*$  transitions indicated by dashed lines which are allowed by the general selection rules ( $E \leftrightarrow E$ ) are forbidden for a limiting rigid rotor. From Herschbach and Swalen [11].

lines. These  $A-E$  doublets may be closely or widely spaced depending on the barrier height and transitions studied. The  $A$  lines will exhibit a pseudorigid rotor spectrum with possible pseudocentrifugal distortion effects if  $n=4$  terms are important. This may or may not be true for the  $E$  lines, depending on whether the odd  $n$  terms are important or not. Furthermore, the odd  $n$  terms can result in the observation of additional transitions which are forbidden for a usual rigid rotor as illustrated in Fig. 12.8. General selection rules are summarized in Table 12.5. Derivation of these rules from the symmetry properties of the Hamiltonian are discussed elsewhere [8].

Usually the barrier is determined from the ground torsional state, unless the doublet splittings are unobservable. For the ground torsional state the  $A$  line usually, but not always, appears at a higher frequency than the  $E$  line. When the barrier is high and the asymmetry large, the Stark effect of a given

**Table 12.5** General Selection Rules

Type of Molecule	Hamiltonian Group	Dipole Moment Symmetry	Selection Rules
No symmetry	$C_3^a$	$A$	$A \leftrightarrow A, E \leftrightarrow E$
Plane of symmetry	$D_3^b$	$A_2$	$A_1 \leftrightarrow A_2, E \leftrightarrow E$

<sup>a</sup>Symmetry species of  $C_3$  are  $E$  and  $A$ .

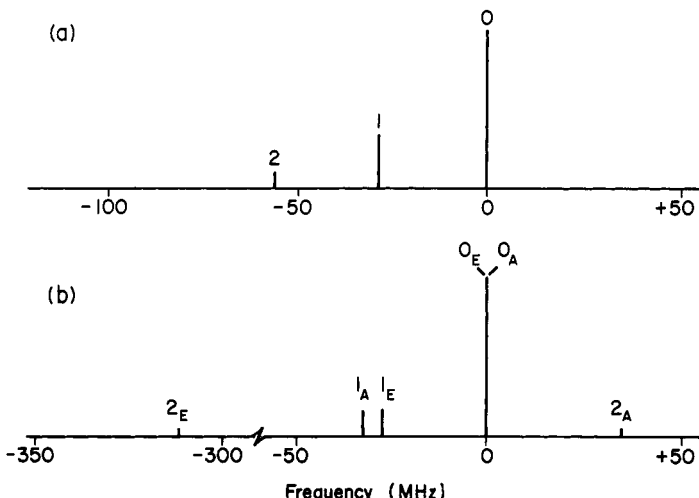
<sup>b</sup>Symmetry species of  $D_3$  are  $E$ ,  $A_1$ , and  $A_2$ .

rotational transition is essentially the same for both the  $A$  and  $E$  lines. If, however, the barrier is not sufficiently high or if the asymmetry is small, the  $E$  lines can show first-order Stark effects which arise because of the presence of the odd  $n$  terms in the Hamiltonian. If the nuclear statistical weights are taken into account, the intensity ratio of the  $A$  and  $E$  lines is 1:1 for the normal methyl group, whereas for the deuterated methyl group, the ratio is 11:16 with the  $E$  line stronger [27]. This applies to molecules with a planar frame and for those with a frame of no symmetry. These characteristics can be useful aids in distinction and assignment of the rotational spectra. It may be pointed out, however, that the barrier has been observed to change upon deuteration of the methyl group due to vibrational effects (for a tabulation see [43]).

If quadrupole coupling is present in addition to hindered internal rotation, the analysis is further complicated, especially if the contributions are of the same order of magnitude. In favorable cases, where the quadrupole and internal rotation coupling are independent of each other, the internal rotation and quadrupole perturbations are simply additive. This has been found, for example, in the acetyl halides ( $\text{CH}_3\text{COX}$ ) [55, 56]. Discussions of magnetic hyperfine interactions [57] in molecules with internal rotation, and quadrupole hyperfine interactions [58] for molecules with a  $C_s$  frame and  $C_{2v}$  top are available.

### Rotational Spectra in Excited Torsional States: $V_6$ Effects

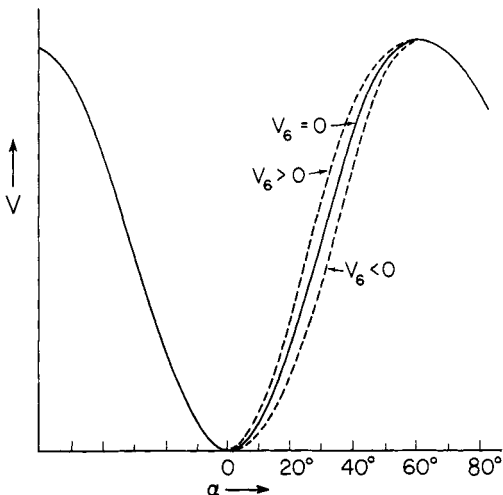
In addition to the transitions in the ground torsional state ( $v=0$ ), rotational transitions associated with excited torsional states ( $v \neq 0$ , called satellite lines) are often observable. Because of the interaction of molecular vibrations with the internal rotation and overall rotation, the rotational constants are slightly different in the excited torsional states, and hence the satellite lines are shifted from the ground torsional state line. These satellite lines which accompany each ground state rotational line decrease in intensity because of the Boltzmann factor; however, since the torsional frequencies are low, a number of satellite lines can be observable (see Fig. 12.9). Lines arising from other excited vibrational states are generally much weaker. The Stark pattern for the satellite lines will be essentially the same as that for the corresponding line for the ground torsional state. The splitting of the  $A$  and  $E$  satellite lines illustrated in Fig. 12.9



**Fig. 12.9** The ground state and torsional satellites of the  $1_{01} \rightarrow 2_{12}$  rotational transition of propylene oxide. For this molecule the same barrier is obtained for the first three torsional states. (a) The rotational lines of the ground and first two excited torsional states, shown without the internal rotation splitting. (b) The same pattern showing the splitting into the  $v_A$  and  $v_E$  doublets due to the effects of internal rotation. After Herschbach and Swalen [11].

can also be used for determination of the barrier. The analysis, however, can be more difficult because of the contribution of molecular vibrations to the satellite splitting. Fortunately, evidence indicates that the splitting of the  $A$  and  $E$  lines associated with the torsional state  $v$  is, in many cases, due almost entirely to internal rotation, and the vibrational effects may be ignored. In propylene oxide the same barrier is obtained for the first three torsional states [11]. The analysis is then no more difficult than for the ground state, that is, the  $A$  and  $E$  splittings associated with an excited torsional state  $v$  are treated with the working expressions outlined for the ground torsional state. This is particularly advantageous for molecules where the barrier is high enough to make the ground torsional state splittings too small to be observed. Because the perturbation coefficients  $W_{v\sigma}^{(n)}$  increase significantly with  $v$ , the splittings are magnified in excited torsional states and can become observable, thereby allowing the barrier to be determined [59]. The upper limit for resolvable ground state splitting occurs at about  $s=75$  (55 if only parallel transitions are accessible), while for the first and second excited state the upper limit on  $s$  is about 130 and 180, respectively [11].

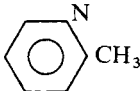
The investigation of excited torsional states is also advantageous for study of the effects of higher terms in the Fourier expansion of the hindering potential. The  $V_6$  constant has been found to be either positive or negative [14]; it modifies the shape of the barrier as demonstrated in Fig. 12.10. If the  $V_6$  term is treated as a perturbation, its contributions change only the values of the perturbation coefficients  $W_{v\sigma}^{(n)}$ . Perturbation calculations have been carried out to give the



**Fig. 12.10** The effect of a  $V_6$  term on the shape of the threefold potential function. The  $V_6$  term does not contribute to either the minimum or maximum of the potential, and the height of the barrier is hence unchanged. A positive  $V_6$  results in a narrower potential well and a broader maximum with the torsional levels becoming more widely separated. A negative  $V_6$  has just the opposite effect. From Fateley and Miller [14].

corrections to  $W_{v\sigma}^{(n)}$  caused by a small  $V_6$  term ( $V_6/V_3 < 5\%$ ) [28, 18]. The corrections, however, enter in such a way that  $V_6$  and  $V_3$  cannot be separately determined from data on a single torsional state  $v$ . Evaluation of the  $V_6$  term requires data from more than one torsional state. If  $V_6$  is important, it is found that the values of  $V_3$  obtained neglecting  $V_6$  vary systematically with torsional state, and by including the effect of a  $V_6$  term, the variation is effectively removed. Some examples of determinations of both  $V_3$  and  $V_6$  are given in Table 12.6. As apparent, the  $V_6$  constants are small compared to  $V_3$ . The variation of  $V_3$  with torsional state, which can be used to determine  $V_6$ , may also result from nonrigidity effects, that is, variations in  $I_\alpha$ ; and if both effects are present, they can be difficult to separate. Physically, as the methyl group rotates, the top is distorted due to a variation in barrier forces closing down slightly [60], for example, at the top of the barrier. Such structural relaxation has been termed torsional flexing [61]. The reduced rotational constant is hence a function of the torsional angle  $F(\alpha)$  and may be expressed in terms of a Fourier expansion. The torsional Hamiltonian is thus more complicated with additional kinetic energy terms being introduced. It has been demonstrated by Lees and Baker [62, 63] in the study of  $\text{CH}_3\text{OH}$  that from the spectrum of a single isotopic species it is impossible in first order to separate the effects of  $V_6$  from those of a variation in  $F$  because the first-order perturbation corrections due to  $V_6$  and torsional flexing are linear dependent. This nonseparability is reflected in a general way from the fact it is possible to transform [64, 65] the torsional Hamiltonian from a system in which  $F$  is a function of torsional angle and  $V_6$

**Table 12.6** Examples of  $V_3$  and  $V_6$  Barrier Evaluations

Molecule	$V_3(\text{cal/mole})$	$V_6(\text{cal/mole})$	Ref.
$\text{CH}_3\text{CH}_3$	2882	20	<sup>a</sup>
$\text{CH}_3\text{CH}_2\text{CN}$	3226	-172	<sup>b</sup>
$\text{CH}_3\text{CHO}$	1145	-31	<sup>c</sup>
$\text{CH}_3\text{COCN}$	1198	-13	<sup>d</sup>
$\text{CH}_3\text{COCOOH}$	972	-10	<sup>e</sup>
	258	-12	<sup>f</sup>

<sup>a</sup>Hirota et al. [67].<sup>b</sup>H. M. Meise, H. Mader, and H. Dreizler, *Z. Naturforsch.*, **31a**, 1228 (1976).<sup>c</sup>Bauder and Günthard [48].<sup>d</sup>G. K. Pandey and H. Dreizler, *Z. Naturforsch.*, **33a**, 204 (1978).<sup>e</sup>R. Meyer and A. Bauder, *J. Mol. Spectrosc.*, **94**, 136 (1982).<sup>f</sup>H. Dreizler, H. D. Rudolph, and H. Mäder, *Z. Naturforsch.*, **25a**, 25 (1970).

is zero, to one in which  $F$  is constant and  $V_6$  is nonzero. A review of this problem has been given by Lees [61], and the importance of considering torsional flexing in the determination of  $V_6$  is pointed out particularly for molecules with light frameworks such as  $\text{CH}_3\text{OH}$ . In this regard, it may be noted that a detailed treatment [66] of a number of isotopic species of  $\text{CH}_3\text{OH}$ , including  $V_6$  and torsional flexing effects, has lead to an essentially zero value for  $V_6 (= -0.07 \pm 0.21 \text{ cm})$ . By measurement of various isotopic forms of ethane [67], and assessing the isotopic effects in the internal-rotation potential constants both  $V_3$  and  $V_6$  have been evaluated (see Table 12.6).

Investigations of the effect on the barrier due to zero-point vibrational averaging and distortion on geometry during internal rotation have been reported [60, 68]. In ethane, calculations indicate that the vibrational averaging correction ( $374 \pm 90 \text{ cal/mole}$ ), which raises the barrier, is larger and of opposite sign to the distortion correction ( $-161 \pm 20 \text{ cal/mole}$ ).

### Stark Effect

As remarked previously, it is possible for certain  $E$  level transitions to exhibit a first-order Stark effect. This is readily demonstrated, as discussed by Lin and Swalen [8]. Consider the Hamiltonian

$$\mathcal{H} = AP_z^2 + BP_x^2 + CP_y^2 + DP_z \quad (12.76)$$

where

$$D = \frac{FW_{vE}^{(1)}\lambda_z I_\alpha}{I_z} \quad (12.77)$$

Because of the presence of the linear  $P_z$  term in this Hamiltonian, the Wang functions are no longer the proper zeroth-order wave functions. For example, an eigenfunction for  $J=1$  and  $K$  odd can be written as

$$\Psi = a\psi(J=1, K=1, M) + b\psi(J=1, K=-1, M) \quad (12.78)$$

where  $a \neq b$ . The expansion coefficients, which can be evaluated in the usual way, are found to depend on both the asymmetry and the barrier. The average of the Stark operator,  $-\mu_z \mathcal{E} \Phi_{zz}$ , may be expressed as follows

$$-\mu_z \mathcal{E} \int \Psi^* \Phi_{zz} \Psi d\tau = \frac{-\mu_z \mathcal{E} (a^2 - b^2) KM}{J(J+1)} \quad (12.79)$$

with  $J=1, K=1$ . Because of the unequal mixing of the  $K$  and  $-K$  symmetric rotor basis functions the first-order Stark effect term is nonvanishing, and a linear Stark effect can thus result for  $K \neq 0, M \neq 0$ . The first-order Stark effect decreases rapidly as the barrier height increases. This mixing of the rigid rotor wave functions is also responsible for the appearance of forbidden transitions. For similar reasons the spectra of asymmetric rotors with very low barriers and  $m \neq 0, \pm 3$  (discussed in Section 8) can show first-order Stark effects.

A general expression for the first-order Stark effect of the  $J \rightarrow J+1, K_{-1}=1$  transitions has been given by Beaudet [69]. For a given  $J \rightarrow J+1, K_{-1}=1$  transition of a prolate rotor the frequency splitting between the  $+|M|$  and  $-|M|$  Stark component is given by

$$\Delta\nu = \frac{8\mu_z \mathcal{E} D |M|}{(B-C)} \left\{ \left[ \frac{1}{J^2(J+1)^2} - \frac{1}{J'^2(J'+1)^2} \right] - \left[ \frac{1}{J^4(J+1)^4} - \frac{1}{J'^4(J'+1)^4} \right] \frac{8D^2}{(B-C)^2} \right\} + \dots \quad (12.80)$$

where  $J' (= J+1)$  is the higher of the two  $J$  levels and  $D$  is the coefficient of the linear  $P_z$  term defined in (12.77). Since the first-order Stark effect is sensitive to the barrier, via the  $D$  constant, it provides a means of determining the barrier. The Stark effect of the  $1_{11} \rightarrow 2_{12}$  transition is illustrated in Fig. 12.11 from the work of Beaudet and Wilson [70] on *cis*-fluoropropylene,  $\text{CH}_3\text{CH}=\text{CHF}$ . The  $A$  and  $E$  transitions were not resolved and four Stark components were found; two linear and two quadratic in the field. One of the second-order Stark components is assigned to the  $|M|=1$  component of the  $A$  transition, and the two components linear in the electric field are assigned to the  $M=+1$  and  $M=-1$  components of the  $E$  transition. The remaining second-order component is assigned to  $M=0$  for both the  $A$  and  $E$  transitions and is not shown in the figure. From the observed splitting of the  $M=+1$  and  $M=-1$  components of the  $E$  transition the barrier height to internal rotation of the methyl group was determined to be 1037 cal/mole, which may be compared with the value 1057 cal/mole obtained from the line splittings. A general theory of the Stark effect in molecules with one or two symmetric tops based on the concept of isometric groups is described by Bossert et al. [71].

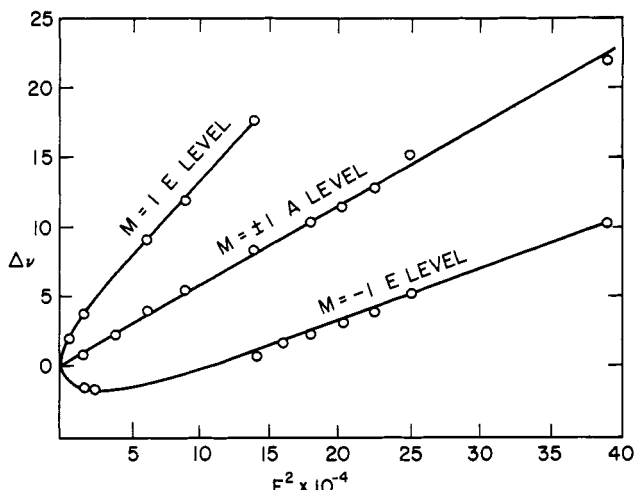


Fig. 12.11 Stark effect of the  $1_{11} \rightarrow 2_{12}$  transition of *cis*-CH<sub>3</sub>CH=CHF. From Beaudet and Wilson [70].

### Example of a Barrier Calculation

As an illustration of the theory we look at a simple example of a barrier height evaluation using the observed splitting of the  $0_{00} \rightarrow 1_{01}$  transition of acetaldehyde, which was found to be  $(v_A - v_E) = 3.0$  MHz. Acetaldehyde is a prolate rotor, and the  $x, y, z$  axes are associated with symbols  $A_{v\sigma}, \dots$ , as follows:  $(x, B_{v\sigma}), (y, C_{v\sigma}), (z, A_{v\sigma})$  where  $A_{v\sigma} > B_{v\sigma} > C_{v\sigma}$  and the  $xz$  plane is taken as the plane of symmetry of the molecule. Employing the structural parameters for acetaldehyde (Table 10 of [27]) we find for the moments of inertia (amu Å<sup>2</sup>)

$$\begin{array}{ll} I_x(I_b) = 49.723 & I_z(I_a) = 8.945 \\ I_y(I_c) = 55.545 & I_\alpha = 3.123 \end{array}$$

If we take the symmetry axis of the methyl group as coaxial with the carbon–carbon bond the direction cosines are

$$\lambda_z = \cos 23^\circ 1' = 0.9204 \quad \lambda_x = \cos 66^\circ 59' = 0.3910$$

with  $\lambda_y = 0$ , since the  $y(c)$  axis is perpendicular to the plane containing the methyl group axis. For the internal rotation parameters we have

$$\begin{array}{ll} \rho_x = 0.02456 & \rho_z = 0.32134 \\ r = 0.6946 & F = 233.0 \text{ GHz} \end{array}$$

We may apply (12.63)–(12.67) to the splitting of the  $0_{00} \rightarrow 1_{01}$  transition, and since  $\lambda_y = 0$  we have  $\Delta C = 0$ . For the  $0_{00}$  level  $E(\kappa) = 0$ ,  $\partial E / \partial A = \partial E / \partial B = 0$ , and we have

$$\Delta E(0_{00}) = 0$$

while for the  $1_{01}$  level  $E(\kappa) = \kappa - 1$ ,  $\partial E / \partial A = 0$ ,  $\partial E / \partial B = 1$ . This gives

$$\Delta E(1_{01}) = \Delta B = B_{0A} - B_{0E}$$

The expression for the splitting ( $\Delta v = v_A - v_E$ ) of the transition is therefore

$$\begin{aligned}\Delta v &= \Delta B = F \rho_x^2 [W_{0A}^{(2)} - W_{0E}^{(2)}] \\ &= 140.54 [W_{0A}^{(2)} - W_{0E}^{(2)}]\end{aligned}$$

From the observed ground torsional state splitting of 3.0 MHz one obtains the difference in the barrier-dependent perturbation coefficients

$$\Delta W_0^{(2)} = W_{0A}^{(2)} - W_{0E}^{(2)} = 0.02135$$

By making use of the following quantities:

$s$	$W_{0A}^{(2)}$	$W_{0E}^{(2)}$	$\Delta W_0^{(2)}$
22	0.01710	-0.008550	0.025650
23	0.01436	-0.007179	0.021539
24	0.01210	-0.006046	0.018146

a linear interpolation yields  $s = 23.06$ , which gives

$$\begin{aligned}V_3 &= \frac{sF}{4.6602} \\ &= \frac{(23.06)(233.0)}{4.6602} = 1153 \text{ cal/mole}\end{aligned}$$

for the barrier height. The conversion factor 4.6602 gives  $V_3$  in cal/mole when  $F$  is expressed in GHz.

## 7 HIGH-BARRIER SYMMETRIC ROTORS

The method for determining barrier heights described for asymmetric rotors, which utilizes splittings of rotational transitions arising from the direct effects of internal rotation, is not applicable for symmetric rotors. To demonstrate this, let us look at the effective rotational Hamiltonian for a symmetric rotor. For a symmetric top with an internal rotor, illustrated in Fig. 12.12,  $B_y = A_x$  and  $\mathcal{P}$  reduces to:  $\mathcal{P} = \rho P_z$ , where  $\rho = I_a/I_z$ . The Hamiltonian of (12.53) can thus be written as

$$\mathcal{H}_{v\sigma} = A_x(P_x^2 + P_y^2) + C_x P_z^2 + F \sum_n W_{v\sigma}^{(n)} (\rho P_z)^n \quad (12.81)$$

where  $F = \hbar^2 I_z / [2I_a(I_z - I_a)]$ . The  $W_{v\sigma}^{(n)}$  are the barrier-dependent perturbation coefficients defined previously. The rigid symmetric rotor functions yield a diagonal matrix for this effective rotational Hamiltonian. The rotational energies for the torsional state  $v\sigma$  are

$$E_{JKv\sigma} = A_x J(J+1) + (C_z - A_x) K^2 + F \sum_n W_{v\sigma}^{(n)} (\rho K)^n \quad (12.82)$$

## Chapter XIII

# DERIVATION OF MOLECULAR STRUCTURES

---

1	INTRODUCTION	647
2	RELATION OF MOLECULAR DIMENSIONS TO MOMENTS OF INERTIA	649
3	SINGLE ISOTOPIC SUBSTITUTION: KRAITCHMAN'S EQUATIONS	656
	Linear Molecules	658
	Symmetric-top Molecules: Location of an Atom on the Symmetry Axis	658
	Symmetric-top Molecules: Location of an Atom off the Symmetry Axis	659
	Asymmetric-top Molecules: Planar	660
	Asymmetric-top Molecules: Nonplanar	661
4	MULTIPLE SUBSTITUTION	665
5	EVALUATION OF STRUCTURES: GENERAL CONSIDERATIONS	667
6	EVALUATION OF EQUILIBRIUM STRUCTURES	672
	Correction for Vibrational Effects	672
	Higher-order Corrections	675
	Equilibrium Structures for Polyatomic Molecules	677
7	EVALUATION OF EFFECTIVE STRUCTURES	679
	Inertial Defect	684
8	EVALUATION OF SUBSTITUTION STRUCTURES	691
9	EVALUATION OF AVERAGE STRUCTURES	706
10	EVALUATION OF MASS-DEPENDENCE STRUCTURES	714
11	DIAGNOSTIC LEAST SQUARES	717

## 1 INTRODUCTION

Microwave spectroscopy provides one of the most widely applicable and accurate methods for evaluation of molecular structures. This structural information is contained in the principal moments of inertia,  $I_a$ ,  $I_b$ ,  $I_c$ , which are derivable from the spectroscopic constants  $A$ ,  $B$ ,  $C$ , that is,

$$I_a = \frac{h}{8\pi^2 A} \quad I_b = \frac{h}{8\pi^2 B} \quad I_c = \frac{h}{8\pi^2 C}$$

with [1]

$$\frac{h}{8\pi^2} = 505,376 \text{ amu } \text{\AA}^2 \text{ MHz}$$

for  $I_a, \dots$ , expressed in atomic mass units-angstrom units squared and  $A, \dots$ , in megahertz. Of course, before the moments of inertia can be related to the bond lengths and bond angles, the job of assigning the rotational spectrum must be accomplished, that is, correlating the spectroscopic constants and the quantum numbers to the spectral lines. Usually, the spectrum of isotopically substituted molecular species must also be studied to provide sufficient data for the evaluation of the structural parameters. Because, however, of the high sensitivity characteristics of microwave spectroscopy such molecular species can, in many cases, be studied in natural abundance.

Molecular structural parameters, in particular bond lengths, have been the major source of data used to obtain a more detailed understanding of the chemical bond. Explanations of observed trends in structural parameters in terms of such concepts as resonance, hybridization, bond order, conjugation, hyperconjugation, ionic character, and nonbonded interactions, have been vigorously pursued since the introduction of the modern concept of a chemical bond. A study of the factors influencing bond lengths and bond angles requires, of course, an appreciation of the accuracy of the derived molecular parameters and the type of structural parameter obtained. Because of the accuracy of the experimental measurements the moments of inertia may be obtained to six or more significant figures. However, evaluation of structural parameters with an accuracy comparable to that of the moments of inertia has proved to be a difficult problem for spectroscopists. The primary source of the problem is not the uncertainties in Planck's constant or the atomic masses but rather the fact that the dimensions of a molecule are affected by its vibrational energy even in its ground vibrational state. Unless corrections are made for these effects, the meaningfulness of the structural parameters, derived from the observed moments of inertia, is limited to much less than six significant figures. Except for diatomic and some simple polyatomic molecules, the explicit correction of the moments of inertia for vibrational contributions has not been possible because of the difficulties in obtaining the required experimental data. Different procedures have been introduced which correct to various degrees for vibrational effects and which have led to different conceptions of interatomic distance. In particular, five types of bond lengths are defined:

1.  $r_e$ , the equilibrium bond length for the hypothetical vibrationless state, evaluated by correction for the effects of vibration including zero-point vibrations, as described in Section 6.
2.  $r_0$ , the effective bond length for the ground vibrational state, calculated from the  $B_0$  or  $I^0$  values as described in Section 7.
3.  $r_s$ , the substitution bond length, derived from the isotopic substitution method described in Section 8.

4.  $\langle r \rangle$  (or  $r_z$ ), the average bond length associated with the average configuration of the atoms, evaluated by a partial correction for the effects of vibration, as described in Section 9.

5.  $r_m$ , the mass dependence bond length, derived from a large number of isotopic species by a first-order treatment of isotopic effects, as described in Section 10.

With the hundreds of molecules that have now been studied by microwave spectroscopy, particularly in the last 10 years, it is no longer possible to provide a reasonably complete compilation of molecular structures in a limited space. In a previous edition of this book [2] a relatively complete compilation to about 1969 was given. Since that time a critical compilation of structures has been given by Harmony et al. [3] covering the period from the late 1940s to halfway through 1977. These authors classify the structural parameters ( $r_e$ ,  $r_0$ ,  $r_s$ ,  $\langle r \rangle$ ) and indicate the range of uncertainty to be associated with the parameters. This is particularly useful as a guide in making realistic evaluations of variations in structural parameters. Another publication [4] lists the best available structural data up to 1974 on more than 1200 molecules.

## 2 RELATION OF MOLECULAR DIMENSIONS TO MOMENTS OF INERTIA

The components of the moment of inertia tensor (see Chapter II, Section 1) may be arranged into a square matrix

$$\mathbf{I} = \begin{bmatrix} I_{xx} & I_{xy} & I_{xz} \\ I_{xy} & I_{yy} & I_{yz} \\ I_{xz} & I_{yz} & I_{zz} \end{bmatrix} \quad (13.1)$$

which is symmetric, with the diagonal elements, or moments of inertia, defined as

$$\begin{aligned} I_{xx} &= \sum_i m_i(y_i^2 + z_i^2) \\ I_{yy} &= \sum_i m_i(x_i^2 + z_i^2) \\ I_{zz} &= \sum_i m_i(x_i^2 + y_i^2) \end{aligned} \quad (13.2)$$

and the off-diagonal elements, or products of inertia, defined as

$$\begin{aligned} I_{yx} &= I_{xy} = -\sum_i m_i x_i y_i \\ I_{zx} &= I_{xz} = -\sum_i m_i x_i z_i \\ I_{zy} &= I_{yz} = -\sum_i m_i y_i z_i \end{aligned} \quad (13.3)$$

In the foregoing equations for the elements of  $\mathbf{I}$ ,  $m_i$  is the mass of the  $i$ th atom,  $x_i, y_i, z_i$  are the corresponding coordinates measured from the origin of a Cartesian coordinate system fixed in the molecule, and the sum is over all atoms of the molecule. The elements of the inertia matrix depend on both the origin and orientation of the coordinate system. The origin, of course, is to be taken at the center of mass. (This choice allows the translational and rotational motions to be treated separately.) For any choice of origin, it is possible to choose an orientation of the coordinate axis in the molecule such that the inertia matrix is diagonal, that is, the products of inertia vanish. These axes for which the products of inertia vanish are called the principal axes, and the diagonal elements of  $\mathbf{I}$  are known as the principal moments of inertia. Our interest lies in the center-of-mass principal moments of inertia since it is these quantities that are determined from an analysis of the rotational spectrum; we shall designate them as  $I_x, I_y, I_z$ .

For a rotation of coordinate axes, the components of a position vector with respect to the "old" and the "new" (rotated) coordinate system are related by a linear transformation. In matrix notation we have simply

$$\mathbf{r} = \mathbf{R}\mathbf{r}' \quad (13.4)$$

or

$$\begin{bmatrix} x \\ y \\ z \end{bmatrix} = \mathbf{R} \begin{bmatrix} x' \\ y' \\ z' \end{bmatrix}$$

where  $\mathbf{R}$  is a square  $3 \times 3$  orthogonal matrix. The primed symbols refer to the new rotated coordinate system which we may consider here to be the principal axis system of the molecule. Under such an orthogonal transformation of coordinates, the transformed moment of inertia matrix  $\mathbf{I}'$  is given by

$$\mathbf{I}' = \tilde{\mathbf{R}}\mathbf{I}\mathbf{R} \quad (13.5)$$

where  $\tilde{\mathbf{R}}$  is the transpose of  $\mathbf{R}$ . The new moment of inertia matrix is said to be obtained by a similarity transformation of  $\mathbf{I}$ . If the transformation takes  $\mathbf{I}$  from an arbitrary system to the principal axis system, the resulting matrix,  $\mathbf{I}'$ , is diagonal. The transformation matrix has a very simple form for the special case for which all but one of the products of inertia vanish, for example,  $I_{xy}$ , which is easily obtainable if initially at least one principal axis (here we take this to be the  $z$  axis) is known. In this particular case, the transformation matrix corresponds to a simple rotation about the  $z$  axis (see Fig. 13.1) that is,

$$\mathbf{R} = \begin{bmatrix} \cos \theta & -\sin \theta & 0 \\ \sin \theta & \cos \theta & 0 \\ 0 & 0 & 1 \end{bmatrix} \quad (13.6)$$

and we may choose the matrix  $\mathbf{R}$  such that it diagonalizes  $\mathbf{I}$  by requiring that

$$\tan 2\theta = \frac{2I_{xy}}{I_{xx} - I_{yy}} \quad (13.7)$$

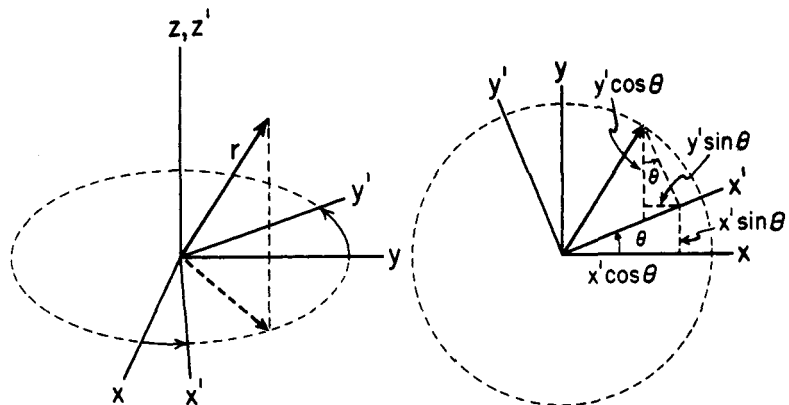


**Fig. 13.1** Rotation of the coordinate axes about the  $z$  axis by an angle  $\theta$  takes the unprimed  $xyz$  coordinate system into the  $x'y'z'$  coordinate system. From the construction, the components of a position vector in the unprimed coordinate system are readily related to those in the primed coordinate system. In particular, the components in the unprimed system are:  $(x' \cos \theta - y' \sin \theta, x' \sin \theta + y' \cos \theta, z')$ . The transformation matrix  $R$  between the primed and unprimed systems is hence given by (13.6) of the text.

The principal moments of inertia may hence be readily calculated by carrying out the matrix multiplication indicated in (13.5) with  $\theta$  determined from (13.7). The principal moment about the  $z$  axis is  $I_z = I_{zz}$ , and the remaining two principal moments may be expressed by the relation

$$I = \left( \frac{I_{xx} + I_{yy}}{2} \right) \pm \left( \frac{I_{xx} - I_{yy}}{2} \right) (1 + \tan^2 2\theta)^{1/2} \quad (13.8)$$

This procedure is applicable, in many cases, since at least one principal axis may often be located from symmetry considerations.

A principal axis is always associated with an  $n$ -fold axis of rotational symmetry,  $C_n$ . When  $n \geq 3$ , the molecule is a symmetric top. The methyl chloride molecule, for example, possesses an axis of threefold symmetry, the axis passing through the chlorine and carbon atoms. In addition, for a symmetric top, any axis passing through the center of mass and perpendicular to the symmetry axis will be a principal axis. This is reflected in the fact that two of the principal moments of inertia are equal. Furthermore, if a molecule has a plane of symmetry, then an axis perpendicular to the symmetry plane is a principal axis. The other two principal axes lie in the symmetry plane and might be obtained, as outlined previously, by consideration of a rotation of coordinate axes in the plane of symmetry.

In general, when none of the principal axes is obvious from symmetry, one can choose any convenient reference system  $x, y, z$  in the molecule and calculate the elements of the inertia tensor from (13.2) and (13.3); one can then diagonalize the tensor to obtain the principal elements [5]. Let us assume that  $R_{xa}$ ,  $R_{ya}$ , and  $R_{za}$  are the cosines of the angles between a principal inertial axis  $a$  and the arbitrary axes  $x, y, z$ ;  $R_{xa} = \cos(x, a)$ , and so on. Since the off-diagonal elements

of the inertia tensor vanish in the principal coordinate system

$$\begin{bmatrix} I_{xx} & I_{xy} & I_{xz} \\ I_{yx} & I_{yy} & I_{yz} \\ I_{zx} & I_{zy} & I_{zz} \end{bmatrix} \begin{bmatrix} R_{xa} \\ R_{ya} \\ R_{za} \end{bmatrix} = I_a \begin{bmatrix} R_{xa} \\ R_{ya} \\ R_{za} \end{bmatrix} \quad (13.9)$$

where  $I_a$  is a constant. When the indicated matrix multiplications are performed and the corresponding elements equated, the three resulting equations, upon rearrangement, can be expressed as

$$(I_{xx} - I_a)R_{xa} + I_{xy}R_{ya} + I_{xz}R_{za} = 0 \quad (13.10)$$

$$I_{yx}R_{xa} + (I_{yy} - I_a)R_{ya} + I_{yz}R_{za} = 0 \quad (13.11)$$

$$I_{zx}R_{xa} + I_{zy}R_{ya} + (I_{zz} - I_a)R_{za} = 0 \quad (13.12)$$

These three simultaneous equations in the three unknown cosines  $R_{xa}$ ,  $R_{ya}$ , and  $R_{za}$  have nontrivial solutions only if the determinant of the coefficients vanishes. Therefore,

$$\begin{vmatrix} I_{xx} - I_a & I_{xy} & I_{xz} \\ I_{yx} & I_{yy} - I_a & I_{yz} \\ I_{zx} & I_{zy} & I_{zz} - I_a \end{vmatrix} = 0 \quad (13.13)$$

Solution of this cubic equation yields three values of  $I_a$  corresponding to the three principal values of the moments of inertia. Each of these values, when substituted for  $I_a$  in (13.10)–(13.12), yields a set of three equations which with the auxiliary relation  $R_{xa}^2 + R_{ya}^2 + R_{za}^2 = 1$  can be solved for the direction cosines between the  $x$ ,  $y$ ,  $z$  system and the axis of the principal element which is substituted. The auxiliary relation is required because (13.10)–(13.12) yield only the ratios of the direction cosines.

It will be convenient to have at our disposal expressions for the moments

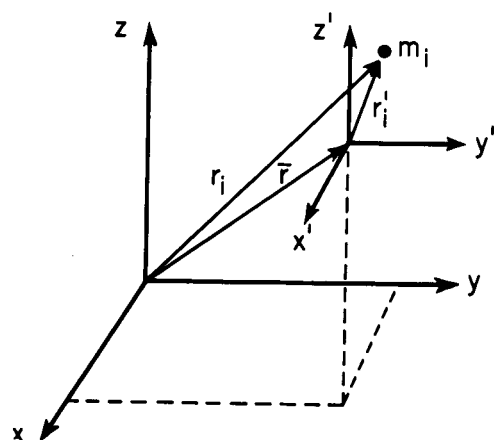


Fig. 13.2 Location of the center of mass and of the  $i$ th atom with respect to an arbitrary origin.

and products of inertia with respect to the center of mass even when the coordinates are measured with respect to an arbitrary origin. In Fig. 13.2 the position vector to the  $i$ th atom measured from the arbitrary origin is designated by  $\mathbf{r}_i$ ; the vector distance of the center of mass from the arbitrary origin is designated by  $\bar{\mathbf{r}}$ ; and  $\mathbf{r}'_i$  represents the distance of the  $i$ th atom from the center of mass. The three vectors are related by the equation

$$\mathbf{r}_i = \bar{\mathbf{r}} + \mathbf{r}'_i \quad (13.14)$$

Multiplying by  $m_i$  and summing over all atoms, we have for the position vector of the center of mass measured from the arbitrary origin

$$\bar{\mathbf{r}} = \frac{\sum_i m_i \mathbf{r}_i}{\sum_i m_i} \quad (13.15)$$

since by definition of the center of mass (sometimes called the first moment equation)

$$\sum m_i \mathbf{r}'_i = 0 \quad (13.16)$$

Hence, the coordinates of the  $i$ th atom measured from the center of mass ( $x'_i, y'_i, z'_i$ ) in terms of the coordinates measured from the arbitrary origin may be expressed by

$$x'_i = x_i - \frac{\sum_i m_i x_i}{\sum_i m_i} \quad (13.17)$$

and so on. Substitution of the above into the general definition of the moments and products of inertia, (13.2) and (13.3), gives

$$I_{xx}(\text{cm}) = \sum_i m_i (y_i^2 + z_i^2) - \frac{(\sum_i m_i y_i)^2}{\sum_i m_i} - \frac{(\sum_i m_i z_i)^2}{\sum_i m_i} \quad (13.18)$$

and so on, and

$$I_{xy}(\text{cm}) = - \sum_i m_i x_i y_i + \frac{(\sum_i m_i x_i)(\sum_i m_i y_i)}{\sum_i m_i} \quad (13.19)$$

and so on. These expressions give the moments of inertia with respect to the center of mass, with the coordinates measured with respect to an arbitrary origin. If the arbitrary origin is chosen as the center of mass, then only the first terms in  $I_{xx}, I_{xy}, \dots$ , are nonvanishing. In any event, use of these equations and subsequent diagonalization of the inertia matrix gives the principal moments of inertia with respect to the center of mass.

When the rotational spectrum of a prospective molecule is being considered, much information about the spectrum to be expected can usually be obtained from moments of inertia evaluated from an assumed structure which is derived from a judicious choice of molecular parameters of similar molecules [6]. When information on similar molecules is not available, a convenient first approximation to the structure may be gained from addition of covalent bond radii given

in Appendix F. A comparison of these idealized bond lengths and the actual bond lengths can also give information on the nature of the bonds. The foregoing expressions are particularly useful for calculation of the moments of inertia since, in many cases, it is convenient to choose an origin for the coordinate system other than the center of mass for evaluation of the coordinates of the atoms. For some simple molecules, the moments of inertia may be readily expressed in terms of the bond lengths and bond angles of the molecule. In Table 13.1 explicit expressions for the principal moments of inertia of a few simple molecules are collected. For large molecules, the evaluation of the Cartesian coordinates of all the atoms becomes a rather tedious task. However, Schwendeman [7] has discussed a computer program for calculation of moments of inertia which is particularly convenient, since it uses directly as input data the structural parameters in the form of bond lengths and bond angles rather than Cartesian coordinates.

**Table 13.1** Expressions for the Moments of Inertia of Some Simple Molecules<sup>a</sup>

Molecule	Moments of Inertia
Diatom, XY	$I = \left( \frac{m_X m_Y}{m_X + m_Y} \right) d_{XY}^2$
Linear, XY <sub>2</sub>	$I = 2m_Y d_{XY}^2$
Linear, XYZ	$I = \frac{1}{M} [m_X m_Y d_{YX}^2 + m_Y m_Z d_{YZ}^2 + m_X m_Z (d_{YX} + d_{YZ})^2]$
Bent, XY <sub>2</sub> <sup>b</sup>	$I_x = 2m_Y d_{XY}^2 \sin^2 \frac{\theta}{2}$ $I_y = \frac{2m_X m_Y}{M} d_{XY}^2 \cos^2 \frac{\theta}{2}$ $I_z = I_x + I_y$
Bent, XYZ <sup>c</sup>	$I_{xx} = \frac{\sin^2(\theta/2)}{M} [m_X(m_Y + m_Z)d_{YX}^2 + m_Z(m_X + m_Y)d_{YZ}^2 + 2m_X m_Z d_{YX} d_{YZ}]$ $I_{yy} = \frac{\cos^2(\theta/2)}{M} [m_X(m_Y + m_Z)d_{YX}^2 + m_Z(m_X + m_Y)d_{YZ}^2 - 2m_X m_Z d_{YX} d_{YZ}]$ $I_{xy} = \frac{\sin(\theta/2) \cos(\theta/2)}{M} [m_X(m_Y + m_Z)d_{YX}^2 - m_Z(m_X + m_Y)d_{YZ}^2]$
Pyramidal, XY <sub>3</sub> <sup>d</sup>	$I_x = I_y = 2m_Y d_{XY}^2 \sin^2 \frac{\theta}{2} + \frac{m_X m_Y}{M} d_{XY}^2 \left( 3 - 4 \sin^2 \frac{\theta}{2} \right)$ $I_z = 4m_Y d_{XY}^2 \sin^2 \frac{\theta}{2}$

**Table 13.1** (Continued)

Molecule	Moments of Inertia
Planar, $ZXY_2^b$	$I_x = 2m_Y d_{XY}^2 \sin^2 \frac{\theta}{2}$ $I_y = \frac{1}{M} \left[ m_Z(2m_Y + m_X)d_{XZ}^2 + 2m_Y(m_X + m_Z)d_{XY}^2 \cos^2 \frac{\theta}{2} + 4m_Y m_Z d_{XZ} d_{XY} \cos \frac{\theta}{2} \right]$ $I_z = I_x + I_y$
Axial symmetric, $ZXY_3^d$	$I_x = I_y = 2m_Y d_{XY}^2 \sin^2 \frac{\theta}{2} + \left( \frac{3m_Y}{M} \right) (m_X + m_Z) d_{XY}^2 \left( 1 - \frac{4}{3} \sin^2 \frac{\theta}{2} \right) + \left( \frac{m_Z d_{XZ}}{M} \right) \left[ (3m_Y + m_X) d_{XZ} + 6m_Y d_{XY} \left( 1 - \frac{4}{3} \sin^2 \frac{\theta}{2} \right)^{1/2} \right]$ $I_z = 4m_Y d_{XY}^2 \sin^2 \frac{\theta}{2}$

<sup>a</sup>The  $d_{ij}$  is the bond distance between atoms  $i$  and  $j$ ,  $M$  is the total mass of the appropriate molecule.

<sup>b</sup>The  $x$  axis corresponds to the  $C_2$  axis, with the  $z$  axis perpendicular to the  $xy$  plane and with  $\theta$  as the  $Y-X-Y$  bond angle.

<sup>c</sup>The remaining off-diagonal elements of the inertia matrix vanish. Here the principal moments of inertia  $I_x$  and  $I_y$  must be evaluated from (13.12) of the text. The  $x$  axis is parallel to the axis bisecting the  $X-Y-Z$  bond angle  $\theta$  with the  $z$  axis perpendicular to the  $xy$  plane. Note that  $I_z = I_{xx} + I_{yy} = I_x + I_y$ .

<sup>d</sup>The  $z$  axis is the  $C_3$  symmetry axis and  $\theta$  is the  $Y-X-Y$  bond angle. Note that the acute angle  $\beta$  between the  $X-Y$  bond and the symmetry axis is related to the bond angle by  $\sin(\theta/2) = (3^{1/2}/2) \sin \beta$ .

For the treatment of a general asymmetric rotor it is sometimes convenient to use another symmetric tensor whose elements are defined as [8]

$$P_{xx} = \sum m_i x_i^2 \quad (13.20)$$

and so on, and

$$P_{xy} = \sum m_i x_i y_i \quad (13.21)$$

and so on. The diagonal elements of  $\mathbf{P}$  are called the planar moments of inertia while the off-diagonal elements are equivalent to the products of inertia except for the sign. (The symbol  $\mathbf{P}$  used here should not be confused with angular momentum which has in earlier chapters also been designated by  $\mathbf{P}$ .) The two matrices are related by the matrix equation

$$\mathbf{I} = d\mathbf{E} - \mathbf{P} \quad (13.22)$$

with  $d = \sum_i m_i(x_i^2 + y_i^2 + z_i^2)$  and with  $\mathbf{E}$  a  $3 \times 3$  unit matrix.  $\mathbf{I}$  and  $\mathbf{P}$  have the same transformation properties; since  $d\mathbf{E}$  is invariant with respect to a similarity transformation, that is, a rotation of axes, the roots are related by

$$I_x = d - P_x \quad (13.23)$$

and so on. Furthermore, we may write

$$2d = I_x + I_y + I_z = 2(P_x + P_y + P_z) \quad (13.24)$$

so that the following relations between the principal moments of  $\mathbf{I}$  and  $\mathbf{P}$  may be given as

$$P_x = \frac{1}{2}(-I_x + I_y + I_z) \quad (13.25)$$

and so on

$$I_x = P_y + P_z \quad (13.26)$$

and so on. Expressions for  $P_y$  and  $P_z$  are obtained by cyclic permutation of the subscripts  $x, y, z$ . Typical elements of  $\mathbf{P}$  computed with respect to the center of mass with an arbitrary origin for the coordinate system have the form

$$P_{xx}(\text{cm}) = \sum_i m_i x_i^2 - \frac{(\sum_i m_i x_i)^2}{\sum_i m_i} \quad (13.27)$$

and so on, and

$$P_{xy}(\text{cm}) = \sum_i m_i x_i y_i - \frac{(\sum_i m_i x_i)(\sum_i m_i y_i)}{\sum_i m_i} \quad (13.28)$$

and so on. When the arbitrary origin of the coordinate system is at the center of mass, the second term of the above expressions vanishes.

### 3 SINGLE ISOTOPIC SUBSTITUTION: KRAITCHMAN'S EQUATIONS

Kraitchman [8] has given a convenient method for calculation of the position of an atom in a molecule which utilizes the changes in moments of inertia resulting from a single isotopic substitution of the atom. Specifically, the principal axis coordinates of the atom are derived; and once a sufficient number of coordinates have been ascertained, the structure of the molecule may be readily evaluated. In the following discussion, we consider the equations developed by Kraitchman for various types of molecules.

The principal moments of inertia of the parent molecule and of the isotopically substituted molecule will be denoted by  $I_x, I_y, I_z$  and  $I'_x, I'_y, I'_z$ , respectively. The coordinates  $x_i, y_i, z_i$  will be measured from the center-of-mass principal axis system of the parent molecule. Furthermore, the molecule is assumed rigid so that the bond distances and angles are unchanged by isotopic substitution.

For the center-of-mass principal axis system of the parent molecule the

elements of  $\mathbf{I}$  are, from (13.18) and (13.19):

$$I_x = I_{xx} = \sum m_i(y_i^2 + z_i^2) \quad (13.29)$$

$$I_y = I_{yy} = \sum m_i(x_i^2 + z_i^2) \quad (13.30)$$

$$I_z = I_{zz} = \sum m_i(x_i^2 + y_i^2) \quad (13.31)$$

$$I_{xy} = -\sum m_i x_i y_i = 0 \quad (13.32)$$

$$I_{xz} = -\sum m_i x_i z_i = 0 \quad (13.33)$$

$$I_{yz} = -\sum m_i y_i z_i = 0 \quad (13.34)$$

If a single isotopic substitution is made for some atom of the molecule, depending on the molecule and the particular atom substituted, both a translation and a rotation of the parent principal axes can result. In many cases at least one of the principal axes of the substituted molecule will remain parallel to a principal axis of the parent molecule. Let the mass of the isotopic atom be denoted by  $m + \Delta m$ , with  $m$  the original mass of the atom. Employing the parent center-of-mass principal axis system with the coordinates of the substituted atom represented by  $x, y, z$ , we find from (13.18) and (13.19) that

$$I'_{xx} = I_x + \Delta m(y^2 + z^2) - \frac{(\Delta my)^2}{M + \Delta m} - \frac{(\Delta mz)^2}{M + \Delta m} = I_x + \mu(y^2 + z^2) \quad (13.35)$$

and similarly that

$$I'_{yy} = I_y + \mu(x^2 + z^2) \quad (13.36)$$

$$I'_{zz} = I_z + \mu(x^2 + y^2) \quad (13.37)$$

$$I'_{xy} = -\mu xy \quad (13.38)$$

$$I'_{xz} = -\mu xz \quad (13.39)$$

$$I'_{yz} = -\mu yz \quad (13.40)$$

where the reduced mass for the isotopic substitution is defined as

$$\mu = \frac{M\Delta m}{M + \Delta m} \quad (13.41)$$

with  $M$  the total mass of the parent molecule. These expressions give us the elements of the inertia matrix with respect to the center of mass of the isotopically substituted molecule in terms of the coordinates measured from the center-of-mass principal axis system of the parent molecule. Diagonalization of the inertial matrix yields the principal moments of inertia of the substituted molecule  $I'_x, I'_y, I'_z$  which are determined experimentally. These equations are now employed for development of expressions for the coordinates  $x, y, z$  of the

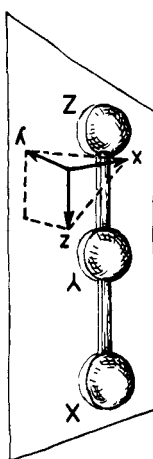


**Fig. 13.3** Illustration of the orientation of the coordinate axes for a linear molecule.

isotopically substituted atom in terms of the principal moments  $I_x$ ,  $I_y$ ,  $I_z$  and  $I'_x$ ,  $I'_y$ ,  $I'_z$ .

### Linear Molecules

Taking the  $z$  axis along the molecular axis (see Fig. 13.3) and noting that only the  $z$  coordinates of the atoms are nonvanishing, we have  $I_z=0$ ,  $I_x=I_y$ . The  $x'y'z'$  axes may be chosen parallel to the  $xyz$  axes; and from (13.35) through (13.40) we have

$$I'_{xy}=I'_{xz}=I'_{yz}=0 \quad (13.42)$$

$$I'_x=I'_{xx}=I_x+\mu z^2 \quad (13.43)$$

$$I'_y=I'_{yy}=I_y+\mu z^2 \quad (13.44)$$

$$I'_z=I_z=0 \quad (13.45)$$

From the equation for  $I'_x$  or  $I'_y$ , we may obtain the distance of the particular substituted atom from the center of mass of the parent molecule; that is

$$|z|=\left[\frac{1}{\mu}(I'_x-I_x)\right]^{1/2}=\left[\frac{1}{\mu}(I'_y-I_y)\right]^{1/2} \quad (13.46)$$

and  $|x|=|y|=0$ . The  $|z|$  thus obtained from the measured  $I$ 's represents the distance of the substituted atom from the center of mass of the molecule.

### Symmetric-top Molecules: Location of an Atom on the Symmetry Axis

The orientations of the principal axes are not altered by isotopic substitution on the symmetry axis (see Fig. 13.4). If we choose the  $z$  axis (and hence  $z'$ ) as the symmetry axis, and taking cognizance of the fact that the  $x$  or  $y$  coordinate

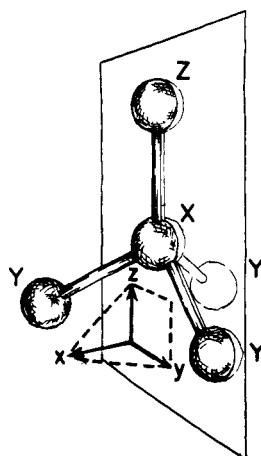


**Fig. 13.4** Illustration of the orientation of the coordinate axes for a symmetric-top molecule.

of any atom on the symmetry axis is zero, we obtain for the inertia elements the same expressions as found for a linear molecule, except that  $I'_z = I_z \neq 0$ . This latter fact, however, has no effect on the determination of the distance  $|z|$  of the substituted atom from the center of mass of the parent molecule which is given by (13.46).

#### Symmetric-top Molecules: Location of an Atom off the Symmetry Axis

Isotopic substitution of an atom which is not on the symmetry axis converts the original symmetric-top to an asymmetric-top molecule. Let the  $z$  axis, as before, be along the symmetry axis. In addition, we may choose the orientation of the  $x$  and  $y$  axes such that the atom to be substituted lies in the  $yz$  plane (see Fig. 13.4). With this choice the coordinates of the substituted atom are  $(0, y, z)$  and (13.35) through (13.40) give

$$I'_{xy} = I'_{xz} = 0 \quad (13.47)$$

$$I'_{yz} = -\mu yz \quad (13.48)$$

$$I'_x = I'_{xx} = I_x + \mu(y^2 + z^2) \quad (13.49)$$

$$I'_{yy} = I_y + \mu z^2 \quad (13.50)$$

$$I'_{zz} = I_z + \mu y^2 \quad (13.51)$$

Since there are no off-diagonal connections to  $I'_{xx}$  we need consider only the submatrix

$$\begin{bmatrix} I_y + \mu z^2 & -\mu yz \\ -\mu yz & I_z + \mu y^2 \end{bmatrix} \quad (13.52)$$

for the substituted molecule. Diagonalization of this matrix yields the two remaining principal moments of inertia,  $I'_y$  and  $I'_z$ . Since the trace and determinant of a matrix are quantities which are invariant under a similarity transformation, we may derive from the above matrix the equations [9]

$$I_y + \mu z^2 + I_z + \mu y^2 = I'_y + I'_z \quad (13.53)$$

$$(I_y + \mu z^2)(I_z + \mu y^2) - \mu^2 y^2 z^2 = I'_y I'_z \quad (13.54)$$

From (13.49) and (13.53) one obtains the relation

$$I_z = I'_y + I'_z - I'_x \quad (13.55)$$

noting  $I_x = I_y$ . Solving (13.53) and (13.54) for  $|y|$  and  $|z|$  and eliminating from these expressions  $I_z$  by means of Eq. (13.55), since  $I_z$  is usually not obtained from an analysis of a symmetric-top spectrum, one obtains finally

$$\begin{aligned} |y| &= \left[ \frac{\Delta I_z}{\mu} \left( 1 + \frac{\Delta I_y}{I_y - I_z} \right) \right]^{1/2} \\ &= \left[ \frac{(I'_x - I'_y)(I'_x - I'_z)}{\mu(I'_x - I'_y - I'_z + I_y)} \right]^{1/2} \end{aligned} \quad (13.56)$$

$$\begin{aligned} |z| &= \left[ \frac{\Delta I_y}{\mu} \left( 1 + \frac{\Delta I_z}{I_z - I_y} \right) \right]^{1/2} \\ &= \left[ \frac{(I'_y - I'_z)(I'_z - I'_y)}{\mu(I'_y + I'_z - I'_x - I_y)} \right]^{1/2} \end{aligned} \quad (13.57)$$

and  $|x|=0$  for the coordinates of the substituted atom in the center-of-mass principal axis system of the original symmetric top. The determination of an accurate  $I'_z$  value for a slightly asymmetric rotor can be difficult. In many cases,  $I'_z$  can be evaluated only with a rather large uncertainty and hence, the coordinates derived will be correspondingly limited in accuracy.

To use the first equations given for  $|y|$  and  $|z|$ ,  $\Delta I_z$  may be replaced by  $\Delta I_x - \Delta I_y$  [see (13.55) or (13.74) where  $\Delta P_x = 0$ ] with an estimate of  $I_z$  if the coordinates are not too sensitive to  $I_z$  as is often the case. On the other hand, as described in Chapter V, observation of "forbidden" transitions can provide an accurate value of the moment of inertia about the symmetry axis,  $I_z$ .

### Asymmetric-top Molecules: Planar

If we choose the  $z$  axis as perpendicular to the molecular plane (see Fig. 13.5), the  $z$  coordinates of all atoms are zero and we have the relation

$$I_x + I_y = I_z \quad (13.58)$$

Substitution of an atom in the plane may result in a rotation of the coordinate axes in the plane; however, the  $z'$  axis will remain parallel to the  $z$  axis. The coordinates of the substituted atom are taken as  $(x, y, 0)$  and (13.35)–(13.40) give

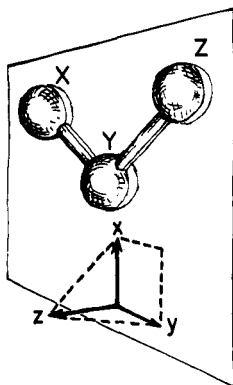


**Fig. 13.5** Illustration of the orientation of the coordinate axes for a planar asymmetric rotor.

$$I'_{xz} = I'_{yz} = 0 \quad (13.59)$$

$$I'_{xy} = -\mu xy \quad (13.60)$$

$$I'_{xx} = I_x + \mu y^2 \quad (13.61)$$

$$I'_{yy} = I_y + \mu x^2 \quad (13.62)$$

$$I'_z = I'_{zz} = I_z + \mu(x^2 + y^2) \quad (13.63)$$

These equations are similar to those for a symmetric-top off-axis substitution and may be treated in the same fashion. Expressions like those of (13.53) and (13.54) are readily obtained which can be solved to give the coordinates of the substituted atom in terms of the changes in the moments of inertia. Explicitly

$$\begin{aligned} |x| &= \left[ \frac{(I'_y - I_y)(I'_x - I_x)}{\mu(I_x - I_y)} \right]^{1/2} \\ &= \left[ \frac{\Delta I_y}{\mu} \left( 1 + \frac{\Delta I_x}{I_x - I_y} \right) \right]^{1/2} \end{aligned} \quad (13.64)$$

$$\begin{aligned} |y| &= \left[ \frac{(I'_x - I_x)(I'_y - I_y)}{\mu(I_y - I_x)} \right]^{1/2} \\ &= \left[ \frac{\Delta I_x}{\mu} \left( 1 + \frac{\Delta I_y}{I_y - I_x} \right) \right]^{1/2} \end{aligned} \quad (13.65)$$

and  $|z|=0$  with  $\Delta I_x = I'_x - I_x$ , and so on.

### Asymmetric-top Molecules: Nonplanar

For the general asymmetric rotor, it is convenient to use the tensor  $\mathbf{P}$  rather than  $\mathbf{I}$ . The principal moments of  $\mathbf{P}$  and  $\mathbf{I}$  are related as given in (13.25). For the center-of-mass principal axis system of the parent molecule, the off-diagonal matrix elements of  $\mathbf{P}$  are

$$\begin{aligned} P_{xy} &= \sum m_i x_i y_i = 0 \\ P_{xz} &= \sum m_i x_i z_i = 0 \\ P_{yz} &= \sum m_i y_i z_i = 0 \end{aligned} \quad (13.66)$$

and the diagonal elements are

$$\begin{aligned} P_x &= P_{xx} = \sum m_i x_i^2 \\ P_y &= P_{yy} = \sum m_i y_i^2 \\ P_z &= P_{zz} = \sum m_i z_i^2 \end{aligned} \quad (13.67)$$

Now for the substituted molecule with respect to the same axes, the elements of  $\mathbf{P}'$  are, from (13.27) and (13.28),

$$P'_{xx} = P_x + \mu x^2 \quad (13.68)$$

and so on, and

$$P'_{xy} = \mu xy \quad (13.69)$$

and so on. The secular equation for the substituted molecule is hence

$$\begin{vmatrix} P_x + \mu x^2 - P' & \mu xy & \mu xz \\ \mu xy & P_y + \mu y^2 - P' & \mu yz \\ \mu xz & \mu yz & P_z + \mu z^2 - P' \end{vmatrix} = 0 \quad (13.70)$$

which is somewhat simpler than the corresponding equation in terms of  $\mathbf{I}$ . The roots of this secular determinant are the planar principal moments  $P'_x$ ,  $P'_y$ ,  $P'_z$ . The coefficients of the polynomial in  $P'$  may be related to the roots [10] giving three equations which may be solved to give the coordinates of the substituted atom

$$|x| = \left[ \frac{\Delta P_x}{\mu} \left( 1 + \frac{\Delta P_y}{I_x - I_y} \right) \left( 1 + \frac{\Delta P_z}{I_x - I_z} \right) \right]^{1/2} \quad (13.71)$$

$$|y| = \left[ \frac{\Delta P_y}{\mu} \left( 1 + \frac{\Delta P_z}{I_y - I_z} \right) \left( 1 + \frac{\Delta P_x}{I_y - I_x} \right) \right]^{1/2} \quad (13.72)$$

$$|z| = \left[ \frac{\Delta P_z}{\mu} \left( 1 + \frac{\Delta P_x}{I_z - I_x} \right) \left( 1 + \frac{\Delta P_y}{I_z - I_y} \right) \right]^{1/2} \quad (13.73)$$

where

$$\begin{aligned} \Delta P_x &= (\frac{1}{2})(-\Delta I_x + \Delta I_y + \Delta I_z) \\ \Delta P_y &= (\frac{1}{2})(-\Delta I_y + \Delta I_z + \Delta I_x) \\ \Delta P_z &= (\frac{1}{2})(-\Delta I_z + \Delta I_x + \Delta I_y) \end{aligned} \quad (13.74)$$

and where  $\Delta I_x (= I'_x - I_x)$ , and so on, are the changes in the principal moments of inertia due to isotopic substitution. The distance of the substituted atom from the center of mass is simply

$$|r| = \left[ \left( \frac{1}{2\mu} \right) (\Delta I_x + \Delta I_y + \Delta I_z) \right]^{1/2} \quad (13.75)$$

The expressions (13.71)–(13.73) can also be written in a more symmetrical form by replacing  $(I_x - I_y)$  by  $(P_y - P_x)$ , and so on:

$$|x| = \left[ \frac{\Delta P_x}{\mu} \left( 1 + \frac{\Delta P_y}{P_y - P_x} \right) \left( 1 + \frac{\Delta P_z}{P_z - P_x} \right) \right]^{1/2} \quad (13.76)$$

Expressions for  $|y|$  and  $|z|$  are obtained by cyclic permutation of  $P_x, P_y, P_z$ .

For substitution of an atom in a symmetry plane which is a principal inertial plane (taken as the  $xy$  plane)  $\Delta P_z = (\Delta I_x + \Delta I_y - \Delta I_z)/2 = 0$ , and (13.76) is simplified to

$$|x| = \left[ \frac{\Delta P_x}{\mu} \left( 1 + \frac{\Delta P_y}{P_y - P_x} \right) \right]^{1/2} \quad (13.77)$$

and likewise

$$|y| = \left[ \frac{\Delta P_y}{\mu} \left( 1 + \frac{\Delta P_x}{P_x - P_y} \right) \right]^{1/2} \quad (13.78)$$

with  $|z|=0$ . These relations can also be derived, starting from (13.70) where elements containing  $z$  vanish. These results can be readily shown to be equivalent to (13.64) and (13.65). Other forms are also possible. Since the change in the planar moment perpendicular to the plane ( $xy$ ) vanishes, the following relations can be written

$$\begin{aligned} \Delta P_x &= \frac{-\Delta I_x + \Delta I_y + \Delta I_z}{2} \\ &= \Delta I_y \\ &= \Delta I_z - \Delta I_x \end{aligned} \quad (13.79)$$

with similar relations for  $\Delta P_y$ . If equilibrium quantities are used, the relation employed will make no difference. When effective ground state moments of inertia are employed, however, slightly different values for the coordinates will be obtained, and the question of which is the preferred expression arises (see Section 8).

Consider the atom to be located as lying on a symmetry axis, which will be a principal inertial axis, say  $z(x=y=0)$ . Hence the changes in the planar moments  $\Delta P_x$  and  $\Delta P_y$  vanish. From (13.73), or (13.70) where only the  $\mu z^2$  term survives, we have

$$|z| = \left( \frac{\Delta P_z}{\mu} \right)^{1/2} \quad (13.80)$$

Alternate forms are readily written since  $\Delta I_z = 0$  and  $\Delta I_x = \Delta I_y$ . Thus (13.80) may be reduced to (13.46).

It is possible to write the transformation between the principal axis system of a parent molecule and an isotopic form in terms of the substitution coordinates of an atom as discussed by Rudolph [11]. The transformation is, in general, a rotation plus a translation

$$\mathbf{r} = \mathbf{R}\mathbf{r}' + \mathbf{t} \quad (13.81)$$

where  $\mathbf{r}$  represents an arbitrary vector for the parent species and  $\mathbf{r}'$  for the isotopic species with

$$\mathbf{R} = -\Delta m \cdot \begin{bmatrix} \frac{xx'}{P_x - P'_x} & \frac{xy'}{P_x - P'_y} & \frac{xz'}{P_x - P'_z} \\ \frac{yx'}{P_y - P'_x} & \frac{yy'}{P_y - P'_y} & \frac{yz'}{P_y - P'_z} \\ \frac{zx'}{P_z - P'_x} & \frac{zy'}{P_z - P'_y} & \frac{zz'}{P_z - P'_z} \end{bmatrix} \quad (13.82)$$

and

$$\mathbf{t} = \frac{\Delta m}{M + \Delta m} \begin{pmatrix} x \\ y \\ z \end{pmatrix} \quad (13.83)$$

For an asymmetric top the six planar moments (parent and single isotopic form) via (13.76) yield the coordinates  $xyz$  of the substituted atom relative to the parent. If the roles of the parent and the substituted species are interchanged, the same data provide the coordinates  $x'y'z$  of the substituted atom relative to the principal axis frame of the isotopic species. Once the signs of the coordinates have been obtained from other considerations, the signs of the elements in the above transformation are uniquely defined. Then the transformation can be constructed without a knowledge (assumed or otherwise) of the complete molecular structure with only a single isotopic substitution required. The accuracy of the transformation will be dependent on the reliability of the coordinates. For substitution in a principal inertia plane ( $xy$ ), the off-diagonal terms of  $R$  involving  $z$  (and  $z'$ ) vanish, and the lower diagonal element is replaced by  $-1/\Delta m$ . The transformation can have a number of applications [11], such as determination of the orientation of the dipole moment in the molecule from the dipole components ( $\mu_a, \mu_b, \mu_c$ ) of the parent ( $\mu$ ) and isotopic form ( $\mu'$ ), aid in transformation of the quadrupole coupling tensor to its principal axis system, and aid in the evaluation of small coordinates (See Section 8). In the former application, for example, only the rotational part of (13.82) is required, and the signs of the components of  $\mu$  and  $\mu'$  are chosen relative to each other such that  $\mu = \mathbf{R}\mu'$  is satisfied.

## 4 MULTIPLE SUBSTITUTION

Kraitchman's procedure may be extended to multiple isotopic substitution which sometimes proved convenient. Consider, for example, the simultaneous isotopic substitution of the equivalent  $Y$  atoms of a bent, triatomic  $X Y_2$  molecule. Let the  $z$  axis be perpendicular to the plane and the  $x$  axis correspond to the twofold symmetry axis (see Fig. 13.5). The orientations of the principal axes are not changed upon double substitution of the  $Y$  atoms. The coordinates of the two substituted atoms are  $(x, y, 0)$  and  $(x, -y, 0)$ , and the isotopic mass of each is  $m + \Delta m$ . Using (13.18) and (13.19) we find

$$I'_{xz} = I'_{xy} = I'_{yz} = 0 \quad (13.84)$$

$$I'_x = I'_{xx} = I_x + 2\Delta m y^2 \quad (13.85)$$

$$I'_y = I'_{yy} = I_y + \mu_2 x^2 \quad (13.86)$$

$$I'_z = I'_{zz} = I_z + 2\Delta m y^2 + \mu_2 x^2 \quad (13.87)$$

where

$$\mu_2 = \frac{2\Delta m M}{(M + 2\Delta m)} \quad (13.88)$$

The coordinates with respect to the parent coordinate system are hence

$$|x| = \left( \frac{\Delta I_y}{\mu_2} \right)^{1/2} \quad (13.89)$$

$$|y| = \left( \frac{\Delta I_x}{2\Delta m} \right)^{1/2} \quad (13.90)$$

and  $|z| = 0$  with  $\Delta I_x = I'_x - I_x$ , and so on, and  $\mu_2$  given by (13.88). These equations might be applied, for example, to data on  $\text{SO}_2$  and  $^{18}\text{OS}^{18}\text{O}$  to give the coordinates of the oxygen atoms.

Another case would be multiple substitution of the equivalent  $Y$  atoms in molecules of the class  $ZXY_3$  having  $C_{3v}$  symmetry. Let the  $z$  axis represent the threefold symmetry axis. If the orientation of the coordinate system is chosen as indicated in Fig. 13.4, one of the  $Y$  atoms will be in the  $yz$  plane. The coordinates of this atom, with respect to the parent coordinate system, will be  $(0, y, z)$ . The coordinates of the remaining  $Y$  atoms are related by a rotation about the  $C_3$  axis, the  $z$  axis. In particular

$$\begin{pmatrix} x_k \\ y_k \\ z_k \end{pmatrix} = \begin{pmatrix} \cos k\omega & -\sin k\omega & 0 \\ \sin k\omega & \cos k\omega & 0 \\ 0 & 0 & 1 \end{pmatrix} \begin{pmatrix} 0 \\ y \\ z \end{pmatrix} \quad (13.91)$$

where  $\omega = 2\pi/3$  and  $k = 1, 2$  give the coordinates of the other two  $Y$  atoms. Application of the above relation gives for the coordinates  $[-(3^{1/2}/2)y, -(1/2)y, z]$  and  $[(3^{1/2}/2)y, -(1/2)y, z]$ . With these coordinates and the mass of each isotopic atom taken as  $m + \Delta m$ , (13.18) and (13.19) give

$$I'_{xz} = I'_{xy} = I'_{yz} = 0 \quad (13.92)$$

$$\Delta I_x = \Delta I_y = \frac{3}{2} \Delta m y^2 + \mu_3 z^2 \quad (13.93)$$

$$\Delta I_z = 3 \Delta m y^2 \quad (13.94)$$

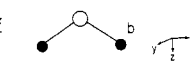
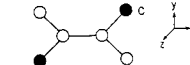
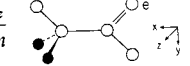
where  $\Delta I_x = I'_x - I_x$ , and so on, and

$$\mu_3 = \frac{3 \Delta m M}{M + 3 \Delta m} \quad (13.95)$$

with  $M$  as usual the mass of the parent molecule. Although the foregoing equations may be solved for the  $|y|$  and  $|z|$  coordinates, the results are of less use, since the moment of inertia about the symmetry axis is usually not determined from the pure rotational spectrum (see, however, Chapter V); but, with the determination of  $z$  from the center-of-mass condition employing the  $z_i$  coordinates of the on-axis  $X$  and  $Z$  atoms, the  $|y|$  coordinate may be found from (13.93).

Explicit expressions for some other types of molecules, where a set of equivalent nuclei is substituted, have been given by Chutjian [12]. A number of disubstitution cases have been considered by Nygaard [13] and the coordinates are expressed in terms of differences in the planar second moments giving rise to more simplified relations. These useful relations are summarized in Table 13.2. The use of double substitution for location of the coordinates in methyl-like groups such as  $\text{CCL}_3\text{F}$  has been discussed [14]. Evaluation of the hydrogen

**Table 13.2** Substitution Coordinates ( $x$ ,  $y$ ,  $z$ ) by Disubstitution for Different Molecular Symmetry<sup>a</sup>

Symmetry	Isotopic Substitution in the Positions	Coordinate Relations			Example Configuration
		$x^2$	$y^2$	$z^2$	
$C_{2v}^z$	$\pm x, 0, z$	$\frac{\Delta P_x}{2\Delta m}$	0	$\frac{\Delta P_z}{\mu_2}$	
$C_{2h}^z$	$\begin{cases} x, & y, 0 \\ -x, & -y, 0 \end{cases}$	$\frac{\Delta P_x}{2\Delta m} \left( 1 + \frac{\Delta P_y}{P_y - P_x} \right)$	$\frac{\Delta P_y}{2\Delta m} \left( 1 + \frac{\Delta P_x}{P_x - P_y} \right)$	0	
$C_2^z$	$\begin{cases} x, & y, z \\ -x, & -y, z \end{cases}$	$\frac{\Delta P_x}{2\Delta m} \left( 1 + \frac{\Delta P_y}{P_y - P_x} \right)$	$\frac{\Delta P_y}{2\Delta m} \left( 1 + \frac{\Delta P_x}{P_x - P_y} \right)$	$\frac{\Delta P_z}{\mu_2}$	
$C_s^{xy}$	$x, y, \pm z$	$\frac{\Delta P_x}{\mu_2} \left( 1 + \frac{\Delta P_y}{P_y - P_x} \right)$	$\frac{\Delta P_y}{\mu_2} \left( 1 + \frac{\Delta P_x}{P_x - P_y} \right)$	$\frac{\Delta P_z}{2\Delta m}$	

<sup>a</sup> $P_x = (-I_x + I_y + I_z)/2$ , etc.,  $\Delta P_x = P'_x - P_x$ , etc. (the change in *principal* planar moments by substitution),  $P_x - P_y = I_y - I_x$ , etc., and  $\mu_2 = M2\Delta m/(m + 2\Delta m)$ . From Nygaard [13]. Equivalent atoms indicated.

<sup>b</sup>Example, furan,  $\text{H}_2\text{O}$ .

<sup>c</sup>Example, planar *trans*-1,2-dichloroethylene.

<sup>d</sup>Example, nonplanar  $\text{H}_2\text{O}_2$  or ethylene ozonide.

<sup>e</sup>Example, acetaldehyde, or aniline.

coordinates of a molecule containing two equivalent methyl groups, for example,  $(\text{CH}_3)_2-X$ , has been described [15]. The coordinates of interest are the symmetric in-plane coordinates ( $\pm x_s, 0, z_s$ ) and the asymmetric out-of-plane coordinates ( $\pm x_a, \pm y_a, z_a$ ). The moments of inertia of the normal (6H), hexadeuterated (6D), and trideuterated (3H3D) species are employed.

## 5 EVALUATION OF STRUCTURES: GENERAL CONSIDERATIONS

When moments of inertia are related to the structural parameters, either of two procedures may be employed. In the first procedure, the molecular structure may be obtained by a best-fitting of calculated and observed moments of inertia of a sufficient number of isotopic species. For example, in the expressions of Table 13.1 which give the moments of inertia in terms of the bond distances and bond angles, the appropriate isotopic masses may be substituted and the molecular parameters found from the solution of the resulting simultaneous equations. Alternately, through the use of the equations considered in Sections 3 through 4 the coordinates of each atom with respect to the principal axes of the parent molecule may be determined, from which the bond distances and bond angles may be easily calculated. One can, of course, choose any one of the molecular species as the "original" or "parent" molecule since within the rigid rotor approximation the structural parameters must be invariant to this choice. For reasons of convenience, however, the normal isotopic species is usually taken as the parent molecule. In application of the equations to a particular molecule the  $xyz$  axes will be identified in some order with the principal axes  $abc$ . It should be noted that the distance between any two atoms of a molecule can be evaluated without knowledge of the other distances, provided the moments of inertia are determined for the species with isotopic substitution for both of these atoms as well as for the original unsubstituted species. Furthermore, since the equations for the moments of inertia, the products of inertia, and the first-moment equations provide relations among the coordinates of the parent molecule, it is not necessary to substitute every atom to determine the structure. The minimum amount of data required for complete determination of the structure is the same for both procedures. It may be noted that the number of structural parameters required to characterize a particular molecule is equal to the number of totally symmetric vibrations. Thus by the evaluation of the number of times the totally symmetric species occurs in the  $\Gamma_{\text{vib}}$  representation, the number of structural parameters is given [16].

For a linear molecule consisting of  $N$  atoms there are  $N$  coordinates or  $(N-1)$  independent internuclear distances to be evaluated. Analysis of the rotational spectrum of a linear molecule yields one moment of inertia for each isotopic species. The moment-of-inertia equation and the first-moment equation

$$I_x = \sum m_i z_i^2, \quad \sum m_i z_i = 0 \quad (13.96)$$

of the parent molecule provide two equations. Therefore, a minimum of  $(N - 2)$  isotopic substitutions is required for a complete evaluation of the structure. Furthermore, only one substitution for a given atom yields independent information. Hence at least one substitution for each  $(N - 2)$  different atoms of the molecule must be made. Knowledge of the coordinates (distance from the center of mass) of two atoms gives the internuclear distance  $d_{ij}$ , that is,

$$d_{ij} = |z_i - z_j| \quad (13.97)$$

We must, however, know whether the atoms lie on the same or opposite sides of the center of mass.

For a diatomic molecule knowledge of the moment of inertia  $I_x$  is sufficient to determine the distance between the two atoms  $m_X$  and  $m_Y$ . In particular (see Table 13.1),

$$d = \left[ \left( \frac{m_X + m_Y}{m_X m_Y} \right) I_x \right]^{1/2} \quad (13.98)$$

For a linear triatomic molecule  $XYZ$  (13.46) and (13.96) allow the calculation of the  $z_i$ 's and hence of the two bond lengths if a single isotopic substitution on either of its three atoms is made. In particular, if the  $X$  atom is isotopically substituted, (13.46) gives the coordinate  $z_X$ , and inserting this into (13.96) yields two relations in the two unknowns  $z_Y$  and  $z_Z$  which may be solved. Equivalently, the moments of inertia for two molecular species gives from Table 13.1 two equations to be solved for the two bond lengths. With more than three atoms, additional isotopic substitutions are required as indicated.

The most common type of symmetric-top molecule, the  $Y_p X Z \dots$  class, has any number  $p$ , greater than two, of symmetrically placed off-axis atoms and any number of atoms  $X, Z, \dots$  along the symmetry axis (the  $z$  axis). Because of the selection rule only one moment of inertia, for example,  $I_x$ , can be found from the spectrum. A single substitution for one of the atoms on the molecular axis allows the distance of that atom from the center of mass to be calculated with (13.46). Substitution of two atoms on the symmetry axis gives the distance between the atoms. Therefore, with  $N$  atoms on the symmetry axis  $N$  isotopic substitutions in addition to the parent molecule will determine the separations between the atoms. When separations of all the atoms on the symmetry axes are thus obtained, only two unknown parameters remain—the bond angle and the  $XY$  bond length. We can obtain these by making a single isotopic substitution on a  $Y$  atom and by using (13.56) and (13.57) to calculate the coordinates of the  $Y$  atom. Alternately, we may employ the inertial equations. If  $y_Y$  represents the perpendicular distance of the  $Y$  atoms from the symmetry axis, the  $z$  axis, and  $z_Y$  the  $z$  coordinate distance of the  $Y_p$  plane from the center of mass, and  $z_i$  the coordinate distance of the  $i$ th atom on the symmetry axis from the center of mass, then the moment of inertia can be written as:

$$I_x = pm_Y \left( \frac{y_Y^2}{2} + z_Y^2 \right) + \sum_i m_i z_i^2 \quad (13.99)$$

with the first moment equation:

$$pm_Y z_Y + \sum_i m_i z_i = 0 \quad (13.100)$$

in which  $m_Y$  represents the mass of Y and  $m_i$  the mass of the  $i$ th atom located on the symmetry axis. The summation extends over all atoms on the symmetry axis but does not include the atoms off this axis. From the geometry of the molecule we can also write

$$d = [(z_X - z_Y)^2 + y_Y^2]^{1/2} \quad (13.101)$$

and

$$\tan \beta = \frac{y_Y}{|z_X - z_Y|} \quad (13.102)$$

where  $d$  is the length of the XY bond and where  $\beta$  is the angle of the bond XY with the symmetry axis. This angle is related to the bond angle YXY, designated  $\theta$ , by:

$$\sin \frac{1}{2}\theta = \sin \frac{\pi}{p} \sin \beta \quad (13.103)$$

With the known  $z_i$  values obtained from isotopic substitutions on the symmetry axis, (13.99) and (13.100) can be employed to give  $y_Y$  and  $z_Y$  and, hence, the bond angle and the XY bond length from (13.101)–(13.103). Conversely, (13.99) through (13.103) are sufficient for calculation of the moment of inertia  $I_x (I_b)$  from assumed bond angles and bond lengths. In Table 13.1 explicit expressions for the moments of inertia in terms of the structural parameters have been given for two of the simplest types of symmetric tops. From the foregoing discussion or the expressions of Table 13.1 it is apparent that a minimum of two molecular species must be studied for the  $XY_3$  type and three for the  $ZXY_3$  type. When a simultaneous solution of the inertial equations is to be considered, then it is obviously simpler if symmetric isotopic substitution of the Y atoms is made.

For an asymmetric-top molecule, all three of its principal moments of inertia can be obtained from the pure rotational spectrum. For a planar molecule, however, only two of these are independent because of the relation given in (13.58) which holds for a rigidly planar molecule. For a planar asymmetric rotor, five moment equations of the parent molecule are available:

$$I_x = \sum m_i y_i^2, \quad I_y = \sum m_i x_i^2, \quad I_{xy} = -\sum m_i x_i y_i = 0, \quad \sum m_i x_i = 0,$$

$$\sum m_i y_i = 0 \quad (13.104)$$

where the z axis is taken perpendicular to the plane. If the x and y coordinates of  $(N-2)$  atoms are determined by means of (13.64) and (13.65), then the remaining four coordinates of the two unsubstituted atoms may be obtained from the solution of the above relations. Therefore, a minimum of  $(N-2)$  isotopic

substitutions at different sites is required for the determination of the complete structure of a planar asymmetric rotor having  $N$  atoms. For a general, non-planar, asymmetric-top molecule, all nine moment equations are available, viz., (13.29)–(13.34) and the three center-of-mass equations. Hence  $(N - 3)$  isotopic substitutions are necessary to fix the complete structure. Expressions for the moments of inertia of some simple asymmetric rotors are given in Table 13.1.

For all types of molecules, if some of the bond lengths or angles are known from symmetry to be equivalent, the minimum number of required substitutions is accordingly reduced. The structures of nonlinear triatomic molecules,  $XY_2$ , can be solved completely from the two independent moments of inertia without isotopic substitution. With the molecule in the  $xy$  plane and the  $x$  axis corresponding to the symmetry axis, we find (see Table 13.1)

$$d = \left[ \frac{1}{2m_Y} \left( \frac{M}{m_X} I_y + I_x \right) \right]^{1/2} \quad (13.105)$$

and

$$\tan \frac{1}{2}\theta = \left( \frac{m_X I_x}{M I_y} \right)^{1/2} \quad (13.106)$$

where  $d$  is the  $X-Y$  bond length and  $\theta$  is the  $YXY$  angle and where  $M (= m_X + 2m_Y)$  is the total mass. For the slightly more complicated case of an  $XYZ$  type, such as  $\text{NOCl}$ , which has three structural parameters, the structure cannot be completely solved from measurements on a single isotopic species. Often some of the dimensions are known with fair precision from electron diffraction, or they can be estimated with confidence from similar molecules. When some molecular parameters are known, fewer substitutions are necessary to complete the structural determination. Substitutions in excess of the minimum number are useful in checking results and simplifying the calculations. Furthermore, additional substitutions are helpful in estimation of the effects of zero-point vibrations when effective moments of inertia are used since the variation of the structural parameters with different choice of data may be observed. Since only the absolute values  $|x|, |y|, |z|$  are obtained, a decision as to the sign of the coordinates must be made from other information. This is really not a serious problem since one usually has a prior knowledge of the arrangement of the atoms in the molecule as well as molecular structure information on the molecule or on similar molecules from other sources, such as infrared or electron diffraction. Also the signs must be such that the center-of-mass conditions  $\sum m_i x_i = 0$ , and so on, and the products of inertia  $\sum m_i x_i y_i = 0$ , and so on, are obeyed (or essentially obeyed for effective rather than equilibrium coordinates). If, for example, the sign of a given coordinate is ambiguous, while others are reasonably obvious, the first-moment equation could be evaluated with both possible signs and the choice made on the basis of how well the relation is satisfied. When the structural calculation is made with both possible signs for an ambiguous coordinate, the derived structure can be used to give a correct sign choice if unreasonable structural parameters are obtained for one

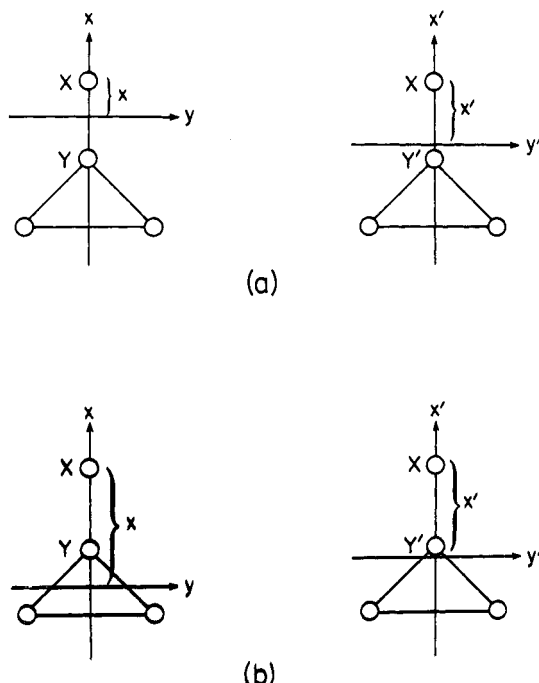


**Fig. 13.6** Determining the relative signs of the coordinates of atoms  $X$  and  $Y$  by isotopic pulling. Note in (a) the coordinate of  $X$  increases when referred to molecule  $X'Y'$  . . . as parent compared to its value relative to  $XY$  . . . as parent. The reverse is true for the center of mass as in (b).

sign as compared to another. If sufficient data are available, it is possible to use the changes in the coordinates of an atom with different parent molecules to determine the signs of the coordinates relative to those of another atom. This procedure is referred to as "isotopic pulling" by Pasinski and Beaudet [17], is particularly useful when little is known about the shape of the molecule. Consider the molecule of Fig. 13.6, with  $m'_x > m_x$  and  $m'_Y > m_Y$ . Isotopic  $X'Y\cdots$  can be used for evaluation of the  $x_X$  coordinate of  $X$  in the parent species  $XY\cdots$ . Likewise, the isotope  $X'Y'\cdots$  can be used for evaluation of the coordinate  $x'_X$  for the parent species  $XY'\cdots$ . The center of mass will be shifted toward  $Y'$  in the  $XY'$  species. Thus, if  $x_X$  is positive as shown in Fig. 13.6a, we will have  $x'_X > x_X$ . On the other hand, if  $X$  and  $Y$  are on the same side of the  $y$  axis, as in Fig. 13.6b, the  $x'_X < x_X$ . Therefore, the increase or decrease in the coordinate locates the relative coordinate position of atoms  $X$  and  $Y$ .

It should be emphasized that here and in previous discussions it has been assumed that the molecule is rigid and therefore that the molecular parameters do not change with isotopic substitution. Hence the equilibrium moments of inertia that correspond to the moments for the vibrationless state where the atoms are at rest should be used in such equations as Kraitchman's equations and the equations of Table 13.1. When effective rather than equilibrium

moments of inertia are used, as is usually the case, a certain amount of ambiguity is introduced into the derived parameters because of the contributions from zero-point vibrations. These effects are particularly troublesome for polyatomic molecules and will be considered in more detail in succeeding sections.

## 6 EVALUATION OF EQUILIBRIUM STRUCTURES

### Correction for Vibrational Effects

Previously, we have recognized that the nuclear framework of a molecule is not rigid and that the nuclei undergo vibrational motions about their equilibrium positions simultaneously with rotation. Since the internuclear distance will be changing as the molecule vibrates, the moments of inertia depend in a complicated way on the vibrational state. Consider, for example, a simple diatomic molecule. We may account for the vibration-rotation interaction to a good approximation by considering the rotational constant, characterizing the rather slow rotational motion as an average value, averaged over the rather rapid vibrational motions of the nuclei. Specifically, we have for the effective rotational constant of the vibrational state  $v$ :

$$B_v = \frac{h}{8\pi^2 I_b^v} = \frac{h}{8\pi^2 \mu} \left\langle \frac{1}{r^2} \right\rangle \quad (13.107)$$

in which  $\mu$  is the reduced mass of a diatomic molecule and  $\langle 1/r^2 \rangle$  is the appropriate average over the vibrational wave function. Now the instantaneous internuclear distance may be expanded about its equilibrium value in terms of the dimensionless vibrational coordinate:

$$\frac{1}{r^2} = \frac{1}{r_e^2} (1 + \xi)^{-2} = \frac{1}{r_e^2} (1 - 2\xi + 3\xi^2 - \dots) \quad (13.108)$$

with  $\xi = (r - r_e)/r_e$ . The vibrational average of  $r^{-2}$  can thus be expressed in terms of the average values of  $\xi$ ,  $\xi^2$ , etc. If the anharmonicity of the potential function is included, that is, the harmonic vibrational wave function is corrected for the presence of a perturbing cubic term ( $V' = h a_0 a_1 \xi^3$ ,  $a_0 = \omega_e^2/4B_e$ ), then the averages are found to be [18]:

$$\langle v|\xi|v \rangle = -a_1 \left( \frac{3B_e}{\omega_e} \right) (v + \tfrac{1}{2}) \quad (13.109)$$

$$\langle v|\xi^2|v \rangle = \left( \frac{2B_e}{\omega_e} \right) (v + \tfrac{1}{2}) \quad (13.110)$$

where  $v$  is the vibrational quantum number,  $\omega_e$  is the classical harmonic vibrational frequency,  $a_1$  is the cubic anharmonic constant (dimensionless), and  $B_e (=h/8\pi^2\mu r_e^2)$  is the equilibrium rotational constant. Hence taking cognizance of (13.107) through (13.110) we have for the effective rotational constant of a vibrating rotator

$$B_v = B_e - \alpha_e (v + \tfrac{1}{2}) \quad (13.111)$$

correct to terms linear in  $(v + \frac{1}{2})$ . The coefficient of the  $(v + \frac{1}{2})$  dependence is given by the expression

$$\alpha_e = -\left(\frac{6B_e^2}{\omega_e}\right)(1+a_1) \quad (13.112)$$

Equation 13.111 is found to be a good approximation to the effective rotational constant. It is evident that even in the ground vibrational state ( $v=0$ ),  $B_0$  differs from  $B_e$  by  $-\alpha_e/2$ . Furthermore, even if the vibration were harmonic ( $a_1=0$ ), a vibrational contribution to the effective rotational constant is realized. Since the anharmonic correction  $a_1$  is usually negative and larger than one,  $\alpha_e$  is positive; the effective rotational constant is less than  $B_e$  and decreases with an increase in the vibrational state.

For polyatomic molecules, expressions similar to (13.111) hold for the effective rotational constants (see Chapter VII)

$$A_v = A_e - \sum_s \alpha_s^a \left( v_s + \frac{d_s}{2} \right) \quad (13.113)$$

$$B_v = B_e - \sum_s \alpha_s^b \left( v_s + \frac{d_s}{2} \right) \quad (13.114)$$

$$C_v = C_e - \sum_s \alpha_s^c \left( v_s + \frac{d_s}{2} \right) \quad (13.115)$$

Alternately, we may define the effective moments of inertia as

$$I_\alpha^v = I_\alpha^e + \sum_s \left( v_s + \frac{d_s}{2} \right) \varepsilon_s^\alpha \quad \alpha = a, b, c \quad (13.116)$$

where the rotation-vibration parameter is given by

$$\varepsilon_s^\alpha = \left( \frac{8\pi^2}{h} \right) (I_\alpha^e)^2 \alpha_s^\alpha \quad (13.117)$$

In the foregoing expressions, the sum is over all vibrations of the molecule counting degenerate ones once;  $v=(v_1, v_2, v_3, \dots, v_s, \dots)$  corresponds to the set of vibrational quantum numbers with  $v_s$  the vibrational quantum number for the  $s$ th vibration having degeneracy  $d_s$ . In asymmetric-top molecules there are no degenerate normal modes of vibration although accidental near-degeneracies are possible. A linear  $XYZ$  molecule, for example, has four modes of vibration (see Fig. 5.1), two of which correspond to bending vibrations in two perpendicular planes; these have the same frequency  $\omega_2$  and the same  $\alpha$  constants and constitute a doubly degenerate vibration ( $d_2=2$ ). The other two remaining modes are stretching vibrations and are nondegenerate;  $\omega_1$ , a stretching vibration of the Y-Z bond ( $d_1=1$ );  $\omega_3$ , a stretching vibration of the Y-X bond ( $d_3=1$ ). The effective rotational constant is thus given explicitly by

$$B_v = B_e - \alpha_1^b(v_1 + \frac{1}{2}) - \alpha_2^b(v_2 + 1) - \alpha_3^b(v_3 + \frac{1}{2}) \quad (13.118)$$

Measurements of  $B_v$  for the ground (0, 0, 0) and the first excited vibrational

states  $(1, 0, 0)$ ,  $(0, 1, 0)$ ,  $(0, 0, 1)$  will allow the evaluation of  $\alpha_1^b$ ,  $\alpha_2^b$ , and  $\alpha_3^b$  and hence  $B_e$  or  $I_b^e$ . Knowledge of the  $\alpha$  constants also gives information on the cubic potential constants as is evident from the definition of  $\alpha_e$  for a diatomic molecule.

For polyatomic molecules there is an additional Coriolis interaction which contributes to the rotational energy; the quantities  $\alpha_s^a$ , etc. depend not only on the harmonic and anharmonic potential constants but also on the Coriolis coupling constants. Because of the additional contributions from Coriolis interactions the effective rotational constants are not simply the average of the inverse of the instantaneous moments. General discussions of the vibrational contributions to the effective moments as well as explicit expressions for the  $\alpha$ 's of some simple molecules have been given [19] (see also Chapter VII). In addition to the contributions from vibration-rotation, the effective rotational constants contain small contributions from centrifugal distortion (see Chapter VIII) and from electron rotation interactions (see Chapter XI).

Naturally, the preferred measure of the distance between two nuclei is the equilibrium bond distance, which is free from the zero-point vibrational effects, and which has a clear physical meaning, that is, the bond distance corresponding to the minimum of the potential energy curve. Figure 13.7 gives an illustration of the lower portion of the potential energy curve for  ${}^7\text{LiF}$ . In principle, the calculation of equilibrium structures is straightforward. Once a sufficient number of vibrational states have been investigated to allow evaluation of the  $\alpha_i$ 's, the equilibrium rotational constants and hence the equilibrium moments of inertia may be obtained. The equilibrium structure may then be calculated as outlined in the previous section. Since the vibrational effects have been corrected for the errors in  $r_e$ , structures are limited only by the experimental uncertainties, uncertainties in fundamental constants such as Planck's constant, and possible uncertainties from electron-rotation effects if these have been ignored.

As we have seen for diatomic and symmetric bent triatomic molecules, only the moments of inertia of a single isotopic species are required for evaluation of the complete structure. For diatomic molecules, then, only one vibrational state need be measured in addition to the ground state if (13.111) holds satisfactorily. If  $(v + \frac{1}{2})^2$  dependence is also important, this adds an additional constant  $\gamma_e$ , and measurements on another excited state are necessary. Once  $B_e$  is determined, the equilibrium bond distance is given by

$$r_e = \left( \frac{\hbar}{8\pi^2 \mu B_e} \right)^{1/2} = \left( \frac{I_b^e}{\mu} \right)^{1/2} \quad (13.119)$$

where  $\mu = m_1 m_2 / (m_1 + m_2)$  is the reduced mass [not to be confused with the  $\mu$  for isotopic substitution defined by (13.41)]. The equilibrium parameters  $B_e$ , and  $r_e$  of some diatomic molecules are displayed in Tables 4.6 and 4.7.

From measurements of  $r_0$  for two or more isotopes of a diatomic molecule it has been pointed out by Laurie [20] that a good approximation to the equilibrium bond distance may be obtained. From (13.156) and (13.155), neglecting higher-order terms and employing  $I_b^e = \mu r_e^2$  and  $\omega_e = (1/2\pi)(f/\mu)^{1/2}$  to separ-

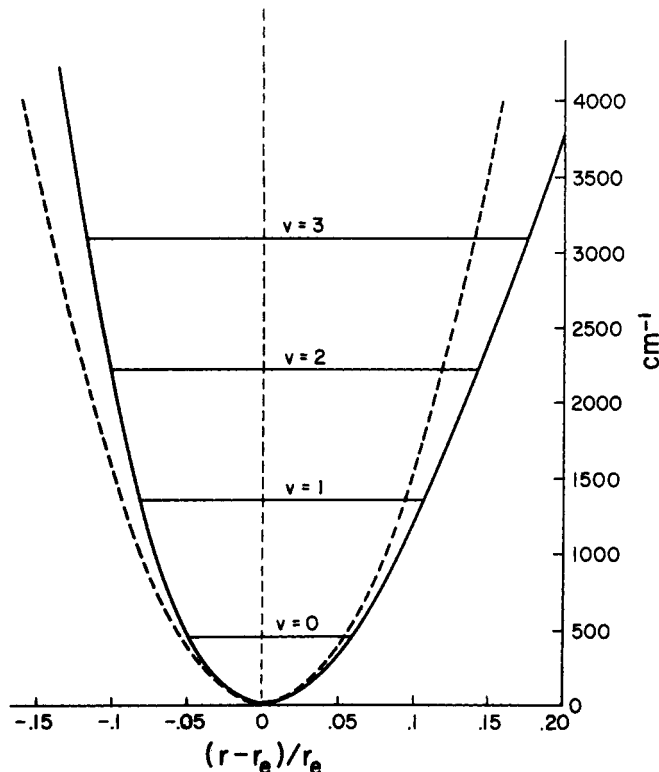


**Fig. 13.7** The solid curve represents the potential function of  ${}^7\text{LiF}$  evaluated from:  $V(\text{cm}^{-1}) = (1.5398 \times 10^5 \text{ cm}^{-1}) \times \xi^2 (1 - 2.7006\xi + 5.10\xi^2 - 8.0\xi^3)$ . The broken curve represents the harmonic part of the potential function. From E. F. Pearson, Ph.D. dissertation, Duke University, 1968.

ate out the reduced mass dependence, one can obtain

$$r_0 = r_e - \left[ \frac{3\hbar(1+a_1)}{4r_e f^{1/2}} \right] \mu^{-1/2} \quad (13.120)$$

By plotting  $r_0$  versus  $\mu^{-1/2}$  and extrapolating  $\mu^{-1/2}$  to zero it is possible to obtain the intercept  $r_e$ . From the  $r_0$  values of HF and DF in Table 13.7 one thus obtains  $r_e = 0.917 \text{ \AA}$ , which agrees with the value obtained by direct correction of the rotational constant for the vibrational effects. This procedure, though, has limited applicability since no simple reduced mass function can be defined for a polyatomic molecule. See, however, Sections 9 and 10.

### Higher-order Corrections

In addition to the gross vibrational effects just discussed, there are higher-order corrections, described later, that are required for a precise evaluation of  $B_e$  and hence of  $r_e$ . In the usual derivation of equilibrium structures from observed rotational spectra for molecules in  ${}^1\Sigma$  states, the interaction of rota-

tion with electronic motions is neglected, and the electrons of each bonded atom are assumed to be concentrated at its nucleus. Actually, of course, these assumptions are not strictly true. There are displacements of the electronic charges due to chemical bonding; and, when the molecule is rotating, the electronic angular momentum is not strictly zero because of the interaction of the electronic and molecular rotational motions. These effects are formally treated in Chapter XI, Section 7. When the  $g$  factor is known, corrections for these effects on  $B_e$  can be simply calculated with (11.135). Not included in (11.135), however, is a small perturbation known as wobble stretching. The nonzero electronic angular momentum causes the rotating nuclear frame to wobble, thus giving rise to a centrifugal-like stretching force which in linear molecules is along the internuclear axis. Corrections for these electronic effects on  $B_e$  originally treated by Van Vleck [21] are further developed and applied to CO by Rosenblum, Nethercot, and Townes [22]. In addition to these electronic perturbations, there is a higher-order correction for vibrational effects known as Dunham's correction that must be applied to give the correct value of  $B_e$  from the Dunham  $Y_{01}$  (generally equated to  $B_e$ ). This Dunham correction of  $B_e$  is given by (4.24). A method for estimation of it together with the wobble-stretching correction will be described.

In general,  $B_e$  for a diatomic molecule can be expressed by

$$B_e = Y_{01} + \delta_1 + \delta_2 + \delta_3 \quad (13.121)$$

where the first correction,  $\delta_1$ , accounts for the electronic effects which are proportional to the rotational  $g$  factor Eq. (11.135),  $\delta_2$  is the wobble stretching correction, and  $\delta_3$  is the Dunham's correction (4.24). Because  $\delta_2$  and  $\delta_3$  both have  $1/\mu^2$  dependence, they can be estimated together from known mass ratios of different isotopic species as follows

$$\frac{B_e}{B'_e} = \frac{B + \delta_2 + \delta_3}{B' + \delta'_2 + \delta'_3} = \frac{\mu'}{\mu} \quad (13.122)$$

where the primed and unprimed quantities represent different isotopic species. With (13.122) and the  $(1/\mu^2)$  dependence of  $\delta_2$  and  $\delta_3$  it can be shown that

$$\delta_2 + \delta_3 = \frac{\varepsilon B'}{(\mu/\mu') - 1} \approx \varepsilon \left( \frac{BB'}{B' - B} \right) \quad (13.123)$$

in which

$$B = Y_{01} + \delta_1 \quad (13.124)$$

and the isotopic discrepancy is defined by

$$\varepsilon = \frac{B}{B'} - \frac{\mu'}{\mu} \quad (13.125)$$

When  $\delta_3$  can be separately evaluated from (4.24),  $\delta_2$  can be found from (13.123). When these corrections are important and are not made, then the derived  $r_e$  values will not be exactly the same for different isotopic species.

**Table 13.3** Rotational Constant Corrections for LiCl, LiF, and LiD (MHz)<sup>a</sup>

Corrections	<sup>7</sup> Li <sup>35</sup> Cl	<sup>7</sup> LiF	<sup>7</sup> LiD
$Y_{01}$	21,181.004	40,329.808	126,905.36
$\delta_1$	-0.978	-1.410	18.80
$\delta_3$	-0.023	0.081	17.2
$\delta_2 + \delta_3$	0.801	1.370	37
$B_e$	21,180.827	40,329.768	126,961

<sup>a</sup>From Pearson and Gordy [23].

The higher-order corrections described have been applied in studies of CO [22], LiD, LiF, and LiCl [23]. Usually the corrections for the electronic effects are larger than the Dunham correction. The corrections for LiD, LiF, and LiCl are illustrated in Table 13.3. Note that for the light LiD molecule all three terms  $\delta_1$ ,  $\delta_2$ , and  $\delta_3$  are rather large and are essentially equal in magnitude. More detailed discussion of these higher-order effects are available [24, 25].

### Equilibrium Structures for Polyatomic Molecules

For a symmetric, bent, triatomic molecule ( $XY_2$ ) there are three non-degenerate normal modes of vibration: a symmetric stretching  $\omega_1$  where the Y atoms move in the same direction along the X-Y bond, an antisymmetric stretching  $\omega_3$  where the Y atoms move in opposite directions along the X-Y bond, and a bending vibration  $\omega_2$ . Therefore, three excited vibrational states must be investigated if the equilibrium constants are to be determined. The equilibrium structure of  $SO_2$  and  $OF_2$  have been determined by Morino et al. [26, 27], from the rotational spectra. The rotational constants for the first excited state of each of the three vibrations  $\omega_1$ ,  $\omega_2$ , and  $\omega_3$  were determined. This information along with the ground state constants gives the constants  $\alpha_s^a$ ,  $\alpha_s^b$ ,  $\alpha_s^c$  which are collected in Table 13.4. With knowledge of the nine vibration-rotation interaction constants, the equilibrium rotational constants are readily obtained

$$A_e = A_{000} + \frac{1}{2}(\alpha_s^a + \alpha_s^b + \alpha_s^c) \quad (13.126)$$

and so on, from which the equilibrium structure can be evaluated by use of (13.105) and (13.106). The equilibrium structures of  $SO_2$  and  $OF_2$  are given in Table 13.5. Within the experimental errors, the relation  $I_c^e = I_a^e + I_b^e$  required for a planar molecule is well satisfied. For  $SO_2$ ,  $\Delta^e = I_c^e - I_a^e - I_b^e = -0.0038$  amu Å while for  $OF_2$ ,  $\Delta^e = -0.0035$  amu Å<sup>2</sup>. Knowledge of the  $\alpha$  constants also allowed the calculation of the cubic force constants [26, 27].

The equilibrium structures for some other symmetric-bent molecules are collected in Table 13.6. That for nitrogen trifluoride (see Table 6.10), trifluoro-

**Table 13.4** Vibration-Rotation Constants, Rotational Constants, and Moments of Inertia for  $\text{SO}_2$  and  $\text{OF}_2$ <sup>a</sup>

s	$\text{SO}_2$			$\text{OF}_2$		
	$\alpha_s^a$	$\alpha_s^b$	$\alpha_s^c$	$\alpha_s^a$	$\alpha_s^b$	$\alpha_s^c$
1	-31.05	50.14	42.83	38.55	65.77	7.18
2	-1175.90	-2.18	16.00	-699.02	42.36	53.28
3	620.02	34.85	32.88	585.02	69.56	115.25
<i>Rotational Constants (MHz)</i>						
	A	B	C	A	B	C
Effective Equilibrium	60,778.79	10,318.10	8,799.96	58,782.630	10,896.431	9,167.412
	60,485.32	10,359.51	8,845.82	58,744.90	10,985.28	9,255.27
<i>Moments of Inertia (amu Å<sup>2</sup>)</i>						
	$I_a$	$I_b$	$I_c$	$I_a$	$I_b$	$I_c$
Effective Equilibrium	8.31756	48.9946	57.4470	8.60006	46.3942	55.1444
	8.35515 <sup>b</sup>	48.7954 <sup>b</sup>	57.1468 <sup>b</sup>	8.60553	46.0189	54.6209

<sup>a</sup>Morino et al. [26, 27].<sup>b</sup>Small corrections from electron-rotation effects have been included for  $\text{SO}_2$ .**Table 13.5** Equilibrium Structures and Various Ground State Structures of  $\text{SO}_2$  and  $\text{OF}_2$ <sup>a</sup>

Structure	$\text{SO}_2$		$\text{OF}_2$	
	r	θ	r	θ
Equilibrium ( $r_e$ )	1.4308	119°19'	1.4053	103°4'
Effective ( $r_0$ )	1.4336	119°25'	1.4087	103°19'
Substitution ( $r_s$ )	1.4312	119°30'	—	—
Mass dependence ( $r_m$ ) <sup>b</sup>	1.4307	119°20'	—	—
Average ( $\langle r \rangle$ )	1.4349	119°21'	1.4124	103°10'

<sup>a</sup>From Morino et al. [26, 27].<sup>b</sup>From Watson [57].

silane (see Table 6.13) and the methyl halides (see Table 6.12) have been given previously, as well as some equilibrium structures for linear triatomic molecules (Tables 5.9 and 5.10). The equilibrium structure for arsenic trifluoride [28] and phosphorous trifluoride [29] have also been reported, as well as FCN [30] and  $\text{CH}_2\text{F}_2$  [31]. For NOCl, the equilibrium structure [32] found is N–O = 1.131

**Table 13.6** Equilibrium Structures of Some Bent Triatomic Molecules

Molecule	$r_e(\text{\AA})$	$\theta_e$
NF <sub>2</sub> <sup>a</sup>	1.3528 ± 0.0001	103°11' ± 2'
O <sub>3</sub> <sup>b</sup>	1.2715 ± 0.0002	117°47' ± 2
GeF <sub>2</sub> <sup>c</sup>	1.7320 ± 0.0009	97.148°
SiF <sub>2</sub> <sup>d</sup>	1.5901 ± 0.0001	100°46' ± 1'
SF <sub>2</sub> <sup>e</sup>	1.58745 ± 0.00012	98.048° ± 0.013°
SeO <sub>2</sub> <sup>f</sup>	1.608	113.8°

<sup>a</sup>R. D. Brown, F. R. Burden, P. D. Godfrey, and I. R. Gillard, *J. Mol. Spectrosc.*, **52**, 301 (1974).

<sup>b</sup>J. C. Depannemaeker and J. Bellet, *J. Mol. Spectrosc.*, **66**, 106 (1977).

<sup>c</sup>H. Takeo and R. F. Curl, Jr., *J. Mol. Spectrosc.*, **43**, 21 (1972).

<sup>d</sup>H. Shoji, T. Tanaka, and E. Hirota, *J. Mol. Spectrosc.*, **47**, 268 (1973).

<sup>e</sup>Y. Endo, S. Saito, E. Hirota, and T. Chikaraishi, *J. Mol. Spectrosc.*, **77**, 222 (1979).

<sup>f</sup>E. Hirota and Y. Morino, *J. Mol. Spectrosc.*, **34**, 370 (1970).

± 0.004 Å, N–Cl = 1.976 ± 0.004 Å, and ONCl = 113°15' ± 11'. For more complicated polyatomic molecules the experimental problem of obtaining sufficient data for evaluating equilibrium structures is rather difficult. Not only must the  $\alpha$ 's for each of the vibrations be obtained, but they must also be measured for a sufficient number of isotopic species to enable a structure evaluation. Furthermore, many of the vibrational frequencies are large, such as those corresponding to bond stretching, and therefore, the populations of these vibrational states are low because of the unfavorable Boltzmann factor. This makes the observation of rotational transitions associated with such states extremely difficult. (Vibrational satellites of low-frequency bending vibrations are, however, usually observable.) As a consequence, it is not usually feasible to acquire enough experimental data to obtain the constants. Theoretical evaluation of the  $\alpha$  constants required knowledge of the potential constants, and except for simple molecules little information on the anharmonic constants is available. One is hence forced to use the effective ground state rotational constants to extract structural information.

## 7 EVALUATION OF EFFECTIVE STRUCTURES

Structures calculated directly from the  $B_v$ 's observed for a particular vibrational state are called effective structures. Here the structural parameters are chosen to reproduce the effective moments of inertia and the corrections described in Section 6 are not applied. For a diatomic molecule, the effective

**Table 13.7** Bond Lengths of some Diatomic Molecules<sup>a</sup>

Molecule	$r_e$	$r_0$	$\langle r \rangle$
HF	0.9170	0.9257	0.9326
DF	0.9171	0.9234	0.9284
TF	0.9177	0.9230	0.9272
$^{16}\text{OH}$	0.9707	0.9800	0.9873
$^{16}\text{OD}$	0.9700	0.9772	0.9825
$^{12}\text{CH}$	1.1198	1.1303	1.1388
$^{12}\text{CD}$	1.1188	1.1265	1.1327
$\text{H}^{35}\text{Cl}$	1.2745	1.2837	1.2904
$\text{H}^{37}\text{Cl}$	1.2746	1.2837	1.2904
$\text{D}^{35}\text{Cl}$	1.2744	1.2813	1.2858
$\text{D}^{37}\text{Cl}$	1.2744	1.2813	1.2858
$\text{T}^{35}\text{Cl}$	1.2746	1.2800	1.2853
$\text{T}^{37}\text{Cl}$	1.2746	1.2800	1.2853
$^{12}\text{C}^{16}\text{O}$	1.1282	1.1309	1.1323
$^{13}\text{C}^{16}\text{O}$	1.1282	1.1308	1.1322
$^{12}\text{C}^{18}\text{O}$	1.1282	1.1308	1.1322
$^{12}\text{C}^{32}\text{S}$	1.5349	1.5377	1.5392
$^{13}\text{C}^{32}\text{S}$	1.5349	1.5376	1.5391
$^{12}\text{C}^{34}\text{S}$	1.5349	1.5377	1.5392
$^{127}\text{I}^{35}\text{Cl}$	2.3209	2.3236	2.3246
$^{127}\text{I}^{37}\text{Cl}$	2.3209	2.3235	2.3245

<sup>a</sup>From Laurie and Herschbach [86]. See [86] for references to the individual molecules.

bond distance  $r_0$  for the ground vibrational state is

$$r_0 = \left( \frac{\hbar}{8\pi^2 \mu B_0} \right)^{1/2} = \left( \frac{I_b^0}{\mu} \right)^{1/2} \quad (13.127)$$

From our previous discussion, it is obvious that any bond distance calculated from  $B_0$  (or  $I_b^0$ ) will differ from the equilibrium internuclear distance  $r_e$ , which must be obtained from  $B_e$  (or  $I_b^e$ ). Furthermore, the distance  $r_0$  does not represent a simple average bond distance, but rather is defined in terms of the reciprocal of the square root of the average inverse square bond distance

$$r_0 = \left\langle \frac{1}{r^2} \right\rangle^{-1/2} \neq r_e \quad (13.128)$$

which is not equal to  $r_e$  even when the vibrations are harmonic. Also, since  $\alpha_e$  depends on the reduced mass via  $B_e$  and  $\omega_e$ ,  $r_0$  can be expected to vary with isotopic substitution. In Table 13.7 the bond lengths of some diatomic molecules are compared. As the effective rotational constant is less than the equilibrium

rotational constant, the  $r_0$  distance is larger than  $r_e$ . The difference is largest for bonds involving light hydrogen atoms where  $r_0$  is about 0.01 Å larger than  $r_e$ . Furthermore, the  $r_0$  values are different for different isotopic species, the variation being particularly large when light atoms such as hydrogen are substituted. Here a big effect on amplitude of vibration results, and the vibrational average over the zero-point vibration is significantly different. For substitution of heavier atoms little effect is observed. On the other hand, the  $r_e$  values are insensitive to isotopic substitution. Since the  $r_e$  refers to the equilibrium position where the nuclei would be at rest, this type of effect does not enter the calculation of  $r_e$  from  $B_e$ . Variations, like those for  $r_0$ , are also found for the average bond distance,  $\langle r \rangle$ , which is also given in Table 13.7. This measure of the bond distance will be discussed more fully in Section 9.

For polyatomic molecules  $r_0$  is no longer simply the  $\langle r^{-2} \rangle^{-1/2}$  because of Coriolis contributions. Also, isotopic data and the assumption that the effective structural parameters are not affected by mass changes are required for evaluation of the structure. Therefore, when more than a minimum number of isotopic species are available, different  $r_0$  structures can be obtained because the molecular vibrations and hence the effective parameters are modified by isotopic substitution. For the linear molecule HCN, four independent moment of inertia equations may be obtained from the data on  $H^{12}C^{14}N$ ,  $H^{13}C^{14}N$ ,  $D^{12}C^{14}N$ , and  $D^{13}C^{14}N$ . These equations may be combined in six different ways to give values of the two bond lengths. The results are given in Table 13.8 along with the  $r_0$  structures of OCS. It is apparent that different  $r_0$  structures are obtained when different isotopic data are used in the calculation. Variations of about 0.01 Å are observed. Obviously the neglect of the zero-point vibrational effects by assumption that  $r_0$  parameters are the same for different isotopic species has seriously limited the accuracy of the derived structural parameters. With more complicated molecules, least-squares fitting techniques are convenient and have been employed. The problem is linearized in the usual way

$$I_i = I_i^0 + \sum_j \left( \frac{\partial I_i}{\partial p_j} \right)_0 \Delta p_j \quad (13.129)$$

where  $I_i$  corresponds to the  $i$ th experimental moment of inertia,  $I_i^0$  represents the  $i$ th moment of inertia calculated from the initial assumed structure, and  $p_j$  is the  $j$ th structural parameter. The derivatives  $\partial I_i / \partial p_j \equiv \Delta I_i / \Delta p_j$  are evaluated by calculating the change in  $I_i^0$  with a small change in  $p_j$  while keeping all other parameters constant. The foregoing expression forms the basis of a least-squares analysis in which the corrections  $\Delta p_j$  to the initial structure are obtained. The process is repeated until the corrections are small enough. A discussion of some computational problems is available [33]. Ambiguities caused by zero-point vibrations are, however, still present.

A particular problem arises if the normal least-squares equations are ill-conditioned. One must then resort to obtaining extra data, or must add restrictive conditions, for example, hold a particular bond length constant or evaluate only certain linear combinations of the parameters using techniques for the

**Table 13.8** Comparison of  $r_0$  Structures of HCN and OCS

<i>Isotopic Species Used</i>	<i>Bond Length (Å)</i>	
	C-H	C-N
<i>HCN<sup>a</sup></i>		
H <sup>12</sup> C <sup>14</sup> N, H <sup>13</sup> C <sup>14</sup> N	1.0674	1.1557
H <sup>12</sup> C <sup>14</sup> N, D <sup>12</sup> C <sup>14</sup> N	1.0623	1.1567
H <sup>12</sup> C <sup>14</sup> N, D <sup>13</sup> C <sup>14</sup> N	1.0619	1.1568
H <sup>13</sup> C <sup>14</sup> N, D <sup>12</sup> C <sup>14</sup> N	1.0625	1.1566
H <sup>13</sup> C <sup>14</sup> N, D <sup>13</sup> C <sup>14</sup> N	1.0624	1.1563
D <sup>12</sup> C <sup>14</sup> N, D <sup>13</sup> C <sup>14</sup> N	1.0658	1.1555
Average	1.0637	1.1563
Range	0.0055	0.0013
<i>OCS<sup>b</sup></i>		
	C-O	C-S
<sup>16</sup> O <sup>12</sup> C <sup>32</sup> S, <sup>16</sup> O <sup>12</sup> C <sup>34</sup> S	1.1647	1.5576
<sup>16</sup> O <sup>12</sup> C <sup>32</sup> S, <sup>16</sup> O <sup>13</sup> C <sup>32</sup> S	1.1629	1.5591
<sup>16</sup> O <sup>12</sup> C <sup>34</sup> S, <sup>16</sup> O <sup>13</sup> C <sup>34</sup> S	1.1625	1.5594
<sup>16</sup> O <sup>12</sup> C <sup>32</sup> S, <sup>18</sup> O <sup>12</sup> C <sup>32</sup> S	1.1552	1.5653
Average	1.1613	1.5604
Range	0.0095	0.0077

<sup>a</sup>From J. W. Simmons, W. E. Anderson, and W. Gordy, *Phys. Rev.*, **77**, 77 (1950); **86**, 1055 (1952).

<sup>b</sup>From C. H. Townes, A. N. Holden and F. R. Merritt, *Phys. Rev.*, **74**, 1113 (1948).

solution of singular systems [34, 35, 36]. When the limits of uncertainties of the structural parameters can be reasonably estimated, the technique of Section 11 can be applied. In some cases, the best that can be done with the available data is to assume some structural parameters from similar molecules and evaluate only certain parameters which ideally do not depend significantly on the assumed parameters (this can be tested). Such structural parameters are useful but less accurate.

The effects of zero-point vibrations are readily manifested when an atom is substituted which lies on a principal axis (e.g., the sulfur atom of SO<sub>2</sub>). If the atom lies on, say, the *x* axis, then in the rigid rotor approximation the corresponding change in the moment of inertia  $\Delta I_x$  must be zero. In practice, however, small changes are observed because of the effects of vibration. These effects present serious problems to the structural determination of molecules with near-axis atoms or atoms near the center of mass. For such atoms, isotopic

**Table 13.9** Comparison of  $r_0$  Structures Obtained from Different Pairs of Moments of Inertia

Calculated From	$\text{SO}_2^a$		$\text{Cl}_2\text{O}^b$	
	$r$	$\theta$	$r$	$\theta$
$(I_a^0, I_b^0)$	1.4322	$119^\circ 32'$	1.6986	$111^\circ 6'$
$(I_a^0, I_c^0)^c$	1.4336	$119^\circ 36'$	1.6994	$111^\circ 8'$
$(I_b^0, I_c^0)^d$	1.4351	$119^\circ 8'$	1.7031	$110^\circ 39'$
Range	0.0029	$0^\circ 28'$	0.0045	$0^\circ 29'$

<sup>a</sup>From Morino et al. [27].

<sup>b</sup>From Herberich et al. [61].

<sup>c</sup>Equivalent to  $I_a^0, I_b^0 + \Delta$ .

<sup>d</sup>Equivalent to  $I_b^0, I_c^0 + \Delta$ .

substitution produces only small changes in the moments of inertia, and these changes may be masked by the zero-point vibration effects. In the well known example of  $\text{N}_2\text{O}$ , the observed moment of inertia for  $^{15}\text{N}^{14}\text{N}^{16}\text{O}$  is slightly larger than for  $^{15}\text{N}^{15}\text{N}^{16}\text{O}$ ; as a consequence, the application of Kraitchman's equation yields an imaginary coordinate for the central nitrogen atom in  $^{15}\text{N}^{14}\text{N}^{16}\text{O}$ , an impossible result for a rigid molecule.

Even for a simple, bent, triatomic molecule where two moments of inertia of one molecular species are sufficient to give the complete structure, ambiguities result because of the finite inertial defect  $\Delta$ . If a molecule is planar in its equilibrium configuration, then

$$I_c^e \pm I_a^e - I_b^e = 0 \quad (13.130)$$

where  $c$  is the axis perpendicular to the plane. However, the effective moments defined by (13.116) have somewhat different vibrational effects associated with the different axes and

$$I_c^v - I_a^v - I_b^v = \Delta \quad (13.131)$$

where  $\Delta$  is called the inertial defect. Although this quantity is very small compared to the moments of inertia, it nevertheless produces ambiguities in structural calculations. In the case of a bent  $XY_2$  molecule, three different structures are obtainable from the three choices of data available, that is, the three pairs:  $I_a^0, I_b^0$ ;  $I_a^0, I_c^0$ ;  $I_b^0, I_c^0$ . This is illustrated in Table 13.9 for  $\text{SO}_2$  and  $\text{Cl}_2\text{O}_2$ . Such effects are particularly large for the light molecules  $\text{H}_2\text{O}$ ,  $\text{D}_2\text{O}$  and  $\text{T}_2\text{O}$  illustrated in Table 13.10. It will be observed that the range in the bond distance decreases as the mass of the vibrating atom increases. On the other hand, it is not clear whether the tendency is for the bond distance to decrease or increase with isotopic substitution. The length, for example, as calculated from  $I_a^0$ ,  $I_b^0$  increases from  $\text{H}_2\text{O}$  to  $\text{T}_2\text{O}$ , whereas it decreases when calculated from the other two combinations. The trend for the average values also included on the

**Table 13.10** Effective Structures of H<sub>2</sub>O, D<sub>2</sub>O, and T<sub>2</sub>O<sup>a</sup>

From	Effective Structures <sup>b</sup>					
	H <sub>2</sub> O		D <sub>2</sub> O		T <sub>2</sub> O	
	r	θ	r	θ	r	θ
(I <sub>a</sub> <sup>0</sup> , I <sub>b</sub> <sup>0</sup> )	0.9560	105.1	0.9567	104.9	0.9570	104.9
(I <sub>a</sub> <sup>0</sup> , I <sub>c</sub> <sup>0</sup> ) <sup>c</sup>	0.9688	106.3	0.9652	105.7	0.9637	105.5
(I <sub>b</sub> <sup>0</sup> , I <sub>c</sub> <sup>0</sup> ) <sup>d</sup>	0.9703	102.9	0.9673	103.3	0.9662	103.5
Range	0.0143	3.4	0.0106	2.4	0.0092	2.0
Average	0.9650 Å	104.8°	0.9631 Å	104.6°	0.9623 Å	104.6°

<sup>a</sup>Data from: (H<sub>2</sub>O) F. C. De Lucia, P. Helminger, R. L. Cook, and W. Gordy, *Phys. Rev.*, **A5**, 487 (1972); (D<sub>2</sub>O) J. Bellet and G. Steenbeckeliers, *Compt. Rend.*, **271B**, 1208 (1970); (T<sub>2</sub>O) F. C. De Lucia, P. Helminger, W. Gordy, H. W. Morgan, and P. A. Staats, *Phys. Rev.*, **A8**, 2785 (1973).

<sup>b</sup>Obtained from different pairs of moments of inertia.

<sup>c</sup>Equivalent to I<sub>a</sub><sup>0</sup>, I<sub>b</sub><sup>0</sup> + Δ.

<sup>d</sup>Equivalent to I<sub>b</sub><sup>0</sup>, I<sub>a</sub><sup>0</sup> + Δ.

table are, however, consistent with the lower zero-point vibrational energy of the heavier isotopic species.

### Inertial Defect

The problem of calculation of inertial defects has been studied in some detail. The vibration-rotation parameters ε<sub>s</sub><sup>α</sup> in (13.116) are separable into harmonic and anharmonic contributions

$$\varepsilon_s^\alpha = \varepsilon_s^\alpha(\text{har}) + \varepsilon_s^\alpha(\text{anhar}) \quad (13.132)$$

(The Coriolis contributions are included in the harmonic part.) Darling and Dennison [37] have shown that the contribution of the anharmonic part of ε<sub>s</sub><sup>α</sup> to the inertial defect vanishes exactly for planar molecules and hence Δ is given by

$$\Delta_{\text{vib}} = \sum_s (v_s + d_s/2) [\varepsilon_s^c(\text{har}) - \varepsilon_s^a(\text{har}) - \varepsilon_s^b(\text{har})] \quad (13.133)$$

Therefore, Δ<sub>vib</sub> correct to terms linear in the vibrational quantum numbers does not depend on the anharmonic potential constants and may be calculated from a knowledge of the harmonic force constants, masses, and geometry of the molecule. Oka and Morino [38] have given a general expression for the inertial defect of a planar molecule. In addition to the contributions from vibrational motion, there are small contributions from centrifugal distortion and electron-rotation interaction, that is

$$\Delta = \Delta_{\text{vib}} + \Delta_{\text{cent}} + \Delta_{\text{elec}} \quad (13.134)$$

where

$$\Delta_{\text{vib}} = \frac{\hbar}{\pi^2 c} \sum_s (v_s + \frac{1}{2}) \sum'_{s'} \frac{\omega_{s'}^2}{\omega_s(\omega_s^2 - \omega_{s'}^2)} [(\zeta_{ss'}^{(a)})^2 + (\zeta_{ss'}^{(b)})^2 - (\zeta_{ss'}^{(c)})^2] + \frac{\hbar}{\pi^2 c} \sum_t \frac{3}{2\omega_t} \left( v_t + \frac{1}{2} \right) \quad (13.135)$$

$$\Delta_{\text{cent}} = -\hbar^4 \tau_{abab} \left( \frac{3}{4} \frac{I_c}{C} + \frac{I_a}{2A} + \frac{I_b}{2B} \right) \quad (13.136)$$

and

$$\Delta_{\text{elec}} = -\frac{m_e}{m_p} (I_c g_{cc} - I_a g_{aa} - I_b g_{bb}) \quad (13.137)$$

In these equations  $\zeta_{ss'}^{(a)}$ , and so on, are the Coriolis coupling constants;  $t$  runs only over the out-of-plane vibrations;  $m_e$  and  $m_p$  are the mass of the electron and proton;  $g_{aa}$ , and so on, are the rotational magnetic moment  $g$  tensor elements. For  $\Delta$  in amu Å<sup>2</sup>, the vibrational frequencies  $\omega_s$  are expressed in cm<sup>-1</sup>; the centrifugal distortion constant  $\hbar^4 \tau_{abab}$  and rotational constants  $A$ ,  $B$ , and  $C$  are expressed in MHz; moments of inertia  $I_a$ , and so on, in amu Å<sup>2</sup>; and  $\hbar/\pi^2 c = 134.901$ . The Coriolis coupling constants are expressed by

$$\zeta^\alpha = \mathbf{L}^{-1} \mathbf{C}^\alpha (\tilde{\mathbf{L}})^{-1} \quad (13.138)$$

The  $\zeta^\alpha$  ( $\alpha = x, y, z$ ) matrices are skew-symmetric, that is  $\tilde{\zeta}^\alpha = -\zeta^\alpha$ . The  $\mathbf{C}^\alpha$  matrices depend only on the masses and molecular geometry. Their evaluation has been discussed by Meal and Polo [39]. The matrix  $\mathbf{L}$  which connects the normal coordinates and the internal coordinates,  $\mathbf{R} = \mathbf{LQ}$ , can be determined from a normal coordinate analysis. If the Coriolis coupling constant  $\zeta_{ss'}^{(\alpha)}$  is to be nonvanishing, the direct product of the symmetry species of the vibrational coordinates  $Q_s$  and  $Q_{s'}$  must contain the species of the rotation  $R_\alpha$  [40]. For example, a nonlinear  $X Y_2$  molecule, which belongs to the point group  $C_{2v}$ , has two vibrational modes ( $\omega_1, \omega_2$ ) of symmetry  $A_1$  and one ( $\omega_3$ : antisymmetric stretch) of symmetry  $B_1$ . The three rotations  $R_x$ ,  $R_y$ , and  $R_z$  under the  $C_{2v}$  group belong to the species  $B_2$ ,  $B_1$ , and  $A_2$ , respectively. Since we have  $A_1 \times B_1 = B_1$ ,  $A_1 \times A_1 = A_1$  for the direct products, it follows that the possible nonvanishing Coriolis constants are  $\zeta_{13}^{(y)}, \zeta_{31}^{(y)}, \zeta_{23}^{(y)}$ , and  $\zeta_{32}^{(y)}$ , ( $y$  is perpendicular to the molecular plane).

The vibrational contribution to  $\Delta$  is the most important, although it has been found that for molecules with out-of-plane electrons, for example, the  $\pi$  electrons in the C=O bond of H<sub>2</sub>CO, the electronic contribution is not negligible. In the case of ozone the electronic contribution is particularly large, amounting to about 10% of the total inertial defect. The calculation of the electronic contribution to the moments of inertia requires a knowledge of the  $g$  tensor of the rotational magnetic moment. Experimental values of the  $g$  tensor have been given in Chapter XI. Good agreement between calculated and observed inertial defects has been obtained for a number of simple planar molecules [41], as illustrated in Table 13.11. Note that the inertial defect does not show a large

## Chapter XIV

# QUADRUPOLE COUPLINGS, DIPOLE MOMENTS, AND THE CHEMICAL BOND

---

1	INTRODUCTION	726
2	FIELD GRADIENTS OF ELECTRONS IN MOLECULES	727
	Simplifying Conditions	730
3	FIELD GRADIENTS OF ATOMIC ELECTRONS	731
4	COUPLING BY UNBALANCED $p$ ELECTRONS	738
5	CORRECTIONS FOR CHARGE ON COUPLING ATOM	741
6	HYBRIDIZED ORBITALS	742
7	PURE COVALENT BONDS—EFFECTS OF ORBITAL OVERLAP	745
8	POLAR BONDS—IONIC CHARACTER FROM QUADRUPOLE COUPLING	748
9	IONIC CHARACTER—ELECTRONEGATIVITY RELATION	753
10	HYBRIDIZATION FROM QUADRUPOLE COUPLING: POSITIVELY CHARGED HALOGENS AND GROUP III ELEMENTS	755
11	MEASUREMENT OF $\pi$ CHARACTER WITH NUCLEAR QUADRUPOLE COUPLING	758
	Symmetrically Bonded Atoms	759
	Involvement of $d$ Orbitals in Double Bonding	762
	$\pi$ Character from the Asymmetry in the Quadrupole Coupling	764
12	HYPERCONJUGATION	767
13	NITROGEN COUPLING	772
14	COUPLING BY CENTRALLY BONDED ATOMS	776
	Group V Elements	776
	Group IV Elements	778
	Group III Elements; Nature of Boron Bonding	780
15	GROUP ELECTRONEGATIVITIES AND QUADRUPOLE COUPLING	783
16	INTERPRETATION OF DIPOLE MOMENTS	788
	Bond Moment	789
	Hybridization Moment of Atomic Orbitals	791

Moment Induced by Internal Fields	794
The Resultant Moment	794
Ionic Character from Dipole Moments	795
Polyatomic Molecules	000

## 1 INTRODUCTION

In Chapter IX we showed how nuclear quadrupole coupling constants are obtained from the hyperfine structure of molecular rotational spectra. Now we shall relate these constants to the electronic structure of the molecule. The coupling constants obtained from the spectra are of the form

$$\chi_z = eQq_z = eQ \left( \frac{\partial^2 V}{\partial z^2} \right) \quad (14.1)$$

where  $e$  is the charge on a proton,  $Q$  is the electric quadrupole moment of the nucleus, and  $\partial^2 V / \partial z^2$  is the electric field gradient evaluated at the coupling nucleus. Since  $Q$  is known for many nuclei (see Appendix E), we shall here consider  $Q$  as a known constant and shall concentrate our attention on  $q$ , which depends on the electronic structure of the molecule. The reference axis  $z$  is fixed in the molecule and is a principal axis of the coupling tensor. In linear or symmetric-top molecules when the coupling nucleus is on the molecular symmetry axis, there is only one observable coupling constant; the reference axis  $z$  is the molecular symmetry axis. In asymmetric-top molecules the coupling is often symmetric about a bond to the atom having the coupling nucleus. In the general case, there will be three principal values,  $\chi_x$ ,  $\chi_y$ , and  $\chi_z$ , in the coupling tensor of each nucleus; but, as explained in Chapter IX, there are at most only two independent coupling constants. Although the coupling constants are obtained with respect to the principal axes, it is usually convenient for interpretation of the coupling to express the coupling constants with respect to a coordinate system  $x$ ,  $y$ ,  $z$ , where the  $z$  axis is along the bond axis of the coupling atom. This transformation may be accomplished without a knowledge of the off-diagonal elements, for example,  $\chi_{ab}$ , if the assumption can be made that the  $x$ ,  $y$ ,  $z$  axes are principal axes of the field gradient tensor (see Chapter IX, Section 4). Since the coupling constants are evaluated in the molecule-fixed reference system, they are independent of rotational state, except for slight centrifugal distortion effects which are generally negligible. Hence coupling constants of molecules measured from microwave rotational spectra are directly comparable to coupling constants measured with pure quadrupole resonance in solids although some differences are expected because of intramolecular interaction in the solids.

The first calculation of a nuclear quadrupole coupling constant in a molecule was that by Nordsieck [1] for HD. Because the bonding in this molecule is essentially through  $s$  orbitals, the very small D coupling observed in molecular beam resonance experiments is due to orbital distortion effects. For this reason the theory derived for HD is not applicable to couplings in the more complex

molecules usually observed with microwave spectroscopy. Approximate methods for interpretation of nuclear quadrupole coupling in complex molecules in terms of chemical bond properties were developed in the early period of microwave spectroscopy by Townes and Dailey [2-4]. These methods were modified and extended by Gordy [5-7]. Molecular orbital treatment of quadrupole coupling of halogen nuclei in unsaturated organic molecules has been given by Bersohn [8] and by Goldstein [9], who showed that the asymmetry in the coupling is due to  $\pi$  bonding by the halogen. Reviews of quadrupole coupling are available [10-15].

Nuclear quadrupole coupling in many atoms is accurately known from atomic beam resonance experiments. The coupling in others can be calculated with useful accuracy when the quadrupole moment is known. The simplest approach to the interpretation of the couplings in molecules is to relate them to known or calculable atomic couplings. This procedure is most suited to application of the valence bond theories and to LCAO molecular orbital theory which expresses the electronic wave functions of the molecule in linear combinations of the atomic functions. Appropriate methods for interpretation of molecular coupling in terms of known atomic couplings are discussed in the following sections.

Although this chapter is primarily devoted to the interpretation of nuclear quadrupole coupling, we give in Section 14 an elementary interpretation of molecular dipole moments in terms of chemical bond properties. While nuclear quadrupole coupling is sensitive only to the charge distribution near the coupling nucleus, the molecular dipole moment depends strongly on the charge distribution over the entire molecule. Information about the electronic structure of molecules obtained from these two molecular parameters is mostly complementary. In some diatomic molecules for which bond ionic character is derivable from both quadrupole coupling and dipole moments, the results are shown to be consistent.

## 2 FIELD GRADIENTS OF ELECTRONS IN MOLECULES

An unscreened electronic charge  $e$  at distance  $r$  from a nucleus will give rise to a potential of  $e/r$  at this nucleus. In a coordinate system  $x, y, z$ , with origin at the nucleus and with  $z$  along the bond axis,  $r=(x^2+y^2+z^2)^{1/2}$ , the electric field gradient at the nucleus due to this electron is

$$\frac{\partial^2 V}{\partial z^2} = \frac{\partial^2}{\partial z^2} \left( \frac{e}{r} \right) = e \frac{\partial}{\partial z^2} (x^2 + y^2 + z^2)^{-1/2} = \frac{e(3 \cos^2 \theta - 1)}{r^3} \quad (14.2)$$

where  $\theta$  is the angle between  $r$  and the reference axis  $z$ . To obtain the contribution by an electron of a molecule to the field gradient at the nucleus of one of its atoms, say atom  $A$ , it is necessary to average the above quantity over the molecular orbital  $\phi_i$  of the electron. Since  $\phi_i$  is normalized so that  $\int \phi_i^* \phi_i d\tau = 1$ , this average may be expressed as

$$q_i^A = e \int \phi_i^* \left( \frac{3 \cos^2 \theta_A - 1}{r_A^3} \right)_i \phi_i d\tau \quad (14.3)$$

The total field gradient  $q^A$  at the nucleus of atom  $A$  due to all the electrons in the molecule is

$$q_{\text{mol}}^A = e \sum_i n_i \int \phi_i^* \left( \frac{3 \cos^2 \theta_A - 1}{r_A^3} \right)_i \phi_i d\tau \quad (14.4)$$

where  $n_i = 1, 2$ , or 0 is the number of electrons in the  $i$ th orbital and the summation is taken over all orbitals of the molecule.

Evaluation of the foregoing integral for all the electrons in a typical molecule seems a formidable problem indeed. However, with reasonable approximations and assumptions, the integral can be evaluated for many molecules to useful accuracy.

Let us consider the field gradient at the nucleus of atom  $A$  caused by the electrons of a diatomic molecule  $AB$ . The molecular orbitals can be expressed as a linear combination of atomic orbitals  $\psi_i^A$  and  $\psi_i^B$  of atoms  $A$  and  $B$ .

$$\phi_i = a_i \psi_i^A + b_i \psi_i^B \quad (14.5)$$

Substitution of this function into (14.4) gives the resultant field gradient at nucleus  $A$  as

$$q_{\text{mol}}^A = e \sum_i n_i \int (a_i \psi_i^{*A} + b_i \psi_i^{*B}) \left( \frac{3 \cos^2 \theta_A - 1}{r_A^3} \right)_i (a_i \psi_i^A + b_i \psi_i^B) d\tau \quad (14.6)$$

where the summation is taken over all electrons of the molecule. Expansion gives

$$\begin{aligned} q_{\text{mol}}^A = & e \sum_i n_i a_i^2 \int \psi_i^{*A} \left( \frac{3 \cos \theta_A - 1}{r_A^3} \right)_i \psi_i^A d\tau \\ & + 2e \sum_i n_i a_i b_i \int \psi_i^{*A} \left( \frac{3 \cos^2 \theta_A - 1}{r_A^3} \right)_i \psi_i^B d\tau \\ & + e \sum_i n_i b_i^2 \psi_i^{*B} \left( \frac{3 \cos^2 \theta_A - 1}{r_A^3} \right)_i \psi_i^B d\tau \end{aligned} \quad (14.7)$$

The last term of (14.7) gives the contributions to the field gradient at the nucleus of atom  $A$  by all the electrons on atom  $B$ . This term is small because of the inverse cube variation of the field gradient with distance and is counterbalanced by an opposite contribution of very nearly the same magnitude from the nuclear charge of  $B$  which has been ignored in (14.2). For these reasons the last term, as well as the contribution from the nuclear charge of  $B$ , will be neglected. The second term on the right is a contribution from the electronic charge in the overlap region and is zero except for electrons in bonding molecular orbitals and is small as compared with the first term on the right, even for bonding orbitals. For reasons described in Section 7, the cross terms for bonding orbitals in the normalization can be neglected, and the wave functions  $\phi_i$  can be normalized by

$$a_i^2 + b_i^2 = 1 \quad (14.8)$$

This normalisation, in effect, divides overlap charge between the two atomic orbitals. Thus, to a good approximation, the coupling field gradient at nucleus  $A$  can be expressed as the summation of the weighted contributions from the electronic charges in the atomic orbitals of atom  $A$ . Thus

$$q_{\text{mol}}^A = \sum_i n_i a_i^2 q_i^A \quad (14.9)$$

where

$$q_i^A = e \int \psi_i^{*A} \left( \frac{3 \cos^2 \theta_A - 1}{r_A^3} \right)_i \psi_i^A d\tau \quad (14.10)$$

and  $a_i^2$  is a measure of the electronic charge density in the  $i$ th atomic orbital  $\psi_i^A$ .

Equation 14.9 is easily generalized to polyatomic molecules for which the wave function  $\phi_i$  must be represented by a linear combination of atomic wave functions of  $N$  atoms

$$\phi_i = \sum_{j=1}^N c_{ji} \psi_{ji} \quad (14.11)$$

where the index  $j$  runs over the different atoms. If effects of overlap distortions and of contributions to the field gradient at the  $k$ th nucleus by electronic and nuclear charges of other atoms of the molecule are neglected, substitution of this wave function in (14.4) yields the field gradient at the nucleus of atom  $k$

$$q_{\text{mol}}^k = \sum_i \sum_j n_i c_{ki} c_{ji} q_{ki,ji} \quad (14.12)$$

where

$$q_{ki,ji} = e \int \psi_{ki}^* \left( \frac{3 \cos^2 \theta_k - 1}{r_k^3} \right)_i \psi_{ji} d\tau \quad (14.13)$$

At most, only overlap terms with atoms bonded to the coupling atom  $k$  need be considered, and generally even these can be neglected. Therefore, the field gradient at the  $k$ th nucleus in a polyatomic molecule is given quite closely by

$$q_{\text{mol}}^k = \sum_i n_i c_{ki}^2 q_{ki,ki} \quad (14.14)$$

where the  $c$ 's are normalized by

$$\sum_j c_{ji}^2 = 1 \quad (14.15)$$

and where  $q_{ki,ki}$  is the field gradient at the  $k$ th nucleus caused by an electron in an atomic orbital  $\psi_{ki}$  of the coupling atom  $k$ .

It should be realized that the atomic orbitals of the atom bonded in the molecule are not necessarily the same as those of the free atoms. The valence shell atomic orbitals  $\psi_{ki}$  might be an admixture of two or more orbitals of the free atom  $k$ . Also, the field gradient at the nucleus of atom  $k$  might differ slightly

from that of the free atom because of changes in nuclear screening. To evaluate the coefficients of  $c_{ki}$  from the observed quadrupole coupling or to predict the coupling from the  $c_{ki}$  values calculated from molecular orbital theory, one must express the atomic orbitals of the bonded atoms in terms of those of the free atoms. Methods for doing this are described in Sections 3-8.

With  $\psi_{ki}$  expressed as a linear combination of hydrogenlike wave functions  $\psi_{nlm_i}$ , the integrals involved in (14.14) will vanish unless  $l'=l\neq 0$  or  $l'=l\pm 2$  and  $m'_i=m_i$ . Many other terms can be ignored on energetic grounds. Cross terms, for example, involving  $s(l=0)$  and  $d(l=2)$  orbitals, although nonvanishing, can be neglected since the integrals are small; also mixing of  $s$  and  $d$  orbitals is usually small, and hence the integral will be multiplied by a small weighting coefficient. Integrals of the type  $n=n', l=l'$  are found to decrease in magnitude with increasing  $n$  or  $l$  (Section 3). The implications of these and other considerations are summarized later.

The coefficients of  $c_{ji}^2$  of (14.11) represent the weights of the various atomic orbital constituents in the molecular orbital  $\phi_i$ . For polyatomic molecules of high symmetry, such as planar organic ringed groups, molecular orbital methods like those described in texts by Coulson [16] or Pullman and Pullman [17] may be used for calculation of the values of these coefficients which can, in principle, be compared with experimental values obtained from nuclear quadrupole couplings. Unfortunately, such calculations give reliable predictions mainly for  $\pi$  orbital densities on the ring carbons, which have no quadrupole moments. Nitrogen atoms, often bonded in unsaturated ringed systems, have quadrupole moments, but the coupling of  $^{14}\text{N}$  is so small as to be difficult to measure accurately in such systems. Quadrupole couplings of halogen atoms attached to planar rings have been treated with molecular orbital theory [8, 18]. Application of molecular orbital theory for prediction of quadrupole coupling for the molecules of low symmetry that are usually observed in microwave spectroscopy is difficult because a high degree of symmetry is required for reduction of unknown parameters of the secular equations. It is evident that quadrupole coupling alone cannot provide very complete information about the molecular orbitals of complex molecules. However, it can give useful information about the bonding to the particular atom for which the quadrupole coupling is measured. Even in the simpler diatomic molecules the unknown parameters are generally more numerous than the measurable coupling constants, and assumptions are necessary in the interpretation of the quadrupole coupling. By correlation of the quadrupole coupling of the same atoms in a number of different molecules, the reasonableness of the approximations and assumptions can be subjected to a consistency test. In this way much has been learned about the nature of chemical bonding.

### Simplifying Conditions

Certain reasonable approximations and assumptions can be made that greatly simplify the evaluation of the field gradients of coupling nuclei as expressed by (14.9) or (14.12). (1) Electrons in closed subvalence shells can be

neglected. Because of spherical symmetry, their resultant contribution is zero except for slight distortion effects such as the Sternheimer corrections [19, 20]. (2) Contributions by electronic charge of  $s$  orbitals of the coupling atom are zero because of spherical symmetry of the  $s$  orbital. (3) Contributions by  $d$  electrons are negligible in comparison to those of  $p$  electrons for most molecules. (4) Contributions by electronic and nuclear charges of atoms other than those of the coupling nuclei approximately cancel and can generally be neglected. (5) The predominant contribution to the field gradient at the nucleus in most molecules is that from  $p$  electrons of the valence shell of the coupling atom. Other orbitals such as  $s$  or  $d$  influence the coupling indirectly by altering the filling of the  $p$  orbitals via hybridization. (6) Contributions by electrons in non-bonding or antibonding electrons in the valence shell of the coupling atoms are the same as those of free atoms except for possible differences in orbital orientation, orbital hybridization, and small effects that are due to change in nuclear screening when there is a formal charge on the coupling atom. (7) Contribution by an electron in a bonding molecular orbital  $i$  to the field gradient at the  $k$ th nucleus is assumed to be that of an electron in the constituent bonding atomic orbital of the coupling atom  $k$  times the weighting coefficient  $c_{ki}^2$ , which gives the fractional contribution of the atomic orbital to the bonding molecular orbital. (8) In calculation of the weighting coefficients  $c_{ki}^2$ , either valence bond theory or molecular orbital theory may be applied, with effects of orbital overlap neglected. (9) Contributions by electrons in hybridized atomic orbitals are taken to be the sum of the contributions by the fractional constituent orbitals, again with effects of orbital overlap neglected.

With these simplifying approximations it is evident that interpretation of the nuclear quadrupole coupling of a bonded atom for which  $Q$  and  $q_{n10}$  are known (Section 3) depends on the degree and manner in which the  $p$  orbitals of the coupling atoms are filled, that is, on the number of unbalanced  $p$  electrons in the valence shell (Section 4).

### 3 FIELD GRADIENTS OF ATOMIC ELECTRONS

The contribution by an electron in an atomic orbital to the field gradient at the atomic nucleus, if effects of electron spin are neglected, can be expressed as

$$q_{nlm_l} = e \int \psi_{nlm_l}^* \left( \frac{3 \cos^2 \theta - 1}{r^3} \right) \psi_{nlm_l} d\tau \quad (14.16)$$

where  $e$  is the electronic charge. The average of  $r$  depends only on  $n$  and  $l$ , and the average of  $\theta$  only on  $l$  and  $m_l$  where  $n$ ,  $l$ , and  $m_l$ , are, respectively, the principal, the orbital angular momentum, and the magnetic quantum numbers. Therefore

$$q_{nlm_l} = e(l, m_l | 3 \cos^2 \theta - 1 | l, m_l) \left( n, l \left| \frac{1}{r^3} \right| n, l \right) = -2e \frac{[3m_l^2 - l(l+1)]}{(2l-1)(2l+3)} \left\langle \frac{1}{r^3} \right\rangle \quad (14.17)$$

In the usual observations in atomic spectra,  $l$  has its maximum projection along

the space-fixed reference axis  $z$  so that  $m_l = l$ , and thus the effective value of  $q$  is

$$q_{nl0} = -\frac{2el}{2l+3} \left\langle \frac{1}{r^3} \right\rangle \quad (14.18)$$

In the bonded atoms where the reference axis is along the  $\sigma$  bond formed by the orbital,  $m_l$  equals zero, and the effective value of  $q$  is

$$q_{nl0} = \frac{2el}{2l+3} \frac{l+1}{2l-1} \left\langle \frac{1}{r^3} \right\rangle \quad (14.19)$$

Comparison of (14.18) and (14.19) shows that

$$q_{nl0} = \frac{l+1}{2l-1} q_{nl1} \quad (14.20)$$

For  $p$  orbitals,  $l=1$  and

$$q_{n10} = -2q_{n11} \quad (14.21)$$

For  $s$  electrons,  $l$  equals zero, and it is evident from (14.18) that the field gradient is zero. The difficulty in evaluation of  $q$  comes in obtaining the average  $\langle 1/r^3 \rangle = \langle n, l | 1/r^3 | n, l \rangle$ . Because of uncertainty in the wave functions, this average cannot be directly calculated with very useful accuracy except for hydrogen or for highly ionized atoms which have hydrogenlike orbitals. However, other measurable quantities, notably the magnetic hyperfine structure and the doublet fine structure, also depend on  $\langle 1/r^3 \rangle$  average, and in many complex atoms the desired values of  $\langle 1/r^3 \rangle$  for  $p$  orbitals can be obtained from measured values of these splittings.

Before discussion of the more accurate, semi-empirical methods for obtaining  $\langle 1/r^3 \rangle$  for  $p$  electrons, let us consider the theoretical relation [21, 22] for hydrogenlike orbitals. If all electrons except the one to be considered are removed, the effective nuclear charge number would be  $Z$ , the atomic number. When relativistic effects are neglected, we would have

$$\left\langle \frac{1}{r^3} \right\rangle = \frac{Z^3}{a_0^3 n^3 l(l+\frac{1}{2})(l+1)} \quad (14.22)$$

where  $a_0$  is the radius of the first Bohr orbit and  $n$  is the total quantum number. Because of the nuclear screening by other electrons in polyelectron alkalilike atoms, the atomic number  $Z$  must be replaced by  $Z_{\text{eff}} = Z - \sigma$  where  $\sigma$  is a screening constant. An obvious difficulty in applying the relation is in obtaining  $Z_{\text{eff}}$ . One procedure is to estimate  $\sigma$  from the observed term energies of the atom by use of the relation [21]

$$E_n = -\frac{RZ_{\text{eff}}^2}{n^2} = -\frac{R(Z-\sigma)^2}{n^2} \quad (14.23)$$

in which  $R$  is the Rydberg constant. Another procedure is to employ the true  $Z$  and alter  $n$  in such a way as to get the term energy

$$E_n = -\frac{RZ^2}{n^{*2}} = -\frac{RZ^2}{(n-\mu)^2} \quad (14.24)$$

where  $\mu$  is the quantum defect or Rydberg correction. A less distorted treatment is to apply corrections to both  $Z$  and  $n$ , but this requires additional relations for evaluation of the two parameters.

Substitution of (14.22) into (14.18) with  $Z_{\text{eff}}$  for  $Z$  yields

$$q_{nl} = -\frac{4eZ_{\text{eff}}^3}{a_0^3 n^3 (l+1)(2l+1)(2l+3)} \quad (14.25)$$

Without quantitative knowledge of the values of  $Z_{\text{eff}}$ , some important qualitative deductions can be made from this formula. (1) We know that the screening will increase rapidly with increase of  $n$  because the higher  $n$  orbitals are, on the average, further from the nucleus and hence more screened by the electrons of the inner shells. Therefore, excited states with  $n$  values greater than those of the valence shells will have  $q$  values considerably less than those of the valence shells not only because of the inverse cube variation with  $n$  but because of the large decrease in  $Z_{\text{eff}}$ . For neutral atoms  $Z_{\text{eff}}$  approaches unity for  $n$  values that are large as compared with the ground state values. (2) Evidence indicates that the  $d$  electrons are more effectively screened from the nucleus than are the  $p$  electrons of the same shell. In addition, the  $q$  value for  $d$  electrons is reduced from that for  $p$  electrons by a factor of  $\frac{2}{3}$  by the change in  $l$  from 1 to 2. Together, these effects cause the  $q$  of  $d$  electrons in most atoms to be less by an order of magnitude than that of  $p$  electrons of the same shell (same  $n$  value). (3) Equation 14.25 also shows why a formal charge on the atom increases, and a negative formal charge decreases, the field gradient of the orbitals. Removal of an electron deletes the screening by that electron and thus increases  $Z_{\text{eff}}$ , whereas addition of an electron correspondingly increases the screening and decreases  $Z_{\text{eff}}$ . According to Slater's rule [23], an electron in an  $s$  or  $p$  orbital of the valence shell has a screening constant of 0.35 for other  $p$  electrons of this shell.

The most widely applicable method for obtaining  $\langle 1/r^3 \rangle$  to useful accuracy for  $p$  electrons in complex atoms makes use of measurements of doublet fine structure. The fine structure splitting is a measure of the spin-orbit coupling which, in turn, is a function of  $\langle 1/r^3 \rangle$ . The well-known formula expressing this relationship [21, 22] is

$$\left\langle \frac{1}{r^3} \right\rangle = \frac{\Delta v}{a_0^3 R \alpha^2 (l + \frac{1}{2}) Z_{\text{eff}} H_r} \quad (14.26)$$

in which  $\Delta v$  is the fine structure doublet frequency in  $\text{cm}^{-1}$ ,  $a_0$  is the radius of the first Bohr orbit,  $R$  is the Rydberg constant,  $\alpha$  is the fine structure constant,  $Z_{\text{eff}}$  is the effective atomic number, and  $H_r$  is a small relativistic correction. Fine structure doublets of  $p$  electrons have been measured for most of the common elements. Obtaining the effective atomic number  $Z_{\text{eff}}$  is difficult. Barnes and Smith [24] have used the term values to obtain  $Z_{\text{eff}}$  values for a

**Table 14.1** Values of  $q_{n10}$  Derived from the Calculations of Barnes and Smith [24]

Atom	Configuration	State	$\left\langle \left( \frac{a_0}{r} \right)^3 \right\rangle^a$	$q_{n10} (10^{15} \text{ esu})^b$
Li	$2p$	$^2P$	0.0387	-0.100
Be	$2s2p$	$^3P$	0.173	-0.45
B	$2p$	$^2P$	0.608	-1.58
C	$2p^2$	$^3P$	1.23	-3.19
N	$2p^3$		(2.46)	-(6.4)
O	$2p^4$	$^3P$	4.29	-11.1
F	$2p^5$	$^2P$	6.55	-17.0
Na	$3p$	$^2P$	0.243	-0.63
Mg	$3s3p$	$^3P$	0.77	-2.00
Al	$3p$	$^2P$	1.28	-3.32
Si	$3p^2$	$^3P$	2.30	-5.97
P	$3p^3$		(3.46)	-(9.0)
S	$3p^4$	$^3P$	4.99	-13.0
Cl	$3p^5$	$^2P$	7.11	-18.6
K	$4p$	$^2P$	0.434	-1.13
Ca	$4s4p$	$^3P$	1.12	-2.91
Ga	$4p$	$^2P$	3.42	-8.88
Ge	$4p^2$	$^3P$	5.61	-14.6
As	$4p^3$		(7.32)	-(19)
Se	$4p^4$	$^3P$	9.36	-24.3
Br	$4p^5$	$^2P$	13.16	-34.2
Rb	$5p$	$^2P$	0.818	-2.12
Sr	$5s5p$	$^3P$	1.93	-5.0
In	$5p$	$^2P$	5.40	-14.0
Sn	$5p^2$	$^3P$	10.5	-27.3
Sb	$5p^3$		12.2	-30.7
Te	$5p^4$	$^3P$	14.0	-36.3
I	$5p^5$	$^2P$	16.8	-43.6
Cs	$6p$	$^2P$	1.20	-3.12
Ba	$6s6p$	$^3P$	2.64	-6.85
Tl	$6p$	$^2P$	9.91	-25.7
Pb	$6p^2$	$^3P$	13.4	-34.8
Bi	$6p^3$		20.4	-53.0

<sup>a</sup>The values of  $\langle (a_0/r)^3 \rangle$  given here are those of Barnes and Smith with the relativistic correction  $H_r$  applied.

<sup>b</sup>Coupling per  $p$  electron for different nuclear isotopes can be obtained with these  $q_{n10}$  values and the  $Q$  values of Appendix E. In MHz units,  $eQq_{n10}(\text{MHz}) = 72.5 Q(10^{-24} \text{ cm}^2) q_{n10}(10^{15} \text{ esu})$ . More precise values of  $eQq_{n10}$  for some nuclei are given in Table 14.2.

large number of excited and/or ionized states of atoms and by projection of these values have concluded that the relation

$$Z_{\text{eff}} = Z - n \quad (14.27)$$

provides a good approximation to  $Z_{\text{eff}}$ . These are similar to the earlier rules [21, 22],  $Z_{\text{eff}} = Z - 2$  for the first period and  $Z_{\text{eff}} = Z - 4$  for higher periods. With values of  $\Delta v$  obtained from the literature and with  $Z_{\text{eff}}$  from (14.27), Barnes and Smith calculated values for  $\langle 1/r^3 \rangle$  for  $p$  orbitals of a large number of elements as shown in Table 14.1. From these values the field gradients  $q_{n10}$  listed in the last column of Table 14.1 are calculated from the relation

$$q_{n10} = -2.596 \left\langle \left( \frac{a_0}{r} \right)^3 \right\rangle \times 10^{15} \text{ esu} \quad (14.28)$$

which is obtained from a combination of (14.26) with (14.19) and substitution of the values for the numerical constants and  $l=1$  for  $p$  electrons. Values for the  $p^3$  configurations, that is, those for the Group V elements N, P, and so on, which have spherically symmetric charge distributions, are considered most questionable by Barnes and Smith because there is no definitive way to infer the doublet splitting equivalent to that of a single  $p$  electron. Consequently, these doubtful values obtained by interpolation are shown in parentheses.

The original tabulation of Barnes and Smith [24] did not include the relativistic correction. They, in effect, tabulated  $\langle (a_0/r)^3 \rangle H_r$ . Although this correction is negligible for first- and second-row elements, it increases with  $Z$  and becomes as large as 10% for elements with  $Z=60$ . Kopfermann [22] provides tabulated numerical values of  $H_r$  for all the elements. In Table 14.1 we have used his tabulation to correct the Barnes and Smith values for the relativistic effect. These corrections lower the magnitude of  $q$ . The values of  $q_{n10}$  listed in Table 14.1 are still not corrected for the Sternheimer polarization [19, 20] which would have the effect of lowering the values slightly more. The accuracy of the field gradients is sufficient, however, for use in most interpretations of molecular quadrupole couplings where other uncertainties are often greater.

The most accurate values of  $q$  are those obtained from atomic beam measurements of the combined magnetic and quadrupole coupling constants commonly designated by  $a$  and  $b$ , respectively, in atoms which have a single unbalanced  $p$  electron in the valence shell. Boron in its ground  ${}^2P_{1/2}$  state has the configuration  $2s^2 2p$  with one  $p$  electron outside the closed  $2s$  subshell. The important halogen atoms have  ${}^2P_{3/2}$  ground states. Each of them lacks the single electron needed to close the  $p$  valence shell and hence has a single unbalanced and unpaired electron. The single electron hole in the  $p$  valence shell of the halogens gives a field gradient of opposite sign to that of a single  $p$  electron outside a closed shell, as in boron. Otherwise, its quadrupole coupling can be treated in a similar manner.

The nuclear magnetic coupling constant of an unpaired non- $s$  electron can be expressed as

$$a = \frac{2\beta\mu_I l(l+1)}{Ij(j+1)} \left\langle \frac{1}{r^3} \right\rangle \quad (14.29)$$

where  $\beta$  is the Bohr magneton,  $\mu_I$  is the nuclear magnetic moment,  $I$  is the nuclear spin, and  $j$  is the total electronic angular momentum quantum number. This expression does not include a small relativistic correction calculated by Casimir [25]. Methods for evaluation of the relativistic corrections are described in Kopfermann's monograph [22] on nuclear moments. The nuclear spins and magnetic moments of all abundant isotopes are now known from magnetic resonance (see Appendix E). Hence, when  $a$  can be measured for atoms having a single unbalanced electron, the  $\langle 1/r^3 \rangle$  value can be evaluated from (14.29). This method gives the most accurate evaluation of  $\langle 1/r^3 \rangle$  for the lighter elements. For heavier elements, however, Koster [26] has pointed out that configuration interaction reduces the accuracy of the values. In addition to possible configuration interaction within the valence shell, there is a slight polarization of the inner electron shells by the asymmetric charge distribution of the valence shell predicted by Sternheimer [20]. Some values of field gradients determined from magnetic hyperfine structure are listed in Table 14.2. Some of these values include corrections for configuration interactions and the Sternheimer correction, as indicated.

When the ratio of the magnetic coupling to the quadrupole coupling constant  $b = -eQq_{nl}$  can be measured for the same unbalanced electron in accurate atomic beam experiments, precise values of the nuclear quadrupole moment  $Q$  can be obtained. The quadrupole coupling in such an atom, in which electron spin is included, is given by

$$b = -eQq_{nl} = -e^2 Q \frac{2l}{2l+3} \left\langle \frac{1}{r^3} \right\rangle \quad (14.30)$$

for the state of maximum projection along  $z$  ( $m_j=j=l+\frac{1}{2}$ ). Division of (14.30) by (14.29) shows that

$$\frac{b}{a} = - \frac{e^2 Q I j(j+1)}{\beta \mu_I (l+1)(2l+3)} \quad (14.31)$$

The more accurate values of  $Q$  listed in Table 14.2 are those obtained from atomic beam experiments.

For interpretation of molecular quadrupole coupling in terms of chemical bond properties we shall need the quantity  $eQq_{n10}$ , which is the nuclear quadrupole coupling of an individual electron in an atomic  $p$  orbital of the valence shell  $n$  having zero angular momentum,  $m=0$ , along the reference axis. This corresponds to the orientation of the symmetry axis of the orbital along the reference axis, as occurs for a  $p$  orbital employed in formation of a  $\sigma$  bond. The  $\pi$  bonds are formed by  $p$  orbitals with  $m=\pm 1$  and therefore have their symmetry axes perpendicular to the reference,  $\sigma$ -bond axis.

In atomic experiments the quadrupole coupling constant  $b$  measured for a

**Table 14.2** Quadrupole Coupling by Atomic *p* Electrons

<i>Nuclear Isotope</i>	<i>Nuclear Spin</i>	$Q$ ( $10^{-24} \text{ cm}^2$ )	<i>Electron</i>	$2(eQq)_{\text{atom}}$ $eQq_{n10}(\text{MHz})$	<i>Ref.</i>
$^{10}\text{B}$	3	+0.0740	2p	-11.83	<sup>a</sup>
$^{11}\text{B}$	$\frac{3}{2}$	+0.0357	2p	-5.39	<sup>a</sup>
$^{14}\text{N}$	1	+0.1	2p	-10	<sup>b</sup>
$^{17}\text{O}$	$\frac{5}{2}$	-0.026	2p	+21	<sup>c</sup>
$^{25}\text{Mg}$	$\frac{5}{2}$	+0.22	3p	-16	<sup>d</sup>
$^{27}\text{Al}$	$\frac{5}{2}$	+0.155	3p	-37.52	<sup>e</sup>
$^{33}\text{S}$	$\frac{3}{2}$	-0.055	3p	+52	<sup>c</sup>
$^{35}\text{Cl}$	$\frac{3}{2}$	-0.0795	3p	+109.74	<sup>f</sup>
$^{37}\text{Cl}$	$\frac{3}{2}$	-0.0621	3p	+86.51	<sup>f</sup>
$^{69}\text{Ga}$	$\frac{3}{2}$	+0.190	4p	-125.0	<sup>g</sup>
$^{71}\text{Ga}$	$\frac{3}{2}$	+0.120	4p	-78.80	<sup>g</sup>
$^{73}\text{Ge}$	$\frac{9}{2}$	-0.224	4p	+224	<sup>h</sup>
$^{75}\text{As}$	$\frac{3}{2}$	+0.29	4p	-400	<sup>c</sup>
$^{79}\text{Br}$	$\frac{3}{2}$	+0.31	4p	-769.76	<sup>i</sup>
$^{81}\text{Br}$	$\frac{3}{2}$	+0.26	4p	-643.03	<sup>i</sup>
$^{115}\text{In}$	$\frac{9}{2}$	+0.82	5p	-899.10	<sup>j</sup>
$^{121}\text{Sb}$	$\frac{5}{2}$	-0.29	5p	+650	<sup>c</sup>
$^{123}\text{Sb}$	$\frac{7}{2}$	-0.37	5p	+830	<sup>c</sup>
$^{127}\text{I}$	$\frac{5}{2}$	-0.79	5p	+292.71	<sup>k</sup>
$^{201}\text{Hg}$	$\frac{3}{2}$	+0.045	6p	-780	<sup>l</sup>
$^{209}\text{Bi}$	$\frac{9}{2}$	-0.4	6p	+1500	<sup>m</sup>

<sup>a</sup>V. S. Korolkov and A. G. Makhanek, *Opt. i Spektroskopiya*, **12**, 163 (1962); *Opt. Spectrosc. USSR (English Transl.)*, **12**, 87 (1962).

<sup>b</sup>See text, Section 13.

<sup>c</sup>Calculated with  $Q$  from Column 3 and  $q_{n10}$  from Table 14.1.

<sup>d</sup>A. Lurio, *Phys. Rev.*, **126**, 1768 (1962).

<sup>e</sup>H. Lew, *Phys. Rev.*, **76**, 1086 (1949).

<sup>f</sup>V. Jaccarino and J. G. King, *Phys. Rev.*, **83**, 471 (1951).

<sup>g</sup>G. F. Koster, *Phys. Rev.*, **86**, 148 (1952).

<sup>h</sup>W. J. Childs, L. S. Goodman, and L. J. Kieffer, *Phys. Rev.*, **120**, 2138 (1960).

<sup>i</sup>J. G. King and V. Jaccarino, *Phys. Rev.*, **94**, 1610 (1954).

<sup>j</sup>T. G. Eck and P. Kusch, *Phys. Rev.*, **106**, 958 (1957).

<sup>k</sup>V. Jaccarino, J. G. King, R. A. Satten, and H. H. Stroke, *Phys. Rev.*, **94**, 1798 (1954).

<sup>l</sup>H. G. Dehmelt, H. G. Robinson, and W. Gordy, *Phys. Rev.*, **93**, 480 (1954).

<sup>m</sup>Robinson et al. [58].

single coupling *p* electron corresponds to the orientation of  $m = \pm 1$  and can be expressed as

$$b = -eQq_{n,1,\pm 1} = \frac{1}{2}eQq_{n10} \quad (14.32)$$

Therefore

$$eQq_{n10} = 2b = 2(eQq)_{\text{atom}} \quad (14.33)$$

Table 14.2 gives values of  $eQq_{n10}$  thus obtained from the measured atomic constant  $b$ . Sometimes  $eQq_{n10}$  derived from atomic spectra is indicated as  $(eQq)_{\text{at}}$ , although this quantity is twice the observable atomic coupling constant  $b$ .  $Q$  is expressed in units of  $\text{cm}^2$ , and sometimes  $q$  is expressed in units of  $\text{cm}^{-3}$ . When this is done, the coupling must be represented by  $e^2Qq$  since  $q(\text{esu}) = eq(\text{cm}^{-3})$ . Also, it is apparent that the coupling in frequency units is  $eQq/h$ . For convenience, however,  $h$  is usually omitted and the coupling constant specified in frequency units simply as  $eQq$ .

#### 4 COUPLING BY UNBALANCED $p$ ELECTRONS

The field gradient which gives rise to the nuclear quadrupole coupling in most molecules is due primarily to an unequal filling of the  $p$  orbitals of the valence shell of the coupling atoms. We shall therefore give a description of the coupling arising from the unbalanced  $p$  electronic charge of the valence shell.

The field gradient at the nucleus of an atom caused by a single electron in an atomic  $p_z$  orbital is, from (14.16),

$$q_z(p_z) = e \left\langle \frac{1}{r^3} \right\rangle \langle 3 \cos^2 \theta_z - 1 \rangle \quad (14.34)$$

where  $e$  is the electronic charge and where the average is taken over the  $p_z$  orbital which has its axis of symmetry along  $z$ . The field gradient  $q_g(p_z)$  of the  $p_z$  electron with reference to some other axis  $g$  that passes through the nucleus can be obtained by a transformation of the angular-dependent term in (14.34) with the relation

$$\langle 3 \cos^2 \theta_g - 1 \rangle = \frac{1}{2}(3 \cos^2 \alpha - 1)\langle 3 \cos^2 \theta_z - 1 \rangle \quad (14.35)$$

where  $\alpha$  is the angle between the symmetry axis of the  $p_z$  orbital and the reference axis  $g$ . With this relation

$$\begin{aligned} q_g(p_z) &= e \left\langle \frac{1}{r^3} \right\rangle \langle 3 \cos^2 \theta_g - 1 \rangle \\ &= \frac{1}{2}e(3 \cos^2 \alpha - 1) \left\langle \frac{1}{r^3} \right\rangle \langle 3 \cos^2 \theta_z - 1 \rangle \end{aligned} \quad (14.36)$$

Therefore, the contribution to the field gradient in the  $g$  direction by an electron in a  $p_z$  orbital may be written as

$$q_g(p_z) = \frac{1}{2}(3 \cos^2 \alpha - 1)q_z(p_z) \quad (14.37)$$

When  $x$  or  $y$  is chosen as the reference axis  $\alpha = 90^\circ$ , and

$$q_x(p_z) = q_y(p_z) = -\frac{1}{2}q_z(p_z) \quad (14.38)$$

Similarly, the gradient of a  $p_x$  electron with reference to the  $y$  or  $z$  axis is

$$q_y(p_x) = q_z(p_x) = -\frac{1}{2}q_x(p_x) \quad (14.39)$$

or of a  $p_y$  electron

$$q_x(p_y) = q_z(p_y) = -\frac{1}{2}q_y(p_y) \quad (14.40)$$

Also,

$$q_x(p_x) = q_y(p_y) = q_z(p_z) = q_{n10} \quad (14.41)$$

where  $q_{n10}$  represents the field gradient due to an electron in atomic orbital with  $l=1$  ( $p$  electron) and  $m_l=0$  (angular momentum zero along the reference axis). The subscript  $n$  represents the total quantum number of the electron orbital. It is evident that the resultant field gradient  $q_g$  due to all the  $p$ -shell electrons is

$$q_g = n_x q_g(p_x) + n_y q_g(p_y) + n_z q_g(p_z) \quad (14.42)$$

where  $n_x$ ,  $n_y$ , and  $n_z$  represents the number, or fractional number, of electrons in the  $p_x$ ,  $p_y$ , and  $p_z$  orbitals respectively. From this relation and from (14.38)–(14.41) it is seen that

$$q_z = -\left(\frac{n_x + n_y}{2} - n_z\right) q_{n10} \quad (14.43)$$

Similarly,

$$q_y = -\left(\frac{n_z + n_x}{2} - n_y\right) q_{n10} \quad (14.44)$$

and

$$q_x = -\left(\frac{n_y + n_z}{2} - n_x\right) q_{n10} \quad (14.45)$$

The quantities within the parentheses represent the unbalanced  $p$  electronic charge of the  $n$  shell of the coupling atom relative to the  $x$ ,  $y$ , or  $z$  axis. It is evident that when the orbitals are symmetrically filled the field gradients are zero with respect to each axis. Thus the completely filled subshells contribute nothing to the coupling, and only the valence shell electrons need be considered.

With (14.43)–(14.45) and with approximations (1)–(9) from Section 2, we can now express the principal elements in the coupling by

$$\chi_x = eQq_x = -(U_p)_x eQq_{n10} \quad (14.46)$$

$$\chi_y = eQq_y = -(U_p)_y eQq_{n10} \quad (14.47)$$

$$\chi_z = eQq_z = -(U_p)_z eQq_{n10} \quad (14.48)$$

with  $e$  the magnitude of the electronic charge and

$$\eta = \frac{\chi_x - \chi_y}{\chi_z} = \frac{3(n_y - n_x)}{n_x + n_y - 2n_z} \quad (14.49)$$

where the unbalanced  $p$  electrons are

$$(U_p)_x = \frac{n_y + n_z}{2} - n_x \quad (14.50)$$

$$(U_p)_y = \frac{n_z + n_x}{2} - n_y \quad (14.51)$$

$$(U_p)_z = \frac{n_x + n_y}{2} - n_z \quad (14.52)$$

The definition of  $U_p$  is such that a positive  $U_p$  corresponds to a  $p$ -electron deficit and a negative  $U_p$  to a  $p$ -electron excess along the reference axis. A deficit of one  $p$  electron in an otherwise closed  $p$  shell with the axis of the electron "hole" oriented along the reference axis would have the value  $U_p = 1$ ; a single  $p$  electron outside a closed shell with its symmetry axis oriented along the reference axis would have the value  $U_p = -1$ . This corresponds to the definition of  $U_p$  employed in the earlier books on microwave spectroscopy [10, 11]; it is convenient for analysis of the halide couplings. The quantity  $f_g = -(U_p)_g$  has been used [14] to designate an excess  $p$  electronic charge along the reference axis  $g = x, y, z$ .

The quantity  $q_{n10}$  used in the discussion of molecules represents the field gradient of an atomic  $p$  electron ( $l=1$ ) of the valence shell  $n$  with the symmetry axis of the  $p$  orbital oriented along the reference axis ( $m=0$ ). The quantity  $eQq_{n10}$  represents the nuclear quadrupole coupling by such an electron. For many atoms,  $eQq_{n10}$  is accurately known from measurements of the atomic hyperfine structure (see Section 3). Measured values are given in Table 14.2. For a single coupling electron, the measured atomic coupling constant is  $b = -eQq_{n,1,\pm 1} = \frac{1}{2}eQq_{n10}$ .

Field gradients  $q_{n10}$  for  $p$  electrons can be calculated theoretically by the method described in Section 3; and, when  $Q$  is known from experiment (values given in Appendix E), semitheoretical values of  $eQq_{n10}$  can be obtained. Usually the coupling constants are given in MHz,  $Q$  in  $\text{cm}^2$ , and  $q$  in esu. The following relation is useful in making numerical calculations

$$\chi_g(\text{MHz}) = -72.5(U_p)_g Q(10^{-24} \text{ cm}^2) q_{n10}(10^{15} \text{ esu}) \quad (14.53)$$

where  $g = x, y, z$  is the reference axis. The quantities  $U_p$  and  $q_{n10}$  are independent of the isotopic number. When the coupling  $\chi_g$  is known for one isotopic species, that for other species of the atom can be calculated with the ratios of  $Q$  given in Appendix E.

With measured or derived values of  $eQq_{n10}$  one can use (14.53) to derive values of  $U_p$  from the measured couplings of molecular constants. These can then be compared with values predicted theoretically from various postulated bond structures, as will be explained in later sections.

An orderly relationship between  $U_p$ , as measured by  $(eQq)_{\text{mol}}/(eQq_{n10})_{\text{atom}}$ , and the internuclear distances for the diatomic halides has been found by

Tiemann [27], who has used the relationship to predict the value of  $\chi_z = -114$  MHz for the  $^{35}\text{Cl}$  coupling in  $\text{Cl}_2$ .

## 5 CORRECTIONS FOR CHARGE ON COUPLING ATOM

If the coupling atom has a formal positive charge, the coupling field gradient per  $p$  electron will be increased over that of the neutral atom because of the reduced nuclear screening. On the other hand, a negative charge on the coupling atom will decrease the coupling. To a first-order approximation, these effects can be taken into account by multiplication of the  $q_{n10}$  for the neutral atom by a correction factor  $(1 + \varepsilon)$  per unit of positive charge on the coupling atom or by the factor  $1/(1 + \varepsilon)$  per unit of negative charge. From the difference in  $q$  for a number of ionized states of free atoms, Townes and Schawlow [11] have estimated values of  $\varepsilon$  for a number of different atoms. These values are given in Table 14.3. If there is a fractional positive charge of  $c^+$  electron units on the coupling atom, (14.46)–(14.48) for the coupling are modified in the molecular orbital treatment used here to

$$\chi_g = -(1 + c^+ \varepsilon)(U_p)_g e Q q_{n10} \quad (14.54)$$

If there is a negative charge of  $c^-$  electron units, they are modified to

$$\chi_g = -\frac{(U_p)_g e Q q_{n10}}{(1 + c^- \varepsilon)} \quad (14.55)$$

where  $g = x, y, z$ . If the coupling atom is bonded by a single bond, as are the halogens,  $c^+$  and  $c^-$  will be numerically equivalent to the ionic character of the bond  $i_c$ , or to the percentage contribution of the ionic structure in the valence bond resonance method employed by Townes and Dailey [2]. In the valence bond resonance method, the resultant  $(U_p)_g$  is the weighted sum of contributions from various resonance structures, that is,  $(U_p)_g = \sum_i c_i (U_p^{(i)})_g$  where  $c_i$  is the fractional importance of the  $i$ th structure and  $(U_p^{(i)})_g$  is the corre-

**Table 14.3** Screening Constants  $\varepsilon$  for Correction of  $p$  Orbital Couplings for Effects of Charges on the Coupling Atom<sup>a</sup>

Atom	$\varepsilon$	Atom	$\varepsilon$	Atom	$\varepsilon$	Atom	$\varepsilon$
Be	0.90	Mg	0.70	Ca	0.60	Sr	0.60
B	0.50	Al	0.35	Sc	0.30	Ga	0.20
C	0.45	Si	0.30	Ge	0.25		
N	0.30	P	0.20	As	0.15	Sb	0.15
O	0.25	S	0.20	Se	0.20	Te	0.20
F	0.20	Cl	0.15	Br	0.15	I	0.15

<sup>a</sup>Values are from *Microwave Spectroscopy* by C. H. Townes and A. L. Schawlow, Copyright 1955, McGraw Hill, Inc. Used with permission of McGraw Hill Book Company.

sponding number of unbalanced  $p$  electrons. The charge correction is applied to the ionic structures by multiplication of the  $(U_p^{(i)})_g$  by the factor  $1+\varepsilon$  or  $(1+\varepsilon)^{-1}$  depending on the sign of the charge on the coupling atom of the  $i$ th structure. If the ionic character is such as to produce a closed shell on the coupling atom, as is the case on the halogen in the contributing structures  $X(\text{Hal})^-$ , the halogen has zero coupling for this structure. Therefore the charge correction has no effect on the overall coupling when it is taken to be the weighted contributions from the various contributing structures in the valence bond resonance treatment. For this reason, the charge correction need not be included in the treatment of the halogen coupling except for ionic structures for which a positive charge is on the coupling atom.

Effects of charges on atoms of the molecule other than the coupling one are usually negligible. For example, an unscreened electronic charge of  $\frac{1}{4}e$  on the  $z$  axis at a distance of 2.1 Å (the bond length of BrCl) from the coupling nucleus would contribute a field gradient  $q_z$  of only  $0.026 \times 10^{15}$  esu. Although such effects of charge are enhanced (on the order of a factor of 10) by polarization of the electron cloud [20, 28] on the coupling atom, the total effect of  $0.2 \times 10^{15}$  esu is still small in comparison with the field gradient of  $20 \times 10^{15}$  esu for a  $p_z$  electron in the valence shell of Cl or of a field gradient of  $34 \times 10^{15}$  esu for a similar electron in Br. In the following discussions we shall neglect the effects of charges on neighboring atoms caused by ionic character of covalent bonds.

Because the same charge corrections are applied to all principal elements of the coupling tensor, as indicated by (14.54) and (14.55), these corrections cancel from (14.49) and thus have no effect on the asymmetry parameter  $(\chi_{xx} - \chi_{yy})/\chi_{zz}$  of the coupling.

## 6 HYBRIDIZED ORBITALS

If an electron is in an  $sp$  hybridized atomic orbital of a coupling atom  $A$  represented by

$$\psi_a = a_s \psi_s + a_p \psi_p \quad (14.56)$$

its field gradient with reference to the  $z$  axis will be

$$q_z(a) = e \int \psi_a^* \left( \frac{\partial^2 V}{\partial z^2} \right) \psi_a d\tau = a_s^2 q_z(s) + a_p^2 q_z(p) \quad (14.57)$$

However, the average of  $(\partial^2 V)/(\partial z^2)$  over the  $s$  orbital is zero,  $q(s)=0$ , because of spherical symmetry. The overlap integral of these orthogonal orbitals is zero, and the normalization is represented by  $a_s^2 + a_p^2 = 1$ . Therefore (14.57) can be expressed as

$$q_z(a) = a_p^2 q_z(p) = (1 - a_s^2) q_z(p) \quad (14.58)$$

If  $\psi_a$  is a constituent of a  $\sigma$  bonding orbital  $\psi_\sigma$ , the orbital  $\psi_\sigma$  will be directed along the bond axis chosen as the reference  $z$  axis. The  $p$  component will then be a  $p_z$  orbital, and  $q_z(p) = q_z(p_z) = q_{n10}$ . If  $a^2$  represents the fractional weight of

the component  $\psi_a$  in the molecular orbital  $\psi_\sigma (=a\psi_a+b\psi_b)$  and if there are two electrons in  $\psi_\sigma$ , the field gradient due to the  $\sigma$  bond will be

$$q_z(\sigma) = 2ea^2 \int \psi_a^* \left( \frac{\partial^2 V}{\partial z^2} \right) \psi_a dz = 2a^2(1-a_s^2)q_{n10} \quad (14.59)$$

The other hybridized orbital,  $\psi'_a = a'_s\psi_s + a'_p\psi_p$ , will be normalized if  $a'_s^2 + a'_p^2 = 1$ . Since the total  $s$  character must be unity, that is,  $a'_s^2 + a'_s^2 = 1$ , it follows that  $a'_p^2 = a_s^2$ . This counterhybridized orbital will therefore have a  $p_z$  component with weight  $a'_p^2 = (1 - a_p^2) = a_s^2$  which will contribute to  $q_z$ . The total number of  $p_z$  electrons,  $n_z$ , will depend upon the way this counter-hybridized orbital is filled. If it is a nonbonding orbital having the maximum of two electrons, we find that

$$n_z = 2a^2(1 - a_s^2) + 2a_s^2 \quad (14.60)$$

Thus we see that when the counterhybridized orbital has an unshared pair of electrons, as is true for the  $\sigma$ -bonded halogen atoms, the  $s$  hybridization increases the  $p_z$  electronic charge. If, however, the counterhybridized orbital also forms a bond and has, on the average, less than  $2a^2a_s^2$  electrons,  $n_z$  would be lowered. The total number of unbalanced  $p$  electrons will also depend on the way the  $p_x$  and  $p_y$  orbitals are filled. If each of them has two unshared electrons, as in the halogens, then we would have

$$(U_p)_z = \frac{n_x + n_y}{2} - n_z = 2(1 - a^2)(1 - a_s^2) \quad (14.61)$$

Since

$$q_z = -(U_p)_z q_{n10} = -2(1 - a^2)(1 - a_s^2)q_{n10} \quad (14.62)$$

it is evident that under the assumed conditions the magnitude of the coupling is lowered by the factor  $(1 - a_s^2)$  from that for the nonhybridized  $p_z$  bonding orbital. For a pure covalent bond (no ionic character)  $a^2 = \frac{1}{2}$ , and (14.62) becomes

$$q_z = -(1 - a_s^2)q_{n10} \quad (14.63)$$

Usually  $\pi$  bonds are formed with pure  $p$  orbitals, and hence we shall not consider the hybridization effects of the  $p_x$  and  $p_y$  orbitals. However, it is evident that if  $(n_x + n_y) < 4a^2$ , the magnitude of  $q_z$  would be increased rather than decreased by the above hybridization.

Effects of  $pd$  hybridization are calculated in a similar manner. An electron in a  $pd$  hybridized orbital

$$\psi_a = a_p\psi_p + a_d\psi_d \quad (14.64)$$

will contribute a field gradient at the nucleus of the atom

$$q_z(a) = a_p^2 q_z(p) + a_d^2 q_z(d) \quad (14.65)$$

where  $q(d)$  is the field gradient of a  $d$  electron. Although  $q(d)$  is not zero, it is an order of magnitude less than  $q(p)$  for electrons of the same  $n$  shell (see Section 3).

Furthermore, the  $d$  contribution is generally expected to be much less than the  $p$  contribution,  $a_d^2 \ll a_p^2$ . Hence, we can neglect the last term of (14.65) and, to a good approximation, can express

$$q_z(a) = a_p^2 q_z(p) = (1 - a_d^2) q_z(p) \quad (14.66)$$

If, as before, the orbital  $\psi_a$  is a bonding  $\sigma$  orbital of weight  $a^2$  having a pair of electrons,

$$q_z(\sigma) = 2a^2(1 - a_d^2)q_{n10} \quad (14.67)$$

Although this expression has the same form as (14.59) for  $sp$  hybrids, the overall effect of  $d$  hybridization on the coupling in common molecules is the opposite to that of  $s$  hybridization; that is, whereas  $s$  hybridization lowers the magnitude,  $d$  hybridization raises it. This difference is caused by the fact that in most common elements forming stable molecules with hybridized  $p$  orbitals, the  $s$  orbital of the atom has a pair of electrons, but the  $d$  orbitals are empty. This is best illustrated by the halogens in which the free atoms have the valence shell configuration  $ns^2np^5$ . In the bonded atoms, the counterhybridized  $sp$  orbital will have an unshared pair as described above, but the counterhybridized  $pd$  orbital would be empty. Thus, if the bonding orbital is a  $pd$  hybrid, the total number of the  $p_z$  electrons would be

$$n_z = 2a^2(1 - a_d^2) \quad (14.68)$$

When there are unshared pairs in the  $p_x$  and  $p_y$  orbitals,  $n_x = n_y = 2$ ,

$$(U_p)_z = 2 - 2a^2(1 - a_d^2) \quad (14.69)$$

and

$$q_z = -[2 - 2a^2(1 - a_d^2)]q_{n10} \quad (14.70)$$

which for pure covalent bonds with  $a^2 = \frac{1}{2}$  becomes

$$q_z = -(1 + a_d^2)q_{n10} \quad (14.71)$$

Upon comparison with (14.63) it is seen that for the assumed bonding conditions,  $s$  and  $d$  hybridization are opposed in their effects on the coupling.

If the cross terms between the  $s$  and  $d$  orbitals are neglected, an  $spd$ -hybridized,  $\sigma$ -bonding orbital

$$\psi_a = a_s\psi_s + a_p\psi_p + a_d\psi_d \quad (14.72)$$

will similarly have

$$q_z(\sigma) = 2a^2(1 - a_s^2 - a_d^2)q_{n10} \quad (14.73)$$

One of the other two hybridized orbitals ( $\psi'_a$ ) assumed to be essentially  $s$  in character, an  $sp$  orbital, will have an amount  $a_s^2$  of  $p$  character, while the remaining orbital ( $\psi''_a$ ) essentially  $d$  in character, a  $pd$  orbital, will have an amount  $a_d^2$  of  $p$  character. These conclusions follow from the assumptions and the normalization conditions. If the counterhybridized  $s$  orbital has an unshared pair

and the counterhybridized  $d$  orbital is empty, as assumed above,

$$n_z = 2a^2(1 - a_s^2 - a_d^2) + 2a_s^2 \quad (14.74)$$

If, as when the  $p_x$  and  $p_z$  orbitals have unshared pairs,

$$q_z = -[2 - 2a^2(1 - a_s^2 - a_d^2) - 2a_s^2]q_{n10} \quad (14.75)$$

then the coupling would be

$$\chi_z = -2[1 - a^2(1 - a_s^2 - a_d^2) - a_s^2]eQq_{n10} \quad (14.76)$$

For pure covalent bonds with  $a^2 = \frac{1}{2}$ , this becomes

$$\chi_z = -(1 - a_s^2 + a_d^2)eQq_{n10} \quad (14.77)$$

In these expressions,

$a^2$  = total weight of the atomic orbital  $\psi_a$  in the  $\sigma$ -bonding molecular orbital

$a_s^2$  = amount of  $s$  character of  $\psi_a$

$a_d^2$  = amount of  $d$  character of  $\psi_a$

$1 - a_s^2 - a_d^2$  = amount of  $p$  character of  $\psi_a$

It is evident that the hybridization effects on the coupling will depend on the way the orbitals are filled. From these examples, the method of calculation of effects for other electronic configurations should be evident. Methods for evaluation of  $a^2$  are described in Sections 7 and 8. Applications of this theory are given in various sections to follow.

## 7 PURE COVALENT BONDS—EFFECTS OF ORBITAL OVERLAP

The bonding in the homopolar, diatomic halides consists essentially of a pure covalent, single  $\sigma$  bond with no ionic character to complicate the interpretation. Table 14.4 gives a comparison of the quadrupole couplings of halides  $\text{Cl}_2$ ,  $\text{Br}_2$ , and  $\text{I}_2$  for the free molecules and for condensed molecules in solids. Although the couplings in these molecules cannot be measured with microwave spectroscopy because the molecules are nonpolar, their couplings in the solid state are accurately known from pure quadrupole resonance [29–31] and for the free molecules of  $\text{Br}_2$  and  $\text{I}_2$  they are accurately known from microwave-optical laser double resonance [32, 33]. The free-molecule coupling in  $\text{Cl}_2$  has been reliably inferred [27] from projection of the couplings in  $\text{Br}_2$ ,  $\text{I}_2$ , and other halides. The solid-state coupling in  $\text{I}_2$  is reduced by weak intramolecular bonding [34] revealed by an asymmetry,  $\eta = 0.173$ , in the coupling of  $\text{I}_2$  crystals. The slightly lower coupling for solid  $\text{Cl}_2$  and  $\text{Br}_2$  as compared with couplings for the free molecules also probably results from weak intramolecular bonding in these solids. For comparison with the molecular couplings, accurate values of the nuclear quadrupole couplings in the free atoms, Cl, Br, and I, are known from

**Table 14.4** Observed Nuclear Quadrupole Couplings and Derived Unbalanced *p* Electrons on the Coupling Atom in Cl<sub>2</sub>, Br<sub>2</sub>, and I<sub>2</sub>

<i>Coupling Nucleus</i>	<i>Observed Coupling, χ<sub>z</sub>(MHz)</i>			
	<i>Free Molecule</i>	<i>Ref.</i>	<i>Molecular Solid</i>	<i>Ref.</i>
<sup>35</sup> Cl <sub>2</sub>	(-114)	<sup>a</sup>	-108.95	<sup>d</sup>
<sup>79</sup> Br <sub>2</sub>	810.0(5)	<sup>b</sup>	765	<sup>e</sup>
<sup>127</sup> I <sub>2</sub>	-2452.584(2)	<sup>c</sup>	-2153	<sup>f</sup>
	$U_p = -\chi_z(\text{mol})/(eQq_{n10})$			
Cl <sub>2</sub>	1.039		0.993	
Br <sub>2</sub>	1.052		0.994	
I <sub>2</sub>	1.070		(0.931)	

<sup>a</sup>Projected value obtained by Tiemann [27].

<sup>b</sup>Bettin et al. [32].

<sup>c</sup>Yokozeki and Muenter [33].

<sup>d</sup>Livingston [29].

<sup>e</sup>Dehmelt [30].

<sup>f</sup>Dehmelt [31].

atomic beam resonance. They are listed in Table 14.2. It is thus possible to obtain experimental values of the unbalanced *p* electrons on the bonded halogens in the free molecules as well as in the molecular solids. These experimental values of  $U_p$  are given in the lower part of Table 14.4.

It is of interest to compare the values of  $U_p$  derived from the observed couplings in Table 14.4 with theoretical  $U_p$  values predicted with the assumption of pure *p*-bonding orbitals and with the neglect of effects of bond overlap distortions on the couplings. From the normalization of (14.8) with  $a=b$ , it is seen that  $a^2=\frac{1}{2}$ . Since there are two electrons in the  $\sigma$  bonding orbital, the number of  $p_z$  electrons on each coupling atom is  $n_z=2a^2=1$ . With no hybridization or  $\pi$  bonding, there will be two electrons in each of the nonbonding  $p_x$  and  $p_y$  orbitals, that is,  $n_x=2$  and  $n_y=2$ . Substitution of these values into (14.52) yields

$$(U_p)_z = \frac{n_x + n_y}{2} - n_z = 1 \quad (14.78)$$

for this idealized model of the halogen molecule. The experimental values are

$$(U_p)_z = -\frac{(eQq_z)_{\text{mol}}}{(eQq_{n10=0})_{\text{atom}}} = -\frac{(q_z)_{\text{mol}}}{(q_{n10})_{\text{atom}}} \quad (14.79)$$

The observed values of  $U_p$  in Table 14.4 do not differ grossly from  $U_p=1$ , predicted with the neglect of the effects of overlap orbitals. However, the very close agreement of the solid state values for Cl<sub>2</sub> and Br<sub>2</sub> with the value predicted for the idealized model is probably fortuitous since the interactions in the solid

tend to lower the coupling values. This lowering is most pronounced for  $I_2$  but is evident in the Cl coupling for the substituted methyl halides in solids compared with gases in Fig. 14.3. It is thus reasonable to take the  $U_p$  values derived from the coupling of the free molecules as perturbed only by the covalent bonding. These  $U_p$  values are seen to be 4 to 7% above the unit value. Since the  $s$  hybridization of the bond orbital would reduce rather than increase the coupling in the molecules, it appears that the increase of  $U_p$  above unity is due to effects of bond orbital overlap. Although some increase of  $U_p$  above unity is expected from orbital overlap distortions, the observed increases are much less than those predicted from normalization of (14.80). As shown below, the simple normalizations of (14.8) or (14.9), usually employed in interpretation of nuclear coupling in molecules, predict values much closer to the observed ones.

Now let us consider possible effects of orbital overlap. Instead of the normalization of (14.8), we employ the normalization of the bonding molecular orbital  $\phi = a\psi_a + b\psi_b$ :

$$\int \phi^* \phi d\tau = a^2 \int \psi_a^* \psi_a d\tau + 2ab \int \psi_a^* \psi_b d\tau + b^2 \int \psi_b^* \psi_b d\tau = 1 \quad (14.80)$$

With

$$\int \psi_a^* \psi_a d\tau = 1 \quad \int \psi_b^* \psi_b d\tau = 1 \quad \int \psi_a^* \psi_b d\tau = S_{ab}$$

this becomes

$$a^2 + 2abS_{ab} + b^2 = 1 \quad (14.81)$$

For homopolar molecules considered here,  $a = b$  and

$$a^2 = \frac{1}{2(1 + S_{ab})} \quad (14.82)$$

For  $Cl_2$ , the theoretical value [35] of the overlap integral  $S_{ab}$  is 0.34, and with this value (14.82) indicates that  $a^2 = 0.37$ . Correspondingly,  $n_z = 2a^2 = 0.74$ , and from (14.78)  $(U_p)_z = 2 - 0.74 = 1.26$ . Substitution of this value of  $U_p$  into (14.79) leads to the predicted  $\chi_z(^{35}Cl_2) = -138$  MHz, in poor agreement with the observed value of  $-109.7$  MHz in solids and  $-114$  MHz for free molecules. Inclusion of the overlap term in the normalization requires, however, that we include the cross term, the second term on the right of (14.7) in the evaluation of the field gradient. Inclusion of this term improves the agreement, but only slightly. Precise calculation of this cross term is rather difficult, but its value can be easily approximated by assumption that the overlap charge is concentrated at a distance equal to the covalent radius  $R$  from the nucleus. Since there are two electrons in the bonding orbital, the total overlap charge is  $2e(2a^2S_{ab})$ . From (14.34) with  $\theta = 0$  and  $3 \cos^2 \theta - 1 = 2$ , the field gradient due to an un-screened charge of this magnitude is

$$q_{ab} \approx \frac{8ea^2S_{ab}}{R^3} \quad (14.83)$$

With  $e = 4.80 \times 10^{-10}$  statcoulombs and  $R = 0.99 \times 10^{-8}$  cm,  $S_{ab} = 0.34$ ,  $a^2 = 0.37$  for  $\text{Cl}_2$ , it is seen that  $q_{ab} \approx 0.5 \times 10^{15}$  esu. For one unbalanced  $p$  electron on Cl,  $q_{310} = 19.5 \times 10^{15}$  esu. Thus inclusion of the cross term in (14.7) decreases the magnitude of the coupling by approximately  $0.5/19.5 = 2.5\%$ . The predicted value is changed from  $-138$  to  $-135$  MHz, which is still in poor agreement with the observed value. A similar estimate of the cross term for  $\text{Br}_2$  with  $R = 1.14 \times 10^{-8}$  cm reduces the field gradient by approximately 1%, and the predicted  ${}^{79}\text{Br}$  coupling from 953 to 944 MHz as compared with the observed value of 765 MHz for solids and 810 MHz for free molecules.

Although this estimated correction for the cross term is very approximate, it does indicate that a precise evaluation of this term could not correct for the increase in coupling caused by a lifting of the overlap charge out of the atomic orbital as required by the normalization by (14.81). The relatively good agreement of the observed coupling with that predicted with (14.79) indicates that this normalization gives a more nearly correct representation of the molecular orbital near the nucleus. The implications are that the overlap distortions occur in the outer regions of the orbitals and that the overlap charge signified by the cross term is not produced by the lifting of significant electronic charge density from the area near the nucleus to the outer regions of the orbital, as is implied by the normalization of (14.81). Obviously, such a lifting would be expensive in energy.

The overlap integrals in the pure covalent bonds of these homopolar halides are greater than those of the mixed halides or other polar molecules for which the covalent component of the bonds, and hence the overlap integral  $S_{ab}$ , is reduced by significant ionic character. Furthermore,  $S_{ab}$  is reduced by a difference in the size of the bonded atoms, which results in less complete overlapping of the bonding orbital of the larger atom. Thus the increase in coupling, only 4 to 7% in these homopolar halides, should be the upper limit of that expected from effects of bond orbital overlap distortions on the halide couplings. For bonds formed between atoms differing appreciably in size, such as HI, or bonds such as AgCl that have significant ionic components, the effects of orbital overlap on the coupling should be negligible.

## 8 POLAR BONDS—IONIC CHARACTER FROM QUADRUPOLE COUPLING

To explore the effects of ionic character on the coupling, let us consider the halogen coupling in diatomic polar molecules. These provide the simplest cases although possible hybridization effects may cause some uncertainty. If we allow for possible  $s$  and  $d$  hybridization of the bonding orbital, the coupling is given by (14.76), in which the coefficient  $a^2$  depends on the ionic character of the bond. In a singly bonded diatomic molecule  $AB$  the  $\sigma$ -bonding orbital can be represented by the linear combination

$$\psi_\sigma = a\psi_a + b\psi_b \quad (14.84)$$

and the ionic character of the  $\sigma$  bond may be represented by

$$i_c = |a^2 - b^2| \quad (14.85)$$

With normalization of  $a^2 + b^2 = 1$  it is evident that

$$a^2 = \frac{1+i_c}{2} \quad \text{when } a^2 > b^2 \quad (A \text{ negative}) \quad (14.86)$$

$$a^2 = \frac{1-i_c}{2} \quad \text{when } a^2 < b^2 \quad (A \text{ positive}) \quad (14.87)$$

In the first case,  $a^2 > b^2$ , the negative pole will be on atom  $A$ , assumed to be the coupling atom. We consider this case first. Substitution of  $a^2 = (1+i_c)/2$  into (14.76) gives the quadrupole coupling

$$\chi_z = -[1 - a_s^2 + a_d^2 - i_c(1 - a_s^2 - a_d^2)] \left( \frac{eQq_{n10}}{1 + i_c\epsilon} \right) \quad (14.88)$$

where  $a_s^2$  is the amount of  $s$  character and  $a_d^2$  is the amount of  $d$  character of the bonding orbital and where  $eQq_{n10}$  is the coupling of an atomic  $p$  electron in the orbital  $\psi_{n10}$ . If there is  $s$  hybridization only,

$$\chi_z = -\frac{(1-i_c)(1-a_s^2)eQq_{n10}}{1+i_c\epsilon} \quad \{\text{negative pole on coupling atom}\} \quad (14.89)$$

Here the factor  $1/(1+i_c\epsilon)$  is applied to correct for the change in nuclear screening caused by the negative charge  $c^- = i_c$  on the coupling atom as described in Section 5. Approximate values of  $\epsilon$  are given in Table 14.3. For Cl, Br, and I,  $\epsilon = 0.15$ .

When the positive pole is on the coupling halogen  $A$ , the factor  $(1+i_c\epsilon)$  is applied to account for the decreased nuclear screening (Section 5). With this correction, and with  $a^2 = (1-i_c)/2$ , (14.76) becomes for the positive pole on the coupling atom

$$\chi_z = -[1 - a_s^2 + a_d^2 + i_c(1 - a_s^2 - a_d^2)](1 + i_c\epsilon)eQq_{n10} \quad (14.90)$$

If there is  $s$  hybridization only,

$$\chi_z = -(1+i_c)(1-a_s^2)(1+i_c\epsilon)eQq_{n10} \quad \{\text{positive pole on coupling atom}\} \quad (14.91)$$

It is evident that there are still more unknown parameters in these equations than there are measurable couplings. This is true even for molecules such as BrCl and ICl in which both atoms have measurable couplings. Since  $a_s^2$  and  $a_d^2$  are not necessarily the same on both atoms, there is a possibility of five unknowns. Assumptions or evaluations of some of the parameters from other experiments are required for solution of these equations.

We make the justifiable assumption that hybridization on a halogen is negligible when the halogen is neutral and when it has a greater electronegativity than has the atom to which it is bonded, that is, when it is negatively charged.

Evidence supporting this assumption for the neutral halogen is provided by the quadrupole coupling for nonpolar  $\text{Cl}_2$  and  $\text{Br}_2$  as earlier shown and discussed earlier in this section. Furthermore, the couplings in the free molecules,  $\text{Cl}_2$ ,  $\text{Br}_2$ , and  $\text{I}_2$ , are slightly greater than those predicted for one unbalanced  $p$  electron, not smaller, as would be expected from hybridization. As explained earlier, an increase is expected from orbital overlap. The assumption of negligible effects of hybridization on the negative atom seems required for a reasonable interpretation of the couplings in  $\text{BrCl}$  and in  $\text{IBr}$ , for which the ionic characters are small, and for a consistent interpretation of the quadrupole coupling of both halogens in  $\text{ICl}$ . As explained earlier [7], hybridization on the negative halogen would be quenched by the primary dipole moment, that is, that due to ionic character, whereas hybridization on the positively charged halogen would be induced or supported by the primary moment.

There are inconsistencies in the ionic characters derived from the two halogen couplings in  $\text{BrCl}$ ,  $\text{IBr}$ , and  $\text{ICl}$  that cannot be removed by assumption of  $sp$  hybridization, but can be removed by inclusion of bond orbital overlap distortions in the calculations, as is explained below. The measured couplings in  $\text{BrCl}$  are  $-102.45$  MHz for  $^{35}\text{Cl}$  and  $875.3$  MHz for  $^{79}\text{Br}$ . With these and with the  $(eQq_{n10})_{\text{atom}}$  values for  $^{35}\text{Cl}$  and  $^{79}\text{Br}$  in Table 14.2, one obtains  $i_c = 0.07$  from substitution of the  $^{35}\text{Cl}$  coupling in (14.89), and  $i_c = 0.12$  from substitution of the  $^{79}\text{Br}$  coupling in (14.91) if  $a_s^2 = 0$  in both solutions. Note that the  $i_c$  from the Br coupling is twice that from the Cl coupling. This inconsistency is increased by assumption of  $s$  hybridization on either atom. There is a comparable inconsistency in the  $i_c$  values of  $\text{IBr}$  predicted in the same way from the I and Br couplings. The covalent component of the bonds in both molecules is large,  $\sim 90\%$ , with the overlap integrals  $S_{ab}$  comparable to those of  $\text{Cl}_2$ ,  $\text{Br}_2$ , and  $\text{I}_2$ . Thus to eliminate, or reduce, effects of orbital overlap distortion on the calculations of  $i_c$ , it seems reasonable to use, instead of the  $(eQq_{n10})_{\text{atom}}$ , the  $(eQq_{n10})_{\text{mol}}$  values:  $114$  MHz for  $^{35}\text{Cl}$ ,  $-810.0$  MHz for  $^{79}\text{Br}$ , and  $2452.5$  MHz for  $^{127}\text{I}$ , as obtained from the couplings listed in Table 14.4 for the free molecules  $\text{Cl}_2$ ,  $\text{Br}_2$ , and  $\text{I}_2$ . These values inherently include effects of orbital overlap. With this procedure and with hybridization assumed to be zero on both Cl and Br in  $\text{BrCl}$ ,  $i_c = 0.09$  is predicted from the  $^{35}\text{Cl}$  coupling and  $i_c = 0.07$  from the  $^{79}\text{Br}$  coupling. This inconsistency can now be cleared up by  $2\%$   $s$  hybridization on the positive Br with none on the negative Cl. The resulting  $i_c = 0.09$  is from both coupling atoms. With this procedure the ionic character of  $\text{IBr}$  predicted from the  $^{79}\text{Br}$  coupling is  $0.124$ ; from the  $^{127}\text{I}$  coupling it is  $0.103$ . A consistent value of  $i_c = 0.124$  is then obtainable by assumption of  $2\%$   $s$  hybridization on the positive I with none on the negative Br. See Section 10.

The values of the ionic character of  $\text{ICl}$  derived from the observed molecular coupling of Cl and of I are likewise not consistent if the free atomic values of  $(eQq_{n10})_{\text{atom}}$  are used and the charge correction,  $\varepsilon_c = 0.15$ , is applied with no assumption of hybridization on either element. For example, the  $\chi_z(^{35}\text{Cl}) = -85.8$  MHz with  $(eQq_{n10})_{\text{atom}} = 109.74$  MHz substituted in (14.89) with  $a_s^2 = 0$  gives  $i_c = 0.196$ , whereas  $\chi_z(^{127}\text{I}) = -2928$  MHz with  $(eQq_{n10})_{\text{atom}} = 2292.71$  MHz

with  $a_s^2 = 0$  substituted in (14.91) gives  $i_c = 0.234$ . Assumption of *s* hybridization of the bonding orbital on either element widens this inconsistency. If one uses the  $eQq_{n10}$  values from the free  $\text{Cl}_2$  and  $\text{I}_2$  molecules instead of the free atomic values, an assumption of 5.5% hybridization on the I gives the consistent value of  $i_c = 0.22$ . With this ionic character the bond has only 78% covalent character, and one should obtain a more nearly correct  $eQq_{n10}$  by interpolating the difference between free-molecule coupling of  $\text{Cl}_2$  and of  $\text{I}_2$  and the respective atomic  $eQq_{n10}$  values in proportion to the covalent ionic character ratios in  $\text{ICl}$ . This procedure leads to effective values,  $eQq_{n10}(\text{Cl}) = 113 \text{ MHz}$  and  $eQq_{n10}(\text{I}) = 2417 \text{ MHz}$  in  $\text{ICl}$  and yields the consistent value  $i_c = 0.216$ , with only 3.5% *s* character on the I and none on the Cl. See Section 10.

With no detectable hybridization on the negative halogen in  $\text{BrCl}$ ,  $\text{ICl}$ , or  $\text{IBr}$ , it seems improbable that there would be significant hybridization on other halogens at the negative pole of an ionic bond. In Table 14.5 are listed values of  $i_c$  that have been calculated from the quadrupole coupling of the negatively charged halogens in the specified diatomic molecules. These values were calculated from

$$i_c = 1 + \frac{\chi_z}{eQq_{n10}} \quad (14.92)$$

which is obtained from (14.88) if  $a_s^2$  and  $a_d^2$  are set equal to zero and if the screening correction is neglected.

For the free halogen atoms the coupling per unbalanced *p* electron,  $(eQq_{n10})_{\text{atom}} = 2b$ , is accurately known from atomic beam resonance experiments. See Section 3, Table 14.2. Molecular values of  $(eQq_{n10})_{\text{mol}}$ , which include effects of orbital overlap, are obtained from the free-molecule couplings in the nonpolar halides,  $\text{Cl}_2$ ,  $\text{Br}_2$ , and  $\text{I}_2$ , listed in Table 14.4. These molecular values presumably represent the effective coupling of one unbalanced  $p_z$  electron on the covalently bonded halide atom. They make possible a consistent interpretation of the coupling of both halogens of the mixed halides,  $\text{BrCl}$ ,  $\text{ICl}$ , and  $\text{IBr}$ , as explained previously. Use of the effective molecular  $eQq_{n10}$  would make the predicted  $i_c$  values of Table 14.5 slightly smaller, and inclusion of the negative charge correction would make these values slightly greater. Thus the values of  $i_c$  in Table 14.5 determined by the simple (14.92) have off-setting effects which tend to increase their accuracy.

For all the halogens  $eQq_{n10}$  is accurately known from the atomic coupling constant *b* measured in atomic beam resonance experiments (Table 14.2) and the molecular couplings  $\chi_z$  are accurately known from microwave rotational spectra. Thus the error limits of  $i_c$  are due primarily to the neglect of orbital overlap and possible hybridization effects. For high values of  $i_c$ , 0.75 and above, the predicted values of  $i_c$  become relatively insensitive to hybridization and orbital overlap distortions; for moderate ionic character, these effects on the determination of  $i_c$  are required to be negligible for a consistent interpretation of the coupling of the two nuclei of  $\text{BrCl}$  and  $\text{ICl}$ . Justification for neglect of effects of orbital overlap are provided by the nonpolar molecules  $\text{Cl}_2$  and  $\text{Br}_2$ .

**Table 14.5** Ionic Character Predicted from Quadrupole Coupling of Negative Halogens on Polar Diatomic Molecules

Molecule <i>AB</i>	Observed Coupling $\chi_z$ (MHz) <sup>a</sup>	<i>Predicted Ionic Character</i> $i_c = 1 + \frac{\chi_z}{eQq_{n10}}$	Electronegativity Difference $ x_A - x_B $
<i>Coupling Atom</i> $^{35}\text{Cl}$			
$\text{Cl}_2$	-108.95 <sup>b</sup>	0	0
HCl	-68	0.38	0.85
KCl	0.04	1	2.2
RbCl	0.77	1	2.2
BrCl	-102.4	0.07	0.2
ICl	-85.8	0.22	0.45
AgCl	-37.32	0.66	1.2
AlCl	-8.8	0.92	1.5
InCl	-13.71	0.875	1.5
TlCl	-15.795	0.855	1.5
<i>Coupling Atom</i> $^{79}\text{Br}$			
$\text{Br}_2$	765 <sup>b</sup>	0	0
HBr	532	0.31	0.65
LiBr	37.2	0.95	1.85
KBr	10.24	0.99	2.0
AgBr	307	0.60	1.0
GaBr	106	0.86	1.3
InBr	110.6	0.85	1.3
TlBr	126.3	0.84	1.3
<i>Coupling Atom</i> $^{127}\text{I}$			
HI	-1828.4	0.20	0.4
LiI	-198.15	0.91	1.60
NaI	-259.87	0.89	1.65
KI	86.79	0.96	1.75

<sup>a</sup>Sources for the  $\chi_z$  values may be found in Landolt-Börnstein, *Numerical Data and Functional Relations in Science and Technology*. For a complete reference, see Chapter 1, [65]. Atomic couplings  $eQq_{n10}$  are from Table 14.2; electronegativities, from Appendix G.

<sup>b</sup>For solid-state value, see Table 14.4.

(Section 7) for which the overlap integral is large. For these reasons we believe that the values of ionic character listed in Table 14.5 represent the best available values for these molecules.

We have deliberately selected for consideration here molecules that have low probability for a significant  $\pi$  component in the bonding. Those molecules in which both atoms are halogens are not likely to have significant  $\pi$  bonding

because both atoms have closed  $p$  shells. Furthermore, large atoms of the higher periods of the atomic table—I, Ga, In, Tl—do not form bonds having significant multiple character because their large covalent radii prevent the required orbital overlap. When the multiple bond character is negligible, as for the molecules listed in Table 14.5, the ionic character  $i_c$  of the  $\sigma$  bond orbital represents the total ionic character of the bond. This is not always true. Effects of  $\pi$  character in the bonds are treated in Section 11.

The very small quadrupole couplings observed in essentially ionic molecules of the alkali halides are treated theoretically by Buckingham [36].

## 9 IONIC CHARACTER—ELECTRONEGATIVITY RELATION

Because we shall need the relationship for interpretation of quadrupole coupling in the more complicated molecules, we digress here to describe the relationship between ionic character of  $\sigma$  bonds and the electronegativity difference of the bonded atoms based on the ionic-character values derived from quadrupole coupling of halogens in simple diatomic molecules (Section 8). The values derived are listed in Table 14.5 along with the corresponding electro-

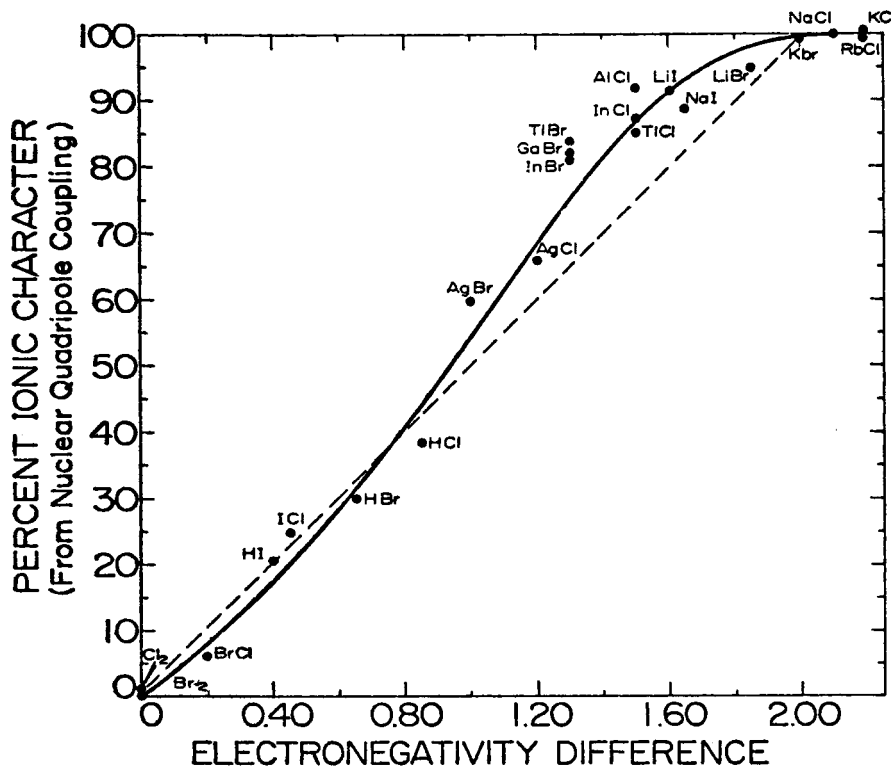


Fig. 14.1 Relation between the ionic character of the bond and the electronegativity difference of the bonded atoms. The ionic character values were derived from nuclear quadrupole coupling of the halogen, as explained in the text.

negativity differences. Figure 14.1 shows a plot of  $i_c$  versus  $|x_A - x_B|$  with these values. Note that the relationship indicates complete ionicity of the bonds for electronegativity differences of 2 or greater. With similar plots on data earlier available, it was shown [6] that the ionic character-electronegativity relationship can be expressed approximately by the very simple and convenient formula

$$i_c = \frac{|x_A - x_B|}{2} \quad \text{for } |x_A - x_B| \leq 2 \quad (14.93)$$

With complete ionicity,  $i_c = 1$  for  $|x_A - x_B| > 2$ . The dotted line in Fig. 14.1 represents this relationship. For bonds having ionic character of 50% or less or for  $|x_A - x_B| \leq 1$ , it is probably as accurate as the electronegativity values justify. For  $|x_A - x_B| > 1$ , the quadrupole coupling indicates a somewhat higher ionicity than indicated by (14.93) although this simple relation can still be used for a quick estimate of the approximate ionicity.

The solid curve of Fig. 14.1 represents closely the correlation of the present data. This curve is a plot of the equation

$$i_c = 1.15 \exp[-(\frac{1}{2})(2 - \Delta x)^2] - 0.15 \quad (14.94)$$

where

$$\Delta x = |x_A - x_B| \leq 2$$

For  $\Delta x > 2$ , the bonds are completely ionic,  $i_c = 1$ , and (14.94) does not apply. Although other equations with different constants might be designed to fit the empirical relationship of Fig. 14.1, the relatively simple formula of (14.93) is probably as accurate as can be justified by the electronegativity values.

The relationship of (14.93), or of (14.94), applies only to single bonds. It does not give the total ionic character of a multiple bond, although it should be applicable to a  $\sigma$  component of a multiple bond whenever the effects of the other bond components on the electronegativity difference can be assessed. Applications of the relation to bonds having  $\pi$  components are made in later sections; examples are shown in Table 14.7.

Since a correct evaluation of ionic character is of great importance in chemistry, we shall attempt to clear up some of the difficulties which have caused chemists to be reluctant to accept the rather large ionic-character values predicted from the ionic character-electronegativity relation based on quadrupole couplings.

Many years ago Pauling [37] recognized that there should be a systematic relationship between the ionic character of a bond and the difference in the electronegativity of the bonded atoms. He obtained the first such correlation on the four hydrogen halides with ionic character, estimated from dipole moments, only three of which had been measured. Since that time his relation has been widely used for estimation of ionic character from electronegativities, and it is still used by some workers, even though it is now known to have been based on an incomplete knowledge of dipole moments. Pauling assumed the ionic character to be  $\mu_{\text{obs}}/eR$ , where  $\mu_{\text{obs}}$  is the measured dipole moment,  $e$  is

the charge on the electron, and  $R$  is the interatomic distance. He thus obtained the ionic character values of 0.17 for HCl, 0.114 for HBr, and 0.049 for HI, in contrast to the values given in Table 14.5 of 0.38, 0.31, and 0.20, respectively. It is now known from the work of Mulliken [38] that a large component due to the orbital overlap charge exists in the dipole moments of the hydrogen halides because of the great difference in the size of the bonded atoms. This overlap moment, not taken into account by Pauling, is in the opposite direction to the primary moment  $\mu_p = i_c eR$ , and for HI is actually larger than the primary moment. Even if the  $i_c$  values used by Pauling for HCl, HBr, and HI had been correct ones, these values ranging from 0.049 to 0.17 could not have been safely projected to give values of high ionicity, and the high value  $i_c = 0.60$  for HF which he used was not based on a measured dipole moment but on an estimated one. It is to Pauling's credit that he recognized the questionable basis of this relationship and warned that it had only qualitative significance. He justified its presentation on the ground that no other method existed for estimation of even approximate values of ionicity. A reinterpretation of the dipole moments of the hydrogen halides is given in Section 16, where it is shown that the ionic character-electronegativity relation derived from dipole moments is consistent with that obtained above from quadrupole couplings.

## 10 HYBRIDIZATION FROM QUADRUPOLE COUPLING: POSITIVELY CHARGED HALOGENS AND GROUP III ELEMENTS

Although the nuclear quadrupole evidence does not indicate hybridization on the negative halogen of a polar bond, there is strong quadrupole evidence for  $sp$  hybridization on the positive element of a polar bond. It is proposed that this difference is due to the fact that hybridization on the positive atom is supported by the primary dipole moment of the polar bond and that hybridization on the negative atom is suppressed by the bond moment. In this section we shall derive from the nuclear quadrupole coupling of the positive atom the amount of such hybridization in a few mixed diatomic halides and in a number of diatomic molecules formed by Group III elements with the halides.

First, we shall consider positively charged halides. In Section 8 it is shown that a consistent interpretation of the two halides in BrCl, IBr, and ICl requires the assumption of small amounts of  $s$  character in the bonding orbital of the positive halide, as indicated in Table 14.6. To obtain this consistency, it was necessary also to use for  $eQq_{n10}$ , the values obtained from the nonpolar halides, Cl<sub>2</sub>, Br<sub>2</sub>, and I<sub>2</sub>. As explained in Section 8, the molecular  $eQq_{n10}$  values must be used to eliminate the effects of bond orbital overlap in these mixed halides that have high covalent character in their  $\sigma$  bonds. We have used the atomic  $eQq_{n10}$  values for calculation of the hybridization on the positive atoms of CIF, BrF, and IF which have high ionic components in their bonds. Also, we have used the atomic  $eQq_{n10}$  for calculation of the hybridization on other positive atoms in

**Table 14.6** Hybridization of Bonding Orbital of Positively Charged Atom of Polar Bonds as Obtained from Nuclear Quadrupole Coupling

Molecule <i>A-B</i>	Hybridized Coupling Atom <i>A</i>	Coupling $\chi_z$ (MHz)	Ionic Character of Bond <i>i<sub>c</sub></i>	<i>s</i> Character of Bonding Orbital of Atom <i>A</i>
BrCl	<sup>79</sup> Br	876.7	0.09 <sup>b</sup>	0.02 <sup>e</sup>
IBr	<sup>127</sup> I	-2753.5	0.12 <sup>b</sup>	0.02 <sup>e</sup>
ICl	<sup>127</sup> I	-2927.9	0.22 <sup>b</sup>	0.05 <sup>e</sup>
ClF	<sup>35</sup> Cl	-145.87	(0.50) <sup>c</sup>	0.18 <sup>f</sup>
BrF	<sup>79</sup> Br	1086.8	(0.58) <sup>c</sup>	0.18 <sup>f</sup>
IF	<sup>127</sup> I	-3438.2	(0.70) <sup>c</sup>	0.20 <sup>f</sup>
BF	<sup>11</sup> B	-4.5	(1.00) <sup>c</sup>	0.28 <sup>g</sup>
AlF	<sup>27</sup> Al	-37.49	(1.00) <sup>c</sup>	0.37 <sup>g</sup>
AlCl	<sup>27</sup> Al	-29.8	0.92 <sup>d</sup>	0.27 <sup>g</sup>
AlBr	<sup>27</sup> Al	-27.9	0.90 <sup>d</sup>	0.25 <sup>g</sup>
AlI	<sup>27</sup> Al	-25.9	0.86 <sup>d</sup>	0.21 <sup>g</sup>
GaF	<sup>69</sup> Ga	-106.5	(1.00) <sup>c</sup>	0.33 <sup>g</sup>
GaCl	<sup>69</sup> Ga	-92.1	0.88 <sup>d</sup>	0.27 <sup>g</sup>
GaBr	<sup>69</sup> Ga	-86.5	0.86 <sup>d</sup>	0.24 <sup>g</sup>
GaI	<sup>69</sup> Ga	-81.1	0.84 <sup>d</sup>	0.21 <sup>g</sup>
InF	<sup>115</sup> In	-723.8	(1.00) <sup>c</sup>	0.33 <sup>g</sup>
InCl	<sup>115</sup> In	-657.5	0.88 <sup>d</sup>	0.27 <sup>g</sup>
InBr	<sup>115</sup> In	-633.2	0.85 <sup>d</sup>	0.25 <sup>g</sup>
InI	<sup>115</sup> In	-607.1	0.83 <sup>d</sup>	0.22 <sup>g</sup>

<sup>a</sup>Coupling from Landolt-Börnstein, *Numerical Data and Functional Relations in Science and Technology*. For a complete reference, see Chapter I, [65].

<sup>b</sup>*i<sub>c</sub>* derived from coupling of negative halogen with  $eQq_{n10}$  determined from the homopolar molecules Cl<sub>2</sub>, Br<sub>2</sub>, and I<sub>2</sub>, as explained in the text.

<sup>c</sup>*i<sub>c</sub>* determined from electronegativity difference by use of (14.93).

<sup>d</sup>*i<sub>c</sub>* derived from coupling of negative halogen by use of (14.92), with  $eQq_{n10}$ (atomic) from Table 14.2.

<sup>e</sup>*s* character  $a_s^2$  derived from (14.91) with coupling in column 3, *i<sub>c</sub>* value in column 4, and  $eQq_{n10}$  from the homopolar molecules Cl<sub>2</sub>, Br<sub>2</sub>, and I<sub>2</sub>, as explained in the text.

<sup>f</sup>*s* character derived from (14.91) with coupling of positive halogen in column 3 and  $\varepsilon = 0.15$  from Table 10.3,  $eQq_{n10}$ (atomic) from Table 14.2 and with *i<sub>c</sub>* value from column 4.

<sup>g</sup>*s* character  $a_s^2$  for Group III elements derived from (14.97) with  $\chi_z$  value in column 3, *i<sub>c</sub>* value in column 4, and  $eQq_{n10}$ (atomic) value from Table 14.2 and  $\varepsilon$  value from Table 14.3.

Table 14.6 for which the *i<sub>c</sub>* is 0.50, or greater. Note that the hybridization is 18 to 20% on the halogens bonded to the highly electronegative F.

The Group III elements, B, Al, Ga, and so on, have the valence shell configuration  $s^2p^1$  and normally would be expected to form single bonds with either a pure *p* orbital, an *sp* hybrid, or an *spd* hybridized orbital. We consider the *spd* hybridized bonding orbital, (14.72), of the coupling atom *A*, analyzed in Section 6. For reasons given there, the coupling of the *d*-orbital component is negligible in comparison with that of the *p* component. The significant effect

of the  $d$  contribution is its reduction of the density of the  $p$  orbital component. The  $p_z$  density of the bonding orbital is reduced by the hybridization to  $a_p^2 = 1 - a_s^2 - a_d^2$ . The counterhybridized  $dp$  orbital does not contribute to the coupling because it is unpopulated in Group III elements. The counterhybridized  $sp$  orbital has a pair of unshared electrons and a  $p_z$  density of  $a_p^2 = 2(1 - a_s^2)$ . The total number of  $p_z$  electrons is  $n_z = 2a^2(1 - a_s^2 - a_d^2) + 2a_s^2$ , as given by (14.74). In the Group III elements the  $p_x$  and  $p_y$  orbitals are unpopulated,  $n_x = 0$ ,  $n_y = 0$ . Thus,

$$(U_p)_z = \frac{n_x + n_y}{2} - n_z = -[2a^2(1 - a_s^2 - a_d^2) + 2a_s^2] \quad (14.95)$$

With  $a^2 = (1 - i_c)/2$  from (14.87) for the positive atom of an ionic-covalent bond, (14.95) can be expressed as

$$(U_p)_z = -[(1 - i_c)(1 - a_s^2 - a_d^2) + 2a_s^2] \quad (14.96)$$

The coupling of a single-bonded Group III element forming the positive pole of an ionic-covalent bond may then be expressed by

$$\chi_z = [(1 - i_c)(1 - a_s^2 - a_d^2) + 2a_s^2](1 + i_c \epsilon)eQq_{n10} \quad (14.97)$$

where  $a_s^2$  and  $a_d^2$  signify the  $s$  and  $d$  character, respectively, of the bonding orbital of the element and  $(1 + i_c \epsilon)$  represents the screening correction for the positive charge.

It is evident from consideration of (14.97) that for the highly ionic bonds generally formed by the Group III elements, the  $s$  character of the bonding orbital is likely to have a much greater effect on the coupling than any probable  $d$  character. For example, let us consider the coupling  $\chi_z$  of  $^{27}\text{Al}$  in AlBr, which has  $i_c = 0.90$ . Although this ionic character is high, all the bonds of diatomic molecules of Group III with halogens listed in Table 14.6 have  $i_c$  greater than 0.80. With  $i_c = 0.90$ , (14.97) becomes

$$\chi_z = [0.10 + 1.9a_s^2 - 0.10a_d^2](1 + 0.90\epsilon)eQq_{n10}$$

If the  $s$  and  $d$  character were equal in this case, the effects of the  $s$  character on the coupling would be 19 times that of the  $d$  character. The effect of the  $s$  character would be to increase the coupling value, whereas the effect of the equal  $d$  character would be to reduce this increase by about 5%. From energy considerations one would expect the  $d$  character to be much lower than, rather than equal to, the  $s$  character. Consequently, in the calculation of the hybridizations listed in Table 14.6 we have neglected possible effects of  $d$  character and have set  $a_d^2 = 0$  in (14.97).

There is no reasonable doubt that the Group III elements have significant  $s$  hybridization of their valence  $p$  orbital when they form single bonds to the more electronegative atoms like the halides. If we set  $a_s^2 = 0$  in the calculation of the  $\chi_z$  coupling of  $^{27}\text{Al}$  in AlBr, just described, the magnitude of the calculated  $\chi_z(^{27}\text{Al})$  would be only 4.9 MHz as compared with the observed value of 27.9 MHz. Inclusion of any  $d$  character would make the calculated value even less

than 4.9 MHz. From the electronegativity differences it is reasonably certain that the bonds of GaF and InF are essentially pure ionic bonds. With  $i_c = 1.00$  substituted in (14.97), the predicted coupling becomes  $\chi_z = 2a_s^2(1 + \varepsilon)eQq_{n10}$ , which is zero if the s hybridization is zero. An s character of 33%,  $a_s^2 = 0.33$ , is required to produce the observed couplings in Ga and InF. In effect, this means that the counterhybridized orbital has  $\frac{1}{3}p_z$  character. Since this counterhybridized orbital has an unshared pair, the number of  $p_z$ -electrons on the Ga or In is  $n_z = \frac{2}{3}$  even though the  $p_z$  electron density in the bonding orbital is entirely on the F. Since bond orbital hybridization usually occurs because it increases the effectiveness of the orbital overlap and hence increases the strength of the covalent component of the bond, one might ask why there would be such large hybridization in a pure ionic bond. The answer must be that the hybridization is induced entirely by the large primary dipole moment of the ionic bond. See the discussion in Section 16.

Comparison of the last two columns of Table 14.6 shows that the general trend is toward increasing hybridization on the positive atom with increasing ionic character of the bond. The highest amount of s hybridization is for the completely ionic bonds formed by the Group III elements with F. There are, of course, individual differences due to other factors, but the effects of ionic character in inducing hybridization on the positive atom are pronounced. Since there is no orbital overlap, the force for hybridization of the atomic orbitals of a completely ionic bond must be the strong electric field of the primary dipole moment. The primary moment will induce a hybridization moment in such a direction as to lower the overall or resultant moment and hence the potential energy. The negative halogen in these molecules has a closed  $sp$  shell, and its polarizability is not great. Significant distortion of these shells would occur through a lifting of  $p$  electron charge into  $d$  orbitals directed toward the positive pole, but this would lead to significant coupling on the negative halogen, in disagreement with the observed coupling of nearly zero for the halogens. Contrast, for example, the nearly zero coupling of Cl in AlCl or InCl with the very large coupling of both Al and In, almost equivalent to that of one unbalanced  $p$  electron. If there were no hybridization on Al or In, removal of the valence  $p$  electron would leave in the ionic structure two electrons on the spherically symmetric s shell, which has no quadrupole coupling.

If there were s hybridization on the negative halogen, it would be expected to be in the bonds of low ionic character where the quenching primary moment is small or in bonds such as HI where there is a large orbital overlap moment in the opposite direction (see Section 16). However, the evidence from quadrupole coupling is against such hybridization (see the discussion of BrCl and IBr in Section 8).

## 11 MEASUREMENT OF $\pi$ CHARACTER WITH NUCLEAR QUADRUPOLE COUPLING

Nuclear quadrupole coupling provides a useful method for investigation of the  $\pi$  character of chemical bonds. When the coupling is axially symmetric

( $\eta=0$ ), as is always true in linear and symmetric-top molecules, the  $\pi$  character can be detected only through its effects on the magnitude of the coupling. Measurements of the  $\pi$  character in this case requires a knowledge of the coupling to be expected if there were no  $\pi$  character in the bond. When the coupling tensor is made asymmetric by  $\pi$  bonding in one plane (double-bond character), the  $\pi$  component can be measured through the observed asymmetry parameter in the coupling tensor. This method is generally more accurate than that which depends on the magnitude of the coupling.

### Symmetrically Bonded Atoms

In linear and symmetric-top molecules there is no observable asymmetry parameter, and one can detect  $\pi$  character only through its effects on the magnitude of the coupling. This method is most applicable to bonds involving a coupling halogen for which the coupling expected for the bond without  $\pi$  character can be estimated from methods derived for single-bonded halogens of diatomic molecules (Sections 7 and 8). We shall illustrate the method for bonds of this type. It is also applicable to symmetrically bonded atoms in asymmetric-top molecules for which the  $\pi_x$  and  $\pi_y$  character is equal and the asymmetry parameter is zero.

In developing the formula for the single-bonded coupling halogen we assumed the  $p_x$  and  $p_y$  orbitals to have unshared pairs. Thus  $n_x=2$  and  $n_y=2$ . In  $\pi$  bonding either the  $p_x$  or the  $p_y$  pair, or both, would be shared. There would be, on the average, only one electron in the  $p$  orbital forming a complete  $\pi$  bond or  $2-\pi_c$  in the halogen orbital which formed a fractional bond of amount  $\pi_c$ . In a symmetrical bond one could not detect the  $\pi_x$  or  $\pi_y$  bonding separately, and hence we designate the total amount of  $\pi$  bonding as  $\pi_c$ . Thus  $n_x+n_y=4-\pi_c$ . The number of  $p_z$  electrons  $n_z$  is determined by (14.60) and (14.86). If we assume the coupling to be on a negative halogen atom of a polar bond (the most common case for halogen bonds in organic molecules), the hybridization for the coupling atom will be negligible, and the unbalanced  $p$  electrons with reference to the bond axis  $z$  will be

$$(U_p)_z = \frac{n_x + n_y}{2} - n_z = 2 - \frac{\pi_c}{2} - (1 + i_\sigma) = \left(1 - i_\sigma - \frac{\pi_c}{2}\right) \quad (14.98)$$

With neglect of the small charge correction, the corresponding coupling on a negative halogen will be

$$\chi_z = -\left(1 - i_\sigma - \frac{\pi_c}{2}\right) eQq_{n10} \quad \{ \text{negative pole of } \sigma \text{ bond on halogen} \} \quad (14.99)$$

and the  $\pi$  character will be

$$\pi_c = 2 \left(1 - i_\sigma + \frac{\chi_z}{eQq_{n10}}\right) \quad (14.100)$$

in which  $i_\sigma$  is the ionic character of the  $\sigma$  bond only. The total ionic character of the bond including both the  $\sigma$  and  $\pi$  components will be

$$i_c = i_\sigma - \pi_c \quad (14.101)$$

If the resultant dipole moment of the bond is such as to put the positive pole on the coupling atom, we must admit of the possibility of *s* hybridization. If there is an  $a_s^2$  amount of hybridization on the coupling halogen, (14.91) becomes

$$\chi_z = - \left[ (1 + i_\sigma)(1 - a_s^2) - \frac{\pi_c}{2} \right] (1 + 0.15i_c) eQq_{n10} \quad \begin{cases} \text{positive pole} \\ \text{of } \sigma \text{ bond on} \\ \text{halogen} \end{cases} \quad (14.102)$$

where the term  $0.15i_c$  is a screening constant for the positive charge on the coupling halogen and where  $i_c = i_\sigma + \pi_c$ .

In Table 14.7 are given the values for the  $\pi$  character of the C- halogen bond in several linear and symmetric-top molecules as estimated from the quadrupole coupling of the halogen. In all, except ICN and CH<sub>3</sub>CCI, (14.100) was used for the calculations, with the ionic character obtained from (14.93). The small possible hybridization in these negative or nearly neutral halogens is neglected. For ICN and CH<sub>3</sub>CCI, for which the positive pole of the  $\sigma$  bond is

**Table 14.7** Bond Character and Resultant Ionic Character for Various Bonds to Halogens Measured from the Halogen Coupling

Molecule	$\chi_z(\text{Hal})(\text{MHz})$ for <sup>35</sup> Cl, <sup>79</sup> Br, or <sup>127</sup> I	<i>Ionic Character of <math>\sigma</math> Bond<sup>a</sup></i> $i_\sigma$	$\pi_c$	<i>Resultant Ionic Character<sup>a</sup></i> $i_c = i_\sigma - \pi_c$
CH <sub>3</sub> Cl	-74.77	0.35	0	0.35
CH <sub>3</sub> Br	577.15	0.25	0	0.25
CH <sub>3</sub> I	-1934	0.13	0.04	0.09
SiH <sub>3</sub> Cl	-40.0	0.55	0.17	0.38
SiH <sub>3</sub> Br	336	0.45	0.22	0.23
SiH <sub>3</sub> I	-1240	0.32	0.28	0.04
GeH <sub>3</sub> Cl	-46.95	0.57	0	0.57
GeH <sub>3</sub> Br	380	0.47	0.06	0.41
CICN	-83.39	0.10	0.28	+0.18
BrCN	685.6	0	0.22	+0.22
ICN	2418.8	+0.12	0.22	+0.34
HCCl	-79.67	0.15	0.24	+0.09
HCCBr	646	0.05	0.22	+0.17
CH <sub>3</sub> CCl	-79.6	0.15	0.24	+0.09
CH <sub>3</sub> CCBr	647	0.05	0.22	+0.17
CH <sub>3</sub> CCI	-2230	+0.07	0.25	+0.32

<sup>a</sup>The positive sign indicates that the positive pole is on the halogen.

on the I, (14.102) is employed with  $a_s^2 = 0$ . There is justification for neglect of  $s$  character when the positive charge on the halogen is small (see Section 8).

The electronegativity values for the halogen atoms that are needed for calculation of the ionic character from (14.93) are taken from Appendix G, except that group electronegativity values of 2.30 for  $\text{CH}_3$ , 2.7 for  $X-\text{C}\equiv\text{C}-$ , and 2.8 for  $\text{N}\equiv\text{C}$  were used [7].

Among the halogen bonds to the hydride group, only those to  $\text{SiH}_3$  show evidence for double-bond character. This bonding can be attributed mainly to contributing structures of the type  $\text{H}_3\text{Si}^-=\text{Cl}^+$ , in which the electron pair on the halogen forms a dative-type  $\pi$  bond with the empty  $d$  orbitals of the Si. From bond-length shortening, the  $\text{Si}-\text{Cl}$  and  $\text{Si}-\text{Br}$  bonds are predicted to have about 10% double-bond character, while those for  $\text{CH}_3-\text{Hal}$  and  $\text{GeH}_3-\text{Hal}$  show no bond shortening attributable to  $\pi$  bonding. Such bonds are also possible with Ge and higher-period elements, but  $\pi$  bond character generally decreases with increasing size of the bond atoms because of less effective orbital overlap. Nevertheless, the quadrupole coupling indicates that the  $\pi$  character in the  $\text{H}_3\text{Si}-\text{Hal}$  bonds increases slightly from Cl to I. Evidently the decrease in electronegativity from Cl to I is responsible for this effect. When, however, there are other halogens bonded to the central atom, as in  $\text{SiCl}_4$ ,  $\text{SiBr}_4$ , and so on, the trend is reversed, that is, the  $\pi$  bonding is greater for the smaller halogen. This reversal is attributable to the difference in effective electronegativity of the group to which the halogen is bonded. For example, the effective electronegativity of the  $\text{Cl}_3\text{Si}$  group is significantly greater than that of  $\text{I}_3\text{Si}$ . The insignificance of  $\pi$  character in the  $\text{CH}_3-\text{halogen}$  bond is due to the fact that no  $d$  orbitals are available on the valence shell of C. Slight amounts of  $\pi$  bonding in these molecules might occur, however, through the mechanism of hyperconjugation.

The results in Table 14.7 show, in agreement with consideration of bond lengths [37], that there is a strong tendency for conjugation of a C-halogen bond with an adjacent triple bond. The  $\pi$  bonding of the C halogen can be ascribed to structures of the form



which contribute from 22 to 28% to the ground state of the halogen cyanides and acetylenes listed in Table 14.7. Because of the positive charge required on the halogens, structures of this type would be expected to decrease in contributions with increasing electronegativity of the halogen from I to Cl. Other things being equal, however, the  $\pi$  bond character would be expected to decrease with increase in size of the halogen. These two opposing effects are evidently responsible for the nearly equivalent  $\pi$  bond character of the chloride, bromide, and iodide bonds in the cyanides and acetylenes.

The  $^{14}\text{N}$  coupling also gives evidence for contributions of structures of the type  $\text{N}^-=\text{C}=\text{Hal}^+$ . Because of the small magnitude of the  $^{14}\text{N}$ , the prediction of the amount of this contribution from the nitrogen coupling is not as reliable as that from the halogen.

## Involvement of *d* Orbitals in Double Bonding

Quadrupole coupling evidence for *d*-orbital involvement in double bonding in  $\text{SiH}_3\text{—Hal}$  and to a lesser extent in  $\text{GeH}_3\text{—Br}$  is shown in Table 14.7. Note that there is no comparable evidence for  $\pi$  bonding in the methyl halides. Since the *d* orbitals of the Group IV elements are normally unoccupied and the *p* shell of a singly bonded halogen is filled, the double bond component is a dative-type bond in which the shared pair is contributed by a *p* orbital of the halogen. The fact that such a double bonded structure as  $\text{X}_3\text{Si}^+ = \text{Hal}^-$  seems to require a positive charge on the very electronegative halogen has caused many to doubt the importance of the structure. Pauling, however, in his well-known treatise on the chemical bond [37] freely postulated such structures to account for bond distances in the silicon halides. The much higher ionic character—of opposite polarity—in the  $\sigma$  component of the bond as revealed by the quadrupole coupling makes this form of double bonding more plausible. For example, (14.93) indicates 55% ionic character for the  $\sigma$  bond in  $\text{SiH}_3\text{Cl}$ , which puts a negative charge of  $0.55e$  on the chlorine. The resultant negative charge on the Cl is reduced to  $0.38e$  by the 17%  $\pi$ -bonding component. This “ $\pi$  feedback” thus makes the charge on the Cl less negative, but not positive. The rather large positive charge of  $0.55e$  in the  $sp_3$  hybrid orbital of the Si significantly reduces the nuclear screening for the *d* orbitals and thus increases their effective electronegativity and tendency for  $\pi$  bonding.

Because of the high electronegativity of the halogens, the group electronegativity of  $(\text{Hal})_3\text{Si}\text{—}$  is appreciably greater than that of  $\text{H}_3\text{Si}\text{—}$ . The same is true for the Ge groups (see Section 15). However, “ $\pi$  feedback” in the halogen groups puts negative charge back on the central atom and alters its electronegativity. In the spherical halides  $\text{Si}(\text{Hal})_4$ ,  $\text{Ge}(\text{Hal})_4$ , and  $\text{Sn}(\text{Hal})_4$ , for which the halogen couplings are known from pure quadrupole resonance, correction for this effect can be taken into account if the number of screening valence electrons is decreased by  $c = 3(i_\sigma - \pi_c)$  in the calculation of the  $(\text{Hal})_3M\text{—}$  group electronegativity from (14.141). Here  $(i_\sigma - i_\pi)$  is the resultant ionic character of each of the halogen bonds. As was shown earlier [7] for the  $M(\text{Hal})_4$  molecule, one can then solve the three equations:

$$\chi_z = - \left( 1 - i_\sigma - \frac{\pi_c}{2} \right) eQq_{n10} \quad (14.103)$$

$$i_\sigma = \frac{x_{\text{Hal}} - x_g}{2} \quad (14.104)$$

$$x_g = \frac{0.31[5 + 3(i_\sigma - \pi_c)]}{r} + 0.50 \quad (14.105)$$

for the three unknowns,  $i_\sigma$ ,  $\pi_c$ , and  $x_g$ , where  $x_g$  is the electronegativity of the  $(\text{Hal})_3M\text{—}$  group. Equation 14.105 is described in Section 15. In these equations,  $\chi_z$  is the halogen coupling,  $x_{\text{Hal}}$  is the halogen electronegativity (3 for Cl, 2.8 for Br, and 2.55 for I) and  $r$  is the covalent radius of  $M$  (1.17 for Si, 1.22 for Ge, and 1.40 for Sn). The resulting values of  $i_\sigma$ ,  $\pi_c$ , and  $x_g$  obtained by this method

**Table 14.8** Bond Properties Derived from the Halogen Quadrupole Coupling in Symmetrical  $X(\text{Hal})_4$  Molecules in the Solid State

Molecule	$\chi_z/eQq_{n10}$	$x_g$	$i_\sigma$	$\pi_c$
$\text{SiCl}_4$	0.37	2.07	0.46	0.33
$\text{SiBr}_4$	0.46	2.02	0.39	0.30
$\text{SiI}_4$	0.58	1.97	0.29	0.26
$\text{GeCl}_4$	0.47	2.07	0.46	0.13
$\text{GeBr}_4$	0.54	2.02	0.39	0.13
$\text{GeI}_4$	0.65	1.96	0.30	0.11
$\text{SnCl}_4$	0.44	1.94	0.53	0.06
$\text{SnBr}_4$	0.50	1.89	0.46	0.08
$\text{SnI}_4$	0.61	1.85	0.35	0.08

are shown in Table 14.8. Although these values are only approximate, they illustrate how quadrupole coupling can be combined with information of other types to provide an understanding of the nature of the bonding in rather complex pentatomic molecules. The  $\pi$  character in these bonds is partly due to hyperconjugation described in Section 12. However, from a consideration of the rather large  $\pi_c$  in  $\text{SnH}_3-\text{Hal}$ , where such hyperconjugation is not significant, it is concluded that the principal mechanisms of the  $\pi$  bonding in the Group IV elements of the third and higher rows involves the  $d$  orbitals. The small amount of  $\pi$  character which results from hyperconjugation should not alter significantly the predicted values. Another assumption—that the screening by  $d$  electrons is the same as that by  $s$  and  $p$  electrons—may cause small errors. This assumption would tend to make the predicted  $x_g$  values slightly too small.

Figure 14.2 shows a plot of double bond character in the Group IV halides

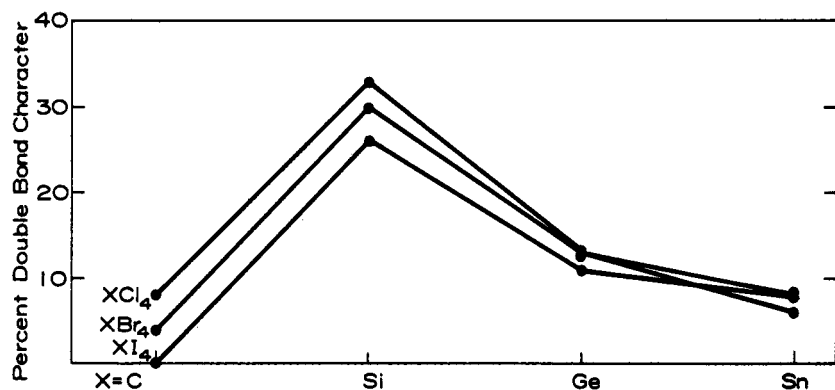


**Fig. 14.2** Double bond character in  $X(\text{Hal})_4$  molecules as derived from the nuclear quadrupole coupling of the halogen.

## Chapter XV

# IRREDUCIBLE TENSOR METHODS FOR CALCULATION OF COMPLEX SPECTRA

---

1	INTRODUCTION	803
2	SINGLE COUPLING NUCLEUS: REDUCED MATRIX ELEMENTS	812
3	PLURAL, UNEQUAL COUPLING	818
4	PLURAL, EQUAL, OR NEARLY EQUAL, COUPLING	823
5	NUCLEAR SPIN-SPIN INTERACTIONS	829
6	RELATIVE INTENSITIES	831
7	ELECTRONIC SPIN INTERACTIONS	835
8	STARK EFFECT	838

### 1 INTRODUCTION

In this section we wish to demonstrate how the irreducible tensor method can be used to extract information on molecular interactions. Direct calculation techniques discussed previously in which wave function expansions are employed to change to a more appropriate basis give rise to particularly complicated expressions. With irreducible tensor methods, such complications are taken care of in the derivation of the relatively simple theorems associated with the theory. Irreducible tensor methods thus provide a highly efficient and powerful way to analyze hyperfine structure arising from plural nuclear coupling, as well as other molecular interactions. Since more applications of these methods are appearing, some familiarity with these techniques is required for an adequate appreciation of the literature on hyperfine interactions, as well as other areas of microwave spectroscopy. The theory of spherical or irreducible tensor operators has been discussed in detail by Rose [1], Edmonds [2], Fano and Racah [3], and Judd [4]. In this section we follow much of the expository discussion given by Cook and De Lucia [5]. Important theories will be simply quoted, and we will concentrate on their application. The reader may consult the previous references for derivations of these theorems.

Discussions and specific applications of irreducible tensor methods to the

analysis of complex spectra have been given by Curl and Kinsey [6], Thaddeus et al. [7], and others [8-44], to cite but a few (see also references cited therein). These include discussions applicable to symmetric tops [15, 19, 24, 26, 28, 29, 38, 40, 42] and molecules with unbalanced electronic angular momentum [6, 12, 20, 32, 35, 36, 39]. Techniques for inclusion of the effects of identical particles in a particularly straightforward way have been given by Cederberg [17]. The theory of hyperfine interactions in molecules with internal rotation has been discussed by Heuvel and Dymanus [21], and Ribeaud et al. [43]; that of nuclear hyperfine interactions in spherical tops, by Michelot et al. [34].

By definition, the quantities  $T_q^{(k)}(q = -k, -k+1, \dots, +k)$  constitute an irreducible tensor of rank  $k$  (an integer) if they transform like the spherical harmonics  $Y_q^{(k)}(\theta, \phi)$  under a rotation. The transformation properties of an irreducible tensor  $\mathbf{T}^{(k)}$  under a rotation of the coordinate system is given by [1]

$$T'_q^{(k)} = \sum_q T_q^{(k)} D_{qq'}^{(k)}(\alpha\beta\gamma) \quad (15.1)$$

where  $T_q^{(k)}$  are the components defined with respect to the old axes,  $T'_q^{(k)}$  are the components with respect to the new or rotated coordinate system, and  $D_{qq'}^{(k)}$  is the  $(2k+1)$  dimensional matrix representation of the rotation operator. The  $D_{qq'}^{(k)}$  depend on the Euler angles  $(\alpha, \beta, \gamma)$  that specify the relative orientation of the two frames. By inverting (15.1) we may express  $T_q^{(k)}$  in terms of the components,  $T'_q^{(k)}$ . Multiplying by  $D_{q'q}^{-1(k)}$  and summing over  $q'$  give

$$T_q^{(k)} = \sum_{q'} (-1)^{q-q'} T'_q^{(k)} D_{-q, -q'}^{(k)} \quad (15.2)$$

where the unitary character of the  $\mathbf{D}^{(k)}$  matrix and the relation

$$D_{q'q}^{-1(k)} = D_{qq'}^{*(k)} = (-1)^{q-q'} D_{-q, -q'}^{(k)} \quad (15.3)$$

have been employed. This relation will be used to express the tensor components  $T_q^{(k)}$  in terms of the components  $T'_q^{(k)}$  with respect to the rotating molecule-fixed principal inertial axis system.

The scalar product of two irreducible tensors  $\mathbf{T}^{(k)}$  and  $\mathbf{U}^{(k)}$  with components  $T_q^{(k)}$  and  $U_q^{(k)}$  is defined as

$$\mathbf{T}^{(k)} \cdot \mathbf{U}^{(k)} = \sum_{q=-k}^k (-1)^q T_q^{(k)} U_{-q}^{(k)} \quad (15.4)$$

The rule for the product of two irreducible tensor operators is specified by

$$\begin{aligned} T_q^{(l)} &= [\mathbf{T}^{(l_1)} \times \mathbf{T}^{(l_2)}]_q^{(l)} \\ &= (2l+1)^{1/2} \sum_{q_1 q_2} (-1)^{-l_1 + l_2 - q} \\ &\quad \times \begin{pmatrix} l_1 & l_2 & l \\ q_1 & q_2 & -q \end{pmatrix} T_{q_1}^{(l_1)} T_{q_2}^{(l_2)} \end{aligned} \quad (15.5)$$

which yields irreducible tensors of rank  $l$ , where  $l$  may be equal to  $|l_1 + l_2| \cdots |l_1 - l_2|$ . Note, in the multiplying of spherical tensors, the ranks are added vectorially

not algebraically. The notation  $T^{(l_1)} \times T^{(l_2)}$  makes clear the origin of the irreducible tensor  $T_q^{(l)}$ . The symbol above in brackets is a  $3j$  symbol and is related to the Clebsch-Gordon coefficients.

The  $3j$  symbol has the property that the value is left unchanged for an even permutation of columns and is multiplied by  $(-1)^{l_1+l_2+l}$  for an odd permutation of columns or for a sign change of all the elements of the second row. Simple algebraic formulas for some special cases are available [2] as well as tabulated numerical values [45]. They may be readily evaluated from their general definition by means of a computer algorithm. They are nonzero only if the elements of the second row sum to zero, that is,  $q_1+q_2-q=0$ , and if  $l_1, l_2, l$  satisfy the triangular condition, that is, a triangle can be formed with the length of each side specified by a quantum number. A very useful orthogonality relation for the  $3j$  symbols is

$$\sum_{m_1 m_2} \begin{pmatrix} j_1 & j_2 & j_3 \\ m_1 & m_2 & m_3 \end{pmatrix} \begin{pmatrix} j_1 & j_2 & j'_3 \\ m_1 & m_2 & m'_3 \end{pmatrix} = \frac{\delta(j_3, j'_3) \delta(m_3, m'_3)}{(2j_3 + 1)} \quad (15.6)$$

To apply the methods of irreducible tensors, the interaction must be written in the form of spherical tensors. In some cases, the interaction can be formulated directly in the form of spherical tensors such as the magnetic and quadrupole interactions [5, 8]. In other cases, it may be convenient to formulate the interaction in Cartesian form. The general hyperfine Hamiltonian in Cartesian tensor form can be expressed as

$$\mathcal{H}_{hfs} = \sum_i^N \left( \frac{1}{8} \mathbf{V}_i : \mathbf{Q}_i + \mathbf{I}_i \cdot \mathbf{C}_i \cdot \mathbf{J} \right) + \sum_i \sum_{j \neq i} (\mathbf{I}_i \cdot \mathbf{D}_{ij} \cdot \mathbf{I}_j) \quad (15.7)$$

The sum is over all coupling nuclei, and the terms represent, respectively, the electric quadrupole (product of two dyadics), magnetic dipole and spin-spin interactions. This, however, presents no serious limitation to the application of irreducible tensor methods, since the elements of a Cartesian tensor can be cast into forms which transform as spherical tensor operators.

The spherical unit vectors  $\mathbf{e}_q^{(1)}$  are defined as [2]

$$\mathbf{e}_0^{(1)} = \mathbf{e}_z, \quad \mathbf{e}_{\pm 1}^{(1)} = \mp(1/\sqrt{2})(\mathbf{e}_x \pm i\mathbf{e}_y) \quad (15.8)$$

The components of a first-rank irreducible tensor  $T_q^{(1)}$  in terms of the Cartesian components ( $T_x, T_y, T_z$ ) of a vector are given by

$$T_q^{(1)} = \mathbf{e}_q^{(1)} \cdot \mathbf{T} = \mathbf{e}_q^{(1)} \cdot (\mathbf{e}_x T_x + \mathbf{e}_y T_y + \mathbf{e}_z T_z) \quad (15.9)$$

which yields

$$T_0^{(1)} = T_z, \quad T_{\pm 1}^{(1)} = \mp(1/\sqrt{2})(T_x \pm iT_y) \quad (15.10)$$

These linear combinations transform as a first-rank spherical tensor. Any interaction written in terms of two vectors can hence be readily formulated in spherical tensor notation. The electric dipole interaction with an external field would be written from (15.4) as

$$\begin{aligned}\mathcal{H}_{\mathbf{E}} &= -\boldsymbol{\mu}^{(1)} \cdot \mathbf{E}^{(1)} = \mathcal{E}_{-1}^{(1)} \mu_{-1}^{(1)} - \mathcal{E}_0^{(1)} \mu_0^{(1)} + \mathcal{E}_1^{(1)} \mu_1^{(1)} \\ &\equiv -\mathcal{E}_x \mu_x - \mathcal{E}_y \mu_y - \mathcal{E}_z \mu_z\end{aligned}\quad (15.11)$$

with  $\boldsymbol{\mu}^{(1)}$  the electrical dipole moment tensor and with the components of the tensors chosen as in (15.10).

A second-rank Cartesian tensor may, in general, be decomposed into three irreducible tensors:

$$\mathbf{T} = \mathbf{T}^{(0)} + \mathbf{T}^{(1)} + \mathbf{T}^{(2)} \quad (15.12)$$

of rank 0, 1, 2. To define the irreducible tensor components in terms of the Cartesian components we first obtain the appropriate unit vectors. The spherical basis vectors may be constructed from (15.5). In particular, the spherical unit vectors obtained by combining  $\mathbf{e}_{q_1}^{(1)}$  and  $\mathbf{e}_{q_2}^{(1)}$  are given by

$$\begin{aligned}\mathbf{e}_q^{(l)} &= (2l+1)^{1/2} \sum_{q_1 q_2} (-1)^q \\ &\times \begin{pmatrix} 1 & 1 & l \\ q_1 & q_2 & -q \end{pmatrix} \mathbf{e}_{q_1}^{(1)} \mathbf{e}_{q_2}^{(1)} \quad (l=0, 1, 2)\end{aligned}\quad (15.13)$$

Employing a table of  $3j$  symbols, one finds

$$\begin{aligned}\mathbf{e}_0^{(0)} &= (1/\sqrt{3})(\mathbf{e}_1^{(1)} \mathbf{e}_{-1}^{(1)} + \mathbf{e}_{-1}^{(1)} \mathbf{e}_1^{(1)} - \mathbf{e}_0^{(1)} \mathbf{e}_0^{(1)}) \\ \mathbf{e}_0^{(1)} &= (1/\sqrt{2})(\mathbf{e}_1^{(1)} \mathbf{e}_{-1}^{(1)} - \mathbf{e}_{-1}^{(1)} \mathbf{e}_1^{(1)}) \\ \mathbf{e}_{\pm 1}^{(1)} &= \pm (1/\sqrt{2})(\mathbf{e}_{\pm 1}^{(1)} \mathbf{e}_0^{(1)} - \mathbf{e}_0^{(1)} \mathbf{e}_{\pm 1}^{(1)}) \\ \mathbf{e}_0^{(2)} &= (\sqrt{2}/\sqrt{3})\mathbf{e}_0^{(1)} \mathbf{e}_0^{(1)} + 6^{-1/2}(\mathbf{e}_1^{(1)} \mathbf{e}_{-1}^{(1)} + \mathbf{e}_{-1}^{(1)} \mathbf{e}_1^{(1)}) \\ \mathbf{e}_{\pm 1}^{(2)} &= (1/\sqrt{2})(\mathbf{e}_0^{(1)} \mathbf{e}_{\pm 1}^{(1)} + \mathbf{e}_{\pm 1}^{(1)} \mathbf{e}_0^{(1)}) \\ \mathbf{e}_{\pm 2}^{(2)} &= \mathbf{e}_{\pm 1}^{(1)} \mathbf{e}_{\pm 1}^{(1)}\end{aligned}\quad (15.14)$$

To define the irreducible tensor components in terms of the Cartesian components we express  $\mathbf{T}$  as a dyadic in terms of its Cartesian components

$$\mathbf{T} = \sum_{g, g'} \mathbf{e}_g \mathbf{e}_{g'} T_{gg'} \quad (g, g' = x, y, \text{ or } z) \quad (15.15)$$

and with the aid of (15.8) and the relation

$$T_q^{(l)} = \mathbf{e}_q^{(l)} \cdot \mathbf{T} \quad (15.16)$$

where  $l=0, 1, 2$  and  $q=-l, -l+1, \dots, +l$ , we find

$$\begin{aligned}T_0^{(0)} &= -(1/\sqrt{3})[T_{xx} + T_{yy} + T_{zz}] & T_0^{(2)} &= 6^{-1/2}[3T_{zz} - (T_{xx} + T_{yy} + T_{zz})] \\ T_0^{(1)} &= -(i/\sqrt{2})[T_{xy} - T_{yx}] & T_{\pm 1}^{(2)} &= \mp \frac{1}{2}[T_{xz} + T_{zx} \pm i(T_{yz} + T_{zy})] \\ T_{\pm 1}^{(1)} &= -\frac{1}{2}[T_{zx} - T_{xz} \pm i(T_{zy} - T_{yz})] & T_{\pm 2}^{(2)} &= \frac{1}{2}[T_{xx} - T_{yy} \pm i(T_{xy} + T_{yx})]\end{aligned}\quad (15.17)$$

It is apparent that if the Cartesian tensor is symmetric and traceless, only the second-rank irreducible tensor is nonvanishing. These relations thus allow an interaction involving first- and second-rank Cartesian tensors to be transformed to irreducible tensor form, where irreducible tensor methods may then be employed.

Consider, for example, the case of the spin-rotation interaction. We may write for the interaction in Cartesian coordinates

$$\mathcal{H}_M = \mathbf{I} \cdot \mathbf{C} \cdot \mathbf{J} \quad (15.18)$$

where all elements are referred to space-fixed axes and  $C$  is a second-rank Cartesian tensor written as a dyadic. To formulate this interaction so that the irreducible tensor techniques may be employed, we decompose  $\mathbf{C}$  as in (15.12) and write the interaction as a sum of scalar products

$$\mathcal{H}_M = \sum_{l=0}^2 N_l [\mathbf{C}^{(l)} \times \mathbf{J}^{(1)}]^{(1)} \cdot \mathbf{I}^{(1)} \quad (15.19)$$

where the elements of  $\mathbf{I}^{(1)}$  and  $\mathbf{J}^{(1)}$  are defined by (15.10) and those of  $\mathbf{C}^{(l)}$  by (15.17). The irreducible products  $[\mathbf{C}^{(0)} \times \mathbf{J}^{(1)}]^{(1)}$ , and so on, are obtained from (15.5). The constants  $N_l$  are appropriate normalization factors such that when (15.19) is written out explicitly it is equivalent to (15.18). The normalization factors are found to be  $N_0 = -1/3^{1/2}$ ,  $N_1 = -1$ , and  $N_2 = -5^{1/2}/3^{1/2}$ . An alternate formulation is also possible in which  $\mathbf{I}^{(1)}$  and  $\mathbf{J}^{(1)}$  are combined to give irreducible tensors of rank 0, 1, and 2 and the scalar products of these with the corresponding irreducible tensors of  $\mathbf{C}$  are formed.

The matrix element equations for irreducible tensor operators, which will be employed in the derivations of the following sections, are briefly summarized below. These theorems are taken from Edmonds [2]. For the basis functions  $|\tau jm\rangle$  that are eigenfunctions of  $\mathbf{j}^2$  and  $j_z$ , the Wigner-Eckart theorem states

$$(\tau' j' m' | T_q^{(k)} | \tau, j, m) = (-1)^{j' - m'} \times \begin{pmatrix} j' & k & j \\ -m' & q & m \end{pmatrix} (\tau' j' || T^{(k)} || \tau j) \quad (15.20)$$

where  $(\tau' j' || T^{(k)} || \tau j)$  is defined as the reduced matrix element, or double-bar matrix element, of  $T^{(k)}$ , it is, however, merely a number. The quantum number  $\tau$ , in general, may be considered a set of quantum numbers required to more clearly specify the state. This factorization theorem shows that the entire projection quantum number dependence of the matrix element is contained in the  $3j$  symbol. A knowledge of the matrix element of any one of the components,  $T_q^{(k)}$ , allows the evaluation of the reduced matrix element.

If the tensor operators  $\mathbf{T}^{(k)}$  and  $\mathbf{U}^{(k)}$  act, respectively, on subsystems 1 and 2 of a system with a subsystem 1 characterized by the angular momentum  $\mathbf{j}_1$  and subsystem 2 by the angular momentum  $\mathbf{j}_2$ , then the matrix elements of the scalar product of these two tensor operators in the coupled basis  $\mathbf{J} = \mathbf{j}_1 + \mathbf{j}_2$  are given by

$$(\tau'_1 j'_1 \tau'_2 j'_2 J' M' | \mathbf{T}^{(k)} \cdot \mathbf{U}^{(k)} | \tau_1 j_1 \tau_2 j_2 JM) = \delta_{JJ'} \delta_{MM'} (-1)^{j_1 + j'_1 + J} \left\{ \begin{matrix} J & j'_2 & j'_1 \\ k & j_1 & j_2 \end{matrix} \right\} \times (\tau'_1 j'_1 || T^{(k)} || \tau_1 j_1) (\tau'_2 j'_2 || U^{(k)} || \tau_2 j_2) \quad (15.21)$$

where the symbol in braces is the  $6j$  symbol, and  $\tau_1$  and  $\tau_2$  represent additional pertinent quantum numbers characterizing subsystems 1 and 2. Numerical

values of the  $6j$  symbol have been tabulated [45], and expressions for certain simple cases are available [2]. The value of a  $6j$  symbol is unaffected by a permutation of the columns or by an interchange of the upper and lower elements in any two columns. They may be conveniently computed from a general formula due to Racah (see Ref. 2, p. 99). Whereas the  $3j$  symbols are involved in the coupling of two angular momenta, the  $6j$  symbol is associated with the coupling of three angular momenta. In particular, they are proportional to the expansion coefficients relating the representation of the coupling scheme  $j_2 + j_3 = j'$ ,  $j' + j_1 = J$  and the representation of the coupling scheme  $j_1 + j_2 = j'$ ,  $j' + j_3 = J$  [see (9.126)]. They are nonzero only if the three numbers of each row and each column satisfy the triangular condition. In applying (15.21) it is important to recognize that  $T^{(k)}$  and  $U^{(k)}$  must be commuting tensor operators.

The relation between the reduced matrix element of a single operator in the coupled and uncoupled representation is given next. For the tensor operator  $T^{(k)}$  acting only on the space of subsystem 1, that is,  $T^{(k)}$  commutes with  $j_2$ , the nonvanishing matrix elements are

$$\begin{aligned} (\tau'_1 j'_1 \tau_2 j_2 J' \| T^{(k)} \| \tau_1 j_1 \tau_2 j_2 J) &= (-1)^{j'_1 + j_2 + J + k} [(2J+1)(2J'+1)]^{1/2} \\ &\quad \times \left\{ \begin{matrix} j'_1 & J' & j_2 \\ J & j_1 & k \end{matrix} \right\} (\tau'_1 j'_1 \| T^{(k)} \| \tau_1 j_1) \end{aligned} \quad (15.22)$$

For  $U^{(k)}$  operating only on subsystem 2, that is,  $U^{(k)}$  commutes with  $j_1$ , the nonvanishing matrix elements are

$$\begin{aligned} (\tau_1 j_1 \tau'_2 j'_2 J' \| U^{(k)} \| \tau_1 j_1 \tau_2 j_2 J) &= (-1)^{j_1 + j_2 + J' + k} [(2J+1)(2J'+1)]^{1/2} \\ &\quad \times \left\{ \begin{matrix} j'_2 & J' & j_1 \\ J & j_2 & k \end{matrix} \right\} (\tau'_2 j'_2 \| U^{(k)} \| \tau_2 j_2) \end{aligned} \quad (15.23)$$

Let  $T^{(k_1)}$  and  $U^{(k_2)}$  be tensor operators acting on subsystem 1 and 2, respectively. The reduced matrix element of the product  $T^{(k_1)} \times U^{(k_2)}$  of these two irreducible operators in the coupled representation, in terms of the reduced matrix elements of the individual operators in the uncoupled representation, is given by

$$\begin{aligned} (\tau' \tau'_1 j'_1 \tau'_2 j'_2 J' \| [T^{(k_1)} \times U^{(k_2)}]^{(k)} \| \tau \tau_1 j_1 \tau_2 j_2 J) &= [(2J+1)(2J'+1)(2k+1)]^{1/2} \\ &\quad \times \sum_{\tau''} \left\{ \begin{matrix} j'_1 & j_1 & k_1 \\ j'_2 & j_2 & k_2 \\ J' & J & k \end{matrix} \right\} (\tau' \tau'_1 j'_1 \| T^{(k_1)} \| \tau'' \tau_1 j_1) (\tau'' \tau'_2 j'_2 \| U^{(k_2)} \| \tau \tau_2 j_2) \end{aligned} \quad (15.24)$$

The symbol in braces, known as a  $9j$  symbol, can be written in terms of the  $3j$  or  $6j$  symbols, and can arise when the coupling of four angular momenta are considered. The sum over the additional classifier  $\tau''$  is usually not required. On the other hand, for a tensor product which involves operators acting on the same subspace,  $\mathbf{jm}$ , the reduced matrix elements are related by

$$(\tau' j' | [T^{(k_1)} \times U^{(k_2)}]^{(k)} | \tau j) = (-1)^{j+j'+k} (2k+1)^{1/2} \\ \times \sum_{\tau'' j''} \left\{ \begin{matrix} k_1 & k_2 & k \\ j & j' & j'' \end{matrix} \right\} (\tau' j' | T^{(k_1)} | \tau'' j'') (\tau'' j'' | U^{(k_2)} | \tau j) \quad (15.25)$$

Such reduced matrix elements can arise, as, for example, in the application of the Wigner-Eckart theorem or (15.21). The summations in the foregoing equation, where  $\tau''$  represents other quantum numbers needed to characterize the state, are usually not required. Derivations of such relationships as given above, applicable to both the rotation group and the point groups, are discussed by Cederberg [17]. The matrix element of a scalar product is a special case of the more general relation of (15.24) with  $k_1 = k_2, k = 0$ . The  $9j$  symbol with two parameters repeated and a single zero element is found to be proportional to a  $6j$  symbol. A short list of expressions for some  $3j$  and  $6j$  symbols which are of particular use here is given in Table 15.1.

An interesting application of the Wigner-Eckart theorem is in the evaluation of the matrix elements of the angular momentum. In particular, we have

$$(J', M'_J | J_q^{(1)} | J, M_J) = (-1)^{J' - M'_J} \begin{pmatrix} J' & 1 & J \\ -M'_J & q & M_J \end{pmatrix} (J' | J^{(1)} | J) \quad (15.26)$$

where  $J_0^{(1)} = J_z$ ;  $J_{\pm}^{(1)} = \mp 1/2^{1/2}(J_x \pm iJ_y)$  are components referred to the space-fixed coordinate system. In this section the space-fixed coordinates will be designated as  $(x, y, z)$ , and the body-fixed coordinates will be designated as

**Table 15.1** Expressions for Certain  $3j$  and  $6j$  Symbols

---

$\begin{pmatrix} J & J & 0 \\ M & -M & 0 \end{pmatrix}$	$= (-1)^{J-M} (2J+1)^{-1/2}$
$\begin{pmatrix} J & J & 1 \\ M & -M-1 & 1 \end{pmatrix}$	$= (-1)^{J-M} \left[ \frac{(J-M)(J+M+1) \cdot 2}{(2J+2)(2J+1)(2J)} \right]^{1/2}$
$\begin{pmatrix} J & J & 1 \\ M & -M & 0 \end{pmatrix}$	$= (-1)^{J-M} \frac{M}{[(2J+1)(J+1)J]^{1/2}}$
$\begin{pmatrix} J & J & 2 \\ M & -M & 0 \end{pmatrix}$	$= (-1)^{J-M} \frac{2[3M^2 - J(J+1)]}{[(2J+3)(2J+2)(2J+1)(2J)(2J-1)]^{1/2}}$
$\left\{ \begin{matrix} a & b & c \\ 0 & c & b \end{matrix} \right\}$	$= (-1)^s \left[ \frac{1}{(2b+1)(2c+1)} \right]^{1/2}$
$\left\{ \begin{matrix} a & b & c \\ 1 & c & b \end{matrix} \right\}$	$= (-1)^{s+1} \frac{2[b(b+1)+c(c+1)-a(a+1)]}{[2b(2b+1)(2b+2)2c(2c+1)(2c+2)]^{1/2}}$
$\left\{ \begin{matrix} a & b & c \\ 2 & c & b \end{matrix} \right\}$	$= (-1)^s \frac{2[3X(X-1)-4b(b+1)c(c+1)]}{[(2b-1)2b(2b+1)(2b+2)(2b+3) \cdot (2c-1)2c(2c+1)(2c+2)(2c+3)]^{1/2}}$

---

where  $s = a+b+c$ ,  $X = b(b+1)+c(c+1)-a(a+1)$

$(x', y', z')$ . To evaluate the reduced matrix element we choose the simplest case for the LHS of the foregoing equation

$$(J', M'_J | J_0^{(1)} | J, M_J) = (J', M'_J | J_z | J, M_J) = M_J \delta_{JJ'} \delta_{M_J M_J}. \quad (15.27)$$

in units of  $\hbar$ . Evaluation of the  $3j$  symbol ( $q=0$ ) from Table 15.1 gives

$$\begin{pmatrix} J & J & 1 \\ M_J & -M_J & 0 \end{pmatrix} = (-1)^{J-M_J} \frac{M_J}{[J(J+1)(2J+1)]^{1/2}}$$

and hence

$$(J || J^{(1)} || J) = [J(J+1)(2J+1)]^{1/2} \quad (15.28)$$

Thus, in general

$$(J, M'_J | J_q^{(1)} | J, M_J) = (-1)^{J-M'_J} \begin{pmatrix} J & 1 & J \\ -M'_J & q & M_J \end{pmatrix} [J(J+1)(2J+1)]^{1/2} \quad (15.29)$$

Note  $-M'_J + q + M_J = 0$ . Replacing the  $3j$  symbol by its equivalent yields the well-known matrix elements

$$(J, M_J | J_0^{(1)} | J, M_J) = M_J \quad (15.30)$$

$$(J, M_J \pm 1 | J_{\pm 1}^{(1)} | J, M_J) = \mp \frac{1}{\sqrt{2}} [(J \mp M_J)(J \pm M_J + 1)]^{1/2} \quad (15.31)$$

Note in the foregoing expression that the upper (or lower) sign applies throughout. Matrix elements for  $J_x$  and  $J_y$  may be readily found from these since

$$J_x = \frac{1}{\sqrt{2}} (J_{-1}^{(1)} - J_{+1}^{(1)}) \quad \text{and} \quad J_y = \frac{i}{\sqrt{2}} (J_{-1}^{(1)} + J_{+1}^{(1)}) \quad (15.32)$$

This yields (in units of  $\hbar$ )

$$(J, M+1 | J_x | J, M) = \frac{1}{2} [(J-M)(J+M+1)]^{1/2} \quad (15.33)$$

$$(J, M-1 | J_y | J, M) = \frac{i}{2} [(J+M)(J-M+1)]^{1/2} \quad (15.34)$$

Likewise, the matrix elements of the angular momentum  $J_q^{(1)}$  referred to the body-fixed axis in the symmetric rotor basis ( $KJM_J$ ) may be obtained by use of (15.1)

$$J_q^{(1)} = \sum_q J_q^{(1)} D_{qq'}^{(k)} \quad (15.35)$$

hence,

$$(K' J' M'_J | J_q^{(1)} | KJM_J) = \sum_{qM''_J} (K' J' M'_J | J_q^{(1)} | K' J' M''_J) (K' J' M''_J | D_{qq'}^{(k)} | KJM_J) \quad (15.36)$$

since from (15.29)  $J_q^{(1)}$  is diagonal in  $K$  and  $J$ . The symmetric rotor functions are related to the  $D$  matrix as follows [5]

$$\psi_{JKM_J}(\alpha\beta\gamma) = (-1)^{M_J - K} [(2J+1)/8\pi^2]^{1/2} D_{-M_J, -K}^{(J)}(\alpha\beta\gamma) \quad (15.37)$$

The matrix elements of  $D_{qq}^{(k)}$  in the symmetric rotor basis may now be obtained from the above identification and are given by [46]

$$(K' J' M'_J | D_{qq}^{(k)} | K J M_J) = (-1)^{M_J - K} [(2J+1)(2J'+1)]^{1/2} \\ \times \begin{pmatrix} J & k & J' \\ M_J & -q & -M'_J \end{pmatrix} \begin{pmatrix} J & k & J' \\ K & -q' & -K' \end{pmatrix} \quad (15.38)$$

where  $K$  is the projection quantum number of the rotational angular momentum  $\mathbf{J}$  in the molecule-fixed frame. Therefore,

$$(K' J' M'_J | J_q'^{(1)} | K J M_J) = (-1)^t [(2J+1)(2J'+1)^2 J'(J'+1)]^{1/2} \\ \times \begin{pmatrix} J & k & J' \\ K & -q' & -K' \end{pmatrix} \sum_{q, M'_J} \begin{pmatrix} J' & 1 & J' \\ M''_J & q & -M'_J \end{pmatrix} \begin{pmatrix} J' & k & J \\ M''_J & q & -M_J \end{pmatrix} \quad (15.39)$$

with  $t = J' - M'_J + M_J - K + 1$  and  $k = 1$  and two of the  $3j$  symbols have been rearranged. Using the orthogonality property of the  $3j$  symbols, (15.6), we obtain

$$(K' J M_J | J_q'^{(1)} | K J M_J) = (-1)^{J+1-K} [(2J+1)J(J+1)]^{1/2} \\ \times \begin{pmatrix} J & 1 & J \\ K & -q' & -K' \end{pmatrix} \quad (15.40)$$

Evaluation of this expression gives the matrix elements of the angular moment components in the molecule-fixed axis system for the symmetric rotor basis

$$(K J M_J | J_\delta'^{(1)} | K J M_J) = K \quad (15.41)$$

$$(K \mp 1 J M_J | J_\pm'^{(1)} | K J M_J) = \mp \frac{1}{\sqrt{2}} [(J \pm K)(J \mp K + 1)]^{1/2} \quad (15.42)$$

Note that the raising and lowering character of the operators is reversed in the two frames, as found in Chapter II.

The components  $J_x'$  and  $J_y'$  are defined in terms of  $J_q'^{(1)}$  as in (15.32), and this yields for the components referred to the molecule-fixed axis system

$$(K-1, J, M_J | J_x' | K, J, M_J) = \frac{1}{2} [(J+K)(J-K+1)]^{1/2} \quad (15.43)$$

$$(K+1, J, M_J | J_y' | K, J, M_J) = \frac{i}{2} [(J-K)(J+K+1)]^{1/2} \quad (15.44)$$

The phase choice in this section is consistent with both  $J_x'$  and  $J_y'$  as real and positive which is consistent with Condon and Shortley [47], but is opposite to the choice used throughout other portions of this text. In application of the techniques discussed in this chapter it is important to use a consistent phase choice throughout.

## 2 SINGLE COUPLING NUCLEUS: REDUCED MATRIX ELEMENTS

By way of introducing the definitions of the reduced matrix elements for the quadrupole and magnetic interaction, we consider first the case of one coupling nucleus. This case has already been discussed in Chapter IX, Section 4; however, we formulate the problem here in terms of irreducible tensors. The quadrupole and magnetic dipole interactions may be developed in terms of irreducible tensor operators [5, 8]. Since the Cartesian tensor for the quadrupole interaction is symmetric and traceless, only second-rank irreducible tensors are needed to characterize this interaction.

$$\mathcal{H}_{hfs} = \mathbf{V}^{(2)} \cdot \mathbf{Q}^{(2)} + \mathbf{m}^{(1)} \cdot \boldsymbol{\mu}^{(1)} \quad (15.45)$$

where  $\mathbf{V}^{(2)}$  is the electric field gradient tensor,  $\mathbf{Q}^{(2)}$  the nuclear quadrupole tensor,  $\mathbf{m}^{(1)}$  the magnetic field tensor, and  $\boldsymbol{\mu}^{(1)}$  the nuclear magnetic dipole tensor. The basis is taken as  $|\tau J I F M_F\rangle$  where  $\tau$  has the usual meaning for an asymmetric rotor and equals  $K$  for a symmetric top. From (15.21) for the matrix elements of a scalar product, we find for the quadrupole interaction

$$(\tau' J' I' F | \mathbf{V}^{(2)} \cdot \mathbf{Q}^{(2)} | \tau J I F) = (-1)^{J+I+F} \begin{Bmatrix} F & I & J' \\ 2 & J & I \end{Bmatrix} (\tau' J' || V^{(2)} || \tau J) (I || Q || I) \quad (15.46)$$

All terms off-diagonal in  $F$  vanish, and the matrix elements are diagonal and independent of the projection quantum numbers  $M_F$ .

In order for the preceding relation to be useful, the reduced matrix element must be evaluated in terms of the usual spectroscopic constants. This is easily accomplished by application of the Wigner-Eckart theorem. The quantum mechanical observable,  $Q$ , termed the nuclear quadrupole moment, is defined via the relation

$$(I, M_I = I | Q_0^{(2)} | I, M_I = I) = \frac{1}{2}(eQ) \quad (15.47)$$

where  $|I, M_I\rangle$  are the nuclear spin basis functions and where  $M_I = I$  corresponds to the nuclear state of maximum alignment along  $z$ . Application of the Wigner-Eckart theorem, (15.20) to (15.47) gives therefore

$$\frac{1}{2}(eQ) = (II | Q_0^{(2)} | II) = \begin{pmatrix} I & 2 & I \\ -I & 0 & I \end{pmatrix} (I || Q^{(2)} || I) \quad (15.48)$$

Expressing the  $3j$  symbol in terms of its algebraic equivalent from Table 15.1, we find for the reduced matrix element of the nuclear quadrupole tensor

$$(I || Q^{(2)} || I) = eQf(I) \quad (15.49)$$

where

$$f(I) = [(2I+1)(2I+2)(2I+3)/8I(2I-1)]^{1/2} \quad (15.50)$$

The reduced matrix element of the field gradient tensor  $\mathbf{V}^{(2)}$  is evaluated in a similar manner. The electric field gradient coupling constant  $q_{J'J}$  is defined as ( $J' \geq J$ )

$$q_{J'J} = (\tau', J', M'_J = J | (\partial^2 V / \partial z^2)_0 | \tau, J, M_J = J) \quad (15.51)$$

and

$$(\tau', J', M'_J = J | V_0^{(2)} | \tau, J, M_J = J) = \frac{1}{2} q_{J'J} \quad (15.52)$$

where  $|\tau JM_J\rangle$  are the rigid rotor basis functions (e.g., the symmetric rotor or asymmetric rotor functions) with  $M_J$  the projection quantum number in the space-fixed frame. It should be noted that in general  $q_{J'J}$  depends on the quantum number  $\tau$ . The Wigner-Eckart theorem yields

$$(\tau' J' J | V_0^{(2)} | \tau J J) = (-1)^{J' - J} \begin{pmatrix} J' & 2 & J \\ -J & 0 & J \end{pmatrix} (\tau' J' || V^{(2)} || \tau J) \quad (15.53)$$

Thus

$$(\tau' J' || V^{(2)} || \tau J) = q_{J'J} f(J') \quad (15.54)$$

where for  $J' \geq J$

$$f(J') = \left[ 2 \begin{pmatrix} J & 2 & J' \\ J & 0 & -J \end{pmatrix} \right]^{-1} \quad (15.55)$$

or explicitly

$$\begin{aligned} f(J') &= \left[ \frac{(2J+1)(2J+2)(2J+3)}{8J(2J-1)} \right]^{1/2} & J' = J, \\ f(J') &= \left[ \frac{(2J+2)(2J+3)(2J+4)}{48J} \right]^{1/2} & J' = J+1, \\ f(J') &= -\left[ \frac{2J(2J+1)(2J+2)}{48(J-1)} \right]^{1/2} & J' = J-1, \\ f(J') &= \left[ \frac{(2J+3)(2J+4)(2J+5)}{48} \right]^{1/2} & J' = J+2, \\ f(J') &= \left[ \frac{2J(2J+1)(2J-1)}{48} \right]^{1/2} & J' = J-2 \end{aligned} \quad (15.56)$$

where for completeness we have also included the case where  $J' < J$  for which  $M'_J = M_J = J'$  in the definition of  $q_{J'J}$ .

In application to specific molecules the quantity  $q_{J'J}$ , which is defined with respect to axes fixed in space, is conveniently re-expressed in terms of the principal inertial axis system ( $x'$ ,  $y'$ ,  $z'$ ) fixed in the molecule, since as previously pointed out, the field gradients with respect to the molecule-fixed axis system are constants independent of the rotational state. We have from the definition of  $q_{J'J}$  and (15.2)

$$\begin{aligned} q_{J'J} &= 2(\tau' J' J | V_0^{(2)} | \tau J J) \\ &= 2 \sum_{q'} (-1)^{-q'} V_{q'}^{(2)} (\tau' J' J | D_{0,-q'}^{(2)} | \tau J J) \end{aligned} \quad (15.57)$$

In the symmetric-top basis we may write from (15.38)

$$\begin{aligned} q_{J'J} &= (-1)^{J-K-q'} [(2J+1)(2J'+1)]^{1/2} \\ &\quad \times \begin{pmatrix} J & 2 & J' \\ J & 0 & -J \end{pmatrix} \begin{pmatrix} J & 2 & J' \\ K & q' & -K' \end{pmatrix} 2V_{q'}^{(2)} \\ &= (-1)^{J-K-q'} [(2J+1)(2J'+1)]^{1/2} [2f(J')]^{-1} \\ &\quad \times \begin{pmatrix} J & 2 & J' \\ K & q' & -K' \end{pmatrix} 2V_{q'}^{(2)} \end{aligned} \quad (15.58)$$

where  $q' = K' - K$ ,  $J' \geq J$ . Note that the latter expression for  $q_{J'J}$  also applies to the case  $J' < J$  with  $f(J')$  as given in (15.56). Usually, the interaction energy is defined as  $\mathbf{V}^{(2)} \cdot \mathbf{Q}^{(2)}$  in spherical tensor notation and as  $\frac{1}{6}\mathbf{V}:\mathbf{Q}$  in the Cartesian notation. For both expressions to be equivalent, a factor of  $6^{-1/2}$  must be included in the definition of the components of  $\mathbf{Q}^{(2)}$  and  $\mathbf{V}^{(2)}$ . The irreducible field gradient tensor components  $V_q^{(2)}$  are thus related to the Cartesian field gradient tensor elements as follows

$$\begin{aligned} 2V_0^{(2)} &= V_{z'z'} \\ 2V_{\pm 1}^{(2)} &= \mp(\sqrt{2}/\sqrt{3})(V_{x'z'} \pm iV_{y'z'}) \\ 2V_{\pm 2}^{(2)} &= 6^{-1/2}(V_{x'x'} - V_{y'y'} \pm 2iV_{x'y'}) \end{aligned} \quad (15.59)$$

In the usual spectroscopic notation, the molecular constants  $eQV_{x'x'}$ , and so on, are the quadrupole coupling constants denoted by  $\chi_{x'x'}$ , and so on.

For a symmetric top with the coupling atom on the symmetry axis, only one of the  $V_q^{(2)}$  is nonvanishing, viz.,  $2V_0^{(2)} = V_{z'z'} = (\partial^2 V / \partial z'^2) \equiv q$ , and the coupling constant for the rotational state  $J, K$  is

$$\begin{aligned} q_{JJ} &= (-1)^{J-K} (2J+1) \begin{pmatrix} J & 2 & J \\ K & 0 & -K \end{pmatrix} \begin{pmatrix} J & 2 & J \\ J & 0 & -J \end{pmatrix} q \\ &= \frac{qJ}{(2J+3)} \left[ \frac{3K^2}{J(J+1)} - 1 \right] \end{aligned} \quad (15.60)$$

which is the usual definition of  $q_{JJ}$  where only diagonal elements in  $J$  are considered, see (9.88). The above is also applicable to a linear rotor where  $K=0$ , and this gives (9.81). For an asymmetric rotor if only diagonal elements in  $J$  are to be considered, it is more convenient to return to the definition of  $q_{JJ}$  and evaluate it in the asymmetric rotor basis as was done in Chapter IX, Section 4. Otherwise, the symmetric top basis may be conveniently employed, and (15.58) applies. Alternately, (15.57) may be evaluated in the asymmetric rotor basis [see also (9.69)].

Usually the interaction energy is sufficiently small that the rotational quantum numbers may be considered good quantum numbers, and only

matrix elements diagonal in  $J$  need be considered. This so-called first-order effect is by far the most important although for quadrupole coupling with nuclei of large  $Q$  second-order effects can be important, as discussed in Chapter IX, Section 6. In what follows, only the matrix elements diagonal in  $J$  will be considered for the magnetic coupling, while for quadrupole coupling general expressions will be given.

For the magnetic spin-rotation interaction we find from (15.21)

$$(\tau JIF|\mathbf{m}^{(1)} \cdot \mu^{(1)}| \tau JIF) = (-1)^{J+I+F} \begin{Bmatrix} F & I & J \\ 1 & J & I \end{Bmatrix} (\tau J|m^{(1)}| \tau J)(I|\mu^{(1)}|I) \quad (15.61)$$

We now consider the evaluation of the reduced matrix element. Conventionally the observable,

$$(I, M_I=I|\mu_z|I, M_I=I)$$

is defined as the magnetic moment,  $g_I \beta_I I$ , and since  $\mu_z \equiv \mu_0^{(1)}$  we have

$$(I, M_I=I|\mu_0^{(1)}|I, M_I=I) = \mu_I = g_I \beta_I I \quad (15.62)$$

where  $\beta_I$  is the nuclear magneton and  $g_I$  is the appropriate nuclear  $g$  factor. For the molecular magnetic field tensor we may employ the following decomposition theorem for first rank tensors [1]

$$(\tau' J'M'|T_q^{(1)}| \tau JM) = \delta_{J'J} \frac{(\tau' J'M'|J_q^{(1)}(\mathbf{J}^{(1)} \cdot \mathbf{T}^{(1)})| \tau JM)}{J(J+1)} \quad (15.63)$$

which relates the matrix elements of  $T_q^{(1)}$  to those of the projection of  $\mathbf{T}^{(1)}$  along the angular momentum  $\mathbf{J}^{(1)}$ . Applying this to  $m_0^{(1)}$  gives

$$\begin{aligned} (\tau JJ|m_0^{(1)}| \tau JJ) &= (\tau JJ|J_0^{(1)}(\mathbf{J}^{(1)} \cdot \mathbf{m}^{(1)})| \tau JJ)/J(J+1) \\ &= \frac{(JJ|J_0^{(1)}|JJ)}{[J(J+1)]^{1/2}} \frac{(\tau JJ|\mathbf{J}^{(1)} \cdot \mathbf{m}^{(1)}| \tau JJ)}{[J(J+1)]^{1/2}} \end{aligned} \quad (15.64)$$

The latter factor may be interpreted as the average magnetic field along  $\mathbf{J}$

$$\langle H_J \rangle = (\tau JJ|\mathbf{J}^{(1)} \cdot \mathbf{m}^{(1)}| \tau JJ)/[J(J+1)]^{1/2} \quad (15.65)$$

and we have

$$(\tau JM_J=J|m_0^{(1)}| \tau JM_J=J) = \{J/[J(J+1)]^{1/2}\} \langle H_J \rangle \quad (15.66)$$

It is recognized that the left-hand side of this equation is the average field in the  $z$  direction, and the above is a relation that is readily derived from the vector model (see Chapter IX, Section 7). The reduced matrix elements can now be found by application of the Wigner-Eckart theorem to (15.62) and (15.66) which yields

$$(I|\mu^{(1)}|I) = g_I \beta_I h(I) \quad (15.67)$$

where

$$h(I) = [I(I+1)(2I+1)]^{1/2} \quad (15.68)$$

and similarly,

$$(\tau J || m^{(1)} || \tau J) = (C_{J,\tau} / g_I \beta_I) h(J) \quad (15.69)$$

where

$$h(J) = [J(J+1)(2J+1)]^{1/2} \quad (15.70)$$

and the spectroscopic constant is defined by

$$C_{J,\tau} = \frac{g_I \beta_I \langle H_J \rangle}{[J(J+1)]^{1/2}} \quad (15.71)$$

Compare this with (9.137) and (9.142). The  $C_{J,\tau}$  depends on the rotational state  $J, \tau$  and is best expressed in terms of the elements of the magnetic coupling tensor with respect to the principal inertial axis system. The derivation now follows closely that discussed in Chapter IX, Section 7. Referring the elements of  $\mathbf{J}^{(1)}$  and  $\mathbf{m}^{(1)}$  to the molecule-fixed  $x'y'z'$  frame, we can write the scalar product in terms of the Cartesian components of the tensors

$$\begin{aligned} \mathbf{J}^{(1)} \cdot \mathbf{m}^{(1)} &= \sum_{q'} (-1)^{q'} J_q'^{(1)} m_{-q'}'^{(1)} \\ &= \sum_g J_g' m_g' \quad (g = x', y', z') \end{aligned} \quad (15.72)$$

For molecules in singlet electronic states the magnetic field arises from the rotation of the molecule and the field components along the molecule-fixed axes may be taken as proportional to the angular velocity, that is,

$$\begin{aligned} m_g' &= (g_I \beta_I)^{-1} \sum_{g'} B_{gg'} \omega_{g'}' \\ &= (g_I \beta_I)^{-1} \sum_{g'} C'_{gg'} J_{g'}' \end{aligned} \quad (15.73)$$

since  $\omega_g' = J_g / I_g$ . Combining this with (15.72) and (15.65) we have (noting that, in general, only the diagonal elements of  $\mathbf{C}$  contribute to the spectrum in first order)

$$C_{J,\tau} = [J(J+1)]^{-1} \sum_g C'_{gg} \langle J_g'^2 \rangle \quad (15.74)$$

where  $J_g'$  are the angular momentum components with respect to the molecule-fixed principal inertial axis system and where the average is taken over the rotational state  $J, \tau$ . The  $C'_{gg'}$  are the coupling constants with respect to the principal axes and are constants independent of the rotational state. This relation agrees with that given previously in (9.143). The quantity  $C_{gg} I_g / g_I = B_{gg}$  is invariant under isotopic substitution.

It is of interest to consider the evaluation of the matrix elements of  $\mathcal{H}_M$  when defined by (15.18). If for simplicity we consider one coupling nuclei, the matrix elements (diagonal in  $J$ ) of the terms in (15.19) are from (15.21):

$$\begin{aligned} (\tau' J I F | [\mathbf{C}^{(l)} \times \mathbf{J}^{(1)}]^{(1)} \cdot \mathbf{I}^{(1)} | \tau J I F) &= (-1)^{J+I+F} \begin{Bmatrix} F & I & J \\ 1 & J & I \end{Bmatrix} \\ &\times (\tau' J | [\mathbf{C}^{(l)} \times \mathbf{J}^{(1)}]^{(1)} | \tau J) (I | I^{(1)} | I) \end{aligned} \quad (15.75)$$

The reduced matrix element  $\langle I|I^{(1)}|I\rangle = [I(I+l)(2I+l)]^{1/2} = h(I)$  is readily obtained from the Wigner-Eckart theorem. The reduced matrix element of the tensor product which involves operators acting on the same subspace is given by (15.25)

$$\langle \tau' J | [\mathbf{C}^{(l)} \times \mathbf{J}^{(1)}]^{(1)} | \tau J \rangle = -\sqrt{3} \begin{Bmatrix} l & 1 & 1 \\ J & J & J \end{Bmatrix} (\tau' J | C^{(l)} | \tau J) (\tau J | J^{(1)} | \tau J) \quad (15.76)$$

As before

$$\begin{aligned} \langle \tau' J' | J^{(1)} | \tau J \rangle &= \delta_{\tau', \tau} \delta_{J', J} [J(J+1)(2J+1)]^{1/2} \\ &= h(J) \end{aligned} \quad (15.77)$$

Collecting terms we have finally

$$\langle \tau' J I F | \mathcal{H}_M | \tau J I F \rangle = (-1)^{J+I+F} h(I) h(J) \begin{Bmatrix} F & I & J \\ 1 & J & I \end{Bmatrix} C_J \quad (15.78)$$

This may be compared to (15.85). Here

$$C_J = -\sqrt{3} \sum_l N_l \begin{Bmatrix} l & 1 & 1 \\ J & J & J \end{Bmatrix} (\tau' J | C^{(l)} | \tau J) \quad (15.79)$$

The  $(\tau' J | C^{(l)} | \tau J)$  are the spectroscopic constants to be evaluated. For a symmetric rotor basis ( $\tau = K$ ) we have

$$\begin{aligned} C_J &= -\sqrt{3}(2J+1) \sum_l (-1)^{J+l-K-q'} \\ &\quad \times \begin{Bmatrix} l & 1 & 1 \\ J & J & J \end{Bmatrix} \begin{pmatrix} J & l & J \\ K & q' & -K' \end{pmatrix} (N_l C'_q)^{(l)} \end{aligned} \quad (15.80)$$

where  $q' = K' - K$  and  $C'_q^{(l)}$  are the components with respect to the molecule-fixed axes and are defined as in (15.17). These are the molecular constants independent of the rotational state. Equation 15.80 is obtained by use of (15.20) to rewrite the reduced matrix element in terms of an ordinary matrix element, followed by transformation of the  $\mathbf{C}^{(l)}$  to principal axes by (15.1), and finally evaluation of the matrix elements in the  $JKM$  basis by (15.38). For a symmetric top with coupling atom on the symmetry axis ( $z'$ ) the off-diagonal elements  $C_{x'y'}$ , and so on, vanish and  $C_{x'x'} = C_{y'y'}$ . Thus the nonvanishing elements are

$$N_0 C'_0^{(0)} = \frac{1}{3} (C_{zz'} + 2C_{x'x'}) \quad (15.81)$$

$$N_2 C'_0^{(2)} = -[(10)^{1/2}/3] (C_{z'z'} - C_{x'x'}) \quad (15.82)$$

and hence in (15.80)  $q' = 0$ ,  $K' = K$ . Evaluating (15.80) we find

$$C_J = C_{x'x'} + (C_{z'z'} - C_{x'x'}) [K^2/J(J+1)] \quad (15.83)$$

which is equivalent to (9.158).

If the previous definition of the reduced matrix elements (15.49) and (15.54)

are substituted into (15.46), the matrix element for the electric quadrupole interaction is

$$\langle \tau' J' IF | \mathbf{V}^{(2)} \cdot \mathbf{Q}^{(2)} | \tau J IF \rangle = (-1)^t (eQq_{J,J'}) f(J') f(I) \begin{Bmatrix} F & I & J' \\ 2 & J & I \end{Bmatrix} \quad (15.84)$$

where  $t = J + I + F$ , and where  $(eQq_{J,J'})$  is the quadrupole coupling constant for the rotational state  $J\tau$ . The quantities  $f(J')$  and  $f(I)$  are specified by (15.56) and (15.50), respectively. For the magnetic interaction (15.61), (15.67), and (15.69) yield

$$\langle \tau J IF | \mathbf{m}^{(1)} \cdot \boldsymbol{\mu}^{(1)} | \tau J' IF \rangle = (-1)^r (C_{J,\tau}) h(J) h(I) \begin{Bmatrix} F & I & J \\ 1 & J & I \end{Bmatrix} \quad (15.85)$$

where  $r = J + I + F$ , and  $h(J)$  and  $h(I)$  are specified by (15.70) and (15.68), respectively. Equations (15.84) and (15.85) yield the usual results for the energy levels ( $J = J'$ ) with replacement of the  $6j$  symbol by its algebraic equivalent. See Table 15.1. In general, once a particular value of  $J$ ,  $I$  and  $F$  is specified, the  $6j$  symbol may be evaluated and hence the corresponding matrix element. This form is particularly convenient because of the ease with which the  $6j$  and  $3j$  symbols may be evaluated by machine computation.

### 3 PLURAL, UNEQUAL COUPLING

We now consider explicitly the derivation of the matrix elements for the case of plural nuclear coupling. For  $N$  nuclei with spins  $I_1, I_2, \dots, I_L, \dots, I_N$  and different coupling energies, it is convenient to employ the coupling scheme

$$\begin{aligned} \mathbf{J} + \mathbf{I}_1 &= \mathbf{F}_1 \\ \mathbf{F}_1 + \mathbf{I}_2 &= \mathbf{F}_2 \\ &\vdots \\ \mathbf{F}_{L-1} + \mathbf{I}_L &= \mathbf{F}_L \\ &\vdots \\ \mathbf{F}_{N-1} + \mathbf{I}_N &= \mathbf{F}_N \equiv \mathbf{F} \end{aligned} \quad (15.86)$$

where  $\mathbf{J}$  is the rotational angular momentum and where the nuclear spins are coupled in order of decreasing coupling energy. The basis functions for this coupling scheme are denoted by

$$|\tau J I_1 F_1 \dots I_L F_L \dots I_N F_N M_F\rangle$$

where  $\tau$  represents any additional quantum numbers, besides the rotational momentum quantum numbers  $J$  and  $M_J$ , that are necessary to specify the unperturbed rotational state. To be specific, we consider the case of three coupling nuclei. The Hamiltonian is

$$\mathcal{H}_{hfs} = \sum_{i=1}^3 \mathbf{V}(i) \cdot \mathbf{Q}(i) + \sum_{i=1}^3 \mathbf{m}(i) \cdot \boldsymbol{\mu}(i) \quad (15.87)$$

Hereafter the explicit rank designation will be omitted. As indicated by the

foregoing equation, the matrix elements of  $\mathcal{H}_{hfs}$  will be composed of a sum of contributions from nucleus 1, 2, and 3.

We wish to show first that the electric or magnetic interaction for the  $L$ th nucleus does not depend on the quantum numbers  $I_{L+1}F_{L+1}\dots F_N$  for the coupling scheme of (15.86). For convenience we consider the case of two nuclei. For nucleus 1 we have the following matrix element to evaluate:

$$(\tau' J'I_1F'_1I_2F'M'_F|\mathcal{H}(1)|\tau JI_1F_1I_2FM_F)$$

where  $\mathcal{H}(1)$  designates, for example, the electric quadrupole or magnetic dipole interaction for nucleus 1. Applying the Wigner-Eckart theorem we have

$$\begin{aligned} (\tau' J'I_1F'_1I_2F'M'_F|\mathcal{H}(1)|\tau JI_1F_1I_2FM_F) &= \delta_{M_F M_{F'}} \delta_{FF'} (2F+1)^{-1/2} \\ &\times (\tau' J'I_1F'_1I_2F'|\mathcal{H}(1)||\tau JI_1F_1I_2F) \end{aligned} \quad (15.88)$$

where the  $3j$  symbol has been evaluated noting that  $\mathcal{H}(1)$  is a scalar and hence  $k=q=0$ . The reduced matrix element may be reduced by use of (15.22) since  $\mathcal{H}(1)$  does not operate on  $I_2$ :

$$\begin{aligned} &(\tau' J'I_1F'_1I_2F|\mathcal{H}(1)||\tau JI_1F_1I_2F) \\ &= \delta_{F_1 F'} (2F+1)[(2F+1)(2F_1+1)]^{-1/2} (\tau' J'I_1F'_1|\mathcal{H}(1)||\tau JI_1F_1) \\ &= \delta_{F_1 F'} \delta_{M_{F_1} M_{F'}} (2F+1)^{1/2} (\tau' J'I_1F'_1M_{F'}|\mathcal{H}(1)|J_I_1F_1M_{F_1}) \end{aligned} \quad (15.89)$$

where we again employ the Wigner-Eckart theorem. Therefore we may write

$$\begin{aligned} (\tau' J'I_1F'_1I_2F'M'_F|\mathcal{H}(1)|\tau JI_1F_1I_2FM_F) &= \delta_{M_F M_{F'}} \delta_{FF'} \delta_{F_1 F'} \delta_{M_{F_1} M_{F_1}} \\ &\times (\tau' J'I_1F'_1M_{F_1}|\mathcal{H}(1)||\tau JI_1F_1M_{F_1}) \end{aligned} \quad (15.90)$$

which shows the matrix elements of  $\mathcal{H}(1)$  depend only on the quantum numbers  $\tau JI_1F_1$ . In general, the matrix elements of  $\mathcal{H}(L)$  are diagonal in all quantum numbers  $F_L I_{L+1} \dots F_N$  and depend only on the quantum numbers  $\tau JI_1F_1 \dots F_L$ . Thus for nucleus 1 we have already discussed the matrix elements; from (15.84) with the appropriate change in notation we have

$$(\tau' J'I_1F_1|\mathbf{V}(1)\cdot\mathbf{Q}(1)|\tau JI_1F_1) = (-1)^{t_1} (eQq_{J'J})_1 f(J') f(I_1) \begin{Bmatrix} F_1 & I_1 & J' \\ 2 & J & I_1 \end{Bmatrix} \quad (15.91)$$

where  $t_1 = J + I_1 + F_1$ , and where  $(eQq_{J'J})_1$  refers to nucleus 1. The quantities  $f(J')$  and  $f(I_1)$  are specified by (15.56) and (15.50), respectively.

For the quadrupole coupling of nucleus 2, (15.21) yields, with  $J \equiv F_2$ ,  $j_2 \equiv I_2$ ,  $j_1 \equiv F_1$ , and  $\tau_1 \equiv \tau JI_1$ ,

$$(\tau' J'I_1F'_1I_2F_2|\mathbf{V}(2)\cdot\mathbf{Q}(2)|\tau JI_1F_1I_2F_2)$$

$$= (-1)^{F_1 + I_2 + F_2} \begin{Bmatrix} F_2 & I_2 & F'_1 \\ 2 & F_1 & I_2 \end{Bmatrix} (\tau' J'I_1F'_1|\mathcal{V}(2)||\tau JI_1F_1)(I_2||Q(2)||I_2) \quad (15.92)$$

The reduced matrix element of the field gradient of nucleus 2 may be reduced to the desired form by application of (15.22) since  $\mathbf{V}(2)$  commutes with  $\mathbf{I}_1$ . This gives

$$(\tau' J' I_1 F'_1 \| V(2) \| \tau J I_1 F_1) = (-1)^{J' + I_1 + F_1} [(2F_1 + 1)(2F'_1 + 1)]^{1/2} \times \begin{Bmatrix} J' & F'_1 & I_1 \\ F_1 & J & 2 \end{Bmatrix} (\tau' J' \| V(2) \| \tau J) \quad (15.93)$$

The contribution that the rank ( $k$ ) makes to the phase factor in (15.22) or (15.23) can obviously be omitted when the rank is even. The reduced matrix element on the right-hand side of this equation is given by (15.54). Therefore, taking cognizance of (15.49), (15.54), and (15.93), we may write for (15.92) for nucleus 2

$$(\tau' J' I_1 F'_1 I_2 F_2 | \mathbf{V}(2) \cdot \mathbf{Q}(2) | \tau J I_1 F_1 I_2 F_2) = (-1)^{t_2} (eQq_{J'J})_2 f(J') f(I_2) [(2F_1 + 1)(2F'_1 + 1)]^{1/2} \begin{Bmatrix} J' & F'_1 & I_1 \\ F_1 & J & 2 \end{Bmatrix} \begin{Bmatrix} F_2 & I_2 & F'_1 \\ 2 & F_1 & I_2 \end{Bmatrix} \quad (15.94)$$

$$\text{where } t_2 = J' + I_1 + I_2 + 2F_1 + F_2.$$

If there were only two coupling nuclei involved, one would stop here, and  $F_2$  would be replaced by  $F$ .

For the quadrupole coupling of nucleus 3, (15.21) yields

$$(\tau' J' I_1 F'_1 I_2 F'_2 I_3 F_3 | \mathbf{V}(3) \cdot \mathbf{Q}(3) | \tau J I_1 F_1 I_2 F_2 I_3 F_3) = (-1)^{F_2 + I_3 + F_3} \begin{Bmatrix} F_3 & I_3 & F'_2 \\ 2 & F_2 & I_3 \end{Bmatrix} (\tau' J' I_1 F'_1 I_2 F'_2 \| V(3) \| \tau J I_1 F_1 I_2 F_2) (I_3 \| Q(3) \| I_3) \quad (15.95)$$

Successive application of (15.22) yields for the reduced matrix elements

$$(\tau' J' I_1 F'_1 I_2 F'_2 \| V(3) \| \tau J I_1 F_1 I_2 F_2) = (-1)^{F'_1 + I_2 + F_2} \times [(2F_2 + 1)(2F'_2 + 1)]^{1/2} \begin{Bmatrix} F'_1 & F'_2 & I_2 \\ F_2 & F_1 & 2 \end{Bmatrix} (\tau' J' I_1 F'_1 \| V(3) \| \tau J I_1 F_1) \quad (15.96)$$

and

$$(\tau' J' I_1 F'_1 \| V(3) \| \tau J I_1 F_1) = (-1)^{J' + I_1 + F_1} [(2F_1 + 1)(2F'_1 + 1)]^{1/2} \times \begin{Bmatrix} J' & F'_1 & I_1 \\ F_1 & J & 2 \end{Bmatrix} (\tau' J' \| V(3) \| \tau J) \quad (15.97)$$

Combination of (15.95)–(15.97) and the definitions of the reduced matrix elements gives for the matrix elements

$$(\tau' J' I_1 F'_1 I_2 F'_2 I_3 F_3 | \mathbf{V}(3) \cdot \mathbf{Q}(3) | \tau J I_1 F_1 I_2 F_2 I_3 F_3) = (-1)^{t_3} (eQq_{J'J})_3 f(J') f(I_3) [(2F_1 + 1)(2F'_1 + 1)(2F_2 + 1)(2F'_2 + 1)]^{1/2} \times \begin{Bmatrix} J' & F'_1 & I_1 \\ F_1 & J & 2 \end{Bmatrix} \begin{Bmatrix} F'_1 & F'_2 & I_2 \\ F_2 & F_1 & 2 \end{Bmatrix} \begin{Bmatrix} F_3 & I_3 & F'_2 \\ 2 & F_2 & I_3 \end{Bmatrix} \quad (15.98)$$

$$\text{where } t_3 = J' + I_1 + I_2 + I_3 + F_1 + F'_1 + 2F_2 + F_3.$$

A similar procedure for the magnetic dipole interaction operator yields the

following matrix elements for the three coupling nuclei.

$$(\tau J I_1 F_1 | \mathbf{m}(1) \cdot \mu(1) | \tau J I_1 F_1) = (-1)^{r_1} (C_{J,\tau})_1 h(J) h(I_1) \begin{Bmatrix} F_1 & I_1 & J \\ 1 & J & I_1 \end{Bmatrix} \quad (15.99)$$

$$(\tau J I_1 F'_1 I_2 F_2 | \mathbf{m}(2) \cdot \mu(2) | \tau J I_1 F_1 I_2 F_2) = (-1)^{r_2} (C_{J,\tau})_2$$

$$\times h(J) h(I_2) [(2F_1 + 1)(2F'_1 + 1)]^{1/2} \begin{Bmatrix} J & F'_1 & I_1 \\ F_1 & J & 1 \end{Bmatrix} \begin{Bmatrix} F_2 & I_2 & F'_1 \\ 1 & F_1 & I_2 \end{Bmatrix} \quad (15.100)$$

$$(\tau J I_1 F'_1 I_2 F'_2 I_3 F_3 | \mathbf{m}(3) \cdot \mu(3) | \tau J I_1 F_1 I_2 F_2 I_3 F_3) = (-1)^{r_3} (C_{J,\tau})_3$$

$$\times h(J) h(I_3) [(2F_1 + 1)(2F'_1 + 1)(2F_2 + 1)(2F'_2 + 1)]^{1/2}$$

$$\times \begin{Bmatrix} J & F'_1 & I_1 \\ F_1 & J & 1 \end{Bmatrix} \begin{Bmatrix} F'_1 & F'_2 & I_2 \\ F_2 & F_1 & 1 \end{Bmatrix} \begin{Bmatrix} F_3 & I_3 & F'_2 \\ 1 & F_2 & I_3 \end{Bmatrix} \quad (15.101)$$

where  $r_1 = J + I_1 + F_1$ ,  $r_2 = J + I_1 + I_2 + 2F_1 + F_2 + 1$ ,  $r_3 = J + I_1 + I_2 + I_3 + F_1 + F'_1 + 2F_2 + F_3$ , and where  $h(J)$  and  $h(I_i)$  are specified by (15.70) and (15.68), respectively. If two coupling nuclei are present, (15.99) and (15.100) apply, with  $F_2$  replaced by  $F$ .

The procedure just outlined may obviously be extended to any number of nuclei. The matrix elements of the electric quadrupole interaction for the  $L$ th nucleus may be written in the form [5]

$$\begin{aligned} & (\tau' F'_0 F'_1 \dots F'_{L-1} F_L | \mathbf{V}(L) \cdot \mathbf{Q}(L) | \tau F_0 F_1 \dots F_{L-1} F_L) \\ &= (-1)^t (e Q q_{J,J'})_L f(J') f(I_L) \begin{Bmatrix} F_L & I_L & F'_{L-1} \\ 2 & F_{L-1} & I_L \end{Bmatrix} \\ & \times \prod_{i=1}^{L-1} [(2F_i + 1)(2F'_i + 1)]^{1/2} \begin{Bmatrix} F'_{i-1} & F'_i & I_i \\ F_i & F_{i-1} & 2 \end{Bmatrix} \end{aligned} \quad (15.102)$$

where the phase factor is determined by

$$t = \sum_{i=1}^{L-1} (F'_{i-1} + I_i + F_i) + (F_{L-1} + I_L + F_L)$$

and  $F_0 = J$ ,  $F'_0 = J'$ , and  $F_N = F$ . As before,  $f(J')$  is given by (15.56) where the expression to be used depends on the value of  $J'$ . Likewise,  $f(I_L)$  is given by (15.50) where the spin of the  $L$ th nucleus is to be substituted.

The matrix elements of the magnetic dipole interaction may be written as [5]

$$\begin{aligned} & (\tau F'_0 F'_1 \dots F'_{L-1} F_L | \mathbf{m}(L) \cdot \mu(L) | \tau F_0 F_1 \dots F_{L-1} F_L) \\ &= (-1)^r (C_{J,\tau})_L h(J) h(I_L) \begin{Bmatrix} F_L & I_L & F'_{L-1} \\ 1 & F_{L-1} & I_L \end{Bmatrix} \\ & \times \prod_{i=1}^{L-1} [(2F_i + 1)(2F'_i + 1)]^{1/2} \begin{Bmatrix} F'_{i-1} & F'_i & I_i \\ F_i & F_{i-1} & 1 \end{Bmatrix} \end{aligned} \quad (15.103)$$

where the phase factor is determined by

$$r = (L-1) + \sum_{i=1}^{L+1} (F'_{i-1} + I_i + F_i) + (F_{L-1} + I_L + F_L)$$

and  $F_0 = F'_0 = J$ , and  $F_N = F$ . The factors  $h(J)$  and  $h(I_L)$  are given, respectively, by (15.70) and (15.68). For both (15.102) and (15.103) in the special case of  $L=1$ , the product  $\prod [ ]^{1/2} \{ \}$  is set equal to one. The diagonal elements yield the hyperfine energy levels to a first-order approximation. Exact energy levels are obtained by construction of the hyperfine energy matrix, which may be factored into blocks of different  $F$ , and subsequent diagonalization. For asymmetric rotors if the symmetric rotor basis is employed, the complete energy matrix of  $\mathcal{H}_r + \mathcal{H}_{hfs}$  must be considered. This amounts to inclusion of the matrix elements of the rotational Hamiltonian in the symmetric-top basis along with those given for the hyperfine Hamiltonian in the coupled basis. A consistent phase choice for the matrix elements should be employed.

In this regard, the rigid rotor Hamiltonian can be conveniently written as

$$\mathcal{H}_r = \frac{1}{2}(B_{x'} + B_{y'})J(J+1) + [B_{z'} - \frac{1}{2}(B_{x'} + B_{y'})]\{J_0'^2 - b(J_{+1}^2 + J_{-1}^2)\} \quad (15.104)$$

with  $b = (B_{y'} - B_{x'})/(2B_{z'} - B_{x'} - B_{y'})$ .

The study of DC≡CCl by Tack and Kukolich [41] provides a simple example of two nuclei with unequal couplings  $J + I_{Cl} = F_1$ ,  $F_1 + I_D = F$ . All the hyperfine components of the  $J=0 \rightarrow 1$  transition are shown in Fig. 15.1. The

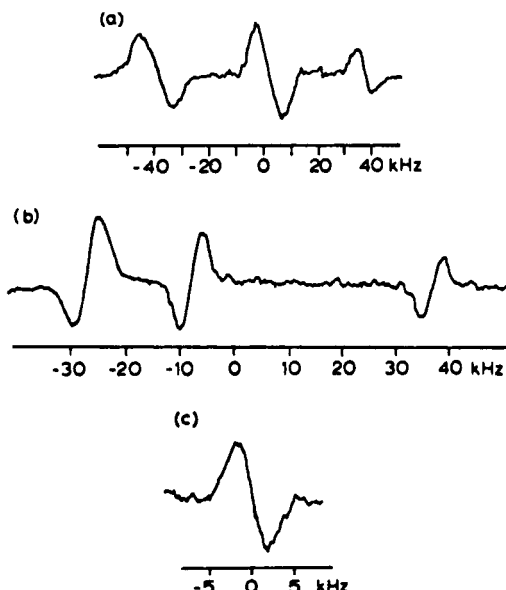


**Fig. 15.1** Molecular beam maser resolution of all hyperfine components of the  $1 \rightarrow 0$  transitions of  $^{35}\text{ClC}\equiv\text{CD}$ . The components are labeled for the  $J=1$  level since all hyperfine matrix elements vanish for  $J=0$  to first order. (a) Recorder tracing of  $F_1 = \frac{3}{2}$  components. Frequencies in kHz relative to 10,358,017 kHz. (b)  $F_1 = \frac{5}{2}$  components. Frequencies relative to 10,377,921 kHz. (c)  $F_1 = \frac{1}{2}$  components. Frequencies relative to 10,393,892 kHz. From Tack and Kukolich [41].

spectrum was analyzed with a hyperfine Hamiltonian consisting of the deuterium quadrupole interaction and chlorine quadrupole and  $^{35}\text{Cl}$  spin-rotation interaction. Second-order quadrupole corrections were calculated for chlorine by perturbation methods (see, e.g., Appendix J) and added to the first-order energies from matrix diagonalization. The coupling constants obtained are:  $eQq(^{35}\text{Cl})=79,739.5(10)$  kHz,  $eQq(\text{D})=202.5(15)$  kHz, and  $C_I(^{35}\text{Cl})=1.3(1)$  kHz.

#### 4 PLURAL, EQUAL, OR NEARLY EQUAL, COUPLING

When the coupling energies are the same or nearly the same, the coupling scheme

$$\begin{aligned} \mathbf{I}_1 + \mathbf{I}_2 &= \mathcal{J}_2 \\ \mathcal{J}_2 + \mathbf{I}_3 &= \mathcal{J}_3 \\ &\vdots \\ \mathcal{J}_{L-1} + \mathbf{I}_L &= \mathcal{J}_L \\ &\vdots \\ \mathcal{J}_{N-1} + \mathbf{I}_N &= \mathcal{J}_N \equiv \mathcal{J} \\ \mathbf{J} + \mathcal{J}_N &= \mathbf{F} \end{aligned} \quad (15.105)$$

is usually employed. This scheme is appropriate in cases such as NaCl where the nuclei have nearly identical quadrupole coupling [13]. It is also particularly convenient when the coupling nuclei are identical and may be exchanged by symmetry operations since some factoring of the energy matrix is then possible.

The basis functions for the foregoing coupling scheme are denoted by

$$|\tau J I_1 I_2 \mathcal{J}_2 \dots I_L \mathcal{J}_L \dots I_N \mathcal{J}_N F M_F\rangle$$

It is convenient for this representation to start with the general  $N$  nucleus problem. From (15.21) with  $\tau_1 \equiv \tau$ ,  $j_1 \equiv J$ ,  $\tau_2 \equiv I_1 I_2 \mathcal{J}_2$ ,  $j_2 \equiv \mathcal{J}_N$  and  $J \equiv F$ , the matrix element for the electric quadrupole interaction of the  $L$ th nucleus is

$$\begin{aligned} & (\tau' J' I_1 I_2 \mathcal{J}'_2 \dots I_L \mathcal{J}'_L \dots I_N \mathcal{J}'_N F | \mathbf{V}(L) \cdot \mathbf{Q}(L) | \tau J I_1 I_2 \mathcal{J}_2 \dots I_L \mathcal{J}_L \dots I_N \mathcal{J}_N F) \\ &= (-1)^{J+\mathcal{J}'_N+F} \begin{Bmatrix} F & \mathcal{J}'_N & J' \\ 2 & J & \mathcal{J}_N \end{Bmatrix} (\tau' J' | V(L) | \tau J) (I_1 I_2 \mathcal{J}'_2 \dots \mathcal{J}'_N | Q(L) | I_1 I_2 \mathcal{J}_2 \dots \mathcal{J}_N) \end{aligned} \quad (15.106)$$

The matrix element for the magnetic dipole interaction of the  $L$ th nucleus can also be written as

$$\begin{aligned} & (\tau J I_1 I_2 \mathcal{J}'_2 \dots I_L \mathcal{J}'_L \dots I_N \mathcal{J}'_N F | \mathbf{m}(L) \cdot \mu(L) | \tau J I_1 I_2 \mathcal{J}_2 \dots I_L \mathcal{J}_L \dots I_N \mathcal{J}_N F) \\ &= (-1)^{J+\mathcal{J}'_N+F} \begin{Bmatrix} F & \mathcal{J}'_N & J \\ 1 & J & \mathcal{J}_N \end{Bmatrix} (\tau J | m(L) | \tau J) (I_1 I_2 \mathcal{J}'_2 \dots \mathcal{J}'_N | \mu(L) | I_1 I_2 \mathcal{J}_2 \dots \mathcal{J}_N) \end{aligned} \quad (15.107)$$

The reduced matrix element of the field tensors which appears in both (15.106)

and (15.107) has been given previously, and the problem reduces to the evaluation of the reduced matrix element of the nuclear quadrupole tensor operator and the reduced matrix element of the magnetic dipole tensor operator. Evaluation of these quantities depends on the number of coupling nuclei in the molecule.

We consider explicitly the case of three coupling nuclei. The reduced matrix element of the nuclear quadrupole tensor operator of nucleus 1,

$$(I_1 I_2 \mathcal{J}'_2 I_3 \mathcal{J}'_3 || Q(1) || I_1 I_2 \mathcal{J}_2 I_3 \mathcal{J}_3)$$

is brought to the desired form by successive application of (15.22), and the matrix elements are found to be given by

$$\begin{aligned} & (\tau' J' I_1 I_2 \mathcal{J}'_2 I_3 \mathcal{J}'_3 F | V(1) \cdot Q(1) | \tau J I_1 I_2 \mathcal{J}_2 I_3 \mathcal{J}_3 F) \\ &= (-1)^{t_1} (eQq_{J'J})_1 f(J') f(I_1) [(2\mathcal{J}_2 + 1)(2\mathcal{J}'_2 + 1)(2\mathcal{J}_3 + 1)(2\mathcal{J}'_3 + 1)]^{1/2} \\ & \quad \times \left\{ \begin{matrix} F & \mathcal{J}'_3 & J' \\ 2 & J & \mathcal{J}_3 \end{matrix} \right\} \left\{ \begin{matrix} \mathcal{J}'_2 & \mathcal{J}'_3 & I_3 \\ \mathcal{J}_3 & \mathcal{J}_2 & 2 \end{matrix} \right\} \left\{ \begin{matrix} I_1 & \mathcal{J}'_2 & I_2 \\ \mathcal{J}_2 & I_1 & 2 \end{matrix} \right\} \end{aligned} \quad (15.108)$$

$$\text{with } t_1 = J + I_1 + I_2 + I_3 + \mathcal{J}_2 + \mathcal{J}'_2 + \mathcal{J}_3 + \mathcal{J}'_3 + F.$$

Similarly, for nucleus 2, successive application of (15.22) and (15.23) bring the reduced matrix element of the quadrupole tensor operator in (15.106) to the desired form. This procedure gives as a final result

$$\begin{aligned} & (\tau' J' I_1 I_2 \mathcal{J}'_2 I_3 \mathcal{J}'_3 F | V(2) \cdot Q(2) | \tau J I_1 I_2 \mathcal{J}_2 I_3 \mathcal{J}_3 F) \\ &= (-1)^{t_2} (eQq_{J'J})_2 f(J') f(I_2) [(2\mathcal{J}_2 + 1)(2\mathcal{J}'_2 + 1)(2\mathcal{J}_3 + 1)(2\mathcal{J}'_3 + 1)]^{1/2} \\ & \quad \times \left\{ \begin{matrix} F & \mathcal{J}'_3 & J' \\ 2 & J & \mathcal{J}_3 \end{matrix} \right\} \left\{ \begin{matrix} \mathcal{J}'_2 & \mathcal{J}'_3 & I_3 \\ \mathcal{J}_3 & \mathcal{J}_2 & 2 \end{matrix} \right\} \left\{ \begin{matrix} I_2 & \mathcal{J}'_2 & I_1 \\ \mathcal{J}_2 & I_2 & 2 \end{matrix} \right\} \end{aligned} \quad (15.109)$$

$$\text{with } t_2 = J + I_1 + I_2 + I_3 + 2\mathcal{J}'_2 + \mathcal{J}_3 + \mathcal{J}'_3 + F.$$

In the case of nucleus 3, (15.23) is used because  $\mathcal{J}_2$  commutes with  $Q(3)$ . This yields specifically

$$\begin{aligned} & (I_1 I_2 \mathcal{J}_2 I_3 \mathcal{J}'_3 || Q(3) || I_1 I_2 \mathcal{J}_2 I_3 \mathcal{J}_3) = (-1)^{\mathcal{J}_2 + I_3 + \mathcal{J}'_3} \\ & \quad \times [(2\mathcal{J}_3 + 1)(2\mathcal{J}'_3 + 1)]^{1/2} \left\{ \begin{matrix} I_3 & \mathcal{J}'_3 & \mathcal{J}_2 \\ \mathcal{J}_3 & I_3 & 2 \end{matrix} \right\} (I_3 || Q(3) || I_3) \end{aligned} \quad (15.110)$$

Therefore, from (15.106)

$$\begin{aligned} & (\tau' J' I_1 I_2 \mathcal{J}_2 I_3 \mathcal{J}'_3 F | V(3) \cdot Q(3) | \tau J I_1 I_2 \mathcal{J}_2 I_3 \mathcal{J}_3 F) = (-1)^{t_3} (eQq_{J'J})_3 f(J') f(I_3) \\ & \quad \times [(2\mathcal{J}_3 + 1)(2\mathcal{J}'_3 + 1)]^{1/2} \left\{ \begin{matrix} F & \mathcal{J}'_3 & J' \\ 2 & J & \mathcal{J}_3 \end{matrix} \right\} \left\{ \begin{matrix} I_3 & \mathcal{J}'_3 & \mathcal{J}_2 \\ \mathcal{J}_3 & I_3 & 2 \end{matrix} \right\} \end{aligned} \quad (15.111)$$

with  $t_3 = J + I_3 + \mathcal{J}_2 + 2\mathcal{J}'_3 + F$ . Note that the matrix elements are diagonal in  $\mathcal{J}_2$ , as follows from (15.110), in contrast to the results for nucleus 1 and 2.

The matrix elements for the magnetic dipole interactions are summarized below

$$\begin{aligned}
 & (\tau J I_1 I_2 \mathcal{J}'_2 I_3 \mathcal{J}'_3 F | \mathbf{m}(1) \cdot \mu(1) | \tau J I_1 I_2 \mathcal{J}_2 I_3 \mathcal{J}_3 F) \\
 & = (-1)^{r_1} (C_{J,\tau})_1 h(J) h(I_1) [(2\mathcal{J}_2 + 1)(2\mathcal{J}'_2 + 1)(2\mathcal{J}_3 + 1)(2\mathcal{J}'_3 + 1)]^{1/2} \\
 & \quad \times \left\{ \begin{matrix} F & \mathcal{J}'_3 & J \\ 1 & J & \mathcal{J}_3 \end{matrix} \right\} \left\{ \begin{matrix} \mathcal{J}'_2 & \mathcal{J}'_3 & I_3 \\ \mathcal{J}_3 & \mathcal{J}_2 & 1 \end{matrix} \right\} \left\{ \begin{matrix} I_1 & \mathcal{J}'_2 & I_2 \\ \mathcal{J}_2 & I_1 & 1 \end{matrix} \right\} \quad (15.112)
 \end{aligned}$$

with  $r_1 = J + I_1 + I_2 + I_3 + \mathcal{J}_2 + \mathcal{J}'_2 + \mathcal{J}_3 + \mathcal{J}'_3 + F$ , and

$$\begin{aligned}
 & (\tau J I_1 I_2 \mathcal{J}'_2 I_3 \mathcal{J}'_3 F | \mathbf{m}(2) \cdot \mu(2) | \tau J I_1 I_2 \mathcal{J}_2 I_3 \mathcal{J}_3 F) \\
 & = (-1)^{r_2} (C_{J,\tau})_2 h(J) h(I_2) [(2\mathcal{J}_2 + 1)(2\mathcal{J}'_2 + 1)(2\mathcal{J}_3 + 1)(2\mathcal{J}'_3 + 1)]^{1/2} \\
 & \quad \times \left\{ \begin{matrix} F & \mathcal{J}'_3 & J \\ 1 & J & \mathcal{J}_3 \end{matrix} \right\} \left\{ \begin{matrix} \mathcal{J}'_2 & \mathcal{J}'_3 & I_3 \\ \mathcal{J}_3 & \mathcal{J}_2 & 1 \end{matrix} \right\} \left\{ \begin{matrix} I_2 & \mathcal{J}'_2 & I_1 \\ \mathcal{J}_2 & I_2 & 1 \end{matrix} \right\} \quad (15.113)
 \end{aligned}$$

with  $r_2 = J + I_1 + I_2 + I_3 + 2\mathcal{J}'_2 + \mathcal{J}_3 + \mathcal{J}'_3 + F$ , and

$$\begin{aligned}
 & (\tau J I_1 I_2 \mathcal{J}_2 I_3 \mathcal{J}'_3 F | \mathbf{m}(3) \cdot \mu(3) | \tau J I_1 I_2 \mathcal{J}_2 I_3 \mathcal{J}_3 F) = (-1)^{r_3} (C_{J,\tau})_3 h(J) h(I_3) \\
 & \quad \times [(2\mathcal{J}_3 + 1)(2\mathcal{J}'_3 + 1)]^{1/2} \left\{ \begin{matrix} F & \mathcal{J}'_3 & J \\ 1 & J & \mathcal{J}_3 \end{matrix} \right\} \left\{ \begin{matrix} I_3 & \mathcal{J}'_3 & \mathcal{J}_2 \\ \mathcal{J}_3 & I_3 & 1 \end{matrix} \right\} \quad (15.114)
 \end{aligned}$$

with  $r_3 = J + I_3 + \mathcal{J}_2 + 2\mathcal{J}'_3 + F + 1$ .

Generalizing the preceding discussion to the case of  $N$  coupling nuclei ( $N > 1$ ), we have for the matrix elements of the quadrupole interaction for the  $L$ th coupling nucleus [5]

$$\begin{aligned}
 & (\tau' J' I_1 I_2 \mathcal{J}_2 \dots I_L \mathcal{J}'_L \dots I_N \mathcal{J}'_N F | \mathbf{V}(L) \cdot \mathbf{Q}(L) | \tau J I_1 I_2 \mathcal{J}_2 \dots I_L \mathcal{J}_L \dots I_N \mathcal{J}_N F) \\
 & = (-1)^t (e Q q_{J,J'})_L f(J') f(I_L) \left\{ \begin{matrix} F & \mathcal{J}'_N & J' \\ 2 & J & \mathcal{J}_N \end{matrix} \right\} \left[ [(2\mathcal{J}_L + 1)(2\mathcal{J}'_L + 1)]^{1/2} \right. \\
 & \quad \times \left. \left\{ \begin{matrix} I_L & \mathcal{J}'_L & \mathcal{J}_{L-1} \\ \mathcal{J}_L & I_L & 2 \end{matrix} \right\} \right] \\
 & \quad \times \prod_{i=L}^{N-1} [(2\mathcal{J}_{i+1} + 1)(2\mathcal{J}'_{i+1} + 1)]^{1/2} \left\{ \begin{matrix} \mathcal{J}'_i & \mathcal{J}'_{i+1} & I_{i+1} \\ \mathcal{J}_{i+1} & \mathcal{J}_i & 2 \end{matrix} \right\} \quad (15.115)
 \end{aligned}$$

where the phase factor is determined by

$$t = J + F + I_N + \mathcal{J}_{L-1} + \prod_{i=L}^{N-1} (I_i + \mathcal{J}_{i+1} + \mathcal{J}'_{i+1}) + 2\mathcal{J}'_L$$

and for the magnetic interaction [5]

$$\begin{aligned}
 & (\tau J I_1 I_2 \mathcal{J}_2 \dots I_L \mathcal{J}'_L \dots I_N \mathcal{J}'_N F | \mathbf{m}(L) \cdot \mu(L) | \tau J I_1 I_2 \mathcal{J}_2 \dots I_L \mathcal{J}_L \dots I_N \mathcal{J}_N F) \\
 & = (-1)^r (C_{J,\tau})_L h(J) h(I_L) \left\{ \begin{matrix} F & \mathcal{J}'_N & J \\ 1 & J & \mathcal{J}_N \end{matrix} \right\} \left[ [(2\mathcal{J}_L + 1)(2\mathcal{J}'_L + 1)]^{1/2} \right. \\
 & \quad \times \left. \left\{ \begin{matrix} I_L & \mathcal{J}'_L & \mathcal{J}_{L-1} \\ \mathcal{J}_L & I_L & 1 \end{matrix} \right\} \right] \\
 & \quad \times \prod_{i=L}^{N-1} [(2\mathcal{J}_{i+1} + 1)(2\mathcal{J}'_{i+1} + 1)]^{1/2} \left\{ \begin{matrix} \mathcal{J}'_i & \mathcal{J}'_{i+1} & I_{i+1} \\ \mathcal{J}_{i+1} & \mathcal{J}_i & 1 \end{matrix} \right\} \quad (15.116)
 \end{aligned}$$

where

$$r = J + F + I_N + \mathcal{J}_{L-1} + \sum_{i=L}^{N-1} (1 + I_i + \mathcal{J}_{i+1} + \mathcal{J}'_{i+1}) + (2\mathcal{J}'_L + 1)$$

In the foregoing expressions  $\mathcal{J}_0 = 0$ ,  $\mathcal{J}_1 = \mathcal{J}'_1 = I_1$ ,  $\mathcal{J}_N = \mathcal{J}$ . For the product factor in (15.115) and (15.116), if the upper product limit is less than the initial value of  $i$ , this factor is to be set equal to one. Likewise the summation term in the expressions for  $t$  and  $r$  is to be set equal to zero if the above condition holds. When  $L = 1$ , the factors in large square brackets in (15.115) and (15.116) are to be set equal to one; the last term  $(2\mathcal{J}'_L)$  in the expression for  $t$  and the last  $r(2\mathcal{J}'_L + 1)$  in that for  $r$  is to be set equal to zero. Note that the matrix elements for a given  $L$  (except  $L = 1, 2$ ) are diagonal in all  $\mathcal{J}$ 's below  $\mathcal{J}_L$  in the coupling sequence [see (15.105)]. Usually only diagonal elements in  $J$  need be considered. Each state may be specified by a given value of  $J$  and  $F$ . Off-diagonal elements can occur for the intermediate quantum numbers  $\mathcal{J}_i$ , and these intermediate quantum numbers can be used to further classify the levels.

The complexity introduced with plural nuclear quadrupole coupling may be illustrated by cyanogen azide ( $N_3CN$ ) with four coupling nuclei, studied by Blackman et al. [22]. The computed and experimental line shapes are shown in Fig. 15.2 for the  $1_{11} \rightarrow 2_{12}$  transition. This transition has 864 hyperfine components. It is difficult to unambiguously assign coupling constants to particular nitrogen atoms in the azide groups. Solution of this problem, as well as considerable simplification on the spectrum, can be obtained, however, by study of  $^{15}N$  isotopically substituted species of cyanogen azide.

Some of the simplification possible when there are identical nuclei in the molecule may be illustrated by specialization of the general expression (15.115) to two coupling nuclei. In particular, for the quadrupole interaction we find

$$(\tau' J' I_1 I_2 \mathcal{J}' F | \mathbf{V}(1) \cdot \mathbf{Q}(1) | \tau J I_1 I_2 \mathcal{J} F) = (-1)^{t_1} (eQq_{J'J})_1 \\ \times f(J')f(I_1)[(2\mathcal{J} + 1)(2\mathcal{J}' + 1)]^{1/2} \begin{Bmatrix} F & \mathcal{J}' & J' \\ 2 & J & \mathcal{J} \end{Bmatrix} \begin{Bmatrix} I_1 & \mathcal{J}' & I_2 \\ \mathcal{J} & I_1 & 2 \end{Bmatrix} \quad (15.117)$$

with  $t_1 = J + I_1 + I_2 + \mathcal{J}' + \mathcal{J} + F$ , and

$$(\tau' J' I_1 I_2 \mathcal{J}' F | \mathbf{V}(2) \cdot \mathbf{Q}(2) | \tau J I_1 I_2 \mathcal{J} F) = (-1)^{t_2} (eQq_{J'J})_2 \\ \times f(J')f(I_2)[(2\mathcal{J} + 1)(2\mathcal{J}' + 1)]^{1/2} \begin{Bmatrix} F & \mathcal{J}' & J' \\ 2 & J & \mathcal{J} \end{Bmatrix} \begin{Bmatrix} I_2 & \mathcal{J}' & I_1 \\ \mathcal{J} & I_2 & 2 \end{Bmatrix} \quad (15.118)$$

with  $t_2 = J + I_1 + I_2 + 2\mathcal{J}' + F$ . Here,  $\mathbf{I}_1 + \mathbf{I}_2 = \mathbf{J}$ ,  $\mathbf{J} + \mathbf{J}' = \mathbf{F}$ .

A study, for example, of (15.117) and (15.118) readily yields an interesting and well-known result when  $I_1 = I_2$  and  $(eQq_{J'J})_1 = (eQq_{J'J})_2$ . Adding the contributions of nucleus 1 and 2, one finds that the elements of the quadrupole coupling matrix may be written as a factor times  $[(-1)^{\mathcal{J}'} + (-1)^{\mathcal{J}}]$ . Hence, it follows that matrix elements of the type  $(\mathcal{J} \pm 1|\mathcal{J})$  vanish, while those of the type  $(\mathcal{J}|\mathcal{J})$  and  $(\mathcal{J} \pm 2|\mathcal{J})$  are nonvanishing, and the matrices for a given  $F$  thus separate into two submatrices of even and odd  $\mathcal{J}$ . This is virtually true for

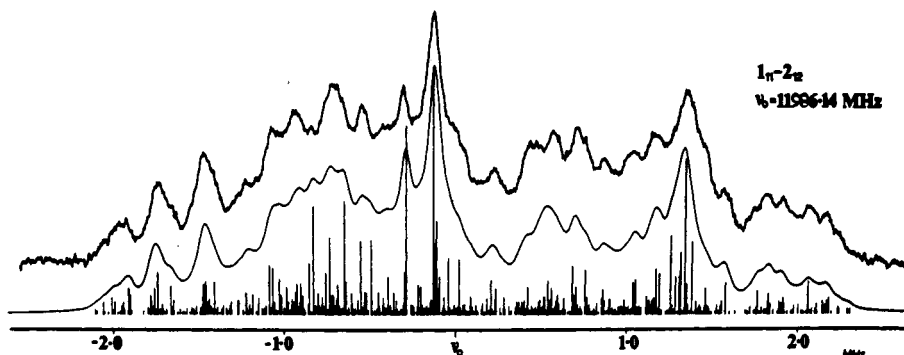


**Fig. 15.2** Comparison of experimental and computed line shape for the  $1_{11} \rightarrow 2_{12}$  transition of cyanogen azide. The quadrupole coupling constants were obtained by comparing the experimental spectral traces with computer simulated traces. The coupling constants found are:  $x_{aa}(1) = 4.82$ ,  $x_{bb}(1) = -0.70$ ;  $x_{aa}(2) = -0.85$ ,  $x_{bb}(2) = 0.70$ ;  $x_{aa}(3) = -0.75$ ,  $x_{bb}(3) = 1.55$ ;  $x_{aa}(4) = -2.27$ ,  $x_{bb}(4) = 1.15$ , where the atom designations indicate the nitrogen position [N(3)-N(2)-N(1)-CN(4)]. From Blackman et al. [22].

NaCl [13] with nonequivalent coupling nuclei and is the case for molecules such as  $\text{COCl}_2$ ,  $\text{D}_2\text{S}$ , where two identical quadrupolar nuclei are involved which occupy identical molecular sites. For a given  $J$ , the submatrices are conveniently grouped into matrices for a given  $F$  with elements within a submatrix labeled by values of  $\mathcal{I}$ . For the case of  $\text{COCl}_2$  ( $I_1 = I_2 = \frac{3}{2}$ ) the possible values of the quantum numbers are:  $\mathcal{I} = 0$ ,  $F = J$ ;  $\mathcal{I} = 1$ ,  $F = J$ ,  $J \pm 1$ ;  $\mathcal{I} = 2$ ,  $F = J$ ,  $J \pm 1$ ,  $J \pm 2$ ;  $\mathcal{I} = 3$ ,  $F = J$ ,  $J \pm 1$ ,  $J \pm 2$ ,  $J \pm 3$ . There are thus seven submatrices (without factoring) corresponding to the various values of  $F$ . Symmetry considerations provide further restrictions, and only certain values of  $\mathcal{I}$  are allowed for a given rotational state  $J_{K_{-1}, K_1}$ . For  $\text{COCl}_2$ , where the rotation  $C_2^b$  interchanges identical chlorine nuclei (Fermions), the total wave function must be antisymmetric with respect to this symmetry operation. A total of  $(2I_1 + 1)(2I_2 + 1) = 16$  spin functions can be constructed. To divide the possible values of  $\mathcal{I}$  into symmetric or antisymmetric spin functions, we note that the lowest  $\mathcal{I}$  state is symmetric when  $I_1$  and  $I_2$  are integral or antisymmetric when  $I_1$  and  $I_2$  are half-integral. The remaining symmetries alternate with increasing values of  $\mathcal{I}$ . Thus, for  $I_1 = I_2 = \frac{3}{2}$ , the  $\mathcal{I} = 0$  (1 spin function) and  $\mathcal{I} = 2$  (5 spin functions) give antisymmetric functions, while  $\mathcal{I} = 1$  (3 spin functions) and  $\mathcal{I} = 3$  (7 spin functions) give symmetric functions. Consider a totally symmetric electronic-vibrational state. For symmetric rotational levels  $A(ee)$ ,  $B_b(oo)$ , only antisymmetric nuclear states ( $\mathcal{I} = 0, 2$ ) exist, while for the antisymmetric rotational levels  $B_a(eo)$ ,  $B_c(oe)$ , only symmetric nuclear states ( $\mathcal{I} = 1, 3$ ) exist. Further discussions for the cases  $I = \frac{3}{2}$  and  $\frac{5}{2}$  are available [48, 49].

As a further specific example we may consider  $\text{D}_2\text{S}$ , where the hyperfine structure of the  $1_{10} \rightarrow 1_{01}$  transition has been studied [16]. The symmetry axis is the  $b$  axis, and the  $1_{10}(B_c)$  and  $1_{01}(B_a)$  levels are antisymmetric with respect to exchange of the two identical deuterium nuclei ( $I_1 = I_2 = 1$ , Bosons). Thus

since  $\mathcal{I}=0$  (symmetric), 1 (antisymmetric) and 2 (symmetric),  $\mathcal{I}$  can take only the value 1 for these rotational levels in order for the total wave function to be symmetric. Specializing (15.117) and (15.118) to the case  $J=1$ ,  $I_1=I_2=\mathcal{I}=1$  with  $(eQq_J)_1=(eQq_J)_2=eQq_J$ , one obtains, for the electric quadrupole energy

$$E_{\text{quad}} = [(-1)^{F+1}] \frac{15}{2} \begin{Bmatrix} F & 1 & 1 \\ 2 & 1 & 1 \end{Bmatrix} eQq_J \quad (15.119)$$

with  $F=0, 1, 2$ . Similar simplified expressions may be obtained for the spin-rotation and spin-spin interactions [16]

$$E_{\text{mag}} = (-1)^F 6 \begin{Bmatrix} F & 1 & 1 \\ 1 & 1 & 1 \end{Bmatrix} C_{J,\tau} \quad (15.120)$$

$$E_{\text{spin-spin}} = (-1)^F 15 \begin{Bmatrix} F & 1 & 1 \\ 2 & 1 & 1 \end{Bmatrix} (JJ|D_0^{(2)}|JJ) \quad (15.121)$$

It may be noted that the expressions for the electric quadrupole and magnetic dipole energies are equivalent to that for a single spin 1 nucleus except for the sign of the quadrupole energy. The calculated  $1_{01} \rightarrow 1_{01}$  transition [28] of D<sub>2</sub>O, which is like that for D<sub>2</sub>S, is compared with the observed pattern in Fig. 15.3.

The hyperfine interaction by three identical nuclei in symmetric tops is also reduced by the symmetry of the rotational wave function, but its calculation is more involved than that for two nuclei, described previously. The reader is directed to the references cited previously.

The two coupling schemes considered in (15.86) and (15.105) are equivalent in that they lead to the same hyperfine structure, and one coupling scheme or coupling order does not offer any great advantage over the other (excluding symmetry considerations) if the energy matrix is diagonalized. The choice of one coupling scheme over the other rests on the first-order approximation being significantly better in one scheme than in the other so as not to require matrix diagonalization. To this end, other coupling schemes, which are mixtures of the two considered, may prove useful. For example, if two nuclei (spins  $I_2$  and  $I_3$ ) have comparable couplings which are smaller than that of a third nucleus (spin  $I_1$ ), the coupling scheme  $J+I_1=F_1$ ,  $I_2+I_3=\mathcal{I}$ ,  $\mathcal{I}+F_1=F$  may prove more convenient. This is particularly true if  $I_2$  and  $I_3$  arise from identical particles. Symmetry restrictions will then limit the possible values of  $\mathcal{I}$  associated with a given rotational level and these restrictions can more easily be introduced into the matrix elements.

The matrix elements of  $\mathcal{H}_{hfs}$  in this representation may be readily evaluated using the procedures already discussed; that for nucleus (1) is, for example, given by (15.84) and (15.85). For nucleus 2 and 3 we would have, for example,

$$(\tau' J' I'_1 I'_2 I'_3 \mathcal{I}' F | \mathcal{H}_Q(L) | \tau J I_1 I_2 I_3 \mathcal{I} F) = (q_{J'J})_L f(J')$$

$$\times (-1)^{[(2F_1+1)(2F'_1+1)]^{1/2}} \begin{Bmatrix} F & \mathcal{I}' & F'_1 \\ 2 & F_1 & \mathcal{I} \end{Bmatrix} \begin{Bmatrix} J' & F'_1 & I_1 \\ F_1 & J & 2 \end{Bmatrix} \quad (15.122)$$

$$\times (I_2 I_3 \mathcal{I}' || Q(L) || I_2 I_3 \mathcal{I})$$

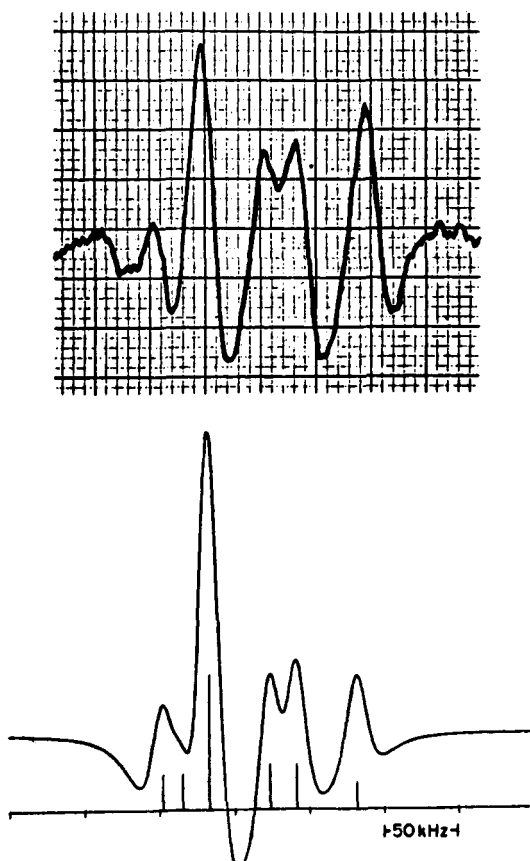


**Fig. 15.3** Theoretical hyperfine pattern (lower figure) of the  $1_{10} \rightarrow 1_{01}$  transition of  $\text{D}_2\text{O}$  compared with the observed pattern (upper figure). The structure is due to the magnetic and quadrupole coupling by the two identical D nuclei. It was calculated by irreducible tensor methods and observed with a molecular beam maser. The transition falls at the submillimeter wave frequency of 317 GHz. From Garvey and De Lucia [28].

with  $t = 2F_1 + J' + F + J' + I_1$  and  $L = 2$  or  $3$ . The reduction of the reduced matrix element follows from (15.22) for  $L = 2$  and (15.23) for  $L = 3$ . Symmetry restrictions for identical particles can be conveniently introduced at this stage in evaluation of the  $6j$  symbol arising from this reduction.

## 5 NUCLEAR SPIN-SPIN INTERACTIONS

We may consider nuclear spin-spin interaction by reference to a specific example,  $\text{D}^{13}\text{C}^{14}\text{N}$ , studied by Garvey and De Lucia [23]. In addition to the quadrupole and spin-rotation interactions of nitrogen and deuterium, and the spin-rotation interaction of  $^{13}\text{C}$ , there is a spin-spin interaction involving the nuclear spins of nitrogen and carbon, and nitrogen and deuterium. The

direct spin-spin interaction may be written in Cartesian form as

$$\begin{aligned}\mathcal{H}_{\text{spin-spin}} &= \mathbf{I}_C \cdot \mathbf{D}_{CD} \cdot \mathbf{I}_D + \mathbf{I}_C \cdot \mathbf{D}_{CN} \cdot \mathbf{I}_N \\ &= \mathbf{I}_3 \cdot \mathbf{D}_{32} \cdot \mathbf{I}_2 + \mathbf{I}_3 \cdot \mathbf{D}_{31} \cdot \mathbf{I}_1\end{aligned}\quad (15.123)$$

The spin-spin interaction between deuterium and nitrogen is negligibly small due to the  $1/r^3$  dependence of the coupling constant and the large D-N separation. Since the largest interaction involves nitrogen, the coupling scheme

$$\begin{aligned}\mathbf{J} + \mathbf{I}_1 &= \mathbf{F}_1 \\ \mathbf{F}_1 + \mathbf{I}_2 &= \mathbf{F}_2 \\ \mathbf{F}_2 + \mathbf{I}_3 &= \mathbf{F}\end{aligned}$$

is appropriate, where the subscripts 1, 2, 3 refer to the nitrogen, deuterium and carbon atoms, respectively. The elements of the Cartesian coupling tensor are defined by

$$(D_{LK})_{ij} = -\frac{3x_i x_j - \delta_{ij} r^2}{r^5} \frac{\mu_L \mu_K}{I_L I_K} \quad (15.124)$$

where  $I_L$  and  $I_K$  are the nuclear spins and  $\mu_L$  and  $\mu_K$  the corresponding magnetic dipole moments of nuclei  $L$  and  $K$ . Here  $\mathbf{r}$  defines the relative position vector of nucleus  $K$  with respect to  $L$ . Rewriting the interaction in spherical tensor form, noting that  $\mathbf{D}$  is a traceless and symmetric Cartesian tensor, we have

$$\mathcal{H}_{\text{spin-spin}} = -\sqrt{\frac{5}{2}} [\mathbf{D}_{32}^{(2)} \times \mathbf{I}_2^{(1)}]^{(1)} \cdot \mathbf{I}_3^{(1)} - \sqrt{\frac{5}{2}} [\mathbf{D}_{31}^{(2)} \times \mathbf{I}_1^{(1)}]^{(1)} \cdot \mathbf{I}_3^{(1)} \quad (15.125)$$

where  $\mathbf{D}^{(2)}$  is a second-rank spherical tensor and the normalization factor has been chosen such that  $D_0^{(2)} = D_{zz}$ . Application of (15.21) to the first term of (15.125) gives

$$\begin{aligned}(JI_1 F'_1 I_2 F'_2 I_3 F) - \sqrt{\frac{5}{2}} [\mathbf{D}_{32}^{(2)} \times \mathbf{I}_2^{(1)}]^{(1)} \cdot \mathbf{I}_3^{(1)} |JI_1 F_1 I_2 F_2 I_3 F) \\ = (-1)^{F_2 + I_3 + F + 1} \left\{ \begin{matrix} F & I_3 & F'_2 \\ 1 & F_2 & I_3 \end{matrix} \right\} (I_3 || I_3^{(1)} || I_3) \\ \times \sqrt{\frac{5}{2}} (JI_1 F'_1 I_2 F'_2) || [\mathbf{D}_{32}^{(2)} \times \mathbf{I}_2^{(1)}]^{(1)} || JI_1 F_1 I_2 F_2) \quad (15.126)\end{aligned}$$

The latter tensor product is composed of tensor operators which operate on different subspaces; therefore application of (15.24) yields

$$\begin{aligned}(JI_1 F'_1 I_2 F'_2) || [\mathbf{D}_{32}^{(2)} \times \mathbf{I}_2^{(1)}]^{(1)} || JI_1 F_1 I_2 F_2) &= [(2F_2 + 1)(2F'_2 + 1)3]^{1/2} \\ &\times \left\{ \begin{matrix} F'_1 & F_1 & 2 \\ I_2 & I_2 & 1 \\ F'_2 & F_2 & 1 \end{matrix} \right\} (JI_1 F_1 || D_{32}^{(2)} || JI_1 F_1) (I_2 || I_2^{(1)} || I_2) \quad (15.127)\end{aligned}$$

Since  $\mathbf{D}^{(2)}$  commutes with  $\mathbf{I}_1$  we apply (15.22)

$$\begin{aligned}(JIF'_1 || D_{32}^{(2)} || JI_1 F_1) &= (-1)^{J+I_1+F_1+2} [(2F_1 + 1)(2F'_1 + 1)]^{1/2} \\ &\times \left\{ \begin{matrix} J & F'_1 & I_1 \\ F_1 & J & 2 \end{matrix} \right\} (J || D_{32}^{(2)} || J) \quad (15.128)\end{aligned}$$

Collection of terms gives

$$\begin{aligned}
 & (J|I_1 F'_1 I_2 F'_2 I_3 F) - \sqrt{\frac{5}{2}} [\mathbf{D}_{32}^{(2)} \times \mathbf{I}_2^{(1)}]^{(1)} \cdot \mathbf{I}_3^{(1)} |J I_1 F'_1 I_2 F'_2 I_3 F) \\
 & = (-1)^{F_2 + I_3 + F + J + I_1 + F_1 + 1} \left[ \frac{15}{2} (2F_2 + 1)(2F'_2 + 1)(2F_1 + 1)(2F'_1 + 1) \right]^{1/2} \\
 & \quad \times \left\{ \begin{array}{ccc} F & I_3 & F'_2 \\ 1 & F_2 & I_3 \end{array} \right\} \left\{ \begin{array}{ccc} J & F'_1 & I_1 \\ F_1 & J & 2 \end{array} \right\} \left\{ \begin{array}{ccc} F'_1 & F_1 & 2 \\ I_2 & I_2 & 1 \\ F'_2 & F_2 & 1 \end{array} \right\} \\
 & \quad \times (J||D_{32}^{(2)}||J)(I_3||I_3^{(1)}||I_3)(I_2||I_2^{(1)}||I_2)
 \end{aligned} \tag{15.129}$$

Similarly, application of (15.21) to the second term of  $\mathcal{H}_{\text{spin-spin}}$  and subsequent use of (15.22) and (15.24) gives finally for the matrix elements

$$\begin{aligned}
 & (J|I_1 F'_1 I_2 F'_2 I_3 F) - \sqrt{\frac{5}{2}} [\mathbf{D}_{31}^{(2)} \times \mathbf{I}_1^{(1)}]^{(1)} \cdot \mathbf{I}_3^{(1)} |J I_1 F'_1 I_2 F'_2 I_3 F) \\
 & = (-1)^{F_2 + I_3 + F + F'_1 + I_2 + F_2} \left[ \frac{15}{2} (2F_2 + 1)(2F'_2 + 1)(2F_1 + 1)(2F'_1 + 1) \right]^{1/2} \\
 & \quad \times \left\{ \begin{array}{ccc} F & I_3 & F'_2 \\ 1 & F_2 & I_3 \end{array} \right\} \left\{ \begin{array}{ccc} F'_1 & F'_2 & I_2 \\ F_2 & F_1 & 1 \end{array} \right\} \left\{ \begin{array}{ccc} J & J & 2 \\ I_1 & I_1 & 1 \\ F'_1 & F_1 & 1 \end{array} \right\} (J||D_{31}^{(2)}||J) \\
 & \quad \times (I_1||I_1^{(1)}||I_1)(I_3||I_3^{(1)}||I_3)
 \end{aligned} \tag{15.130}$$

The reduced matrix element of the rotation-dependent operator is found from the Wigner-Eckart theorem

$$(J||D^{(2)}||J) = 2f(J)(JJ|D_0^{(2)}|JJ) \tag{15.131}$$

and  $(JJ|D_0^{(2)}|JJ)$  can be taken as the spectroscopic constant to be determined. More often the small effects of the spin-spin interaction can be accurately accounted for by calculation of  $D_0^{(2)}$  from the molecular geometry. Likewise we have

$$(I_\alpha||I_\alpha^{(1)}||I_\alpha) = h(I_\alpha) \tag{15.132}$$

with  $h(I_\alpha)$  defined in (15.68).

## 6 RELATIVE INTENSITIES

In the interpretation of rotational hyperfine spectra the relative intensities of the transitions are required. This may also be readily formulated in terms of irreducible tensor methods. The line strength of the transition  $\tau' J' \alpha' F' \rightarrow \tau J \alpha F$  is defined by [2]

$$S(\tau' J' \alpha' F' \rightarrow \tau J \alpha F) = \sum_{q M_F M'_F} |(\tau' J' \alpha' F' M'_F | \mu_q^{(1)} | \tau J \alpha F M_F)|^2 \tag{15.133}$$

where  $\mu_q^{(1)}$  are the components of the irreducible electric dipole moment tensor operator [ $\mu_0^{(1)} = \mu_z$ ,  $\mu_{\pm 1}^{(1)} = \mp(1/2^{1/2})(\mu_x \pm i\mu_y)$ ] and where  $\tau J$  specifies the pure rotational state. To be able to discuss plural nuclear coupling we let  $\alpha$  stand for the set of intermediate momenta in the coupling scheme. From the Wigner-Eckart theorem

$$(\tau' J' \alpha' F' M'_F | \mu_q^{(1)} | \tau J \alpha F M_F) = (-1)^{F' - M'_F} \begin{pmatrix} F' & 1 & F \\ -M'_F & q & M_F \end{pmatrix} (\tau' J' \alpha' F' || \mu^{(1)} || \tau J \alpha F) \quad (15.134)$$

Thus

$$S(\tau' J' \alpha' F' \rightarrow \tau J \alpha F) = |(\tau' J' \alpha' F' || \mu^{(1)} || \tau J \alpha F)|^2 \sum_{q M_F M'_F} \left| \begin{pmatrix} F' & 1 & F \\ -M'_F & q & M_F \end{pmatrix} \right|^2 \quad (15.135)$$

The last term in this equation can be rewritten as

$$\begin{aligned} \sum_{q M_F M'_F} \left| \begin{pmatrix} F' & 1 & F \\ -M'_F & q & M_F \end{pmatrix} \right|^2 &= \sum_q \sum_{M_F M'_F} \begin{pmatrix} F' & 1 & F \\ -M'_F & q & M_F \end{pmatrix} \begin{pmatrix} F' & 1 & F \\ -M'_F & q & M_F \end{pmatrix} \\ &= \sum_q \sum_{M_F M'_F} \begin{pmatrix} F' & F & 1 \\ -M'_F & M_F & q \end{pmatrix} \begin{pmatrix} F' & F & 1 \\ -M'_F & M_F & q \end{pmatrix} \end{aligned} \quad (15.136)$$

with the aid of the symmetry properties of the  $3j$  symbol. The sum over  $M_F$  and  $M'_F$  is equal to  $\frac{1}{3}$ . This follows from the orthogonality property of the  $3j$  symbols in (15.6). Thus the sum over the three components of  $q$  gives unity, and we have finally for (15.133)

$$S(\tau' J' \alpha' F' \rightarrow J \alpha F) = |(\tau' J' \alpha' F' || \mu^{(1)} || \tau J \alpha F)|^2 \quad (15.137)$$

Evaluation of the reduced matrix element depends on the coupling scheme.

For a single coupling nucleus  $\alpha$  stands for  $I$  which does not change during a transition, and (15.22) gives

$$\begin{aligned} (\tau' J' I F' || \mu^{(1)} || \tau J I F) &= (-1)^{J' + I + F + 1} [(2F + 1)(2F' + 1)]^{1/2} \begin{Bmatrix} J' & F' & I \\ F & J & 1 \end{Bmatrix} \\ &\times (\tau' J' || \mu^{(1)} || \tau J) \end{aligned} \quad (15.138)$$

The square of the preceding reduced matrix element gives the strength of the hyperfine transition according to (15.137)

$$S(\tau' J' I F' \rightarrow \tau J I F) = (2F + 1)(2F' + 1) \begin{Bmatrix} J' & F' & I \\ F & J & 1 \end{Bmatrix}^2 |(\tau' J' || \mu^{(1)} || \tau J)|^2 \quad (15.139)$$

The reduced matrix element  $(\tau' J' || \mu^{(1)} || \tau J)$  which represents the intensity of the unsplit rotational transition  $\tau' J' \rightarrow \tau J$  may be omitted in evaluation of the relative intensities of the hyperfine transitions. If it is desired, this reduced matrix element may be evaluated by first expressing  $\mu_q^{(1)}$  by means of (15.1), in terms of the dipole moment components  $\mu_q^{(1)}$  along the molecule-fixed axes. The matrix elements of  $\mu_0^{(1)}$  in the symmetric rotor basis may then be obtained by application of (15.38) and finally the reduced matrix element can be found from the Wigner-Eckart theorem. For asymmetric rotors  $|(\tau' J' || \mu^{(1)} || \tau J)|^2$  is related to the line strength  $\lambda_g$  introduced in Chapter VII.

We may define a relative intensity of a particular hyperfine line by first

summing over  $F$  and  $F'$  and rearranging the  $6j$  symbol

$$\begin{aligned} \sum_{F,F'} S(\tau' J' IF' \rightarrow \tau J IF) \\ = \sum_{F'} (2F'+1) \sum_F \left[ (2F+1) \left\{ \begin{matrix} 1 & J & J' \\ I & F' & F \end{matrix} \right\} \left\{ \begin{matrix} I & J & F \\ 1 & F' & J' \end{matrix} \right\} \right] |(\tau' J'| \mu^{(1)} | \tau J)|^2 \quad (15.140) \end{aligned}$$

The sum over the term in brackets is  $(2J'+1)^{-1}$  by the orthogonality property of the  $6j$  symbols. Likewise, the sum over the initial  $F'$  states from  $|J'-I|$  to  $J'+I$  [for  $J' > I$  and  $J' < I$  number of  $F'$  values are  $(2I+1)$  and  $(2J'+1)$ , respectively] is  $(2J'+1)(2I+1)$ . Hence

$$\sum_{F,F'} S(\tau' J' IF' \rightarrow \tau J IF) = (2I+1) |(\tau' J'| \mu^{(1)} | \tau J)|^2 \quad (15.141)$$

The relative line strength of a hyperfine line is the ratio of (15.139) to (15.141) [11]

$$\begin{aligned} s(J' IF' \rightarrow J IF) &= \frac{S(J' \tau' IF' \rightarrow J \tau IF)}{\sum_{FF'} S(J' \tau' IF' \rightarrow J \tau IF)} \\ &= \frac{(2F+1)(2F'+1)}{(2I+1)} \left\{ \begin{matrix} J' & F' & I \\ F & J & 1 \end{matrix} \right\}^2 \quad (15.142) \end{aligned}$$

where the notation for  $s$  takes into account that it is independent of  $\tau, \tau'$ . Furthermore, it is clear that

$$\sum_{FF'} s(J' IF' \rightarrow J IF) = 1 \quad (15.143)$$

As discussed by Rudolph [11], these results can be used to give the unsplit line, corrected for the effects of quadrupole coupling, without actual assignment of the hyperfine structure. The transition frequency of a given hyperfine line  $J' \tau' IF' \rightarrow J \tau IF$  is (to first-order)

$$\nu = \nu_r + E_Q(J \tau IF) - E_Q(J' \tau' IF') \quad (15.144)$$

where  $\nu_r$  is the transition frequency  $J' \tau' \rightarrow J \tau$  if no hyperfine structure were present. If we multiply each hyperfine component by its relative intensity and sum over all components, we have

$$\sum_{FF'} \nu \cdot s = \nu_r \sum_{FF'} s + \sum_{FF'} \{E_Q(J \tau IF) - E_Q(J' \tau' IF')\} s \quad (15.145)$$

By substituting from (15.84) for  $E_Q$ , one can show from orthogonality relations of the  $6j$  symbol that the sums on the right-hand side vanish identically, yielding [11]

$$\nu_r (J' \tau' \rightarrow J \tau) = \sum_{FF'} \nu (J' \tau' IF' \rightarrow J \tau IF) s(J' IF' \rightarrow J IF) \quad (15.146)$$

Therefore, the unsplit frequency is given to first-order by the intensity-weighted average of the multiplet frequencies. This allows, in principle, the evaluation of  $\nu_r$  without a detailed analysis of the *hfs* patterns and assignment of individual  $F' \rightarrow F$  components. The  $\nu_r$ 's can then, of course, be used to give the rotational

constants. Partially resolved or coinciding components are properly accounted for by choice of the intensity weighted mean or center-of-gravity of the multiplet. Of course there are problems in application where weak components with large frequency displacements are not observed.

The relative intensities for the two representations discussed previously require evaluation of the reduced matrix element of (15.137). For the case of unequal coupling since  $\mathbf{I}_i$  commutes with  $\mu^{(1)}$ , successive application of (15.22) can be used to bring the reduced matrix element

$${}_1 I_2 \dots I_N F'_N || \mu^{(1)} || \tau J I_1 F_1 I_2 \dots I_N F_N$$

to the desired form

$$(\tau' J' || \mu^{(1)} || \tau J)$$

For  $N$  nuclei the relative intensities for unequal coupling are given by [5]

$$S(J' F'_1 \dots F'_N \rightarrow J F_1 \dots F_N) = |C(J' F'_1 \dots F'_N \rightarrow J F_1 \dots F_N)|^2 \quad (15.147)$$

where

$$C(J' F'_1 \dots F'_N \rightarrow J F_1 \dots F_N) = (-1)^t \prod_{i=1}^N [(2F_i + 1)(2F'_i + 1)]^{1/2} \begin{Bmatrix} F'_{i-1} & F'_i & I_i \\ F_i & F_{i-1} & 1 \end{Bmatrix} \quad (15.148)$$

and

$$t = \sum_{i=1}^N (I_i + F'_{i-1} + F_i) + N \text{ with } F_0 = J, F'_0 = J' \text{ and } F_N = F$$

For evaluation of the relative intensities of the hyperfine transitions in the equal or nearly equal coupling scheme, the reduced matrix element

$$(\tau' J' I_1 I_2 \mathcal{J}_2 \dots I_L \mathcal{J}_L \dots I_N \mathcal{J}_N F' || \mu^{(1)} || \tau J I_1 I_2 \mathcal{J}_2 \dots I_L \mathcal{J}_L \dots I_N \mathcal{J}_N F)$$

must first be evaluated. Since the  $\mathcal{J}$ 's commute with  $\mu^{(1)}$ , (15.22) gives

$$\begin{aligned} (\tau' J' I_1 F' || \mu^{(1)} || \tau J \dots \mathcal{J}_N F) &= (-1)^{J' + \mathcal{J}_N + F + 1} [(2F + 1)(2F' + 1)]^{1/2} \\ &\times \begin{Bmatrix} J' & F' & \mathcal{J}_N \\ F & J & 1 \end{Bmatrix} (\tau' J' || \mu^{(1)} || \tau J) \end{aligned} \quad (15.149)$$

The resulting relative intensities for equal coupling are [5]

$$S(J' \dots \mathcal{J}_N F' \rightarrow J \dots \mathcal{J}_N F) = |C(J' \dots \mathcal{J}_N F' \rightarrow J \dots \mathcal{J}_N F)|^2 \quad (15.150)$$

where

$$C(J' \dots \mathcal{J}_N F' \rightarrow J \dots \mathcal{J}_N F) = (-1)^t [(2F + 1)(2F' + 1)]^{1/2} \begin{Bmatrix} J' & F' & \mathcal{J}_N \\ F & J & 1 \end{Bmatrix} \quad (15.151)$$

and  $t = J' + \mathcal{J}_N + F + 1$  with  $\mathcal{J}_N = \mathcal{J}$ . If the intermediate  $F_i$  (or  $\mathcal{J}_i$ ) are not good

quantum numbers, the first-order intensities given by (15.148) and (15.151) may not be adequate. The matrix of  $\mathbf{C}$  must then be transformed by means of a similarity transformation to the basis which diagonalizes the hyperfine Hamiltonian, that is,

$$\mathbf{C}' = \tilde{\mathbf{T}}_i \mathbf{C} \mathbf{T}_f \quad (15.152)$$

where  $\mathbf{T}_i$  diagonalizes the energy matrix of the initial state of the transition and  $\mathbf{T}_f$  diagonalizes the energy matrix of the final state. The squares of the elements of  $\mathbf{C}'$  yield the relative intensities.

## 7 ELECTRONIC SPIN INTERACTIONS

The oxygen molecule, which has a  $^3\Sigma$  ground state, is a classic example of a diatomic molecule having both spin-rotation and electronic spin-spin interactions. Its microwave spectrum, analyzed in some detail in Chapter IV, Section 2, is most simply treated by irreducible tensor methods [50, 51].

Exclusive of centrifugal distortion and nuclear coupling isotopes, the  $^3\Sigma$  oxygen Hamiltonian (Chapter IV, Section 2) may be written as

$$\mathcal{H} = BN^2 + \gamma \mathbf{N} \cdot \mathbf{S} + \frac{2}{3}\lambda(3S_z^2 - S^2) \quad (15.153)$$

where the first term is the rotational part  $\mathcal{H}_r$ , the second term is the spin-rotation part  $\mathcal{H}_{sr}$ , and the last term is the spin-spin interaction [50, 51]  $\mathcal{H}_{ss}$ . Here  $S_z$  is the body-fixed component of the electron spin along the internuclear axis,  $\mathbf{N}$  is the rotational angular momentum, and  $\mathbf{S}$  is the total electron spin operator. Evaluation of the matrix elements of this Hamiltonian allows the energy levels to be evaluated by direct diagonalization of the energy matrix. The appropriate basis functions are  $|S, N, J, M_J\rangle$  where the total angular momentum  $\mathbf{J} = \mathbf{S} + \mathbf{N}$ . The operators  $\mathbf{J}^2$ ,  $J_z$ ,  $\mathbf{N}^2$  and  $\mathbf{S}^2$  are diagonal in this basis. It is readily seen that the matrix elements for  $\mathcal{H}_r$  and  $\mathcal{H}_{sr}$  are given by

$$\langle S, N, J, M_J | \mathcal{H}_R | S, N, J, M_J \rangle = BN(N+1) \quad (15.154)$$

$$\langle S, N, J, M_J' | \mathcal{H}_{sr} | S, N, J, M_J \rangle = \frac{1}{2}\gamma[J(J+1) - N(N+1) - S(S+1)] \quad (15.155)$$

noting  $\mathbf{N} \cdot \mathbf{S} = \frac{1}{2}[\mathbf{J}^2 - \mathbf{N}^2 - \mathbf{S}^2]$ .

The matrix elements for the spin-spin term may be conveniently evaluated by application of irreducible tensor methods by writing this term in terms of the space-fixed components of  $\mathbf{S}$ , that is,  $\mathcal{H}_{ss} = \frac{2}{3}\lambda(\sum \Phi_{iz'}\Phi_{jz'}S_iS_j - \mathbf{S}^2)$ , where  $\Phi_{iz'}$  is the direction cosine between the body-fixed  $z'$  axis and the space-fixed  $i$  axis ( $i=x, y, z$ ). In Cartesian tensor form

$$\begin{aligned} \mathcal{H}_{ss} &= \lambda \mathbf{S} \cdot \mathbf{T} \cdot \mathbf{S} \\ &= \lambda \sum_{i,j} S_i S_j T_{ij} \end{aligned} \quad (15.156)$$

where  $T_{ij} = \frac{2}{3}(3\Phi_{iz'}\Phi_{jz'} - \delta_{ij})$ . This may be written in spherical tensor form as

$$\mathcal{H}_{ss} = \sum_{l=0}^2 N_l [\mathbf{S}^{(1)} \times \mathbf{S}^{(1)}]^{(l)} \cdot \mathbf{C}^{(l)}; N_l = (-1)^l \quad (15.157)$$

with  $\mathbf{S}^{(1)}$  the first rank spherical tensor form of the first rank Cartesian tensor  $\mathbf{S}$  defined via (15.10), and  $\mathbf{C}^{(l)}$  is the  $l$ th rank ( $l=0, 1, 2$ ) spherical tensor form of  $\mathbf{T}$  defined via (15.17). In this particular case,  $\mathbf{C}^{(l)}=0$  except for  $l=2$ . Therefore

$$\mathcal{H}_{ss} = \lambda [\mathbf{S}^{(1)} \times \mathbf{S}^{(1)}]^{(2)} \cdot \mathbf{C}^{(2)} \quad (15.158)$$

From (15.21) we have

$$(N', S, J, M_J | \mathcal{H}_{ss} | N, S, J, M_J) = (-1)^{S+N'+J} \begin{Bmatrix} J & N' & S \\ 2 & S & N \end{Bmatrix} \times (S || [\mathbf{S}^{(1)} \times \mathbf{S}^{(1)}]^{(2)} || S) (N' || C^{(2)} || N) \quad (15.159)$$

Application of (15.25) gives for the reduced matrix element of the electron spin

$$(S || [\mathbf{S}^{(1)} \times \mathbf{S}^{(1)}]^{(2)} || S) = \sqrt{5} \begin{Bmatrix} 1 & 1 & 2 \\ S & S & S \end{Bmatrix} [(S || S^{(1)} || S)]^2 \quad (15.160)$$

Here  $S=1$ , and the  $6j$  symbol is equal to  $\frac{1}{6}$ . From the Wigner-Eckart theorem, it follows from the matrix element  $(S, M_S = S | S_0^{(1)} | S, M_S = S) = S$  that

$$(S || S^{(1)} || S) = [S(S+1)(S+2)]^{1/2} = \sqrt{6} \quad (15.161)$$

Similarly, application of the Wigner-Eckart theorem gives

$$(N' || C^{(2)} || N) = (-1)^{N'-M_N} (N', M_N | C_0^{(2)} | N, M_N) \begin{pmatrix} N' & 2 & N \\ -M_N & 0 & M_N \end{pmatrix}^{-1} \quad (15.162)$$

where  $C_0^{(2)} = (2/6^{1/2})(3\Phi_{zz'} - 1)$ . Evaluation of the direction cosine elements for a linear molecule gives

$$(N' || C^{(2)} || N) = -\frac{4}{\sqrt{6}} \left[ \frac{N(N+1)(2N+1)}{(2N-1)(2N+3)} \right]^{1/2} \delta_{N', N} + 2 \left[ \frac{(N+1)(N+2)}{(2N+3)} \right]^{1/2} \delta_{N', N+2} + 2 \left[ \frac{N(N-1)}{(2N-1)} \right]^{1/2} \delta_{N', N-2} \quad (15.163)$$

The matrix elements of the Hamiltonian are hence given by the sum of (15.154), (15.155), and (15.159) with cognizance of (15.160), (15.161), and (15.163). The Hamiltonian is diagonal in  $J, M_J$ , and  $S$ , and since  $S=1$  for each value of  $J$ , we have  $N=J-1, J$  and  $J+1$  with  $J=1, 2, \dots$ . For  $J=0$ ,  $N=1$ . The energy matrix may hence be factored into a set of  $3 \times 3$  blocks except for  $J=0$  which is  $1 \times 1$ . To take into account distortion effects, the constants  $B$ ,  $\gamma$ , and  $\lambda$  may be expanded in terms of  $N$ . For the diagonal matrix elements, the constants are expanded as in (4.57). For the off-diagonal term ( $N'=J+1 | N=J-1$ ),  $\lambda = \lambda_0 + \lambda_1(J^2 + J + 1)$ . Elaboration of this theory and calculation of transition strengths are given in the dissertation of Steinbach [51].

The complexity of the spectra of polyatomic molecules with unpaired electron spins is illustrated in Fig. 15.4 for  $\text{CF}_3$  which has a doublet electronic ground state with three identical coupling nuclei—the first such molecule analyzed by

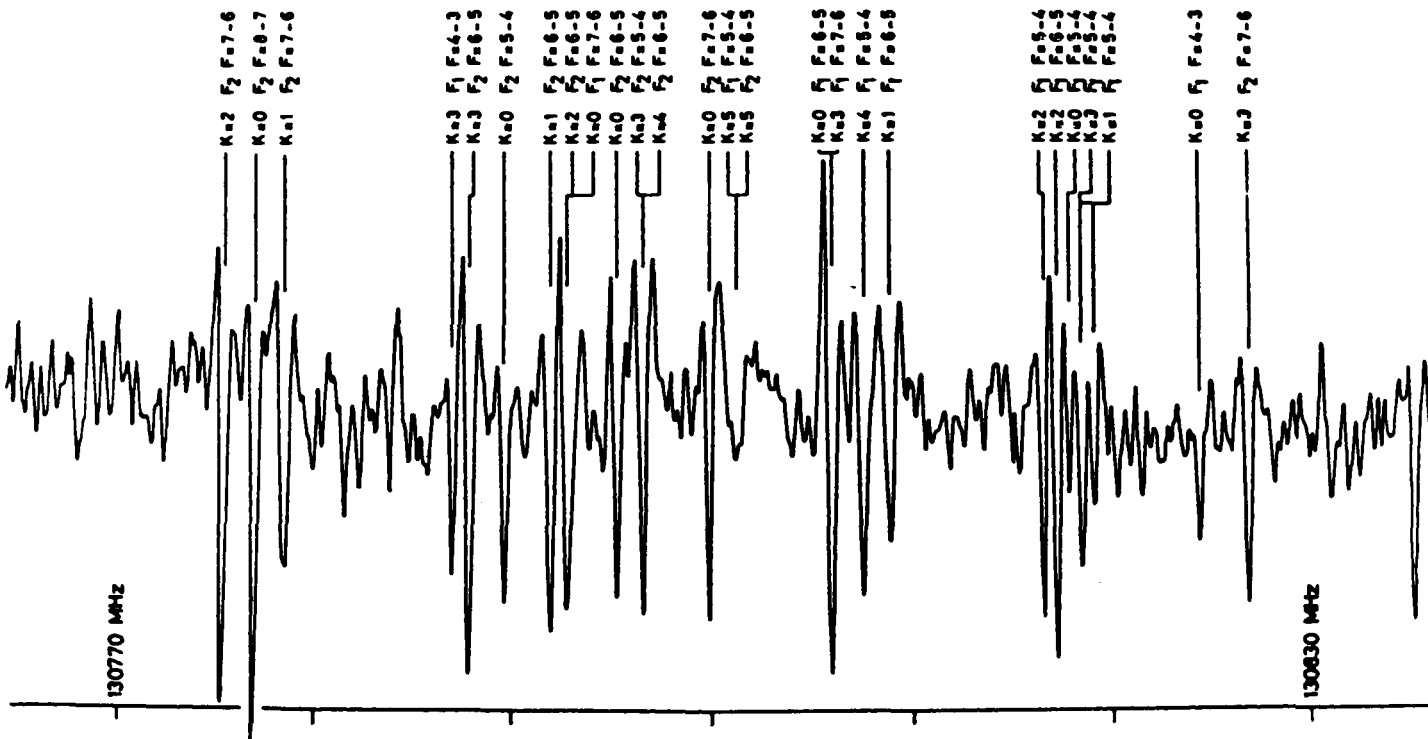


**Fig. 15.4** Observed spectrum of the  $N=6 \leftarrow 5$  transition of  $\text{CF}_3$ . The spectrum was synthesized from batches of records, each covering a region 10 MHz wide and representing the accumulation of 400 scans at a repetition rate of 5 Hz. The spectrum consists of  $K$  components split into many lines by the spin-rotation and the hyperfine interactions. From Endo et al. [39].

microwave spectroscopy. The hyperfine Hamiltonian is significantly complicated by the presence of the electronic spin momentum. The coupling scheme employed is  $\mathbf{J} = \mathbf{N} + \mathbf{S}$  and  $\mathbf{F} = \mathbf{J} + \mathbf{I}_0$  with  $\mathbf{I}_0 = \mathbf{I}_1 + \mathbf{I}_2 + \mathbf{I}_3$ . A detailed analysis by Endo et al. [39] allowed evaluation of the spin-rotation constants, the Fermi interaction parameter, and the diagonal elements of the dipole-dipole hyperfine interaction tensor. Elements of the latter tensor split the  $K=1$  level in first order. A discussion of the Hamiltonian may be found elsewhere [39, 35, 20].

Varied applications of irreducible tensor methods to diatomic molecules with electronic spin momentum are given in the book by Mizushima [44].

## 8 STARK EFFECT

As a final example we consider the Stark effect for a linear or symmetric top molecule with a single quadrupole coupling nucleus. For a coupling nucleus with large nuclear spin  $I$ , a direct diagonalization of the energy matrix may be more appropriate than a perturbation treatment. The matrix elements of the Stark effect Hamiltonian will hence be considered. With the electric field  $\mathcal{E}$  along the space-fixed axis  $z$ , the Hamiltonian has the form

$$\mathcal{H}_{\mathcal{E}} = -\mathcal{E}\mu_0^{(1)} \quad (15.164)$$

The basis functions are  $|KJIFM_F\rangle$ , and from the Wigner-Eckart theorem we have

$$(K'J'IF'M_F|\mathcal{H}_{\mathcal{E}}|KJIFM_F) = -\mathcal{E}(-1)^{F'-M_F} \begin{pmatrix} F' & 1 & F \\ -M_F & 0 & M_F \end{pmatrix} \times (K'J'IF'|\mu_0^{(1)}|KJIF) \quad (15.165)$$

Further reduction of the matrix is accomplished with the theorem of (15.22)

$$(K'J'IF'|\mu_0^{(1)}|KJIF) = (-1)^{J'+I+F+1} [(2F+1)(2F'+1)]^{1/2} \times \begin{Bmatrix} J' & F' & I \\ F & J & 1 \end{Bmatrix} (K'J'|\mu_0^{(1)}|JK) \quad (15.166)$$

Application of the Wigner-Eckart theorem again gives

$$(K'J'M_J|\mu_0^{(1)}|KJM_J) = (-1)^{J'-M_J} \begin{pmatrix} J' & 1 & J \\ -M_J & 0 & M_J \end{pmatrix} (K'J'|\mu_0^{(1)}|K, J) \quad (15.167)$$

Projection of  $\mu_0^{(1)}$  on the molecule-fixed axis with (15.2) yields

$$(K'J'M_J|\mu_0^{(1)}|KJM_J) = \sum_{q'} (-1)^{-q'} \mu_q^{(1)} (K'J'M_J|D_{0,-q'}^{(1)}|KJM_J) \quad (15.168)$$

For a linear or symmetric-top molecule only,  $\mu_0^{(1)} \equiv \mu$  is nonzero. The matrix element of  $\mathbf{D}^{(1)}$  may be evaluated from (15.38); thus  $K' = K$  throughout, and

$$(KJ'M_J|\mu_0^{(1)}|KJM_J) = \mu(-1)^{M_J-K} [(2J+1)(2J'+1)]^{1/2} \times \begin{pmatrix} J & 1 & J' \\ M_J & 0 & -M_J \end{pmatrix} \begin{pmatrix} J & 1 & J' \\ K & 0 & -K \end{pmatrix} \quad (15.169)$$

Therefore

$$(KJ'M_J|\mu_0^{(1)}|KJM_J) = \mu(-1)^{M_J-K} [(2J+1)(2J'+1)]^{1/2} \times \begin{pmatrix} J & 1 & J' \\ K & 0 & -K \end{pmatrix} \quad (15.170)$$

For  $J'=J$ ,  $(KJ|\mu_0^{(1)}|KJ) = \mu K(2J+1)^{1/2}/[J(J+1)]^{1/2}$ , for  $J'=J+1$ ,  $(KJ+1|\mu_0^{(1)}|KJ) = \mu[(J+1)^2 - K^2]^{1/2}/(J+1)^{1/2}$  and for  $J'=J-1$ ,  $(KJ-1|\mu_0^{(1)}|KJ) = -\mu(J^2 - K^2)^{1/2}/J^{1/2}$ . For a linear molecule,  $K=0$ , which implies that all diagonal elements vanish.

The matrix elements for  $\mathcal{H}_g$  are thus given by (15.165) with the auxiliary equation (15.166) and the values of  $(J'|\mu_0^{(1)}|J)$ . To these may be added the matrix elements for the rigid rotor, the magnetic spin-rotation interaction, and the nuclear quadrupole interaction. The zero-field frequencies are found by setting  $\mathcal{E}=0$ , and the Stark shifts are found by setting  $\mathcal{E}$  to the desired field value and diagonalizing the energy matrix for each value of  $M_F$ . Since the energy matrix of the total Hamiltonian is no longer diagonal in  $F$  with the addition of  $\mathcal{H}_g$ , a truncated matrix of appropriate dimensions must be chosen.

If there is more than one coupling nucleus, additional quantum numbers will appear in the reduced matrix element of (15.165). Equation (15.22) may be repeatedly used until the reduced matrix element appears in its most reduced form. This will introduce products of  $6j$  symbols.

It may be noted that the general form of (15.167) written in terms of  $\mu_q^{(1)}$  ( $q=0, \pm 1$ ) yields the matrix elements of the dipole moment tensor in terms of the constant components along the body-fixed axis with the aid of (15.2). The matrix elements of  $\mathbf{D}^{(1)}$  are the matrix elements of the first rank spherical components of the usual direction cosines,  $\Phi$ .

## References

1. M. E. Rose, *Elementary Theory of Angular Momentum*, Wiley, New York, 1957.
2. A. R. Edmonds, *Angular Momentum in Quantum Mechanics*, Princeton Univ. Press, Princeton, N.J., 1960.
3. U. Fano and G. Racah, *Irreducible Tensorial Sets*, Academic, New York, 1959.
4. B. R. Judd, *Operator Techniques in Atomic Spectroscopy*, McGraw-Hill, New York, 1963.
5. R. L. Cook and F. C. De Lucia, *Am. J. Phys.*, **39**, 1433 (1971).
6. R. F. Curl, Jr., and J. L. Kinsey, *J. Chem. Phys.*, **35**, 17 (1961).
7. P. Thaddeus, L. C. Krishner, and J. H. N. Loubser, *J. Chem. Phys.*, **40**, 257 (1964).
8. N. F. Ramsey, *Molecular Beams*, Clarendon Press, Oxford, England, 1956.
9. W. H. Flygare and W. D. Gwinn, *J. Chem. Phys.*, **36**, 787 (1962).
10. H. P. Benz, A. Bauder, and Hs. H. Günthard, *J. Mol. Spectrosc.*, **21**, 156 (1966).
11. H. D. Rudolph, *Z. Naturforsch.*, **23a**, 540 (1968).
12. A. Carrington, B. J. Howard, D. H. Levy, and J. C. Robertson, *Mol. Phys.*, **15**, 187 (1968).

13. J. W. Cederberg and C. E. Miller, *J. Chem. Phys.*, **50**, 3547 (1969).
14. G. L. Blackman, R. D. Brown, and F. R. Burden, *J. Mol. Spectrosc.*, **36**, 528 (1970).
15. S. G. Kukolich, and S. C. Wofsy, *J. Chem. Phys.*, **52**, 5477 (1970).
16. F. C. De Lucia and J. W. Cederberg, *J. Mol. Spectrosc.*, **40**, 52 (1971).
17. J. W. Cederberg, *Am. J. Phys.*, **40**, 159 (1972).
18. E. Herbst and W. Steinmetz, *J. Chem. Phys.*, **56**, 5342 (1972).
19. J. T. Hougen, *J. Chem. Phys.*, **57**, 4207 (1972).
20. I. C. Bowater, J. M. Brown, and A. Carrington, *Proc. R. Soc. London, Ser. A* **333**, 265 (1973).
21. J. E. M. Heuvel and A. Dymanus, *J. Mol. Spectrosc.*, **47**, 363 (1973).
22. G. L. Blackman, K. Bolton, R. D. Brown, F. R. Burden, and A. Mishra, *J. Mol. Spectrosc.*, **47**, 457 (1973).
23. R. M. Garvey and F. C. De Lucia, *J. Mol. Spectrosc.*, **50**, 38 (1974).
24. R. M. Garvey, F. C. De Lucia, and J. W. Cederberg, *Mol. Phys.*, **31**, 265 (1976).
25. J. T. Murray, W. A. Little, Q. Williams, and T. L. Weatherly, *J. Chem. Phys.*, **65**, 985 (1976).
26. H. K. Bodenseh, W. Hüttner, and P. Nowicki, *Z. Naturforsch.*, **31a**, 1638 (1976).
27. A. Dymanus, "Beam Maser Spectroscopy," in *MTB International Reviews of Science, Physical Chemistry Series 2*, Vol. 3 *Spectroscopy*, D. A. Ramsay, Ed., Butterworths and University Park Press, 1976.
28. R. M. Garvey and F. C. De Lucia, *Can. J. Phys.*, **55**, 1115 (1977).
29. S. G. Kukolich, G. Lind, M. Barfield, L. Faehl, and J. L. Marshall, *J. Am. Chem. Soc.*, **100**, 7155 (1978).
30. W. Hüttner, H. K. Bodenseh, P. Nowicki, and K. Morgenstern, *J. Mol. Spectrosc.*, **71**, 246 (1978).
31. K. P. R. Nair, J. Hoeft, and E. Tiemann, *Chem. Phys. Lett.*, **58**, 153 (1978).
32. J. M. Brown and T. J. Sears, *J. Mol. Spectrosc.*, **75**, 111 (1979).
33. K. P. R. Nair, J. Hoeft, and E. Tiemann, *J. Mol. Spectrosc.*, **78**, 506 (1979).
34. F. Michelot, B. Bobin, and J. Moret-Bailey, *J. Mol. Spectrosc.*, **76**, 374 (1979).
35. J. T. Hougen, *J. Mol. Spectrosc.*, **81**, 73 (1980).
36. Y. Endo, S. Saito, and E. Hirota, *J. Chem. Phys.*, **74**, 1568 (1981).
37. H. A. Fry and S. G. Kukolich, *J. Chem. Phys.*, **76**, 4387 (1982).
38. A. M. Murray and S. G. Kukolich, *J. Chem. Phys.*, **77**, 4312 (1982).
39. Y. Endo, C. Yamada, S. Saito, and E. Hirota, *J. Chem. Phys.*, **77**, 3376 (1982).
40. S. G. Kukolich and C. D. Cogley, *J. Chem. Phys.*, **76**, 1685 (1982); **77**, 581 (1982).
41. L. M. Tack and S. G. Kukolich, *J. Mol. Spectrosc.*, **94**, 95 (1982).
42. C. D. Cogley, L. M. Tack, and S. G. Kukolich, *J. Chem. Phys.*, **76**, 5669 (1982).
43. M. Ribeaud, A. Bauder, and Hs. H. Günthard, *J. Mol. Spectrosc.*, **42**, 441 (1972).
44. M. Mizushima, *The Theory of Rotating Diatomic Molecules*, Wiley, New York, 1975.
45. Numerical values have been tabulated by M. Rotenberg, R. Bivens, N. Metropolis, and J. K. Wooten, *The 3j and 6j Symbols* MIT Press, Cambridge, Mass., 1959.
46. Equation 15.38 may be obtained by application of (4.62) of Ref. 1 or (4.6.2) of Ref. 2 and the definition of the symmetric rotor functions.
47. E. U. Condon and G. H. Shortley, *Theory of Atomic Spectra*, Cambridge University Press, Cambridge, England, 1959.
48. G. W. Robinson, and C. D. Cornwell, *J. Chem. Phys.*, **21**, 1436 (1953).
49. J. S. Rigden and L. Nygaard, *J. Chem. Phys.*, **44**, 4603 (1966).
50. W. Steinbach and W. Gordy, *Phys. Rev.*, **A8**, 1753 (1973).
51. W. Steinbach, Ph.D. dissertation, Duke Univ., 1974.

# NOTES ON MATRIX MECHANICAL METHODS

---

To facilitate the understanding of certain parts of this book by those not well versed in matrix mechanical methods, we give here a concise description of elements essential to interpretation of microwave spectra.

## PROPERTIES OF SPECIAL MATRICES

We start by considering the properties of some special matrices. There are two types of matrices that are of particular importance in quantum mechanics. They are Hermitian matrices and unitary matrices. Before defining these it is useful to define the transpose and Hermitian adjoint matrix.

The transpose of  $\mathbf{A}$  denoted by  $\tilde{\mathbf{A}}$  is obtained from  $\mathbf{A}$  by an interchange of rows and columns thus

$$\tilde{A}_{nm} = A_{mn} \quad (\text{A.1})$$

The transpose of a column matrix is a row matrix.

The Hermitian adjoint  $\mathbf{A}^\dagger$  of a matrix  $\mathbf{A}$  we obtain by transposing  $\mathbf{A}$  and taking the complex conjugate of each element, that is,

$$\mathbf{A}^\dagger = (\tilde{\mathbf{A}})^* \quad (\text{A.2})$$

or in terms of the matrix elements

$$A_{nm}^\dagger = (\tilde{A}_{nm})^* = A_{mn}^* \quad (\text{A.3})$$

where the asterisk signifies complex conjugation.

A matrix  $\mathbf{A}$  is said to be Hermitian if it is equal to its Hermitian adjoint, that is,

$$\mathbf{A} = \mathbf{A}^\dagger \quad (\text{A.4})$$

or for the elements

$$A_{nm} = A_{mn}^* \quad (\text{A.5})$$

The operators of quantum mechanics representing observables are Hermitian operators since such operators yield real eigenvalues and expectation values. The matrix corresponding to a Hermitian operator is likewise a Hermitian matrix. A Hermitian matrix whose elements are real is a symmetric matrix

for which

$$\mathbf{A} = \tilde{\mathbf{A}} \quad (\text{A.6})$$

A matrix  $\mathbf{A}$  is unitary if its inverse is equal to its Hermitian adjoint

$$\mathbf{A}^{-1} = \mathbf{A}^\dagger \quad (\text{A.7})$$

hence

$$\mathbf{A}\mathbf{A}^{-1} = \mathbf{A}\mathbf{A}^\dagger = \mathbf{E} \quad (\text{A.8})$$

where  $\mathbf{E}$  is a unit matrix ( $E_{nm} = \delta_{nm}$ ) also commonly designated  $\mathbf{I}$ . A real unitary matrix

$$\mathbf{A}^{-1} = \tilde{\mathbf{A}} \quad (\text{A.9})$$

is an orthogonal matrix. Transformations between different orthonormal basis systems are accomplished by unitary matrices. Unitary transformations have the property that they preserve the value of a scalar product, which is naturally required since the observable quantities are obtained from scalar products and must hence be independent of the choice of basis system. A unitary transformation is a generalization to complex space of an orthogonal transformation in real space.

## MATRIX REPRESENTATION OF WAVE FUNCTIONS AND OPERATORS

In wave mechanics, the dynamical variables or observables are represented by linear operators. Each linear operator,  $A$ , has an eigenvalue equation associated with it.

$$A\phi_n = a_n\phi_n \quad (\text{A.10})$$

where  $\phi_n$  is the eigenfunction and  $a_n$  the corresponding eigenvalue of the operator  $A$ . The most important operator is the energy or Hamiltonian operator  $\mathcal{H}$ . The solution of its eigenvalue equation, the Schrödinger equation, yields the energy levels (eigenvalues) and energy eigenstates (eigenfunctions) of the quantum system. In matrix mechanics, the quantum mechanical operators are represented by matrices, and the problem of solving the eigenvalue equation (a differential equation) is replaced by the problem of diagonalizing a matrix.

Consider a set of linearly independent functions  $\phi_1, \phi_2, \dots, \phi_n, \dots$ , such as the set of eigenfunctions generated by the solution of an eigenvalue equation. Throughout our discussion we employ a single index to distinguish the various members of the set  $\{\phi_n\}$  of basis functions. If more than one quantum number is required in order to specify the basis functions, then the index  $n$  must be regarded as standing for the complete set of quantum numbers, viz.,  $n = i, j, k, \dots$ . We shall assume that the basis functions are orthogonal and normalized, i.e.,

$$(\phi_n | \phi_m) = \int \phi_n^* \phi_m d\tau = \delta_{nm} \quad (\text{A.11})$$

where the Kronecker delta is defined by

$$\delta_{nm} = \begin{cases} 0 & \text{if } n \neq m \\ 1 & \text{if } n = m \end{cases} \quad (\text{A.12})$$

Frequently the notation  $(\phi_n|\phi_m)$  is further abbreviated to  $(n|m)$ . The basis functions are said to form a complete set in that any arbitrary wave function may be expanded in terms of them. An arbitrary function  $\psi$  can hence be expressed as

$$\psi = \sum_n C_n \phi_n \quad (\text{A.13})$$

where the  $C$ 's are the expansion coefficients or coordinates of  $\psi$  referred to the basis  $\{\phi_n\}$  and are defined by

$$C_n = (\phi_n|\psi) \quad (\text{A.14})$$

The function  $\psi$  is uniquely specified by enumeration of the coefficients  $C_n$  (in general complex). These may be written as a column matrix

$$\begin{bmatrix} C_1 \\ C_2 \\ \vdots \\ C_n \\ \vdots \end{bmatrix} \quad (\text{A.15})$$

In the language of matrix mechanics we refer to this as the matrix representation of  $\psi$  referred to the basis  $\{\phi_n\}$ . The basis system is, of course, arbitrary, and a different basis may be chosen. Then, however, the list of elements in the column matrix will be altered, and a different matrix representation will be obtained.

The scalar product of two functions  $\chi$  and  $\psi$  denoted by  $(\chi|\psi)$  is given by the product of a row matrix and a column matrix

$$(\chi|\psi) = \int \sum_n B_n^* \phi_n^* \sum_n C_n \phi_n d\tau = \sum_n B_n^* C_n = [B_1^* B_2^* \cdots B_n^* \cdots] \begin{bmatrix} C_1 \\ C_2 \\ \vdots \\ C_n \\ \vdots \end{bmatrix} \quad (\text{A.16})$$

Note that the first factor in the scalar product is the Hermitian adjoint of the column matrix representing  $\chi$ . If the two functions are orthogonal, the above scalar product will vanish.

The matrix representation of the operator  $A$  in the basis  $\{\phi_n\}$  is defined by the equation

$$A_{nm} = (\phi_n|A|\phi_m) = \int \phi_n^* A \phi_m d\tau \quad (\text{A.17})$$

The array of numbers (called matrix elements) calculated by the above relation

may be written as a square matrix **A**, that is,

$$\begin{bmatrix} A_{11} & A_{12} & A_{13} & \dots & \dots \\ A_{21} & A_{22} & \dots & \dots & \dots \\ A_{31} & \dots & \dots & \dots & \dots \\ \vdots & \vdots & \vdots & \ddots & \ddots \end{bmatrix} \quad (\text{A.18})$$

The operator matrix depends on the basis chosen and will have different forms in different basis systems. If the operator represents a measurable quantity, the matrix operator is Hermitian and its elements satisfy (A.5).

The matrix of the sum of two operators **C** ( $=\mathbf{A}+\mathbf{B}$ ) is just the sum of the matrices representing the operators **A** and **B** in the basis  $\{\phi_n\}$ . Hence, the elements of **C** are defined by

$$C_{nm} = A_{nm} + B_{nm} \quad (\text{A.19})$$

The matrix of the product operator **C** ( $=\mathbf{AB}$ ) is obtained from the matrix of **A** and **B** by the usual rule for multiplication of two matrices. The matrix elements of the matrix operator **C** are hence given by

$$C_{nm} = \sum_k A_{nk} B_{km} \quad (\text{A.20})$$

Note that all elements are defined with respect to the same basis. Similarly, the matrix for the product of any number of operators is obtained by multiplication of the corresponding matrices. In general,  $\mathbf{AB} \neq \mathbf{BA}$  since matrix multiplication is noncommutative. Any matrix **A** does, however, commute with its inverse and with a unit matrix **E**; any two diagonal matrices will also commute. If basis functions are chosen which are simultaneous eigenfunctions of two operators **A** and **B**, the corresponding matrices will be diagonal [see (A.33)] and hence commute. This is analogous to the statement that if a function is an eigenfunction of two operators, then the operators commute.

We are now in a position to rewrite any equation of wave mechanics in matrix form. In matrix mechanics, for example, operation on a function  $\psi$  with an operator **A** is represented by the product of a square matrix **A** times the column matrix representing  $\psi$ . The result is a new column matrix (or function). With this in mind and taking cognizance of the definition of a scalar product, we may write

$$(\psi | A | \psi) = [C_1^* C_2^* \cdots C_n^* \cdots] \begin{bmatrix} A_{11} & A_{12} & A_{13} & \dots & \dots \\ A_{21} & A_{22} & \dots & \dots & \dots \\ A_{31} & \dots & \dots & \dots & \dots \\ \vdots & \vdots & \vdots & \ddots & \ddots \end{bmatrix} \begin{bmatrix} C_1 \\ C_2 \\ \vdots \\ C_n \\ \vdots \end{bmatrix} \quad (\text{A.21})$$

This gives the average or expectation value of an observable represented by the operator **A**, for the quantum state  $\psi$ . Evaluation of the average value of an observable thus requires a knowledge of the matrix elements of the operator in a given basis and the expansion coefficients of the state  $\psi$  in that basis.

## CHANGE OF BASIS

Many times it is advantageous to change from one basis to another. Two salient questions then arise: first, how the coordinates of a wave function, that is, its matrix representation, are related in the two basis systems and second, how the matrix of an operator is related in the two basis systems.

Let the connection between the original orthonormal basis functions  $\{\phi_n\}$  and the new set of basis functions  $\{\phi'_n\}$  be written

$$\phi'_n = \sum_m S_{mn} \phi_m \quad n = 1, 2, \dots \quad (\text{A.22})$$

with

$$S_{mn} = (\phi_m | \phi'_n) \quad (\text{A.23})$$

The coefficients  $S_{mn}$  define a square matrix  $\mathbf{S}$ , a transformation matrix, which is a unitary matrix. This insures, for example, that if the original basis functions are orthonormal, then the transformed basis remains orthonormal. If the functions  $\phi_n$  and  $\phi'_n$  are regarded as elements of two column matrices, (A.22) may be written in matrix form as

$$\begin{bmatrix} \phi'_1 \\ \phi'_2 \\ \vdots \\ \phi'_n \\ \vdots \end{bmatrix} = \tilde{\mathbf{S}} \begin{bmatrix} \phi_1 \\ \phi_2 \\ \vdots \\ \phi_n \\ \vdots \end{bmatrix} \quad (\text{A.24})$$

where  $\tilde{\mathbf{S}}$  is the transpose matrix of  $\mathbf{S}$ . The relation between the expansion coefficients of a given wave function  $\psi$  in the two different basis systems is found as follows

$$\psi = \sum_n C_n \phi'_n = \sum_{n,m} S_{mn} C'_m \phi_m = \sum_m C_m \phi_m \quad (\text{A.25})$$

where

$$C_m = \sum_n S_{mn} C'_n \quad (\text{A.26})$$

which gives the old coefficients or coordinates in terms of the new ones. The transformation may be equivalently written as

$$\begin{bmatrix} C_1 \\ C_2 \\ \vdots \\ C_n \\ \vdots \end{bmatrix} = \mathbf{S} \begin{bmatrix} C'_1 \\ C'_2 \\ \vdots \\ C'_n \\ \vdots \end{bmatrix}, \quad \begin{bmatrix} C'_1 \\ C'_2 \\ \vdots \\ C'_n \\ \vdots \end{bmatrix} = \mathbf{S}^\dagger \begin{bmatrix} C_1 \\ C_2 \\ \vdots \\ C_n \\ \vdots \end{bmatrix} \quad (\text{A.27})$$

Note that if the elements of  $\mathbf{S}$  are real, then both the basis functions and coordinates transform in the same manner.

The basis functions  $\{\phi_n\}$  generate a representation of the operator  $A$  through the relation

$$A_{nm} = (\phi_n | A | \phi_m) \quad (A.28)$$

while in terms of the basis functions  $\{\phi'_n\}$ , the operator matrix is defined by

$$A'_{nm} = (\phi'_n | A | \phi'_m) \quad (A.29)$$

The relation between the matrix  $\mathbf{A}$  and  $\mathbf{A}'$  is found by use of (A.22) in the foregoing equation

$$\begin{aligned} A'_{nm} &= \left( \sum_k S_{kn} \phi_k | A | \sum_l S_{lm} \phi_l \right) \\ &= \sum_{k,l} S_{kn}^* S_{lm} (\phi_k | A | \phi_l) \\ &= \sum_{k,l} (\tilde{S}_{nk})^* A_{kl} S_{lm} \\ &= \sum_{k,l} S_{nk}^\dagger A_{kl} S_{lm} \end{aligned} \quad (A.30)$$

In matrix form

$$\mathbf{A}' = \mathbf{S}^\dagger \mathbf{A} \mathbf{S} \quad (A.31)$$

This gives the matrix representation of the operator referred to the new basis in terms of the matrix representation of the operator in the old basis and of the unitary transformation  $\mathbf{S}$  connecting the two basis systems. The matrix  $\mathbf{A}$  is said to be transformed from the  $\phi_n$  representation to the  $\phi'_n$  representation by a similarity transformation. If the transformation has the property that it converts  $\mathbf{A}$  to diagonal form, then it may be referred to as a principal axis transformation. If  $\mathbf{A}$  is Hermitian, then because of the unitary character of  $\mathbf{S}$ ,  $\mathbf{A}'$  is also Hermitian [1]. Furthermore, the form of an equation is unaltered [2] by a transformation such as  $\mathbf{S}$ , and the eigenvalues of a matrix are invariant to a change of basis [3]. If the transformation matrix is real, as is often the case, then (A.31) reads

$$\mathbf{A}' = \tilde{\mathbf{S}} \mathbf{A} \mathbf{S} \quad (A.32)$$

## DIAGONALIZATION OF MATRICES: EIGENVALUES AND EIGENFUNCTIONS

In treating spectra we are especially interested in the eigenfunctions and eigenvalues of Hermitian operators. If the eigenfunctions  $\psi_1, \psi_2, \dots, \psi_n, \dots$  of a Hermitian operator are known and these functions are used as basis functions for construction of the matrix of this operator, then the matrix will

be diagonal. This follows from the orthonormality of the eigenfunctions

$$\langle \psi_m | A | \psi_n \rangle = a_n \langle \psi_m | \psi_n \rangle = a_n \delta_{mn} \quad (\text{A.33})$$

The elements  $a_n$  of the diagonal matrix are the eigenvalues of the operator  $A$ . The diagonal representation of the operator matrix is hence of special interest. Even if the eigenfunctions are initially unknown, it is possible to find a transformation which will diagonalize the operator matrix by means of a similarity transformation. Consider the operator matrix  $\mathbf{A}$  with respect to some orthonormal basis  $\phi_1, \phi_2, \dots, \phi_n, \dots$ . Let the basis functions  $\psi_1, \psi_2, \dots, \psi_n, \dots$ , the eigenfunctions of  $A$ , be related to the arbitrary basis functions by

$$\psi_n = \sum_m S_{mn} \phi_m \quad (\text{A.34})$$

The  $\mathbf{A}$  matrix will be transformed from the  $\phi$  representation to the  $\psi$  representation by

$$\mathbf{S}^\dagger \mathbf{A} \mathbf{S}$$

and for this basis the transformed matrix must be diagonal with elements  $\mathcal{A}_{mn} = a_n \delta_{mn}$  so that

$$\mathbf{S}^\dagger \mathbf{A} \mathbf{S} = \mathcal{A} \quad (\text{A.35})$$

If we premultiply by  $\mathbf{S}$ , since  $\mathbf{S} \mathbf{S}^\dagger = \mathbf{S}^\dagger \mathbf{S} = \mathbf{E}$ , we have

$$\mathbf{A} \mathbf{S} = \mathbf{S} \mathcal{A} \quad (\text{A.36})$$

and for the matrix elements

$$\sum_m A_{km} S_{mn} = \sum_m S_{km} \mathcal{A}_{mn} = S_{kn} a_n = \sum_m \delta_{km} S_{mn} a_n \quad (\text{A.37})$$

or

$$\sum_m (A_{km} - \delta_{km} a_n) S_{mn} = 0 \quad (\text{A.38})$$

Hence, if the transformation diagonalizes the matrix, we are led to a set of simultaneous linear equations defining the  $S_{mn}$  in terms of the  $a_n$  and the  $A_{km}$ . For a given value of  $n$ , (A.38) gives a set of linear equations corresponding to the various values of  $k$ ; these have nontrivial solutions for the  $S_{1n}, S_{2n}, \dots$  if—and only if—the determinant of the matrix of coefficients vanishes

$$|A_{km} - \delta_{km} a_n| = 0 \quad (\text{A.39})$$

The roots of this equations (the secular determinant or secular equation) in  $a_n$  provide the eigenvalues  $a_1, a_2, \dots$ ; by substitution of each of the eigenvalues into the set of (A.38) the corresponding  $\mathbf{S}$  matrix may be evaluated. The  $n$ th eigenvalue, for example, yields the  $n$ th column of  $\mathbf{S}$  that is  $S_{1n}, S_{2n}, \dots$ ; these are the expansion coefficients of the eigenfunction  $\psi_n$  in the basis  $\{\phi_n\}$ . The

columns of  $\mathbf{S}$  are also referred to as the eigenvectors of the matrix  $\mathbf{A}$ . In evaluating the  $S_{nm}$  use is made of the normalization condition, that is,

$$\sum_k S_{nk} S_{nk}^* = 1 \quad (\text{A.40})$$

In summary, the diagonalization of the matrix representation of the operator which is tantamount to the solution of the secular equation gives the eigenvalues. The determination of the transformation matrix  $\mathbf{S}$  which diagonalizes the operator matrix yields the eigenfunctions. In the text, the secular equation is arrived at from a slightly different point of view, viz., by a rewriting of the eigenvalue equation in matrix form.

Of particular importance is the diagonalization of the Hamiltonian matrix. The diagonalization of  $\mathbf{H}$  can be simplified by a knowledge of the operators which commute with the Hamiltonian. If an operator  $A$  commutes with  $\mathcal{H}$  then

$$[\mathcal{H}, A] = \mathcal{H}A - A\mathcal{H} = 0 \quad (\text{A.41})$$

The matrix representation of this equation based on functions which are eigenfunctions of  $A$ , so that  $\mathbf{A}$  is diagonal, is

$$\mathcal{H}_{nm}(A_{mm} - A_{nn}) = 0 \quad (\text{A.42})$$

It therefore follows that  $\mathcal{H}_{nm}$  vanishes if the states  $n$  and  $m$  belong to different eigenvalues of  $A$  ( $A_{nn} \neq A_{mm}$ ). The  $\mathcal{H}$  matrix will hence factor into submatrices with each submatrix involving states with the same eigenvalues for  $A$ . In many cases, more than one operator will commute with  $\mathcal{H}$ . The greatest simplification will result if basis functions are chosen which are simultaneous eigenfunctions of the complete set of commuting operators. The operators which may be considered are not only the commuting observables such as the square of the angular momentum  $P^2$  but also what we might classify as symmetry operators, operators which leave  $\mathcal{H}$  invariant and hence commute with  $\mathcal{H}$ . Consideration therefore of the symmetry of the Hamiltonian also facilitates solution of the diagonalization problem.

## References

1. If  $\mathbf{A}$  is Hermitian we may write  $\mathbf{A}' = \mathbf{S}^\dagger \mathbf{A}^* \mathbf{S}$ ; taking the Hermitian adjoint we have  $(\mathbf{A}')^\dagger = (\mathbf{S}^\dagger \mathbf{A}^* \mathbf{S})^\dagger = \mathbf{S}^\dagger \mathbf{A} \mathbf{S} = \mathbf{A}'$  showing that the Hermiticity is invariant.
2. In the matrix equation  $\chi = \mathbf{A}\psi$  if we multiply by  $\mathbf{S}^\dagger$  then  $\chi' = \mathbf{S}^\dagger \chi = \mathbf{S}^\dagger \mathbf{A}\psi = \mathbf{S}^\dagger \mathbf{A} \mathbf{S} \mathbf{S}^\dagger \psi = \mathbf{A}'\psi$  showing the transformed equation has the same form.
3. The eigenvalues are solutions of the secular equation  $|\mathbf{A} - a\mathbf{E}| = 0$ . Since  $|\mathbf{AB}| = |\mathbf{A}||\mathbf{B}|$  and  $\mathbf{S}^\dagger \mathbf{S} = \mathbf{E}$ , we may write

$$|\mathbf{A} - a\mathbf{E}| = |\mathbf{A} - a\mathbf{E}| |\mathbf{S}^\dagger \mathbf{S}| = |\mathbf{S}^\dagger| |\mathbf{A} - a\mathbf{E}| |\mathbf{S}| = |\mathbf{S}^\dagger \mathbf{A} \mathbf{S} - a\mathbf{E}| = |\mathbf{A}' - a\mathbf{E}|$$

Hence the eigenvalues do not depend on the choice of basis.

# CALCULATION OF THE EIGENVALUES AND EIGENVECTORS OF A HERMITIAN TRIDIAGONAL MATRIX BY THE CONTINUED FRACTION METHOD

---

When the matrix representation of the Hamiltonian operator has a tri-diagonal form

$$\begin{bmatrix} H_{11} & H_{12} & & & & & \\ H_{21} & H_{22} & H_{23} & & & & \\ & \ddots & \ddots & \ddots & & & \\ & & H_{k,k-1} & H_{k,k} & H_{k,k+1} & & \\ & & & \ddots & \ddots & \ddots & \\ & & & & H_{n,n-1} & H_{n,n} & \end{bmatrix} \quad (B.1)$$

the secular equation may be written in continued fraction form. The discussion given by Swalen and Pierce<sup>1</sup> on the continued fraction method will be followed here.

Let  $\mathbf{S}$  be a unitary transformation which diagonalizes  $\mathbf{H}$ , that is,

$$\mathbf{S}^\dagger \mathbf{H} \mathbf{S} = \Lambda \quad (B.2)$$

where  $\Lambda$  is a diagonal matrix. Denoting by  $\mathbf{s}$  a column of  $\mathbf{S}$ , we have for a particular eigenstate the system of homogeneous linear equations

$$(\mathbf{H} - \lambda \mathbf{E}) \mathbf{s} = 0 \quad (B.3)$$

where  $\lambda$  is an element of  $\Lambda$  and  $\mathbf{E}$  is a unit matrix.

To develop the continued fraction about the  $k$ th diagonal element of  $\mathbf{H}$ , let the eigenvector  $\mathbf{s}$  be written as

$$\mathbf{s} = N_k \begin{bmatrix} \vdots \\ \sigma_{k-1} \\ 1 \\ \sigma_{k+1} \\ \vdots \end{bmatrix} \quad (B.4)$$

The column matrix is an unnormalized eigenvector of  $\mathbf{H}$  with the  $k$ th element set equal to unity, and  $N_k$  is the appropriate normalization factor defined explicitly by the equation

$$|N_k|^{-2} = 1 + \sum_{\alpha} [\sigma_{k+\alpha}^* \sigma_{k+\alpha} + \sigma_{k-\alpha}^* \sigma_{k-\alpha}] \quad (B.5)$$

Here and in following equations when the subscript  $k+\alpha$  occurs, the running index  $\alpha$  takes on the values  $1, 2, \dots, n-k$ ; whenever the subscript  $k-\alpha$  appears,  $\alpha$  takes on the values  $1, 2, \dots, k-1$ . The simultaneous equations of relation (B.3) may be written in terms of the elements of the relative eigenvector, the  $k$ th equation is

$$H_{k,k-1}\sigma_{k-1} + (H_{kk} - \lambda) + H_{k,k+1}\sigma_{k+1} = 0 \quad (B.6)$$

Employing the  $(k+\alpha)$ th and  $(k-\alpha)$ th equations we obtain the following recursion relation for the elements of the relative eigenvector

$$\frac{\sigma_{k\pm\alpha}}{\sigma_{k\pm\alpha\mp 1}} = \frac{-H_{k\pm\alpha, k\pm\alpha\mp 1}}{H_{k\pm\alpha, k\pm\alpha} - \lambda + H_{k\pm\alpha, k\pm\alpha\pm 1}(\sigma_{k\pm\alpha\pm 1}/\sigma_{k\pm\alpha})} \quad (B.7)$$

Defining the recursion relation

$$R_{k\pm\alpha} = \lambda - H_{k\pm\alpha, k\pm\alpha} - h_{k\pm\alpha\pm 1}^2/R_{k\pm\alpha\pm 1} \quad (B.8)$$

with

$$h_{k\pm\alpha}^2 = |H_{k\pm\alpha, k\pm\alpha\mp 1}|^2 \quad (B.9)$$

we may write the above recursion relation for the  $\sigma$ 's in compact form

$$\frac{\sigma_{k\pm\alpha}}{\sigma_{k\pm\alpha\mp 1}} = \frac{H_{k\pm\alpha, k\pm\alpha\mp 1}}{R_{k\pm\alpha}} \quad (B.10)$$

The components defined by (B.7) or (B.10) constitute an eigenvector only if (B.6) is satisfied. Note that the limits on  $\alpha$  specified above arise because the quantity  $R_{k\pm\alpha}$  or  $h_{k\pm\alpha}$  is zero when  $(k-\alpha) < 1$  or  $(k+\alpha) > n$ .

If the expressions for  $\sigma_{k-1}$  and  $\sigma_{k+1}$  are inserted in the  $k$ th simultaneous equation, (B.6), one obtains the continued fraction form of the secular equation

$$\lambda = H_{kk} + \frac{h_{k+1}^2}{R_{k+1}} + \frac{h_{k-1}^2}{R_{k-1}} \quad (B.11)$$

The above expression represents the  $k$ th development (the leading term is  $H_{kk}$ ) of the continued fraction form of the secular equation. There are  $n$  such developments corresponding to the  $n$  possible values of  $k$ .

To evaluate the eigenvalues of  $\mathbf{H}$ , we may use a first-order iterative procedure. If interest lies in the  $k$ th eigenvalue and if the off-diagonal elements are small, then  $H_{kk}$  will most nearly approximate the  $k$ th eigenvalue. Substitution of this initial approximation to  $\lambda$  on the right-hand side of (B.11) gives an improved approximation to the eigenvalue. Note that the quantities  $R_{k+1}$  and  $R_{k-1}$  are functions of  $\lambda$ . The improved approximation may now be inserted in (B.11) to give a better approximation, and this process may be continued until the desired accuracy is obtained.

A much more efficient procedure is to use the Newton-Raphson technique, a second-order iterative procedure. Let the function  $f_k(\lambda)$  be defined as

$$f_k(\lambda) = \lambda - H_{kk} - \frac{h_{k+1}^2}{R_{k+1}} - \frac{h_{k-1}^2}{R_{k-1}} \quad (\text{B.12})$$

The roots of  $f_k(\lambda)$  are the eigenvalues of  $\mathbf{H}$ . There are  $n$  functions  $f(\lambda)$  which may be defined; the above equation gives the  $k$ th development of  $f(\lambda)$ . If  $f_k(\lambda)$  is expanded about the  $i$ th approximation  $\lambda^{(i)}$  to an eigenvalue, then

$$f_k(\lambda) = f_k(\lambda^{(i)}) + f'_k(\lambda^{(i)})(\lambda - \lambda^{(i)}) \quad (\text{B.13})$$

where higher-order terms are neglected. From this, we see that for  $f_k(\lambda)$  to be zero the next approximation  $\lambda^{(i+1)}$  should be chosen as

$$\lambda^{(i+1)} = \lambda^{(i)} - \frac{f_k(\lambda^{(i)})}{f'_k(\lambda^{(i)})} \quad (\text{B.14})$$

in which

$$\begin{aligned} f'_k(\lambda) &= \frac{df_k(\lambda)}{d\lambda} \\ &= 1 + \left( \frac{h_{k+1}}{R_{k+1}} \right)^2 \left[ 1 + \left( \frac{h_{k+2}}{R_{k+2}} \right)^2 (1 + \dots) \right] \\ &\quad + \left( \frac{h_{k-1}}{R_{k-1}} \right)^2 \left[ 1 + \left( \frac{h_{k-2}}{R_{k-2}} \right)^2 (1 + \dots) \right] \end{aligned} \quad (\text{B.15})$$

As before, with an initial approximation to the eigenvalue, the function  $f_k(\lambda)$  and its derivative are evaluated, and (B.14) is employed to give an improved approximation. The iterations may be continued until the change in the eigenvalue is small enough to be ignored. This second-order iterative procedure yields the eigenvalues much more rapidly. Since the sum of the diagonal elements of  $\mathbf{H}$  is equal to the sum of the eigenvalues of  $\mathbf{H}$ , that is,

$$\sum_k H_{kk} = \sum_k \lambda_k \quad (\text{B.16})$$

one of the eigenvalues may be computed without solution of the continued fraction equation.

The derivative  $f'_k(\lambda)$  is also related to the normalization constant  $N_k$ . By insertion of (B.10) into (B.5) it can be shown that

$$f'_k(\lambda) = 1 + \sum_{\alpha} (\sigma_{k+\alpha}^* \sigma_{k+\alpha} + \sigma_{k-\alpha}^* \sigma_{k-\alpha}) \quad (B.17)$$

for any  $\lambda$ . If  $\lambda$  is, in particular, an eigenvalue of  $\mathbf{H}$ , that is, (B.11) is satisfied, then  $f'_k(\lambda)$  is related to the normalization constant of the eigenvector

$$|N_k|^2 = \frac{1}{f'_k(\lambda)} \quad (B.18)$$

For convergence that is rapid and to the desired root, both the choice of the initial approximation to the eigenvalue and the choice of development are important. For  $\lambda'$  an eigenvalue of  $\mathbf{H}$ , the best development may be defined as the  $k$ th if

$$f'_k(\lambda') \leq f'_{k \pm \alpha}(\lambda') \quad \alpha = 1, 2, 3, \dots \quad (B.19)$$

from which it follows that

$$\sigma_{k \pm \alpha}^* \sigma_{k \pm \alpha} \leq \sigma_k^* \sigma_k \quad (B.20)$$

for all values of  $\alpha$ . Suppose  $f(\lambda)$  is developed about some arbitrary position  $k'$ . Then, with  $\lambda^0$  as a good approximation to the true eigenvalue  $\lambda'$ , one evaluates  $f'_{k'}(\lambda^0)$ . If the largest term in  $f'_{k'}(\lambda^0)$  is  $\sigma_{k'+j}^* \sigma_{k'+j}$ , then the best development is the  $k$ th, where  $k = k' + j$ .

Although the discussion has focused on the solution of tridiagonal matrices, it may be applied in other cases since it is possible to transform a general Hermitian matrix into tridiagonal form.<sup>2</sup>

## References

1. J. D. Swalen and L. Pierce, *J. Math. Phys.*, **2**, 736 (1961). The reader is also directed to the following additional references on the continued fraction method: (a) G. W. King, R. M. Hainer, and P. C. Cross, *J. Chem. Phys.*, **11**, 27 (1943). (b) M. W. P. Strandberg, *Microwave Spectroscopy*, Wiley, New York, 1954. (c) D. W. Posener, *J. Chem. Phys.*, **24**, 546 (1956). (d) L. Pierce, *J. Math. Phys.*, **2**, 740 (1961).
2. W. Givens, *J. Assoc. Comp. Mach.*, **4**, 298 (1957), and Oak Ridge National Laboratory Report ORNL-1574, March 3, 1954.

## Appendix C

# THE VAN VLECK TRANSFORMATION

---

We wish, in this section, to consider a perturbation technique which has found extensive application. Let the Hamiltonian of interest be divided into two parts

$$\mathcal{H} = \mathcal{H}_0 + \lambda \mathcal{H}' \quad (C.1)$$

where  $\mathcal{H}'$  is referred to as the perturbing Hamiltonian and  $\mathcal{H}_0$  the unperturbed or zero-order Hamiltonian. The parameter  $\lambda$  is introduced for mathematical convenience in keeping track of the various orders of perturbation. It may be considered to vary between 1 and 0 with  $\mathcal{H}$  reducing to  $\mathcal{H}_0$  when  $\lambda=0$ ; when  $\lambda=1$  the full effect of the perturbation is experienced. The eigenfunctions and energy eigenvalues of the unperturbed problem will be denoted by  $\psi_{tr}^0$  and  $E_{tr}^0$ , respectively. The  $E_{tr}^0$ , as the index  $r$  ranges over its values, are a set of near-degenerate or degenerate energy levels while those for the various values of  $t$  are assumed to be more widely separated. In general,  $r$  and  $t$  may each represent a set of quantum numbers. In this basis system,  $\{\psi_{tr}^0\}$ ,  $\mathcal{H}_0$  is diagonal

$$(t, r | \mathcal{H}_0 | t', r') = \delta_{tt'} \delta_{rr'} E_{tr}^0 \quad (C.2)$$

whereas  $\mathcal{H}'$  will, in general, have matrix elements both diagonal and off-diagonal in the two quantum numbers

$$(t, r | \mathcal{H}' | t', r') \neq 0$$

The Hamiltonian matrix is shown schematically in Fig. C.1. To obtain a tractable solution to the energy levels of  $\mathcal{H}$  we seek a unitary transformation such that the transformed Hamiltonian matrix, denoted by  $\tilde{\mathcal{H}}$ , will have no

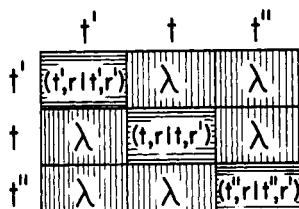


**Fig. C.1** A small portion of the energy matrix is depicted. Each diagonal block represents a group of nearly degenerate energy levels. The diagonal blocks are connected by off-diagonal elements arising from the perturbation term in  $\mathcal{H}$ .

first-order elements connecting states of different  $t$ . As a consequence, matrix elements joining different  $t$ , that is, connections between the various groups of near-degenerate levels, will be reduced in size and can hence be ignored. This yields a set of smaller submatrices (diagonal in  $t$ ) to be solved for the energy levels.

The transformed Hamiltonian matrix takes the form

$$\bar{\mathcal{H}} = \mathbf{T}^\dagger \mathcal{H} \mathbf{T} = \bar{\mathcal{H}}_0 + \lambda \bar{\mathcal{H}}_1 + \lambda^2 \bar{\mathcal{H}}_2 + \dots \quad (\text{C.3})$$

in which the transformed matrix is represented by a power series in the parameter  $\lambda$ , and we restrict ourselves to terms to second-order ( $\lambda^2$ ). The transformation matrix may be expressed as

$$\mathbf{T} = e^{i\lambda S} = \mathbf{E} + i\lambda \mathbf{S} - \frac{1}{2}\lambda^2 \mathbf{S}^2 - \dots \quad (\text{C.4})$$

where the exponential function is defined by the power series expansion and with  $S$  Hermitian,  $T$  is unitary. We hence have from (C.3)

$$\begin{aligned} \bar{\mathcal{H}}_0 &+ \lambda \bar{\mathcal{H}}_1 + \lambda^2 \bar{\mathcal{H}}_2 + \dots \\ &= (\mathbf{E} - i\lambda \mathbf{S} - \frac{1}{2}\lambda^2 \mathbf{S}^2 + \dots)(\mathcal{H}_0 + \lambda \mathcal{H}')(\mathbf{E} + i\lambda \mathbf{S} - i\lambda^2 \mathbf{S}^2 - \dots) \\ &= \mathcal{H}_0 + \lambda[\mathcal{H}' + i(\mathcal{H}_0 \mathbf{S} - \mathbf{S} \mathcal{H}_0)] \\ &\quad + \lambda^2[\mathbf{S} \mathcal{H}_0 \mathbf{S} + i(\mathcal{H}' \mathbf{S} - \mathbf{S} \mathcal{H}') - \frac{1}{2}(\mathbf{S}^2 \mathcal{H}_0 + \mathcal{H}_0 \mathbf{S}^2)] + \dots \end{aligned} \quad (\text{C.5})$$

For all this to be true for all values of  $\lambda$ , the coefficients of like powers of  $\lambda$  must be equal. Therefore, to second-order

$$\bar{\mathcal{H}}_0 = \mathcal{H}_0 \quad (\text{C.6})$$

$$\bar{\mathcal{H}}_1 = \mathcal{H}' + i(\mathcal{H}_0 \mathbf{S} - \mathbf{S} \mathcal{H}_0) \quad (\text{C.7})$$

$$\bar{\mathcal{H}}_2 = \mathbf{S} \mathcal{H}_0 \mathbf{S} + i(\mathcal{H}' \mathbf{S} - \mathbf{S} \mathcal{H}') - \frac{1}{2}(\mathbf{S}^2 \mathcal{H}_0 + \mathcal{H}_0 \mathbf{S}^2) \quad (\text{C.8})$$

The first equation tells us that the matrix  $\bar{\mathcal{H}}_0$  is identical to  $\mathcal{H}_0$ . The remaining relations give the first- and second-order contributions to  $\bar{\mathcal{H}}$  in terms of  $\mathcal{H}$  and the transformation matrix  $S$ .

Writing (C.7) in terms of its matrix elements, we have

$$(t, r | \bar{\mathcal{H}}_1 | t', r') = (t, r | \mathcal{H}' | t', r') + i(t, r | \mathcal{H}_0 \mathbf{S} - \mathbf{S} \mathcal{H}_0 | t', r') \quad (\text{C.9})$$

Now we wish to choose the transformation such that no first-order connections exist between the diagonal  $t$  block and the rest of the matrix, i.e.,

$$(t, r | \mathcal{H}_1 | t', r') = 0 \quad \text{for } t' \neq t \quad (\text{C.10})$$

Such connections are thereby reduced to second-order; they appear in  $\mathcal{H}_2$ . This condition from (C.9) requires that  $S$  be chosen so that

$$(t, r | S | t', r') \{(t, r | \mathcal{H}_0 | t, r) - (t', r' | \mathcal{H}_0 | t', r')\} = i(t, r | \mathcal{H}' | t', r') \quad (\text{C.11})$$

or

$$(t, r | S | t', r') = \frac{i(t, r | \mathcal{H}' | t', r')}{E_{tr}^0 - E_{t'r'}^0} \quad (\text{C.12})$$

where we have taken cognizance of the fact that  $\mathcal{H}_0$  is diagonal in the basis chosen. Similarly from (C.7) or the Hermitian property of  $\mathbf{S}$  we find

$$(t', r' | S | t, r) = \frac{-i(t', r' | \mathcal{H}' | t, r)}{E_{tr}^0 - E_{t'r'}^0} \quad (C.13)$$

The remaining elements of  $\mathbf{S}$  may be conveniently set equal to zero,

$$(t, r | S | t, r') = 0 \quad (C.14)$$

$$(t', r' | S | t'', r'') = 0 \quad \text{for } t', t'' \neq t \quad (C.15)$$

From this latter choice of the elements of  $\mathbf{S}$  we have

$$(t, r | \bar{\mathcal{H}}_1 | t, r') = (t, r | \mathcal{H}' | t, r') \quad (C.16)$$

for the elements of the  $t$ -block and

$$(t', r' | \bar{\mathcal{H}}_1 | t'', r'') = (t', r' | \mathcal{H}' | t'', r'') \quad (C.17)$$

for  $t', t'' \neq t$ . The transformation thus affects connections of the type  $(t|t')$  only.

With our choice of elements of  $\mathbf{S}$ , the desired effect of reducing elements of the type  $(t|t')$  in  $\mathcal{H}$  to  $\lambda^2$  has been accomplished. Without the transformation, the  $(t|t)$  block could be separated from the rest of the matrix only if terms in  $\lambda \mathcal{H}'$  were neglected. See Fig. C.1. In the transformation process, elements of the  $(t|t)$  block are modified. We now proceed to evaluate this modification by considering the contribution of  $\bar{\mathcal{H}}_2$ . The matrix elements diagonal in  $t$  are given by

$$\begin{aligned} (t, r | \bar{\mathcal{H}}_2 | t, r') &= \sum_{t'', r''} [E_{t''r''}^0 (t, r | S | t'', r'') (t'', r'' | S | t, r') \\ &\quad + i(t, r | \mathcal{H}' | t'', r'') (t'', r'' | S | t, r') - i(t, r | S | t'', r'') (t'', r'' | \mathcal{H}' | t, r')] \\ &\quad - \frac{1}{2} (E_{tr}^0 + E_{t'r'}^0) (t, r | S | t'', r'') (t'', r'' | S | t, r')] \end{aligned}$$

Employing Eqs. (C.12) and (C.13) and collecting terms gives

$$(t, r | \bar{\mathcal{H}}_2 | t, r') = \frac{1}{2} \sum'_{t'', r''} (t, r | \mathcal{H}' | (t'', r'') (t'', r'' | \mathcal{H}' | t, r') \left( \frac{1}{E_{tr}^0 - E_{t''r''}^0} + \frac{1}{E_{tr'}^0 - E_{t''r''}^0} \right) \quad (C.18)$$

The term  $t'' = t$  is excluded from the sum. If only one level is present in the  $t$  block, viz.,  $r' = r$ , then the above reduces to the second-order energy contribution of ordinary nondegenerate perturbation theory

$$\sum'_{t''r''} \frac{(t, r | \mathcal{H}' | t'', r'') (t'', r'' | \mathcal{H}' | t, r)}{E_{tr}^0 - E_{t''r''}^0} \quad (C.19)$$

where the  $E_{t''r''}^0$  are not near  $E_{tr}^0$ .

Recapitulating, we can neglect the connections between the  $(t|t)$  block and the rest of the matrix, since these have been reduced by the transformation to order  $\lambda^2$ . Diagonalization of this smaller matrix yields the energy levels of the group of near-degenerate or degenerate states, the matrix elements of the  $(t|t)$

block being given to second-order by

$$(t, r | \bar{\mathcal{H}} | t, r') = (t, r | \mathcal{H}_0 | t, r') + (t, r | \mathcal{H}' | t, r') + \frac{1}{2} \sum'_{t'', r''} (t, r | \mathcal{H}' | t'', r'') (t'', r'' | \mathcal{H}' | t, r') \\ \times \left( \frac{1}{E_{tr}^0 - E_{t''r''}^0} + \frac{1}{E_{tr'}^0 - E_{t''r''}^0} \right) \quad (\text{C.20})$$

with  $t'' \neq t$ ,  $(t, r | \mathcal{H}_0 | t, r') = \delta_{rr'} E_{tr}^0$  and  $\mathcal{H}'$  the perturbation.

In the text, this perturbation procedure is employed in the discussion of the Stark effect of asymmetric rotors; in the discussion of internal and over-all rotation it is exploited to give approximate diagonalization in the internal rotation quantum number.

## Appendix D

# FUNDAMENTAL CONSTANTS AND CONVERSION FACTORS

---

### *Fundamental Physical Constants<sup>a</sup>*

Speed of light	<i>c</i>	$(2.997925 \pm 0.000001) \times 10^{10}$ cm/sec
Electronic charge	<i>e</i>	$(4.80298 \pm 0.00007) \times 10^{-10}$ esu
		$(1.60210 \pm 0.00002) \times 10^{-20}$ emu
Avogadro's constant	<i>N</i>	$(6.02252 \pm 0.00009) \times 10^{23}$ molecules/mole
1 amu	<i>M(C<sup>12</sup>)</i> /12	$(1.66043 \pm 0.00002) \times 10^{-24}$ g
Electron rest mass	<i>m<sub>e</sub></i>	$(9.10908 \pm 0.00013) \times 10^{-28}$ g
Proton rest mass	<i>m<sub>p</sub></i>	$(1.67252 \pm 0.00003) \times 10^{-24}$ g
Neutron rest mass	<i>m<sub>n</sub></i>	$(1.67482 \pm 0.00003) \times 10^{-24}$ g
Planck's constant	<i>h</i>	$(6.62559 \pm 0.00016) \times 10^{-27}$ erg sec
Fine structure constant (e <sup>2</sup> /hc)	<i>α</i>	$(7.29720 \pm 0.00003) \times 10^{-3}$
Bohr magneton (eħ/2m <sub>e</sub> c)	<i>β</i>	$(9.2732 \pm 0.0002) \times 10^{-21}$ erg/gauss
Nuclear magneton (eħ/2m <sub>p</sub> c)	<i>β<sub>I</sub></i>	$(5.05050 \pm 0.00013) \times 10^{-24}$ erg/gauss
Boltzmann's constant	<i>k</i>	$(1.38054 \pm 0.00006) \times 10^{-16}$ erg/deg
Rydberg constant	<i>R<sub>∞</sub></i>	$(1.0973731 \pm 0.0000001) \times 10^5$ cm <sup>-1</sup>
Bohr radius	<i>a<sub>0</sub></i>	$(5.29167 \pm 0.00002) \times 10^{-9}$ cm

### *Conversion Factors and Equivalents*

1 electron-volt/particle	= 1.60210 × 10 <sup>-12</sup> erg
	= 8065.73 cm <sup>-1</sup>
	= 23061 cal/mole
1 calorie (thermochemical)	= 4.184 × 10 <sup>7</sup> erg
1 erg	= 1.50930 × 10 <sup>20</sup> Mc
1 statvolt	= 299.8 volt
Standard volume, <i>V<sub>0</sub></i>	= 22413.6 cm <sup>3</sup> /mole
Gas constant, <i>R<sub>0</sub></i>	= 0.082053 liter atm/mole deg
	= 82.055 cm <sup>3</sup> atm/mole deg
	= 1.9872 cal/mole deg
Degree Kelvin (°K)	T(°K) = T(°C) + 273.15
Rotational constant	$B(\text{Mc}) = \frac{5.05376 \times 10^5}{I_b(\text{amu } \text{\AA}^2)}$
Stark effect constant	$\mu\mathcal{E} = 0.50344 \text{ (MHz)/(debye volt/cm)}$
Reduced barrier height	$s = \frac{4.6602 V_3(\text{cal/mole})}{F(\text{GHz})}$

<sup>a</sup>From E. R. Cohen and J. W. M. DuMond, *Rev. Mod. Phys.*, **37**, 537 (1965). The unified scale of atomic masses is used throughout (C<sup>12</sup> = 12).



## Appendix E

# ISOTOPIC ABUNDANCES, MASSES, AND MOMENTS

---

The relative isotopic abundances have been taken from the compilation of G. H. Fuller, *Nuclear Data Tables*, 1959. The masses are after J. H. E. Mattauch, W. Thiele, and A. H. Wapstra, *Nuclear Phys.*, **67**, 1 (1965). The nuclidic masses are for the new unified scale, which is based on the assignment of mass 12 to the isotope  $^{12}\text{C}$ . The last place quoted in the masses is uncertain.

The nuclear spins and moments are from a compilation by G. H. Fuller and V. W. Cohen, *Appendix I to Nuclear Data Sheets*, May 1965. The zero spins enclosed by parentheses are based on the absence of observable hyperfine structure. A diamagnetic correction has been applied to the nuclear magnetic moments values listed.

## Isotopic Abundances, Masses, and Moments

Atomic Number	Element	Symbol	Mass Number	Mass (amu)	Relative Abundance (%)	Spin	Nuclear Magnetic Dipole Moment $\mu$	Nuclear Electric Quadrupole Moment $Q$ [in units of barns ( $10^{-24}$ cm $^2$ )]
							(in units of nuclear magnetons)	
1	Hydrogen	H	1	1.00782519	99.9850	$\frac{1}{2}$	2.79278	0.0028
			2	2.0141022	0.01492	1	0.85742	
2	Helium	He	3	3.0160297	$1.37 \times 10^{-4}$	$\frac{1}{2}$	-2.1276	-0.0008
			4	4.0026031	99.999863	0		
3	Lithium	Li	6	6.015125	7.42	1	0.82201	-0.04
			7	7.016004	92.58	$\frac{3}{2}$	3.2564	
							$\left(\frac{^6\text{Li}}{^7\text{Li}}\right)^a = 0.0176 \pm 0.0010$	
4	Beryllium	Be	9	9.012186	100	$\frac{3}{2}$	-1.1776	$\pm 0.03$
5	Boron	B	10	10.0129388	19.61	3	1.8007	0.08
			11	11.0093053	80.39	$\frac{3}{2}$	2.6885	0.04
							$\left(\frac{^{10}\text{B}}{^{11}\text{B}}\right)^a = 2.084 \pm 0.002$	
6	Carbon	C	12	12.0000000	98.893	0		
			13	13.0033544	1.107	$\frac{1}{2}$	0.7024	
7	Nitrogen	N	14	14.0030744	99.6337	1	0.4036	0.01
			15	15.0001077	0.3663	$\frac{1}{2}$	-0.2831	0.0000845
8	Oxygen	O	16	15.9949150	99.759	0		
			17	16.999133	0.0374	$\frac{5}{2}$	-1.8937	-0.026
			18	17.9991600	0.2039	0		
9	Fluorine	F	19	18.9984046	100	$\frac{1}{2}$	2.6287	

10	Neon	Ne	20	19.9924405	90.92	(0)		
			21	20.993849	0.257	$\frac{3}{2}$	-0.6618	0.09
			22	21.9913847	8.82	(0)		
11	Sodium	Na	23	22.989771	100	$\frac{3}{2}$	2.2176	0.11
12	Magnesium	Mg	24	23.985042	78.70	(0)		
			25	24.985839	10.13	$\frac{5}{2}$	-0.8553	0.22
			26	25.982593	11.17	(0)		
13	Aluminum	Al	27	26.981539	100	$\frac{5}{2}$	3.6414	0.15
14	Silicon	Si	28	27.976929	92.21	(0)		
			29	28.976496	4.70	$\frac{1}{2}$	-0.5553	
			30	29.973763	3.09	(0)		
15	Phosphorus	P	31	30.973765	100	$\frac{1}{2}$	1.1317	
16	Sulfur	S	32	31.9720737	95.0	0		
			33	32.971462	0.760	$\frac{3}{2}$	0.6434	-0.055
			34	33.967865	4.22	(0)		
			36	35.967090	0.0136	(0)		
17	Chlorine	Cl	35	34.968851	75.529	$\frac{3}{2}$	0.82183	-0.079
			37	36.965899	24.471	$\frac{3}{2}$	0.68411	-0.062
18	Argon	A	36	35.967545	0.337	(0)	$\left(\frac{^{35}\text{Cl}}{^{37}\text{Cl}}\right)^a = 1.26878 \pm 0.00015$	
			38	37.962728	0.063	(0)		
			40	39.9623842	99.600	(0)		
19	Potassium	K	39	38.963710	93.10	$\frac{3}{2}$	0.3914	0.09
			40	39.964000	0.01181	4	-1.298	-0.07
			41	40.961832	6.88	$\frac{3}{2}$	0.2148	$\pm 0.11$
							$\left(\frac{^{41}\text{K}}{^{39}\text{K}}\right)^a = 1.220 \pm 0.002$	

## Isotopic Abundances, Masses, and Moments

<i>Atomic Number</i>	<i>Element</i>	<i>Symbol</i>	<i>Mass Number</i>	<i>Mass (amu)</i>	<i>Relative Abundance (%)</i>	<i>Spin</i>	<i>Nuclear Magnetic Dipole Moment <math>\mu</math> (in units of nuclear magnetons)</i>	<i>Nuclear Electric Quadrupole Moment <math>Q</math> [in units of barns (<math>10^{-24}</math> cm<math>^2</math>)]</i>
20	Calcium	Ca	40	39.962589	96.97	(0)		
			42	41.958625	0.64			
			43	42.958780	0.145	$\frac{7}{2}$	-1.317	
			44	43.955491	2.06			
			46	45.95369	0.0033			
			48	47.95253	0.185			
21	Scandium	Sc	45	44.955919	100	$\frac{7}{2}$	4.7564	-0.22
22	Titanium	Ti	46	45.952632	7.93			
			47	46.951769	7.28	$\frac{5}{2}$	-0.7884	
			48	47.947950	73.94	0	-1.1040	
			49	48.947870	5.51	$\frac{7}{2}$	-1.1040	
			50	49.944786	5.34			
			51	49.947164	0.24	6	3.3470	
23	Vanadium	V	50	50.943961	99.76	$\frac{7}{2}$	5.148	0.27
24	Chromium	Cr	50	49.946055	4.31			
			52	51.940513	83.76			
			53	52.940653	9.55	$\frac{3}{2}$	-0.4744	-0.03
			54	53.938882	2.38			
25	Manganese	Mn	55	54.938050	100	$\frac{5}{2}$	3.468	0.4
26	Iron	Fe	54	53.939617	5.82			
			56	55.934936	91.66			
			57	56.935398	2.19	$\frac{1}{2}$	0.0905	
			58	57.933282	0.33			

27	Cobalt	Co	59	58.933189	100	$\frac{7}{2}$	4.649	0.4
28	Nickel	Ni	58	57.935342	67.88			
			60	59.930787	26.23			
			61	60.931056	1.19			
			62	61.928342	3.66			
			64	63.927958	1.08			
29	Copper	Cu	63	62.929592	69.09	$\frac{3}{2}$	2.226	-0.18
			65	64.927786	30.91	$\frac{3}{2}$	2.385	-0.17
							$\left(\frac{^{63}\text{Cu}}{^{65}\text{Cu}}\right)^a = 1.0806 \pm 0.0003$	
30	Zinc	Zn	64	63.929145	48.89	(0)		
			66	65.926052	27.81	(0)		
			67	66.92715	4.11	$\frac{5}{2}$	0.8757	0.17
			68	67.924857	18.57	(0)		
			70	69.925334	0.62			
31	Gallium	Ga	69	68.925574	60.4	$\frac{3}{2}$	2.016	0.19
			71	70.924706	39.6	$\frac{3}{2}$	2.562	0.12
							$\left(\frac{^{69}\text{Ga}}{^{71}\text{Ga}}\right)^a = 1.5867 \pm 0.0004$	
32	Germanium	Ge	70	69.924252	20.52	(0)		
			72	71.922082	27.43	(0)		
			73	72.923463	7.76	$\frac{9}{2}$	-0.8792	-0.22
			74	73.921181	36.54	(0)		
			76	75.921405	7.76	(0)		
33	Arsenic	As	75	74.921596	100	$\frac{3}{2}$	1.439	0.29
34	Selenium	Se	74	73.922476	0.87	(0)		
			76	75.919207	9.02	(0)		
			77	76.919911	7.58	$\frac{1}{2}$	0.534	
			78	77.917314	23.52	0		

## Isotopic Abundances, Masses, and Moments

<i>Atomic Number</i>	<i>Element</i>	<i>Symbol</i>	<i>Mass Number</i>	<i>Mass (amu)</i>	<i>Relative Abundance (%)</i>	<i>Spin</i>	<i>Nuclear Magnetic Dipole Moment <math>\mu</math> (in units of nuclear magnetons)</i>	<i>Nuclear Electric Quadrupole Moment <math>Q</math> [in units of barns (<math>10^{-24}</math> cm<math>^2</math>)]</i>
35	Bromine	Br	80	79.916527	49.82	0		
			82	81.916707	9.19	(0)		
			79	78.918329	50.537	$\frac{3}{2}$	2.106	0.31
			81	80.916292	49.463	$\frac{3}{2}$	2.270	0.26
36	Krypton	Kr	78	77.920403	0.354			
			80	78.916380	2.27			
			82	81.913282	11.56	(0)		
			83	82.914131	11.55	$\frac{9}{2}$	-0.970	0.23
			84	85.911503	56.90	(0)		
			86	85.910616	17.37	(0)		
37	Rubidium	Rb	85	84.911800	72.15	$\frac{5}{2}$	1.3527	0.28
			87	86.909187	27.85	$\frac{3}{2}$	2.7506	0.14
							$\left(\frac{^{85}\text{Rb}}{^{87}\text{Rb}}\right)^a = 2.0669$	$\pm 0.0005$
38	Strontium	Sr	84	83.913430	0.56			
			86	85.909285	9.86	(0)		
			87	86.908892	7.02	$\frac{9}{2}$	-1.093	0.36
			88	87.905641	82.56	(0)		
39	Yttrium	Y	89	88.905872	100	$\frac{1}{2}$	-0.1373	

40	Zirconium	Zr	90	89.904700	51.46			
			91	90.905642	11.23	$\frac{5}{2}$	-1.303	
			92	91.905031	17.11			
			94	93.906313	17.40			
			95	94.905839	15.72	$\frac{5}{2}$		
			96	95.908286	2.80			
41	Niobium	Nb	93	92.906382	100	$\frac{9}{2}$	6.167	-0.22
42	Molybdenum	Mo	92	91.906810	15.84	(0)		
			94	93.905090	9.04	(0)		
			95	94.905839	15.72	$\frac{5}{2}$	-0.9135	
			96	95.904674	16.53	(0)		
			97	96.906022	9.46	$\frac{5}{2}$	-0.9327	
			98	97.905409	23.78	(0)		
			100	99.907475	9.63	(0)		
44	Ruthenium	Ru	96	95.907598	5.51	$\frac{5}{2}$	-0.63	
			98	97.905289	1.87			
			99	98.905936	12.72	$\frac{5}{2}$	-0.63	
			100	99.904218	12.62			
			101	100.905577	17.07	$\frac{5}{2}$	-0.69	
			102	101.904348	31.61			
			104	103.905430	18.58			
45	Rhodium	Rh	103	102.905511	100	$\frac{1}{2}$	-0.0883	
46	Palladium	Pd	102	101.90561	0.96			
			104	103.90401	10.97			
			105	104.90506	22.23	$\frac{5}{2}$	-0.6015	
			106	105.903479	27.33			
			108	107.903891	26.71			
			110	109.90516	11.81			

$$\left( \frac{^{97}\text{Mo}}{^{95}\text{Mo}} \right)^a > \pm 1$$

## Isotopic Abundances, Masses, and Moments

<i>Atomic Number</i>	<i>Element</i>	<i>Symbol</i>	<i>Mass Number</i>	<i>Mass (amu)</i>	<i>Relative Abundance (%)</i>	<i>Spin</i>	<i>Nuclear Magnetic Dipole Moment <math>\mu</math></i> <i>(in units of nuclear magnetons)</i>	<i>Nuclear Electric Quadrupole Moment <math>Q</math></i> <i>[in units of barns (<math>10^{-24} \text{ cm}^2</math>)]</i>
47	Silver	Ag	107	106.905094	51.35	$\frac{1}{2}$	-0.1135	
			109	108.904756	48.65	$\frac{1}{2}$	-0.1305	
48	Cadmium	Cd	106	105.906463	1.215			
			108	107.904187	0.875			
			110	109.903012	12.39	(0)		
			111	110.904188	12.75	$\frac{1}{2}$	-0.5950	
			112	111.902763	24.07	(0)		
			113	112.904409	12.26	$\frac{1}{2}$	-0.6224	
			114	113.903360	28.86	(0)		
49	Indium	In	116	115.904762	7.58	(0)		
			113	112.904089	4.28	$\frac{9}{2}$	5.523	0.82
			115	114.903871	95.72	$\frac{9}{2}$	5.534	0.83
50	Tin	Sn	112	111.90484	0.96			
			114	113.902773	0.66			
			115	114.903346	0.35	$\frac{1}{2}$	-0.918	
			116	115.901745	14.30	(0)		
			117	116.902958	7.61	$\frac{1}{2}$	-1.000	
			118	117.901606	24.03	(0)		
			119	118.903313	8.58	$\frac{1}{2}$	-1.046	
			120	119.902198	32.85	(0)		
			122	121.903441	4.72			
			124	123.905272	5.94			

51	Antimony	Sb	121 123	120.903816 122.904213	57.25 42.75	$\frac{5}{2}$ $\frac{7}{2}$	3.359 2.547	-0.29 -0.37
						$\left(\frac{^{123}\text{Sb}}{^{121}\text{Sb}}\right)^a = 1.274717$ $\pm 0.000010$		
52	Tellurium	Te	120 122 123 124 125 126 128 130	119.90402 121.903066 122.904277 123.902842 124.904418 125.903322 127.904476 129.906238	0.089 2.46 0.87 4.61 6.99 18.71 31.79 34.48	$\frac{1}{2}$ $\frac{1}{2}$ (0) (0) (0)	-.7359 -0.8871	
53	Iodine	I	127	126.904470	100	$\frac{5}{2}$	2.808	-0.79
54	Xenon	Xe	124 126 128 129 130 131 132 134 136	123.9061 125.904288 127.903540 128.904784 129.903509 130.905085 131.904161 133.905397 135.907221	0.096 0.090 1.919 26.44 4.08 21.18 26.89 10.44 8.87	$\frac{1}{2}$ $\frac{3}{2}$ (0) (0) (0)	-0.7768 0.6908 -0.12	
55	Cesium	Cs	133	132.90536	100	$\frac{7}{2}$	2.579	-0.003
56	Barium	Ba	130 132 134 135 136 137	129.90625 131.9051 133.90461 134.9056 135.90430 136.90550	0.101 0.097 2.42 6.59 7.81 11.32	$\frac{3}{2}$ (0) $\frac{3}{2}$ (0) $\frac{3}{2}$	0.8372 0.9366	0.18 0.28

## Isotopic Abundances, Masses, and Moments

Atomic Number	Element	Symbol	Mass Number	Mass (amu)	Relative Abundance (%)	Spin	Nuclear Magnetic Dipole Moment $\mu$	Nuclear Electric Quadrupole Moment $Q$ [in units of barns ( $10^{-24}$ cm $^2$ )]
							(in units of nuclear magnetons)	
57	Lanthanum	La	138	137.90500	71.66	(0)	$\left(\frac{^{137}\text{Ba}}{^{135}\text{Ba}}\right)^a = 1.543 \pm 0.003$	$\begin{aligned} & \pm 0.8 \\ & 0.22 \end{aligned}$
			138	137.90691	0.089	5		
			139	138.90614	99.911	$\frac{7}{2}$		
58	Cerium	Ce	136	135.9071	0.193		$\left(\frac{^{138}\text{La}}{^{139}\text{La}}\right)^a \simeq \mp 3.5$	
			138	137.90583	0.250			
			140	139.90539	88.48			
			142	141.90914	11.07			
59	Praseodymium	Pr	141	140.90760	100	$\frac{5}{2}$	4.5	-0.06
60	Neodymium	Nd	142	141.90766	27.11			
			143	142.90978	12.17	$\frac{7}{2}$	-1.1	-0.6
			144	143.91004	23.85			
			145	144.91254	8.30	$\frac{7}{2}$	-0.71	-0.3
			146	145.91309	17.22			
			148	147.91687	5.73			
			150	149.92092	5.62			
							$\left(\frac{^{143}\text{Nd}}{^{145}\text{Nd}}\right)^a = 1.893 \pm 0.016$	

62	Samarium	Sm	144	143.91199	3.09			
			147	146.91487	14.97	$\frac{7}{2}$	-0.90	< $\pm 0.7$
			148	147.91479	11.24			
			149	148.91718	13.83	$\frac{7}{2}$	-0.75	< $\pm 0.7$
			150	149.91728	7.44			
			152	151.91976	26.72			
			154	153.92228	22.71			
63	Europium	Eu	151	150.91984	47.82	$\frac{5}{2}$	3.464	0.95
			153	152.92124	52.18	$\frac{5}{2}$	1.530	2.42
64	Gadolinium	Gd	152	151.91979	0.200			
			154	153.92093	2.15			
			155	154.92266	14.73	$\frac{3}{2}$	-0.27	1.3
			156	155.92218	20.47			
			157	156.92403	15.68	$\frac{3}{2}$	-0.36	1.5
			158	157.92418	24.87			
			160	159.92712	21.90			
65	Terbium	Tb	159	158.92535	100	$\frac{3}{2}$	$\pm 1.7$	
66	Dysprosium	Dy	156	155.9239	0.0524			
			158	157.92445	0.0902			
			160	159.92520	2.294			
			161	160.92695	18.88	$\frac{5}{2}$	$\pm 0.42$	$\pm 1.1$
			162	161.92680	25.53			
			163	162.92876	24.97	$\frac{5}{2}$	$\pm 0.58$	$\pm 1.3$
			164	163.92920	28.18			
							$\left(\frac{^{163}\text{Dy}}{^{161}\text{Dy}}\right)^a = 1.18 \pm 0.15$	
67	Holmium	Ho	165	164.93042	100	$\frac{7}{2}$	4.1	3.0
68	Erbium	Er	162	161.92874	0.136			
			164	163.92929	1.56			
			166	165.93031	33.41			

## Isotopic Abundances, Masses, and Moments

Atomic Number	Element	Symbol	Mass Number	Mass (amu)	Relative Abundance (%)	Spin	Nuclear Magnetic Dipole Moment $\mu$ (in units of nuclear magnetons)	Nuclear Electric Quadrupole Moment $Q$ [in units of barns ( $10^{-24}$ cm $^2$ )]		
69	Thulium	Tm	167	166.93206	22.94	$\frac{7}{2}$	-0.56	2.8		
			168	167.93238	27.07					
			170	169.93556	14.88					
	Ytterbium	Yb	169	168.93425	100	$\frac{1}{2}$	-0.229			
			168	167.9342	0.135					
			170	169.93502	3.03					
70	Lutetium	Lu	171	170.93643	14.31	$\frac{1}{2}$	0.4930			
			172	171.93636	21.82					
			173	172.93806	16.13	$\frac{5}{2}$	-0.679	3.0		
			174	173.93874	31.84					
			176	175.94268	12.73					
			175	174.94064	97.41	$\frac{7}{2}$	2.23	5.6		
71			176	175.94266	2.59	7	3.18	8.0		
Hafnium	Hf	175	175.94266	2.59						
		174	173.94036	0.18						
		176	175.94157	5.20						
		177	176.94340	18.50	$\frac{7}{2}$	0.61	3			
		178	177.94388	27.14	(0)					
		72			179	178.94603	13.75	$\frac{9}{2}$	-0.47	3
					180	179.9468	35.24	(0)		
Hafnium	Hf	177	176.94340	18.50						
		178	177.94388	27.14						
		179	178.94603	13.75						
		180	179.9468	35.24						
Hafnium	Hf	175	175.94266	2.59						
		176	176.94340	18.50						
		177	177.94388	27.14						
		178	178.94603	13.75						
		179	179.9468	35.24						
		180	180.9476	1.00						

$$\left(\frac{^{175}\text{Lu}}{^{176}\text{Lu}}\right)^a = 0.71 \pm 0.01$$

$$\left(\frac{^{177}\text{Hf}}{^{178}\text{Hf}}\right)^a = 0.99 \pm 0.02$$

73	Tantalum	Ta	180	179.94754	0.0123			
			181	180.94801	99.9877	$\frac{7}{2}$	2.36	4.2
74	Tungsten	W	180	179.94700	0.135			
			182	181.94830	26.41	(0)		
			183	182.95032	14.40	$\frac{1}{2}$	0.117	
			184	183.95103	30.64	(0)		
			186	185.95444	28.41	(0)		
75	Rhenium	Re	185	184.95306	37.07	$\frac{5}{2}$	3.172	2.6
			187	186.95583	62.93	$\frac{5}{2}$	3.204	2.6
							$\left(\frac{^{185}\text{Re}}{^{187}\text{Re}}\right)^a = 1.056 \pm 0.005$	
76	Osmium	Os	184	183.95275	0.018			
			186	185.95387	1.59			
			187	186.95583	1.64	$\frac{1}{2}$	0.067	
			188	187.95608	13.3			
			189	188.95830	16.1	$\frac{3}{2}$	0.6566	0.8
			190	189.95863	26.4			
			192	191.96145	41.0			
77	Iridium	Ir	191	190.96064	37.3	$\frac{3}{2}$	0.18	1.3
			193	192.96301	62.7	$\frac{3}{2}$	0.18	1.2
78	Platinum	Pt	190	189.95995	0.0127			
			192	191.96115	0.78			
			194	193.96273	32.9	(0)		
			195	194.96481	33.8	$\frac{1}{2}$	0.6060	
			196	195.96497	25.3	(0)		
			198	197.96790	7.21			
79	Gold	Au	197	196.96654	100	$\frac{3}{2}$	0.14486	0.58
80	Mercury	Hg	196	195.96582	0.146			
			198	197.966756	10.02	(0)		
			199	198.968279	16.84	$\frac{1}{2}$	0.5027	

## Isotopic Abundances, Masses, and Moments

<i>Atomic Number</i>	<i>Element</i>	<i>Symbol</i>	<i>Mass Number</i>	<i>Mass (amu)</i>	<i>Relative Abundance (%)</i>	<i>Spin</i>	<i>Nuclear Magnetic Dipole Moment <math>\mu</math></i> (in units of nuclear magnetons)	<i>Nuclear Electric Quadrupole Moment <math>Q</math></i> [in units of barns ( $10^{-24}$ cm $^2$ )]
81	Thallium	Tl	200	199.968327	23.13	(0)	-0.5567	0.45
			201	200.970308	13.22	$\frac{3}{2}$		
			202	201.970642	29.80	(0)		
			204	203.973495	6.85	(0)		
82	Lead	Lb	203	202.972353	29.50	$\frac{1}{2}$	1.6115	1.6274
			205	204.974442	70.50	$\frac{1}{2}$		
			204	203.973044	1.48	0.5895	0.5895	
			206	205.974468	23.6	(0)		
83	Bismuth	Bi	207	206.975903	22.6	$\frac{1}{2}$	4.080	-0.34
			208	207.976650	52.3	(0)		
			209	208.980394	100	$\frac{9}{2}$		
			232	232.03812	100	-0.35	4.1	
90	Thorium	Th	234	234.04090	0.0056	$\frac{7}{2}$	4.1	
			235	235.04392	0.7205			
			238	238.05077	99.2739			

<sup>a</sup>Quadrupole moment ratio.

## Appendix F

# BOND RADII

---

Covalent Radii ( $\text{\AA}$ )<sup>a</sup>

Atom	Single Bond Radius	Double Bond Radius	Triple Bond Radius
H	0.32 <sup>b</sup>		
B	0.81	0.71	0.64
C	0.772	0.667	0.603
N	0.74	0.62	0.55
O	0.74	0.62	0.55
F	0.72	0.60	
Si	1.17	1.07	1.00
P	1.10	1.00	0.93
S	1.04	0.94	0.87
Cl	0.99	0.89	
Ge	1.22	1.12	
As	1.21	1.11	
Se	1.17	1.07	
Br	1.14	1.04	
Sn	1.40	1.30	
Sb	1.41	1.31	
Te	1.37	1.27	
I	1.33	1.23	

Van Der Waals Radii ( $\text{\AA}$ )

	H	1.2			
N	1.5	O	1.40	F	1.35
P	1.9	S	1.85	Cl	1.80
As	2.0	Se	2.00	Br	1.95
Sb	2.2	Te	2.20	I	2.15
$\text{CH}_3$	2.0				
$\text{C}_6\text{H}_6$	1.70	= half-thickness of benzene molecule			

<sup>a</sup>From L. Pauling, *Nature of the Chemical Bond*, 3rd ed., Cornell Univ. Press, Ithaca, N.Y., 1960. The bond length  $r_{AB}$  between

(continued)

two atoms *A* and *B* is given by

$$r_{AB} = r_A + r_B - \beta |x_A - x_B|$$

where  $r_A$  and  $r_B$  are the covalent radii of atoms *A* and *B*;  $x_A$  and  $x_B$  are the corresponding electronegativities. A table of electronegativities is given in Appendix G. The empirical constant  $\beta$  is assigned the following values:

$\beta = 0.08 \text{ \AA}$ , for bonds involving one (or two) first-row atom(s).

$\beta = 0.06 \text{ \AA}$ , for bonds between Si, P, or S and a more electronegative atom not in the first row.

$\beta = 0.04 \text{ \AA}$ , for bonds between Ge, As, or Se and a more electronegative atom not in the first row.

$\beta = 0.02 \text{ \AA}$ , for bonds between Sn, Sb, or Te and a more electronegative atom not in the first row.

$\beta = 0$ , for bonds between C and elements of Groups V, VI, and VII not in the first row.

$\beta = 0.06 \text{ \AA}$ , for bonds to hydrogen.<sup>b</sup>

<sup>b</sup>From W. Gordy, W. V. Smith, and R. T. Trambarulo, *Microwave Spectroscopy*, Wiley, New York, 1953.

# Appendix G

## ELECTRONEGATIVITIES OF THE ELEMENTS

---

*Electronegativities as Derived from*

Atomic Number	Element	Atomic Radius and Nuclear Screening <sup>a</sup>	Bond Energies <sup>b</sup>	Selected Value <sup>c</sup>
1	H	2.17	2.1	2.1 <sub>5</sub>
2	He	—	—	—
3	Li	0.96	1.0	0.95
4	Be	1.38	1.5	1.5
5	B	1.91	2.0	2.0
6	C	2.52	2.5	2.5
7	N	3.01	3.0	3.0
8	O	3.47	3.5	3.5
9	F	3.94	4.0	3.9 <sub>5</sub>
10	Ne	—	—	—
11	Na	0.90	0.9	0.9
12	Mg	1.16	1.2	1.2
13	Al	1.48	1.5	1.5
14	Si	1.82	1.8	1.8
15	P	2.19	2.1	2.1
16	S	2.58	2.5	2.5
17	Cl	3.00	3.0	3.0
18	A	—	—	—
19	K	0.82	0.8	0.80
20	Ca	1.03	1.0	1.0
21	Sc	1.3	1.3	1.3
22	Ti	1.6	1.6	1.6
	V <sup>III</sup>	1.4	1.35	1.4
23	V	V <sup>IV</sup> V <sup>V</sup>	1.7 1.9	1.65 ~1.8
				1.9
	Cr	Cr <sup>II</sup> Cr <sup>III</sup> Cr <sup>IV</sup>	1.3 1.5 2.2	1.5 1.6 ~2.1
24				1.4 1.6 2.2
	Mn	Mn <sup>II</sup> Mn <sup>III</sup> Mn <sup>VII</sup>	1.3 1.5 2.6	1.4 1.5 2.5
25				

*Electronegativities as Derived from*

<i>Atomic Number</i>	<i>Element</i>	<i>Atomic Radius and Nuclear Screening<sup>a</sup></i>	<i>Bond Energies<sup>b</sup></i>	<i>Selected Value<sup>c</sup></i>
26	Fe		1.65 1.8	1.7 1.8
27	Co		1.7	1.7
28	Ni		1.7	1.8
29	Cu	Cu <sup>I</sup> Cu <sup>II</sup>	1.8 2.0	1.8 2.0
30	Zn	Zn <sup>II</sup>	1.5	1.5
31	Ga	1.48	1.6	1.5
32	Ge	1.77	1.7	1.8
33	As	2.04	2.0	2.0
34	Se	2.35	2.3 (2.4)	2.4
35	Br	2.68	2.8	2.8
36	Kr	—	—	—
37	Rb	0.79	0.8	0.8
38	Sr	0.98	1.0	1.0
39	Y	1.21	1.2(1.3)	1.2
40	Zr	1.48	1.4 (1.6)	1.5
41	Nb	1.7	~1.6	1.7
42	Mo	Mo <sup>IV</sup> Mo <sup>VI</sup>	1.6 2.1	~1.6 ~2.1
43	Tc	Tc <sup>V</sup> Tc <sup>VII</sup>	1.9 2.3	1.9 2.3
44	Ru		2.05	2.0
45	Rh		2.1	2.1
46	Pd		2.0	2.0
47	Ag		1.8	1.8
48	Cd		1.5	1.5
49	In	In <sup>I</sup>	1.36	1.5
50	Sn	Sn <sup>II</sup> Sn <sup>IV</sup>	1.61 1.8	1.65 (1.7) 1.8
51	Sb	Sb <sup>III</sup> Sb <sup>V</sup>	1.82 2.1	1.8 (1.8) 1.8
52	Te		2.08	2.1
53	I		2.36	2.6 (2.5)
54	Xe	—	—	—
55	Cs		0.78	0.7
56	Ba		0.93	0.85 (0.9)
57	La		1.2	1.1
58	Ce	Ce <sup>III</sup>	1.2	1.05
59	Pr		1.2	1.1
60	Nd		1.2	~1.2
61	Il		1.2	~1.2

*Electronegativities as Derived from*

<i>Atomic Number</i>	<i>Element</i>	<i>Atomic Radius and Nuclear Screening<sup>a</sup></i>	<i>Bond Energies<sup>b</sup></i>	<i>Selected Value<sup>c</sup></i>
62	Sm	1.2		~1.2
63	Eu	1.1		~1.1
64	Gd	1.2		~1.2
65	Tb	1.2		~1.2
66	Dy	1.2		~1.2
67	Ho	1.2		~1.2
68	Er	1.2		~1.2
69	Tm	1.2		~1.2
70	Yb	1.1		~1.1
71	Lu	1.2		~1.2
72	Hf	1.4	~1.3	1.4
73	Ta <sup>III</sup>	1.3	~1.4	1.3
	Ta <sup>V</sup>	1.7		1.7
74	W <sup>IV</sup>	1.6	~1.6	1.6
	W <sup>VI</sup>	2.0	~2.1	2.0
75	Re <sup>V</sup>	1.8		1.8
	Re <sup>VII</sup>	2.2		2.2
76	Os		2.1	2.0
77	Ir		2.1	2.1
78	Pt		2.1	2.1
79	Au		2.3	2.3
80	Hg <sup>I</sup>		1.8	1.8
	Hg <sup>II</sup>		1.9	
81	Tl <sup>I</sup>	1.34	1.5	1.5
	Tl <sup>III</sup>		1.9	1.9
82	Pb <sup>II</sup>	1.56	1.6	1.6
	Pb <sup>IV</sup>		1.8	1.8
83	Bi	1.8	1.8	1.8
84	Po	2.0	2.0	2.0
85	At	2.2	~2.4	2.2
86	Rn	—	—	—
87	Fa	0.76	~0.7	0.7
88	Ra	0.92	~0.8	0.9
89	Ac	1.1	1.0	1.1
90	Th <sup>II</sup>	1.0	1.1	1.0
	Th <sup>IV</sup>	1.4		1.4
91	Pa <sup>III</sup>	1.3	~1.4	1.3
	Pa <sup>V</sup>	1.7		1.7
92	U <sup>IV</sup>	1.5	1.3	1.4
	U <sup>VI</sup>	1.9		1.9
93	Np	1.1		~1.1
94	Pu	1.3		~1.3
95	Am	1.3		~1.3

*Electronegativities as Derived from*

<i>Atomic Number</i>	<i>Element</i>	<i>Atomic Radius and Nuclear Screening<sup>a</sup></i>	<i>Bond Energies<sup>b</sup></i>	<i>Selected Value<sup>c</sup></i>
96	Cm	1.3		~1.3
97	Bk	1.3		~1.3
98	Cf	1.3		~1.3

<sup>a</sup>From method derived by W. Gordy, *Phys. Rev.*, **69**, 604 (1946).

<sup>b</sup>Pauling's scale [*J. Am. Chem. Soc.*, **54**, 3570 (1932)] extended by Haissinsky [*J. Phys. Radium*, **7**, 7 (1946)].

<sup>c</sup>Values selected by Gordy and Thomas from those derived by four different methods [*J. Chem. Phys.*, **24**, 439 (1956)].

## Appendix H

# COMPUTATIONAL PROCEDURE FOR THE VIBRATIONAL EIGENVALUE PROBLEM

---

Relation between internal ( $S$ ) and normal ( $Q$ ) coordinates

$$S = LQ$$

Vibrational, kinetic, and potential energy matrices

$$2T = \tilde{S}G^{-1}\dot{S}, 2V = \tilde{S}FS$$

Vibrational secular determinant ( $GF$  nonsymmetric)

$$GFL = L\Lambda \rightarrow |GF - E\lambda| = 0$$

$\Lambda$  diagonal matrix of eigenvalues  $\lambda_k$ ,  $L$  eigenvector matrix,  $E$  a unit matrix.

- \* Diagonalize symmetric kinetic energy matrix and normalize orthogonal eigenvector matrix

$$\tilde{L}_G^0 GL_G^0 = \Lambda_G, L_G = L_G^0 \Lambda_G^{1/2} [(L_G)_{ij} = (L_G^0)_{ij} (\lambda_G^{1/2})_j]$$

$\Lambda_G$  diagonal matrix of eigenvalues  $\lambda_G$  of  $G$ . Nonorthogonal transformation  $L_G$  matrix thus defined so

$$L_G \tilde{L}_G = G$$

- \* Transformation  $L_G$  operates on  $F$  to give a new secular determinant

$$L_G \tilde{L}_G F L_G \tilde{L}_G^{-1} L = L \Lambda$$

$$\bar{F} L_F = L_F \Lambda \rightarrow |\bar{F} - E\lambda| = 0$$

$$\bar{F} = \tilde{L}_G F L_G \quad \text{and} \quad L_F = L_G^{-1} L$$

- \* Diagonalization of the symmetric transformed  $F$ -matrix gives the frequencies and the orthogonal eigenvector matrix

$$\tilde{L}_F \bar{F} L_F = \Lambda$$

- \* The orthogonal eigenvector matrix gives the original nonorthogonal transformation matrix

$$L = L_G L_F$$

**\* Computational checks**

$$\mathbf{L}\tilde{\mathbf{L}} = \mathbf{G}, \tilde{\mathbf{L}}\mathbf{F}\mathbf{L} = \Lambda$$

The eigenvalue problem in the form  $\mathbf{FL} = \mathbf{G}^{-1}\mathbf{L}\Lambda$  or  $|\mathbf{F} - \mathbf{G}^{-1}\lambda| = 0$  can be solved by the same sequence of steps.  $\mathbf{F}$  and  $\mathbf{G}$  matrices in terms of symmetry coordinates may, of course, be used.

# ENERGIES AND RELATIVE INTENSITIES OF NUCLEAR QUADRUPOLE HYPERFINE STRUCTURE

---

The function  $Y(J, I, F)$  and the relative intensities are tabulated for the most common nuclear spins  $I = \frac{1}{2}, 1, \frac{3}{2}, \frac{5}{2}, \frac{7}{2}$  and  $\frac{9}{2}$ . The  $Y(J, I, F)$  is defined as

$$Y(J, I, F) = \frac{\frac{3}{4}C(C+1) - I(I+1)J(J+1)}{2(2J+3)(2J-1)I(2I-1)}$$

where

$$C = F(F+1) - I(I+1) - J(J+1)$$

and  $F$  takes on the values

$$J+I, J+I-1, \dots, |J-I|$$

The quadrupole energies are given by

$$E_Q = \left[ \frac{eQq_J(2J+3)}{J} \right] Y(J, I, F)$$

Here the appropriate  $q_J$  for a linear, symmetric, or asymmetric rotor must be used (see Chapter IX). The relative intensities [see e.g., (15.142)] have been normalized such that the sum of the intensities of the various hyperfine components of a transition is 100. The intensities for the  $J+1 \rightarrow J$  transitions are obtained by reversal of the arrows in the entries for  $J \rightarrow J+1$ . Thus the entries for  $F \rightarrow F+1$  correspond to  $F+1 \rightarrow F$  and those for  $F \rightarrow F-1$  to  $F-1 \rightarrow F$ .

## Relative Intensities

J	F	Y(JIF)	J→J+1			J→J	
			F→F+1	F→F	F→F-1	F↔F+1	F→F
$I=\frac{1}{2}$							
0	$\frac{1}{2}$	0	66.667	33.333	0	0.0	0.0
1	$\frac{3}{2}$	0	60.000	6.667	0	0.0	55.556
	$\frac{1}{2}$	0	33.333	0.0	0	11.111	22.222
2	$\frac{5}{2}$	0	57.143	2.857	0	0.0	56.000
	$\frac{3}{2}$	0	40.000	0.0	0	4.000	36.000
3	$\frac{7}{2}$	0	55.556	1.587	0	0.0	55.102
	$\frac{5}{2}$	0	42.857	0.0	0	2.041	40.816
4	$\frac{9}{2}$	0	54.545	1.010	0	0.0	54.321
	$\frac{7}{2}$	0	44.444	0.0	0	1.235	43.210
5	$\frac{11}{2}$	0	53.846	0.699	0	0.0	53.719
	$\frac{9}{2}$	0	45.454	0.0	0	0.826	44.628
6	$\frac{13}{2}$	0	53.333	0.513	0	0.0	53.254
	$\frac{11}{2}$	0	46.154	0.0	0	0.592	45.562
7	$\frac{15}{2}$	0	52.941	0.392	0	0.0	52.889
	$\frac{13}{2}$	0	46.667	0.0	0	0.444	46.222
8	$\frac{17}{2}$	0	52.632	0.310	0	0.0	52.595
	$\frac{15}{2}$	0	47.059	0.0	0	0.346	46.713
9	$\frac{19}{2}$	0	52.381	0.251	0	0.0	52.355
	$\frac{17}{2}$	0	47.368	0.0	0	0.277	47.091
10	$\frac{21}{2}$	0	52.174	0.207	0	0.0	52.154
	$\frac{19}{2}$	0	47.619	0.0	0	0.227	47.392
11	$\frac{23}{2}$	0	52.000	0.174	0	0.0	51.985
	$\frac{21}{2}$	0	47.826	0.0	0	0.189	47.637
12	$\frac{25}{2}$	0	51.852	0.148	0	0.0	51.840
	$\frac{23}{2}$	0	48.000	0.0	0	0.160	47.840
13	$\frac{27}{2}$	0	51.724	0.128	0	0.0	51.715
	$\frac{25}{2}$	0	48.148	0.0	0	0.137	48.011
14	$\frac{29}{2}$	0	51.613	0.111	0	0.0	51.605
	$\frac{27}{2}$	0	48.276	0.0	0	0.119	48.157
15	$\frac{31}{2}$	0	51.515	0.098	0	0.0	51.509
	$\frac{29}{2}$	0	48.387	0.0	0	0.104	48.283

## Relative Intensities

J	F	$Y(J, I, F)$	$J \rightarrow J+1$		$J \rightarrow J$		
			$F \rightarrow F+1$	$F \rightarrow F$	$F \rightarrow F-1$	$F \leftrightarrow F+1$	$F \rightarrow F$
$I=1$							
0	1	0.0	55.556	33.333	11.111	0.0	0.0
1	2	0.050000	46.667	8.333	0.556	0.0	41.667
	1	-0.250000	25.000	8.333	0.0	13.889	8.333
	0	0.500000	11.111	0.0	0.0	11.111	0.0
2	3	0.071429	42.857	3.704	0.106	0.0	41.481
	2	-0.250000	29.630	3.704	0.0	5.185	23.148
	1	0.250000	20.000	0.0	0.0	5.000	15.000
3	4	0.038888	40.741	2.083	0.033	0.0	40.179
	3	-0.250000	31.250	2.083	0.0	2.679	28.009
	2	0.200000	23.810	0.0	0.0	2.646	21.164
4	5	0.090909	39.394	1.333	0.013	0.0	39.111
	4	-0.250000	32.000	1.333	0.0	1.630	30.083
	3	0.178571	25.926	0.0	0.0	1.620	24.306
5	6	0.096154	38.462	0.926	0.006	0.0	38.300
	5	-0.250000	32.407	0.926	0.0	1.094	31.148
	4	0.166667	27.273	0.0	0.0	1.091	26.182
6	7	0.100000	37.778	0.680	0.003	0.0	37.677
	6	-0.250000	32.653	0.680	0.0	0.785	31.765
	5	0.159091	28.05	0.0	0.0	0.783	27.422
7	8	0.102941	37.255	0.521	0.002	0.0	37.187
	7	-0.250000	32.813	0.521	0.0	0.590	32.153
	6	0.153846	28.889	0.0	0.0	0.590	28.299
8	9	0.105263	36.842	0.412	0.001	0.0	36.795
	8	-0.250000	32.922	0.412	0.0	0.460	32.414
	7	0.150000	29.412	0.0	0.0	0.460	28.952
9	10	0.107143	36.508	0.333	0.001	0.0	36.474
	9	-0.250000	33.000	0.333	0.0	0.368	32.597
	8	0.147059	29.825	0.0	0.0	0.368	29.456
10	11	0.108696	36.232	0.275	0.001	0.0	36.206
	10	-0.250000	33.058	0.275	0.0	0.302	32.730
	9	0.144737	30.159	0.0	0.0	0.302	29.857
11	12	0.110000	36.000	0.231	0.000	0.0	35.980
	11	-0.250000	33.102	0.231	0.0	0.252	32.830
	10	0.142857	30.435	0.0	0.0	0.252	30.183
12	13	0.111111	35.803	0.197	0.000	0.0	35.787
	12	-0.250000	33.136	0.197	0.0	0.213	32.907
	11	0.141304	30.667	0.0	0.0	0.213	30.454
13	14	0.112069	35.632	0.170	0.000	0.0	35.620
	13	-0.250000	33.163	0.170	0.0	0.183	32.968
	12	0.140000	30.864	0.0	0.0	0.183	30.682

## Relative Intensities

J	F	Y(J, I, F)	J→J+1			J→J	
			F→F+1	F→F	F→F-1	F↔F+1	F→F
<i>I=1 (continued)</i>							
14	15	0.112903	35.484	0.148	0.000	0.0	35.474
	14	-0.250000	33.185	0.148	0.0	0.158	33.017
	13	0.138889	31.035	0.0	0.0	0.158	30.876
15	16	0.113636	35.354	0.130	0.000	0.0	35.345
	15	-0.250000	33.203	0.130	0.0	0.139	33.056
	14	0.137931	31.183	0.0	0.0	0.139	31.044
<i>I=3/2</i>							
0	3/2	0.0	50.000	33.333	16.667	0.0	0.0
1	5/2	0.050000	40.000	9.000	1.000	0.0	35.000
	3/2	-0.200000	21.000	10.667	1.667	15.000	4.444
	1/2	0.250000	8.333	8.333	0.0	13.889	2.778
2	7/2	0.071429	35.714	4.082	0.204	0.0	34.286
	5/2	-0.178571	24.490	5.224	0.286	5.714	17.286
	3/2	0.0	16.000	4.000	0.0	7.000	8.000
	1/2	0.250000	10.000	0.0	0.0	5.000	5.000
3	9/2	0.083333	33.333	2.315	0.066	0.0	32.738
	7/2	-0.166667	25.463	3.023	0.085	2.976	21.769
	5/2	-0.050000	19.133	2.296	0.0	3.827	14.745
	3/2	0.200000	14.286	0.0	0.0	2.857	11.429
4	11/2	0.090909	31.818	1.488	0.028	0.0	31.515
	9/2	-0.159091	25.785	1.959	0.034	1.818	23.583
	7/2	-0.071429	20.741	1.481	0.0	2.377	18.060
	5/2	0.178571	16.667	0.0	0.0	1.786	14.881
5	13/2	0.096154	30.769	1.036	0.013	0.0	30.594
	11/2	-0.153846	25.888	1.369	0.016	1.224	24.437
	9/2	-0.083333	21.694	1.033	0.0	1.612	19.904
	7/2	0.166667	18.182	0.0	0.0	1.212	16.970
6	15/2	0.100000	30.000	0.762	0.007	0.0	29.890
	13/2	-0.150000	25.905	1.010	0.008	0.879	24.882
	11/2	-0.090909	22.316	0.761	0.0	1.162	21.041
	9/2	0.159091	19.231	0.0	0.0	0.874	18.357
7	17/2	0.102941	29.412	0.584	0.004	0.0	29.338
	15/2	-0.147059	25.887	0.775	0.005	0.662	25.128
	13/2	-0.096154	22.750	0.583	0.0	0.877	21.797
	11/2	0.153846	20.000	0.0	0.0	0.659	19.341
8	19/2	0.105263	28.947	0.462	0.003	0.0	28.896
	17/2	-0.144737	25.854	0.613	0.003	0.516	25.270
	15/2	-0.100000	23.068	0.461	0.0	0.685	22.330

## Relative Intensities

J	F	Y(J, I, F)	J→J+1			J→J	
			F→F+1	F→F	F→F-1	F↔F+1	F→F
<i>I=3/2 (continued)</i>							
9	13/2	0.150000	20.588	0.0	0.0	0.515	20.074
	21/2	0.107143	28.571	0.374	0.002	0.0	28.534
	19/2	-0.142857	25.816	0.497	0.002	0.414	25.353
	17/2	-0.102941	23.310	0.374	0.0	0.549	22.722
10	15/2	0.147059	21.053	0.0	0.0	0.413	20.640
	23/2	-0.108696	28.261	0.309	0.001	0.0	28.233
	21/2	-0.141304	25.778	0.412	0.001	0.339	25.401
	19/2	-0.105263	23.500	0.309	0.0	0.450	23.021
11	17/2	0.144737	21.429	0.0	0.0	0.338	21.090
	25/2	0.110000	28.000	0.260	0.001	0.0	27.978
	23/2	-0.140000	25.740	0.346	0.001	0.283	25.428
	21/2	-0.107143	23.653	0.260	0.0	0.376	23.255
12	19/2	0.142857	21.739	0.0	0.0	0.282	21.457
	27/2	0.111111	27.778	0.222	0.001	0.0	27.761
	25/2	-0.138889	25.704	0.295	0.001	0.239	25.442
	23/2	-0.108696	23.778	0.222	0.0	0.318	23.442
13	21/2	0.141304	22.000	0.0	0.0	0.239	21.761
	29/2	0.112069	27.586	0.191	0.000	0.0	27.573
	27/2	-0.137931	25.671	0.254	0.001	0.205	25.447
	25/2	-0.110000	23.883	0.191	0.0	0.273	23.596
14	23/2	0.140000	22.222	0.0	0.0	0.205	22.017
	31/2	0.112903	27.419	0.166	0.000	0.0	27.408
	29/2	-0.137097	25.640	0.222	0.000	0.178	25.447
	27/2	-0.111111	23.971	0.166	0.0	0.237	23.723
15	25/2	0.138889	22.414	0.0	0.0	0.178	22.236
	33/2	0.113636	27.273	0.146	0.000	0.0	27.264
	31/2	-0.136364	25.611	0.195	0.000	0.156	25.443
	29/2	-0.112069	24.047	0.146	0.0	0.207	23.830
	27/2	0.137931	22.581	0.0	0.0	0.156	22.425
<i>I=5/2</i>							
5/2	0.0	44.444	33.333	22.222	0.0	0.0	
7/2	0.050000	33.333	9.524	1.587	0.0	28.571	
1	5/2	-0.160000	17.143	12.190	4.000	15.873	1.905
	3/2	0.140000	6.222	9.333	6.667	15.556	6.667
	9/2	0.071429	28.571	4.409	0.353	0.0	27.161
	7/2	-0.121429	19.400	6.450	0.816	6.173	11.922
2	5/2	-0.071429	12.245	6.612	1.143	8.571	3.429
	3/2	0.071429	6.857	5.418	1.058	8.000	9.148

## Relative Intensities

J	F	Y(J, I, F)	J→J+1			J→J	
			F→F+1	F→F	F→F-1	F↔F+1	F→F
<i>I</i> = $\frac{5}{2}$ (continued)							
3	$\frac{1}{2}$	0.200000	2.963	3.704	0.0	5.185	1.481
	$\frac{11}{2}$	0.083333	25.926	2.525	0.120	0.0	25.325
	$\frac{9}{2}$	-0.100000	19.697	3.848	0.265	3.247	15.713
	$\frac{7}{2}$	-0.100000	14.550	4.157	0.340	4.850	9.095
	$\frac{5}{2}$	-0.006667	10.393	3.628	0.265	5.102	4.898
	$\frac{3}{2}$	0.110000	7.143	2.381	0.0	4.286	2.593
4	$\frac{1}{2}$	0.200000	4.762	0.0	0.0	2.646	2.116
	$\frac{13}{2}$	0.090909	24.242	1.632	0.052	0.0	23.932
	$\frac{11}{2}$	-0.086364	19.580	2.532	0.110	1.994	17.164
	$\frac{9}{2}$	-0.107792	15.598	2.785	0.135	3.064	12.121
	$\frac{7}{2}$	-0.037662	12.256	2.463	0.096	3.333	8.571
	$\frac{5}{2}$	0.071429	9.524	1.587	0.0	2.910	6.349
5	$\frac{3}{2}$	0.178571	7.407	0.0	0.0	1.852	5.556
	$\frac{15}{2}$	0.096154	23.077	1.140	0.026	0.0	22.896
	$\frac{13}{2}$	-0.076923	19.373	1.785	0.054	1.347	17.767
	$\frac{11}{2}$	-0.110256	16.138	1.981	0.064	2.098	13.770
	$\frac{9}{2}$	-0.053846	13.350	1.758	0.043	2.314	10.795
	$\frac{7}{2}$	0.050000	10.999	1.122	0.0	2.043	8.780
6	$\frac{5}{2}$	0.050000	10.999	1.122	0.0	2.043	8.780
	$\frac{3}{2}$	0.166667	9.091	0.0	0.0	1.299	7.792
	$\frac{17}{2}$	0.100000	22.222	0.840	0.014	0.0	22.107
	$\frac{15}{2}$	-0.070000	19.160	1.324	0.029	0.970	18.021
	$\frac{13}{2}$	-0.110909	16.440	1.475	0.034	1.522	14.736
	$\frac{11}{2}$	-0.063636	14.051	1.312	0.022	1.691	12.196
7	$\frac{9}{2}$	0.036364	11.988	0.833	0.0	1.499	10.372
	$\frac{7}{2}$	0.159091	10.256	0.0	0.0	0.950	9.307
	$\frac{19}{2}$	0.102941	21.569	0.645	0.009	0.0	21.491
	$\frac{17}{2}$	-0.064706	18.963	1.020	0.017	0.731	18.166
	$\frac{15}{2}$	-0.110860	16.619	1.140	0.020	1.153	15.339
	$\frac{13}{2}$	-0.070136	14.529	1.014	0.013	1.286	13.128
8	$\frac{11}{2}$	0.026923	12.692	0.641	0.0	1.142	11.470
	$\frac{9}{2}$	0.152846	11.111	0.0	0.0	0.722	10.390
	$\frac{21}{2}$	0.105263	21.053	0.511	0.005	0.0	20.998
	$\frac{19}{2}$	-0.060526	18.788	0.809	0.011	0.571	18.134
	$\frac{17}{2}$	-0.110526	16.729	0.906	0.012	0.903	15.735
	$\frac{15}{2}$	-0.074737	14.873	0.806	0.008	1.009	13.780
9	$\frac{13}{2}$	0.020000	13.217	0.508	0.0	0.897	12.263
	$\frac{11}{2}$	0.150000	11.765	0.0	0.0	0.566	11.199
	$\frac{23}{2}$	0.107143	20.635	0.414	0.004	0.0	20.595
	$\frac{21}{2}$	-0.057143	18.634	0.658	0.007	0.458	18.115

## Relative Intensities

J	F	$Y(J, I, F)$	$J \rightarrow J+1$			$J \rightarrow J$	
			$F \rightarrow F+1$	$F \rightarrow F$	$F \rightarrow F-1$	$F \leftrightarrow F+1$	$F \rightarrow F$
$I = \frac{5}{2}$ (continued)							
10	$\frac{19}{2}$	-0.110084	16.799	0.737	0.008	0.726	16.005
	$\frac{17}{2}$	-0.078151	15.129	0.656	0.005	0.813	14.255
	$\frac{15}{2}$	0.014706	13.622	0.413	0.0	0.722	12.858
	$\frac{13}{2}$	0.147059	12.281	0.0	0.0	0.455	11.826
	$\frac{25}{2}$	0.108696	20.290	0.343	0.003	0.0	20.260
	$\frac{23}{2}$	-0.054348	18.498	0.545	0.005	0.375	18.076
	$\frac{21}{2}$	-0.109611	16.844	0.611	0.005	0.596	16.196
	$\frac{19}{2}$	-0.080778	15.326	0.543	0.003	0.668	14.611
1	$\frac{17}{2}$	0.010526	13.944	0.342	0.0	0.594	13.318
	$\frac{15}{2}$	0.144737	12.698	0.0	0.0	0.373	12.325
	$\frac{27}{2}$	0.110000	20.000	0.288	0.002	0.0	19.977
	$\frac{25}{2}$	-0.052000	18.379	0.459	0.003	0.313	18.029
12	$\frac{23}{2}$	-0.109143	16.873	0.514	0.004	0.498	16.335
	$\frac{21}{2}$	-0.082857	15.482	0.458	0.002	0.559	14.887
	$\frac{19}{2}$	0.007143	14.205	0.28-	0.0	0.497	13.684
	$\frac{17}{2}$	0.142857	13.044	0.0	0.0	0.312	12.731
	$\frac{29}{2}$	0.111111	19.753	0.246	0.001	0.0	19.735
	$\frac{27}{2}$	-0.050000	18.273	0.391	0.003	0.265	17.979
13	$\frac{25}{2}$	-0.108696	16.891	0.439	0.003	0.422	16.437
	$\frac{23}{2}$	-0.084541	15.608	0.391	0.002	0.474	15.105
	$\frac{21}{2}$	0.004348	14.421	0.245	0.0	0.421	13.981
	$\frac{19}{2}$	0.141304	13.333	0.0	0.0	0.265	13.069
	$\frac{31}{2}$	0.112069	19.540	0.212	0.001	0.0	19.526
	$\frac{29}{2}$	-0.048276	18.179	0.338	0.002	0.228	17.928
14	$\frac{27}{2}$	-0.108276	16.903	0.379	0.002	0.363	16.514
	$\frac{25}{2}$	-0.085931	15.711	0.337	0.001	0.407	15.280
	$\frac{23}{2}$	0.002000	14.603	0.212	0.0	0.362	14.226
	$\frac{21}{2}$	0.140000	13.580	0.0	0.0	0.227	13.353
	$\frac{33}{2}$	0.112903	19.355	0.185	0.001	0.0	19.343
	$\frac{31}{2}$	-0.046774	18.095	0.294	0.001	0.197	17.879
15	$\frac{29}{2}$	-0.107885	16.909	0.331	0.002	0.315	16.573
	$\frac{27}{2}$	-0.087097	15.797	0.294	0.001	0.353	15.424
	$\frac{25}{2}$	0.0	14.758	0.184	0.0	0.314	14.431
	$\frac{23}{2}$	0.138889	13.793	0.0	0.0	0.197	13.596
	$\frac{35}{2}$	0.113636	19.192	0.162	0.001	0.0	19.182
	$\frac{33}{2}$	-0.045455	18.019	0.259	0.001	0.173	17.831
	$\frac{31}{2}$	-0.107524	16.912	0.291	0.001	0.276	16.619
	$\frac{29}{2}$	-0.088088	15.870	0.259	0.001	0.310	15.544
	$\frac{27}{2}$	-0.001724	14.892	0.162	0.0	0.275	14.606
	$\frac{25}{2}$	0.137931	13.979	0.0	0.0	0.173	13.806

*Relative Intensities*

J	F	Y(J, I, F)	J→J+1			J→J	
			F→F+1	F→F	F→F-1	F↔F+1	F→F
<i>I=7/2</i>							
0	7/2	0.0	41.667	33.333	25.000	0.0	0.0
1	-9/2	0.050000	30.000	9.722	1.944	0.0	25.463
	-7/2	-0.142857	15.278	12.698	5.357	16.204	1.058
	-5/2	0.107143	5.357	9.643	10.000	16.071	8.929
2	11/2	0.071429	25.000	4.545	0.455	0.0	23.636
	-9/2	-0.096939	16.883	6.926	1.190	6.364	9.470
	-7/2	-0.081633	10.476	7.483	2.041	9.167	1.905
	-5/2	0.025510	5.612	6.531	2.857	8.929	0.071
	-3/2	0.153061	2.143	4.286	3.571	6.000	4.000
3	13/2	0.083333	22.222	2.618	0.160	0.0	21.635
	-11/2	-0.071429	16.827	4.196	0.406	3.365	12.787
	-9/2	-0.097619	12.311	4.885	0.661	5.276	6.629
	-7/2	-0.047619	8.598	4.838	0.850	5.952	2.721
	-5/2	0.035714	5.612	4.209	0.893	5.612	0.638
	-3/2	0.119048	3.274	3.175	0.694	4.464	0.0
	1/2	0.178571	1.488	2.083	0.0	2.679	0.893
4	15/2	0.090909	20.455	1.697	0.071	0.0	20.148
	-13/2	-0.055195	16.485	2.785	0.175	2.074	14.005
	-11/2	-0.097403	13.054	3.338	0.275	3.365	9.324
	-9/2	-0.071892	10.124	3.428	0.337	3.977	5.899
	-7/2	-0.009276	7.660	3.127	0.325	4.012	3.527
	-5/2	0.065399	5.268	2.494	0.212	3.571	2.012
	-3/2	0.132653	4.000	1.556	0.0	2.750	1.185
	1/2	0.178571	2.778	0.0	0.0	1.620	1.157
5	17/2	0.096154	19.231	1.188	0.036	0.0	19.051
	-15/2	-0.043956	16.120	1.974	0.087	1.404	14.460
	-13/2	-0.094322	13.374	2.400	0.134	2.318	10.794
	-11/2	-0.082418	10.974	2.504	0.159	2.797	7.947
	-9/2	-0.032053	8.900	2.318	0.146	2.893	5.820
	-7/2	0.036630	7.139	1.865	0.087	2.652	4.329
	-5/2	0.107143	5.682	1.136	0.0	2.110	3.435
	-3/2	0.166667	4.545	0.0	0.0	1.273	3.273
6	19/2	0.100000	18.333	0.877	0.020	0.0	18.219
	-17/2	-0.035714	15.789	1.470	0.048	1.012	14.607
	-15/2	-0.090909	13.510	1.801	0.073	1.689	11.635
	-13/2	-0.087662	11.484	1.893	0.085	2.060	9.246
	-11/2	-0.045455	9.700	1.764	0.075	2.156	7.385
	-9/2	0.018831	8.152	1.421	0.043	1.998	6.015
	-7/2	0.090909	6.838	0.855	0.0	1.603	5.128
	-5/2	0.159091	5.769	0.0	0.0	0.962	4.808

## Relative Intensities

J	F	Y(J, I, F)	J→J+1			J→J	
			F→F+1	F→F	F→F-1	F↔F+1	F→F
<i>I=7/2 (continued)</i>							
7	$\frac{21}{2}$	0.102941	17.647	0.674	0.012	0.0	17.569
	$\frac{19}{2}$	-0.029412	15.502	1.135	0.029	0.764	14.620
	$\frac{17}{2}$	-0.087750	13.558	1.398	0.043	1.283	12.141
	$\frac{15}{2}$	-0.090498	11.808	1.476	0.049	1.576	10.099
	$\frac{13}{2}$	-0.054137	10.245	1.379	0.042	1.659	8.463
	$\frac{11}{2}$	0.006787	8.866	1.111	0.023	1.545	7.213
	$\frac{9}{2}$	0.079670	7.670	0.663	0.0	1.242	6.351
	$\frac{7}{2}$	0.153846	6.667	0.0	0.0	0.741	5.926
8	$\frac{23}{2}$	0.105263	17.105	0.534	0.008	0.0	17.050
	$\frac{21}{2}$	-0.024436	15.256	0.903	0.018	0.597	14.573
	$\frac{19}{2}$	-0.084962	13.563	1.115	0.027	1.007	12.458
	$\frac{17}{2}$	-0.092105	12.024	1.181	0.030	1.242	10.682
	$\frac{15}{2}$	-0.060150	10.634	1.105	0.026	1.312	9.227
	$\frac{13}{2}$	-0.001880	9.391	0.889	0.014	1.225	8.084
	$\frac{11}{2}$	0.071429	8.296	0.528	0.0	0.985	7.254
	$\frac{9}{2}$	0.150000	7.353	0.0	0.0	0.585	6.768
9	$\frac{25}{2}$	0.107143	16.667	0.433	0.005	0.0	16.626
	$\frac{23}{2}$	-0.020408	15.043	0.734	0.012	0.479	14.500
	$\frac{21}{2}$	-0.082533	13.546	0.910	0.018	0.810	12.661
	$\frac{19}{2}$	-0.093037	12.173	0.965	0.020	1.003	11.094
	$\frac{17}{2}$	-0.064526	10.922	0.903	0.017	1.062	9.787
	$\frac{15}{2}$	-0.008403	9.791	0.727	0.009	0.993	8.735
	$\frac{13}{2}$	0.065126	8.781	0.430	0.0	0.798	7.940
	$\frac{11}{2}$	0.147059	7.895	0.0	0.0	0.472	7.422
10	$\frac{27}{2}$	0.108696	16.304	0.359	0.004	0.0	16.274
	$\frac{25}{2}$	-0.017081	14.859	0.609	0.008	0.393	14.417
	$\frac{23}{2}$	-0.080418	13.518	0.756	0.012	0.666	12.794
	$\frac{21}{2}$	-0.093576	12.279	0.802	0.013	0.826	11.393
	$\frac{19}{2}$	-0.067833	11.142	0.752	0.011	0.876	10.208
	$\frac{17}{2}$	-0.013485	10.104	0.604	0.006	0.820	9.235
	$\frac{15}{2}$	0.060150	9.167	0.357	0.0	0.659	8.476
	$\frac{13}{2}$	0.144737	8.333	0.0	0.0	0.389	7.944
11	$\frac{29}{2}$	0.110000	16.000	0.302	0.003	0.0	15.976
	$\frac{27}{2}$	-0.014286	14.698	0.513	0.006	0.382	14.332
	$\frac{25}{2}$	-0.078571	13.484	0.637	0.009	0.557	12.882
	$\frac{23}{2}$	-0.093877	12.357	0.678	0.009	0.692	11.617
	$\frac{21}{2}$	-0.070408	11.314	0.635	0.008	0.735	10.534
	$\frac{19}{2}$	-0.017551	10.356	0.510	0.004	0.688	9.629
	$\frac{17}{2}$	0.056122	9.482	0.300	0.0	0.553	8.905
	$\frac{15}{2}$	0.142857	8.696	0.0	0.0	0.326	8.370

## Relative Intensities

J	F	Y(J, I, F)	J→J+1		J→J		
			F→F+1	F→F	F→F-1	F↔F+1	F→F
$I = \frac{7}{2}$							
12	$\frac{31}{2}$	0.111111	15.741	0.257	0.002	0.0	15.722
	$\frac{29}{2}$	-0.011905	14.558	0.438	0.004	0.278	14.249
	$\frac{27}{2}$	-0.076950	13.449	0.545	0.006	0.473	12.940
	$\frac{25}{2}$	-0.094030	12.414	0.579	0.007	0.588	11.788
	$\frac{23}{2}$	-0.072464	11.451	0.543	0.006	0.625	10.790
	$\frac{21}{2}$	-0.020876	10.561	0.436	0.003	0.585	9.945
	$\frac{19}{2}$	0.052795	9.744	0.256	0.0	0.470	9.254
	$\frac{17}{2}$	0.141304	9.000	0.0	0.0	0.276	8.724
13	$\frac{33}{2}$	0.112069	15.517	0.222	0.001	0.0	15.502
	$\frac{31}{2}$	-0.009852	14.433	0.378	0.003	0.238	14.170
	$\frac{29}{2}$	-0.075517	13.413	0.471	0.005	0.406	12.977
	$\frac{27}{2}$	-0.094089	12.457	0.501	0.005	0.505	11.920
	$\frac{25}{2}$	-0.074138	11.563	0.470	0.004	0.537	10.996
	$\frac{23}{2}$	-0.023645	10.732	0.377	0.002	0.504	10.203
	$\frac{21}{2}$	0.050000	9.964	0.221	0.0	0.404	9.544
	$\frac{19}{2}$	0.140000	9.259	0.0	0.0	0.237	9.022
14	$\frac{35}{2}$	0.112903	15.323	0.194	0.001	0.0	15.310
	$\frac{33}{2}$	-0.008065	14.323	0.330	0.003	0.207	14.096
	$\frac{31}{2}$	-0.074245	13.379	0.411	0.004	0.353	13.001
	$\frac{29}{2}$	-0.094086	12.490	0.438	0.004	0.439	12.205
	$\frac{27}{2}$	-0.075525	11.656	0.410	0.003	0.467	11.164
	$\frac{25}{2}$	-0.025986	10.876	0.329	0.002	0.438	10.418
	$\frac{23}{2}$	0.047619	10.152	0.193	0.0	0.351	9.787
	$\frac{21}{2}$	0.138889	9.483	0.0	0.0	0.206	9.277
15	$\frac{37}{2}$	0.113636	15.152	0.170	0.001	0.0	15.141
	$\frac{35}{2}$	-0.006494	14.224	0.290	0.002	0.181	14.026
	$\frac{33}{2}$	-0.073108	13.345	0.362	0.003	0.309	13.016
	$\frac{31}{2}$	-0.094044	12.515	0.385	0.003	0.385	12.109
	$\frac{29}{2}$	-0.076690	11.733	0.361	0.002	0.410	11.303
	$\frac{27}{2}$	-0.027989	10.999	0.290	0.001	0.384	10.598
	$\frac{25}{2}$	0.045566	10.314	0.170	0.0	0.308	9.995
	$\frac{23}{2}$	0.137931	9.677	0.0	0.0	0.181	9.497

 $I = \frac{9}{2}$ 

0	$\frac{9}{2}$	0.0	40.000	33.333	26.667	0.0	0.0
1	$\frac{11}{2}$	0.050000	28.000	9.818	2.182	0.0	23.636
	$\frac{9}{2}$	-0.1333333	14.182	12.929	6.222	16.364	0.673
	$\frac{7}{2}$	0.091667	4.889	9.778	12.000	16.296	10.370
2	$\frac{13}{2}$	0.071429	22.857	4.615	0.527	0.0	21.538

*Relative Intensities*

J	F	$Y(J, I, F)$	$J \rightarrow J+1$			$J \rightarrow J$	
			$F \rightarrow F+1$	$F \rightarrow F$	$F \rightarrow F-1$	$F \leftrightarrow F+1$	$F \rightarrow F$
<i>I = <math>\frac{9}{2}</math> (continued)</i>							
3	$\frac{1}{2}$	-0.083333	15.385	7.161	1.455	6.462	8.084
	$\frac{3}{2}$	-0.083333	9.455	7.879	2.667	9.455	1.212
	$\frac{5}{2}$	0.005952	4.952	6.966	4.082	9.333	0.381
	$\frac{7}{2}$	0.130952	1.796	4.490	5.714	6.286	5.714
	$\frac{9}{2}$	0.83333	20.000	2.667	0.190	0.0	19.429
	$\frac{11}{2}$	-0.055556	15.111	4.376	0.513	3.429	11.077
	$\frac{13}{2}$	-0.091667	10.989	5.245	0.909	5.495	5.285
	$\frac{15}{2}$	-0.061111	7.576	5.387	1.323	6.364	1.732
4	$\frac{1}{2}$	0.005556	4.815	4.913	1.701	6.190	0.136
	$\frac{3}{2}$	0.083333	2.653	3.918	2.000	5.102	0.327
	$\frac{5}{2}$	0.152778	1.048	2.444	2.222	3.143	2.571
	$\frac{7}{2}$	0.090909	18.182	1.733	0.086	0.0	17.882
	$\frac{9}{2}$	-0.037879	14.631	2.921	0.226	2.118	12.134
	$\frac{11}{2}$	-0.086580	11.539	3.625	0.392	3.526	7.722
	$\frac{13}{2}$	-0.079545	8.876	3.906	0.551	4.308	4.480
	$\frac{15}{2}$	-0.037879	6.612	3.826	0.673	4.545	2.245
5	$\frac{1}{2}$	0.020563	4.714	3.448	0.727	4.321	0.854
	$\frac{3}{2}$	0.081169	3.152	2.836	0.679	3.714	0.152
	$\frac{5}{2}$	0.132576	1.891	2.069	0.485	2.800	0.015
	$\frac{7}{2}$	0.166667	0.889	1.333	0.0	1.630	0.593
	$\frac{9}{2}$	0.096154	16.923	1.215	0.044	0.0	16.746
	$\frac{11}{2}$	-0.025641	14.170	2.078	0.115	1.435	12.490
	$\frac{13}{2}$	-0.080128	11.724	2.626	0.196	2.439	9.052
	$\frac{15}{2}$	-0.085470	9.566	2.892	0.269	3.055	6.344
6	$\frac{1}{2}$	-0.057692	7.682	2.910	0.318	3.329	4.275
	$\frac{3}{2}$	-0.010684	6.052	2.712	0.326	3.306	2.755
	$\frac{5}{2}$	0.043803	4.662	2.331	0.280	3.030	1.697
	$\frac{7}{2}$	0.096154	3.497	1.790	0.168	2.545	1.018
	$\frac{9}{2}$	0.138889	2.545	1.091	0.0	1.891	0.655
	$\frac{11}{2}$	0.166667	1.818	0.0	0.0	1.091	0.727
	$\frac{13}{2}$	0.100000	16.000	0.898	0.025	0.0	15.887
	$\frac{15}{2}$	-0.016667	13.769	1.551	0.065	1.036	12.567

*Relative Intensities*

J	F	Y(J, I, F)	J→J+1			J→J	
			F→F+1	F→F	F→F-1	F↔F+1	F→F
<i>I=9/2 (continued)</i>							
7	23/2	0.102941	15.294	0.691	0.015	0.0	15.217
	21/2	-0.009804	13.427	1.200	0.039	0.783	12.528
	19/2	-0.069193	11.726	1.543	0.065	1.356	10.240
	17/2	-0.087104	10.183	1.731	0.087	1.737	8.322
	15/2	-0.074284	8.792	1.776	0.098	1.941	6.741
	13/2	-0.040347	7.549	1.689	0.095	1.984	5.470
	11/2	0.006222	6.448	1.477	0.075	1.879	4.485
	9/2	0.058069	5.487	1.141	0.039	1.636	3.771
	7/2	0.108974	4.667	0.667	0.0	1.259	3.339
	5/2	0.153846	4.000	0.0	0.0	0.735	3.265
8	25/2	0.105263	14.737	0.547	0.010	0.0	14.682
	23/2	-0.004386	13.137	0.956	0.025	0.612	12.440
	21/2	-0.064912	11.666	1.234	0.041	1.066	10.503
	19/2	-0.086403	10.320	1.390	0.054	1.373	8.849
	17/2	-0.078070	9.095	1.433	0.061	1.543	7.459
	15/2	-0.048246	7.986	1.368	0.058	1.586	6.316
	13/2	-0.004386	6.993	1.198	0.044	1.510	5.406
	11/2	0.046930	6.117	0.924	0.023	1.320	4.723
	9/2	0.100000	5.348	0.535	0.0	1.016	4.278
	7/2	0.150000	4.706	0.0	0.0	0.588	4.118
9	27/2	0.107143	14.286	0.444	0.007	0.0	14.246
	25/2	0.0	12.889	0.778	0.017	0.491	12.334
	23/2	-0.061275	11.596	1.008	0.027	0.859	10.662
	21/2	-0.085434	10.403	1.140	0.036	1.111	9.215
	19/2	-0.080532	9.309	1.178	0.040	1.253	7.980
	17/2	-0.053922	8.310	1.126	0.037	1.293	6.947
	15/2	-0.012255	7.406	0.987	0.028	1.234	6.106
	13/2	0.038515	6.595	0.760	0.014	1.081	5.456
	11/2	0.093137	5.879	0.437	0.0	0.831	5.006
	9/2	0.147059	5.263	0.0	0.0	0.478	4.785
10	29/2	0.108696	13.913	0.368	0.005	0.0	13.883
	27/2	0.003623	12.676	0.646	0.012	0.403	12.224
	25/2	-0.058162	11.523	0.839	0.019	0.707	10.758
	23/2	-0.084382	10.454	0.950	0.025	0.916	9.476
	21/2	-0.082189	9.466	0.984	0.027	1.037	8.368
	19/2	-0.058162	8.557	0.942	0.025	1.072	7.427
	17/2	-0.018307	7.727	0.826	0.019	1.025	6.648
	15/2	0.031941	6.975	0.635	0.009	0.898	6.030
	13/2	0.087719	6.303	0.364	0.0	0.690	5.581
	11/2	0.144737	5.714	0.0	0.0	0.396	5.319

## Relative Intensities

J	F	$Y(J, I, F)$	$J \rightarrow J+1$			$J \rightarrow J$	
			$F \rightarrow F+1$	$F \rightarrow F$	$F \rightarrow F-1$	$F \leftrightarrow F+1$	$F \rightarrow F$
$I = \frac{9}{2}$ (continued)							
11	$\frac{3}{2}$	0.110000	13.600	0.310	0.003	0.0	13.576
	$\frac{29}{2}$	0.006667	12.490	0.545	0.008	0.337	12.115
	$\frac{27}{2}$	-0.055476	11.452	0.709	0.014	0.592	10.814
	$\frac{25}{2}$	-0.083333	10.483	0.804	0.017	0.769	9.665
	$\frac{23}{2}$	-0.083333	9.583	0.833	0.019	0.871	8.661
	$\frac{21}{2}$	-0.061429	8.749	0.798	0.017	0.902	7.799
	$\frac{19}{2}$	-0.023095	7.983	0.700	0.013	0.864	7.075
	$\frac{17}{2}$	0.026667	7.282	0.358	0.006	0.757	6.488
	$\frac{15}{2}$	0.083333	6.650	0.307	0.0	0.581	6.043
	$\frac{13}{2}$	0.142857	6.087	0.0	0.0	0.332	5.755
12	$\frac{33}{2}$	0.111111	13.333	0.264	0.002	0.0	13.315
	$\frac{31}{2}$	0.009259	12.328	0.465	0.006	0.285	12.012
	$\frac{29}{2}$	-0.053140	11.384	0.606	0.010	0.502	10.844
	$\frac{27}{2}$	-0.082327	10.499	0.689	0.013	0.654	9.805
	$\frac{25}{2}$	-0.084138	9.672	0.714	0.014	0.742	8.889
	$\frac{23}{2}$	-0.064010	8.903	0.685	0.012	0.769	8.094
	$\frac{21}{2}$	-0.026973	8.190	0.601	0.009	0.737	7.417
	$\frac{19}{2}$	0.022343	7.535	0.461	0.004	0.646	6.858
	$\frac{17}{2}$	0.079710	6.938	0.262	0.0	0.496	6.422
	$\frac{15}{2}$	0.141304	6.400	0.0	0.0	0.282	6.118
13	$\frac{35}{2}$	0.112069	13.103	0.228	0.002	0.0	13.088
	$\frac{33}{2}$	0.011494	12.186	0.402	0.005	0.245	11.916
	$\frac{31}{2}$	-0.011092	11.320	0.524	0.007	0.432	10.858
	$\frac{29}{2}$	-0.081379	10.506	0.596	0.009	0.562	9.910
	$\frac{27}{2}$	-0.084713	9.741	0.619	0.010	0.639	9.068
	$\frac{25}{2}$	-0.066092	9.027	0.594	0.009	0.663	8.330
	$\frac{23}{2}$	-0.030172	8.362	0.521	0.007	0.636	7.696
	$\frac{21}{2}$	0.018736	7.746	0.399	0.003	0.557	7.164
	$\frac{19}{2}$	0.076667	7.181	0.227	0.0	0.427	6.737
	$\frac{17}{2}$	0.140000	6.667	0.0	0.0	0.243	6.424
14	$\frac{37}{2}$	0.112903	12.903	0.199	0.001	0.0	12.891
	$\frac{35}{2}$	0.013441	12.059	0.351	0.004	0.212	11.826
	$\frac{33}{2}$	-0.049283	11.261	0.458	0.006	0.375	10.860
	$\frac{31}{2}$	-0.080496	10.506	0.521	0.007	0.489	9.989
	$\frac{29}{2}$	-0.085125	9.796	0.541	0.008	0.556	9.211
	$\frac{27}{2}$	-0.067802	9.129	0.519	0.007	0.578	8.524
	$\frac{25}{2}$	-0.032855	8.505	0.455	0.005	0.554	7.926
	$\frac{23}{2}$	0.015681	7.925	0.349	0.002	0.486	7.419
	$\frac{21}{2}$	0.074074	7.388	0.198	0.0	0.372	7.003
	$\frac{19}{2}$	0.138889	6.897	0.0	0.0	0.211	6.685

*Relative Intensities*

<i>J</i>	<i>F</i>	<i>Y(J, I, F)</i>	<i>J</i> → <i>J</i> +1			<i>J</i> → <i>J</i>	
			<i>F</i> → <i>F</i> +1	<i>F</i> → <i>F</i>	<i>F</i> → <i>F</i> -1	<i>F</i> ↔ <i>F</i> +1	<i>F</i> → <i>F</i>
<i>I</i> = $\frac{9}{2}$ ( <i>continued</i> )							
15	$\frac{39}{2}$	0.113636	12.727	0.175	0.001	0.0	12.717
	$\frac{37}{2}$	0.015152	11.946	0.309	0.003	0.186	11.743
	$\frac{35}{2}$	-0.047675	11.205	0.403	0.004	0.329	10.855
	$\frac{33}{2}$	-0.079676	10.503	0.459	0.006	0.429	10.050
	$\frac{31}{2}$	-0.085423	9.839	0.477	0.006	0.488	9.327
	$\frac{29}{2}$	-0.069227	9.214	0.458	0.005	0.507	8.683
	$\frac{27}{2}$	-0.035136	8.627	0.401	0.004	0.487	8.119
	$\frac{25}{2}$	0.013062	8.078	0.307	0.002	0.427	7.634
	$\frac{23}{2}$	0.071839	7.568	0.174	0.0	0.326	7.230
	$\frac{21}{2}$	0.137931	7.097	0.0	0.0	0.185	6.912

## Appendix J

# NUCLEAR QUADRUPOLE SECOND-ORDER CORRECTION ENERGIES FOR LINEAR OR SYMMETRIC-TOP MOLECULES

---

To obtain  $E_Q^{(2)}$ , the entries given are to be multiplied by the factor

$$\left(\frac{(eqQ)^2}{B}\right) \times 10^{-3}$$

$J$	$F$	$K=0$	$K=1$	$K=2$	$K=3$	$K=4$	$K=5$	$K=6$
$I=\frac{3}{2}$								
0	$\frac{3}{2}$	-10.4167						
1	$\frac{1}{2}$	-6.0000	-9.4688					
	$\frac{3}{2}$	-2.2500	-10.8750					
	$\frac{1}{2}$	0.0000	-11.7188					
2	$\frac{7}{2}$	-4.0999	-5.6487	-7.2885				
	$\frac{5}{2}$	-2.1866	2.4561	-3.8875				
	$\frac{3}{2}$	10.4167	5.2082	-10.4170				
	$\frac{1}{2}$	0.0000	11.7188	0.0000				
3	$\frac{7}{2}$	-3.0864	-3.8520	-5.3818	-5.3758			
	$\frac{5}{2}$	-1.9290	0.2170	3.4721	1.717119			
	$\frac{3}{2}$	6.0000	3.4466	-2.6042	-7.3244			
	$\frac{1}{2}$	2.2500	5.6668	10.4170	0.0000			
4	$\frac{11}{2}$	-2.4652	-2.8917	-3.9090	-4.7287	-4.0384		
	$\frac{9}{2}$	-1.6904	-0.5944	1.8570	3.1549	-0.8835		
	$\frac{7}{2}$	4.0998	2.8205	-0.4613	-4.0782	-5.2500		
	$\frac{5}{2}$	2.1866	3.5660	6.4915	7.3240	0.0000		
5	$\frac{13}{2}$	-2.0482	-2.3084	-2.9800	-3.7373	-4.0366	-3.1171	
	$\frac{11}{2}$	-1.4935	-0.8679	0.7160	2.3783	2.6536	-0.5096	
	$\frac{9}{2}$	3.0864	2.3715	0.4443	-2.0424	-4.0004	-3.9066	
	$\frac{7}{2}$	1.9290	2.6111	4.2779	5.7901	5.2500	0.0000	
6	$\frac{15}{2}$	-1.7500	-1.9198	-2.3779	-2.9701	-3.4295	-3.4365	-2.4684
	$\frac{13}{2}$	-1.3333	-0.9447	0.0971	1.4220	2.4120	2.2022	-0.3188
	$\frac{11}{2}$	2.4652	2.0288	0.8175	-0.8767	-2.5661	-3.5684	-3.0065
	$\frac{9}{2}$	1.6904	2.0749	3.0805	4.2634	4.8839	3.9066	0.0000

<i>J</i>	<i>F</i>	<i>K=0</i>	<i>K=1</i>	<i>K=2</i>	<i>K=3</i>	<i>K=4</i>	<i>K=5</i>	<i>K=6</i>
<i>I</i> = $\frac{5}{2}$								
0	$\frac{5}{2}$	-5.8333						
1	$\frac{7}{2}$	-2.8930	-6.1475					
	$\frac{5}{2}$	-2.0829	-3.6386					
	$\frac{3}{2}$	-0.5400	-8.2350					
2	$\frac{9}{2}$	-1.8039	-3.1402	-4.8439				
	$\frac{7}{2}$	-1.8039	2.6858	-0.8261				
	$\frac{5}{2}$	4.9478	0.0657	-3.9850				
	$\frac{3}{2}$	-0.1968	5.6991	-5.1118				
	$\frac{1}{2}$	0.0000	-0.8333	-2.0832				
3	$\frac{11}{2}$	-1.2767	-1.9108	-3.2421	-3.5571			
	$\frac{9}{2}$	-1.4773	0.3006	3.1402	-0.4417			
	$\frac{7}{2}$	2.0002	0.7866	-1.6667	-1.7969			
	$\frac{5}{2}$	1.8072	1.7500	0.7640	-3.5926			
	$\frac{3}{2}$	0.5400	1.7341	3.0208	-2.6368			
	$\frac{1}{2}$	0.0000	0.8333	2.0833	0.0000			
4	$\frac{13}{2}$	-0.9753	-1.3193	-2.1601	-2.9227	-2.6497		
	$\frac{11}{2}$	-1.2289	-0.4042	1.4534	2.4952	-0.3603		
	$\frac{9}{2}$	0.9756	0.6127	-0.2797	-1.1141	-0.9101		
	$\frac{7}{2}$	1.5081	1.2013	0.3300	-0.9597	-2.4238		
	$\frac{5}{2}$	0.8856	1.2000	1.7349	1.2654	-2.2500		
	$\frac{3}{2}$	0.1968	0.7918	2.0910	2.6368	0.0000		
5	$\frac{15}{2}$	-0.7835	-0.9894	-1.5290	-2.1682	-2.5167	-2.0281	
	$\frac{13}{2}$	-1.0446	-0.6066	0.5031	1.6706	1.8734	-0.3198	
	$\frac{11}{2}$	0.5225	0.3992	0.0704	-0.3410	-0.6301	-0.5106	
	$\frac{9}{2}$	1.1840	0.9640	0.3562	-0.4822	-1.2888	-1.6970	
	$\frac{7}{2}$	0.8928	0.9656	1.0935	1.0039	0.2435	-1.8228	
	$\frac{5}{2}$	0.2756	0.6230	1.4861	2.3272	2.2500	0.0000	
6	$\frac{17}{2}$	-0.6519	-0.7844	-1.1456	-1.6258	-2.0431	-2.1421	-1.5948
	$\frac{15}{2}$	-0.9052	-0.6482	0.0404	0.9144	1.5623	1.4089	-0.2855
	$\frac{13}{2}$	0.2900	0.2466	0.1258	0.0453	-0.2204	-0.3361	-0.3097
	$\frac{11}{2}$	0.9468	0.8020	0.3961	-0.1836	-0.7938	-1.2316	-1.2380
	$\frac{9}{2}$	0.8283	0.8321	0.8202	0.7229	0.4239	-0.2394	-1.4762
	$\frac{7}{2}$	0.2958	0.5081	1.0693	1.7527	2.1803	1.8228	0.0000

<sup>a</sup>Numerical calculations were made by J. W. Simmons and W. E. Anderson. From W. Gordy, W. V. Smith, and R. F. Trambarulo, *Microwave Spectroscopy*, Wiley, New York, 1953.

# AUTHOR INDEX

---

Numbers in parentheses are reference numbers and indicate that the author's work is referred to although his name is not mentioned in the text. Numbers in *italics* show the pages on which the complete references are listed.

## Index Terms

## Links

### **A**

Adachi, M.	627 (155)	<i>644</i>		
Albritton, D. L.	106 (68)	<i>122</i>	361 (135)	388
Aldrich, P. D.	222 (123)	<i>226</i>		
Aleksandrov, A. P.	313 (40)	<i>385</i>		
Alexander, A. J.	146 (63)	<i>171</i>		
Aliev, M. R.	195 (72)	206 (72)	224	285 (122)
	286 (124)	288 (124)	296	307 (31)
	313 (40, 461)	329 (72)	338 (72)	357 (72)
	381 (72)	382 (72, 198)		385 389
Alix, A.	313 (43)	<i>385</i>		
Allan, A.	380 (164)	<i>388</i>		
Allen, C. L.	<i>411</i>			
Allen, H. C., Jr.	246 (13)	251	(13)	293
	341 (87)	<i>386</i>		
Allen, L. C.	789 (74)	<i>802</i>		
Allen, W. C.	<i>411</i>	512 (36)	532 (36)	534 (36)
	546 (36)	<i>565</i>		
Almy, G. M.	110 (83)	<i>122</i>		
Altman, R. S.	<i>155</i>			
Amano, T.	106 (70)	107 (75)	116 (96, 99)	<i>122</i>
	169 (140)	<i>173</i>	559 (108)	560 (94)
	564 (108, 111)	<i>567</i>		
Amat, G.	133 (8, 13)	135 (15)	<i>169</i>	
	185 (19, 22)	187 (19)	201 (22)	223

## Index Terms

## Links

	282 (108)	284 (108)	286 (108)	295
	304 (13)	360 (131)	384	387
Amiot, C.	208 (102)	225		
Andersen, U.	534 (39)	565	598 (52)	618 (52)
	623 (52)	641		
Anderson, P. W.	50 (6)	69		
Anderson, T. G.	96 (43)	121	145 (54)	165 (125)
	166 (132)	170	172	
Anderson, W. E.	682	896		
Andolfatto, M. K.	500			
Andresen, U.	276 (85)	295		
Arnold, W.	773 (55)	802		
Asprey, L. B.	380 (169)	389		
Attanasio, A.	282 (113)	295		
Autler, S. H.	273 (69)	277 (69)	279 (69)	294
	492 (36)	503		
Aval, G. M.	488 (34)	503		
Avery, L. W.	146 (60)	147 (60)	171	
Avirah, T. K.	228 (48)	228	267 (43)	268 (48, 51)
	294	629 (168)	644	690 (54)
	722			
Aynsley, E. E.	411			
Azrak, R. G.	635 (186)	645		

## **B**

Babcock, H. D.	106 (69)	122		
Baiocchi, F. A.	154 (89)	157 (89)	159 (89)	160 (98, 100)
	161 (100)	171		
Baird, D. H.	619 (99)	643		
Baird, J. C.	444 (61)	449		
Bak, B.	231	502	534 (37)	565

## Index Terms

## Links

	627 (153)	644	691 (55)	698 (63)
	722			
Baker, J. G.	4 (32)	7 (32, 62)	8	143 (35)
	170	186 (25)	187 (29)	223
	273 (62)	288 (136)	294	296
	360 (127)	383 (212)	387	390
	444 (61)	449	498 (49)	501
	504	602 (62)	642	
Balikci, B.	360 (130)	387		
Ball, J. A.	116 (98)	123		
Balle, T. J.	5 (41)	9	155 (85)	156 (86)
	159 (86)	160 (101)	161 (102)	
	171			
Bardeen, J.	423 (20)	427 (37)	448	
Barfield, M.	804 (29)	840		
Barnes, C. E.	560 (96)	567		
Barnes, R. G.	733 (24)	734 (24)	801	
Baron, P. A.	639 (215)	646		
Barrett, A. H.	5 (49)	9	115 (90)	122
Barriol, J.	320 (58)	351 (58)	385	
Barsuhn, J.	145 (58)	170		
Bartell, L. S.	706 (89)	723		
Bassompierre, A.	727 (13)	801		
Bates, H. F.	535			
Battaglia, A.	273 (71)	294		
Bauder, A.	133 (7)	169	181	186 (26)
	187 (26, 35)	223	276 (86)	282 (113)
	295	598 (48)	600 (58)	603 (48)
	603	604 (71)	618 (48, 51)	622 (124, 126)
	623 (51, 129, 140)		624 (48)	624
	626	641	689 (52)	701 (68)

## Index Terms

## Links

	722	804 (10, 43)	839	
Bauman, L. E.	628 (164)	633 (176)	638 (164)	644
Beason, E. B.	321			
Beaudet, R. A.	231	272 (59)	294	604 (69)
	605 (70)	642	671 (17)	704 (75)
	721	723		
Bedard, F. D.	115 (95)	123		
Beers, Y.	354 (132)	387	441 (48)	449
	560 (99)	567		
Beeson, E. L.	181 (77)	200 (77)		214 (78)
	224	502		
Bell, M. B.	146			
Bell, R. P.	636 (204)	645	672 (18)	721
Bellama, J. M.	216 (108)	225	415	770
Bellet, J.	349 (102)	351 (142)	360 (128)	361 (102)
	366 (102)	369 (142)	387	679
Bellott, E. M., Jr.	267 (38)	294	635 (183)	645
Belov, S. P.	2 (14)	8	193 (59)	194
	201 (80)	202 (59, 80)	224	383 (216)
	389			
Bender, C. F.	789 (72)	802		
Bendtsen, J.	351	502		
Benedict, W. S.	192 (51)	224	341 (86)	386
	712 (95)	724		
Benson, R. C.	516 (57)	534 (33, 35, 57)		535 (33)
	536 (60)			
	537 (61)	565	695 (62)	723
Benz, H. P.	804 (10)	839		
Berendths, B. T.	51			
Beringer, R.	552 (74)	553 (74)	554 (77)	556 (76)
	557 (76)	561 (74)	566	

## Index Terms

## Links

Bernard, P.	357 (125)	359 (125)	387	
Bersohn, R.	397 (12)	425 (24)	448	727 (8)
	730 (8)	767 (8)	800	
Bertram, M.	220 (119)	225		
Bettin, N.	745 (32)	801		
Bevan, J. W.	153 (78)	171	221 (120)	225
Bhattacharya, B. N.	493 (39)	497 (40)	500 (40)	503
	535			
Bird, G. R.	444 (61)	449	619 (99)	643
Bird, R. B.	487 (31)	503		
Birnbaum, G.	50 (9)	51	54 (9)	69
Birss, F. W.	286 (126)	296		
Bivens, R.	426 (36)	439 (36)	447 (36)	449
	805 (45)	838 (45)	840	
Bjarnov, E.	380 (171)	389		
Bjørseth, A.	216 (106)	225		
Blackman, G. L.	145 (55)	170	804 (14, 22)	826 (22)
	840			
Blake, G. A.	164 (131)	172		
Blaker, J. W.	246 (14)	293		
Blanch, G.	577 (16)	640		
Bleaney, B.	188 (37)	223		
Blickensderfer, R.	534 (26)	565		
Blukis, U.	231			
Bobin, B.	804 (34)	840		
Bodenseh, H. K.	135 (14)	169	181	183 (13)
	223	411	500	706 (80)
	723	804 (26, 30)	840	
Bogey, M.	96 (44)	98 (44)	121	133 (7)
	164 (122)	169	172	411
Boggia, L. M.	321			

## Index Terms

## Links

Boggs, J. E.	51 689 (48)	502 722	620 (103)	643
Bohn, R. K.	267 (36)	293	634 (178)	645
Boland, M. R.	636 (198)	645		
Bolton, K.	635 (193) 840	645	804 (22)	826 (22)
Boone, D. W.	502			
Borchert, S. J.	268 (46)	294		
Borgers, T. R.	369 (145)	388	636 (203)	645
Born, M.	150 (74)	171		
Born, W.	80 (7)	120		
Bossert, W.	598 (49) 626	604 (71) 641	622 (126)	626 (126)
Botskor, I.	3 (28) 632 (174)	8 645	501 (52)	504
Böttcher, C. J. F.	799 (80)	802		
Boucher, D.	415 641	421 766	597 (43) 770	600 (43)
Bouchy, A.	269 (55) 351 (58) 643	294 385 689 (53)	320 (58) 387 722	349 (111) 620 (108)
Bowater, I. C.	560 (91) 840	567	804 (20)	838 (20)
Bowen, H. J. M.	653 (6)	721		
Bowen, K. H.	160 (99)	172		
Bradley, R. H.	360 (126)	387		
Bragg, J. K.	248 (18) 413 (9)	293 416 (10)	392 (9) 427 (9)	406 (10) 448
Bransford, J. W.	444 (62)	449		
Bray, P. J.	767 (42)	772 (44)	801	
Breivogel, F. W.	797			

## Index Terms

## Links

Breslow, R.	695 (62)	723		
Bridge, N. J.	488 (33)	503		
Brier, P. N.	288 (136)	296	360 (126, 130)	
	361 (126)	387		
Brim, W. W.	192 (52)	224		
Britt, C. O.	51	502	620 (103)	
	643	689 (48)	722	
Brittain, A. H.	380 (173)	389		
Broida, H. P.	105 (66)	122		
Brookbanks, D. M.	360 (127)	387		
Brossel, J.	3 (21)	8		
Broten, N. W.	146 (60)	147 (60)	171	
Brown, J. M.	115 (89)	122	560 (91, 96)	
	567	804 (20, 32)	838 (20)	840
Brown, R. D.	145 (55)	170	679	710
	804 (14, 22)	826 (22)	840	
Brown, W. G.	768 (43)	801		
Buck, L.	649 (4)	721		
Buckingham, A. D.	458 (5)	462 (5)	488 (33)	496 (5)
	501 (5)	503	539 (62, 65)	542 (65)
	566	753 (36)	801	
Budenstein, P. P.	2 (10)	8		
Buhl, D.	87 (34)	121	144 (50)	145 (56)
	147 (50)	163 (112)	164 (116, 121)	
	170	172		
Bunker, P. R.	135 (20)	170	193 (56, 58)	224
	285 (116)	296	304 (18)	382 (18)
	383 (202, 210)		385	389
	620 (112)	643	677 (25)	722
Burden, F. R.	679	710	804 (14, 22)	826 (22)
	840			

## Index Terms

## Links

Burenin, A. V.	2 (12) 201 (80) 383 (216)	8 225 386	152 (75) 349 (96) 390	171
Burg, A. B.	781 (64)	802		
Burie, J.	415	770		
Burkhard, D. G.	571 (7) 643	582 (7)	623 (132)	639
Burrus, C. A.	1 (3) 115 (81) 180 495 (43) 511 (8) 802	2 (10) 118 (103) 417 (18) 496 (44) 520 (8) 448 500 (43) 565 778 (57)	7	109 (81) 137 448 503 778 (57)
Butcher, S. S.	231 645	477 (20)	503	638 (210)
Buxton, L. W.	154 (84) 161 (103)	159 (84) 162 (103)	160 (103) 171	
Bykov, A. D.	285 (123)	296		

## C

Cade, P.	789 (71)	802		
Cahill, P.	84 (16) 497	121 500	443 (52)	449
Callomon, J. H.	649 (4)	721		
Caminati, W.	380 (177) 636 (199)	389 645	624	635 (194)
Campbell, E. J.	5 (41) 159 (84) 171	9 160 (101) 221 (122)	154 (84) 161 (103) 222 (122)	155 162 (102) 226
Careless, A. J.	181 (31) 296	187 (31) 415	223 770	288 (133)
Carpenter, J. H.	288 (137)	296	351 (115)	351

## Index Terms

## Links

	354 (115)	380 (168)	381 (115)	387
	421	766	770	
Carreira, L. A.	628 (163)	638 (163)	644	
Carrier, L. A.	628 (164)	638 (164)	644	
Carrington, A.	5 (44) 87)	6 (53)	9	558 (85,
	559 (87)	559	560 (91, 96)	
	561 (85, 105)	564 (106)	567	804 (12,
	20)			
	838 (20)	839		
Casabella, P. A.	772 (44)	801		
Casimir, H. B. G.	392 (3) 801	404 (3)	448	735 (25)
Casleton, K. H.	421	766	770	
Castle, J. G., Jr.	552 (74) 566	553 (74)	556 (76)	561 (74)
Cazzoli, G.	143 (32) 181 384 32)	148 (70) 299 (3) 389	160 (101) 351 (3) 415	170 380 (176) 678 (30,
	722	770		
Cederberg, J. S.	804 (13, 16, 24) 16)	809 (17)	823 (13)	827 (13,
	828 (16)	840		
Cervellati, R.	635 (194)	645	678 (32)	722
Chan, M. Y.	304 (19) 385	341 (19) 389	369 (19)	382 (200)
Chan, S. I.	369 (145) 636 (201)	388 638 (201)	477 (19) 645	503
Chan, Y.	367 (141)	388		
Chance, K. V.	160 (99)	172		

## Index Terms

## Links

Chang, Tsu-Shen	181 (6)	223		
Chantry, G. W.	5 (39)	7 (39)	9	
Chanussot, J.	360 (128)	387		
Chao, S.	629 (168)	644		
Charo, A.	166 (135)	173	560 (101)	567
Charpentier, L.	618 (96)	643		
Chen, M. M.	216 (115)	216	225	
Cheung, A. C.	5 (50)	9		
Chikaraishi, T.	381 (193)	389	679	
Childs, W. J.	737			
Choplin, A.	276 (91)	278 (91)	295	
Christensen, D.	231	698 (63)	723	
Christiansen, J. J.	147 (67)	151 (67)	171	231
	411	502	627 (153)	644
Christy, A.	109 (79)	114 (79)	122	
Chu, F. Y.	195 (67)	198 (67)	201 (67)	215 (67)
	224			
Chung, K. T.	304 (19)	326 (65)	341 (19)	369 (19)
	385			
Churchwell, E.	6 (52)	9	115 (92)	122
	300 (5)	384		
Chutjian, A.	666 (12)	721		
Clark, A. H.	710			
Clark, W. W.	81 (10)	82 (13)	84 (10)	89 (10)
	107 (74)	116 (74)	120	351
Cleeton, C. E.	188 (36)	223		
Cleveland, F. F.	307 (26)	311	385	
Clough, S. A.	304 (16)	326 (66)	385	
Clouser, P. L.	85 (31)	121		
Codding, E. G.	624			
Coester, F.	458 (6)	462 (6)	466 (6)	503

## Index Terms

## Links

Cogley, C. D.	804 (40, 42)	840		
Cohen, E. A.	288 (135)	296	349 (110)	355 (110)
	387			
Cohen, E. R.	857			
Cohen, M. H.	397 (13)	399 (13)	448	767 (41)
	801			
Cohen, V. W.	859			
Cohn, E. R.	51			
Coles, D. K.	392 (7)	415 (41)	436 (41)	448
	456	506 (1)	565	
Combs, L. L.	267 (36)	293		
Condon, E. U.	446 (64)	449	459 (7)	468 (7)
	478 (7)	503	524 (14)	565
	811 (47)	840		
Cook, J. M.	560 (103)	567		
Cook, R. L.	7 (69)	10	100 (59)	107 (71)
	122	228 (48)	228	265 (34)
	267 (36), (43)	268 (48, 51)	292 (150)	293
	294	296	300 (7)	313 (49)
	343 (91, 147, 163)		344 (91)	345 (92)
	346 (91)			
	347 (91)	349 (97)	351 (7, 155)	352 (93)
	353 (91, 97)	361 (7, 91)	364 (7)	366 (91)
	375 (93, 155)	376 (157)	378 (157, 163)	379 (156, 161)
	380 (155, 163)	381 (97)	384	388
	497	498 (47)	500	502
	504	551 (72)	566	628 (166)
	629 (166, 168)	630 (166)	633 (176)	
	644	649 (2)	690 (54)	710 (93)
	721	724	803 (5)	805 (3)

## Index Terms

## Links

	810 (5)	812 (5)	821 (5)	825 (5)
	834 (5)	839		
Cool, T. A.	3 (22)	8		
Cooper, T. A.	145			
Corbelli, G.	187 (29)	223	380 (179)	389
Comet, R.	351	421	766	770
Cornwell, C. D.	421	425 (23)	448	492 (38)
	503	766	770	827 (48)
	840			
Costain, C. C.	141 (30)	170	188 (39)	190 (43)
	224	357 (121)	387	477 (20)
	503	617 (85)	621 (85)	635 (181)
	638 (210)	642	645	688 (44)
	691 (58)	694 (58)	698 (58)	722
Coulson, C. A.	730 (16)	793 (16)	793	796 (13)
	801			
Cowan, M.	2 (6)	7	75	
Cox, A. I.	678 (29)	722		
Cox, A. P.	187 (33)	223	273 (74)	276 (74)
	295	380 (173)	389	616 (81)
	617 (81)	627 (149)	642	644
Cox, J. T.	180 (7)	511 (6)	514 (6)	516 (6)
	550 (70)	565		
Coxon, J. A.	115 (86)	122		
Crable, G. F.	472 (15)	474 (16)	503	
Crawford, B. L.	581 (22)	583 (22)	640	
Crawford, B. L., Jr.	308 (37)	385		
Creswell, R. A.	90 (29)	121	144 (48)	145 (48,53)
	146	170	421	268 (50)
	294	369 (144)	381 (185)	388

## Index Terms

## Links

	624	689 (51)	722	766
	770			
Cross, L. C.	653 (6)	721		
Cross, P. C.	31 (5)	35	229 (1)	232 (1)
	234 (1)	236 (1)	242 (1)	246 (1, 11)
	259 (23)	262 (23)	282 (111)	
	292	295	302 (11)	340
	372 (11)	384	416 (17)	448
	849 (1)	852		
Curl, R. F., Jr.	207 (96, 97)	225	231	267 (41)
	268 (49)	294	381 (195)	389
	444 (61)	449	500 (51)	504
	560 (103)	567	618 (97)	622 (125)
	626 (125)	633 (177)	635 (185, 188)	
	643	645	679	682 (35)
	717 (35)	720 (35)	722	804 (6)
	839			
Currie, G. N.	561 (105)	567		
Curry, J.	87 (36)	121		
Curtiss, C. F.	487 (31)	503		
Cyvin, B. N.	307 (33)	311 (33)	385	
Cyvin, J. J.	713 (99)	724		
Cyvin, S. J.	307 (32)	311 (33)	373 (150)	377 (151)
	385	388	706 (89)	723
Czieslik, W.	534 (39, 44, 48)	541 (49)	565	
<b>D</b>				
Dailey, B. P.	231	421	495 (45)	496 (46)
	500 (45)	501	504	506 (4)
	511 (4)	533 (4)	540 (4)	565
	624 (145)	644	727 (2)	741 (2)
	766	770	772 (2)	779 (60)

## Index Terms

## Links

	800	802		
Dakin, T. W.	456			
Dal Borgo, A.	181	415	770	
Damaison, J.	421	766	770	
Damburg, R. J.	193 (54)	224		
Dang-Nhu, M.	208 (103)	225		
Dangoisse, D.	351 (142)	369 (142)	388	
Danielis, V.	383 (209)	389		
Daniels, J. M.	561 (104)	567		
Darling, B. R.	282 (104)	295		
Darling, B. T.	304 (12)	384	674 (19)	684 (37)
	721			
Das, T. P.	397 (14)	448	727 (12)	767 (12)
	801			
Davidson, E. R.	789 (72)	802		
Davies, P. B.	160 (93)	161 (93, 108)	171 202 (81)	
	225	357 (123)	359 (123)	387
Davis, R. W.	351 (152)	351	371 (153)	372 (153)
	380 (171)	388		
Decius, J. C.	282 (111)	295	302 (11)	372 (11)
	384			
de Hemptinne, M.	421	766	770	
Dehmelt, H. G.	399 (15)	448	737 (58)	737
	745 (30, 34)	746 (30)	767 (40)	770
	782 (65)	801		
de Leeus, F. H.	797			
Delfino, A. B.	269 (54)	294		
Delpuech, J. J.	689 (53)	722		
De Lucia, F. C.	2 (8)	3 (17, 23)	4 (23)	7
	75	81 (10)	83 (32)	84 (10, 28)

## Index Terms

## Links

85 (32)	86 (28)	89 (10)	96 (42)
100 (59)	107 (74)	116 (74)	120
131 (3)	141 (22)	143 (22)	144 (49)
145 (22)	164 (126, 131)		164
165 (126, 131)	166 (135)	169	172
190 (47)	191 (47)	192 (47)	
214	224	299 (3, 4)	343 (91)
344 (91)	345 (92)	346 (91)	347 (91)
349 (95, 97, 106)			351 (3)
351			
352 (93)	353 (91, 97, 106, 108)		361 (91)
366 (91)	375 (93, 156)	379 (156, 161)	381 (97)
384	386	434	444 (63)
449	560 (101)	567	702 (71)
710 (93)	723	803 (5)	
804 (16, 23, 28)	805 (3)	810 (5)	812 (5)
821 (5)	825 (5)	827 (16)	828 (16, 28)
829 (23, 28)	834 (5)	839	
Demaison, J.	291 (149)	296	313 (44)
	351 (58)	369 (143)	385
	415	597 (43)	600 (43)
	641	706 (79)	723
Demtroder, W.	4 (31)	8	
Demuyck, C.	96 (44)	98 (44)	121
	172	411	
Dendl, G.	324 (61)	386	502
Dennison, D. M.	29 (2)	32 (2)	35
	69	175 (1)	181 (6)
	189 (42)	193 (42)	201 (79)
	282 (104)	295	304 (12)
	384	386	324 (60)
			582 (7, 24)

## Index Terms

## Links

	603 (66)	618 (92)	639	642
	674 (19)	684 (37)	721	
Depannemaeker, J. C.	679			
Derr, V. E.	82	535	797	
DeSantis, D.	772 (50)	802		
Destombes, J. L.	96 (44)	98 (44)	121	164 (122)
	172	351 (142)	369 (142)	388
	411			
Di Cianni, N.	339 (82)	343 (82)	346 (82)	374 (82)
	378 (82)	386	710	
Dickman, R. L.	165 (130)	172		
Diercksen, G. H. F.	164 (118)	172		
DiGaicom, A.	273 (80)	295		
Dijkerman, H. A.	619 (101)	643		
Disch, R. L.	539 (65)	542 (65)	566	
Dixon, R. N.	110 (84)	122		
Dixon, T. A.	5 (46)	9	96 (41, 43)	97 (43, 48)
	121	154 (89)	157 (89)	159 (89)
	160 (98, 100)	161 (100)	163 (110)	164 (119)
	165 (125)	166 (132)	171	
Dixon, W. B.	231	698 (63)	723	
Dobyns, V.	595 (39)	597 (39)	641	
Dodd, R. E.	411			
Donohue, J.	653 (6)	721		
Dorain, P. B.	561 (104)	567		
Doraiswamy, S.	272 (57)	294		
Dorney, A. J.	338 (76)	360 (76)	386	
Dossel, K.-F.	181	415	501	516 (51)
	533 (51)	534 (49, 51)	546 (51)	566
	625	770		
Dousmanis, G. C.	109 (80)	115 (80)	122	432 (38)

## Index Terms

## Links

	444 (53, 58)	449	540 (67)	544 (67)
	552 (79)	554 (79)	566	
Dowling, J. M.	306 (24)	307 (25)	322 (59)	324 (25, 59)
	385	688 (44)	722	
Dreizler, H.	247 (16)	276 (84, 89)	293	295
	321	324 (61)	351	386
	421	502	534 (37, 39)	565
	572 (9)	597 (43)	598 (46, 52)	
	600 (43)	603	615 (78)	617 (83)
	618 (46, 52, 95)	643	621 (118, 120)	622 (122)
	623 (52, 136)	624 (144)	625 (123)	625
	639	641	667 (15)	721
	766	770	773 (55)	802
Drew, D. A.	216 (106)	225		
Drigas, T. M.	766	770		
Dubrulle, A.	351 (142)	369 (142)	388	415
	421	597 (43)	600 (43)	641
	766	770		
Duckett, J. A.	706 (83)	710 (84)	723	
DuMond, J. W. M.	857			
Duncan, J. L.	218 (118)	225	299 (166)	373 (147)
	378 (147)	380 (164, 166, 175, 180)		388
	603 (67)	642	712 (96)	724
Dunham, J. L.	73 (4)	78 (4)	120	
Dunmur, D. A.	539 (65)	542 (65)	566	
Durig, J. R.	216 (111, 115)	216	225	271 (56)
	272 (56)	294	598 (53)	621 (54)
	624	626 (53)	626	637
	641	666 (14)	721	
Dyer, P. N.	558 (87)	559 (87)	567	
Dyke, T. R.	153 (76)	161 (108)	171	

## Index Terms

## Links

Dymanus, A.	84 (26)	86 (26)	121	133 (6)
	141 (26)	143 (42)	169	411
	445	497	535	600 (57)
	619 (101)	642	797	804 (21, 27)
	840			
<b>E</b>				
Eagle, D. F.	481 (25)	503		
Eck, T. G.	737			
Eckart, C.	306 (22)	385		
Eckhardt, W.	1 (4)	7		
Edmonds, A. R.	426 (34)	439 (34)	448 (34)	449
	803 (2)	805 (2)	807 (2)	831 (2)
	839			
Edwards, H. D.	51			
Edwards, T. H.	341 (90)	386		
Ekkers, J.	5 (40)	9	276 (86)	295
	604 (71)	642		
El-Sayed, M. A.	5 (45)	9		
Ellder, J.	115 (94)	123		
Endo, Y.	97 (49)	116 (101)	121	381 (193)
	389	560 (95, 102)		567 603
	(67)			
	624	642	679	804 (36,
	39)			
	837 (39)	840		
Engerholm, G. G.	639 (213)	646		
Englebrecht, L.	617 (83)	642		
Erickson, N. R.	166 (134)	173		
Erlandsson, G. E.	190 (45)	224		
Esbitt, A. S.	619 (100)	643		
Eshbach, J. R.	506 (3)	511 (3)	520 (3, 11)	525 (3)

## Index Terms

## Links

	546 (3)	565		
Espositi, C. D.	143 (32)	148 (70)	170	635 (194)
	645	678 (30)	722	
Evenson, K. M.	105 (66)	106 (67)	115 (87, 89)	122
	560 (97)	567		
Ewig, C. S.	602 (60, 64)	603 (60, 68)	618 (60)	642
<b>F</b>				
Fabris, A. R.	559 (89)	567		
Faelhl, L.	804 (29)	840		
Fano, U.	458 (3)	503	803 (3)	839
Fantoni, A. C.	321			
Farag, M. S.	267 (36)	293		
Farukane, U.	772 (48)	801		
Fateley, W. G.	574 (14)	601 (14)	640	
Favero, P. G.	109 (82)	122	143 (32)	148 (70)
	170	181	231	273 (78)
	295	415	444 (56)	449
	498 (49)	504	678 (30)	722
	770			
Feenberg, E.	17 (1)	31 (1)	35	
Feld, B. T.	392 (5)	448		
Feldman, P. A.	146			
Ferigle, S. M.	306 (23)	385		
Fermi, E.	136 (21)	170		
Fernandez, J.	477 (19)	503	636 (201)	638 (201)
	645			
Filgueira, R. R.	321	380 (179)	389	
Findlay, F. D.	4 (33)	8	144 (51)	170
Finnigan, D. J.	380 (173)	389		
Fitzky, H. G.	84 (17)	121		
Fleming, J. W.	5 (42)	7 (42)	9	

## Index Terms

			<u>Links</u>
Fletcher, W. H.	308 (37)	385	
Fliege, E.	625		
Flygare, W. H.	5 (40) 91) 155 160 (101, 104) 162 (102, 104) 273 (65, 75) 421 500 514 (9) 517 (17) 533 (21, 23, 28, 32, 58) 534 (17, 23, 32, 40, 57) 536 (58, 60) 541 (58) 565 766 804 (9)	9 156 (86) 171 294 441 (49) 503 516 (21, 23, 28, 32, 57) 530 (16) 535 (19, 25, 33) 537 (58, 61) 545 (17, 20, 24) 624 770 839	154 (84) 155 (84, 86) 161 (102, 104) 222 (124) 295 411 481 (24) 512 (17, 20, 30, 36, 40) 516 532 (18, 20, 30, 36, 40) 535 540 (17, 66) 546 (17, 36, 40) 695 (62) 780 (62) 802
Flynn, G. W.	273 (74)	276 (74)	277 (93) 295
Foley, H. M.	97 (47) 554 (81) 736 (20)	121 566 742 (20, 28)	444 (57) 531 (20) 801
Ford, L. H.	341 (89)	386	
Ford, R. G.	276 (92)	281 (100)	295 624
Forti, P.	380 (179)	389	
Foster, P. D.	444 (63) 534 (19, 24)	449 535 (19, 24)	512 (20) 545 (20) 565
Fox, K.	195 (63, 71) 338 (79)	206 (63, 71) 360 (79)	207 (71) 386
Fraley, P. E.	341 (88)	386	

## Index Terms

## Links

Freedman, J. N.	326 (66)	386		
Frenkel, L.	4 (35)	8	179 (4)	181
	205	223		
Freund, R. S.	772 (50)	802		
Freund, S. M.	144 (44)	170	558 (86)	567
Fristrom, R. E.	291 (140)	296		
Friz, E.	369 (146)	388		
Fröhlich, H.	50 (5)	69		
Frosch, R. A.	97 (47)	121	444 (57)	449
	554 (81)	566		
Fry, H. A.	421	766	770	804 (37)
	840			

Fujii, O.	493 (40)	497 (40)	500 (40)	503
Fukuyama, T.	713 (98)	717 (102)	724	
Fuller, G. H.	859			
Fuller, M. J.	632	636 (200)	645	

## **G**

Gailar, N.	712 (95)	724		
Galica, J.	288 (138)	296		
Gallagher, J. J.	82	111 (85)	115 (95)	116 (85)
	122	444 (55)	449	535
	797			
Gallaher, K. L.	704 (73)	723		
Gamo, I.	312 (39)	385		
Garrison, A. K.	84 (20)	121	141 (24)	170
Garvey, R. M.	3 (24)	8	298 (2)	384
	804 (23, 28)	828 (28)	829 (23, 28)	840
Gaumann, T.	272 (58)	294		
Gauthier, L.	338 (75)	360 (75)	386	
Gaylord, A. S.	628 (162)	638 (162)	644	
Gebbie, H. A.	4 (33)	8	144 (51)	170

## Index Terms

## Links

Gegenheimer, R.	183 (13)	223		
Genzel, L.	1 (4)	7		
Georghiou, C.	287 (128)	288 (136)	296	381 (201)
	389	501		
Gerry, M. C. L.	146	181 (30)	181	187 (30)
	195 (69)	202 (82)	205 (82)	207 (69, 92)
	208 (94)	216 (82)	221 (121)	223
	226	307 (29)	338 (81)	343 (178)
	351 (152, 174)	351	361 (133)	371 (152)
	380 (29, 171, 174, 178)	385		498 (48)
	504			
	635 (184)	645	688 (45)	700 (67)
	706 (84)	710 (84)	722	
Gershstein, L. I.	2 (14)	8	193 (59)	194
	201 (80)	202 (59, 80)	224	
Geschwind, S.	411	415	770	
Ghosh, D. K.	321			
Ghosh, S. N.	800 (81)	802		
Giguere, P. T.	164 (121)	172		
Gilliam, O. R.	51	414	520 (10)	565
	679			
Gillies, C. W.	704 (73)	723		
Givens, W.	852 (2)	852		
Glorieux, P.	277 (94)	295		
Godfrey, P. D.	144 (44)	145 (55)	170	411
	679	710		
Gold, L.	789 (70)	802	979	
Gold, L. P.	82	84 (16)	121	497
	500			
Gold, R.	306 (24)	307 (25)	324 (25)	385
Golden, S.	248 (18)	293	392 (10)	406 (10)

## Index Terms

## Links

416 (10)	448	468 (11)	470 (11)
488 (11)	491 (11)	503	
Goldsmith, M.	304 (13)	384	
Goldsmith, P. F.	165 (130)	172	
Goldstein, J. H.	421	502	727 (9)
	766	770	800
Golub, G. H.	682 (36)	722	
Good, W. E.	188 (38)	224	392 (6)
	436 (41)	448	456
	565		506 (1)
Goodman, L. S.	737		
Gora, E. K.	263 (31)	293	
Gordon, J. P.	3 (20)	8	436 (42)
Gordy, W.	1 (1, 3)	2 (5, 11)	449
	7 (57)	7	47 (2)
	51	54 (8)	50 (8)
	72 (1)	75	67 (18)
	84 (1, 10, 20, 28)		69
	(22, 28, 33)	81 (10)	82 (1)
		85 (1, 21, 30, 33)	86
	87 (37)	89 (10)	102 (61)
	104 (57, 61)	105 (57, 61, 65)	106 (61)
	107 (71, 73)		
	109 (81)	115 (81)	120
	141 (22, 24, 31)	142 (31)	137
	145 (22)	170	144 (47)
	181 (7, 77)	181	180 (7)
	186 (25)	190 (45)	185 (23)
	198 (73)	191 (47)	192 (48)
	214 (78)	200 (77)	201 (73, 77)
	232 (3)	214	223
	292 (159)	256 (22)	257 (22)
		293	268 (22)
		296	349 (98, 106)

## Index Terms

## Links

353 (98, 106)	386	411	414
417 (18)	428	434	435 (39)
444 (54, 56)	448	487 (32)	493 (39)
494 (41)	495 (42)	497 (40)	500 (40)
501 (42)	503	511 (6)	512 (31, 41)
514 (6)	516 (6)	520 (10)	532 (31, 41)
534 (31, 41)	540 (68)	541 (69)	548 (68)
550 (70)	551 (70)	565	623 (141)
635 (187)	644	649 (2)	677 (23)
682	702 (71)	721	727 (5, 10)
737 (58)	737	740 (10)	745 (34)
750 (7)	754 (6)	761 (7)	770
772 (47)	778 (57)	781 (64)	783 (7)
785 (5)	787 (7)	788 (68)	795 (7)
800 (81)	800	835 (50)	840
874	878	896	
Gottlieb, C. A.	116 (98)	123	
Gottlieb, E. W.	116 (98)	123	
Gozzini, G.	273 (71)	294	
Grashoff, M.	445		
Green, S.	6 (56)	9	165 (122)
	168 (136)	172	
Grenier-Beeson, M. L.	185 (19)	187 (19)	223
	384		304 (14)
Griffths, J. E.	779 (59)	802	
Grivet, P.	727 (13)	801	
Groner, P.	598 (53)	621 (54)	624
	641		626 (53)
Gsell, R. A.	216 (108)	225	415
Guarnieri, A.	193 (60)	224	231
	295	321	276 (84)
		500	502

## Index Terms

## Links

	534 (43, 46, 53)	566		
Gudeman, C. S.	96 (43)	121	164 (28)	165 (128)
	166 (132)	172		
Guelachvili, G.	208 (102)	225		
Guélin, M.	165 (127)	168 (136)	169 (136, 138)	172
Guggenheim, E. A.	672 (18)	721		
Guibe, L.	772 (46)	801		
Gunn, H. I.	145 (55)	170		
Günthard, Hs. H.	272 (58)	276 (86)	282 (113)	294
	295	598 (48)	600 (58)	603 (48)
	604 (71)	618 (48, 51, 93)	622 (124, 126)	
	623 (51, 139)	624 (48)	626 (126)	641
	701 (68)	723	804 (10, 43)	839
Gunther-Mohr, G. R.	392 (11)	411	415 (41)	415
	436 (11, 41)	441 (11)	448	770
Gustafson, S.	487 (32)	503	512 (31, 41)	532 (31, 41)
	534 (31, 41)	565		
Gwinn, W. D.	369 (145)	388	421	425 (22)
	448	477 (19)	499 (50)	502
	608 (75)	615 (79)	616 (76)	628 (162)
	636 (201)	638 (162, 201, 206, 211)	639 (213)	
	642	644	766	770
	804 (9)	839		

## **H**

Hadley, G. F.	426 (31)	449		
Haese, N. N.	164 (28)	165 (128)	172	
Hagen, G.	307 (32)	311 (33)	385	
Hahn, E. L.	397 (14)	448	727 (12)	767 (12)
	801			
Hainer, R. M.	31 (5)	35	229 (1)	232 (1)
	234 (1)	236 (1)	242 (1)	246 (1)

## Index Terms

## Links

	259 (23)	262 (23)	292	340
	416 (17)	448	849 (1)	852
Haissinsky	878			
Haland, A.	216 (107)	225		
Hallowell, C. D.	797			
Halonen, L.	369 (146)	388		
Hamer, E.	534 (37)	565		
Hamilton, W. C.	361 (135)	388		
Hamphill, D. C.	633 (177)	645		
Handelman, E. T.	615 (79)	642		
Hannay, N. B.	795 (76)	802		
Hanson, H. M.	195 (61)	224		
Hanyu, Y.	620 (104)	643	689 (48)	722
Hardy, W. A.	137			
Harford, S. L.	411			
Harmony, M. D.	281 (102)	295	636 (197)	645
	649 (3)	691 (56)	721	
Harrington, H. W.	638 (206)	645		
Harris, C. L.	411			
Harris, C. O.	602 (64)	642		
Harris, D. O.	623 (133)	632 (133)	638 (206)	639 (213)
	643	645		
Harris, S. J.	160 (93)	161 (93, 95)	162 (96)	171
Harrop, W. J.	106 (68)	122		
Hasegawa, A.	624			
Hayashi, M.	577 (19)	579 (19)	590 (19)	621 (19)
	624	626	627 (146, 154)	
	632	640	644	
Heath, G. A.	415	770		
Hebb, M. H.	99 (51)	121		
Hebert, A. J.	797			

## Index Terms

## Links

Hecht, K. T.	207 (99)	225	338 (73)	360 (73)
	386	582 (26)	618 (92)	623 (141)
	640	642	644	674 (19)
	721			
Hedberg, K.	706 (89)	723		
Heidelberg, R. F.	444 (61)	449		
Heise, H. M.	502			
Helminger, P.	2 (8)	7	47 (2)	69
	75	96 (42)	121	131 (3)
	164 (126, 131)	166 (135)	169	172
	181 (77)	190 (46)	191 (47)	192 (47)
	200 (77)	214 (78)	214	224
	299 (4)	343 (91)	344 (91)	345 (92)
	346 (91)	347 (91)	349 (97, 106)	
	352 (93)	353 (91, 97, 106, 108)		356 (118)
	361 (91)	366 (91)	375 (93, 156)	379 (155, 161)
	381 (97)	384	386	411
	434	702 (71)	710 (93)	
	723			
Helms, D. A.	84 (25)	90 (25)	121	
	198 (73)	201 (73)	215 (73)	224
Henderson, G.	221 (122)	226		
Henderson, R. S.	435 (40)	449		
Henry, A. F.	552 (77)	554 (77, 80)	556 (77)	566
Henry, J. C.	5 (49)	9	115 (90)	122
Henry, L.	360 (131)	387		
Herberich, G. E.	343 (138)	363 (138)	373 (138)	378 (138)
	388	616	683 (61)	693 (61)
	723			
Herbst, E.	83 (32)	85 (32)	96 (42)	121
	164 (114, 126, 131)	164	165 (126, 131)	166 (135)

## Index Terms

## Links

	172	558 (86)	567	804 (18)
	840			
Herlemont, F.	415	770		
Herrmann, G.	191 (50)	224	426 (32)	449
Herschbach, D. R.	477 (18)	502	574 (11)	577 (18)
	584 (28)	587 (28, 33)	589 (28)	590 (18, 28)
	591 (28, 34)	593 (32)	594 (11, 32)	596 (28)
	599 (11)	601 (11, 59)	602 (18, 28)	612 (28)
	618 (28)	639	680 (86)	686 (42)
	706 (85)	708 (85)	709 (86)	712 (42, 86)
	714 (86)	722		
Herzberg, G.	7 (68)	10	57 (14)	69
	87 (36)	94 (40)	106 (69)	121
	162 (109)	172	211 (104)	225
Herzberg, L.	87 (36)	121		
Heuvel, J. E. M.	600 (57)	642	804 (21)	840
Hickernell, F.	633 (175)	645		
Higgins, R. J.	267 (36)	293		
Hill, A. G.	483 (26)	497 (26)	503	
Hill, E. L.	108 (76)	111 (76)	122	
Hill, R. H.	341 (90)	386		
Hill, R. M.	99 (54)	122	539 (64)	542 (64)
	551 (70)	566		
Hillger, R. E.	340 (84)	386	520 (11)	565
Hills, G. W.	560 (103)	567		
Hinze, J.	784 (67)	802		
Hirakawa, H.	411			
Hirose, C.	187 (34)	223	701 (69)	723
Hirota, E.	97 (49)	106 (70)	107 (75)	116 (96,
	99, 101)			
	121	187 (28, 32)	223	231

## Index Terms

## Links

268 (52)	288 (132)	291 (141)	294
296	381 (189, 192)		389
559 (108)	560 (95, 102)		564 (108, 111)
567			
596 (42)	603 (67)	607 (74)	620 (74)
621 (119)	623 (133)	624	627 (133, 152)
628 (156)	630 (169)	633 (156)	635 (190)
641	649 (4)	677 (26)	678 (26, 31)
679	711 (26)	721	804 (36, 39)
837 (39)	840		
Hirschfelder, J. O.	487 (31)	503	
Hjalmarson, A.	165 (130)	172	
Hobbs, L. M.	164 (115)	172	
Hocker, L. O.	4 (35)	8	
Hocking, W. H.	90 (29)	121	380 (172)
	389	498 (48)	504
			632
Hodgeson, J. A.	444 (62)	449	
Hoeft, J.	81 (11)	84 (19)	87 (38)
	89	120	411
	804 (31, 33)	840	445
Hoffman, J. M.	192 (52)	224	
Høg, J. H.	620 (105)	643	689 (49)
Holden, A. N.	51	137	682
Hollis, J. M.	164 (116, 121)	172	
Holloway, J. H.	380 (164, 181)	388	
Holmgren, S. L.	160 (97)	172	
Holt, C. W.	195 (69)	207 (69, 92)	224
	386		338 (81)
Hølzer, B.	445		
Honda, T.	268 (52)	294	
Honerjäger, R.	89	532 (38, 42, 45)	534 (38, 42, 45)
			565

## Index Terms

## Links

Honig, A.	83 (15)	85 (15)	121	
Hooper, H. O.	767 (42)	801		
Hopfinger, A. J.	272 (60)	294		
Horak, M.	383 (209)	389		
Horsfall, R. B.	110 (83)	122		
Hougen, J. T.	169 (139)	173	193 (56)	224
	304 (18)	382 (18)	385	560 (98)
	567	804 (19, 35)	838 (35)	840
Houston, P. L.	273 (64)	294		
Howard, B. J.	153 (76)	171	804 (12)	839
Howard, C. J.	560 (97)	567		
Howard, J. B.	282 (103)	286 (103)	295	301 (8)
	304 (8)	384	586 (32)	641
	674 (19)	721		
Howard, R. R.	48 (3)	69	539 (63)	542 (63)
	566			
Howe, J. A.	481 (24)	503		
Hoy, A. R.	193 (58)	220 (119)	224	380 (165)
	383 (203)	388		
Hrubesh, L. W.	7 (70)	10		
Hsu, S. L.	624			
Hüber, K. P.	7 (68)	10		
Hiibner, D.	534 (55)	535 (56)	536 (55)	538 (55)
	540 (56)	542 (56)	566	
Hudson, S. D.	626			
Hughes, R. H.	451 (1)	492 (1, 35)	502	
Huguenin, G. R.	165 (130)	172		
Huis zoon, C.	141 (26)	170		
Hunt, R. H.	623 (141)	644		
Huo, W.	789 (71)	802		
Hüttner, W.	411	512 (17, 20)	516 (23)	517 (17)

## Index Terms

## Links

530 (16)	532 (20)	533 (23)	534 (17, 23, 25)
535 (25)	540 (17)	545 (17, 20)	546 (17)
565	804 (26, 30)	840	

### I

Ibers, J. A.	193 (53)	224	
Ibushi, N.	626		
Ikeda, T.	267 (41)	268 (49)	294
	643		618 (97)
Imachi, M.	627 (154)	644	
Ingram, D. J. E.	7 (59)	9	
Irvine, W. M.	115 (94)	123	165 (130)
Irwin, J. C.	623 (132)	643	172
Ito, T.	425 (25)	448	
Ivash, E. V.	582 (25)	640	

### J

Jaccarino, V.	737		
Jache, A. W.	444 (62)	449	
Jackson, R. H.	339 (82)	343 (82, 138)	346 (82)
	363 (138)		
	373 (138)	374 (82, 138)	375 (82)
	378 (82, 138)		
	386	683 (61)	693 (61)
	723		710
Jacobs, G. D.	421	766	770
Jacox, M. E.	145 (59)	171	
Jaeschke, A.	615 (78)	642	
Jaffe, H. H.	784 (67)	802	
Jahn, H. A.	685 (40)	722	
Jalilian, M. R.	626		
Jaman, A. I.	321		
Janda, K. C.	160 (96)	171	

## Index Terms

## Links

Javan, A.	4 (35)	8	273 (79)	295
Jefferts, K. B.	87 (35)	97 (45)	121	163 (111)
	172			
Jen, C. K.	506 (2)	511 (5)	520 (2, 11)	523 (12)
	524 (5)	546 (5)	565	
Jenkins, D. G.	653 (6)	721		
Jenkins, D. R.	185 (24)	223	444 (61)	449
Johns, J. W. C.	145	150 (72)	171	193 (56)
	224	304 (18)	382 (18)	385
Johnson, C. M.	111 (85)	115 (95)	116 (85)	122
	444 (55)	449		
Johnson, D. R.	3 (19)	8	116 (99)	123
	146	149	354 (113)	371 (154)
	375 (154)	387	411	
	559 (108)	564 (108)	567	710
Johnson, R. C.	501			
Johnson, R. D.	608 (75)	642		
Johnson, R. H.	52 (11)	69		
Johnston, M.	184 (15)	223		
Jones, G. E.	2 (7)	7 (69)	7	10
	72 (2)	120	265 (34)	293
	300 (7)	351 (7)	361 (7)	364 (7)
	384			
Jones, H.	3 (28)	4 (30)	7 (30)	8
	273 (63)	294	411	635 (189)
	645			
Jones, L. H.	192 (52)	224	380 (169)	389
Jones, S. R.	288 (136)	296	360 (127)	387
	501			
Joosen, P.	602 (65)	642		
Jordahl, O. M.	586 (31)	640		

## Index Terms

Joyner, C. H.

154 (89)

161 (100)

Judd, B. R.

426 (35)

839

Jurek, R.

360 (128)

387

## **K**

Kabar, R. K.

688 (46)

Kaercher, A.

246 (14)

Kagann, R. H.

202 (82)

225

Kakar, R. K.

116 (97)

643

Kalasinsky, K. S.

624

Kalasinsky, V. F.

624

Karakida, K.

216 (114)

Karlsson, H.

618 (97)

Karo, A. M.

789 (74)

Karplus, R.

51 (10)

Karyakin, E. N.

152 (75)

Kasai, P. H.

231

Kastler, A.

3 (21)

Kasuya, T.

321

Kato, Y.

772 (48)

Kauppinen, J.

194

Kaushik, V. K.

321

Kawashima, Y.

187 (33)

Keenan, M. R.

5 (41)

159 (86)

161 (102, 106)

Keller, C.

689 (52)

Keller, H. J.

282 (113)

## Links

157 (89)

171

439 (35)

449

803 (4)

387

689 (46)

293

205 (82)

207 (95)

216 (82)

123

620 (106)

632

620

216

225

643

802

54 (12)

69

171

621 (114)

643

8

421

766

770

801

223

678 (29)

722

9

155 (85)

156 (86)

160 (101, 106)

162 (102) 171

722

295

## Index Terms

## Links

Keller, R. A.	499 (50)	502	504	639 (213)
	646			
Kellogg, J. M. B.	392 (1)	448	466 (9)	503
Kemble, E. C.	475 (17)	503	586 (31)	640
Kemp, J. D.	570 (1)	639		
Kennard, O.	653 (6)	721		
Kenney, C. N.	7 (60)	9	65 (17)	70
	444 (61)	449	727 (15)	801
Kerr, C. M. L.	115 (89)	122		
Kewley, R.	185 (24)	223	250	267 (41)
	294	321	633 (177)	645
Kieffer, L. J.	737			
Kikuchi, Y.	381 (189)	389	677 (26)	711 (26)
	722			
Kilb, R. W.	231	577 (17)	578 (17)	583 (27)
	592 (27)	594 (37)	600 (27)	605 (27)
	607 (37)	640		
Kilpatrick, J. E.	639 (212)	646		
Kim, H.	351 (120)	357 (120)	387	499 (50)
	502	504	639 (213)	646
King, G. C.	31 (5)	35		
King, G. W.	112	246 (1)	292	340
	416 (17)	448	849 (1)	852
King, J. G.	737			
King, W. C.	2 (5)	7		
Kinsey, J. L.	444 (61)	449	804 (6)	839
Kirby, C.	144 (46)	146 (64)	147 (62)	170
	415	700 (65)	723	770
	781 (63)	802		
Kirchheimer, J.	773 (53)	802		
Kirchhoff, W. H.	328 (68)	343 (163)	354 (68, 113)	361 (68)

## Index Terms

## Links

363 (37, 68)	364 (37)	370 (68)	371 (68, 137, 154)
375 (68, 154)	378 (137, 163)		380 (163)
386			
617 (87)	642	710	
Kirschner, S. M.	208 (100)	225	338 (77)
	386		360 (77)
Kirtman, B.	602 (60)	603 (60, 68)	617 (89)
	642		618 (60, 89)
Kitchin, R. W.	267 (43)	294	628 (166)
Kivelson, D.	247 (17)	251 (21)	293
	311 (21, 38)	314 (50)	305 (21)
	324 (21)	343 (38)	33 (50)
	385	375 (38)	378 (38)
	618 (88, 90)	473 (14)	617 (88)
		503	
Kiwada, K.	626	642	
Kizer, K. L.	624	666 (14)	721
Klauss, K.	307 (36)	385	
Klein, G. P.	354 (113)	387	
Klemperer, W.	82	87 (39)	121
	153 (76)	154 (89)	144 (44)
	156	157 (89)	155
	161 (93, 95, 99, 108)	159 (89)	156 (89)
	163 (113)	162 (96, 100)	160 (93)
	225	164 (114)	170
	357 (123)	166 (81)	202 (81)
	415	359 (123)	411
	770	387	434
		558 (86)	567
		802	979
Kneizys, F. X.	326 (66)	386	
Kneubuhl, F.	272 (58)	294	
Knöckel, H.	745 (32)	801	
Knopp, J. V.	623 (127, 130)	643	

## Index Terms

## Links

Kohima, T.	620 (106)	643		
Kohler, F.	3 (29)	8		
Kohler, J. S.	582 (24)	640		
Kojima, T.	231	624	689 (47)	722
Kondo, K.	436 (43)	449		
Kopfermann, H.	732 (22)	733 (22)	735 (22)	801
Korolkov, V. S.	737			
Koster, G. F.	735 (26)	737	801	
Kraemer, W. P.	164 (118)	172		
Kraitchman, J.	231; 415	655 (8)	721	770
Kramers, H. A.	99 (50)	121		
Kreiner, W. A.	207 (98)	225	616	
Krischer, L. C.	143 (36)	170	216 (108, 112)	
	225	231	415	426 (33)
	436 (33)	438 (33)	443 (33, 52)	
	447 (33)	449	594 (38)	597 (38)
	600 (55)	641	700 (66)	723
	770			
Krishner, L. C.	804 (7)	839		
Kronig, R. de L.	29 (4)	35	175 (3)	223
Kroto, H. W.	7 (63)	9	133 (9)	144 (46)
	145 (9)	145	146 (60, 63)	147 (60)
	169	181 (31)	187 (31)	216 (116)
	223	225	282 (110)	288 (110, 133)
	295	415	500	571 (4)
	639	700 (65)	723	770
	781 (63)	802		
Krüger, H.	399 (15)	448		
Krupnov, A. F.	2 (12)	7 (13)	8	152 (75)
	171	193 (59)	194	201 (80)
	202 (59, 80)	224	349 (96)	386

## Index Terms

## Links

Kuchitsu, K.	216 (114)	216	225	373 (150)
	388	649 (4)	706 (89)	713 (97, 100)
	717 (102)	721	723	
Kuczkouski, R. L.	143 (36)	170	415	649 (3)
	704 (73, 76)	721	723	770
Kudian, A. K.	195 (68)	207 (68)	224	
Kuhler, M.	618 (96)	643		
Kuijpers, P.	84 (26)	86 (26)	121	133 (6)
	143 (42)	169	445	
Kuiper, T. B. H.	116 (97)	123		
Kukolich, S. G.	222 (123, 125)	226	415	421
	436 (44)	449	516 (28)	516
	533 (28)	535	565	766
	770	804 (15, 29, 37, 40)		840
Kundle, A. C.	444 (62)	449		
Kunstmann, K.	231	502	627 (153)	644
Kupecek, P.	360 (132)	387		
Kurland, R. J.	687 (43)	722		
Kusch, P.	737			
Kutner, M. L.	166 (133)	173		
Kwan, Y. Y.	288 (135)	296	603 (66)	642
Kwei, G. H.	477 (18)	500 (51)	503	
Kwok, S.	146			

## **L**

Laane, J.	380 (169)	389		
Lada, C. J.	116 (98)	123		
Lafferty, W. J.	267 (40)	268 (50)	294	321
	349 (104)	387	628 (161)	644
	649 (3)	721		
Lainé, D. C.	3 (25)	8		
Lamb, W. E.	141 (29)	170	392 (5)	448

## Index Terms

## Links

Landolt-Börnstein	7 (65) 423 (19) 504 756 (65)	9 445 (19) 623 (143)	292 (151) 448 644	296 502 (53) 752 (65)
Landsberg, B. M.	135 (20) 421 723	170 571 (4) 766	383 (204, 210)	389 706 (82)
Larkin, D. M.	493 (41)	494 (41)	503	
Larsen, N. W.	623 (135, 137)	643		
Laurie, V.	276 (91)	278 (91)	295	
Laurie, V. W.	259 (26) 296 485 (28) 501 638 (209) 674 (20) 706 (85, 89) 714 (86) 802	265 (33) 415 487 (28) 607 (72) 642 680 (86) 708 (85) 721	291 (142) 457 (2) 494 (2) 617 (86) 644 686 (42) 709 (86) 770	293 458 (2) 501 (2) 628 (158) 649 (3) 703 (20) 712 (42, 86) 779 (61)
Le Fevre, R. J. W.	799 (78)	802		
Leacock, R. A.	623 (141)	644		
Leavell, S.	635 (188)	645		
LeCroix, C. K.	622 (125)	626 (125)	643	
Lee, M. C.	276 (88)	295		
Lees, R. M.	143 (34) 385 642	170 387 682 (34)	318 (54) 602 (61) 720 (34)	361 (133) 603 (61) 722
Legell, H.	598 (47)	641		
Legon, A. C.	7 (66) 155 (80, 85, 91) 159 (80, 86)	10 155 160 (106)	153 (78) 156 (80, 86) 171	154 (80) 157 (80) 221 (120)

## Index Terms

## Links

	221	222 (124)	225	635 (184)
	645			
Legrand, J.	277 (94)	295		
Levine, I. N.	627 (147)	644		
Levy, D. H.	5 (43)	9	558 (87)	559 (87)
	559	561 (105)	564 (106)	567
	804 (12)	839		
Lew, H.	737			
Li, Y. S.	216 (111, 115)	216	225	271 (56)
	272 (56)	294	598 (53)	624
	626 (53)	626	637	641
	666 (14)	721		
Lide, D. R.	4 (34)	8	84 (16)	107 (72)
	121	143 (36, 41)		144 (41, 52)
	170	231	259 (25)	261 (25)
	268 (45)	291 (140)	293	296
	321	363 (137)	371 (137)	378 (137)
	388	497	500	501
	502	563 (107)	567	571 (3)
	584 (29)	608 (29)	613 (29)	615 (29)
	617 (29, 86)	639	642	
Lin, C. C.	231	444 (60)	449	572 (8)
	579 (8)	582 (8)	583 (27)	584 (29)
	587 (8)	592 (8, 27)	594 (8)	599 (8)
	600 (27)	603 (8)	605 (27)	608 (8,
	29)			
	609 (29)	610 (8, 29)	611 (29)	612 (8)
	613 (8, 29)	614 (8)	615 (8, 29)	617 (29)
	623 (129)	627 (129)	639	643
Lind, G.	804 (29)	840		
Lindfors, K. L.	492 (38)	503		

## Index Terms

## Links

Lindsey, D. C.	351 (155)	375 (155)	380 (155)	388
Linke, R. A.	165 (127)	172		
Linzer, M.	556 (82)	567		
Lister, D. G.	572 (10)	620 (109)	624	635 (191)
	639	643	645	
Little, G. B.	688 (45)	722		
Little, R.	411			
Little, W. A.	804 (25)	840		
Liu, B.	164 (117)	172		
Livingston, R.	414	426 (30)	449	520 (10)
	565	745 (29)	770 (29)	801
Ljunggren, S. O.	689 (50)	722		
Lo, M.-K.	512 (17, 20)	517 (17)	532 (20)	534 (17, 19)
	535 (19)	540 (17)	545 (17, 20)	546 (17)
	565			
Long, M. W.	426 (27)	448		
Longuet-Higgins, H. C.	539 (65)	542 (65)	566	620 (113)
	643			
Lord, R. C.	628 (163)	638 (163)	644	
Lorentz, H. A.	48 (4)	69		
Loubser, J. H. N.	426 (33)	436 (33)	438 (33)	447 (33)
	449	804 (7)	839	
Louck, J. D.	282 (107)	295	304 (20)	385
Lovas, F. J.	81 (11)	82 (14)	89 (11)	89
	120	164 (116)	172	354 (113)
	387	411	501	649 (3)
	721			
Low, W.	458 (4)	468 (4)	478 (4)	503
Lowe, R. S.	321			
Loyd, R. C.	691 (56)	722		
Lucas, N. J. D.	351 (170)	380 (170)	389	559 (89)

## Index Terms

## Links

567

Lucken, E. A. C.

772 (49)

802

Lum, D. K.

633 (176)

645

Luntz, A. C.

638 (206, 208, 211)

639 (213)

645

Lurio, A.

737

772 (50)

802

Lutz, H.

502

622 (122)

625 (122)

625

643

Lyons, H.

191 (49)

224

## M

McAfee, K. B.

492 (35)

503

779 (59)

802

McCormick, R. V.

144 (45)

170

McDonald, C. C.

556 (84)

561 (84)

567

Macdonald, J. N.

7 (66)

10

572 (10)

628 (165)

639

644

McDowell, R. S.

192 (52)

224

McGurk, J. C.

273 (65)

294

500

512 (40)

532 (40)

534 (40)

546 (40)

565

Macke, B.

277 (94)

295

McKean, D. C.

380 (164, 174, 181)

388

McKinney, P. M.

622 (125)

626 (125)

643

McKnight, J. S.

105 (65)

122

MacLeod, J. M.

146 (60)

147 (60)

171

McNaught, I.

307 (28)

385

McRae, G. A.

207 (95)

225

Mäder, H.

276 (84)

295

598 (52)

603

618 (52)

623 (52)

641

Maes, S.

181

185 (20)

187 (35)

223

Mahler, L.

421

766

770

Mahler, R. J.

105 (66)

122

Makhanek, A. G.

737

Maki, A. G.

4 (34)

8

144 (52)

146

## Index Terms

## Links

	149	170	200 (75)	224
	649 (3)	357 (124)	387	721
Makushkin, Y. S.	285 (123)	296		
Mallinson, P. D.	380 (180)	389		
Malloy, T. B., Jr.	228 (48)	228	267 (36, 43)	
	268 (47, 51)	293	294	
	628 (163, 167)	629 (168)	633 (176)	
	638 (163)	644	690 (54)	722
Maltesen, G.	773 (53)	802		
Mandel, M.	83 (15)	85 (15)	121	
Mann, D. E.	291 (140)	296		
Manning, M. F.	189 (41)	193 (41)	224	
Manns, K.	89			
Manson, E. L.	84 (10, 28)	86 (28)	87 (37)	89 (10)
	120			
Marcuse, D.	141 (23)	170		
Margenau, H.	554 (80)	566		
Mariella, R. P.	558 (86)	567		
Marino, R. A.	772 (46)	801		
Markov, V. N.	201 (80)	225		
Maroor, J.	421	766	770	
Marshall, J. L.	804 (29)	840		
Marshall, M. D.	155			
Marshall, S. A.	485 (27)	493 (27)	503	
Marstokk, K.-M.	216 (106)	225	272 (61)	294
	320 (56)	321	351 (142)	369 (142)
	385	388	635 (195)	645
Martin, D. H.	7 (62)	9		
Martin, M. C.	704 (74)	723		
Maslovskij, A. V.	2 (14)	8	193 (59)	201 (80)
	202 (59, 80)	224		

## Index Terms

## Links

Masson, M. A.	689 (53)	722		
Mata, F.	704 (74)	723		
Matamura, C.	216 (114)	225		
Mathier, E.	598 (50)	623 (137)	641	643
Mathur, S. N.	281 (102)	295	691 (56)	722
Matsumara, K.	500			
Matsumura, C.	143 (38, 41)	144 (41)	170	181 (117)
	217 (117)	225	621 (119)	643
	717 (102)	724		
Matsumura, M.	216			
Mattauch, J. H. E.	859			
Matthews, H. E.	146			
Mays, J. M.	496 (46)	501	504	779 (60)
	802			
Mazur, U.	704 (76)	723		
Mazzariol, E.	373 (147)	378 (147)	388	
Meakin, P.	623 (133)	632 (133)	643	
Meal, J. H.	285 (117)	296	373 (149)	388
	685 (39)	709 (39)	722	
Meeks, M. L.	5 (49)	9	115 (90)	122
Meerts, W. L.	202 (84)	203 (86)	204 (84)	205 (85)
	225	411	618 (110)	620 (110)
	621 (110)	643		
Meier, J.	622 (124)	643		
Meise, H. M.	603			
Meister, A. G.	306 (24)	307 (25)	324 (25)	385
Mennicke, J.	183 (13)	223		
Merritt, F. R.	51	137	682	
Messelyn, J.	277 (94)	295		
Messer, J. K.	2 (9)	8		
Metropolis, N.	426 (36)	439 (36)	447 (36)	449

## Index Terms

## Links

	805 (45)	838 (45)	840	
Meyer, H.	773 (52)	802		
Meyer, R.	598 (50)	603	618 (93)	641
Michelot, F.	338 (79)	360 (79)	386	804 (34)
	840			
Mikhaylov, V. M.	195 (72)	206 (72)	224	
Millen, D. J.	7 (66)	10	153 (78)	154 (80)
	155 (80)	159 (80)	171	221 (120)
	221	225	343 (138)	363 (138)
	373 (138)	378 (138)	388	627 (148)
	635 (182, 184)	644	683 (61)	693 (61)
	723			
Miller, C. E.	804 (13)	823 (13)	827 (13)	840
Miller, F. A.	574 (14)	601 (14)	640	
Miller, S. L.	99 (53)	121		
Miller, T. A.	559 (88)	561 (105)	564 (106)	567
	772 (50)	802		
Milligan, D. E.	145 (59)	171		
Mills, I. M.	195 (66)	206 (88)	220 (119)	224
	287 (129)	296	369 (144, 146)	370 (144)
	373 (147)	377 (159)	378 (147)	380 (167)
	381 (183, 185)	388	674 (19)	706 (83)
	721	723		
Minton, T. K.	155 (85)	156 (86)	159 (86)	171
Mirri, A. M.	109 (82)	122	181	231, 273
	(78)			
	295	373 (147)	378 (147)	388
	444 (56)	449	624	635 (194)
	645	678 (32)	722	
Mishra, A.	804 (22)	826 (22)	840	
Mitchell, A. D.	653 (6)	721		

## Index Terms

## Links

Miyahara, A.	411			
Mizushima, M.	7 (67) 105 (66) 195 (65) 425 (25) 478 (22) 503 838 (44)	10 106 (62, 67) 224 444 (59) 485 (30) 550 (70) 840	99 (54, 58) 115 (88) 383 (214) 448 487 (30) 566 804 (44)	104 (62) 122 389 469 (12) 495 (30) 804 (44)
Mizushima, S.	571 (5)	639		
Mjöberg, P. J.	154 (82) 722	155 (83)	171	689 (50)
Mochel, A. R.	620 (103)	643		
Mohamad, A. B.	216 (111)	225		
Mohan, N.	313 (43)	385		
Møllendal, H.	216 (106) 320 (56) 385	225 321 388	272 (61) 351 (142) 635 (195)	294 369 (142) 645
Moller, K. D.	623 (136)	643		
Möller, T.	445			
Molloy, T. B., Jr.	628 (166)	644		
Moloney, M. J.	600 (55)	642		
Montagutelli, J.	338 (75)	360 (75)	386	
Montgomery, J. A., Jr.	6 (56)	9	165 (122)	172
Moret-Bailly, J.	338 (74, 79) 804 (34)	360 (74, 79) 840		386
Morgan, H. W.	190 (47) 353 (106) 723	191 (47) 387 766	224 421 770	349 (106) 702 (71)
Morgenstern, K.	181	411	804 (30)	840
Morino, Y.	3 (18) 122	8 149	107 (75) 181 (117)	116 (96, 99) 187 (28, 34)

## Index Terms

## Links

	217 (117)	223	225	231
	285 (118)	291 (143)	296	298 (1)
	341 (85)	373 (148)	381 (182, 184, 188)	
	384	386	388	559 (108)
	564 (108, 110)	567	621 (119)	628 (156)
	633 (156)	643	677 (26)	
	679	683 (27)	684 (38)	685 (41)
	686	706 (88)	711 (26, 88)	
	713 (98, 100)	722		
Morris, M.	145 (57)	164 (120)	170	172
Morrison, J. A.	216 (112)	225	415	770
Morse, P. M.	73 (3)	120		
Morton, R. J.	627 (148)	644		
Muenter, J. S.	153 (77)	158 (92)	171	415
	457 (2)	458 (2)	485 (28)	487 (28)
	494 (2, 29)	497 (29)	500 (29)	501 (2)
	500	745 (33)	770	801
Müller, A.	313 (43)	385		
Muller, N.	421	766	770	
Mulliken, R. S.	108 (77)	109 (79)	114 (79)	122
	130 (2)	169	239 (5)	242 (5)
	293	747 (35)	755 (38)	768 (43)
	790 (75)	791 (35)	798 (35)	801
Mun, I. K.	633 (175)	645		
Murchison, C. B.	381 (187)	389		
Murray, A. M.	804 (38)	840		
Murray, J. T.	804 (25)	840		
Murty, A. N.	635 (185)	645		
Muse, J. D.	288 (137)	296		
Myers, R. J.	231	425 (22)	448	608 (75)
	616 (76)	621 (114)	622 (125)	626 (125)

## Index Terms

## Links

642

### N

Nair, K. P. R.	445	625	804 (31, 33)	840
Nakagawa, I.	149 (71)	171		
Nakagawa, J.	626	627 (155)	632	644
Nakagawa, T.	149	381 (184, 188)		389
Nakata, M.	717 (102)	724		
Nandi, R. N.	321	636 (198)	645	
National Bureau of Standards	7 (64)	9		
Naylor, R. E., Jr.	608 (77)	612 (77)	615 (77)	642
Nelson, A. C.	415			
Nelson, J. F.	624			
Nelson, R.	231	421	627 (150)	644
	765 (39)	766	770	801
Nemes, L.	285 (119)	296	313 (45)	385
	706 (79)	723		
Nethercot, A. H.	75 (9)	80 (9)	120	511 (7)
	545 (7)	548 (7)	565	676 (22)
	722			
Neuenschwander, M.	689 (52)	722		
Neumann, R. M.	202 (81)	225	357 (123)	359 (123)
	387			
Newman, M.	352 (112)	387		
Nielsen, A. H.	127 (1)	169	674 (19)	721
Nielsen, H. H.	131 (4)	132 (4)	133 (8, 13)	169
	182 (12)	185 (17, 22)		201 (22, 79)
	223	232 (2)	282 (105, 108)	284 (108)
	286 (108)	292	295	301 (9)
	304 (9, 13)	384	582 (23)	640
	674 (19)	721		

## Index Terms

## Links

Nielsen, J. T.	773 (53)	802		
Niroomand-Rad, A.	286 (125)	296	367 (141)	382 (200)
	388			
Nishikawa, T.	766	770		
Nixon, J. F.	133 (9)	145 (9)	145	169
Nixon, J. R.	216 (116)	225	500	
Nolan, F. J.	246 (14)	293		
Nolting, H.-P.	89			
Nordsieck, A.	392 (4)	448	726 (1)	800
Norris, C. L.	273 (65)	294	411	500
	512 (40)	532 (40)	534 (40)	536 (61)
	546 (40)	565	780 (62)	802
Nösberger, P.	598 (51)	618 (51)	623 (51)	641
	701 (68)	723		
Novick, S. E.	160 (93)	161 (93, 95, 108)		162 (96)
	171	313 (48)	315 (48)	385
Nowicki, P.	411	804 (26, 30)	840	
Nuckolls, R. G.	191 (49)	224		
Nygaard, L.	231	502	620 (105)	623 (135)
	627 (153)	643	666 (13)	689 (49)
	698 (63)	704 (13)	721	773 (53)
	802	827 (49)	840	
Nyman, L.-Å.	165 (130)	172		
<b>O</b>				
O'Konski, C. T.	727 (14)	740 (14)	767 (14)	772 (14)
	801			
O'Reilly, J. M.	574 (13)	627 (151)	640	644
Oak Ridge National				
Laboratory	852 (2)	852		
Oda, M.	695 (62)	723		

## Index Terms

## Links

Oelfke, W. C.	623 (141)	644		
Ogata, T.	616 (81)	617 (80)	642	
Ohashi, O.	145			
Ohl, R. S.	2 (10)	8		
Oka, T.	3 (26)	8	143 (33)	146 (60)
	147 (60)	170	195 (62, 67, 70)	
	197 (70)	198 (67, 70)	199 (70)	201 (67)
	206 (70)	207 (96, 98)	215 (67)	224
	273 (65, 67)	276 (90)	285 (114, 118, 120)	
	291 (143)	294	295	298 (1)
	341 (85)	357 (125)	359 (125)	373 (148)
	384	386	388	411
	421	684 (38)	685 (41)	686
	706 (87)	711 (88)	712 (90)	722
	766	770		
Okaya, A.	442 (50)	449		
Olofsson, H.	165 (130)	172		
Olson, W. B.	200 (75)	224	341 (87)	357 (124)
	386			
Oppenheimer, J. R.	150 (74)	171		
Oppenheimer, R.	80 (7)	120		
Orville-Thomas, W. J.	180 (7)	223	571 (6)	639
Otake, M.	181 (117)	187 (28)	217 (117)	223
	225			
Overend, J.	381 (187)	382 (196)	389	
Owen, N. L.	572 (10)	624	628 (160)	635 (193)
	639	644		
Oxton, I. A.	380 (181)	389		
Oyamada, M.	626	627 (154)	644	
Ozier, I.	195 (68)	202 (82, 84)	203 (86)	204 (84)
	205 (82, 85)	206 (89)	207 (68, 90)	

## Index Terms

## Links

208 (94, 101)	216 (82)	224	338 (78, 81)
360 (78)	361 (78, 133)	386	618 (110)
620 (110)	621 (110)	643	

## **P**

Pake, G. E.	17 (1)	31 (1)	35
Palke, W. E.	602 (60)	603 (60, 68)	618 (60)
Palmer, P.	145 (57)	164 (120)	170
Pandey, G. K.	276 (89)	295	534 (50)
	603	625	566
Papousek, D.	2 (14)	8	667 (15)
	202 (59)	224	721
Parent, G. R.	193 (55, 57, 59)	383 (207)	389
Parker, P. M.	307 (29)	380 (29)	385
	286 (125)	296	315 (53)
	326 (65)	328 (67)	341 (19, 89)
	369 (19)	382 (199)	367 (141)
Pascal, P.	385	388	
Pasinski, J. P.	536 (59)	566	
	671 (17)	721	
Pauling, L.	72	73 (5)	120
	38 (1)	69	
	754 (37)	761 (37)	770 (37)
	795 (37)	801	873
Pearsall, C. S.	878		
Pearson, E. F.	501		
	72 (1)	82 (1)	90 (29)
	120	143 (39, 43)	144 (39, 43, 45, 48)
	145 (48, 53)	170	288 (138)
	294	296	357 (120)
	387	411	540 (68)
	544 (68)	566	541 (69)
	780 (62)	677 (23)	722
Pearson, P. K.	802		
Pearson, R., Jr.	164 (117)	172	
	3 (19)	8	149
	278 (91)	295	276 (91)

## Index Terms

## Links

Peau, E. W.	147 (68)	171		
Pedersen, T.	285 (115)	286 (127)	296	623 (135, 137)
	643			
Pekeris, C. L.	73 (6)	77 (6)	120	
Pence, D. T.	291 (142)	296		
Penfield, H.	116 (98)	123		
Penney, W. G.	468 (10)	481 (10)	503	
Penrose, R. P.	188 (37)	223		
Penzias, A. A.	87 (35)	97 (45)	121	
Peter, R.	247 (16)	293		
Peters, C. W.	623 (141)	644		
Pickett, H. M.	267 (42)	282 (112)	294	349 (110)
	355 (110)	387	635 (192)	645
Pierce, L.	231	246 (10)	293	339 (82)
	343 (82, 153)	346 (82)	374 (82, 153)	
	378 (153)	378 (82)	386	388
	421	574 (12, 13)	594 (12, 37)	
	597 (38)	607 (37)	621 (116)	
	627 (146, 150)	639	643	698 (64)
	700 (64, 66)	710	723	765 (39)
	766	770	801	849 (1)
	852			
Pierre, G.	208 (102)	225		
Pillai, M. G. K.	311			
Piltch, N. D.	96 (43)	121	164 (28)	165 (128)
	172			
Pinkstone, J.	560 (96)	567		
Pitzer, K. S.	570 (1)	571 (3)	639 (212)	639
	646			
Plambeck, R. L.	166 (134)	173		
Pliva, J.	380 (162)	382 (197)	388	

## Index Terms

## Links

Plyler, E. K.	192 (51)	224	341 (86)	386
	712 (95)	724		
Pochan, J. M.	516 (23, 32)	532 (32)	533 (23)	534 (23, 32)
	565			
Polacco, E.	273 (71)	294		
Pollnow, G. F.	272 (60)	294		
Polo, S. R.	285 (117)	296	307 (30)	373 (149)
	385	388	685 (39)	709 (39)
	722			
Polyansky, O. L.	383 (216)	389		
Porter, A. P.	411			
Posener, D. W.	339 (83)	386	436 (46)	441 (47)
	449	849 (1)	852	
Pote, C. S.	649 (4)	721		
Poussigue, G.	208 (103)	225		
Powell, F. X.	107 (72)	116 (99)	122	371 (154)
	375 (154)	388	559 (108)	563 (107)
	564 (107)	567	710	
Poynter, R. L.	421	704 (75)	723	766
	770			
Prakash, V.	51			
Pratto, M. R.	259 (27)	293	471 (13)	473 (13)
	503			
Pringle, W. C.	638 (205)	645		
Propin, R. Kh.	193 (54)	224		
Pulay, P.	307 (35)	385		
Pullman, A.	730 (17)	801		
Pullman, B.	730 (17)	801		
Putley, E. H.	7 (62)	9		
<b>Q</b>				
Quade, C. R.	618 (94)	620 (106)	623 (127, 138)	

## Index Terms

## Links

627 (129)      632      642      689 (47)  
722

### **R**

Rabi, I. I.	29 (4)	35	175 (3)	223
	392 (1)	448	466 (9)	503
Racah, G.	479 (23)	503	803 (3)	839
Rademacher, H.	29 (3)	35	175 (2)	223
Radford, H. E.	115 (87, 89)	122	552 (78)	554 (78)
	556 (78, 82)	557 (78, 82)	558 (82)	560 (97)
	566			
Ralowski, W. M.	689 (50)	722		
Ralston, A.	246 (8)	293		
Ramadier, J.	135 (15)	169		
Ramaprasad, K. R.	269 (54)	294	624	
Ramsey, D. A.	6 (53)	9	649 (3)	721
Ramsey, N. F.	392 (1)	404 (16)	448	466 (9)
	503	804 (8)	812 (8)	839
Rank, D. M.	5 (50)	9		
Ransil, B. J.	789 (73)	799 (73)	802	
Rao, CH. V. S. R.	377 (160)	388		
Rao, D. R.	4 (35)	8		
Rao, K. N.	192 (52)	224	341 (88)	386
Rastrup-Andersen, J.	231	444 (62)	449	502
	627 (153)	644	698 (63)	723
	773 (53)	802		
Rastrup-Andersen, N.	421	766	770	
Rawson, E. B.	552 (77)	554 (77)	556 (77)	566
Ray, B. S.	233 (4)	293		
Raymonda, J.	87 (39)	121	411	434
Read, W. G.	155	221 (122)	222 (122, 125)	226
Reed, P. R.	616			

## Index Terms

## Links

Reiche, F.	29 (3)	35	175 (2)	223
Reif, F.	397 (13)	399 (13)	448	767 (41)
	801			
Reike, C. A.	768 (43)	801		
Reinartz, J. M. L. J.	411			
Renwanz, E. F.	89			
Reuger, L. J.	191 (49)	224		
Rhodes, I.	577 (16)	640		
Ribeaud, M.	598 (50)	600 (58)	623 (140)	641
	644	804 (43)	840	
Rigden, J. S.	231	827 (49)	840	
Rimmer, D. F.	351			
Rinehart, E. A.	616	620 (106)	643	689 (47)
	722			
Rinehart, P. B.	616			
Ring, H.	781 (64)	802		
Riveros, J. M.	627 (149)	632 (170)	644	
Robertson, J. C.	804 (12)	839		
Robiette, A. G.	181	343 (178)	369 (146)	380 (171, 178)
	381 (185)	388	706 (83)	710 (84)
	723			
Robinson, G. W.	425 (23)	448	827 (48)	840
Robinson, H. G.	737 (58)	737	745 (34)	770
	801			
Rock, S. L.	500	512 (40)	532 (40)	534 (40)
	546 (40)	565		
Rodriguez-Kuiper, E. N.	116 (97)	123		
Rogers, S. C.	153 (78)	154 (80)	155 (80)	159 (80)
	171	221 (120)	221	225
Rohart, F.	617 (82)	642		
Rohwer, F.	534 (53)	566		

## Index Terms

## Links

Ronn, A. M.	273 (77)	276 (77)	295	
Rose, M. E.	459 (8)	468 (8)	478 (8)	503
	803 (1)	815 (1)	839	
Rosenberg, A.	195 (68)	207 (68, 90)	224	
Rosenblum, B.	75 (9)	80 (9)	120	511 (7)
	545 (7)	548 (7)	565	676 (22)
	722			
Rosenthal, E.	421	766	770	
Rosenthal, J.	444 (62)	449		
Rotenberg, M.	426 (36)	439 (36)	447 (36)	449
	805 (45)	838 (45)	840	
Rothman, L. S.	304 (16)	385		
Roussy, G.	5 (39)	7 (39)	9	269 (55)
	294	320 (58)	349 (111)	351 (58)
	385	387	620 (108)	643
	689 (53)	722		
Rowell, R. L.	488 (34)	503		
Ruben, D. J.	415	770		
Rudolph, H. D.	3 (29)	8	231	247 (16)
	262 (29, 30)	276 (85)	291 (149)	293
	295	324 (62)	369 (143)	386
	388	595 (40)	603	615 (78)
	616	625	628 (157)	641
	644	664 (11)	700 (11)	704 (72)
	721	723	773 (55)	802
	804 (11)	833 (11)	839	
Ruitenberg, G.	620 (102)	643		
Rusk, J. R.	51	84 (21)	121	141 (25)
	170			
Russell, J. W.	369 (145)	388	636 (203)	645
Ryan, R. R.	380 (169)	389		

## Index Terms

Rydbeck, O. E. H.

115 (94)

## Links

### **S**

Saff, E. B.

383 (213)

389

Sage, M. L.

621 (117)

643

Saito, S.

3 (18)

8

97 (49)

116 (96, 99, 101)

121

123 169

(140)

173

291 (146)

296

381 (189, 191, 193)

389

559 (108)

560 (93, 100, 102)

564 (108, 111)

567

603 (67)

624

642

677 (26)

679

683 (27)

711 (26)

722

804 (36, 39)

837 (39)

840

Sams, R. L.

149

200 (75)

224

357 (124)

387

Sanders, T. M.

109 (80)

115 (80)

122

444 (53)

449

552 (79)

554 (79)

566

Sarachman, T. N.

231

Sarka, K.

383 (205)

389

Sastray, K. V. L. N.

83 (32)

85 (32)

96 (42)

107 (71)

121

164 (126)

164

165 (126)

166 (135)

172

231

250

268 (49)

294

534 (43)

551 (72)

566

Satten, R. A.

737

Sawodny, W.

307 (35)

385

Saykally, R. J.

5 (47)

9

145 (54)

164 (119)

165 (125)

166 (134)

170

172

Scappini, F.

193 (60)

224

273 (78)

295

351

421

534 (47)

566

598 (52)

618 (52)

623 (52)

641

## Index Terms

## Links

	766	770		
Schaefer, H. F.	164 (117)	172		
Schäfer, F.	411			
Schaffter, W. H.	674 (19)	721		
Scharpen, L. H.	265 (32)	293	485 (28)	487 (28)
	503	633 (175)	638 (207, 209)	645
Schatz, P. N.	311			
Schawlow, A. L.	1 (2)	7	50 (7)	54 (13)
	65 (7)	69	188 (40)	224
	246 (12)	251 (12)	293	415 (41)
	425 (21)	436 (21, 41)	448	478 (22)
	491 (21)	492 (37)	503	727 (11)
	740 (11)	741	770	772 (11)
	801			
Schempp, E.	772 (45)	801		
Schimizer, T.	273 (66)	294		
Schlapp, B.	99 (52)	121		
Schmalz, T. G.	273 (65)	294	536 (61)	566
Schmeltekopf, A. L.	106 (68)	122	363 (137)	371 (137)
	378 (137)	388		
Schmidt, R. E.	632			
Schnabel, E.	190 (44)	224	357 (122)	359 (122)
	387			
Schottlander, M.	231			
Schwartz, J.	276 (91)	278 (91)	295	
Schwarz, R. F.	432 (38)	449	540 (67)	544 (67)
	566			
Swendeman, R. H.	247 (15)	251 (20)	259 (24, 26)	293
	421	624	632 (172)	632
	645	649 (3)	654 (7)	681 (33)
	701 (33)	704 (33)	706 (78)	714 (33)

## Index Terms

## Links

	721	766	770	
Schwinger, J.	51 (10)	69		
Schwoch, D.	291 (149)	296	369 (143)	388
Scott, T. A.	773 (51)	802		
Sears, T. J.	560 (96)	567	804 (32)	840
Seiler, H.	231	615 (78)	642	773 (56)
	802			
Seip, H. M.	713 (99)	724		
Sekino, S.	766	770		
Serenellini, S.	678 (30)	722		
Serratrice, G.	689 (53)	722		
Shaffer, W. H.	131 (4)	132 (4)	169	182 (9)
	223			
Shapin, S. M.	152 (75)	171	201 (80)	225
	383 (216)	389		
Sharbaugh, A. H.	415	502	770	
Sharma, S. D.	272 (57)	294		
Shenk, B.	81 (12)	89 (12)	121	
Sheridan, J.	7 (66)	10	137	145
	411	415	624	626
	628 (165)	635 (193)	644	770
	772 (47)	801		
Shiki, Y.	624	626		
Shimizu, T.	3 (26)	8	442 (51)	449
Shimoda, K.	3 (27)	8	273 (65, 72)	
	294	436 (43)	442 (51)	449
Shimoda, K. S.	273 (70)	294		
Shoemaker, R. L.	512 (18, 20, 30)	514 (9)	516 (23, 32)	
	532 (18, 20, 30)	533 (23, 32)		
	534 (18, 20, 23, 30, 32, 35)		535 (20)	540 (66)
	545 (20, 24)	565		

## Index Terms

## Links

Shoji, H.	381 (194)	389	679	
Shoolery, J. N.	502			
Shortley, G. H.	446 (64)	449	459 (7)	468 (7)
	478 (7)	503	811 (47)	840
Shulman, R. G.	133 (10)	169	495 (45)	496 (46)
	500 (45)	504		
Sidran, M.	246 (14)	293		
Silver, S.	182 (9)	223		
Silvey, G.	137			
Silvey, J.	411			
Simmons, J. W.	144 (47)	170	428	435 (39)
	449	502	682	896
Simmons, N. P. C.	133 (9)	145 (9)	169	216 (116)
	225	500		
Simpson, J. B.	148 (69)	171		
Sinnott, K. M.	600 (56)	642	766	770
Skaarup, S.	691 (55)	722		
Slater, J. C.	733 (23)	785 (23)	801	
Slawsky, Z. I.	324 (60)	386		
Small, C. E.	288 (137)	296		
Smith, A. G.	144 (47)	170	428	
Smith, D. F.	382 (196)	389		
Smith, D. L.	616 (81)	617 (81)	642	
Smith, D. S.	207 (96)	225		
Smith, J. G.	148 (69)	171	179 (5)	202 (83)
	223	225	288 (137)	296
	351 (142, 170)	369 (142)	380 (170, 173)	388
	421	678 (28)	717 (101)	722
	724	766	770	
Smith, J. W.	799 (79)	802		
Smith, L. G.	571 (2)	639		

## Index Terms

## Links

Smith, W. L.	195 (66)	224		
Smith, W. V.	1 (1)	7	48 (3)	50 (8)
	54 (8)	69	144 (47)	170
	232 (3)	293	474 (16)	503
	539 (63)	542 (63)	566	727 (10)
	733 (24)	734 (24)	740 (10)	801
	874	896		
Smyth, C. P.	795 (76)	802		
Snyder, L. E.	87 (34)	115 (91)	121	144 (50)
	145 (56)	147 (50, 66)	163 (112)	164 (116, 121)
	170	172	300 (6)	384
Somerville, W. B.	6 (51)	9		
Soper, P. D.	155 (85, 87, 91)	155	156 (86)	159 (86)
	171			
Sørensen, G. L.	773 (53)	802		
Sørensen, G. O.	307 (34)	385	421	620 (105)
	643	689 (49)	704 (74)	722
	766	770		
Speirs, G. K.	380 (175)	389		
Špirko, V.	2 (14)	8	193 (55, 57, 59)	194
	202 (59)	224	383 (207)	389
Spitzer, R.	639 (212)	646		
Srivastava, G. P.	635 (181)	645		
Srivastava, S. L.	51			
Staats, P. A.	190 (47)	191 (47)	224	349 (106)
	353 (106)	387	702 (71)	723
Starck, B.	213 (105)	225	649 (4)	721
Steenbeckeliers, G.	349 (102)	361 (102, 134)		366 (102)
	370 (134)			
	387			
Steinbach, W.	2 (11)	8	99 (57)	100 (57, 60)

## Index Terms

## Links

	102 (61)	103 (60)	104 (57, 61)	
	106 (61)	122	835 (50)	836 (51)
	840			
Steiner, P. A.	455	493 (42)	495 (42)	501 (42)
	503			
Steinfeld, J. I.	273 (64)	294		
Steinmetz, W.	804 (18)	840		
Steinmetz, W. E.	265 (35)	267 (35)	293	633 (175)
	645			
Stelman, D.	591 (35)	641		
Stephens, P. J.	458 (5)	462 (5)	496 (5)	501 (5)
	503			
Sternheimer, R. M.	731 (19)	735 (19)	736 (20)	742 (20, 28)
	801			
Stiefvater, O. L.	274 (83)	277 (97)	278 (98)	279 (99)
	295	632 (171)	645	
Stitch, M. L.	83 (15)	85 (15)	121	
Stølevik, R.	713 (99)	724		
Stolze, M.	534 (55)	535 (56)	536 (55)	538 (55)
	540 (56)	542 (56)	566	
Stolze, W. H.	534 (56)	535 (56)	540 (56)	542 (56)
	566			
Stone, J. M. R.	145	193 (55, 57)	224	380 (165)
	383 (202, 206)	388		
Stone, N. W. B.	4 (33)	8	144 (51)	170
Stone, R. G.	516 (23, 32)	532 (32)	533 (23)	534 (23, 32)
	565			
Stouffs, P.	349 (105)	387		
Strandberg, M. W. P.	7 (58)	9	52 (11)	69
	99 (55)	122	246 (9)	293
	339 (83)	340 (84)	386	483 (26)

## Index Terms

## Links

	497 (26)	501	503	506 (3)
	511 (3)	520 (3)	525 (3)	546 (3)
	551 (73)	561 (73)	565	849 (1)
	852			
Strauch, R.	797			
Strauss, H. L.	369 (145)	388	636 (203)	645
Street, K.	797			
Strey, G.	307 (36)	377 (160)	381 (186)	385
	388			
Stroke, H. H.	737			
Strow, L. L.	354 (116)	387		
Su, C. F.	321			
Suenram, R. D.	281 (101)	295	501	623 (131)
	643			
Sugden, T. M.	7 (60)	9	65 (17)	70
	181 (30)	181	185 (24)	187 (30)
	223	444 (61)	449	727 (15)
	801			
Sugie, M.	717 (102)	724		
Sullivan, T. E.	4 (35)	8	179 (4)	181
	205	223		
Sumberg, D. A.	382 (199)	389		
Sundaram, S.	307 (26)	385		
Sung, E.	636 (197)	645		
Sutherland, G. B. B. M.	188 (39)	224		
Sutter, D.	617 (83)	618 (96)	622 (122)	642
Sutter, D. H.	415	501	516 (51)	
	533 (51, 58)	534 (27, 37, 44, 48, 54, 58)		
	535 (27, 56)	536 (54, 58)	537 (58)	538 (55)
	540 (56)	541 (48, 58)	542 (56)	546 (51)
	565	625	770	

## Index Terms

## Links

Sutton, L. E.	653 (6)	721		
Suzean, P.	360 (128)	387		
Suzuki, M.	502	534 (46)	566	
Svidzinskii, K. K.	426 (29)	448		
Swalen, J. D.	193 (53)	224	246 (10)	293
	502	572 (8)	574 (11)	579 (8)
	582 (8)	587 (8, 32)	592 (8)	593 (32)
	594 (8, 1, 32)	599 (8, 11)	601 (11)	603 (8)
	608 (8)	610 (8)	612 (8)	617 (85)
	621 (85)	639	641	849 (1)
	852			
Szalanski, L. B.	624	700 (67)	723	
Szanto, P. G.	5 (47)	9	96 (43)	121
	145 (54)	164 (119)	165 (125)	170
	172			

## T

Tack, L. M.	804 (41)	822 (41)	840	
Taft, H.	506 (4)	511 (4)	533 (4)	540 (4)
	565			
Takagi, K.	291 (143)	296	624	712 (90)
	723			
Takami, M.	3 (27)	8	116 (101)	123
	411			
Takeo, H.	381 (192, 195)	389	679	717 (102)
	724			
Takeyama, H.	772 (48)	801		
Takuma, H.	442 (51)	449		
Tan, B. T.	291 (149)	296	369 (143)	388
	616	625		
Tanaka, K.	500			
Tanaka, T.	291 (144)	296	381 (190, 194)	389

## Index Terms

## Links

	500	679		
Tang, C. L.	4 (38)	8		
Tannenbaum, E.	231	608 (75)	616 (76)	642
Tarrago, G.	133 (8)	169	185 (22)	186 (27)
	201 (22)	208 (103)	223	225
	282 (108)	284 (108)	286 (108)	295
	304 (14)	384		
Taylor, R. C.	415	770		
Teller, E.	184 (14)	223		
Terman, F. W.	773 (51)	802		
Thaddeus, P.	6 (54, 56)	9	165 (124, 127)	166 (133)
	168 (136)	169 (136, 138)	172	426 (33)
	436 (33)	438 (33)	443 (33, 52)	
	447 (33)	449	804 (7)	839
Thiele, W.	859			
Thomas, C. H.	421	624	765 (39)	766
	770	801		
Thomas, E. C.	415	501	770	
Thomas, L. F.	415	770		
Thompson, I.	179 (5)	223	421	766
	770			
Thompson, J. C.	181			
Thorne, L. R.	501			
Thornton, D. D.	5 (50)	9		
Thorson, W. R.	149 (71)	171		
Thyagarajan, G.	307 (26)	385		
Tieglear, H. L.	512 (40)	532 (40)	534 (40)	546 (40)
	565			
Tiemann, E.	81 (11)	82 (14)	87 (38)	89 (11)
	89	120	411	445
	741 (27)	745 (27, 32)		801

## Index Terms

## Links

	804 (31, 33)	840		
Tigelear, H. L.	500			
Timms, P. L.	616 (81)	617 (81)	642	
Tinkham, M.	99 (55)	122	551 (73)	561 (73)
	566			
Tischer, R.	81 (11)	89 (11)	89	99 (56)
	120	122	532 (38, 42, 45)	
	534 (38, 42, 45)	565		
Tobiason, F. L.	706 (78)	723		
Tolles, W. M.	615 (79)	642		
Tolman, C. A.	639 (213)	646		
Toman, S.	380 (162)	388		
Tong, C. C.	271 (56)	272 (56)	294	
Tong, C. K.	637			
Törning, T.	81 (11)	84 (18, 26)	86 (26)	87 (38)
	89 (18)	120	133 (6, 12)	135 (12)
	137 (12)	143 (42)	169	190 (44)
	224	357 (122)	359 (122)	387
	411			
Townes, C. H.	1 (2)	3 (20)	5 (50)	7
	50 (7)	51	54 (13)	65 (7)
	69	75 (9)	80 (9)	83 (15)
	85 (15)	99 (53)	109 (80)	115 (80)
	120	133 (10)	137	169
	188 (40)	224	246 (12)	251 (12)
	267 (69)	273 (69)	279 (69)	293
	392 (11)	411	415	423 (20)
	425 (21)	427 (37)	432 (38)	436 (11, 21)
	441 (11)	444 (53)	448	458 (4)
	468 (4)	478 (4, 21)	491 (21)	492 (36)
	495 (45)	500 (45)	503	511 (7)

## Index Terms

## Links

	540 (67)	544 (67)	545 (7)	548 (7)
	552 (79)	554 (79)	565	676 (22)
	682	722	727 (2, 11)	740 (11)
	741 (2, 11)	741	770	772 (2, 11)
	779 (60)	800		
Toyama, M.	298 (1)	384		
Trambarulo, R.	185 (23)	223	800 (81)	802
Trambarulo, R. F.	1 (1)	7	50 (8)	54 (8)
	69	232 (3)	293	727 (10)
	740 (10)	801	874	896
Treacy, E. B.	441 (48)	449		
Trinkaus, A.	625			
Trowell, P. L.	216 (111)	225		
True, N. S.	634 (178)	645		
Trueblood, M. B.	143 (39, 43)	170		
Tsuchiya, S.	624			
Tucker, K. D.	166 (133)	173		
Turner, B. E.	6 (54)	9	115 (93)	123
	145 (57)	147 (65)	164 (120)	165 (123)
	170	171	172	
Tycko, D.	742 (28)	801		
Tyler, J. K.	137	145	411	500
	635 (191)	645	797	
Typke, V.	320 (57)	328 (71)	333 (71)	354 (114)
	385	625	701 (70)	723
<b>U</b>				
Uehara, H.	564 (110)	567		
Uhlenbeck, G. E.	189 (42)	193 (42)	224	
Ulenikov, O. N.	285 (123)	296		
Ulich, B. L.	164 (116)	172		
Unland, M. L.	273 (75)	295		

## Index Terms

## Links

Urban, S.	2 (14)	8	193 (59)	202 (59)
	224			
<b>V</b>				
VanderHart, D.	512 (21)	532 (21)	534 (21)	565
Van Dijk, F. A.	141 (27)	170		
van Eijck, B. P.	269 (53)	294	328 (70)	333 (70)
	386	444 (63)	449	602 (65)
	632 (173)	642	645	705 (77)
	723			
Van Vleck, J. H.	50 (5)	69	80 (8)	108 (76)
	109 (78)	111 (76)	115 (78)	119 (8)
	120	122	239 (7)	293
	392 (8, 11)	436 (11)	441 (11)	448
	475 (17)	503	524 (13)	544 (13)
	565	586 (31)	640	676 (21)
	721			
van Wachem, R.	497	797		
Varga, R. S.	383 (213)	389		
Varma, R.	7 (70)	10	624	
Veazey, S. E.	85 (30)	121		
Venkatachar, A. C.	415	770		
Venkateswarlu, P.	186 (25)	195 (65)	223	321
	635 (187)	645		
Verdier, P. H.	617 (98)	619 (98)	643	
Verhoeven, J.	535			
Volltrauer, H. N.	632 (172)	632	645	
<b>W</b>				
Wacher, P. E.	471 (13)	473 (13)	503	
Wacker, P. F.	259 (27)	293		
Wagner, J.	182 (8)	223		
Wagner, R. S.	624 (145)	644		

## Index Terms

## Links

Wahlgren, U.	164 (117)	172		
Walden, M.	160 (97)	172		
Walden, R. T.	300 (7)	351 (7)	361 (7)	364 (7)
	384			
Walksley, C. M.	6 (52)	9	115 (92)	122
	300 (5)	384		
Walsh-Bakke, A. M.	304 (17)	385		
Walton, D. R. M.	146 (63)	147 (62)	171	
Wang, J. H. S.	415	534 (26, 33)		565
	770			
Wang, S. C.	239 (6)	250 (6)	251 (6)	293
Wapstra, A. H.	859			
Warren, I. D.	635 (196)	645		
Watson, J. K. G.	195 (64, 66)	196 (64)	206 (63)	208 (100)
	216 (112)	224	282 (106)	285 (121)
	286 (106, 124)	288 (124, 131, 134)		295
	304 (15)	313 (42, 47)	314 (51)	318 (51)
	320 (51, 55)	325 (55, 63)	326 (63)	327 (55, 64)
	328 (55, 63)	329 (63, 72)	330 (64)	335 (140)
	336 (64)	338 (72, 76, 80)	339 (64, 72, 80)	
	342 (64)	357 (64, 72)	360 (76, 80)	361 (64, 76)
	364 (139)	367 (140)	371 (140)	376 (158)
	380 (165)	381 (72)	385	388
	667 (16)	677 (24)	678 (57)	691 (57)
	714 (57)	717 (57, 101)		721 724
Watson, W. A.	415	770		
Wayne, F. D.	115 (89)	122		
Weatherly, T. L.	426 (27)	448	481 (25)	501
	503	804 (25)	840	
Weber, A.	306 (23)	385		
Weber, J.	485 (27)	493 (27)	503	

## Index Terms

## Links

Weinreb, S.	5 (49)	9	115 (90)	122
Weiss, M. T.	501			
Weiss, R.	799 (77)	802		
Weiss, V. W.	273 (75)	295	411	
Weisskopf, V. F.	50 (5)	69		
Welch, W. J.	5 (50)	9		
Wells, J. A.	268 (47)	294	628 (167)	644
Wells, J. S.	105 (66)	115 (87)	122	
Wells, P. R.	784 (66)	789 (66)	802	
Welsh, W. M.	104 (64)	106 (64)	122	
Welti, D.	623 (137)	643		
Wendling, P.	615 (78)	642		
Wentink, T., Jr.	483 (26)	497 (26)	503	
West, B. G.	104 (63)	106 (63)	122	469 (12)
	503			
Westerkamp, J. F.	133 (11)	169		
Wharton, L.	82	789 (70)	797	802
Wheatley, P. J.	653 (6)	721		
Whiffen, D. H.	148 (69)	171	421	653 (6)
	721	766	770	
White, H. W.	732 (21)	733 (21)	735 (21)	801
White, K.	477			
White, K. G.	498 (47)	502	504	
White, M. S.	502			
White, R. L.	415 (41)	432 (38)	434 (45)	436 (41, 45)
	449	540 (67)	544 (67)	566
White, W. F.	276 (88)	295		
Whitehead, M. A.	784 (67)	802		
Whittle, M. J.	187 (29)	223	360 (126)	387
Wick, G. C.	524 (15)	565		
Wiese, J.	534 (48, 54)	536 (54)	541 (48)	566

## Index Terms

				<u>Links</u>
Wilardjo, L.	304 (19)	341 (19)	369 (19)	385
Wilcox, W. S.	502			
Wilf, H. W.	246 (8)	293		
Wilke, W.	190 (44) 387	224	357 (122)	359 (122)
Willemot, E.	351 (142)	369 (142)	388	
Williams, G.	624			
Williams, J. R.	415	770		
Williams, N. H.	188 (36)	223		
Williams, Q.	426 (27) 503	448 804 (25)	481 (25)	501 840
Willis, R. E.	82 (13)	121		
Wilson, E. B., Jr.	38 (1) 120 247 (17) 276 (74, 77, 82) 282 (103, 111) 293 304 (8) 315 (52) 372 (11) 470 (11) 502 584 (29) 604 (70) 612 (77) 617 (29, 98) 628 (159) 632 (170, 171) 635 (183, 186, 196) 687 (43)	65 (16) 185 (16) 267 (38) 277 (77) 283 (111) 295 305 (21) 319 (50) 384 488 (11) 503 586 (32) 605 (27, 70) 613 (29) 619 (98, 100) 632 633 (159) 636 (186, 200) 721	69 187 (16) 273 (74, 77, 82) 279 (82) 286 (103) 301 (8, 10) 311 (21) 324 (21) 451 (1) 491 (11) 581 (21) 592 (27) 608 (29, 77) 615 (29, 77) 621 (115) 621 (115) 674 (19) 722	73 (5) 223 273 (74, 77, 82) 279 (82) 289 (139) 302 (11) 314 (50) 339 (50) 468 (11) 492 (1, 35) 583 (27) 600 (27) 609 (29) 616 (77) 621 (115)

## Index Terms

## Links

Wilson, P. W.	87 (35) 389	97 (45)	121	381 (195)
Wilson, S.	168 (137)	173		
Winn, J. S.	160 (99)	172		
Winnewisser, B. P.	3 (16) 135 (16) 288 (138) 383 (210) 706 (81)	8 136 (20) 296 386 723	84 (24) 143 (43) 349 (94) 389 632	121 169 380 (172) 632
Winnewisser, G.	3 (16) 70 121 149 268 (22, 52) 333 (69) 356 (69, 118) 384 498 (48) 644	6 (52) 84 (25) 144 (48) 170 293 349 (94) 358 (119) 386 500 700 (67) 770	8 90 (25, 29) 145 (48, 53) 256 (22) 300 (5) 351 (155) 375 (155) 421 504 723	67 (18) 115 (92) 145 257 (22) 328 (69) 351 380 (155, 171) 497 623 (142) 766
Winnewisser, M.	3 (16) 84 (23) 135 (14, 16) 146 152 (67) 257 (22) 293 356 (117) 502 644	8 90 (25) 136 (14) 147 (67) 169 268 (22, 52) 288 (138) 296 375 (117) 551 (72) 700 (67)	67 (18) 107 (71, 73) 144 (48) 150 (73) 250 288 (138) 349 (94) 386 566 706 (80)	70 121 145 (48, 53) 151 (67, 73) 256 (22) 291 (147) 351 500 623 (142) 723
Winther, F.	135 (17)	170		

## Index Terms

## Links

Winton, R. S.	141 (31)	170	181	623 (142)
	644			
Wodarczyk, F. J.	273 (82)	276 (82)	279 (82)	295
Wofsy, S. C.	202 (81)	225	357 (123)	359 (123)
	387	415	770	804 (15)
	840			
Wolf, A. A.	426 (28)	448		
Wolf, S. N.	216 (109, 113)	225	415	770
Wolfe, P. N.	426 (26)	448		
Wollrab, J. E.	7 (61)	9	282 (109)	295
	590 (121)	616	622 (121)	643
Woods, R. C.	5 (46)	9	96 (41, 43)	
	97 (43, 48)	121	145 (54)	163 (110)
	164 (119, 128)	165 (125, 128)		166 (132)
	170	172	273 (77)	276 (77)
	295	597 (44)	641	
Wooten, J. K.	426 (36)	439 (36)	447 (36)	449
	805 (45)	838 (45)	840	
Wyse, F. C.	85 (33)	87 (37)	121	
<b>Y</b>				
Yajima, T.	273 (72, 81)	294	295	
Yallabandi, K. K.	328 (67)	341 (89)	386	
Yamada, C.	500	804 (39)	837 (39)	840
Yamada, K.	135 (18)	147 (68)	150 (73)	170
	288 (130)	291 (147)	296	356 (117)
	375 (117)	387	700 (67)	723
Yokozeki, A.	745 (33)	801		
Young, A. T.	383 (215)	389		
Young, L. D. G.	383 (215)	389		
<b>Z</b>				
Zacharias, J. R.	392 (1)	448	466 (9)	503

## Index Terms

Zare, R. N.                    106 (68)  
                                  378 (137)

Zeiger, H. J.                3 (20)

Zeil, W.                     183 (13)

Zijderveld, G. R. D.      619 (101)

Zimmerer, R. W.            104 (62)

Zinn, J.                     477 (19)  
                                  645

Ziurys, L. M.                166 (134)

Zukerman, B.                115 (93)  
                                  164 (120)

## Links

122                            363 (137)            371 (137)

388

8

223

643

106 (62)                  122

503                          636 (201)            638 (201)

173

116 (97)                  123

170                          172

# **SUBJECT INDEX**

---

<b><u>Index Terms</u></b>	<b><u>Links</u></b>				
<b>A</b>					
Absorption, optimum region for:	122	133	133	133	
diatomic molecules	120				
linear molecules	139	140			
symmetric-top molecules	212	213			
Absorption cells:					
attenuation constant	43				
cavity	5	160	198	223	
double resonance modulation	276	279			
free space	3	84			
high temperature	82	84			
parallel plate	493				
Stark modulation	492	493			
Absorption coefficient:					
asymmetric-top molecules	263				
diatomic molecules	117	118			
general formula, with Lorentzian line shape	42				
linear molecules	138				
measurement of	43				
symmetric-top molecules	208				
Angular momenta:					
average values of, in asymmetric rotor basis	247	248	253	254	
	271				
classical	11				
time rate of change	13	15			
commutation rules	16	17	19	21	
	282	314	318	584	

## Index Terms

## Links

molecule -fixed axes	21			
space-fixed axes	16	17		
eigenfunctions	27			
eigenvalues	17			
matrix elements, <i>see</i> Matrix elements, angular				
momentum operators	15	16	23	
raising and lowering	17	18	21	
spin	19	20		
phase convention	19	811		
transformation properties under $V$	237	315		
Anharmonicity, Fermi resonance	136	187	219	286
Anharmonicity constant, $\omega_e x_e$	74			
relation to spectroscopic constants	77	79		
table of	83	86	88	90
Assignment of spectra	258	264	273	491
	492	686		
Associated Legendre polynomials	28			
Asymmetric rotor	227			
analysis of spectra for rotational constants	269			
assignment of spectra	258	264	273	491
	492	686		
branches	254	257	258	
notation	257			
centrifugal distortion	287	288	297	339
	361			
Coriolis interaction	285	286	289	
energy levels, rigid rotor	232			
algebraic expressions	244	245		
example calculation	26	27	248	249
notation of	229	230	232	

## Index Terms

## Links

sum rules	341	342	851	
energy matrix	240	241		
intensities	256			
peak absorption coefficient	263			
internal motions	569			
<i>See also</i> Internal rotation				
matrix elements	24	235	236	250
	290			
nuclear magnetic coupling	435	816	817	827
	828			
nuclear quadrupole coupling	413	429	436	814
	827	828		
nuclear spin statistics	66	440	441	600
	827	828		
representations	236			
selection rules	254			
slightly asymmetric rotors	250	417	418	474
Stark effect	468	488	603	604
structures	291	292	678	679
	683	684	696	702
	703	710	711	713
	717			
vibration, correction to rotational constant	281	288		
effect on energy levels	281			
wave functions	29	60	61	233
	237	247		
example calculation	248	249		
symmetry classification	60	61	241	
Zeeman effect	515	530	534	535
	617			

## Index Terms

		<u>Links</u>		
Asymmetric rotor group V	238			
Asymmetry parameter:				
in asymmetric rotors, inertial	229	250	251	
in quadrupole coupling	398	407	739	764
Atomic masses	859			
Atomic number, effective	732	733	735	785
Atomic term energy	732	733		
Atom-molecule, complexes	5	160		
force constants	162			
structure	161			
$\alpha$ -type transitions	256			
Avogadro's constant	857			
Avoided-crossing technique for,				
internal rotation barriers	205	620	621	
K-level separations	202			
<b>B</b>				
Back-Goudsmit effect	521			
Band spectra	265	633	634	
frequency relations	266			
Barriers, hindered rotation, table of	603	616	624	
Barrier tunneling	188	575	576	632
Basis functions	842	843		
Bohr magneton	857			
Bohr radius	857			
Boltzmann distribution law	39	619		
Boltzmann's constant	857			
Bond length:				
average $\langle r \rangle$	649	706		
evaluation of	706			
relation to $r_0$ and $r_e$	707			
effective $r_0$	648	679		

## Index Terms

## Links

evaluation of	679				
equilibrium $r_e$	648	674			
evaluation of	672				
mass dependence $r_m$	649	714			
evaluation of	714				
substitution $r_s$	648	691	692		
evaluation of	691				
relation to $r_0$ and $r_e$	693				
Born-Oppenheimer expansion parameter	150	151	285	328	
Bose-Einstein statistics	62				
<i>b-type</i> transitions	256				
<b>C</b>					
Casmir's function, <i>see</i> Y(J,L,F)					
Center of mass	653				
Centrifugal distortion	297				
asymmetric rotors	287	288	297	339	
	361	617			
derivation of P4 Hamiltonian for	287	288	301		
first-order	313	344			
higher-order	339				
diatomic molecules	74	75	78	79	
	304				
with electronic angular momentum	94	95	99	110	
	111				
energy matrix, form of	340	342	349	352	
matrix elements	340	344	354		
Hamiltonian, general	325				
orthorhombic form	326	327			
number of terms	327				
Padé	383	384			

## Index Terms

## Links

reduced, derivation of	324			
asymmetric-top reduction	329			
symmetric-top reduction	333			
standard form	327			
number of terms	327			
linear molecules	127	131	132	
spherical tops	207	208	338	339
	360	361		
symmetric rotors	177	185	191	197
	200	201	322	337
	338	357		
Centrifugal distortion constants:				
approximation for methyl halides	181	182		
bent triatomic, expression for	311	312		
dectic	333	339		
defect	370			
determinable combinations	335			
diatomic, expression for	77	304		
evaluation from spectra	339			
choice of Hamiltonian	361			
effect of representation	354	356		
relations between representation	356			
rigid rotor basis method	343			
semirigid rotor basis method	347	348		
extremal properties	313			
isotopic relations	312	313		
linear triatomic, expression for	127			
octic	333	335	338	339
planarity relations	321	323	366	
quartic	319	320	322	330

## Index Terms

## Links

	333	334	338	
relation to $\tau_{\alpha\beta\gamma\delta}$ , asymmetric rotor	320	322	330	331
	337			
symmetric rotor	323	324		
relation between A and S reduction	335			
sextic	331	332	334	337
	338			
calculation of	288	382		
enumeration of	326			
sum rules	341	342		
table of, asymmetric rotors	321	343	350	352
	353	355	381	
diatomic molecules	75	76	83	88
	90	98	106	108
linear molecules	142	148	155	161
	164	168		
spherical tops	381			
symmetric rotors	181	192	201	202
	221	381		
vibration effects	368			
Centrifugal distortion constants $\tau_{\alpha\beta\gamma\delta}$ :				
calculation of	305			
definition of	287	303	305	311
	312			
nonvanishing of, asymmetric tops	316			
in first-order	314	315		
symmetric tops	323	324		
planarity relations	322	367		
potential constants, from	372			

Character table:

## Index Terms

## Links

C <sub>3</sub> group	578				
V group	238				
Chemical analysis	7	301			
Chi-square distribution	362				
Clebsch-Gordon coefficients	446	459	468	478	
	805				
<i>See also</i> Three-j symbol					
Coherence splitting, creeper	274	279	280		
Commutation rules, <i>see</i> Angular momenta					
Commutator	328				
Complexes:					
atom-molecule	5	160			
hydrogen bonded	5	153	221		
Constants of rotational motion	13	20	23	24	
	229				
Continued fraction, evaluation of energy levels of asymmetric rotor	849				
Conversion factors	857				
Coordinates, structural, <i>see</i> Kraitchman's equations					
Coriolis coupling constants:					
calculation of	685				
expression for bent XY <sub>2</sub>	709				
expression for linear XYZ	708				
rule for nonvanishing of	285	685			
sum rules	285				
Coriolis force	131				
Coriolis interaction:					
asymmetric rotors	289				
linear molecules	128				
symmetric rotors	183	219	607		
Correlation coefficients	362	363			

## Index Terms

Correlation diagram:

asymmetric rotor	230
Mathieu eigenvalues	576
$^2\Pi$ states	112
Covalent bond radii, table of	873
Crystal harmonic generator	1      2
<i>c</i> -type transitions	256

## **D**

Degrees of freedom	301
Detectors	2
Diagnostic least squares, for structural parameters	717
Diatomic molecules	71
bond lengths	76      83      86      88
	90      106      680
centrifugal distortion	74      75      78      79
	94      95      99      110
	111      304
Dunham's solution	78
with electronic angular momentum	87      90      444      550
	551      835      836      838
energy levels	71      78      79      87
	90      107
intensities	103      104      117
peak absorption coefficient	117
$\Lambda$ -type doubling	107
nuclear magnetic coupling	432      444
nuclear quadrupole coupling	407      426      444      445
nuclear spin statistics	63      64
selection rules	34      72      74      92
	95      102      112      113

## Links

## Index Terms

## Links

Stark effect	451	484		
vibration, effect on energy levels	72	78		
wave functions	28			
Zeeman effect	509	520	521	529
	530	532	550	551
Dimers, <i>see</i> Hydrogen bonding				
Dipole moment matrix elements, asymmetric rotor	259	262	263	
<i>l</i> -doublets	133	482		
linear	33			
Λ-doublets	113	562		
inversion doublets	33	482		
symmetric rotor	31	33	35	
Dipole moments:				
direction of	498	544		
effects of, centrifugal distortion	497	498		
isotopic substitution	494	496	497	
vibration	496	497		
from intensity measurements	492	493		
from Stark splitting measurements	493			
example calculation	473	474		
tables of	495	497	498	500
enhanced	154	156		
induced	195	206	207	
interpretation of	788			
bond moment	789	794	795	799
	800			
hybridization moment	791			
induced moment	794	798		
ionic character from	754	755	795	
overlap moment	790	791		

## Index Terms

## Links

primary moment	790			
Direction cosine, symmetry under $V$	255	469		
Direction cosine matrix elements:				
asymmetric rotor	259	468	471	
linear	33			
symmetric rotor	31	32		
Dissociation energy	74	77		
Doppler broadening	45			
Doppler frequency shift	45			
Double resonance	3	4	143	273
assignment aid	276			
four-level system	280			
line profiles	279	280		
information from	3	4	273	
three-level system	274			
line profiles	274	277		
Dunham constants	78	79		
relation to potential constants	79			
table of	83	86	88	90
Dunham correction, to rotational constant	79	80	676	677
Dunham's solution, diatomic	78			
<b>E</b>				
Eckart conditions	306	308	311	
Effective rotational constant	74	79	108	128
	129	131	182	281
	672			
Eigenvalue equation	842			
Eigenvalues, methods of finding	24	846	879	880
Einstein coefficients	33	38	39	
Electric field gradient in atoms	731			
from atomic beam measurements	735			

## Index Terms

## Links

configuration interaction correction	736				
from doublet find structure	733				
effects of formal charge	733				
effects of screening	732	733			
relativistic correction	735	736			
Sternheimer polarization correction	735	736			
table of $q_{n10}$	734	737			
Electric field gradient in molecules:					
approximations and assumptions	730	731			
calculation of	727	738			
formal charge corrections	741	742			
hybridization effects	742				
interpretation of quadrupole coupling					
constants	745	755			
See also					
Nuclear quadrupole coupling					
unbalanced p-electrons	738				
units	738				
Electronegativities	753	762	763	783	
	795	875			
values of	761	778	783	785	
	875				
Electronic angular momentum, coupling cases	91				
molecules in, $\Pi$ or $\Delta$ states	107	169			
$^2\Sigma$ states	94	166	836		
$^3\Sigma$ states	98	835	836		
molecules with, hyperfine structure	444				
notation	87	90	91		
tables of derived constants	98	106	164	165	
	168	557	564		

## Index Terms

## Links

Zeeman effect	549			
Electronic corrections to:				
inertial constants	80	546	675	
inertial defect	684			
Electron paramagnetic resonance of gases	552			
molecular constants derived from	557	564		
Stark effect	561			
Electronic spin -spin interaction	99	835		
Energy ellipsoid	14	15		
Energy level index for asymmetric rotors, $K_{-1}, K_1, \tau$	229	230	232	
Equilibrium structure, tables of	76	83	86	88
	90	106	143	149
	217	219	220	678
	679	680		
Euler's angles	29			
Euler's equations of motion for free rotation	13			
Euler's theorem on homogeneous functions	715			
<b>F</b>				
Fermi-Dirac statistics	62			
Fermi resonance	136	187	219	286
Fine structure constant	857			
Forbidden transitions, internal rotation	599	604		
spherical tops	195	205		
line strengths	206			
selection rules	206			
Stark effect	489	491	562	
symmetric tops	194			
interaction term	197			
line strengths	198			
selection rules	197	200		
Force constants, <i>see</i> Potential constants				

## Index Terms

Four group, *see* Asymmetric rotor group

Frequencies of transitions:

<i>l</i> -doublet	133	135
$\Lambda$ -doublet	113	
rotational:		
in diatomic molecules	72	74
Hund's case (a)	93	
$^3\Sigma$ states	102	
in linear molecules	127	128
degenerate bending mode	131	
in symmetric rotors	177	179
degenerate bending mode	185	
rotation-inversion	191	
of some rotational transitions, in asymmetric rotors	266	

Frequency, of inversion	188	194
-------------------------	-----	-----

<i>F</i> -test	364	
----------------	-----	--

Fundamental constants, table of	857	
---------------------------------	-----	--

## **G**

<i>g</i> -factor, electron spin $g_s$	549	550
molecular $g$ , asymmetric rotor	516	
general definition of	508	
linear molecules	509	
symmetric rotor	513	
molecules with electronic angular momentum	550	551
molecules with nuclear coupling	519	520
origin in $^1\Sigma$ molecules	523	
molecular $g$ tensor elements $g_{gg}$ definition	527	
effects of isotopic substitution	544	545
from microwave spectra	512	516
nuclear spin $g_l$	429	520

## Links

## Index Terms

G-matrix, *see* Vibrational energy

Gyromagnetic ratio 429 507

## **H**

Hamiltonian:

centrifugal distortion:					
asymmetric rotor	303	313	317	325	
	331	333			
linear molecule	127				
spherical top	338	339			
symmetric top	178	337	338		
Coriolis coupling	285	289			
electric polarizability	485				
harmonic oscillator	282	283			
hyperfine, general	805	818			
internal rotation	584	585	587	590	
	606	609			
torsional	585				
<i>K</i> -level splitting in symmetric tops	338				
magnetic susceptibility	529				
molecules with electronic angular momentum,					
Hund's coupling case (a)	92				
$^2\Sigma$ states	94	95	97	167	
$^3\Sigma$ states	99	100	835		
nuclear magnetic coupling (I-J)	430	438	805	818	
nuclear quadrupole coupling	396	404	439	805	
	818				
solid state	396				
Padé	383				
reduced, centrifugal distortion	331	333	337		
rigid rotor:					

## Links

## Index Terms

## Links

asymmetric-top	232	233	250	
reduced	233	250		
linear molecule	72	126		
spherical-top	23	23		
symmetric-top	23	176		
ring puckering	638			
spin-rotation interaction	94	100		
spin-spin interactions	100	805	830	835
Stark effect	452			
vibration-rotation	130	184	282	284
	289			
expanded form	284			
general (nonlinear)	282			
Zeeman effect	507			
nuclear magnetic	509			
Harmonic oscillator, <i>see</i> Hamiltonian				
Hermitian, definition of, matrix	234	841		
operator	19			
High resolution spectroscopy	2	3	5	141
	441			
High temperature spectroscopy	82	143	144	
Homogeneous function	714			
Euler's theorem	715			
Hybridization:				
from nuclear quadrupole coupling	755			
table of	756			
relation to bond angle	777			
relation to dipole moment	749	750	758	794
	795			
rule	749	750		

## Index Terms

Hydrogen bonded complexes:

asymmetric-tops	157	222	
bridge lengths	155	161	221
enhanced dipole moment	154	156	
force constants	158	159	
linear	153		
symmetric tops	221		

Hydrogen bonding in rotational isomers

Hyperconjugation from quadrupole coupling

table of

Hund's coupling cases

case (a)

case (b)

Hypergeometric series

## **I**

Inertial defect

effect on structure calculations	683	684	691	703
	705	712		
expression for	684			
information on, planarity	687	688	691	
torsional vibrations	689	690		
substitution	691			
tables of	686	687	689	703

Intensity of absorption, asymmetric -top

diatomic molecule	117		
forbidden transitions	198	206	
general theory	37		
integrated	43		
linear molecules	138		
nuclear hyperfine structure	445	831	881

## Links

## Index Terms

## Links

irreducible tensor methods	831			
peak	43	117	138	209
	263			
Stark effect	489			
with quadrupole coupling	491			
symmetric-top molecule	208			
Zeeman effect	514	518	519	522
	549			
Intensity measurements, relative	619	620		
Internal axis method	582			
Internal rotation	570			
barriers, effects of vibration	600	602	603	
from avoided crossing method	205	620	621	
from relative intensities	618			
from rotational fine structure	591	612		
example calculation	605	606		
from satellite frequency pattern	617	618		
tables of	603	616	624	
classical kinetic energy	583			
Coriolis effects	607			
denominator corrections	591			
direct diagonalization methods	598			
effective principal axis system	592			
forbidden transitions	599	604		
free internal rotation	609			
Hamiltonian, derivation of	582			
high-barrier approximation:				
derivation of effective rotational Hamiltonian	585	590	591	
higher-order effects	593			
methyl group equilibrium orientation	624	625		

## Index Terms

## Links

methyl group tilt	625			
molecules with low sixfold barriers	612			
distortion effects	617			
Zeeman effect	617			
molecules with twofold barriers	620	622	623	
nuclear statistical weights	600			
perturbation coefficients	587	621	622	
table of	588	589		
potential function	573	602	608	631
$V_6$ effects	602			
evaluation of	600			
pseudocentrifugal distortion effects	596	597		
pseudorigid rotor	591			
quadrupole and magnetic coupling	600			
selection rules	592	599	600	607
	610	612	615	
spectra in, ground torsional state	598			
excited torsional states	600	601		
Stark effect	603	604	615	
symmetric rotor	606	607	609	610
	617			
torsional energy levels	574			
two-top molecules	621	622		
vibration-rotation interactions	600	617	618	
Interstellar space molecules	5	6	96	115
	116	145	163	300
Inversion	187			
frequency	188	189	194	
effect of isotopic substitution	193			
hyperfine structure	435	436	441	

## Index Terms

## Links

potential, illustration of	188				
selection rules	34	188			
Stark effect	481	482			
Ionic character, definition of	749	754	759	760	
	762	790	796	797	
	799				
from dipole moments	754	755	795		
table of values	797	798			
from quadrupole coupling	748	772			
table of values	752				
tables of values	752	756	760	763	
	770	797	798		
Ionic character-electronegativity relation	753	798	799		
Ions, <i>see</i> Radicals and ions					
Irreducible tensor, definition of	804				
from Cartesian tensors	805				
matrix element theorems	807	815			
transformation properties	804				
Irreducible tensor methods	803				
electronic spin-spin interaction	835				
nuclear quadrupole and magnetic interaction	812				
relative intensities	831				
nuclear spin-spin interaction	829				
rotational angular momentum, matrix elements	809				
Stark effect	838	839			
Isotopic abundances, table of	859				
Isotopic relations	81	285	312	313	
distortion constants	312	313			
Dunham's constants	81				
Isotopic shrinkage of bonds	713	714			

## Index Terms

## Links

### **J**

Jacobi diagonalization procedure 246

### **K**

K-level splitting 196 229 230 232  
    avoided crossing from 202  
    expressions for 201 251 266 357  
    360  
    forbidden transitions from 196  
Kraitchman's equations 656  
    choice of 663 704  
    multiple isotopic substitution 665  
    single isotopic substitution 657

### **L**

Laplace's equation, in quadrupole coupling 395 400 407  
Large amplitude motions 149 187 382 383  
    706

*See also* Internal rotation; Ring, puckering

Lasers 3 4 219 299  
Least squares analysis 270 271 361 681  
    682 701 702 717  
Legendre equation 28  
Linear molecules 125  
    centrifugal distortion 127  
    energy levels 126  
    Fermi resonance 136  
    intensities 138  
        peak absorption coefficient 138  
    *t*-type doublet spectra 133  
    matrix elements 126  
    nuclear magnetic coupling 136 432  
    nuclear quadrupole coupling 136 137 407 426

## Index Terms

## Links

		814		
quasi-linear		149	706	
selection rules		34	127	130
		133		131
Stark effect		451	481	
structures		143		
tables of		143	145	146
		165	682	694
vibration, effect on energy levels		128		
level notation		130		
wave function		28		
Zeeman effect		509	520	529
		533		530
Line shape, Doppler		45	46	
illustration of, Doppler-broadened		47		
first and second derivative		53		
pressure-broadened		49	50	
instrumental distortion		50		
Lorentzian		48	51	
Van Vleck-Weisskopf		50		
Line strength		259	262	263
		595	831	
definition of		259	831	
properties of		263		
relation to matrix elements of, angular momentum	263		595	
dipole moment		259	262	263
direction cosine		262	471	
sum rules		262	263	
Line width		44		
collision with walls		52		

## Index Terms

## Links

Doppler	45	
modulation and detection effects	53	54
in molecular beams	52	
natural	44	45
power effects	50	
pressure broadening	43	47
table of	51	
<i>L</i> -matrix, <i>see</i> Vibrational energy		
Lórentzian line shape function	48	
<i>l</i> -type doubling, linear molecules	129	
constants, table of	135	137
spectra	133	
Stark effect	481	
symmetric-top molecules	183	
spectra	185	
<i>Λ</i> -type doubling	107	552
expressions for	110	
in electron paramagnetic resonance	552	
spectra	113	
<i>L</i> -uncoupling	107	
correction to rotational constant	80	546     675

## **M**

Magnetic moment:

electron spin	549	
molecular	506	549
origin	523	
nuclear spin	429	520
orbital angular momentum	549	
Magnetic susceptibility	528	
anisotropy in, table of	532	

## Index Terms

## Links

bulk	524			
calculation of	536			
table of atomic susceptibilities	537			
Magnetic -susceptibility tensor	524	529	531	
Magneton, Bohr	857			
nuclear	857			
Manning potential	189			
Maser	3	141	436	
resolution and spectra from	3	441	822	829
Mathieu's equation	577			
eigenfunctions and eigenvalues	577			
Matrix, diagonalization of	246	352	846	
continued fraction method	849			
Givens method	352			
Jacobi method	246	352		
Matrix elements:				
angular momentum	18	234	340	344
	354	397	399	595
	809			
relation to direction cosine matrix elements	406			
asymmetric rotor	24	235	236	250
	290			
dipole moment	31	33	113	133
	259	262	263	482
	562			
direction cosine	31	32	259	468
	471			
internal rotation	594	595	610	613
	614			
linear molecule	126	127		

## Index Terms

## Links

nuclear magnetic coupling (I-J)	404	439	817	818
	821	825		
nuclear quadrupole coupling	404	427	428	440
	818	821	825	
reduced, <i>see</i> Reduced matrix elements				
spherical-top	23			
symmetric-top	23			
vibrational coordinates	283	672		
vibrational momentum	283			
Matrix mechanical methods	841			
Microwave region, extent of		1		
Modulation	53	54	276	279
	492			
double resonance	276	279		
Stark	492			
Molecular quadrupole moments	538			
from line width	542			
table of	532	541		
tensor elements	539			
relation to elements of g and x	539			
from Zeeman effect	540			
Molecular structures, <i>see</i> Structure				
Moment of inertia	649	653		
average configuration	708			
expressions for	708	709		
calculation of	649			
effective	673			
electronic corrections	546			
expressions for	654	655		
mass-dependence	715			
of methyl group, evaluation of	703	712		

## Index Terms

## Links

relation to structural parameters	656			
substitution	695	715	716	
Moment of inertia tensor	649			
derivatives of	284	306		
inverse	282			
derivatives of	284	305		
expansion of	284			
transformation property	650			
Momentum sphere	14			
Morse potential	74			
illustration of	74			
<b>N</b>				
Natural lifetime in state	44	45		
Natural line width	44	45		
Near-axis atoms, location of	664	698		
Normal equation matrix	362			
Nuclear hyperfine structure, effects of identical nuclei	440	441	804	826
table of relative intensities	881			
Nuclear magnetic coupling, asymmetric tops	435			
general theory	429			
irreducible tensor methods	815	831		
linear and diatomic molecules	432			
magnetic field, origin of	431	432		
magnetic field at coupling nucleus	433	435		
molecules with electronic angular momentum	97	98	444	
in Zeeman effect	551	552		
more than one coupling nucleus	436	818	831	
in paramagnetic resonance of gases	554			
with quadrupole coupling	436	818	831	
selection rules	432	434	437	445

## Index Terms

		<u>Links</u>			
in Stark effect	464				
symmetric tops	433	441			
in Zeeman effect	518				
Nuclear magnetic coupling constants, $C_{ji}$ ,					
expressions for	430	432	434	435	
	816	817			
information from	432				
table of	434	443			
Nuclear magnetic moments, table of	859				
Nuclear masses, table of	859				
Nuclear quadrupole coupling:					
asymmetric tops	413	416	425	429	
	439				
example calculation	417	418			
derivation of Hamiltonian	399				
general theory	392	399			
irreducible tensor methods	812	818	831		
linear and diatomic molecules	136	137	407	423	
with magnetic coupling	436	818	831		
in paramagnetic resonance of gases	555				
second-order corrections	426	815	823		
table of	895	896			
selection rules	398	408	412	417	
	425	432	434	437	
	445				
in solids	395				
in Stark effect	458	478			
symmetric tops	412	425			
two or more nuclei	423	439	440	818	
	831				

## Index Terms

## Links

in Zeeman effect	518			
Nuclear quadrupole coupling constants, atomic p-electrons, table of	737			
determination of principal elements	418	419	422	664
effects of vibration	444	445		
$g_{ji}$ , expressions for	405	406	408	412
	416	813	814	
relation to electronic structure	726			
in centrally bonded atoms	776			
group electronegativities	783			
hybridization	755	777		
hyperconjugation	767			
ionic character	748	772		
in nitrogen ring compounds	772			
$\pi$ character	758	775	776	780
	783			
pure covalent bonds	745			
tables of	411	415	420	421
	443	445		
Nuclear quadrupole moments	395	396	401	403
	812			
from atomic beam measurements	736	737		
tables of	737	859		
Nuclear spins, determination of, from microwave spectra	413			
table of	859			
Nuclear spin -spin interaction	441	805	829	
Nuclear statistical weights	61	210	440	441
	600	827	828	
table of	64	65		

<u>Index Terms</u>	<u>Links</u>
<b>O</b>	
Oblate symmetric rotor	176 229 230 236
Operator matrix	843 844
change of basis	845 846
diagonalization of	246 352 846 849
Orthorhombic symmetry	315
Overlap integral	747 789
<b>P</b>	
Padé Hamiltonian	383 384
Partition function	54 118 138 211
Paschen-Back effect	462 521
P-branch	254
Perturbation theory, contact transformation	286
ordinary	286 855
Van-Vleck transformation	286 287 474 475
	477 586 590 595
	613 853
Phase convention	19 811
Phase-sensitive detection	53 54 492
$\pi$ character from quadrupole coupling	758 775 776 780
	783
from asymmetry of coupling	764
due to hyperconjugation	767
involvement of $d$ orbitals	762
from magnitude of coupling	758
tables of	760 763 766 770
$\pi$ feedback	762
$\pi$ transitions:	
in Stark effect	454
in Zeeman effect	509 519 521 522
Planar moments of inertia	655 656
Planck's constant	857

## Index Terms

## Links

Planck's radiation law	39			
Polarizability, electric	484			
Population of energy states	54			
fraction of molecules, general definition	55			
in rotational states	56			
in vibrational states	55	118	138	211
inversion of	3	40		
Potential barriers, internal rotation, table of	603	616	624	
Potential constants:				
anharmonic	83	381	382	
from centrifugal distortion constants	372			
sources of information	373			
tables of	375	378	379	
multiple solution problem	379	380		
relation to Dunham's constants, diatomic molecule	79			
table of	83			
Potential function	74	78	283	301
	374			
illustration of	74	675		
Potential function for hindered rotation	573	608	622	631
effect of $V_6$ term	602			
illustration of	573	631		
Potential function for ring puckering	638			
Power absorption	43			
fractional, calculation of	119	120	139	211
Power attenuation constant of absorption cell, $\alpha_c$	43			
Power saturation	50			
Pressure broadening	43	47		
Principal axes of inertia	12	649		
location from symmetry	651			
Principal axes of quadrupole coupling constant				

<u>Index Terms</u>	<u>Links</u>			
tensor, determination of	418	419	422	664
Principal axis coordinates, evaluation of by				
isotopic substitution	656			
in asymmetric -tops	660	666	667	
in linear molecules	658			
sign of coordinates	670	671		
in symmetric -tops	658	665	666	
Principal axis method	581	582		
Principal moments of inertia	12	649		
expressions for	654	655		
Products of inertia	649	653		
Prolate symmetric rotor	176	229	230	236
Pseudorotation	639			
Pumping	3	273		
<b>Q</b>				
$Q$ -branch	254			
Quadrupolar center, effective	542			
Quasi-linear molecules	149	706		
criterion	150			
<b>R</b>				
Radiation density	38			
Radicals and ions	5	6	96	106
	163			
Ray's asymmetry parameter $\kappa$	229			
Ray's operator $H(\kappa)$	233			
$R$ -branch	254			
Reduced angular momentum, $P$ , internal rotation	584	591		
Reduced barrier height	577	857		
Reduced distortion Hamiltonian, <i>see</i> Centrifugal distortion				
Reduced energy, asymmetric rotor	232	250		
coefficients in perturbation expansion of $W(bp)$	252			

## Index Terms

		<u>Links</u>		
relation between Ray's $E(\mathbf{k})$ and Wang's $W(b)$	253			
submatrices	240	241		
matrix elements of	235	236	250	
symmetry classification of	241			
table of	244			
Reduced mass	73			
for inversion	189	192	193	
for isotopic substitution	657	665	668	
Reduced matrix element, for irreducible operators	807			
Reduced moment of inertia, internal rotation	574	583	584	
Reduced nuclear statistical weight, g,	57	64	210	
Reduced rotational constant F, internal rotation	584			
Reduced Stark coefficients	470			
$\rho$ -type triplet	98			
$\rho$ -vectors	307			
Ring:				
conformation	627	688		
puckering	636			
Rotating coordinate system	12	232		
conditions on	306			
Rotational constants:				
conversion factor	857			
dependence on vibrational quantum numbers	74	79	128	129
	131	182	281	288
	672			
tables of, asymmetric-tops	231	678		
diatomic molecules	75	76	83	86
	88	90	98	106
	677			
linear molecules	132	140	142	143

## Index Terms

## Links

	145	146	148	155
	161	164	168	693
symmetric tops	181	192	201	202
	205	217	218	220
	221			
Rotational isomerism	501	627		
table of isomers	632			
Rotational kinetic energy, classical	12	14		
Rotational spectrum, assignment of	258	264	273	491
	492			
Rotation of coordinate axes, transformation matrix	650			
Rotators, classification of	71	72	126	176
	227			
Rydberg constant	857			
<b>S</b>				
<i>s</i> character, in terms of bond angle	777			
Schrodinger equation	24	25		
Second moments, electron charge distribution	542			
Secular equation, derivation of	24	25	846	847
Selection rules:				
asymmetric-top	254			
basis for	33			
diatomic molecules	34	72	74	92
	95	102	112	113
electron paramagnetic resonance	555			
internal rotation	592	599	600	607
	610	612	615	
inversion spectra	34	188		
linear molecules	34	127	130	131
	133			
<i>l</i> -type doubling	133			

## Index Terms

## Links

Λ-type doubling	113			
nuclear hyperfine structure	398	408	412	417
	425	432	434	437
	445			
pure quadrupole resonance	398			
Stark effect	454	462	464	466
	471	479		
symmetric-tops	34	177	185	188
	196	197	200	
from symmetry	58			
Zeeman effect	509	513	518	519
	522			
σ transitions:				
in Stark effect	454			
in Zeeman effect	509	519	521	522
Six-j symbol	425	426	447	448
	807			
symmetry	808			
tables of	809			
Slater's rules	733			
Slightly asymmetric rotors	250	417	418	474
Slightly nonplanar molecules	477	636	687	688
Spherical tensors, <i>see</i> Irreducible tensors				
Spherical top	23	195	205	338
	339	360	361	381
Spin operators	19	20		
Spin-orbit coupling constant.	108	109	111	
Spin-rotation interaction constant	94	100		
Spin-spin interaction constant	99	831		
Spin uncoupling	107	111		
Standard deviation of least-squares fit	362			

## Index Terms

## Links

Standard error in least-squares parameter	362				
Stark effect	451				
anisotropic polarizabilities from	484				
assignment aid	491	492			
asymmetric-tops	468	488			
dipole moments from	493				
tables of	156	495	497	498	
	500				
forbidden transitions	489	491	562	604	
fourth-order	457	458	472	473	
	487	494	495		
high frequency	277				
intermediate field case with one quadrupolar nucleus	465	481			
internal rotation	477	603	604	615	
inversion doublets	481	482			
irreducible tensor methods	838	839			
<i>K</i> -type doublets	475				
<i>l</i> -type doublets	482				
linear and symmetric-top molecules	451	481			
$M_j$ , evaluation of	471	472	476	492	
with magnetic hyperfine structure	464				
modulation with	492				
paramagnetic resonance of gases	561				
patterns	455	456	472	477	
	490				
relative intensities	489	491			
secondary standards for measurement of Stark splittings	493	494			
selection rules	454	462	464	466	
	471	479			
strong-field case, with one quadrupolar nucleus	462	480			

<u>Index Terms</u>		<u>Links</u>			
plural nuclear coupling	464	480	481		
weak-field case with one quadrupolar nucleus	459	478			
Stark effect constant	857				
Statistical weights, <i>see</i> Nuclear statistical weights					
Structural parameters, number of	667				
Structure, evaluation of	647				
average structure	706				
from diagnostic least squares	717				
effective structure	679				
equilibrium structure	672				
from least squares	681	682	701	702	
mass-dependence structure	714				
substitution structure	691				
example calculation	693				
with small coordinates	664	698			
Structures:					
in asymmetric tops	291	292			
tables of	678	679	683	684	
	702	703	710	711	
	713				
in complexes	153	221			
tables of	155	161	221		
in diatomic molecules	77				
tables of	76	83	86	88	
	90	106	680		
in linear molecules	143	163			
tables of	143	145	146	149	
	165	682	694		
in symmetric tops	213				
tables of	214	219			

## Index Terms

## Links

vibrational effects on	214	215	680	694
	702	712	717	
estimation of	704	714		
Student's <i>t</i> distribution	363			
Sum rules	262	263	285	341
	342	851		
Surface spherical harmonics	28	804		
<i>s</i> -vectors	307			
Symmetric rotor	175			
centrifugal distortion	177	185	191	197
	200	201	322	337
	338	357		
energy levels	175			
forbidden transition	194			
intensities	208			
peak absorption coefficient	209			
internal rotation	606	607	609	610
	617			
inversion	34	187		
<i>K</i> -level splitting, from avoided crossing	202	620	621	
from forbidden transitions	194			
<i>l</i> -type doubling	183			
matrix elements	21	31	35	234
nuclear magnetic coupling	433	441	817	
nuclear quadrupole coupling	412	425	814	
nuclear spin statistics	64	210	441	
selection rules	34	177	185	188
	196	197	200	
Stark effect	451	481	482	484
structures	213			

## Index Terms

tables of	214	219		
vibration, effect on energy levels	182	219	607	
wave functions	29	810	811	
Zeeman effect	512	520	528	529
	533			
Symmetry number $\sigma$	57	58	63	66
	209	210		

## **T**

Term symbols	91			
Thermal equilibrium, Boltzmann's law	39			
Three-j symbol	804	805	809	
symmetry	805			
tables of	809			
Torsional angle	572			
Torsional energy levels	574			
Torsional frequency	575	619	620	
from intensity measurements	618			
Torsional satellite lines	600	601		
Transformation:				
contact	286			
Van Vleck	286	287	474	475
	477	586	590	595
	613	853		
to diagonalize asymmetric rotor energy matrix	245			
of moment of inertia tensor	650			
between parent and isotopic form	664			
Transformation coefficients, in coupling three angular momenta	425	808		
two angular momenta	808			

## **U**

Unbalanced $p$ electrons $U_p$	740			
--------------------------------	-----	--	--	--

## Index Terms

	<u>Links</u>
Uncertainty principle	44
Unitary matrix	842
Unitary transformation	325      846
 <b>V</b>	
Valence orbitals, hybridized:	
$sp_2$	774
$sp_3$	776
Van Vleck transformation	286      287      853
in internal rotation	586      590      595      613
in Stark effect	474      475      477
Van Vleck-Weisskopf line shape function	50
Van der Waals complexes, <i>see</i> Atom-molecule complexes	
Van der Waals radii, bond	873
$V_6$ Barrier term	573      602
Vector model:	
Hund's case (a)	92
Hund's case (b)	94      95
nuclear coupling	400
nuclear quadrupole coupling, two nuclei	424
strong-field Stark effect, molecule with	
nuclear coupling	463
symmetric-top	176
Stark effect	453
weak-field Stark effect, symmetric-top with	
nuclear coupling	460
Zeeman effect	506
Vibration, effects on energy levels:	
asymmetric-top	281
diatomic molecules	72      78
linear molecules	128
symmetric-tops	182      219      607

<u>Index Terms</u>	<u>Links</u>			
Vibrational energy, coordinates	282	301	307	308
<i>G</i> matrix, etc.	302	307	308	311
	372	374	376	377
	879	880		
Hamiltonian	282	283		
secular equation	372	879		
solution of	879	880		
Vibrational frequency, from intensity measurement	183	618		
relation to spectroscopic constants	77			
Vibrational modes:				
resulting on dimer formation	157			
triatomic linear molecule	129			
triatomic nonlinear molecule	677			
Vibrational potential function, <i>see</i> Potential function				
Vibration-rotation constants, expression for, asymmetric -tops	288			
Vibration-rotation Hamiltonian	282			
expansion of	284			
order of magnitude classification	285			
perturbation solution	286			
Vibration-rotation perturbation parameter	285	328		
Vibration-torsion-rotation interactions	600	617	618	
<b>W</b>				
Wang asymmetry parameter	250	251		
Wang functions	239			
transformation properties under V	242			
Wang operator: $\mathsf{H}$ (b)	250			
Wang transformation	239	240		
Wave function:				
asymmetric rotor	29	60	61	233
	237	247		
example calculation	248	249		

## Index Terms

		<u>Links</u>		
internal rotation	585	609	610	
inversion	187			
linear molecule	28			
matrix representation	843			
for nuclear hyperfine states	446	459	478	
nuclear spin	63			
torsional function	577	578	580	
Wigner-Eckart theorem	807			
Wigner $6j$ symbol, <i>see</i> Six- $j$ symbol				
Wobble-stretching correction to rotational constant	80	675		
<b>Y</b>				
Y(J,I,F)	408			
table of	881			
<b>Z</b>				
Zeeman effect:				
asymmetric tops	515	530	534	535
	617			
determination of, molecular quadrupole moments	538			
second moments electron distribution	542			
sign of dipole moment	544			
electronic corrections to inertial constants, relation to g factor	546			
evaluation of anisotropic magnetic susceptibility	528			
general theory	506			
linear and diatomic molecules	509	520	529	530
	533			
magnetism in ${}^1\Sigma$ states, origin of	523			
molecules with electronic angular momentum	549			
molecules with nuclear coupling	518			
relative intensities	514	518	519	522

## Index Terms

selection rules	509	513	518	519
	522			
symmetric tops	512	520	528	529
	533			
tables of derived constants	512	516	532	541
	545			
transition between Zeeman components, electron				
paramagnetic resonance	552			
Stark effect	561			
Zero-point vibrations:				
effect on structures	214	215	680	694
	702	712	717	

## Links